Hydrochemistry and Hydrology of the Coastal Dune area of the Western Netherlands

Pieter Jan Stuyfzand

kiwa

HYDROCHEMISTRY AND HYDROLOGY OF THE COASTAL DUNE AREA OF THE WESTERN NETHERLANDS

Cover : decomposing leaf on decalcified dune sand at the bottom of a flow-through lake. The released organics reduce sulphate and ferric hydroxides, and both reaction products combine into a black iron monosulphide precipitate downgradient.

Photo : *F. Lüers*

CIP-DATA KONINKLIJKE BIBLIOTHEEK, DEN HAAG

Stuyfzand, Pieter Jan

Hydrochemistry and hydrology of the coastal dune area of the Western Netherlands / Pieter Jan Stuyfzand. - Nieuwegein : KIWA, Afd. Onderzoek & Advies. - I11.
Also publ. as thesis Vrije Universiteit Amsterdam, 1993. -
With index, ref - With summary in Dutch.
ISBN 90-74741-01-0
NUGI 816
Subject headings : hydrochemistry / hydrology ; Western Netherlands.

VRIJE UNIVERSITEIT

HYDROCHEMISTRY AND HYDROLOGY OF THE COASTAL DUNE AREA OF THE WESTERN NETHERLANDS

ACADEMISCH PROEFSCHRIFT

ter verkrijging van de graad van doctor aan
de Vrije Universiteit van Amsterdam,
op gezag van de rector magnificus
dr. C. Datema,
hoogleraar aan de faculteit der letteren,
in het openbaar te verdedigen
ten overstaan van de promotiecommissie
van de faculteit der aardwetenschappen
op dinsdag 25 mei 1993 te 15.30 uur
in het hoofdgebouw van de universiteit, De Boelelaan 1105

door

PIETER JAN STUYFZAND

geboren te Haarlem

Promotor	:	prof.dr. G.B. Engelen
Copromotor	:	dr. C.A.J. Appelo
Referenten	:	prof.dr. G. Matthess
		dr. W.M. Edmunds

To my parents Do and Jan
To Loredana and Eugenie

CONTENTS

PREFACE . 13

SUMMARY 15
SAMENVATTING 21

1. INTRODUCTION
1.1 General significance of hydrochemistry . 27
1.2 Coastal plains and dunes in general 28
1.3 The coastal dune area of the Western Netherlands as a test site . 29
1.4 Previous hydrochemical studies in the dunes 31
1.5 Scope and outline of this study 34
1.6 Dissolved constituents under consideration . 36

2. THE HYDROCHEMICAL FACIES ANALYSIS
Abstract 39
2.1 General 39
2.2 Principles and definitions 41
2.3 Acquisition and screening of hydrochemical data . 42
2.3.1 Needed data in general 43
2.3.2 Sampling groundwater : problems and recommendations . 43
2.3.3 Checking the accuracy of chemical analyses 48
2.3.4 Estimating missing values 50
2.4 Defining the facies 51
2.4.1 Classification of water types . 51
2.4.2 The redox index 55
2.4.3 A water quality index 58
2.4.4 A relevant mineral saturation index . 60
2.4.5 Water temperature . 61
2.5 Identifying the origin . 61
2.6 Mapping 62
2.6.1 Suggestions for associations and differentiations . 63
2.6.2 Coding and nomenclature 63
2.7 Interpretation 63
2.8 Concluding remarks . 65

3. HYDROLOGY OF THE COASTAL AREA
Abstract . 67
3.1 General 67
3.2 Physiography 68
3.2.1 Situation and climate . 68
3.2.2 Geology 68
3.2.3 Geomorphology 73
3.2.4 Parent materials and soils . 74
3.2.5 Dune vegetation 75
3.3 Hydrogeological structure 76
3.4 Natural groundwater recharge in dunes . 78

3.4.1 Gross precipitation 78
3.4.2 Natural groundwater recharge as a function of vegetation . 78
3.4.3 Natural groundwater recharge in 1850 and 1980 81
3.4.4 Transit time in the vadose zone 81
3.5 Analytical approximations for a fresh dune water lens . 83
3.5.1 The Ghyben-Herzberg principle 83
3.5.2 General assumptions and their validity . 84
3.5.3 Size and shape 84
3.5.4 Time of formation 85
3.5.5 Dispersion across the fresh-salt water interface 88
3.6 Palaeohydrology and early-historical hydrology : the Quarternary period till 1850 AD . 91
3.6.1 The Pleistocene 91
3.6.2 The Holocene till 1000 AD 91
3.6.3 The Holocene from 1000 till 1550 AD 93
3.6.4 The Holocene from 1550 till 1850 AD . 95
3.7 Historical hydrology : the period after 1850 AD . 96
3.7.1 The period from 1850 - 1903 . 96
3.7.2 The period from 1903 - 1955 . 98
3.7.3 The period from 1955 - 1976 . 102
3.7.4 The period from 1976 - 1990 . 104
3.7.5 The period after 1990 104
3.8 Major changes during the past 5000 years : synthesis and areal extent . 105
3.9 Actual groundwater flow systems 108
3.9.1 Definitions 108
3.9.2 The coastal area anno 1981 109
3.9.3 The Maassluis system 109
3.9.4 The North Sea system . 109
3.9.5 Dune systems . . . 111
3.9.6 Polder systems 112
3.9.7 Artificial recharge systems . 113
3.10 Special flow cases 113
3.10.1 Gravity-driven collapse and volumetric compensation 113
3.10.2 Rain water lenses 113
3.10.3 Flow-through dune lakes 117
3.11 Concluding remarks . 120

4. HYDROCHEMICAL FACIES ANALYSIS OF THE COASTAL AREA
Abstract 121
4.1 General 121
4.2 Hydrochemical data collection and screening . 122
4.2.1 Inventory of all available data 122
4.2.2 Screening and ranking 122
4.2.3 Collection and analysis of 2500 samples 123
4.3 Construction and presentation of regional maps . 125
4.3.1 Starting-points 125
4.3.2 Origin detection 125
4.3.3 Maps, sections and typical analyses 126
4.4 Discussion of the discerned hydrosomes and their facies . 127
4.4.1 The connate, marine Maassluis hydrosome (M) . . . 127
4.4.2 The relict, Holocene transgression hydrosome (L) . 131
4.4.3 The actual North Sea hydrosome (S) . . . 136
4.4.4 Coastal dune hydrosomes (D) . 138
4.4.5 Polder hydrosomes (P) 142
4.4.6 Artificial recharge hydrosomes (A) . 142
4.4.7 Important mixed hydrosomes 150
4.5 Interpretation of the regional patterns . 151
4.5.1 Facies chains 151
4.5.2 Flow patterns and life cycle . 151

4.5.3 Geochemical structure of the subsoil 154
4.5.4 Water table fluctuations, land-use and environmental pollution . 154
4.6 Subregional application to flow-through dune lakes 159
4.7 Local application to a moist dune slack 163
4.8 Concluding remarks . 166

5. COMPOSITION OF BULK PRECIPITATION
Abstract 167
5.1 General 167
5.2 Measurement 167
5.2.1 Bulk precipitation as a fraction of total atmospheric deposition . 167
5.2.2 Problems 168
5.2.3 Monitoring stations . 169
5.3 Mean composition 169
5.3.1 General considerations . 169
5.3.2 Sea spray contribution 172
5.3.3 Continental mineral aerosols . 173
5.3.4 Biogenic inputs . 173
5.3.5 Air pollution . . 174
5.4 Spatial variations 176
5.4.1 Regional patterns 176
5.4.2 Gradients perpendicular to the shore line south of Zandvoort aan Zee . 176
5.5 Variations with time 179
5.5.1 Trends 179
5.5.2 Variations in annual means . 182
5.5.3 Seasonal fluctuations 182
5.5.4 Episodes 182
5.5.5 During a shower . 186
5.6 Concluding remarks . 186

6 FROM RAIN WATER TO THE UPPER DUNE WATERS
Abstract 187
6.1 General 188
6.2 Description of sites and groundwater sampling 188
6.3 Hydrological boundary conditions 193
6.3.1 Gross precipitation and groundwater recharge . 193
6.3.2 Position of the water table 194
6.3.3 Vegetation water lenses and the transit times within . 194
6.3.4 Artificial dispersion by sampling 197
6.4 Geochemistry of dune sand and dune peat 199
6.4.1 Dune sand as parent material . 199
6.4.2 Dune sand in soil zone . . 202
6.4.3 Dune peat 205
6.5 Changes "en route" from rain water to the upper dune waters . 205
6.5.1 Review of processes 205
6.5.2 The changes, in a bird's-eye view . 206
6.5.3 Throughfall . . . 207
6.5.4 Litter leachate . 210
6.5.5 Soil moisture 211
6.6 Spatial variations in the composition of upper dune water . 213
6.6.1 Presentation of results 213
6.6.2 Effects of spatial variations in bulk precipitation chemistry 214
6.6.3 Effects of different vegetation covers 219
6.6.4 Effects of differences in decalcification 221
6.6.5 Effects of different kinds of dune peat interaction 227
6.6.6 Effects of differences and changes in thickness of the unsaturated zone . 230
6.7 Fluctuations in the composition of upper dune water . . 233

6.7.1 Main causes . 233
6.7.2 Trends . 234
6.7.3 Fluctuations in annual means . 237
6.7.4 Seasonal fluctuations . 240
6.7.5 Effects of dispersion . 249
6.8 Important fluxes . 252
6.8.1 Interception deposition . 252
6.8.2 Storage in biomass . 256
6.8.3 N_2-fixation . 256
6.8.4 Decalcification rates . 257
6.9 Concluding remarks . 260

7. CHEMICAL EVOLUTION OF INTRUDING DUNE, RHINE AND NORTH SEA WATER DOWNGRADIENT
Abstract . 263
7.1 General . 264
7.2 Geochemistry of marine Holocene and selected Pleistocene deposits . 264
7.3 Bergen dune water towards the Geestmerambacht polder . 265
7.3.1 Situation and collection of hydrochemical data . 265
7.3.2 Heterogeneities in the upper 30 meters . 267
7.3.3 Heterogeneities further downgradient . 267
7.3.4 The generalized evolution over 7 km . 267
7.4 Zandvoort dune water towards the Haarlemmermeer polder . 279
7.4.1 Situation and collection of hydrochemical data . 279
7.4.2 Heterogeneities in the upper 30 meters . 279
7.4.3 Heterogeneities and discontinuities further downgradient . 279
7.4.4 The generalized evolution over 9 km . 284
7.4.5 Groundwater dating . 289
7.5 Rhine water intruding into dune water . 292
7.5.1 Situation and collection of hydrochemical data . 292
7.5.2 Some calculations . 292
7.5.3 Areal patterns in cross section . 293
7.5.4 The generalized quality evolution downgradient . 298
7.5.5 Dating . 302
7.6 Intruding North Sea water . 304
7.6.1 Situation and collection of hydrochemical data . 304
7.6.2 Intrusion into relict Holocene transgression water . 304
7.6.3 Intrusion into dune water . 307
7.7 Comparison of field data with column experiments by Beekman . 310
7.8 Conclusions . 311

8. CHEMICAL MASS BALANCES FOR DUNE GROUNDWATER
Abstract . 313
8.1 Definition, purpose and limitations . 313
8.2 General set-up . 314
8.2.1 Principles . 314
8.2.2 Normal sequence in the procedure . 317
8.3 Carbon-13 . 320
8.4 Shallow groundwater in contrasting dune areas . 322
8.4.1 Presentation of balances . 322
8.4.2 Intercomparison of H^+ budgets . 322
8.4.3 Dissolution of $CaCO_3$ by strong and weak acids . 326
8.5 Bergen dune water downgradient . 328
8.5.1 Presentation of balances . 328
8.5.2 Intercomparison of H^+ budgets . 329
8.5.3 Check by carbon-13 . 331
8.6 Concluding remarks . 332

CONCLUSIONS . 333

CONCLUSIES 337

REFERENCES . 341

UNITS AND ABBREVIATIONS 359

SUBJECT INDEX . 363

ENCLOSURES (in separate portfolio) :

1.1. Location and physiographic subdivision of the Noordwijk - Camperduin area, with some historical developments during the past 500 years.
1.2 The most relevant piezometers and miniscreens sampled in the Noordwijk - Camperduin area.
1.3 Areal distribution of aquitards 1D through 1H, at or close to the base of the Holocene deposits, separating the first and second aquifer in the Noordwijk - Camperduin area.
1.4 Areal distribution of aquitards 2A through 2E, separating the second and third aquifer in the Noordwijk - Camperduin area.
2.1 Isohypses of mean phreatic level in the Noordwijk - Camperduin area, for the year 1981.
2.2 Isohypses of mean fresh-water head in the second aquifer at 25 to 30 m-MSL in the Noordwijk - Camperduin area, for the year 1981.
2.3 Contour lines of equal mean difference in hydraulic head between the first and second aquifer in the Noordwijk - Camperduin area, for the year 1981.
2.4 Isohypses of mean salt-water head in the third aquifer at 80 to 130 m-MSL in the Noordwijk - Camperduin area, for the year 1981.
3.1 Isohypses of reconstructed mean phreatic level in the coastal dunes in the Noordwijk - Camperduin area, before 1850 when (semi)natural conditions prevailed.
3.2 Contour lines of equal drawdown of the water table in the coastal dunes in the Noordwijk - Camperduin area, in the period 1850 - 1981.
3.3 Contour lines of equal depth to the fresh-brackish water interface (300 mg Cl^-/l) in the Noordwijk - Camperduin area, for the period 1976-1990.
3.4 Contour lines of equal rise of the fresh-brackish water interface (300 mg Cl^-/l) in the Noordwijk - Camperduin area, in the period 1910 - 1981.
4.1 Areal distribution of groundwater flow systems in the second aquifer at 25 to 30 m-MSL, in the Noordwijk-Camperduin area, for the period 1976-1990.
4.2 Areal distribution of hydrosomes and their chemical facies in the second aquifer at 25 to 30 m-MSL, in the Noordwijk - Camperduin area, for the period 1976 - 1990.
4.3 Areal distribution of chemical water types in the second aquifer at 25 to 30 m-MSL, in the Noordwijk - Camperduin area, for the period 1976 - 1990.
4.4 Areal distribution of hydrosomes and their chemical facies at 80 ± 5 m-MSL, in the Noordwijk - Camperduin area, for the period 1976 - 1990.
4.5 Areal distribution of chemical water types at 80 ± 5 m-MSL, in the Noordwijk - Camperduin area, for the period 1976 - 1990.
5 Cross sections over the coastal dunes north of the river Old Rhine, showing the areal distribution of hydrosomes and their chemical facies.
6 Cross sections over the coastal dunes north of the river Old Rhine, showing the areal distribution of chemical water types.
7 Longitudinal section over the coastal dunes from Camperduin to Monster, showing the areal distribution of hydrosomes and their chemical facies, and chemical water types.
8 Legend to codes for hydrosomes and hydrochemical facies discerned in the coastal area.
9 Legend to lithological units in well drilling logs and hydrogeological units.

PREFACE

My apologies to those who thought to rush through a normal-sized Ph.D thesis. Numerous figures with extensive captions, the detailed contents and subject index may speed up your search for the desired information.

This thesis satisfies two needs : the completion of academic research at the Institute of Earth Sciences of the Vrije Universiteit of Amsterdam (IvA-VU), which started in August 1978; and the integration of many investigations conducted at KIWA, the Waterworks' Testing and Research Institute, Research & Consultancy Division, where I am employed since February 1981. The material covered is expected to be of general interest to hydrochemists, geochemists, hydrologists, ecologists, geologists, geomorphologists, pedologists and everybody interested in the regional situation of the study area : the coastal dunes and adjacent polders in between Monster (Province South Holland) and Camperduin (Province North Holland).

My acknowledgements are directed to those who inspired and corrected me, the financiers who believed in me, the many unknown who contributed to the patrimony of data collected since 1850, the many unnamed analysts who performed tedious work for me on highly variable, capricious samples, the many colleagues and family members who contributed in several ways, and those who supported my too prolonged dedication to "the book".

To start with Prof.dr. G.B. Engelen, the promotor, his powers of observation in the field and holistic thinking inspired me greatly. The whole manuscript and especially chapter 2 on the Hydrochemical Facies Analysis benefitted much from his suggestions for improvement. I thank him for his faith, the freedom he gave me and his patience since I left IvA-VU. The enthusiasm, personality and profound scientific knowledge of Dr. Tony Appelo, the co-promotor, conduced to a strong stimulation and many corrections. I thank Dr. Mike Edmunds and Prof.dr. G. Matthess, the referees, for their inspiring and constructive criticisms on the manuscript, and Professor G. Matthess also for his hospitality at the "Geologisch-Paläontologisches Institut" in Kiel.

I wish to extend my sincere thanks to Ing. Frans Lüers, co-worker and room-mate at KIWA since 1991, for his many contributions : the conversion of WORDMARC text files into WP5.1., the styling in 2 columns, all the computer drawings, data handling, carefully reading the entire text and eliminating many of the errors that crept in, the innumerable suggestions for improving the readability, mental support and the cover photo. Other colleagues at KIWA provided valuable suggestions for improvement of parts of the text : Dr. Willem Koerselman, Ir. Kees Maas, Ir. Jos Peters and Ir. Henk Vinkers. Prof.dr. W.H.O. Ernst gave valuable comments on chapter 1 and 6, and Prof.dr. W.G. Mook read the sections on environmental isotopes.

The following organizations raised the direct financial funds for carrying out this investigation or the printing of the enclosures :
(1) the Netherlands' Waterworks Association (VEWIN), which assigns research in the general interest of its members (the public drinking water supply companies), to KIWA. This study formed part of the topics "quality changes of surface water upon artificial recharge", "trace elements in groundwater", and "ecological aspects of artificial recharge", since February 1981;
(2) the Institute of Earth Sciences of the Vrije Universiteit of Amsterdam (IvA-VU), by engaging me during the period August 1978 till February 1981, analysing 1780 water samples, bailer drilling of three multilevel wells, etc; and
(3) the Municipal Water Supply Co. of Amsterdam (GW), the Provincial Water Supply Co. North Holland (PWN N.V.) and the Provincial Authority of North Holland (Water & Environment Dept.), by a grant for printing the enclosures. I express my gratitude to Ir. Theo Olsthoorn, Ing. R.A. Schuurmans, Drs. Fred van de Vegte, Drs. Bart Korf and Ir. Piet Veel for their confidence.

I am greatly indebted to the water supply companies GW, PWN N.V., the Dune Water Supply Co. of South Holland (N.V. DZH), the Water Supply Co. Zuid-Kennemerland (WLZK), the Energy & Water Supply Co. of Rijnland (EWR N.V.) and the Drinking Water Supply Co. Westland (WDM), and the Provincial Authorities of

North and South Holland (Water & Environment Depts.), for their numerous contributions. They gave very substantial support in chemical analyses, hospitality at their laboratories, assistance in groundwater sampling, generous supply of data and access to their extensive "data cemeteries". They also ordered me (KIWA) to carry out various investigations in the study area, which yielded many essential data, and allowed KIWA to publish them.

For a huge bulk of analytical work I should like to address my acknowledgements to the following laboratories, with citation of the principal contact persons only, under whose skillful supervision the many unnamed analysts generally did the job : the Water & Soil Laboratory of IvA-VU (Mrs. Tiny Bäer); the Laboratory of GW (Ing. Jos Bouma and Ing. Dick van de Gugten); the Laboratory of PWN N.V. (Drs. H.J.M. Lips, Drs. Bart Schultink, Ir. Janny Willemsen-Zwaagstra); the Laboratory of N.V. DZH (Ir. Jan van Puffelen); the Laboratory of EWR N.V. (Ir. D. Mus, Drs. Arie de Ruyter); the Radiochemical Laboratory of the Netherlands' Energy Research Foundation (ECN, Dr. Hans van der Sloot); the Centre for Isotope Research (Mr. Harm-Jan Streurman, Prof.dr. W.G. Mook); and the Laboratory for Inorganic Analysis and Materials of KIWA (Ing. Hans van der Jagt).

I also wish to specify my sincere thanks to some of those who assisted in various remarkable ways : Drs. Anton Rijsdijk and my brother-in-law Drs. Roelof Stuurman, in those days students, did an excellent job during their final practical work under my supervision. Ing. Lester Reiniers (Prov. Authority North Holland) organized the installation of four multilevel wells in the Bergen dune area, assisted in sampling groundwater, sampled groundwater on strategic positions on my request and kept me informed on the last data obtained from the provincial groundwater monitoring network. Mr. Tim Spierings (†) drilled the three most used multilevel wells. Drs. Paul Baggelaar taught me the power of redundant pleonasms with superfluous information repeated and rehearsed all over again. Ing. Maarten Nieuwland constructed the initial hydrochemical data base and carried out many SPSS-runs. The data base was further developed at KIWA by Ing. Gerrit Nauta and Ing. Theodoor van der Kooi. Mr. Hans Vermeulen prepared high-quality, photographic under- and overlays of many drawings. Sabicas (†), the absolute king of flamenco guitar, made the many monastic jobs a lot more agreeable.

And last but not least, my family. My father Jan skillfully converted all my drawings-by-hand, into a high-quality technical version, in an astonishingly rapid way. It was an immense job, and I sincerely hope to please him with this book. My sister Marjorie ordered, synthesized and visualized part of the historical data : an enormous and tremendously tedious piece of work indeed. My mother Do and mother-in-law Rosa deputized in numerous ways. Without their baby-sitting, cooking and shopping this book would have been delayed even more. I thank my wife Loredana for her patience and lifting me up from the swamp of science into the more elevated orbitals of real life.

Zandvoort aan Zee, The Netherlands
March, 1993

Pieter Jan Stuyfzand

SUMMARY

For a thematic, alphabethical listing of the principal issues of this study, reference is made to the conclusions, following chapter 8 in the main text.

Introduction

In this thesis an integrated approach of the hydrochemistry and hydrology of Holland's coastal dune area is offered, with emphasis on the chemical composition of groundwater. A regional survey of the coastal dune area in between Camperduin (North Holland) and Monster (South Holland) forms the starting point of a detailed exploration of the processes that are responsible for the observed, extreme chemical variations of groundwater, both in space and time. This exploration starts with general descriptions and proceeds with increasing detailed information and interpretation. Due attention is paid to historical developments, atmospheric deposition, the complex transformation of rain water into shallow groundwater, the chemical evolution within various water bodies down the hydraulic gradient over 0.8-10 km towards their intrusion front, and chemical mass balances. The latter indicate the most plausible reactions that occurred and their respective contribution to the observed water quality.

The study area contains one of the most varied, extensive, unspoilt coastal dune areas in Western Europe, adjacent to the most densely populated and industrialized polder area of the world. We are faced therefore with a wide spectrum of natural variations and strong anthropogenic impacts, side by side as well as superimposed. Internationally these dunes perhaps still are somewhat exceptional in their very prominent role as fresh groundwater reservoirs for drinking water supply to the densely populated polder area behind, where other water sources are scarce due to the high salinity of groundwaters and serious pollution of surface waters. The high pollution loads of rain water and of the rivers Rhine and Meuse recharging the dune aquifers, make hydrochemical research highly relevant to the custody of both a vital drinking water supply and an already stressed nature reserve.

Chapter 2

The HYdrochemical Facies Analysis (HYFA) is introduced as a new method to map the chemistry of groundwater in complex situations with abundant data. The essence of this method consists of the mapping of water bodies with a specific origin (the *hydrosomes*, like North Sea, Rhine, polder and dune water), and characteristic hydrochemical zones (the *facies*) within each hydrosome.

The HYFA consists of five successive steps : (1) the gathering and selection of hydrochemical data; (2) the objective determination of the hydrochemical facies of each sample; (3) the identification of its origin, using amongst others specific environmental tracers; (4) the construction and description of maps and cross sections presenting the spatial distribution of discerned hydrosomes and the different facies within each hydrosome; and (5) the interpretation of maps and cross sections, leading to the recognition and understanding of facies chains (evolution lines) in the direction of groundwater flow within each hydrosome.

The facies is determined by integration of 4-5 more or less independent facies-parameters : (a) the chemical water type, which includes in one code the chlorinity, alkalinity, most important cation and anion, and a base exchange index; (b) the redox level, as deduced from the concentrations of O_2, NO_3^-, SO_4^{2-}, Fe, Mn, H_2S and CH_4; (c) a water quality index, either a new pollution index for general purposes or phosphate classes for hydro-ecological studies; (d) the most relevant mineral saturation index for the system; and if useful (e) the water temperature on site.

For groundwater the available sampling facilities and devices are discussed, together with sampling problems and some guidelines for obtaining representative samples and maintaining them so by preservation techniques. How to recognize and correct for the dissolution of suspended fines upon addition of acids to unfiltered samples for storage, is indicated. Tests to check the accuracy of chemical analyses consist of the ionic balance, comparison of the calculated with measured electrical

conductivity (or total dissolved solids), and a check on internal chemical consistency. Some improvements to these classical tests are presented. And several ways to estimate the concentrations of missing or mistrusted main constituents are reported.

Chapter 3

Hydrological maps are presented to a scale 1:200,000 for the 900 km^2 area north of the Old Rhine. They comprise : historical developments during the past 500 years; the areal distribution of important aquitards; isohypses of the reconstructed mean phreatic level around 1850 AD and of actual piezometric heads at different depths; the drawdown of the water table in the period 1850-1981; the depth to the actual position of the fresh - brackish water interface; the rise of this interface in the period 1910-1981; and the areal distribution of groundwater flow systems.

The mean natural groundwater recharge is established for common dune vegetation covers, by using lysimetric data mainly. It varies from -0.58 to 0 m/y for reeds to +0.62 m/y for bare dune sand, respectively. Annual variations and mean seasonal fluctuations are shown as well.

Analytical solutions for the calculation of the size and shape of a fresh dune water lens, its time of formation and dispersion across the fresh-salt water interface are passed in review. The solution for the time of formation by Brakel (1968) and Bakker (1981) is extended to account for anisotropy. Dispersion across an undisturbed interface in 1910 AD could be modelled with a transversal dispersivity of 0.0025 - 0.01 m.

Geological information, palaeogeographical maps and intensive measurements since about 1850 AD have been used, to reconstruct the palaeohydrology of the area. The Holocene transgressions salinized the whole aquifer system at least to the top of the marine Maassluis Formation at 100-270 m-MSL, which still contains connate water.

Changes of the groundwater table with respect to mean sea level, reveal that a deep freshening prevailed in the dunes from 3800 BC till 1600 AD in connection with enlargement of the coastal barriers. The fresh dune water pocket contracted in the period 1853-1957 in its western and central parts, for at least 7 reasons.

The phreatic level consequently dropped by 2-8 m, the fresh-salt water interface rose by 5-100 m and the mean thickness of the brackish transition zone in the central dune area expanded in the vicinity of the drawdown centres from 10-20 to 20-50 m. Large-scale artificial recharge since about 1955 and a reduced abstraction of dune groundwater led to a fast return of high groundwater levels, and to the pushing back of the fresh-salt water interface.

A shallow freshening dominated in the former peat bogs from 3000 BC till about 900 AD. The central parts of the deep polders resalinized since 900 AD due to drainage and peat digging, Dunkirke transgressions and the reclamation of lakes in the period 1550-1875 AD. The area in between the younger dunes and the deep polders experienced, after this reclamation, a gradual supersession of shallow, old dune water pockets by polder water (river Rhine water mixed with local rain water), and water from the younger dunes.

The actual situation is described by the presence of 5 groundwater flow systems, in order of decreasing size and age : the supraregional Maassluis system, which is driven mainly by compaction of finegrained Lower-Pleistocene and Tertiary marine deposits and man-made drainage; the North Sea system, that has been strongly activated since the reclamation of lakes; various dune systems of different order; several man-made polder systems; and diverse man-made artificial recharge systems.

Field evidence and an analytical solution are presented for the so-called rain water lenses on top of infiltrated surface water that migrated laterally. Again, a transversal dispersivity of 0.0025 m yields the best prediction for the transition zone between both groundwaters. Most dune lakes exhibit an essential in- and output through exfiltration of groundwater and infiltration respectively, and therefore belong to the flow-through type. Effects of these lakes on the groundwater flow pattern and fluctuations of the phreatic level are demonstrated.

Chapter 4

Application of the Hydrochemical Facies Analysis to the study area revealed the presence of six hydrosome types. These are, in order of decreasing age : (1) the more than 2 million y old, connate, marine Maassluis hydrosome, with a deep anoxic, salinized, calcareous and unpolluted facies; (2) the relict, Holocene transgression hydrosome, that formed 8000-300 y ago in either a lagoonal, tidal flat and estuarine environment behind coastal barriers (the marsh type) or in an open marine environment (the coastal type). It is slowly bleeding out in the deep polders, with a deep anoxic, salinized, calcareous and unpolluted facies; (3) the actual North Sea hydrosome, which makes part of the man-enforced, North Sea flow system that originated about 1000 y ago. The most common facies is reduced, calcareous, unpolluted and without base exchange; (4) several coastal dune hydrosomes, that originated mainly in between 3800 and 200 BC and exhibit a large diversity of facies; (5) several polder hydrosomes, most of

which originated upon the reclamation of deep lakes in the period 1500-1880 AD. The general facies is freshened, (deep) anoxic, calcareous and polluted or unpolluted; and (6) several artificial recharge hydrosomes. Most of them originated after 1955 AD. The common facies is polluted, (sub)oxic to reduced, either salinized or without base exchange, and calcareous.

The actual distribution of the recognized hydrosomes and their hydrochemical facies is shown on maps (1:200,000) and in cross sections, and interpreted. For each hydrosome and the most common facies a typical analysis of major and trace constituents is given, forming a valuable check-list for natural backgrounds in hydrochemistry in the specified environments. The best environmental tracers for recognition of each hydrosome are discussed.

Eight facies chains are recognized along flow paths ranging from 0.4 to 12 km in length. They relate to freshening dune water, salinizing North Sea water, freshening polder water and various artificial recharge waters. The most evolved chain is the freshening dune chain near Bergen, starting in decalcified dunes and terminating in the deep Geestmerambacht polder. It contains five different evolution lines in optima forma : from polluted to unpolluted, from acid (pH4) to basic (pH8.5), from oxic to methanogenic, from "without base exchange" to a strong positive base exchange (by freshening), and from fresh to brackish by mixing with and transition into relict Holocene transgression water. The accompanying sequence in water types is from F_*NaCl, F_0NaCl, F_1CaMix, F_2CaMix, F_2CaHCO_3, F_2CaHCO_3+, F_2MgHCO_3+, F_3NaHCO_3+, F_4NaHCO_3+, to B_5NaCl+.

The areal distribution of hydrosomes and their facies is shown on a smaller scale around flow-through lakes in between Katwijk aan Zee and Scheveningen, and for a moist dune slack south of Egmond aan Zee. The passage of bottom sludge in dune lakes, and a shallow depth to the groundwater table around flow-through lakes and in moist to wet dune slacks, has a crucial effect on the facies, especially on the redox index (reduced to deep anoxic) and phosphate levels (slightly to strongly eutrophic). The high biological productivity of flow-through lakes in the dunes is explained by the focusing of (sub)regional groundwater flow and nutrient transport towards the lake.

Chapter 5

Compositional variations of bulk precipitation are demonstrated by carefully synthesizing the results for 93 coastal stations in the study area during the period 1930-1990. Many data from unpublished reports and data files are considered, including original and unpublished data from the famous network used by Leeflang (1938), after careful examination of the materials and methods applied.

The chemical composition is explained by contributions from sea spray (>50% on coastal dunes for Na^+, Cl^-, K^+, Mg^{2+}, B, Li^+ and Sr^{2+} separately), continental mineral aerosols (>50% for Al, Sc, SiO_2, Rb^+, Th and Ti, each), biogenic inputs (especially PO_4^{3-} and NH_4^+), and anthropogenic pollution (>50% for most heavy metals, F^-, NO_3^-, NH_4^+, SO_4^{2-} and organic microcontaminants, each).

Spatial variations are dominated by gradients in sea spray deposition perpendicular to the North Sea shoreline, a nationwide northward gradient of diminishing air pollution, and local emission centres, especially those in the glasshouse district, urban areas and industries in the IJmond. The dune strip within the first km to the high water line, receives additional SO_2 and probably NO_x inputs through mediation of sea spray and calcareous dust.

The record of Cl^-, NO_3^-, NH_4^+, pH and sea-salt-corrected SO_4^{2-} has been reconstructed for the period since the 1930s. Trends are recognized for NO_3^- and NH_4^+ (increasing), pH (strongly depending on the buffering by regional dust supplies), sea-salt-corrected SO_4^{2-} (increasing till 1970 and decreasing since then) and Cl^- (high in the period 1967-1977). Seasonal variations are discussed using a 10 and 20 years monitoring on the coastal background station "De Kooy" and the coastal station "Monster" in the glasshouse district, respectively. And variations on a smaller time scale are presented, for maritime and continental episodes, dry and wet periods, and during one shower.

Chapter 6

The chemical metamorphosis of rain water into the upper dune groundwaters is shown and explained by comparison of bulk precipitation, throughfall, litter leachate, soil moisture and groundwater, on well defined locations. The major constituents, 19 trace elements, several organic microcontaminants and the natural isotope oxygen-18 were examined. The upper groundwater was monitored for several years using multilevel wells equipped with miniscreens, and four 625 m^2 lysimeters, on 28 plots that form a representative cross section of the natural environments in coastal dunes. An extensive list of the mean hydrochemical composition on these plots, provides a reference table on natural backgrounds, which include, however, effects of atmospheric pollution, acidification and, on several plots, a drawdown of the water table.

The concepts "*vegetation water lens*" and "*pure*

vegetation groundwater" are introduced, as the vegetation cover proved to have a dominant impact. Simple hydrological calculations of the transit time in the vadose and shallow groundwater zone, and the thickness of both a vegetation water lens and the mixing zone between two pure vegetation groundwaters, compared well with hydrochemical observations.

Passage of the vegetation canopy as throughfall and percolation through the litter layer lead to a substantial increase of SO_4^{2-}, NO_3^-, PO_4^{3-} and K^+ by evaporation, interception deposition (SO_4^{2-} and NO_3^-) and leaching of leaves and mineralization of litter (NO_3^-, PO_4^{3-} and K^+).
Sea buckthorn (*Hippophaë*) excells in the highest concentrations of NO_3^- in litter leachate and groundwater (related to N_2 fixation), and pines (*Pinus nigra* ssp. *nigra*) in the highest SO_4^{2-} (by evaporation and interception deposition) and lowest NO_3^- concentration in groundwater (by uptake). As the litter leachate passes through the active root zone, K^+, PO_4^{3-} and NO_3^- are preferentially withdrawn from the water phase again. This nutrient cycling leads to low concentrations of PO_4^{3-} and K^+. The raised atmospheric deposition causes NO_3^- to leak to a much higher degree to the groundwater zone.

Spatial variations of the dune water composition are discussed in terms of spatial variations of bulk precipitation chemistry, effects of 8 different types of vegetation cover, differences in geochemistry (calcareous versus decalcified dune sand, with and without intercalated dune peat) and variations of the mean thickness of the unsaturated zone. A mean position of the groundwater table >0.5 m below the surface yields a (sub)oxic facies. The most reactive constituents of dune sand are shell debris, ferromagnesian silicates (like hornblende), plagioclase and Fe- and Al-hydroxides. Their weathering yields a major contribution to Ca^{2+}, HCO_3^-, SiO_2, Fe, Mn, Al, As, Li^+, Rb^+, Sr^{2+} and U dissolved in groundwater. The atmosphere supplies the bulk or all of Na^+, Cl^-, SO_4^{2-}, NO_3^-, Br^-, K^+, Mg^{2+} and probably Cu, F^-, I, Pb, Se, V and Zn.

Long-term changes in the composition of shallow dune groundwater are composed of an overall increase in total dissolved solids, a specific rise of NO_3^- and Ca^{2+}, and a rise followed by a decrease, in SO_4^{2-}. These are largely connected with changes in vegetation cover, atmospheric deposition and a drawdown of the water table. Annual and seasonal fluctuations in the chemistry of pure vegetation groundwaters are shown to be extremely high, which appears characteristic for a dynamic coastal environment. The main causes are discussed and seasonal fluctuations of the biological, atmospherical and hydrological type are discerned. Both annual and seasonal Cl^- fluctuations, with the years 1974, 1977 and 1979 and the month November as recognizable extremes, proved useful in shallow groundwater dating, notwithstanding smoothing by dispersion. Effects of hydrodynamic dispersion (in the porous medium) and artificial dispersion by various sampling facilities are calculated and compared with observations.

The following fluxes of dissolved major constituents are quantified for selected vegetation covers in both calcareous and decalcified dunes : interception deposition, storage in biomass, N_2-fixation and decalcification rates. The contribution of interception deposition (= dry deposition minus the dry deposition on a bulk rain collector) to the total deposition of SO_x and NO_x + NH_y varied for mosses, dune shrub, oaks and pines (without edge effects) from 50 to 75%.
$CaCO_3$ leaching is highest under sea buckthorn (*Hippophaë*) and lowest under Corsican pine, and is favoured by interaction with dune peat above the water table. The decalcification depth as calculated with a simple balance, compared well with geochemical observations on old dune soils (200-5500 y) in primarily calcareous dunes. However, field data suggest an accellerated $CaCO_3$ leaching during the initial period, when there is still clacium carbonate left in the root zone. This period lasts about 17 years for each percent of $CaCO_3$ in the parent material.

Chapter 7

Changes in concentration of major constituents, trace elements and the isotopes ^3H, ^{13}C and ^{18}O are presented for dune, Rhine and North Sea water, from recharge towards their intrusion front. They are shown in detailed well logs, in specific cross sections and along a generalized flow path down the hydraulic gradient at specific locations. The flow paths selected, vary in length from 0.8 km for Rhine water which escaped from direct recovery, to 6-10 km for dune and North Sea water flowing towards reclaimed lakes.

Evolution lines, which the three hydrosomes have in common, are made up of several fronts downgradient due to redox reactions, cation exchange and displacement. Fronts in connection with environmental pollution could be traced back in dune and Rhine water only, as North Sea groundwater was not examined in detail at shallow depth. An acidification front in shallow groundwater was exclusively found in the decalcified dunes north of Bergen.

The position of redox fronts is related mainly to the geochemical zonation (availability of organic matter), flux of the mobile oxidants O_2, NO_3^- and SO_4^{2-}, and antecedent water table fluctuations

(leaching). Oxygen and nitrate generally survive the dune sands, but are completely consumed in the sandy North Sea deposits at 1-5 m-MSL (dune and Rhine water) or deeper where the present sea floor cut through these deposits. Sulphate reduction and methanogenesis are quantitatively important for dune water only (generally not for Rhine and North Sea water), in connection with its relatively low flux of oxidants. It occurs where well developed dune or basal peat or specific Holocene clastic aquitards are passed. The highest Fe and As levels are encountered in the anoxic sulphate (meta)stable zone. Uranium is strongly mobilized in the lower parts of the suboxic zone, where U roll front deposits are dissolved, and it probably precipitates as UO_2 where Fe is mobilized.

Specific exchange zones develop behind each intrusion front in analogy with the ion chromatographic effects demonstrated with column experiments by Beekman (1991). A fresh dune water intrusion into brackish Holocene transgression water results in (a) a broad exchange zone with specific patterns for Na^+, K^+, Li^+, Rb^+, Ca^{2+}, Mg^{2+}, Sr^{2+}, NH_4^+ and SiO_2, and (b) several secundary reactions in consequence of strongly reduced Ca^{2+} concentrations (dissolution of fluorapatite-like phases), raised HCO_3^- levels and increased pH (dissolution of gibbsite and precipitation of a manganous siderite). The intrusion of North Sea water at 60-100 m-MSL into dune water leads to a very narrow exchange zone with opposite reactions and a clear mobilization of Fe, Mn and Ba^{2+}. The displacement of dune water by recharged Rhine water is to be considered as a salinization as well, with similar reactions in many respects. The exchange zone is wider due to the lower displacing capacity of Rhine water (Σcations = 8.6 instead of 515 meq/l for coastal North Sea water).

The environmental pollution record of precipitation is reflected in dune water by decreasing levels downgradient for the mainly atmogenic trace elements Se, Cu, F^-, Zn, Pb, Sb and V (in decreasing order of depth of penetration) and organohalogens adsorbable to activated carbon, and by the tritium and sea-spray-corrected SO_4^{2-} patterns.
Recharged Rhine water shows well conserved patterns for Cl^-, SO_4^{2-} and tritium, a smoothed pattern for dissolved organic matter, and breakthrough of Na^+, Mg^{2+}, K^+, F^- and PO_4^{3-} in dune sand after about 1.2, 3, 5, 5 and 30 pore flushes, respectively.

An acidification front was observed in dune groundwater north of Bergen exclusively, at about 5 m below ground level, i.e. 3 m below the phreatic level. The pH rapidly increases in the front from about 4.5 to 6, with a concomitant decline of Al concentrations and a remarkable mobilization of Be, Cd, Co, Li^+, Ni, Rb^+ and Zn. These trace ions probably reach the extreme levels observed by dissolution of "roll-deposits", which form downgradient of the advancing acid front. Concentration peaks of the trace cations are separated probably by ion chromatographic effects, in order of increasing distance down the hydraulic gradient, and concomitantly increasing pH : Pb < Cu < Al < {Be $\cong$ Rb $\cong$ Zn $\cong$ Cd} < {Co $\cong$ Ni} < Li. The position of the acid front coincides with the redox cline, and it is calculated that denitrification and the reduction of $Fe(OH)_3$ contribute in this case for about 60% to the acid buffering.

Dune water that formed after 1953, was dated using the technique of history matching. Years with an anomalous atmospheric input of tritium, $\delta^{18}O$ and Cl^- could be traced back in detailed vertical hydrochemical logs. Dune water older than 70 years could be dated using (1) a $\delta^{18}O$ front, which matched a strong drawdown of the water table in the area in the period 1880-1920, and (2) ^{14}C radiometry, with the approach of Pearson & Hanshaw (1970). A maximum age of 800 years was deduced for very deep dune water in the Haarlemmermeer polder. Rhine water, that was recharged since 1957, could be dated with even more details in a cross section, by matching the combined chloride and tritium input record.

Chapter 8

Chemical mass balances are composed here of a set of 25-50 reaction equations in appropriate order and the sum of all resulting mass transfers between bulk precipitation and dune groundwater. A general set-up of the balance approach is presented, consisting in this complicated case of 31 consecutive steps. In addition to water-rock interaction, also reactions at the interface of the upper soil with the atmosphere (like interception deposition) and vegetation (for instance uptake) are considered.

Mass balances for 4 shallow vegetation groundwaters in contrasting dune areas revealed the main sources and sinks of the strong acids H_2SO_4, HNO_3 and HF on the one hand, and carbonic acid on the other. Interception deposition constitutes the main source of the strong acids, and is generally followed in second position by nitrification and, in case of fast growing pines, by the uptake of cations. Respiration generally yields the bulk of carbonic acid, except for pines in decalcified dunes where dry soil conditions and the lack of reactive $CaCO_3$ hamper an effective transfer of CO_2 gas to the water phase. Reaction with $CaCO_3$ explains the higher contribution of CO_2 produced by respiration in calcareous dunes as compared to

decalcified dunes.

Strong acids are neutralized in the calcareous dunes, mainly by reduction of the base saturation of the exchange complex in the upper unsaturated zone. In decalcified dunes, various sinks of strong acids can be assigned, the most important being : the uptake of anions under fast growing pines, SO_4^{2-} adsorption (or the formation of jurbanite-like phases), the dissolution of gibbsite and the HCO_3^- buffer, which is mainly formed by interaction with decomposing organic matter. The dissolution of $CaCO_3$ and free drainage constitute the main sink of carbonic acid in calcareous and decalcified dunes, respectively.

Mass balances were also drawn up for 5 samples of Bergen dune groundwater down the hydraulic gradient, from close to the water table in the younger dunes towards exfiltration in the polder area. They revealed the strong impact of atmospheric pollution in the upper zone, and further downgradient the increasing effects of methanogenesis, cation exchange due to freshening and dissolution of apatites, including the conversion of fluor- into hydroxyapatite. The present supply of strong acids to dune water (waters <50 y old) is about 13 times higher than the natural background supply to dune water (waters >150-200 y old).

Carbon-13 data assisted in the distinction between $CaCO_3$ dissolution by strong atmospheric acids and the dissolution by carbonic acid, regard ing shallow dune groundwater without interference of dune peat. Interaction with dune peat results in a rather uniform $\delta^{13}C$ value of -16‰, by the overwhelming effect of isotopic exchange between the relatively small quantity of dissolved HCO_3^- and the hugh reservoir of CO_2 in soil air and organic matter in the peat. The mass balance for ^{13}C in deep dune waters containing high methane concentrations, corresponded well with observations if a $\delta^{13}C$ value of +30‰ is assumed for the CO_2 originating from methanogenesis.

SAMENVATTING

De belangrijkste conclusies uit deze studie staan op thema en alfabetisch gesorteerd, vermeld in "Conclusies", volgend op hoofdstuk 8.

Inleiding

In deze dissertatie wordt een integrale benadering van de hydrochemie en hydrologie van Holland's kustduinen geboden, waarbij de chemische samenstelling van het grondwater centraal staat. Een regionale kartering van het 100 km lange, 10 km brede kustduingebied tussen Camperduin (Noord Holland) en Monster (Zuid Holland) vormt het uitgangspunt voor een gedetailleerde verkenning van de processen die verantwoordelijk zijn voor de extreme en veelsoortige variaties in grondwaterchemie, die zowel in ruimte als tijd zijn waargenomen. Deze verkenning begint algemeen beschrijvend en vervolgt met steeds gedetailleerder informatie met verder voerende interpretatie. Daarbij wordt volop aandacht geschonken aan achtereenvolgens : historische ontwikkelingen in het studiegebied, atmosferische depositie, de ingewikkelde transformatie van regenwater in ondiep duingrondwater, de verdere chemische evolutie binnen diverse waterlichamen langs stroombanen met een lengte van 0,8-10 km (van infiltratiepunt richting drain, pompput of kwel in de droogmakerijen), en tenslotte chemische massabalansen. Dergelijke balansen bestaan uit een opsomming van de meest aannemelijke reacties die zijn opgetreden, met de individuele bijdrage aan de waargenomen watersamenstelling.

Het studiegebied bevat zo ongeveer de grootste, meest gevarieerde en nog ongerepte kustduinen van West-Europa. Aan dit langgerekte natuurgebied grenst het dichtst bevolkte en meest geïndustrialiseerde poldergebied ter wereld. Dat leidt tot conflicterende belangen en een breed spectrum aan natuurlijke variaties en antropogene invloeden. Internationaal gezien nemen de Hollandse kustduinen een bijzondere plaats in door hun grote betekenis als drinkwaterbron voor de achterliggende, dichtbevolkte polders. Andere drinkwaterbronnen zijn daar schaars vanwege hoge zoutconcentraties in het grondwater en de ernstige vervuiling van het oppervlaktewater. De verontreiniging van regenwater op de duinen en van het Rijn- en Maaswater, dat er in een zevental gebieden kunstmatig geïnfiltreerd wordt, maken hydrochemisch onderzoek uiterst relevant voor de bewaking van zowel een vitale drinkwatervoorziening als een zwaar onder druk staand natuurreservaat.

Hoofdstuk 2

Een algemeen toepasbare, nieuwe methode voor het in kaart brengen van de grondwaterchemie in ingewikkelde gebieden met veel gegevens, vormt het thema van hoofdstuk 2. Het betreft de HYdrochemische Facies Analyse (HYFA). De essentie van deze methode schuilt in het karteren van waterlichamen met een specifieke herkomst (de *hydrosomen*, zoals Noordzee-, Rijn-, polder- en duin-water), en kenmerkende hydrochemische zones daarbinnen (de *facies*). De facies wordt bijvoorbeeld beschreven door de kenmerken zuur of kalkrijk, aëroob of anaëroob, verontreinigd of schoon, verzoet of verzilt, en koud of warm.

De HYFA bestaat uit 5 stappen : (1) het verzamelen en selecteren van hydrochemische gegevens; (2) de objectieve bepaling van de hydrochemische facies; (3) de vaststelling van de herkomst van het water, o.a. met behulp van gidsparameters (herkenbare tracers); (4) de constructie en beschrijving van kaarten en doorsneden met de ruimtelijke verbreiding van de onderscheiden hydrosomen en de verschillende facies daarbinnen; en (5) de interpretatie van het kaartmateriaal, door ontrafeling van de aanwezige evolutielijnen langs stroombanen binnen elk hydrosoom.

De bepaling van de facies geschiedt, met vrijheden voor wie de HYFA toepast, op basis van : (a) het chemische watertype, dat in één code informatie herbergt t.a.v. de chloride concentratie, alkaliteit, het dominante kation en anion, en een basenuitwisselingsindex; (b) het redoxniveau, zoals afgeleid uit de concentraties van O_2, NO_3^-, SO_4^{2-}, Fe, Mn, H_2S en CH_4; (c) een waterkwaliteitsindex, bestaande uit een algemene verontreinigingsindex of b.v. fosfaat-klassen; (d) de meest relevante mineraalverzadigingsindex voor het chemische systeem, b.v. de kalkverzadigingsindex; en indien nuttig en noodzakelijk (e) de watertemperature ter plaatse.

Richtlijnen voor uitvoering van regionaal hydrochemisch onderzoek worden gegeven, met aandacht voor bemonsteringsperikelen, gegevenscontrole en het schatten van ontbrekende waarnemingen. Gidsparameters komen in algemene zin aan de orde.

Hoofdstuk 3

Hier worden de in Bijlagen 1-4.1 gegeven hydrologische kaarten beschreven, en wordt algemene informatie verstrekt over de voeding, vorm en vorming van zoetwaterlenzen in duingebieden. De kaarten beslaan het gebied ten noorden van de Oude Rijn, ongeveer 900 km^2 groot. Zij tonen de ruimtelijke verbreiding van belangrijke slecht-doorlatende pakketten, de gereconstrueerde grondwaterstand rond 1850, de actuele stijghoogten op verschillende diepten, de grondwaterstandsverlaging in de periode 1850-1981, de actuele diepteligging van het zoet-brak grensvlak (300 mg Cl^-/l), de verandering daarin in de periode 1910-1981, en de ruimtelijke verbreiding van grondwaterstromingsstelsels.

Geologische informatie, paleogeografische kaarten en intensieve metingen sinds ongeveer 1850 zijn aangewend om de paleohydrologie van het gebied te ontrafelen. De Holocene transgressies verziltten de hele ondergrond ten minste tot de top van de mariene Maassluis Formatie op 100-270 m-NAP. De zeewaartse ontwikkeling van een serie parallelle strandwallen langs Hollands kust in de periode van 3800 tot 200 v.Chr. bracht de eerste ontwikkeling van relatief geïsoleerde rijen van ondiepe zoetwaterlenzen. De jonge duinvorming in de periode 1000-1200 leidde tot het gedeeltelijk aaneenrijgen van deze lenzen en dientengevolge tot verdere groei die tot circa 1600 duurde.

Door samenloop van 7 oorzaken, waaronder grondwaterwinning, nam het volume van de hoofdlens sterk af in de periode 1853-1957, vooral in de westelijke en centrale delen. Bijgevolg daalde de grondwaterstand met 2-8 m, kwam het zoet-zout grensvlak met 5-100 m omhoog en nam de dikte van de brakke overgangszone in de nabijheid van onttrekkingen toe van 10-20 tot 20-50 m. Grootschalige kunstmatige infiltratie sinds ongeveer 1955 en een afgenomen diep-duinwaterwinning leidden tot snel herstel van hoge grondwaterstanden en het langzaam terugduwen van het zoet-zout grensvlak.

In voormalige veenmoerassen achter de duinen verzoette de bovengrond locaal in de periode 3000 v.Chr. tot 900 na Chr. Maar sinds 900 verziltten de centrale delen van de diepe polders weer door drainage, veendelving, Duinkerken transgressies en drooglegging van meren in de periode 1550-1875 AD. Het gebied tussen de jonge duinen en de diepe polders kreeg, na deze drooglegging, te maken met een geleidelijke verdringing van ondiepe duinwaterlenzen onder de strandwallen, door polderwater (bestaande uit Rijnwater vermengd met locaal regenwater), en toestromend water uit de jonge duinen.

De actuele situatie wordt beschreven door 5 grondwaterstromingsstelsels, in volgorde van afnemende grootte en ouderdom : het Maassluis systeem, dat voornamelijk gedreven wordt door drainage van de droogmakerijen en compactie van fijnkorrelige Onder-Pleistocene en Tertiaire, mariene sedimenten; het Noordzee systeem, dat sterk geactiveerd is sinds de drooglegging van meren; duinsystemen van verschillende orde; antropogene poldersystemen; en diverse kunstmatige infiltratiesystemen.

Het bestaan van decimeters tot enkele meters dikke regenwaterlenzen op geïnfiltreerd oppervlaktewater dat lateraal afstroomt, wordt met veldwaarnemingen aangetoond. Analytische formules voor de lensdikte, dikte van de onderliggende mengzone en verblijftijd in de lens worden gegeven en blijken zeer goed aan te sluiten bij de waarnemingen. Voor de transversale dispersiviteit van duin- en strandzand moet dan 2,5 mm worden aangehouden. De meeste duinmeren vertonen een essentiële grondwaterbijdrage in de waterbalans, bestaande uit kwel aan de stroomopwaartse kant en wegzijging aan de stroomafwaartse zijde. Effecten van deze zogenaamde *doorstroom-meren* (kwelplassen) op het grondwaterstromingspatroon en fluctuaties in de grondwaterstand worden getoond.

Hoofdstuk 4

De Hydrochemische Facies Analyse wordt hier toegepast op het studiegebied. Er zijn 6 typen waterlichamen (hydrosomen) onderscheiden, in volgorde van afnemende ouderdom : (1) het meer dan 2 miljoen jaar oude, ingesloten, mariene Maassluis hydrosoom, met een diep anoxische (methaanrijke), verzilte, kalkrijke en onverontreinigde facies; (2) het relicte, Holocene transgressie hydrosoom, dat 8000-300 jaar geleden gevormd werd in hetzij een lagunair, wadden en estuarien milieu achter de strandwallen (het moerastype), hetzij een open marien milieu (het kusttype). Het bloedt langzaam leeg in de diepe polders, met een diep anoxische, verzilte, kalkrijke en onverontreinigde facies; (3) het actuele Noordzee hydrosoom, dat deel uitmaakt van het door de mens versterkte Noordzee stromingsstelsel, dat ongeveer 1000 jaar geleden in gang werd gezet. De facies is meestal gereduceerd, kalkrijk, onverontreinigd en zonder basenuitwisseling; (4) diverse kustduinhydrosomen, die tussen 3800 en 200 v.Chr. ontstonden en een grote variatie aan facies vertonen; (5) verscheidene polder hydrosomen, die grotendeels ontstonden naar aanleiding van de drooglegging van meren in de periode 1500-1880. De facies is doorgaans verzoet, (diep) anoxisch, kalkrijk en verontreinigd of onverontreinigd; en (6) enkele hydrosomen, die door kunstmatige infiltratie zijn ontstaan na 1955. De meest voorkomende facies is verontreinigd, kalkrijk, (sub)oxisch tot gereduceerd, en hetzij verzilt of zonder basenuitwisse-

ling.

De actuele ruimtelijke verdeling van de onderscheiden hydrosomen en hun facies is in beeld gebracht op de kaarten in Bijlagen 4.2-7. Voor elk hydrosoom en de meest algemene facies wordt een representatieve chemische analyse van hoofd- en sporenbestanddelen gegeven. De resulterende lijst geeft tevens de natuurlijke achtergrondwaarden voor de diverse grondwatersoorten in verschillende milieus. De beste gidsparameters (tracers) voor herkenning van elk hydrosome worden aangegeven.

Er zijn 10 faciesketens (met typische chemische evolutiepatronen) waargenomen langs stroombanen met een lengte varierend van 0,4 tot 12 km. Zij hebben betrekking op verzoetend duinwater, verziltend Noordzeewater, verzoetend polderwater en verschillende infiltratiewateren.

De meest gedifferentieerde keten ligt langs een stroombaan van verzoetend duinwater bij Bergen (Noord Holland) : van infiltratie in de kalkarme duinen tot exfiltratie in de diepe Geestmerambacht polder. Zij bevat 5 evolutielijnen in optima forma : van verontreinigd tot onverontreinigd, van zuur (pH4) tot basisch (pH8,5), van oxisch (aëroob) tot methaanrijk, van "zonder basenuitwisseling" tot een sterk positieve basenuitwisseling (door verzoeting), en van zoet tot brak door menging met en overgang in relict Holocene transgressiewater. De vergezellende opeenvolging van watertypen is van F_*NaCl, F_0NaCl, F_1CaMix, F_2CaMix, F_2CaHCO_3, F_2CaHCO_3+, F_2MgHCO_3+, F_3NaHCO_3+, F_4NaHCO_3+, naar B_5NaCl+.

De ruimtelijke verbreiding van hydrosomen en hun facies op kleinere schaal wordt getoond voor doorstroom-meren in de duinen tussen Katwijk aan Zee en Scheveningen, en voor een vochtige duinvallei ten zuiden van Egmond aan Zee. De passage van bodemslib in duinmeren, en een ondiepe grondwaterstand rond doorstroom-meren, in vochtige en natte duinvalleien, hebben een cruciaal effect op de facies, vooral op de redox index (gereduceerd tot diep anoxisch) en fosfaat concentraties. De hoge biologische productiviteit van doorstroom-meren in duinen wordt verklaard door de optredende convergentie van stroombanen aan de kwelzijde, de daardoor verhoogde nutriëntentoevoer, en de chemische en biologische vastlegging van nutriënten in het meer.

Hoofdstuk 5

De zeer grote variaties in chemische samenstelling van regenwater (opgevangen met een altijd open trechter) worden getoond aan de hand van meetresultaten afkomstig van 93 kuststations in het studiegebied, die ergens in de periode 1930-1990 operationeel waren. Hierbij zijn veel gegevens uit ongepubliceerde rapporten en gegevensbestanden verwerkt, waaronder de originele en ongepubliceerde gegevens uit het beroemde netwerk dat Leeflang (1938) gebruikte. De toegepaste materialen en methoden zijn zorgvuldig in beschouwing genomen.

De gemiddelde chemische samenstelling wordt verklaard uit bijdragen door verstoven zeezout (>50% op kustduinen voor Na^+, Cl^-, K^+, Mg^{2+}, B, Li^+ en Sr^{2+} afzonderlijk), continentale minerale aërosolen (>50% voor Al, Sc, SiO_2, Rb^+, Th en Ti afzonderlijk), biogene bronnen (vooral PO_4^{3-} en NH_4^+), en antropogene verontreiniging (>50% voor de meeste zware metalen, F^-, NO_3^-, NH_4^+, SO_4^{2-} en organische microverontreinigingen afzonderlijk).

Ruimtelijke variaties worden beheerst door gradiënten in verstoven zeezout loodrecht op de Noordzeekust, een nationale noordwaartse gradiënt van afnemende luchtverontreiniging, en locale emissiecentra, vooral die in het kassendistrict (bij Monster), stedelijke gebieden en de IJmond. De duinstrook op minder dan 1 km tot de hoogwaterlijn, ontvangt extra SO_2 depositie en waarschijnlijk NO_x depositie door toedoen van hygroscopisch werkend zeezout en kalkrijk stof dat het gevormde zuur gedeeltelijk opsoupeert.

Het langjarige verloop van Cl^-, NO_3^-, NH_4^+, pH en voor-zeezout-gecorrigeerd SO_4^{2-}, is gereconstrueerd voor de periode sinds 1930. Daarin zijn trends te zien voor NO_3^- en NH_4^+ (toename), pH (regionaal verschillende trends, sterk afhankelijk van zuurbufferende stof-inwaai), voor-zeezout-gecorrigeerd SO_4^{2-} (toename tot 1970, afname sedertdien) en Cl^- (hoog in de winderige periode 1967-1977). Gemiddelde seizoensfluctuaties worden getoond en besproken aan de hand van 10 en 20 jaar waarnemen op resp. het achtergrondstation "De Kooy" langs de kust bij Den Helder, en het kuststation "Monster" in het kassendistrict. Ook de variaties op kleinere tijdschaal worden gepresenteerd, voor maritieme en continentale episodes, droge en natte perioden, en tijdens een enkele bui.

Hoofdstuk 6

De chemische transformatie van regenwater in ondiep duingrondwater wordt in beeld gebracht door tussentijdse opnames van doorval, strooiselpercolaat en bodemvocht. Daarna komen de zeer grote variaties in de samenstelling van ondiep duinwater, zowel in ruimte als tijd, aan de orde. Met minifilters uitgeruste waarnemingsputten en de vier lysimeters te Castricum, elk 625 m^2 groot en 2,5 m diep, zijn voor dit onderzoek op totaal 28 proefperken gedurende enkele jaren in de periode 1979-1983 bemonsterd.

De begrippen "*vegetatie-waterlens*" en "*puur*

vegetatie-grondwater" worden geïntroduceerd, daar uiteenlopende typen begroeiing aan ondiep grondwater een duidelijk herkenbaar "watermerk" opleggen. Eenvoudige, hydrologische berekeningen van de verblijftijd in de onverzadigde en verzadigde zone, en de dikte van zowel een vegetatie-waterlens als de onderliggende mengzone, kwamen goed overeen met hydrochemische waarnemingen.

De passage door het bladerdak en de strooiselllaag leiden tot een aanzienlijke toename van SO_4^{2-}, NO_3^-, PO_4^{3-} and K^+ door verdamping, droge depositie (SO_4^{2-} en NO_3^-) en bladuitloging en de vertering van strooisel (NO_3^-, PO_4^{3-} en K^+). Duindoorn (*Hippophaë rhamnoides)* munt uit door de hoogste concentraties NO_3^- in strooiselpercolaat en grondwater (door N_2-binding), en dennen (*Pinus nigra* ssp. *nigra*) door de hoogste SO_4^{2-} (t.g.v. verdamping en droge depositie) en laagste NO_3^- concentraties in grondwater (door opslag in biomassa). Tijdens passage van strooiselpercolaat door de wortelzone worden K^+, PO_4^{3-} en NO_3^- preferent weer onttrokken aan het doorsijpelend bodemvocht. Deze nutriëntenkringloop leidt tot (zeer) lage concentraties PO_4^{3-} en K^+ in grondwater onder goed groeiende planten. Een door luchtverontreiniging verhoogd atmosferisch aanbod zorgt ervoor dat NO_3^- aanzienlijk meer dan K^+ en PO_4^{3-}, doorlekt naar het ondiepe grondwater.

Ruimtelijke variaties in de samenstelling van ondiep duingrondwater worden getoond en verklaard in termen van ruimtelijke variaties in regenwaterchemie, de effecten van 8 typen begroeiing, verschillen in geochemie (kalkrijk versus kalkloos duinzand, met en zonder passage van duinveen) en variaties in de gemiddelde dikte van de onverzadigde zone. Een gemiddelde positie van de grondwaterspiegel dieper dan 0,5 m beneden maaiveld brengt een (sub)oxische (aërobe) facies met zich mee. De meest reactieve bestanddelen van duinzand bestaan uit schelpfragmenten, de donker gekleurde ferromagnesiumsilicaten (zoals hoornblende), plagioklaas en Fe- en Al-hydroxiden. Hun verwering levert de grootste bijdrage aan in grondwater opgelost Ca^{2+}, HCO_3^-, SiO_2, Fe, Mn, Al, As, Li^+, Rb^+, Sr^{2+} en U. De atmosfeer verschaft het leeuwedeel van of alle Na^+, Cl^-, SO_4^{2-}, NO_3^-, Br^-, K^+, Mg^{2+} en waarschijnlijk Cu, F^-, I, Pb, Se, V en Zn.

Gemiddelde veranderingen in de samenstelling van ondiep duingrondwater op de lange termijn (1910-1990) bestaan uit een algehele toename van de totale hoeveelheid opgeloste stoffen, een specifieke stijging van NO_3^- en Ca^{2+}, en een toename gevolgd door een afname voor SO_4^{2-}. Deze wijzigingen houden verband met veranderingen in begroeiing, atmosferische depositie en een gemiddelde daling van de grondwaterspiegel. Jaarlijkse schommelingen en seisoensfluctuaties in de chemie van pure vegetatie-grondwateren zijn bijzonder groot, hetgeen zeer kenmerkend is voor kustduinen. De hoofdoorzaken hiervan worden besproken en seizoensfluctuaties van het biologische, atmosferische en hydrologische type worden onderscheiden. Zowel jaarlijkse schommelingen als seizoensfluctuaties in Cl^- concentratie, met de jaren 1974, 1977 en 1979 en de maand november als herkenbare extremen, bleken goede aanknopingspunten voor de datering van zeer ondiep duingrondwater, ondanks afvlakking door dispersie. De berekende effecten van hydrodynamische dispersie (in het poreuze medium) en kunstmatige dispersie door verschillende filtertypen kwamen voor grondwater onder eiken en schraler begroeide vegetatietypen goed overeen met waarnemingen.

De volgende fluxen van opgeloste hoofdbestanddelen zijn voor kenmerkende begroeiingstypen gekwantificeerd, zowel in de kalkrijke als kalkloze duinen : interceptiedepositie (= droge depositie minus de droge depositie op een altijd open regenvanger), opslag in biomassa, N_2-binding en de snelheid van ontkalking. De bijdrage van interceptiedepositie aan de totale atmosferische depositie van SO_x en NO_x + NH_y varieerde voor mossen, duindoorn, eiken en dennen (zonder bosrandeffecten) van 50 tot 75%. De ontkalkingssnelheid is het hoogst onder duindoorn (*Hippophaë rhamnoides)* en het laagst onder Corsicaanse den (*Pinus nigra* ssp *nigra*), en wordt verhoogd door interactie met duinveen boven de waterspiegel. De berekende ontkalkingsdiepte op basis van een simpele lineaire balans, kwam goed overeen met geochemische waarnemingen in primair kalkrijke duinen voor zover het oudere duinbodems betrof (200-5500 jaar). Grondmonsters in zeer jong duinzand wijzen er echter op, dat de ontkalking in het begin, wanneer er zich nog kalk in de wortelzone bevindt, sneller verloopt. Deze beginperiode van versnelde uitloging duurt ongeveer 17 jaar voor elk gewichtsprocent kalk in het moedermateriaal.

Hoofdstuk 7

Veranderingen in de concentratie van hoofdbestanddelen, sporenelementen en de isotopen ^3H, ^{13}C en ^{18}O worden gepresenteerd voor duin-, Rijn- en Noordzeewater, van infiltratiepunt tot hun intrusiefront (waar het water met een andere herkomst verdringt). Dit wordt getoond door middel van gedetailleerde minifilteropnames, opnames langs 120 m diepe en 10 km lange dwarsdoorsneden en langs een gegeneraliseerde stroombaan stroomafwaarts. De geselecteerde stroombanen variëren in lengte van 0.8 km voor Rijnwater dat aan directe terugwinning ontsnapte, tot 6-10 km voor duin- en Noordzeewater stromend naar de diepe droogmakerijen.

Evolutielijnen, die de 3 hydrosomen gemeenschappelijk hebben, bestaan uit het optreden van enkele fronten in stroomafwaartse richting, naar aanleiding van redoxreacties, basenuitwisseling en verdringing. Fronten in verband met milieuverontreiniging konden alleen in duin- en Rijnwater worden aangetoond, daar het Noordzeegrondwater niet in detail op geringe diepte onderzocht was. Een verzuringsfront in ondiep grondwater werd uitsluitend in de kalkloze duinen ten noorden van Bergen gevonden.

De positie van redoxfronten is vooral gerelateerd aan de geochemische zonering (beschikbaarheid van organisch materiaal), de flux van de mobiele oxydatoren O_2, NO_3^- en SO_4^{2-}, en vroegere grondwaterstandsfluctuaties (uitloging). Zuurstof en nitraat overleven in het algemeen de duinzand formatie, maar worden volledig opgesoupeerd in de zandige Noordzee afzettingen op 1-5 m-NAP (duin- en Rijnwater) of dieper, waar de huidige zeebodem deze afzettingen erodeerde. Sulfaatreductie en methaanvorming zijn kwantitatief alleen voor duinwater belangrijk (doorgaans niet voor Rijn- noch voor Noordzeewater), ten gevolge van zijn relatief lage aanvoersnelheid en concentratie van oxydatoren. Beide processen treden op waar goed ontwikkeld duin- of basisveen gepasseerd moeten worden, of specifieke, Holocene klastische slecht-doorlatende pakketten. De hoogste Fe en As niveaus worden in de anoxisch-sulfaat(meta)stabiele zone waargenomen. Uranium wordt sterk gemobiliseerd in de lagere regionen van de suboxische zone, waar U "roll-front-afzettingen" (ontstaan door een soort chemisch bezem- of bulldozer-effect) oplossen, terwijl het waarschijnlijk neerslaat als UO_2 als Fe gemobiliseerd wordt.

Achter elk intrusiefront ontwikkelen zich specifieke uitwisselfronten, in analogie met de ionchromatographische effecten die b.v. Beekman (1991) in kolom experimenten aantoonde. De indringing van zoet duinwater in brak Holoceen transgressiewater in de polders resulteert in (a) een brede uitwisselzone met specifieke patronen voor Na^+, K^+, Li^+, Rb^+, Ca^{2+}, Mg^{2+}, Sr^{2+}, NH_4^+ en SiO_2, en (b) enkele secundaire reacties ten gevolge van sterk verlaagde Ca^{2+} concentraties (oplossing van fluorapatiet), toegenomen HCO_3^- niveaus en verhoogde pH (oplossing van gibbsiet en het neerslaan van een mangaanhoudende sideriet). De verdringing van duinwater door Noordzeewater op 60-100 m-NAP leidt tot een smalle uitwisselzone met reacties tegengesteld aan de zojuist genoemde reacties, en een duidelijke mobilisatie van Fe, Mn en Ba^{2+}. De verdringing van duinwater door geïnfiltreerd Rijnwater dient eveneens als een verzilting te worden opgevat, met in veel opzichten vergelijkbare reacties. De uitwisselzone is echter breder door de geringere verdringingscapaciteit van Rijnwater (Σkationen = 8.6 in plaats van 515 meq/l voor Noordzeewater langs de kust).

De historische ontwikkeling van de luchtverontreiniging manifesteert zich in duinwater door middel van in stroomafwaartse richting afnemende concentraties van de voornamelijke atmosferisch gedeponeerde sporenelementen Se, Cu, F^-, Zn, Pb, Sb en V (in volgorde van afnemende penetratiediepte) en aan actieve kool adsorbeerbare organohalogenen, en door de tritium en zee-zout-gecorrigeerde SO_4^{2-} patronen. Geïnfiltreerd Rijnwater vertoont goed bewaard gebleven patronen voor Cl^-, SO_4^{2-} en tritium, een afgevlakt patroon voor opgeloste organische stof, en de doorbraak van Na^+, Mg^{2+}, K^+, F^- en PO_4^{3-} in duinzand na resp. ongeveer 1,2, 3, 5, 5 en 30 poriedoorspoelingen.

Een verzuringsfront in duingrondwater was alleen aantoonbaar in de kalkloze duinen ten noorden van Bergen, op ongeveer 5 m beneden maaiveld, i.e. 3 m beneden de grondwaterspiegel. De pH loopt in het front snel op van ongeveer 4,5 tot 6, met een gelijktijdige afname van de Al concentratie en een opmerkelijke mobilisatie van Be, Cd, Co, Li^+, Ni, Rb^+ en Zn. Deze sporenelementen bereiken de waargenomen piekconcentraties waarschijnlijk door oplossing van de eerder genoemde "roll-front-afzettingen", die zich stroomafwaarts van het opdringende zuurfront vormen. De concentratiepieken worden waarschijnlijk van elkaar gescheiden door ion-chromatographische effecten. Hun penetratieafstand is, in volgorde van toenemende afstand stroomafwaarts, hetgeen overeenkomt met toenemende vastleggings-pH : Pb < Cu < Al < {Be $\cong$ Rb $\cong$ Zn $\cong$ Cd} < {Co $\cong$ Ni} < Li. De positie van het zuurfront valt samen met de redoxcline (overgang van aëroob naar anëroob). Volgens berekening draagt de denitrificatie en de reductie van $Fe(OH)_3$ in dit geval voor ongeveer 60% bij aan de zuurbuffering.

Na 1953 gevormd duinwater kon gedateerd worden met behulp van de techniek van "geschiedenis-vergelijking". Jaren met een afwijkende atmosferische aanvoer van tritium, $\delta^{18}O$ en Cl^- konden in gedetailleerde verticale hydrochemische profielen teruggevonden worden. Duinwater ouder dan 70 jaar werd gedateerd via (1) een $\delta^{18}O$ front, dat samenvalt met een sterke daling van de grondwaterspiegel in het studiegebied in de periode 1880-1920, en (2) ^{14}C radiometrie, met de benadering van Pearson & Hanshaw (1970). Een maximale ouderdom van 800 jaar werd vastgesteld voor zeer diep duinwater in de Haarlemmermeer polder. Rijnwater, dat sinds 1957 kunstmatige geïnfiltreerd wordt, kon nog veel gedetailleerder gedateerd worden in een dwarsdoorsnede, dankzij ondubbelzinnige en talrijkere aanknopingspunten

in de gecombineerde chloride en tritium verlopen van de aanvoer.

Hoofdstuk 8

Chemische massabalansen bestaan hier uit een set van 25-50 reactievergelijkingen in de juiste volgorde en de som van alle resulterende stofoverdracht tussen regenwater en duingrondwater. Een algemene opzet van de balansbenadering wordt gegeven, in dit geval bestaande uit 31 opeenvolgende stappen. Naast interacties tussen water en vaste fasen, worden ook diverse reacties aan het scheidingsvlak tussen bodem en atmosfeer (zoals droge depositie) en de begroeiing (o.a. opslag) in beschouwing genomen.

De massabalansen voor 4 ondiepe vegetatiegrondwateren in kalkrijke en kalkloze duinen brachten de belangrijkste bronnen en neutraliserende reacties aan het licht, voor enerzijds de sterke zuren H_2SO_4, HNO_3 en HF, en anderzijds koolzuur. De droge depositie vormt de hoofdbron van de sterke zuren, en nitrificatie neemt doorgaans de tweede plaats in, tenzij er snel groeiende dennen in het spel zijn, want dan is het de opname van kationen. Ademhaling is in het algemeen de grootste leverancier van koolzuur, met uitzondering van dennen in kalkloze duinen waar een droge bodem en het gebrek aan reactieve kalk een effectieve overdracht van CO_2 gas naar de waterfase in de weg staan. De reactie met kalk verklaart ook de hogere CO_2 bijdrage door ademhaling in kalkrijke duinen in vergelijking met die in kalkloze duinen.

Sterke zuren worden in de kalkrijke duinen voornamelijk geneutraliseerd door verdringing van geadsorbeerd Ca^{2+} door oprukkend H^++Al^{3+}, hetgeen leidt tot een geleidelijke afname van de basenverzadiging van het uitwisselcomplex in de onverzadigde zone. In de ontkalkte duinen is geen sprake van één enkele dominerende reactie die het sterke zuur neutraliseert. De belangrijkste reacties die de sterke zuren daar bufferen zijn : de opname van anionen onder snel groeiende dennen, SO_4^{2-} adsorptie (of de vorming van jurbaniet-achtige fasen), de oplossing van gibbsiet en de HCO_3^- buffer, die voornamelijk tot stand komt door ontledende organische stof. Kalkoplossing en vrije drainage vormen de belangrijkste afvoerwegen voor koolzuur in resp. de kalkrijke en kalkloze duinen.

Massabalansen zijn ook opgesteld voor 5 monsters duingrondwater uit de ontkalkte duinen van Bergen, langs een stroombaan van dicht onder de grondwaterspiegel tot exfiltratie in het poldergebied. Zij onthullen de grote invloed van luchtverontreiniging op de bovenste grondwaterzone. Verder stroomafwaarts zien we een toename van de effecten van methaanvorming, basenuitwisseling als gevolg van verzoeting, en de oplossing van fluorapatiet. De huidige aanvoer van sterke zuren voor recent duinwater (<50 jaar oud) is ongeveer 13 maal hoger dan de aanvoer onder natuurlijke omstandigheden (duinwater >150-200 jaar oud).

Koolstof-13 gegevens droegen bij aan het onderscheiden van kalkoplossing door sterke atmosferische zuren en kalkoplossing door koolzuur, althans wat ondiep duinwater zonder duinveenpassage betreft. Interactie met duinveen leidt tot een tamelijk uniforme $\delta^{13}C$ waarde van -16‰, door het overheersende effect van isotoop-uitwisseling tussen de relatief geringe hoeveelheid opgelost HCO_3^- en de enorme voorraad CO_2 in bodemlucht en organisch materiaal in het veen. De massabalans voor ^{13}C in diep duinwater met hoge methaanconcentratie, stemt goed overeen met de waarnemingen indien een $\delta^{13}C$ waarde van +30‰ wordt aangenomen voor het koolzuur dat bij het onstaan van methaan vrijkomt.

Chapter 1

INTRODUCTION

1.1 General significance of hydrochemistry

The chemical composition of water in relation to the earth's crust, constitutes the focus of the science called geohydrochemistry or, simply, hydrochemistry. Water quality makes part of the primordial environmental factors determining which flora and fauna will thrive and which material will dissolve or form by precipitation. The significance for life on earth was already well-known in ancient Oriental civilizations, where groundwater was exploited for drinking water supply, irrigation and medical application.

Plinius wrote in 74 AD : "Tales sunt aquae quales terrae per quas fluunt" or, translated very freely, "the composition of water reflects the material it contacted". Unconsciously, he stated the first law in geohydrochemistry (Edmunds, 1981). As a second law can be added : "That material also derives some characteristics from the circulating water, which it acquired upgradient, and may buffer therefore exogenic quality changes of circulating water by a change in its own composition". And the third law may read : "The composition of groundwater also reflects the composition of its recharge, in part independently of the material it contacted".

The first law has been successfully applied for instance in epidemiological research for goitre in The Netherlands (Gezondheidsraad, 1932) or fluorosis in the world, in prospecting for ores (Runnells et al., 1992) and oil and gas (Schoeller, 1955), in water technology by filtration of acid water over marble and in hydrology to visualize flow patterns (Van Oldenborgh, 1915a, 1916; Mazor, 1976; this thesis : sections 4.5.3, 4.6, 6.6.5 and 7.4.3).

The second law is illustrated by the phenomenon of cation-exchange, which has been widely applied for a long time to soften drinking and industrial waters using geological materials (mainly zeolites), and to furnish a key to the past or future for hydrologists interested in the dynamics of flow systems (Versluys, 1916; Ribbius, 1925; this thesis : section 4.5.2 and chapter 7).

And the third law provides tools to : (1) trace back the origin or, more precisely, localize the recharge area of groundwater, for instance by using the conservative tracers ^{18}O and Cl^- (Mazor, 1992; this thesis : sections 4.3.2 and 4.4); and (2) dating groundwater not only by means of the famous radionuclides tritium and carbon-14 (for instance Mook, 1989; this thesis : sections 7.4.5 and 7.5.5), but also using the technique of history matching. This technique implies that either chemical evidence is sought in the sampled groundwater, of a dated event at or close to the land surface, or the time-shift is determined that is required to obtain the best overlap between an undulating time-series of a conservative tracer in groundwater and its recharge (this thesis : sections 6.7, 7.4.5 and 7.5.5).

The combination of the first and second law has led in a later stage, during the past decades, to the development of a quantitative framework for the investigation of natural waters, as presented in Stumm & Morgan (1981) and reflected in multicomponent, speciation and mineral equilibria computer programs, like WATEQF (Plummer et al., 1976), in hydrogeochemical manipulation programs like PHREEQE (Parkhurst et al., 1980), and in combined reaction-transport models, like the model of Schulz & Reardon (1983) and PHREEQM (Nienhuis et al., 1987).

In hydrology, contributions from hydrochemistry in addition to those cited above, consist of possibilities to assess the degree of mixing of different water types within a reservoir, and to calculate the natural groundwater recharge from concentrations of Cl^- in bulk precipitation and groundwater (Heymann, 1927; Schoeller, 1960; Schulz, 1972; Mazor & George, 1992).

In environmental research hydrochemistry is one of the most economic, sensitive and relevant pollution sensors. Economic for the possibility of direct measurement without complicated extractions prior to analysis, sensitive because of an analytically more agreeable surrounding matrix (water molecules) as compared to the solid phases in soil or hardrock, and relevant on account of a direct selection of the mobile phases. These aspects also

explain the success of hydrochemistry in pedological research.

And in geomorphology we are confronted with the most spectacular impact of hydrochemistry : karst landscapes with their lapies surfaces, impressive caves, sinkholes and travertine deposits.

1.2 Coastal plains and dunes in general

Sedimentary coastal plains, like those in the Western Netherlands, are amongst the most densely populated areas in the world. Coastal defence, land reclamation, land subsidence, acid sulphate soils, intricate drainage and irrigation networks, artificial replenishment of aquifers, sea ports and environmental pollution all fit into the general scenery, sooner or later. Although surface and groundwater constitute vast reservoirs, their quality is or will become poor by salinization, excessive manuring, the application of pesticides, acid rain, an increased mineralization of drained peaty soils, chemical wastes, sewage effluents etc.

When these problems are recognized, many different institutions become involved in the monitoring of water quality, in order to measure and predict the diffusion of pollution, check for potability and irrigatability, make alarming or reassuring reports for politicians and help hydrologists in the calibration of models simulating the flow of the last droplets of pre-industrial groundwater. A huge amount of water analyses is generated in the course of time, not rarely from poor samples obtained at the wrong places and, also by lack of integration with all available information, many erroneous conclusions are likely to be drawn.

An important reason for difficulties in interpretation, is the complicated hydrochemical nature of coastal plains. Typical is a very broad spectrum in :

- the origin of groundwaters. Their recharge may consist of for example coastal seawater, river or rain water, and mixed water from a lagoon or estuary;
- salinity, which depends among others on the origin, mixing, vegetation, distance to the coast and the dissolution of evaporites;
- alkalinity, being close to zero in decalcified dunes and amounting to 60 meq/l in methane-rich lagoonal groundwaters in equilibrium with calcite;
- redox potential, varying from oxic in the upper dune sands to anoxic, methanogenic in lagoonal peaty clay;
- the extent of ion exchange, for example due to salt water intrusion or acidification; and
- pollution, in consequence of varied human activities.

To this complexity are to be added the high natural dynamics due to coastal progradation or erosion, fast vegetational successions and periodicity of onshore winds.

With a more systematic approach in hydrochemistry, for which chapter 2 in this thesis offers a framework, and with integration of all relevant information contained in hydrological, geological, pedological, palaeogeographical, geobotanical and environmental pollution maps, a more rational water quality monitoring and management should become feasible.

Coastal dunes

One of the most striking features of many coastal zones are the dunes, where outstanding scenic variations are combined with a wealth of animal and plant life (Salisbury, 1952; Ranwell, 1972; Croin Michielsen, 1974; Adriani et al., 1980). Strong gradients in wind velocity, sea spray deposition and vegetation perpendicular to the coast, large differences in micro-climate for instance between north and south slopes, humidity gradients from wet dune valleys to arid circumstances in exposed sand ridges, all within a distance ranging from 10 m to 10 km, contribute to the unique, small-scale diversity of this particular landscape. A genuine field laboratory for natural sciences indeed, especially when we consider the high dynamics of this aeolian environment.

These important nature reserves, a status not attributed to all, are continuously threatened, however, by man's activities like : residential development, industrial settlement, catchment for public drinking water supply, coastal defence, cultivation of flower bulbs, forestry, transport facilities (highways, railroads, canals), military exercises and recreation, which includes golf playing on dune golfcourses (Boorman, 1977; Salman, 1989; Bijvoet & Taal, 1991). No wonder that one of the outcomes of the first European coastal dune congress held in Leiden (Netherlands) in 1987, was the establishment of a European Union for Dune conservation and Coastal management (EUDC).

It can be stated in general, that hydrochemical studies on coastal dune aquifer systems abroad, which go further than the exclusive use of Cl^- for the distinction between fresh dune and salt ocean water; are scarce in accessible literature.

From Belgium there are publications by Lebbe & De Breuck (1979), who discovered high sulphate groundwaters in the vicinity of a dune water catchment area, where iron sulphides were oxidized in consequence of lowered water tables. And Lebbe & Walraevens (1989) and Lebbe et al. (1990) explained the spatial distribution of freshened, equilibrated and salinized water types, with historical and palaeogeographical data in combina-

tion with hydrological computer simulations.

In the USA, Magaritz & Luzier (1985) observed Ca-Na and Ca-Mg exchange reactions, the oxidation of organic matter in Quarternary sediments with sulphate reduction, and the production of mineral coatings and cements of pyrite and siderite.

A brief listing and superficial discussion of few analyses on dune groundwaters were obtained from Wichmann (1980) regarding the German North Sea islands, from Gorham (1958) for a small dune system in the UK, and from Campbell & Bate (1991), who report on dune groundwater as an important source of nitrogen for surf-zone phytoplankton in South Africa. Contributions from The Netherlands are discussed in section 1.4.

1.3 The coastal dune area of the western Netherlands as a test site

The coastal dunes and adjacent polders of the Western Netherlands make part of the south-eastern, North Sea coastal plain, extending from Denmark to northern France (Fig.1.1). These lowlands are characterized by coastal dunes on-shore or off-shore (on barrier islands), by estuaries, polders and tidal flats. The study area is composed of an uninterrupted coastal dune belt, about 100 km long and 8 km wide at most, in between Hoek van Holland and Camperduin, and a flat, polder landscape largely below sea level and protected from the sea by these dunes and by dikes. It can be considered representative for coastal dunes largely fixed by natural and planted vegetation (Fig.1.2), in a temperate climate with predominating onshore winds. Further physiographic information is given in section 3.2.

The densely populated area (2000 inhabitants/km^2) suffers from all environmental evils of modern times, but still contains one of the most fully developed, extensive coastal dune areas in Western Europe (Westhoff, 1989; Salman, 1989). We therefore are faced with a wide spectrum of natural variations and anthropogenic impacts, side by side as well as superimposed.

Internationally these dunes perhaps still are somewhat exceptional in their very prominent role as fresh groundwater reservoirs for drinking water supply to the densely populated polder area behind, where other water resources are scarce due to the high salinity of groundwaters and heavy pollution of surface waters. The high pollution loads of rain water and the rivers Rhine and

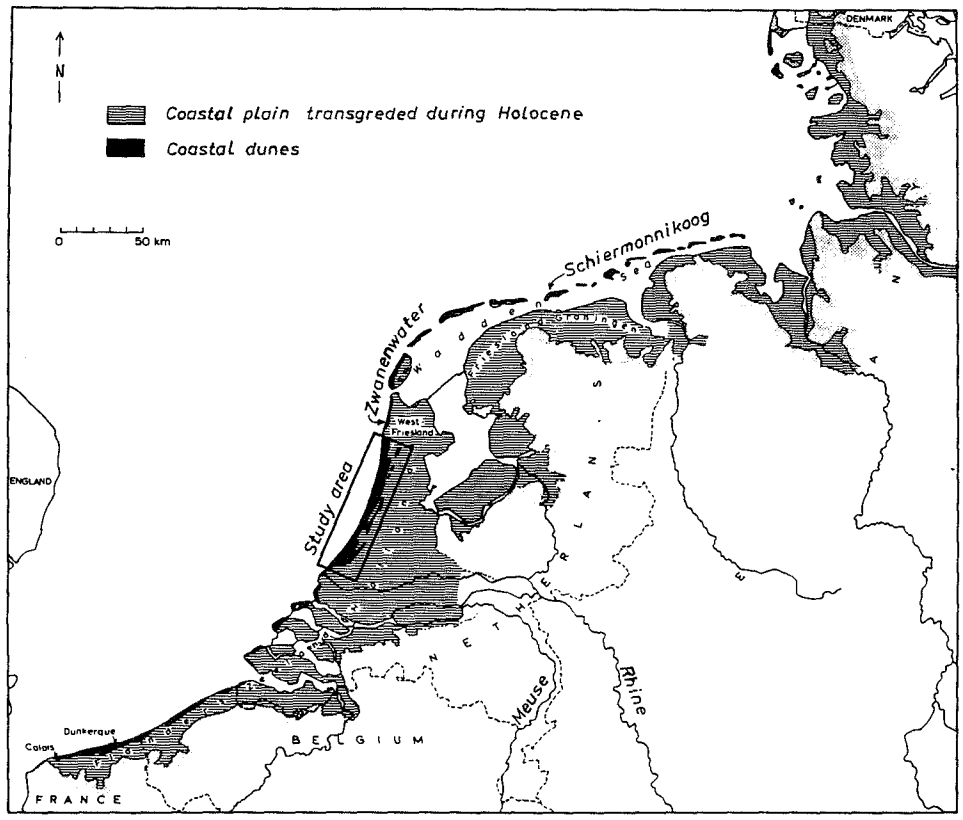

FIG. 1.1 The studied coastal area of the Western Netherlands (modified from Roeleveld, 1974).

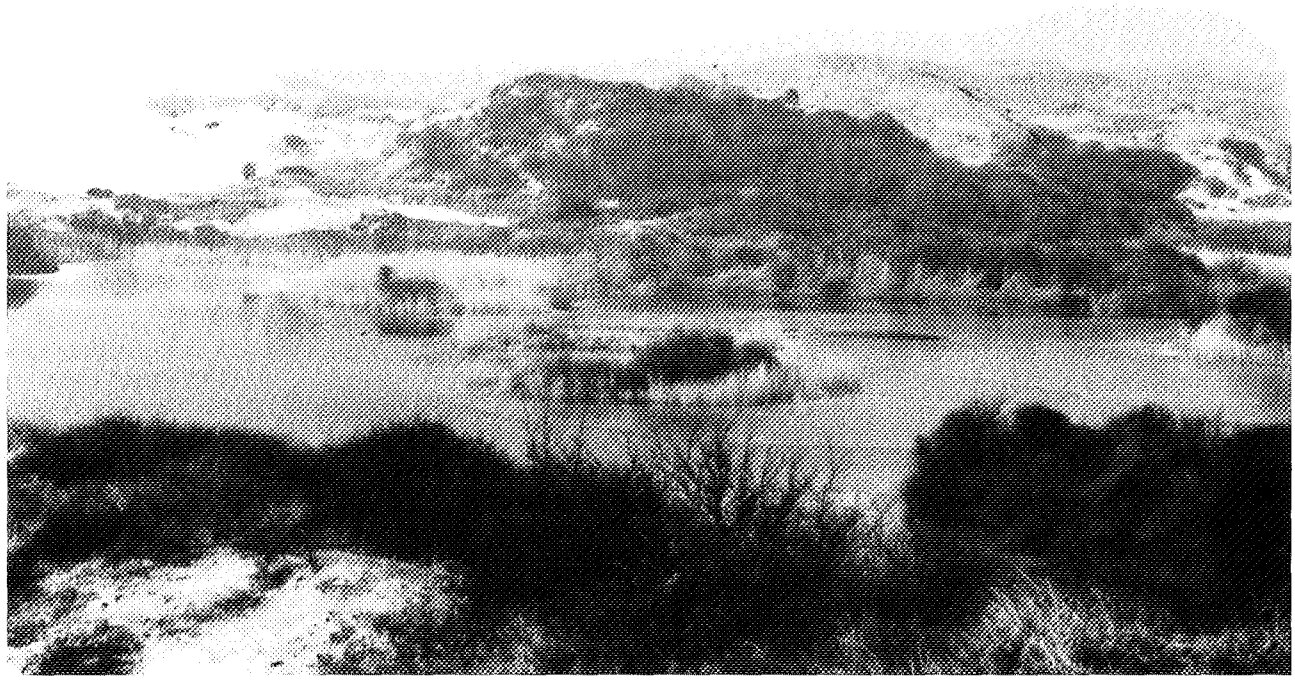

FIG. 1.2 Impression of the coastal dunes of the Western Netherlands, that are largely fixed by natural and planted vegetation.

Meuse, that recharge the dune aquifers locally, make hydrochemical research highly relevant to the custody of both a vital drinking water supply and an already stressed nature reserve.

The area was also judged ideal for this research because of : (a) its abundant historical, physiographical and environmental data; (b) the unique amount of groundwater observation facilities, as a result of intensive hydrological monitoring from the beginning of this century and detailed hydro-ecological research since the late 1980s; and (c) proximity to the research institute and the laboratoria involved in this study.

Water supply and nature conservation : a love-hate relationship

The vast stock of fresh dune water, which has been of paramount importance to the supply of drinking water to the Western Netherlands since 1853, probably saved the dunes as a landscape (Carriere, 1929). Nevertheless the allocation of large dune areas as a drinking water catchment, has been and still is a matter in dispute, especially from an ecological point of view. The exploitation of dune water resulted in a large scale lowering of water tables by 2-3 metres on average (Bakker, 1981) and the disappearance of highly appreciated, phreatophytic plant communities (Van Zadelhoff, 1981).

The digging of spreading basins when artificial replenishment became necessary (Fig.1.3), changed the local, natural landscape (Steenkamp et al., 1981). And the large scale artificial recharge since the late 1950s (Enclosure 1.1), with eutrophic and polluted surface water notwithstanding pretreatment, created new conditions in favour of ruderal plant species (Londo, 1966; Van Zadelhof, 1981; Van der Meulen, 1982; Van Dijk, 1984).

A more harmonious symbiosis in the dunes, between nature conservation and drinking water supply, is sought today in five sanitation measures (Sprey et al., 1990; Peters et al., 1992) : (1) a further reduction in the abstraction of autochthonous dune groundwater; (2) a hydro-ecological optimization of the open artificial recharge, by hydrological isolation (prevention of dispersion of allochthonous waters in the dunes) and by modification of monotonous spreading basins into more varied water courses with bays and islands ; (3) deep well recharge at the expense of recharge by surface spreading; (4) the removal of treatment facilities and buildings from the dunes; and (5) further pretreatment of the surface waters, that are used to recharge the aquifers.

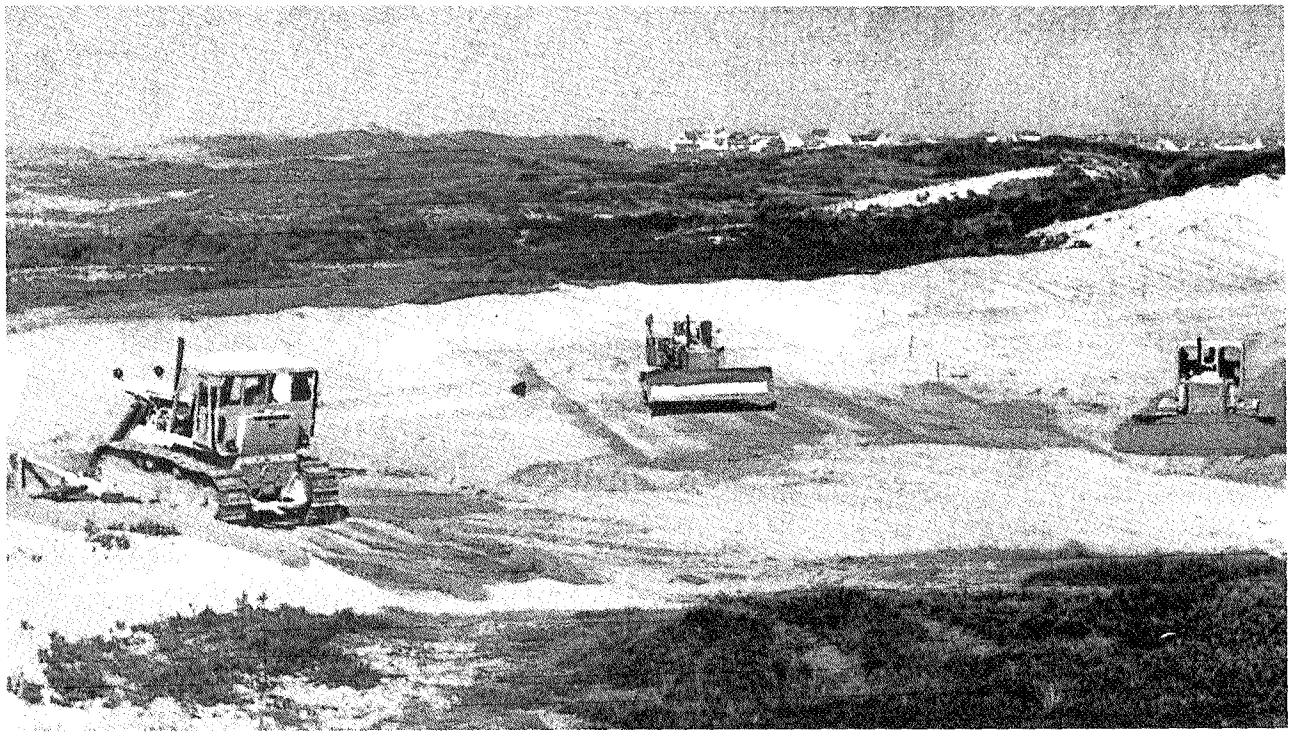

FIG. 1.3 Disturbance of the original dune landscape for the sake of artificial recharge with pretreated river Rhine water in the Leiduin spreading area (Photo derived from Duyve & Stijger, 1957). The village of Zandvoort aan Zee can be seen on the horizon.

1.4 Previous hydrochemical studies in the dunes

The pioneers

The first analysis of coastal dune water in The Netherlands was published in 1854 by Von Baumhauer, when the recharge mechanism of fresh dune water was still a matter of fierce debate between adherents to the theory of condensation of atmospheric water vapour, and the theory of recharge through direct precipitation (De Vries, 1982).

Dubois (1909) and Van der Sleen (1912) published more extensive analyses of dune groundwater obtained at various depths, and recognized the importance of the dissolution of shell fragments and silicates and the more or less successive reduction of oxygen, nitrate, ferric compounds and sulphate in the transition zone of yellow to dark grey dune sand. Sulphate-reducing bacteria were indeed isolated from Holocene aquitards in the dunes by Von Wolzogen Kühr (1922). Van der Sleen also presented in his Ph.D. thesis valuable information on the chemical and mineralogical composition of dune sand and deeper formations. He noted that groundwaters with an excess of sodium carbonate ($NaHCO_3$-waters) were generally coffee-coloured, and coupled a raised mobility of the responsible dissolved organics to the low Ca^{2+} concentrations.

He erroneously attributed, however, their origin to the weathering of Na-containing silicates in deep fluviatile aquitards. Versluys (1916) correctly explained for the first time their genesis in groundwater in the dunes and elsewhere, in terms of cation-exchange. Sodium was exchanged for calcium, where it is to be expected that the salt water has been displaced (recently) by fresh, calcareous water. His later publication in Economic Geology (Versluys, 1931) remained unnoticed by textbook writers like Hem (1970, p.137) and Matthess (1982, p.103), who credited Renick (1924) for the discovery of cation-exchange phenomena in groundwater bodies.

Heymann (1925, 1927) studied iodine concentrations of dune groundwater, in a period of intensive epidemiological research for goitre in The Netherlands. He concluded that rainwater, the leaching of shell fragments in dune sand and vegetation formed the main sources of iodine. He did not recognize, however, the significant contribution from peat and marine aquitards, probably in consequence of the oxidation of ferrous-iron in his anoxic samples upon exposure to the atmosphere. Iodide is indeed co-precipitated by iron(III) hydroxides (Sugawara et al., 1958), and when iodate is formed upon oxidation of iodide, this is partly

immobilized by sorption to iron hydroxide as well (Ullman & Aller, 1985). A higher atmospheric input of total iodine to a lysimeter covered with marram, as compared to its drainage output, led Heymann (1927) to the conclusion that iodine was lost by bioaccumulation and volatilization.

In the same publication, Heymann demonstrated perhaps for the first time, that chloride can be used to determine the natural recharge of dune groundwater below a scanty vegetation. An excellent agreement was obtained between a two years chloride and water balance for a rain gauge and shallow lysimeter. Heymann also recommended, however, to calculate the natural recharge for woodlands from Cl^--measurements on bulk precipitation and shallow groundwater. Thereby he neglected the importance of the additional dry deposition of sea spray on dense and tall vegetations, as demonstrated by Wind (1952) and Minderman & Leeflang (1968).

Leeflang (1940), who was known for his research into the quality of precipitation in the coastal dunes south of Zandvoort aan Zee (Leeflang, 1938), concluded that the dissolution of shell fragments in dune and sea sand is accompanied by the addition of oxidizable proteins, present in between the many growth zones of a shell and as overall coatings of the shells.

Piston flow

It was recognized and demonstrated in the early 1950s in the coastal dunes of The Netherlands (Van Doorn, 1951; Wind, 1952), that water transport in a sandy, unsaturated zone occurs more or less as piston (plug) flow. The experiments with radioactive tracers by Zimmerman et al. (1966) and field observations on tritium profiles, which correlated well with the tritium record of precipitation (Andersen & Sevel, 1974) gained more publicity however.

Piston flow of fast flowing groundwater, from spreading basins towards drainage canals, had been noticed in the mid 1960s (Huisman & Van Haaren, 1965) and has been illustrated more extensively by Stuyfzand (1986d). Seasonal chloride fluctuations in recharged Rhine water could be easily traced back in groundwater as far as 150 m from the spreading basins (Fig.1.4).

After the introduction of miniscreens for detailed groundwater sampling in the late 1970s, piston flow could be demonstrated also for groundwater below an unsaturated zone receiving recharge by precipitation only (Groeneveld, 1977; Van Duijvenbooden, 1979; Meinardi, 1983b,c). Annual fluctuations in the tritium record of precipitation could be satisfactorily matched by Van Duijvenbooden with a vertical tritium log for dune water near Monster (south of Den Haag [The Hague]).

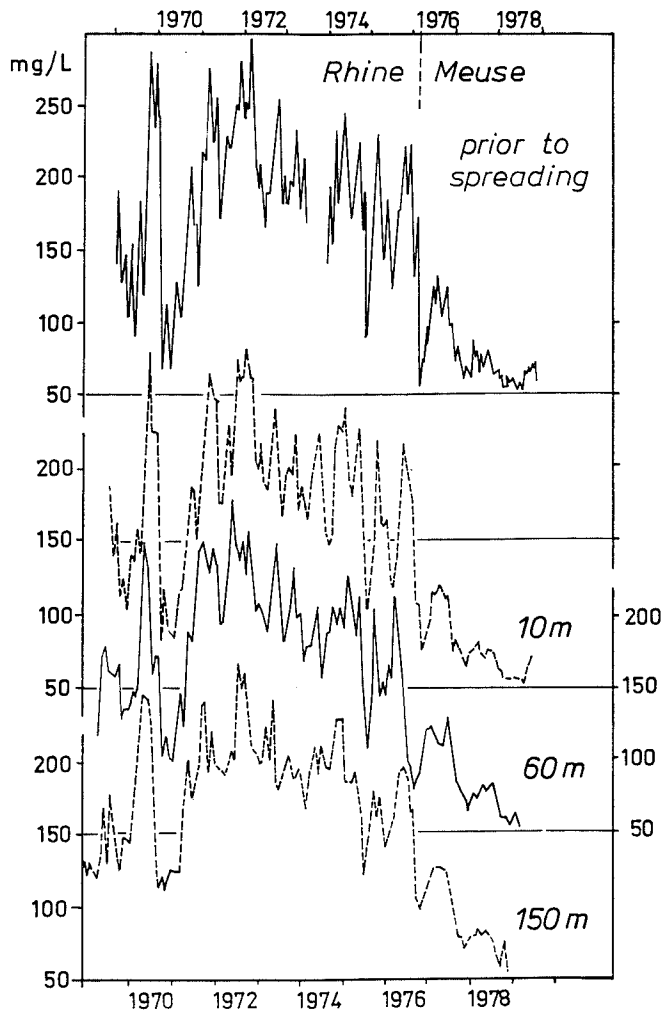

FIG. 1.4 Piston flow of recharged river Rhine and Meuse water in the upper aquifer of the Scheveningen spreading area, as demonstrated by a very small smoothing of Cl^- peaks during 150 metres of subsoil passage. Based on measurements using piezometers with a 1 m long well screen. The travel time in the subsoil to the wells investigated, was 35, 126 and 210 d, respectively.

Effects of vegetation on dune water composition

Wind (1952) studied the composition of water in the unsaturated zone of dunes as a function of three vegetation types : a poor, dry dune vegetation, oak and pines. He applied a unique, but protracted extraction of soil solution from 1 m long soil samples, using a displacement technique with distilled water containing fluorescein as indicator. Groundwater beneath oak and pines exhibited much higher levels for Cl^-, HCO_3^-, total hardness, Chemical Oxygen Demand and colour, than beneath the scanty vegetation.

And it was concluded that soil amendments to stimulate growth of pines and oaks had a strong effect on the concentration of NO_3^- and organic substances in soil moisture.

Results obtained with four giant lysimeters near Castricum (section 6.2), each with a different vegetation (barely a vegetation, dune shrub, oak and pines), were published by Minderman & Leeflang (1968), Tollenaar & Rijckborst (1975) and Stuyfzand (1984d, 1987a). Although each of these investigations yielded new insights in effects and processes, several questions have to be raised with regard to their representativity. The results also contain effects of soil amendments, some interaction of water with the materials used for construction of the lysimeters, and quality changes during the residence time (at least one week) of the water drained into a collection tank.

Artificial recharge

Relatively many publications deal with the quality changes of surface waters upon artificial recharge in the dunes. Most studies were and still are largely inspired by questions regarding the fate of pollutants upon detention in spreading basins (Fig.1.5) and upon passage of the dunes aquifer system, before recollection, post-treatment and distribution as drinking water. They can be subdivided into those, which focus on major constituents (Baars, 1957; Baars & Le Cosquino de Bussy, 1960; Huisman & Van Haren, 1965; Leeflang, 1965; Lips et al., 1969; Haasnoot & Leeflang, 1971; Van Puffelen, 1979 and 1985; Stuyfzand, 1986d; Stuyfzand & Steinmetz, 1990), trace elements (Stuyfzand et al., 1984; Stuyfzand, 1991d), organic micro-contaminants (Piet & Zoeteman, 1980; Smeenk, 1984; Piet & Smeenk, 1985; Hrubec et al., 1986; Te Welscher & Smeenk, 1988; Te Welscher, 1989), microbiology (Baars, 1957; Hoekstra, 1984) and toxicology (Van der Gaag, 1984).

Quality changes upon deep well recharge were reported by Appelo et al. (1979), Van Puffelen, 1984; Van Beek & Van Puffelen (1987), Stuyfzand (1977, 1989i) and Rutte (1990). The areal distribution of recharged Rhine water in the subsoil was first studied by Engelen & Roebert (1974), who recognized the penetration of Rhine water into the deep aquifer on sites where aquitards are lacking or poorly developed. Problems with the recognition of recharged Rhine and Meuse water against the varied autochthonous dune groundwaters have led several authors, however, to wrong pictures of the areal distribution of these water bodies.

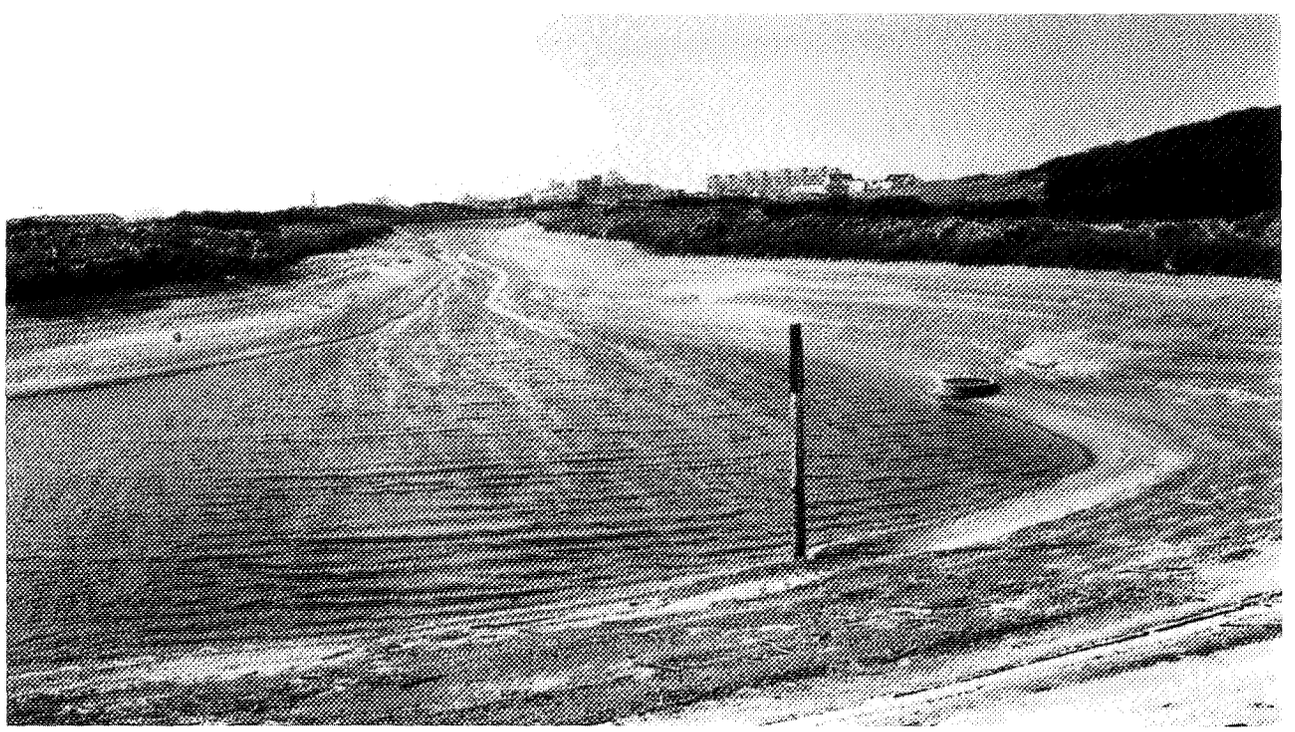

FIG. 1.5 Spreading basin 8.4.2 in the Scheveningen area during low water level. The inlet of pretreated river Meuse water can be seen on the right hand side, and the city of Scheveningen on the horizon (photo by E. Wanders, DZH-archive).

1.5 Scope and outline of this study

Scope

The previous studies yielded valuable bits of information without integration into a systematic analysis of processes and relations with for instance the hydrogeochemical zonation, groundwater flow pattern and record of water table fluctuations, land use and environmental pollution. This thesis aims at such an integration, including the supply of new bits of information.

More specifically it aims at :

1. The development of a sophisticated hydrochemical mapping system for areas with a high complexity and abundant data. The resulting maps and cross sections should provide clear information on the most important hydrochemical characteristics, including the degree of pollution and the origin of the water;

2. The specification of the baseline geohydrochemical conditions for the coastal dune aquifers, which are characterized by a large range of natural environments. Knowledge of the natural backgrounds for the various dissolved species, enables long-term changes and incipient pollution to be identified, and the present extent of uncontaminated groundwater to be mapped. Only when the principal hydrogeochemical processes in the aquifers are established, their role in the release and attenuation of solutes, both natural and anthropogenic, during infiltration and flow downgradient can be predicted;

3. The assessment of the impact of atmospheric deposition and various site-specific factors on the hydrochemistry of the upper few metres of dune groundwater. Factors intended here, are the distance to the coast, vegetation cover, depth of decalcification of dune sand, and thickness of the unsaturated zone. These factors help to explain the extreme variability in the hydrochemistry of dune groundwater and need careful examination in the design of monitoring networks. On the other hand knowledge of their interferences with groundwater quality, may be useful in those landscape ecological studies, where the composition of groundwater is considered a major factor.

4. The overall assessment of the impact of various types of environmental pollution on groundwater in the area : atmospheric pollution on autochthonous dune water; fluvial pollution on

FIG. 1.6 An impression of the Hoogovens industrial steel complex in the younger dune area to the north of the North Sea Canal, being a local pollution source of among others dust, heavy metals, SO_2, NO_x, F (as CaF_2 and HF) and PAHs.

Rhine water, which flushes the drainage and shipping network in the polders adjacent to the dunes, and recharges aquifers in the polder area; fluvial pollution on pretreated Rhine and Meuse waters, which feed spreading basins and recharge-wells in the dunes for subsequent recovery as part of the preparation of drinking water; and pollution by groundwater abstraction itself. The lowering of water tables leads to increased oxidation of peat and iron sulphides, whereas upconing and mixing disrupt the original stratification of fresh and salt groundwater;

5. The application of hydrochemistry as an aid in the solution of specific hydrological problems : the determination of the origin of groundwater by recognition through specific natural tracers; visualization of actual flow patterns by mapping groundwaters of various origin and characteristics; verification of flow velocities by groundwater dating; reconstruction of the palaeohydrological environments in order to establish the present stage of evolution of the flow systems; the determination of the degree of mixing within and between flow systems; and a quantification of the propagation of quality fluctuations in groundwater along flow paths.

Information on the latter is required for an optimal monitoring of groundwater, by aiding in the choice of the ideal well position, screen length, diameter of riser and frequency of sampling. It may also yield the dispersivity of the porous medium, which constitutes an essential parameter for predicting the breakthrough and areal extent of a pollutant downgradient of its entrance into the aquifer system.

Outline

In this thesis the logical sequence for regional hydrochemical surveys is followed, from low to higher levels of abstraction and interpretation, and simultaneously from general towards more detailed information (Fig.1.7). But before doing so, the so-called "Hydrochemical Facies Analysis" is presented in chapter 2 as a sophisticated hydrochemical mapping procedure. It leads to the distinction of water bodies (hydrosomes) with a specific origin and geohydrochemical zones (facies) within these waterbodies.

In chapter 3 the first and second step in the sequence are taken by elucidation of the physiography and hydrology of the study area.
After presentation of the areal distribution of

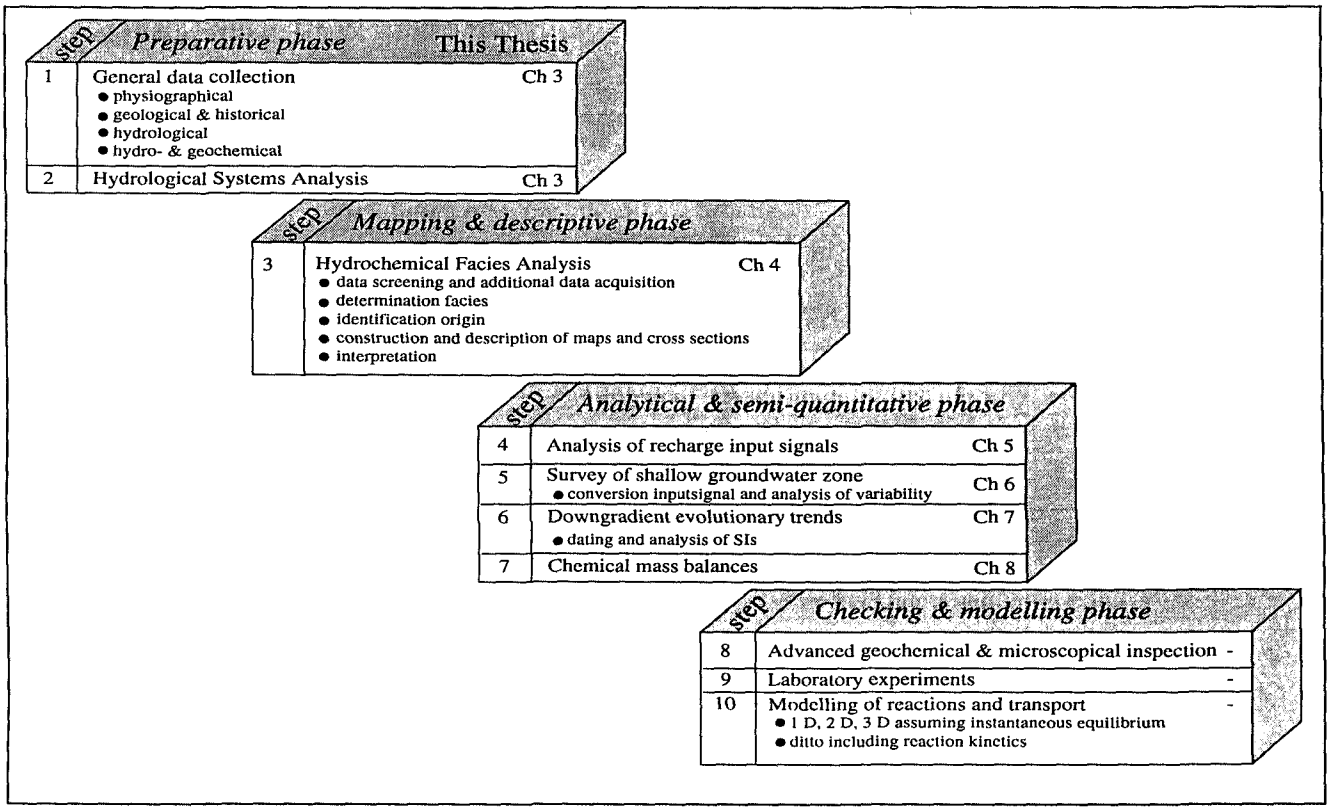

FIG. 1.7 The logical sequence for regional chemical surveys of groundwater, from low to higher levels of abstraction and interpretation, and simultaneously from general towards more detailed information. Note that there is an essential feed-back from the steps 3 and 6 to the hydrological systems analysis (step 2).

geologically well-defined aquitards, the water-balance, the principles of the formation of fresh water lenses, and a palaeohydrological and historical record, the groundwater flow patterns are analysed using the hydrological systems approach as proposed by Engelen et al. (1988).

The third step follows in chapter 4, where the Hydrochemical Facies Analysis is applied to the coastal area of the Western Netherlands. Maps and cross sections are presented with the areal distribution and compositional variations of the many discerned waterbodies. For interpretation purposes, evolutionary quality trends downgradient are searched after and related to the groundwater flow patterns, life cycle of each waterbody, the geochemical structure of the subsoil, and environmental changes near the land surface, as in land-use, atmospheric deposition, fluvial pollution and water table fluctuations.

Chapter 5 presents the fourth step for the dune water body, to which the main focus is directed in the following chapters. The mean composition of bulk precipitation on the study area is unravelled in its main contributions from sea spray, continental mineral aerosols, biogenic inputs and air pollution. Very pronounced variations in space and time are shown and discussed.

The fifth step is taken in chapter 6, which deals with the quality changes from bulk precipitation to the upper dune groundwaters and with the impressive spatial and temporal variability in the composition of the latter.

Chapter 7 forms the sixth step, by showing the detailed compositional evolution of dune water, recharged river Rhine water and North Sea water downgradient, in their respective flow systems from recharge towards discharge or intrusion front. And finally, in chapter 8 preliminary chemical mass balances are drawn up as the seventh step, for shallow groundwater in contrasting dune areas, and for selected points along a deep flow path of Bergen dune groundwater.

The last three steps in Fig.1.7, which ideally constitute the final phase of regional chemical surveys of groundwater and involve detailed checking and modelling, have thus not been reached here. Future research may therefore start at this point.

1.6 Dissolved constituents under consideration

The considered species and their notation

The main focus of this study is directed upon inorganic ions and compounds dissolved in groundwater, together with the organic sum parameters DOC (Dissolved Organic Carbon) and COD (Chemical Oxygen Demand as measured by the consumption of $KMnO_4$). Attention is incidentally paid to the isotopes ^3H (tritium), ^{13}C, ^{14}C and ^{18}O, the organic sum parameters AOCl (non-volatile organohalogens adsorbable to activated carbon) and VOCl (volatile organohalogens), PAHs (Polycyclic Aromatic Hydrocarbons), and some specific xenobiotics.

The investigated inorganics are listed in Table 1.1, with information regarding their geochemical character, mean concentration levels for soil material on earth (after Rahn, 1975) and for selected recharge waters, the drinking water standards for the European Community (EC, 1980), the upper background levels for natural groundwater in The Netherlands as proposed by LBS (1988), and the dominating ionic form in groundwater without consideration of complexes. The upper background levels have been incorporated by MILBOWA (1991) as target values for groundwater in the Dutch National Environmental Policy Plan.

Throughout this thesis the notation of the inorganics is as follows. Elements or compounds are denoted by a specific ionic form (for instance Ca^{2+}), on the condition that (1) colloids and suspended fines have been excluded prior to their analysis or do not contribute significantly to their analytical results, and (2) the specified ionic form predominates in the water phase. In practically all other cases, elements are denoted by their chemical symbol without indication of any ionic form (for example Al and Pb). This means that all major constituents, Fe and Mn generally excluded, are represented by the ionic form as indicated in Table 1.1. Silica and orthophosphate are denoted for simplicity by SiO_2 and PO_4^{3-}, respectively. The only trace elements which can be savely and generally denoted by a specific ionic form, are Ba, Br, F, Li, Rb and Sr (Table 1.1). It should be realized, however, that the many exceptions to a general ionic form notation are ignored for the sake of simplicity. Analytical results always refer to the total dissolved concentration, except for PO_4^{3-}, NH_4^+, Br^- and I, which exclude organic compounds.

Subdivision of the inorganics

The inorganic constituents are generally subdivided into main constituents and trace elements (TEs). As no clear definition exists in hydrochemistry, it is proposed here, in analogy with geochemistry, to declare 0.1 percent of the total dissolved solids (TDS in mg/l) as the upper limit for TEs. In water with 100 (unpolluted groundwater in decalcified areas), 1,000 (river Rhine water) and 50,000 (ocean water) mg TDS/l, the upper limit for TEs then becomes 0.1, 1 and 50 mg/l, respectively, which is in harmony with a negligible contribution to the ionic balance.

TABLE 1.1 The inorganic constituents of water under consideration, subdivided into major compounds and trace elements, in alphabetical order.

ELEMENTS/COMPOUNDS Symbol	Name	Molecular weight kg/m³	geo-chemical group ##	MEAN CONCENCENTRATION world soil [1]	ocean water [2]	rain water [3]	Rhine water [4]	Meuse water [5]	MPC drinking water [6]	Maximum backgrounds Netherlands [7]	Predominant ionic form in groundwater
MAIN CONSTITUENTS				*ppm*	*mg/l*	*mg/l*	*mg/l*	*mg/l*	*mg/l*	*mg/l*	
Ca	Calcium	40.08	Li+(Hy)	13,700	422	2	77.8	64.6	150	-	Ca^{2+}
CH_4	Methane	16	Si	-	<0.01	<0.01	<0.01	<0.01	-	-	CH_4
Cl	Chloride	35.453	Hy	100	19,805	15	151	54	150	100	Cl^-
CO_3	Carbonate	60.02	Si	20,000	3	0	<1	<1	-	-	CO_3^{2-}
Fe	Iron	55.847	Si	38,000	0.002	0.05	<0.01	0.82	0.2		Fe^{2+}, Fe^{3+}
HCO_3	Bicarbonate	61.02	Si	-	145	0	155	161	$>60^S$		HCO_3^-
H_2CO_3	Carbonic acid	62.02	Si	-	-	0.7	-	-	-		H_2CO_3
K	Potassium	39.1	Li+(Hy)	13,600	408	0.6	6.2	5.1	12^A		K^+
Mg	Magnesium	24.305	Hy+(Li)	6,300	1,322	1.0	11.6	7.4	50		Mg^{2+}
Mn	Manganese	54.938	Li	850	<0.01	0.03	0.05	0.12	0.05		Mn^{2+}, Mn^{4+}
Na	Sodium	22.99	Hy	6,300	11,020	8.0	83.1	33.4	120^R	-	Na^+
NH_4	Ammonium	18.04	Li	$1,290^B$	0.03	1.21	0.85	0.82	0.2	$2.6\text{-}12.9^L$	NH_4^+
NO_3	Nitrate	62.0	Li	-	0.3	3.5	17.0	15.2	50	24.8	NO_3^-
O_2	Oxygen	15.9994	Hy+(Li)	490,000	890,000	11.0	8.3	9.6	>2	-	O_2
PO_4	Orthophosphate	94.97	Si	2,448	0.06	0.05	1.16	0.98	6.1^T	$1,2\text{-}9.2^L$	PO_4^{3-}
SiO_2	Siliciumdioxide	60.08	Li	706,200	4.4	0.2	5.2	7.3	-	-	H_4SiO_4
SO_4	Sulphate	96.06	Hy+(Ch)	2,547	2,775	8.0	71	57	150	150	SO_4^{2-}
TRACE ELEMENTS				*ppm*	*µg/l*	*µg/l*	*µg/l*	*µg/l*	*µg/l*	*µg/l*	
Ag	Silver	107.87	Ch	0.1	0.29	<0.05	<1	<1	10	-	Ag^+
Al	Aluminum	26.9815	Li	71,300	5	99	≤270	-	200	-	Al^{3+}
As	Arsenic	74.922	Ch+(Si)	5	2.5	<0.8	2.4	2.7	50	10	AsO_2^-, AsO_4^{3-}
Au	Gold	196.967	Si+(Ch/Hy)	0.003	0.011	-	-	-	-	-	Au^+
B	Boron	10.811	Hy+Li	10	4,600	<5	122	120	1,000	-	$B(OH)_3$
Ba	Barium	137.327	Li	500	30	3	86	62	500	50	Ba^{2+}
Be	Beryllium	9.0122	Li	6	0.0006	<0.02	0.01	<0.05	-	-	Be^{2+}
Br	Bromide	79.904	Hy+(Li)	5	67,300	150	230	130	-	300	Br^-
Cd	Cadmium	112.41	Ch	0.5	0.11	0.11	0.33	0.5	5	1.5	Cd^{2+}
Ce	Cerium	140.12	Li	80	0.0052	0.31	-	-	-	-	Ce^{3+},Ce^{4+}
Co	Cobalt	58.933	Si	8	0.1	0.34	0.8	<0.5	-	20	Co^{2+}
Cr	Chromium	51.996	Li	200	0.2	0.7	2.6	1.6	50	1	Cr^{3+}, CrO_4^{2-}
Cs	Cesium	132.905	Li	5	0.3	0.09	-	-	-	-	Cs^+
Cu	Copper	63.546	Ch	20	0.9	3.2	4.1	5.6	100	15	Cu^{2+}, Cu^+
Eu	Europium	151.965	Li	(2.3)	0.00013	0.02	-	-	-	-	Eu^{3+}, Eu^{2+}
F	Fluoride	18.9984	Li+(Hy)	200	1,300	27	240	378	1,100	500	F^-
Hf	Hafnium	178.49	Li	6	<0.008	-	-	-	-	-	Hf^{4+}
Hg	Mercury	200.59	Ch	0.01	0.03	0.04	0.04	0.13		0.05	Hg_2^{2+}, Hg^{2+}, Hg^0
I	Iodine	126.904	Li+(Hy)	5	60	4	8	7		-	I^-, IO_3^-
La	Lanthanum	138.91	Li	40	0.012	-	-	-			La^{3+}
Li	Lithium	6.941	Li+(Hy)	30	170	<0.6	18	8			Li^+
Lu	Lutetium	174.97	Li	(0.7)	0.00015	-	-	-		-	Lu^{3+}
Mo	Molybdenum	95.94	Si+(Ch/Hy)	2	10	<0.1	2			5	MoO_4^{2-}
Nd	Neodymium	144.24	Li	(40)	0.0092	-	-	-	-	-	Nd^{3+}
Ni	Nickel	58.69	Si	40	0.7	0.6	4.3	6.2	50	15	Ni^{2+}
Pb	Lead	207.2	Ch+(Si)	10	0.03	10.4	1.5	3.5	50	15	Pb^{2+}
Rb	Rubidium	85.47	Li	100	120	≤0.5	-	-	-	-	Rb^+
Sb	Antimony	121.75	Ch	(1)	0.3	0.89	0.3		10		$Sb(OH)_3^0$, $Sb(OH)_6^-$
Sc	Scandium	44.956	Li	7	0.0007	0.038	-	-	-		Sc^{3+}
Se	Selenium	78.96	Ch+(Hy)	0.01	0.09	<0.16	0.35	<0.6	10		SeO_3^{2-}, SeO_4^{2-}
Sm	Samarium	150.36	Li	(7)	0.00045	0.06	-	-	-	-	Sm^{2+}, Sm^{3+}
Sn	Tin	118.71	Si+(Ch)	10	0.8	-	-			10	Sn^{2+}, Sn^{4+}
Sr	Strontium	87.62	Li+(Hy)	300	8,100		(450)			-	Sr^{2+}
Ta	Tantalum	180.948	Li	(2)	<0.003		-				Ta^{5+}
Tb	Terbium	158.925	Li	(1)	0.00014						Tb^{3+}
Te	Tellurium	127.60	Ch+(Hy)	(<0.01)	<0.06	-					Te^{2+}, Te^{4+}, Te^{6+}
Th	Thorium	232.038	Li	6	0.0004	<0.03					Th^{4+}
Ti	Titanium	47.88	Li	4,600	1	3.8					TiO^{2+}
Tl	Thallium	204.38	Ch+(Li)	(1.5)	-	-	-				Tl^+, Tl^{3+}
U	Uranium	238.03	Li	1	3.3	0.02	0.9	-			UO_2^+
V	Vanadium	50.942	Li	100	1.9	2.0	2.0	2.8			$V(OH)_3^0$, VO^{2+}, VO_4^{3-}
W	Tungsten	183.85	Li+(Si)	(2)	0.1	-	0.09	-			WO_4^{2-}
Yb	Ytterbium	173.04	Li	3	0.00082	-	-	-	-	-	Yb^{2+}, Yb^{3+}
Zn	Zinc	65.39	Ch	50	2	15	26	48	100	150	Zn^{2+}

: Ch = Chalcophile (sulphide form); Hy = Hydrophile (preference for dissolved phase, especially in oceanwater); Li = Lithophile (silicate form); Si = siderophile (iron form); (Ch). etc. = moderately chalcophile, etc.

[1] = according to Rahn (1975); [2] = after Van der Sloot (1979); [3] = bulk precipitation along North Sea coast south of Zandvoort, 1 km inland, after Stuyfzand (1991a); [4] = river Rhine water at Vuren for 1980-1983, 0.45 µm filtrated, based on data in RIWA (1980-1983) and in Van der Sloot et al. (1985); [5] dito Meuse near Heusden for 1980-1983, 0.45 µm filtrated, based on data in RIWA (1980-1983); [6] = Maximum Permissible Concentration according to EC (1980); [7] = dissolved in groundwater, according to LBS (1988) and MILBOWA (1991).

A = exemption possible in special cases; B = including NO_3 and organic N, expressed as NH_4; L = low value for sandy areas, high value for clay and peat areas; R = with a 80% percentile for the past 3 years; S= guideline EC (1980); T = total phosphate.

The investigated elements are grouped in Table 1.1 according to a modification, introduced here, of Goldschmidt's geochemical classification of the elements (see for instance Krauskopf, 1967). To the three groups discerned by Goldschmidt, chalcophile (those concentrated in sulphides), lithophile (elements generally occurring in or with silicates) and siderophile (those which preferentially occur with native iron), a fourth group has been added : the group hydrophile (those which prefer to dissolve in water). This classification bears as a matter of fact also a hydrochemical significance, because it indicates important conditions for mobilization in aqueous solutions : the chalcophiles generally in oxidizing, the lithophiles in acid, the siderophiles in weak reducing and the hydrophiles in most environments.

Those elements are judged hydrophilic, which exhibit a migration coefficient "Mig" as defined by Perelman (1972), superior to 1, where

$$Mig = \frac{C_w \cdot 10^6}{C_s \cdot TDS} \qquad (1.1)$$

with : C_w = concentration in water, i.c. ocean water in Tabel 1.1 (mg/kg); C_s = concentration in the earth crust, i.c. of mean soil material on earth from Table 1.1 (mg/kg); TDS = Total Dissolved Solids in water, i.c. ocean water in Table 1.1 (mg/l).

Elements with $0.1 \leq Mig \leq 1$, are considered "moderately hydrophilic".

Units of analysis

The results of hydrochemical analysis have been reported as far as possible in mg/l or µg/l, which still is the commonly used standard unit, at least in Western Europe. Fluxes are expressed in mg m^{-2} d^{-1}, and chemical mass balances are drawn up in either µmol/l or µmol m^{-2} d^{-1}. For conversion of several units, reference is made to Table 1.2.

The ^3H activity is, as usual, given in TU (tritium units), equivalent to a concentration of one tritium atom per 10^{18} hydrogen atoms or roughly 10^{-16} mg/l. This is equivalent to an activity of 0.119 Bq/l (3.19 pCi/l or 7.2 disintegrations per minute per litre water). The half-life of tritium is 12.43 years (Mook, 1989). Tritium decays (β-) to the stable helium isotope ^3He.

Carbon-13 concentrations are expressed as the relative deviation of the ^{13}C : ^{12}C isotope ratio from a specific carbon reference standard, here PDB (a Belemnite in the Pee Dee Formation) :

$$\delta^{13}C = 10^3 \cdot \left[\frac{(^{13}C/^{12}C)_{sample}}{(^{13}C/^{12}C)_{PDB}} - 1 \right] \qquad (1.2)$$

with $\delta^{13}C$ in ‰ versus PDB standard.
About 1.1 % of inorganic carbon is composed of the stable ^{13}C isotope.

Carbon-14 activities are given in pmc (percentage of modern carbon), where ^{14}C measurements are related to a standard oxalic acid. This acid is meant to closely represent the specific activity of carbon in naturally growing plants in 1950 (before significant thermonuclear contributions), yielding 13.56 disintegrations per minute for each gram of carbon. The true half-life of ^{14}C is 5730 years (Mook, 1989). Radiocarbon decays (β-) to the stable ^{14}N isotope.

The heaviest, stable isotope of oxygen is ^{18}O. Its concentration in the water molecule is given as the relative deviation of the ^{18}O : ^{16}O isotope ratio from an ocean water standard (V-SMOW = Vienna Standard Mean Ocean Water) :

$$\delta^{18}O = 10^3 \cdot \left[\frac{(^{18}O/^{16}O)_{sample}}{(^{18}O/^{16}O)_{V\text{-}SMOW}} - 1 \right] \qquad (1.3)$$

with $\delta^{18}O$ in ‰ versus V-SMOW standard.
In absolute terms, the ^{18}O concentration of water samples roughly amounts to 2000 mg/l.

TABLE 1.2 Important conversion factors for hydrochemical data, in alphabetical order.

from	to	multiply with
ha^{-1} y^{-1}	m^{-2} d^{-1}	$2.74 \cdot 10^{-7}$
kg ha^{-1} y^{-1}	mg m^{-2} d^{-1}	0.274
lb $acre^{-1}$ y^{-1}	mg m^{-2} d^{-1}	0.307
meq/l	mg/l	MW/|z|
meq/l	mmol/l	$\|z^{-1}\|$
mg m^{-2} d^{-1}	mg/l	v_w^{-1}
µg/g (air)	µg/m^3 (air)	1.2923
mol l^{-1}	mg/l	MW
mol ha^{-1} y^{-1}	mg/l	$2.74 \cdot 10^{-4}$ MW/v_w
mol ha^{-1} y^{-1}	mol/l	$2.74 \cdot 10^{-7}/v_w$
mS/m	µS/cm	10
ppm (air)	µg/m^3 (air)	0.022414 MW^{-1}
TU	Bq/l	0.119

|z| = absolute value of electrical charge; MW = molecular weight in g/mole; v_w = water flux in mm/d.

Chapter 2

THE HYDROCHEMICAL FACIES ANALYSIS

Abstract

The HYdrochemical Facies Analysis (HYFA) is introduced as a new procedure to map and diagnose the major factors accounting for regional variations in hydrochemistry, the results from environmental pollution and hydrological disturbances, like artificial recharge, included. It consists of five successive steps : (1) the gathering and selection of hydrochemical data; (2) the objective determination of the hydrochemical facies (characteristics) of each sample; (3) the identification of its origin, using among others specific environmental tracers; (4) the construction and description of maps and cross sections presenting the spatial distribution of discerned hydrosomes (water bodies, each with a distinct origin) and the different facies (hydrochemical zones) within each hydrosome; and (5) the interpretation of maps and cross sections, leading to the recognition and understanding of facies chains (evolution lines) in the direction of groundwater flow within each hydrosome.

For groundwater the available sampling facilities and devices are discussed, together with sampling problems and some guidelines for obtaining representative samples and maintaining them so by preservation techniques. How to recognize and correct for the dissolution of suspended fines upon addition of acids to unfiltered samples for storage, is indicated. Tests to check the accuracy of chemical analyses consist of the ionic balance, comparison of the calculated with measured electrical conductivity (or total dissolved solids), and a check on internal chemical consistency. Some improvements to these classical tests are presented. And several ways to estimate the concentrations of missing or mistrusted main constituents are reported.

The facies is determined by integration of 4-5 more or less independent facies-parameters : (a) the chemical water type, which includes in one code the chlorinity, alkalinity, most important cation and anion, and a base exchange index; (b) the redox level, as deduced from the concentrations of O_2, NO_3^-, SO_4^{2-}, Fe, Mn, H_2S and CH_4; (c) a water quality index, either a new pollution index for general purposes or phosphate classes for hydro-ecological studies; (d) the most relevant mineral saturation index for the system; and if useful (e) the water temperature on site.

2.1 General

Good hydrochemical maps are indispensable in water resources allocation, the optimization of monitoring networks, water pollution control and the set-up of combined transport-reaction models. They also form the most effective communication tool for transfer of water quality data in a geographical context, either from expert to expert or from expert to policy-maker.

However, as compared to geology, pedology and hydrology, the mapping of hydrochemical data lagged behind. The initial lack of sufficient data and monitoring wells with a short well screen, probably prevented the construction of mature hydrochemical maps. Hem (1970) still advised in his famous textbook to use symbols at each sampling point to represent the quality observed there, or to prepare isogram maps by drawing lines of equal concentration of dissolved solids or single ions. In many areas the amount of groundwater observation facilities and available hydrochemical data, and the hydrochemical complexity through environmental pollution and hydrological disturbances have reached a level that necessitate the (additional) preparation of more sophisticated maps.

The HYdrochemical Facies Analysis (HYFA) as presented here, offers an approach to sophisticated mapping, and is applied to the coastal area of the Western Netherlands in chapter 4. It can be defined as a procedure to map and diagnose all major factors accounting for regional variations in hydrochemistry. The result is similar to a geological, pedological or hydrological map including cross sections and documented interpretation (Fig.2.1). Geological formations, soil classes or flow systems are discerned on the basis of their genesis. Hydrosomes are likewise defined as water bodies with a specific origin. And the litho-stratigraphical facies, soil horizons or flow branches are substituted for by different hydrochemical facies (zones), within each hydrosome.

	geology	*pedology*	*groundwater*	
			hydrology	*chemistry*
GENETICAL UNIT	formation	soil type	flow system	water body (hydrosome)
example	Westland Formation	Podzol	North Sea	Dune Water
ZONES WITHIN UNIT	sedimentary facies	horizon	flow branch	hydrochemical facies
examples	younger dune sand	A_0	4th order (local)	acid, polluted
	older dune sands	A_1	3d order (subregional)	acid, (sub)oxic
	beach sands	A_2	2nd order (regional)	calcareous, anoxic
	shallow marine sands	B	1th order (supraregional)	ditto, deep anoxic
	lagoonal clay	B_2		ditto, freshened
	basal peat	C		

FIG. 2.1 Comparison of the mapping of geological, pedological, hydrological and hydrochemical data, with a first grouping according to the genesis or origin, and subsequent subdivision on the basis of specific characteristics.

Back (1960, 1966) introduced the term "hydrochemical facies" to denote the sum of all the primary chemical characteristics of water, in analogy with the significance of facies (Latin for face) in stratigraphy as Walther defined it in 1893 (cited in Krumbein & Sloss, 1963).
Back described the facies by the chemical water type, for instance Na-Ca-HCO_3 water, as based on the dominant and next-dominant cation and anion. Although this is an important aspect, it surely does not give a satisfactory summation of all important hydrochemical characteristics, which should include information on the salinity, alkalinity, redox level, degree of pollution, agressivity towards minerals, and temperature as well.

A HYFA may be considered as supplementary to and as an integral part of the hydrological systems analysis (HSA) founded by Toth (1963) and elaborated further by Engelen & Jones (1986). The main issue of a HSA is the mapping of nested groundwater flow systems of different order, each connecting a recharge area with one or more discharge areas. Hydrochemistry is used as a tool there to show the actual flow patterns, to verify flow velocities by dating, to reconstruct palaeohydrological environments in order to establish the present stage of evolution of the flow systems, and to determine the degree of mixing within and between systems (Mazor, 1976; Wallick & Toth, 1976; Stuyfzand, 1989f). On the other hand, a HYFA surely needs the results of a HSA, as an aid in the delimitation of hydrosomes and in the overall interpretation.

Classical approaches to depict and understand variations in hydrochemistry, consider either chemical water types, like Palmer (1911), Sulin (1935), Alekin (1953), Back (1966) and Pawlow & Schemiakin (1967, cited in Matthess, 1990); or chemical formula (Kurlov, 1928); or quality indices, like Richards (1954), Horton (1965), Prati et al. (1971) and Heinonen & Herve (1987); or graphs each representing a single sample, like Rogers (1917), Collins (1923) and Stiff (1951); or plots of many samples into a nomograph (Schoeller, 1955) or in triangles, like Piper (1944) and Durov (1948); or a genetic classification (White, 1957a and b); or hydrochemical zones imposed by climate and depth (Chebotarev, 1955) or altitude (Shipovalov, 1984); or redox zones (Froelich et al., 1979; Champ et al., 1979; Berner, 1981; Edmunds et al., 1984).

Each method is intended for a specific purpose and has its own merits. However, for more sophisticated mapping purposes they lack a holistic view on water quality with a general applicability. This makes them unsuitable on their own for a HYFA in complex situations with abundant data, which may have to deal with complicated, man-induced situations, for instance due to upconing of salt water during groundwater abstraction, artificial recharge, bank filtration (induced recharge) and environmental pollution in addition to all natural variations.

An alternative approach to classify water types, is formed by cluster analysis (Schulz, 1977; Pedroli, 1990; Frapporti et al., 1990; Ruiz et al.,

1990). However, there are many disadvantages attached to this statistical method for general application : (1) the boundaries of each cluster (water type) are not clearly defined and depend on the sample population. This results in difficulties when adjacent maps, prepared with the same technique, are to be compared. Besides, each new sample added to the data base will require a new cluster analysis on the increased population; (2) (log)normality and statistical independence of all data have to be assumed, which is only partly true; (3) very much variation is not tolerated, leading for instance to exclusion of interesting extremes from the data set, restriction of the number of chemical variables and an a priori division of the remaining samples; and (4) a discriminant analysis, with its implicit assumptions is required for revelation of the relative importance of all hydrochemical variables in discriminating between the clusters.

2.2 Principles and definitions

The HYFA consists of five consecutive steps :
(1) the acquisition and screening of hydrochemical data;
(2) the objective, computerizable determination of the hydrochemical facies of each sample from a more or less complete chemical analysis (Fig.2.2). It is determined by combination of 4-5 more or less independent facies-parameters : the chemical water type, redox index, a water quality index (a pollution index for general purposes or an eutrophication potential index for hydro-ecological studies), the most relevant mineral saturation index for the system, and if useful water temperature;
(3) identification of the hydrosome for each sample, using natural tracers in combination with the facies and eventually with geochemical information superimposed on the groundwater flow pattern;
(4) the construction and description of maps and cross sections presenting the areal extent of discerned hydrosomes and their facies; and finally
(5) their interpretation.
These steps are discussed in sections 2.3 through 2.7, respectively.

A *hydrosome* is defined, more or less in analogy with the stratigraphical concept "lithosome" (Krumbein & Sloss, 1963), as a water (Greek : ὑδωρ = hydro) body (Greek : σωμα = soma) with a specific origin, for instance coastal dune groundwater recharged by local rain water versus intruded sea water. A hydrosome is composed of watervolumes constituting a facies chain, facies complex or facies unit in decreasing order (Fig.2.3). On the other hand, the coexistence of several hydrosomes in a certain kind of landscape may be considered a hydrochemical district or province (Fig.2.3). Examples are coastal plains, inland fluvial plains, inland carbonate terrains, volcanic areas, intramontane depressions without discharge and alpine crystalline areas.

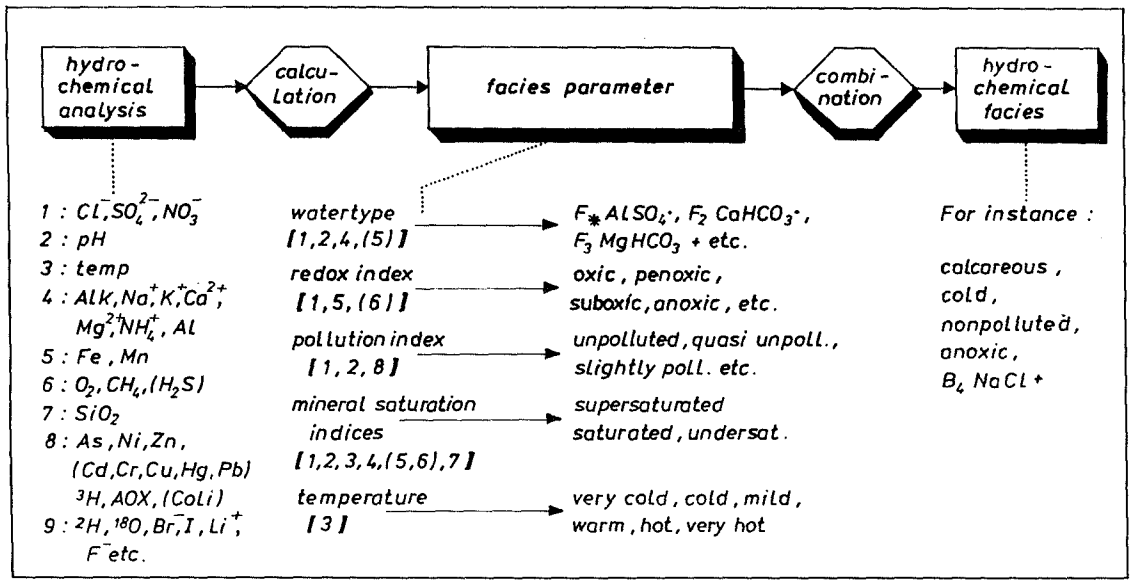

FIG. 2.2. Outline of the computation of the hydrochemical facies with the required chemical analyses, and their destination in the calculation of facies-parameters (within brackets = omissible). 9 = normally for determination of the origin only.

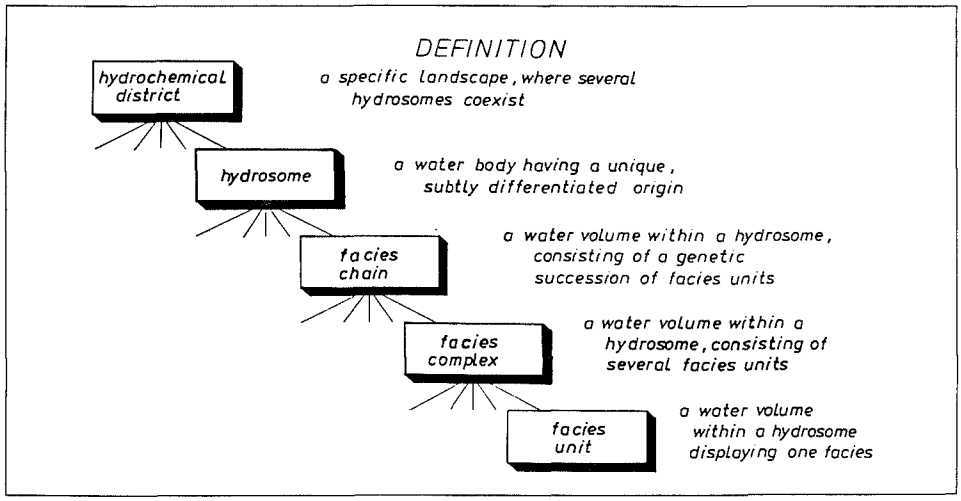

FIG. 2.3. Hierarchical organisation of the concepts facies unit, facies complex, facies chain, hydrosome and hydrochemical district, together with their definition.

A hydrosome generally displays many different facies, due to changes in recharge composition and flow patterns, and due to chemical processes between water and its porous medium. In complex situations the total number of facies may be confusingly and unnecessarily high. In that case several water types have to form a so-called association and/or several facies-parameters need omission. Suggestions for sensible associations as well as for further differentiations in monotonous situations are given in section 2.6.1, suggestions for nomenclature and coding of hydrosomes and their facies follow in section 2.6.2.

A *facies chain* or sequence is defined as a systematic hydrochemical evolution in the direction of (ground) water flow, either within one hydrosome or through several hydrosomes.
When such chains are recognized and can be related to the areal distribution of geochemical zones, the evolution of the hydrological system and the record of environmental pollution and land-use, the last step in the HYFA has been taken.

2.3 Acquisition and screening of hydrochemical data

Obviously, before starting any sampling campaign all available data should be collected and scrutinized in order to identify our gaps in knowledge. Many existing data are easily overlooked, especially in densely populated countries with a long history of hydrochemical research with numerous institutions involved. Additional efforts are required to find the so-called "fugitive sources", i.e. unpublished project reports, governmental agency file documents, memoranda, old handwritten data files etc. Existing data must be examined very critically, however, as the long way to reliable results is fraught with pitfalls, as we shall see. For the same reason a sampling campaign must be carefully prepared with due consideration of all technical aspects.

The hydrochemical analyses needed for a HYFA and those which can be missed or estimated are elucidated in section 2.3.1. The available sampling facilities and sampling devices for groundwater are discussed in section 2.3.2, together with the most important pitfalls in sampling groundwater and with some guidelines for obtaining representative samples and maintaining them so by preservation techniques.
How to recognize and correct for the dissolution of suspended fines upon addition of acids to unfiltered samples for storage, is indicated there as well. Sampling problems with other waters than groundwater are treated elsewhere : rain water in Galloway & Likens (1978), Ridder et al. (1984) and section 5.2.2; surface waters in Hem (1970) and Golterman et al. (1978); and vadose waters in Litaor (1988), Ross & Bartlett (1990) and Merkel & Grossmann (1992).

Tests to check the accuracy of chemical analyses are presented in section 2.3.3. And several ways to estimate the concentrations of missing or mistrusted main constituents are reported in section 2.3.4.

For storage, retrieval and hydro(geo)chemical, statistical and graphical manipulations of water analyses, a geographical data base coupled to manipulation modules is indispensable. A data base of that kind, CHEMCAL, has been developed

at KIWA for a VAX minicomputer by Van der Kooi & Stuyfzand (1987). A similar data base for a PC, though necessarily more restricted in size and possibilities, has been prepared at the Free University of Amsterdam (VU) by Biesheuvel et al. (1988).

2.3.1 Needed data in general

The ideal HYFA is performed on a large database, containing the required chemical analyses (Fig.2.2) of high reliability on sufficient samples, that were collected within the period under consideration, well distributed over the study area and covering recharge waters, groundwaters and discharged surface waters.

The chemical analysis of a sample should preferably consist of (Fig.2.2) :

(1) *a complete analysis*, which includes all major constituents (Cl^-, SO_4^{2-}, alkalinity, Na^+, K^+, Ca^{2+}, Mg^{2+}), macro-nutrients (NO_3^-, NH_4^+, PO_4^{3-}, K^+, SiO_2), Fe, Mn, pH and temperature, in order to determine most facies-parameters and the ionic balance (for checking the analytical results; section 2.3.3). In surface and groundwaters with pH<5 also Al and dissolved organic carbon (DOC) need consideration. It is advised to include the electrical conductivity (EC) in a complete analysis, as an additional instrument to check its accuracy (section 2.3.3). Another reason to include DOC, also when pH>5, is the redox interpretation of raised Fe and Mn concentrations in surface and groundwaters containing O_2 or NO_3^- (section 2.4.2).

(2) *specific analyses* for a single facies-parameter : O_2, CH_4, As, Cd, Cr, Cu, Hg, Ni, Pb, Zn, ^3H, chlorinated hydrocarbons adsorbable to activated coal (AOCl) and thermotolerant *Escherichia coli* bacteria (not necessary in most groundwaters); and if useful

(3) *additional analyses* of isotopes, trace elements, organic microcontaminants or gases, in order to determine the origin in difficult cases or for other special purposes.

In reality, few samples with such an extensive analysis will occupy the regional hydrochemical database. However, there are several methods to estimate missing values for incomplete analyses (section 2.3.4), while the lack of several specific analyses can be circumvented by the determination of the redox and pollution index on a reduced set of analyses (Fig.2.2). Furthermore, several specific constituents can be assumed zero or close to zero, when the hydrological and hydrochemical position of the sample and the factors and processes controlling the concentration of these constituents are well-known (section 4.3.1).

Analyses performed prior to the period under consideration can be included only, if the well screen is judged sufficiently distant from the former and actual boundaries of the hydrosome in situ.

2.3.2 Sampling groundwater : problems and recommendations

Sampling facilities

Groundwater sampling facilities can be subdivided into three categories :

(1) natural, like springs and caves;

(2) man-made occasional, like temporary piezometers during or after drilling, soil cores which need squeezing or centrifugation, and a well point sampler or so-called hydropunch. The latter is a sampling tool connected to a small diameter drive pipe as described by Kerfoot (1984) and Edge & Cordry (1989); and

(3) man-made semi-permanent, like pumping wells and gas wells, both having screens often exceeding 5 m, and observation wells. Observation wells can be subdivided into : (a) piezometers — single, in clusters (together in separate boreholes) or nested (many at different depths in one borehole) — normally having a screen 0.5-2 m long; and (b) multilevel samplers equipped with miniscreens. The latter are usually attached to a central support pipe and have a screened length inferior to 0.1 m.

Many types of these multilevel samplers have been developed since the mid 1970s, as hydrochemical profiling in aquifers became increasingly important for preventive monitoring, clean-up studies and scientific work. Atakan et al. (1974) published details on the construction and use of one of the first versions in Germany. C. Maas developed in 1974 at the National Institute for Drinking Water Supply (RID) the type, that was described by Snelting (1979) and has been used in this study. An example, with attachment to piezometers and with details about well completion, is presented in Fig.2.4. Its installation and simultaneous vacuum sampling are shown in Fig.2.5.

Pickens et al. (1978) introduced at the same time a version with the sample riser tubes inside the support pipe, which reduces the risk on short-circuiting of water from different layers, and with a different type of screen. Constructions equipped with a small reservoir above the miniscreen, a valve at its bottom and a gas entry tube appeared in 1981 (Vasak et al., 1981; Morrison & Brewer, 1981). They allow sampling of groundwater below the suction level (> 8 m) with minimization of oxidation/reduction reactions when an inert gas is used to blow out the sample.

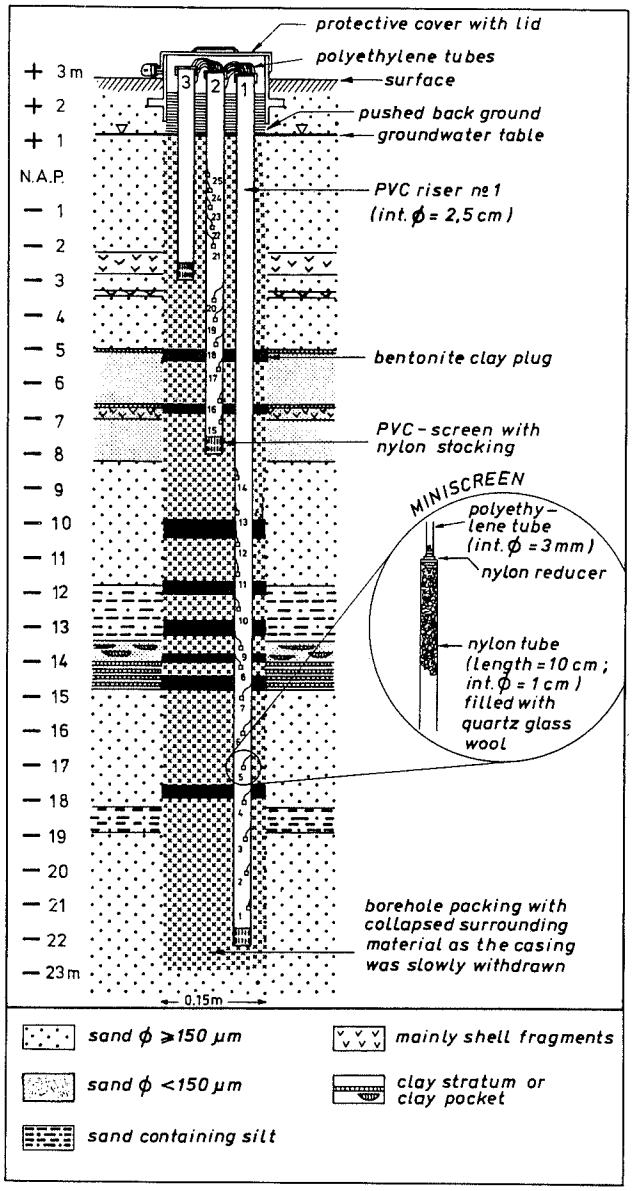

FIG. 2.4 Bailer drilled borehole 24H.470 equipped with miniscreens of the type described by Snelting (1979), for sampling groundwater by suction as shown in Fig.2.5.

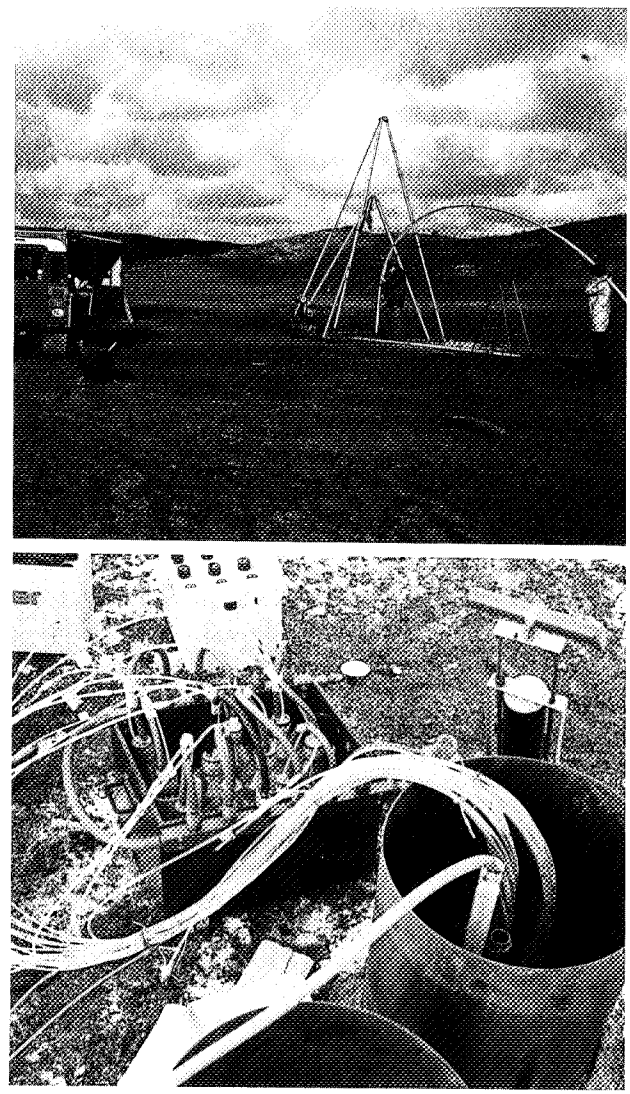

FIG. 2.5 Installation of a miniscreened observation well and the simultaneous sampling of groundwater from 1-12 miniscreens by means of a vacuum system with quick couplings and hand pump.

Sampling devices

A sampling device is defined here as a mechanism to pull up water from any sampling facility described above. An overview of available portable types of groundwater sampling devices is presented in Table 2.1, giving some operational limitations and the chemical parameters that can be analysed in samples thus obtained, without serious losses or gains. Barcelona et al. (1984) and Nielsen & Yeates (1985) compared several advantages and disadvantages of most devices, which may help to choose the right device for a specific problem.

Problems

The most frequent problems met in sampling groundwater from piezometers or miniscreens in unconsolidated sediments, are arranged in Table 2.2. For each problem discerned, the diagnosis, chemical consequences, prophylaxis and symptom abatement are indicated. The long list, which is discussed more in detail by Stuyfzand (1983a), reveals the high chances of totally unrepresentative water samples, if preventive measures are ignored. As a general rule, the larger the physicochemical differences between the natural groundwater and substances introduced during well installation (drilling fluids, seals and backfills), the stronger and longer the well installation trauma (Walker, 1983) will be.

TABLE 2.1 Comparison of 12 groundwater sampling devices, regarding some operational and hydrochemical limitations (Modified from Pohlmann & Hess, 1988). It is assumed that the monitoring wells are properly installed and constructed of materials suitable for detection of the parameters of interest, and that the device is cleaned, operated properly and constructed of suitable materials.

Device	Approxim. maximum sample depth@ (m)	Minimum well diameter (cm)	Sample delivery rate or volume*	INORGANIC							ORGANIC				RADIOACTIVE		BIOLOGY
				EC	pH	Re-dox	Major ions	Trace metals	NO_3^-, F^-	Gases	Nonvo-latile	Vola-tile	DOC	AOCl	Ra-dium	Gross α & β	Coli-forms
GRAB																	
Open bailer	NL	1.3	variable	++	+	-	++	++	++	-	++	-	+	++	++		++
Point-source bailer	NL	1.3	variable	++	++	++	++	++	++	++	++	++	++	++	++	-	++
Syringe sampler	NL	3.8	0.04-0.8L	++	++	++	++	++	++	-	++	-	+	++	++	++	++
POSITIVE DISPLACEMENT (Submersible)																	
Bladder pump	120	3.8	0-500 L/h	++	++	++	++	++	++	++	++	++	++	++	++	++	++
Helical rotor	50	5.0	0-300 L/h	++	++	++	++	++	++	++	++	++	++	++	++	++	++
Piston gas drive	150	3.8	0-100 L/h	++	++	-	++	++	++	-	++	-	+	++	++	++	-
Centrifugal	variable	7.6	variable	++	+		++	+	++		+		+	++	++	++	
SUCTION LIFT																	
Peristaltic	8	0.3	0-100 L/h	++	+	+	++	+	++		++		+	++	++		++
Centrifugal	9	0.3	variable	++	+	+	++	+	++		++		+	++	++		++
Handpump	8.5	0.3	0-100 L/h	++		+	++	++	++		++		+	++	++		++
GAS CONTACT																	
Gas-lift	variable	2.5	variable	+			+	+	+		-			+	-		
Gas-drive	50	0.3	0- 50 L/h	++	+	+	++	+	++	-	++	-	+	++	++	-	-

@ = depth to waterlevel in well; * = average ranges based on typical field conditions (L = liter); ++ = very suitable for high quality data; + = can be suitable to obtain moderate to good quality data; - = unsuitable; NL = no limit

TABLE 2.2 The diagnosis, chemical consequences, prophylaxis and symptom abatement of problems frequently met in sampling groundwater from piezometers or miniscreens in unconsolidated sediments.

DESCRIPTION	DIAGNOSIS	CHEMICAL CONSEQUENCES	PROPHYLAXIS	SYMPTOM ABATEMENT
Invasion of drilling fluids and additives into formation surrounding new wells	analyse drilling fluid and its specific tracers during each flushing prior to definite sampling.	* drilling fluid sampled * cation exchange * redox reactions * sorption to neoformed $Fe(OH)_3$ * dissolution additives * sorption to additives	install observation well by hammering or pushing down (bailer drilling without fluids still results in the introduction of mixed groundwater standing in the casing)	* limitation of drilling fluids * limitation of additives * wait for natural equilibration by ground water flow, or * help equilibration by frequent, protracted pumping
short circuit	compare depth-quality and depth-head relations with quality-measurements during flushing and head-measurements afterwards.	* leakage water sampled or a mixture with desired water	apply watertight connections and noncorrosive materials	* use sampling device with packers * or, in case of leaky risers, lower sampling device to bottom and evacuate mainly above
chemical interaction with screen, riser or sampling device	exposure experiments in laboratory	too high or too low concentrations	all contacting materials must be inert	* protracted flushing (>3 times) * reduce contact time by sampling at bottom of well, or raise the discharge of the pump.
extraction from original environment	* effervescence of sample, * development of turbidity upon standing * measure changes in open vessel	1.degassing (CO_2, CH_4, VOCs) 2.introduction of O_2 3.change of temperature 4.introduction atmospheric dust	1.maintain pressure in device 2.exclude atmospheric contact 3.isolate sample 4.exclude atmospheric contact.	1.avoid suction 2.proper sample conservation 3.measurement in field 4.shield the sampling site
presence of suspended fines	* initial turbidity * examine residue on membrane	* interference with analytical method * dissolution upon acidification of sample for storage * raised concentrations for colloidal particles (Fe, Al)	* reduce flow velocity in vicinity of well * apply screens with right meshes and packing * use screens without sand trap	* filtration in-situ over <0.45 µm membrane, avoiding atm. contact. * reduce discharge of pump, or * flush abundantly, if this helps
mixing of different watertypes in well	development of turbidity upon standing, without atmospheric contact	1.inconsistent analysis (O_2-Fe, NO_3^--CH_4, ^3H-^{14}C) 2.precipitation of $Fe(OH)_3$ or $Al(OH)_3$ or $CaCO_3$	* apply miniscreens * minimize flushing	1. impossible 2. proper sample conservation

Seven ways of leakage or shortcircuiting in monitoring wells are shown in Fig.2.6. The evil of leaky risers, made of PVC or stainless steel, is widely disseminated in monitoring networks, as shown by Stuyfzand (1982, 1983a), Toussaint (1987) and Lebbe et al. (1989).

Additional problems arise when pumping wells with their longer screens and larger diameters are to be sampled : instationarity of flow around the well and well field, urges a prolonged discharge in a normal or identical abstraction scenery for the whole well field (Schmidt, 1977; Nightingale & Bianchi, 1980; Blaszyk & Gorski, 1981); and a progressive clogging of the well may change the mixing ratio of contributing water types and/or lead to the development of an anoxic zone around the screen (Van Beek & Kooper, 1980).

Cased and uncased monitoring and pumping wells in hard rock lead to still further complications. Water from the macropores having strong circulation, is inevitably mixed with water from the micropores where circulation is limited but high buffer capacities prevail (Edmunds, 1981).

Check and correction for contribution of suspended fines

Suspended and colloidal particles cannot be easily and completely removed from solution, because their size spectrum may overlap with truly dissolved matter (Stumm & Morgan, 1981; Edmunds, 1981). For conveniency and more or less by convention, matter retained by a 0.45 µm filter paper is designated as suspended fines.

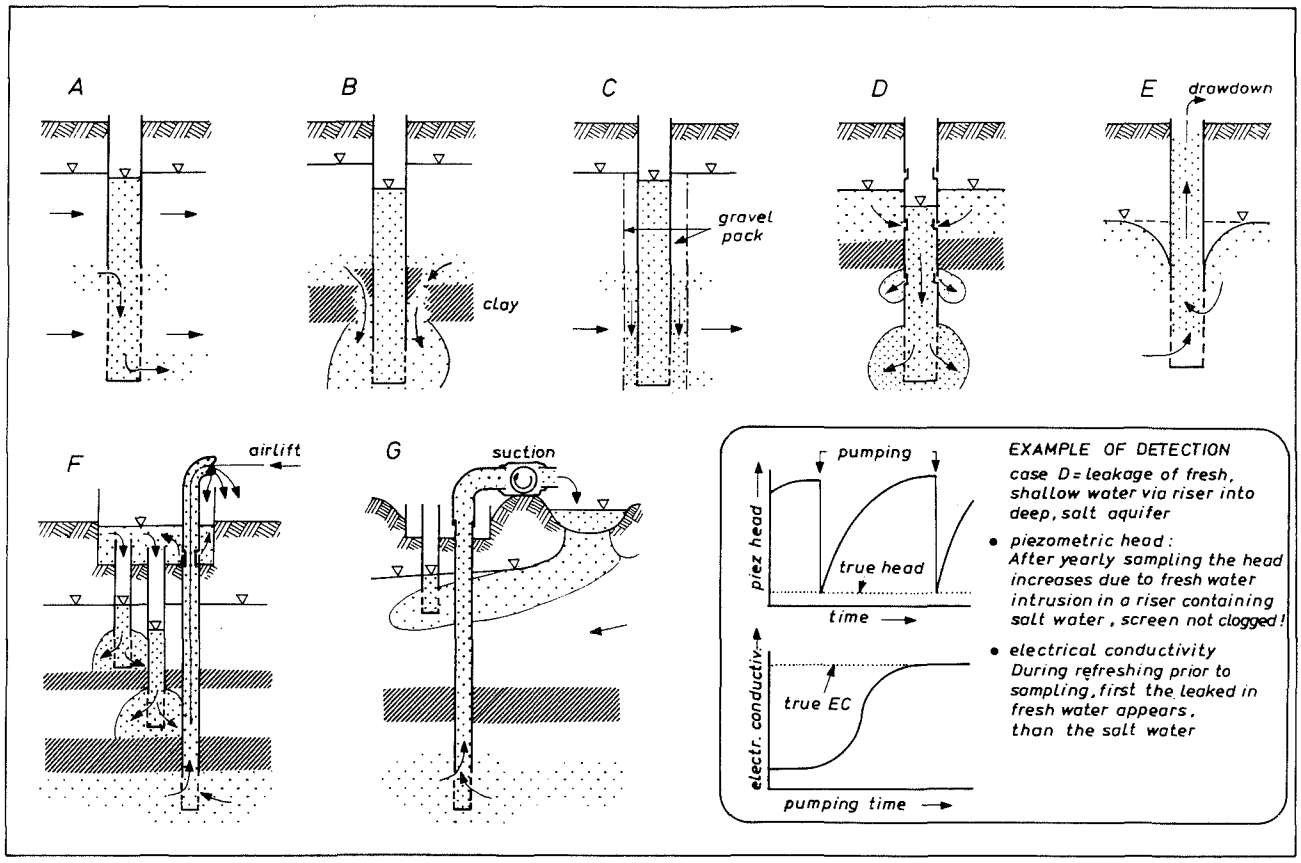

FIG. 2.6 Seven different ways of leakage or shortcircuiting in monitoring wells, with an example of detection for case D. A = screen too long in aquifer where also vertical flow occurs; B = pierced aquitard insufficiently sealed; C = gravel pack applied to whole borehole in finer grained aquifer; D = leaky riser, at connections; E = depression cone by heavy pumping, draws the upper groundwater layer towards the screen; F = discharged water is spilled into the housing of a piezometer nest and drained by piezometers without cap; G = discharged deep groundwater recharges local groundwater flowing to shallow piezometer.

In groundwater studies general interest focuses on the truly dissolved solids, because suspended fines must be considered largely as an artefact, as opposed to surface water. Recently, however, evidence has accrued showing that colloidal material may exist in significant concentrations in undisturbed groundwater as well (Ryan & Gschwend, 1990; Magaritz et al., 1990; Matthess, 1990). Herzog et al. (1991) discuss the many pros and cons of groundwater sample filtration. The advantages strongly outbalance the disadvantages for most trace elements.

Filtration offers the fastest way with the best removal efficiency of suspended matter. The common use of a 0.45-µm membrane filter must be considered as a compromise between the highest possible filtration speed, the easiest exclusion of air contact, and complete separation of suspended matter.

Investigations of surface water by Kennedy et al. (1974) and of groundwater by Edmunds (1981) and Hettinga & Stuyfzand (1991), indicate that the trace element content in particular is strongly affected by very fine suspended matter, which can pass through these filters and which is not necessarily stopped by 0.1-µm screens either. Kennedy et al. found that the pH after acidification and the storage time of the sample determine the effect of the passage of the particles.

Checking and correcting trace element analyses of groundwater for a contribution of suspended fines seems warranted, as acidification is an essential part of conservation for many trace elements, and filtration of groundwater is often discarded, because of convenience, lack of any "visible" suspended matter or an unstable character under atmospheric conditions. A check or correction can be performed only when typical indicators of suspended particles should be regarded as virtually insoluble under the hydrogeochemical conditions prevailing in the aquifer (Stuyfzand, 1987c). Aluminium for instance, is a good indicator of suspended clay in case of groundwater with 6 < pH < 8.5 and without significant complex-formation by among others fluoride, dissolved organic substances and sulphate.

Table 2.3 shows a strong positive correlation between Al (as a measure of the quantity of suspended clay) and Ti, V, Sc, Ce, Th, Cr, Lu, Hf, and Zn (r^2 >0.5), for unfiltered, anoxic, pH 7-8 dune groundwater in The Netherlands. The constant Ce:Cr:Hf:Lu:Sc:Th ratio of 100:112:4.5:0.3:17:17 also coincides fairly closely with that for clay samples from other parts of The Netherlands, being 100:100:8:0.5:15:15 (dr. H.A. Van Der Sloot, Energy Research Centre of The Netherlands [ECN], pers. comm).

TABLE 2.3 Concentrations of various trace elements in 67 unfiltered, anoxic, pH 7-8 dune groundwater samples after acidification for storage, with and without correction for a contribution of suspended clay particles. Aluminium was considered to derive from the dissolution of suspended clay, when its concentration was above 10 µg/l, and a correction was made using linear regression with Al according to Eq.2.1. The range of uncorrected Al concentrations was 1-2161 µg/l (Fragment from Stuyfzand, 1987c).

	Content uncorrected**			Content corrected***
	Range (µg/l)	Linear regression	r^2	Range (µg/l)
Ti(α)*	<2–138	Ti = 0.064 Al	0.98	<2
V(α)	0.08–4.27	V = (160 + 1.9 Al)·10^{-3}	0.98	0.08–0.30
Sc(α)	0.001–0.551	Sc = (5.1 + 0.24 Al)·10^{-3}	0.98	0.001–0.010
Th(α)	<0.004–0.570	Th = 2.5·10^{-4} Al	0.93	<0.004–0.016
Ce(α)	<0.024–3.730	Ce = (45 + 1.43 Al)·10^{-3}	0.89	<0.024
Cr(α)	<0.1–4.0	Cr = 0.3 + 0.0016 Al	0.82	<0.1–0.5
Lu(α)	<0.001–0.009	Lu = 4·10^{-6} Al	0.71	<0.001–0.002
Hf(α)	<0.004–0.122	Hf = 6.3·10^{-5} Al	0.70	<0.004–0.010
Zn(α)	<0.1–14	Zn = 2.9 + 0.006 Al	0.65	0.1–7
Pb	0.2–4	Pb = 0.4 + 0.003 Al	0.45	0.2–1

* α = Neutron activation analysis after preconcentration on activated carbon.
** Without correction for suspended clay; total number of samples examined: 67.
*** Without correction if Al ≤ 20 µg/l (n = 11) or Al > 20 (r^2 < 0.5) and with correction for Al if Al > 20 and $r^2 \geq 0.5$.

In the far right-hand column of Table 2.3, concentrations of these Trace Elements (TEs) were corrected for positive interference by suspended clay as follows :

$$TE_{corr} = TE_{meas} - b \cdot (Al - 10) \qquad (2.1)$$

where b is the regression constant in TE = c + b.Al, and 10 = the average concentration (µg/l) in samples practically unaffected by clay.

Effects on the main constituents could be neglected, whereas no strong linear relation was found between Al on the one hand and As, Ag, Co, Cu, Eu, F^-, Fe, Hg, Mn, Nd, Ni, Sb, Se, and Tb on the other (r^2 < 0.25). This means that these TEs, Fe and Mn cannot be corrected for a contribution of suspended fines by using Eq.2.1. In case of no filtration, their concentration must therefore be considered as an upper boundary, and should be checked for a contribution of other fines, like colloidal iron hydroxides. Such a correction is much more difficult and questionable, however, and stresses the importance of filtration on site prior to acidification.

Sample conservation

Various components in groundwater samples are quite unstable above the ground because, among others, pressure, gas composition and temperature of the environment differ from those at the screen level from which the sample was obtained. Sampling and filtration are also certainly not conducive to maintaining the original balance. If no consideration is given to proper storage of sam-

ples, it is possible to carry out a perfect analysis on an originally representative sample, which completely lost its identity. The stabilizing reagents that are to be added (after any filtration), the material of the storage vessel and the permissible storage time before analysis, if the sample is kept in a cool (4°C), dark place (!) are given for a number of inorganic parameters in Table 2.4.

2.3.3 *Checking the accuracy of chemical analyses*

Did one succeed in taking representative samples and store them properly in spite of all perils previously described, then there are still several rocks in the laboratory on which the research can split, aside from broken bottles. Errors arising in the laboratory can be classified as random analytical, systematic analytical and administrative. A lot of misery can be avoided by asking the laboratory of your choice about their quality control system (Kirchmer, 1983), and by sending every now and then identical samples and standards to different laboratories, including a few using totally different analytical methods.

Fortunately there are several tests to check the accuracy of chemical analyses of main constituents, preferably of course before the remainders of the sample left the laboratory through the sink. These are based on the ionic balance, electrical conductivity, residue on evaporation, internal chemical consistency, and comparison with samples from the same or similar environment. A combination of these methods is advised.

Ionic balance

When all main constituents have been analysed, an ionic balance (IB) can be drawn up (Fig.2.7). It is defined as follows :

$$IB = 100 \cdot \left(\frac{\Sigma k - \Sigma a}{\Sigma k + \Sigma a} \right) \qquad (2.2)$$

in which Σk = sum of cations (meq/l); and Σa = sum of anions (meq/l).

A simplified calculation of Σk and Σa is shown in Fig.2.7. It includes the often neglected transformation of H^+ and OH^- activity as obtained by pH measurement, into its concentration; that part of

TABLE 2.4 Survey of sample storage techniques for inorganic chemical investigation of groundwater (From Stuyfzand, 1987c). Unstable samples are, for instance, anoxic samples through miniscreens operating under vacuum or through air lifting. Stable samples are, for example, samples containing oxygen and no iron taken with a point-source bailer or bladder pump.

	Filtering[a]		Storage vessel[b]	Stabilising agents	Maximum storage time
	Unstable samples	Stable samples			
Electrical conductivity (20°C)	−/+	±	P/B	−	12 h
pH[c]	−	−	P/B[d]		6 h[n]
Cl^-	±	+	P/B/G		14 days[o], > 1 year[k]
SO_4^{2-}		+	P/B/G	−	7 days[o], > 1 year[k]
HCO_3^-, CO_3^{2-}[e]		−/+	P/B/G[e]	−	6–12 h[k], 24 h[p]
$NO_3^- + NO_2^-$		+	P/B/G	H_2SO_4[f]	30 days[n], 8 days[o]
NO_3^-		+	P/B/G	$HgCl_2$	18–100 days[n]
NO_2^-		−	P/B/G	$HgCl_2$	7 days[n], 0 days[o]
PO_4^{3-}		++	B[d]	[m]	< 2 days[n]
Total phosphate		++	B[d]	HNO_3[g]	Unlimited[o]
F^-	+	+	P	−	14 days[n], > 30 days[q]
Br^-	+	+	P/B	−	2 days[n]
Na^+	+	+	P[d]	HNO_3[g]	½ year[n], > 1 year[k]
K^+	+/++	+/++	P[d]	HNO_3[g]	½ year[n], > 1 year[k]
Ca^{2+}	−	++	P[d]	HNO_3[g]	½ year[n], > 1 year[k]
Mg^{2+}	−/+	++	P[d]	HNO_3[g]	½ year[n], > 1 year[k]
Fe	−	++	P[d]	HNO_3[g]	½ year[n], > 1 year[k]
Mn		++	P[d]	HNO_3[g]	½ year[n], > 1 year[k]
Hg		−/++	P[d]	$HNO_3 + K_2Cr_2O_7$[h]	30 days[n]
Ag		++	P[d]	HNO_3[g]	30 days[n]
Other metals		++	P[d]	HNO_3[g]	½ year[n]
NH_4^+		−	P/B/G	H_2SO_4[f]	6–30 days[n], 16 days[o]
N-Kjeldahl		−	P/B/G	H_2SO_4[f]	30 days[n]
SiO_2		++	P[d]	HNO_3[g]	> 1 year[k]
(^{18}O, ^2H, ^3H)[c]		−	G	−	> ½ year[l]
^{13}C			G	KI/I_2[i]	14 days[i]
^{14}C			P/B/G	−	2–7 days[l]
Free CO_2[c]			B	−	6 h
H_2S[c]	−	−	B	Zn-acetate[j]	7 days[n], 1 day[p]
O_2[c]	−	−	G	−	6 h

[a] ++ = necessary; + = recommended; − = not advised.
[b] P = polyethylene, B = boron silicate, G = glass
[c] From a closed full vessel.
[d] Vessels rinsed out with HNO_3 and distilled water.
[e] Permeability of polyethylene to O_2 and CO_2 must be low, good lid construction is very important.
[f] Up to pH 1.5.
[g] Up to pH < 2.
[h] Up to pH 0.5 and 0.05% $K_2Cr_2O_7$.
[i] Five drops (15 g I_2 and 30 g KI per 1000 ml).
[j] 1 M, 2 ml per l.
[k] Groundwater findings, Free University Laboratory, Institute of Earth Sciences, Amsterdam, The Netherlands.
[l] Prof. W.G. Mook, Laboratory for Isotope Physics, State University of Groningen, The Netherlands, personal communication.
[m] Addition of HNO_3 recommended where storage time > 2 days, notwithstanding low hydrolysis of organic P.
[n] K.R. Huibregtse and J.H. Moser, *Handbook for Sampling and Sample Preservation of Water and Wastewater*, US Dept. of Commerce, Nat. Techn. Inf. Serv., PB-259946, 1976, 257 pages.
[o] W. Funk, *Vom Wasser*, 48 (1977) 75–87.
[p] M.R. Scalf, J.F. McNabb, W.J. Dunlap, R.L. Cosby and J. Fryberger, *Manual of Groundwater Sampling Procedures*, NWWA/EPA Series, 1981, 93 pages.
[q] C.L. Chakrabarti, K.S. Subramanian, J.E. Sueiras and D.J. Young, *J. Am. Water Works Assoc.*, 70 (1978) 560–565.

1. *Conversions (mg/l to meq/l, pH to H^+). Specification data entry : HCO_3^- = total alkalinity as HCO_3^-, if pH < 8.3 or if CO_3^{2-} unknown; CO_3^{2-} = phenolphthalein alkalinity (pH = 8.3). N.B. : PO_4^{3-}-conversion to mmol/l*

Cl^-	= Cl^-/35.453	Na^+	= Na^+/22.9898
SO_4^{2-}	= SO_4^{2-}/48.0288	K^+	= K^+/39.0983
HCO_3^-	= HCO_3^-/61.02	Ca^{2+}	= Ca^{2+}/20.04
CO_3^{2-}	= CO_3^{2-}/30.01	Mg^{2+}	= Mg^{2+}/12.1525
NO_3^-	= NO_3^-/62.	NH_4^+	= NH_4^+/18.04
NO_2^-	= NO_2^-/46.006	Fe^{2+}	= Fe/27.93
F^-	= F/19.	Mn^{2+}	= Mn/27.45
PO_4^{3-}	= PO_4^{3-}/94.971	Al^{3+}	= Al/8.993
		H^+	= 10.**(3.-pH)

2. *Simplified calculation of : $H_2PO_4^-$, which is not included in alkalinity; ionic strength (i); and activity coefficient for monovalent ions (γ_1).*

$H_2PO_4^- = PO_4^{3-}[1 + 10.0**(pH - 7.21)]$

$i = 0.0005*[Cl^-+HCO_3^-+NO_3^-+NO_2^-+F^-+H^++Na^++K^++H_2PO_4^-+2.*(SO_4^{2-}+CO_3^{2-}+Ca^{2+}+Mg^{2+}+Fe^{2+}+Mn^{2+})+3.*Al^{3+}]$

$\gamma_1 = 10.**[-0.5*[\sqrt{(i)}/(\sqrt{(i)}+1.)-0.3*i]]$

3. *Calculation of sum of cations (Σk) and anions (Σa).*

$\Sigma a = Cl^-+HCO_3^-+SO_4^{2-}+NO_3^-+NO_2^-+CO_3^{2-}+F^-+H_2PO_4^-$

$\Sigma k = H^+/\gamma_1+Na^++K^++Ca^{2+}+Mg^{2+}+NH_4^++Fe^{2+}+Mn^{2+}+Al^{3+}$

4. *Calculation including organic anions (AORG) according to Oliver et al. (1983), if pH < 5, where DOC = Dissolved Org. Carbon (in mg/l).*

IF (pH ≤ 5) THEN.
KORG = 10.**(0.039*pH**2. -0.9*pH-0.96)
AORG = KORG*DOC/(100*KORG+H^+/10)
IF (AORG > HCO_3^-) Σa = Σa+AORG-HCO_3^-
ENDIF

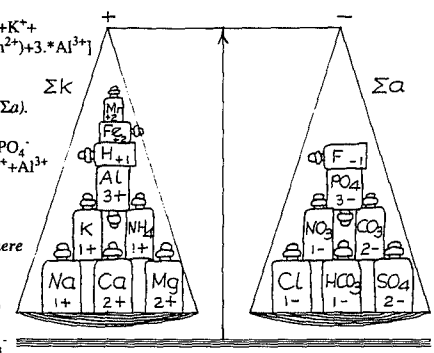

FIG. 2.7 The ionic balance, one of the most powerful checks on correctness of main constituents, with its stepwise calculation.

orthophosphate, which is not included in the determination of alkalinity; and organic anions in so far not included in alkalinity, according to a procedure presented by Oliver et al. (1983). However, the most accurate calculation of an ionic balance if organic anions can be ignored, is offered by computer programs like WATEQF (Plummer et al., 1976).

The balance is judged square, if : | IB | < 2%, if Σa+Σk > 8 meq/l; | IB | < 3%, if Σa+Σk = 2-8 meq/l; and | IB | < 5%, if Σa+Σk < 2 meq/l.

Electrical conductivity

The electrical conductivity of water (EC) at standard temperature (in The Netherlands 20°C), is a measure of its total dissolved solids (TDS). When all main constituents have been analysed, EC can be calculated and compared to the measured EC, as a check of the accuracy of their analysis. The calculation is no easy matter at all, as there are no simple relations in a natural mixed solution, between concentrations or activities and EC, due to interactions of electrical and ionic nature (Harned & Owen, 1958; Robinson & Stokes, 1965; Tanji, 1969; Hem, 1982). This appears also from the rather low accuracy and the limited range of application of calculation methods presented among others by Guillerd (1941), Blanquet (1946), Dunlap & Hawthorn (1951), Logan (1961), McNeal et al. (1970), Tanji & Biggar (1972), Rossum (1949, 1975) and Golterman et al. (1978).

An accurate method, not earning a medal for elegancy but performing much better than all above mentioned methods, was presented by Stuyfzand (1983c) with updates in Stuyfzand (1987b), applicable to the range of 0.2-12,000 meq Σa+Σk/l or an EC in between 10 and 200,000 µS/cm. The average percentage error amounts to 2.3 ± 1.9% , and in the range of 8-1200 meq Σa+Σk/l it is 1.9 ± 1.5% . The method consists essentially of a dialling system (Fig.2.8), which selects out of 6 transformed and adjusted methods described in literature, the best for a given sum of cations and anions and for a certain anion-ratio.

Using this method, an analysis will earn the mark "good", if the calculated EC approximates the accurately measured EC in such a way, that : | δEC | < 10% , if Σk+Σa < 8 meq/l; | δEC | < 5% , if 8 < Σk+Σa < 1,200 meq/l; and | δEC | < 9% , if Σk+Σa > 1,200 meq/l, where :

$$\delta EC = 100 \cdot \left(\frac{EC_{meas} - EC_{calc}}{EC_{meas}} \right) \qquad (2.3)$$

These requirements can even be tightened for more selected water types, as indicated in a discussion of several cases by Stuyfzand (1983b). Differences in temperature (temp,°C) during measurement can be corrected for, according to TNO (1976) and Thomas (1986), by :

$$EC_{20} = EC_t \cdot [1 + 0.023 \cdot (20 - temp)] \qquad (2.4)$$

where EC_{20} = electrical conductivity [µS/cm] at temp = 20°C; EC_t = ditto at temp = t°C.

Residue on evaporation

The Residue on Evaporation at 180 °C (RE), can be calculated as follows :

$$RE = Na^+ + K^+ + Ca^{2+} + Mg^{2+} + NH_4^+ + Fe + Mn + Al + SiO_2 + Cl^- + SO_4^{2-} + NO_3^- + 0.5(\text{Alkalinity as } HCO_3^-) + PO_4^{3-} + DOC \qquad (2.5)$$

where all concentrations are expressed in mg/l.

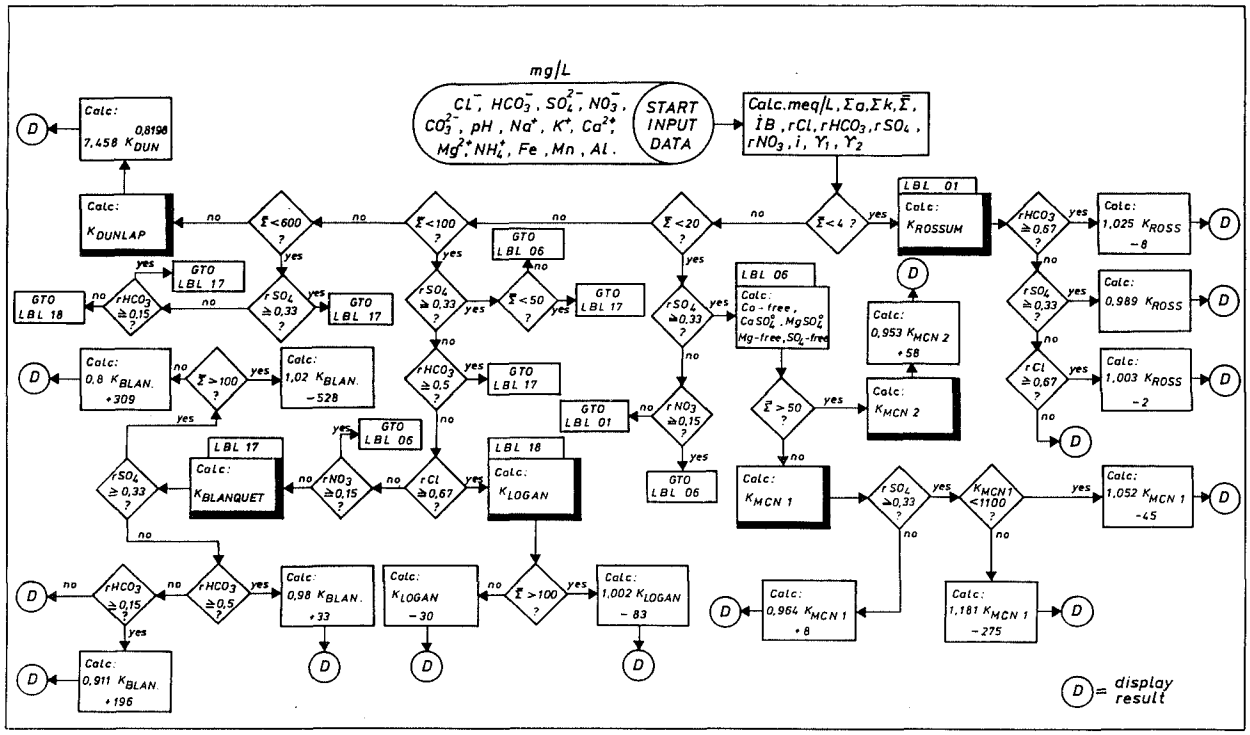

FIG. 2.8 Flow chart for the calculation of the Electrical Conductivity (EC) according to Stuyfzand (1987b). The heavy blocks indicate the calculation according to a modified version of the method by Rossum (1975), McNeal et al. (1970), Logan (1961), Blanquet (1946) or Dunlap & Hawthorne (1951). $rSO_4 = SO_4^{2-}/\Sigma a$ in meq/l; $rHCO_3$, rCl and rNO_3 as rSO_4; $\bar{\Sigma} = (\Sigma k + \Sigma a)/2$; i = ionic strength; γ_1 = activity coefficient monovalent ions; γ_2 = ditto divalent ions; K_{BLAN} = EC calculated with Blanquet's method.

An analysis is judged OK, if $|\delta RE| < 10\%$ (definition δRE similar to δEC in Eq.2.3). The calculation of RE suffers from inaccuracies when dealing with waters rich in Ca^{2+} and SO_4^{2-}, or in NO_3^- or with a low pH (Hem, 1970).

Internal chemical consistency

Internal chemical consistency couples of groundwater samples are for instance O_2- Fe or NO_3^- - Fe (if pH > 4), NO_3^- - CH_4, Al - pH and ^3H - ^{14}C. For instance, when concentrations of O_2, NO_3^- and tritium are high, with pH in between 5.5 and 9, then iron, methane and aluminium should normally be low, whereas carbon-14 cannot approach zero. An inconsistency may point at analytical errors, insufficient conservation, sampling errors or mixing, either by sampling or in the aquifer. An unbiased inconsistency using miniscreens points at mixing in the aquifer, whereas such an inconsistency obtained from a very long well screen of a pumping well, indicates the mixing of different water types in the well (mixing by sampling).

Comparison

Large differences in chemical analysis as compared to all previous samples in a time series or to a sample taken in the neighbourhood from the same stable environment, are suspect. And when peaks in the time series of different monitoring wells coincide with the sampling date or date of analysis, something went wrong that particular day, because it is extremely unlikely that peaks arrive on exactly the same day at monitoring wells.

2.3.4 *Estimating missing values*

It will undoubtedly occur that not all main constituents were analysed in some of the most critical samples. Sometimes it is possible to calculate the concentration of the missing or mistrusted ion(s), thereby heavily relying on a square ionic balance. This presupposes correctness of all other main components, and well established relations between two or more parameters, like between electrical conductivity and the sum of anions or between alkalinity and ammonium (Stuyfzand, 1988b).

After giving a few conversions of ancient parameters to modern ones, three cases of increasing complexity are discussed in order to illuminate the estimation of missing values.

Conversion of old-fashioned parameters
In hydrochemical reports written around the beginning of this century, which may be extremely valuable in approximating natural backgrounds, old-fashioned expressions were used to denote the concentration of for instance Fe (Fe_2O_3), SO_4^{2-} (SO_3^{2-}) and HCO_3^- ($CaCO_3$ or $NaHCO_3$ or free + half-bound CO_2).
A general conversion formula for compound A_aB_b to A_cB_d, both expressed in mg/l, is :

$$A_cB_d = A_aB_b \cdot \frac{(\ MW\ of\ A_cB_d\ )}{(\ MW\ of\ A_aB_b\ )} \cdot \frac{a}{c} \qquad (2.6)$$

where : MW = molecular weight (g/mol). For instance 5 mg Fe_2O_3/l = 3.5 mg Fe/l.
Conversions to alkalinity as HCO_3^- in mg/l are :

$$HCO_3^- = 2.77 \cdot (free + half\text{-}bound\ CO_2) \qquad (2.7)$$

$$HCO_3^- = 61.02 \cdot (\frac{NaHCO_3}{84.01} + \frac{TotH}{2.8}) \qquad (2.8)$$

$$HCO_3^- = 61.02 \cdot (\frac{Na_2CO_3}{106} + \frac{TotH}{2.8}) \qquad (2.9)$$

where : $NaHCO_3$ = excess alkalies as $NaHCO_3$, in mg/l; Na_2CO_3 = idem as Na_2CO_3, in mg/l; and TotH = total hardness in german degrees = 5.6 (Ca^{2+}+Mg^{2+}) in mmol/l.

Case 1 :
Is only one major constituent (X in mg/l) lacking, then its concentration can be easily calculated using the ionic balance directly :

$$X = |\ \Sigma a - \Sigma k\ | \cdot \frac{MW_x}{Z_x} \qquad (2.10)$$

where MW_x = molecular weight of X (g/mol); and Z_x = charge of X. X may also stand for [Na^++K^+, expressed as Na^+], [Ca^{2+}+Mg^{2+}, expressed as Ca^{2+}] or [SO_4^{2-}+NO_3^-, expressed as SO_4^{2-}].

Case 2:
Are there two missing or mistrusted values of major constituents, a cation and an anion, whereas EC has been correctly measured, then both values can be accurately calculated using an iterative procedure, which stops when the calculated EC approximates the measured EC within for instance one percent (Stuyfzand, 1983c).

During the successive approximations, starting with zero meq/l for both ions, the difference between the measured and calculated EC is divided by 100 each time, giving ΔEC/100. The first time this amount is added as meq/l to the lower of Σa and Σk, for instance Σk, whereas Σa is raised to the level of Σk + ΔEC/100. The next times ΔEC/100 is added to both. The whole procedure can be easily included in any computerprogram for the calculation of EC according to the method by Stuyfzand (1983c, 1987b).

Case 3:
Are there three missing values of major constituents, one cation and two anions or vice versa, whereas EC was not measured, then there still is a chance to complete the analysis, on the following conditions :
· one ion can be assumed zero, because it is the small partner of an internal consistency couple (section 2.3.3) and its partner was analysed, for instance Fe was >0.5 mg/l, so that NO_3^- can be assumed zero; and
· one of the other missing ions can be reliably estimated by regression with a measured ion or parameter (like NH_4^+ or colour). Such regressions generally hold for a specific water type or group of water types only, so that the hydrochemical position of the sample must be assessed first. A missing ion can also be calculated by assuming equilibrium with a mineral phase (for instance Ca^{2+} from calcite or Al from gibbsite), for which thermodynamic data are well established.

The concentration of the remaining ion is subsequently calculated using Eq.2.10.

2.4 Defining the facies

The hydrochemical facies of a water sample is determined by combination of 4-5 more or less independent facies-parameters, each of which (except for the temperature) is derived from a specific lumped quality index as calculated from its own set of chemical analyses (Fig.2.2). The aspects considered, are the chemical water type, redox index, a water quality index (either a pollution index for general purposes, or phosphate classes for hydro-ecological studies), the most relevant mineral saturation index for the system, and if useful water temperature. Their determination, information and significance are treated in the next sections.

2.4.1 Classification of water types

General aspects
In a review of 17 methods to classify natural waters according to their chemical composition,

Konzewitsch (1967) concluded : "Really the absence of an efficacious classification causes a lot of difficulties in the progress to study the chemical composition of natural waters and had already paralysed, is paralysing now and will paralyse a gradual and successful development in this branch of natural sciences". This pessimistic prediction has been falsified, but the increased knowledge has not led to any production of more sophisticated, surveyable hydrochemical maps. In my opinion a further development of classification systems may contribute to achieve this.

The hydrochemical classification system proposed by Stuyfzand (1986a/b, improved in 1989g) has several advantages over the systems discussed by Konzewitsch (1967) and Matthess (1982, 1990) and more recent methods, and is therefore recommended. First of all, it combines four essential aspects in a logical code (Fig.2.9) : the chlorinity, alkalinity, most important cation and anion and a new base exchange index. The latter results in a more sophisticated and better diagnosis of cation exchange due to fresh or salt water intrusion as compared to other base exchange indices. Its earlier denomination of otherwise (very) rare water types through a new principle of family support in the denomination of the most important cation and anion, makes the method more effective in the diagnosis of processes like acidification ($AlSO_4$ groundwater), cation exchange ($MgHCO_3$ and MgCl groundwater), air pollution (NH_4SO_4, HNO_3 and HCl rain water) and excessive applications of fertilizers (KNO_3 groundwater).

The determination of a water type implies the successive calculation of the main type, type, subtype and class of a water sample, each of which contributes to the total code (and name) of the water type (Fig.2.9). These levels of subdivision are consecutively discussed below.

Main types, by Cl^-

Chlorinity determines the main type, as indicated in Table 2.5, because of (a) its paramount importance in the determination of the origin of waters (sections 2.5 and 4.3.2), (b) its indicative value of the thalassogenic mineralization of water (by sea or rock salt) and (c) its relevancy to aquatic flora and fauna (Redeke, 1922; Anonymous, 1959;

TABLE 2.5. Division in main types on the basis of the chloride concentration.

Main type	code	chloride concentration meq/l	chloride concentration mg/l
oligohaline	G	<0.141	0 - 5
oligohaline-fresh	g	0.141 - 0.846	5 - 30
fresh	F	0.846 - 4.231	30 - 150
fresh-brackish	f	4.231 - 8.462	150 - 300
brackish	B	8.462 - 28.206	300 - 1,000
brackish-salt	b	28.206 - 282.064	1,000 - 10,000
salt	S	282.064 - 564.127	10,000 - 20,000
hyperhaline	H	>564.127	> 20,000

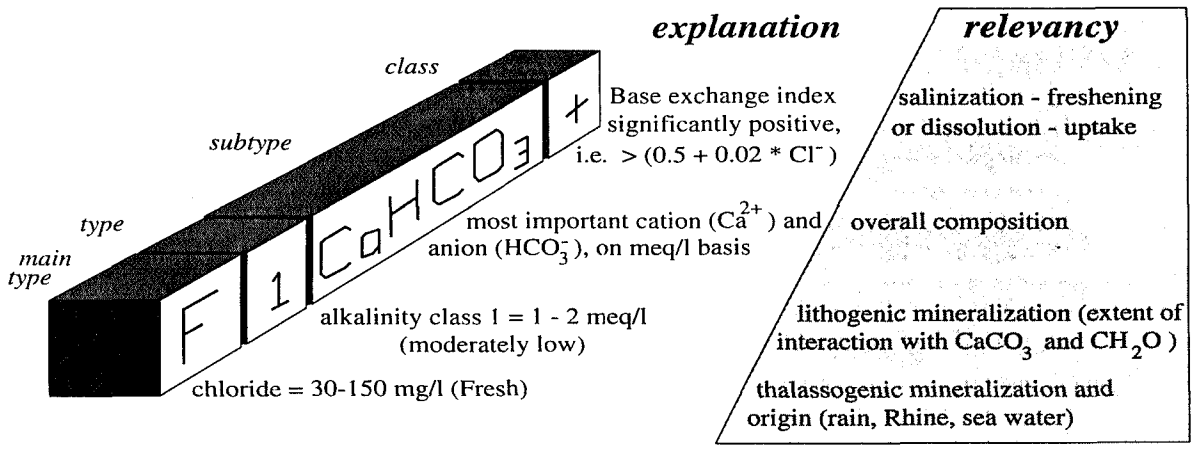

Fig. 2.9. The hydrochemical classification system of water types by Stuyfzand (1989g), with its coding in 9 positions. The example is called "a fresh, moderately low alkalinity, calciumbicarbonate water with a positive base exchange index (BEX)". The latter is often due to intrusion of fresh water into a previously saltier subsoil. In that case the term "freshened" is applicable. Note that the "+" in the code does not indicate the charge of a $CaHCO_3$ complex.

Heerebout, 1970) and to the potential use of water to man (Hem, 1970). The boundaries in Table 2.5 are based on criteria discussed in Stuyfzand (1986b).

Types, by alkalinity
Each main type is subdivided into 9 types according to alkalinity (Table 2.6), which in many situations is an excellent reaction progress variable or, in other words, a measure for the lithogenic mineralization of water (Eriksson, 1987; chapter 7 of this thesis). For most natural waters with 4.5 < pH < 9.5 alkalinity equals HCO_3^- + CO_3^{2-} in meq/l, of which CO_3^{2-} can be ignored if pH < 8.2.

TABLE 2.6 Subdivision of main types into 9 types according to alkalinity, on a 2log-basis.

type	alkalinity as HCO_3^-		
	meq/l	mg/l	@
very low	< ½	< 31	*
low	½ - 1	31 - 61	0
moderately low	1 - 2	61 -122	1
moderate	2 - 4	122 -244	2
moderately high	4 - 8	244 -488	3
high	8 - 16	488 -976	4
very high	16 - 32	976-1953	5
rather extreme	32 - 64	1953-3905	6
extreme	> 64	> 3905	7

@ : code = ^{2}log(upper boundary of type, in meq/l), if upper boundary ≥ 1 meq/l; else code = *

Subtypes, by the dominating cation and anion
The most important cation and anion determine the subtype in a way that bears a resemblance to the traditional assignment of a chemical water type. The direct preponderance in the ionic balance is decisive there, whereas here the support of geohydrochemical family members is included (Fig.2.10). Further details including a computer program, are given by Stuyfzand (1989g). This grouping method has the important advantage that otherwise very rare water types like $AlSO_4$, KNO_3, HCl, HNO_3, MgCl and $MgHCO_3$ water, are assigned much earlier than when a single ion is required to occupy >50% of the sum of cations or anions in meq/l for nomination. On the other hand the assignment is more substantial by the geo-
hydrochemical family support, than when the dominant cation and anion (without family support) are chosen on the basis of the highest share in the sum of cations and anions in meq/l. Both aspects considerably increase the diagnostic value of the classification system.

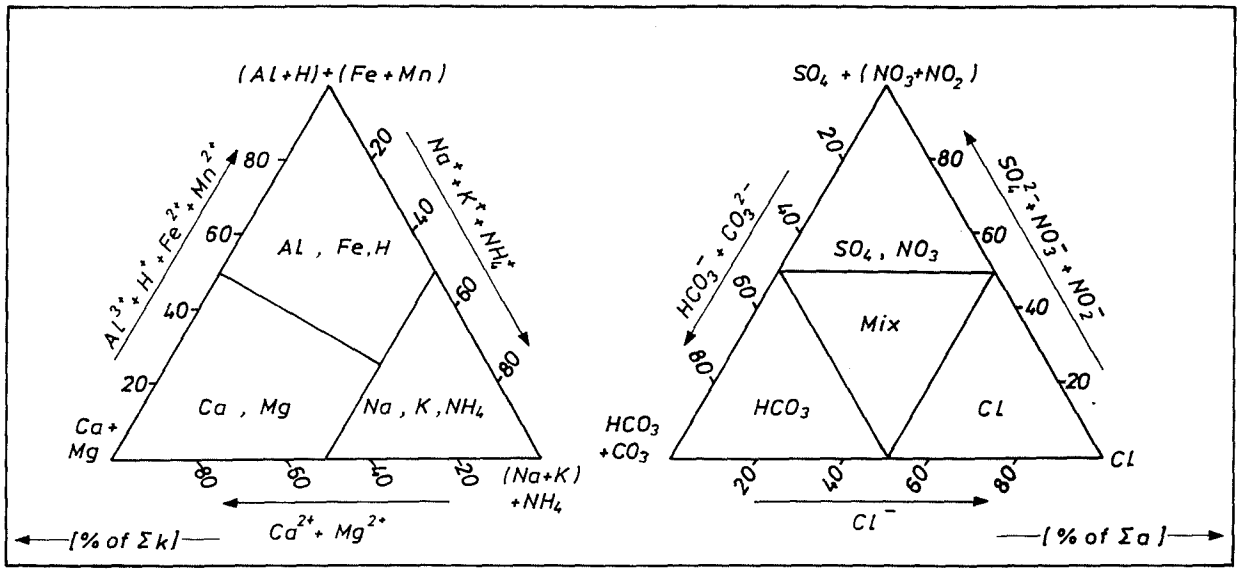

FIG. 2.10. Subdivision of types into subtypes on the basis of the proportional share of main constituents in the sum of the cations (left) and anions (right), both in meq/l. First of all, the dominating hydrochemical family at the vertices of each triangle is determined, for instance the [Al+H+Fe+Mn]- and [SO_4+NO_3+NO_2]-families. Then the strongest couple within a family (in brackets at the vertices) is selected, where present, for example [Al+H]. If now Al is superior to H^+, and SO_4^{2-} superior to [NO_3+NO_2] the subtype becomes "$AlSO_4$". The strongest family members discovered to date are placed in the appropriate fields inside the triangles.

Methods nominating all ions contributing for >20% to the sum of cations or anions in meq/l, like the method of Szczukariew & Priklonski (cited in Jankowski & Jacobson, 1989), result in long codes and too many subtypes. The "Mix" anion family is introduced here, and refers to water in which no anion family makes up more than 50% of the sum of the anions.

Classes, by the base exchange index

Finally, each subtype is subdivided into 3 classes (Table 2.7) according to a base exchange index introduced by Stuyfzand (1985a) : BEX (Base EXchange in meq/l), which is the meq-sum of the typically marine cations Na^+, K^+ and Mg^{2+}, corrected for a contribution of sea salt :

$$BEX = [Na^+ + K^+ + Mg^{2+}]measured - 1.0716 \cdot Cl^- \quad (2.11)$$

In previous publications BEX has also been called the "marine cations excess". The factor 1.0716 is equal to $\{[Na^+ + K^+ + Mg^{2+}]/Cl^-\}$ in meq/l for mean ocean water (Riley & Skirrow, 1975). It is hereby assumed that : (1) all the Cl^- ions are of marine origin (Eriksson, 1952); (2) fractionation of the main constituents of sea water during spray formation can be ignored (Duce & Hoffman, 1976), so that the atmospheric Na^+, K^+ and Mg^{2+} contribution to fresh water exclusively depends on the Cl^- concentration; (3) Cl^- behaves conservatively; and (4) the three marine cations exchange together for calcium (see Eq.2.12).

For sea salt corrections of the individual ions, reference is made to section 5.3.2.

The class boundaries at ± (0.5 + 0.02 Cl^-) are somewhat untightened with respect to previous publications (± ½√Cl^-). They form a threshold against (a) the expected errors in chemical analyses, which adequately offset one another in the ionic balance, and (b) waters without base exchange, that derive from silica terrains where more Na^+, K^+ and Mg^{2+} ions than Cl^- ions dissolve by chemical breakdown of silicates. Under specific conditions it can be more convenient to incorporate this release or the release of Mg^{2+} from dolomite, into BEX by direct subtraction.

If the ionic balance of water is not sufficiently in equilibrium, it is pointless calculating BEX and nothing should be printed at the ultimate position of the watertype code in Fig.2.9. To check this, 1.5(Σk - Σa) is used as a measure of ionic imbalance in the manner indicated in Table 2.7.

Other base exchange indices were proposed by Versluys (1916, 1931), Schoeller (1934) and Delecourt (1941), respectively: $Na^+/\{Na^+ + Ca^{2+} + Mg^{2+}\}$, $\{Cl^- - (Na^+ + K^+)\}/Cl^-$ and $(Na^+ + K^+)/Cl^-$, all on a meq/l basis. The most important objections to these indices are : (1) being a ratio, they do not provide information on the amount of ions exchanged; (2) being without thresholds, an imbalance by other causes is too easily attained. Ocean water already exhibits a positive Schoeller-ratio, for instance; and (3) also Mg^{2+} is generally involved in the base exchange, often on the same side as Na^+ and K^+ (see below).

TABLE 2.7 Subdivision of subtypes into 3 classes, based on the Base EXchange index BEX, which is defined as the meq-sum of $Na^+ + K^+ + Mg^{2+}$ corrected for a contribution of sea salt (Eq.2.11). Under ideal conditions (no other sources and sinks for Na^+, K^+ and Mg^{2+}), which prevail in The Netherlands, BEX constitutes an unambiguous cation exchange parameter. Where other sources or sinks of the typically marine cations are suspected, BEX requires another interpretation and can be neutrally called the marine cations surplus or deficit. Σk, Σa = sum of cations and anions, respectively.

Class code	base exchange index (BEX)	INTERPRETATION if base exchange only process	INTERPRETATION if other processes relevant	conditions for BEX, in meq/l
	negative	salinized	marine cations deficit	$< -(0.5 + 0.02\ Cl^-)$ and $< 1.5(\Sigma k - \Sigma a)$
	zero	without base exch.@	marine cations equilibrium	$> -(0.5 + 0.02\ Cl^-)$ and $< +(0.5 + 0.02\ Cl^-)$ and **
	positive	freshened	marine cations surplus	$> +(0.5 + 0.02\ Cl^-)$ and $> 1.5(\Sigma k - \Sigma a)$

** = $| BEX + \frac{(\Sigma k - \Sigma a)}{|\Sigma k - \Sigma a|} . (0.5 + 0.02\ Cl^-) | > 1.5 |\Sigma k - \Sigma a|$

@ = indicative of adequate flushing with water of constant composition, or syngenesis with and stagnant in porous medium.

BEX and the intrusion of salt and fresh water
The intrusion of fresh or salt groundwater generally leads to the following, simplified empiric cation exchange process, not only in The Netherlands (Stuyfzand, 1986b), but also elsewhere in the world with comparable conditions, as can be deduced from data regarding the UK (for instance Howard & Lloyd, 1983), the USA (Chapelle & Knobel, 1983), Belgium (Lebbe & Walraevens, 1989) and Indonesia (Kloosterman, 1989) :

$$aCa^{2+} + [bNa, cK, dMg]\cdot Exchanger \leftrightarrows [aCa]\cdot Exchanger + bNa^{+} + cK^{+} + dMg^{2+} \quad (2.12)$$

with the meq-balance : $2a = b + c + 2d$.

Upon fresh water intrusion, Ca^{2+} expels, grosso modo, the previously adsorbed, marine cations Na^{+}, K^{+} and Mg^{2+} from the exchanger. The above exchange reaction proceeds from left to right then, leading to a significantly positive BEX (or $[Na^{+}+K^{+}+Mg^{2+}]$surplus). The reverse reaction occurs during salt water intrusion. This means that BEX constitutes an excellent base exchange index indeed, on the condition that other sources and sinks of Na^{+}, K^{+}, Mg^{2+} and Cl^{-} can be neglected. Such ideal conditions prevail in the upper aquifer systems of The Netherlands, which are largely composed of quartz sands without evaporites and dolomites. A significantly positive BEX can then be translated into freshening (displacement of saltier groundwater), a significantly negative BEX into salinization (displacement of fresher groundwater), and a BEX = 0 into adequate flushing with water of constant composition.

Na^{+}, K^{+} and Mg^{2+} do not always ad- or desorb simultaneously during salt or fresh water intrusion respectively (section 7.7), which means that their individual concentrations corrected for a contribution of sea salt, do not always indicate the right direction of displacement. Minor quantities of NH_4^{+}, Fe, Mn, Li^{+} and Sr^{2+} are involved in the exchange reaction as well (chapter 7). Deviations from reaction 2.12 are quantitatively insufficient, however, to influence the sign of BEX (Fig.7.25), which pleads for this classification parameter as an indicator of salinization or freshening.

Complications
The following cases demand a quite different interpretation of BEX : (1) dissolution of minerals which contain Na, K and/or Mg, such as dolomite, albite, olivine and serpentinite; (2) mineralization of biomass; (3) leaching, dissolution or drainage/infiltration of fertilizers or manure; (4) dolomitization and other transformations of minerals; (5) new formation (synthesis) of minerals comprising Na, K and/or Mg; (6) synthesis of biomass; and (7) significant atmospheric deposition of anthropogenic or volcanic Cl_2 gas.

The complications 1-3 can produce a significant marine cation surplus (positive BEX), whereas the complications 4-7 may cause a significant marine cation deficit (negative BEX). In The Netherlands, complication 3 can be encountered on a large scale in the upper tens of metres of groundwater in agricultural areas, whereas the complications 2 and 6 are generally limited to the upper metres of groundwater in woodlands.

Another type of complication is formed by a decrease of BEX from high to lower positive values downgradient, where surface water with an original marine cation surplus (positive BEX) recharges, artificially or spontaneously, an aquifer system which previously exhibited marine cation equilibrium (no base exchange). The change is explained by exchange of the excess $(Na^{+}+K^{+}+Mg^{2+})$ for Ca^{2+}. When in this case the intruding surface water also contains more Cl^{-}, then the "salt" water intrusion is accompanied, after the breakthrough of Cl^{-}, by a paradoxal freshened facies! (section 4.4.5 and 4.4.6).

2.4.2 The redox index

The mobility, dissolution, degradation and toxicity of inorganic and organic substances in or in contact with the water phase, strongly depend on the redox potential (E_H) of the system (Stumm & Morgan, 1981). The direct measurement of E_H with electrodes runs into practical problems, however, and is handicapped by unreliable results (Lindberg & Runnells, 1984) or difficulties in quantitative thermodynamic interpretation (Peiffer et al., 1992). Unfortunately the same holds for its calculation from a single redox pair like Fe^{2+}/Fe^{3+} (Lindberg & Runnells, 1984; Kölling, 1986; Barcelona et al.,1989).

Therefore the suggestion by Stumm (1984) was followed to deduce the redox level from all redox sensitive main components of water, i.e. O_2, NO_3^{-}, SO_4^{2-}, Fe, Mn, CH_4 and eventually H_2S. This led to the semi-empirical redox indexing as outlined in Fig.2.11 and Table 2.8. The following 7 redox levels are discerned there, in order of decreasing concentrations of oxidants :

0 : *oxic*, with O_2 concentrations close to (super)saturation;
1 : *penoxic*, with nearly ("pene" in Latin) as high O_2 concentrations as in the oxic environment. By definition, the O_2 concentration must be in between 1 mg/l and 90% saturation. Nitrate is stable in this environment;

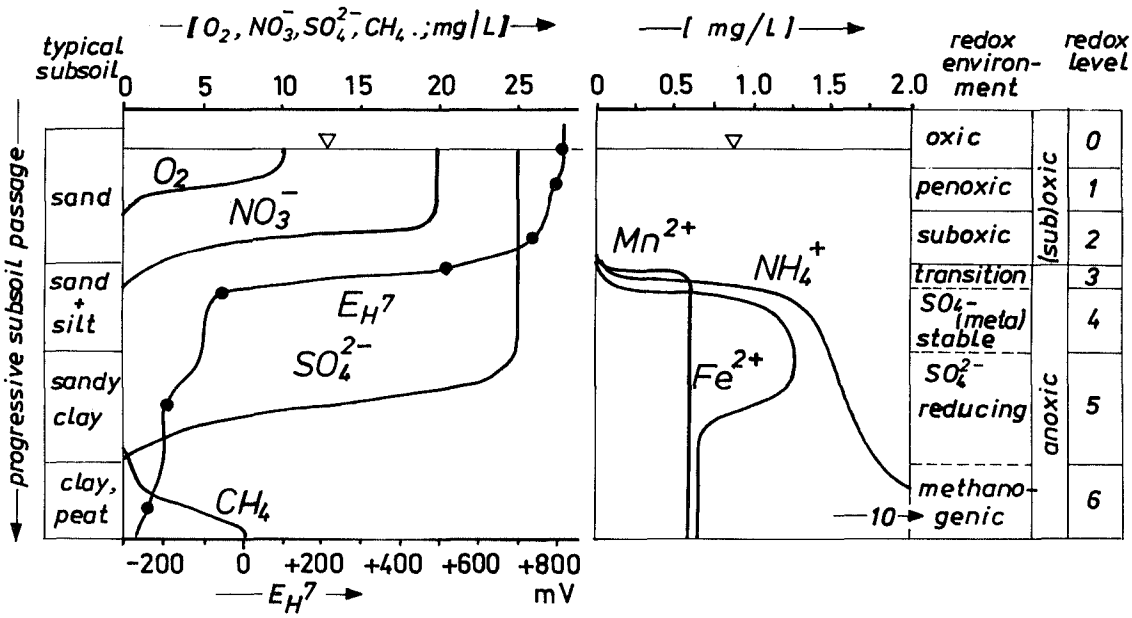

FIG. 2.11 General classification of the natural redox environment, based on the presence or absence of the main redox components of water : O_2, NO_3^-, SO_4^{2-}, Fe, Mn and CH_4. Subsoil passage is assumed as piston flow in a system, which is closed from the atmosphere and progressively richer in organic carbon. The initial O_2, NO_3^- and SO_4^{2-} concentrations (at the water table) are set at 10, 20 and 25 mg/l, respectively. The indicative redox potentials at pH = 7 (E_H7) are derived from Stumm & Morgan (1981).

TABLE 2.8 Practical criteria for the determination of the redox index (modified after Stuyfzand, 1988a). For each level the relevant redox reaction and indicative redox potential at pH = 7 (E_H7) are given. Concentrations in mg/l. Equilibrium O_2 concentrations with the atmosphere at sea level ($\{O_2\}$sat.) according to Peters (1984).

redox level	redox environment	reaction	equation	typical E_{H7} (mV)	determination with complete analysis (mg/l)							ditto, incomplete analysis (mg/l)				assoc redox level	typical E_H (mV) meas. @
					O_2	NO_3^-	Mn^{2+}	Fe^{2+}	SO_4^{2-}	H_2S	CH_4	NO_3^-	Mn^{2+}	Fe^{2+}	SO_4^{2-}		
0	oxic	oxygen (super)saturation	$O_2(g)+H_2O$ <--> $O_2 + H_2O$	+820	A	(≥1)	(<0.1)	(<0.1)	(C)	(-)	(<0.2)	≥1	(<0.1)	(<0.1)	(C)		
	penoxic	aerobic respiration	O_2+CH_2O <--> $CO_2 + H_2O$	+800	B	(≥1)	(<0.1)	(<0.1)	(C)	(-)	(<0.2)	≥1	(<0.1)	(<0.1)	(C)	0-2	+330 à +430
1	suboxic	denitrification	NO_3^- + 5/4CH_2O <--> ½N_2 + ¼CO_2 + HCO_3^- + ¾H_2O	+740	<1	≥1	(<0.1)	(<0.1)	(C)	(-)	(<0.2)	≥1	(<0.1)	(<0.1)	(C)		
3	transition	reduction manganese	MnO_2+ ½CH_2O + 3/2CO_2 + ½H_2O <--> Mn^{2+} + 2HCO_3^-	+520	(<0.5)	<0.5	≥0.1	<0.1		(-)	(<0.2)	<0.5	≥0.1	<0.1			
4	SO_4 (meta) stable	reduction iron	$Fe(OH)_3$+½CH_2O+¼CO_2 --> Fe^{2+} + 2HCO_3^- + ¾H_2O	- 50	(<0.5)	<0.5		≥0.1			(<0.5)	<0.5		≥0.1	C		≤ +160
5	SO_4-reducing	reduction sulphate	SO_4^{2-} + 2CH_2O -->HS + H_2O + CO_2 + HCO_3^-	-190	(<0.5)	<0.5			D		(<1)	<0.5			D		
5	fermenting	methanogenesis	CO_2 + 2CH_2O --> CH_4 + 2CO_2 + 2H_2O	-240	(<0.5)	<0.5			E		(≥1)	<0.5			E		

+ , - = yes/no H_2S-smell in field ; . = no requirement ; ( ) = if unknown, no requirement ; A = $O_2 \geq 0.9\{O_2\}$sat. ; B = $1 \leq O_2 < 0.9\{O_2\}$sat. ; C = $SO_4^{2-} \geq 0.9\{SO_4\}_o$; D = $0.1\{SO_4\}_o < SO_4^{2-} < 0.9\{SO_4\}_o$ if $Cl^- \leq 300$ mg/l and else $0.5\{SO_4\}_o \leq SO_4^{2-} < 0.9\{SO_4\}_o$; E = $SO_4^{2-} \leq 0.1\{SO_4\}_o$ or $SO_4^{2-} \leq 3$, if $Cl^- \leq 300$ mg/l and else $SO_4^{2-} < 0.5\{SO_4\}_o$; $\{O_2\}$sat. = $14.594 - 0.4\,t + 0.0085\,t^2 - 97 \cdot 10^{-6}\,t^3 - 10^{-5} \cdot (16.35 + 0.008\,t^2 - 5.32/t) \cdot Cl$, in which t = temp. in °C and Cl^- = chloride in mg/l ; $\{SO_4\}_o$ = original SO_4^{2-}-concentration in mg/l; @ : where pH = 7-9.

2 : *suboxic*, with O_2 levels clearly below (in Latin "sub") oxic, i.e. < 1 mg/l and $NO_3^- \geq 1$ mg. In this zone nitrate is either stabile or nearly completely reduced;
3 : *transition*, from the above zones containing oxygen and with a relatively high E_H (typically > +300 mV in pH7-9 groundwater) to the zones without (in Latin "an") oxygen and with a low E_H (typically < +160 mV in pH7-9 groundwaters). By definition, there must be a characteristic rise in Mn concentration (> 0.1 mg/l) without accompanying Fe-increase. The sharp E_H-decrease in the transition zone is also called the redoxcline;
4 : *sulphate (meta)stable*, with O_2 and NO_3^- concentrations below detection and with approximately conservative behaviour of sulphate. More than 90% of the sulphate concentration entering this zone, has to be conserved, which allows only a very weak sulphate reduction. In this anoxic zone Fe^{2+} generally attains it highest concentrations, due to the characteristic reduction of iron(III) hydroxides and the lack of iron sulphide precipitation;
5 : *sulphate reducing*, with 10-90% sulphate reduction in case of fresh water ($Cl^- \leq 300$ mg/l) and 10-50% in case of brackish and salt water (Cl^- >300 mg/l). The reason for discrimination between fresh and brackish/salt water is given below in the discussion on prohibitive and non-prohibitive mixing. The water generally exhibits a penetrating H_2S smell, notwithstanding very low concentrations due to FeS and FeS_2 formation; and
6 : *methanogenic*, if >50-90% of the sulphate has been reduced (percentage depending on salinity, see above). Methane concentrations typically exceed 1 mg/l, whereas the concentrations of NH_4^+, PO_4^{3-}, HCO_3^- and fulvic acids may reach high and even extreme levels.

In case of chemical desinfection, Cl_2 or O_3 and side products need to be considered, and the redox level can become *hyperoxic*. The basic assumptions pertaining to the above discerned 7 redox levels are : (a) the successive oxidation of organic material in a closed system by oxidants decreasing in strength, as shown in Fig.2.11; and (b) the absence of mixing of water from different redox environments.

Prohibitive and non-prohibitive mixing
In two cases the above mentioned mixing is not prohibitive in the assignment of the redox level. The first case concerns penoxic and suboxic water (levels 1 and 2, respectively). Nitrate may be reduced to N_2 in aquatic systems even if the bulk phase still contains some dissolved oxygen (Stumm & Morgan, 1981). The reduction takes place then in anoxic micro-environments, for instance a buried rootlet in aeolian sand, and the N_2 released is not reoxidized in the penoxic bulk phase because of strong kinetic hindrance. Hence, the boundary between penoxic and suboxic is not coupled to the first signs of denitrification, but has been set at an O_2 level of 0.5 mg/l, which Huisman & Van Haaren (1965) consider as a true boundary condition for general denitrification.

The second case concerns groundwater showing significant but incomplete sulphate reduction (level 5). Such water, which is generally brackish or salt (for instance sample 19B.109 in Table 4.2), is often observed to contain rather high amounts of dissolved methane as well (> 1 mg/l), although Martens & Berner (1974) concluded, that methane is formed only when >90% of the original sulphate has been reduced. Contrary to the first case, methane is considered capable to reduce sulphate sufficiently fast (Rudd & Taylor, 1980; Reeburgh, 1982; Iversen & Jørgensen, 1985; Hovland et al., 1987). The coexistence therefore may point at the release of methane from deep anoxic micro-environments to a less reduced bulk solution, in combination with either a slow reaction rate (perhaps due to low temperatures, lack of the right micro-organisms or quickly rising gas bubbles, that contain the CH_4) or fast mixing in consequence of sampling.

Hence, methane concentrations are not considered decisive, instead the amount of sulphate reduction is used to discriminate between level 5 and 6. The 90% of Martens & Berner (1974) is used for fresh water only ($Cl^- \leq 300$ mg/l), whereas 50% results in a better separation for brackish and salt waters. It should be stated, that sulphate may remain metastable in specific deep anoxic environments (redox level 5-6), for instance due to the lack of the right bacteria and nutrients (Edmunds et al., 1984). In that case the redox environment (sulphate (meta)stable) cannot be translated into the right redox potential or level. Sulphate metastable conditions probably do not prevail in the upper 40 metres of the aquifer system in the coastal area of the Western Netherlands, however, because Von Wolzogen-Kühr (1922) isolated the right bacteria (*Microspira desulphuricans*) up to a depth of 35 m-MSL and demonstrated the occurrence of sulphate reduction also in deep sand samples.

In all other cases mixing or re-aeration is diagnosed and coded "m" when notwithstanding sufficient data, no redox level can be assigned following the criteria listed in Table 2.8. Low levels of nitrate in otherwise perfectly anoxic or deep anoxic water, should be considered critically, and neglected if oxidation of ammonium may have occurred in the sample container or upon filtration.

The same holds for low sulphate concentrations as measured with ICP-AES in deep anoxic water high in DOC, because organic sulphur is included in that particular analysis of sulphate (Edwards et al., 1992). Data in Noij et al. (1989) and Edwards et al. (1992) suggest that 0.02-0.12 mg SO_4^{2-}/l may derive from each mg DOC/l.

Incomplete analyses, the original sulphate concentration, E_H-measured, Fe and Mn

Incomplete analyses may be circumvented as indicated in Table 2.8. Knowledge of the original NO_3^- and SO_4^{2-} content is even more essential then. The original SO_4^{2-} concentration, $\{SO_4\}_o$, can be deduced from Cl^-, when a strong correlation between SO_4^{2-} and Cl^- is known or can be assumed, like in case of river Rhine water (see Eq.7.3). In coastal plains without dissolution of gypsum and without oxidation of sulphide minerals, a linear mixing formula for shallow dune water and coastal sea water may suffice.

For brackish water (Cl^- > 300 mg/l), composed of dune and North Sea water, it can be approximated by : $\{SO_4\}_o$ = 20 + 0.14 Cl^- (mg/l). Sulphate reduction (level 5) is concluded then, when the SO_4^{2-} concentration falls in between 10 and 90% of $\{SO_4\}_o$ for fresh water and in between 10 and 50% for brackish and salt water.

Notwithstanding their drawbacks, redox measurements may still assist in the determination of the redox level (Fig.2.11) : values in between +330 and +420 mV generally correspond with oxygenated waters (level 0-1) and values ≤ +160 mV indicate depletion of oxygen and nitrate (Edmunds et al., 1987), i.e. level ≥ 3. Note that redox measurements do not correspond with the thermodynamic equilibrium redox potential for standard conditions at pH = 7 and 25°C (E_H7 in Fig.2.11).

Values of pH below 4 and contents of dissolved organic carbon exceeding about 10 mg/l may tackle the assumption, that concentrations of total Fe or Mn superior to 0.1 mg/l point at anoxic conditions. The same problem is observed, where Fe(III)-containing colloids dissolve in acidified samples. And on the other hand, Fe and Mn concentrations below 0.1 mg/l have also been observed in deep anoxic groundwaters, where the precipitation of manganous siderite is postulated (section 7.3.4, zone VIII, Miscellania). Nitrate and sulphate are therefore better indicators of redox conditions than total iron.

2.4.3 A water quality index

Pollution Indices (PI) and Water Quality Indices (WQI) were developed for surface waters mainly, like the PI by Prati et al. (1971) and Dresscher & Van der Mark (1976), and the WQI by Horton (1965), Brown et al. (1970) and Heinonen & Herve (1987). The choice should depend on the purpose of the map, as there probably does not exist a single quality index satisfying all needs. Hence, two indices are proposed here, one as an example of a widely applicable PI, which may serve general purposes, and another as an example of a simple WQI for restricted purposes.

The pollution index POLIN

This index is based on six quality aspects (A-F, Table 2.9), each having an equal weighting factor and a logarithmic character :

A : pH, as a measure of either acidification or eutrophication (in the bloom period);

B : (NO_3^- + SO_4^c) as a measure of the effects of an excessive application of fertilizers or manure spreading. Sulphate is corrected for both a contribution of sea salt and the transformation of 1 mole NO_3^-/l into 0.67 moles SO_4^{2-}/l upon its oxidation of pyrite. The factor 0.67 may also be considered as a weighting factor of SO_4^{2-} relative to NO_3^-, which approximates the NO_3^-/SO_4^{2-}-ratio in several water standards.

High levels of (NO_3^-+SO_4^c) may also indicate: (1) the oxidation of sulphide minerals due to lowered water tables or due to mining activities; (2) degeneration or dying off of vegetation; (3) strong air pollution with NO_x, SO_2 and/or $(NH_4)SO_4$; and (4) dissolution of gypsum;

C : the sum of several trace elements in unfiltered samples, as a measure of pollution with environmental hazardous heavy metals and As. A weighting factor is included in accordance with their respective drinking water standards for the European Community (EC, 1980);

D : the sum of halogenated hydrocarbons adsorbable to activated coal (AOCl), expressed as chloride, as a measure of pollution by mobile xenobiotics with a general occurrence (Feenstra, 1987). It should be realized, however, that high concentrations of chloride (> 750 mg/l), iodide (> 60 µg I^-/l or > 80 µg IO_3^-/l) and sulphide (> 5 mg/l) may bias the AOCl determination (Grøn, 1990). In specific cases other organic sum parameters, like the sum of PAHs or selected pesticides, may constitute an alternative to AOCl;

E : the amount of colony forming units on a feed substrate, of thermotolerant *Escherichia coli* bacteria (44°C), as a measure of faecal contamination; and

F : tritium activity as a measure of pollution with radioactive substances and as an indirect measure of potential modern pollution with organic microcontaminants (Noordsij et al., 1985).

Fresh groundwater without tritium originated before 1955 (Fig.5.7 and 7.19) and has a fair

chance to exhibit low concentrations of organic micropollutants for two reasons : (1) the emissions of mobile, environmental pollutants strongly increased after 1955; and (2) the older groundwater experienced more losses due to a longer period of degradation and more sorption along a longer flow path in the subsoil.

Originally, the scores of A-F were classified and averaged (Stuyfzand, 1988a). A numerical solution is presented in Tabel 2.9. A minimum number of quality aspects (A-F) and trace elements is required for the calculation of POLIN. In the case of groundwater, *E. coli* counts can generally be assumed zero. And when tritium is lower than 8 T.U., AOCl often approaches to zero as well (Noordsij et al., 1985).

The nomenclature and examples of discerned pollution classes are given in Table 2.10. Not always environmental pollution will be the cause of raised values for the index. For instance, a very high pH is typical for playa lakes or lakes with a natural, high degree of eutrophication; very low pH values may be due to dissolved vulcanic gases; high SO_4^{2-} concentrations corrected for a sea salt contribution are also typical for gypsiferous terrains or terrains containing pyrite oxidizing naturally; and high NO_3^- contents are also caused by leaching of guano deposits or by N_2-fixation by among others *Hippophaë rhamnoides* (dune shrub). Nevertheless, for human consumption those waters may be considered unfit, a criterium that has been included in the rating of pollution classes and in the weighting of several constituents considered.

TABLE 2.10 Nomenclature of discerned pollution classes, with examples from The Netherlands. The pollution index POLIN has a logarithmic character.

name of pollution class	POLIN	example
unpolluted	<0.5	>100 years old, deep dune water
quasi unpolluted	0.5 - 1.5	shallow, calcareous dune water
slightly polluted	1.5 - 2.5	shallow, acid dune water
moderately polluted	2.5 - 3.5	bulk precipitation anno 1980
polluted	3.5 - 4.5	pretreated Rhine water for AR
heavily polluted	4.5 - 5.5	river Rhine during low flow
very heavily polluted	5.5 - 6.5	municipal sewage effluent
extremely polluted	>6.5	industrial sewage effluent

AR = Artificial Recharge.

TABLE 2.9 Determination of the logarithmic pollution index POLIN, by averaging the quality aspects A through F. These parameters are a measure of, respectively : acidification or eutrophication (A), the excessive application of fertilizers or manure spreading (B), pollution with environmental hazardous heavy metals and As (C), pollution by mobile xenobiotics with a general occurrence (D), faecal contamination (E), and pollution with radio-active substances as well as mobile xenobiotics (F). N = number of quality aspects participating in calculation (minimum = 2).

$$POLIN = \frac{(A + B + C + D + E + F)}{(N - \frac{N}{6})} \qquad \text{with:}$$

$$A = 1.333 \cdot |pH - 7|$$

$$B = \frac{\ln\{10 \cdot [\frac{NO_3^-}{62} + SO_4^c]\}}{ln2} \qquad \text{[mg/l]}$$

, *if* $\{\ \} > 1$, *otherwise* $B = 0$

, *where* $SO_4^c = 0.67 \cdot (\frac{SO_4^{2-}}{96.06} - \frac{0.0232 \cdot Cl^-}{35.453})$ *if* > 0, *otherwise* $SO_4^c = 0$

$$C = \frac{1}{\ln 2} \cdot \ln\{\frac{[\frac{As+Cr+Ni+Pb}{50} + \frac{Cu+Zn}{100} + \frac{Cd}{5} + Hg]}{0.01n}\} \qquad \text{[µg/l]}$$

, *if* $\{\ \} > 1$, *otherwise* $C = 0$; n = *number of elements considered (minimum of* $n = 3$*)*

$$D = \frac{\ln(AOCl)}{\ln 2} \quad \text{, if } AOCl > 1, \text{ otherwise } D = 0 \qquad \text{[µg Cl/l]}$$

$$E = \log(E.\ Coli) + 1 \quad \text{, if } E.\ Coli > 0.1, \text{ otherwise } E = 0 \qquad \text{[counts/l]}$$

$$F = \frac{\ln(tritium)}{\ln 2} - 3 \quad \text{, if tritium} > 8\,TU, \text{ otherwise } F = 0 \qquad \text{[TU]}$$

The water quality index "Phosphate"
A WQI for restricted hydro-ecological purposes may be exclusively based on the concentration of orthophosphate, which is considered as one of the most critical eutrophying nutrients for moist or wet ecosystems (Vollenweider, 1976; Schindler, 1981). Nitrogen ions (mainly NO_3^- and NH_4^+) are considered less critical, as a deficit can be made up through N_2-fixation by blue-green algae, cyano-bacteria or symbiotic bacteria. Hence, a simple division into 8 mappable phosphate classes may be employed as an index to denote eutrophication hazards (Table 2.11).

It should be realized, however, that low phosphate levels do not necessarily indicate a low trophic status of the system, either because this means that all dissolved phosphate had been taken up by algae during a bloom period, or because high flow velocities may still result in a high nutrient load (Vollenweider, 1976; Van Dijk, 1984). On the other hand high phosphate concentrations may not be synonymous to hypertrophic conditions, as such groundwater may remain beyond the reach of the rooting system, or other environmental conditions like temperature, pH or E_H may be unfavourable to growth.

TABLE 2.11 Orthophosphate as a water quality index denoting eutrophication hazards.

class		PO_4^{3-} as:		
no	name	mg PO_4^{3-}/l	mg PO_4–P/l	µmol P/l
0	atrophic	< 0.004	< 0.001	< 0.04
1	oligotrophic	0.004 – 0.016	0.001 – 0.005	0.04 – 0.16
2	mesotrophic	0.016 – 0.063	0.005 – 0.020	0.16 – 0.66
3	slightly eutrophic	0.063 – 0.25	0.020 – 0.082	0.66 – 2.63
4	eutrophic	0.25 – 1.0	0.082 – 0.33	2.63 – 10.5
5	strongly eutrophic	1.0 – 4	0.33 – 1.31	10.5 – 42.1
6	hypertrophic	4 – 16	1.31 – 5.23	42.1 – 168
7	strongly hypertrophic	16 – 64	5.23 – 20.9	168 – 674
8	extremely hypertrophic	> 64	> 20.9	> 674

2.4.4 A relevant mineral saturation index

Calculation of the degree of saturation of a water sample with respect to various solid phases may yield insight into the reactive phases contributing to the dissolved ions, and into the further quality evolution when the liquid phase is assumed to reach equilibrium with the solid phases. Saturation indices may thus form a reaction progress variable in the examination of evolutionary trends in water quality data, both in space and time. Although it is uncommon that only one mineral dictates the solution's composition, one mineral is generally observed to have a dominant effect. The saturation index for that particular mineral is considered as an interesting facies parameter for mapping purposes.

The saturation index of water with a particular mineral m (SI_m) is generally defined as :

$$SI_m = \log \frac{IAP}{K_s} \qquad (2.13)$$

where : IAP = Ion Activity Product of the mineral-water reaction in the sample [on a mol/kg water basis]; and K_s = the corresponding solubility product in pure water, adjusted to the temperature and pressure of the sample.

This means that water with a $SI_m = 0$, is in equilibrium with the mineral considered, with a $SI_m < 0$ it is undersaturated and will tend to dissolve the mineral when it is met, and with a $SI_m > 0$ it is oversaturated and may deposit the mineral.

An excellent computer program, that iteratively calculates for a multicomponent, natural system the speciation of dissolved inorganic substances in water and many mineral equilibria, is WATEQF presented by Plummer et al. (1976), or the further extended PC-version WATEQX by Van Gaans (1989). Of course, the resulting SIs must be interpreted with great care, for at least four reasons : (a) analytical errors (especially pH and E_H) or mixing phenomena may bias the calculation; (b) organic complexes are generally ignored; (c) minerals in nature are never pure whereas they are assumed so in the program; and (d) kinetics may be so slow that equilibrium will never be attained like in case of the chronic supersaturation of most groundwaters with respect to quartz.

In this context one of the most relevant and scientifically best established mineral equilibria will be discussed as an example, namely that for calcite (SI_c). An accurate, relatively simple, direct calculation was presented by Stuyfzand (1989b). It requires fewer data (temperature, EC, pH, alkalinity as HCO_3^-, Ca^{2+} and SO_4^{2-}) and can easily operate on simple programmable pocket calculators.

Analytical problems may easily cause deviations from calcite equilibrium yielding SI_c values of 0 ± 0.3, and waters with an SI_c in between -0.3 and -1.0 may reside in aquifers which still contain a large amount of carbonate rock. It was found empirically, that below -1.0 virtually no calcite traces are present any more (Edmunds & Kinniburgh, 1986; Stuyfzand et al., 1992b), with direct consequences for Ca^{2+}, alkalinity and pH in the water phase. The facies may therefore be described as acid when $SI_c < -1.0$, and otherwise as calcareous. A further subdivision is presented in Table 2.12, including additional hydrochemical data as observed in the coastal dune aquifer system of the Western Netherlands.

TABLE 2.12 Division into five calcite saturation classes, with some additional hydrochemical information as observed in the coastal aquifer system of the Western Netherlands.

level code	name	SI_c	accompanying composition in dunes: pH	Alkalinity as mg HCO_3^-/l	Ca^{2+} mg/l	Al µg/l	examples in coastal area
v	very agressive	< -5.0	< 5	<5	<10	>700	groundw. 0-3 m-MGL in NDD
a	agressive	-3.0 to -5.0	5-6	5-30	2-50	50-700	groundw. 3-5 m-MGL in NDD
l	slightly agressive	-1.0 to -3.0	6-6.7	30-61	15-200	<100	groundw. 5-15m-MGL in NDD
c	equilibrium	-1.0 to +0.3	6.7-8	61-1000	4-2500	<20	all groundwaters in SDD
p	supersaturated	> +0.3	> 7.5	30-3500	4-450	1-300	surface and groundw. with **

** = high concentrations of Mg^{2+}, PO_4^{3-} and DOC; NDD = Northern Dune District (decalcified); SDD = Southern Dune District (calcareous); MGL = Mean Groundwater Level.

2.4.5 Water temperature

In areas with thermal waters at shallow depth or in surveys, that extend down to considerable depths, temperature may constitute a major process variable, contributing significantly to the spatial variability in hydrochemistry. Water temperature determines to a large degree the kinetics and level of mineralization of biomass and the kinetics and level of mineral dissolution or precipitation. The most spectacular example is SiO_2 that may even be used as a geothermometer for hot springs (Fournier & Potter, 1982). It seems justifiable therefore to include this physical parameter in the description of the hydrochemical facies.

Temperature is subdivided in Table 2.13 into 6 classes according to several criteria : human sensorial observation, microbiological activity and solubility of quartz and calcite.

TABLE 2.13 Nomenclature and characteristics of discerned temperature classes.

temperature class (°C)	name	characteristics: Microbiological activity (%) A	B	solubility quartz* (mg/l)	solubility calcite@ (mg/l)
< 5	very cold	0	<10	<5.7	>243
5 - 15	cold	0-10	10- 50	5.7 - 8.0	243-212
15 - 25	mild	10-60	50-100	8.0 - 10.8	212-183
25 - 40	warm	60-90	100- 80	10.8 - 16.4	183-144
40 - 80	hot	90- 0	80- 0	16.4 - 42.0	144- 72
> 80	very hot	0	0	>42.0	<72

A = percent degradation of phenanthrene after 5 days, by a natural microbial population (dr. G. Schraa, LU Wageningen The Netherlands, pers. comm.): B = relative, general microbial reaction rate (Paul & Clarke, 1987); * = SiO_2 in pure water according to Siever (1962); @ = $CaCO_3$ in rain water with pH = 4.42, Ca^{2+} = 0.85 and NH_4^+ = 1.0 mg/l, after complete nitrification and equilibration with calcite under fixed P_{CO2}= 1 kPa (= 0.01 atm).

2.5 Identifying the origin

In his classical papers White (1957a & b) discerned marine, meteoric, connate, metamorphic, magmatic, volcanic, plutonic and juvenile water. The marine and meteoric waters are essentially cyclic, they are still recharged by sea and rain water respectively, as opposed to connate waters. He defined connate water as "fossil interstitial water of unmetamorphosed sediments and extrusive volcanic rocks and water that has been driven from them", for instance by compaction and cleavage respectively. The inclusion of migrated water in this definition, constitutes in fact a contradiction with the term connate (Latin for originated together with). Nevertheless we adhere, for the sake of simplicity, to White's definition.

A further subdivision is useful, especially regarding the meteoric waters forming the best potable category, and waters of mixed origin :

1. Autochthonous meteoric water : rain water before and after infiltration in situ, without long transport beyond the local geomorphological unit, like dune water occurring as surface and groundwater within coastal dunes;
2. Allochthonous meteoric water, as opposed to the former. River Rhine water largely stemming from the Alps, in its fluvial plain in The Netherlands is a nice example; and
3. Estuarine and lagoonal waters as the result of mixing between allochthonous meteoric and marine waters in their respective environment.

Tracers

Where contrasts in chemistry between waters of different origin are strong and well understood, the origin can be easily identified by analysis of one or a few specific tracers. Chloride or ^{18}O should suffice for instance to distinguish fresh coastal dune waters from intruded ocean water. The distinction between marine and connate salt water

may require, however, the whole hydrochemical fingerprint, composed of the analysis of all main constituents, several trace elements and natural isotopes (White, 1957a,b; Mazor, 1976; Lloyd et al., 1982; Stuyfzand, 1989f, 1992). Obviously the more complex the history of a water body by mixing before or after burial and by all kinds of mutilating hydrogeochemical processes, the more difficult will be the diagnosis, like in case of the deep and very saline groundwaters throughout the Canadian Shield (Fritz, 1983). In such complex situations the position of the sample in both space and time should be considered as well (Fig.2.12). A hydrological systems analysis is indispensable thereby. It must be stressed however, that a hydrosome will not always coincide with a groundwater flow system, due to instationarity of earth processes. For instance, when coastal dunes are formed in a formerly marine environment, the expanding, fresh dune water flow system will discharge saline waters first.

The ideal tracer for origin detection, possesses characteristic concentration levels for waters of dissimilar origin, which are sufficiently large for analytical and statistical detection, and such a tracer should behave conservatively upon subsoil passage. Conservative behaviour can generally be assumed for the anions Cl^- and Br^-, constituents of the watermolecule (^2H, ^3H, and ^{18}O), inert gases (He, Ar) and persistent organic micropollutants with a very low octanol-water distribution coefficient (for instance Na-dikegulac). When chemical equilibrium can be assumed in a flow system, also nonconservative constituents may form valuable labels, like B, F^-, I, K^+, Li^+, Mg^{2+}, Mo, Sr^{2+} and V. Trace elements without charge like $B(OH)_3$ and trace anions, which do not easily substitute for ubiquitous OH-groups of the solid phases are to be preferred then.

Tracers for origin detection may be obtained before infiltration (meteoric and marine waters), by chemical reaction with the porous medium (juvenile water) or both (all other waters, including meteoric and marine water). Tracers can also be classified on the basis of the anthropogenic contribution to their concentration, as natural, semi-natural and wholly anthropogenic. In river Rhine water for instance, these are ^{18}O, Cl^- and bisdichloro(iso)propylethers, respectively (Stuyfzand, 1985b; see also section 4.4.6).

The thermal anomaly of water may form a powerful physical tracer. Autochthonous meteoric, allochthonous meteoric and volcanic or related groundwaters may be diagnosed by their orthothermal, hypo- or slightly hyperthermal and strongly hyperthermal character, respectively. Hypothermal is defined here, somewhat different from Schoeller (1962), as more than 2°C below, orthothermal as equal ± 2°C to, slightly hyperthermal as 2-4°C above, moderately hyperthermal as 4-20°C above and strongly hyperthermal as >20°C above mean shallow groundwater temperature for a similar (nonthermal) area where groundwater is recharged by local precipitation.

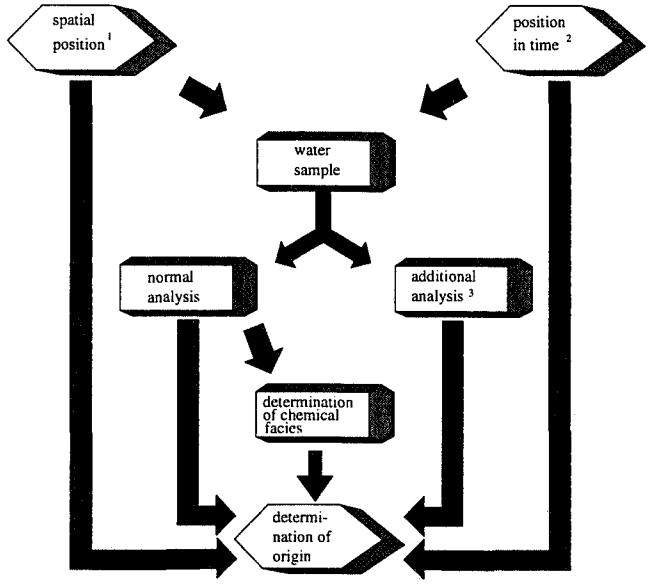

FIG. 2.12 Determination of the origin of groundwater. In easy cases the analysis of major constituents may suffice, whereas very difficult situations require all the bits of information indicated. 1 = geology, hydrology, vegetation cover, geomorphological unit, distance to coast, etc.; 2 = environmental pollution, decalcification time, changes in land-use (historical developments in area); 3 = TEs, isotopes, organic micropollutants.

2.6 Mapping

When the hydrosome and facies have been determined for all selected water samples, maps and cross sections showing their areal distribution can be constructed. However, first an inventory of all available variation of facies and hydrosomes should be made, the purpose of the map must be defined, the scale and desired or admissable complexity of the map should be harmonised and all discernable entities on the map should be given a logical code. For a clear description of map and cross sections an unambiguous nomenclature has to be introduced.

Some useful associations and differentiations are suggested in order to reduce or raise the complexity. Examples of concise codings and nomenclature are given for coastal plains.

2.6.1 Suggestions for associations and differentiations

The theoretical maximum number of 8640 water types, 7 redox levels, 8 pollution classes, 5 calcite saturation levels and 6 temperature classes, already lead to the absurd total maximum number of about $14.5 \cdot 10^6$ facies. Although perhaps 99% of these combinations does not exist in nature, and only 1% of the remaining combinations may be encountered in a regional survey, associations will generally be needed anyhow.

In coastal districts with strongly diverging salinities, the association of the main types G + g + F + f into F (fresh) and B + b into B (brackish) in the chemical water type, can be advantageous. For large scale studies where the hydrological interpretation is of major concern, the omission of all subtypes within the chemical water type and of all redox, pollution, saturation and temperature levels may be profitable (Stuyfzand, 1989d). The discerned redox, pollution and calcite saturation levels may be aggregated into much less facies parameters, as illustrated in Table 2.15. And for instance the temperature may be cut out, when differences are small or irrelevant enough for neglect.

A further differentiation may be needed for specific purposes or in case of extremely monotonous situations. This can be done easily by a more subtle subdivision of the pollution and saturation indices and temperature, by adding more chlorinity levels to the chemical water type, by subdivision of the anion Mix in the chemical water type into MiF, MiC, MiS, MiN and MiCl when F^-, (HCO_3^-+ CO_3^{2-}), SO_4^{2-}, (NO_3^-+NO_2^-), and Cl^- respectively are to some degree predominant, or even by adding new facies parameters, like a radiation index.

2.6.2 Coding and nomenclature

The hydrosome together with its facies may be coded in full fig as follows : C_{abcd}-water type, where "C" stands for an alphabetical character in capital denoting the hydrosome, "abcd" stands for four aggregated, undercast, alphabetical characters which indicate the redox, pollution, mineral saturation and temperature level respectively, and the water type follows the coding in Fig.2.9.

On complicated maps with many hydrosomes and facies, such a coding may result in too long codes. Each code should be converted then into a specific colour and number, which is described in the legend. Each hydrosome should be depicted in a specific basic colour, and the different facies within in gradations of that colour (see Enclosures 4, 5 and 7).

The alphabetical characters preferably form a logical abbreviation of what they stand for. For coastal plains this may result in the coding of discerned hydrosomes according to Table 2.14. Suggestions for the coding of hydrochemical facies parameters (abcd + water type) are given in Table 2.15, with options for few and many associations.

TABLE 2.14 Major hydrosomes, defined as water bodies with a specific origin, in coastal plains, in alphabetical order. Local = autochthonous; remote = allochthonous.

HYDROSOME code	name	origin	main recharge mechanism
A	Artificial recharge	remote meteoric	pumps
B	river Banks	local meteoric	precipitation
C	Creek ridge	local meteoric	precipitation
D	coastal Dunes	local meteoric	precipitation
E	Estuary	rm + cyclic marine	floods, pumps
F	Fluvial	remote meteoric	floods, pumps
J	Juvenile	juvenile	heat
L	Lagoon & tidal flats	cyclic marine + rm	density, pumps
M	connate Marine	connate marine	none, compaction
P	marsh land & Polder	local & remote meteoric	pumps, precip.
S	open Sea, near shore	cyclic marine	density, pumps
U	remote Uplands	remote meteoric	precipitation
V	Vulcanic, magmatic and plutonic	meteoric &/or connate	precip., heat

rm = remote meteoric.

Not all facies-parameters are needed in the code to describe the facies. For example, "D_{ceno}" or more concisely "D" with option II in Table 2.15, denotes calcareous (c), nonpolluted (n), (sub)oxic (o) coastal Dune water without base exchange (e), in case of a coastal district (Table 2.14). The omission of "ceno" is allowed, because c, e, n and o are considered the standard state of a hydrosome and are opposite to a, f+s, p and r, respectively. The nomenclature may be structured as follows : abcd-water type-C, for instance a calcareous, cold, nonpolluted, anoxic F_2CaHCO_3+ dune water. The water type may be described as indicated in Fig.2.9.

2.7 Interpretation

The final objective of a HYFA consists of the interpretation of the areal distribution of hydrosomes and their facies, in terms of (ground) water

TABLE 2.15 Hydrochemical facies parameters, in alphabetical order for two situations : Option I when few associations are needed and Option II when more associations are required.

OPTION I : FEW ASSOCIATIONS			OPTION II : MANY ASSOCIATIONS		
Hydrochemical facies-parameter code	name	specification	Hydrochemical facies-parameter code	name	specification
CHEMICAL WATERTYPE			*BASE EXCHANGE INDEX (BEX)*		*see Table 2.7*
**	all watertypes	Fig.2.9	(e)	equilibrated	without base exchange
			f	freshened	with positive BEX
			s	salinized	with negative BEX
REDOX LEVEL		*see Table 2.8*	*REDOX LEVEL*		*see Table 2.8*
d	deep anoxic	redox index = 6	d	deep anoxic	redox index = 6
(o)	(sub)oxic	redox index = 0-2	(o)	(sub)oxic	redox index = 0-2
r	reduced (anoxic)	redox index = 3-5	r	reduced (anoxic)	redox index = 3-5
m	mixed	redox index = 0-6	m	mixed	redox index = 0-6
POLLUTION INDEX (POLIN)		*see Table 2.10*	*POLLUTION INDEX (POLIN)*		*see Table 2.10*
(n)	natural (nonpolluted)	polin < 1.5	(n)	natural (nonpolluted)	polin < 2.5
p	polluted	polin = 1.5 - 3.5	p	polluted	polin ≥ 2.5
t	strongly polluted	polin = > 3.5	-	-	-
CALCITE SATURATION LEVEL (SI_c)		*see Table 2.12*	*CALCITE SATURATION INDEX (SI_c)*		*see Table 2.12*
a	acid (agressive)	$-5.0 < SI_c < -1.0$	a	acid (agressive)	$SI_c < -1.0$
(c)	calcareous (saturated)	$SI_c > -1.0$	(c)	calcareous	$SI_c > -1.0$
v	very acid (agressive)	$SI_c < -5.0$	-	-	-
TEMPERATURE LEVEL		*see Table 2.13*			
(f)	cold	temp. < 15 C			
h	hot	temp. > 40 °C			
w	warm	temp. = 15 - 40 °C			

( ) = as the standard facies omissible in the code, in order to promote a short code and to nominate special features only;
SI = log {ion activity product/ solubility constant}. ** = for coding see Fig.2.9.

flow patterns, the life cycle of each hydrosome within the dynamic geological and geomorphological boundary conditions, the geochemical structure of the subsoil and the record of water table fluctuations, land-use and environmental pollution.

This is largely accomplished by detection and description of all major evolution or succession lines in the facies in the direction of groundwater flow within and beyond each hydrosome. Examples of evolution lines are :

(a) from polluted with for instance SO_4^{2-}, NO_3^-, K^+, heavy metals, tritium and persistent xenobiotics, to unpolluted through : (a) elimination processes as filtration, sorption, breakdown and decay; and (b) increasing age of the water beyond the onset of industrialization (Edmunds et al., 1982; Stuyfzand, 1984e);

(b) from acid to basic by weathering reactions with the porous medium, which consume acids like H_2CO_3, H_2SO_4 and HNO_3 and produce alkalinity (Eriksson, 1987);

(c) from oxic to anoxic-methanogenic by continued oxidation of organic matter in a system closed from the atmosphere, which results in a typical order of consumption of oxidants in water (Froelich et al., 1979; Champ et al., 1979; Edmunds et al., 1984), and to an increase of alkalinity (Stuyfzand, 1989a);

(d) from equilibrium between the exchange complex of the porous medium and its interstitial water to ion exchange and side reactions, during and long after displacement by another hydrosome (Versluys, 1931; Stuyfzand, 1985a), as happens when fresh dune water intrudes into a coastal aquifer containing salt water;

(e) from fresh to brackish or saline by hydrodynamic dispersion across the boundaries of adjacent hydrosomes, or by continued evapotranspiration. The latter may lead to evolution lines described by Hardie & Eugster (1978) and Jankowski & Jacobson (1989); and

(f) from low pressure and temperatures to elevated ones, by way of downward migration of groundwater or by subsidence of its porous medium. The reverse may also occur as happens with water squeezed out of compacting clay, and a combination of both is observed where meteoric water first descends in a recharge area and subsequently ascends in a discharge zone. An increase of temperature and pressure may lead to K^+- and Mg^{2+}-

depletion by recrystallization of compacting clay (Muller, 1967), to hyperfiltration (Freeze & Cherry, 1979) and an increase of overall salinity by a reduction of the cation exchange capacity (Schoeller, 1955).
Ascending groundwater may become supersaturated with respect to minerals and dissolved gases like CH_4. The resulting supersaturation with respect to methane may lead to the formation of gas bubbles which may rise much faster than the groundwater. The upward migrating bubbles may be blocked by an aquitard, under which they accumulate and form a gas reserve.

The evolution lines mentioned above, determine together the normal hydrochemical evolution of a hydrosome in the direction of groundwater flow, which leads to a typical, prograde facies sequence or chain. A retrograde facies evolution is defined, in analogy with the concept of retrograde metamorphism in petrology, as the return to a lower grade of evolution in the direction of (ground) water flow. Examples are the re-aeration of anoxic groundwater in a seepage lake, and renewed pollution by mixing with injected waste water. Another complicated evolution pattern arises, when sanitation measures have their effect on groundwater, such that pollution first increases and subsequently decreases downgradient. This may be called an inversion.

An important factor in the chemical evolution is the order of encounter of various minerals or rocks by the water as it moves through the flow system (Freeze & Cherry, 1979; Palmer & Cherry, 1985). On a fixed position within the system the normal evolution in the course of time is the reverse of the above mentioned evolution lines (a), (b), (c) and (d), in consequence of breakthrough and leaching.

2.8 Concluding remarks

The hydrochemical facies analysis proposed, integrates five fundamental facies parameters into a more holistic view on hydrochemistry in a spatial perspective. The purpose is to diagnose and map the major factors accounting for variations in hydrochemistry, the results of environmental pollution and hydrological disturbances, like artificial recharge, included.

Certainly, many data are required for an optimal performance and this may not always be feasible. The whole procedure is made flexible enough to cope with lacking data, for instance by calculation of the redox and pollution index from a reduced set of chemical analyses, by association of several redox levels and by cutting out facies parameters for which data are missing. On the other hand, further differentiations in monotonous situations can be easily adopted. And in specific cases it may be advantageous to modify the facies parameters or add new ones.

The method has been applied to a coastal plain, as shown in chapter 4, but should be applicable, after modifications, to every hydrochemical district, like inland fluvial plains, inland carbonate terrains, volcanic areas, intramontane depressions without discharge and alpine crystalline areas.

Chapter 3

HYDROLOGY OF THE COASTAL AREA

Abstract

Hydrological maps are presented to a scale 1:200,000 for the 900 km^2 area north of the Old Rhine. They comprise : historical developments during the past 500 years; the areal distribution of important aquitards; isohypses of the reconstructed mean phreatic level around 1850 AD and of actual piezometric heads at different depths; the drawdown of the water table in the period 1850-1981; the depth to the actual position of the fresh - brackish water interface; the rise of this interface in the period 1910-1981; and the areal distribution of groundwater flow systems.

The mean natural groundwater recharge is established for common dune vegetation covers, by using lysimetric data mainly. It varies from -0.58 to 0 m/y for reeds to +0.62 m/y for bare dune sand, respectively. Annual variations and mean seasonal fluctuations are shown as well.

Analytical solutions for the calculation of the size and shape of a fresh dune water lens, its time of formation and dispersion across the fresh-salt water interface are passed in review. The solution for the time of formation by Brakel (1968) and Bakker (1981) is extended to account for anisotropy. Dispersion across an undisturbed interface in 1910 AD could be modelled with a transversal dispersivity of 0.0025 - 0.01 m.

Geological information, palaeogeographical maps and intensive measurements since about 1850 AD have been used, to reconstruct the palaeohydrology of the area. The Holocene transgressions salinized the whole aquifer system at least to the top of the marine Maassluis Formation at 100-270 m-MSL, which still contains connate water.

Changes of the groundwater table with respect to mean sea level, reveal that a deep freshening prevailed in the dunes from 3800 BC till 1600 AD in connection with enlargement of the coastal barriers. The fresh dune water pocket contracted in the period 1853-1957 in its western and central parts, for at least 7 reasons.

The phreatic level consequently dropped by 2-8 m, the fresh-salt water interface rose by 5-100 m and the mean thickness of the brackish transition zone in the central dune area expanded in the vicinity of the drawdown centres from 10-20 to 20-50 m. Large scale artificial recharge since about 1955 and a reduced abstraction of dune groundwater led to a fast return of high groundwater levels, and to a pushing back of the fresh-salt water interface.

A shallow freshening dominated in the former peat bogs from 3000 BC till about 900 AD. The central parts of the deep polders resalinized since 900 AD due to drainage and peat digging, Dunkirke transgressions and the reclamation of lakes in the period 1550-1875 AD. The area in between the younger dunes and the deep polders experienced, after this reclamation, a gradual supersession of shallow, old dune water pockets by polder water (river Rhine water mixed with local rain water), and water from the younger dunes.

The actual situation is described by the presence of 5 groundwater flow systems, in order of decreasing size and age : the supraregional Maassluis system, which is driven mainly by compaction of finegrained Lower-Pleistocene and Tertiary marine deposits and man-made drainage; the North Sea system, that has been strongly activated since the reclamation of lakes; various dune systems of different order; several man-made polder systems; and diverse man-made artificial recharge systems.

Field evidence and an analytical solution are presented for the so-called rain water lenses on top of infiltrated surface water that migrated laterally. Again, a transversal dispersivity of 0.0025 m yields the best prediction for the transition zone between both groundwaters. Most dune lakes exhibit an essential in- and output through exfiltration of groundwater and infiltration respectively, and therefore belong to the flow-through type. Effects of these lakes on the groundwater flow pattern and fluctuations of the phreatic level are demonstrated.

3.1 General

The hydrology of coastal dune aquifers is extremely intriguing because of the occurrence of fresh water floating on salt water, and the relative ease to observe this groundwater with piezometers or miniscreens reaching depths rarely superior to 150 m. Small scale variations in groundwater depth, natural recharge and aquifer characteristics, the occurrence of flow-through lakes and the possibility to visualize flow-patterns using natural hydrochemistry as a label, all add to the perception of coastal dunes as a field laboratory for

groundwater hydrologists. But, there is also a need for research, at least in the densely populated Western Netherlands, with its many conflicting interests and environmental problems (sections 1.2 and 1.3).

The physiographical, historical and hydrological information contained in this chapter, constitutes the first and second step in the logical sequence for regional chemical surveys of groundwater (Fig.1.7), as presented in this thesis. The main focus of regional hydrology is directed on the 900 km^2 area north of the mouth of the Old Rhine (Fig.3.1), for which hydrological and hydrochemical maps to a scale of 1 to 50,000 were prepared by Stuyfzand (1985a, 1987d, 1988b, 1989a). Those four separate sheets are united here into one sheet to a scale of 1 to 200,000. This necessitated updates due to new data and due to the mapping of angles and strips of land not investigated before.

The area to the south of the Old Rhine has been included here in longitudinal sections, the description of the palaeohydrology and historical hydrology, the description of flow systems (without maps) and the general topic on flow-through lakes, for which it offered the best field data. Reference is made to Stuyfzand et al. (1993) for 1:50,000 hydrogeological maps of a large part of the coastal area to the south of the Old Rhine.

3.2 Physiography

3.2.1 Situation and climate

The coastal area is situated at the edge of the Rhine delta, in the southeastern marginal part of the North Sea basin (Fig.1.1 and 3.1), approximately at 4°30' E and 52°30' N. The area is about 100 km long and 15 km across, with an altitude of 6 m-MSL to 52 m+MSL (Mean Sea Level).

The climate can be defined as a temperate, rainy, marine, west coast climate. According to Köppen's classification system it is a Cfb climate, which indicates a temperate rainy climate, moist in all seasons and with the warmest month under 22°C. The predominant wind blows from the southwest, mean air temperature is about 10°C and mean annual precipitation amounts to 0.82 m. For further details reference is made to section 3.4 (precipitation and evaporation), KNMI (1972, 1983) and Bakker et al. (1979). The latter also summarized microclimatological studies in the coastal dunes.

3.2.2 Geology

Geological formations to a depth of 250 m-MSL are of main interest to this study. They consist of unconsolidated sediments of Quarternary age, deposited in (peri)marine, aeolian, paludal, fluvial and even glacial environments. A longitudinal geological section over the studied area is shown in Fig.3.2, and a cross section just south of Zandvoort aan Zee in Fig.3.3. The areal distribution of four Quarternary key formations in The Netherlands is shown in Fig.3.4. The approximate age and sedimentary environment of the discerned formations are indicated in Fig.3.5.

Pleistocene deposits are present in the whole area below 8 to 35 m-MSL, to a depth of more than 300 m-MSL in the south and more than 450 m-MSL in the north. Its lower parts clearly dip northward, at least in between Monster and IJmuiden, under an angle averaging 0.1° (Fig.3.2). The top of the marine Maassluis Formation is found therefore at about 120 m-MSL below The Hague and at 230-290 m-MSL north of the North Sea Canal (Fig.3.4A). Saalian glacial deposits like boulder clay, glaciolimnic varved clays and coarse grained sandr deposits are present in between 30 and 105 m-MSL, north of Hillegom and south of Alkmaar (Fig.3.4B and Enclosure 1.4). The borders of the discerned Haarlem and Wijk aan Zee glacial basins are composed of buried ice-pushed ridges, reflecting the south-westernmost margin of the inland-icesheet in The Netherlands. Continental Eemian deposits have been found in the glacial basin of Wijk aan Zee (Breeuwer et al., 1979), whereas marine Eemian deposits occur over a large northern and a smaller southern part of the study area (Fig.3.4C). Fine grained deposits of the Eemian, Drente and Kedichem Formations, which constitute important aquitards, have been mapped on Enclosure 1.4, with subdivision according to their stratigraphical position and sedimentary environment (section 3.3).

The Holocene Westland Formation is composed of coastal barrier and coastal plain deposits and covers Weichselian or Eemian deposits everywhere (Fig.3.4D). The formation is further differentiated in Fig.3.6. The areal extent of fine-grained and peaty, Calais deposits, which constitute important aquitards at or near the base of the Holocene (section 3.3), is shown in Enclosure 1.3.

A concise description of the geological history is integrated in section 3.6, dealing with the hydrological evolution of the study area till 1850 AD. Detailed descriptions are given by Jelgersma et al. (1970), Zagwijn & Van Staalduinen (1975), Zagwijn (1985, 1986), Westerhoff et al. (1987), Roep et al. (1991) and Van der Valk (1992).

Sections and year of reclamation of lakes

Pumping stations and artificial recharge

Topographical names referred to in text

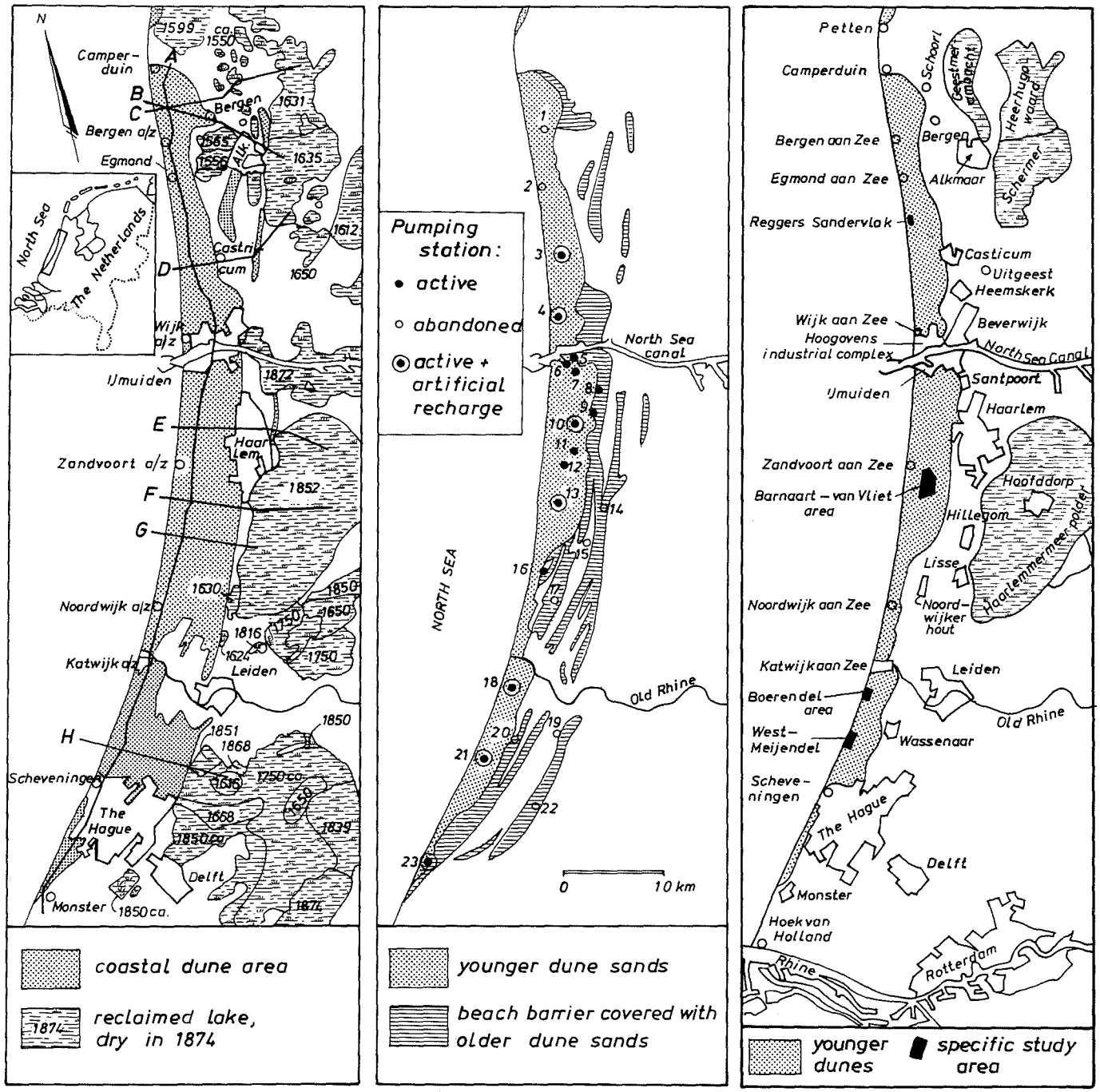

FIG. 3.1 Situation of the coastal area of the Western Netherlands, with several landscape units, pumping stations for drinking water supply (with data in Table 3.6) and the position of longitudinal and cross sections.

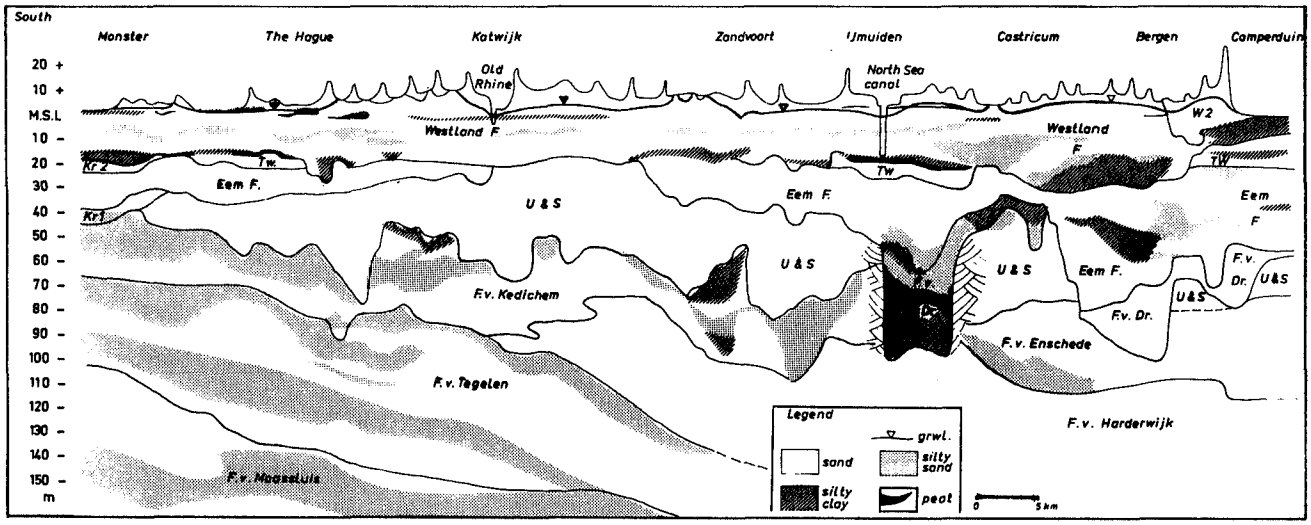

FIG. 3.2 Longitudinal, geological section over the coastal dunes from Camperduin to Monster (A in Fig.3.1), with formations whose age and sedimentary environment are indicated in Fig.3.5. W2 = Westland Formation poor in lime; Tw = Twente F.; U&S = Urk and Sterksel F.; F.v.Dr. = Drente F.; F = Formation.

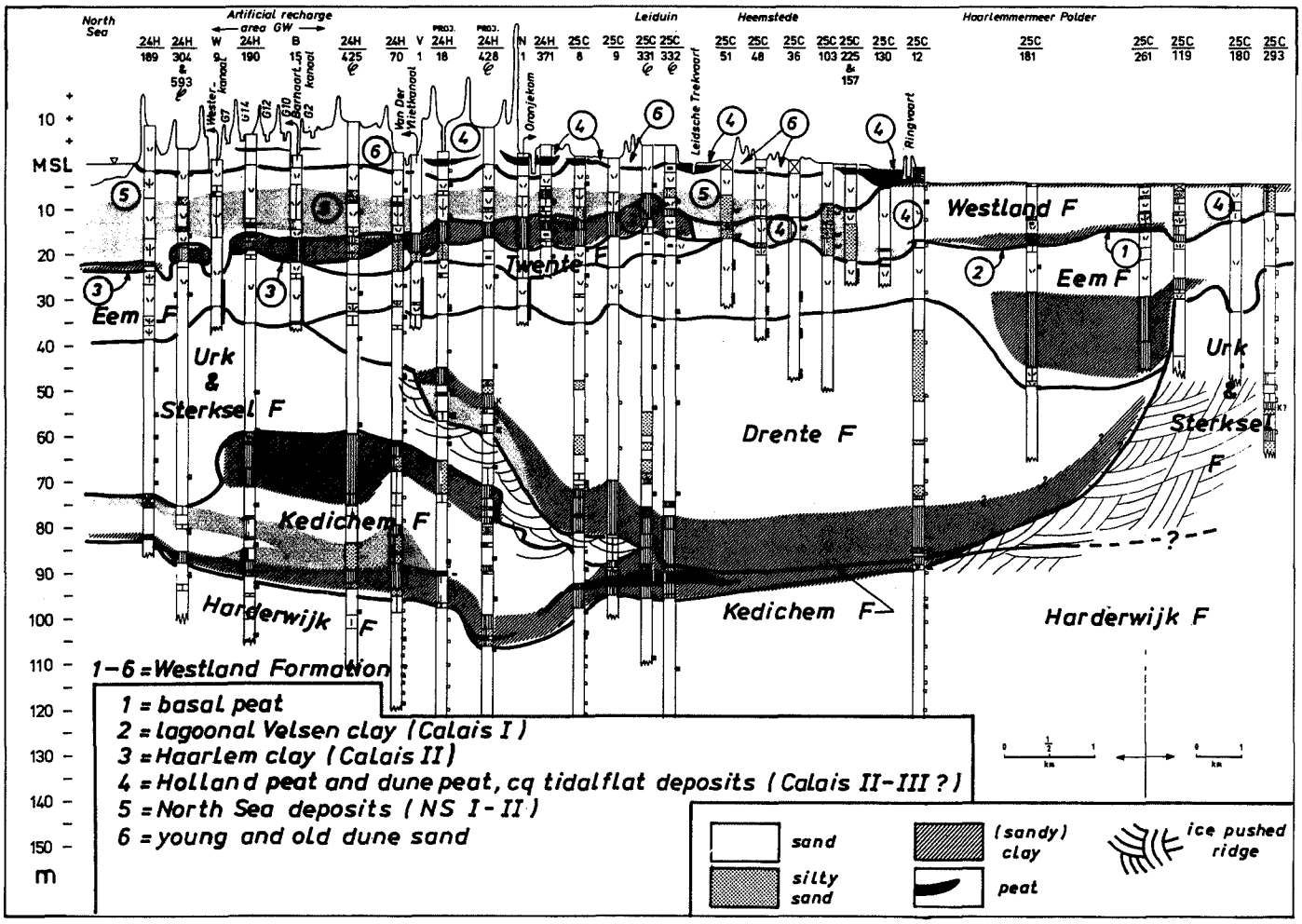

FIG. 3.3 Geological cross section over the coastal dunes 2 km south of Zandvoort aan Zee (F in Fig.3.1).

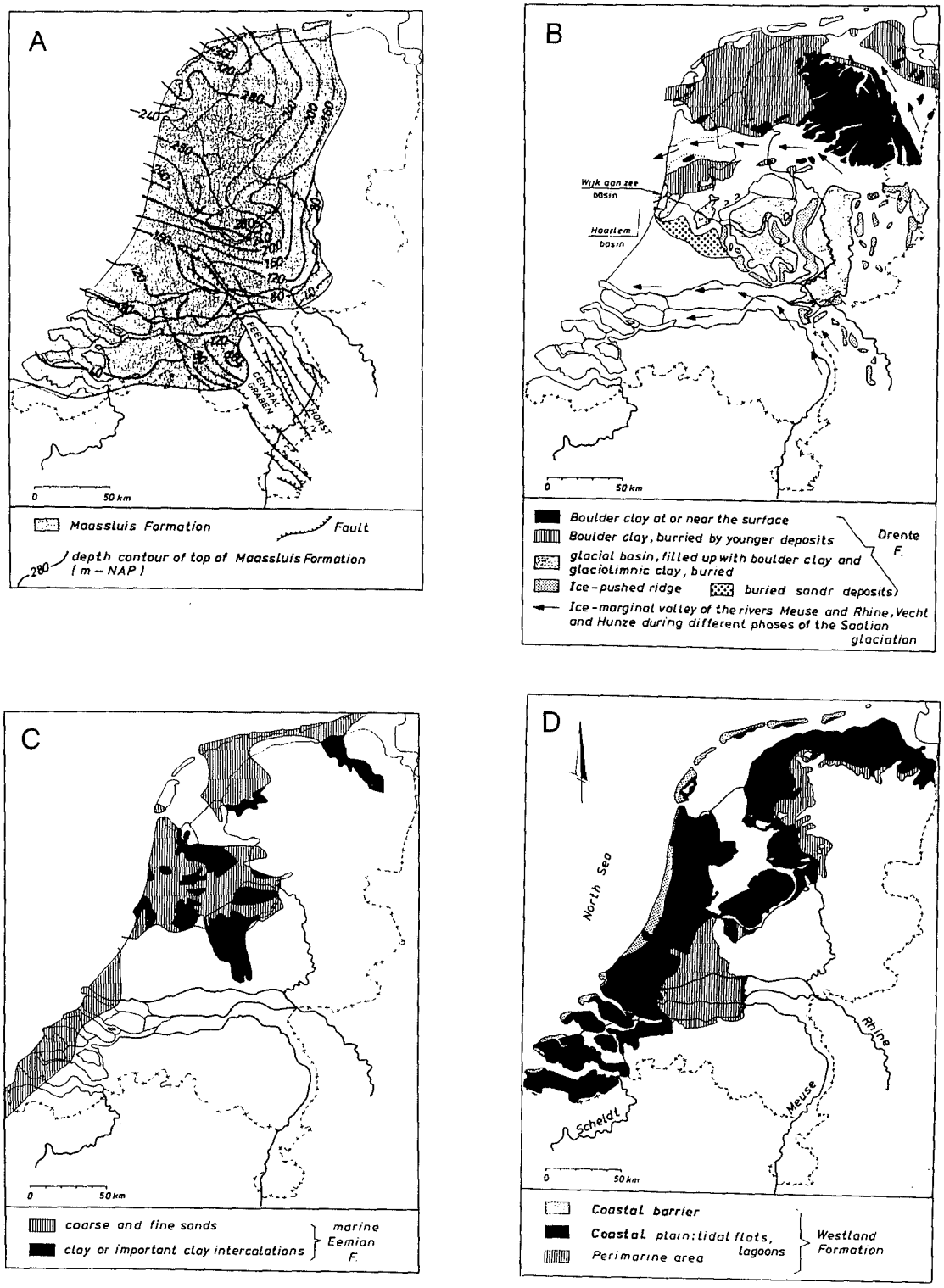

FIG. 3.4 Areal distribution of four geological key formations of Quarternary age in The Netherlands; A : the marine Maassluis Formation (simplified after Zagwijn & Van Staalduinen, 1975), with modifications for North Holland after Breeuwer et al., 1979); B : the glacial Drente Formation with preserved glacial phenomena caused by the Saalian glaciation (simplified after Zagwijn & Van Staalduinen, 1975), with modifications for North Holland after Breeuwer et al., 1979); C : the marine Eemian Formation (after Jelgersma, 1976, with modifications for North Holland after Breeuwer et al., 1979; and own interpretation); and D : the (peri)marine Westland Formation with depositional environments during the younger Holocene (modified after Hageman, 1969, and Zagwijn & Van Staalduinen, 1975).

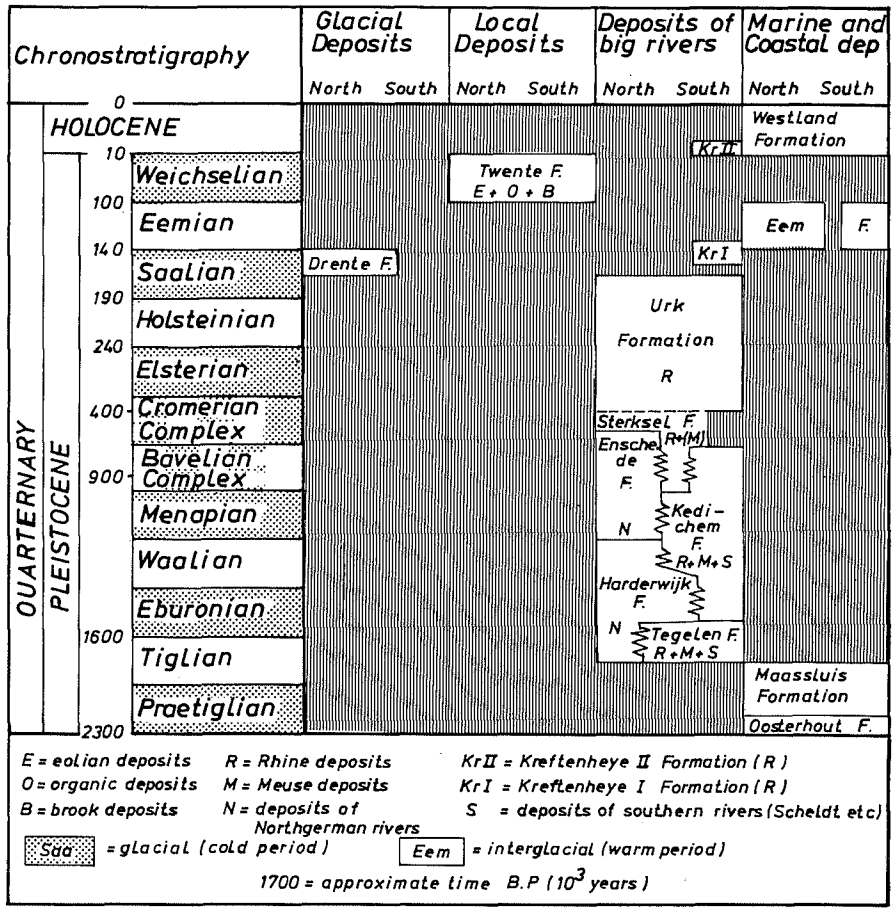

FIG. 3.5. Quarternary formations in the coastal area of the Western Netherlands arranged according to age and genesis. Based on information in Zagwijn & Van Staalduinen (1975), Breeuwer et al. (1979) and Zagwijn (1985).

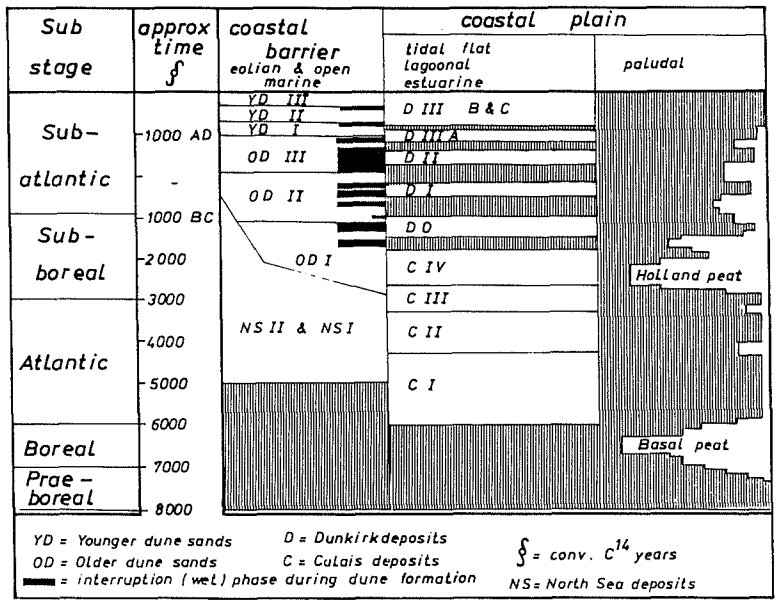

FIG. 3.6. Holocene deposits in the coastal area of the Western Netherlands, arranged according to age and sedimentary environment. Based on data in Jelgersma et al. (1970), Zagwijn & Van Staalduinen (1975) and Zagwijn (1986).

3.2.3 Geomorphology

The geomorphology of the area, whose younger dunes have been studied among others by Van Dieren (1934) and Klijn (1981), can be schematized by a typical sequence of units perpendicular to the coast line, as indicated in Fig.3.7. The main units are, from the North Sea shore inland : the beach, younger dunes, beach barrier and beach plain landscape, shallow polders and reclaimed lakes (deep polders), whose areal extent is shown in Fig.3.1 and, with more details, in Enclosure 1.1.

A *polder* is defined as a low lying flat area with controlled water levels and protection from surrounding high water levels (see also Fig.3.29). Shallow polders and reclaimed shallow lakes are intercalated in the beach barrier and beach plain landscape north of Beverwijk, where the distance between parallel barriers or between the younger dunes and a singular beach barrier is rather long. Compaction and oxidation of dewatered peat is the main cause of subsidence of the polder land.

The dune coast belongs to the on-shore type, according to the classification system proposed by Olson & Van der Maarel (1989). The younger dunes are classified as blow-out dunes, whereas the older dunes are residual (Olson & Van der Maarel, 1989).

Primary dune valleys, which originate after the cut-off of a beach plain from beach action, are lacking in the younger dunes in the study area. All dune valleys and plains evolved there by downward wind channeling between the arms of a blow-out form, and therefore belong to the secondary type. One of the most striking features of these dune valleys and deflation plains, is the practically horizontal position of their floor (Dubois, 1909). Gevers (1826) already recognized, that the altitude of this floor was conditioned by the position of the groundwater table. More precisely, the floor is the result of the aeolian erosion of dry dune sand

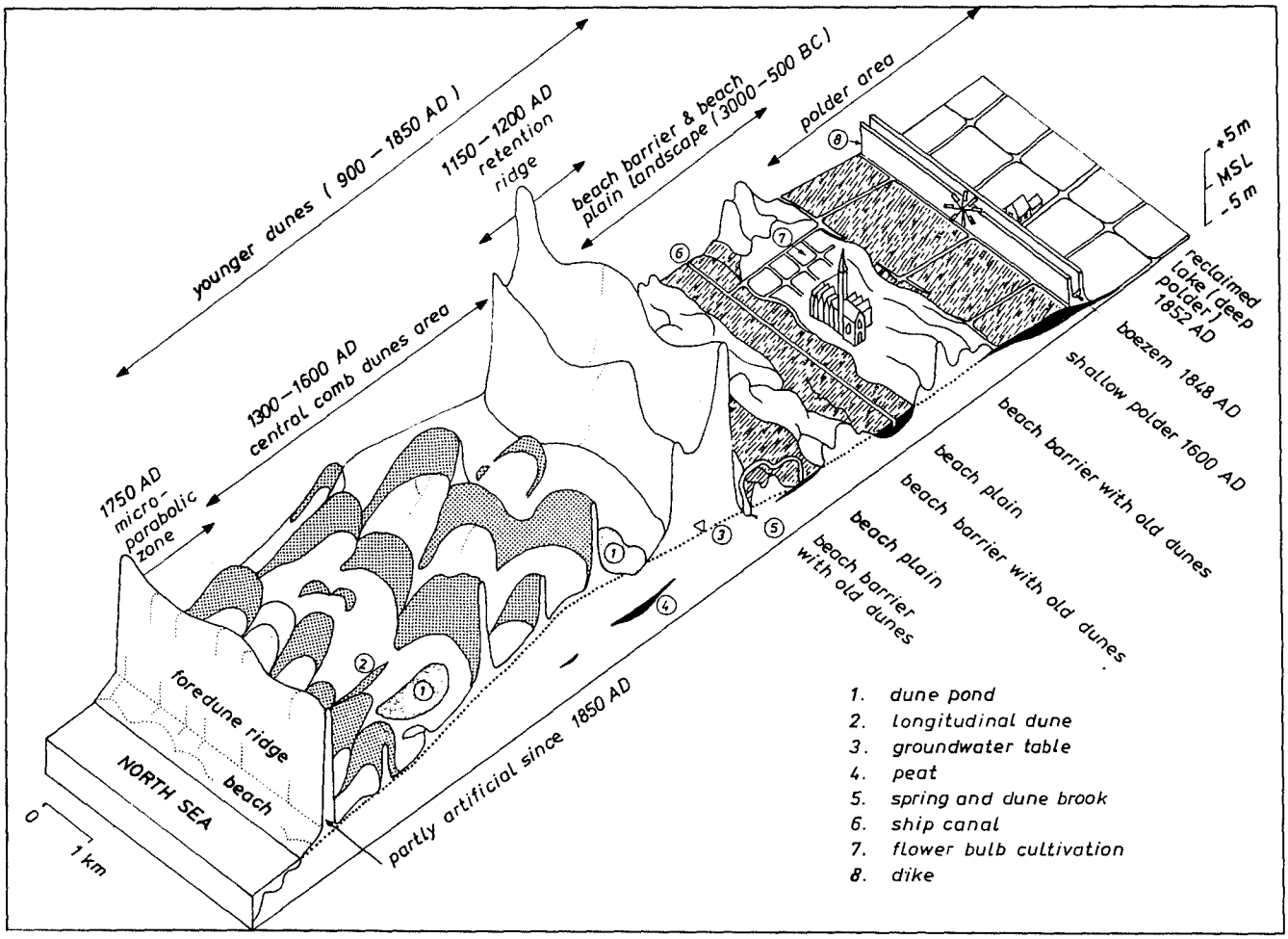

FIG. 3.7 Schematized cross section over the coastal area south of Zandvoort aan Zee, showing the geomorphological units in little disturbed form.

up to the top of the capillary fringe during the period of its formation (Fig.3.8A). The small thickness of the capillary fringe (0.2-0.3 m, Dubois, 1909; Lindenbergh, 1941; Wind, 1952) and rather small seasonal fluctuations in the groundwater table of about 0.4-0.7 m (Bakker, 1981), allow to assume that this period approximately coincides with the mean position of the groundwater table.

The (sub)horizontal position of the floor can be explained by the rather flat position of the groundwater table in the dunes, in connection with the relatively high permeability of dune sand (12 m/d). It is important to notice, that the position of most valley floors in the dunes has not changed during the past 150 years, notwithstanding a considerable decline of groundwater tables. Natural and planted vegetation as well as twigs and branches spread over susceptible areas, resulted in a complete fixation of the formerly wandering dunes (Fig.3.8B). This phenomenon has been utilized to reconstruct palaeo-isohypses of the mean groundwater table around 1850 AD (section 3.6.4).

3.2.4 Parent materials and soils

In between Egmond aan Zee and Bergen aan Zee an important transition zone exists, from calcareous younger dunes (>2% $CaCO_3$) in the south to dunes poor in lime (<0.4% $CaCO_3$) in the north (Enclosure 1.1; Bijhouwer, 1926; Eisma, 1968). The fair dune sands poor in lime, have a lower $Fe(OH)_3$ and feldspar content but higher concentration of tourmaline (section 6.4.1). They consist mainly of reworked glacial sands of Saalian age, with admixing of relative few, Holocene, marine shells (Eisma, 1968). A prolonged leaching of these sands has contributed further to their extreme deficiency in lime (section 6.8.4).

The transition zone marks the position of a former tidal inlet, which became completely choked about 900 AD (Jelgersma et al., 1970). The calcareous yellowish dune sands derive mainly from Rhine deposits and reworked, marine Eemian deposits, with a primarily moderate to high lime content, and with strong admixing of Holocene, marine shells.

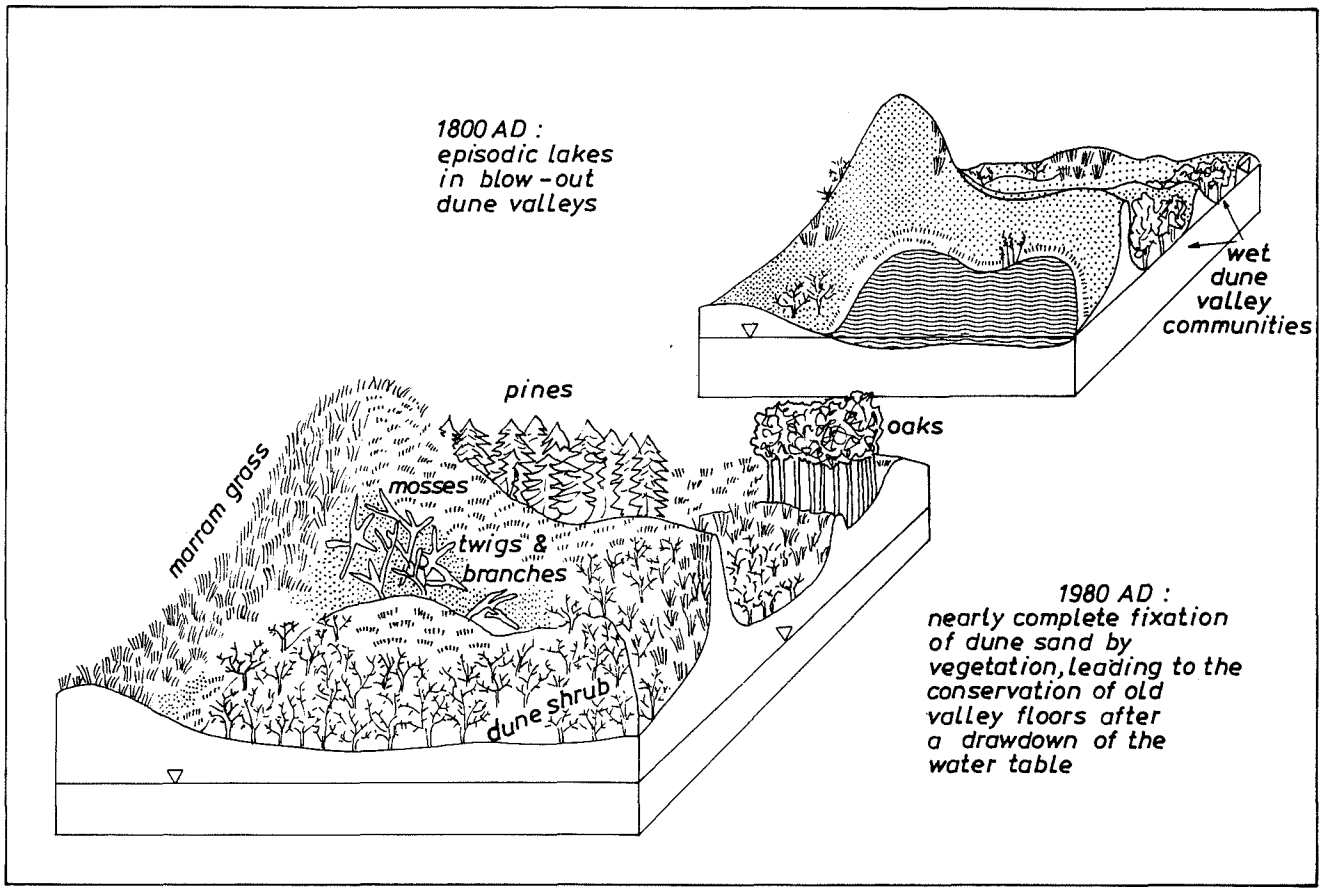

FIG. 3.8 Subhorizontal dune valley floors, shortly after their aeolian formation and flooded with groundwater (A), and their preservation after a lowering of groundwater tables (B).

Most soils are poorly developed in the younger dunes. They may be classified as entisols or inceptisols according to the 7th approximation (USDA, 1960). Decalcification of the calcareous sands (sections 6.4.2 and 6.8.4) may have proceeded to several decimeters after the formation of an organic horizon. These aspects become more pronounced inland (Figs. 6.9 and 6.57) with increasing age of the landscape (Fig.3.7), as is well-known from studies abroad (Salisbury, 1925; Olson, 1958; Wilson, 1960; James & Wharfe, 1989) and in The Netherlands (Boerboom, 1963; Adriani & Van der Maarel, 1968; Jungerius, 1990). Features of gleying may be notable in the slacks.

The process of podzolization is manifest under conifers (Wardenaar & Sevink, 1992), especially in the older dunes and younger dunes poor in lime, but in general it is insufficiently mature to reach the stage of a true spodosol. Decalcification has reached a depth of 1-3 metres in the older, primarily calcareous dunes (section 6.8.4). Animal manuring and cultivation for centuries, have led to the development of brown earthy soils (probably inceptisols) in several dune slacks and on quarried beach barriers (Vos, 1984).

Parent materials in the beach plains, shallow and deep polders consist of heavy clay, peat, sand and all their mixtures. Most soils on these young Holocene sediments are weakly developed, due to shortage of time (Pons & Van Oosten, 1974). They are to be classified as histosols on peat and otherwise as entisols or inceptisols. Soil formation is restricted to physical ripening, leading to subsidence and cracking; chemical ripening, leading to desalinization, cation exchange, oxidation (mainly of organic matter and iron sulphides), decalcification and the formation of acid sulphate soils notably in the deep reclaimed lakes; and the formation of a humic topsoil (Pons & Van Oosten, 1974). Detailed soil maps have been published by Van der Meer (1952), De Roo (1953), Van Wallenburg (1966), Pons & Van Oosten (1974) and Vos (1984).

3.2.5 Dune vegetation

Vegetation types are distributed in the coastal dunes, very roughly, in zones parallel to the coast line, and coincide partly with the geomorphological zones (Doing, 1966, 1988). From the first dune ridge inland, on average an ever increasing density and/or height of vegetation is found : the first dune ridge is covered mainly by dune grasses, like marram (*Ammophila arenaria*); the microparabolic dune zone by a mosaic of mosses (*Tortula ruralis* and *Hyphnum cupressiforme*), dune grasses (*Phleum arenarium* and *Corynephorus canescens*), dewberry (*Rubus caesius*), creeping willow (*Salix repens*) and low sea buckthorns (*Hippophaë rhamnoides*); the central zone composed of comb dunes and extensive dune valleys, by dune grasses, sea buckthorn and the dune shrubs hawthorn (*Crataegus monogyna*), birch (*Betula pubescens*), spindle-tree (*Euonymus europaeus*), etc.; the terminal accumulation ridge forming the landward limit of the younger dunes, by planted pines (*Pinus nigra subsp. nigra* and *Pinus sylvestris*); and the older dunes directly bordering the retention ridge, by planted and indigenous oaks (*Quercus robur*).

This pattern is traversed by innumerable exceptions and more subtle gradients, connected with differences in for instance exposition to the wind and sun, depths to the groundwater, stages of succession and interferences by man. The younger dunes poor in lime, north of Bergen aan Zee are covered relatively little by sea buckthorn, and by heather (*Calluna vulgaris*) instead, whereas planted pine (*Pinus nigra subsp. nigra* and *Pinus maritima* mainly) also occupies large areas in the central zone. For further details and maps reference is made to Van Zadelhoff (1981), Doing (1988) and Kruijsen et al. (1992).

Changes in vegetation cover during the period 1850-1980, are related to local (re)afforestations, marram plantations and the drying up of the dunes due to groundwater exploitation, all by the end of the 19th and during the first half of the 20th century (Westhoff, 1989). They comprise the increase of dry dune vegetation, oaks and pines at the expense of bare dunes and wet dune slack communities. A quantification for the younger dunes is presented in Table 3.5 and discussed in section 3.4.3. All changes together led to the present aspect of complete fixation by vegetation covers, a unique situation in the past 1000 years indeed. Additional factors for the expansion of dry dune shrub, were the advent of myxomatosis in the 1950s, which strongly reduced the number of rabbits, and the planting of *Hippophaë rhamnoides* as an aid to sand stabilization (Boorman, 1977; Ernst, 1984).

Not only the drying up of wet dune slacks, but also the artificial recharge with eutrophic surface waters and the topography of both submerged sand pits and dug recharge facilities contributed to the disappearance of many oligotrophic phreatophytes in that period (Londo, 1966; Bakker et al., 1979; Van Dijk, 1984). Recent changes in vegetation comprise the dissemination of (dune) reeds (*Phragmites*), also beyond the sphere of influence of recharged eutrophic surface waters (Bakker et al., 1979), and the rapid conquest of the dunes by an exotic moss (*Campylopus introflexus*) as described by Van der Meulen (1988). Recent changes in dune management consist of the stimulation of wandering dunes in selected areas, and the local felling of pine woods (Van der Meulen et al., 1987).

3.3 Hydrogeological structure

The spatial distribution of aquifers and aquitards is shown in a longitudinal section over the younger dunes, running over a distance of 100 km from Monster in the south to Camperduin in the north (Fig.3.9), and in a cross section over the city of Haarlem (Fig.3.10). Geological, sedimentological and hydraulic characteristics of the recognized aquifers and aquitards are listed in Table 3.1.

The aquitards have been subdivided largely on the basis of their stratigraphical position and sedimentary environment, in contrast with less detailed, regional surveys conducted by DGV-TNO (Lageman & Homan, 1979; Speelman & Houtman, 1979) and ICW (1976 and 1982). Whereas those studies focused mainly on the mapping of the aquifers, the aquitards are given more consideration here, because of their clear influence on flow systems and their great hydrochemical impact.
Maps have therefore been prepared with the areal distribution of the main aquitards at the base of the Holocene (Enclosure 1.3), which separate the first from the second aquifer, and of several Pleistocene aquitards in between the second and third aquifer (Enclosure 1.4). These maps cover the study area to the north of the Old Rhine, which constitutes the main focus of this chapter. It is astonishing that similar hydrogeological maps were not prepared before, for an area that earns the mark "data paradise" and has received so much hydrological attention. About 5500 well drilling logs were selected for the construction of Enclosure 1.3 and some 600 for Enclosure 1.4. They stem from the archives of : (1) four water supply companies, respectively the Provincial Water Supply Co. of North-Holland Ltd. (PWN), Water Supply Co. of South-Kennemerland (WLZK), Municipal Water Supply Co. of Amsterdam (GW) and Energy and Water Supply Co. of Rijnland Ltd. (EWR); (2) the National Institute for Drinking Water Supply (RID); and (3) the National Geological Survey (RGD).

Reference is made to Stuyfzand (1985a, 1987d, 1988b and 1989a) for the areal extent of shallower, Holocene aquitards within the first aquifer (1A, 1B, 1C and 1F), further descriptions of the presented sections and maps, and other cross sections. Similar aquitard maps as presented in Enclosures 1.3 and 1.4, were prepared for a large part of the study area south of the Old Rhine, by Stuyfzand et al. (1993).

TABLE 3.1 Characteristics of the aquifers and aquitards discerned in Fig.3.9 and 3.10. K_h = median horizontal permeability; c_v = median vertical flow resistance; D = thickness.

AQUIFERS				AQUITARDS				
nr.	geological unit (fig.3.5 & 3.6)	description	K_h (m/d)	nr.	geological unit (fig.3.5 & 3.6)	description	c_v (d)	D (m)
	West- YD I-III	younger dune sand	12		Westland F.:			
	land OD I-III	older dune sand	12	1A	dune peat	Holland peat in dunes	100-15,000	0,05-1
	F. NS I-II	open marine sand	5-20	1B	DI	heavy estuarine clay	150,000	2
	C II-IV	tidal flat/gully sand	5-10	1C	NS I/II	open marine, silty fine sand	200	3
				1C'	NS I/II	as 1C, estuarine or tidal inlet	200	10
	Twente F.	eolian fine coversand	5	1D	CIII?	silty clay	5,000	5
II	Kr. F. 1 & 2	fluvial sands	5-20?	1E	CIII	Bergen clay (silty)	50,000	12
	Eem F.	coarse marine sands	40	1F	CII-IV, DO-III	clay & Holland peat	?	1-10
	U & S F.	coarse fluvial sands	30		CII	tidal flat sandy clay		2
				1G	CI	lagoonal Velsen clay	20,000	2
	Eem F.	coarse marine sands	20-40		basal peat	strongly compacted peat		0,4
III_A	Drente F.	fluvioglacial coarse sands	40					
	U & S F.	coarse fluvial sands	30	1H	Twente F.	silty clay	1,000?	
	Enschede F.	coarse fluvial sands	40					
				2A	Eem F.	marine sandy clay	500-40,000	2-30
III_B	Kedichem F.	fluvial sands	25	2B	Eem F.	continental fine sand & peat	?	10
	Harderwijk F.	coarse fluvial sands	50	2C	Drente F.	glaciolimnic varved clay	100,000	20
				2D	Drente F.	boulder clay	5,000	6
IV	Tegelen F.	fluvial (fine) sands	10-30	2E	Kedichem F.	loam, sandy clay & peat	100-4,000	1-15
	Tegelen F.	fluvial (fine) sands	10-30	3A	Enschede F.	loam, sandy clay	1,000	6
	Maassluis F.	marine sands	5-30?	3B	Tegelen F.	loam, sandy clay & peat	500-2,000	2-10
				4	Tegelen F.	loam, sandy clay	?	5-10
VI	Maassluis F.	marine fine sands	5-10	5	Maassluis F.	marine sandy clay	?	?

F. = Formation; Kr. = Kreftenheye; U & S = Urk and Sterksel.

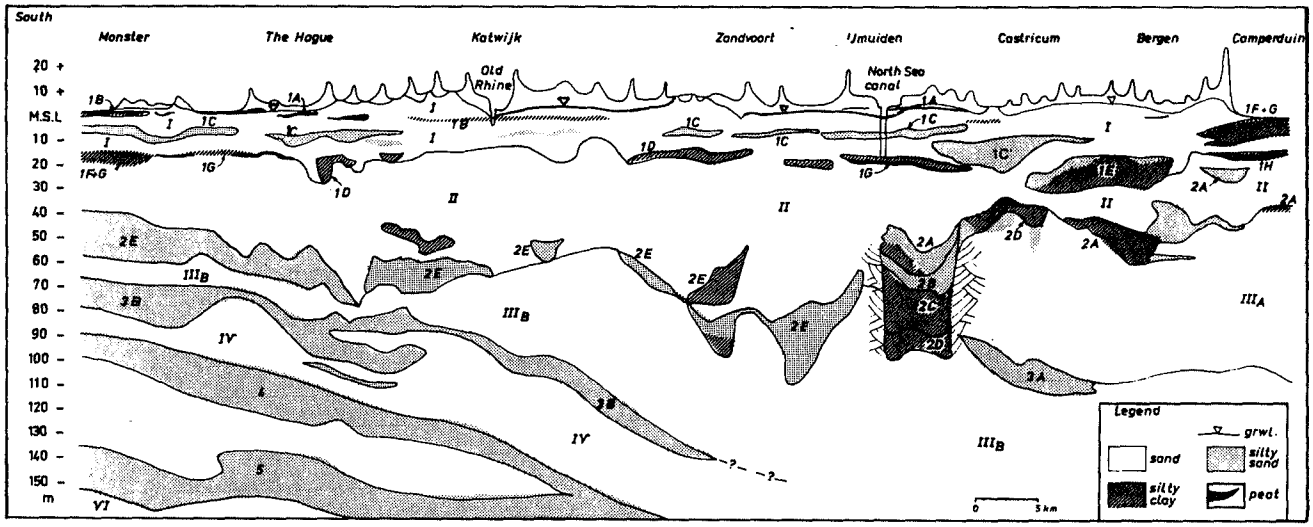

FIG. 3.9 Longitudinal section over the Monster-Camperduin coastal dune area (A in Fig.3.1), with the hydrogeological subdivision. The aquifers (numbered I-VI) and aquitards (coded 1A-H, 2A-E, 3A-B, 4 and 5) are characterized in Table 3.1.

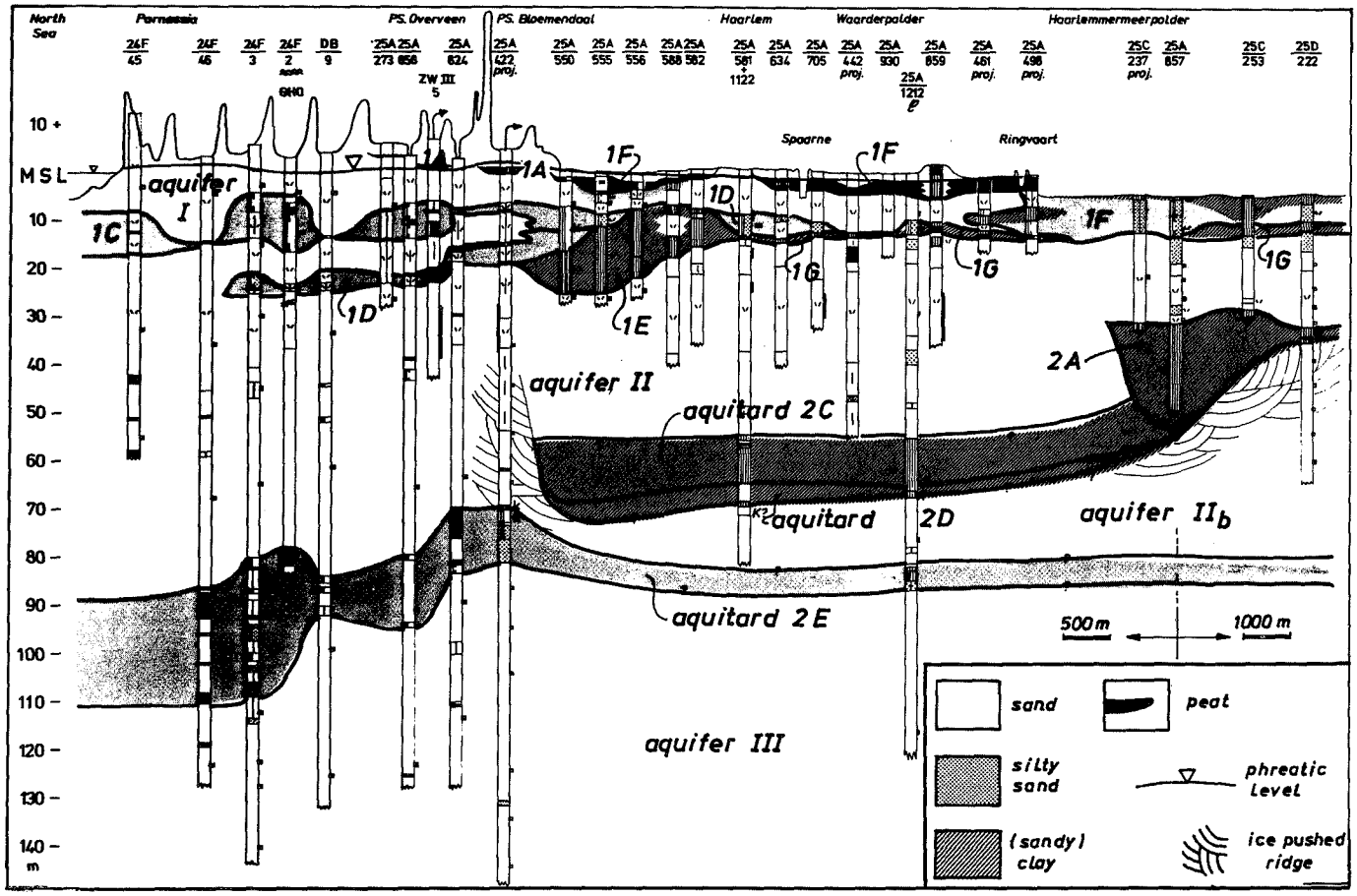

FIG. 3.10 Hydrogeological cross section over the coastal dunes near the city of Haarlem (E in Fig.3.1). The aquifers (numbered I-VI) and aquitards (coded 1A-G and 2A-E) are characterized in Table 3.1. For legend to lithological units in well drilling logs, see Enclosure 9.

Superposition of all aquitard maps may reveal the position of the recharge focus areas for deep confined aquifers. They can be considered as vertical shafts of high permeability, which convey the bulk of water arriving at great depths. Examples are discussed in section 4.5.3.

3.4 Natural groundwater recharge in the dunes

3.4.1 Gross precipitation

Mean gross precipitation on the coastal dunes north of the mouth of the Older Rhine, with due corrections for the so-called wind effect (Braak, 1945; Van Leeuwen, 1972; Warmerdam, 1981), amounts to 0.82 m/y for the period 1947-1981 (Stuyfzand, 1988b). Isohyets reveal an inland increase in gross precipitation up to the landward limit of the younger dunes (Fig.3.11). This may be related to (a) a gradual warming up of maritime air masses above land, which is further stimulated by a decrease in albedo with increasing vegetation inland, and (b) a slight orographic effect.

The 10 years moving average of annual gross precipitation (Fig.3.12), does not reveal any systematic change during the period 1740-1990. Distinct wet and dry periods occurred, however (Fig.3.12; Labrijn, 1945; Bakker, 1981).

Mean monthly, gross precipitation varies according to Fig.3.14. During the months February through June, it amounts to 50 ± 5 mm/month. For the remaining period mean monthly totals vary in between 72 and 104 mm, with a maximum around November.

3.4.2 Natural groundwater recharge as a function of vegetation

Annual means

The difference between gross precipitation (*P*) and all evaporation losses (*E*) yields the precipitation excess. This is about equal to the natural groundwater recharge (*N*) in dunes without significant surface discharge. In what can be called the first scientific publication on the hydrology of coastal dunes, Rutgers Van Rozenburg et al. (1891) concluded that the mean precipitation excess for coastal dunes as a whole should figure about 40% of gross precipitation, an amount that still holds against modern insights.

Observations since 1941 on four giant lysimeters near Castricum, each 2.5 m deep with a surface of 625 m^2 and with different vegetation, yielded close estimates of *N* under different kinds of representative vegetation units for dunes, during their growth and after reaching maturity (Wind, 1958 and 1960; Minderman & Leeflang, 1968; PWN, 1972; Stuyfzand, 1986c). Additional data from small lysimeters covered with some mosses and dune grasses south of Zandvoort (Stuyfzand, 1988b) and from literature (Bakker, 1981; Meinardi, 1976; Liebscher, 1970) permitted the construction of a refined scale of mean annual *N* under vegetation units of increasing density, height or moisture supply (Table 3.2). Mean annual values, which are normalized to a gross precipitation of 820 mm/y, vary in between +0.62 m for bare dunes and +0.21 to -0.58 m for dune lakes full of reeds, respectively, with true evapo(transpi)ration rates (E) of about 0.2 and 0.6-1.4 m/y, respectively.

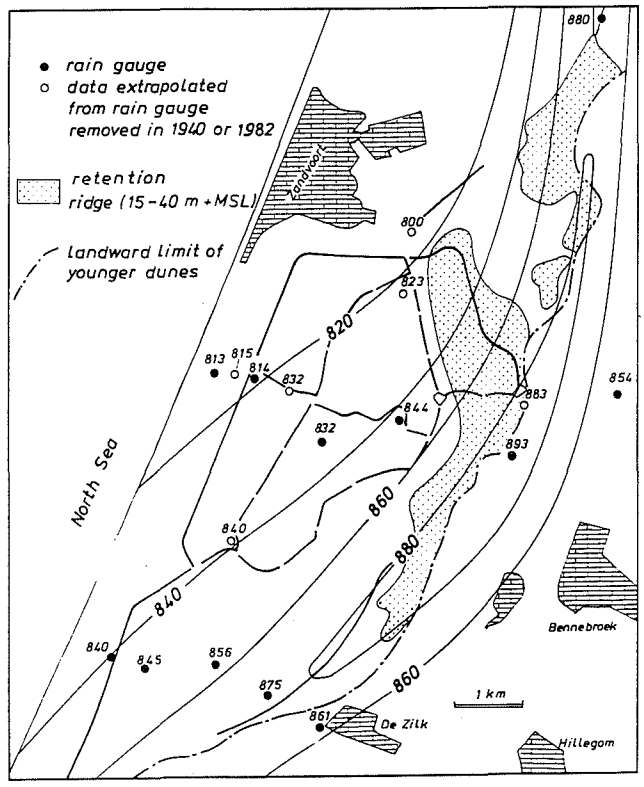

FIG. 3.11 Isohyets of mean annual gross precipitation on the coastal dune area near Zandvoort aan Zee, for the period 1983-1986. Measurements were carried out using gauges at ground-level and in so-called "English position" : funnel at 40 cm above ground-level, surrounded by an earthen wall 40 cm high, 300 cm in diameter and an outer slope of 14°. Van Leeuwen (1972) demonstrated that the rain gauges in English position yielded 2% less gross precipitation than the gauges at ground-level, which practically eliminates the otherwise strong wind effect leading to an underestimation of rainfall.

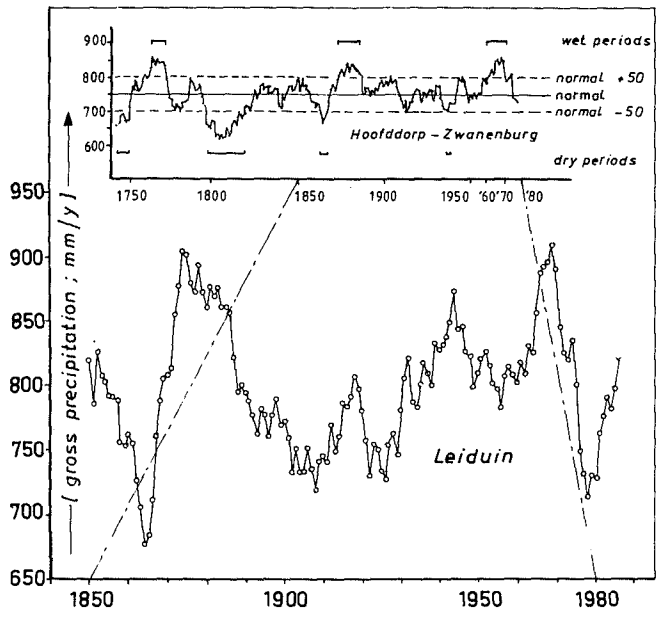

Fig. 3.12 Ten years moving average of annual gross precipitation on the coastal dune area near Zandvoort aan Zee (Leiduin; from Stuyfzand, 1988b) and the reclaimed lake Haarlemmermeer (Hoofddorp-Zwanenburg; from Bakker, 1981).

Quantitative measurements of gross precipitation (in the open), throughfall, stemflow, litter leachate and percolating soil moisture below the root zone (section 6.5) were integrated in Table 3.3 to yield insight into the contribution of each of the three evaporation terms : interception (by the overground parts of vegetation), soil evaporation (from the unvegetated soil surface, litter included) and transpiration. Interception appears the most important term for the vegetation types on land, whereas soil evaporation is the only term for bare dune sand. Transpiration rates are lower for dune shrub than for oak and pines, and may reach maximum values in reed stands.

Annual fluctuations

Variations in annual recharge are large and most pronounced below scanty vegetation covers, as evidenced by observations on the lysimeters near Castricum (Table 3.4).

Growth of dune shrub, oak and pines during their initial 13 years, is clearly accompanied by a declining recharge, as can be deduced from the increasing percentage of gross precipitation which evaporates (Fig.3.13). Since about 1953 the

TABLE 3.2 Mean annual water balance for coastal dunes with different vegetation covers, in order of increasing evapo(transpi)ration. Additional data are : f = concentration factor by evaporation; and t = modal transit time in a 3 m thick unsaturated zone with a mean moisture content of 6.5% by volume.
P = gross precipitation; N = precipitation excess; E = true evapo(transpi)ration; %E = 100(E/P); f = P/N.

vegetation type	P	N	E	%E	f	t	foot note
		mm/year		(%)		(d)	
bare, very few mosses	820	623	197	24	1,3	114	I
bare, some marram	820	613	207	25	1,3	116	II
mosses, dewberry, bare	820	519	301	37	1,6	137	III
moss carpet	820	492	328	40	1,7	145	est
mosses, dry grass, bare	820	476	344	42	1,7	150	IV
poor, dry dune vegetation	820	459	361	44	1,8	155	V
rather poor, see foot note *	820	426	394	48	1,9	167	XIII
sea buckthorn, <50% mosses	820	410	410	50	2,0	174	est
sea buckthorn, <50% grass	820	394	426	52	2,1	181	est
rich, dry dune vegetation	820	377	443	54	2,2	189	V
heather	820	369	451	55	2,2	193	II, VII
dry deciduous, open structure	820	369	451	55	2,2	193	V
dense dune shrub, dry nor wet	820	344	476	58	2,4	207	VI
wet, tall grasses and herbs	820	328	492	60	2,5	217	VIII
oaks, dry nor wet	820	303	517	63	2,7	235	IX
wet dune slack vegetation	820	238	582	71	3,5	299	V
wet deciduous forest	820	238	582	71	3,5	299	V
dry pines	820	197	623	76	4,2	361	V
pines, dry nor wet	820	141	679	83	5,8	505	X
wet pines	820	74	746	91	11,1	962	V
open water	820	49	771	94	-	-	XI
reeds in dune lake	820	205/-580	615/1400	75/171			XII

I = lys.1 Castricum (Stuyfzand, 1986); II = Liebscher, 1970; III = lys. Zwarteveld (Stuyfzand, 1986); IV = lys. Oranjekom (Stuyfzand, 1986); V = Bakker, 1981; VI = lys.2 Castricum (Stuyfzand, 1986); VII = Meinardi (1976); VIII = SWNBL, 1988; IX = lys.3 Castricum (Stuyfzand, 1986); X = lys.4 Castricum (Stuyfzand, 1986); XI = KNMI.; XII = Burian, 1971; Bernatowicz et al., 1976; Koerselman & Beltman, 1988; XIII = Schroeder (1988), extrapolated; est = estimated. * = rather poor dry dune vegetation : if mosses and <50% low sea buckthorns; or if grasses and <50% sea buckthorns; or if mosses, grasses and bracken; or if carpetted with short grasses.

TABLE 3.3 Mean annual totals (1947-1981) of gross precipitation, evapo(transpi)ration (with differentiation) and excess precipitation (≈ natural recharge) for coastal dunes lacking a vegetation cover and covered with either dune shrub, oaks or pines, where the water table stands 2.3 m below the surface. Synthesis of data collected on the four lysimetric plots near Castricum and on the plots dune shrub-1 (D_1), oaks-2 (O_2) and pines-3 (P_3) of this study south of Zandvoort aan Zee. For locations see Fig.6.2.

mm/year	bare dune sand	dune shrub (*Hippophaë*)	oaks (*Quercus robur*)	pines (*Pinus nigra*)
gross precipitation	820	820	820	820
interception	0	162[a]	230[a,c,#]	360[a,d,e,§]
soil evaporation	197[b]	174[g]	115[a]	150[a,f]
transpiration [**]	0	139	170	170
excess precipitation	623[b]	345[b]	305[b]	140[b]

[**] = calculated as rest term; a = Stuurman (1984); [b] = measured with lysimeters near Castricum, Stuyfzand (1986); [c] = Dolman & Oosterbaan (1986); [d] = Mulder (1983); [e] = Wind (1954); [f] = Berhane & Van de Coevering (1987); [g] = estimated, by taking the mean value of bare dune sand and pines; [#] = stemflow < 1% during summer period and 5% during winter (Dolman, 1987); [§] = stemflow = 20 mm/y (Mulder, 1983).

vegetation covers of the lysimeters can be considered hydrologically mature. This is demonstrated by the linear relationship of annual recharge with annual gross precipitation (Table 3.4). Somewhat better relationships are obtained by consideration of a hydrological year starting in February or March (Stuyfzand, 1986c), and by consideration of the previous year as well.

Annual fluctuations of N result in annual fluctuations of the position of the groundwater table by about 0.4-0.7 m (Bakker, 1981).

TABLE 3.4 Linear regression of annual groundwater recharge (N) and annual gross precipitation (P), for bare dune sand and selected hydrologically mature vegetation covers of coastal dunes in The Netherlands. Based on lysimetric observations by the Provincial Water Supply Co. of North-Holland Ltd. (PWN) near Castricum in the period 1957-1981. Minimum values coincide with 1971 or 1976, maximum values with 1966 or 1979.

vegetation cover	regression equation (N & P in m/year)		N (m/y) 1957-1981 minimum[a]	N (m/y) 1957-1981 maximum[b]
bare	$N = 0.91 \cdot P - 0.123$	0.98	0.42	0.87
dune shrub	$N = 0.75 \cdot P - 0.306$	0.93	0.18	0.59
oak	$N = 0.82 \cdot P - 0.370$	0.93	0.14	0.57
pine	$N = 0.56 \cdot P - 0.321$	0.84	0.00	0.34

a = with P-minimum = 0.63 m/y; b = with P-maximum = 1.10 m/y

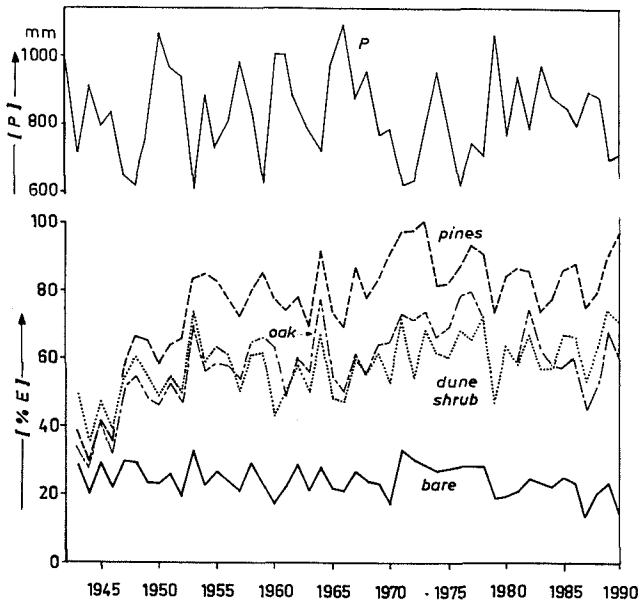

FIG. 3.13 Variations in annual gross precipitation (P) and the percentage of evapotranspiration (%E = 100E/P) by selected vegetation types, during the period 1942-1986. Based on data obtained at the lysimetric station of PWN, west of Castricum. Growth of vegetation led to a steady increase of evapotranspiration losses during the period 1940-1955, after which the vegetated lysimeters reached hydrological maturity (%E hardly affected by further growth).

Seasonal fluctuations
Variations in monthly means of the precipitation excess are shown for selected vegetation units in Fig.3.14. These data derive from small lysimeters (1 m^2 and 1 m deep, with poor vegetation and negligible soil moisture storage), and from the four lysimeters near Castricum. The Castricum data were corrected for storage of soil moisture and perched groundwater, according to Stuyfzand (1986c). It can be deduced for average conditions, that bare dunes or dunes with a poor vegetation are recharged during the whole year, with the lowest precipitation excess in May-June and highest in November-December; and that densely vegetated dunes receive a precipitation excess during the period August/September - April only, whereas a soil moisture deficit develops in the remaining period. This means that groundwater under densely vegetated dunes is recharged after restoration of the soil moisture deficit, which takes about two months where the phreatic level stands about 2½ m below the surface.

Seasonal fluctuations in N induce seasonal fluctuations in the position of the groundwater table by 0.4-0.7 m (Bakker, 1981). The groundwater table generally rises in areas with a shallow phreatic level (<0.5 m below the surface), in the period September-February, and in areas where it stands deeper than about 1 m, in the period November-April. The deeper the phreatic level and the higher the evapotranspiration losses, the longer is the delay (Bakker, 1981; Stuyfzand & Moberts, 1987a).

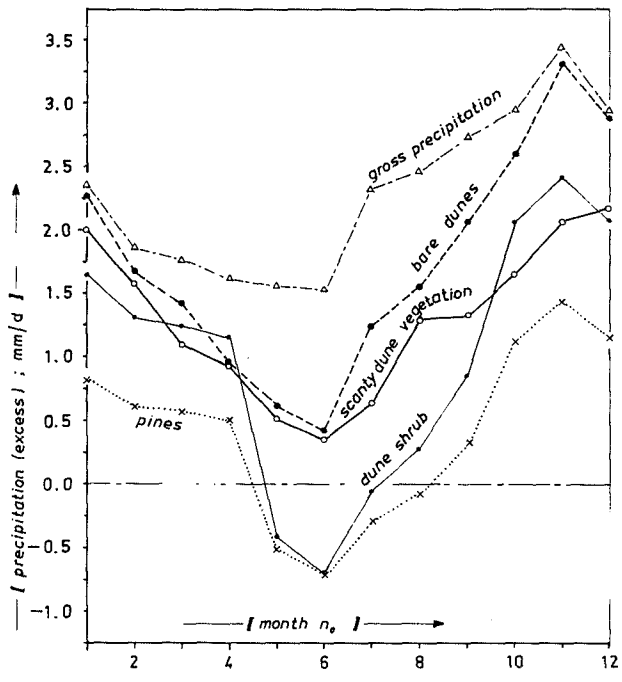

FIG. 3.14 Mean monthly gross precipitation and precipitation excess under different vegetation types.

Depression focused recharge?
Is the groundwater below dune tops recharged at a higher rate than below dune valleys, or do we have depression focused recharge? There are two mechanisms pleading for the latter : (1) overland flow along dune slopes, when dry dune sands are repelling water (Rutin, 1983; Jungerius & De Jong, 1989); and (2) soil moisture flow towards the valley bottom, which may be generated when a dry soil is wetted, the wetted zone is sloping due to topography and a higher permeability pathway is formed for the wetted zone (McCord & Stephens, 1987).

However, their effects are probably small as compared to the lower precipitation excess in dune valleys in consequence of the generally denser and taller vegetatation. The answer is therefore probably no. This does not necessarily mean that the phreatic level is always higher below dune tops, because the slope of the local or subregional groundwater level may be too steep.

3.4.3 Natural groundwater recharge in 1850 and 1980

In 1850 land-use of the younger dune area, to the north of the mouth of the Older Rhine was as indicated in Table 3.5. Apart from small urban areas and several cultivated dune slacks, natural conditions prevailed and N was approximately 0.41 m/y. Round about 1980 land-use had changed in favour of built-up areas, dry dune vegetations, oak and pine plantations at the expense of bare dunes, wet dune slack communities and open water, leading to a net 17% decrease in N and leaving 0.34 m/y.

The total surface occupied by the younger dunes diminished with nearly 5 km^2 mainly due to excavations for the sea port of IJmuiden and North Sea Canal.

3.4.4 Transit time in the vadose zone

By matching peaks in precipitation with those in the drainage of 1 and 4½ m deep lysimeters having a scanty vegetation cover, it can be deduced that soil wetting fronts descend on average 1 m/week (Fig.3.15). Hydrochemical data reveal, however, that labelled water descends about eightfold slower under similar conditions (Stuyfzand, 1984e and 1986c) than the water pulse. This agrees with general consensus that water transport in sandy aquifers

TABLE 3.5 Comparison of land-use for the younger dune area in between the mouth of the older Rhine and the village Camperduin, in 1850 and 1980, with indication of the annual evapo(transpi)ration for each unit and for the whole area. Based on data obtained from topographical maps and data in Bakker et al. (1979).

land use within younger dunes	1850 AD Area km²	1850 AD Area %	1850 AD E@ mm/y	1980 AD Area km²	1980 AD Area %	1980 AD E@ mm/y
bare	33.7	19.3	197	7.1	4.1	197
dry dune veget.	81.3	46.4	361	95.3	56.3	402
wet dune veget.	38.1	21.8	582	5.2	3.0	582
dry, decid. forest	2.5	1.5	451	7.6	4.7	451
wet, decid. forest	10.0	5.8	582	13.1	7.6	582
dry, pines	<0.1	<0.1	623	13.3	7.7	623
wet, pines	<0.1	<0.1	746	5.7	3.3	746
open water	8.2	4.6	771	2.5	1.5	771
open urban	0.8	0.4	450#	2.7	1.6	574*
dense urban	0.3	0.2	550#	17.6	10.2	700**
total	176.9	100.0	412	172.0	100.0	482

@ = where annual gross precipitation is 820 mm; # = no export by sewers; * = 0.6*P* evaporated and 0.1*P* exported by sewers; ** = 0.25*P* evaporated and 0.6*P* exported by sewers.

approaches piston flow (Van Doorn, 1951; Wind, 1952; Zimmerman et al., 1966; Andersen & Sevel, 1974).

The transit time in the unsaturated zone and capillary fringe (t_v, in d), together the vadose zone (Fig.6.1), becomes easy to calculate under the assumption of piston flow :

$$t_v = \frac{(hV + \varepsilon c)}{N} \qquad (3.1)$$

where h = thickness unsaturated zone (m); V = mean moisture content of unsaturated zone (fraction by volume); ε = porosity of capillary fringe (fraction by volume); *c* = thickness of capillary fringe (m); *N* = precipitation excess (m/d).

The annual mean moisture content of the unsaturated zone in dune sand is, practically independent of the type of vegetation cover, 6.5 % by volume (Wind, 1952; Stuyfzand, 1991b). Seasonal fluctuations are very strong, however, especially in the upper 40 cm (Ten Harkel, 1992a). The thickness of the capillary fringe in dune sand amounts to circa 0.25 m and the porosity of dune sand in the capillary fringe is about 40% (Rutgers Van Rozenburg et al., 1891; Dubois, 1909; Lindenbergh, 1941; Wind, 1952).

Insertion of these values into Eq.3.1, yields mean transit times in the vadose zone as a function of the depth to the groundwater table (= h + c) and N, as depicted in Fig.3.16. Below a high retention ridge covered with pines the transit time may figure 10-15 years, whereas about 4 months suffice to reach a 2 metres deep groundwater table below a scanty vegetation.

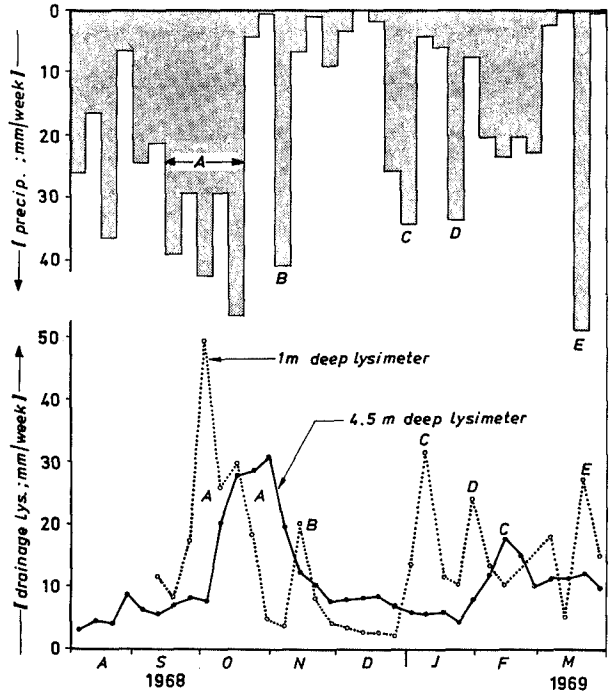

FIG. 3.15 The delayed response of the drainage of 1 m² lysimeters with scanty vegetation cover, to gross precipitation in the dunes south of Zandvoort aan Zee (modified after Van Leeuwen, 1972). The soil wetting front moves at a rate of ca. 8 m/y.

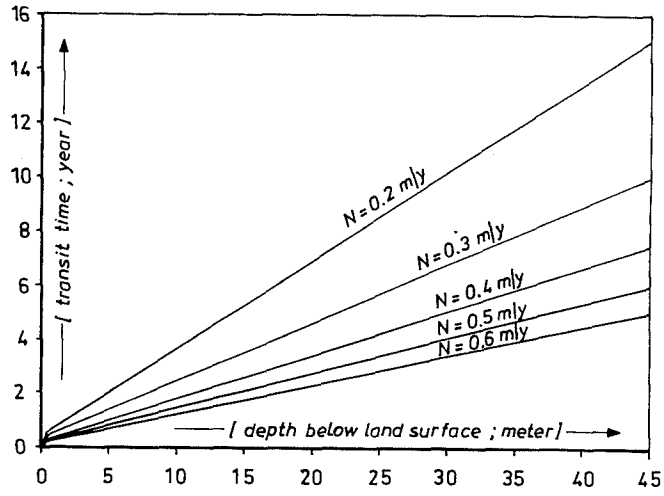

FIG. 3.16 Mean transit time of soil moisture to reach the groundwater table, as a function of its depth and the natural recharge (N). Calculated using Eq.3.1, with V = 0.065 , ε = 0.4 and c = 0.25 m.

For simplicity it has been assumed that soil wetting fronts are descending vertically in the vadose zone, in a plane paralleling the soil surface, without any formation of fingers as observed in the laboratory by Glass et al. (1989) and in dune sand, recognizable up to a depth of about 0.5 m, by Dekker & Jungerius (1990). Complications by overland flow along dune slopes, when dry dune sands are repelling water (Rutin, 1983; Jungerius & De Jong, 1989), have been ignored in these calculations as well.

3.5 Analytical approximations for a fresh dune water lens

3.5.1 The Ghyben-Herzberg principle

Where dunes develop along the sea margin of coastal lowlands that were previously invaded by the sea, the infiltrating precipitation excess will form a fresh water lens. This was realized in the 19th century, when Du Commun (1828), Badon-Ghyben (1889) and Herzberg (1901) formulated, independently, the principle of fresh groundwater floating on stagnant salt groundwater (Fig.3.17A), such that in equilibrium :

$$Z_\infty = \frac{\rho_f H_\infty}{\rho_s - \rho_f} \qquad (3.2)$$

where :
Z_∞ = depth to fresh-salt water interface in equilibrium (time = ∞) [m-MSL]; H_∞ = elevation of groundwater table in equilibrium [m+MSL]; ρ_f = density fresh water, normally 1.0 [kg/l];
ρ_s = density salt water, in The Netherlands often 1.023 [kg/l].
The density of water (ρ in kg/l) can be calculated from :

$$\rho = 1 + 8.05 \cdot 10^{-7} \cdot RE - 6.5\,10^{-6} \cdot (t - 4 + 2.2\,10^{-4} \cdot RE)^2 \qquad (3.3)$$

where : t = temperature [°C]; RE = Residue on Evaporation at 180°C [mg/kg]. RE can be calculated using Eq.2.5, from chlorinity (mg Cl^-/kg water) or electrical conductivity (EC, in µS/cm at 20°C):

$$RE = 1.805\ Cl^- + 30 \qquad (3.4)$$

$$RE = 0.69778\ EC \qquad (3.5)$$

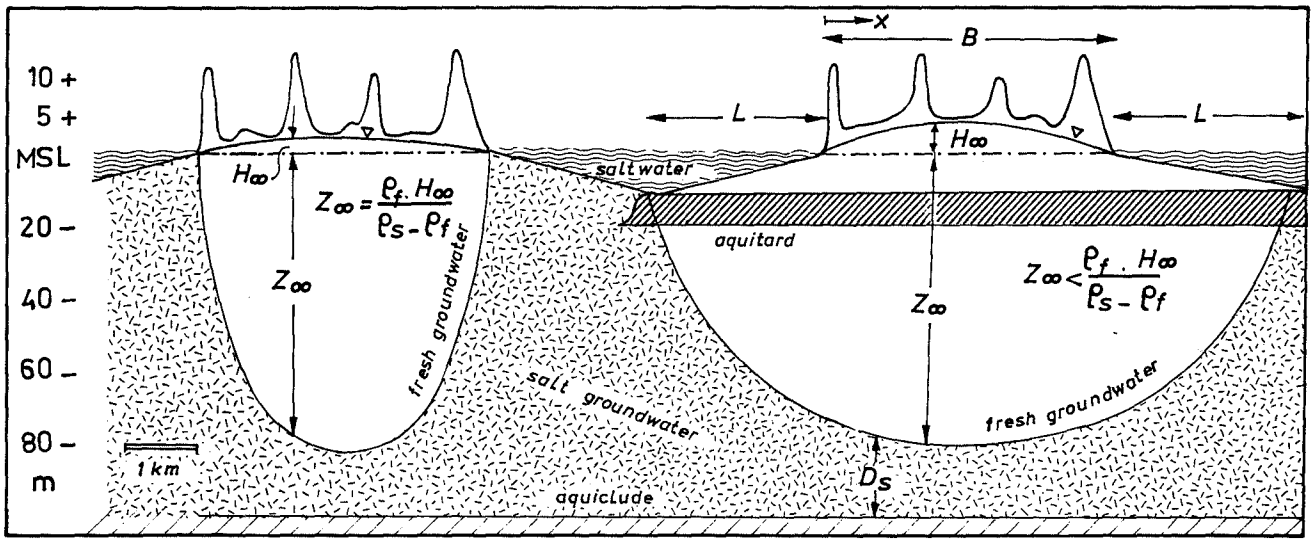

FIG. 3.17 A : the Ghyben-Herzberg principle of fresh groundwater floating on stagnant salt groundwater (Eq.3.2). B : the real geometry of a fresh water lens, with a much shallower depth to the fresh-salt water interface in equilibrium (Z_∞) than predicted from the elevation of the groundwater table (H_∞), due to vertical flow and anisotropy of the porous medium ($K_h > K_v$). L_∞ = length of the fresh water tongue; D_s = thickness of the aquifer system saturated with salt water.

Although the Ghyben-Herzberg principle explained the occurrence of fresh groundwater in salty coastal plains satisfactorily for the first time, a predicted depth of the interface at 42.6H was rarely met along the North Sea coast with ρ_s = 1.023 kg/l (Van Oldenborgh, 1916; Bakker, 1981). Discrepancies with experimental data stimulated many hydrologists to arrive at improved analytical approximations, for a review see for instance Reilly & Goodman (1985).

In the following sections practical, analytical solutions are presented, most of them without derivation, for the calculation of, in order, the size and shape of a fresh water lens, its time of formation and dispersion across the fresh-salt water interface. Beforehand, the underlying general assumptions are given and commented upon. Realistic examples are presented and further applications follow in sections 3.6 and 3.7, where the hydrological evolution of the coastal area is discussed.

3.5.2 General assumptions and their validity

In the next sections regarding the time of formation, shape and size of the fresh water lens, it is generally assumed that : (a) the upper boundary of the flow region involves a phreatic surface with precipitation; (b) the land surface is composed of an infinite, stable dune strip without surface discharge and surrounded by salt water; (c) natural groundwater recharge is constant and uniformly distributed in space; (d) the aquifer system is sufficiently deep to contain the fresh water lens and underlying salt water; (e) the interface is sharp (immiscible fluids); (f) salt water conditions are steady; (g) the porous medium and both fluids are homogeneous; and (h) the density of both fluids is equal in all directions.

In practice the conditions a and d are quite acceptable for the study area, whereas the others may pose severe restrictions. Indeed, coastal accretion and erosion are more normal than coastal stability. Natural recharge is not constant on a time scale of several decades (Fig.3.12 and 3.13) and decreases by more than 50% inland (Table 3.2). The interface is at least 8 m wide (section 3.5.5). Salt water conditions are not steady due to eustatic sea level fluctuations, storm surges and periodical inundations of land behind the dunes. And the density of salt groundwater may decrease inland as well as in the direction of river mouths cutting through the beach barrier. The most problematic condition is formed, however, by the constraint of homogeneity of the porous medium. The areal distribution of aquitards in Enclosures 1.3. and 1.4 illustrates the great heterogeneity, whereas isohypses of the groundwater table in Enclosure 2.1 reveal an asymmetrical water table and the importance of groundwater flow parallel to the coast line, clearly reflecting the distribution of the discerned aquitards.

Analytical 2D-approaches therefore may yield valuable conclusions only, if uniform areas with negligible groundwater flow parallel to the coast and sufficiently long and stable periods are selected, if lateral inhomogeneities are taken into account, for instance by glueing together two complete calculations for the whole section, one with the low and one with the high vertical resistance of the western and eastern part respectively, and if due consideration is given to their calibration.

3.5.3 Size and shape

The two-dimensional size and shape of a fresh dune water lens in equilibrium (Fig.3.17A), can conveniently be approximated by analytical solutions proposed by Van der Veer (1977). Advantages are : a two-dimensional approach instead of the essentially one-dimensional Badon Ghyben - Herzberg principle, easy incorporation of anisotropy at least when the salt water is stagnant (Bakker, 1981), the inclusion of the possibility for salt water flow directed landwards or seawards, and, compared with numerical solutions, its ease of computation requiring a simple iteration after a first estimate for the so-called "modified fresh water discharge" q^* (Stuyfzand, 1985a).

After incorporation of anisotropy, the position of the groundwater table above mean sea level reads :

$$H_\infty = \sqrt{-[A(x')^2 + 2Ex'] \cdot \frac{F+A}{F+1} - E^2 \cdot \frac{1-A-F}{(F+1)(1-A)}} \qquad (3.6)$$

The position of the sharp interface below MSL is then given by :

$$Z_\infty = \sqrt{\frac{-A(x')^2 + 2Ex'}{(F+A)(F+1)}} \qquad (3.7)$$

And the length of the fresh water tongue below the sea (L_∞ , Fig.3.17) then becomes :

$$L_\infty = \frac{q^*}{N'} - \frac{B}{2} \qquad (3.8)$$

where :

$A = N'/K'$ $\qquad E = q^*/K'$

$F = \delta/\gamma$ $\qquad K' = \sqrt{(K_h K_v)}$

$N' = N\sqrt{(K_h/K_v)}$ $\quad x' = -(L+x)\sqrt{(K_v/K_h)}$

$\gamma = 1 + (q_s\rho_s)/(q^*\rho_f)$ $\qquad \delta = (\rho_s - \rho_f)/\rho_f$

$$q^* = 0.5BN.\{ 1 - A [\frac{1 - F - A}{(1-A)(F+A)}] \}^{-½}$$

$$q_s = K_s D_s(\Delta H_s/\Delta X_s)$$

in which :
B = width of the dune belt [m]; D_s = thickness of aquifer system saturated with salt water (Fig.3.17) [m]; $\Delta H_s/\Delta X_s$ = hydraulic head gradient in aquifer saturated with salt water, X inland positive [-]; K_h = horizontal permeability [m/d]; K_v = vertical permeability [m/d]; K_s = K_h in parts of aquifer system saturated with salt water [m/d]; K' = fictive isotropic permeability [m/d]; N = natural groundwater recharge [m/d]; N' = fictive isotropic N [m/d]; q^* = modified fresh water discharge [m^2/d]; q_s = salt water discharge [m^2/d]; x = distance to the mean tide line, inland positive [m]; x' = fictive isotropic x [m].

When more than one aquifer and one aquitard are involved, K_h and K_v are calculated as follows :

$$K_h = \frac{\sum_{i=1}^{n} K_i D_i}{D_{tot}} \qquad (3.9)$$

$$K_v = \frac{D_{tot}}{\sum_{i=1}^{n} C_i} \qquad (3.10)$$

where : C_i = vertical resistance to flow of layer i [d]; D_i = thickness of layer i [m]; D_{tot} = total thickness [m]; K_i = horizontal permeability of layer i [m/d].
In multilayered media few iterations are required, after a first estimate of H_∞ and Z_∞, to determine the participating formations and their contribution to K_h and K_v.

A realistic example, representative of younger dunes in the Western Netherlands with a well developed Holocene aquitard, is shown as the anisotropic 2D-case in Fig.3.17B. In reality, the shape of the fresh-salt water interface is less smooth and displays saw-teeth around aquitards (Enclosures 5-6).

Effects of different widths of the dune belt (B), salinities of the salt water (ρ_s) and changes in the natural groundwater recharge (N) and in the resistance to vertical flow (Σc_i) of participating aquitards, are shown in Fig.3.18, because they cannot be easily deduced from the rather complicated analytical formulae. The chosen values for these parameters are within the range of natural variations in the Western Netherlands.

The following conclusions can be drawn from Fig.3.18 : An increase in width of the dune belt gives a nearly linear increase of H_∞, Z_∞ and L_∞. A rise of the density of the salt water results in a nonlinear increase of H_∞ and a nonlinear decrease in Z_∞ and L_∞. A rise of the natural recharge manifests itself in an increase of H_∞, Z_∞ and L_∞, which is about equal to $\sqrt{(N_2/N_1)}$. And an increase in vertical flow resistance leads to a very substantial, nonlinear rise of H_∞ and L_∞ and to a rather small, nonlinear decrease in Z_∞.

Effects of salt water flow inland are shown for a 5 km wide dune belt in Fig.3.18 as well. An increase in the salt water gradient leads to a moderate increase of Z_∞ and decrease in H_∞, whereas L_∞ remains practically uneffected. Narrowing the dune belt under a constant salt water gradient inland, accentuates these effects exponentially, because of its strong impact on the parameter γ in Eqs.3.6 and 3.7.

3.5.4 Time of formation

A fresh water lens may develop in an aquifer, previously saturated with salt water, after the formation of coastal dunes on top of a beach barrier. The time which is needed to attain a fraction of the ultimate depth in equilibrium, τ, can be calculated with an approximation by Brakel (1968, in Bakker, 1981), after multiplying with two correction factors according to Stuyfzand (1985a) :

$$\tau = \frac{f_1 f_2}{2} \cdot [\frac{4NK_h(\rho_s - \rho_f)}{(0.25\pi\varepsilon B)^2 \rho_s}]^{-\frac{1}{2}} \cdot \ln[\frac{1+\frac{Z_t}{Z_\infty}}{1-\frac{Z_t}{Z_\infty}}] \qquad (3.11)$$

where :
f_1 = correction factor equal to the relative increase in volume of a fresh water lens due to anisotropy of the porous medium (Fig.3.19) :

$$f_1 = \frac{H_a + Z_a \cdot [1 + \frac{2L}{B}] - L^2 \cdot \frac{(\tan\alpha + \tan\beta)}{\pi B}}{H_i + Z_i} \qquad (3.12)$$

with :
α = mean slope of the sea floor on the seaward face [°], in The Netherlands about 0.4°; β = ditto landward face (in The Netherlands close to zero) [°]; H_a = elevation of groundwater table in equilibrium, in anisotropic two-dimensional (2D) situation [m+MSL]; H_i = ditto for isotropic 1D-situation [m+MSL]; Z_a = depth to fresh-salt water interface in equilibrium, in anisotropic 2D-situation [m-MSL]; Z_i = ditto for isotropic 1D-situation [m-MSL].

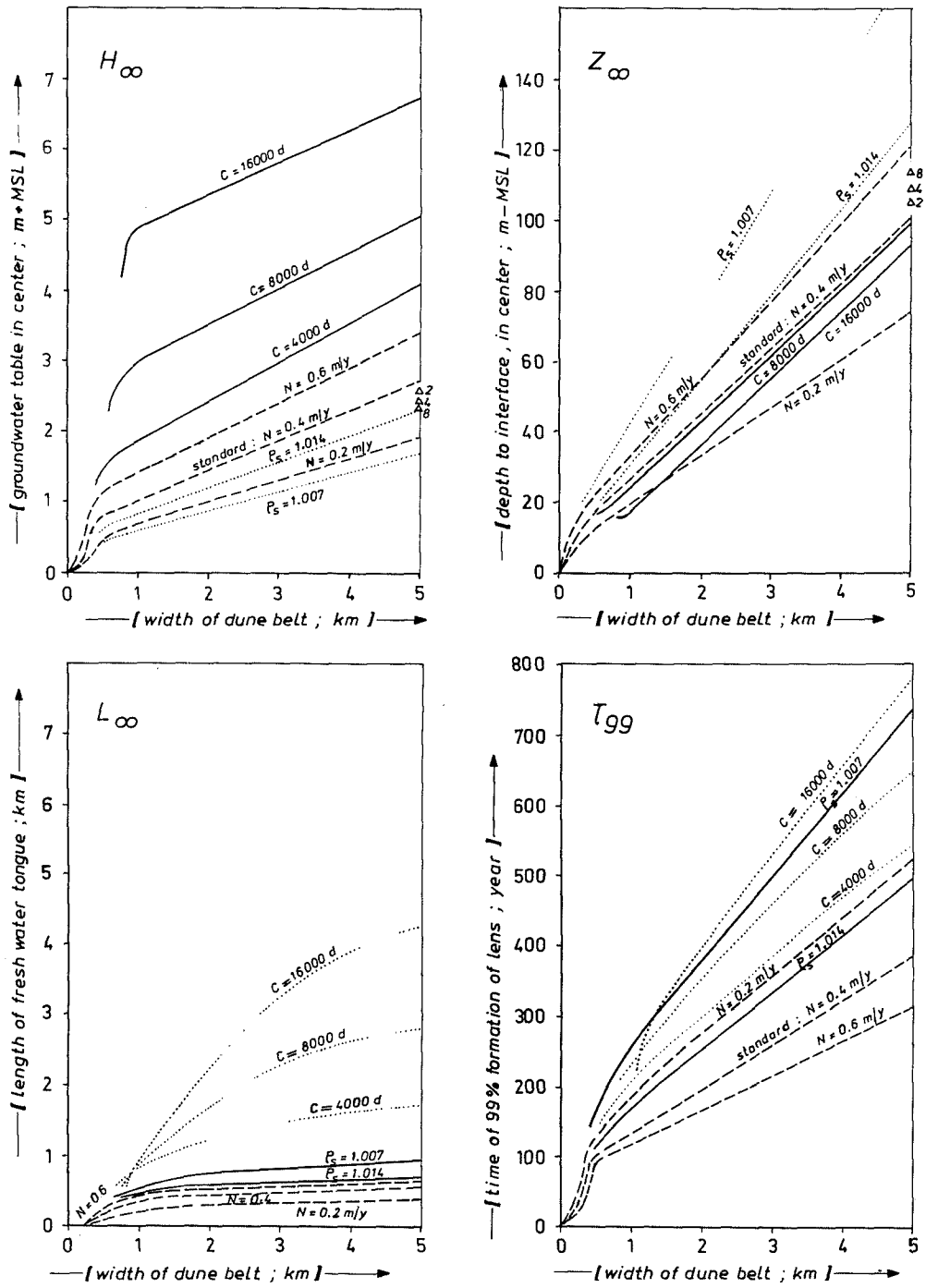

FIG. 3.18 Influence of the width of the dune belt (B), natural groundwater recharge (N), density (ρ_s), resistance to vertical flow of the involved aquitards (C = c_v) and salt water flow inland, on the equilibrium height of the water table at x = ½B (H_∞), the equilibrium depth to the fresh-salt water interface at x = ½B (Z_∞), the length of the fresh water tongue in equilibrium (L_∞) and time of 99% formation of the lens (τ_{99}).
For the selected cases all other variables are maintained standard, being :
*N = 0.4 m/y; K_h = [(H_∞+ 12)*10 + (Z_∞- 17)*35]/(H_∞+ Z_∞) if $Z_\infty \geq$ 17 m-MSL and [(H_∞+ 12)*10]/(H_∞+ Z_∞) if Z_∞= 12 to 17 m-MSL and else 10 m/d; c = 1000 d; ρ_s = 1.022; $\Delta H_s/\Delta X_s$ = 0 (no salt water flow); $\alpha = 0.4^o$; $\beta = 0^o$.*
Effects of salt water flow on H_∞ and Z_∞ are given for B = 5000 m only, with K_s= 35 m/d and D_s= 150 - Z_∞ : Δ2 = $\Delta H_s/\Delta X_s = 2.10^{-4}$; Δ4 = $\Delta H_s/\Delta X_s = 4.10^{-4}$; Δ8 = $\Delta H_s/\Delta X_s = 8.10^{-4}$;
The densities 1.007, 1.014 and 1.022 correspond with water of 12 °C having a chlorinity of 5000, 10000 and 15000 mg/l, respectively.

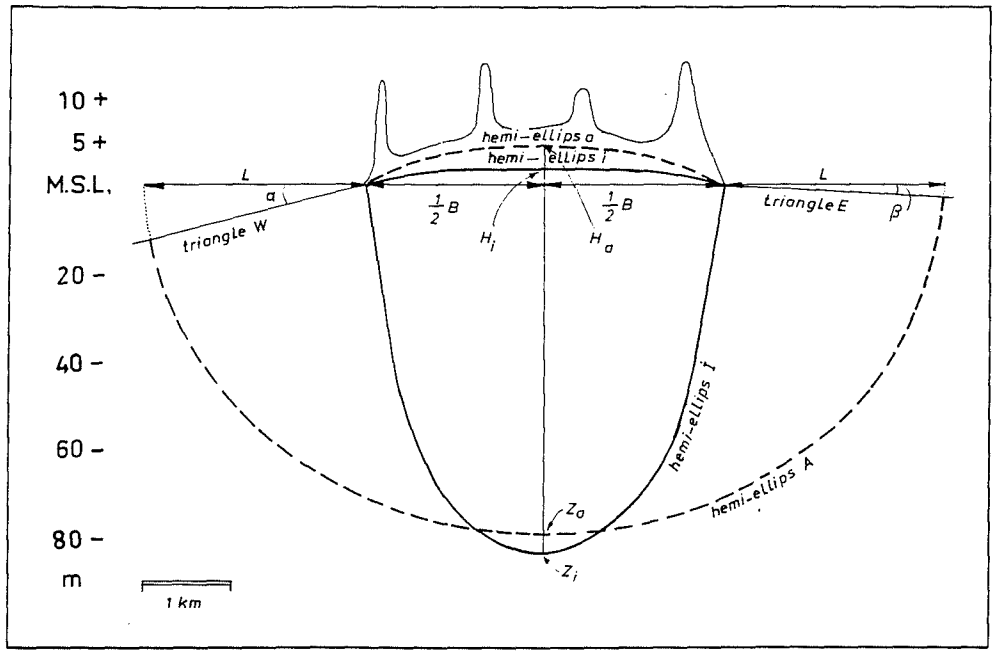

Fig. 3.19 The relative volumetric increase of the fresh water lens in consequence of vertical flow and anisotropy of the porous medium ($K_h > K_v$). This increase constitutes the correction factor f_1 in Eqs.3.11 and 3.12, with which the time of formation of a fresh water lens can be approximated. The factor f_1 (in this particular example being 2.1) can be approximated by consideration of the surfaces occupied by the hemi-ellipses A, a, I and i (note that, due to vertical exaggeration, the horizontal axis is their longitudinal axis) and the triangles E and W.
Constants in this case : N = 0.4 m/y; B = 4000 m; K_h = 28 m/d; c (anisotropic) = 8000 d; c (isotropic) = 3 d; ρ_s= 1.022; $\Delta H_s/\Delta X_s$ = 0 (no salt water flow); α = 0.4°; β = 0°; L = length of fresh water tongue. For definition of H_a, H_i, Z_a and Z_i see Eq.3.12.

And f_2 = correction factor in order to achieve the best fit with a more accurate, numerical solution by Bakker (1981) :

$$f_2 = 1.1693 + 1.2616\,(\frac{H_t}{H_\infty}) - 4.3889(\frac{H_t}{H_\infty})^2 + 3.669(\frac{H_t}{H_\infty})^3 \qquad (3.13)$$

with R^2 = 0.97 for $0.1 \le (H_t/H_\infty) \le 0.99$.
The magnitude of the correction factor f_1 depends most on the vertical flow resistance of aquitards within the flow domain of the lens : for c = 3, 1000, 4000 and 16000 d, with all other variables standard as indicated in Fig.3.18, it becomes 1, 1.25, 1.8 and 2.5, respectively. In the example presented in Fig.3.19, f_1 amounts to 2.1. The magnitude of f_2 varies in between 1.2 and 1.75.

The progress in the formation of a fresh water lens is shown in Fig.3.20, for an isotropic and anisotropic case. Growth proceeds almost linearly with time during the first 55%, which results in an advance of the expanding fresh water lens under the current boundary conditions, at x = ½B, of about 1.1 and 0.5 m/y for the isotropic and anisotropic case, respectively. For practical reasons 99% is taken as the state of equilibrium. Olsthoorn (1989) arrived at a comparable velocity for the isotropic case, with a numerical approach.

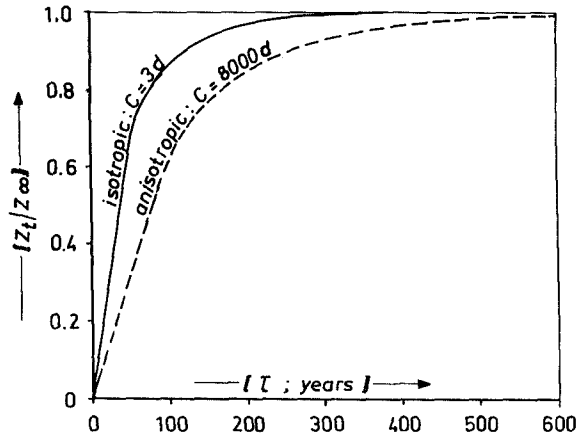

FIG. 3.20 Progress in the formation of a fresh water lens as a function of time, for an anisotropic and isotropic schematisation. Same boundary conditions as in Fig.3.19.

A decrease in natural recharge and density of the salt water and an increase in width and vertical flow resistance, raise the 99% formation time (Fig.3.18). Salt water flow inland has little effect on τ_{99} as there is a relatively small effect on Z_∞ (compare Δ2, Δ4 and Δ8 in Fig.3.18).

3.5.5 *Dispersion across the fresh-salt water interface*

The sharp interface between fresh and salt groundwater, which had to be assumed in the previous sections, has never been observed in reality. At the beginning of the 20th century, before large scale withdrawal of dune water from the second aquifer, the thickness of the transition zone between fresh dune water and salt North Sea water varied in the study area from 8 to 50 metres (Fig.3.21). The lowest values were found in the Zandvoort area at about 1-2.5 km from the High Water Line (HWL), where the groundwater divide for deep dune water was situated at that time. An increase can be concluded from that zone both seawards and inland, and is related to the length of subhorizontal flow as we shall see.

The main fundamental cause for the origin of a transition zone is hydrodynamic dispersion in the porous medium, which is activated by (a) normal circulation patterns within the fresh water lens, (b) natural changes in the shape of a fresh water lens, for instance by coastal erosion or accretion, long term changes in recharge and eustatic sea level fluctuations, (c) natural changes in salt water flow below the lens and (d) anthropogenic changes, as in case of pumping or artificial recharge.

An analytical approximation

A useful analytical solution was given by Bear & Todd (1960) and Verruijt (1971), for dispersive mixing between two fluids (here one fresh, the other salt) in a steady position. They flow in the same subhorizontal direction with equal velocity in an isotropic medium, without any mixing at their starting point of flow (Fig.3.22). The equation describing concentration as a function of time and the perpendicular distance to the interface then becomes, by the second diffusion law of Fick :

$$\frac{\partial c'}{\partial t} = D \cdot \frac{\partial^2 c'}{\partial z^2} \quad (3.14) \quad \text{with:} \quad c' = \frac{C - C_f}{C_s - C_f}$$

where : c' = the relative concentration of the conservative tracer [-]; C = concentration of conservative tracer [mg/l]; C_f = concentration of conservative tracer in upper, fresh fluid [mg/l]; C_s = ditto in the lower, salt fluid [mg/l]; D = hydrodynamical dispersion coefficient [m^2/d]; t = time [d]; z = shortest distance to the interface, upward positive [m].

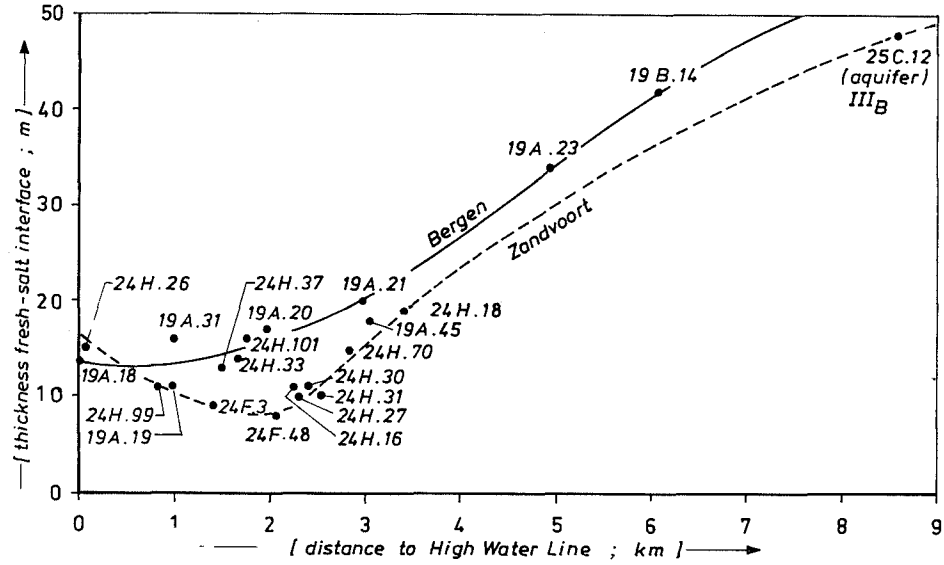

FIG. 3.21 Variation of the quasi-natural thickness of the transition zone (195 < Cl⁻ < 16340 mg/l) between fresh dune and salt North Sea water, with the distance of the observation wells to the mean high water line. Based on observations in the Bergen and Zandvoort area respectively, in the period 1903-1916, before the exploitation of deep dune groundwater started.

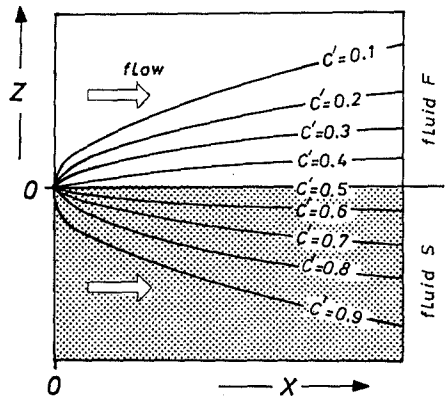

FIG. 3.22 The dispersive mixing between fresh and salt groundwater, in case of a steady position of both fluids, an equal flow velocity in the same subhorizontal direction, an isotropic medium and no mixing at the starting point of flow (slightly modified after Verruijt, 1971).

The hydrodynamical dispersion coefficient equals in this one-dimensional, dispersive flow case, the transversal dispersion coefficient D_T [m^2/d]:

$$D_T = \alpha_T v_w + D_d \qquad (3.15)$$

where : α_T = transversal dispersivity of the porous medium [m]; v_w = migration velocity of water or conservative tracer = flow velocity in the pores [m/d]; D_d = molecular diffusion coefficient [m^2/d], for Cl^- in porous media at 10°C being about 4 10^{-5} m^2/d (section 4.5.2).
In case of a fresh water lens with active internal circulation, yielding a v_w of about 0.01-0.06 m/d for the deepest flow line, and with α_T = 0.01 m, the diffusion coefficient contributes for about 10-30% to D_T.
With the boundary conditions C = C_f for t = 0 and z > 0, and C = C_s for t = 0 and z < 0, the analytical solution of Eq.3.14 becomes, for t > 0 and with neglect of diffusion (D_d = 0 in Eq.3.15) :

$$c'_{x,z} = 0.5\left[\,1 - erf\left(\frac{z}{2\sqrt{\alpha_T X}}\right)\right] \qquad (3.16)$$

where : $c'_{x,z}$ = c' as a function of X and z; X = total distance travelled in the direction of parallel flow [m]; erf = error function (max = +1 ; min = -1) [-].
Abramowitz & Stegun (1965) give the following approximation for erf, accurate to 0.0005 :

$$erf(X) = 1 - (1 + aX + bX^2 + cX^3 + dX^4)^{-4} \qquad (3.17)$$

where : a = 0.278393; b = 0.230389; c = 0.000972; d = 0.078108.
This equation holds for positive X only. Negative X are coped with by entering their absolute value in Eq.3.17 and taking -erf(X).

For practical reasons, the mixing zone can be delineated by c' = 0.01 and c'= 0.99, which implies a transition from 195 to 16,340 mg Cl^-/l when dealing with fresh and salt water of 30 and 16,500 mg Cl^-/l, respectively. The value c' = 0.01 implies that erf(z/[$2\sqrt{\alpha_T X}$]) be 0.98, which is true if z/[$2\sqrt{\alpha_T X}$] equals 1.645. This means $z = 3.29\sqrt{\alpha_T X}$, and the total width of the symmetrical transition zone ($D_{1\text{-}99}$) now becomes, in m :

$$D_{1\text{-}99} = 6.58\sqrt{\alpha_T X} \qquad (3.18)$$

Calculations compared with field data
Two chloride logs are presented in Fig.3.23, one close to the deep groundwater divide at that time (500 m in 1912) and the other about 4000 m downgradient inland. An excellent agreement is obtained with the calculated transition zone for well 19A.19 (Fig.3.23), using Eq.3.16 with X = 500 m, α_T = 0.01 m and 30 and 17,000 mg Cl^-/l for the fresh dune and salt North Sea end members. Discrepancies between the observed and calculated logs for well 19B.14 (Fig.3.23) can be attributed mainly to fresh water intrusion (Cl^- was 152 mg/l in 1912 and 32 mg/l in 1979 at 93 m-MSL).

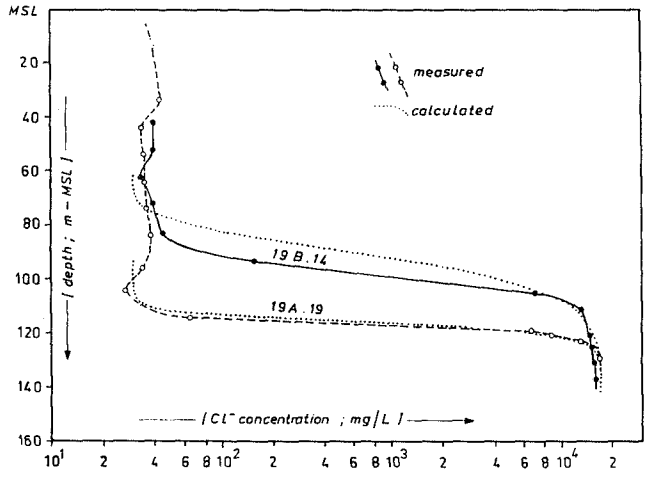

FIG. 3.23 Comparison of observed and calculated Cl^- logs for two piezometer nests in coastal dunes north of Bergen in 1912, before the onset of deep dune water exploitation. Observations on piezometers with a 1 m long screen derive from Van Oldenborgh (1915a). Calculations are based on Eq 3.16, using α_T = 0.01 m, X = 500 m for 19A.19 and 4000 m for 19B.14, 30 mg Cl^-/l for fresh dune water and 17,000 mg Cl^-/l for salt North Sea water.

For two situations D_{1-99} was calculated with Eq.3.18, using 0.01 m for α_T, as this value suited the data in Fig.3.23 :
(1) a free, symmetrical, isolated fresh water lens, i.e. without constraints imposed by the porous medium and with stagnant salt groundwater (see Fig.3.45). The result of calculation is shown in Fig.3.24A. Salt water flow is restricted to half the thickness of the mixing zone, in order to satisfy the condition of parallel flow. Although the boundary conditions differ in this flow case from the assumptions pertaining to Eq.3.18 — in course of time the lower parts of the transition zone are depleted in salt to some extent — , this equation still yields a good approximation as shown by Uffink (1990, p.132); and (2) a free, asymmetrical, salt-nested fresh water lens (see Fig.3.45), with a strong salt water flow inland. The calculated transition zone (Fig.3.24B) corresponds reasonably well with the field observations shown in Fig.3.21.

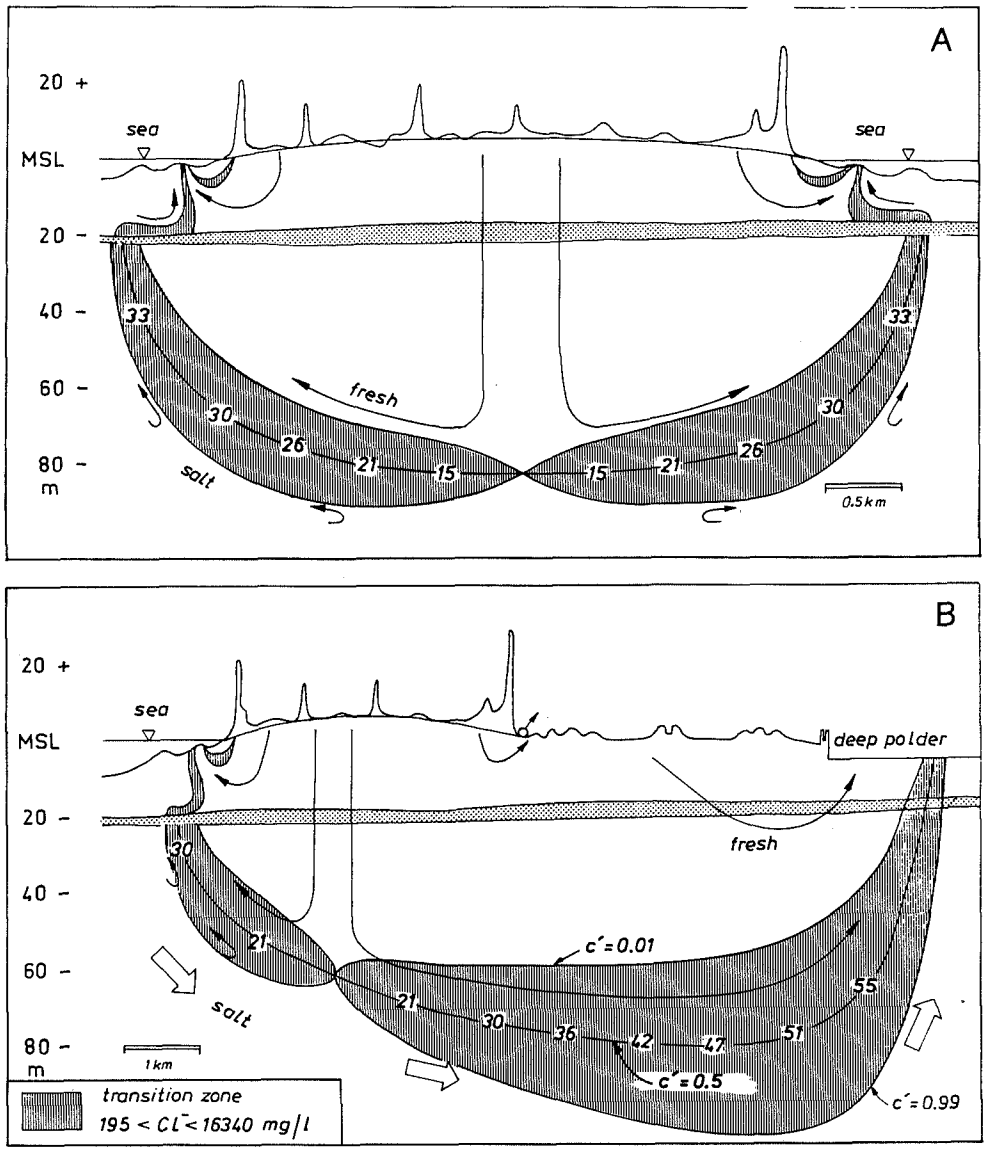

FIG. 3.24 Calculated hydrodynamic dispersion across the fresh/salt water interface of a symmetrical lens with stagnant salt groundwater (A) and an asymmetrical lens with salt groundwater flow (B), using Eq.3.18 with α_T= 0.01 m and X = 0 below the deep groundwater divide. Note that the narrowing of the transition zone in the second aquifer close to the stippled aquitard, is only apparent due to effects of vertical exaggeration. The transition zone in the upper aquifer has not been calculated but is based on observations by Lebbe (1981) and Cooper et al. (1964).
Numbers indicate the thickness of the transition zone D_{1-99} in m.

The calculated, very thin zone below and fringing the deep groundwater divide, is in both cases not realistic, however, mainly due to changes in the position of the groundwater divide and water table. As long as the transition zone is situated within a single aquifer, effects of anisotropy probably do not disrupt the practical validity of Verruijt's approximation, but will or must be included in the transversal dispersivity, which as a matter of fact also contains here some effects of diffusion.

3.6 Palaeohydrology and early-historical hydrology : the Quarternary period till 1850 AD

Although man already had its strong impact on and some knowledge of the hydrological situation in the Western Netherlands before 1850 AD, as evidenced by dikes, drainage canals, reclaimed land and river improvements, the true hydrological history started afterwards. It was about then, that the first groundwater observations were performed and documented (Rutgers Van Roozenburg et al., 1891), that the first groundwater was exploited and distributed for drinking water supply, from the dunes south of Zandvoort for the city of Amsterdam (Leeflang, 1974), and that the origin and movement of groundwater gradually became understood (De Vries, 1982). Let us start here with the palaeohydrology, which covers the period till 1000 AD, and the early-historical hydrology afterwards, and continue in section 3.7 with the period after 1850 AD.

The hydrological evolution of the study area during the whole Quarternary period, can be reconstructed on the basis of palaeogeographical studies conducted by Zagwijn (1974, 1986). The deduced evolution, with special attention to alternating and simultaneous fresh and salt water intrusions, is shown on a long time scale in Fig.3.25 and in detail for the past 7000 years in Fig.3.26. A brief description of the discerned stages is given below.

3.6.1 The Pleistocene

The prolonged deposition of clay-rich sediments in a marine and coastal environment during the Upper Tertiary, continued during the Early Pleistocene. The resulting Oosterhout Formation and Maassluis Formation contained and probably still contain connate brackish and salt water, entrapped under semi-stagnant conditions. This holds especially for the area north of the North Sea Canal, where the top of the Maassluis formation is found at great depth, namely below 240 m-MSL (Fig.3.4A).

A significant westward shift of the coastline occurred during the Upper Tiglian, some 1.8 million years ago. A substantial fluvial complex formed in the subsequent 1.6 million years, during which fresh water may have circulated actively and freshened the Upper-Maassluis Formation to some extent (Appelo & Geirnaert, 1983), mainly south of the North Sea Canal where its top reaches shallower depths (Fig.3.4A). A very deep circulation of fresh groundwater during glacial periods, was probably limited by deep permafrost.

The area north of Hillegom was invaded by a large North-European sheet of inland-ice during the Saalian glacial (Fig.3.4B and Enclosure 1.4). Permafrost probably occurred in the upper tens of metres of the soil during the most severe episodes, whereas fresh groundwater may have circulated during less cold episodes.

The onset of the Eemian interglacial caused a new transgression of the North Sea some 130,000 years ago, first through deeply incised valleys and former glacial basins and finally covering a large northern and small southern part of the area (Fig.3.4C). Salt water was included in the Eemian Formation and invaded the underlying deposits by its higher density.

The Weichselian glacial did not bring any cover of inland-ice but resulted again in a drop of the sea level by ca. 120 m, in permafrost and freshening. The Eemian salinization was probably washed out completely in this period, which lasted some 90,000 years. Only in very heavy glaciolacustrine varve clay and thick Eemian clay basins some traces could have been preserved.
The permafrost, with a thickness of approximately 20 metres (De Gans, 1991), may have resulted in cryoconcentration of salts in unfroozen groundwater just below freezing groundwater from which they were excluded and dissipated (Pomper, 1977). These brackish waters were probably washed out as well after melting of the permafrost.

3.6.2 The Holocene till 1000 AD

Sealevel rose with the melting of the Weichselian inland-ice. This continued during the first half of the Holocene period, till 5000 BC at a rather constant rate approximating 1 metre each century and slowing down to negligible rates around 3500 BC. Since then the relative sea level rise roughly amounts to 0.1 metre each century and is largely dominated by land subsidence (Zagwijn, 1986). The Holocene invasion of the area by the North Sea occurred in at least 10 distinct transgression phases (Fig.3.6).

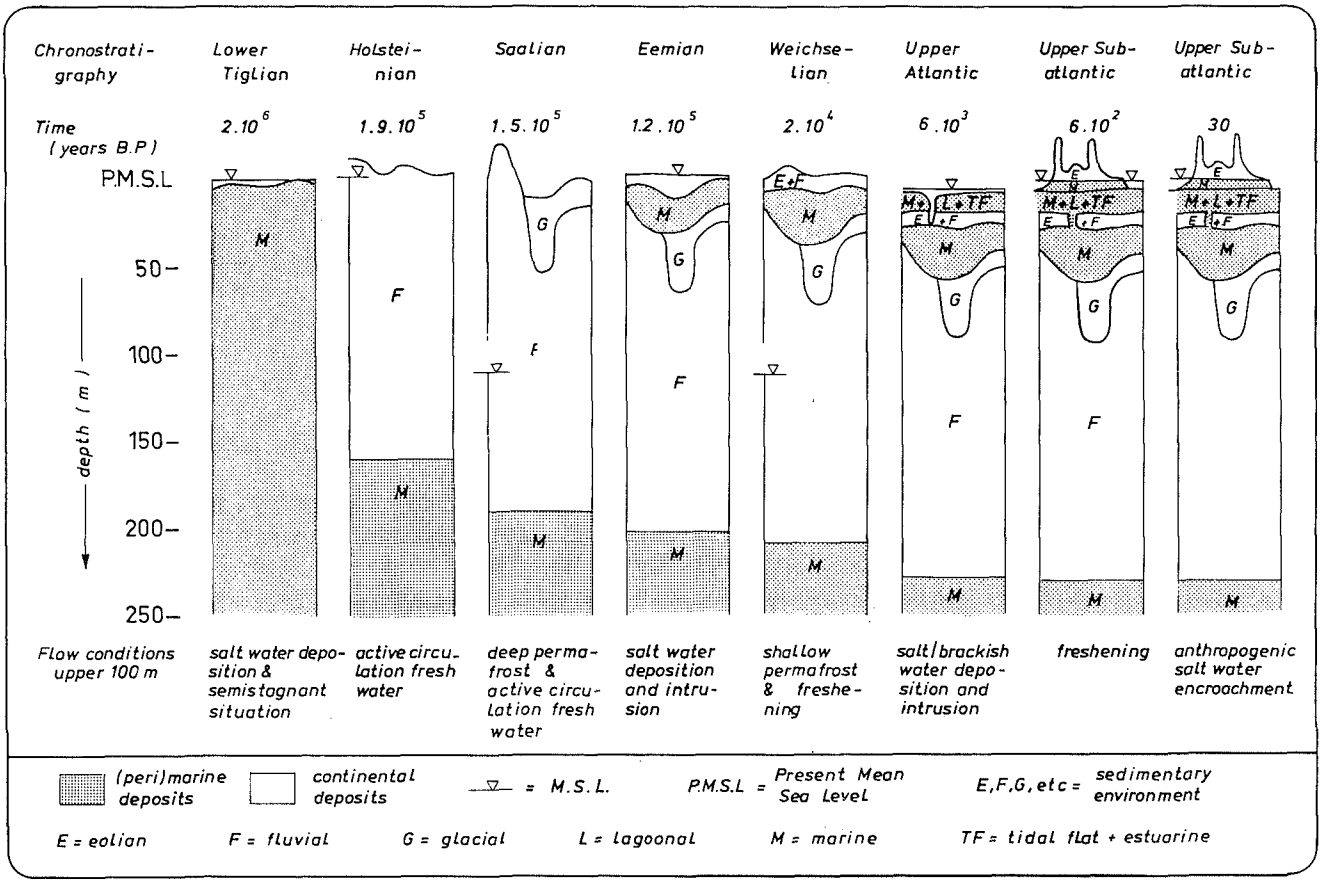

FIG. 3.25. Scheme of the geological and hydrological evolution of the coastal district of the Western Netherlands during the Quarternary period, with emphasis on sedimentary environments and flow conditions in the upper 100 metres.

The so-called "Basal peat" was formed in a landward shifting, fresh coastal swamp environment in between 6000 and 7000 BC. In the early Atlantic around 6000 BC, the area was drowned by a shallow brackish lagoon. Gradually the area changed into a tidal flat with less protection from the open sea by a landward migrating, discontinuous coastal barrier (Fig. 3.26, 5000 BC). The intrusion of North Sea and brackish waters took advantage of local and subregional marine erosion of basal peat and heavy lagoonal clay. The mechanism of intrusion consisted mainly of density driven flow (Versluys, 1918), which was calculated by Van der Molen (1989) and Gieske (1991) to reach a depth of 200-450 m in areas without resistant aquitards, within 50-400 years.

All residual, deep fresh water was forced out of the system or mixed with the invaded salt and brackish waters. North of the North Sea Canal the highest salinities were probably attained in consequence of remoteness from the river mouths (Fig.3.27 : 5500 BC). It should be realized that since this intrusion, density differences between groundwater offshore and in the tidal flats may have been sufficiently large for lateral intrusion as well (Witt & Wit, 1982).

Coastal barriers were formed seaward of the former one(s) in the period from 3800 BC till about 200 BC, due to a slowing down of the sealevel rise, an increase in the affluence of sediment and possibly a lowering of the tidal range. This led to the preservation of several barriers, each with its own, independent fresh water lens, separated by beach plains which acted as their drainage levels (Fig.3.26, 500 AD).

Around 3000 BC four tidal inlets cut through the coastal barrier system (Fig.3.27). Near Bergen-Alkmaar (inlet 1) and Beverwijk (inlet 3) North Sea water invaded and minor quantities of Rhine water were discharged. Near Katwijk (inlet 5) and Hoek van Holland (outlet 6) much larger quantities of Rhine water were discharged. In the period 3000 till 1250 BC the tidal inlet near Bergen gradually narrowed and nearly closed. The inlet near Beverwijk shifted to the north, narrowed considerably but gained in importance as an outlet for Rhine water. And the Old Rhine inlet gradually changed into the main outlet for the Rhine.

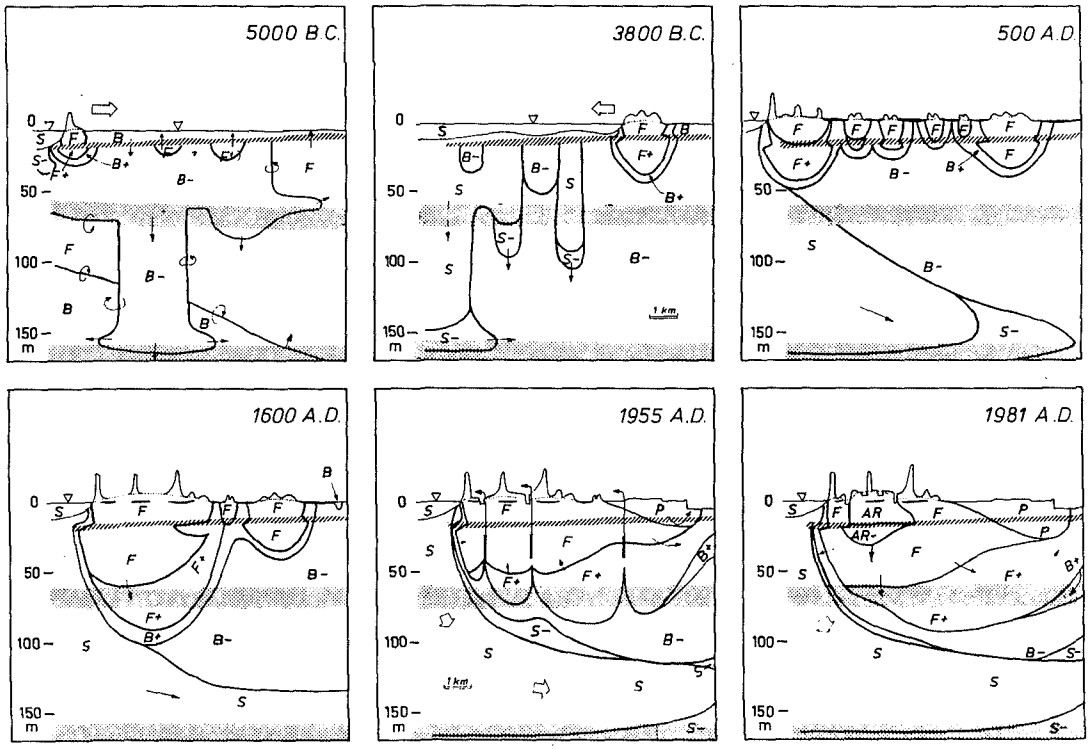

FIG. 3.26. Scheme of the geological and hydrochemical evolution of the coastal dune area of the Western Netherlands in the Haarlem - Hillegom area, during the past 7000 years.
AR = artificially recharged Rhine water; P = polder water, mainly composed of Rhine water; F = fresh (since 3000 BC dune water only); B = brackish (300 < Cl ⁻ < 10,000 mg/l); S = salt; + = freshened; - = salinized; + nor - = without base exchange.

The reduced marine influence manifested itself in the formation of low and later high moors in the coastal plain, the so-called "Holland peat" (Fig.3.27 : 1250 BC). Where high moors developed, fresh water pockets may have formed (De Ruiter, 1990).

The outlet near Castricum, the so-called Oer-IJ estuary (outlet 3 in Fig.3.27), practically silted up about 200 BC (Jelgersma et al., 1970), the remnants of the former Bergen inlet completely closed in 900 AD (Pons & Van Oosten, 1974) and the river mouth of the Old Rhine became choked around 850 AD (Van der Meer, 1952).

The shape and size of the fresh water lenses in Fig.3.26 (500 AD) were calculated using formula 3.6 through 3.8 with N = 0.4 m/y, appropriate hydraulic constants, present-day or estimated widths of the coastal barriers (250-2500 m), ρ_s= 1.022 and no salt water flow. The assumption about the density of the salt water is rather critical, because of its strong impact on the equilibrium depth to the fresh-salt interface (Fig.3.18). The high chlorinity is assumed because of the open marine environment along the western shore line of the beach barriers at the time of their formation and a sufficiently large distance to the river mouths for the considered section.

The 99% formation time of the fresh water lenses as calculated with Eq.3.11, varies in between 30 and 450 years for the considered barriers with a width of 250 and 2500 m, respectively (Fig.3.18).

3.6.3 The Holocene from 1000 till 1550 AD

Around 1000 AD, marine erosion resulted in an eastward shift of the coastline, a steepening of the sea floor and the formation in ca. 200 years of the younger dunes, which were blown over several older dune ridges and over several interspaced beach plains rich in peat (Zagwijn, 1984). Many small hydrological dune systems were thus united into one 4 to 5 km wide dune system, wider than any old dune system before. Consequently the fresh water lens had to expand according to Eqs.3.6 -3.8, as all other boundary conditions remained practically constant (Fig.3.26, 1600 AD).

This growth probably took 250-400 years in order to reach 99% of the new equilibrium state, a time-span obtained by applying Eq.3.11 to several cross sections with subtraction of the time which would have been required to attain the previous size and shape under the new circumstances (Stuyfzand, 1985a, 1987d, 1988b).

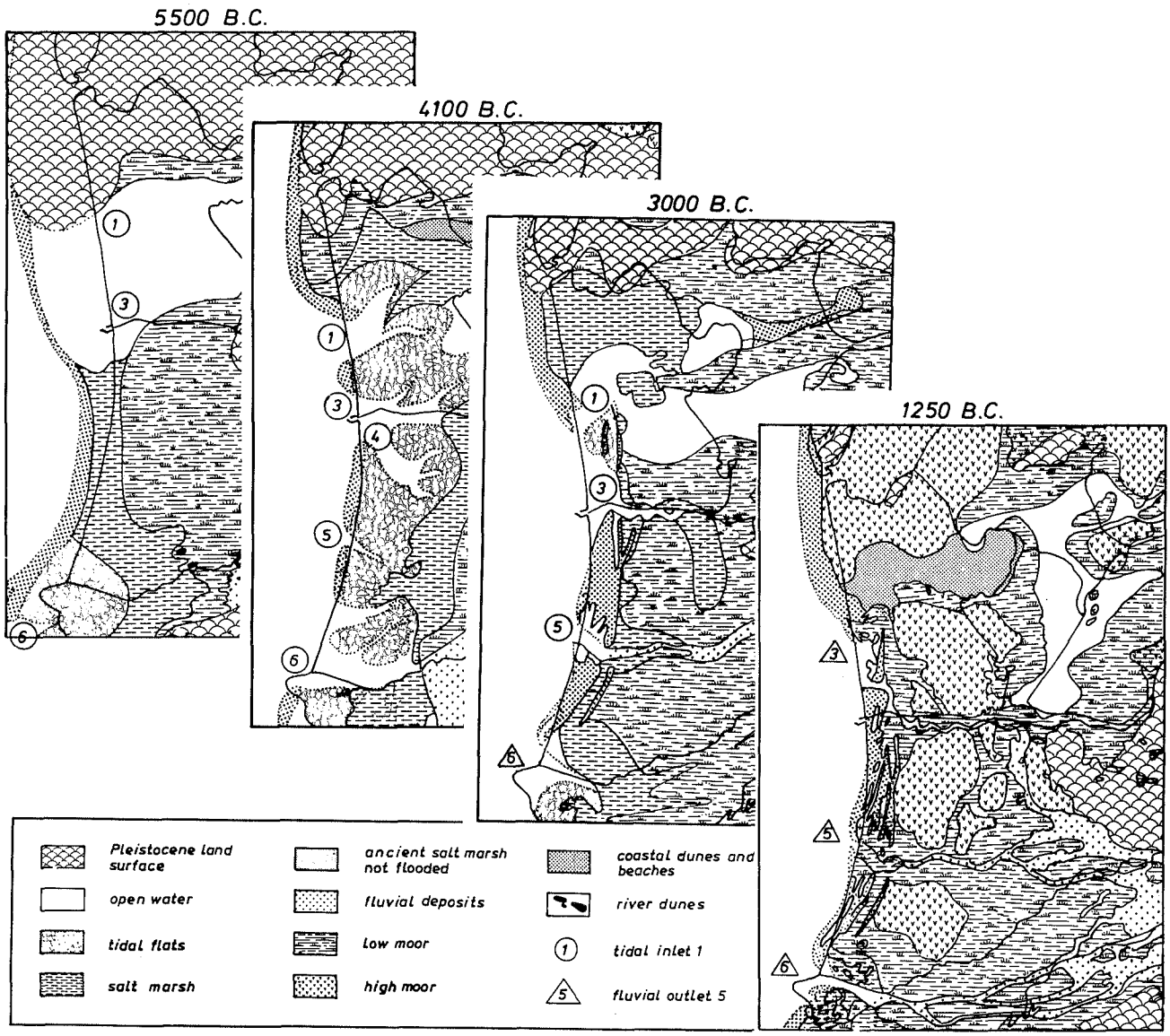

FIG. 3.27 Palaeogeographical situation of the Western Netherlands around 5500, 4100, 3000 and 1250 BC (redrawn fragments from maps by Zagwijn, 1986). The Holocene transgression yielded the most saline conditions for the longest time in the study area, to the north of the North Sea canal in the neighbourhood of Bergen-Alkmaar (inlet 1). Numbering of tidal inlets, with time of main activity within brackets was slightly modified after Roep et al. (1991) : 1 = Alkmaar-Bergen (6000-1650 BC); 2 = Uitgeest (not shown; 4400-3100 BC); 3 = Oer-IJ (5000-1250 BC; continued as fluvial outlet 1250-50 BC); 4 = Hoofddorp (5000-4000 BC); 5 = Oude Rijn (4400-2600 BC; continued as Old Rhine outlet 2600 BC - 850 AD); 6 = Rijswijk-Hoek van Holland (6000-4300 BC; continued as Rhine outlet).

Geological evidence from dated peat layers clearly reflects the rise in the groundwater table during and up to at least three centuries after widening of the dune system (Fig.3.28). This agrees well with the calculated 250-400 years, when we consider that the ultimate groundwater table submerged the shallowest wet dune soils, that were studied by Zagwijn (1984). The expanding fresh water lens generated freshening water types within and around the lens (Fig.3.26, 1600 AD; see further section 4.4), and some salinization along its sides due to volumetric compensation.

The area behind the dunes was strongly influenced in this period by man and Dunkirk III transgressions especially from the north. Already since 800 AD marshland was drained and peat was dug for heating mainly (Hallewas, 1984). The resulting land subsidence and increased marine invasions especially in the period 1100-1200 AD, necessitated the building of an extensive network of dykes and dams, which was more or less completed around 1200 AD. Nevertheless vast peat lands were

lost to the sea slightly north of Alkmaar, whereas erosional scars in the form of lakes gradually enlarged in a northeasterly direction by wave action. Part of the lakes was directly formed due to peat cutting and dredging, especially in the area south of the Old Rhine.
The disappearance of the raised peat bogs together with marine transgressions caused the vanishing or contraction of the shallow fresh water lenses there, if these existed at all.

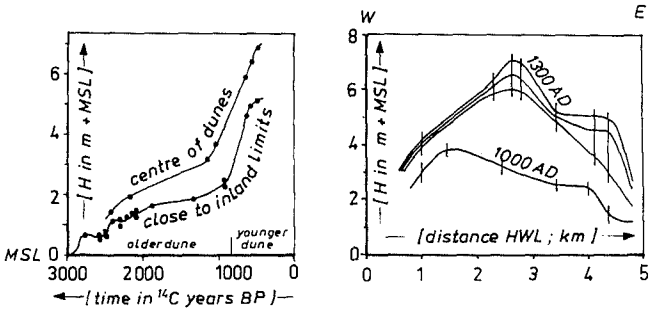

FIG. 3.28 Changes in the height of the water table in coastal dunes south of Zandvoort, as deduced from the position of dated, wet dune soils and dated peat levels corrected for compaction (From Zagwijn, 1984).

The beach barrier and beach plain landscape was dewatered since about 1000 AD, as evidenced by still existing canals especially in the surroundings of The Hague (De Mulder et al., 1983).

3.6.4 The Holocene from 1550 till 1850 AD

Lakes behind the dunes north of Castricum, near Lisse and near Leidschendam-Voorschoten were reclaimed during this period (Fig.3.1 and Enclosure 1.1), using wind mills. The more difficult lakes followed after 1850 AD when mechanical pumps arrived. An intricate network of drainage ditches was dug into the new or recuperated land, in order to discharge excessive seepage water to strategical positions, where it was pumped out on the so-called boezem.

The *boezem* is the main water course in the polder landscape (Fig.3.29). It is composed of interconnected lakes and canals, with the highest controlled water level in the surroundings, which is often well above the adjacent polder surface. The boezem served in this period mainly as a drainage artery and as a storage reservoir to tide over periods in which discharge to the sea or Rhine was impossible.

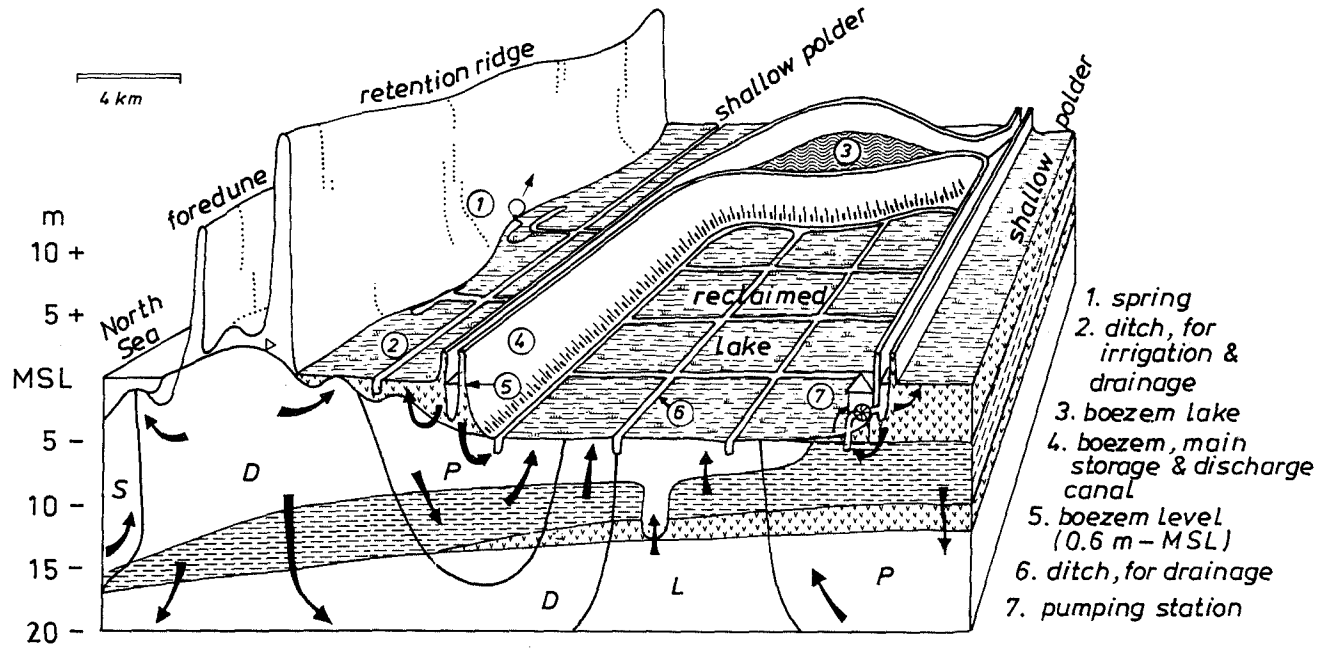

FIG. 3.29 Hydrological scheme of a deep Dutch polder (a reclaimed lake), with surrounding shallow polders, the boezem and flow patterns. D = dune water; L = relict Holocene transgression water; P = polder water; S = North Sea water.

The artificial lowering of the base level in the reclaimed lakes with 2-5 meters, triggered an eastward expansion of the younger dunes flow system, generated polder flow systems in between dunes and reclaimed lakes, and enhanced the intrusion of North Sea water (Fig.3.26, 1955 AD).

The polder system partly substituted for isolated dune water lenses, which had not been incorporated into the enlarged younger dunes system. There are two main reasons for this change. First, the beach barrier and beach plain landscape was gradually transformed into a shallow polder area, especially since the 18th century when large parts of the older dune ridges were levelled for the cultivation of flower bulbs. These bulbs require a sandy soil with shallow groundwater tables and a dense network of canals, drainage and irrigation ditches (Van der Meer, 1952). And second, the rain water was exported by sewers in built-up areas, especially since ± 1920 AD. Most shallow polders were pumped already since about 1670 AD (Van der Meer, 1952).

On a local scale the water table dropped in the younger dunes, for various reasons. Cultivation and drainage of dune valleys in the younger dunes, started for instance in the Breesaap near IJmuiden around 1600 AD (Pruissers et al., 1991) and in the drainage area of the Hoepbeek near Castricum (Enclosure 3.1) around 1820. The quarrying of dune sand from the retention ridge notably since the 18th century, was accompanied by the digging of a drainage canal penetrating hundreds of metres into the dunes near Hargen (north of Schoorl) and Overveen. Also the construction of shipping canals and discharge canals, like the Uitwateringskanaal near Scheveningen (in between 1850 and 1909) and the Scheveningsch Canal (before 1850) strongly increased the drainage of the local dune area. And coastal erosion especially north of Egmond aan Zee (Enclosure 1.1; Rakhorst, 1991) and south of Scheveningen (Klijn, 1981; Wiersma, 1991) had a strong impact. In 1823 a dyke was completed north of Camperduin, as a substitution for the coastal dunes, which had been completely eroded away by the North Sea. The coastal defence in the Scheveningen - Hoek van Holland area and to the north of Bergen aan Zee consisted of the construction of breakwaters, somewhere in the period 1790-1900.

Mean phreatic levels around 1850 AD have been reconstructed for the dunes in the Noordwijk-Camperduin area (Enclosure 3.1), by contouring the position of dune valleys and deflation plains unaffected by excavation or recent erosion, from detailed topographic maps (1 to 5,000 or 10,000). The principle is explained and justified in section 3.2.3. Dune brooks and other topographical details have been derived from a map prepared by Uitwaterende Sluizen in 1781 and from the first official topographical maps 1:50,000 in the period 1850-1900 (Wolters-Noordhoff, 1990).

3.7 Historical hydrology : the period after 1850 AD

As stated at the beginning of the previous section, 1850 AD may be seen as the onset of the era of historical hydrology in The Netherlands. Since then an ever multiplying amount of hydrological data and hydrological reports has been produced, especially regarding the studied coastal area, where the exponential growth of population was the largest in the country.

The beginning of the new era coincides with the start of public drinking water supply in 1853, using shallow groundwater from the dunes south of Zandvoort aan Zee for the city of Amsterdam. Groundwater abstraction from the dunes is shown to be one of the main transformers of the hydrological situation in this period. It is dominated by salinization, declining water tables and artificial recharge. The changes in a cross section north of Scheveningen (Fig.3.30) illustrate what happened in many dune areas. The deep expansion of recharged river water and the change over from river Rhine to Meuse water, are however unique for this dune area.

3.7.1 The period 1850 - 1903

This episode is dominated by three major events. The first is the reclamation of several deep lakes with steam power : the Haarlemmermeer in 1852, Wijkermeer and IJ in 1872 and several polders east of The Hague (Fig.3.1 and Enclosure 1.1). The nature of their effect has been described already in the previous section dealing with the period 1550-1850 AD. Flow systems in dunes and adjacent polders in between Monster and Leidschendam and in between Lisse and Heemskerk became influenced now by their deep artificial base levels.

The second event is the digging of the North Sea Canal in the period 1865-1876, in order to improve the access to the sea port of Amsterdam. Low water levels in this canal (0.5 m-MSL), caused a very heavy drainage of the cleaved dunes, with former water levels well above 8 m+MSL, and consequently triggered a strong salinization of the deep groundwaters. Another effect was the introduction of sea water into the surface water of the canal mainly by locking through the sluices.

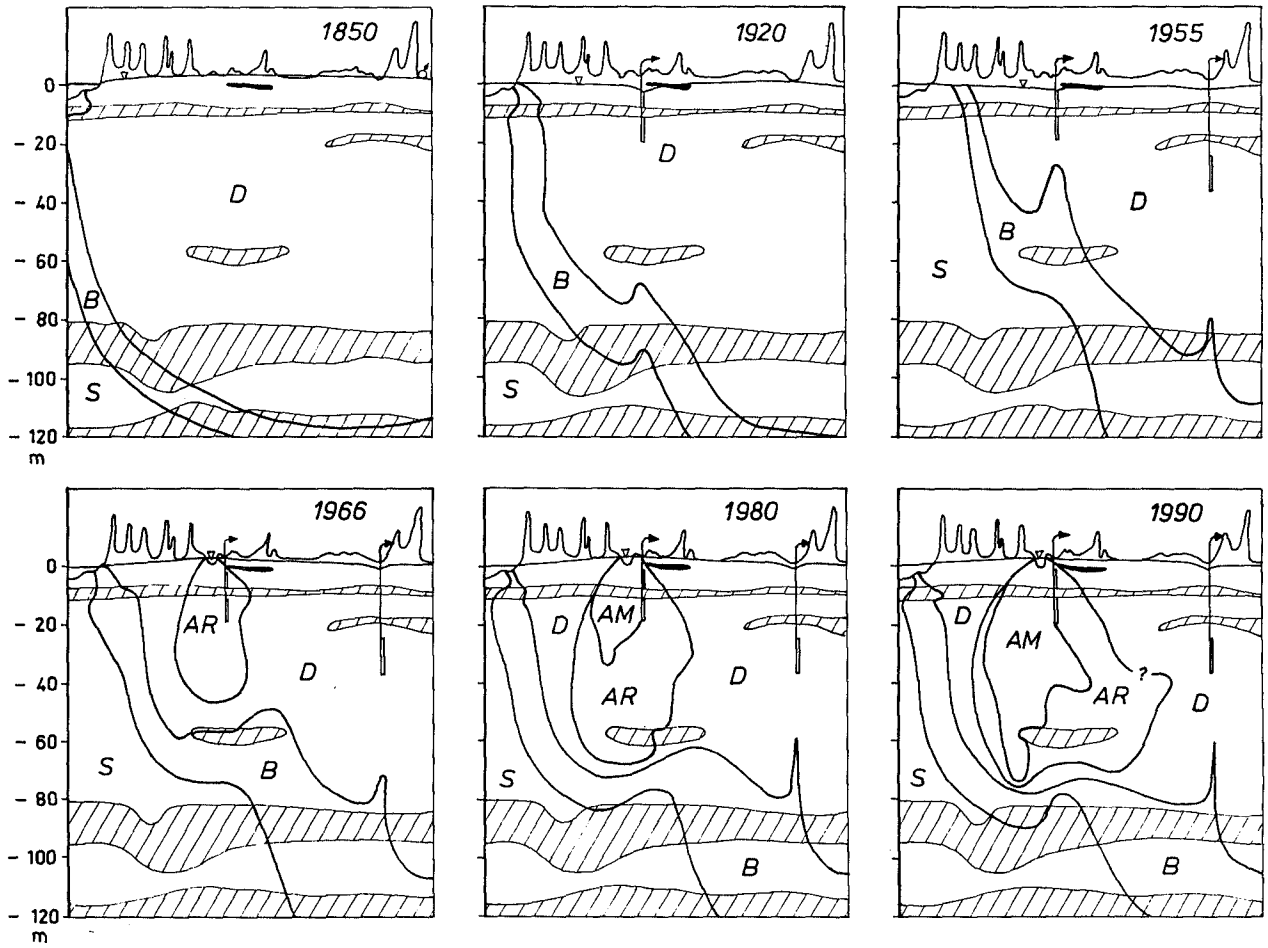

FIG. 3.30 Salinization till 1956 AD and subsequent freshening in a cross section over the West-Meijendel dunes, north of Scheveningen (see Fig.3.1), in the period 1850-1990. Groundwater pumping started in the west in 1874 and in the east around 1930. Artificial recharge of river Rhine water commenced in 1956. The intake of Rhine water was closed in 1976, in order to continue the recharge with river Meuse water of lower salinity. AM = fresh, artificially recharged Meuse water; AR = fresh, artificially recharged Rhine water; B = brackish water (300 < Cl^- < 10,000 mg/l); D = fresh, dune water; S = salt North Sea water.

And the third is the gradual increase in dune water exploitation from the upper aquifer, for drinking water supply. After Leiduin in 1853, the following pumping stations were put in operation : Scheveningen in 1874, Katwijk in 1878, Wijk aan Zee and Bergen in 1885, Monster in 1887, Overveen and Voorburg in 1898, and IJmuiden-West in 1899 (Table 3.6 and Fig.3.1).
Dune water was abstracted from the upper aquifer by dug channels and shallow wells. The total production was 17.10^6 m^3 for the year 1900 (Fig.3.31). The rising water demand was met by extension or deepening of the channel system or by increasing the number of wells. The groundwater table gradually dropped, as can be seen in Fig.3.32. By 1903 water tables reached about their minimum level in the catchment area of Amsterdam, south of Zandvoort, after 50 years of exploitation (Fig.3.32). It has been calculated that the fresh-salt water interface was drawn up about 5 metres there at that time (Stuyfzand, 1988b p.86-89; Fig.3.35 this thesis).

With the completion of the last steam pumping station at the former mouth of the Old Rhine in 1880, the level of Rijnlands Boezem could be maintained at a constant level of 0.6 m-MSL. This triggered a further increase in the cultivation of flower bulbs at the expense of older dune ridges (Van der Meer, 1952), and caused a further supersession of old dune flow systems by shallow polder systems. The more precise water level control was induced by ever increasing economical

constraints : a fall could be followed by irreversible land subsidence, by the disintegration of building foundations and canal linings, by crossing the interests of agriculture, navigation and later also of recreation and nature preservation.

The boezem received an additional task : the flushing of the main water courses, which suffered from salt pumped out of reclaimed lakes and from pollution caused by domestic sewage effluent and industrial wastes (Van Rees Vellinga et al., 1981).

3.7.2 The period 1903 - 1955

The most important feature of this episode is the wide application of deep wells for pumping dune water from the second aquifer. This gradually resulted in true mining and salinization problems (Fig.3.26, 1955 AD).

With the strongly disputed Ghyben-Herzberg principle (section 3.5.1) in mind, the director of the municipal watersupply of Amsterdam, Pennink, commanded in 1902 the discovery of a vast stock of fresh water in the dunes south of Zandvoort aan Zee. The results have been documented by Hoogesteeger (1905). In the subsequent 30 years deep dune water was more or less explored in all other areas (Dubois, 1909; Beijerink et al., 1909; Van Oldenborgh, 1915a, 1915b, 1916; RvD, 1933). The depth to the fresh-brackish interface (300 mg Cl^-/l) was detected around the following pumping stations, in order from north to south : at about 130 (Bergen), 110 (Castricum), 60 (Wijk aan Zee), 120 (IJmuiden-North), 140 (Bloemendaal), 110 (Leiduin), 55 (Katwijk), 110 (Scheveningen) and 55 m-MSL (Monster).

TABLE 3.6 Data on all groundwater pumping stations for drinking water supply in the coastal dunes of the Western Netherlands, in order from north to south. The numbers correspond with the locations in Fig.3.1.

PUMPING STATION		water	ABSTRACTION				ARTIFICIAL RECHARGE			Cl^--CONCENTRATION mg/l		
nr.	location	supply company (anno 1991)	since	stopped	total 1989 10^6 m^3	depth 1989 @ m-MSL	since	total 1989 10^6 m^3	source ##	onset abstraction	before closedown or artificial recharge	anno 1989
1	Bergen	PWN	1885	-	2.4	9-69				31	-	75
2	Egmond a. Zee	PWN	1915	1961	0.2*	5-10	-	-	-	47	82	-
3	Castricum	PWN	1924	-	24.0	4-39	1957	20.8	B,A[1]	40	48	178
4	Wijk a. Zee	PWN	1885		13.0	2-40	1975	12.3	B,A[2]	38	69	122
5	IJmuiden-North	WLZK	1916		0.2	26-66	-	-	-	36	280	-
6	IJmuiden-West	WLZK	1899		0.5	27-37				54[a]	-	150
7	IJmuiden-South	WLZK	1964		1.6	25-38				39		62
8	Santpoort	WLZK	1940		1.6	22-44				42[d]		53
9	Bloemendaal	WLZK	1904		1.1	25-45	-	-	-	31	-	70
10	Overveen	WLZK	1898		9.5	0-6+25-40	1975	1.0	B	32	43	78
11	Kraantje Lek	WLZK	1964		1.0	22-35	-	-	-	27	-	42
12	Bentveld	WLZK	1929		0.2	25-38	-	-	-	29	168[b]	45
13	Leiduin	GW	1853	-	66.0	0-3+25-35	1957	56.8	B	30	57	121
14	Bennebroek	PWN	1933	1948	0.7*	27-43	-	-	-	55	87	-
15	Hillegom	GH	1925	1982	1.6*	25-33				28	191	-
16	Noordwijk	EWR	1919	-	1.5	20-30				29	-	62
17	Voorhout	GVh	1929	1956	0.2*	25-35?	-	-	-	40	373	-
18	Katwijk	EWR	1878	-	22.3	0-3+25-30	1940	20.4	E,D[3]	55	33	93
19	Voorschoten	GVs	1909	1970	0.2*	25-35?	-	-	-	51	424	-
20	Wassenaar	GW	1928	1969	2.6*	25-35?	-	-	-	21	45	-
21	Scheveningen	DZH	1874	-	48.2	0-18+25-40	1955	51.8	C,D[4]	32	55	61
22	Voorburg	VWM	1898	1960	2.0*	25-35?	-	-	-	75	280	-
23	Monster	WDM	1887	-	5.1	0-10	1970	5.4	F,D[5]	86[c]	186	80

a = 1957; b = 1962, since then Cl^- lowered due to reduced abstraction; c = 1926; d = 1962; * = total during best years; @ = or before closedown;
: A = Rhine water from Lake IJssel near Andijk; B = Rhine water from Lekkanaal Nieuwegein; C = Rhine water from Lek near Bergambacht; D = Meuse water from Afgedamde Maas near Brakel; E = Rhine boezem water from adjacent polder; F = Rhine boezem water from Delflands boezem;
1 = since 2nd quarter 1989; 2 = since June 1981; 3 = since May 1988 in southern area; 4 = since March 1976; 5 = since November 1983.

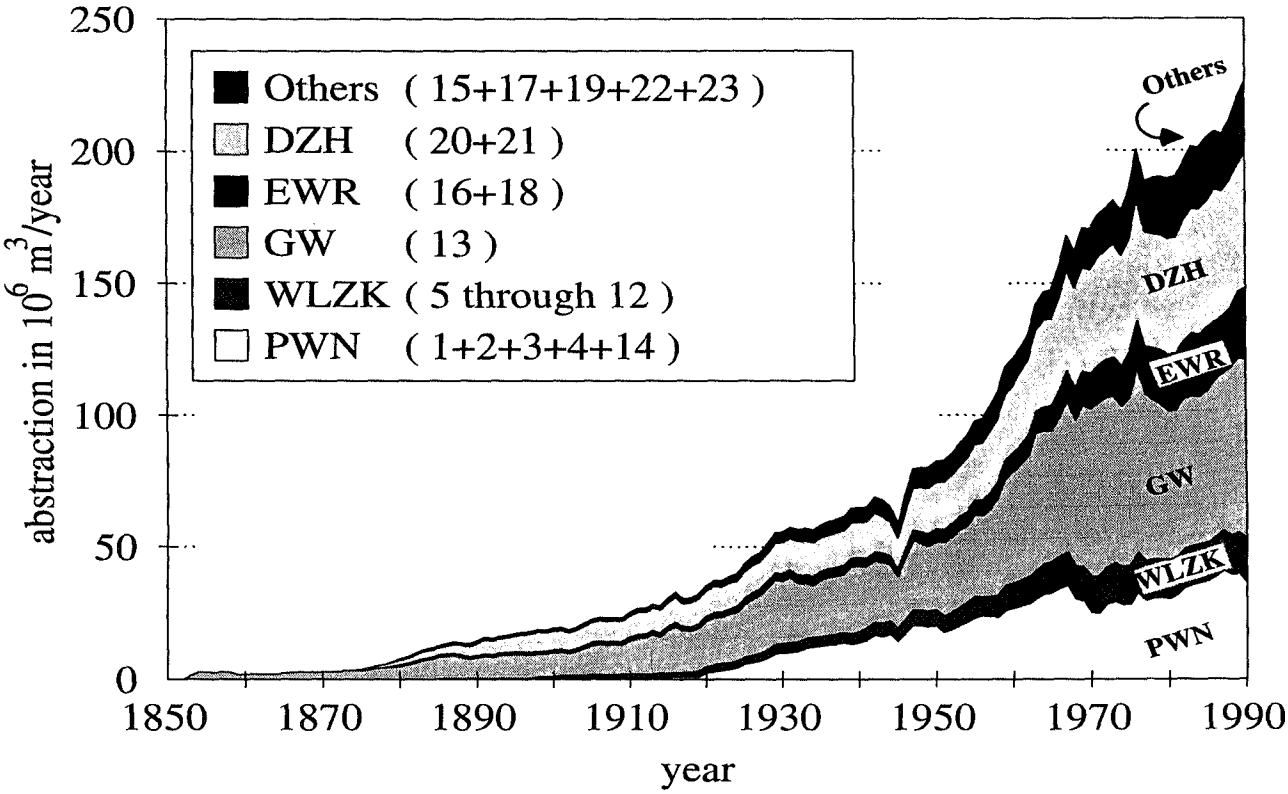

FIG. 3.31 Historical annual totals of groundwater abstraction from the dunes, for public drinking water supply by the indicated companies (for explanation see Units and Abbreviations). The numbers refer to the pumping stations in Fig.3.1 and Table 3.6.

The first batteries of deep pumping wells for public water supply were completed in 1903 in the dunes south of Zandvoort aan Zee. The already existing pumping stations followed rapidly, forced by a growing demand for drinking water, and most of the 12 new pumping stations in this period (Table 3.6 and Fig.3.1) exploited deep dune water. The total abstraction rapidly increased from $17 \cdot 10^6$ to 96.10^6 m^3/year (Fig.3.31). The mining of the deep dune water resulted of course in a strong decline of the piezometric head in the second aquifer (Fig.3.33) and caused a rise of the fresh-salt water interface (Figs. 3.34 and 3.35).

Industry became another important consumer of dune groundwater especially in urban areas, like Alkmaar, Beverwijk, IJmuiden, Haarlem, Katwijk and The Hague and in the industrial zone north of IJmuiden, where the Hoogovens steel production complex settled in 1918. In urban areas dune water was abstracted from the second aquifer mainly, in quantities increasing from approximately $7 \cdot 10^6$ to approximately $50 \cdot 10^6$ m^3/y by the end of this period. Hoogovens and Royal Paper Mills Van Gelder & Sons Ltd, both in the IJmuiden area, had the largest abstraction of deep dune water, about $20 \cdot 10^6$ m^3/y each.

Synchronous to the mining of deep dune water, several important events reduced the natural recharge of the dunes and increased their discharge. After settlement of the Hoogovens steel production complex in 1918, major extensions of the harbour of IJmuiden, first mainly a fishing port, followed in 1930 (and 1968). These led to further losses of younger dunes and enhanced the drainage of dune water and further salinization.

Most changes in land-use of the younger dunes in between 1850 and 1980, took shape and had their initial effects in this period (Table 3.5) : The increase in built-up areas meant the export of rain and sewer water out of the younger dunes especially in IJmuiden, Katwijk aan Zee and The Hague. Changes in dune vegetation (section 3.2.5) resulted in a net decrease in natural recharge as well. Lysimetric observations with different vegetations near pumping station Castricum, demonstrated this already after about ten years of growth (Fig.3.13; Wind, 1958) and contributed to the decision to halt further afforestations of the dune water catchment areas.

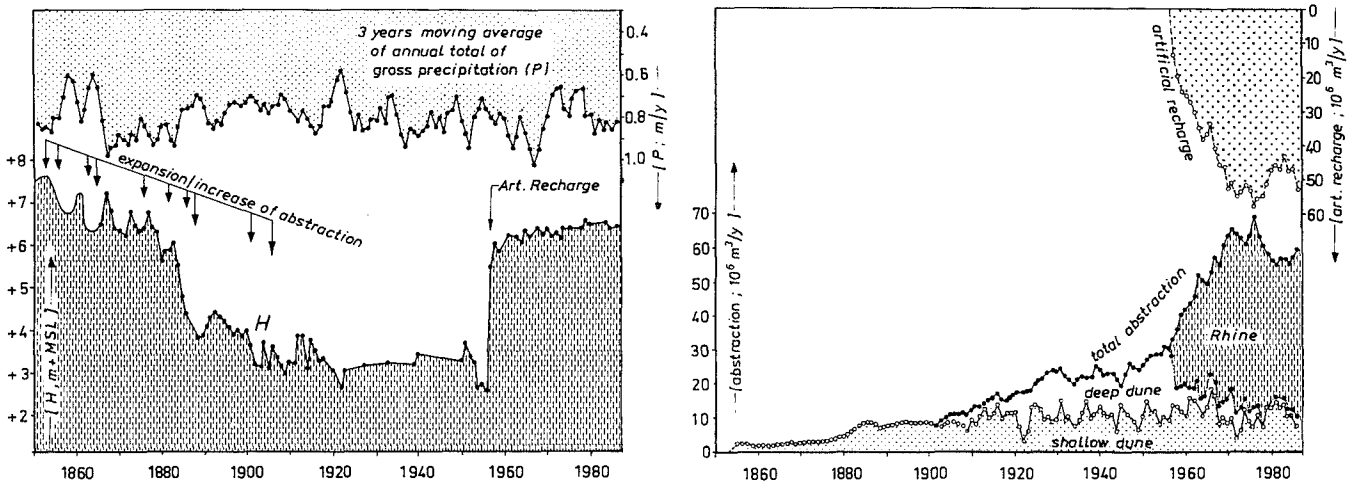

FIG. 3.32 Historical changes in : the annual mean position of the groundwater table (H) in the centre of the dunes south of Zandvoort aan Zee; the 3-years moving average of local gross precipitation (P); and groundwater withdrawal and replenishment in the Zandvoort area by Gemeentewaterleidingen. Art. Recharge = start of artificial recharge with pretreated Rhine water.

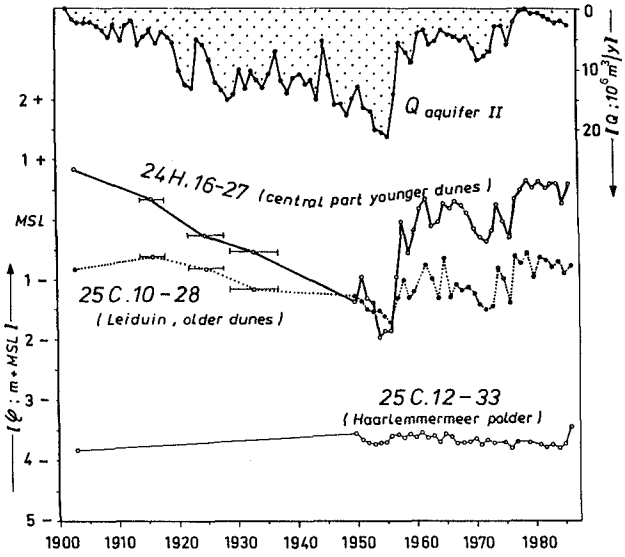

FIG. 3.33 Historical changes of the piezometric head of fresh dune water in the second, semi-confined aquifer south of Zandvoort aan Zee, as related to the abstraction (Q) of dune water from the second aquifer by pumping station Leiduin (no. 13 in Fig.3.1). Groundwater is withdrawn in the close surroundings of piezometer 24H.16-27, about 1 km from 25C.10-28 and 4 km from 25C.12-33.

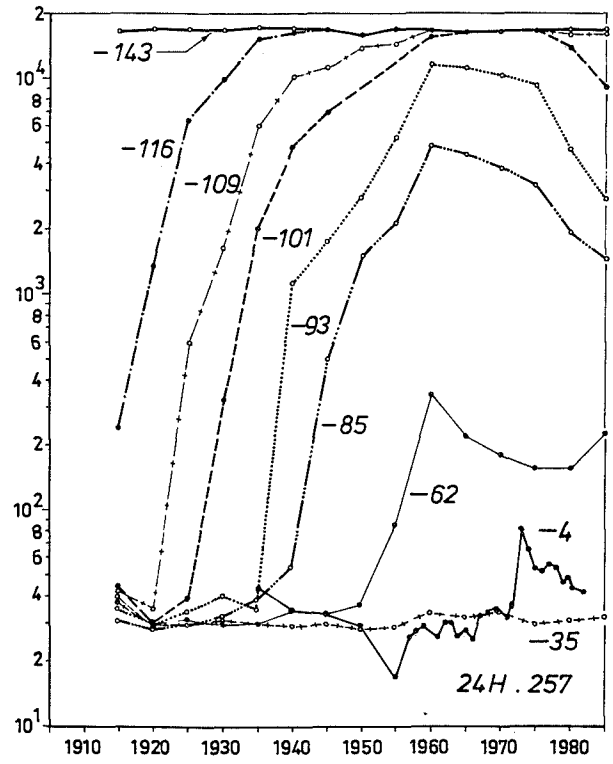

FIG. 3.34 Salinization phenomena in piezometer nest 24H.257, about 2 km east of Zandvoort aan Zee, in between two groundwater abstractions : well field Bentveld (no. 12 in Fig.3.1) and the Boog canal (part of the catchment area Leiduin, no. 13 in Fig.3.1). The fresh-brackish water interface rose by 51 m in the period 1915-1960, after which it slightly subsided due reduced rates of pumping.

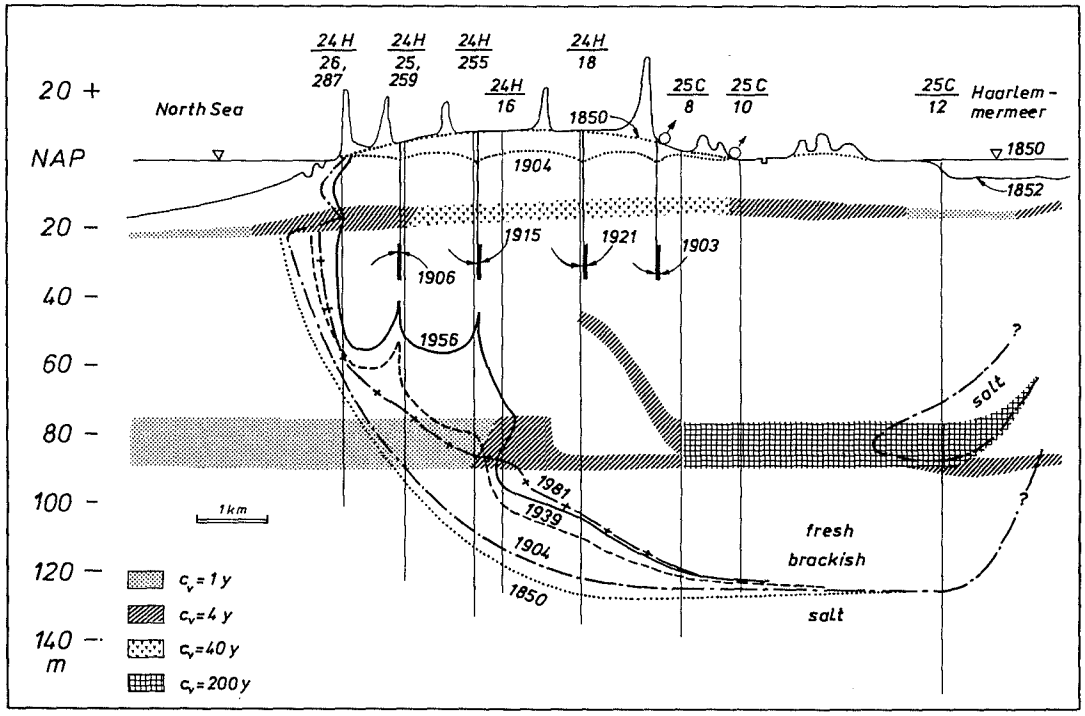

FIG. 3.35 Changes in the position of the fresh-salt water interface (8250 mg Cl⁻/l) in a schematized cross section over the dunes south of Zandvoort aan Zee. The year 1850 represents the calculated natural situation; 1903 yields the situation observed after 50 years of shallow dune water abstraction, just before the onset of deep dune water exploitation; 1956 gives the observed situation before the start of artificial recharge; and 1981 represents the situation observed after 25 years of artificial recharge, about 130 years after reclamation of the Haarlemmermeer.

Increases in (sub)urban areas and flower bulb cultivation lots on the beach barriers, led to a further expansion of the polder flow system at the expense of old dune flow systems, especially near Alkmaar, Beverwijk, Haarlem and The Hague.

In the deep reclaimed lakes, where methane-rich groundwater wells up by itself, numerous gas wells were installed since 1895 for domestic energy supply on farms (Ribbius, 1898; De Voogd, 1941; Bol, 1991). Details on their construction and operation are given in Fig.3.36. The gas yield generally is 1 m^3 for each 10-15 m^3 of water, while the mean water yield is about 2 m^3/h (ICW, 1982) and in several polders like the Haarlemmermeer even 4 m^3/h (De Voogd, 1941).
Around 1941 there were some 1000 gas wells operating in the deep polders in the study area, which resulted in an annual groundwater discharge of nearly $20 \cdot 10^6$ m^3. Along the western borders of the reclaimed lakes, this groundwater is composed of fresh dune or polder water, more to the centre it becomes brackish or saline. The gas wells thus contributed to the attraction of deep dune water and, according to calculations by De Gruyter and Molt (1950) and ICW (1976 and 1982) to salinization of the surface waters.

Another important change in most reclaimed lakes was the deeper dewatering to comply with the needs of modern agriculture. In the Haarlemmermeer for instance, mean winter levels in the ditches near Hoofddorp dropped from an initial 4.5 m-MSL to 5.3 m-MSL in 1900 to 5.8 m-MSL in 1930, while the total land subsidence amounted to only 0.3 and 0.4 m respectively (Bijl, 1933).

In 1932 the Zuiderzee was closed off from the North Sea by a long dam (Afsluitdijk) with large discharge sluices. Lake IJssel was born and turned gradually into a fresh water lake receiving most water from the river IJssel, a branch of the river Rhine (Fig.3.37). This freshening was also of vital importance to the flushing of the polders north of the line Haarlem - Amsterdam. Their waters had remained brackish because of isolation from the fresh river Rhine tributaries, in contrast to the area south of the line Haarlem - Amsterdam (Fig.3.37).

The first artificial recharge projects aimed at getting rid of waste water. The earliest and still operational facility is formed by a sludge basin next to each drinking water treatment plant, where the wash water of rapid sand filters is conducted to and

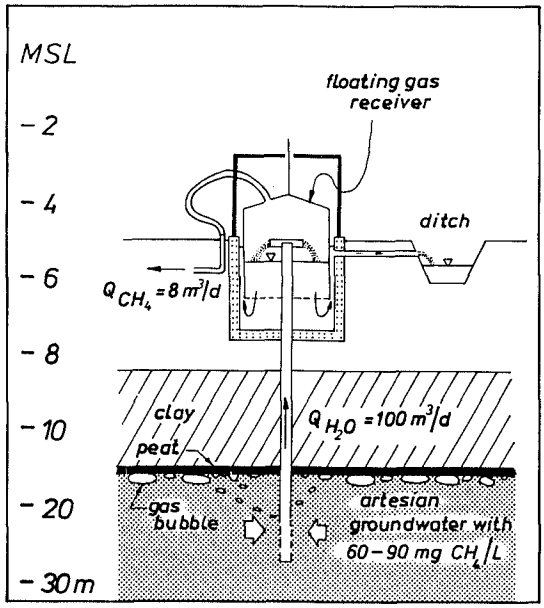

FIG. 3.36 Construction and principle of a gas well for domestic energy supply on farms, as applied in deep polders with artesian, methane-rich groundwater (modified from De Voogd, 1941). The discharged groundwater of 10 °C is in several cases used for cooling purposes as well. The composition of the gas is 79-86% CH_4, 9-12% CO_2 and 4-10% N_2. Q = discharge.

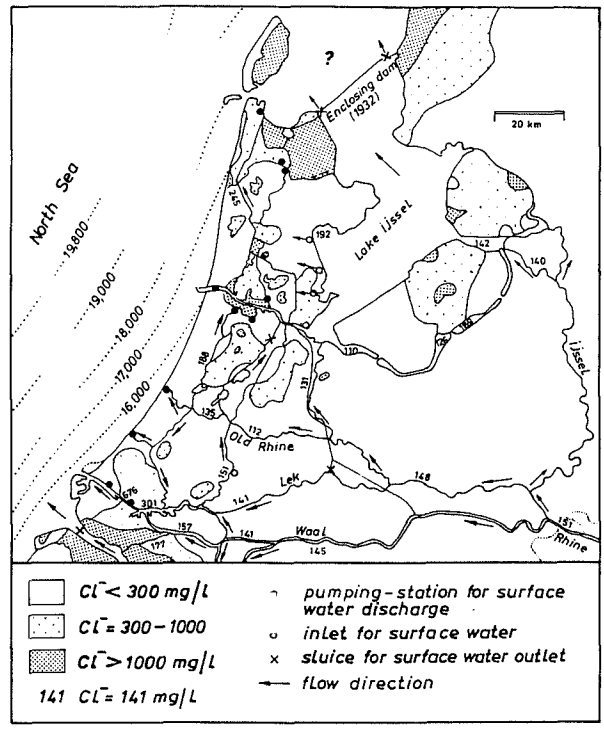

FIG. 3.37 Surface water management (simplified from Van de Ven et al., 1986) and mean chlorinity of surface waters in the study area and their surroundings. Chlorinity of Rhine tributaries refers to the period 1980-1983 (based on data in Stuyfzand, 1985b), that of North Sea water to the period 1977-1978 (calculated from data in RWS, 1979), that of polders in the province of North Holland to the period 1977-1987 (from ICW, 1976 & 1982; Stuyfzand, 1987a, 1988b and 1989a and PWS, 1981).

where its supernatant water disappears by lateral infiltration or by discharge into neighbouring ditches. Quite large volumes are involved, about 5% of the drinking water production on site.
The first and only one waste water recharge operation in the dunes started, probably at the beginning of the 20th century, on a very small scale near Zandvoort aan Zee, where untreated sewage effluent was spread over excavated dune pits.

From May 1923 till April 1928 $7 \cdot 10^6$ m³ of deep dune water from a construction trench for new sluices in the sea port of IJmuiden, was spread over dune valleys near Wijk aan Zee pumping station (PWN, 1924-1928). This was the first project aiming at recharge of aquifers for drinking water supply. The first project compensating for lowered water tables due to groundwater exploitation, was the artificial recharge of an agricultural polder called Mariënduin near pumpingstation Leiduin, where $5 \cdot 10^5$ m³ of boezem water is pumped to annually since 1924, mainly from April till November.

And in 1940 the first surface water for artificial recharge and recovery for drinking water supply was spread in the dunes south of Katwijk (location 18 in Fig.3.1 and Table 3.6). This was the prelude to the next period.

3.7.3 The period 1955 - 1976

This period is largely dictated by a rapid expansion of surface spreading facilities to recharge the overcropped dunes with surface waters, in combination with a strong decline in the pumping of deep dune water. The preparation of drinking water from Rhine, Meuse, Lake IJssel or different types of polder water by dune infiltration, commonly involves a pretreatment near the intake, transport to the dunes, recharge and recovery in the dunes and a post-treatment (Fig.3.38).

After Scheveningen in 1955 five dune areas followed : Leiduin in April 1957, Castricum in August 1957, Monster in 1970, Wijk aan Zee in 1975 and Overveen in 1975 (Table 3.6 and Fig.3.1). Growing water demands necessitated a steady increase in recharge (Fig.3.39) and recollection. This was achieved by extension of recharge facilities at the expense of natural dune valleys and by intensification of the process by changing from intermittent

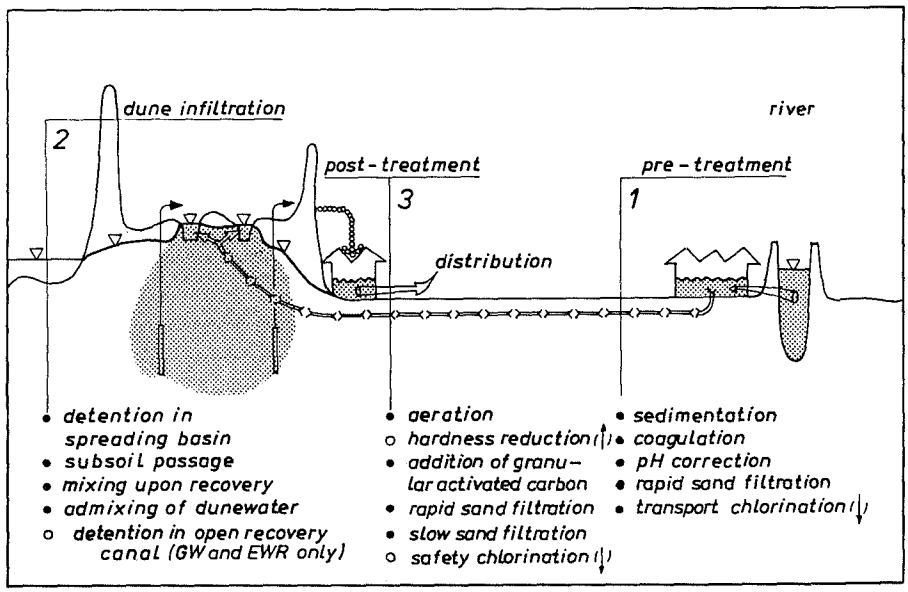

FIG. 3.38 The common preparation of drinking water from polluted surface water by subsequently a pre-treatment near the intake, transport to the dunes, dune infiltration (i.e. recharge and recovery in the dunes) and post-treatment, as practized in The Netherlands. o = not common, increasingly (↑) or decreasingly (↓) applied.

recharge to permanent recharge (Katwijk in 1968), by further pretreatment in order to reduce the clogging of basin floors (Leiduin and Castricum in 1974, Scheveningen in 1976, Monster in 1983 and Katwijk in 1988) and by raising the gradient between recharge and recollection in various ways. For further hydrological details about the six spreading plants reference is made to Stuyfzand (1984f, 1986d).

Groundwater levels rapidly increased in and adjacent to the recharge areas (Fig.3.32), while a significant overdose of recharge as compared to recollection pushed down the local fresh-salt interface (Figs. 3.30 and 3.35, in the western part).

Due to salinization three pumping stations with wells in the second aquifer had to close : Voorhout in 1956, Voorburg in 1960 and Voorschoten in 1970 (Table 3.6 and Fig.3.1). In order to relieve the salinizing pumping stations IJmuiden-North and Bentveld, new pumping stations were put in operation : IJmuiden-South and Kraantje Lek, respectively (Table 3.6 and Fig.3.1). For economical reasons and due to problems with capacity and quality, Egmond aan Zee was closed down in 1961. Wassenaar closed in 1969 but was more or less incorporated into the well field of Scheveningen.

Many industrial abstraction wells were closed down in this period as well, because of salinization (mainly in the IJmuiden harbour area), other quality problems, technological changes etc. The drastical reduction in groundwater pumping by Hoogovens and Royal Paper Mills Van Gelder & Sons Ltd in the IJmuiden harbour area, was compensated for by import of pretreated river Rhine water by pipeline since 1957. On the other hand Hoogovens increased the local pumping of salt groundwater at a depth of 130 to 180 m-MSL for cooling purposes, from a few millions since 1951 to some 20 millions of m^3/y in the 1980s.

The harbour of IJmuiden was enlarged and deepened and its piers extended in 1968. This brought the total loss of younger dunes at about 4 km^2. In the period 1966-1970 the Hoogovens steel production complex expanded in a northward direction, which led to a strong drop of local water tables by heavy drainage of construction pits. The drained groundwaters were recharged in the neighbourhood, a practice that gradually became a regulation for excavation works in The Netherlands. Rain water intercepted by roofs and roads in the new northern area of Hoogovens, is conducted to a recharge ditch along its northeastern boundaries.

Since 1964 about 10^6 m^3 of sewage effluent from Zandvoort aan Zee are treated annually and spread over new basins situated within its famous circuit. And finally, there is a flower bulb cultivation area called Het Langeveld near pumping station Noordwijkerhout, where polder water with a high Rhine water component is pumped up to since about 1957, in order to compensate for losses mainly due to groundwater pumping for drinking water supply.

Submerged sand pits, which were excavated on a relatively large scale by suction since the late 1950s and now constitute lakes for recreation, increased the exfiltration of dune or brackish waters or increased infiltration rates of boezem and polder waters. Examples north of the Old Rhine are the Oosterduinmeer and Lake Geestmerambacht, respectively.

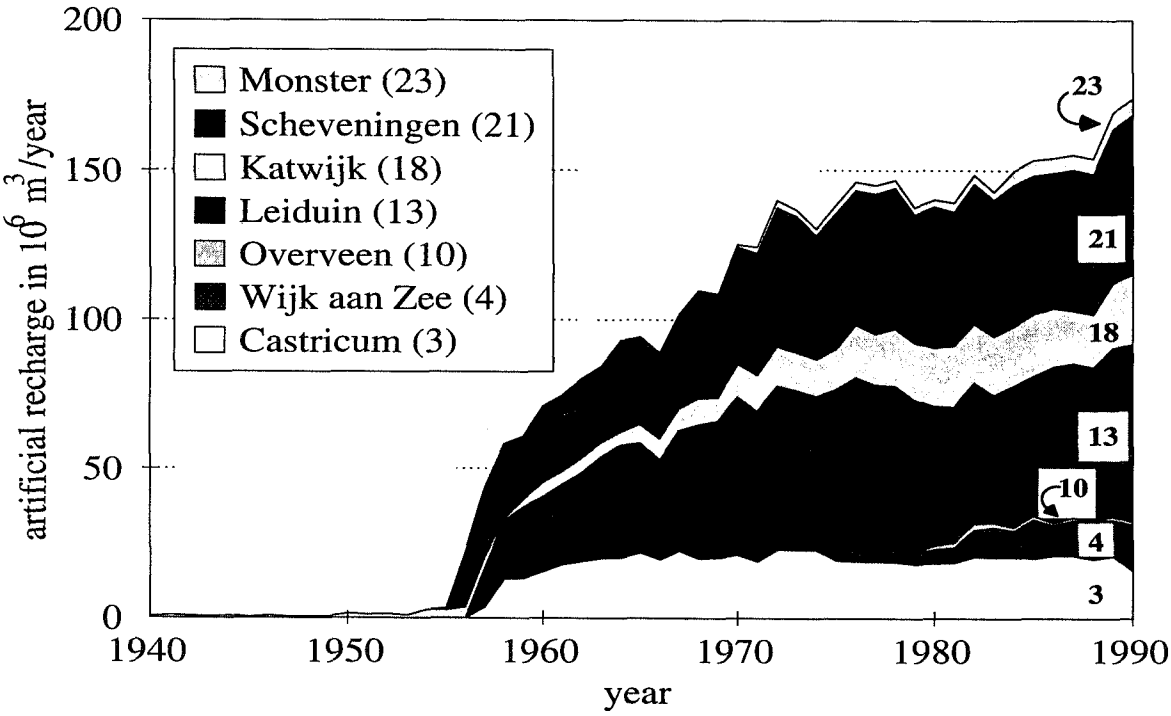

FIG. 3.39 Historical changes in the annual totals of surface water recharge by spreading in seven dune areas situated in the Western Netherlands.

3.7.4 The period 1976 - 1990

Hydrological conditions remained nearly unchanged in this period. There was no further extension of recharge facilities, the quantity of recharged surface water was kept at a nearly constant level, and the pumping of deep dune water was not reduced any further. One pumping station for drinking water supply had to be abandoned, Hillegom, due to risks of contamination with herbicides used in the cultivation of flower bulbs. Pumping station Noordwijkerhout is running now the risk of a forced closure for the same reasons.

Experiments with deep well recharge have been conducted since 1973 on several dune locations with coordination by KIWA (Olsthoorn, 1982; Peters, 1985). Only one or two injection wells were involved on each site, so that the hydrological impact is limited to their close vicinity. In 1990 the first pilot plant studies were put in operation near pumping station Castricum and Scheveningen. About $4 \cdot 10^6$ m^3 of highly pretreated surface water is annually feeding about 20 recharge wells on each location.

Basic hydrological data are shown for the year 1981, representing the period after 1976 : isohypses of mean piezometric heads at different depths (Enclosure 2) and contour lines of equal depth to the fresh-brackish water interface (Enclosure 3.3). The schematized situation in a cross section is shown in Fig.3.26 and 3.35. Groundwater flow systems in this period are discussed in section 3.9.

Enclosure 3.3 reveals the present existence of three fresh, dune water pockets of considerable size: a circular dune hydrosome in the north around Bergen, and two elongate dune hydrosomes, one in the middle around Castricum and the other in the south around Zandvoort aan Zee. Three isolated fresh polder hydrosomes reaching deeper than 20 m-MSL can be diagnosed : one in the north in the shallow polder Geestmerambacht, one around Hoofddorp in the centre of the Haarlemmermeer and one in the southeast corner of the Haarlemmermeer, where the Westeinder Plassen recharge the aquifer system.

3.7.5 The period after 1990

The final period is too short yet for conclusions, but permits to depict some future developments for the younger dune area. The necessity for nature conservation has urged the water supply companies to start with several sanitation measures which also have an important hydrological bearing :

(1) the cutback of the abstraction of autochthonous dune groundwater in selected areas, which should lead to the return of wet dune slacks there;

(2) the reduction of the subterranean expansion of allochthonous surface water, that recharges the dune aquifers artificially, by a more effective recovery;

(3) large scale application of deep well recharge and recovery, in order to cope with increasing water demands and to partly substitute for open recharge. This substitution should lead to a reduction of the impact of artificial recharge on the landscape and to the return of more natural fluctuation patterns for the surface water and groundwater levels;
(4) the use of alternative sources for artificial recharge when a calamity blocks one river intake, so that a rapid decline of water tables can be prevented;
(5) further pretreatment of the surface water to be infiltrated, in order to meet the so-called Dutch Infiltration Act for Soil Protection (VROM, 1992). Filtration over granular activated carbon and hyperfiltration are considered (Van Dijk, 1992);
(6) the curtailment of large, non-indigenous pine woods, which also reduces evapotranspiration losses; and
(7) the local admission of aeolian erosion, to stimulate the development of new dune slacks.

3.8 Major changes during the past 5000 years : synthesis and areal extent

Synthesis

From the extensive prehistorical and historical record presented in the previous sections, several events during the past 5000 years had an overwhelming, large scale impact on recent groundwater hydrology. They are plotted versus time for the dunes and deep polders separately, together with their effect on the groundwater table, in Fig.3.40. Several aspects refer exclusively to the situation along a transection south of Zandvoort aan Zee up to the Haarlemmermeer polder. It is assumed that all groundwaters in the study area were salt or brackish before 3800 BC, the upper 100 to 240 metres by the Holocene Calais transgressions and the deeper waters by stagnant, Lower Pleistocene, connate salt water.

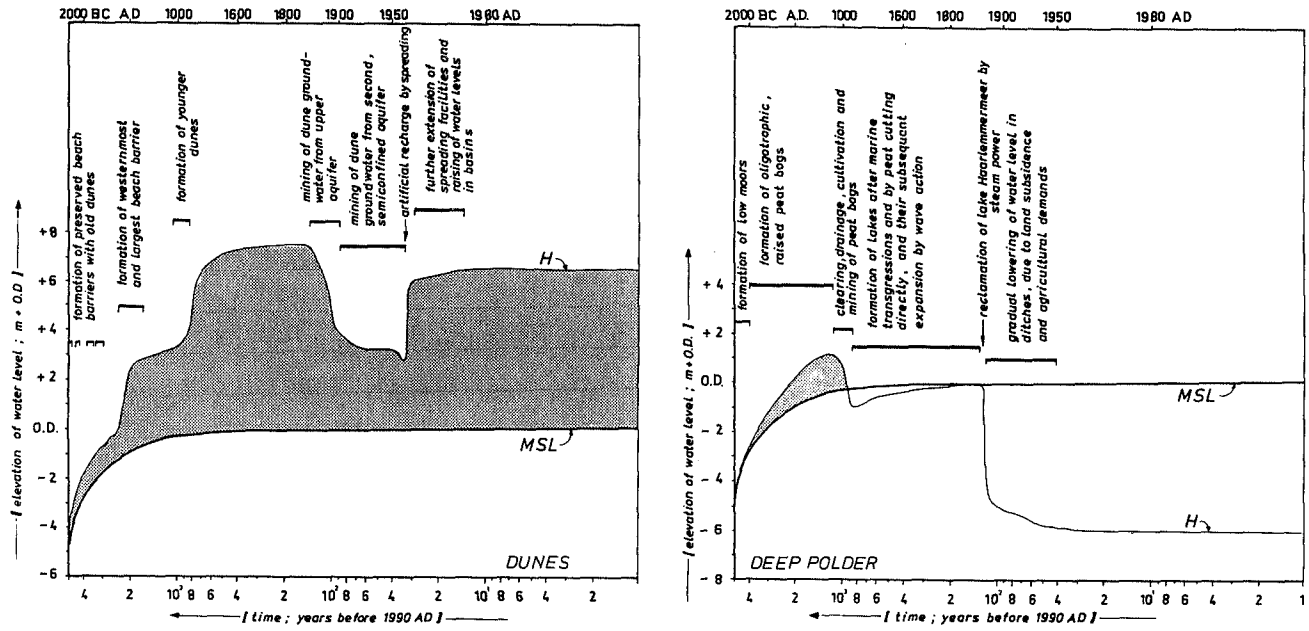

FIG. 3.40 Prehistorical and historical changes in the elevation of Mean Sea Level (MSL), the groundwater table in the centre of the widest dune belt at the time (H), and the groundwater table in deep polders (H), together with the major hydrological events. The elevation of groundwater tables and time of reclamation refer to the situation along a transection south of Zandvoort aan Zee. In several areas deep lakes were reclaimed as early as 1630 AD with the aid of wind mills.

Changes of the groundwater table with respect to mean sea level, reveal that a deep freshening prevailed in the dunes from 3800 BC till 1600 AD in connection with enlargement of the coastal barriers and after 1957 AD by artificial recharge, while a shallow freshening probably dominated in the former peat bogs from 3000 BC till about 900 AD. The fresh dune water pocket contracted in the period 1853-1957 in its western and central parts due to mining (Fig.3.30), while the central parts of the deep polders salinized mainly since 900 AD due to drainage and peat digging, Dunkirke transgressions and the reclamation of lakes.

The area in between the younger dunes and the deep polders experienced, after reclamation of the deep lakes, a gradual supersession of shallow old dune water pockets by polder water and an eastward expansion of young dune water. Polder waters, and locally waters from the younger dunes are still freshening the western parts of the deep reclaimed lakes (Fig.3.26, 1981 AD). The presence of basal peat and Velsen clay (aquitard 1G) in the Nieuw Vennep area strongly reduces the exfiltration of the still advancing dune water in the western parts of the Haarlemmermeer (Fig.3.41). This water could be pumped for drinking water supply.

Areal extent of changes during the past 150 years in the younger dunes

The major, hydrological changes in the younger dunes, during hydro-historical times, comprise a net drawdown of the groundwater table and a net rise of the fresh-brackish water interface. The areal extent of these phenomena is shown on maps for the area north of the Old Rhine (Enclosure 3.2 and 3.4 respectively). These maps have been reproduced in a simplified form in Fig.3.41.

The drawdown of the water table refers to the year 1981 as compared to 1850 AD, for which isohypses are presented in Enclosures 2.1 and 3.1 respectively, the one around 1850 on the basis of a geomorphological survey, the principle of which is explained in section 3.2.3. The change in the position of the fresh-brackish water interface refers to the year 1981 with respect to the period 1903-1920, when the lower boundaries of the dune water pocket became explored and some salinization already had taken place (Fig.3.35).

It can be concluded from Fig.3.41, that there are 11 areas displaying an anomalously high rise of the interface (>20 m), on several locations in combination with an extreme drawdown of the groundwater table (>4 m). These areas correspond with the most heavily exploited dune areas, and in case of site 5, also a strong drainage by the North Sea canal is contributing to the extreme drawdown of the water table and salinization. The most affected sites are : the Bergen area (1-2), IJmuiden area (5) and the large Overveen-Zandvoort-De Zilk area (6-9), with a drawdown of 1-3.5, 8 and 2-8 m, and a rise of the interface by 20-45, 100 and 30-55 m, respectively.

In between these 11 areas a smaller rise of the fresh-brackish water interface is found, which is inherent to the induced flow patterns. It is important to notice that the interface also moved downwards in certain dune areas, often since or shortly after the start of artificial recharge, which allowed a strong reduction in the pumping of deep dune water. This means, that salinization phenomena have even been worse than depicted in Fig.3.41. Around pumping station Castricum and Leiduin the fresh-brackish interface rose by 0.5-1.0 m/y in the period 1920-1955. South of the Old Rhine, salinization phenomena were severe as well. The fresh-brackish water interface in the Scheveningen area, ascended by about 60 m and the lateral intrusion of North Sea water into the upper aquifer reached about 300 m inland (Fig.3.30).

A comparison of all dune water catchment areas with consideration of separate well clusters, leads to the following risk factors, which enhance the chance of salinization :

(a) a long duration, high rate and high intensity of the abstraction;

(b) a shallow depth to the initial fresh-salt water interface, a short distance to the coastline and the lack of an aquitard with sufficiently high vertical flow resistance in between the well screen and initial fresh-salt water interface;

(c) the presence of an aquitard with high vertical flow resistance and a large lateral extent in between the well screens and groundwater table; and

(d) a restricted lateral flow due to another well field upgradient, or the presence of vertical semi-pervious boundaries. These are composed of the glacial basins filled with clay-rich sediments in the IJmuiden area, and clay-rich faults or strata in ice-pushed ridges surrounding the glacial basins.

It is important to notice, that a rise of the fresh-brackish water interface is generally accompanied by a strong widening of the whole transition zone between fresh and salt water close to the well field and much less in adjacent areas (Fig.3.42). This is caused by dispersion both in a transversal and longitudinal direction, in combination with fluctuations in pumping rates. When a well is temporarily closed down for several months due to a raised salinity, the brackish upconing below its screen may collapse by gravity (section 3.10.1) in an undoubtedly changed flow field and mix with unaffected fresh groundwater.

Coastal erosion and increased evapotranspiration by pines had a major contribution to the large scale drawdown of the groundwater table in the dunes north of Bergen (Enclosure 3.2).

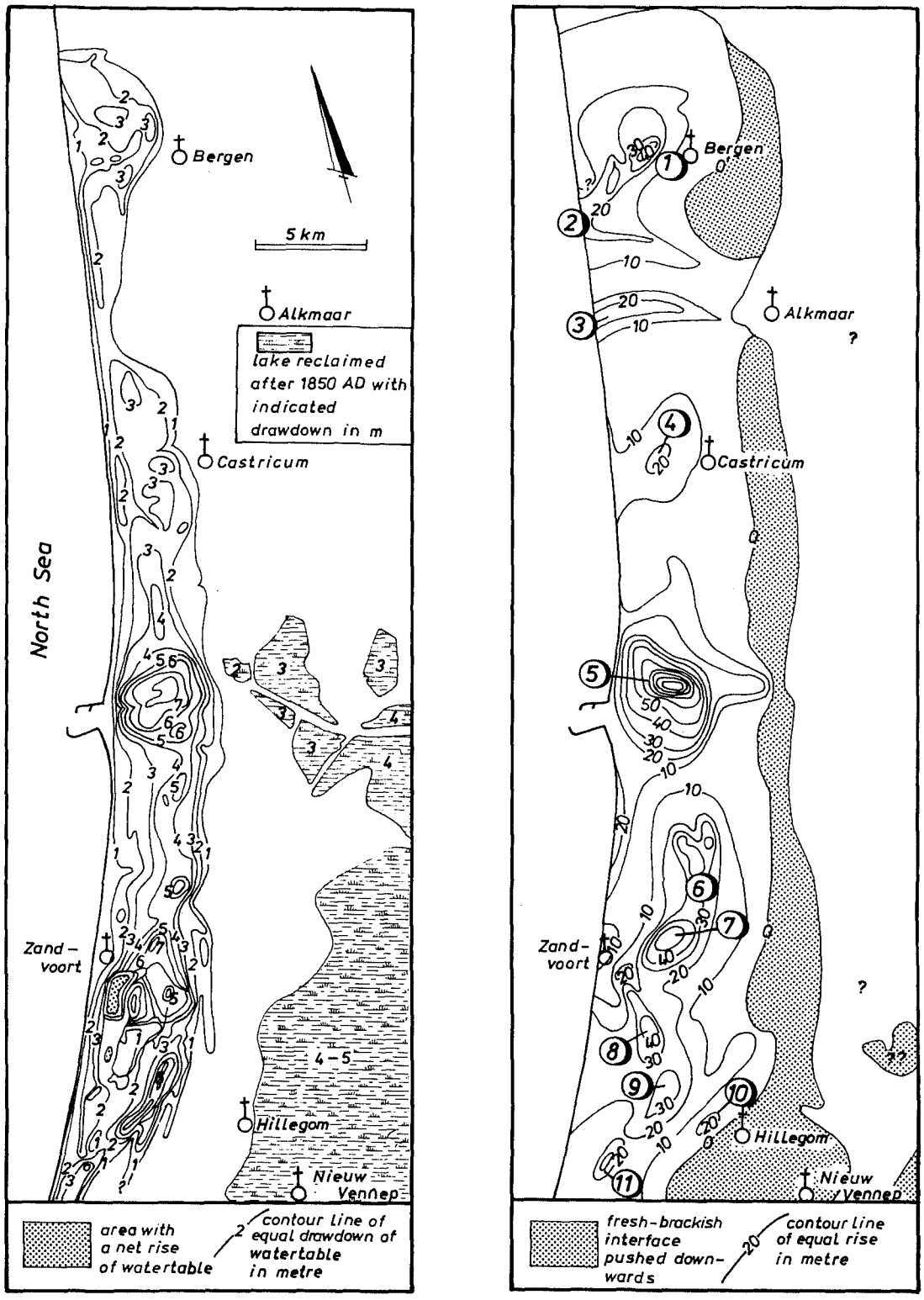

FIG. 3.41 Areal extent of changes in the position of the groundwater table and fresh-brackish (300 mg Cl⁻/l) water interface, in the period 1850-1981 and 1910-1981 respectively (simplified after Enclosures 3.2 and 3.4, respectively). 1 = pumping station Bergen; 2 = southern fringe of the Bergen dune hydrosome; 3 = northern fringe of the Castricum dune hydrosome; 4 = pumping station Castricum; 5 = IJmuiden sea port area with several well fields; 6 = pumping station Overveen; 7 = Boog canal and pumping station Bentveld; 8 = centre of the Leiduin catchment area; 9 = Ooster canal (part of pumping station Leiduin); 10 = pumping station Hillegom; 11 = pumping station Noordwijk.

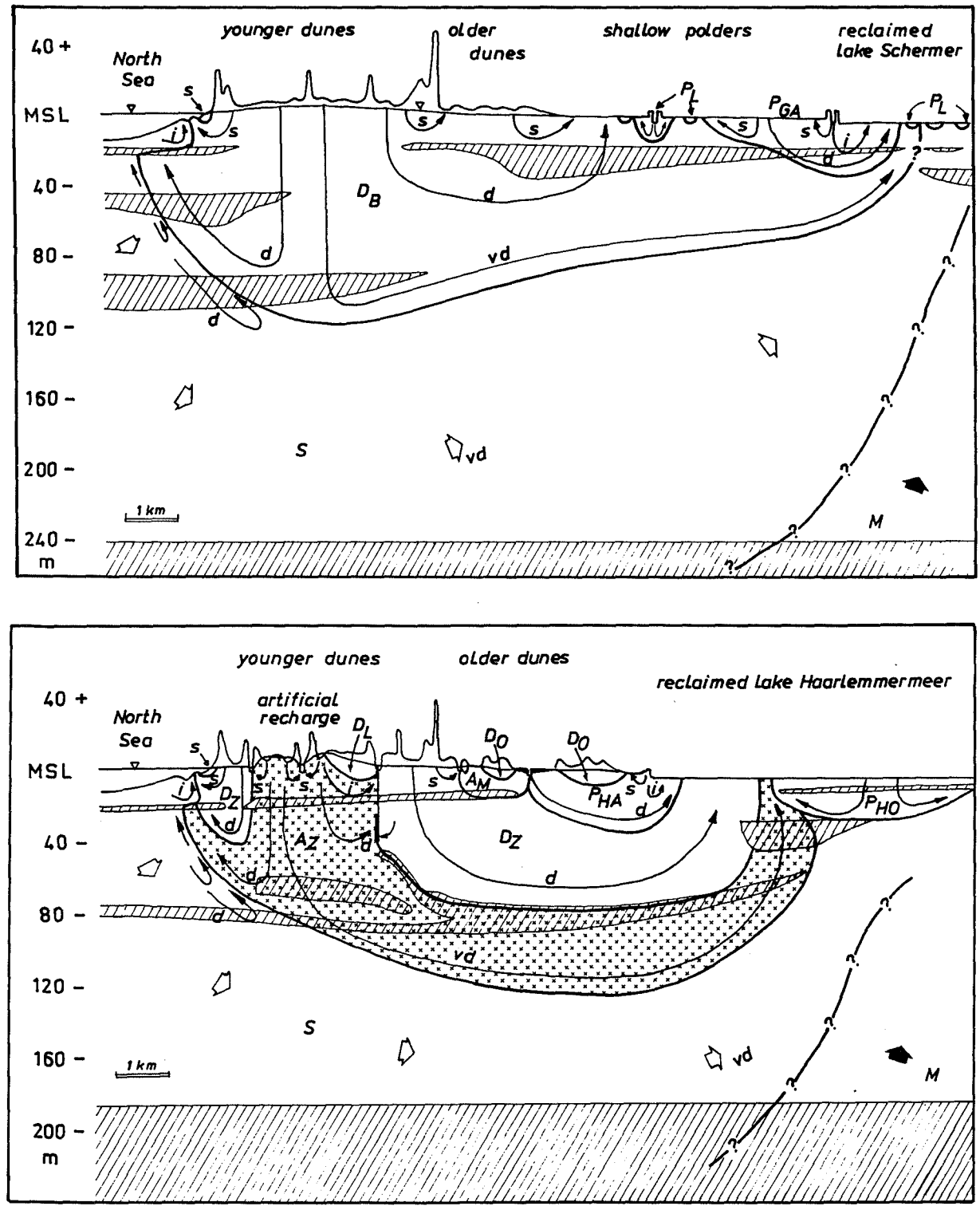

FIG. 3.44 Schematized cross section with the distribution of groundwater flow systems (GFSs) and their main flow branches, for the Bergen-Alkmaar area (without artificial recharge) and for the Zandvoort-Hoofddorp area (with artificial recharge). Coding of flow systems according to Table 3.7, in alphabetical order : A_M = Mariënduin artificial recharge GFS; A_Z = Zandvoort artificial recharge GFS; D_B = Bergen dune GFS; D_O = old dune GFS; D_Z = Zandvoort dune GFS; M = Maassluis marine GFS; P_{GA} = Geestmerambacht polder GFS; P_{HA} = Haarlem polder GFS; P_{HO} = Hoofddorp polder GFS; P_L = local polder GFS; S = North Sea GFS.
Coding of flow branches as follows : d = deep; i = intermediate; s = shallow; vd = very deep.

It may be called therefore a man-enforced GFS. Piezometric levels at 130 m-MSL (Enclosure 2.4) clearly reveal the flow towards the Schermer and Haarlemmermeer polder and towards a deep well field in the IJmuiden harbour area, where Hoogovens is pumping salt groundwater.

TABLE 3.7 Discerned groundwater flow systems (GFSs) in the Western Netherlands, with several characteristics. The GFS types in order of decreasing age and the individual GFSs in alphabethical order.

Groundwater flow system code	name	order @	maximum size§ (km) L	B	d	origin years before 1990 AD	main causes of flow **
MARINE SYSTEMS							
M	Maassluis	5	700	400	0.5	$<2*10^6$	C, L
NS	North Sea	4	1200	50	0.2	8000 ##	L, G
DUNE SYSTEMS							
D_B	Bergen	3	12	12	0.12	5000	N, L, Q
D_C	Castricum	3	18	11	0.11	1650-2500	N, L, Q
D_E	Egmond	2	12	7	0.02	1000-2000	N, L
D_L	local lenses	1	1	0.8	0.01	<33-50	N, Q
D_M	Monster	3	12	3?	0.03	1650-2550	N, L, Q
D_N	Noordwijk	3	10	3	0.04	1650-2550	N, L
D_O	Older dunes	1-2	1	0.5	0.01	3000-5800	N, L, Q
D_S	Scheveningen	3	19	11	0.10	1650-2550	N, L, Q
D_Z	Zandvoort	3	30	14	0.12	1650-2550	N, L, Q
POLDER SYSTEMS (north of Old Rhine only)							
P_{AA}	Akersloot-Assendelft	2	17	5	0.06	350-410	L, N
P_{BW}	Braassem & Westeinder	3	27	6?	0.07	350	L, N
P_E	Eiland	3	8	6	0.06	350	L, N
P_{GA}	Geestmerambacht	3	12	6	0.06	360-440	L, N
P_{HA}	Haarlem	2	25	5	0.05	110-140	L, N
P_{HO}	Hoofddorp	2	5	3	0.03	<140	L, N
P_L	shallow, local	1	0.5	0.1	0.00	110-400	L, N
P_{IJ}	IJ & North Sea Canal	2-3	18	5	0.04	110	L, N
P_Z	Zaan	3	12	5	0.04	350	L, N
ARTIFICIAL RECHARGE SYSTEMS							
A_B	sludge basins	1	0.2	0.2	0.04	<33-50	R
A_C	Castricum	2	2	1	0.05	33	R, Q
A_D	deep, local	1	0.2	0.2	0.07	<15	R
A_E	sewage effluent Zandvoort	2	4	1	0.10	ca 80	R, Q
A_K	Katwijk	2	4	3?	0.07	50	R, Q, L
A_L	Langeveld polder	2	2	1.5	0.03	32	R, Q, L
A_M	Mariënduin polder	1	4	1	0.01	ca 66	R, L, Q
A_{Mo}	Monster	2	2	1	0.03	20	R, Q
A_O	Overveen	1	1	0.5	0.04	15	R, Q
A_S	Scheveningen	2-3	9	7	0.10	35	R, Q, L
A_W	Wijk aan Zee	1-2	1	0.5	0.02	15	R, Q
A_Z	Zandvoort	2-3	9	6	0.10	33	R, Q, L

** : C = compaction; G = density gradients; L = drainage of reclaimed lakes; N = precipitation; Q = abstraction; R = artificial recharge; @ : 4-5 = supraregional; 3 = regional; 2 (sub)regional; 1 = local; ## = the actual flow system : about 1000 y. § : L = length; B = width; d = depth

Generally there are four distinct North Sea flow branches (Fig.3.44) :
- a shallow branch below the beach, from the upper swash line flowing back to the low tide mark (Lebbe, 1981);
- an intermediate branch situated approximately seaward of the low tide mark and above the upper fresh water tongue (in the upper parts of the second aquifer). Flow is directed inland, driven by salt groundwater losses by mixing with and shear forces exerted by dune water flowing upwards (Cooper et al., 1964);
- a deep branch very similar to the intermediate branch, however directed towards and along the seaward face of the fresh-salt water interface in the second aquifer and deeper; and
- a very deep branch passing the point of maximum depth of the fresh-salt water interface and flowing further inland under the influence of the strongly drained, reclaimed lakes or deep polders.

3.9.5 Dune systems

Dune systems of different order are present : The regional Bergen, Castricum, Zandvoort, Noordwijk and Scheveningen systems of third order are nested into the North Sea GFS. The first three are shown on Enclosure 4.1, the latter two are situated in between Noordwijk aan Zee and Katwijk aan Zee, and in between Katwijk aan Zee and Monster, respectively (Fig.4.8). The subregional Egmond system of second order is largely restricted to the upper aquifer and parts of aquitard 1E in between Bergen aan Zee and Egmond aan Zee, and is partly nested into the North Sea, Bergen and Castricum flow systems. And the local, younger and older dune systems of first order are embedded in subregional artificial recharge systems (as so-called rain water lenses) and polder systems, respectively. Further details about the analytical modelling and occurrence of rain water lenses are given in section 3.10.2.

The origin of all (sub)regional, dune flow systems can be dated in between 3800 and 200 BC. They expanded during and after the formation of the younger dunes (950-1180 AD), and contracted in the period 1850-1957 AD mainly in their western and central parts, due to exploitation. They expanded substantially since the reclamation of deep lakes in the period 1600-1853 AD, in an eastward direction. The latter expansion was accompanied by a strong seaward shift in the position of the groundwater divide in the second aquifer (Enclosure 2.2), which contributed to the contraction in the western parts.

The older dune flow systems contracted strongly or disappeared completely since about 1700 AD, for two reasons : (1) large parts of the older dunes gradually became levelled and traversed by numerous ditches and canals, which drain local rain water during the wet season and supply boezem water (containing a high percentage of Rhine water) for irrigation and recharge; and (2) local rain water, which previously fed the older dune systems, is discharged since about 1920 by sewers to the boezem outside the older dunes area.

Five distinct flow branches can be recognized within regional dune GFSs today (Fig.3.44) :
- a shallow branch in the upper aquifer, which is directed towards the low tide mark on the beach;

· a shallow branch in the upper aquifer, which discharges into dune brooks east of the retention ridge or in ditches cutting through adjacent older dunes.
· a deep, relatively short branch down into the second aquifer and discharging at the top of the seaward fresh water tongue;
· a deep, long branch mainly in the second aquifer running into a shallow polder; and
· a very deep branch, which reaches the third aquifer and exfiltrates in a reclaimed lake.

The dune flow systems can be classified on the basis of their shape and boundary conditions (Fig.3.45) : the Bergen system as quasi-circular, asymmetrical, semi-forced and salt-nested; the Egmond system as elongated, asymmetrical, forced and fresh-nested; the Castricum, Zandvoort, Noordwijk and Scheveningen systems as elongated, asymmetrical, semi-forced and salt-nested; the rain water lenses as elongated, (a)symmetrical, free or (semi)forced and fresh-nested; and the older dune systems as elongated, quasi-symmetrical, semi-forced or free and fresh-nested.

3.9.6 Polder systems

These systems are completely man-made. The main drainage and flushing artery in the polder landscape, the so-called boezem with its relatively high water level at about 0.6 m-MSL, acts by strong infiltration losses as a line source (Fig.3.29). Relatively shallow polders on one or both sides of the boezem act as partial sinks for the boezem and as planar sources for deeper polders in the neighbourhood (Engelen & de Ruiter-Peltzer, 1986).

The following systems of different order are recognized north of the Old Rhine : the regional Geestmerambacht, Eilandspolder, Zaan, IJ & North Sea Canal and Braassemer & Westeinder polder flow systems of third order (Enclosure 4.1); the subregional Akersloot-Assendelft, Haarlem and Hoofddorp polder flow systems of second order (Enclosure 4.1); and local, very shallow polder systems of first order, which are recharged by precipitation on small plots surrounded by drains and small ditches.

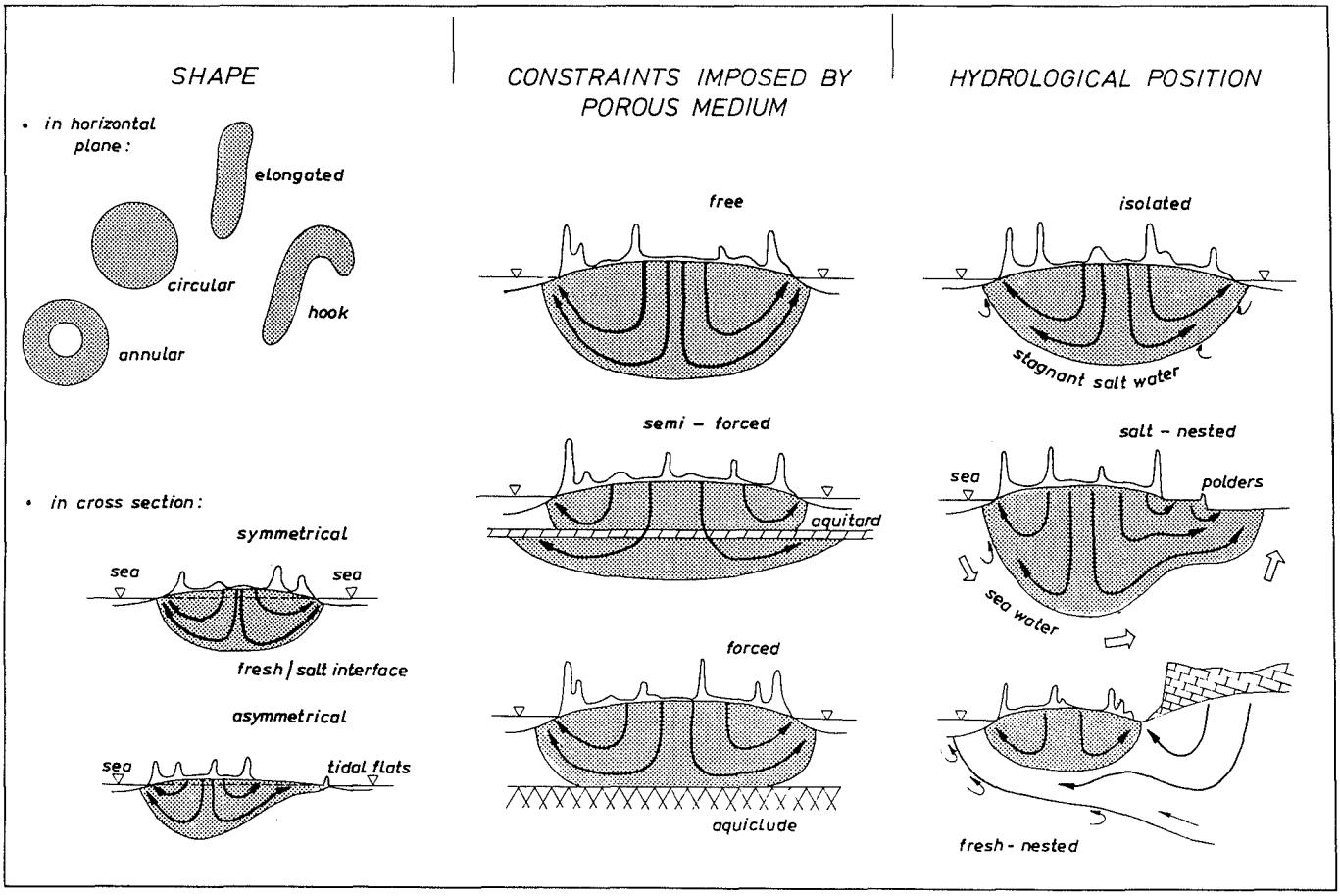

FIG. 3.45 Classification of coastal dune groundwater flow systems, on the basis of their shape and several boundary conditions. The subdivision into free, semi-forced, forced, symmetrical and asymmetrical follows Beukeboom (1976).

The origin of all these systems coincides in general with the date of reclamation of adjacent lakes or lowering of the drainage level of adjacent polders. In the beach barrier and beach plain landscape the cultivation of flower bulbs and the expansion of (sub)urban areas contributed to a further expansion of polder systems (section 3.6.4). Shallow, intermediate and deep flow branches are shown in Fig.3.44.

3.9.7 Artificial recharge systems

These systems are characterized by a controlled pumpage of allochthonous surface water or groundwater, pretreated or not, into open basins or recharge wells, which are situated well above the intake surface level. The main difference with a polder flow system therefore is the higher topographical position of the recharge area, and the controllability of recharge and of quality (by pretreatment and selective intake).

The following systems of different order have been recognized in 1981 : the (sub)regional Castricum, Wijk aan Zee, Zandvoort aan Zee, Katwijk, Scheveningen and Monster recharge systems of fourth order. The first and third are shown on Enclosure 4.1; and to the north of the Old Rhine the local Hoogovens, Overveen, Zandvoort's sewage effluent, Mariënpolder, Langevelder polder and several sludge basin and deep well recharge systems of fifth order (some shown on Enclosure 4.1).

The subregional systems consist exclusively of open recharge systems for drinking water supply, which largely discharge into drainage canals, drains or wells (Fig.4.11). They expanded mainly in the period 1957-1976. Shallow, intermediate, deep and very deep flow branches are shown in Fig.3.44.
Very characteristic is the large spread in detention times, both in the spreading basins (<1 to >40 days) and in the subsoil (40 days to > 40 years). About 80% of the infiltrate is recovered on most recharge sites, from the upper aquifer after a modal transit time in the subsoil of 40-135 days. The remaining part is recovered after 0.5-50 years from the aquitards 1C, 1C' or 1D (5-20%) and from the deep aquifer II (1-15%).

3.10 Special flow cases

In the younger dunes three interesting groundwater flow phenomena were observed : the gravity driven collapse of brackish upconings, which is accompanied by volumetric compensation (section 3.10.1), the formation of so-called rain water lenses on top of infiltrated surface water migrating in a lateral direction (section 3.10.2), and a particular flow pattern around flow-through lakes (section 3.10.3).

3.10.1 Gravity driven collapse and volumetric compensation

The start of artificial recharge meant the close down of many deep wells in dune catchment areas which were previously mined. Although this resulted in a general, slow pushing down of the fresh-salt water interface, as expected, locally a poorly understood, salinization was observed. Good examples have been documented in the recharge area south of Zandvoort aan Zee (Stuyfzand, 1988b).

The mechanism behind this salinization is shown in Fig.3.46. The gravity driven collapse of the denser brackish upconings after close down of deep wells, creates an upward flow along its flanks towards the resulting gap. The phenomenon is to be considered as a temporary, man-induced, local GFS. It is similar to the process called volumetric compensation in the surroundings of a salt diapir (G.B. Engelen, pers. comm.).

3.10.2 Rain water lenses

General
A rain water lens is defined as a shallow lens of autochthonous groundwater (recharged by local precipitation) on top of infiltrated allochthonous surface water migrating laterally. The term was probably introduced by dutch hydro-ecologists, who studied the nutrient status of wetland systems adjacent to areas with (1) large scale artificial or induced recharge of groundwater by eutrophic surface waters, like river Rhine and Meuse water, or (2) decalcified sandy hills. It is generally used to denote a thin, shallow layer of nutrient-poor, autochthonous groundwater or acid groundwater similar to rain water, on top of eutrophic, more mineralized groundwater of different origin.

Bakker (1981), Van Dijk & Bakker (1984) and Van Dijk & de Groot (1987) concluded, however, that no well defined precipitation water layer develops on top of the infiltrated groundwater in the coastal dunes, because of hydrodynamic dispersion. Their conclusion is based on field evidence mainly from specific locations where lenses are ill-developed indeed, and on bad evidence. Their discrimination between dune and infiltrated river water contains errors by nonconservative behaviour of the (semi)natural tracers K^+ and F^- applied, and by larger natural variations of the K^+ and F^- concentration in shallow dune water, both blurring the assumed contrast (Stuyfzand & Stuurman, 1985; Stuyfzand & Moberts, 1987a,b).

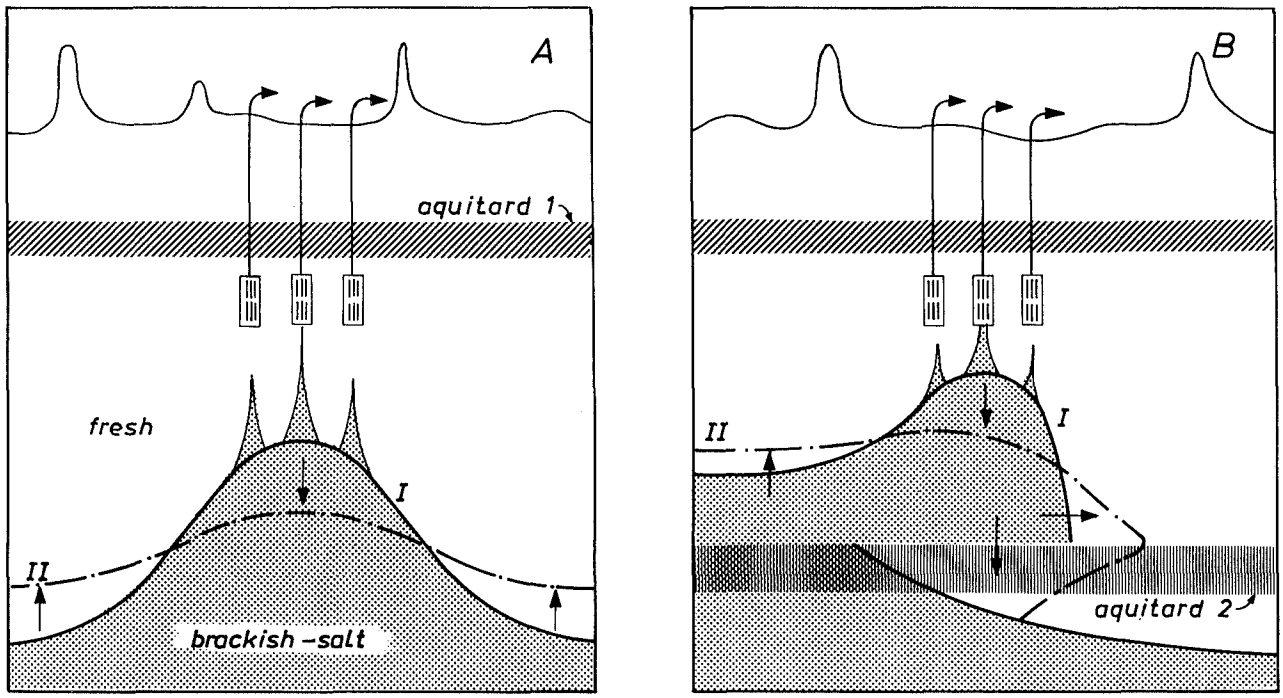

FIG. 3.46 Salinization in the bordering areas of brackish upconings by volumetric compensation, upon close down of deep wells. Arrows indicate the direction of groundwater flow after close down. I = during pumpage; II = after close down; A : without second aquitard and without lateral salt-water encroachment; B : contrary to A.

Evidence from the coastal dunes

Rain water lenses on top of infiltrated Rhine water could be clearly demonstrated for the first time in the catchment area south of Zandvoort aan Zee (Stuyfzand & Stuurman, 1985), using multilevel wells with miniscreens and both Cl^- and $\delta^{18}O$ as a tracer (Fig.4.9). Pretreated Rhine water was introduced on 20 April 1957 in the investigated area. The observation wells are aligned in a row approximately heading downgradient, in between spreading basins in the west and a recollection canal about 1 km to the east (Fig.3.47). The phreatic head drops from about 7 m+MSL in the spreading basins and the supply canal, which feeds the basins, to 2 m+MSL in the recollection canal, and exceeds the piezometric head in the second aquifer by 2-6 m in consequence of a well-developed aquitard 1D (c_v = 14,600 d) at 16-20 m-MSL (Fig.3.47). Aquitard 1C (c_v = 100 d) at 6-11 m-MSL has a much smaller influence on the hydraulic head distribution. The main source of Rhine water for the miniscreened wells, is the supply canal.

The distribution of the recognized rain water lens, infiltrated Rhine water and deep dune water, including their transition zone (10-90%), is shown in Fig.3.48. It is concluded that the thickness of the well-developed rain water lens and its transition zone with river Rhine water increase downgradient, as expected. River Rhine water has reached the recollection canal and, close to the spreading areas, the second aquifer. This corresponds well with the transit times in the subsoil, both calculated and established hydrochemically (section 7.5.5). In between spreading basin 1 and the strongly recharging supply canal a relatively thick lens developed (well 477 in Fig.3.48), due to a small hydraulic gradient. A flow component parallel to both recharge facilities explains the remarkable shape of this lens.

Rain water lenses have also been clearly demonstrated in other infiltration areas : near Castricum (Stuyfzand, 1985a), south of the area discussed above and in the Scheveningen area (Stuyfzand & Moberts, 1987a,b), and in the area south of Katwijk (Stuyfzand, 1990a).

The available field data sustain some general conclusions about the occurrence of rain water lenses. Their development is stimulated by a low flow velocity, a long distance to the banks of the spreading basin that recharges the allochthonous water below the lens, a high precipitation excess, and sufficiently stable boundary conditions. This generally means that they hardly develop in the recharge-recollection areas with closely interspaced

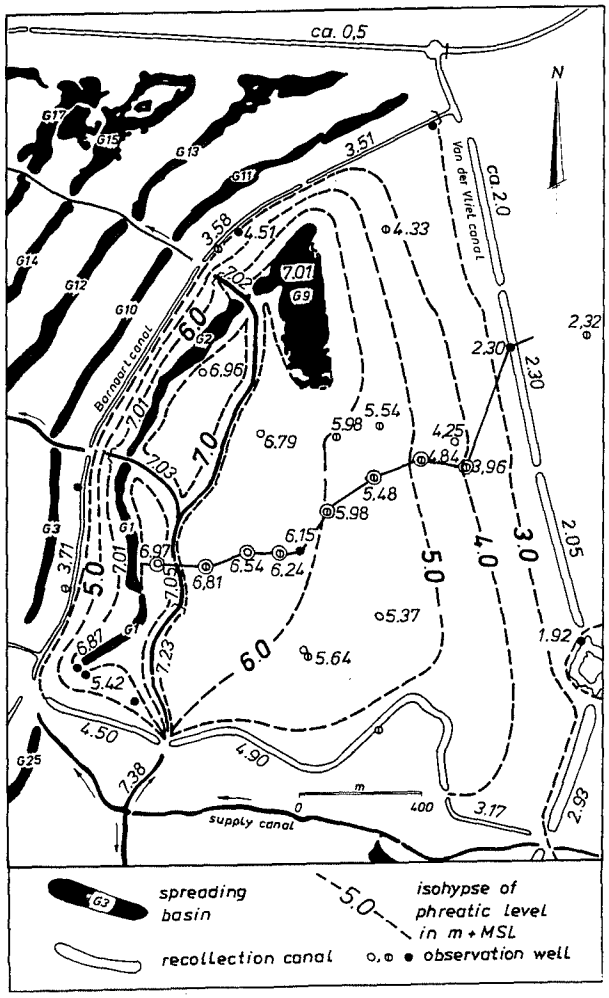

FIG. 3.47 The position of miniscreened observation wells and the groundwater flow pattern in the Barnaart - Van der Vliet dune area (see Fig.3.1) within the artificial recharge area of Gemeentewaterleidingen (A), and the hydraulic head distribution in section on 1 June 1984 (B).

basins and recoveries. The transit time in the subsoil is too short and fluctuations in water level may easily disrupt the tiny lens by an enhanced dispersion.

Modelling

When a steady-state, primarily horizontal and completely indispersive flow are assumed for the situation sketched in Fig.3.49A, we obtain according to Darcy's law :

$$q = -K_h D_x \frac{dH}{dX} \tag{3.19}$$

and because of continuity

$$q = N\,X \tag{3.20}$$

where D_x = thickness of rain water lens at distance X [m]; H = phreatic head [m+MSL]; K_h = horizontal permeability [m/d]; N = precipitation excess [m/d]; q = recharge and discharge of precipitation water [m^2/d]; X = distance to the closest bank of the relevant spreading basin, as measured in the horizontal plane along the flow line [m].

Combination of Eq.3.20 with Eq.3.19 yields :

$$D_x = \frac{-NX \cdot dX}{K_h \cdot dH} \tag{3.21}$$

For the representative situation of two aquifers separated by an aquitard (Fig.3.49B), the position of the water table H can be approximated by a solution given by Huisman & Olsthoorn (1983):

$$H = C_1 e^{-\frac{X}{\lambda}} + C_2 e^{\frac{X}{\lambda}} + Nc_v + \varphi_x \tag{3.22A}$$

where : C_1, C_2 = integration constants to be obtained from the boundary conditions; c_v = vertical hydraulic resistance of the aquitard [d]; $\lambda = \sqrt{(K_h D c_v)}$ = the leakage factor [m/d]; D = Z'+ ½(H_0 + H_X) ≈ mean thickness of upper aquifer [m]; φ_x = piezometric head in second aquifer at X = X [m+MSL]; Z' = position of upper face of the aquitard [m-MSL].

For Eq.3.22A the following general conditions must be satisfied : no radial resistance; $\varphi_x = a + bX$ (a and b are constants); and $D \gg H_0 - H_x$ (H at X=0 and X=X, respectively).

When the piezometric heads were measured in the upper and second aquifer at X = 0 and X = M (M > 0), then the boundary conditions can be specified as : H = H_0 and $\varphi_x = \varphi_0$ at X = 0, H = H_M and $\varphi_x = \varphi_M$ at X = M, and

$$\varphi_x = \varphi_0 + \frac{\varphi_M - \varphi_0}{M} X \tag{3.22B}$$

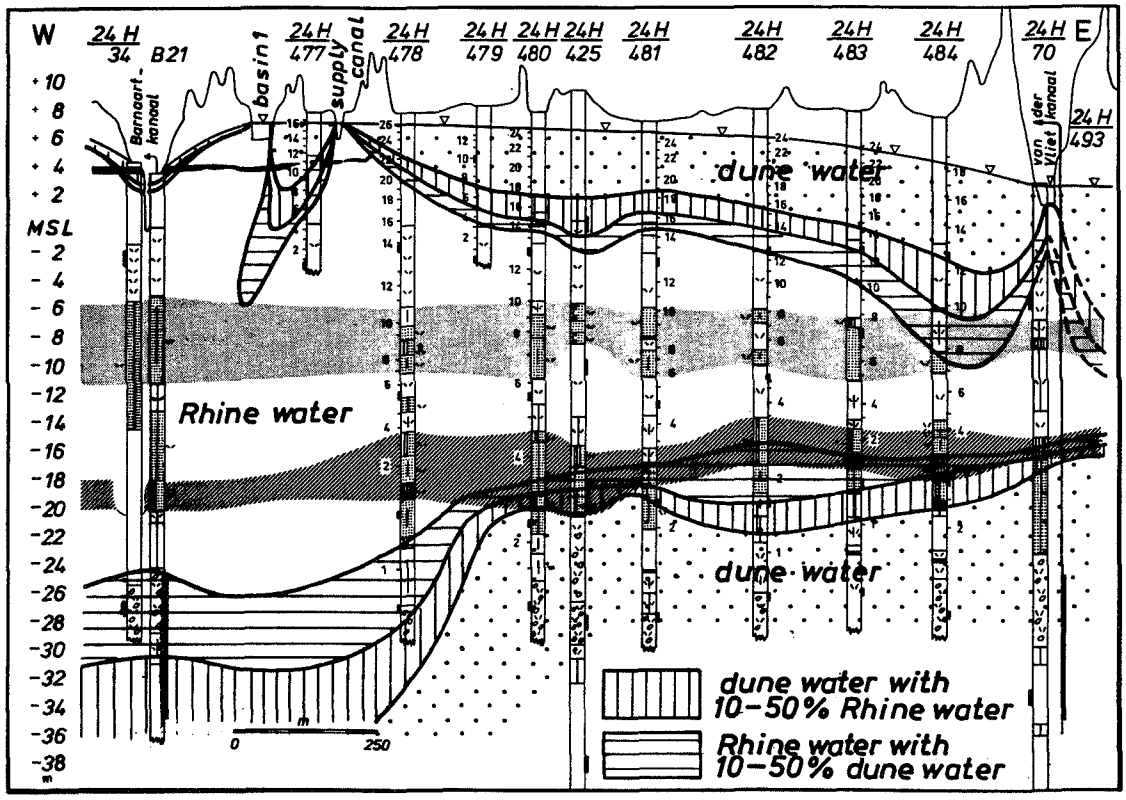

FIG. 3.48 The distribution of a more or less stationary rain water lens on top of infiltrated Rhine water in the cross section depicted in Fig.3.47, in March 1981. Deep dune water is being displaced by Rhine water in the second aquifer below 20 m-MSL. Groundwater flow in between the strongly recharging supply canal and basin 1, contains a component perpendicular to the section.

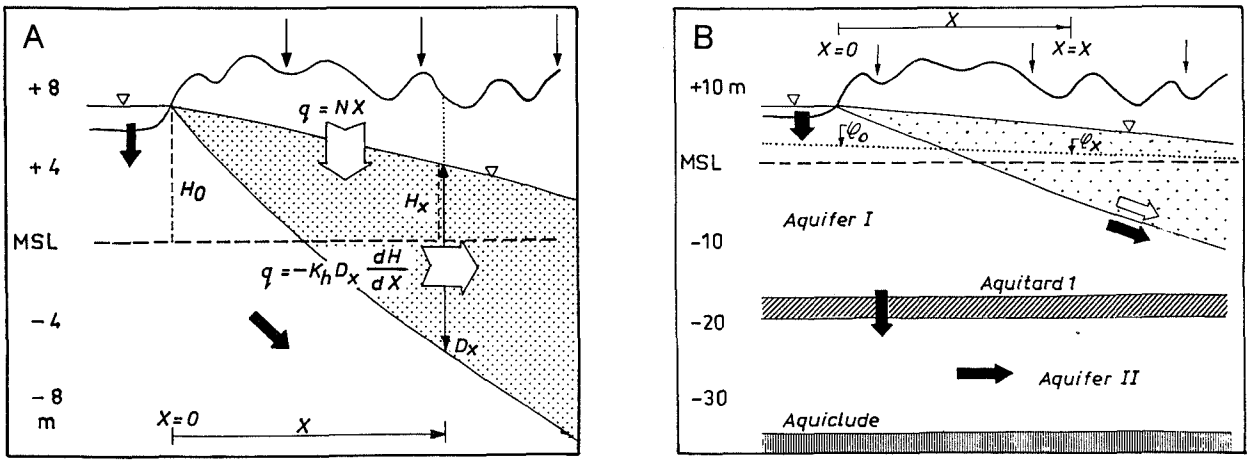

FIG. 3.49 Scheme of a rain water lens (stippled) on top of infiltrated surface water migrating laterally, with important parameters and water balance for calculation of its thickness (A), and the situation in case of two aquifers with a declining piezometric head in the second aquifer (B). For definition of parameters see explanation to Eqs.3.19 and 3.20.

These conditions yield :

$$C_1 = H_o - C_2 - Nc_v - \varphi_o \qquad (3.22C)$$

$$C_2 = \frac{H_M - (H_o - Nc_v - \varphi_o)\, e^{-\frac{M}{\lambda}} - Nc_v - \varphi_M}{e^{\frac{M}{\lambda}} - e^{-\frac{M}{\lambda}}} \qquad (3.22D)$$

After insertion of Eqs.3.22A and 3.22B into Eq.3.21 and differentiation we obtain :

$$D_x = \frac{NX}{K_h \cdot \{ \frac{C_1 e^{-\frac{X}{\lambda}}}{\lambda} - \frac{C_2 e^{\frac{X}{\lambda}}}{\lambda} - \frac{\varphi_m - \varphi_o}{M} \}} \qquad (3.23)$$

With Eqs.3.22A-D and Eq.3.23 the stationary position of a rain water lens can be calculated, from the piezometers at the bank of the spreading basin (X=0) towards and beyond the piezometers at X = M. Additional boundary conditions are : $D_x < (Z' + H_x)$ and $X \geq 0$.

Calculations using Eq.3.23 compare very well with observations in the cross section shown in Fig.3.48 (see Table 7.4), and in other dune areas (Stuyfzand & Moberts, 1987a,b; Stuyfzand, 1990a).

Dispersion

The interface between both fluids is not sharp (Fig.3.48) in consequence of hydrodynamic dispersion, in analogy to the interface between fresh dune and salt North Sea water (section 3.5.5). As a matter of fact Eq.3.16 can also be used to predict dispersion across the interface in this situation, because both fluids move subhorizontally in the same direction. However, the thickness of the transition zone should be inferior to twice the thickness of the rain water lens then.

The chemical contrast between both fluids is smaller than for dune and sea water, so that the delineation of the observed transition zone becomes more difficult. The definition of the mixing zone is therefore somewhat untightened by taking the relative concentration of the conservative tracer of infiltrated surface water c' = 0.1 and c' = 0.9 (see Eq.3.14) as its upper and lower boundary, respectively. The total width of the symmetrical transition zone ($D_{10\text{-}90}$) then becomes in m:

$$D_{10\text{-}90} = 3.624 \sqrt{\alpha_T X} \qquad (3.24)$$

Calculations using Eq.3.24 compare very well with observations in the cross section shown in Fig.3.48 (see Table 7.4), and in other dune areas (Stuyfzand & Moberts, 1987a,b; Stuyfzand, 1990a), by taking for α_T = 0.0025 m. Note that in these publications an α_T = 0.01 m was found, but the definition of α_T was different : (α_T)there is 4 * (α_T)here = 4 * (α_T)conventional. Van Dijk & De Groot (1987) needed an α_T = 0.05 m in order to fit the calculated with the observed transition zone. Their higher value also contains, however, the considerable effects of mixing within flow-through dune lakes (next section) and errors in the delineation of the mixing zone due to the use of nonideal tracers. The low value observed here, corresponds well to observations on fine-grained sandy aquifers elsewhere (Uffink, 1990; Lebbe, 1983).

Other lens types

Other types of groundwater lenses can be modelled in a similar way. For instance lenses composed of groundwater that is recharged in an area with a specific vegetation cover, the so-called vegetation water lenses (section 6.3.3). Or a peat water lens, composed of groundwater which passed thick anoxic dune peat with a high flow resistance, in a flow field with predominantly subhorizontal flow (section 6.6.5).

3.10.3 Flow-through dune lakes

General

Flow-through lakes, also called water-table window lakes, are defined as lakes which receive the bulk of their water by groundwater exfiltration along their upgradient shoreline and discharge most water through infiltration along their downgradient shoreline (Born et al., 1979). In the coastal dunes many lakes belong to this category, because the in- and output of surface runoff can generally be neglected. As a matter of fact practically all dune lakes, spreading basins of course excluded, have at least some groundwater in- and output. The first author to recognize the throughput of groundwater in Dutch dune lakes, was Londo (1971), who studied lake Grote Vogelmeer west of Haarlem. Also Van Dijk & Meltzer (1981) noticed the possibility of groundwater throughput in dune lakes.

A groundwater contribution to the water balance of lakes is recognized as an essential supply of nutrients, especially SiO_2 (for diatoms; Hurley et al., 1985) and PO_4^{3-} (in case of exfiltration of eutrophic groundwater; Van Dijk, 1984), and acid buffering components like HCO_3^- (Kenoyer & Anderson, 1989; Cook et al., 1991). For further hydrochemical details around flow-through lakes in the dunes reference is made to section 4.6.

Further hydrological consequences as observed in dunes north of Scheveningen

An extremely large number of dune lakes is observed in the dunes north of Scheveningen and south of Katwijk aan Zee, in between the North Sea and the westernmost spreading basins. The southern part of this area is shown in Fig.3.50, together with the position of two rows of observation wells, that were used for hydrological and hydrochemical research. The lakes generally are shallow (< 1 m), well mixed and surrounded by and containing phreatophytes (mainly reeds). The deeper ones are (semi)permanent and the others dry up during summer or soon after a prolonged period of low water levels in the spreading basins.

The high number of dune lakes is related to (1) the presence of spreading basins, where a relatively high water level is maintained, and (2) either the complete absence of a recovery or the presence of a recovery with a low-yield, to their west. These spreading basins are therefore drained on their west flank mainly by the North Sea, as can be deduced from the isohypses in Fig.3.50.

Chemical contrasts between groundwater in the capture and release zone of a flow-through lake (Fig.4.30) and between infiltrated Meuse water and autochthonous dune water (section 4.4.6) were used, in combination with hydrological data and temperature measurements (Fig.3.51B), to visualize the flow patterns (Stuyfzand & Moberts, 1987a,b).

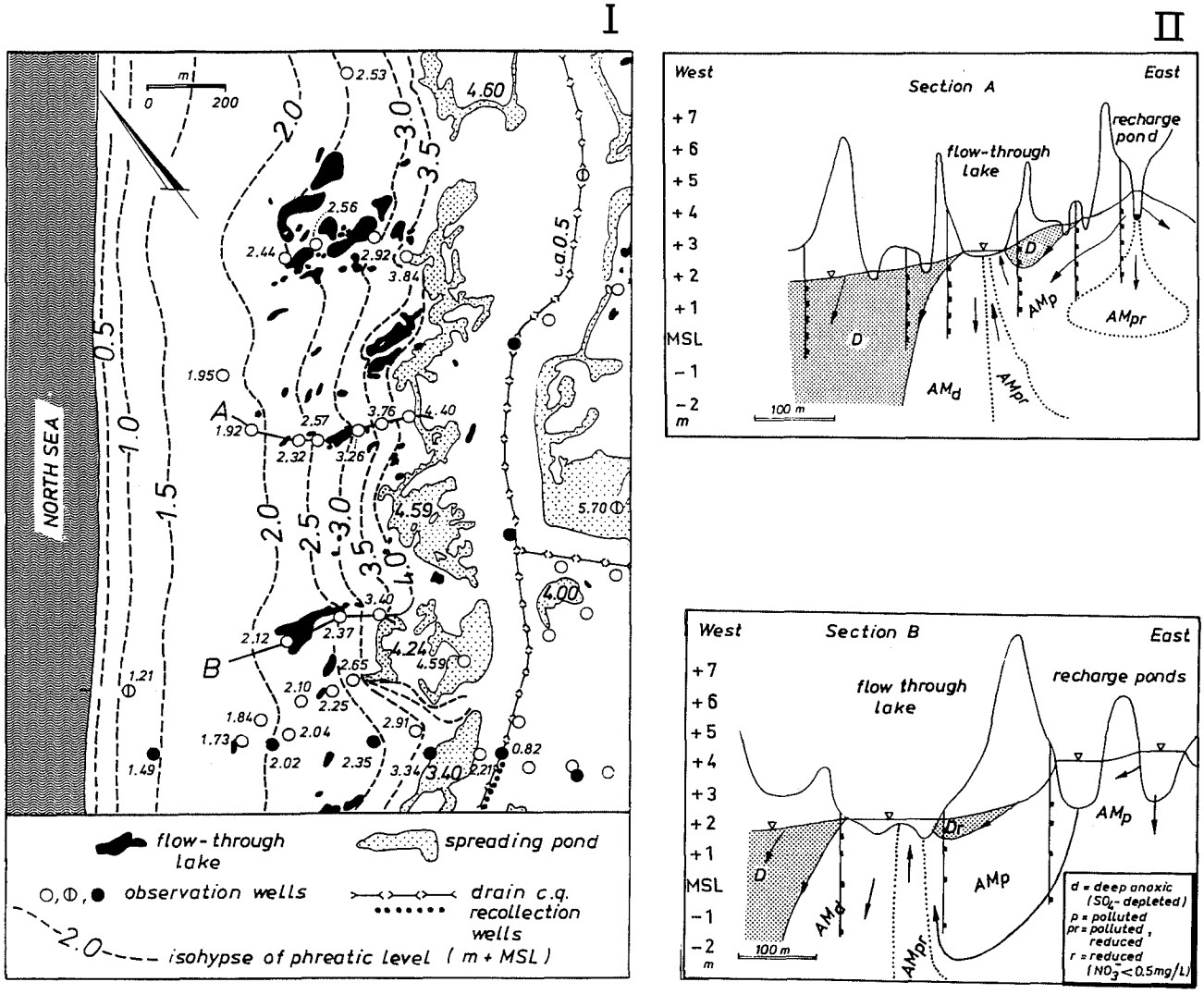

FIG. 3.50 I : Flow-through dune lakes in West-Meijendel (see Fig.3.1) adjacent to spreading ponds, with isohypses of the mean phreatic level for 1985 and the position of two rows of observation wells. II : The areal distribution of infiltrated Meuse water (AM) and autochthonous dune water (partly as rain water lenses; D) along the indicated sections A and B, with the deduced flow patterns. For further explanation of chemical zones (d,p,r) see section 4.6.

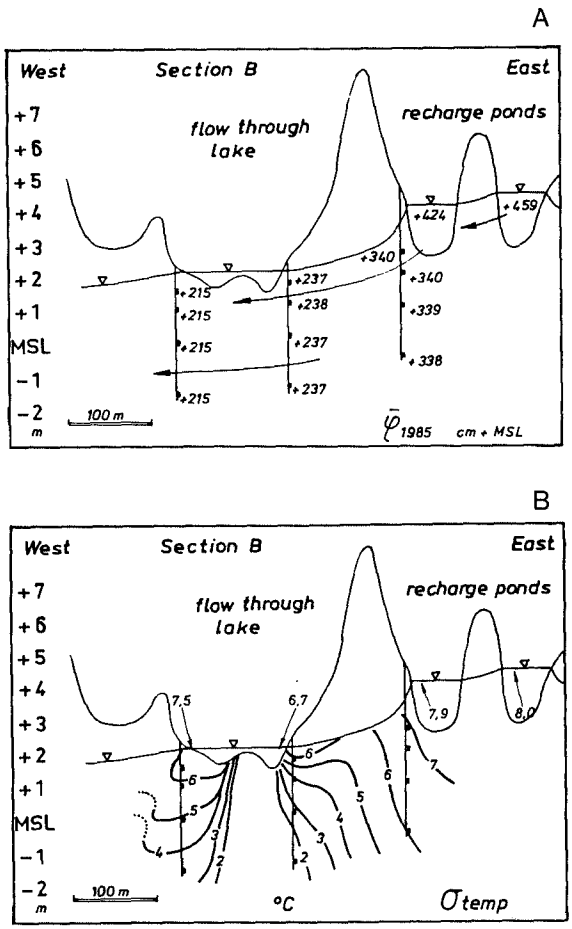

FIG. 3.51 A : Mean hydraulic head distribution for 1985 along section B in Fig.3.50, with the erroneous flow pattern as deduced from head measurements alone. B : The seasonal fluctuations of groundwater temperature (given as the standard deviation from mean annual temperature) in section B indicate an upward flow along the upgradient shore line (strongly reduced fluctuations by heat exchange with the porous medium) and downward flow along the downgradient shore line (restored amplitude of fluctuation by heat exchange with the atmosphere in the dune lake). The correct flow pattern is shown in Fig.3.50.

Hydraulic head measurements alone can be quite misleading (Fig.3.51A), because the vertical head gradients are too small in permeable sand to be noticed with conventional measurements accurate to 0.5 cm.

The patterns in Fig.3.50 demonstrate : (a) exfiltration on the upgradient parts (the capture zone) and discharge along the downgradient shore line (the release zone) of flow-through lakes; (b) the presence of weakly developed rain water lenses in between the spreading basins and the first, large flow-through lakes at about 100-150 m; (c) a predominant contribution of Meuse water to the water balance of these first lakes, which are therefore considered as making part of the Meuse groundwater flow system; (d) a well developed rain water lens downgradient of these first lakes; and (e) still further downgradient the presence of autochthonous dune water floating on North Sea water at great depth. Flow-through lakes in this zone belong to the dune groundwater flow system.

Flow-through lakes may have a strong effect on fluctuations of the phreatic level, as illustrated in Fig.3.52A. Upgradient of a large, (semi)permanent flow-through lake fluctuations are reduced (compare wells 9 and 10 upgradient of lake e_N in Fig.3.52A), due to the so-called open-water effect (increase in porosity from 40% in dune sand to 100% in the lake). And downgradient of an episodic flow-through lake fluctuations strongly increase (compare wells F and D on either side of lake f_o in Fig.3.52A). This is caused by elimination of the strong recharge function of a flow-through lake in its downgradient parts, as soon as it dries up.

Flow-through lakes also have a profound effect on the flow pattern in plan (schematized in Fig.3.52B). The lake behaves like a hydrological short-circuit, or as Winter (1986) puts it, as a thin layer of high permeability which focuses the regional flow towards it. This does not only happen in vertical section (Fig.3.50) but evidently also in plan, where we see convergence of flow lines in the capture zone and divergence in the release zone.

A perpendicular orientation to (sub)regional groundwater flow, an elongate shape and a large distance between the upgradient and downgradient side probably enhance interference with the groundwater flow pattern, both in section and plan (Fig.3.52B).

Modelling

Some interesting tools exist to model the groundwater flow pattern around flow-through lakes. A complicated 2D analytical solution for two selected flow cases around flow-through lakes, has been given by Townley & Davidson (1988). The 2D finite difference model FLOWNET by Van Elburg et al. (1986, 1991) was applied by Stuyfzand et al. (1992b) to a wet dune slack at the island Schiermonnikoog, and a finite-difference, 3D advection-dispersion model was applied by Krabbenhoft et al. (1990).

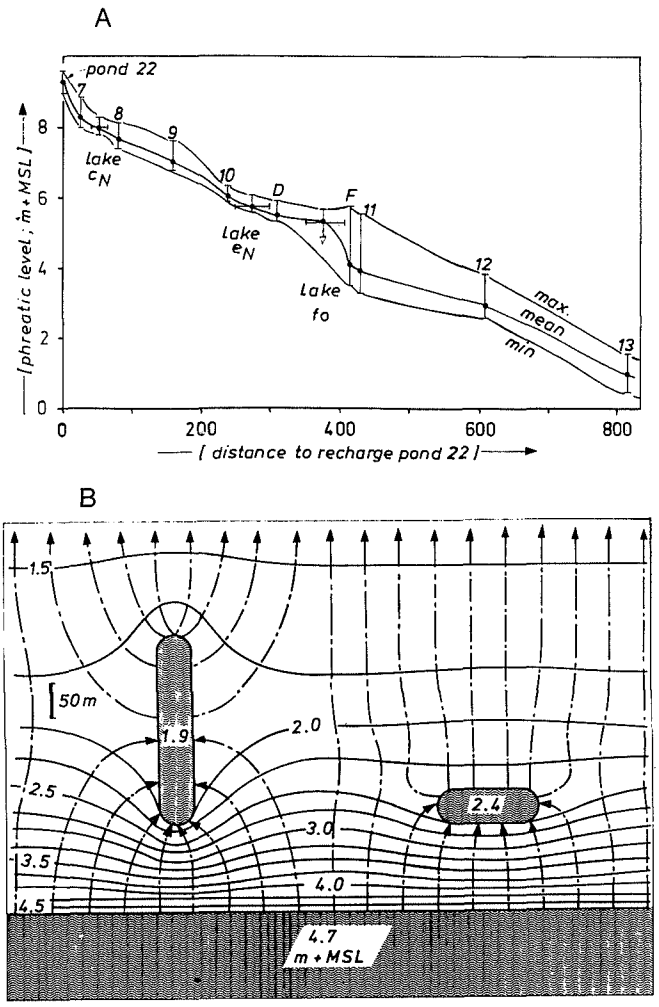

FIG. 3.52 Effects of flow-through lakes on the phreatic level. A : impact on fluctuations along a row of piezometers in the Boerendel area south of Katwijk aan Zee in 1988. B : impact on the groundwater flow pattern in plan.

Before modelling, additional field data are required, however, on the presumed exponential decrease of exfiltration and discharge offshore (McBride & Pfannkuch, 1975; Born et al., 1979), the contribution of evapotranspiration to water losses from the lake, and the hydraulic resistance offered by bottom sludge. Stuyfzand & Moberts (1987b) demonstrated the strong effect of the latter two factors on the flushing rate of a flow-through lake, by way of a simple water balance.

3.11 Concluding remarks

The original complexity of the hydrology of the study area, through alternating fresh and salt water intrusions, has been further raised by man. Land reclamation, drainage, flushing of the drainage arteries with river Rhine or Lake IJssel water, groundwater pumping and artificial recharge in the dunes, all contribute to a highly vulnerable and dynamic hydrological system. A hydrological steady state never occurred during the Holocene, which should be taken into account when calibrating hydrological 2D and 3D steady state models.

Today, hydro-ecologists urge hydrologists to optimize groundwater abstraction, artificial recharge and recollection in the dunes, in order to achieve the best water quality and natural fluctuations of the phreatic level in the root zones or lakes. Rain water lenses and flow-through lakes, as demonstrated here, therefore deserve special attention.

The next chapter will reveal that regional hydrochemical patterns will help to further visualize flow patterns and reveal the impact of fresh and salt water intrusions, even if these are no longer active. Examples of groundwater dating are presented in section 6.7 and in chapter 7.

Chapter 4

HYDROCHEMICAL FACIES ANALYSIS OF THE COASTAL AREA

Abstract

Application of the Hydrochemical Facies Analysis to the study area revealed the presence of six hydrosome types. These are, in order of decreasing age : (1) the more than 2 million y old, connate, marine Maassluis hydrosome, with a deep anoxic, salinized, calcareous and unpolluted facies; (2) the relict, Holocene transgression hydrosome, that formed 8000-300 y ago in either a lagoonal, tidal flat and estuarine environment behind coastal barriers (the marsh type) or an open marine environment (the coastal type). The marsh type is slowly bleeding out in the deep polders, with a deep anoxic, salinized, calcareous and unpolluted facies; (3) the actual North Sea hydrosome, which makes part of the man-enforced, North Sea flow system that originated about 1000 y ago. The most common facies is reduced, calcareous, unpolluted and without base exchange; (4) several coastal dune hydrosomes, that originated mainly in between 3800 and 200 BC and exhibit a large diversity of facies; (5) several polder hydrosomes, as part of relict and, above all, man-made polder flow systems. The latter originated upon the reclamation of deep lakes in the period 1500-1880 AD. The general facies is freshened, (deep) anoxic, calcareous and polluted or unpolluted; and (6) several artificial recharge hydrosomes, as part of man-made flow systems. Most of them originated after 1955 AD. The common facies is polluted, (sub)oxic to reduced, either salinized or without base exchange, and calcareous.

The actual distribution of the recognized hydrosomes and their hydrochemical facies is shown on maps (1:200,000) and in cross sections, and interpreted. For each hydrosome and the most common facies a typical analysis of major and trace constituents is given, forming a valuable check-list for natural backgrounds in hydrochemistry in the specified environments. The best environmental tracers for recognition of each hydrosome are discussed.

Ten facies chains are recognized along flow paths ranging from 0.4 to 12 km in length. They relate to freshening dune water, salinizing North Sea water, freshening polder water and various artificial recharge waters. The most evolved chain is the freshening dune chain near Bergen, starting in decalcified dunes and terminating in the deep Geestmerambacht polder. It contains five different evolution lines in optima forma : from polluted to unpolluted, from acid (pH4) to basic (pH8.5), from oxic to methanogenic, from "without base exchange" to a strong positive base exchange (by freshening), and from fresh to brackish by mixing with and transition into relict Holocene transgression water. The accompanying sequence in water types is from F_*NaCl, F_0NaCl, F_1CaMix, F_2CaMix, F_2CaHCO_3, F_2CaHCO_3+, F_2MgHCO_3+, F_3NaHCO_3+, F_4NaHCO_3+, to B_5NaCl+.

The areal distribution of hydrosomes and their facies is shown on a smaller scale around flow-through lakes in between Katwijk aan Zee and Scheveningen, and for a moist dune slack south of Egmond aan Zee. The passage of bottom sludge in dune lakes, and a shallow depth to the groundwater table around flow-through lakes and in moist to wet dune slacks, have a crucial effect on the facies, especially on the redox index (reduced to deep anoxic) and phosphate levels (slightly to strongly eutrophic). The high biological productivity of flow-through lakes in the dunes is explained by the focusing of (sub)regional groundwater flow and nutrient transport towards the lake.

4.1 General

The HYdroChemical Facies Analysis (HYFA) presented in chapter 2, is applied here to the 1500 km^2 coastal area of the Western Netherlands, in between Monster and Camperduin (Fig.3.1). The main focus is directed, however, on the 900 km^2 area north of the mouth of the Old Rhine, for which hydrological and hydrochemical maps to a scale of 1 to 50,000 were prepared by Stuyfzand (1985a, 1987d, 1988b, 1989a). Those four separate sheets are united here into one sheet to a scale of 1 to 200,000. This necessitated updates due to (1) new data, (2) a gradual development of the HYFA, and (3) the mapping of angles and strips of land not investigated before. For hydrochemical maps of a large part of the area to the south of the Old Rhine, reference is made to Stuyfzand et al. (1993).

The application of HYFA constitutes the mapping and descriptive phase of regional chemical surveys of groundwater (Fig.1.7). The regional application to groundwater in the period 1976-1990, which is considered as the actual state, forms the bulk of this chapter. Further details on the chemical evolution and chemical processes along flow paths within selected hydrosomes, are given in ch.7 and 8.

A subregional application of HYFA to flow-through dune lakes in between Katwijk aan Zee and Scheveningen is presented in section 4.7. And a local application to the moist dune valley Reggers Sandervlak south of Egmond aan Zee, is given in section 4.8. The pollution index has been substituted for in these applications by phosphate as a water quality index, because of more direct hydro-ecological relevancy. As a matter of fact, eutrophication phenomena have been clearly observed in these areas (Van Dijk, 1984; Den Hoed et al., 1987; Nijssen, 1990; Grootjans et al., 1988).

4.2 Hydrochemical data collection and screening

4.2.1 Inventory of all available data

About 10,000 complete and 5,000 incomplete chemical analyses (definition in section 2.3.1), on regionally distributed groundwater samples in the coastal area in between Monster and Camperduin, were selected from several sources : the archives of RIVM, PWS, Hoogovens and the water supply companies PWN, WLZK, GW, EWR and DZH; a vast stock of unpublished and published reports; and records based on own field campaigns. The data pertain to groundwater from temporary piezometers, single piezometers, piezometer nests, multilevel wells equipped with miniscreen, pumping wells and gas wells, in the period 1880-1992.

About 70% came from the younger dunes, 25% from the beach barrier and beach plain landscape and 5% from the deep polders. On average 25, 60, 10, 5 and <1% was pumped from a depth of <20, 20-50, 50-85, 85-150 and >150 m-MSL, respectively. The 15,000 analysed samples were obtained from about 3000 different sites, each with, on average, three sampled depths and two samples repeated after a considerable time. Nearly 80% of all samples was collected north of the Old Rhine. From the 10,000 complete analyses about 8% contained information on several up to 40 trace elements, 6% on natural isotopes (mainly ^{18}O and ^{3}H), 3% on organic micropollutants and incidentally micro-organisms, and 1% on methane.

Complementary information on the position and shape of the transition zone in between fresh and salt groundwater, was obtained from geo-electrical sensors installed in monitoring wells, geo-electrical bore-hole logs and surface geo-electrical surveys using the Schlumberger arrangement. The latter surveys were documented by Van Dam & Meulenkamp (1967), Van Dongen (1969), Lageman (1979), Speelman & Senden (1979) and Cornelissen (1980).

4.2.2 Screening and ranking

The 15,000 analyses were judged on four criteria : quality of the sample, quality of analysis, profundity of analysis (number of parameters examined) and relevancy of the sample.

Quality of groundwater samples

This aspect was checked against the problems listed in Table 2.2, as far as possible with all available information regarding the well, sampling device and sampling protocol.

About 5% of all samples required removal from the database by strong admixing of drilling fluids in insufficiently developed wells. Another 5% was clearly affected by leakage of shallow groundwater into deep risers (Fig.2.6, especially case D), often evident from raised SO_4^{2-} levels or strongly reduced SiO_2 concentrations, typical for shallow dune groundwaters. Especially Pb (15% of Pb analyses) but also Zn, Cd and Sn suffered from their well-known initial mobilization from fresh PVC screens and PVC risers (Boelens, 1959; Poels & Dibbets, 1982; Parker et al., 1990). A more constant delivery of Cu by screens made entirely of copper, which was common practice before 1953, spoiled 30% of the Cu-analyses. Degassing of deep groundwaters resulted in far too low Ca^{2+} and HCO_3^- concentrations and too high pH values, by precipitation of calcite, in 5% of all samples.

Endemic (80%) was the impact of oxygenation of anoxic samples rich in Fe^{2+}, on orthophosphate, because of common practice to filtrate the samples in the laboratory prior to its analysis. In that way $Fe(OH)_3$-flocs are removed together with PO_4^{3-} in samples that were not acidified (Bray et al., 1973; Stuyfzand, 1983a, 1987c).

About 10% of all samples was obtained using the poorest sampling device of all : air-lift (Fig.4.1). Although this led to a general pH increase by 0.3-0.8 units, in most cases the analysis of major constituents was little affected by desisting from any filtration and by acidification of the subsample for metals. Lack of filtration of groundwater apparently free from suspended fines, and subsequent acidification for conservation resulted in raised concentrations for many sensible trace elements (Table 2.3) by dissolution of clay (50% of all samples). Many samples could be corrected, however, using Al as an indicator and regression parameter (section 2.3.2).

And finally about 20% of all samples was obtained from pumping wells and gas wells with an unacceptably long well screen (>10 m), leading to a high degree of mixing of different water types.

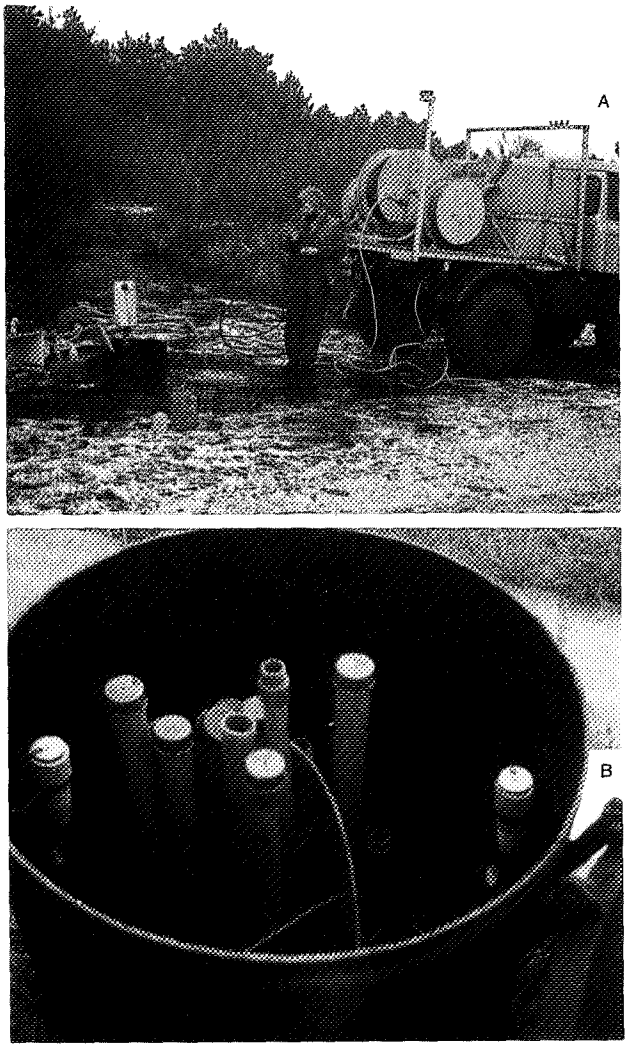

Fig. 4.1 A : Sampling of groundwater with air-lift, the quickest but poorest sampling device of all. Discontinuous flow is regulated by a buffer barrel mounted to the riser; B : An example of a piezometer nest equipped with permanent electrical conductivity sensors for direct salinity readings.

Quality and profundity of a (reported) analysis
The quality was checked by calculation of the ionic balance and electrical conductivity (section 2.3.3), by analysis of the internal chemical consistency against the hydrological backgrounds of the sample (section 2.3.3) and by comparison with samples from the same or similar environments. About 5% of all samples was judged to have a completely unreliable analysis and was discarded from the database. In many cases trace element analyses were of poor quality due to many kinds of interferences or useless due to too high detection limits.

A very extensive, high quality analysis on a sample of high quality yields a high profundity. This may rank the sample as a prototype for a specific hydrochemical facies of a given hydrosome. Missing values of trace constituents like heavy metals, organic microcontaminants and natural isotopes in samples from that hydrosome with the same hydrochemical facies, can then be estimated from its prototype. About 500 samples satisfied the criteria for a high profundity.

Relevancy of a sample
The relevancy was judged both in a time and spatial perspective. No relevancy by old age and significant changes in the close surroundings of the sampling point led to skipping (10%), a high relevancy of an incomplete analysis stimulated to estimate missing values (10%).

After scrutiny 5000 complete and 2500 incomplete analyses survived, which is 50% of the preselected 15,000 samples. Listings containing the majority of screened, complete analyses of samples taken to the north of the Old Rhine, have been included in Stuyfzand (1985a, 1987d, 1988b and 1989a). Only the most important sample localities are shown on Enclosure 1.2.

4.2.3 Collection and analysis of 2500 samples

Collection
During several campaigns in the period November 1977 - January 1983 the author collected about 1750 regionally distributed groundwater samples from single piezometers, piezometer nests and multilevel wells equipped with miniscreens. In the period 1984-1991 he conducted field campaigns in cooperation with water supply companies and the Provincial Authority of North Holland, which resulted in another 750 samples.

An evacuation of at least three times the water content of riser plus well screen, preceded the sampling. However, this refreshening was continued in (semi)confined groundwater, until stability was reached in EC- and pH-logs of the water discharged. About 85% of the samples was obtained by vacuum, 5% by a point source bailer after flushing under vacuum or air-lift, and 10% by air-lift. Most samples were 0.45 µm membrane filtered in situ, those obtained by air-lift and many samples by vacuum from miniscreens, were not filtered.

Filtration was discarded in air-lifted samples and initially in samples from miniscreens as well, because this was feared to affect the sample composition. Chemical instability of dissolved substances was caused there by CO_2 losses and oxygenation. In case of miniscreens, oxygen

remained and leaked into the vacuum pumped bottles, in which water from the miniscreens was sucked (Fig.2.5). Filtration of anoxic water rich in dissolved Fe^{2+} from miniscreens with a low yield (1 liter in ≥½ hour), was indeed observed to lead to filtration of $Fe(OH)_3$ flocks formed on site. In many cases this lack of filtration caused no anomalies with equivalent filtered samples. Yet, it was decided in 1988 to routinely apply filtration on site to all samples obtained from miniscreens, in order to exclude subjective criteria and avoid uncertainties connected with later corrections for suspended fines. The latter especially regards the many trace elements to which the correction procedure using Eq.2.1 does not apply (section 2.3.2).

For samples with analysis of trace elements (TEs), isotopes or chlorinated hydrocarbons adsorbable to activated coal (AOCl) in addition to major constituents, bailer drilled observation wells with a well screen length ≤2 m were considered mainly. The wells selected, had been flushed and sampled at least three times in a 1-3 years period prior to sampling for extensive analysis, in order to check for the condition of the facility and to reduce suspended matter and deleterious interactions with screen and riser.

Analysis

Temperature, EC, pH and occasionally CO_2, O_2 and redox potential (Eh) were measured onsite. Alkalinity and again pH and EC were measured in the laboratory, directly after sampling. The portion to be analysed for most trace elements, Ca^{2+}, Mg^{2+}, Fe, Mn, SiO_2 and PO_4 (both ortho and total) was directly acidified to pH=1.5 using HNO_3-suprapure and was stored in the dark at 4 °C in polyethylene vessels rinsed out with HNO_3, distilled water and the water to be sampled.

Main constituents were analysed in all samples with conventional, well-standardized analytical methods, which need no further description, at the laboratories of VU, PWN, GW, EWR, DZH and KIWA, which participated in inter-laboratory comparison studies. It is noteworthy, however, that a new method for the determination of DOC, introduced in 1981, gave lower results by 33%.

Different methods of analysis of trace elements were applied to a total of 500 samples by ECN, PWN, GW, DZH and KIWA. The latter four used more or less conventional methods : Atomic Absorption Spectrophotometry (AAS) with a graphite furnace, matrix modifiers (MM) and occasionally standard addition (SA) for : Ag, Al, B, Ba^{2+}, Be, Cd, Co, Cr, Cu, Li^+, Mo, Ni, Pb, Rb^+, Sn, Te, Ti, Tl and V; AAS-hydride with MM and SA for : As, Hg, Sb and Se; AAS-flame for Fe, Mn, Sr^{2+} and Zn; potentiometry after ion-chromatographic separation for Br^-, F^- and I (total inorganic); and a selective electrode for F^-.

The KIWA laboratory has recognized since about 1988, that groundwater requires a special approach, which deviates from standardized AAS-methods for water as described by the Dutch Normalization Institute (NNI). The instability of groundwater, special matrix and the presence of several valencies for redox-sensitive elements (often due to oxygenation above ground) necessitate a specific receipt of matrix modifiers and background corrections for each element (Van der Jagt & Stuyfzand, 1991). Hettinga & Stuyfzand (1991) observed that about 10 µg Al/l, 0.3 µg Pb/l and 0.04 µg Cd/l derived from their sampling and filtration equipment. This stresses the importance of sampling blancs in the field, which are subjected to the whole sequence of sampling, sample pretreatment, conservation and analytical procedures. The correction for blancs is common practice in analytical procedures in the laboratory, but does not include what happens before arrival at the laboratory. The increased knowledge of all pitfalls resulted in the selection of the more recent data with a correction for field-blancs, where a choice could be made.

Neutron activation analysis (NAA) after preconcentration of most elements on activated carbon, was carried out at The Netherlands Energy Research Foundation (ECN, Petten). The elements considered are : Ag, Al, Au, Ba^{2+}, Br^-, Ce, Co, Cr, Cs, Cu, Eu, Fe, Hf, Hg, I, La, Lu, Mn, Mo, Nd, Ni, Rb^+, Sb, Sc, Se, Sm, Sn, Sr^{2+}, Ta, Tb, Th, Ti, U, V, W, Yb and Zn. For analytical details reference is made to Van der Sloot (1976) and Van der Sloot et al. (1983). The NAA-analysis of Al, Co, Eu, Fe, La, Mo, Se, Sn, V and Zn after preconcentration on activated carbon was previously tested on (1) penoxic, fresh groundwater, (2) anoxic-methanogenic, fresh groundwater and (3) anoxic, sulphate-stable salt groundwater, by recovery of added radioactive isotopes (Stuyfzand, 1979). Recovery was >95%, except for La (62-76% in all samples) and for V, Se and Eu in salt groundwater (90%).

Natural isotopes were analysed in 400 samples at the Centre for Isotope Research (CIR, Groningen) : the radioactive ^3H and ^{14}C by proportional gas counting, and the stable ^2H, ^{13}C and ^{18}O by mass spectrometry (MS), as specified by Mook (1989). Non-volatile chlorinated hydrocarbons adsorbable to activated coal (AOCl) were analysed in 40 samples by PWN and KIWA, by microcoulometry after stripping to remove volatile organohalogens.

The more sophisticated sampling procedures and direct data controll resulted in a low amount of samples rejected from the database (3%) as compared to data derived from archives and literature (27%), and in an overall higher quality of the data.

4.3 Construction and presentation of regional maps

4.3.1 Starting-points

Maps to a scale of 1 : 200,000 had to satisfy both the hydrologist, hydro-ecologist, policy-maker and geohydrochemist. Due to a far too high number of hydrochemical facies in the complex coastal area of the Western Netherlands, it was judged convenient to present surveyable maps with many associations of hydrochemical facies and to add a separate hydrochemical facet map, displaying one particular aspect, namely the chemical water type.

Many facies were therefore associated according to option II in Table 2.15. This resulted in the mapping of the facies by combination of the base exchange index (freshened, salinized or without base exchange), redox index ((sub)oxic, reduced or deep anoxic), pollution index (unpolluted or polluted) and calcite saturation index (acid or calcareous). Temperature was excluded as there was too little variation (generally within 11 ± 2°C).

Concentrations of heavy metals, As, tritium, AOCl and thermotolerant Coli bacteria had to be estimated for many samples, in order to determine the pollution index POLIN. This was done by interpolation of the results of neighbouring groundwater samples, or by taking the results of a prototype of that particular hydrosome and facies. For instance, from a detailed study on relatively few, but well selected samples in the coastal area of the Western Netherlands, it was concluded that (deep) anoxic dune groundwater below the extensive Holocene aquicludes 1D, 1E and 1F+G and sufficiently remote from their borders, does not contain measurable amounts of tritium, AOCl and Cd, Cr, Cu, Hg, Ni, Pb and Zn (sections 7.3 and 7.4). And Coli bacteria were never detected in any groundwater, except for small areas bordering septic tanks or polluted influent surface waters (Baars, 1957; Hoekstra, 1984).

Hydrosomes and their facies were coded according to Table 2.14 and 2.15 (option II), respectively. Boundaries between hydrosomes of similar chlorinity were set at their 50% mixing divide, thus between fresh Dune, Polder and Artificial recharge water, and between salt connate Marine water, North Sea water and relict, coastal Holocene transgression water. Between two hydrosomes of quite different chlorinity a mixing zone was introduced : (D/S) between dune and North Sea water, with Cl^- = 300-15,500 mg/l; (D/L) between dune and relict Holocene transgression water (L), with Cl^- = 300-variable (best judgement); and (P/L) between polder and relict Holocene transgression water (L), with Cl^- = 500-variable (best judgement). Mixing zones with a strong preponderance of one end-member were coded for instance (D+L), indicating Dune water with admixture of relict Holocene transgression water (L).

The hydrochemical facet map was based on the chemical classification of water types as outlined in section 2.4.1. For the sake of simplicity the main types oligohaline through fresh-brackish have been associated into fresh (F = Cl^- < 300 mg/l) and the main types brackish and brackish-salt into brackish (B = 300 < Cl^- < 10,000 mg/l).

4.3.2 Origin detection

The groundwater flow systems discerned in section 3.9 and the superimposed hydrochemical facies, reveal the presence of six hydrosome types in the studied area (Table 4.1). These are in alphabetical order regarding their code (within brackets), which follows Table 2.14 : Artificial recharge (A), coastal Dunes (D), relict Holocene transgression, among others in a Lagoonal environment (L), connate Marine (M), Polder (P) and open Sea (S). Each of the types A, D and P consists of several individual hydrosomes with a regional, subregional or local extension (Table 3.7), whereas the others occur as a single hydrosome of supraregional dimension. The relict, Holocene transgression hydrosome has been subdivided into the marsh type (L) and coastal type (LC).

The origin of water, or rather its hydrosome, was identified mainly on the basis of one or several of the hydrochemical labels (tracers) listed in Table 4.1. These environmental tracers cannot be applied without a check on all kinds of spatial and temporal variation. Occasionally, seasonal and/or annual quality fluctuations were available to assist in the identification. For a general discussion on tracers for origin detection, reference is made to section 2.5.

The combination of two conservative tracers, like chloride and ^{18}O, and chloride and bromide (Fig.4.2) is highly recommended, as the individual tracer may not result in a clear distinction between two hydrosomes, especially when the seasonal fluctuations in both hydrosomes overlap (Fig.4.9). The distinction between coastal dune groundwater and recharged river Rhine or Meuse water, is not only relevant to the coastal plain of the Western Netherlands, but also to the fluvial plain of both rivers. These waters recharge Pleistocene aquifers there, either spontaneously or by induced recharge in the neighbourhood of groundwater pumping stations (Stuyfzand, 1989c).

TABLE 4.1 The major hydrosome types and their hydrochemical recognition, in the study area. For further data on the chemical composition of pretreated river Rhine, river Meuse and Lake IJsselmeer water, reference is made to the annual reports of the Water transporting company Rijn-Kennemerland Ltd (WRK), and the water supply companies GW and DZH. In bold type = the best tracer.

Hydrosome	code	age of water y before 1993	VARIATION OF ANNUAL MEANS[1] OR COMPOSITION[2] Cl^- mg/l	HCO_3^- mg/l	SO_4^{2-} mg/l	F^- µg/l	K^+ mg/l	Mg^{2+} mg/l	$-\delta^{18}O$ ‰	^3H TU[§]	RECOMMENDED TRACERS (for ( ), [ ], { }, @ and HFP see foot notes)
Artificial recharge :											
· Meuse	AM	0-17	58-67	179-200	48-67	280-460	4.5-5.3	8.2-9.8	7.5	100-220	**^3H**, (F^-), {Cl^-}, (@), HFP
· Rhine, Lek	AR	0-38	114-228	136-169	61-103	160-400	5.5-9.9	10.2-13.7	9.3	50-600	**$\delta^{18}O/Cl^-$** (Fig.4.9), Br^-/Cl^- (Fig.4.2), (Mg^{2+}), (@), {Cl^-}, (temp)
· Rhine, IJsselmeer	AR	0-12	132-220	121-141	111-153	130-200	7.3-9.3	11.8-14.0	8?	40-160	{Cl^-}, [SO_4^{2-}/Cl^-], (Mg^{2+}), **HFP**
· polder Monster	AP	10-23	128-207	230-260	180-232	250	21-27	20-27	6?	-	**Br^-/Cl^-** (Fig.4.2),[SO_4^{2-}/Cl^-],{Cl^-},(K^+, Mg^{2+})
· polder Katwijk	AP	0-53	80-214	220-280	70-130	200-400	10-22	14-20	6.5		{Cl^-}, (B,F,I,V,K^+, Mg^{2+}), Sr/Ca, (@), **HFP**
Polder[3] :											
· Geestmerambacht	P	0-3000?	200-330	230-260	130-220		13-17	23-33	5?		**$\delta^{18}O/Cl^-$** (Fig.4.2), **HFP**, (@)
· Haarlem	P	0-150	120-240	230-290	125-180		10-22	15-33	5-6		**$\delta^{18}O/Cl^-$** (Fig.4.2), **HFP**, (@)
Dune	D	0-1000	10-300	0-1200	0-200	10-1500	0.2-50	2-50	6-8	0-180	**$\delta^{18}O/Cl^-$** (Fig.4.9); Br^-/Cl^- (Fig.4.2); HFP
North Sea	S	0-1000	14,500-17,500	180-1000	1000-2400	50-440	250-310	1000-1250	2-4	0-40	**$\delta^{18}O/Cl^-$** (Fig.4.2), {Cl^-}, {HCO_3^-}
Relict Holocene :											
· marsh type 2#	L	300-5800	2000-5000	>1,000	0-100	10-100	50-100	90-200	4-5	0	{Cl^-}, {HCO_3^-}, **HFP**, $\delta^{18}O/Cl^-$
· marsh type 1	L	5800-8000	5000-12,000	500-1000	100-1000	10-150	100-150	200-600	3-5	0	{Cl^-}, {HCO_3^-}, **HFP**
· coastal type	LC	1000-5800	12,000-15,000	300-500	1000-2000	10-300	100-250	500-1000	2-4	0	{Cl^-}, {HCO_3^-}, **HFP**
Connate Maassluis	M	>2·10[6]	5000-13,500	300-500	400-800	100-200	50-100	300-700	3-5		NH_4^+/HCO_3^- (Fig.4.5); SO_4^*/Cl^- (Fig.4.5), DOC/HCO_3^-, **HFP**

[1] = regarding the surface water prior to spreading (artificial recharge hydrosomes) or prior to spontaneous infiltration (polder hydrosomes); [2] = regarding Dune, North Sea, relict Holocene transgression and connate Maassluis water; 3 = since 1975, estimated from fragmentary data set; § = surface water without correction for radioactive decay, groundwater as sampled in 1980-1985; ( ) = if system sufficiently flushed (adsorption complex in equilibrium), and if well checked on anomalous concentrations in adjacent hydrosome; [ ] = if redox conditions remain favourable to stability of compound, and if well checked on anomalous concentrations in adjacent hydrosome; { } = if well checked on anomalous concentrations in adjacent hydrosome; (@) = specific, persistent hydrophylic xenobiotics (for Rhine : bisdichloro(iso)propylethers, bentazone, tetrachloro-orthophtalic acid and Na-dicegulac), if system sufficiently flushed; HFP = Hydrochemical Finger Print; # = connate water in the Bergen clay excluded (Cl^- = 10,000-16,000 mg/l; see sample 19B.109-16 in Table 4.3).

The identification of each hydrosome type and of selected polder and artificial recharge hydrosomes will be discussed in combination with their areal distribution and facies in section 4.4.

4.3.3 Maps, sections and typical analyses

The areal distribution of hydrosomes (with their hydrochemical facies) and chemical water types, is separately presented in : plan at about 30 and 80 m-MSL respectively, for the area to the north of the Old Rhine (Enclosures 4.2-4.5); four cross sections up to a depth of 150 m-MSL, respectively near Bergen, Castricum, Haarlem and Leiduin (Enclosures 5-6); and one longitudinal section running over the younger dunes from Camperduin in the north to Monster in the south (Enclosure 7). The position of all sections is shown in Fig.3.1.

The areal distribution of hydrosomes, their facies and chemical water type is also shown in two schematized cross sections up to a depth of 260 m-MSL: near Bergen-Alkmaar, where the fresh dune water lens was only little affected by excessive pumping and artificial recharge of the dunes is lacking (Fig.4.3); and south of Zandvoort aan Zee across the Leiduin catchment area, where inordinate pumping caused a severe salinization and necessitated artificial recharge of the dunes with river Rhine water in 1957 (Fig.4.4). These sections also differ in the following respects : the depth of decalcification of dune sand in the upper aquifer (up to 20 m near Bergen and < 2 m (unsaturated zone only) south of Zandvoort aan Zee); the position of hydrochemically important aquitards (like the Bergen clay at 15-30 m-MSL near Bergen and the glaciolimnic Drente clay at 70-80 m-MSL in the Leiduin area); the salinity of relict Holocene transgression water (higher in the Bergen area where the Bergen tidal inlet was situated); the position of chloride inversions (in the Bergen clay and Drente clay, respectively); and the unique occurrence of a fresh dune water enclave in the Leiduin area at about 100 m-MSL. In 1910 it was still connected with the main dune hydrosome, but salinization led to its amputation.

A list of all 50 HYFA map units is presented in Table 4.2, the hydrosomes in approximate order of increasing age, and the facies within each hydrosome in alphabetical order. This table has been reproduced as Enclosure 8, in order to facilitate the

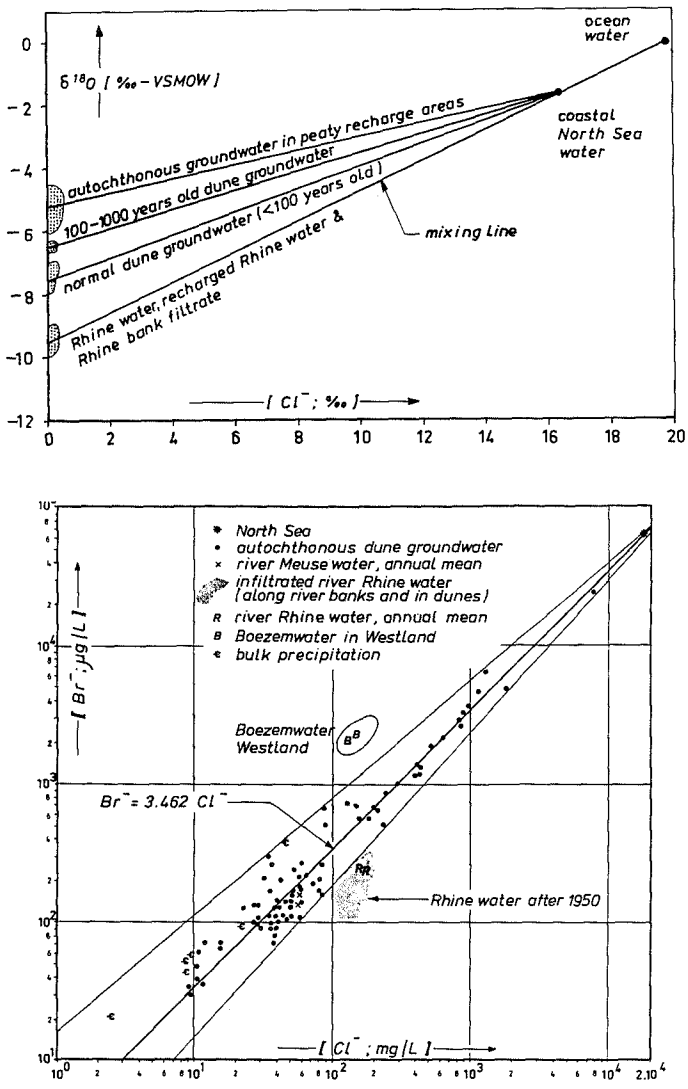

FIG. 4.2 Recognition of selected hydrosomes by their position in a $\delta^{18}O$-Cl^- and Br^--Cl^- diagram.

reading of this chapter and the enclosures 4-7. It gives a short explanation to the HYFA-codes and lists the most common chemical water types for each facies.

Results of representative chemical analyses are listed for the most frequently encountered facies of each hydrosome type, in Tables 4.3 (major constituents) and 4.4 (trace elements and isotopes). They have been ordered approximately in the same way as Table 4.2. The following discussion of hydrosomes and their identification, areal extent and facies follows more or less the chronological sequence of their formation. Information on the nature and extent of chemical reactions, is given in chapters 7 and 8.

4.4 Discussion of the discerned hydrosomes and their facies

4.4.1 The connate, marine Maassluis hydrosome (M)

Relatively low carbon concentrations, both inorganic (as HCO_3^-) and organic (as DOC), in combination with a strong depletion of SO_4^{2-} and high concentration of NH_4^+, which normally point at a strong interaction with organic carbon, distinguish this hydrosome from the other brackish and saline groundwaters (Fig.4.5). Also uncommon are the rather strong depletion of K^+ (K^* being -3.2 mmol/l) despite a not so negative BEX (-17.1 meq/l), and the high concentrations of Co and Sb.

The exact mechanisms that have led to this remarkable composition, remain unclear. Diagenetic changes in compacting clay, like the fixation of K^+ or the exchange of NH_4^+ for K^+, may play a role. And the combination of a strong sulphate depletion (7.3 mmol/l) with the lack of an about double as high HCO_3^- production (see Eqs.4.2A and 4.2B), may point at sulphate reduction by upward migrating methane from a deeper source, leading to the following reaction :

$$CH_4 + SO_4^{2-} + Ca^{2+} + Fe(OH)_3 + 0.25\ CH_2O(NH_3)_{0.08} + (n\text{-}3.5)\ H_2O \rightarrow FeS\cdot nH_2O + CaCO_3 + 0.02\ NH_4^+ + 0.23\ H_2CO_3^* + 0.02\ HCO_3^- \quad (4.1)$$

This reaction is obtained by taking Eq.8.47 + Eq.8.14 - Eq.8.30B (see Tables 8.2-8.4). It should be verified by checking for secundary calcite (which may form cements) in the Maassluis Formation, and by analysis of the ^{13}C content of this precipitated, secundary calcite (should be very low, about -40 ‰ ; Van Straaten, 1991).

The Cl^- concentration (5,000 - 13,500 mg/l) is lower than in present day coastal North Sea water (Cl^- = 15,500 - 17,000 mg/l). This may be related to the admixing of fresh river water during sedimentation of the Maassluis Formation or to freshening during later continental phases. The high Br^- concentration and $\delta^{18}O$ value (-3.75 ‰ with Cl^- = 11,200 mg/l at 337 m-MSL in well 30D.207) indicate anyhow, that the salt has not been derived from a salt dome, but is of direct marine origin.

The Maassluis hydrosome is probably present at a supraregional scale within aquitard 5 and underlying sediments, which make part of the Maassluis Formation (Fig.3.2 and 3.4A) and Oosterhout Formation. It has been found in each of 9 available piezometer nests in the province of North Holland, north of the North Sea Canal, at 10-40 m below the

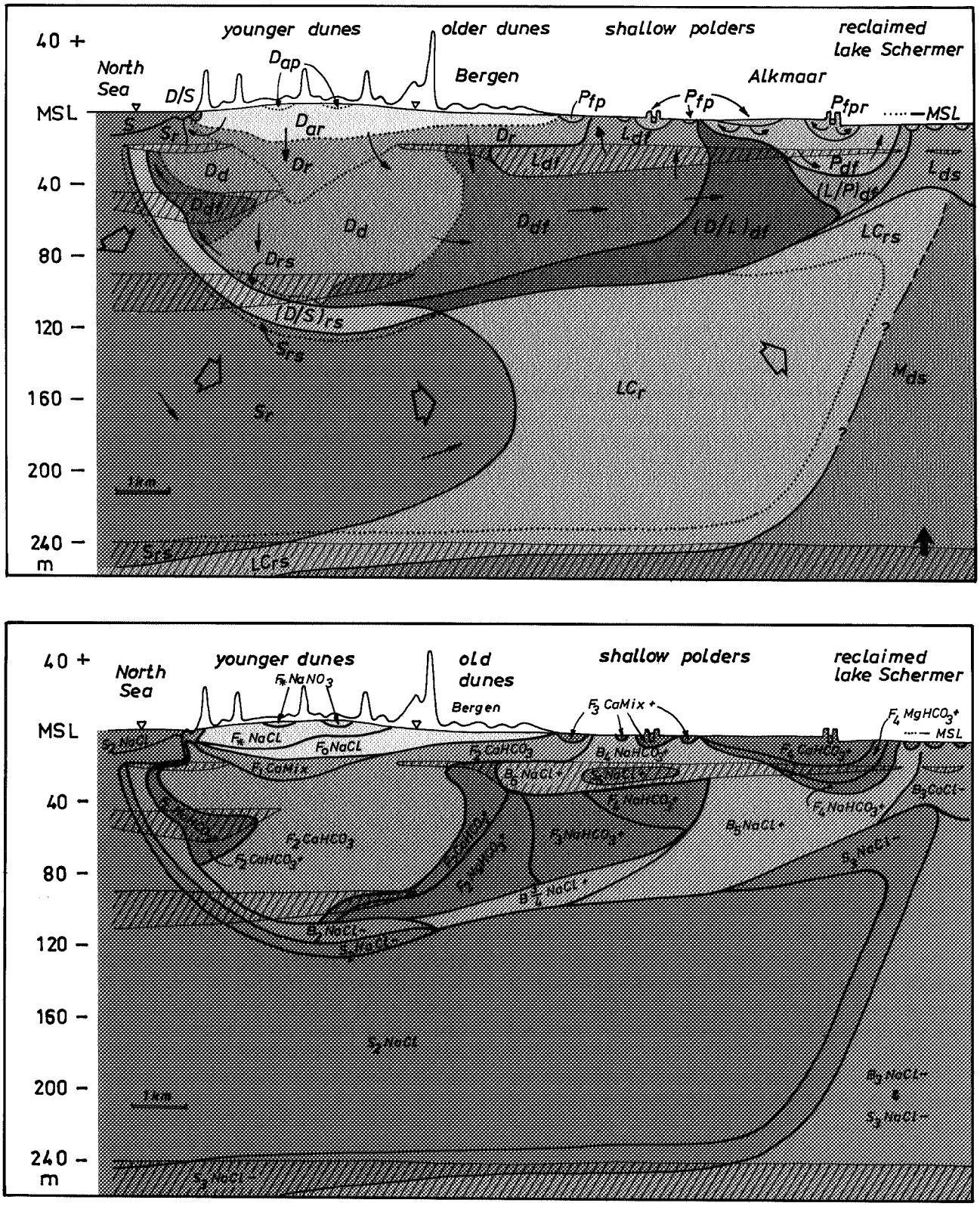

FIG. 4.3 Schematized cross sections over the coastal dunes near Bergen, with the areal distribution of hydrosomes, their hydrochemical facies and chemical water types, in the period 1975-1990 AD. For location of the profile see B in Fig.3.1. Hatched areas indicate the aquitards. The legend to the HYFA codes is given in Table 4.2 and Enclosure 8.

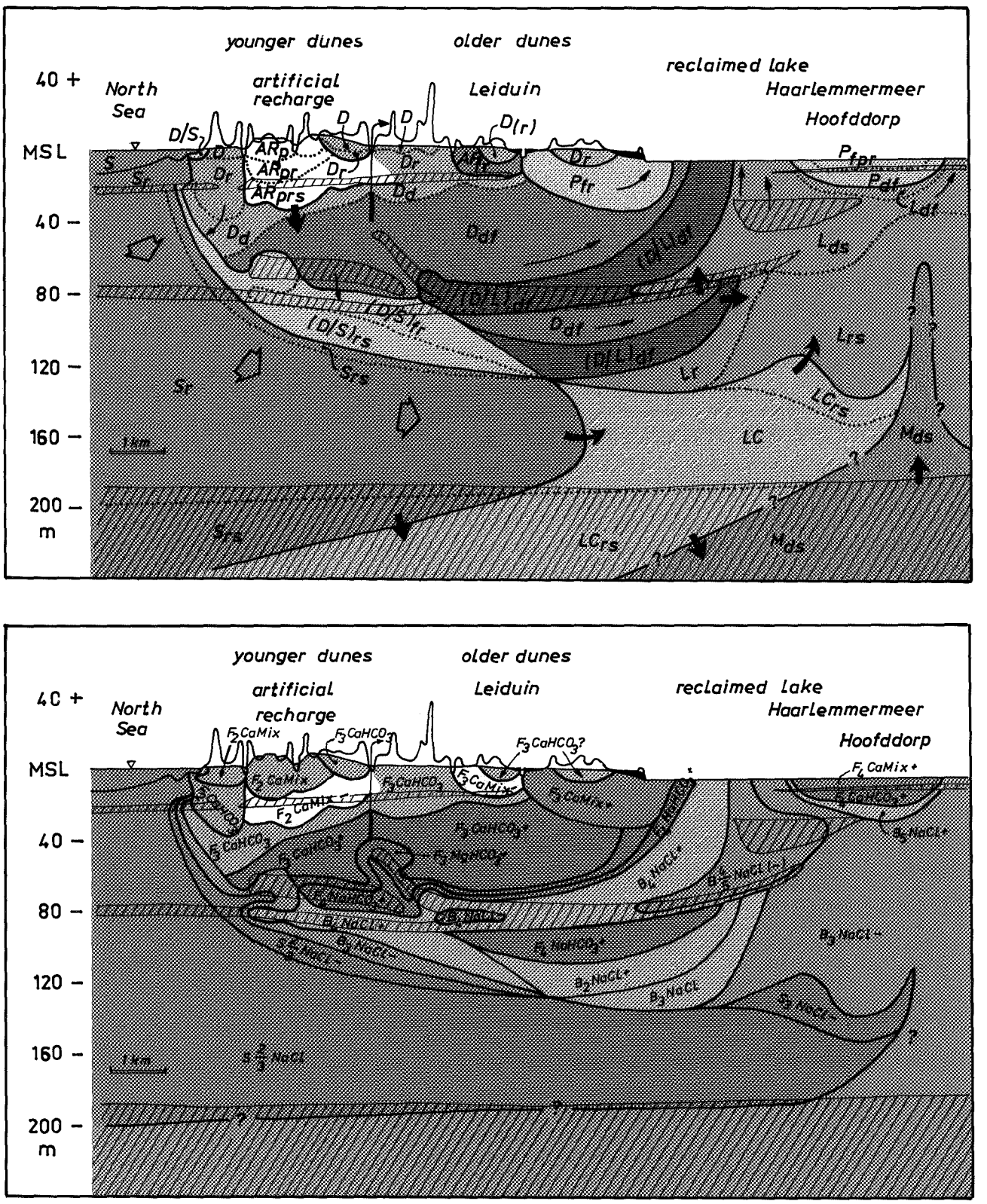

FIG. 4.4 Schematized cross section over the coastal dunes south of Zandvoort aan Zee across the Leiduin catchment area, with the areal distribution of hydrosomes, their hydrochemical facies and chemical water types, in the period 1975-1990 AD. For location of the profile see F in Fig.3.1. Hatched areas indicate the aquitards. The legend to the HYFA codes is given in Table 4.2 and Enclosure 8.

TABLE 4.2 Listing and explanation of all 50 HYFA map units, with the most frequently encountered chemical water type for each facies. Also available as Enclosure 8.

Map unit	explanation	common water types
FRESH, ARTIFICIAL RECHARGE HYDROSOMES		
AE_{df}	Sewage effluent Zandvoort; deep anoxic, freshened, (calcareous, unpolluted)	F_3-F_4CaHCO_3+, F_3NaHCO_3+
AE_{fpr}	Sewage effluent Zandvoort; freshened, polluted, reduced, (calcareous)	F_3-F_4CaMix+
AM_{fpr}	Meuse[@]; freshened, polluted, reduced, (calcareous)	F_2CaMix+
AM_p	Meuse[@]; polluted, (calcareous, [sub]oxic, without base exchange)	F_2CaMix, F_2CaHCO_3
AM_{pr}	Meuse; polluted, reduced, (calcareous, without base exchange)	F_3CaMix, F_3CaHCO_3
AP_{df}	Polder[@]; deep anoxic, freshened, (calcareous, unpolluted)	F_3-F_4CaHCO_3+
AP_{fp}	Polder[@]; freshened, polluted, (calcareous, [sub]oxic)	F_2CaMix+
AP_{fr}	Polder[@]; freshened, polluted, reduced, (calcareous)	F_3CaMix+, F_3CaHCO_3+
AP_r	Polder[@]; reduced, (calcareous, unpolluted, without base exchange)	F_3CaMix, F_3CaHCO_3
AR_{fr}	Rhine[@]; freshened, reduced, (calcareous, unpolluted)	F_2NaMix+, F_2NaCl+, F_2MgMix+, F_2MgCl+
AR_p	Rhine[@]; polluted, (calcareous, [sub]oxic, without base exchange)	F_2CaMix, F_2NaMix
AR_{pr}	Rhine; polluted, reduced, (calcareous, without base exchange)	F_2CaMix
AR_{prs}	Rhine[@]; polluted, reduced, salinized, (calcareous)	F_2CaMix-, F_2CaCl-
FRESH, POLDER HYDROSOMES		
P_{df}	Deep anoxic, freshened, (calcareous, unpolluted)[@]	F_4CaHCO_3+, F_4-F_5MgHCO_3+, F_4-F_5NaHCO_3+
P_{fp}	Freshened, polluted, (calcareous, [sub]oxic)[@]	F_3CaMix+, F_3CaHCO_3+
P_{fpr}	Freshened, polluted, reduced, (calcareous)	F_3CaMix+, B_4NaCl+
P_{fr}	Freshened, reduced, (calcareous, unpolluted)[@]	F_3CaHCO_3+, F_3CaMix+
FRESH, DUNE HYDROSOMES		
D	(calcareous, [sub]oxic, unpolluted, without base exchange)[@]	F_2CaMix, F_2CaHCO_3
D_{ap}	Acid, polluted, ([sub]oxic, without base exchange)[@]	F_*NaCl, F_*NaNO_3, F_*CaMix
D_{ar}	Acid, reduced, (unpolluted, without base exchange)[@]	F_*NaCl, F_0NaCl, F_0CaMix
D_d	Deep anoxic, (calcareous, unpolluted, without base exchange)[@]	F_2-F_3CaHCO_3
D_{df}	Deep anoxic, freshened, (calcareous, unpolluted)[@]	F_2-F_4CaHCO_3+, F_2-F_4MgHCO_3+, F_3-F_5NaHCO_3+
D_{ds}	Deep anoxic, salinized, (calcareous, unpolluted)[@]	F_2-F_3CaCl-, F_2-F_3MgCl-, F_2-F_3NaCl-
D_{fr}	Freshened, reduced, (calcareous, unpolluted)	F_3MgCl+, F_3NaCl+
D_p	Polluted, (calcareous, [sub]oxic, without base exchange)[@]	F_3CaNO_3, F_2-F_3CaMix, F_3CaHCO_3
D_{pr}	Polluted, reduced, (calcareous, without base exchange)[@]	F_2CaSO_4, F_3CaMix, F_3CaHCO_3
D_r	Reduced, (calcareous, unpolluted, without base exchange)[@]	F_1-F_2CaMix, F_2-F_3CaHCO_3
D_{rs}	Reduced, salinized, (calcareous, unpolluted)	F_2CaCl-, F_2NaCl-
BRACKISH AND SALINE, UNMIXED HYDROSOMES		
LC_r	relict Holocene coastal type[@]; reduced, (calcareous, unpolluted, without base exchange)	S_3-S_4NaCl
LC_{rs}	relict Holocene coastal type; reduced, salinized, (calcareous, unpolluted)	S_3-S_4NaCl-
L_d	relict Holocene marsh type[@]; deep anoxic, (calcareous, unpolluted, without base exchange)	B_5-B_6NaCl, S_5-S_6NaCl
L_{df}	relict Holocene marsh type[@]; deep anoxic, freshened, (calcareous, unpolluted)	B_4-B_6NaCl+, S_5-S_6NaCl+,
L_{ds}	relict Holocene marsh type[@]; deep anoxic, salinized, (calcareous, unpolluted)	B_3-B_4CaCl-, B_3-B_5NaCl-, S_5NaCl-
L_r	relict Holocene marsh type; reduced, (calcareous, unpolluted, without base exchange)	B_3-B_5NaCl
M_{ds}	connate Maassluis[@]; deep anoxic, salinized, (calcareous, unpolluted)	B_3NaCl-, S_3NaCl-
P_d	Polder, north of Old Rhine, deep anoxic, (calcareous, unpolluted, without base exchange)	B_3NaCl
P_r	North Sea canal polder; reduced, (calcareous, unpolluted, without base exchange)	B_4NaCl
S	North Sea[@]; (calcareous, [sub]oxic, unpolluted, without base exchange	S_2NaCl
S_r	North Sea[@]; reduced, (calcareous, unpolluted, without base exchange)	S_2-S_4NaCl
S_{rs}	North Sea; reduced, salinized, (calcareous, unpolluted)	S_2-S_4NaCl-
MIXED HYDROSOMES, BRACKISH OR SALINE		
$(AR/D/S)_{fr}$	Artificial Rhine, Dune and North Sea; freshened, reduced, (calcareous, unpolluted)	B_3NaCl+
$(D/L)_{df}$##	Dune and relict Holocene marsh type[@]; deep anoxic, freshened, (calcareous, unpolluted)	B_4-B_6NaCl+, B_5-B_6NaHCO_3+
$(D/S)_{ds}$	Dune and North Sea; deep anoxic, salinized, (calcareous, unpolluted)	B_3-B_4NaCl-, S_4NaCl-
$(D/S)_{fr}$	Dune and North Sea; freshened, reduced, (calcareous, unpolluted)	B_3-B_4NaCl+
$(D+S)_{rs}$	Dune with some North Sea[@]; reduced, salinized, (calcareous, unpolluted)	B_2-B_3CaCl-, B_3MgCl-
$(D/S)_{rs}$	Dune and North Sea[@]; reduced, salinized, (calcareous, unpolluted)	B_2-B_3CaCl-, B_2-B_3NaCl-, S_2-S_3NaCl-
$(L+D+S)_{ds}$	relict Holocene with some Dune and North Sea; deep anoxic, salinized, (calcareous, unpolluted)	B_5NaCl-
$(L+P)_{df}$	relict Holocene with some Polder; deep anoxic, freshened, (calcareous, unpolluted)	B_4-B_5NaCl+
$(L/P)_{ds}$	relict Holocene and Polder; deep anoxic, salinized, (calcareous, unpolluted)	B_3-B_4CaCl-, B_4-B_5NaCl-
$(P/L)_{df}$	Polder and relict Holocene; deep anoxic, freshened, (calcareous, unpolluted)	B_5NaCl+

@ = listing of chemical analysis in Tables 4.3 and 4.4; ## = also $(D+L)_{df}$

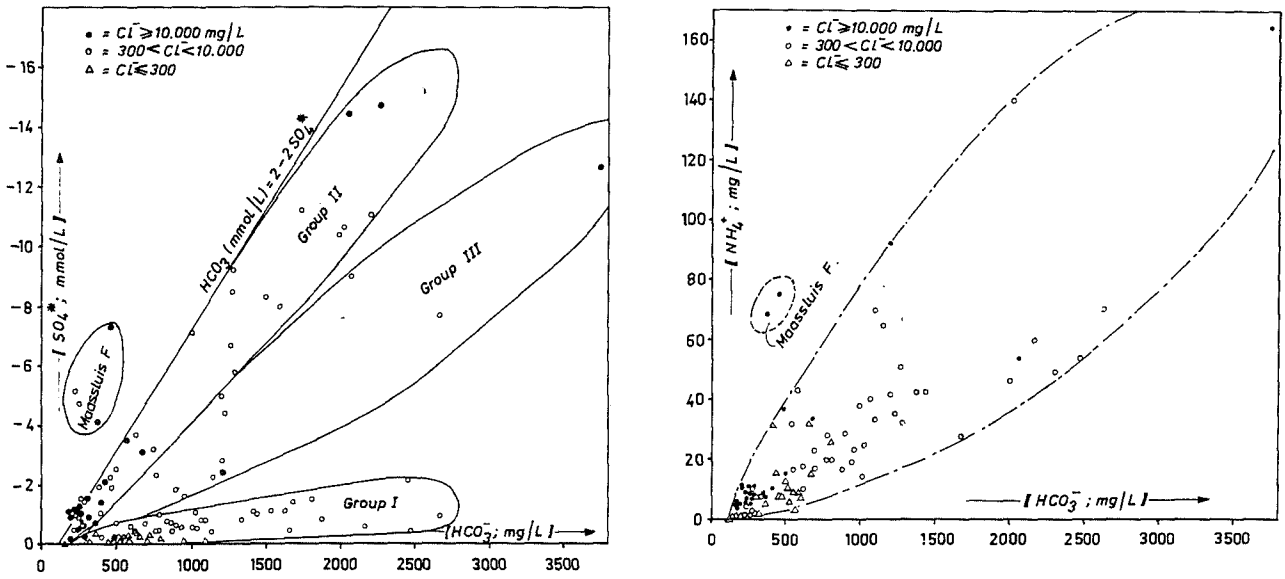

FIG. 4.5 The exceptional composition of connate, marine Maassluis water as compared to (deep) anoxic groundwaters in the second and third aquifer, belonging to the hydrosomes L (300 < Cl⁻ ≤ 16500 mg/l), S (15,000 < Cl⁻ ≤ 17,000 mg/l), D (Cl⁻ ≤ 300 mg/l) or P (Cl⁻ ≤ 300 mg/l). Group I = relatively low contribution of sulphate-reduction and high contribution of methanogenesis to alkalinity; Group II = relatively high contribution of sulphate-reduction and low contribution of methanogenesis to alkalinity; Group III = high contribution of both sulphate-reduction and methanogenesis to alkalinity.
SO_4^* = sulphate corrected for a contribution of sea salt (see Table 5.5). A negative value indicates sulphate reduction.

top of the Maassluis Formation, which is situated there at 230-290 m-MSL (see also Fig.4.3). The same holds for each of five abandoned piezometer nests north of Scheveningen, where Maassluis water with a Cl^- content of 8,000-13,000 mg/l was found repeatedly in the period 1910-1946 below intruded North Sea water, deeper than 160 m-MSL (deduced from DZH files).

It is probable that Maassluis water is ascending in the centre of deep reclaimed lakes. At 75 m-MSL, about 100 m above the Maassluis Formation, water with the same characteristics was obtained from piezometer nest 25C.340 in the centre of the Haarlemmermeer polder (Fig.4.4).

Sample 19A.259 in Tables 4.3 and 4.4 forms a prototype of the Maassluis hydrosome. The facies is in general calcareous, unpolluted, deep anoxic and salinized, leading to the code M_{ds}. The redox index is sulphate-reducing or methanogenic, the pollution index around 0.5 and the calcite saturation index close to zero. The water type is B_3NaCl- or S_3NaCl-

4.4.2 The relict, Holocene transgression hydrosome (L)

These brackish and saline groundwaters were formed 300 till 8000 years ago during the Holocene transgressions. This lumped hydrosome is characterized by a large hydrochemical variety, due to strong variations in salinity and in the deposition and erosion of reactive Holocene aquitards, both in space and time, during its formation. For simplicity three members are discerned :
(a) the young, marsh type (L^{m2}), which formed in a sedimentary environment composed of lagoons, marshes (partly high moors) and estuaries, behind a well developed coastal barrier with few tidal inlets;
(b) the ancient marsh type (L^{m1}), which formed in a sedimentary environment composed of tidal flats, lagoons, marshes (low moors) and estuaries, behind a less protective coastal barrier with many coastal inlets; and
(c) the coastal type (LC), which originated in the present dune and beach barrier area, seaward of the most inland beach barrier, or in the Bergen inlet before deposition of the Bergen clay.

Density currents and diffusion partly obscured the original hydrochemical contrasts, which hampers the mapping of these three members. An attempt was made for the cross section to the south of Zandvoort aan Zee (Fig.4.6). It shows the normal, downward succession of L^{m2}, L^{m1} and LC water, which corresponds with a downward increase in age and chlorinity and a downward decrease in alkalinity. Difficulties in the distinction between the members L^{m1} and L^{m2} necessitated their association into L on all other maps (Fig.4.3 and 4.4; Enclosures 4, 5 and 7).

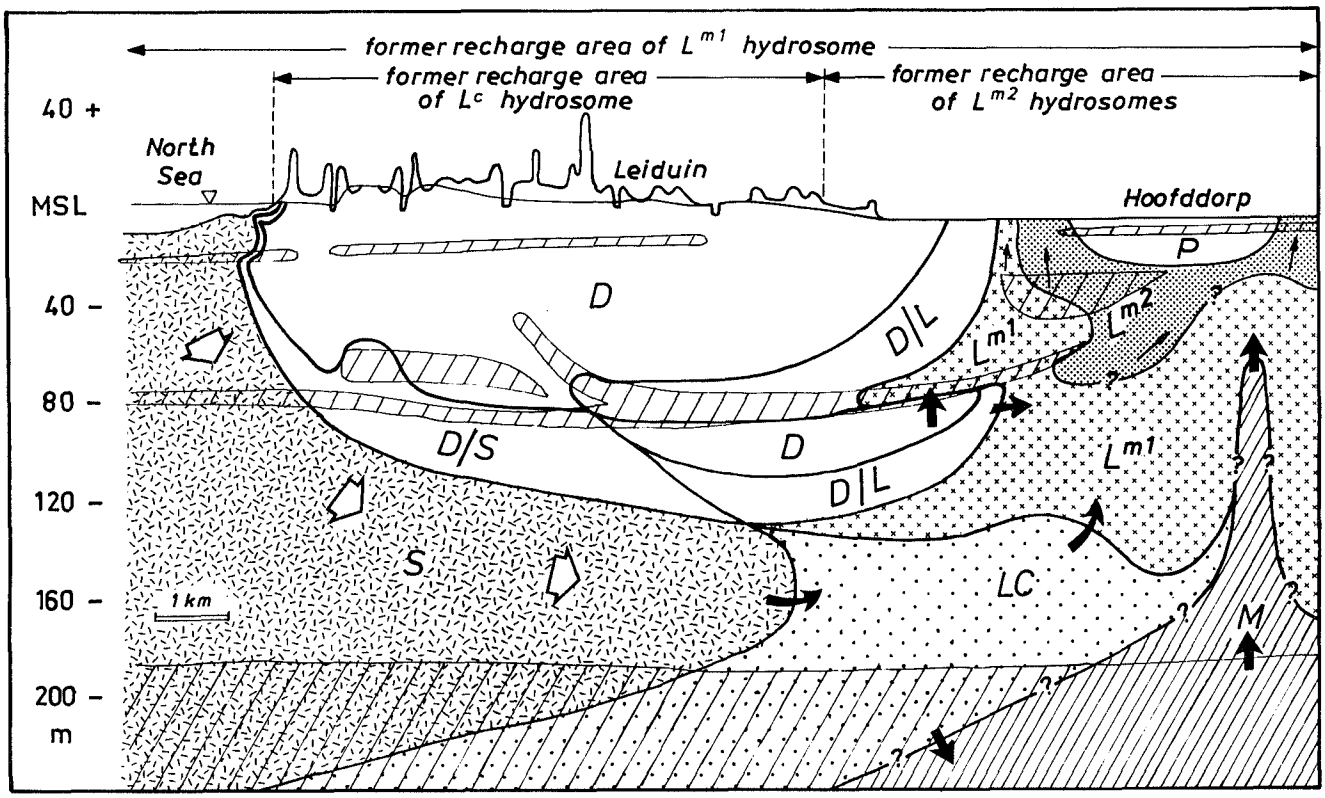

FIG. 4.6 The position of brackish and saline hydrosomes in a cross section over the Zandvoort - Hoofddorp area (same section as Fig.4.4), with subdivision of the relict, Holocene transgression hydrosome (L), into three members : the coastal type (LC), ancient marsh type (L^{m1}) and young marsh type (L^{m2}). The approximate recharge area of these members is indicated.
D = dune hydrosome (also containing nested, artificial recharge and polder hydrosomes; not shown); M = Maassluis hydrosome; P = Hoofddorp polder hydrosome; S = (actual) North Sea hydrosome; D/L = mixing of D with L.

Current recharge is lacking for all members, due to further protection of the area from the sea by man-made dykes and sluices. The epithet "relict" has been added in order to distinguish this lumped hydrosome from the others, which make part of their own groundwater flow system. Expansion of the North Sea, coastal dune and polder systems occurs at the expense of the relict waters, which are bleeding out in seepage areas, mainly in the deep polders (reclaimed lakes).

The marsh types (L^{m} or L)
Relict waters of the marsh type can generally be recognized by their brackish character and very high to extreme alkalinity (Table 4.1). In comparison with the coastal type, the mean chlorinity is lower, due to the admixing of river water or autochthonous rainwater on the less inundated parts. The hydrogencarbonate concentrations are higher because of detention in or passage of Holocene clay and peat layers, rich in shells and unstabilized organic matter (further explained below).

The ancient marsh type originated before the start of formation of the Holland peat around 3800 BC. It is characterized by a higher chlorinity and lower alkalinity than the young marsh type, because of stronger marine influences and the absence of the very reactive Holland peat and younger clays. In case of an age superior to 5000-6000 y, parts of the ancient marsh type originated even before the formation of the aquitards 1D, 1E and 1F, in broad, sandy tidal inlets and gullies cutting through the basal Holocene aquitard 1G or Weichselian aquitard 1H.

With a (moderately) high alkalinity (8-16 meq/l) and raised chlorinity, these waters cannot easily be discerned from the coastal type. The higher chlorinities for the marsh type are found to the north of the North Sea Canal, where little diluted North Sea water invaded the area (Fig.3.27). North of Camperduin the young, marsh type exhibits a relatively high chlorinity. This is caused by proximity to the Zijper inlet (just ouside the study area), which formed in the period 900-1100 AD, and facilitated

TABLE 4.3 Major constituents of recharge and groundwaters in the coastal area of the Western Netherlands, grouped on the basis of hydrosomes and ordered according to their position on a facies chain.

piezo-meter no.	sample depth m+MSL	subsoil flow m	subsoil age y	temp °C	EC 20°C µS/cm	pH	Cl^-	SO_4^{2-}	HCO_3^-	NO_3^-	PO_{4T}	Na^+	K^+	Ca^{2+}	Mg^{2+}	Fe	Mn	NH_4^+	SiO_2	DOC	COD #	O_2	CH_4	watertype	redox	polin	SI_C	code
							mg/L																					
CONNATE MARINE MAASSLUIS WATER																												
19A.259	-338	<100?	$2 \cdot 10^6$	16.0	29670	7.4	11000	840	461	<0.2	6.2	6000	100	310	630	4.10	0.52	75.3	13.9	3.5		<0.2		S_3NaCl-		0.4	0.35	M_{DS}
NORTH SEA WATER BEFORE AND AFTER INTRUSION																												
North Sea	0	0	0	10.5	39000	8.1	16800	2355	160	3	0.51	9350	346	350	1122	<0.1	<0.1	0.4	0.9	2.4	.	9.4	.	S_3NaCl	0	1.8[D]	0.50	S
24H.259	-105	800	80	11.5	40700	7.2	16300	2294	253	<1	2.78	9208	330	357	1080	6.4	0.46	6.1	10.5	4.9	-	<0.2	-	S_3NaCl	4	0.6	-0.15	S_R
24H.018	-132	3370	165	12.0	38750	7.6	16800	2120	260	<1	1.50	9500	310	400	1080	11.0	0.63	7.0	11.5	4.3	-	<0.2	-	S_3NaCl	4	0.5	0.19	S_R
24H.190	-75	1300	130	12.0	27000	6.8	10865	1534	334	<0.2	0.61	5500	70	1150	613	14.9	1.57	13.0	30.0	4.6	-	<0.2	-	S_3NaCl-	4	0.5	0.14	$(S+D)_{RS}$
24H.189	-60	500	90	11.0	17970	6.8	7873	1032	293	<0.5	0.7	3593	20.6	1314	222	27.2	1.30	7.5	17.4	-	.	<0.2	-	B_3NaCl-	4	0.5	0.19	$(S/D)_{RS}$
24H.450	-90	5500	450	11.8	2450	7.0	690	2	385	<0.1	2.10	205	12	280	27	5.5	0.36	5.4	20.0	6.1		<0.2	-	B_3CaCl-	6	0.5	0.28	$(D+S)_{DS}$
24H.189	-55	520	100	11.0	930	7.4	243	3	313	<0.2	0.48	66	3.0	154	7.0	5.0	0.33	1.1	22.2	-		<0.2	-	F_3CaCl-	6	0.5	0.35	D_{DS}
RELICT HOLOCENE TRANSGRESSION WATERS																												
25C.012	-165	7700	3000?	12.5	36000	7.1	14752	2132	290	<1	0.92	8218	249	459	990	12.8	0.56	10.6	12.0	5.8	-	<0.2	-	S_3NaCl	4	0.5	-0.07	LC_R
19B.161	-124	6500	5000?	12.0	39320	7.1	16100	2100	315	<1	4.1	9500	310	400	995	4.7	0.39	11.0	12.2	1.9	-	<0.2	-	S_3NaCl	4	0.5	-0.14	LC_R
19B.109	-16	<5	5000	11.0	38900	7.1	14262	780	3752	<0.2	62.7	8317	256	343	1131	1.21	0.56	164	57.6	71.1	-	<0.2	>12.6	S_6NaCl+	6	0.5	0.90	L_{DF}
19B.049	-67	?	6000?	11.0	16100	7.0	5850	5	1290	<0.2	4.80	2825	88	728	310	14.0	0.70	19.1	34.0	-	84.0	<0.2	-	B_3NaCl-	6	0.5	0.8	L_{DS}
25C.342	-28	?	?	11.3	10250	7.3	3200	3	1200	<0.2	6.43	1950	61	145	195	9.7	0.30	14.2	25.3	18.0	46.2	<0.2	-	B_3NaCl	6	0.5	0.42	L_D
19A.182	-30	.	5000_L	10.5	7450	7.7	1765	41	2458	<0.2	≥37	1395	84	81	215	5.40	0.53	123	65.0	-	-	<0.2	>15	B_6NaCl+	6	0.5	0.97	$(D+L)_{DF}$
RAIN AND COASTAL DUNE WATER, DECALCIFIED DUNES NEAR BERGEN																												
rain	3	0	0	10.0	68	4.4	15	8	0	3.5	0.04	8	0.6	2	1.0	0.05	0.03	1.21	0.2	1.5	4.9	11.0	<0.05	F_eNaCl	.	2.8	-6.5	D_{AP}
14C.041	6.5	3_V	1	10	140	4.3	19	16	0	22.6	0.04	15	1.1	2	1.6	0.29	0.05	0.05	11.2	4.4	17.4	2.0	<0.05	F_eNaNO_3	1	3.2	-6.6	D_{AP}
14C.041	+3.5	5_V	3	10	180	5.7	41	20	13	<0.1	0.43	21	2.8	5	5.4	3.43	0.13	0.19	18.6	1.7	7.3	0.3	<0.01	F_eNaCl	2	1.9	-4.1	D_{AP}
19A.326	-12.5	14_V	18	10	209	6.2	41	24	23	<0.5	0.15	24	1.7	13	2.7	0.7	0.03	0.23	15.1	3.6	13.9	0	-	F_eNaCl	4	1.2	-2.9	D_{AR}
19A.326	-23.5	29_V	30	10	388	7.6	50	47	106	<0.2	0.3	31	2.0	47	3.3	0.4	0.13	0.34	13.3	2.8	11.9	<0.2	0.14	F_1CaMix	4	1.4	-0.29	D_R
19A.159	-93	2500	250	10.5	303	7.6	29	1	156	<0.2	0.43	15	1.2	48	2.5	1.22	0.13	0.45	17.6	4.7	16.6	<0.2	9.1	F_2CaHCO_3	6	0.5	-0.15	D_D
19B.014	-92	4000	350	10.7	323	8.1	33	0	169	<0.5	0.83	24	9.5	13	21	0.69	0.04	0.83	22.9	2.9	11.5	<0.2	5.0	F_2MgHCO_3+	6	0.4	-0.20	D_{DF}
19B.088	-44	6500	600	10.8	696	8.5	35	0	398_A	<0.5	10.56	155	11.5	3	3.1	0.62	0.04	6.19	17.4	20.0	84.9	<0.2	18.2	F_3NaHCO_3+	6	0.7	-0.12	D_{DF}
COASTAL DUNE WATER, CALCAREOUS DUNES SOUTH OF ZANDVOORT AAN ZEE																												
24H.470	0	3_V	1	10.0	357	7.8	30	27	143	25.2	<0.10	18	0.9	56	4.5	<0.05	<0.05	0.05	4.3	3.3	10.8	2.0	<0.05	F_2CaMix	.	2.4	0.04	D
24H.471	-9	13_V	20	10.0	452	7.5	30	27	235	<0.5	1.06	17	1.2	83	3.6	4.54	0.40	0.50	24.0	3.0	-	<0.2	-	F_2CaHCO_3	4	1.6	0.11	D_R
24H.481	-28	30_V	60	10.5	479	7.5	30	6	286	<0.5	1.20	17	3.5	84	8.7	1.26	0.34	1.5	55.6	3.1	8.2	<0.2	3.8	F_2CaHCO_3	5	0.2	0.20	D_D
24H.500	-45	500	100	10.8	554	7.1	33	0	345	<0.2	3.40	21	7.4	90	10.0	3.9	0.42	1.9	29.0	6.0	-	<0.2	-	F_2CaHCO_3+	6	0.1	-0.08	D_{DF}
24H.450	-57	1500	300	11.3	604	7.5	31	1	397	<0.5	2.50	20	17.9	45	44.2	1.83	0.22	3.1	24.7	4.2	15.0	<0.2	-	F_2MgHCO_3+	6	0.3	0.04	D_{DF}
24H.600	-49	5500	650	11.5	1014	7.4	58	0	639	<0.5	3.03	180	23.1	44	22.2	0.84	0.09	3.3	15.9	15.2	-	<0.2	-	F_4NaHCO_3+	6	0.1	0.12	D_{DF}
25C.294	-30	8000	900	11.7	2274	7.9	515	81	533	<0.5	15.9	520	21.0	13	14.0	3.15	0.25	2.15	36.4	47.0	-	<0.2	-	B_4NaCl+	5	0.3	-0.09	$(D+L)_{FR}$
POLDER WATER BEFORE AND AFTER INFILTRATION, GEESTMERAMBACHT																												
Before inf.	-0	0	0	10.9	-	7.9	301	205	248	10.9	3.86	182	16.8	121	33.7	0.38	0.20	2.55	9.6	-	50.0	6.8		B_3CaMix+	.	4	0.56	P_{FP}
19B.173	-9	9_V	?	10.0	1200	7.2	136	69	536	<0.2	6.4	77	20	140	37.0	7.0	0.70	15.5	59.9	12.0	34.4	<0.2	-	F_4CaHCO_3+	5	0.8	0.29	P_{FR}
19B.173	-25	25_V	?	11.0	1150	7.3	154	0	540	<0.5	4.6	62	37	77	76	4.1	0.26	8.0	28.7	9.0	39.0	<0.2	-	F_4MgHCO_3+	6	0.2	0.16	P_{DF}
19B.182	-30	30_V	.	11.0	-	7.6	250	33	952	<0.2	10.8	320	40.7	47	60.3	3.6	0.21	19.3	-	-	-	-		F_4NaHCO_3+	6	<0.5	0.43	P_{DF}
POLDER WATER BEFORE AND AFTER ARTIFICIAL RECHARGE, BOERENDEL AREA SOUTH OF KATWIJK AAN ZEE																												
Before inf.	8.5	0	0	10.5	752	8.7	110	95	220	1.6	0.80	65	13.5	85.3	16.0	0.21	0.14	0.93	3.0	13.0	33.0	9.5	<0.05	F_2CaMix+	1	3.0	1.22	AP_{FP}
30E.b01	5	50	0.2	10.5	1080	7.6	150	6	500	<0.2	11.00	100	22	110	18.0	5.00	0.71	17.0	27.8	13.0	30.0	<0.2	-	F_4CaHCO_3+	6	1.5	0.56	AP_{DF}
30E.b03	-2	240	1.5	10.5	809	7.4	122	58	300	<0.2	2.5	75	14.0	82	17.0	11.0	0.64	0.8	15.6	9.7	27.0	<0.2	-	F_3CaMix+	5	1.8	0.12	AP_{FR}
30E.b07	-6	45	5?	10.5	914	7.4	150	75	304	<0.2	0.73	88	3.4	120	8.9	4.3	0.74	2.8	17.8	9.8	24.0	<0.2	-	F_3CaMix	5	1.5	0.19	AP_R
PRETREATED RHINE WATER BEFORE AND AFTER ARTIFICIAL RECHARGE, NORTH OF SCHEVENINGEN																												
Before inf.	8	0	0	12.6	804	7.8	152	67	162	19.2	0.18	90	6.2	77	11.5	0.04	0.01	0.06	5.0	3.0	9.8	6.0	<0.05	F_2CaMix		3.6[B]	0.23	AR_P
30G.193	0.1	50	0.1	12.5	815	7.7	152	67	170	19.4	0.18	90	6.2	80	11.5	0.04	<0.01	<0.05	4.5	2.3	-	3	-	F_2CaMix	1	2.9	0.14	AR_P
24H.484	-15	800	17.1	10.0	859	7.6	156	71	243	<1	0.49	56	2.2	125	5.1	7.09	0.84	0.64	21.6	4.7	-	<0.2	-	F_2CaMix-	4	2.8	0.35	AR_{PR}
30G.619	-53	200	20	10.0	973	7.75	188	98	186	<0.5	1.73	144	3.6	66	4.9	1.03	0.06	1.02	15.9	3.4	-	<0.2	-	F_2NaCl+	4	2.5	0.08	AR_{FR}
30E.160	-79	300	21	10.5	1090	7.8	225	87	218	<0.5	0.27	121	19.3	53	42.2	0.64	0.11	0.23	15.0	4.2	-	<0.2	-	F_2MgCl+	4	2.1	0.14	AR_{PR}
PRETREATED MEUSE WATER BEFORE AND AFTER ARTIFICIAL RECHARGE, NORTH OF SCHEVENINGEN																												
Before inf.	3	0	0	11.4	572	7.7	61	59	190	14.8	0.20	35	4.8	76	8.9	0.07	0.04	0.07	5.0	5.1	12.8	7.9	<0.05	F_2CaMix	1	3.8[C]	0.15	AM_P
30G.193	0.1	50	0.1	11.3	573	7.7	61	60	196	11.8	0.32	35	4.9	75	8.9	0.04	<0.01	0.02	4.0	3.8	7.0	-	-	F_2CaMix	1-2	3.2	0.12	AM_P
30G.616	-30	100	5	10	610	7.8	69	78	192	<0.2	-	51	6.1	75	6.7	0.56	-	0.39	10.5	3.2	8.5	<0.5	-	F_2CaMix+	4	≥2	0.20	AM_{FPR}

A = + 17 mg CO_3^{2-}/l; B: Coli = 13 counts/l; C: Coli = 28; D: Coli = 1; L = relict Holocene end-member; V = vertical distance; # = as $KMnO_4$.

several marine inundations in the period 1000-1550 AD (Pons & Van Oosten, 1974).

The connate Holocene seawater in the Bergen clay (sample 19B.109-16 in Tables 4.3 and 4.4; the S_6NaCl+ water at 15-25 m-MSL east of Bergen in Fig.4.3) is hard to classify. Its approximate seawater chlorinity pleads for the coastal type, but the extreme alkalinity and stagnant position turn the scale into the marsh type.

The samples 19B.109, 19B.049 and 25C.342 in Tables 4.3 and 4.4 are prototypes for the relict L hydrosome of the marsh type. Their facies is unpolluted, calcareous, deep anoxic and, depending on its hydrological position, either freshened, salinized or without base exchange. This results in the following codes : L_{df}, L_d and L_{ds}, respectively. The chemical water types belonging to these facies are listed in Table 4.2. The pollution index is always around 0.5 (unpolluted) and the calcite saturation index around +0.6. This supersaturation is probably

TABLE 4.4 Trace elements and isotopes in recharge and groundwaters in the coastal area of the Western Netherlands, grouped on the basis of hydrosomes and ordered according to their position on a facies chain.

piezo-meter no	sample depth m+MSL	Al µg/l	As µg/l	B µg/l	Ba^{2+} µg/l	Be ng/l	Br^- µg/l	Cd µg/l	Co µg/l	Cu µg/l	Cr µg/l	F^- µg/l	I µg/l	Li^+ µg/l	Mo µg/l	Ni µg/l	Pb µg/l	Rb^+ µg/l	Sb ng/l	Se ng/l	Sr^{2+} µg/l	U µg/l	V µg/l	Zn µg/l	AOCl µg/l	^3H TU	$\delta^{13}C$ ‰	$\delta^{18}O$ ‰
CONNATE MARINE MAASSLUIS WATER																												
19A.259	-323	-	6.9	-	180	<50	55000	·	7.0	0.3		100	2.0			1.2			2700		6500			<10				
NORTH SEA WATER BEFORE AND AFTER INTRUSION																												
N.Sea	0	5	2.5	3900	40	<10	56000	0.18	0.2	1.4	1	1200	55	160	10.7	0.9	0.7	103	200	90	7100	2.6	1.9	5		25	-	-1.3
24H.259	-105	25	8	-	120	<10	58000	-	1.1	<6		240	73	175	6.2	4	<3	9.6	-	-	7000	<0.05	1.3	26		<3	-11.1	-1.3
24H.018	-132	<5	8		140	-	55000	-	0.1	-		40	137	165	5.6	5	<3	10.0	-	13	7000	<0.05	-	25	-	<3	-	-1.3
24H.190	-75	-	-		150	·	35000	-	-		-	70	312	175	<0.1	-	-	-	-	-	12000	-	-	-	<4	<3		-
24H.189	-60	2	<1.3		41	·	18700	-	0.3		<3	<100	24	-	<1.5	3	<3	<0.5	<10		6124	<0.05	<0.1	6	<4	<3		
24H.450	-90	5	0.9		310	·	2955	-	-	2	-	50	17	28	1.3	-	-	3.1	-	-	2000	<0.01	0.2	28	<4	<3		
24H.189	-55	<100	-		300	·	860	<0.05	-	<5	<3	<100	12	-	<0.1			<0.5	50		-	-	-	-	<4	<3		
RELICT HOLOCENE TRANSGRESSION WATERS																												
25C.012	-165	-	-	-	120	-	55000	-	-	-		10	120	170	3.8	-		10.0			7000		-	-	<4	~		
19B.161	-124	-	0.3	-	200	-	39000	-	4.8	1.5		280	70	150	0.6	5.5		-	-		7000	-	8.3	<10	-	-		
19B.109	-16	23	5.7		120	-	63000	-	3.9	3.2		290	3550	155	<0.5	5.3					7000	-	12.0	10	15§	?		
19B.049	-67	-	-		-	-	-	-	-	-	-	-	-	-	-	-	-	-			-	-	-	-	-	-		
25C.342	-24	<20	0.4		520		10800	<0.1	0.1	<0.6	1.5	-	-	-	<0.1	<0.6	<2	<2			1567	0.01	2.8	<2		0	-	-
19A.182	-30	<20	11.0		17	-	9400	-	9.0	-	-	420	2590	52	<0.5	5.5	-	-			2100	-	2.5	120		<2	+10.1	-6.44
RAIN AND COASTAL DUNE WATER, DECALCIFIED DUNES NEAR BERGEN																												
rain	-	72	0.8	<5	4	<20	65	0.22	0.3	8	0.7	56	-	0.6	<0.6	0.6	15.0	0.4?	890	<160	3	0.02	3.5	29	15	25		-7.8
14C.041	6.5	2600	<1	<50	44	260	-	0.6	1.2	7.7	<1	80	2	5	<0.1	7	3.8	2.8	<500	<1000	<100	-	7.4	60	-	-	-	-7.2
14C.041	+3.5	68	6	<50	<10	<50	-	0.2	<1.0	1.8	2	≤10	2	9	<0.5	4	0.5	1.8	<500	<1000	60		<1	26	10		-	-7.2
19A.326	-12.5	45	1	<100	<10	<50	-	<0.1	<1.0	<1	<1	≤10	3	1	<0.5	<0.5	≤1.0	0.5	<500	<1000	100		<1	7	9		-22.2	-7.0
19A.326	-23.5	<50	1	<100	11	<50	-	<0.1	<1.0	<1	<1	≤10	-	1	<0.5	<0.5	≤1.0	0.8	<500	<1000	170		<1	7	7		-	-7.2
19A.159	-93	9	1.0	<100	21	60	90	<0.1	<1.0	-	<0.5	30	2	3	<0.5	≤1.0	≤1.0	<0.3	<500	<1000	190		<0.5	15	<4	0	-8.8	-6.6
19B.014	-92	17	1.0	-	31	<50	120	<0.1	<1.0	<5	0.2	100	5	5	<0.5	≤1.0	≤1.0	<0.3	<500	<1000	160		<0.5	5	<4	0	-	-
19B.088	-44	240	1.0	<100	<5	100	120	≤0.1	<1.0	<5	6.9	1500	29	6	<0.5	≤1.0	≤1.0	2.2	<500	<1000	<50		15	3	<4	0		
COASTAL DUNE WATER, CALCAREOUS DUNES SOUTH OF ZANDVOORT AAN ZEE																												
24H.470	0	9	<1.0	<100	12	<10	105	0.1	0.2	8	<1	180		4	-	1.8	0.7	<0.5	85	130	250	0.16	0.2	25		76	-11.5	-7.3
24H.471	-9	16	5	<100	20	<10	105	<0.1	<0.1	<0.1	<1	50	-	5	0.3	1.5	<1	<2	52	50	400	<0.01	0.3	3	-	48	-	-7.3
24H.481	-28	9	2	50	11	<10	105	<0.1	0.1	<1	<1	70		6	<0.1	<1	<0.5	-	37	25	420	<0.05	0.3	<2	<4	<2	-8.8	-7.4
24H.500	-45	-	-	-	-	<10	-	<0.1	-	<1	<1	60	-	-	<0.5	<1	<1	-	-	13	-	<0.05	-	<10	<4	<2	-	-
24H.450	-57	3	1.2		72	<10	-	<0.1	0.2	<1	<1	220	:	6	<0.5	<0.5	<1			11	320	0.08	1.5	9	<4	<2	-7.9	-6.8
24H.600	-49	3	1.0		32	<10	180	<0.1	0.1	<1	1	240	-	8	0.2	<1	<1		-	25	280	<0.01	2.0	5	<4	<6	-	-6.5
25C.294	-30	-	0.7	-	74	-	-	<0.1	-	<1		690	1	10	<0.5	0.6	<1	:	26	-	250	-	2.5		<4	0		-
POLDER WATER BEFORE AND AFTER INFILTRATION, GEESTMERAMBACHT																												
Before inf.	0	300	-	500	25	-	-	-	-	-	-	-		25		-	-				600			-		-		
19B.173	-9	<20	0.1	-	27	-	-	<0.1	-	<0.6	<0.5	-		-		<0.6	<2				1040			<6		19		
19B.173	-25	<20	0.1		146			<0.1	-	<0.6	<0.6	-				<0.6	<2				810			<6		<5		
19B.182	-30	-	-	-	-			-	-	-	-	-				-	-				-			-		-		
POLDER WATER BEFORE AND AFTER ARTIFICIAL RECHARGE, BOERENDEL AREA SOUTH OF KATWIJK AAN ZEE																												
Before inf.	8.5	170	4.0	115	23	-	385	0.06	-	7	-	235	15	6	<1	3.9		1.3			510		5.3	2		60		-5.9
30E.b01	5	140	32	530	54	-	795	0.06	-	-	-	270	31	8	<1	2.9		1.8			810		5.1	<2		-		-
30E.b03	-2	85	27	350	165		555	0.05	-			200	16	6	<1	1.5		<0.5	-		630		2	14		-		-
30E.b07	-6	310	1.6	280	97		685	0.17				90	15	4	<1	1.0		<0.5	-		590			16		24		-6.0
PRETREATED RHINE WATER BEFORE AND AFTER ARTIFICIAL RECHARGE, NORTH OF SCHEVENINGEN																												
Before inf.	8	35	<1.0	100	120	10	200	0.15	<1.0	4.0	2.3	200	5?	17		4.0	1.4	-	<500	<600	450	-	1.0	12	80	105		-9.4
30G.pp193	0.1	<20	<1.0	100	120	<10	200	0.1	0.5	2.7	<3	195	-	17	-	2.4	1.0	-	-	40	460	0.21	0.6	9	37	105		-9.4
24H.484	-15	<20	15	<100	61	-	207	<0.1	0.1	0.8	0.7	60	4	12	<0.1	<2	<1	0.2		25	550	<0.05	0.2	3	24	175		-9.4
30G.619	-53	3	<1.3	-	52		-	-	<0.1	0.6	-	280	-		-	2	<3	-		20	326	<0.01	<0.1	4	15	150		-9.3
30E.160	-79	2	<1.3	-	18				0.5	-		<100	-			?	5			20	501	<0.05	<0.1	3	15	50		-9.2
PRETREATED MEUSE WATER BEFORE AND AFTER ARTIFICIAL RECHARGE, NORTH OF SCHEVENINGEN																												
Before inf.	4	43	1.4	130	64	<50	150	0.13	0.6	6.3	1.0	370	6?	7		5.0	2.7	-	<1000	<600	-		1.4	37	53	150		-7.2
30G.pp193	0	<20	4	140	40	<50	150	0.6	0.5	4	0.8	340	-	7		3.5	2.1	-	-	<600	230	-	1.6	35	35	150	-	-7.6
30G.616	-30	-	-	-	-	-	-	-	-	-	-	-	-	-	-	-	-	-	-	-	-	-	-	-	-	-	-	-

§ = unreliable due to high I and Cl^-.

connected with raised levels of Mg^{2+}, PO_4^{3-} and organic acids, which are known to inhibit the precipitation of calcite (Reddy, 1977; Reddy & Wang, 1980; Inskeep & Bloom, 1986; Griffioen, 1992). Furthermore, the SI_c is probably too high, because the complexation of Ca^{2+} to organic acids has not been included in the calculation of SI_c.

The freshened facies is encountered mainly downgradient of the advancing dune or polder hydrosomes. The salinized facies is largely restricted to the deeper polders. The relatively low alkalinity water types B_3CaCl- and B_3NaCl- have been found in the Heerhugowaard area and Hoofddorp area respectively, where Holocene aquitards are lacking.

The coastal type (LC)

The relict coastal waters probably originated during and after the formation of the beach barrier most inland around 3800 BC, till about 1000 AD, when the actual coast line was approached. The main difference with actual North Sea water therefore is, that the relict coastal sea waters infiltrated on sites now occupied by land, and that they are older than 1000 y. Chemical differences are slight. Relict coastal seawater probably exhibits a lower ^{14}C activity (not investigated yet), and a somewhat lower chlorinity, due to a more distributed Rhine discharge through three tributaries : south of The Hague (still active), near Katwijk (Old Rhine till 850 AD) and Castricum (Oer IJ till 50 BC).

The actual North Sea hydrosome pushed these high salinity and low alkalinity LC waters at least 6 km inland (section 4.4.3), where they are now situated below the marsh type. From north to south the areal extent of LC water strongly decreases (Fig.4.7), in accordance with the palaeohydrology and Early-historical hydrology of the study area.

The samples 25C.12-165 and 19B.161-124 in Tables 4.3 and 4.4 constitute prototypes of LC water. Their facies is unpolluted, calcareous, anoxic (sulphate (meta)stable) and without base exchange, with code LC_r. A salinized facies is observed where LC water is intruding in an upward direction (Figs 4.3, and 4.4).

Chloride inversions

Major extensions of L are situated landward of the coastal dune hydrosomes and in between the coastal dune hydrosomes of Bergen and Castricum. In the latter area the so-called Bergen clay was deposited in a deep tidal inlet with high salinity, as evidenced by connate water with Cl^- up to 15,000 mg/l, sampled at semi-stagnant localities (19B.109 and 19B.170). The syngenetic L-waters in the Bergen clay impose a "*connate Cl^--inversion*" with dune or polder waters flowing around or below, and with various degrees of freshening by these waters. Other connate Holocene inversions within thick, heavy clay and peat beds are shown on Enclosure 3.3.

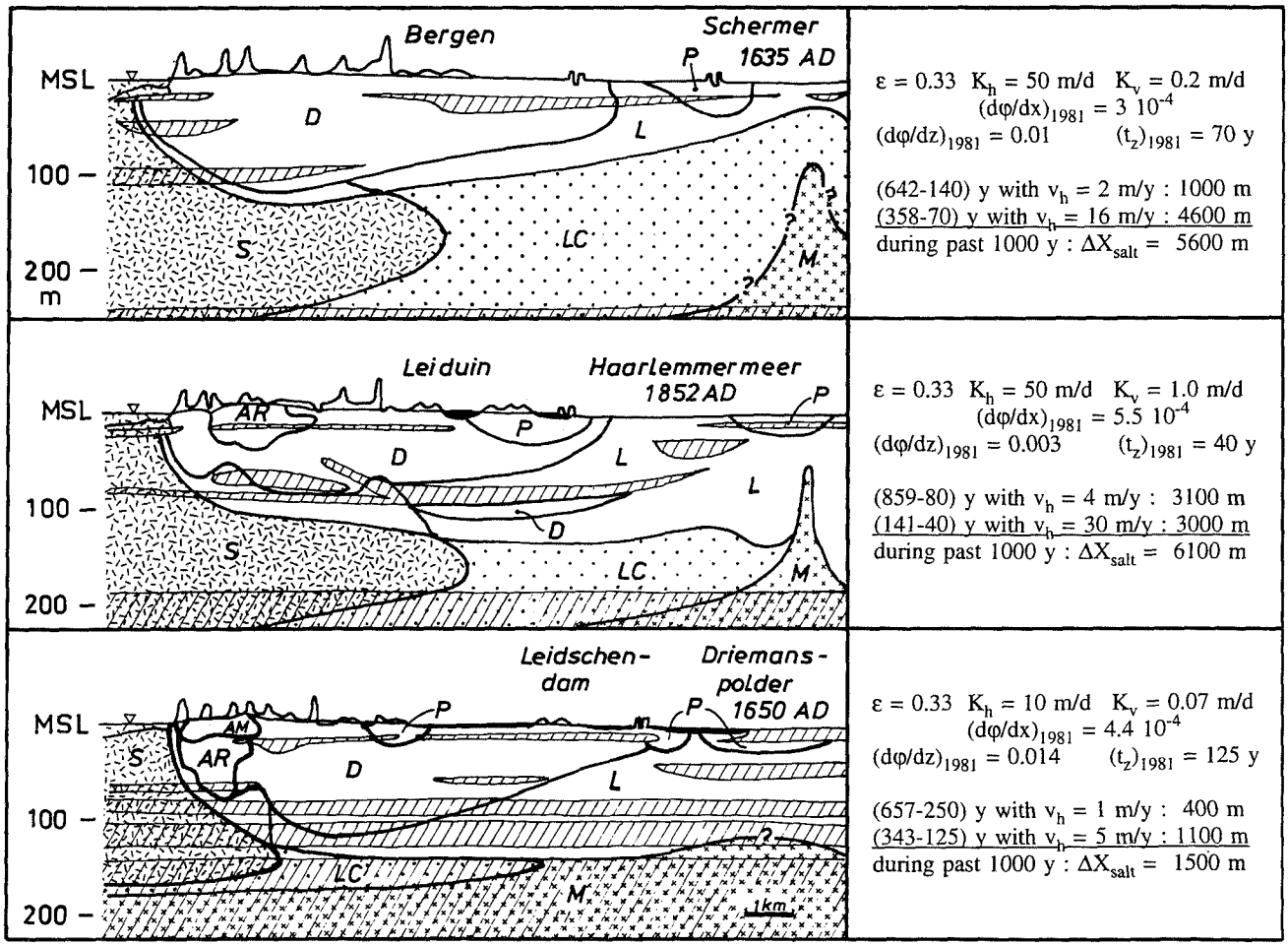

FIG. 4.7 The areal distribution of actual North Sea water (S; <1000 y old), coastal relict Holocene transgression water (LC; 1000-5800 y old) and connate Maassluis water (M; $2 \cdot 10^6$ y old), in a cross section over Bergen (B in Fig.3.1), Leiduin (F in Fig.3.1) and Leidschendam (north of The Hague; H in Fig.3.1). The hydrochemically determined position of the inland intrusion front of North Sea water coincides well with the hydrological calculations presented. D = dune water; L = relict Holocene transgression water of the marsh type; P = polder water; ε = porosity; K_h, K_v = resp. horizontal and vertical permeability; $d\varphi/dx$ = piezometric head gradient at about 130 m-MSL; $d\varphi/dz$ = vertical hydraulic head gradient at the HWL; t_z = transit time during vertical flow to a depth of 130-150 m-MSL near the HWL; v_h = horizontal migration velocity of water.

A different kind of inversion by relict Holocene transgression waters is probably found in the aquitards 2A-2D within the glacial basins of Wijk aan Zee and Haarlem. They form the "*intruded inversion type*" shown on Enclosure 3.3, and are slowly flushed by dune water. Their chlorinity varies in between 300 and 9,500 mg/l, depending on the permeability of the aquitard, the distance to the upgradient face of the aquitard and the hydrological position. An Eemian origin of this salt inversion cannot be rejected here, but seems unlikely, as the period of fresh water circulation in between the Eemian and Holocene transgression lasted about 90,000 years (section 3.6.1).

The extreme alkalinity of the marsh type
Prolonged contact with abundant organic material led to extreme HCO_3^-, NH_4^+, PO_4, DOC, $\delta^{13}C$ and CH_4 concentrations and a typical yellowish, beerlike appearance, which is attributed to humic and fulvic acids. Extreme HCO_3^- concentrations are generated where the following two reactions take place : (1) the simultaneous reduction of sulphate and ferric hydroxides by decomposing organic material (represented simply by CH_2O), leading to the formation of an iron sulphide :

$$2.25\ CH_2O + Fe(OH)_3 + SO_4^{2-} \rightarrow FeS + 2\ HCO_3^- + 0.25\ H_2CO_3 + 2.5\ H_2O \quad (4.2A)$$

$$3.75\ CH_2O + Fe(OH)_3 + 2\ SO_4^{2-} + 0.25\ H_2CO_3 \rightarrow FeS_2 + 4\ HCO_3^- + 2.25\ H_2O \quad (4.2B)$$

and (2) fermentation followed by direct consumption of the CO_2 produced, by the dissolution of shell fragments :

$$2\ CH_2O + CaCO_3 + H_2O \rightarrow CH_4 + Ca^{2+} + 2\ HCO_3^- \quad (4.3)$$

An additional source of HCO_3^- in this system is the dissolution of calcite as a side effect of : (a) exchange of Ca^{2+} for adsorbed Na^+, K^+ and Mg^{2+} upon freshening (Eq.6.14 to the right); (b) the mixing of fresh with salt water; (c) the oxidation of organic matter, yielding organic acids which dissolve calcite and complex Ca^{2+} (Eq.8.30C); and (d) conditions favourable to reach calcite supersaturation, through inhibition of calcite precipitation by the Mg^{2+} exchanged, and by the PO_4^{3-} and organic acids released upon oxidation of organic matter. This combined source may explain about 10-30% of the total concentration of HCO_3^-. It should be realized that decomposing organic material also contains significant amounts of NH_4^+ and PO_4^{3-}, which are mobilized as well (Table 8.2) and give rise to a positive correlation with HCO_3^- (Fig.4.5, 7.5 and 7.11).

Most relict Holocene transgression waters with little admixing, belong to group II and III in Fig.4.5. Samples of group II plot closely to the straight line $HCO_3^- = 2 - 2 \cdot SO4^*$ in mmol/l, which indicates that reaction 4.2 strongly dominates. Samples of group III exhibit the additional effects of reaction 4.2, as does sample 19B.109-16 from Table 4.3. It has the highest HCO_3^- concentration observed, namely 3752 mg/l (=61.5 mmol/l). For this particular sample 25 mmoles HCO_3^- are indeed explained by reaction 4.2, when an original HCO_3^- concentration before entrapment of about 2-4 mmol is assumed. This leaves approximately 33.5 mmol for reaction 4.3 and the additional sources, and would yield, with 30% of 61.5 mmol/l for the lumped additional source, $\{33.5 - 0.3 \cdot 61.5\}/2 =$ 7.53 mmol/l = 120 mg CH_4/l. And it would yield, with an original Ca^{2+} concentration calculated from the chlorinity at 304 mg/l (using Eq.5.7), and an additional 33.5/2 mmol/l = 671 mg, about 975 mg Ca^{2+}/l. Both concentrations contrast with the analysis presented in Table 4.1. This is explained by further processes, the removal of methane from the solution and exchange of marine cations by Ca^{2+}, respectively.

The removal of CH_4 can be quantified as at least 120 mg/l minus its maximum solubility at a pressure of 263 kPa (= 2.6 atmosphere) which is taken for the sampling depth of 16 m below ground surface. With a solubility of 29.9 mg CH_4/l at 10°C and 101 kPa pressure, and with a mean composition of marsh gas of 82% CH_4 (Brandes, 1985), we obtain for 263 kPa a maximum solubility of 2.6*29.9*0.82 = 64 mg/l. The much lower CH_4 analysis (13 mg/l) may indicate that a maximum of 51 mg methane was lost during sampling or during transfer from the sampling pipette to the headspace or from the headspace to the gas chromatograph. Anyhow, at least half of the calculated methane concentration was thus lost not in the laboratory but by natural processes in the aquitard. Natural compaction of the aquitard may have triggered the lateral or upward migration of gas bubbles.

The removal of 975 (calculated) - 343 (observed) = 631 mg Ca^{2+}/l (i.e. 31.5 meq/l) can largely be attributed to cation exchange as a result of freshening (Eq.2.12 to the right). The analysis yields a BEX, according to Eq.2.11, of +30.4 meq/l, which is the amount of exchanged marine cations and approximately equals the 31.5 meq Ca^{2+}/l lost.

4.4.3 The actual, North Sea hydrosome (S)

This hydrosome originated about 1000 years ago, when the North Sea coast approached its present position after some retreat during the preceeding 1200 years. It constitutes in essence, the young flow

branch of a much older North Sea hydrosome of much larger dimensions, and flows inland since about 1000 AD. Intruded coastal North Sea water can, in many situations, be easily recognized by its typical chlorinity in between 14,500 and 17,500 mg/l depending on the distance to the actual Rhine estuary (Fig.3.37). Another criterium is its usually low alkalinity as compared to the relict L-hydrosomes. The low alkalinity is connected with infiltration through a sandy sea floor in an open marine environment and with the passage of few and ill-developed Holocene aquitards. A high alkalinity is associated with many transgreded sea waters, that infiltrated through tidal flat, lagoonal or estuarine deposits. Chemical contrasts with coastal, relict Holocene transgression water (LC) are very small in the north of the study area (500-1000 mg Cl^-/l at best), and somewhat more pronounced (1000-5000 mg Cl^-/l) to the south of the North Sea Canal (see also section 4.4.2).

Actual North Sea water occurs on a supraregional scale west of and below the coastal dune hydrosomes, down to the top of the Maassluis Formation (Fig.4.3 and 4.4, Enclosures 5 and 7).
Their inland intrusion front is, according to chemical observations, situated at approximately 6 km from the HWL (Fig.4.7), at least to the north of the Old Rhine. In the neighbourhood of The Hague a deep fresh water lens and the shallow position of the aquitards 2E (Kedichem Formation), 3B (Tegelen Formation) and 4 (Maassluis Formation) impede a high intrusion rate. The intrusion front is observed there at about 2 km inland (Fig.4.7).

The hydrochemically determined, inland position of the intrusion front is not contradicted by hydrological calculations. Their results are presented for three cross sections in Fig.4.7. Darcy's law was applied (Eq.7.11) with the constants quoted in Fig.4.7, for the situation before and after reclamation of the lakes Schermer, Haarlemmermeer and Driemanspolder (with nearby Zoetermeersche polder), respectively. The estimated flow velocity before reclamation, certainly is the most critical parameter in these calculations. That flow is driven by both a horizontal density gradient inland (especially in the south) and an early drainage of shallow polders (in between the coastal dunes and reclaimed lakes). The estimates correspond with those made by Wit & Witt (1982). The influence of fresh water tongues below the sea has been neglected.

A relatively shallow depth to the top of unmixed, coastal North Sea water is found below land, where the coastal dune belt is very narrow or absent (north of Camperduin along the Hondsbossche Zeewering and north of Katwijk; Fig.4.8 and Enclosure 7), with the exception of the narrow dunes to the south of The Hague. The shallow position of many aquitards (1C, 1G, 2E, 3B and 4) and coastal erosion south of Scheveningen strongly delay the inland North Sea intrusion there.
A shallow depth is also observed where inordinate pumping resulted in a strong North Sea water intrusion, as happened south of Wijk aan Zee (Enclosure 4.2).

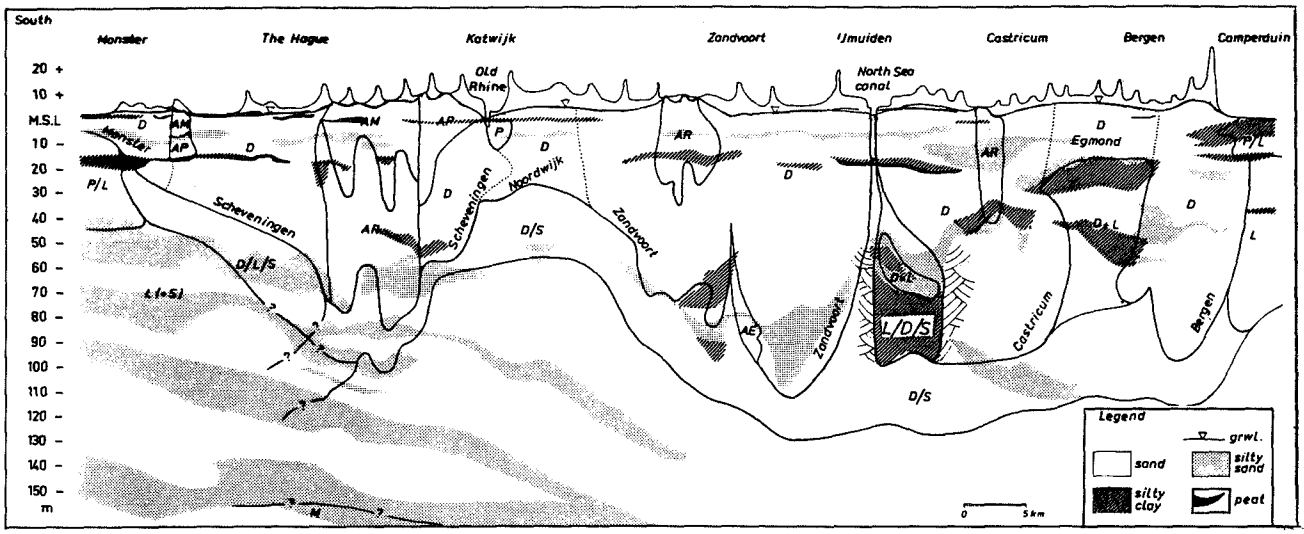

FIG. 4.8 Longitudinal section over the Monster - Camperduin coastal dune area (A in Fig.3.1), with the areal distribution of hydrosomes (simplified after Enclosure 7). AE, AM, AP, AR = artificially recharged sewage Effluent, river Meuse, Polder and river Rhine water, respectively; D = dune water; L = relict Holocene transgression water (marsh type); P = polder water; S = actual North Sea water; (X/Y) = mixing of X and Y; (X+Y) = mixing of X with some Y.

The samples 24H.259 and 24H.018 in Tables 4.3 and 4.4 form prototypes of intruded North Sea water. The major changes with respect to coastal North Sea water, are related to the passage of anoxic Holocene aquitards, rich in unstabilized organic matter, shell fragments and diatom sceletons. This leads to increases for HCO_3^-, Ca^{2+}, PO_4^{3-}, NH_4^+, Fe, Mn, DOC, SiO_2, Ba^{2+} and I, and to decreases in pH, O_2 and NO_3^-. Decreases in F^-, Mo, Rb^+ and V are probably related to sorption phenomena. The changes are discussed further in section 7.6.

The general facies is calcareous, reduced and either without base exchange or salinized. This leads to the codes S_r or S_{rs}, respectively. A salinized facies is restricted to fringes of the hydrosome. The redox index is in general sulphate-(meta)stable, the calcite saturation index close to zero and the pollution index around 0.5 . The water type is predominantly S_2-S_3NaCl. or S_2-S_4NaCl-. The salinized facies makes part of a facies chain from North Sea to dune water along the western face of dune hydrosomes, which is discussed in section 7.6.3.

4.4.4 *Coastal dune hydrosomes (D)*

Coastal dune waters can be recognized rather easily, where dispersion smoothened seasonal and annual fluctuations, by a low chlorinity (25-80 mg/l), $\delta^{18}O$-values in between -6.0 and -7.7 ‰ V-SMOW, and a normal Br-/Cl--ratio (Fig.4.2). Shallow dune groundwaters, however, may display very strong quality fluctuations and exhibit a wide chlorinity spectrum (10-500 mg Cl-/l) and a high δ18O variability (-4.5 to -9.5 o/oo), in dependence on vegetation type and distance to the coast (chapter 6). In order to distinguish it then from a shallow flow branch of an artificial recharge hydrosome of highly variable composition as well, may require consideration of additional environmental tracers, like tritium, B, F^-, I, K^+, V and specific organic microcontaminants, which exhibit relatively low concentrations in dune water (Tables 4.1, 4.3 and 4.4). Dune and recharged river Rhine water can be most accurately discerned in a $\delta^{18}O/Cl^-$ diagram (Fig.4.9).

Seasonal quality fluctuations can be very strong in the upper few metres (section 6.7), whereas a group of 2-3 extreme years is retraceable, under favourable circumstances, up to a depth of about 20 metres below the water table (sections 7.3.2 and 7.4.5).

The dune hydrosomes partly coincide with the dune flow systems discussed in section 3.9.5 and listed in Table 3.7. The areal extent of all 7 (sub)regional dune hydrosomes in the younger dune area, is shown in Fig.4.8, and with the various facies on Enclosure 7. The largest one is found around Zandvoort aan Zee, for which there is hydrochemical evidence that it extended about 1 km to the north of the North Sea Canal before its digging in 1865-1876. The least disturbed of the four large ones, is the Bergen hydrosome, which lacks any artificial recharge and experienced a relatively small-scale drawdown of the water table and small-scale salinization (Enclosures 3.2 and 3.4).

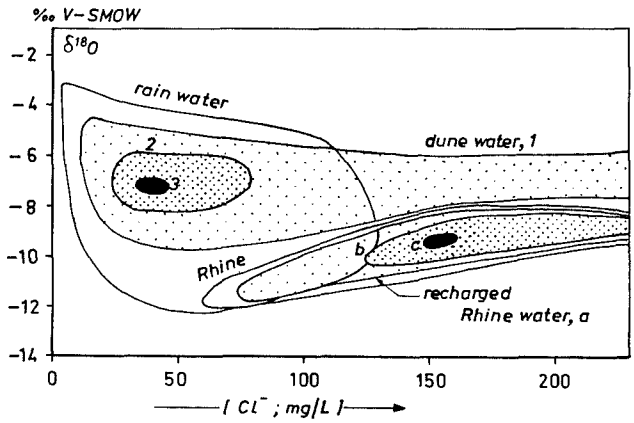

FIG. 4.9 Recognition of coastal dune water and recharged river Rhine water by their position in a detailed $\delta^{18}O/Cl^-$ diagram, with variation of focus from a highly variable recharge composition (rain and Rhine water, respectively) to a well-mixed composition in the second, semi-confined aquifer. 1 = circumference of plot for all 450 pure, dune groundwater samples in the study area; 2 = ditto, in the vicinity of the spreading area to the south of Zandvoort aan Zee, and with a subsoil detention time of 5-15 y (100 samples); 3 = as 2, with a subsoil detention time of 25-100 y (40 samples).
a = circumference of plot for all pure, recharged river Rhine water samples, in the spreading area to the south of Zandvoort aan Zee (calculated, assuming an attenuation by about 6% in the spreading basins); b = ditto, observed in 140 samples with a subsoil detention time of 3-20 y in the upper aquifer and Holocene aquitards ; c = observed, in the second aquifer (5 samples).

The 11 facies discerned in Table 4.2, are discussed below in approximate order of encounter along a flow path from the centre of the younger dunes towards the intrusion front against relict Holocene transgression water in the second or third aquifer (Fig.4.3 and 4.10).

Acid and polluted (D_{ap})
This facies occupies appproximately the upper two metres of the Bergen dune hydrosome, which receives its recharge from dunes primarily poor and

strongly depleted in $CaCO_3$ (<0.1% , Enclosure 1.1). On a very local scale similar groundwater occurs as an upper sheet in older dunes, like in the vicinity of Duinrel, Wassenaar.

Prototypes of this facies are the samples 14C.041+6.5 and +3.5 in Tables 4.3 and 4.4. The pH is below 6.0, tritium is probably about 20 TU in the late 1980s, and AOCl varies in between 10 and 70 µg/l, largely depending on the type of vegetation (section 6.6.3). Concentrations of most trace elements (TEs) are relatively high (Table 4.4), due to enhanced mobilities of atmogenic TEs and an increased leaching in acid environments (section 6.6.4). The calcite saturation index SI_c is below -3.0, the pollution index around 3.0, the redox index is penoxic to suboxic, and the base exchange index does not deviate significantly from zero.

The normal water type is F_*NaCl, testifying of a predominant contribution of sea spray to bulk composition. Less common water types are F_*AlNO_3, F_*NaNO_3, and F_*CaMix.

Acid and reduced (D_{ar})
This facies occurs below the acid, polluted facies down to a maximum depth of 15 m-MSL in the Bergen dune hydrosome (Fig.4.3 and 4.10). Sample 19A.326-12.5 in Tables 4.3 and 4.4 forms a prototype. The pollution index drops to values in between 1 and 2.5, mainly thanks to a higher pH and lower concentrations for NO_3^-, heavy metals and AOCl. With depth the calcite saturation index increases from -4 to -1, whereas the redox index changes to sulphate-(meta)stable. The water types F_*-F_0NaCl and F_0CaMix belong to this facies.

Polluted (D_p) or polluted and reduced (D_{pr})
Dune groundwaters with this facies are calcareous and without base exchange. They are confined to the upper 0.1-3 m in calcareous dunes (south of Bergen aan Zee). Some examples of the overall composition are given in Tables 6.13-6.16. The polluted facies was observed in the following situations :
(1) Below a relatively dense and tall vegetation (especially oak and pines) without peat interference. A well developed vegetation cover leads to increases in interception deposition of atmospheric SO_2, NO_x, NH_4^+, TEs and organohalogens, to evapotranspiration and raised mobilities for several constituents (section 6.6.3). The resulting water type normally is F_2- F_3CaMix or F_3CaHCO_3, the pollution index may score 3.2.
(2) Below strongly oxidizing peat. When the groundwater table is lowered below a previously submerged, deep anoxic peat layer, a strong oxygenation by soil air will speed up mineralization. This may lead to (a) NO_3^--levels up to 400 mg/l when no iron sulphides are involved; (b) SO_4^{2-} concentrations up to 400 mg/l by oxidation of iron sulphides downgradient of the peat, by the NO_3^- mobilized; or (c) elevated levels for both NO_3^- and SO_4^{2-}, when also iron sulphides become exposed to soil air. The resulting water types are F_3CaNO_3 or F_2CaSO_4, the pollution index may rise to 3.2.
(3) In urban or industrial areas like The Hague, Katwijk aan Zee and IJmuiden (Fig.4.10). Here, additional sources of pollution are composed of leaky sewers, fertilizers and black earth for gardens, waste spills, waste dumps and the like. Common water types are F_2- F_3CaMix and F_2CaSO_4.

The standard facies : calcareous, (sub)oxic, unpolluted and without base exchange (D)
This facies is observed in the upper metres of groundwater below dry dunes, where the average thickness of the unsaturated zone exceeds 0.5 m. A maximum thickness of about 5 metres is reached where peat is lacking and vegetation scarce (Fig.4.10). The lower boundary is normally formed by either anoxic marine sea sands underlying the dune sands, or dune peat.

Sample 24H.470 in Tables 4.3 and 4.4 forms a prototype of this facies. There is close equilibrium with ubiquitous shell fragments ($-0.1 < SI_c < 0.3$) and with the cation exchange complex ($BEX \approx 0 \pm 0.5$ meq/l). Concentrations of several TEs (notably Cu, F^-, Se and Zn) and AOCl clearly point at influences of atmospheric pollution, leading to a pollution index of about 1-2½. The redox index is penoxic to suboxic. The normal water types are F_2CaHCO_3 and F_2CaMix. The latter is associated with (a) a short distance to the coast leading to a high load of sea spray; and/or (b) rather high NO_3^- concentrations by N_2-fixation by symbionts of *Hippophaë rhamnoides* (dune shrub) and atmospheric NO_x deposition (section 6.6.3 and 6.8.3).

Reduced (D_r)
This calcareous, unpolluted water without base exchange, is either sulphate-(meta)stable or sulphate-reduced. This means, by definition, that it contains in any case at least 3, generally >10 mg SO_4^{2-}/l. Reduced dune water has a general occurrence in the upper aquifer and intercalated or basal Holocene aquitards 1C, 1D and 1C' of the calcareous dunes (south of Bergen), below the (sub)oxic facies D_p or D. Its presence in the second aquifer is an important indication of the upgradient absence of deep anoxic, Holocene aquitards, which normally possess a high hydraulic resistance. Its presence is therefore often translated into the close vicinity of a recharge focus area for this semi-confined aquifer (section 4.5.3).

There are five such recharge focus areas in the younger dunes, with reduced dune water in the

second aquifer : west of Bergen to a maximum depth of 50 m-MSL, west of Castricum to a maximum depth of 65 m-MSL, in between IJmuiden and Zandvoort aan Zee in the western parts to a maximum depth of 85 m-MSL, in between Zandvoort aan Zee and Noorwijk aan Zee to a maximum depth of 45 m-MSL and in between Katwijk aan Zee and Loosduinen in the western parts to a maximum depth around 50 m-MSL (Fig.4.10, Enclosures 4 and 7). The lower boundary generally coincides with the presence of an aquitard, which is met at great depth (85 m-MSL) in a restricted area north of Zandvoort aan Zee (Fig.4.10 and Enclosure 4.4).

Prototypes of facies D_r are the samples 24H.471 and 19A.326-23.5 in Tables 4.3 and 4.4. The main changes with respect to the (sub)oxic facies D, are the raised concentrations of constituents typically bound to reduced conditions : Fe, Mn and As by dissolution of the omnipresent iron hydroxide coatings of sand grains, NH_4^+ and PO_4^{3-} from decomposing organic matter and SiO_2 from diatom sceletons, radiolaria and silicified reed in the marine sea sands below dune sand and in fine-grained marine aquitards.

The pollution index decreases with depth from about 2 to 0.8 thanks to a pH around 7.5, no NO_3^- and a tritium activity decreasing from a maximum of 180 TU (measured in 1979) to practically zero, very low levels of heavy metals and concentrations of AOCl decreasing from a mean value of 20 to below detection (<4 µg/l). The common water type is F_2-F_3CaHCO_3, whereas F_1-F_2CaMix only occurs in the Bergen dune hydrosome at the contact with facies D_{ar}. The greatest depth of F_2CaHCO_3 water is found in a restricted area north of Zandvoort aan Zee (Enclosure 7B), testifying of low CO_2-levels in the unsaturated zone and very little interaction with CO_2 producing aquitards.

Deep anoxic (D_d)

This facies also implies equilibrium with calcite, no pollution and the lack of base exchange. It surrounds the former reduced facies (D_r) in the Holocene aquitards 1A, 1B, 1E and 1F+G and in the (semi)confined aquifer II and IIIa (Figs. 4.3 and 4.4, and Enclosures 4-7). A maximum depth of 95-100 m-MSL is reached in both the Bergen and Castricum

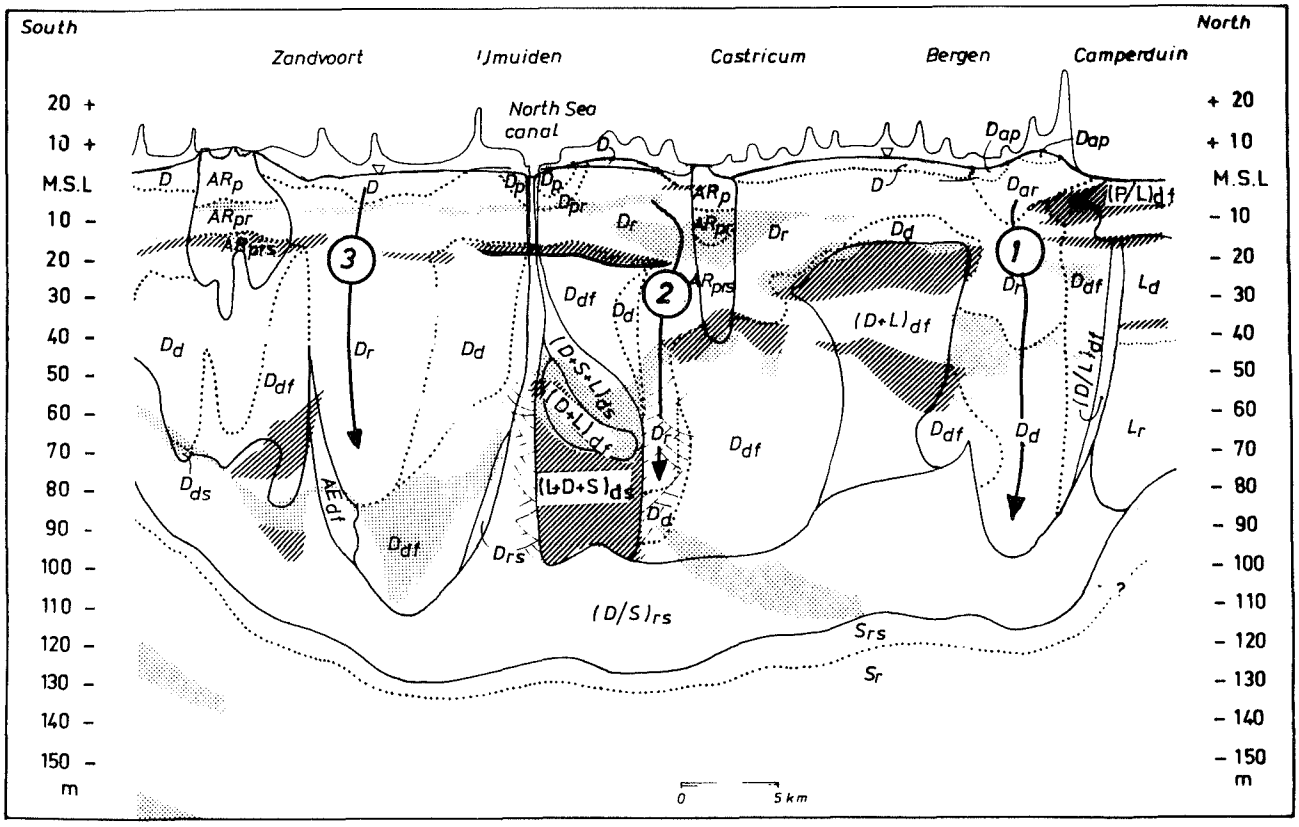

FIG. 4.10 Areal distribution of hydrosomes and their hydrochemical facies in a longitudinal section over the younger coastal dunes, from Zandvoort aan Zee to Camperduin (northern part of Enclosure 7). The recharge focus areas (1-3), which convey the bulk of dune water to the deep aquifers, are characterized below 20 m-MSL by a relatively low redox index (reduced instead of deep anoxic), and the lack of a positive base exchange.

dune hydrosome. Such a deep penetration coincides again with the upgradient presence of a recharge focus area for the deep aquifer, because less flushed parts of the deep aquifer still exhibit a deep anoxic, freshened facies. Deep anoxic dune water is also encountered on a local scale in the first aquifer below anoxic dune peat (section 6.6.5).

Prototypes are the samples 24H.481 and 19A.159 in Tables 4.3 and 4.4. The major changes with respect to reduced facies (D_r) are : the complete reduction of sulphate, methanogenesis leading to CH_4 levels often in between 3 and 20 mg/l, the increase of HCO_3^- by both reactions (see Eqs 4.2 and 4.3), further increases of NH_4^+, PO_4^{3-} and SiO_2, and decreases in Fe and As by formation of sulphide minerals. The general water type is F_3CaHCO_3, whereas F_2CaHCO_3 is found in the Bergen dune hydrosome only.

Freshened and reduced (D_{fr})
Only a small part of the reduced waters obtains, without further SO_4^{2-} losses, a freshened aspect. The bulk changes first into deep anoxic water and then into freshened, deep anoxic (section 4.5.1). The rather anomalous facies D_{fr} is observed mainly in the western part of a dune hydrosome, where it is expanding after first a strong contraction due to pumping, and subsequently a restoration of the seaward fresh water flows since the spreading of surface water. A second requirement is the lack of deep anoxic Holocene aquitards. The combination of both is encountered to the west of the spreading area Castricum (Enclosure 5.2). The water types observed, are F_3NaCl+ and F_3MgCl+.

Freshened and deep anoxic (D_{df})
This wide-spread calcareous and unpolluted facies forms the outer shell of the regional and subregional dune hydrosomes, mainly on their inland side, where the eastward fresh-water flow has been extended within the period 1000-1880 AD in consequence of the formation of the younger dunes and the reclamation of deep lakes. The freshened D_{df} facies has a regional occurrence in the western parts of the Bergen and Castricum hydrosomes exclusively, because only there aquitards with a high cation exchange capacity (CEC) are situated at relatively shallow depth (aquitards 2A and 2D respectively). In the third aquifer below the glacial basin of Haarlem, a very deep and long dune water tongue with a freshened facies occurs (Enclosures 3.3 and 5). In its southern parts east of Zandvoort aan Zee, this tongue was cut off from its recharge area by salt water intrusion, thus forming a fresh water enclave (Fig.4.4).

Prototypes of this facies are the samples 24H.500, 24H.450, 24H.600, 19B.014 and 19B.088 in Tables 4.3 and 4.4. As compared to facies D_d, the base exchange index changed to significantly positive values (from about +0.5 to a maximum of +14 meq/l), due to exchange of Na^+, K^+ and Mg^{2+} for Ca^{2+}. In this exchange other constituents are involved as well : Sr^{2+} and NH_4^+ (not always) adsorb, whereas Li^+ and possibly Rb^+ desorb. It is probable that the following secundary reactions occur (section 7.3.4 and 7.4.4) : a further dissolution of calcite, visible in an increase for HCO_3^- and pH; dissolution of a Ca-F-compound, which is triggered by the strong decrease in Ca^{2+}; sorption or precipitation of SiO_2; and the precipitation of a manganous siderite stimulated by the HCO_3^- and pH increase.

A typical zonation of freshened water types is common, as a result of ion-chromatographic effects upon displacement of brackish to salt water by fresh water (Stuyfzand, 1986a; sections 7.3, 7.4 and 7.7). From F_2CaHCO_3 dune water without base exchange in the Bergen hydrosome towards its intrusion front, the following water types are met in general order (Fig.4.3) : F_2CaHCO_3+ , F_2MgHCO_3+ , F_3NaHCO_3+ and F_4NaHCO_3+ . Starting with more calcareous F_3CaHCO_3 water without base exchange with 90 instead of 50 mg Ca^{2+}/l, the chain becomes near Zandvoort aan Zee (Fig.4.4) : F_3CaHCO_3+ , F_3MgHCO_3+ and F_3- or F_4NaHCO_3+. With a further Ca^{2+} increment to 130 mg/l in F_3CaHCO_3 water, the chain near Wijk aan Zee and south of Hillegom is reduced to : F_3CaHCO_3+ and F_4NaHCO_3+. Further details are presented in section 4.5.1.

These normal sequences are interrupted locally by (1) lithological heterogeneities, as in intercalated clay lenses where the freshening is slowed down by low permeability and high CEC, and (2) younger salinization phenomena, that are most frequently encountered at the base and western side of the dune hydrosomes (see next facies below). The freshened facies chain continues in the $(D/L)_{df}$ mixing zone (section 4.4.7) and in the adjacent L-hydrosome (section 4.4.2).

Deep anoxic and salinized (D_{ds}), or reduced and salinized (D_{rs})
Both salinized facies do not make part of the above facies chain. They should be present on many locations as an outer shell of the (sub)regional dune hydrosomes along their westward face, in consequence of coastal erosion (especially north of Bergen aan Zee), dune water mining and the reclamation of deep lakes, which led to a westward shift of the groundwater divide in the second aquifer. However, it has not been detected on a large scale due to a small thickness of this zone and, locally, the restoration of fresh water flows since the spreading of surface water. The most prominent examples are observed in local upconings below deep pumping wells (Enclosure 5.3).

Sample 24H.189-55 in Tables 4.3 and 4.4 forms

a prototype of this calcareous, unpolluted water. As compared to facies D_{df}, the base exchange index changed to significantly negative values (up to -4 meq/l) due to adsorption of Na^+, K^+ and Mg^{2+}. Other chemical characteristics are discussed together with the wide-spread mixing zone $(D/S)_{rs}$, in section 4.4.7. The D_{ds} facies is in fact the end-point for the facies chain from intruded North Sea water towards salinized dune water. The most common water types are F_2CaCl- and F_2NaCl-. Where salt water intrudes into a system which previously was in an intermediate stage of freshening, F_2MgCl- water may be formed (section 7.6.3).

Close to the transition of D_{ds} into $(D/S)_{rs}$, the redox index may change into "reduced" due to dominating effects of unaltered high SO_4^{2-} concentrations in the intruded North Sea water over the complete reduction of low sulphate levels in dune water.

4.4.5 Polder hydrosomes (P)

The fresh polder hydrosomes can generally be distinguished from coastal dune waters, at least where dispersion smoothened quality fluctuations, by way of : a higher Cl^- content (60-300 as compared to 20-60 mg/l in eastward flowing dune waters), higher concentrations of SO_4 and/or HCO_3^-, and higher concentrations of DOC, B, I, V and persistent xenobiotics. Ethylene thiourea (ETU), a decay product of the widely applied fungicide ethylene bisdithiocarbamate (Frakes, 1988) on flower bulb cultivation lots, is an example of a sufficiently stable, hydrophilic xenobiotic to acquire a wide-spread occurrence in groundwater in polder areas (Lagas et al., 1990).

The differences with dune water are caused by : (a) a significant contribution of river Rhine water flushing the boezems (10-90%, varying both in space and time) and of brackish seepage waters, to their recharge; (b) a more reactive subsoil by a higher content of iron sulphides and organic matter in the thicker and less pervious Holocene aquitards; and (c) a more intensive land-use by irrigation, drainage and application of fertilizers and pesticides.

In polders receiving less Rhine water, higher $\delta^{18}O$-levels due to evaporation on insufficiently drained land and the export of low $\delta^{18}O$ winter rains (Meinardi, 1983c), may form an additional tracer (Fig.4.2). Especially in the southwestern part of the study area, south of The Hague, a remarkably high Br^-/Cl^- ratio characterizes the polder waters. This is due to the mineralization of methylbromide, that is used on a large scale for soil fumigation in intensive horticulture glasshouses (Wegman et al., 1983).

The polder hydrosomes to the north of the Old Rhine largely coincide with the polder flow systems discussed in section 3.9.6 and listed in Table 3.7. For a large scale areal distribution of the highly dynamic polder hydrosomes south of the Old Rhine, reference is made to Engelen & De Ruiter-Peltzer (1986) and De Ruiter (1990). An interesting question not yet answered, is whether P-hydrosomes still contain relict, autochthonous fresh water, that infiltrated either in the period from 2000 BC till about 1000 AD in high moor areas (Engelen & De Ruiter-Peltzer, 1986; Beekman & Appelo, 1989), or in between the mining of the peat bogs and the reclamation of lakes.

Samples 19B.173 and 19B.182 in Tables 4.3 and 4.4 form prototypes of the Geestmerambacht polder hydrosome, invading into a formerly brackish to salty subsoil. Major changes with respect to the recharge mixture, which is composed of Schermer boezem and local rain water, are related to the oxidation of unstabilized organic matter in the Holocene aquitards 1F and 1E or 1G and to cation exchange due to freshening.

It should be noted, that a positive base exchange index in most polder waters can be partly or wholly inherited from the recharging boezem itself. Partial inheritance dominates in the Geestmerambacht, where relict Holocene transgression water had to be displaced first and part of the positive BEX is also explained by this freshening. Complete inheritance applies to the Haarlem polder hydrosome, where it displaced fresh older dune systems.

The general facies at shallow depths is freshened, reduced and polluted (P_{fpr}). Pollution partly stems from high SO_4^{2-} and probably high AOCl levels. At greater depths (>2-5 m below ground level) the facies becomes freshened and reduced (P_{fr}), if deep anoxic, Holocene aquitards are lacking. This is the case in the Castricum and Haarlem area (Enclosure 5). And the encounter of deep anoxic, Holocene aquitards, for instance in the Geestmerambacht area (Enclosure 4.2), changes the facies into freshened and deep anoxic (P_{df}). All waters are calcareous (SI_c close to zero). An acid, reduced facies was not observed, although acid sulphate soils are not uncommon in our polders (Pons & Van Oosten, 1974). Such a facies is probably restricted to the unsaturated zone (which has not been considered) or is remedied by liming. The most common water types are indicated in Table 4.2.

4.4.6 Artificial recharge hydrosomes (A)

Discussion is limited to the larger artificial recharge hydrosomes, which correspond to the six subregional, artificial recharge flow systems discerned in Table 3.7. These can be subdivided according to the source of their recharge waters, into three groups, in chronological order : Polder (AP), Rhine (AR) or Meuse (AM). For information on the interesting

sewage effluent hydrosome of Zandvoort aan Zee (AE; Enclosures 5 and 7), reference is made to Stuyfzand (1988b).

A general scheme for spreading and recovery in the dunes, is presented in Fig.4.11. It shows that the total effect of dune infiltration is composed of quality changes in the spreading basins, the subsoil and recollection system, where on average 20% autochthonous dune water is admixed. Oxic conditions prevail in the spreading basins due to equilibration or supersaturation with atmospheric oxygen. In the basin banks (Fig.4.12) and the phreatic aquifer downgradient, oxygen is partly consumed and most nitrate conserved, leading to a (sub)oxic facies. Passage of sludge at the basin floor (Fig.4.13) creates anoxic to deep anoxic conditions, whereas the passage of dune peat and the Holocene aquitards 1C-1G generally leads to a reduced facies.

The situation described here, may strongly change in the near future due to the sanitation measures 2-5 mentioned in section 3.7.5. In this context the main issues will be a reduction or stabilization of the areal extent of artificial recharge hydrosomes in the dunes, and strong quality improvements of the imported surface waters.

FIG. 4.12 The basin banks of a recharge basin in the Zandvoort aan Zee spreading area exposed during low water level. The intake of river Rhine water was suspended in order to exclude a pollution wave on the river. The high permeability of the sandy basin banks and low permeability of bottom sludge (Fig.4.13), may result in about 80% of all recharge passing through these banks.

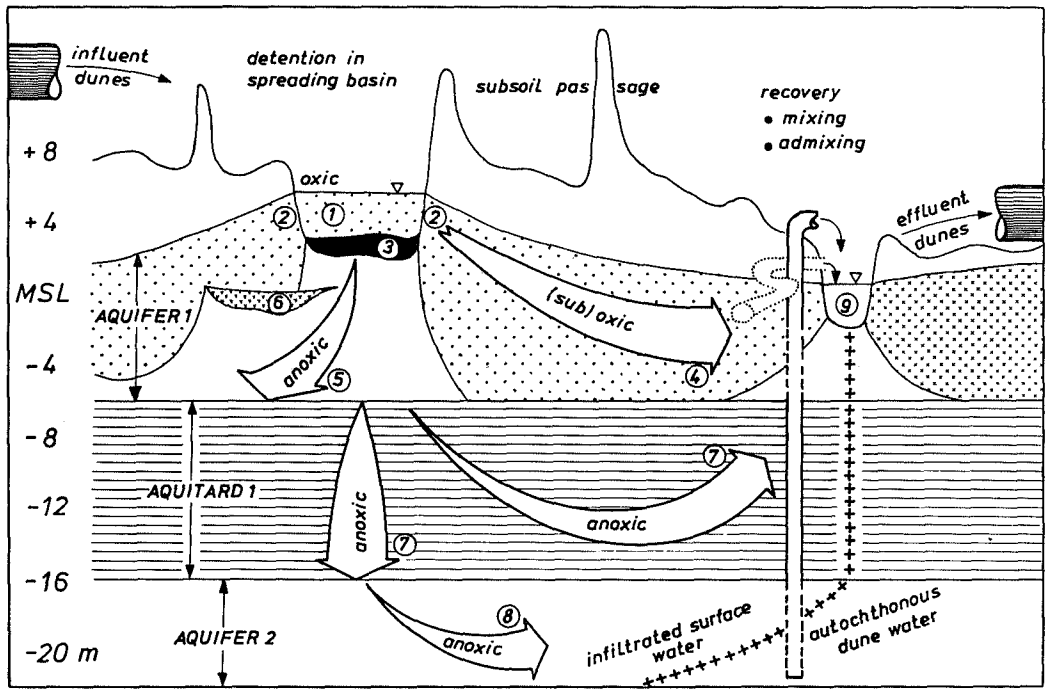

FIG. 4.11 Scheme of the process called open dune infiltration, with its relevant hydrological and hydrogeochemical compartments, in order : 1 = spreading basin, oxic; 2 = basin banks, (sub)oxic; 3 = sludge at basin floor, (deep) anoxic; 4 = phreatic first aquifer, composed of dune and sea sand, (sub)oxic; 5 = semi-confined first aquifer, composition as 3 or 6, (deep) anoxic; 6 = dune peat, (deep) anoxic; 7 = first aquitard (1C-1G), composed of Holocene, marine and tidal flat deposits, anoxic; 8 = second, confined aquifer, composed of Pleistocene coarse sands, anoxic; 9 = recovery system : shallow and deep wells, shallow drains and drainage canals.

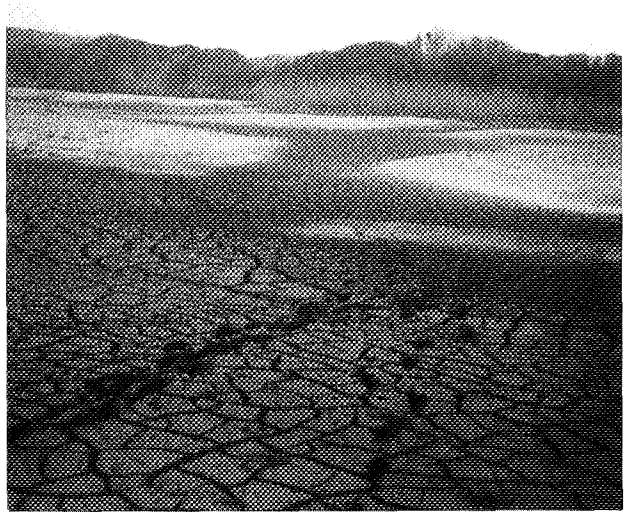

FIG. 4.13 Sludge at the bottom of spreading basin 11 in the Scheveningen area, in 1981. Since its operation started in 1956, no sludge has ever been removed. The hydrological disadvantages of sludge accumulation are obvious. There are, however, some hydrochemical advantages : complete denitrification, reduction of many chlorinated hydrocarbons and the immobilization of many heavy metals.

Polder (AP)

The Katwijk and Monster artificial recharge hydrosomes partly belong to the polder group. Their areal extent is shown on Enclosure 7. Near Katwijk it reached the second aquifer especially in the western and southern parts, where aquitard 1B is lacking or ill-developed and where shallow recollection is far from complete (Fig.4.14). Near Monster the artificial recharge by spreading started later than elsewhere and the polder water still had not reached aquifer II in 1985.

The polder group is to be considered at least partly as a relict hydrosome, because recharge was changed over to pretreated Meuse water near Monster in 1983 and in the southern part of the Katwijk spreading plant in 1988. The main reason to abandon the intake of polder water was the very high concentration of nutrients (NH_4^+, PO_4^{3-} and K^+), leading to unacceptable algal blooms in both recharge and adjacent flow-through ponds, as well as the appearance of ruderal plant species in both (Van der Meulen, 1982; Van Dijk, 1984).

The recharged polder waters can be recognized as discussed under their "spontaneous" P-hydrosome (section 4.4.5). The following fingerprint of the recharged polder water near Katwijk, proved to be useful in its distinction from shallow dune water, in the upper aquifer with transit times inferior to 6 years (Stuyfzand, 1990a) : Cl^- = 120±40 mg/l, HCO_3^->240 mg/l, NO_3^-<1 mg/l, K^+ = 6-22 mg/l, Mg^{2+} = 12-20 mg/l, DOC = 8-14 mg/l, PO_4 = 0.5-12 mg/l, As = 6-60 µg/l, B = 200 µg/l, I = 7-32 µg/l, V = 1-7 µg/l and Sr^{2+}/Ca^{2+} > 0.005 on a mg/l basis. These levels are, except for NO_3^-, generally higher than those for shallow dune water, but form unreliable diagnostic tools when used individually.

Samples 30E.b01, 30E.b03 and 30E.b07 in Tables 4.3 and 4.4, are prototypes of the Katwijk artificial recharge hydrosome of the polder type. Major changes with respect to its recharge water are composed of : increases of HCO_3^-, PO_4, NH_4^+, I, CH_4 and decreases in O_2, NO_3^- and SO_4^{2-}, due to decomposition of unstabilized organic matter (OM), which accumulated in (deep) anoxic sludge at the banks and bottom of spreading ponds; an increase for Ca^{2+}, HCO_3^- and Sr^{2+} by further dissolution of calcite in sludge and dune sands, due to a raised production of CO_2 and organic acids in connection with continued oxidation of OM in a methanogenic system; a rise of SiO_2 and possibly Ba^{2+} by dissolution of diatom skeletons and silicified reed in sludge and aquitards; increases for Fe, Mn and As by reduction and dissolution of ferric hydroxides in dune sands; and a Ba^{2+} increase by dissolution of barite in deep anoxic sludge and dune sands, which is triggered by sulphate reduction.

Where the porous medium was insufficiently flushed with polder water, PO_4^{3-}, F^-, Na^+, K^+, Mg^{2+}, Li^+, Ni and V are retained by sorption (Figs. 4.14 and 4.15). Na^+, K^+ and Mg^{2+} are exchanged for Ca^{2+} (Eq.2.12 to the left), especially in aquitards and also in dune sands more remote from the spreading ponds. This sorption is illustrated for PO_4^{3-}, K^+ and Mg^{2+} in a cross section from the westernmost spreading basins to the North Sea (Fig.4.14). The concentration curves of F^-, Li^+, Ni and V along a 700 m long flow path in the upper aquifer towards the North Sea (Fig.4.15), demonstrate that the order of increasing retardation probably is : F^- < Li^+ < V < Ni. However, the Ni and V curves are also influenced by increasing concentrations in the polder water recharged. The concentration patterns of vanadium (probably present as VO_4^{3-}) strongly resemble those of PO_4^{3-}. The latter were not only influenced by an exponential increase of its input in the period 1956-1972, but also by a very pronounced mobilization from (deep) anoxic sludge at the bottom of the spreading basins in the 1980s (Fig.4.28; Stuyfzand, 1990a).

In the upper aquifer within the first 700 metres of flow, the common facies is freshened and reduced to deep anoxic, leading to the codes AP_{fr} and AP_{df} with the water types $F_3CaMix+$ and F_3CaHCO_3+ .

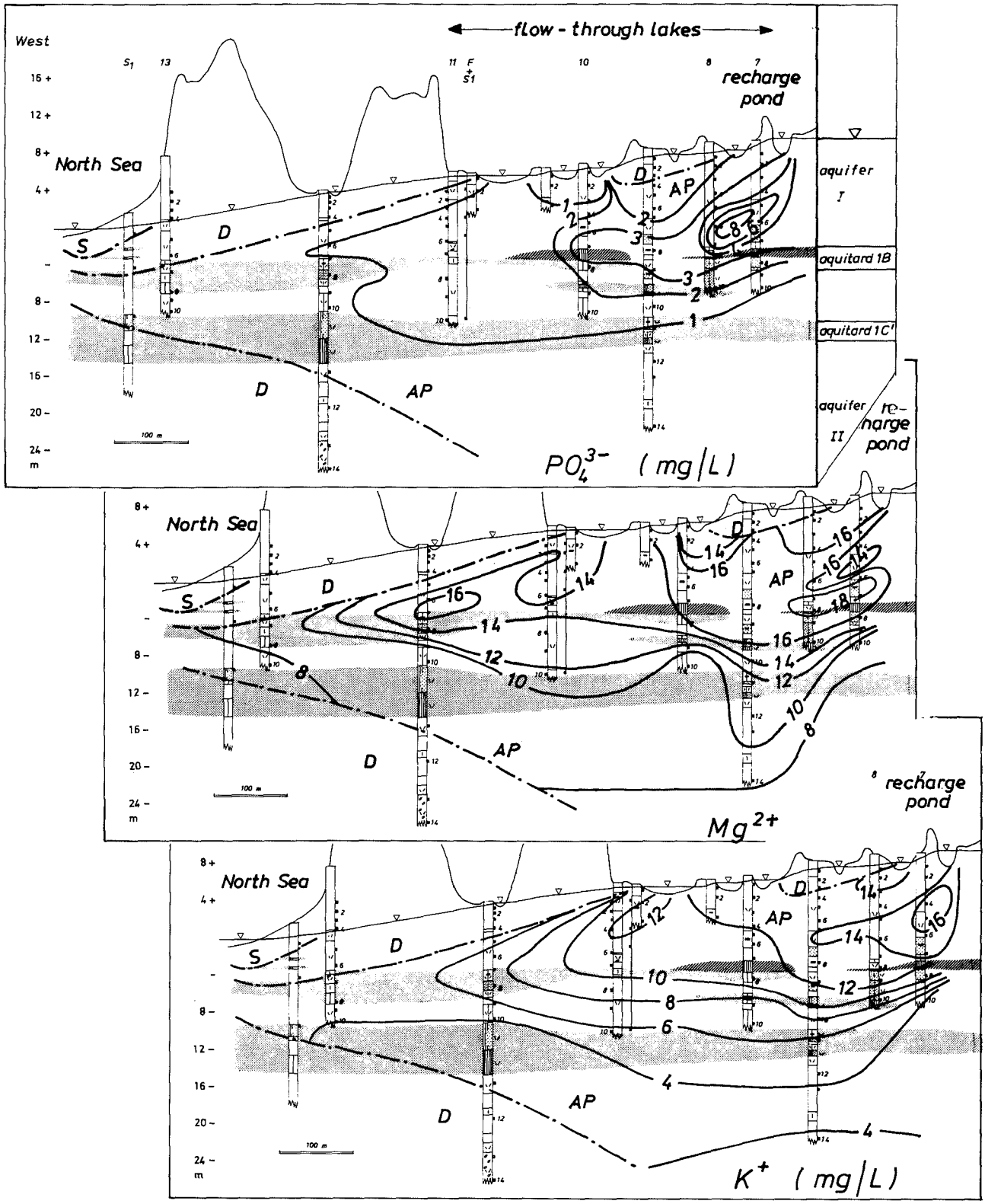

FIG. 4.14 Areal distribution pattern for artificially recharged boezem water (AP), dune water (D) and North Sea water (S), and the concentration patterns of phosphate, potassium and magnesium in a cross section over the Boerendel area (4 km south of Katwijk aan Zee; see Fig.3.1) in March-June 1988. These ions are adsorbed below 4-8 m-MSL and at about 300 (PO_4^{3-}), 500 (K^+) and 700 m (Mg^{2+}) distance from the spreading pond.

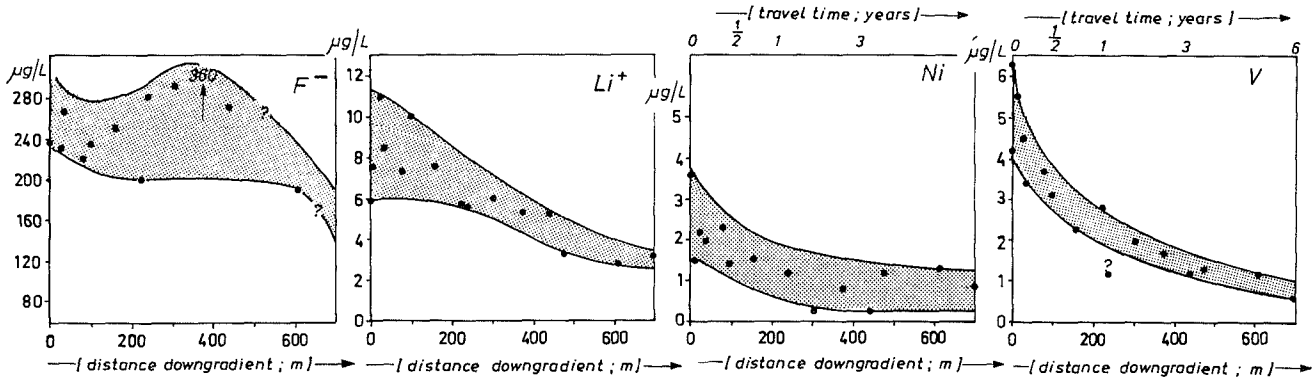

FIG. 4.15 Changes in concentration of fluoride, lithium, nickel and vanadium in recharged polder water in the Boerendel area (see Fig.3.1), along a 700 m long flow path in the upper aquifer, in April 1988, that is after 32 years of artificial recharge. Based on samples from two rows of wells equipped with miniscreens. Fluoride is breaking through (for 50%) at 700 m distance, which yields a retardation factor R_F (see Eq.7.5) of 32/6 = about 5. The retardation of the other trace elements is estimated at : R_{Li} = 32/2 = about 16; R_{Ni} = 32/0.5 = 64; and R_V = 32/1 = 32.

The positive base exchange index is completely inherited from the polder water recharged, and therefore reflects the breakthrough of Na^+, K^+ and Mg^{2+} (Fig.4.14). Beyond about 700 m of flow and in the aquitards 1B or 1C' the base exchange index approaches zero, which reflects their sorption, and the facies becomes AP_r with the water types F_3CaMix and F_3CaHCO_3. Recharged polder water is always very close to equilibrium with calcite. It is unpolluted, thanks to (1) a relatively low AOCl, because no chlorination for transport is applied, (2) a relatively low tritium activity, and (3) the presence of highly reactive, (deep) anoxic bottom sludge in the spreading basins, which captures many chalcophile heavy metals and forms an excellent barrier to chlorinated hydrocarbons by sorption and breakdown.

Rhine (AR)

The Castricum, Wijk aan Zee, Zandvoort aan Zee and Scheveningen artificial recharge hydrosomes belong to the Rhine group. Their areal extent is shown on Enclosures 4.2, 5 and 7. Near Scheveningen it reaches the greatest depth, namely up to 85 m-MSL in aquitard 3B (survey in 1981). This is related to the highest recharge/recollection-ratio, relatively low hydraulic resistivities of the Holocene aquitards and the configuration of recharge and recollection facilities. The size of the Wijk aan Zee and Castricum artificial recharge hydrosomes is relatively small, mainly due to a low recharge/recollection-ratio and the approach of a closed system, where practically all infiltrated surface water is recollected close to the spreading area. A shorter period of recharge and the presence of effective aquitards (1A and 1G), explain why the second aquifer had not been reached yet around 1981 in the Wijk aan Zee area. The Scheveningen artificial recharge hydrosome is to be considered as a relict hydrosome, because recharge was gradually changed over to pretreated Meuse water in the period 1976-1978.

The Rhine water recharged, can be recognized unambiguously from dune water in a $\delta^{18}O/Cl^-$- or Br^-/Cl^--diagram, because of its relatively low ^{18}O and Br^- content when Cl^- might overlap (Fig.4.9). Normal mean levels for the recharged Rhine water are $\delta^{18}O$ = -9.4 ‰ V-SMOW, Br^- = 200 µg/l and Cl^- = 155 mg/l , as compared to -7.2 ‰ V-SMOW, 140 µg/l and 40 mg/l, respectively, for mean dune water. The Cl^--discrepancy implies that the intrusion of Rhine water can be considered in most cases as a mild salinization. Characteristic organic micropollutants with a high mobility and stability like bisdichloro(iso)propylethers (Smeenk, 1984; Noordsij et al., 1985), bentazone (Noij et al., 1989; Smeenk et al., 1990), tetrachloro-orthophtalic acid (Smeenk et al., 1990) and Na-dicegulac (Hopman et al., 1990) may also form diagnostic tracers, although their historical input is known only since the 1980s - 1990s.

The low $\delta^{18}O$ value for Rhine water is related to the fact that about 45% of the Rhine water comes from Switzerland and about 30% from central and southern Germany. Precipitation there has a much lower ^{18}O content than in The Netherlands, because its concentration in the vapour phase is constantly lowered by raining out from oceanic air, moving inland and uphill (Mook, 1989). The low Br^-/Cl^- ratio is explained by the low Br content of salt waste from the salt mines in NE France, which is discharged to the tributary Moesel (Geirnaert, 1973).

Some quality changes in the spreading basins as a function of the detention time, are shown in Fig.4.16. Uptake by algae leads to a progressive depletion of the nutrients PO_4^{3-}, NH_4^+, NO_3^- and

SiO_2, which subsequently accumulate in sludge at the basin floor. Ca^{2+} and TIC decrease and pH increases downstream due to uptake of CO_2 by algae and CO_2 stripping. This biogenic softening is accompanied by a significant deposition of calcite. Trihalomethanes (THMs) formed during chlorination for transport, are clearly removed by natural stripping. As a result of various processes, like stripping, adsorption to neoformed organic matter and photochemical degradation, the taste strongly improves. Fluctuations in salt concentration are progressively smoothed (see Cl^- in Fig.4.16) mainly by wind driven currents. Fluctuations of nutrients and oxygen behave in a more complex way, with a tendency to increase downstream in connection with the periodicity of algal blooms and the accompanying progressive depletion of nutrients and production of O_2 downstream.

Several quality changes in the upper (sub)oxic phreatic aquifer, in between recharge basins and recovery, are depicted in Fig.4.17. These changes largely determine the composition of the recovered infiltrate, as about 80% of the recharged Rhine water is forced to flow through this aquifer. The mean results for two recharge systems are presented, one after 2 months of operation in the Scheveningen area, and the other after 12 years of operation in the Castricum area. In both cases the pretreated Rhine water was still heavily polluted, due to a bad quality at the intake and only a simple pretreatment (without coagulation).

It can be concluded that the strongest quality improvement takes place in the basin proximal zone, during the first 3-5 metres of subsoil passage and that relatively little changes in this respect after 12 years of operation. This is especially true for the processes nitrification, biodegradation of dissolved organic matter, taste improvement and removal of colloidal Fe and Mn. Phosphate is slowly breaking through, however, which after several years contributed to the eutrophication of nearby, moist to wet ecosystems (Van Dijk, 1984). The facies normally is polluted, calcareous, (sub)oxic and without base exchange, leading to the code A_p (sample 30G.193 in Tables 4.3 and 4.4). The pollution index is about 3.0, mainly due to high levels for SO_4^{2-}, NO_3^-, tritium and AOCl, of which the latter is clearly raised in consequence of chlorination for transport. The most frequent water types are F_2CaMix and F_2NaMix. Further details are given in the literature referred to in section 1.4.

Where the recharged Rhine water encounters either anoxic sludge in the spreading basins or dune peat, the above facies changes to reduced or even deep anoxic. In the first aquitard and second aquifer with detention times superior to 5 years, a calcareous, reduced, polluted and salinized facies dominates, leading to the code A_{prs} (sample 24H.484 in Tables 4.3 and 4.4). The redox index is sulphate-(meta)stable, the pollution index around 2.7, and the water type either F_2CaMix- or F_2CaCl- . Quality changes of Rhine water which escaped from direct

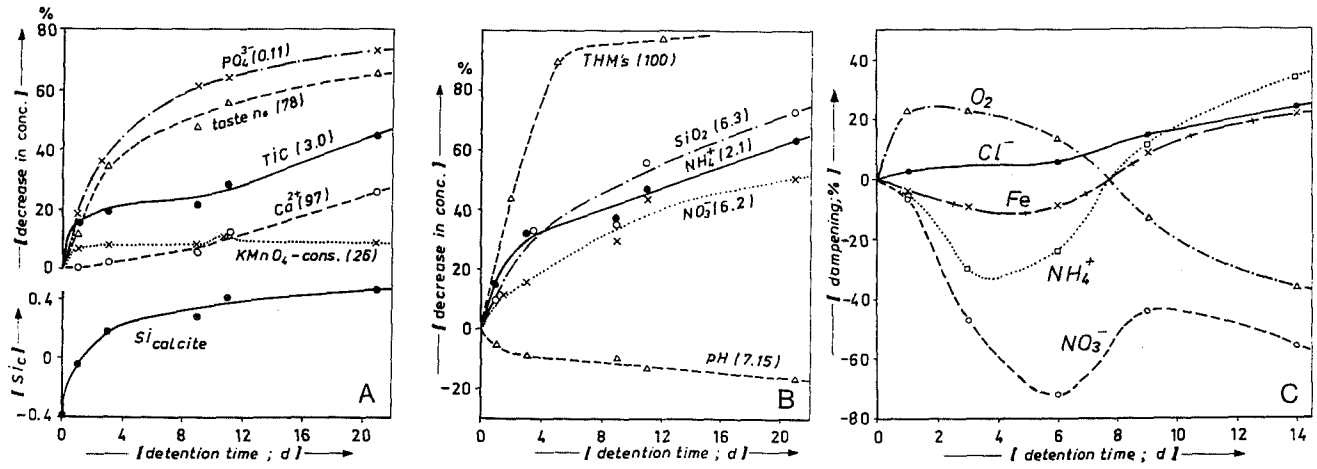

FIG. 4.16 Effects of detention time of pretreated Rhine water in spreading basins, on mean concentration levels and mean damping of seasonal quality fluctuations. Within brackets : the original mean concentration or mean standard deviation to annual means. Number of observations : 52/y. A and B : Scheveningen area (site 21 in Fig.3.1), pond 11 (horiz. flow velocity v_h = 40 m/d), period 1964-1965; C : Zandvoort area (site 13), basins 4-7 connected in series (v_h = 150 m/d) and basin 12 (v_h = 50 m/d), period 1964-1966. The smoothing was calculated by taking 100 (1 - S_x/S_o), where S_o = quadratic mean standard deviation to annual means for Meuse water in the spreading pond; and S_x = ditto for Meuse water during subsoil passage.

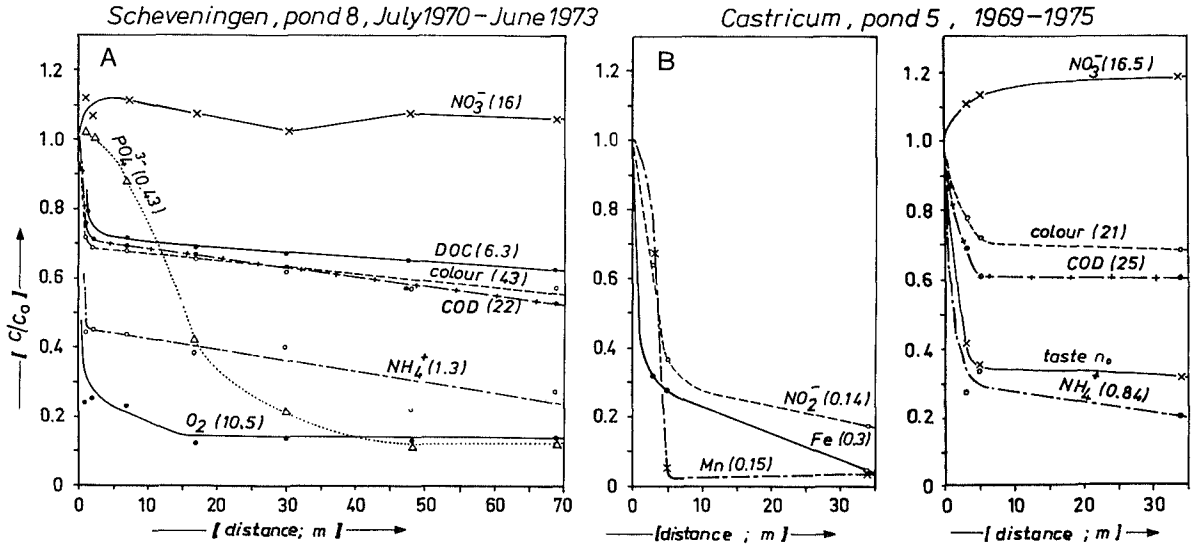

FIG. 4.17 Mean quality changes of pretreated Rhine water upon subsoil passage in the upper, (sub)oxic aquifer in between the spreading basin and recovery, for 2 systems : A = pond 8 in the Scheveningen area (site 21 in Fig.3.1), after 2 months of operation, during the period July 1970 through June 1973 (groundwater flow velocity v_h = 1 m/d); B = pond 5 in the Castricum area (site 3), after 12 years of operation during the period 1969 - 1975 (v_h = 2.5 m/d). Number of observations : 52/y for pond 8 and 26/y for pond 5. Within brackets : the mean concentration or standard deviation before infiltration, in spreading pond. C/C_o = concentration related to concentration in spreading pond.

recovery and displaced dune water over a distance of 800 m in the upper aquifer and Holocene aquitards, are discussed in detail in section 7.5.

A freshened A_{fr} facies with the water types F_2NaCl+, $F_2NaMix+$, F_2MgCl+ and $F_2MgMix+$ has been found only in the Scheveningen area (samples 30G.619 and 30E.160 in Tables 4.3 and 4.4). This facies occurs in the lower parts of the Rhine hydrosome, where the first Rhine water (from the late 1950s) displaced brackish waters, that nearly had reached the upper aquifer in consequence of overexploitation.

Meuse (AM)

The Meuse group is composed of the southern part of the Katwijk, the upper Scheveningen and upper Monster artificial recharge hydrosome, shown on Enclosure 7. The largest size and deepest penetration is found north of Scheveningen, where it had reached a maximum depth of about 40 m-MSL in 1981, that is after 5-6 years, and 70 m-MSL in 1990 (Fig.3.30).

Infiltrated Meuse water, the pretreatment of which includes a coagulation, is in many respects quite similar to coastal dune water, also in $\delta^{18}O$ and Br^-/Cl^--ratio (Table 4.1 and Fig.4.2). It can be recognized most easily, amidst coastal dune groundwater, by its elevated tritium activity (about 100 against 20 TU in 1981). The difference is connected mainly with an increased contamination of Meuse water by cooling water from nuclear power plants. If certain conditions are fullfilled, however, also F^- and K^+ may form valuable tools (Stuyfzand & Moberts, 1987a,b). Those conditions are : first, the sorption complex of the subsoil must be in equilibrium with Meuse water, which was determined experimentally for dune sands in a retrospective study at about 3-7 times the travel time for water (Stuyfzand, 1986d; Stuyfzand, 1991d); and second, raised F^- or K^+ levels for the local dune water must be excluded by checking for an atmospheric F-source (shallow depth, low Ca^{2+}), for biogenic K^+-sources (decomposing fresh organic matter in woods or in sea gull breeding areas) and for geochemical K^+-sources (cation exchange upon freshening). Recharged Meuse water strongly deviates form recharged Rhine and polder waters, by its lower Cl^- concentration (Table 4.1).

Several quality changes in the upper (sub)oxic phreatic aquifer, in between recharge basins and recovery, are shown in Fig.4.18. The data refer to a system, that was previously flushed by recharged Rhine water for about 21 years and since 3 years by Meuse water of much better quality. The data presented, therefore contain the effects of desorption or leaching of substances retained from Rhine water. Desorption explains the typical peaks for PO_4^{3-}, As, Cu and Ni downgradient, of which those of PO_4^{3-} and As and those of Cu and Ni approximately coincide. The retardation factor (see Eq.7.5) of Cu and Ni appears to be 10 times higher than that of PO_4^{3-} and As, in this system.

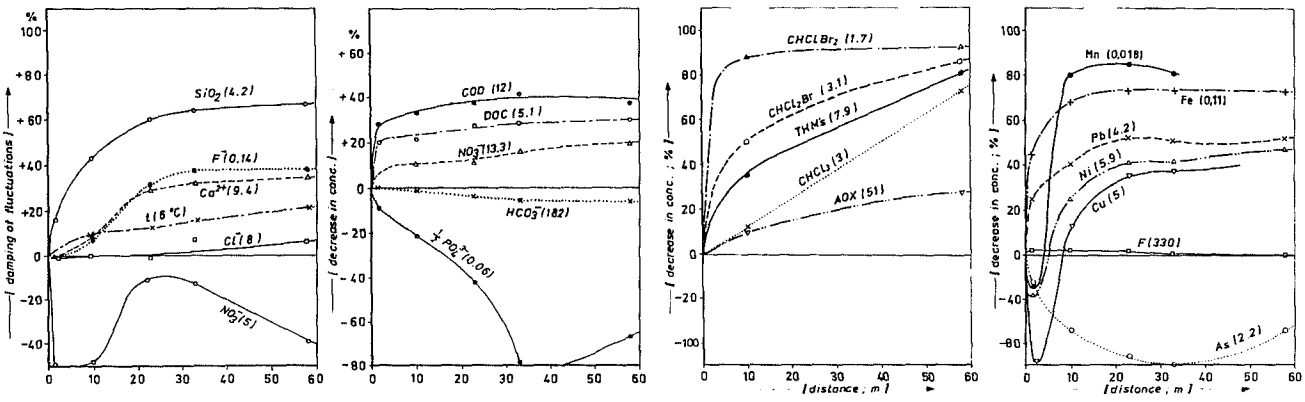

FIG. 4.18 Mean quality changes of pretreated Meuse water upon subsoil passage in the upper, (sub)oxic aquifer in between spreading pond and recovery, during the period 1979-1983. Pond 13 in the Scheveningen area (site 21 in Fig.3.1), after 21 years of Rhine infiltration and 3 years of Meuse recharge (groundwater flow velocity = 0.5 - 1 m/d), 13 observations/y. Within brackets : the original mean concentration c.q. mean standard deviation for pond 13, in mg/l for main constituents, µg/l for trace elements and organic micropollutants, in mmol/l for TIC and °C for temperature. The damping was calculated by taking 100 (1 - S_x/S_o), where S_o = quadratic mean standard deviation to annual means for Meuse water in the spreading pond, and S_x = ditto for Meuse water during subsoil passage.

Concentrations of Na^+, K^+, Mg^{2+}, Cl^-, SO_4^{2-}, Br^-, F^- and SiO_2 as well as the taste do not change significantly in this strongly flushed system (sample 30G.193 in Tables 4.3-4.4). The low NH_4^+ concentrations and calcite equilibrium of the pretreated Meuse water result in minor changes of Ca^{2+}, HCO_3^- and TIC (Fig.4.18). DOC and NH_4^+ behave in a similar way as described for Rhine water. Trihalomethanes are removed for about 80% after 60 m of subsoil passage by biodegradation (Smeenk, 1984). The higher removal rate for brominated species correlates with their higher chemical instability (Schwarzenbach & Giger, 1985). Chloroform exhibits a more sluggish removal, due to (a) the requirement of a reductive dechlorination in an environment where at least nitrate is reduced (Bouwer & McCarthy, 1983; Hrubec et al., 1986, 1988), and (b) a slow denitrification in this (sub)oxic system where only 20% of the original nitrate is reduced.

Seasonal fluctuations of SiO_2, F^-, Ca^{2+} and temperature, in order of decreasing efficiency, are progressively smoothed by sorption, in a system where piston flow is demonstrated by Cl^- behaviour (Fig.4.18). Further details on quality changes in this system are presented by Stuyfzand (1986d, 1989e), Smeenk (1984) and Hoekstra (1984). The facies is calcareous, penoxic to suboxic, moderately polluted and without base exchange, leading to the code AM_p. Also here chlorination for transport from the Meuse towards the dunes contributes to pollution by raising AOCl, which is only partly removed (Fig.4.18). The encounter of anoxic dune peat or sludge changes the above facies into reduced or even deep anoxic.

Where Meuse water is displacing Rhine water in the Scheveningen area, a very mild form of freshening occurs (sample 30G.616). The facies at this greater depth is calcareous, sulphate-(meta)stable, freshened and probably moderately polluted, which results in the code A_{fpr}. And where the relatively nutrient-poor Meuse water displaces the very eutrophic, infiltrated polder water, a slow elution of the nutrients PO_4^{3-}, NH_4^+ and K^+ is observed (Fig.4.19). The retardation factor R_i as defined in Eq.7.5, is about 10 for these three nutrients. This is relatively low for phosphate and high for K^+ and NH_4^+, because dune sand flushed with Rhine and Meuse water normally exhibits a R_i of 20-55, 5 and 4, respectively (Stuyfzand, 1986d, 1989e). The discrepancy is explained by the anoxic environment, in which phosphate is more mobile (Sanyal & De Datta, 1991), and by the much higher concentration levels in the infiltrated polder water. Although the R_is are about equal, a much sharper elution front can be observed in Fig.4.19 for K^+ as compared to NH_4^+ and PO_4^{3-}. For further details reference is made to Stuyfzand et al., 1991.

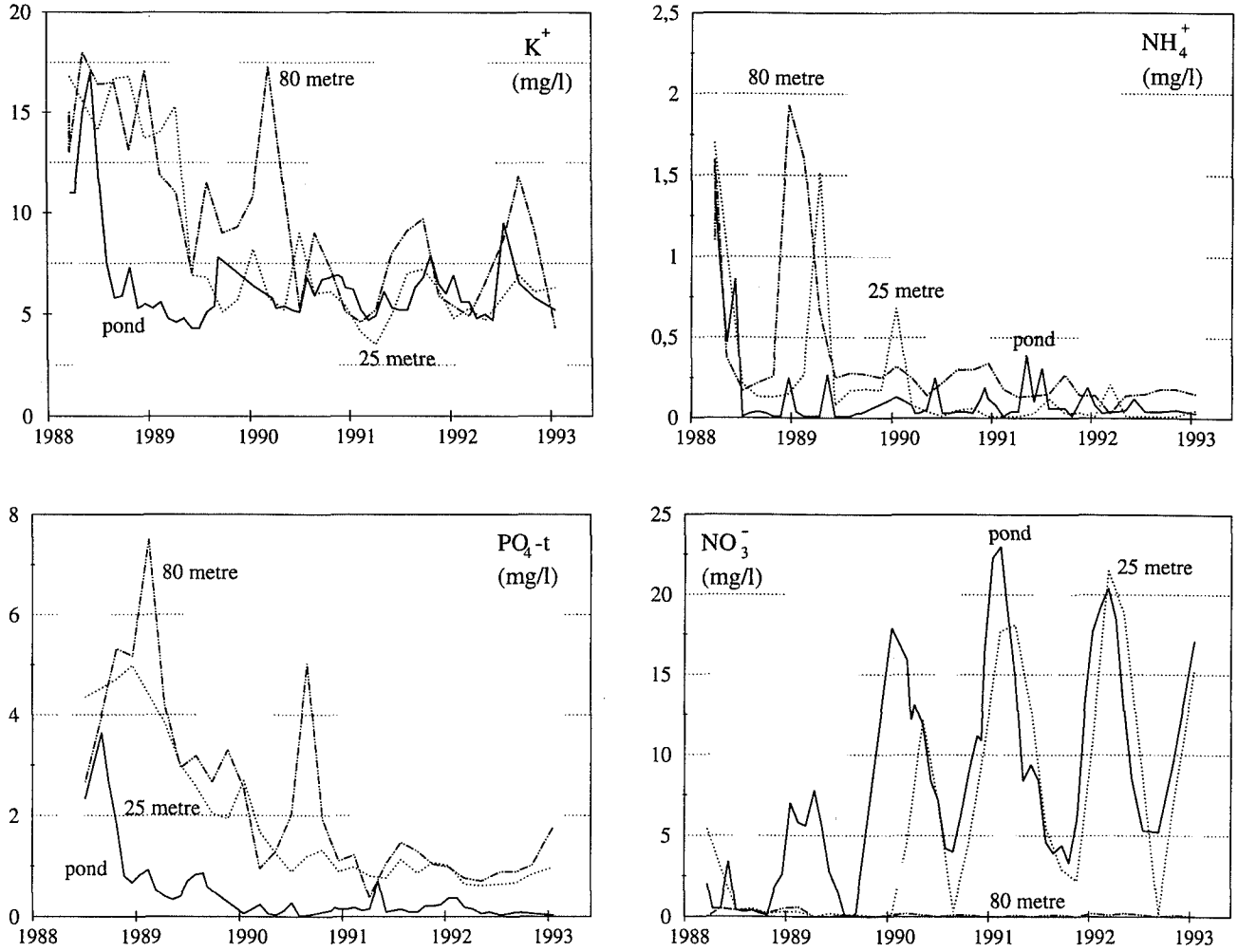

FIG. 4.19 Development of nutrient concentrations in recharged surface water before and after 25 and 80 m subsoil passage, in the Boerendel area (see Fig.3.1), following the change over from strongly eutrophic polder to slightly eutrophic Meuse water as influent. Meuse water was introduced on 5 July 1988, sludge was removed from the recharge basin in November 1989 (which explains the rapid breakthrough of NO_3^- afterwards at 25 m), and sludge was removed from the flow-through lake in between 25 and 80 m in February 1990. Approximate groundwater flow velocity is 1 m/d. 1 = change from polder to Meuse water; 2 = sludge removal from recharge basin; 3 = ditto from flow-through lake.

4.4.7 Important mixed hydrosomes

Their size and position in a large facies chain, make it worthwhile to discuss the following mixing zones between hydrosomes : $(D/L)_{df}$ and $(D/S)_{rs}$.

The deep anoxic, freshened transition zone from D to L

In between the (sub)regional, dune hydrosomes (D) and the supraregional, relict Holocene transgression hydrosome (L) the transition zone "(D/L)" is found. It occurs mainly along the landward side of the coastal dune hydrosomes, but also in between the Bergen and Castricum dune hydrosomes, where the Bergen clay (aquitard 1E) still delivers L-water (Fig.4.10; Enclosures 4-7).

Samples 19A.182 and 25C.294 in Tables 4.3 and 4.4 form prototypes. The facies is also calcareous (supersaturated) and unpolluted. The base exchange index varies from +8 to +40 meq/l, with the highest values in association with the Bergen clay. The water types are : B_5 to B_6NaHCO_3+ and B_4 to B_6NaCl+.

The reduced, salinized transition zone from S to D

In between the supraregional North Sea hydrosome (S) and the seaward face of the regional dune hydrosomes (D), the transition zone "(D/S)" occurs. A maximum thickness of about 100 m is observed in the IJmuiden area (Fig.4.10), where the Castricum and Zandvoort dune hydrosomes strongly contracted due to cleavage of the dunes by the sea port of

IJmuiden and the North Sea Canal, and by over-exploitation for industrial use and drinking water supply.

Samples 24H.190, 24H.189-60 and 24H.450-90 in Tables 4.3 and 4.4 form prototypes in the direction of the North Sea intrusion. The facies is also calcareous and unpolluted. The base exchange index ranges from -4 to -120 meq/l. The water types are successively : S_2 or S_3NaCl-, B_2 or B_3NaCl- and B_2CaCl-. Incidentally also B_3MgCl- is found (section 7.6.3).

4.5 Interpretation of the regional patterns

A general interpretation is structured by subsequent consideration of facies chains (evolutionary trends) and the influences of (a) hydrology, or more specifically the groundwater flow patterns and life cycle of each hydrosome, (b) the geochemical structure of the subsoil and (c) environmental changes, like input fluctuations, water table fluctuations and changes in land-use.

4.5.1 Facies chains

Facies chains are defined as a genetic succession of facies units, not necessarily restricted to one hydrosome. They represent specific evolutionary trends in water quality downgradient, and are therefore outstanding guidelines for discussion and interpretation. This requires, however, that the flowpath is accurately known.

The main facies chains are specified in Fig.4.20 and have been nominated after their primary characteristics. Most of them contain, in the direction of groundwater flow, the prograde evolution or succession lines a-e as described in section 2.7. Several facies chains are further illuminated and discussed in detail in chapter 7 : the initially low alkalinity, freshening dune chain (section 7.3), the initially medium alkalinity, freshening dune chain (section 7.4), the salinizing, artificial Rhine chain (section 7.5), the polder intruding, salinizing North Sea chain (section 7.6.2) and the dune intruding, salinizing North Sea chain (section 7.6.3).

It should be noted that the salinizing North Sea chain, that intrudes into dune water along its seaward face, is a relict feature now in those areas, where excessive groundwater pumping stopped and/or artificial recharge reversed the intrusion process. The Meuse/polder, artificial recharge chain is observed in the Katwijk and Monster spreading areas, the Meuse/Rhine chain only in the Scheveningen spreading area, and the Rhine chain in the Castricum, Wijk aan Zee, Overveen and Leiduin spreading areas.

The freshening dune chain, which occurs along the eastward, deep and very deep flow branches of (sub)regional dune groundwater flow systems, is subdivided into three types on the basis of the initial alkalinity. The low initial alkalinity in decalcified dunes north of Bergen aan Zee, results in the most differentiated chain with an acid, polluted facies at the beginning. A very high initial alkalinity and Ca^{2+} concentration in the Wijk aan Zee area, leads to the least differentiated chain, because the raised Ca^{2+}-levels block the issue of the $MgHCO_3$+ water type. Although Mg^{2+} increases downgradient of the $CaHCO_3$+ water type, as it normally does, the high Ca^{2+} levels prevent Mg^{2+} to become the dominant ion before Na^+ takes over this position. The initially high Ca^{2+} and HCO_3^- concentrations in this area arise by way of an enhanced dissolution of shell fragments, due to a raised atmospheric deposition of acidifying gases (SO_2 and NO_x) in the neighbourhood of the Hoogovens industrial complex, and a high CO_2 supply in methanogenic environments after passing through both dune peat and basal peat.

An interesting short, freshening dune chain of the initially low alkalinity type, is observed about 10 km to the north of the study area, in the relatively very young, Zwanenwater dune area (Fig.4.21). This dune complex was formed in between 1600 and 1800 AD and is composed of sand with a primarily low $CaCO_3$ content (< 1%). It is underlain by a well developed aquitard complex (1F + 1G) at shallow depth, which still contains brackish water (Cl^- about 1000 mg/l), and therefore points at a very slow flushing. Further details are given by Stuyfzand & Lüers (1992a).

4.5.2 Flow patterns and life cycle

The areal distribution of a freshened, salinized and {Na+K+Mg}-equilibrated facies corresponds well with the dynamic flow patterns described in sections 3.8 and 3.9.

The freshened facies is encountered, where fresh dune and polder waters are expanding or expanded in the past. The large areal extent is explained by (1) the general presence of brackish to saline groundwaters prior to the genesis of the coastal dune and polder hydrosomes, and (2) the relatively low displacing power of fresh waters. Their cation concentrations (Σcations = 6 meq/l) are low compared with the relatively high concentrations of marine cations to be exchanged (about 43 meq/l water for medium coarse sandy aquifers with CEC = 10 meq/kg dry weight, and about 1000 meq/l

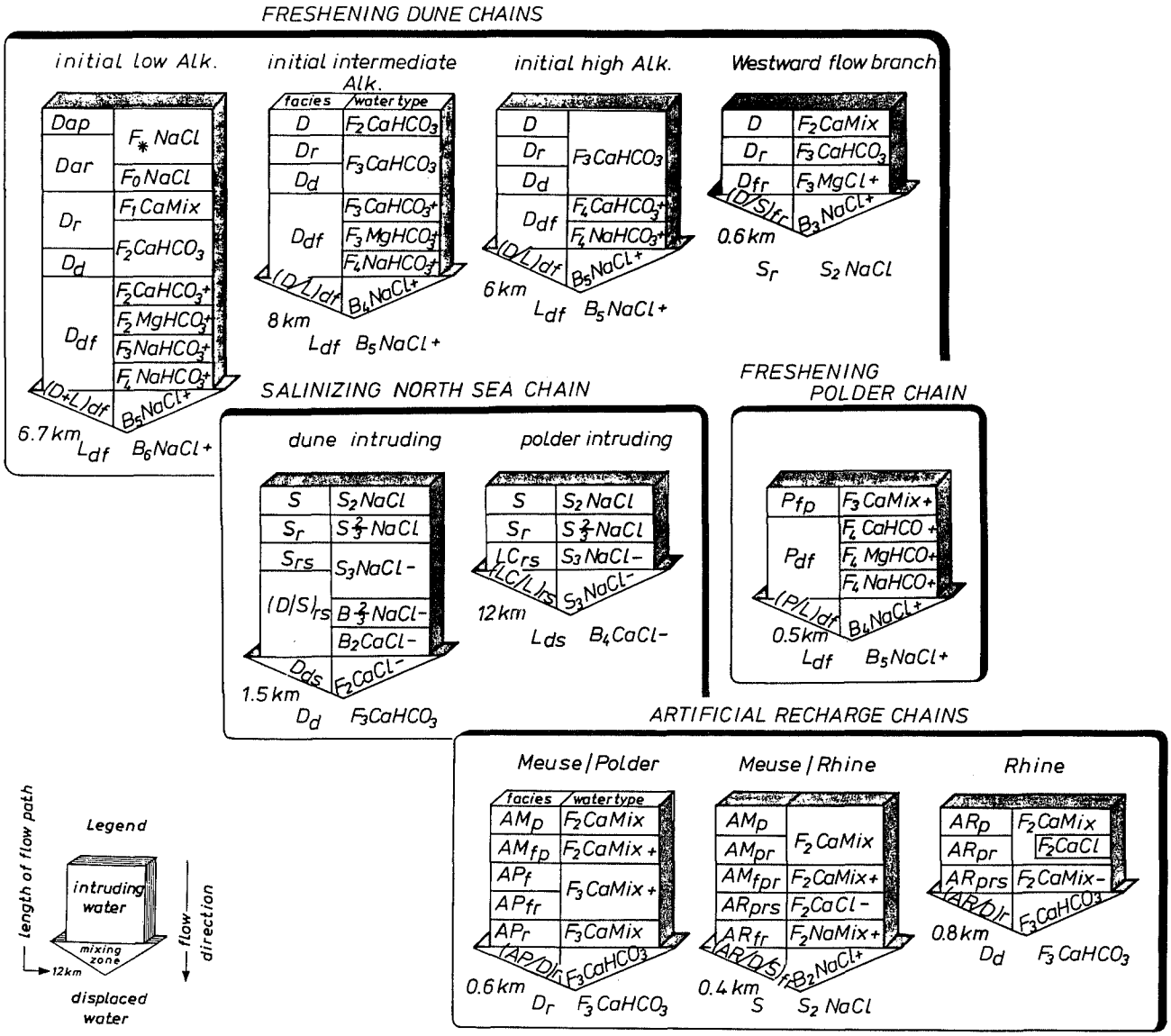

FIG. 4.20 Specification of the 10 main facies chains encountered in the coastal area in between Monster and Camperduin. Each chain represents a typical evolutionary trend down the hydraulic gradient. If the actual flow system persists, then the upper facies will expand downgradient and gradually force the other facies and hydrosomes out of the groundwater flow system.

water for clay-rich aquitards). When the exchange process is strongly simplified to the displacement of all adsorbed cations by the cations in fresh dune water, it already takes 7 to 165 pore flushes to equilibrate most aquifers and several aquitards, respectively. This may require a considerable time indeed, in the order of centuries to millennia.

Equilibrium with the cation adsorption complex has generally been attained by dune water in : (a) the whole upper aquifer, where time was sufficient and the CEC low enough for complete removal of any residual Na^+, K^+ and Mg^{2+}; (b) the second aquifer, only in the western parts of the regional dune hydrosomes, where fresh dune water flushed the porous medium for approximately 2000 years (Figs. 3.26 and 4.4); and (c) the recharge focus areas for the second and deeper aquifers, by virtue of a high flushing rate and the lack of high CEC aquitards (Fig.4.10). A freshened facies of dune water in the second aquifer is observed in the western parts, exclusively where the exchanging aquitards possess a high CEC, exhibit a considerable thickness, and are situated at greater depth (Fig.4.3). The latter reduces the amount of pore flushes with fresh water since the origin or enlargement of the dune system. Another situation of a freshened facies in the

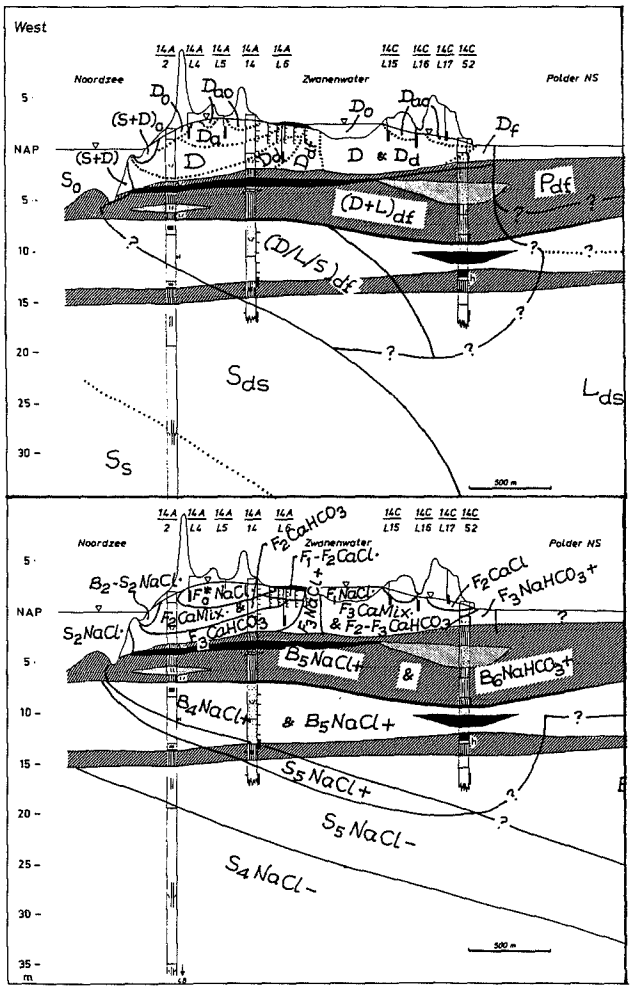

FIG. 4.21 Example of a short, freshening dune chain of the initially low alkalinity type (indicated by arrow), as observed about 10 km to the north of the study area, in the relatively very young Zwanenwater dune area. The chain is composed of : D_a (acid, (sub)oxic Dune water), D_{ar} (acid, reduced), D_r (reduced), D_d (deep anoxic), D_{df} (deep anoxic, freshened), $(D+L)_{df}$ (Dune with some relict Holocene transgression water, deep anoxic and freshened) and $(D/L/S)_{df}$ (a deep anoxic, freshened mixture of dune water, relict, Holocene transgression water and actual North Sea water). The deep dune water in its intrusion front, is 250 years old at most.

western parts of dune water in the second aquifer is encountered, where a previous salt water intrusion is pushed back again after cessation of pumping from this aquifer or after artificial recharge.

A salinized facies is observed below the western flank of the regional dune hydrosomes, where North Sea water expands or expanded at the expense of fresh dune water. It is encountered also below the polders, where Holocene transgression waters displaced fresh or less saline water. And in the younger dunes, salinized Rhine water is found in the vicinity of its intrusion front, where dune water is displaced. A similar calculation as presented above, explains the widely distributed facies "without base exchange", of North Sea water (Σcations ≅ 515 meq/l) and its relatively confined, salinized facies, notwithstanding large scale intrusion, in terms of a nearly 100 fold higher displacing power compared with fresh water.

So, the areal distribution of a freshened, salinized and {Na+K+Mg}-equilibrated facies correspond well with the palaeohydrology of the area. The high diversity, as observed in the study area, testifies of dynamic flow systems and too short stagnant periods, if they existed at all, to fade out the original hydrochemical stratifications by diffusion, even those in the relict Holocene transgression waters. Effects of molecular diffusion can be calculated using a slightly modified Eq.3.16, by substituting $C_{x,t}$ for c' and taking $v_w = 0$ in Eq.3.15 :

$$C_{x,t} = C_i \left[1 - erf\left(\frac{x}{2\sqrt{D_d t}}\right)\right] \qquad (4.4)$$

where : C_i = concentration of marker of a specific, homogeneous water body before diffusion started [mg/l]; $C_{x,t}$ = concentration of that marker at distance x from the boundary of that specific water body, at time t since stagnant flow triggered the manifestation of diffusion [mg/l]; x = distance travelled by the marker [m]; D_d = diffusion coefficient [m^2/d]; t = time since the start of diffusion [d]; erf ( ) = error function of ( ), see Eq.3.17.

In this equation it is assumed that the concentration of the marker of the specific waterbody is constant, and that the adjacent water body does not contain the marker. In reality the concentration of the marker will drop in the specific waterbody by diffusive losses, so that Eq.4.4 will exaggerate diffusive mixing to some extent. With a D_d of about $4 \cdot 10^{-5}$ m^2/d for Cl^- at 10°C in a porous medium (Li & Gregory, 1974; Volker, 1961; Beekman, 1991), at 10 and 20 m distance from the specific groundwater body a maximum value of 10% admixing is calculated for the adjacent hydrosome or facies after 1250 and 5000 years of diffusion, respectively. And 50% mixing is achieved at 10 and 20 m after 7,500 and 30,000 years, respectively. These results indicate that the original hydrochemical variations of the relict, Holocene transgression hydrosome within a zone of 10-20 m, have been smoothed by diffusion, but not wiped out completely. This agrees well with the survival of various 10-20 m thick, Holocene chloride inversions (section 4.4.2; Enclosure 3.3).

Recent changes in the flow pattern may also disrupt the simple interpretation of the base

exchange index. The appearance of a freshened facies at shallow depth below pumping wells may be a precursor of salinization. In that case, freshened water is forced out of an exchanging aquitard (originally downgradient) back into the previously equilibrated aquifer. Part of the acquired Na^+, K^+ and Mg^{2+} is exchanged again for Ca^{2+} in the aquifer, but the remaining fraction may remain sufficient to yield a freshened facies. In ion-chromatographic terms this phenomenon can be explained by first a self-sharpening front of intruding fresh water, followed by a broadening front of back-flushing water (dr. C.A.J. Appelo, pers. comm.). Such a situation is probably present to the south of Zandvoort aan Zee (Fig.4.4) and explains the wide-spread extension of F_3CaHCO_3+ water in the formerly overexploited, central dune area, above strongly exchanging aquitards at 60-80 m-MSL.

4.5.3 Geochemical structure of the subsoil

Geochemistry has a strong impact on the facies, also for the already mineralized North Sea, polder, Rhine and Meuse waters. The most important reactive phases calcite and organic matter are considered here exclusively. Cation exchanging phases and other reactive solid phases are discussed in chapters 6-8.

The general occurrence of shell fragments composed of aragonite and calcite in Holocene and Eemian deposits, and fast reaction rates explain that most groundwaters are in close equilibrium with calcite, leading to a calcareous facies. Lack of calcite is reflected in acid dune groundwater only, where the unsaturated zone and upper metres are completely decalcified. In the deep continental Harderwijk Formation, which generally does not contain any $CaCO_3$ (Van der Sleen, 1912), no agressivity towards $CaCO_3$ has been observed, because the overall composition of the upgradient hardened groundwater hardly changes.

Most aquitards with a large areal extent and with a high resistance to vertical flow (Fig.3.9), have a pronounced impact on the chemical composition of percolating groundwater. The interactions are similar to those described for sea water in anoxic, marine sediments (Sholkovitz, 1973; Berner, 1971; Rijsdijk, 1983) and lake water in anoxic, lacustrine muds (Golterman, 1975; Emerson, 1976). In essence, they are driven mainly by a strong decomposition of unstabilized organic matter, leading to a relatively high redox index — sulphate-reducing or methanogenic — and high concentrations of HCO_3^-, PO_4^{3-}, NH_4^+, CH_4 and DOC.

This is well illustrated in Fig.4.22, where high HCO_3^- and low SO_4^{2-} levels in the upper parts of the second aquifer in the dune area clearly correspond with the presence of Holocene aquitards at the base of the upper aquifer. There are four major gaps in the basal Holocene aquitards, respectively west of Bergen, west of Castricum, north of Zandvoort aan Zee and north of Noordwijk aan Zee (numbered 1-4 in Fig.4.22). They constitute the recharge focus areas of the second and even third aquifer in the coastal dune area (Fig.4.10). The basal Holocene aquitards rank as follows, in order of decreasing geochemical impact : the Bergen clay (aquitard 1E with HCO_3^- = 1000-2500 mg/l) > Velsen clay on top of basal peat (aquitard 1G with HCO_3^- = 400-1000 mg/l) > aquitard 1D (including the Haarlem clay, with HCO_3^- = 300-450 mg/l). Other illustrations are offered by so-called dune peat groundwater (section 6.6.5), and a relatively high redox index for relict, Holocene transgression waters of the marsh type and polder groundwaters. The latter two contacted more Holocene peat and clay as compared to North Sea and dune groundwaters, respectively.

The areal distribution of a deep anoxic facies coincides in general with a low pollution index. This is explained by the reduction of NO_3^- and SO_4^{2-}, by a more effective immobilization of heavy metals through coprecipitation in iron sulphides and sorption to clay and organic matter, by dehalogenation of many halogenated hydrocarbons in this specific redox environment (Smeenk, 1984; Hrubec et al., 1986), and in many cases by a relatively high age, beyond the onset of the industrial epoch.

4.5.4 Water table fluctuations, land-use and environmental pollution

Changes in water table, landuse and atmospheric pollution have no effect of course on the connate Maassluis hydrosome and relict Holocene transgression waters. Coastal North Sea water is clearly affected by many sources of pollution (Weichart, 1973), but the sampled North Sea groundwaters are probably too old to show any signs.

Dune water

These waters have been affected by : (a) a regional lowering of the water table in the period 1850-1960, (b) changes in vegetation cover notably since about 1920, and (3) atmospheric pollution, which strongly increased in the period 1920-1980 (section 5.5.1).

The lowering of the groundwater table by pumping and drainage, led to a drop of the $\delta^{18}O$-values from about -6.5±0.2 to -7.2±0.2 ‰ for the whole younger dune area (section 7.4.5). The inherent expansion of the unsaturated zone led to (further) oxidation of DOC and $NH4^+$ in a system open to the atmosphere (section 6.6.6). This signifies that more oxidants remained available for oxidation in the closed system below the water table.

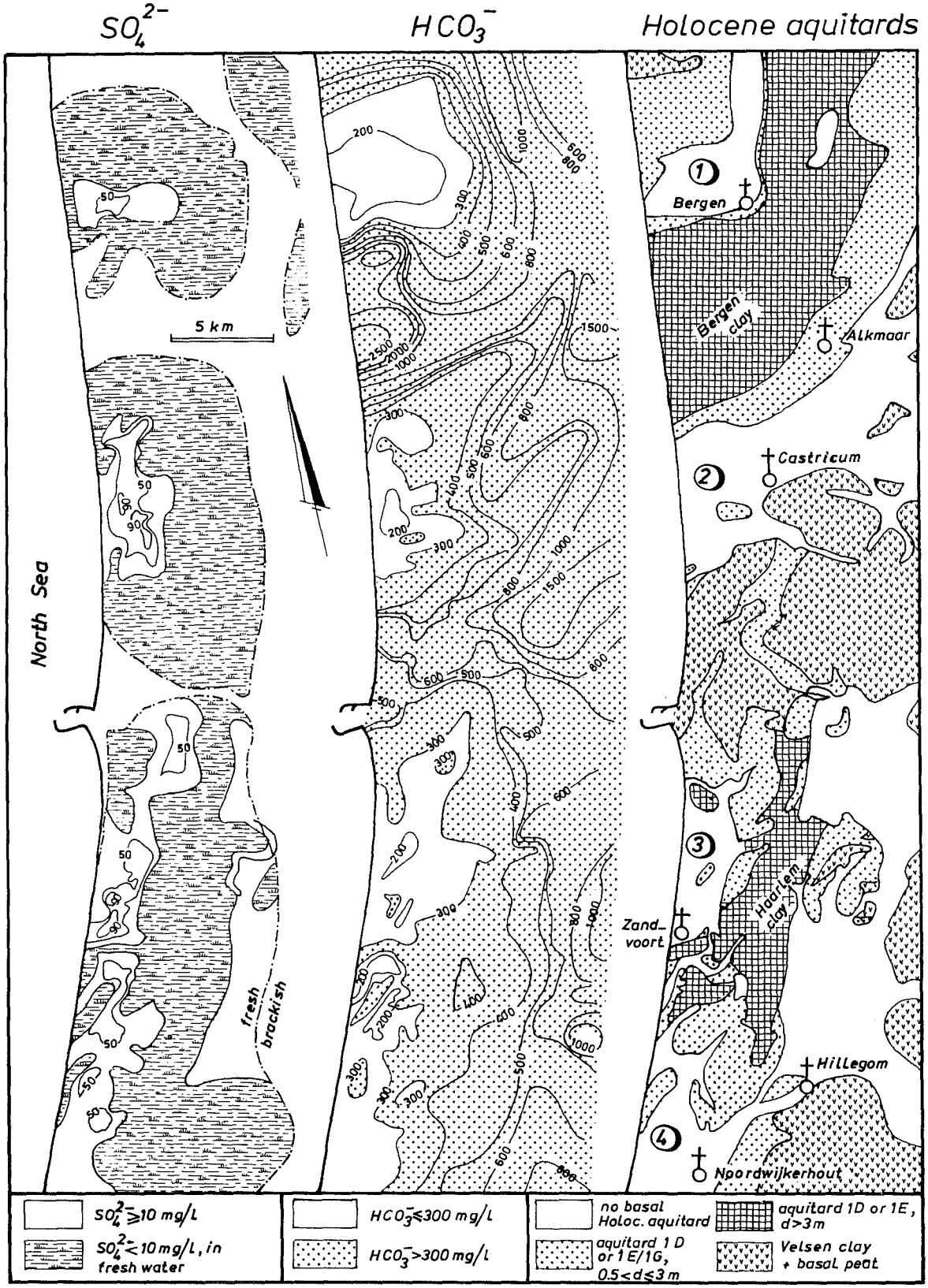

FIG. 4.22 Relation between the presence of Holocene aquitards at the base of the first aquifer and the HCO_3^- and SO_4^{2-} concentrations of groundwater in the upper parts of the second aquifer (at 30 m-MSL), north of the Old Rhine, in the period 1976-1992. The areas numbered 1-4, constitute recharge focus areas for the second aquifer in the dunes.

Consequently, the (sub)oxic zone could expand and, temporarily, the SO_4^{2-} levels had to rise somewhat by oxidation of iron sulphides, at least in areas where vegetation did not change much.

On a local scale, especially close to drainage canals and pumping wells, anoxic dune peat and iron sulphides became exposed to soil air and rapidly oxidized. High NO_3^- concentrations in connection with the oxic decomposition of peat, oxidized iron sulphides at greater depth, so that the overall result was an increase in SO_4^{2-} concentrations and locally a polluted facies. The most pronounced effect on deep dune groundwater pumped for drinking water supply, was observed in the Castricum catchment area where deep Holocene aquitards (1D-1G) are lacking (gap 2 in Fig.4.22). The SO_4^{2-} increase is accompanied there exclusively by a similar increase for Ca^{2+} (both about 1.2 mmol/l), a negligible increase of Fe (0.07 mmol/l) and a negligible pH decrease from 7.3 to 7.2 (Fig.4.23).

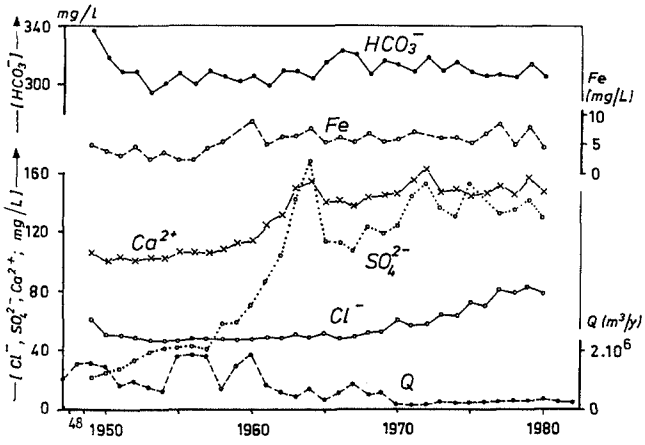

FIG. 4.23 The increase of Ca^{2+} and SO_4^{2-} concentrations in pumped, deep dune groundwater west of Castricum is mainly due to a drawdown of the phreatic level below dune peat and the concomitant oxidation of iron sulphides and dissolution of shell fragments. The slowly increasing Cl^- concentrations reflect the growth of pines planted in the 1930s in the catchment area. Time series for the raw water from all pumping wells of group G, screened at 23-36 m-MSL.

Overall reactions, that explain both a Ca^{2+} production equal to the amount of SO_4^{2-} mobilized, and an unchanged alkalinity, are :

$$0.6\ FeS_2 + 2.25\ O_2 + 0.9\ H_2O + 1.2\ CaCO_3 \rightarrow 0.6\ Fe(OH)_3 + 1.2\ Ca^{2+} + 1.2\ SO_4^{2-} + 1.2\ CO_2 \quad (4.5)$$

$$1.2\ FeS \cdot nH_2O + 2.4\ O_2 + 1.2\ CaCO_3 \rightarrow 1.2\ FeCO_3 + 1.2\ SO_4^{2-} + 1.2\ Ca^{2+} + 1.2n\ H_2O \quad (4.6)$$

Reaction 4.5 requires all the carbondioxide formed to be lost to the atmosphere prior to arrival at the groundwater table. With a low natural recharge under pines, that form the predominant vegetation cover of the close surroundings of the pumping wells of group G, this could be true (sections 6.8.4 and 8.4.2). Reaction 4.6 constitutes, however, a more elegant explanation to be checked by solid phase research on site. The siderite ($FeCO_3$) precipitation can be considered in this case as an ion exchange of Ca^{2+} for Fe^{2+}. The condition of (super)saturation of the pumped water with respect to siderite, is satisfied. And the oxidation of sulphide may indeed consume all the oxygen or nitrate (for simplicity not considered here), and thereby leave the ferrous iron unharmed. This requires an excess of iron sulphides to be present or necessitates a flow velocity superior to the reaction rate (Postma et al., 1991).

The increased vegetation and air pollution resulted in raised deposition rates for SO_2, NO_x, NH_4^+, F^-, heavy metals (among others Cd, Cu, Pb, Sb, V and Zn) and organic micro-contaminants (for instance PAHs and chlorinated hydrocarbons). This is reflected in a polluted facies in the upper 0.1-3 metres of (sub)oxic dune water, and in a decrease of the pollution index with depth (Table 4.3). This decrease is caused by sorption of heavy metals and AOCl, decay of tritium, breakdown of halogenated hydrocarbons and an increasing age of the water beyond the onset of industrialisation. Notwithstanding a possible retention of SO_4^{2-}, an acid facies contributes to a polluted facies through the mobilization of heavy metals (sections 6.6.4 and 7.3.4). Another important change is the expansion of dune shrub (*Hippophaë rhamnoides*), which fix N_2 and thereby assist in the enlargement of the (sub)oxic and polluted zones.

Sulphate concentrations of dune groundwater today, exceed those of 50-75 years ago in the recharge focus areas of the second aquifer (Fig.4.24). This has been caused by expansion of the (sub)oxic zone, raised atmospheric inputs of NO_3^- and SO_4^{2-}, local oxidation of iron sulphides and an increased downward flux by pumping. These changes contribute to the large areal extent of the reduced or more precisely sulphate-(meta)stable facies, as observed today in the second aquifer in the younger dunes (Enclosure 4.2).

Polder water

These waters have been influenced mainly by : changes in the proportion of river Rhine water, which was drastically raised around 1880 AD south

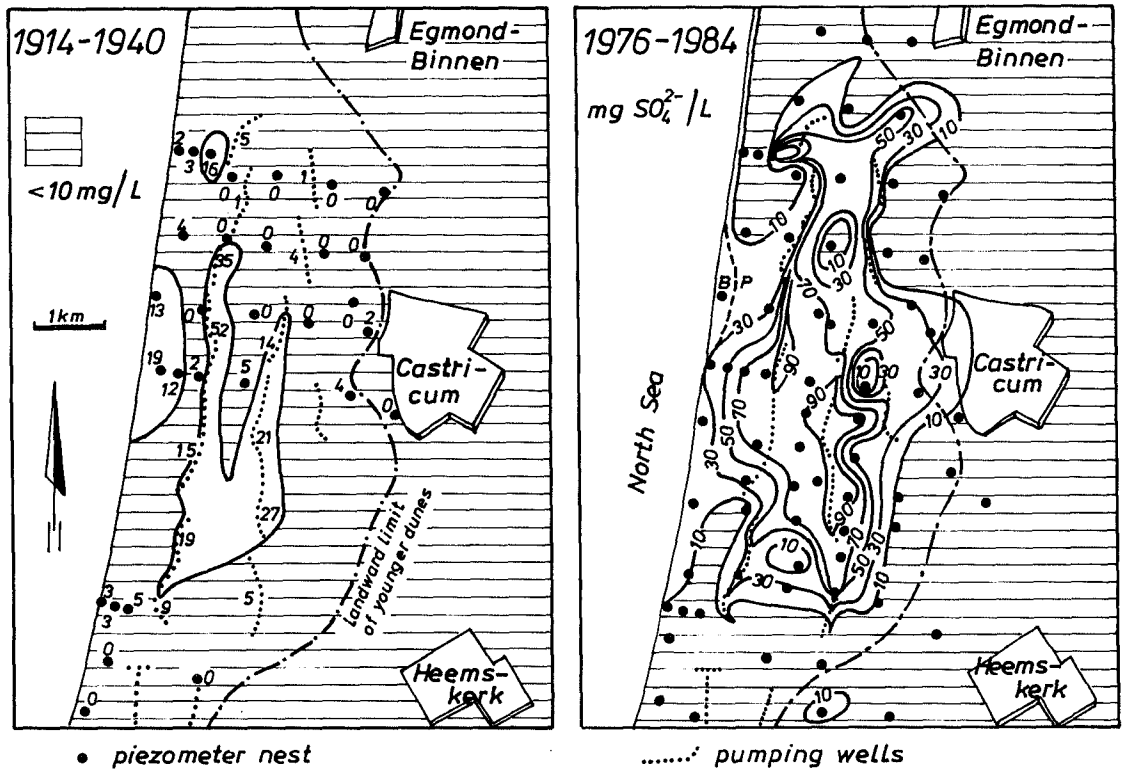

FIG. 4.24 Contour lines of equal SO_4^{2-} concentration in groundwater at about 30 m-MSL in the second aquifer in between Wijk aan Zee and Egmond aan Zee, for the period 1914-1940 and 1976-1984, respectively. Increases of SO_4^{2-} are related to changes in hydrology, vegetation and air pollution, and are restricted to the recharge focus area for the second aquifer, where deep anoxic Holocene aquitards in between the upper and second aquifer are lacking. The effects of $FeS_{(2)}$ oxidation predominate in zones with extreme increases.

of the North Sea Canal and around 1940 AD to the north; the pollution history of the river Rhine (Fig.4.25, left); increased quantities of locally discharged sewage effluents and industrial wastes roughly until the 1960s, when many sewage treatment plants were put in operation; and intensification of agriculture, leading to raised levels for nitrate, pesticides like ethylene thiourea and 1.2-dichloropropane (Lagas et al., 1990) and, more locally, Br^- (Wegman et al., 1978). How deep these pesticides and their decay products penetrated and which AOCl levels are actually present, is practically unknown. A polluted facies is assumed for shallow polder waters.

Recharged surface water

These waters have been influenced by the pollution record of their source at the intake (see Fig.4.25 for the Rhine), by changes in pretreatment, by a selective intake and by the frequency of sludge removal from the spreading basins (which was higher when pretreatment was less rigourous). The quality development of the imported river Rhine water upon arrival at the dunes is shown in Fig.4.25 (right). The overall result is, that recharged surface waters generally are polluted, however to a lower degree in aquitards and the second aquifer by virtue of a protracted, beneficial subsoil passage (section 7.5).

There is a tendency for most infiltrated waters to become less polluted in the upper aquifer since the late 1970s, mainly in consequence of sanitation measures in the Rhine fluvial basin, further pretreatment by coagulation, and a reduced chlorination for transport. This chlorination leads to the formation of, among others, trihalomethanes (Rook, 1974), dihaloacetonitriles (Peters et al., 1989), bromate (Bull & Kopfler, 1991), halogenated acetic acids and chlorate (Versteegh et al., 1990) and AOCl (Smeenk, 1984). The overall quality improvement creates a distortion of the normal prograde quality evolution downgradient : somewhere downgradient a pollution peak is observed, which stems from the previous, more polluted period. The migration of this peak is generally retarded by sorption phenomena (section 7.5) and smoothed by both sorption and dispersion.

In the period 1974-1978 the calcite saturation index of pretreated river water increased from agressive (-0.4) to supersaturated (+0.15). This change is caused by : (a) the reduced NH_4^+

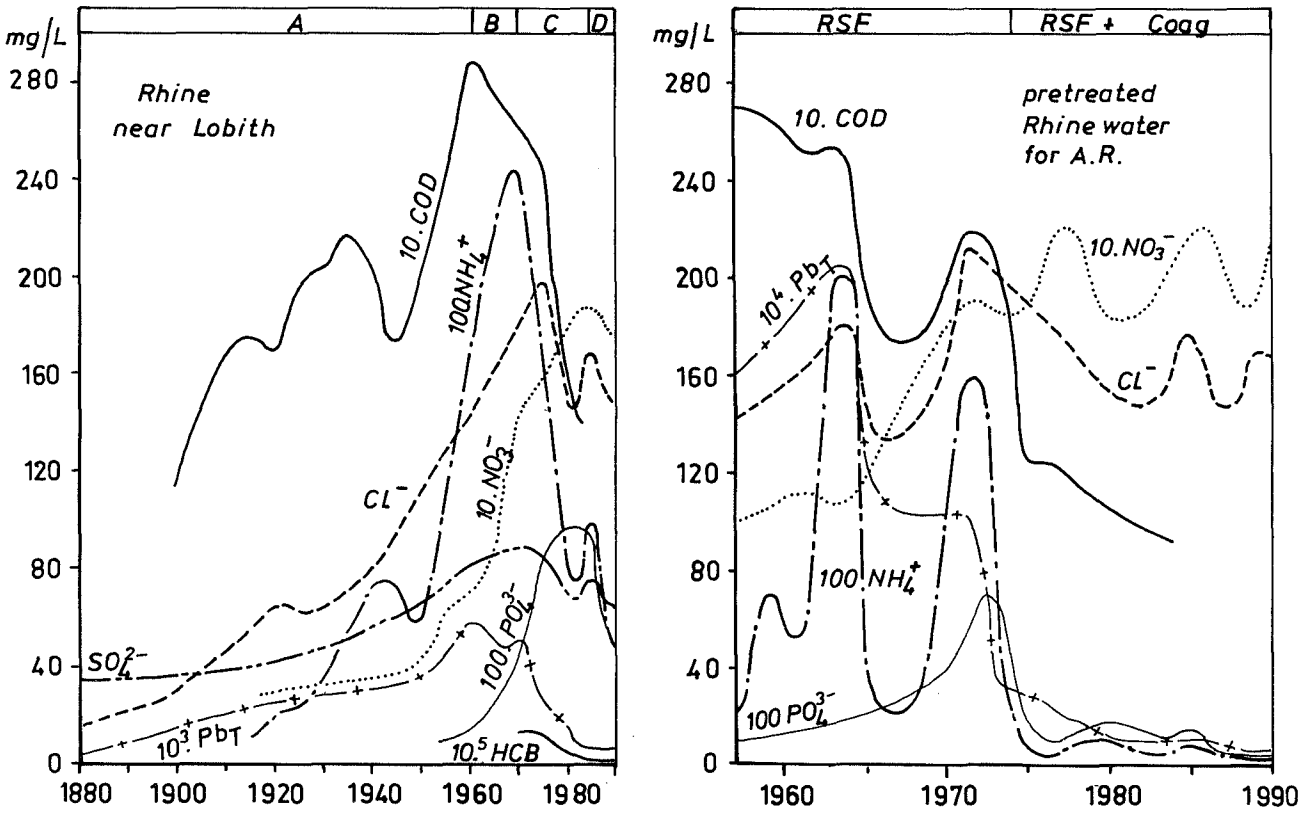

FIG. 4.25 Schematized quality development of the river Rhine near the German border during the past century, and pretreated Rhine water upon arrival at the dunes south of Zandvoort aan Zee. Phases for the Rhine near German border : A = steady increase in pollution; B = sanitation measures on organic load and heavy metals; C = further reduction of heavy metals and treatment of sewage effluent; D = PO_4 treatment, NTA as a substitute for phosphates in detergents. Pretreatment : RSF = rapid sand filtration; Coag = coagulation. Data derived from Molt (1961), annual reports of RIWA, RWS, GW, DZH and unpublished data files.

concentrations in the Rhine, which upon rapid sand filtration lead to less nitrification and thereby generate less H^+; (b) further pretreatment by coagulation including a pH correction since mid-1974 in case of Rhine water, for recharge sites Castricum, Wijk aan Zee and Leiduin; and (c) the change over from Rhine to coagulated Meuse water in 1976 for recharge site Scheveningen. The resulting calcite supersaturation and the lower NH_4^+ concentrations also in the pretreated river water, led to a predictable decline in $CaCO_3$ dissolution during subsoil passage (Fig.4.26).

Sludge was regularly removed from spreading basins in the Castricum and Leiduin recharge areas, before the addition of a coagulation step to pretreatment. During periods of prolonged sludge formation without removal, the redox level could drastically change from (sub)oxic to anoxic, as evidenced by denitrification and mobilization of NH_4^+, Fe, Mn and organics (Fig.4.27), and a retarded mobilization of phosphate (Fig.4.28).

The phosphate mobilization peak is in both depicted cases strongly retarded by sorption. The retardation can be quantified by the retardation factor R_{PO4}, being the ratio of the phosphate migration velocity and the migration velocity of the water phase or Cl^- (Eq.7.5). In case of pond 13.1 in the Scheveningen area R_{PO4} is about 22, and in case of pond 40 in the Katwijk spreading area it amounts to 11. The about double as high retardation in the Scheveningen area is explained by : (1) the predominant (sub)oxic boundary conditions, in which ferric hydroxides are stable and add to the adsorption capacity of the porous medium, (2) relatively low concentrations of dissolved humic substances that compete for sorption sites and may complex phosphate (Sanyal & De Datta, 1991); (3) relatively little complexation of phosphate by Ca^{2+}, Mg^{2+} and Fe^{2+}; and (4) overall lower phosphate concentrations. The behaviour of PO_4^{3-} is further complicated by the presence of both a slow and fast sorption reaction (De Groot, 1981), seasonal fluctuations in redox level ([sub]oxic in winter, (deep) anoxic in summer), interaction with dune peat (both

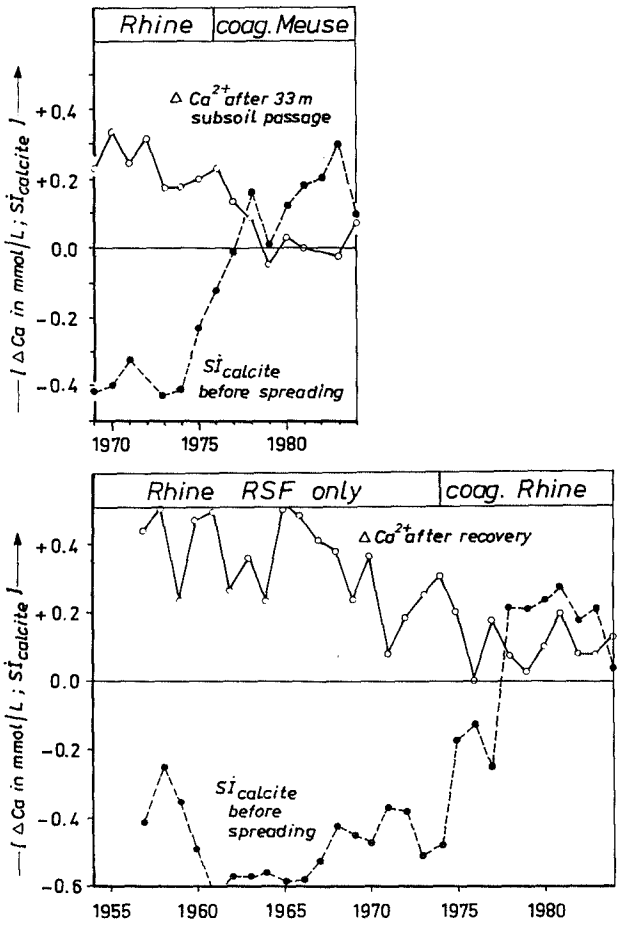

FIG. 4.26 Changes in the annual mean, calcite saturation index of pretreated Rhine and Meuse water and their effect on $CaCO_3$ dissolution during dune infiltration in the Leiduin and Scheveningen area (resp. sites 13 and 21 in Fig.3.1). The $CaCO_3$ dissolution is indicated as ΔCa, being the difference between the annual mean Ca^{2+} concentration in pretreated river water before infiltration and after recollection or 33 m subsoil passage.

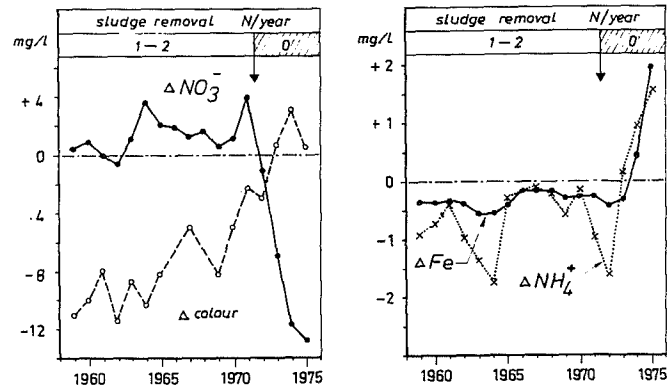

FIG. 4.27 The development of anoxic conditions following the suspended removal of sludge from the floor of spreading basin 5 in the Castricum area. Quality changes during subsoil passage are given as the difference in concentration between groundwater from an observation well 2 m below the centre of the basin floor, and surface water in basin 5. The mean subsoil travel time to this well was circa 2 days. A positive Δ indicates an increase during subsoil passage.

a source and sink), removal of phosphate loaded sludge, and aquifer fouling in the basin proximal zone, where deep bed filtration may increase the adsorption capacity of the aquifer (Stuyfzand, 1986d, 1989e).

4.6 Subregional application to flow-through dune lakes

The HYFA was also applied on a subregional scale, to two areas rich in flow-through dune lakes, both adjacent to spreading areas (Fig.4.29). Instead of the pollution index, the water quality index phosphate was used, because of more relevancy in these hydro-ecological study areas where eutrophication is of major concern.

The areas diverge in their hydrological and hydrochemical setting : pretreated river Meuse water relatively poor in phosphate is infiltrated in West-Meyendel (part of the Scheveningen spreading area; see Fig.3.1), where the low hydraulic resistance of aquitard 1C results in a strong vertical flow component; and eutrophic polder water is recharged in the Boerendel area (part of the Katwijk spreading area; see Fig.3.1), where aquitards 1B + 1C' of high hydraulic resistance induce a strong lateral flow component. The hydraulic gradient between the spreading ponds and the North Sea HWL amounts to 4.5 m over 600 m for West-Meyendel and 9 m over 800 m for the Boerendel area.

Artificial recharge started in both areas around 1956. For Meyendel the surface water intake was changed over from little pretreated Rhine to further pretreated Meuse water in 1976. The Rhine water recharged was never as eutrophic, however, as the polder water that was used for spreading in the Boerendel area till July 1988.

Comparison

The cross sections in Fig.4.29 reveal that the infiltrated polder water migrated indeed about double as far laterally as the Meuse water, due to the higher hydraulic resistance of aquitards 1B + 1C' as compared to 1C, and due to the higher hydraulic gradient. More flow-through lakes therefore receive

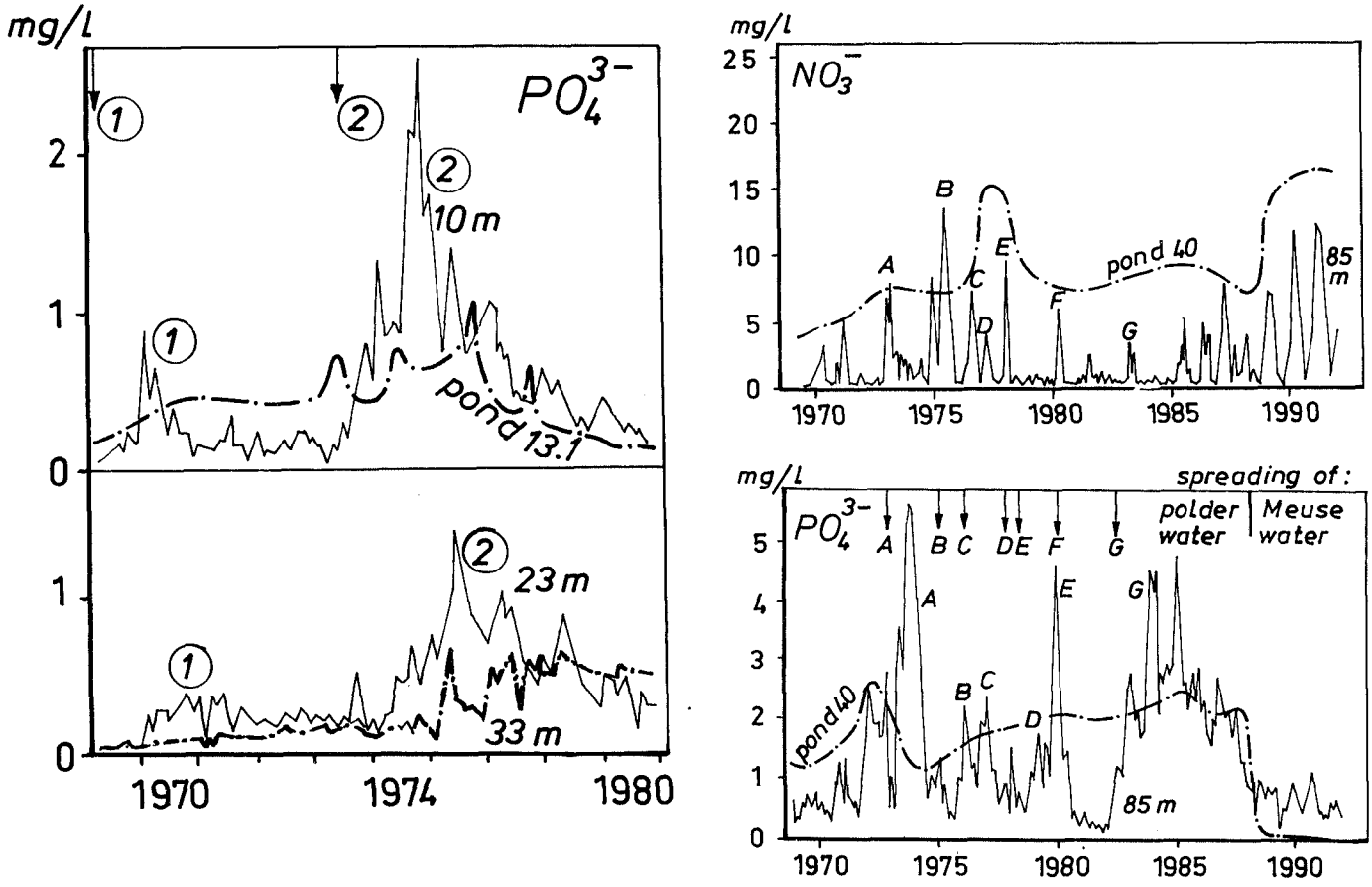

FIG. 4.28 The complex behaviour of orthophosphate during subsoil passage in the Scheveningen (pond 13.1) and Katwijk spreading area (pond 40). Sludge removal from the basin floor (indicated by arrows A-E) and atmospheric exposition of basin sludge (without removal) during a recharge stop (indicated by arrows 1-2) are preceded by an exponential increase of the PO_4^{3-} concentration. This is due to clogging (being the reason for countermeasures) and the development of (deep) anoxic conditions, leading to the mobilization of retained phosphate. Removal of the sludge and oxygenation lead to a drastic return to more normal levels. In the Scheveningen area a gradual breakthrough of PO_4^{3-} can be inferred from the wells at 23 and 33 m distance. The mean, subsoil migration velocity of the Rhine water from pond 13.1 and polder water from pond 40 was 0.8 and 2 m/d, respectively.

a large inflow from infiltrated surface water in the Boerendel area than in West-Meyendel. Rain water lenses are clearly present in both areas (see also section 3.10.3). The low permeability of aquitard 1B + 1C' retards the displacement of deep dune groundwater below the infiltrated polder water.

The phosphate levels of ground and surface waters in the Boerendel area (for specifications see Fig.4.14) exceed those in West-Meyendel, as expected. The general decrease downgradient can be explained in terms of (a) adsorption, leading to a retardation factor of 10-50 (Stuyfzand, 1986d; section 4.5.4), and (b) the phosphate input record, with a strong increase from 0.6 in 1966 to about 2.0 mg PO_4^{3-}/l since 1971 (Stuyfzand, 1990a).

Storage and release of phosphate in anoxic sludge at the bottom of spreading ponds, leads to a relatively phosphate depleted flow through the banks of spreading ponds and a phosphate enriched flow through the bottom sludge, both in the Boerendel (Fig.4.14 and 4.29) and West Meyendel area (Fig.4.29).

The phosphate patterns of infiltrated Meuse water in West-Meyendel (Fig.4.29) reveal also that phosphate is mobilized on three locations : (1) in the upper aquifer at some distance from the spreading ponds, due to desorption of phosphate, that was adsorbed during the preceding Rhine water flushing; (2) in aquitard 1C, where the decomposition of organic matter releases some phosphate; and (3) in bottom sludge at the infiltrating parts of flow-through lakes.

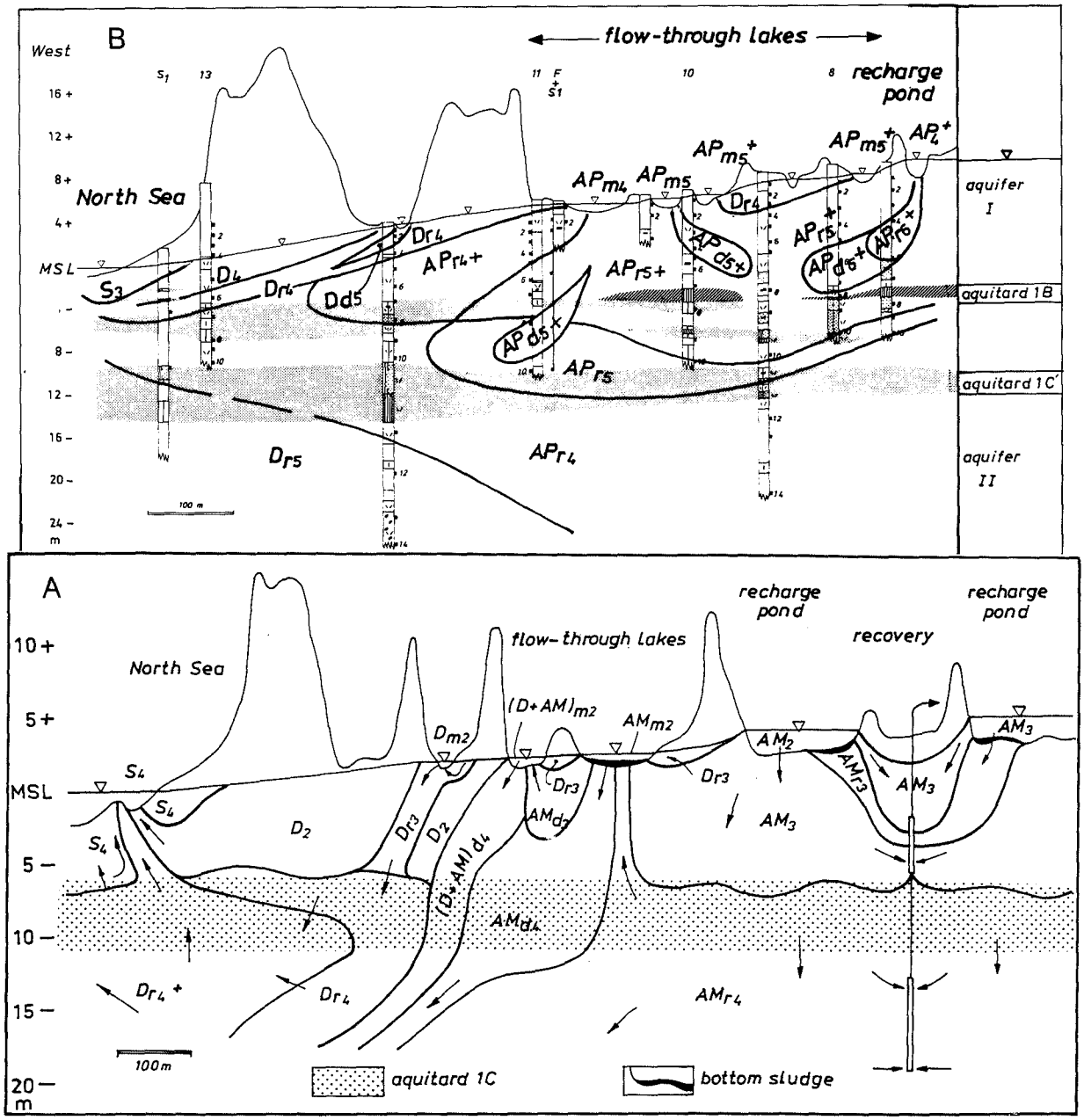

DUNE WATER

D_2 = (sub)oxic, mesotrophic
D_4 = (sub)oxic, eutrophic
D_{d5} = deep anoxic, strongly eutrophic
D_{m2} = mixed, mesotrophic
D_{r3} = reduced, slightly eutrophic
D_{r4} = reduced, eutrophic
$D_{r4}+$ = as D_{r4}, freshened
D_{r5} = reduced, strongly eutrophic

MIXED DUNE AND MEUSE WATERS

$(D+AM)_{m2}$ = mixed, mesotrophic
$(D+AM)_{d4}$ = deep anoxic, eutrophic

RECHARGED MEUSE WATER

AM_2 = (sub)oxic, mesotrophic
AM_3 = (sub)oxic, slightly eutrophic
AM_{d3} = deep anoxic, slightly eutrophic
AM_{d4} = deep anoxic, eutrophic
AM_{m2} = mixed, mesotrophic
AM_{r3} = reduced, slightly eutrophic
AM_{r4} = reduced, eutrophic

NORTH SEA WATER

S_3 = (sub)oxic, slightly eutrophic

RECHARGED POLDER WATER

AP_4+ = (sub)oxic, eutrophic, freshened[1]
AP_{d5} = deep anoxic, strongly eutrophic
$AP_{d6}+$ = deep anoxic, hypertrophic, freshened[1]
AP_{m4} = mixed, eutrophic
$AP_{m5}+$ = mixed, strongly eutrophic, freshened[1]
AP_{r4} = reduced, eutrophic
AP_{r5} = reduced, strongly eutrophic
$AP_{r5}+$ = reduced, strongly eutrophic, freshened[1]
$AP_{r6}+$ = reduced, hypertrophic, freshened[1]

' = inherited from the polder water itself, pointing at breakthrough of Na^+, K^+ and Mg^{2+}

Note : all waters are calcareous and without base exchange, unless stated otherwise.

FIG. 4.29 Cross sections over flow-through dune lakes in between the North Sea and westernmost spreading basins, showing the areal distribution of hydrosomes and their hydrochemical facies. A = schematized situation in the period 1980-1985 for West-Meyendel (for location see Fig.3.1), where pretreated river Meuse water relatively poor in phosphate is infiltrated; B = situation in March-June 1988 for the Boerendel area (for location see Fig.3.1), where strongly eutrophic polder water was recharged till 5 July 1988.

Interaction with bottom sludge and vegetation in flow-through lakes generally yields nice geochemical tracers of groundwater flow (Fig.4.30). During both upward flow in the groundwater capture zone and downward flow in the discharge zone, deep anoxic sludge, plant roots and algal mats are encountered. Their passage leads to complete denitrification and often complete sulphate reduction, strong increases for DOC and HCO_3^-, and an accentuation of fluctuations for among others K^+, HCO_3^- and DOC (Fig.4.31; Stuyfzand & Moberts, 1987b).

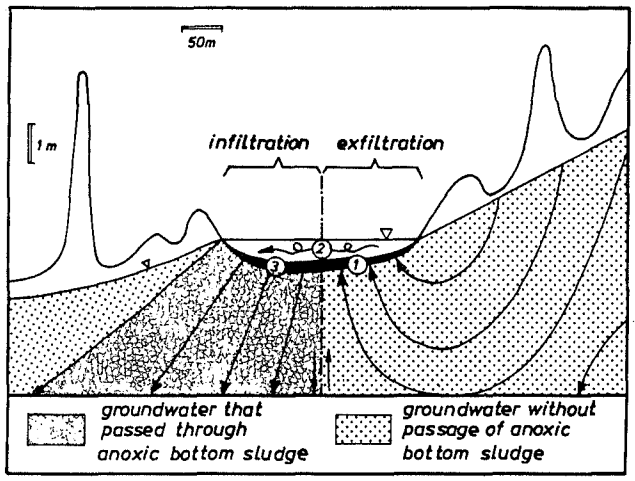

FIG. 4.30 Passage of anoxic bottom sludge, the root zone and algal mats in flow-through dune lakes, both in the capture zone (1) and release zone of groundwater (3), yields geochemical tracers of groundwater flow. Groundwater flowing towards the lake is (sub)oxic or sulphate-(meta)stable. The groundwater released in the downgradient parts of the lake is (deep) anoxic, i.e. completely denitrified and (completely) depleted in sulphate, and contains raised levels of DOC, HCO_3^-, Ca^{2+}, Fe and PO_4^{3-}. During its flow through the lake (zone 2) the water is strongly depleted in Fe, Mn, CO_2, Ca^{2+}, PO_4^{3-}, NH_4^+ and SiO_2 by aeration, biological uptake and (co)precipitation.

This interaction with bottom sludge in flow-through lakes yielded a more consistent hydrochemical pattern and better diagnosis of groundwater flow in West-Meijendel than in the Boerendel area (Fig.4.29), for two reasons : (1) in West-Meijendel there is less interaction with biomass and bottom sludge in the spreading pond upgradient of the flow-through lake. This yields a stronger contrast between the captured and released groundwater; and (2) the hydrological situation in the Boerendel area is more complex due to the presence of a chain of five flow-through lakes in this particular cross section, and due to severe clogging of their floor (Fig.4.32A and B). That clogging may reduce the amount of water passing through and thus increases the risk of missing this deep anoxic water in monitoring wells.

Quality changes of exfiltrated groundwater in the flow-through lake are composed of : (a) CO_2 removal by air-stripping and uptake during photosynthesis; (b) precipitation of calcite due to these CO_2 losses; (c) oxidation of Fe^{2+} and Mn^{2+} by aeration, leading to the precipitation of ferric hydroxides (Fig.4.32C); (d) uptake of NH_4^+, PO_4^{3-} and SiO_2 by algae and vegetation (SiO_2 especially by diatoms); and (e) coprecipitation of PO_4^{3-} with $Fe(OH)_3$ and $CaCO_3$.

The higher nutrient loads of polder water as compared to Meuse water, induce an overall higher redox index (reduced versus (sub)oxic; Fig.4.29) for two reasons. First, they raise the biological production of the spreading ponds, which results in more sludge formation and a higher consumption of oxidants upon passage of this mainly organic sludge. And second, the much higher NH_4^+ concentrations in polder water imply a higher oxygen consumption by nitrification.

The freshened facies of infiltrated polder water in the upper aquifer up to about 700 m downgradient of the spreading ponds, is completely inherited from the polder water itself (BEX = +1.2 meq/l). The loss of K^+ and Mg^{2+} further downgradient by sorption (Fig.4.14), leads to the change from a freshened facies to the facies "without base exchange" further downgradient. Meuse water generally exhibits a too small, inherited, positive BEX (≤+0.5 meq/l) to be significant.

Dune groundwater in the Holocene aquitard and in the aquifer below, has a freshened facies in the West-Meyendel area and the facies "without base exchange" in the Boerendel area. This difference is explained by a much more serious North Sea water intrusion in the West-Meyendel area prior to the artificial recharge. The abstraction of shallow dune groundwater resulted in a water table below MSL, so that North Sea water could even intrude laterally into the upper aquifer (Fig.3.30). Artificial recharge since 1956 led to a clear pushing back of the salt water and caused the cation exchange responsible for the observed freshened facies.

Hydro-ecological spinoff

Flow-through dune lakes within the sphere of influence of spreading ponds, attract groundwater with high concentrations and fluxes of phosphate, ammonia or nitrate and siliciumdioxide, and fix part of these nutrients in biomass (both living and accumulated in bottom sludge) and part of the phosphate in precipitated calcite and ferric hydroxides. This explains the large extent of ruderal plant species in and around these flow-through

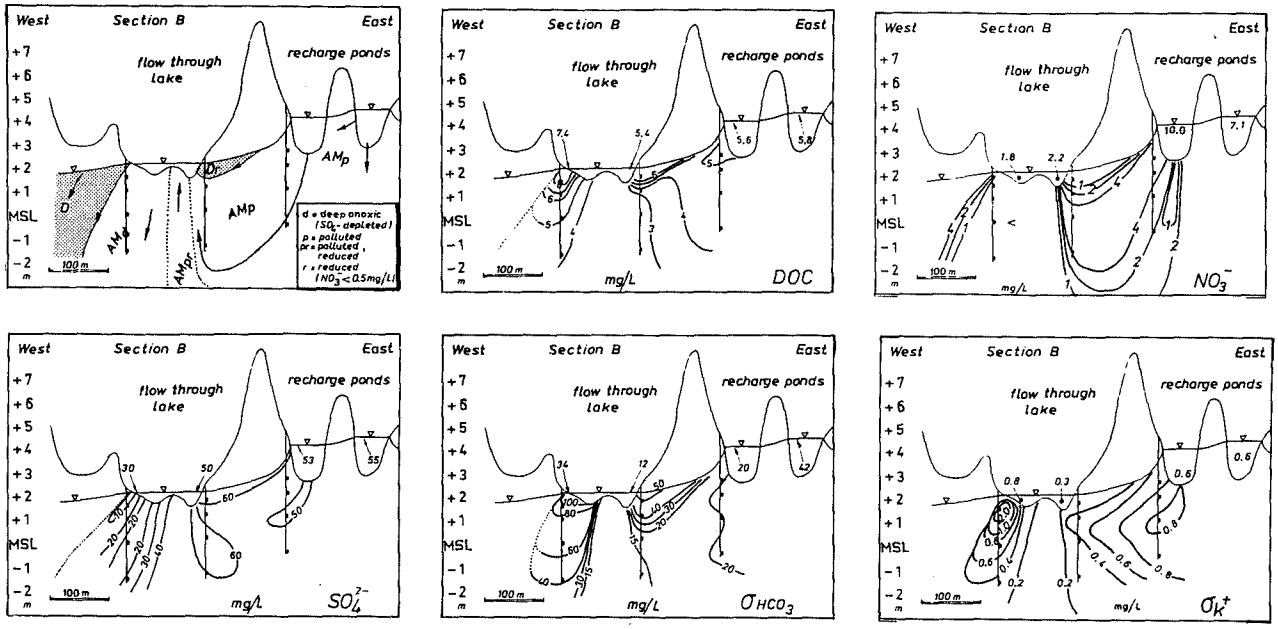

FIG. 4.31 Areal distribution of hydrosomes (AM = recharged Meuse; D = Dune) and their facies, mean concentrations of Dissolved Organic Carbon, nitrate and sulphate, and seasonal fluctuations of HCO_3^- and K^+ concentrations (expressed as the standard deviation σ from the annual mean), in cross section B of Fig.3.50 during the year 1985.

lakes (Londo, 1966; Van Dijk, 1984), and the high accumulation rate of sludges mainly composed of organic matter, at the bottom of these lakes (Fig.4.32A).

However, also large, (semi)permanent flow-through lakes without any influence of artificial recharge will yield a high flux of nutrients, because of their hydrological short-circuiting (section 3.10.3). They will also act as an oasis for animals, that forage elsewhere and create an additional input of nutrients by their excrements. And sufficiently deep flow lines, that exfiltrate in these lakes, may pass geological formations with decomposing organic matter and soluble diatom skeletons, and thereby add to a significant natural PO_4^{3-}, NH_4^+ and SiO_2 supply.

The latter statement clarifies that wet dune slacks in areas affected by artificial recharge cannot return to their original mesotrophic or slightly eutrophic state, solely by further pretreatment of surface waters to be infiltrated and the removal of sludges from spreading ponds and flow-through lakes. Also the hydraulic gradient must be reduced, which will decrease the flux and the depth of the deepest flow lines drained.

4.7 Local application to a moist dune slack

And finally, the HYFA was applied on a local scale to the moist dune slack "Reggers Sandervlak", about 5 km to the south of Egmond aan Zee (Fig.3.1). This valley experienced a drawdown of the phreatic level to about 1 m below ground surface for various reasons (Stuyfzand & Moberts, 1987a), and a return to moist conditions since the 1980s due to the combination of a reduced pumping of dune groundwater since 1958 and relatively wet years since 1976.

Instead of the pollution index, the water quality index phosphate was used also here, because of more relevancy in this hydro-ecological study area where eutrophication is of major concern. In contrast to the flow-through lakes discussed above, artificial recharge has no direct influence on this area. The mean spatial distribution of hydrosomes and their hydrochemical facies is shown in a cross section perpendicular to the shoreline and parallel to groundwater flow (Fig.4.33). Discussion is limited to the different facies of the dune hydrosome to a depth of 2 m-MSL.

FIG. 4.32 An impression of some aspects typical for flow-through dune lakes close to spreading ponds in the Boerendel area (for location see Fig.3.1) during low water levels (in 1991) : A = a 15 cm thick bottom sludge, composed of about 50% organic matter; B = 0.6 m loss of hydraulic head in the groundwater release zone, due to clogging of the lake bottom; C = exfiltration of anoxic, recharged polder water with oxidation of Fe^{2+} to a brownish precipitate of $Fe(OH)_3$; D = black iron monosulphide (probably hydrotroillite) in dune sand along the shore of lake 2H22, testifying of sulphate reduction.

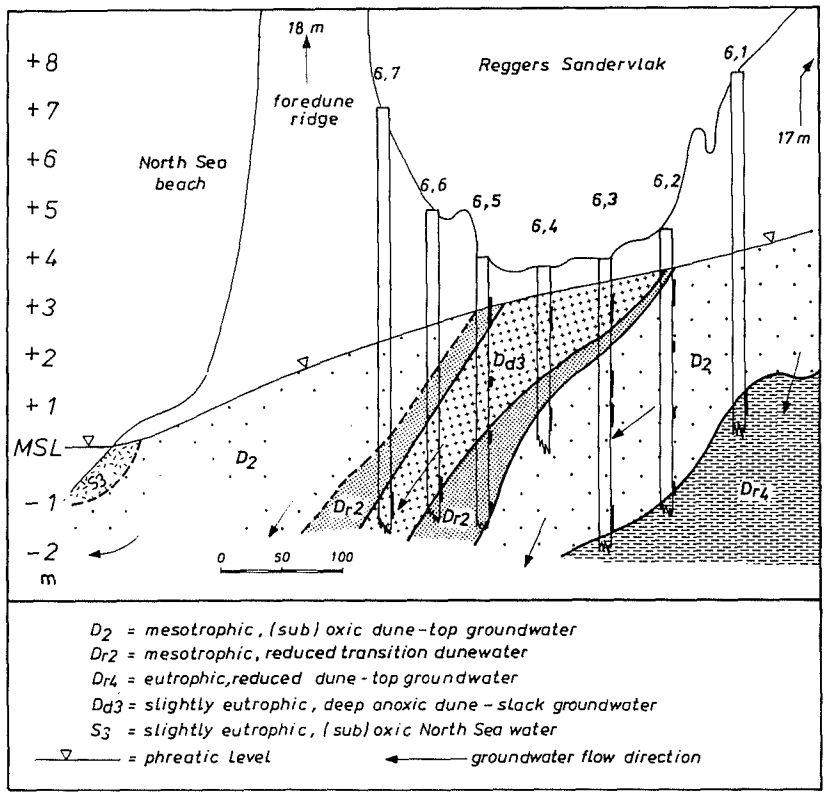

FIG. 4.33 Cross section over the moist dune slack "Reggers Sandervlak", 5 km to the south of Egmond aan Zee (see Fig.3.1), showing the mean areal distribution of hydrosomes and their hydrochemical facies. Based on 10 surveys in the period October 1984 - September 1985.

From east to west (towards the North Sea), the following facies can be discerned :

(1) shallow dune-top groundwater, showing little interaction with decomposing organic matter, and consequently low DOC (≤ 3 mg/l) and high NO_3^- (≥ 1 mg/l) concentrations. The facies is mesotrophic, (sub)oxic (D_2), calcareous and without base exchange, and associated with the water type F_2CaHCO_3. It extends down to a maximum depth of 2 m-MSL close to the axis of the dune slack, which is oriented parallel to the coastline.

(2) deep dune-top groundwater, showing interaction with decomposing organic matter in the marine sea sands below the dune sand, and consequently with higher PO_4^{3-} concentrations (ca 0.5 mg/l) and without NO_3^-. The facies (D_{r4}) is eutrophic, reduced (anoxic, sulphate-stable), also calcareous and without base exchange, and associated with the water type F_3CaHCO_3. It is found below 0-2 m-MSL up to the western border of the dune slack.

(3) transition water (D_{r2}) between dune-top and dune-valley groundwater. It has a mesotrophic, reduced facies, is calcareous and without base exchange, and combines with the water type F_3CaHCO_3.

(4) dune-valley groundwater, which is characterized by a strong interaction with decomposing organic matter in the valley floor, leading to a high DOC (> 10 mg/l), complete denitrification and significant SO_4^{2-} reduction. The facies thereby becomes slightly eutrophic, deep anoxic (D_{d3}) and is also calcareous and without base exchange, and the water type is F_3CaHCO_3. This water is found at shallow depth in the lower parts of the dune slack and extends to increasing depths downgradient. Uptake by an increasing vegetation cover and the removal of vegetation by mowing, reduce the leaching of phosphate.

(5) about the same transition water as mentioned under 3.

(6) similar dune-top groundwater as described under 1, however with higher concentrations of airborne sea salts due to a shorter distance to the HWL. Consequently, the water type changes from F_2CaHCO_3 to F_2CaMix.

The patterns described above, clearly demonstrate the flow paths below a moist dune slack with a rather dense vegetation cover and with predominance of downward over upward flow on an annual flux basis. The concave, lower boundary of

the dune-valley groundwater corresponds with a decrease of the precipitation excess, from the inland dune top with scanty vegetation cover towards the slack.

Hydro-ecological spinoff
The presence of natural groundwater with higher phosphate levels at relatively shallow depth, forms an additional eutrophication hazard when a flow-through lake would develop upon a further rise of the phreatic level in the area.

The present extension of ruderal plant species in the dune slack (Den Hoed et al., 1987) may relate to : (1) the dying back of the previous dry dune vegetation; (2) relatively strong fluctuations of the phreatic level to which for example reeds are well adapted; and (3) perhaps an increased phosphate deposition by beach sands blown over the foredune ridge, sands to which more algal coatings are attached than in the past, in consequence of eutrophication of the North Sea. Freshly blown sand grains from the foreshore proved to be an essential nitrogen source for marram grass (Fay & Jeffrey, 1992).

4.8 Concluding remarks

Application of the Hydrochemical Facies Analysis to the very complex situation in the coastal area of the Western Netherlands with a well documented palaeohydrological record, revealed interesting hydrochemical patterns and processes and additional hydrological details. The produced maps may satisfy : (a) those who design groundwater monitoring networks and want the strategic positions (downgradient of hydrosome and facies boundaries) and need to know the relevant quality parameters (for instance, the analysis of organic micropollutants and heavy metals in old, deep anoxic dune water is a waste of money for certain); (b) hydrologists looking for the recharge focus areas of semi-confined aquifers, a chemical visualization of flow patterns, and the present stage of evolution of flow systems; (c) hydrochemists interested in modelling and searching for the best flow lines and all relevant processes that must be taken into account; and (d) hydro-ecologists studying natural or anthropogenic changes in flora and fauna, that may be linked to changes in saturation, redox or pollution index, the chemical water type or origin.

The palaeohydrological evolution of the study area is clearly reflected in the actual distribution of hydrosomes and their facies chains. But also the reverse is true, a principle that helps the hydrologist to reconstruct palaeohydrological data where they are scarce. However, the same geochemical memory effects, that render hydrochemistry a valuable tool in the analysis of flow patterns, may spoil a desired verdict on the actual state — expanding, steady or contracting — of a flow system. A freshened facies for instance, may point at either an actual, fresh water intrusion downgradient, or a steady flow system, in which chemical equilibrium lags behind. It may even be relict, when the fresh hydrosome is contracting at some further distance by salt water intrusion. This situation is clearly present along the central, lower face of many dune hydrosomes, where a relict, freshened facies may rest on top of a salinized facies. The latter facies is at least locally also relict, due to a restored fresh water flow after the close down of many pumping wells or the start of artificial recharge.

The low ages of fresh groundwaters and spatial distribution of water types in connection with the geological and anthropogenic evolution of the area, indicate a very dynamic, quickly responding aquifer system, at least in the upper 150 meters. Traces from the Holocene transgression have been preserved as Cl^- inversions within the fresh water lens, only in very heavy clay beds of 10-20 m thick at various levels down to 100 m-MSL. An interesting, fresh dune water reserve is presently accumulating in the south-west corner of the Haarlemmermeer polder near Nieuw Vennep. Basal peat and Velsen clay hamper there the exfiltration of fresh dune water flowing inland. A further salinization of drainage water in deep polders is to be expected especially to the south of the North Sea Canal, where the relict, Holocene transgression waters are less saline and will be substituted for by actual North Sea water of high salinity, which is advancing with a calculated migration velocity of 5-30 m/y. Future research should focus on this salinization and the discrimination between actual North Sea water (<1000 y old) and relict Holocene transgression water of the coastal type (>1000 y old), for instance by using radiocarbon.

Chapter 5

COMPOSITION OF BULK PRECIPITATION

Abstract

Compositional variations of bulk precipitation are demonstrated by carefully synthesizing the results for 93 coastal stations in the study area during the period 1930-1990. Many data from unpublished reports and data files are considered, including original and unpublished data from the famous network used by Leeflang (1938), after careful examination of the materials and methods applied.

The chemical composition is explained by contributions of sea spray (>50% on coastal dunes for Na^+, Cl^-, K^+, Mg^{2+}, B, Li^+ and Sr^{2+} separately), continental mineral aerosols (>50% for Al, Sc, SiO_2, Rb^+, Th and Ti each), biogenic inputs (especially PO_4^{3-} and NH_4^+), and anthropogenic pollution (>50% for most heavy metals, F^-, NO_3^-, NH_4^+, SO_4^{2-} and organic microcontaminants, each).

Spatial variations are dominated by gradients in sea spray deposition perpendicular to the North Sea shoreline, a nationwide northward gradient of diminishing air pollution, and local pollution centres, especially those in the glasshouse district, urban areas and the IJmond. The dune strip within the first km to the high water line, receives additional SO_2 and probably NO_x inputs through mediation of sea spray and calcareous dust.

The record of Cl^-, pH, NO_3^-, NH_4^+ and sea-salt-corrected SO_4^{2-} has been reconstructed for the period since the 1930s. Trends are recognized for NO_3^- and NH_4^+ (increasing), pH (strongly depending on buffering by regional dust supplies), sea-salt-corrected SO_4^{2-} (increasing till 1970 and decreasing since then) and Cl^- (high in the period 1967-1977). Seasonal variations are discussed using a 10 and 20 years monitoring on the coastal background station "De Kooy" and the coastal station "Monster" in the glasshouse district, respectively. And variations on a smaller time scale are presented, for maritime and continental episodes, dry and wet periods, and during one shower.

5.1 General

A close inspection of the input signal for each hydrosome, including both spatial and temporal variations, constitutes the fourth step in regional chemical surveys of groundwater (Fig.1.7). The most relevant and complicated input signal for this study is the atmospheric deposition, to which this chapter is directed.

Atmospheric deposition significantly contributes to the composition of coastal dune groundwater in three ways : (a) directly by the deposition of sea spray, gases like SO_2 and NO_x, trace elements, organic microcontaminants etc., which are dissolved in infiltrating rain water; (b) indirectly through the supply of acid or acidifying components which stimulate the dissolution of reactive phases from the porous medium; and (c) in a complex way by its profound effect on vegetation, which has a large impact on groundwater quality (section 6.6.3). Atmospheric deposition constitutes an essential source of nutrients to the normally mesotrophic dune vegetations (Van der Valk, 1974) and, on the other hand, regulates growth of salt-intolerant species through its extreme sea spray loads (Boyce, 1954; Sloet van Oldruitenborgh & Heeres, 1969), or strongly reduces the vitality of many species through noxious pollution (for instance ozone, oxides and heavy metals).

The composition of precipitation on a bulk collector is chosen here as a measure of the atmospheric input (for backgrounds see section 5.2.1). Such a gauge is always opened to the atmosphere and therefore collects both precipitation and dry fallout.

The data presented in this chapter derive from the so-called fugitive sources (section 2.3), annual and quarterly reports, literature and own observations in the dunes south of Zandvoort aan Zee. Further details and extensive listings are given by Stuyfzand (1991a).

5.2 Measurement

5.2.1 Bulk precipitation as a fraction of total atmospheric deposition

The measurement of total atmospheric deposition is an extremely complex matter, because there are three phases involved : gases, solid particles and water with dissolved substances. These phases influence one another in dependency of the nature

and exposition of the impacted surface. The collection of precipitation in the open, constitutes an attractive alternative by virtue of relative simplicity of measurement and interpretation. Three generic types of precipitation collectors are commonly used in precipitation chemistry studies (Galloway & Likens, 1978) : bulk (collects precipitation and dry fallout in the same container), wet/dry (automated collectors that collect precipitation separately from dry fallout) and wet-only (collects precipitation exclusively).

All precipitation stations in the Western Netherlands used bulk collectors till April 1988, and most information to date has been collected with this type. The following question therefore becomes highly relevant : "do samples obtained with a bulk collector represent total atmospheric deposition, wet deposition only or neither of the two"?

Results presented in section 6.8.1, reveal that a bulk collector intercepts only 5-15% less sea spray as compared to dunes with a scanty vegetation cover (mosses and low grasses), but on average 50-67% less for ions that are also deposited in a gaseous form (SO_2, NO_x, NH_y, HF). And taller vegetations intercept on average more than twice as much sea spray as a bulk collector. Samples from a bulk collector are therefore considered to comprise the total atmospheric deposition, so far as gaseous contributions can be ignored, on terrains with a vegetation canopy up to approximately 0.1 m above ground. However, for elements that are originally mainly bound to the more insoluble aerosols, like most heavy metals and the heavier polycyclic aromatic hydrocarbons (PAHs), total deposition can only be approached, if any filtration is excluded and suspended matter is completely digested before chemical analysis.

A bulk collector intercepts considerably more in coastal areas than a wet-only collector (section 5.3.1), and consequently is not representative of wet deposition.

5.2.2 Problems

Low concentration levels, long collection periods in order to obtain the volume required for analysis, wrong materials and other pitfalls may have a deleterious effect on the composition of precipitation samples (Ridder et al., 1984). Several problems together with their prophylaxis or symptom abatement are listed in Table 5.1.

Where the results from different networks have to be used for the reconstruction of a time series or for the preparation of isoconcentration maps, as was the case in this study, the various sampling and sample treatment procedures need careful comparison. The most important points of examination are : how often was the funnel cleaned from dust or bird droppings, was there any filtration facility mounted in between funnel and container, was there any addition of acids to the container before insertion, how long was the sampling interval, was there any filtration in the laboratory and how well were the (remaining) particles digested for chemical analysis? Without these insights interpretation becomes futile and the integration of data obtained from differently operating networks hazardous, especially regarding elements that are originally mainly bound to the more insoluble aerosols, like most heavy metals and the heavier PAHs.

TABLE 5.1 Common problems in sampling precipitation for chemical analysis, with their prophylaxis or symptom abatement.

problems	prophylaxis and symptom abatement
accuracy of chemical analysis	indicate required detection limits, send identical samples to different laboratories, add standards, pH-measurement on site.
biodegradation #	add 5 ml H_2SO_4 (pH3), in which $CuSO_4$ has been dissolved (5 g/l), to empty 5 liter-bottle.
bird droppings	apply bird scarer (nylon wires fitted around funnel; model KNMI); clean the funnel thoroughly from droppings if nonetheless hit.
chemical interaction with collector	use inert materials (no rubber, metals, PVC etc.)
congelation	glow-lamp and thermostat.
dissolution of dust particles	short collection period (14d), or prevent dust from entering into container (see ad insects)
dissolution or escape of gases	short collection period (14d), conservation or direct analysis in laboratory.
evaporation from the container	apply waterseal and a short collection period (14d).
growth of algae in container	opaque white sample container protected against daylight, e.g. using the current KNMI-model.
insects	pyrex glass-wool wad in funnel outlet, to be replaced after each sampling; or a 450 μm sieve in bottle-neck.
interception of local dust	rim of funnel at 1.5 m above ground, which should not be bare, but preferentially covered with grass.

= Van Noort (1985).

5.2.3 Monitoring stations

The most important bulk collectors in the coastal area with a regular monitoring of several quality parameters for at least one year, are shown in Fig.5.3. Further information on these 93 stations is given in Stuyfzand (1991a).

The first network satisfying the above conditions, operated in the period 1933-1939 under supervision of Leeflang (1938), with most collectors in the dunes south of Zandvoort aan Zee. The best bulk precipitation network operated in the period 1978-1987 under supervision of the Royal Netherlands Meteorological Institute (KNMI) and National Institute of Public Health (RIVM). The results have been published in annual reports (KNMI-RIVM, 1978-1988). After a few optimizations during the first years most of the errors and problems listed in Table 5.1 were solved.

Many other networks, notably those directed by the National Institute for Drinking Water Supply (RID) and the Netherlands's Waterworks Association (VEWIN; Van de Meent et al., 1984), by TNO (IG-TNO, 1959-1978), Hoogovens (Visser, 1969), the Provincial Water Authority of North Holland (PWS, 1973-1988; Vermeulen, 1977) and VU (south of Zandvoort aan Zee; Stuyfzand, 1991b), yielded valuable data especially on major constituents, notwithstanding minor imperfections as compared to the KNMI/RIVM-network. Some of the materials and methods applied in all above mentioned networks, can be compared in Table 5.2.

5.3 Mean composition

5.3.1 General considerations

The weighted mean annual composition of bulk precipitation is shown in Table 5.3 for several locations less than 10 km distant from the North Sea shore line. Data on other trace elements and several group parameters for organic contaminants are given in Tables 5.4 and 6.16, respectively.

Most concentrations are very high as compared to continental rain of natural background (Table 5.3), due to the high load of air-borne sea salts in consequence of proximity to the North Sea, and due to air pollution. The common water type is g_*NaCl, the redox index 0 (oxic), the pollution index about 3 (moderately polluted), the phosphate level around 2 (mesotrophic) and the calcite saturation index below -6 indicating strong agressivity.

As stated in section 5.2.3, the KNMI-results in Table 5.3 suffer least from sampling errors. The RID-collectors probably yield an overestimation for Cd and Zn due to interaction with the metal rig to which the collector was mounted, and for nutrients due to bird droppings. These interferences are even more pronounced for the DZH-gauges. The PWS-collectors deviate by anomalous concentrations of Fe, Cr and Zn, which is explained by a separate digestion of filtered dust in a so-called Teflon-bomb (200°C, 5 MPa + HNO_3).

Bulk versus wet-only

Bulk deposition can be compared with wet deposi-

TABLE 5.2 Comparison of material and methods for the most important precipitation-chemistry networks before 1988.

	collection period	sampling frequency per year	height of funnel above ground [m]	funnel diameter in cm	material of funnel	protection from daylight	bird scarer	special features (see footnotes)
GW (33-39)	2-3 m	4-5	?	30.6	glass	yes	no	1
IG-TNO	4 w	13	1.2	30.0	glass/PVC	no	no	1
Hoogovens	4 w	13	1.2	30.8	glass	no	no	1
PWS	1d-1m$^{\alpha}$	365-12$^{\alpha}$	1.8	22.6	HD-PE	@	half	2
RID-VEWIN	2 w	24	1.5	22.6	vulcathene	β	yes?	3
KNMI-RIVM	2 w	12	1.5	22.6	HD-PE	yes	yes	4
VU #	2 w	24	1.5	28.5	HD-PE	yes	yes	5

= dune area south of Zandvoort aan Zee, November 1980 - December 1981; α = pH measured in daily samples (was lower than in monthly samples; Vermeulen, 1977); β = for daily samples (pH, NH_4^+, NO_3^-, Na^+ and SO_4^{2-}) in black painted bottle; 1 = samples were probably filtrated in the laboratory, no sieve in funnel; 2 = no sieve in funnel, filtration of monthly samples (Cl^-, F^-, Na^+, Ca^{2+}, heavy metals) in laboratory ECN, addition of 40 cc 65% HNO_3 p.a. to container before insertion (thereby suspended Cd, Cu and Pb will dissolve for >95%), and digestion of residue in tephlon-bomb (HNO_3, 200°C, 50 atm.) for Cr, Fe, V and Zn; 3 = container daily emptied in other container kept in refrigerator at 4°C, no information on filtration, probably performed in RID-laboratory, probably without additional digestion of suspended matter; 4 = 450 μm sieve in funnel, conservation of samples in dark at 4°C, addition of 30 cc 0.2 M $HClO_4$ to a separate container for heavy metals before insertion, filtration in laboration over 250 μm PE-filter, before analysis $HClO_4$ is adjusted to 0.2 M; 5 = glass-wool wad in funnel, filtration and acidification in laboratory for part of sample to be analysed on metals.

TABLE 5.3 Survey of the weighted mean annual composition of bulk precipitation on the coastal (dune) area of the Western Netherlands. X^* = sea-salt-corrected concentration of X, using Eq.5.7 and Table 5.5.

parameter		Leiduin					De Kooy	Bergen	Castricum	Wijk a/Zee	Scheveningen	Kolhorn	Beverwijk	natural background	
	unit				bulk	wet-only									
no. station (Fig.5.3)		53	8	3	3	3	2	5	6	7	9	12	18	cont.[C]	mar.[M]
period	(+1900)	37-39	79-81	83-87	88-89	88-89	83-87	79-81	79-81	79-81	79-81	79-81	79-81		
network		GW	RID	KNMI	KNMI	KNMI	KNMI	RID	RID	RID	DZH	PWS	PWS		
samples	(n)	14	72	60	24	24	60	70	72	71	26	36	36	-	-
dist. HWL	m	5610	5850	5850	5850	5850	4750	3620	2000	900	360	14800	5950	>6E+5	0
P-chem	mm/y	803	822	813	-	-	692	930	898	979	584	861	853	-	-
P-meteo	mm/y	866	880	838	788	788	832	888	927	895	894	-	-	800	800
EC 20°C	µS/cm	39	65	50	62	48	66	63	66	112	356	-	-	-	-
Cl^-	mg/l	6.6	7.8	7.1	10.0	6.9	11.8	9.6	10.7	23.0	80.7	9.8	9.9	0.1	7.4
SO_4^{2-}	mg/l	5.5	6.0	4.8	5.5	4.3	5.4	6.5	7.1	9.7	21.8	6.6	9.0	0.4	1.3
NO_3^-	mg/l	0.1	3.2	2.8	3.3	2.5	3.3	3.4	3.5	4.0	10.3	4.1	5.5	0.1	≤0.1
HCO_3^-	mg/l	2.8	0	0	0	0	0	0	0	0	28.5	0	0	0.1@	0.1@
PO_4^{3-}	mg/l	-	0.09	0.02	0.03	0.02	0.02	0.20	0.16	0.10	1.46	-	-	≤0.02	≤0.02
F^-	µg/l	-	-	24	31	17	27	-	-	158	83	48	69	<10	<10
pH		4.8	4.27	4.45	4.48	4.46	4.48	4.38	4.45	4.42	5.00	4.28	4.1	5.3@	5.3@
Na^+	mg/l	2.8	4.1	3.9	5.6	3.9	6.6	5.5	6.2	12.9	47.8	-	-	0.02	4.1
K^+	mg/l	-	0.31	0.22	0.33	0.23	0.31	0.37	0.42	0.72	3.1			0.02	0.14
Ca^{2+}	mg/l	1.7	0.9	0.6	0.8	0.5	0.7	0.9	1.3	2.0	8.2			<0.01@	0.15@
Mg^{2+}	mg/l	1.4#	0.6	0.5	0.6	0.45	0.8	0.7	0.8	1.7	5.5			<0.01	0.47
NH_4^+	mg/l	0.51	1.12	1.12	1.24	0.92	1.40	1.44	1.25	1.43	3.38	-	-	0.02	0.04
Fe	mg/l	<0.02	0.07	0.13	0.12	0.05	0.11	0.04	0.05	0.12	0.56	0.29	0.60	<0.02	<0.02
Mn	µg/l	<30	20	10	8	4	5	20	30	50	40	-	-	<4	<4
As	µg/l	-	1.3	-	-	-	<0.8	0.8	1.3	0.8	3.9	-	-	<0.8	<0.8
Cd	µg/l		0.25	0.11	0.11	0.17	0.11	0.3	0.7	0.44	2.28	0.51	0.57	<0.1	<0.1
Cr	µg/l		0.4	-	-	-	0.7	1.3	0.5	0.3	2.3	1.1	2.4	<0.3	<0.3
Cu	µg/l		14.5	5.1	4.0	2.9	3.2	8.2	12.1	8.0	9.6	6.6	10.2	<3	<3
Ni	µg/l		1.9	1.2	0.65	0.49	0.6	1.2	1.3	1.6	6.0	-	-	<0.5	<0.5
Pb	µg/l		17.1	12.4	9.1	8.1	10.4	14.0	15.0	19.2	28.9	22.4	42.1	<8	<8
V	µg/l		-	3.1	2.1	1.6	2.0	-	-	-	-	-	-	<1.6	<1.6
Zn	µg/l	-	50	16	-	-	15	87	60	101	718	128	138	<15	<15
COD	mg/l	-	5.3				-	4.8	4.8	4.9	11.3			-	
DOC	mg/l	-	1.6	-	-	-	1.4	1.7	1.7	1.6	5.6	-	-	-	-
SO_4^*	mg/l	4.6	4.9	3.8	4.1	3.4	3.8	5.2	5.6	6.5	10.5	5.2	7.6	≤0.3	0.3
Na^*	mg/l	-0.9	-0.2	-0.1	0.1	0.0	-0.1	0.2	0.3	0.1	2.9	-	-	-0.1	+0.1
K^*	mg/l	-	0.15	0.07	0.12	0.09	0.07	0.17	0.20	0.25	1.44			0.0	0.0
Ca^*	mg/l	1.6	0.7	0.5	0.6	0.34	0.5	0.7	1.1	1.5	6.5			<0.01	0.0
Mg^*	mg/l	1.0#	0.1	0.0	-0.1	-0.0	0.0	0.1	0.1	0.2	0.1	-	-	0.0	0.0

GW = Gemeentewaterleidingen Amsterdam, calculated from original data; RID = Rijks Instituut voor Drinkwatervoorziening, calculated from screened data in Van de Meent et al., 1984; KNMI = Kon. Ned. Meteorologisch Instituut, calculated from data in KNMI-RIVM (1983-1987); DZH = Duinwaterbedrijf Zuid-Holland, calculated from data files; # : probably too high by analytical problems; C, M = resp. continental and maritime, both based on data in Galloway et al. (1982), Vong (1990), Hicks & Artz (1992) and this study, assuming negligible contributions from calcareous dust; @ = higher in areas receiving calcareous dust; P-chem, P-meteo = gross precipitation on collector 1.5-1.8 m and 0 m above surface, resp.

tion on the station Leiduin (Table 5.3). We deduce that a coastal background, bulk collector at 6 km from the High Water Line of the North Sea (HWL) intercepts about 45% more sea spray constituents (Na^+, Cl^-, K^+, Mg^{2+}), 30% more anthropogenic gases (SO_4^{2-}, NH_4^+ and NO_3^-), and 66-173% more regional dust (Ca^{2+}, Fe, Mn). This agrees fairly well with observations by Ridder et al. (1984) close to De Bilt (about 45 km to the east). Proximity of the North Sea yielded more dry deposited sea spray at Leiduin (45 as compared to 25% for De Bilt).

Total versus dissolved

Bulk precipitation was collected on station Petten (No.43 in Fig.5.3) in the period July 1974 through June 1976 by Cambray et al. (1979), and analysed on total and dissolved concentrations of trace elements and chloride. Their results (Table 5.4) permit to discern groups on the basis of the percentage in solution (not bound to suspended matter) : (a) the little hydrophylic group with ≤ 33% dissolved, composed of Al, Fe, Sc and Th; (2) the moderately hydrophylic group with 33-67% dissolved, represented by Ce, Co, Cr, Cs, Sb and Zn; and (3) the hydrophylic group with ≥ 67% dissolved, made up of Br^-, Cl^-, Cu, Mn, Ni, Pb, Rb^+, Se and V. Note that the latter group considerably deviates from the hydrophylic group in Table 1.1, as defined on the basis of Perelman's migration coefficient relating to ocean water. The difference is mainly connected with the low pH of rain water, which raises the mobility of most TEs.

TABLE 5.4 Survey of weighted mean annual concentrations of trace elements in bulk precipitation (with and without filtration), in air, upon congruent dissolution of either clay in The Netherlands or the average soil on earth (both in aqua dest. to Al = 100 µg/l), and in ocean water diluted to Cl^- = 19.3 mg/l.

	Petten (station 43)			De Kooy[C]	Coastal	dissolved	dissolved	diluted
	total[A]	dissolved[A]	air[B]	(station 2)	dunes	clay[D]	dust[U]	seawater[E]
	µg/l	µg/l	ng/m³	µg/l	µg/l	µg/l	µg/l	µg/l
Cl^-	48,000	48,000	3,360	11,800	-		0.1	19,300
Ag	-	<0.05	-	-	<0.05[F]	-	1.4E-4	2.9E-4
Al	530	<94	200	99	88[K]	100	100	0.005
As	<4	<3.6	4.8	<0.8	-	0.04	0.007	0.003
B	-	-	54[S]	<5	-	-	0.014	4.6
Ba^{2+}			8[S]	3	<12[K]	0.7	0.7	0.03
Be	-	-	0.04[S]	-	<0.02[P]	-	0.008	6.E-7
Br^-	155	150	78	(47)	-		0.007	66
Cd	-	<1.8	1.0[R]	0.11		-	7.0E-4	1.1E-4
Ce	0.83	0.31	0.23	-		0.14[I]	0.07	5.2E-6
Co	0.56	0.34	0.30	<0.9		0.04	0.011	1.0E-4
Cr	3.7	1.2	4.0	0.7		0.31	0.28	2.0E-4
Cs	0.18	0.09	0.21	-		0.04	0.007	3.0E-4
Cu	24.0	16.5	<8	3.2	-	-	0.03	9.0E-4
Eu	-	-	-	-	0.02[F]	0.003	0.002	1.3E-7
F^-	-	-	71[S]	27	32[K]	-	0.28	1.3
Fe	600	98	375	110	77[K]	48	53	0.002
Hg	-	-	0.6[R]	0.04	-	-	1.4E-5	3.0E-5
I			-	-	4.0[G]		0.007	0.06
In			-		≤0.01[T]	-	1.4E-4	1.0E-4
La			0.5[R]		1.39[T]	0.077	0.056	1.2E-5
Li^+	-	-	-	-	≤0.6[K]	-	0.042	0.17
Mn	30	24	18.7	5	21[K]		1.2	4.0E-4
Mo	-	-	0.8[R]	-	-		0.003	0.01
Ni	6.7	6.6	9.4	0.6		-	0.06	7.0E-4
Pb	31	24	124	10.4	-	0.3[I]	0.014	3.0E-5
Rb^+	<5	<3.6	<9	-	≤0.5[K]	0.4	0.14	0.12
Sb	1.55	0.89	3.2		0.3[F]	0.002	0.001	3.0E-4
Sc	0.23	0.038	0.054	-	0.006[T]	0.04	0.01	7.0E-7
Se	0.69	0.50	1.24	<0.16	-	-	1.4E-5	9.0E-5
SiO_2	-	-	850[R]	-	170[K]	79-963[M]	990	6.2
Sm			-		0.06[T]	0.014	0.008	4.5E-7
Sr^{2+}	-	-	2[S]		-	-	0.42	8.0
Th	0.13	<0.03	0.041	-	<0.1[F]	0.05	0.008	4.0E-7
Ti	-	-	<20[R]	3.8	-	6.5[I]	6.45	0.001
U	-	-	-	-	0.02	-	0.0014	0.003
V	7.4	5.0	11.6	2.0	-	0.2[I]	0.14	0.002
Zn	85	29	97	15	-	0.6[I]	0.07	0.002

A = Cambray et al. (1979); B = Peirson et al. (1974); C = 1983-1987 (KNMI,1983-1987); D = calculated from analyses on dutch clay samples, by dr. H.A. Van der Sloot (ECN); E = calculated from mean ocean water in Riley & Skirrow (1975); F = Conrads & Buijsman (1973); G = Heymann, 1927; H = Luten, 1977; I = Stuyfzand (1983); K = Stuyfzand (1991); M = soluble (79) - bound (963); N = Van Aalst et al. (1983), p.44; P = Van Puffelen (1986); R = calculated from data in Diederen & Guicherit (1981); S = Van Jaarsveld & Onderlinden (1986); T = Navarre et al. (1980); U = average composition of soil material on earth according to Rahn (1975).

Acidity, acid buffering and potential acidity

The following calculations show that anthropogenic NO_x gases and sulphur species (mainly SO_2 gas) contribute for about 40 and 60% respectively to the high acidity of most rain waters. And also that NH_3, which is largely derived from animal manure, and Ca^{2+} (from calcareous dust) are the most important neutralizing compounds (75 and 25%, respectively). They buffer about 75% of the acidity. As a matter of fact, electroneutrality is required both for the strongly acid rain water as a whole and for its dissolved sea salts, yielding respectively :

$$Cl^- + 2\ SO_4^{2-} + NO_3^- + F^- = H^+ + Na^+ + K^+ + NH_4^+ + 2\ Ca^{2+} + 2\ Mg^{2+} \qquad (5.1)$$

$$Cl_m^- + 2\ SO_{4m}^{2-} = Na_m^+ + K_m^+ + 2\ Ca_m^{2+} + 2\ Mg_m^{2+} \qquad (5.2)$$

with all concentrations in mol/l and X_m = concentration of X in dissolved, marine salts.

Subtraction of Eq.5.2 from Eq.5.1, assuming all Cl^- to be derived from sea spray ($Cl^- = Cl_m$) and substituting X^* for $X - X_m$, yields (in mol/l):

$$2\ SO_4^* + NO_3^- + F^- = H^+ + Na^* + K^* + NH_4^+ + 2\ Ca^* + 2\ Mg^* \qquad (5.3)$$

As the concentrations for F^-, Na^*, K^* and Mg^* can generally be ignored in the coastal dunes (Table 5.3), a rearranged Eq.5.3 reduces to :

$$H^+ = 2\ SO_4^* + NO_3^- - NH_4^+ - 2\ Ca^* \qquad (5.4)$$

Expressed in words, the acidity of bulk precipitation is equal to the concentration of sulphuric and nitric acid minus the concentration of the neutralizing substances ammonia and calcium carbonate. Inserting the data for Leiduin and De Kooy in the period 1983-1987 yields the conclusion stated above, which agrees with similar calculations by Asman et al. (1981).

The potential acidity of rain water (H^+_{pot}) is raised by a possible nitrification of ammonium :

$$NH_4^+ + 2O_2 \rightarrow NO_3^- + 2H^+ + H_2O \qquad (5.5)$$

Assuming 100% nitrification, yields (in mol/l) :

$$H^+_{pot} = 2\ SO_4^* + NO_3^- + NH_4^+ - 2\ Ca^* \qquad (5.6)$$

The potential acidity of bulk precipitation at Leiduin was, in 1979-1981 and 1988-1989, 1590 and 1420 mol H^+ ha^{-1} y^{-1}, respectively. The mean contributions of SO_x, NO_x and NH_x to the potential acidity for Leiduin and De Kooy are 40, 25 and 35%, respectively. The neutralization of this acidity by constituents dissolved in rain water, reduces to only 12%.

Mean contributions of sea spray, continental mineral aerosols, biogenic matter and anthropogenic pollution to the composition of bulk precipitation in the period 1979-1987, are discussed below.

5.3.2 *Sea spray contribution*

It is common practice to correct concentrations of Na^+, K^+, Ca^{2+}, Mg^{2+} and SO_4^{2-} in precipitation for a contribution of sea spray, in order to quantify the non-marine part of dissolved constituents or more specifically, the anthropogenic pollution levels (Asman et al., 1981). Although Na^+ is commonly preferred as a tracer of sea spray, being considered without other contributions, Cl^- is chosen here. The reason is, that vulcanic and anthropogenic emissions have a negligible effect on the high Cl^- levels in bulk precipitation in this coastal area (Vermeulen, 1977), and that Na^+ behaves nonconservatively upon subsoil passsage, contrary to Cl^- (see Eq.2.12). Whether the Cl losses from sea salt particles due to pH-lowering reactions (Möller, 1990) are nicely balanced by Cl gains from anthropogenic sources, is unknown. Anyhow, Duce & Hoffman (1976) conclude that the fractionation of the main constituents of sea water during spray formation can be properly ignored.

With this assumption, the correction becomes :

$$X^* = X - \alpha_x Cl^- \qquad (5.7)$$

where X^* = non-marine concentration of constituent X; X = concentration of X measured; Cl^- = chloride content measured; and α_x = (X/Cl^-) in sea water.

Appropriate values for α_x, as calculated from data in Riley & Skirrow (1975) and assuming similarity of coastal North Sea water to mean ocean water, are listed in Table 5.5, both on a mg/l and mol/l basis.

TABLE 5.5 Correction factor α_x in Eq.5.7, in order to correct concentrations of various components for a contribution of sea spray, on either a mg/l or mol/l basis. This factor also applies to groundwater to be corrected for a contribution of mixed ocean water or North Sea water.

mayor/trace constituents	factor mg/l	factor mol/l
Na^+	0.5564	0.8581
K^+	0.0206	0.0187
Ca^{2+}	0.0213	0.0188
Mg^{2+}	0.0668	0.0974
SO_4^{2-}	0.1401	0.0517
B	$2.30 \cdot 10^{-4}$	$7.541 \cdot 10^{-4}$
Br^-	$3.48 \cdot 10^{-3}$	$1.543 \cdot 10^{-3}$
F^-	$7.19 \cdot 10^{-5}$	$1.341 \cdot 10^{-4}$
Li^+	$9.34 \cdot 10^{-6}$	$4.773 \cdot 10^{-5}$
Mo	$5.17 \cdot 10^{-7}$	$1.913 \cdot 10^{-7}$
Rb^+	$6.06 \cdot 10^{-6}$	$2.513 \cdot 10^{-6}$
Sr^{2+}	$4.21 \cdot 10^{-4}$	$1.702 \cdot 10^{-4}$

Results of calculation on annual means are shown in Table 5.3. With the focus on the best data obtained (Leiduin and De Kooy in the period 1983-1987), it is concluded (Fig.5.1) that Na^+ and Mg^{2+} originate exclusively from sea spray, Cl^- for >97%, K^+ for about 70%, Ca^{2+} for 30% and SO_4^{2-} roughly for 25% , at about 5 km from the HWL, in areas relatively remote from industrial emission centres. Obviously a shorter distance to the HWL and a longer distance to the industrial areas should raise the maritime contributions for Cl^-, K^+, Ca^{2+} and SO_4^{2-} significantly (section 5.4).

Trace elements in bulk precipitation with a significant maritime contribution probably are (Fig.5.1) : B (>54%), Br^- (80%), Li^+ (>28%), Mo (>10%), Rb^+ (≥20%) and Sr^{2+} (80%). Algal biomass in sea spray may contribute significantly to concentrations of organic carbon, I_{total}, NO_3^-, NH_4^+, PO_4^{3-}, and organic N and P.

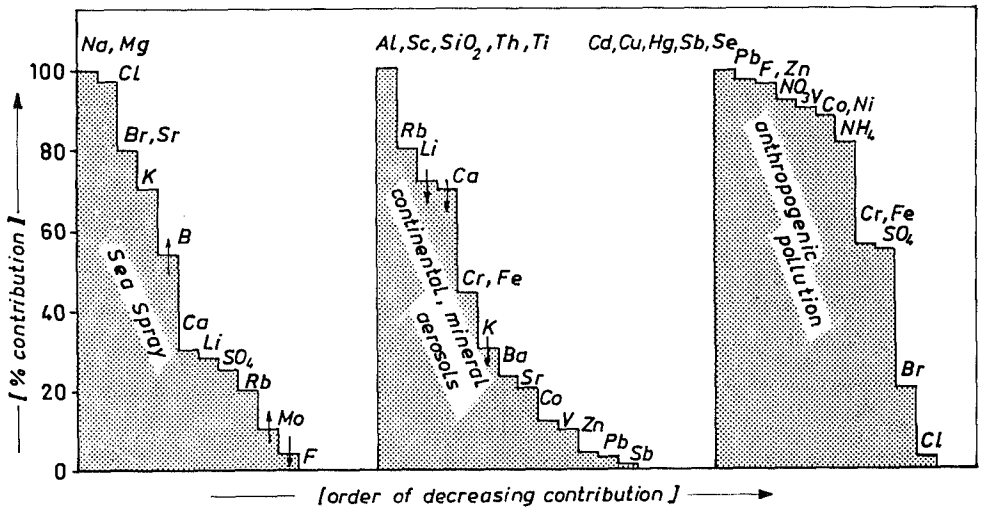

FIG. 5.1 Mean annual contribution of sea spray, continental mineral aerosols and anthropogenic pollution to several main constituents of and trace elements in bulk precipitation, in the Western Netherlands at about 5 km from the high water line of the North Sea and relatively remote from industrial centres. Constituents with a contribution ≥1% have been plotted exclusively. ↑ , ↓ = plotted contribution to be considered as a lower and upper limit, respectively.

5.3.3 Continental, mineral aerosols

Aluminium, SiO_2 or Sc are generally considered as the best suitable indicator of mineral aerosols derived from the continents as a result of the weathering of rock and the erosion of soils (Rahn, 1975; Cambray et al., 1979; Arimoto & Duce, 1987). It is thereby assumed that those dust particles congruently dissolve in precipitation and in any acids added. Al-Si-Sc ratios in bulk precipitation near Petten (Table 5.4) and south of Zandvoort aan Zee (Table 5.6) confirm that Al can also be used alone. The presence of other Al sources, like the combustion of coal and oil (Diederen & Guicherit, 1981) is thus neglected.

Using either the world's average soil composition as a reference, as published by Rahn (1975), or the mean composition of clay in The Netherlands (Table 5.4), we then calculate : a high contribution (>67%) from continental mineral aerosols for Rb^+, Sc, SiO_2, Th, Ti and probably Be and Li^+; an intermediate contribution (33-67%) for Cr and Fe, and probably Ce and Cs as well; and a low contribution (<33%) for Ba^{2+}, Br^-, Cd, Co, Cu, F^-, Hg, I, Mn, Ni, Pb, Sb, Se, Sr^{2+}, V, Zn, most major constituents and probably As, Eu and La (Fig.5.1). These results agree well with those published by Rahn (1975) and Arimoto & Duce (1987).

Another potentially important constituent of continental mineral aerosols, which would remain largely beyond consideration if Al was used as a unique tracer, is limestone ($CaCO_3$). The Ca^*/Ca^{2+} ratio can be conveniently considered as an upper limit for this contribution (70%, Fig.5.1), because other Ca-containing dust sources, both natural (like clay minerals and anorthite) and man-made (cement), cannot be easily separated. A cement industry causes important emissions of Ca containing dust in the IJmond area near the Hoogovens steal production complex, where it clearly buffers the pH of otherwise very acid rain water in this high SO_2 and NO_x emission centre (Fig.5.3). In a way, their vicinity constitutes a beneficial industrial combination indeed!

5.3.4 Biogenic inputs

Biogenic contributions to the composition of bulk precipitation may consist of bird-droppings, insect-droppings, plant and animal debris, marine plankton in sea spray, plant volatiles, micro-organisms, etc.

Rain gauges without a device to keep birds away, probably intercept more bird droppings than their surroundings. This justifies the application of preventive measures and data correction procedures. Asman et al. (1982) studied the desastrous influence of bird-droppings on the chemistry of bulk precipitation. It can be concluded from their results, and from the generally observed low orthophosphate levels in bulk precipitation obtained from gauges with an effective bird-scarer (Buijsman, 1989b), that total PO_4-levels superior to about 0.10 mg/l or orthophosphate concentra-

tions exceeding 0.05 mg/l, are highly suspect of interference with at least one bird-dropping on the equipment, and that phosphate is the most reliable correction parameter for this type of bias.

The correction procedure, as based on data in Asman et al. (1982) and Stuyfzand (1986d : Fig.7.6), becomes for samples with PO_4^{3-} > 0.05 mg/l :

$$X_{cbd} = X - \beta_x \cdot (PO_4^{3-} - 0.05) \qquad (5.8)$$

where X_{cbd}= concentration of constituent X corrected for bird droppings [mg/l]; X = measured concentration of X [mg/l]; PO_4^{3-}= measured orthophosphate content [mg/l]; β_x= correction factor depending on X : β_{NH4}= 3.4; β_{TOC}= 2.9; β_{NO2}= 1.06; β_{SO4}= 0.5; β_{Ca}= 0.45; β_K= 0.41; β_{Na}= 0.32; β_{Cl}= 0.15; and β_{Mg}= 0.08.

Values for β_{NH4} are to be lowered when raised NO_3^- levels point at a partial nitrification. Also pH and HCO_3^- levels are generally raised in consequence of the relatively high lime content of bird droppings, but a correction remains hazardous.

The excellent positive linear relationship between TOC, NH_4^+ and K^* on the one hand and orthophosphate on the other, is illustrated in Fig.5.2, where data mainly from Tabel 5.3 are plotted. Obviously, the collector near Scheveningen, which was situated close to a breeding colony of sea gulls, suffered most from bird droppings, all RID-stations to some extent and none of the KNMI-gauges was affected by virtue of an effective bird-scarer.

Corrected data and data unaffected by bird droppings still contain about 1.4 mg/l organic carbon (TOC), 0.8 mg/l total organic NH_4 (deduced from data in Van Puffelen, 1986), as much organic phosphate as orthophosphate (in between 0.02 and 0.05 mg/l, Van Puffelen, 1986; Buijsman, 1989b) and a maximum of about 2 µg/l organic iodine (Heymann, 1925 and 1927). These amounts are considerable and those of N and P form a significant nutrient input to dune ecosystems. Further investigations into the exact nature of the compounds involved and microscopic examinations are required to trace back their provenance. Also local dust may constitute a significant source, as soil dust generally contains high amounts of nutrients bound to organics (Timperley et al., 1985).

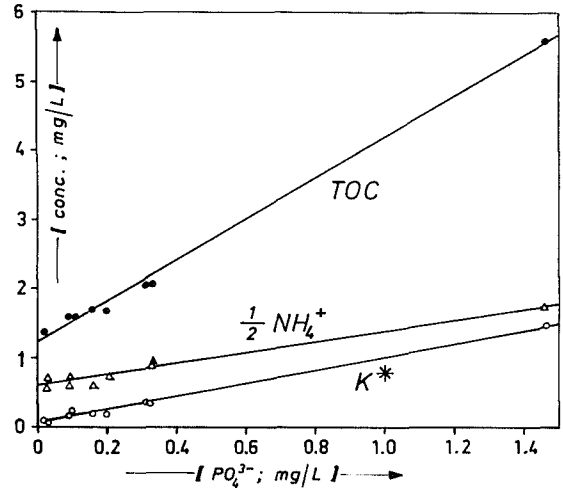

FIG. 5.2 Plot of Total Organic Carbon (TOC), NH_4^+ and K^+ corrected for sea spray (K^*) in mean annual bulk precipitation, versus orthophosphate. PO_4^{3-} is considered, above 0.05 mg/l, as an indicator of interference with bird droppings. Most observations stem from Table 5.3.

5.3.5 *Air pollution*

Sources of man-made atmospheric pollution are nowadays innumerable and their products are trespassing the most desolate corners on earth.

Classical, primary pollutants are carbon monoxide, nitrogen oxides (NO_x), hydrocarbons, sulphur oxides (SO_x) and particulates, which are put into the air mainly by transportation, fuel combustion (stationary), industrial processes and solid waste disposal (Stoker & Seager, 1972). The anomalous ammonia emissions from farm-yard manure in The Netherlands (Van Breemen et al., 1982; Heij & Schneider, 1991) are considered here as an anthropogenic pollution as well.

With the inevitable uncertainties about natural backgrounds for bulk precipitation (Table 5.3) and about the degree of chemical digestion of several trace elements bound to particulates before analysis (notably Cr and Fe), we estimate the contribution of pollution as indicated in Fig.5.1. A high contribution (>67%) is found for many heavy metals (including more elements than indicated in Fig.5.1; Rahn, 1975; Arimoto & Duce, 1987), F^-, NO_3^- and NH_4^+; an intermediate contribution (33-67%) for Cr, Fe and SO_4^{2-}; and a low contribution (<33%) for Br^-, Cl^- and all those constituents, that ranked high in a sea spray and/or continental mineral aerosol contribution (Fig.5.1).

Not shown, but surely having a very high man-made contribution (>90%) are (see also Table 6.16) : halogenated hydrocarbons, giving rise to about 13 µg AOCl/l (Ten Harkel, 1992; Van der Neut, 1992) and about 0.45 µg VOCl/l (KNMI-RIVM, 1981); PAHs with summed concentrations up to 0.53 µg/l (KNMI-RIVM, 1983-1988) and more recently 0.1 µg/l (Ten Harkel, 1992); mono-

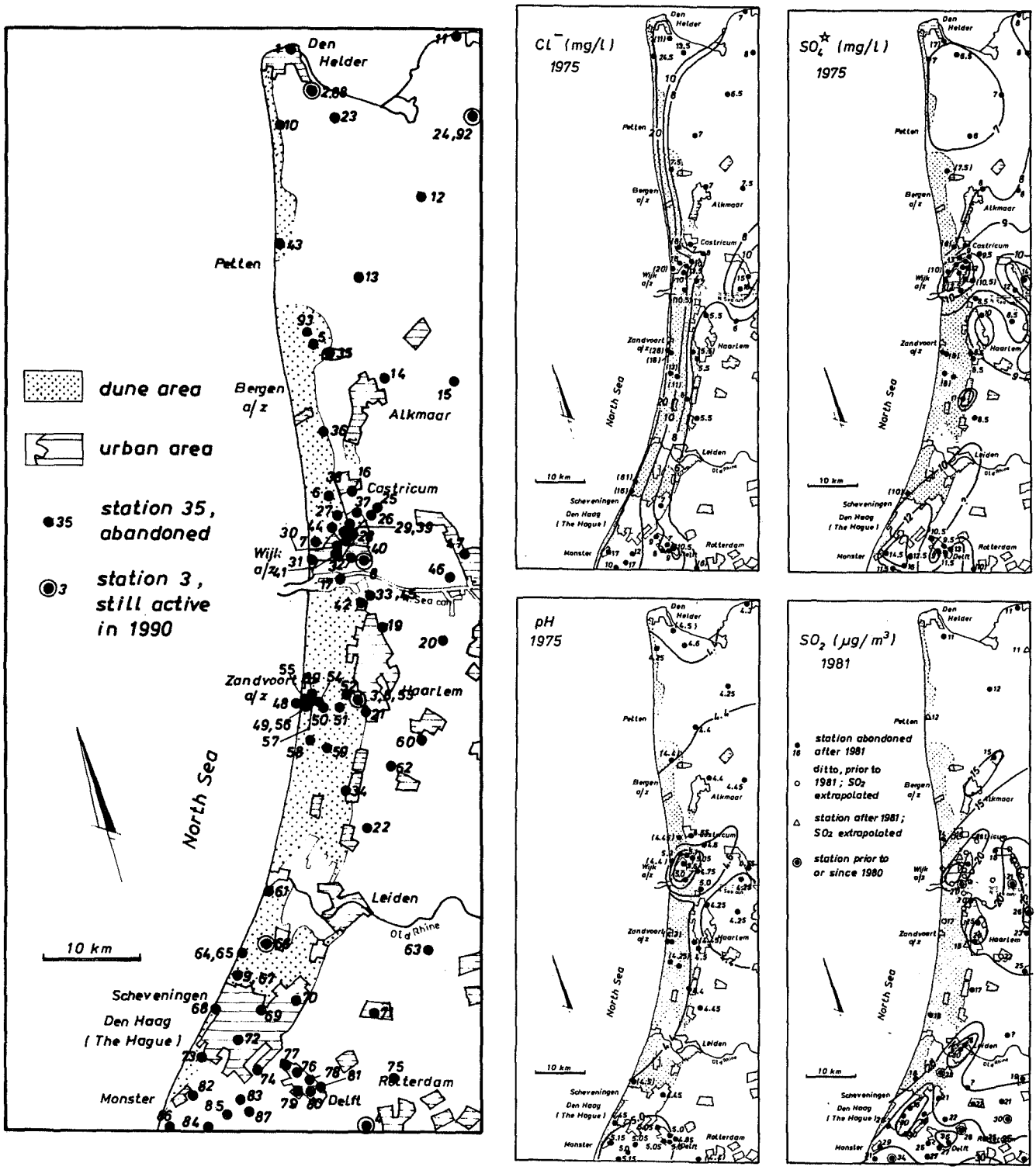

FIG. 5.3 Location map of precipitation-chemistry stations and iso-concentration maps for weighted means of Cl^-, SO_4^{2-} corrected for sea spray (SO_4^*) and pH in bulk precipitation on the coastal area of the Western Netherlands during the year 1975, and for the arithmetic mean of SO_2 gas in the air during the year 1981. Data obtained from stations before or after 1975, by cross correlation, are within brackets.

cyclic aromatics like benzene, toluene and xylenes, generally within 0.01 and 0.06 µg/l (KNMI-RIVM, 1983); and individual pesticides like lindane (γ-HCH) and hexachlorobenzene (Van Puffelen, 1986; KNMI-RIVM, 1979-1988) and atrazine, simazine and bentazon (Van Zoonen et al., 1988), all generally within 0.01 and 0.1 µg/l. Relatively high concentrations of pesticides are expected in the glasshouse district to the south of The Hague, and in flower bulb cultivation areas.

5.4 Spatial variations

5.4.1 Regional patterns

Gradients in sea spray deposition perpendicular to the North Sea shoreline (Leeflang, 1938; Vermeulen, 1977), a nationwide northward gradient in air pollution (KNMI, 1978-1988; RIVM, 1984-1989) and superimposed subregional gradients around industrial zones and cities (Visser, 1969; IG-TNO, 1959-1978; Vermeulen, 1977; Ridder, 1978; Ernst, 1984), dictate most spatial variations in the chemistry of bulk precipitation on the study area.

This can be deduced from Fig.5.3, showing the pattern for annual means of Cl^-, SO_4^* and pH during 1975, a year without exceptional sea spray deposition nor extreme atmospheric pollution (Fig.5.5) and within a period having the highest density of stations scattered over the coastal area of the Western Netherlands.

The use of data from different networks introduced differences in the materials and methods applied. This led to diffulties in comparability of the analytical results, especially regarding : NH_4^+ and NO_3^- due to differences in the prevention of bird droppings and alteration; pH for the above reasons and by differences in the length of the collection period, which has a strong effect on the amount of and exposition time to suspended reactive dust (Vermeulen, 1977; Ridder, 1978); and heavy metals by differences in (a) interaction of precipitation with the collector rig and funnel, (b) filtration and (c) digestion of suspended dust. These troubles have been accounted for as far as possible in constructing the spatial patterns as shown in Fig.5.3.

The SO_4^* pattern closely corresponds with the pattern for arithmetic mean concentrations of SO_2 in the air, even though the latter refers to 1981 (Fig.5.3). This similarity was to be expected for two reasons : SO_4^* is formed from SO_2 by oxidation, and the emission pattern did not change much in the period 1975-1981.

Areas suffering most from atmospheric pollution are : the glasshouse district in the southwest corner, the so-called Zaan region to the north of the North Sea Canal and the surroundings of the Hoogovens industrial complex. The pollution of bulk precipitation is not limited to raised SO_4^* levels, but includes elevated concentrations of among others dust, heavy metals, PAHs, F^- and, as can be deduced from Fig.5.3 and from Ridder (1978), Cl^-. An important source of this anthropogenic Cl^-, is the combustion of plastics. The high pH values (>5) in the glasshouse district and around Hoogovens are related to high dust immissions which neutralize acid rain for >80% .

5.4.2 Gradients perpendicular to the shore line south of Zandvoort aan Zee

The data set published by Leeflang (1938) is considered the best national reference regarding the chemistry of bulk precipitation before the second world war. He considered six rain gauges perpendicular to the North Sea coast line, about 2.5 km south of Zandvoort aan Zee, 0.44, 2.28, 3, 5.6, 48 and 80 km inland, during the period 1933-1937. Materials and methods of his investigation are summarized in Table 5.2.

It was therefore a happy surprise to detect in a mount of dusty papers in the archives of the Municipal Water Supply Co. of Amsterdam, where Leeflang was employed, in addition to all raw data regarding the period 1933-1937, unpublished data for the preceding years 1930-1932 and the subsequent years 1938 and 1939. A listing, elaboration and discussion of these data is given by Stuyfzand (1991a). The years 1938 and 1939 offered an additional monitoring at 0.13 km inland.

The latter data are presented as weighted mean values in Table 5.6, together with results obtained along practically the same section in 1981 and 1982, respectively, reaching 165 km inland. The results of Cl^-, SO_4^*, NO_3^-, NH_4^+, Ca^* and the isotopes ^{18}O and ^3H are plotted versus the distance to the high water line, in Fig.5.4. It is convenient for the discussion to discern two distinct zones, the inland zone behind the inner dune fringe, and the younger coastal dune area.

The inland zone, from 165 to 5.5 km distance to the HWL

Within this zone the following changes are observed in the direction of the HWL (Fig.5.4) : Sea salts (notably Cl^-, Na^+ and Mg^{2+}) increase exponentially, by the gradual settling and wash out of sea spray aerosols in the landward direction, as observed elsewhere (Eriksson, 1952; Bätjer & Kuntze, 1963; Edwards & Claxton, 1964).

The anthropogenic pollutants SO_4^*, NO_3^- (not in 1938-1939) and NH_4^+ decrease, due to the increasing off-wind position with respect to the

TABLE 5.6 Weighted mean annual composition of bulk precipitation as a function of the distance to the North Sea high water line (HWL), for the period 1938-1939 (calculated from unpublished data GW), 1981 and 1982. Differences in sea salt concentrations between the three periods relate to annual variations in storm frequencies and storm characteristics. The NO_3^- and NH_4^+ contents during the years 1981 and 1982 significantly exceed those in the period 1938-1939, due to an increased fuel combustion and production of farm-yard manure, respectively. Differences in sea-salt-corrected concentrations of Na^+ and Mg^{2+} are probably caused by systematic deviations in the analysis of Cl^-, Na^+ and Mg^{2+} in the three laboratories involved (1938-1939 = GW; 1981 = VU; and 1982 = GU). Mg^* of 1938-1939 is probably too high!

		1938-12-22 till 1940-2-9						1981			Feb.1982-Jan.1983			
location/plot		foredune ridge	mosses -1	grasses -2		Lei-duin	Hil-versum	mosses -1	artificial rech area	Lei-duin	dune shrub-1	pines -3	oaks -2	Lei-duin
dist.HWL	m	125	430	2270	2990	5590	48000	340	1000	5850	650	1675	3150	5850
samples	n	9	9	9	9	9	9	24	24	24	12	12	12	24
P-chem	mm/y	817	772	747	824	798	733	795	755	885	790	662	734	705
RE 180°C	mg/l	78	41	29	24	22	16	-	-	-	-	-	-	-
EC 20°C	µS/cm	136	68	48	43	42	31	153	104	61	95	71	67	56
Cl^-	mg/l	29.5	15.3	10.0	7.9	7.1	3.5	38.7	23.5	8.7	19.3	13.9	11.5	7.9
SO_4^{2-}	mg/l	9.1	5.8	5.1	5.3	5.5	5.8	9.2	6.8	5.5	9.1	6.7	6.7	6.5
NO_3^-	mg/l	1.6	0.5	0.3	0.2	0.1	0.1	4.0	4.4	2.8	4.2	3.6	3.6	3.3
HCO_3^-	mg/l	4.5	2.6	2.2	1.9	1.6	1.8	<0.5	<0.5	0.5	<0.5	<0.5	<0.5	<0.5
PO_4^{3-}	mg/l	-	-	-	-	-	-	<0.1	<0.1	0.11	0.04	0.05	0.05	0.20
F^-	µg/l	-	-	-	-	-	-	-	-	-	32	31	34	40
pH		-	-	-	-	4.8#	-	4.22	4.17	4.42	4.23	4.28	4.24	4.30
Na^+	mg/l	14.4	6.7	5.3	3.4	2.9	1.4	20.3	12.0	4.8	10.7	7.7	6.4	4.6
K^+	mg/l	-	-	-	-	-	-	0.86	0.65	0.36	0.66	0.50	0.58	0.29
Ca^{2+}	mg/l	4.5	2.6	2.2	1.9	1.6	1.8	2.1	1.5	0.7	2.1	2.2	1.8	0.8
Mg^{2+}	mg/l	2.7	1.7	1.3	1.4	1.5	1.1	2.5	1.6	0.6	1.8	1.1	0.9	0.6
NH_4^+	mg/l	0.63	0.44	0.42	0.62	0.54	0.61	0.96	0.97	1.05	0.79	0.77	0.91	1.38
SiO_2	mg/l	1.9	1.7	1.6	1.2	0.9	1.3	<1	<1	-	0.19	0.14	0.17	-
Al	µg/l	-	-	-	-	-	-	<200	<200	-	72	101	92	72
Fe	µg/l							<250	<250	50	48	97	87	65
Mn	µg/l							<150	<150	20	16	18	30	26
$\delta^{18}O$	‰	-	-	-	-	-	-	-7.08	-7.14	-7.36	-	-	-	-
colour	mg Pt/l	2.6	2.0	1.9	2.0	1.6	1.6							
COD[a]	mg/l	9.1	5.1	5.1	6.0	4.6	5.8	-	-	-	-	-	-	-
SO_4^*	mg/l	5.0	3.7	3.7	4.2	4.5	5.3	3.8	3.5	4.3	6.4	4.8	5.1	5.4
Na^*	mg/l	-2.0	-1.8	-0.3	-1.0	-1.1	-0.6	-1.2	-1.1	-0.0	-0.0	-0.0	0.0	0.2
K^*	mg/l	-	-	-	-	-	-	0.06	0.17	0.18	0.26	0.21	0.34	0.13
Ca^*	mg/l	3.9	2.3	1.7	1.6	1.8	2.0	1.3	1.0	0.5	1.7	1.9	1.6	0.6
Mg^*	mg/l	0.7	0.7	0.6	0.9	1.0	0.9	-0.1	0.0	0.0	0.5	0.2	0.1	0.1
TIN	µmol/l	61	32	28	38	32	34	118	125	103	112	101	109	130

a = chemical oxygen demand by and expressed as $KMnO_4$; X^* = X corrected for sea salt; TIN = $NH_4^+ + NO_3^- + NO_2^-$; # = deduced from pH/HCO_3^--relations elsewhere (Stuyfzand, 1991a); P-chem = gross annual precipitation on bulk collector for chemical investigation (5-10% underestimated by position of funnel about 1.5 m above ground).

main emission centres of SO_2, NO_x and NH_3, in combination with losses by dry and wet deposition during easterly winds.

Oxygen-18 increases through the preferential raining out of the heavier oxygen isotope from oceanic air masses in the landward direction (Dansgaard, 1964). And tritium decreases by preferential raining out of the heavier hydrogen isotope from continental air masses in the seaward direction (Roether, 1967 cited in Matthess, 1982).

The younger dune zone, from 5.5 to 0 km distance to the HWL

Within this zone the following changes are observed in the direction of the HWL (Fig.5.4) :

Sea salts increase even more rapidly than before, due to a very rapid fall-out of the larger sea spray aerosols within the first 5 km (Rosśknecht et al., 1973). For ^{18}O the continued rise plots as a straight line. Ca^* and SiO_2 increase, probably in connection with a growing contribution of local dust, which contains among others SiO_2 and calcareous shell debris, due to raised wind speeds and a reduced vegetation cover.

NH_4^+ continues to decrease up to 1-1½ km from the HWL and shows little changes beyond that point in 1981-1982, whereas in 1938-1939 an increase occurred. The latter is perhaps connected with the raised organics (as deduced from colour and $KMnO_4$-consumption) in the first few

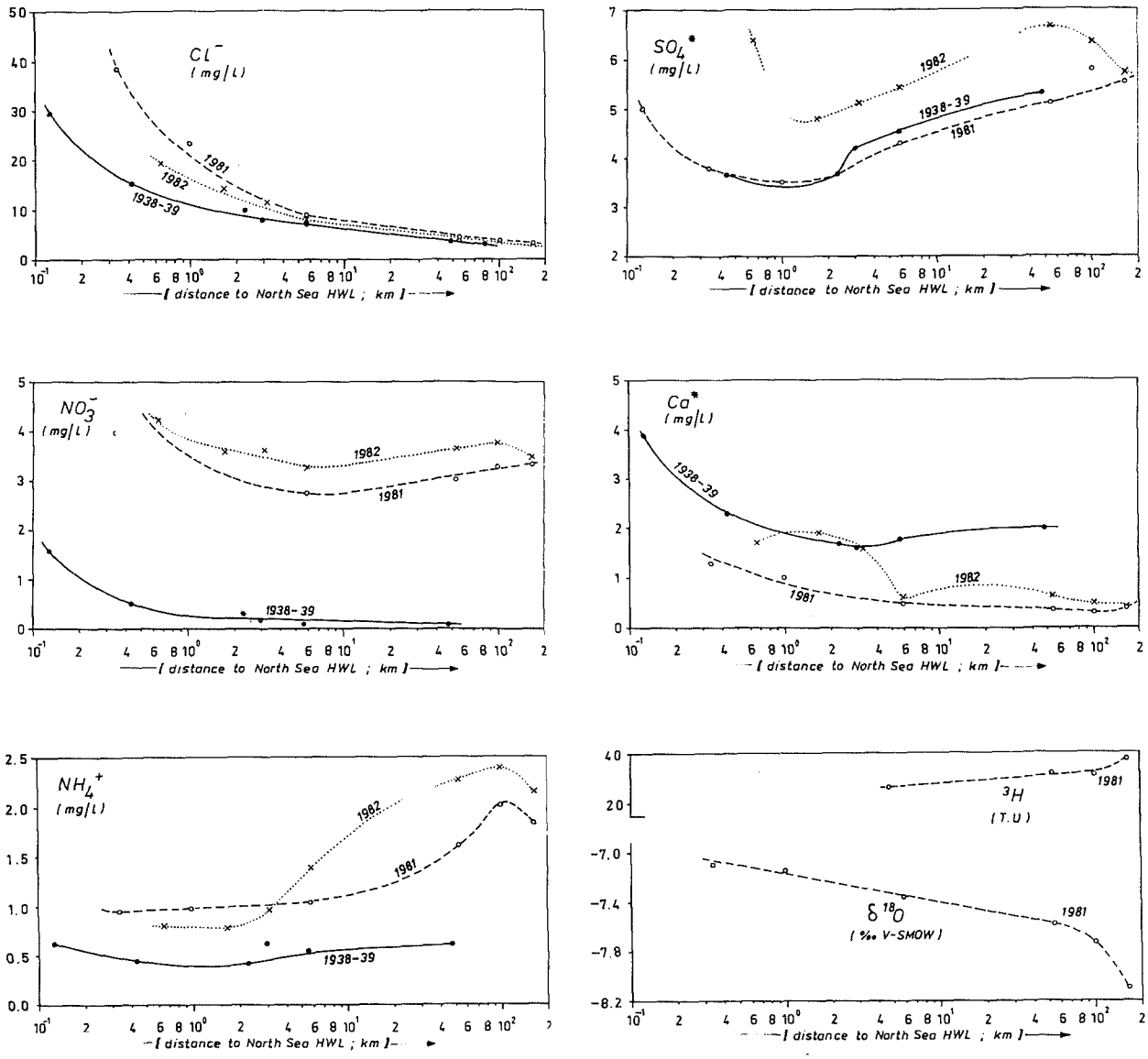

FIG. 5.4 Variation of weighted mean annual composition of bulk precipitation with the distance to the North Sea high water line (HWL), for 1938-1939, 1981 and 1982 respectively (based on data in Table 5.6 and, regarding observations at 53, 100 and 165 km, on KNMI, 1981 and 1982). See also text ad Table 5.6. X = X corrected for sea spray contribution.*

hundreds of metres from the HWL. Marine algae in sea spray or as coatings of sand grains could form the source of the organic material intercepted. Nitrate also increases, which may be related to the combined effects of more interception of organics (see above) and more NO_x sorption to surfaces receiving hygroscopic sea spray and reactive calcareous dust (see below).

SO_4^* continues to decrease up to 1-1½ km from the HWL but increases rapidly upon further approachment. This increase should be seen in relation to the increase of NO_3^-, and has not been previously described to my knowledge. It is explained as the result of an increased sorption of SO_2 and NO_x to an increasingly favourable surface, by virtue of deposited hygroscopic sea salt and calcareous dust. A wetted, reactive surface is indeed known to absorb more atmospheric acid gases (Fowler, 1978). A rapid transformation of these absorbed gases into acids on moist salt surfaces, and the fast consumption of these acids by reaction with calcareous dust, lead to further

absorption, in analogy with the principle of Le Chatelier & Van 't Hoff, formulated in 1888 : "Any external change in volume, temperature or concentration of one of the reacting compounds in a system in equilibrium, is counteracted by that system".

Evidence for this hypothesis is offered by unpublished results obtained with the predecessor of Leeflang's network, consisting of about the same stations but equipped with funnels made of tinned copper. Concentrations of sea-salt-corrected sulphate were much higher than those in precipitation collected with inert funnels, and the discrepancy exhibits a linear positive relation to the Cl^- concentration (Stuyfzand, 1991a).

Representativity

The gradients shown for bulk precipitation south of Zandvoort aan Zee, probably are representative for large parts of the coastal dune area of the Western Netherlands north of The Hague, with the exception of the surroundings of the Hoogovens industrial complex.

It is to be expected, however, that considerable local deviations occur mainly due to differences in wind exposition, as shown by Edwards & Claxton (1964), Randall (1970), Ranwell (1972), Van der Valk (1974) and Veelenturf (1982). An important source of deviations on a larger scale, is the chlorinity of the sea water (Veelenturf, 1982), the altitude of the foredune ridge (Veelenturf, 1982), and the bending of the coastline with respect to the predominant storm direction (Stuyfzand, 1986d). The latter can be corrected for by taking, instead of the shortest distance to the HWL, the distance along this wind direction, which is N260°W for the Western Netherlands according to Van Straaten (1961).

5.5 Variations with time

We consider here subsequently : long-term variations (trends), variations in annual means (exceptional years), seasonal fluctuations as based on monthly means, specific episodes (continental versus maritime, and wet versus dry periods), and variations during one shower.

5.5.1 Trends

Hiatus in the data record and changes in sample locality, methodology of sampling, analytical procedures and sample conservation interfere with the reconstruction of the record of compositional variations of bulk precipitation (Ridder, 1978), from the earliest reliable observations in 1930 to date. Nonetheless an attempt was made for Cl^-, SO_4^*, NO_3^-, NH_4^+ and pH in bulk precipitation on coastal stations (Fig.5.5), by selecting the best data, by data control and by cross correlation to fill up gaps. The changes in SO_4^* are probably parallelled by among others F^-, PAHs and dust, and those for NO_x by Pb and Br^* till 1985 (introduction of unleaded gasoline), as these atmospheric constituents have a common source.

Comparison with the reconstructed changes of the national SO_2, NO_x and NH_3 emissions (Fig.5.6), leads to the following conclusions, when a similar pattern is assumed for NO_x and NH_3 in Western Europe as a whole and a somewhat delayed decrease for SO_2 :

Concentrations of nitrate and ammonium in bulk precipitation increased in the period 1930-1980, more or less in analogy with the NO_x and NH_3 emissions, which are mainly related to fuel combustion and the production of farm-yard manure, respectively. After 1980 their levels seem to have stabilized. Concentrations of SO_4^* increased till 1967 (coal combustion) and gradually decreased afterwards, due to a switch over from coal to natural gas in The Netherlands, and from coal to nuclear power elsewhere. Also developments in exhaust-gas treatment and, according to Sluyter & Olsthoorn (1992) the import of S-poor fuels contributed to the decrease. This agrees with the national SO_2 emissions and with regional SO_2 concentration levels (Fig.5.5, inset SO_4^*). A linear positive relation ($r = 0.95$) was found between annual mean air SO_2 concentration levels and the SO_4^* content of bulk precipitation (Fig.6.39).

Changes in pH correspond best with those for SO_4^*, the Hoogovens industrial area near Beverwijk excluded. The lowest pH values during a period of at least several years, were measured in between 1962 and 1970, when SO_2 emissions culminated (Vermeulen, 1977). The remarkably high pH near Beverwijk is caused by $CaCO_3$-rich dust emissions in the area, which probably diminished in the period 1979-1985. This local anomaly clearly illustrates the influence of an acid buffering dust deposition on the pH of precipitation. The low pH for coastal background stations in the period 1962-1970, therefore not only results from trends in the emission of acidifying gases, but also from trends in the emission of acid buffering aerosoles and gases. The deposition levels of acid buffering fly-ash (generated during coal combustion) probably were high till the late 1960s and since then drastically decreased by a partial switch over first to oil and then to natural gas, in combination with an increasing exhaust-gas treatment.

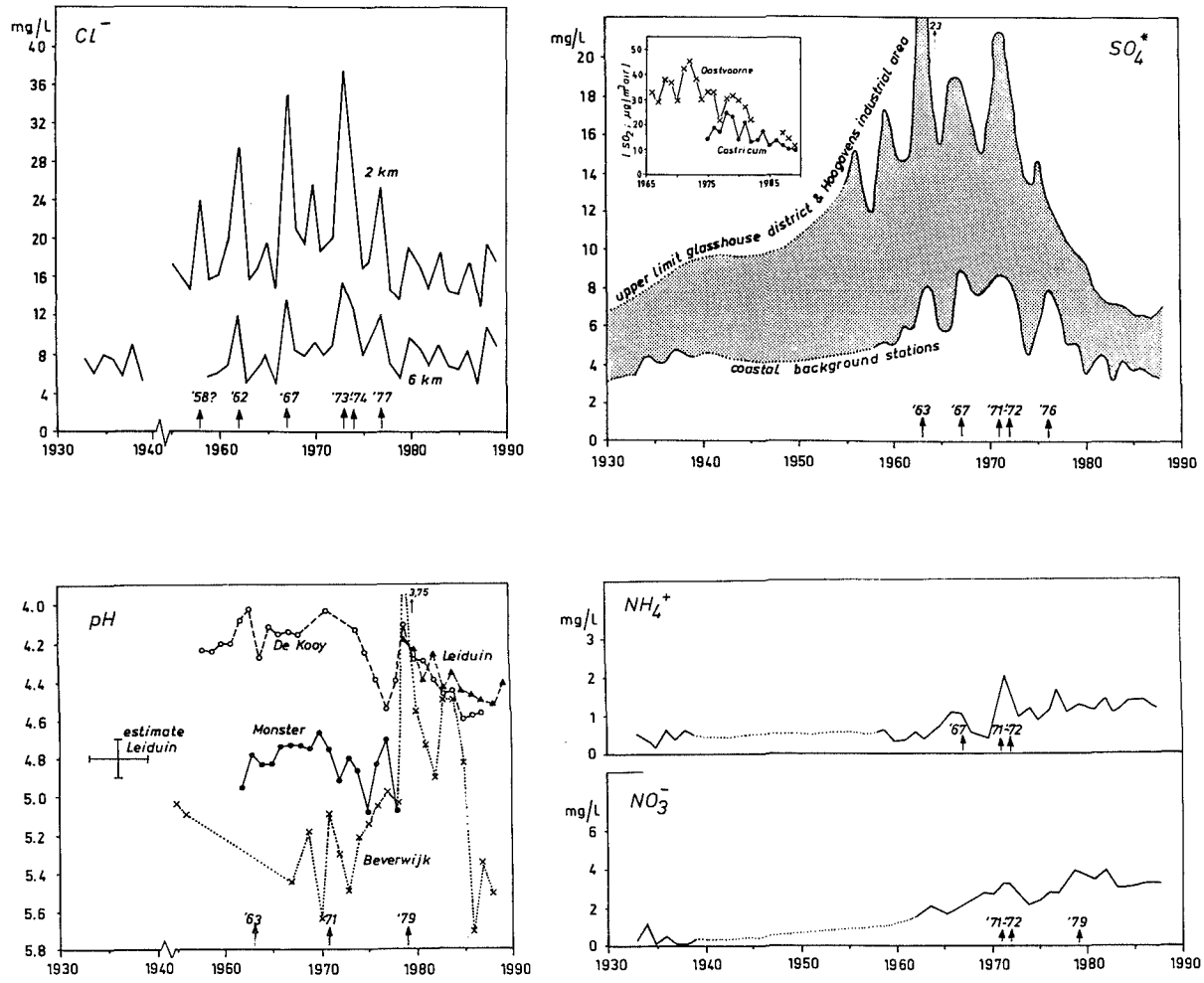

FIG. 5.5 Changes in annual weighted means of Cl^-, SO_4^*, NO_3^-, NH_4^+ and pH in bulk precipitation on the Western Netherlands, during the period 1930-1990. Exceptional years with high concentrations and low pH, are indicated by an arrow. The inset in the SO_4^* graph gives the mean SO_2 concentration in air for two coastal stations.

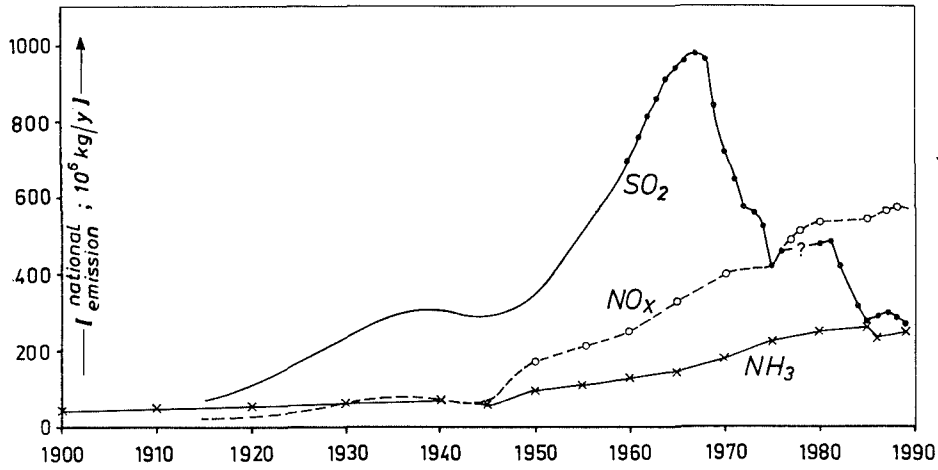

FIG. 5.6 Changes in annual, atmospheric emissions of SO_2, NO_x and NH_3 in The Netherlands, during the period 1910-1990. Based on various sources (see Stuyfzand, 1991a).

However, the steady increase of acid buffering ammonia in the period 1950-1980 (Fig.5.6) counteracted these changes.

A hypothetical trend that cannot be demonstrated by lack of relevant and good data, is composed of an increase of organic PO_4 and NH_4 in connection with the eutrophication of coastal North Sea water. During the formation of sea spray more marine algae could be emitted and beach dust may be loaded with more algal coatings than before. The eutrophication of coastal North Sea water is mainly due to eutrophication of river Rhine and Meuse water, and dredging activities in the sea port of Rotterdam (Van Buuren, 1988; Baan et al., 1991).

Isotopes

The nearest station with a long data record on natural isotopes, is situated in the city of Groningen, about 165 km to the north-east of Zandvoort aan Zee. National distribution patterns of tritium and oxygen-18 reveal that Groningen is sufficiently representative for the study area (Stuyfzand, 1991a).

The record of weighted annual mean concentrations of ^{18}O and activities of ^{3}H since 1965 and 1950 respectively, is shown in Fig.5.7. The $\delta^{18}O$ record is based on Groningen exclusively, whereas the tritium record had to be reconstructed as follows : data before 1958 were derived from Roether (1967, in Matthess, 1982) after correction for a more oceanic position, those for the period 1958-1969 stem from observation station Valentia (Ireland) after multiplication with 2 to account for a more continental position (deduced from Roether, 1967 in Matthess, 1982), those for the period 1970-1972 relate to station Bilthoven about 50 km to the south-west of Zandvoort aan Zee (Mattern & Strackee, 1973), and those after 1972 were measured in Groningen.

Tritium levels in precipitation since 1954 significantly exceed the natural activity of about 5 TU. Since that year the record was dictated mainly by above ground, nuclear weapon tests, which culminated in 1963-1964 and generated tritium, and by a slow exchange between the atmo- and stratosphere. The latter still leaks tritium to the atmosphere since the thermonuclear moratorium in 1964 reduced the number of above ground nuclear explosions significantly (Mook, 1989).

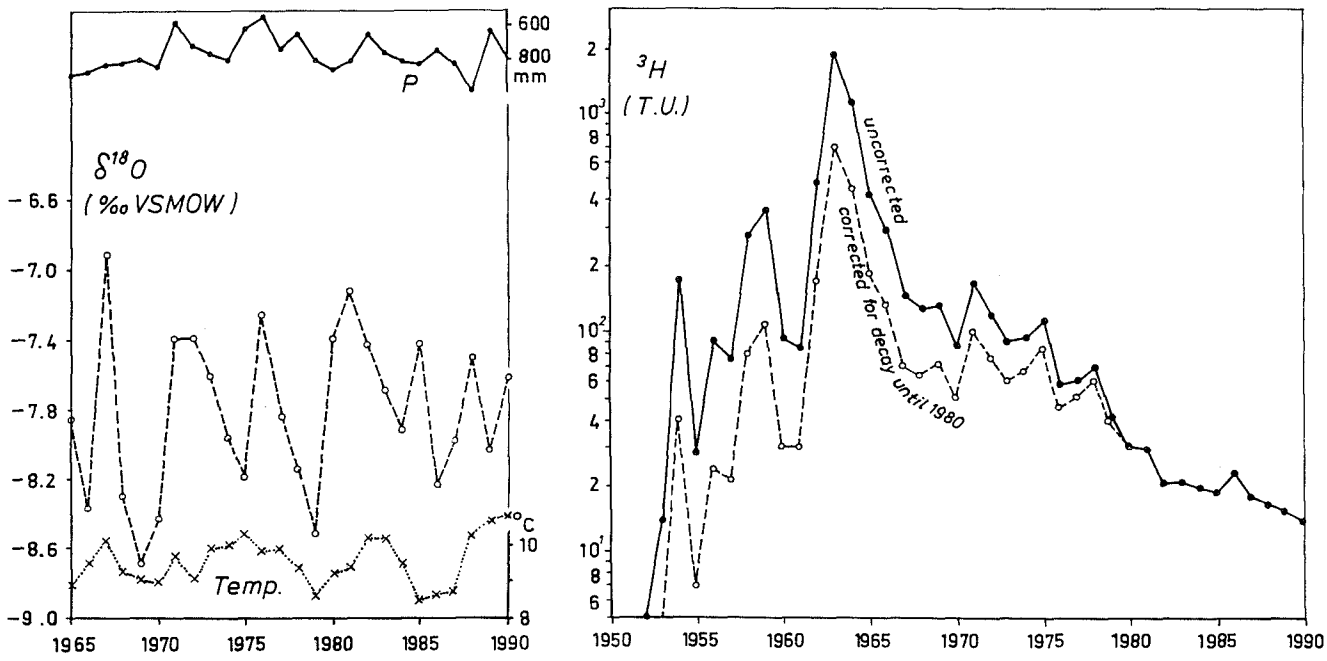

FIG. 5.7 Changes in annual weighted means of oxygen-18 and tritium in bulk precipitation on station Groningen (165 km NW of Zandvoort aan Zee), which is considered representative for the study area. Based on data obtained from the Centre for Isotope Research, University of Groningen (^{18}O and, since 1973 ^{3}H), and various sources regarding ^{3}H before 1973 (see text).

5.5.2 Variations in annual means

Chloride concentrations fluctuated more at random, although the period 1967-1977 can be distinguished from the preceding and following decennium by significantly higher levels (Fig.5.5). High concentrations in bulk precipitation coincide with years subject to a high storm frequency and/or a few exceptional storms, like 1967, 1973, 1974 and probably 1990 (no data yet).

Continental years, with exceptional pollution levels and relatively low Cl^- concentrations were (Fig.5.5) : 1963 (SO_4^* , pH), 1967 (SO_4^* and NH_4^+), 1971 and 1972 (both SO_{4*}^*, NO_3^- and NH_4^+, 1971 also pH), 1976 (SO_4^*) and 1979 (NO_3^-). The year 1979 was relatively wet and 1971, 1972 and 1976 were relatively dry. During most maritime years, with raised Cl^- concentrations, pollution levels were relatively low (1958, 1962, 1973, 1974 and 1977). The wet year 1967 was an exception, being high in both pollution load and Cl^-.

The curve for oxygen-18 seems to correlate in a complex way with annual mean temperature, the amount of precipitation and precipitation chemistry (Fig.5.7). A high temperature, low amount of precipitation and a high load of sea salts appear favourable to high ^{18}O concentrations. This agrees with the oceanic origin and well-known temperature effect (Mook, 1989).

5.5.2 Seasonal fluctuations

Mean seasonal fluctuations in the composition of bulk precipitation are shown in Fig.5.8 for two stations : De Kooy, a coastal background station, during the period 1978-1987 with reduced SO_2 emissions; and Monster, a coastal station in the glasshouse district (south of The Hague) with raised pollution loads, also due to consideration of a relatively more polluted period, 1959-1978, regarding among others SO_4^*, F^- and dust.

All presented data show a remarkable, more or less sinusoidal seasonal fluctuation :
During the winter semester (October-March), which is characterized by a high frequency of southwesterly storms, sea salts are showing their maximum concentrations, as evidenced by Cl^-. The peak is generally found in November, the month with the highest storm frequency and strongest winds (KNMI, 1972).

The seasonal wave for SO_4^*, dust (see ash residu), F^-, PAHs (not shown, see Brasser, 1980), Ca^*, NO_3^- and NH_4^+ is somewhat retarded with respect to the Cl^--wave. Their maximum falls somewhere in between February and May. This largely corresponds with their emission peaks (among others a raised combustion of fossil fuels for heating purposes in winter, and a peak in NH_3 emissions from animal manure in February till May) and with relatively low rainfall. The latter promotes the formation of dust and reduces the otherwise diluting power of abundant precipitation.

During the summer semester maximum values are observed for DOC (median 2.8 mg/l versus 0.3 for the winter semester; Van Noort, 1985) and K^* (Fig.5.8, De Kooy). This may be due to a contribution from plant or animal debris in the vegetative period, as suggested for K^+ by Boström et al. (1989).

The behaviour of pH strongly depends on site specific circumstances. Maximum H^+ concentrations were observed near Monster in the period November-April (Fig.5.8). The H^+ curve strongly resembles the Cl^--curve and is opposite to the curve of the residue of ashes. This points at a predominant influence of pH-buffering dust particles, which are relatively low in concentration during the more windy, maritime months. This pattern is representative for an area and a period with strong air pollution.
The highest H^+ concentrations at the coastal background station De Kooy occurred, however, in the period April-July. This is explained by the predominant effect of acid, continental air masses in this period with low rainfall, in areas remote from anthropogenic dust sources.

Isotopes
Mean seasonal fluctuations are shown for oxygen-18 and tritium in Fig.5.9, together with their monthly minima and maxima. Those for ^{18}O closely correlate with temperature (Yurtsever & Gat, 1981). High tritium activities are generally observed in the period May - August. This is explained by mixing between the stratosphere and troposphere at high latitudes in early spring, so that ^3H, originally deposited in the stratosphere high-altitude by nuclear explosions, can return to the troposphere (Mook, 1989).

5.5.3 Episodes

An episode is defined here as a period shorter than a season, characterized by a specific chemical composition of bulk precipitation in connection with special meteorological circumstances.
Examples are : maritime versus continental episodes, episodes with extreme air pollution or sea spray deposition, dry versus wet episodes, etc. One characteristic analysis of bulk precipitation for respectively a maritime, continental, dry and wet episode is listed in Table 5.7.

Maritime episodes can be discerned from continental episodes by their higher sea salt concentrations and lower concentrations of typical components of air pollution (SO_4^*, NO_3^-, F^-, Br^*, NH_4^+, Ca^*, Al, Pb, V; Table 5.7).

Especially the NH_4^+/Na^+ ratio constitutes an excellent expression for the continentality of precipitation (Asman et al., 1981), generally being high during continental and low during maritime winds.

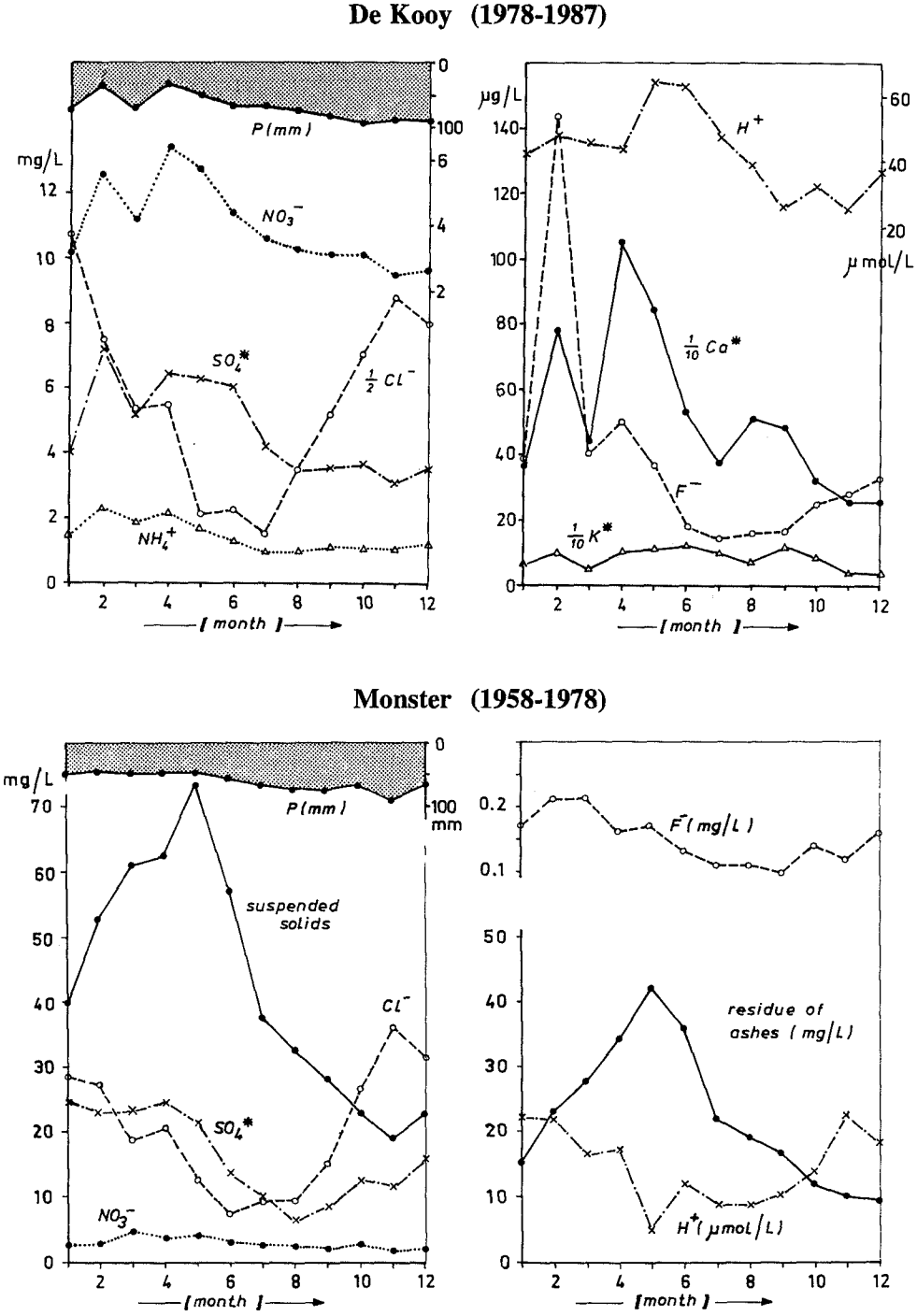

FIG. 5.8 Mean seasonal variations in the composition of bulk precipitation near De Kooy (weighted monthly means, 1978-1987, calculated from data in KNMI-RIVM, 1978-1987) and Monster (weighted monthly means, 1958-1977, calculated from data in IG-TNO, 1958-1978). De Kooy is station 2 and Monster station 82 in Fig.5.3.

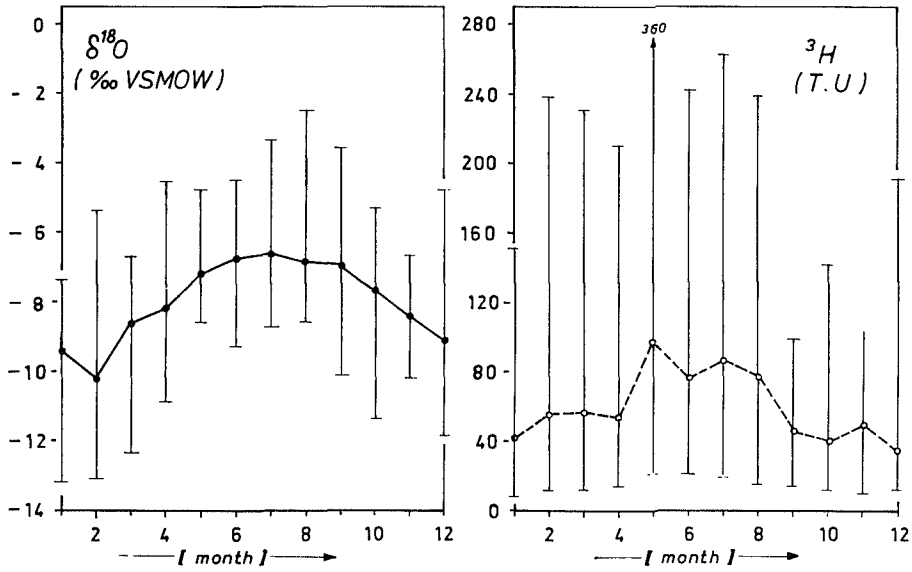

FIG. 5.9 Mean seasonal variations in the oxygen-18 concentration and tritium activity of bulk precipitation on Groningen in the NE-Netherlands (weighted monthly means, 1968-1987 for ^{18}O and 1970-1987 for ^{3}H, calculated with data obtained from the Laboratory of Isotope Physics Groningen). Monthly minima and maxima are shown as well.

TABLE 5.7 Compositional variations of bulk precipitation in the coastal area of the Western Netherlands, during meteorologically conditioned episodes. Data from De Kooy derive from Asman et al. (1981).

parameter	unit	DE KOOY (station 2) maritime period	DE KOOY (station 2) continental period	VU-1 (station 56) dry episode	VU-1 (station 56) wet episode
period	(+1900)	78?	78?	Aug-81	Oct-81
network		ECN	ECN	VU	VU
samples	(n)	21?	21?	1	1
dist.HWL	m	4750	4750	340	340
P (chem)	mm/14d	-	-	10	102
EC 20°C	µS/cm	-	-	334	89
Cl^-	mg/l	8.9	2.5	83.0	22.0
SO_4^{2-}	mg/l	5.2	9.4	19.5	3.6
NO_3^-	mg/l	2.7	6.4	13.1	1.6
PO_4^{3-}	mg/l	-	-	<0.1	<0.1
F^-	µg/l	21	53	-	-
pH		-	-	3.96	4.30
Na^+	mg/l	4.7	1.2	45.3	11.2
K^+	mg/l	0.24	0.19	2.17	0.46
Ca^{2+}	mg/l	0.44	0.72	6.3	<1.1
Mg^{2+}	mg/l	0.73	0.29	5.6	1.4
NH_4^+	mg/l	0.78	2.45	1.2	0.3
Fe	mg/l	0.04	0.08	<0.05	<0.05
Mn	mg/l	0.004	0.013	<0.05	<0.05
Al	µg/l	43	97	-	-
Br^-	µg/l	43	21		
Pb	µg/l	14.5	33.2		
V	µg/l	2.1	4.3	-	-
SO_4^*	mg/l	4.0	9.1	7.8	0.5
Na^*	mg/l	-0.3	-0.2	-0.4	-0.9
K^*	mg/l	0.06	0.14	0.51	0.02
Ca^*	mg/l	0.3	0.7	4.5	0.1
Mg^*	mg/l	0.1	0.1	0.05	-0.07

VU-1 = own measurements during a 2 weeks period in 1981. P-chem = precipitation on a bulk collector with funnel at 1.5 m above ground;

A 14 days period, with about ten times as much rainfall but with a similar level of air pollution (the NH_4^+/Na^+ ratio is practically equal), yields approximately ten times lower levels for components of air pollution like SO_4^*, NO_3^- and dust as deduced from SiO_2 (Table 5.7). Several constituents of bulk precipitation show indeed a positive relation with the reciprocal of rain depth, which reads :

$$C = a + \frac{b}{P} \qquad (5.9)$$

where C = concentration [mg/l]; a and b are constants; and P = rain depth [mm/period].
This formula implies a constant background level (a) and a constant air pollution (b) in a variable water volume (P). Eq.5.9 is obeyed well by SO_4^* (r=0,88), in biweekly samples from station 55 to the south of Zandvoort aan Zee in the period December 1980 - December 1981 (Fig.5.10), and to a significant level by NO_3^- (r=0,79), NH_4^+ (r=0,76) and Ca^* (r=0,71) as well. Variations in the level of air pollution prevent the relation from being perfect. Eq.5.9 cannot be applied to sea salts, because of too strong variations in the natural emission of sea spray.

The wet episode from 13 October till 2 November 1981 with 10.2 cm of rain fall, exhibited an extremely low SO_4^* concentration of 0.5 mg/l (Table 5.7). This value approaches the natural

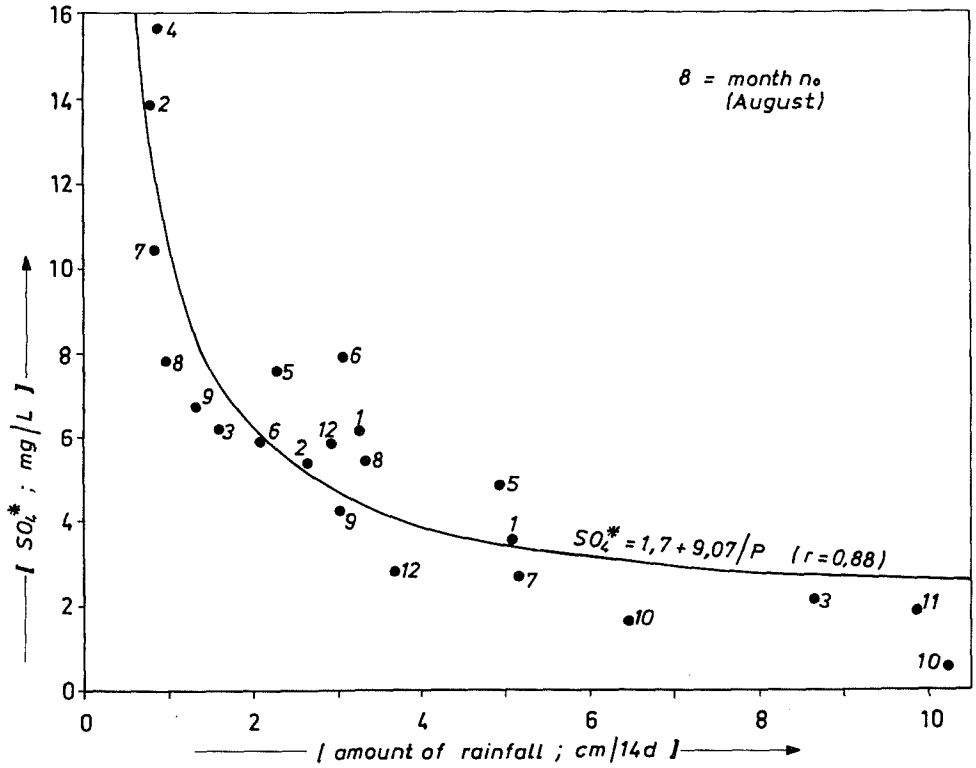

FIG. 5.10 Relationship between the rain depth in 14-days periods, and sea-salt-corrected sulphate in bulk precipitation on station 55 to the south of Zandvoort aan Zee, during the period December 1980 - December 1981.

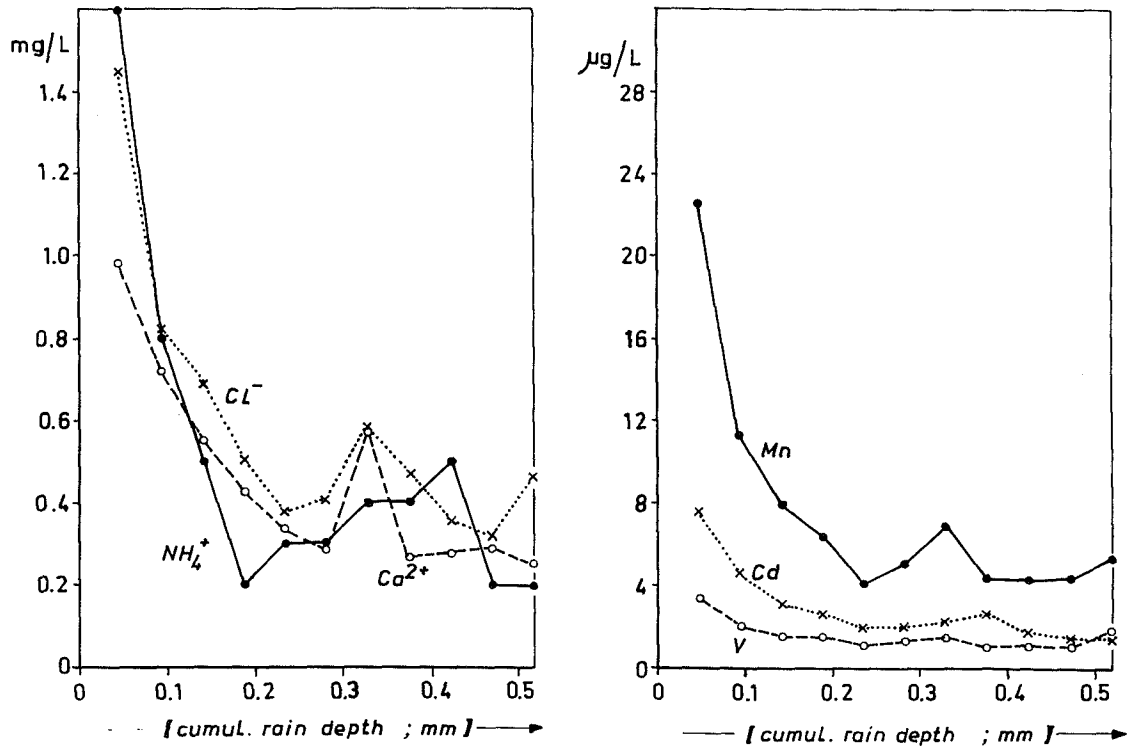

FIG. 5.11 The concentration decrease for some main and trace constituents of bulk precipitation during one shower near Utrecht, about 50 km to the south-east of Zandvoort aan Zee (based on data in Luten, 1977).

backgrounds of 0.3 mg/l (Table 5.3). Although the concentrations of nitrate and ammonium were very low as well, they still are about ten times their natural background. This can be explained by a longer residence time of anthropogenic NO_x compounds in the atmosphere as compared to SO_2 (Erisman, 1992), and a biogenic input together with sea spray from the North Sea (section 5.3.4; Fig.5.4).

5.5.4 During a shower

The sampling of equal amounts of precipitation during one shower, generally shows a continuous decrease for dissolved and suspended constituents (Beilke & Georgii, 1968; Luten, 1977). This is illustrated for a shower approximately 50 km to the south-east of Zandvoort aan Zee (Fig.5.11).

The phenomenon is explained by the so-called raining-out and washing-out of air constituents. Raining-out is defined as the dissolution or suspension of particles in water droplets within the clouds, where also upward air movements occur. The washing-out process takes place, on the contrary, by downward migrating raindrops from the cloud basis to the ground surface.
The process can be described by Eq.5.9 as well.

5.6 Concluding remarks

Bulk precipitation exhibits, in coastal areas with predominantly on-shore winds, an extreme compositional variability both in space and time. This can be explained by (a) proximity of the sea, which is a highly variable source of aerosols, (b) a strong gradient in the deposition of sea spray perpendicular to the shore line, and (c) a high solubility of sea spray. Anthropogenic sources strongly contribute to this variability in the Western Netherlands, especially regarding substances that also occur in a gaseous form (S, N, F), many heavy metals and organic microcontaminants.

The spatial patterns observed, can be traced back in the composition of shallow dune groundwater, as will be shown in section 6.6.2. The discerned trends in air pollution, exceptional years and seasonal fluctuations in precipitation chemistry, can also be detected in dune groundwater as demonstrated in section 6.7 and in chapter 7. In several cases this can be used to date shallow dune groundwater.

Most of the data underlying this study, necessarily refer to filtered precipitation samples with a relatively mild digestion of suspended dust particles. This means that the total atmospheric deposition on a bulk collector can be considerably higher for elements removed upon filtration and not digested upon sample pretreatment. On the other hand, the true chemical composition of precipitation just before infiltration can be overestimated in this way, for two reasons : (a) the contact time of rain water with suspended fines can be unnaturally long in a sample container, and (b) the acids dosed for digestion may strongly exceed the "natural" acidifying processes before infiltration. The latter consist of evaporation and a more effective absorption of acidifying gases to natural surfaces, as compared to a bulk collector.

These problems are only partly solved with wet-only collectors with a sieve in the bottle-neck, because the finer dust particles, which are collected during the shower, still pass the sieve and may dissolve in the pre-acidified bottle.

Chapter 6

FROM RAIN WATER TO THE UPPER DUNE WATERS

Abstract

The chemical metamorphosis of rain water into the upper dune groundwaters is shown and explained by comparison of bulk precipitation, throughfall, litter leachate, soil moisture and groundwater, on well defined locations. The major constituents, 19 trace elements, several organic microcontaminants and the natural isotope oxygen-18 were examined. The upper groundwater was monitored for several years using multilevel wells equipped with miniscreens, and four 625 m^2 lysimeters, on 28 plots that form a representative cross section of the natural environments in coastal dunes. An extensive list of the mean hydrochemical composition on these plots, provides a reference table on natural backgrounds, which include, however, effects of atmospheric pollution, acidification and, on several plots, a drawdown of the water table.

The concepts "*vegetation water lens*" and "*pure vegetation groundwater*" are introduced, as the vegetation cover proved to have a dominant impact. Simple hydrological calculations of the transit time in the vadose and shallow groundwater zone, and the thickness of both a vegetation water lens and the mixing zone between two pure vegetation groundwaters, compared well with hydrochemical observations.

Passage of the vegetation canopy as throughfall and percolation through the litter layer lead to a substantial increase of SO_4^{2-}, NO_3^-, PO_4^{3-} and K^+ by evaporation, interception deposition (SO_4^{2-} and NO_3^-) and leaching of leaves and mineralization of litter (NO_3^-, PO_4^{3-} and K^+). *Hippophaë* excells in the highest concentrations of NO_3^- in litter leachate and groundwater (related to N_2 fixation), and pines (*Pinus nigra* ssp. *nigra*) in the highest SO_4^{2-} (by evaporation and interception deposition) and lowest NO_3^- concentration in groundwater (by uptake). As the litter leachate passes through the active root zone, K^+, PO_4^{3-} and NO_3^- are preferentially withdrawn from the water phase again. This nutrient cycling leads to low concentrations of PO_4^{3-} and K^+. The raised atmospheric deposition causes NO_3^- to leak to a much higher degree to the groundwater zone.

Spatial variations of the dune water composition are discussed in terms of spatial variations of bulk precipitation chemistry, effects of 8 different types of vegetation cover, differences in geochemistry (calcareous versus decalcified dune sand, with and without intercalated dune peat) and variations of the mean thickness of the unsaturated zone. A mean position of the groundwater table >0.5 m below the surface yields a (sub)oxic facies. The most reactive constituents of dune sand are shell debris, ferromagnesian silicates (like hornblende), plagioclase and Fe- and Al-hydroxides. Their weathering yields a major contribution to Ca^{2+}, HCO_3^-, SiO_2, Fe, Mn, Al, As, Li^+, Rb^+, Sr^{2+} and U dissolved in groundwater. The atmosphere supplies the bulk or all of Na^+, Cl^-, SO_4^{2-}, NO_3^-, Br^-, K^+, Mg^{2+} and probably Cu, F^-, I, Pb, Se, V and Zn.

Long-term changes in the composition of shallow dune groundwater are composed of an overall increase in total dissolved solids, a specific rise of NO_3^- and Ca^{2+}, and a rise followed by a decrease, in SO_4^{2-}. These are largely connected with changes in vegetation cover, atmospheric deposition and a drawdown of the water table. Annual and seasonal fluctuations in the chemistry of pure vegetation groundwaters are shown to be extremely high, which appears characteristic for a dynamic coastal environment. The main causes are discussed and seasonal fluctuations of the biological, atmospherical and hydrological type are discerned. Both annual and seasonal Cl^- fluctuations, with the years 1974, 1977 and 1979 and the month November as recognizable extremes, proved useful in shallow groundwater dating, notwithstanding smoothing by dispersion. Effects of hydrodynamic dispersion (in the porous medium) and artificial dispersion by various sampling facilities are calculated and compared with observations.

The following fluxes of dissolved major constituents are quantified for selected vegetation covers in both calcareous and decalcified dunes : interception deposition, storage in biomass, N_2-fixation and decalcification rates. The contribution of interception deposition (= dry deposition minus the dry deposition on a bulk rain collector) to the total deposition of SO_x and $NO_x + NH_y$ varied for mosses, dune shrub, oaks and pines (without edge effects) from 50 to 75%. $CaCO_3$ leaching is favoured by interaction with dune peat above the water table, highest under *Hippophaë* and lowest under Corsican pine. The decalcification depth as calculated with a simple balance, compared well with geochemical observations in primarily calcareous dunes on a long time scale (200-5500 y). However, field data suggest an accellerated $CaCO_3$ leaching during the initial period, which lasts about 17 years for each percent $CaCO_3$ originally present.

TABLE 6.1. Characteristics of the 28 monitoring plots for the upper 0.3-3 metres of dune groundwater, with a mean gross precipitation (P) of 820 mm/y. N = Excess precipitation = P-E , where E = evapotranspiration; %E = 100 (E/P); f = solute concentration factor by evaporation losses = P/N; t_v = transit time in vadose zone; t_d = transit time from the water table to sampling points within vegetation water lens.

monitoring plot n_o	name	specification of vegetation	GEOCHEMISTRY decalc depth* m-surf	dune peat @	TOPOGRAPHY distance HWL m	surface altitude m+MSL	HYDROLOGICAL BOUNDARY CONDITIONS groundwater level (m-surf) mean	lowest	highest	N m/y	%E	f	transit time t_v d	t_d d
MINISCREENS, DUNES POOR IN CALCITE, NORTH OF BERGEN														
S	scanty	20% bare, 80% mosses and grasses	13	-	950	9.7	3.1	3.1	3.1	0.50	39	1.6	210	30-465
H	heather	*Calluna vulgaris*	20	h	1400	5.0	2.1	2.1	2.1	0.37	55	2.2	220	80-750
P_4	pines-4	*Pinus nigra ssp nigra* (8m, 58y)	20	-	800	4.8	2.9	2.9	2.9	0.14	83	5.8	710	315-2295
P_5	pines-5	*Pinus maritima* (15m, 82y)	18		3000	6.0	3.7	3.7	3.7	0.20	76	4.2	592	35-1095
PIEZOMETERS, CALCAREOUS DUNES SOUTH OF EGMOND														
G_4	grasses-4	40% grasses, 30% dune reed, 30% creeping willow	<0.1		340	3.8	0.4	0.6	0.1	0.25	70	3.3	160	410
G_5	grasses-5	70% grasses, 20% creeping willow, 10% dune reed	<0.1		360	3.8	1.1	1.4	0.9	0.33	60	2.5	170	620-755
LYSIMETERS, CALCAREOUS DUNES, WEST OF CASTRICUM														
S_L	bare-L	85% bare, 15% mosses	<0.1		2000	3.8	2.2	2.2	2.2	0.62	24	1.3	135	<10-155
D_L	dune shrub-L	*Hippophaë rhamnoides* mainly (2½ m, 40y)	<0.1		2040	3.8	2.3	2.5	2.2	0.34	58	2.4	250	<10-280
O_L	oaks-L	*Quercus robur* (8 m, 40y), undergrowth of birdcherry	<0.1		2115	3.8	2.3	2.5	2.2	0.30	63	2.7	285	<10-315
P_L	pines-L	*Pinus nigra ssp nigra* (13m, 40y)	<0.1		2200	3.8	2.4	2.5	2.2	0.14	83	5.8	625	<10-680
MINISCREENS, CALCAREOUS DUNES SOUTH OF ZANDVOORT														
M_1	mosses-1	60% mosses, 20% grasses and 20% bare	0.05		325	2.8	1.6	1.7	1.4	0.52	37	1.7	130	110-900
M_2	mosses-2	uninterrupted carpet of mosses	0.2		2500	7.8	1.7	2.0	1.3	0.49	40	1.7	145	15-595
M_3	mosses-3	70% mosses, 30% *Hippophaë rhamnoides* (<1 m)	0.3		2725	7.6	2.5	2.3	2.9	0.43	48	1.9	210	15-850
G_1	grasses-1	80% grasses, 20% bare	<0.1		2100	7.6	0.7	0.8	0.6	0.38	54	2.2	125	20-850
G_2	grasses-2	grasses and herbs	0.3	-	2650	7.7	0.3	0.4	0.1	0.33	60	2.5	115	90-975
G_3	grasses-3	80% grasses, 20% low shrubs	1.3	+e	3310	3.6	3.1	3.5	2.8	0.33	60	2.5	315	45-750
B_1	bracken-1	*Pteridium aquilinum*, see foot note #	2.0	-	3485	4.4	4.1	4.4	3.7	0.41	50	2.0	310	320
B_2	bracken-2	*Pteridium aquilinum*, see foot note #	1.3	+p	3115	2.5	2.1	2.3	1.8	0.41	50	2.0	195	20
D_1	dune shrub-1	*Hippophaë rhamnoides* (1 m)	<0.1	-	625	3.8	2.7	2.9	2.4	0.38	54	2.2	250	305
D_2	dune shrub-2	*Hippophaë rhamnoides* (2 m)	0.3	-	1685	6.3	2.4	2.7	2.1	0.38	54	2.2	230	190
D_3	dune shrub-3	60% *Hippophaë rhamnoides* (1m), 40% grasses	1.3	tp	3175	3.9	3.7	4.0	3.4	0.38	54	2.2	310	115
D_4	dune shrub-4	mixed composition, see foot note A	0.3	+e	1145	3.7	2.1	2.3	1.8	0.41	50	2.0	330	390-1140
O_1	oaks-1	90% *Quercus robur* (7m, 80y), 10% Acer (8m)	1.4	te	3260	3.9	3.5	3.8	3.1	0.31	62	2.7	365	140-1035
O_2	oaks-2	*Quercus robur* (6m, 80y)	1.3-1.7	-	3200	3.5	3.0	3.3	2.6	0.31	62	2.7	330	140-565
O_3	oaks-3	*Quercus robur* (7m, 80y)	1.5		3245	3.9	3.6	3.9	3.2	0.31	62	2.7	375	45-95
P_1	pines-1	*Pinus nigra ssp nigra* (10m, 30y)	0.4		1515	5.7	2.2	2.5	2.0	0.14	83	5.8	590	315-1355
P_2	pines-2	*Pinus nigra ssp nigra* (10m, 30y)	0.4	-	1635	5.1	1.6	1.9	1.4	0.14	83	5.8	490	625
P_3	pines-3	*Pinus nigra ssp nigra* (8m, 30y)	0.1	t	1700	7.1	2.9	3.2	2.6	0.20	76	4.2	495	35-1605

@ : + = clearly present, always in saturated zone; +p = clearly present, permanently in unsaturated zone; +e = clearly present, episodically in unsaturated zone; t = in traces, always in saturated zone; te = in traces, episodically in unsaturated zone; tp = in traces, permanently in unsaturated zone; h = humic top layer 0.1 m thick; - = absent; A = 45% *Hippophae rhamnoides*, 30% dewberry, 15% grasses and 10% creeping willow; HWL = mean high water line of North Sea; # = 1½ - 2 m high, mainly grasses from mid-November till mid-May. t_v = total transit time in vadose zone; t_d = transit time from water table up to the deepest observation well within the pure vegetation water sampled; * = decalcification depth.

and 6.4 in Fig.4.33 were involved, yielding the dune valley groundwater discussed in section 4.7. Groundwater was sampled twice by Pruijt (1984) on the plot grasses-5, approximately 1.5 m below the mean water table, in the period June - September 1983. For further details on both plots and well construction, reference is made to Pruijt (1984) and Stuyfzand & Moberts (1987a).

The lysimeters west of Castricum

Four giant lysimeters with different vegetation covers are situated west of Castricum, in the dune water catchment area of PWN, close to each other at about 2100 m from the North Sea (Fig.6.2). The vegetation cover of the four lysimeters in summer 1983 is shown in Fig.6.3.

PWN sampled their drainage waters by bailer from a central collection tank in the subsoil, on a monthly basis during the period March 1946 till January 1962 and since March 1988, and on a weekly basis during the period January 1980 till March 1988. The period mainly considered here, is restricted to March 1980 till March 1983, because of elaboration of those data by Stuyfzand (1984d) and for the sake of better comparison with the many data collected south of Zandvoort aan Zee.

The effective depth of the lysimeters (2.5 m), the presence of a groundwater table within the lysimeters (Fig.6.4) and their size (25 by 25 m) justify the assumption that the drainage solute represents a spatial average for upper dune groundwater on the specific site. The lysimeters were completed in 1940. The bare lysimeter remained without vegetation cover except for small patches of mosses, which are still suppressed by weeding. It has always been covered with bare twigs and branches for protection against aeolian erosion. Their presence must be considered as a source of

FIG. 6.3 The four lysimeters west of Castricum in summer 1983.

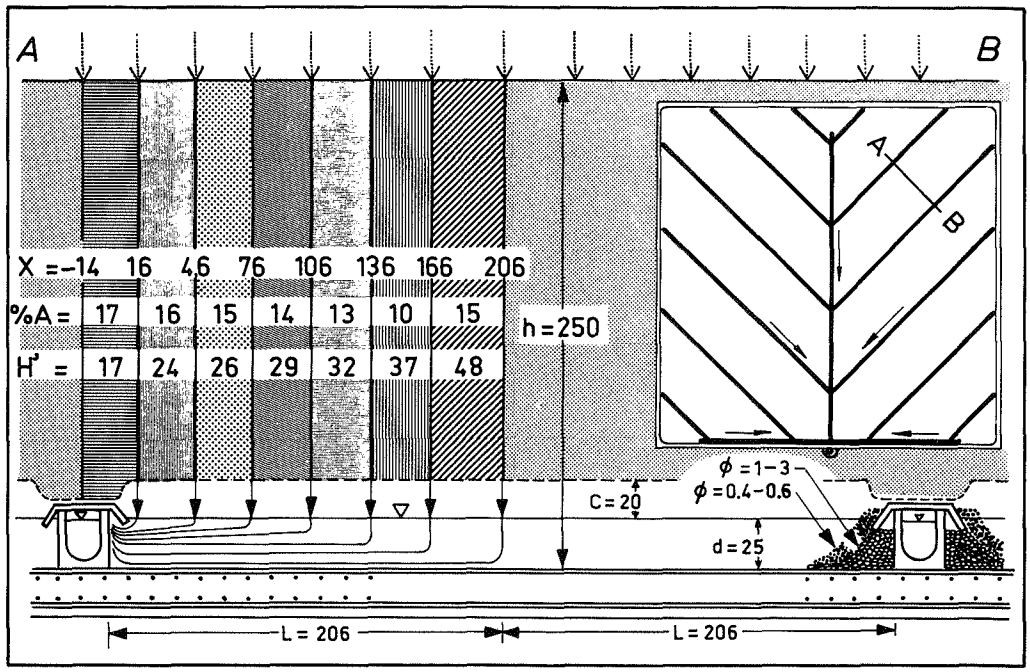

FIG. 6.4 Cross section of segment AB of a lysimeter west of Castricum, with information on hydrological compartments and their drainage. The inset gives the position of the cross section and a view from above on the drainage system. All measures in cms. X = distance of a water parcel to drain wall; %A = total surface of lysimeter (in %) within shown distance interval; H' = total water content in lysimeter to be displaced before arrival at the drains; c = capillary fringe; d = groundwater zone; h = total depth; L = distance of water divide to wall of drain.

several compounds. The protection measure has been common practice in coastal dune management, so that the representativity of this lysimeter remains intact, at least in this respect. However, in 1942 a 1 cm thick layer of black soil was deposited erroneously, and in 1946 20 kg of KCl was deposited for a tracer experiment.

The soil of the lysimeters vegetated with either dune shrub, oak or pines, was amended in the period 1942-1945 by several centimeters of black soil and compost, and fertilizers were added in the period 1946-1951 (Hiege, 1987). Even after 30-40 years this may still explain raised concentrations of several compounds (section 6.6.1). Soil amendment may have been common practice for oak and pine plantations in the dunes, but certainly not for the natural dune shrubs.

For further details regarding the construction of the lysimeters, reference is made to Van Nievelt (1941). The development of juvenile vegetation since 1941 has been documented by Hiege (1987).

The miniscreened observation wells south of Zandvoort aan Zee

In the dune water catchment area of the Municipal Water Supply Co. of Amsterdam (GW), multilevel wells equipped with miniscreens (same type as in Fig.2.4) were sampled on 18 monitoring plots. One to ten miniscreens in 1-3 boreholes were sampled on each plot on a monthly or bimonthly basis for 1-4 years, generally within the period March 1979 till February 1983 (the exact period for each plot is indicated in Table 6.13). Detailed information on site specific conditions for each monitoring plot, is given by Stuyfzand (1991b). Fig.6.5 gives an impression of the plots called mosses-1 and oaks-1.

The miniscreens considered here, are positioned within the upper 0.3-3 metres below the mean groundwater table, in the calcareous dune sand formation. They are sufficiently distant from the vegetation border upgradient, to exclude any significant admixing of deeper groundwater, which originated under a vegetation cover different from the one indicated in Table 6.1. This aspect was checked for by hydrochemical logs using miniscreens to delineate the thickness of the local vegetation water lens, or by hydrological calculations (section 6.3.3).

The miniscreens were installed in bailer drilled wells (Fig.2.5), in most cases without the addition of water. After an equilibration period of at least 3 months during which the miniscreens were flushed 2-3 times, sampling for complete analysis started. Each time about 0.5 liter was used for flushing the

FIG. 6.5 The monitoring plots mosses-1 and oaks-1 by the end of October 1980. The plot mosses-1, with bulk precipitation collector VU.1 in the foreground and multilevel well 24H.470 in the background, is situated close to the foredune ridge and is practically unaffected as yet by decalcification. The plot oaks-1, with an undergrowth of bracken, is situated in the older dunes about 3 km from the foredune ridge and is decalcified to a depth of 1.4 - 1.7 m. The 60 liter vessel was used to export the groundwater pumped during well development, in order to avoid the adverse effects of irrigation-return flow. During regular monitoring the groundwater necessary for flushing the facility and bottles, was disposed of, always on the downgradient side of the well.

facility and bottles, after which 1-2 liters were collected for determinations on site and further analysis in the laboratory.

Filtration of the water samples was discarded for reasons outlined in section 4.2.3. Clay particles from the aquifer matrix or from clay seals were not significantly included in most samples, as indicated by Al concentrations in samples directly acidified to pH 1.5, being below 20 µg/l after three months of conservation. Besides, aluminium and other analyses agreed well with those of 0.45 µm membrane-filtered samples from incidentally sampled piezometer screens in the same environment. Lack of filtration led to enhanced levels, mainly for Al and several trace elements, on the plots mosses-2, mosses-3 and grasses-1. These data were corrected according to Eq.2.1 with the regression constants listed in Table 2.3. Additional data on trace elements in 0.45 µm membrane filtered samples, were obtained for mosses-1, mosses-2 and grasses-2 in November 1991. These data have been used in this survey, if the older data were affected by omission of filtration or if the new data contained information on trace elements not yet analysed.

6.3 Hydrological boundary conditions

6.3.1 Gross precipitation and groundwater recharge

Mean gross precipitation (*P*) on the plots studied, amounts to 0.82 m/y for the period 1947-1981 (Stuyfzand, 1988b). For the average period under consideration here (1980 through 1982), *P* was 0.84 m/y without the occurrence of extreme years. Therefore, the values for the natural groundwater recharge (*N*) in Table 3.2 could be used directly or were extrapolated to the specific vegetation cover with

due consideration of local moisture supply. Thus derived or estimated values of N are listed in Table 6.1 for the 28 plots studied, and refer to mean annual conditions.

The percentage of P that evaporates (%E), is listed in Table 6.1 as well, and varies from 24% for the bare lysimeter west of Castricum to 83% for most pine-plots. This evapo(transpi)ration will concentrate the remaining ions by a factor f, which equals P/N for ions with conservative behaviour. Values of f are listed in Table 6.1 as well. They vary from 1.3 for the bare lysimeter west of Castricum to 5.8 for most pine-plots.

Further details on annual and seasonal variations of P and N are given in section 3.4.1 and 3.4.2, respectively. Variations of annual means of f are shown in Fig.6.40A.

6.3.2 *Position of the water table*

The mean position of the groundwater table on the 28 plots varied in between 0.3 and 4.1 m below the surface, with 24 plots deeper than 1.5 m (Table 6.1). Dry dunes therefore dominate in this survey. This is in harmony with present average conditions and related to the historical drawdown of the water table (section 3.7, Enclosure 3.2). The relatively shallow position of the water table on the plots G_1 and G_2 is connected with their position adjacent to spreading areas, and that on the plots G_4 and G_5 corresponds with relatively low pumping rates in the surroundings.

The position of the groundwater table fluctuated during the monitoring period (roughly 1980 through 1982 for most plots) by 0 to 0.7 m, as calculated from the maxima and minima listed in Table 6.1. This "total" fluctuation, on average over a 3-years period, was unnaturally small for (a) the lysimeters (0-0.25 m), in consequence of their drainage level 0.25 m above the bottom (Fig.6.4), and (b) the plots G_1 and G_2 (0.2-0.3 m), where a more stable position of the water table was imposed by steady artificial recharge in the bordering areas. On the other 22 plots, the total fluctuation amounted to 0.5-0.7 m, which is within the natural range given by Bakker (1981).

Seasonal fluctuations of the water table on these 22 plots exhibit a natural, sinusoidal pattern, with a maximum around March-April and a minimum around September-October (Figs. 6.44 and 6.45).

6.3.3 *Vegetation water lenses and the transit time within*

It is convenient to further differentiate hydrochemical facies within a large hydrosome, when small-scale variations need to be mapped, for instance only shallow groundwater in a (natural) recharge area with a patchy vegetation cover or land-use. This example connects very well with the situation to be analysed in this chapter. The overwhelming effect of the vegetation cover on the composition of shallow dune groundwater (section 6.6.3) and the shape of groundwater zones with a specific vegetational finger print, inspired to the distinction of vegetation water lenses, and where the impact of vegetation is masked by interaction with dune peat, dune peat lenses (Fig.6.6).

Definitions

A *vegetation water lens* is defined as a groundwater body, receiving its recharge for >50% from precipitation on a specific vegetation unit. Examples are shown in Fig.6.6, where two pine-water lenses are floating on dune shrub-water in a cross section perpendicular to groundwater flow. The pine-water could be discerned from dune-shrub water by a higher Cl^- and lower NO_3^- concentration.

The lower boundary of the upper lens is blurred by mixing with the adjacent lens in consequence of dispersive flow (section 3.10.2), and by gradual boundaries between different vegetation covers. It is therefore useful to introduce the term "*pure vegetation water*", which refers for practical reasons, to groundwater receiving its recharge for >80% from precipitation on the indicated vegetation unit.

It was ascertained that the miniscreens used for the hydrochemical characterization of each monitoring plot, sampled the upper, pure vegetation water. This was done by (1) hydrochemical logs using multilevel wells equipped with miniscreens, which enable us to delineate the thickness of the upper vegetation water lens and the transition zone (20-80% admixing), and/or (2) hydrological calculations, which are elucidated below.

Calculations

When a steady-state, primarily horizontal and completely indispersive flow in a homogeneous, isotropic aquifer with uniform recharge are assumed for the situation sketched in Fig.6.7, we obtain the same formula as for a rain water lens (Eq.3.21 in section 3.10.2) :

$$D_x = \frac{-N\,X\,dX}{K_h\,dH} \qquad (6.1)$$

however, with : D_x = thickness of vegetation water lens at distance X [m]; N = natural recharge [m/d]; H = phreatic head [m+MSL]; K_h = horizontal permeability [m/d]; X = distance to the edge of the surrounding vegetation unit upgradient, as measured in the horizontal plane along the groundwater flow line [m].

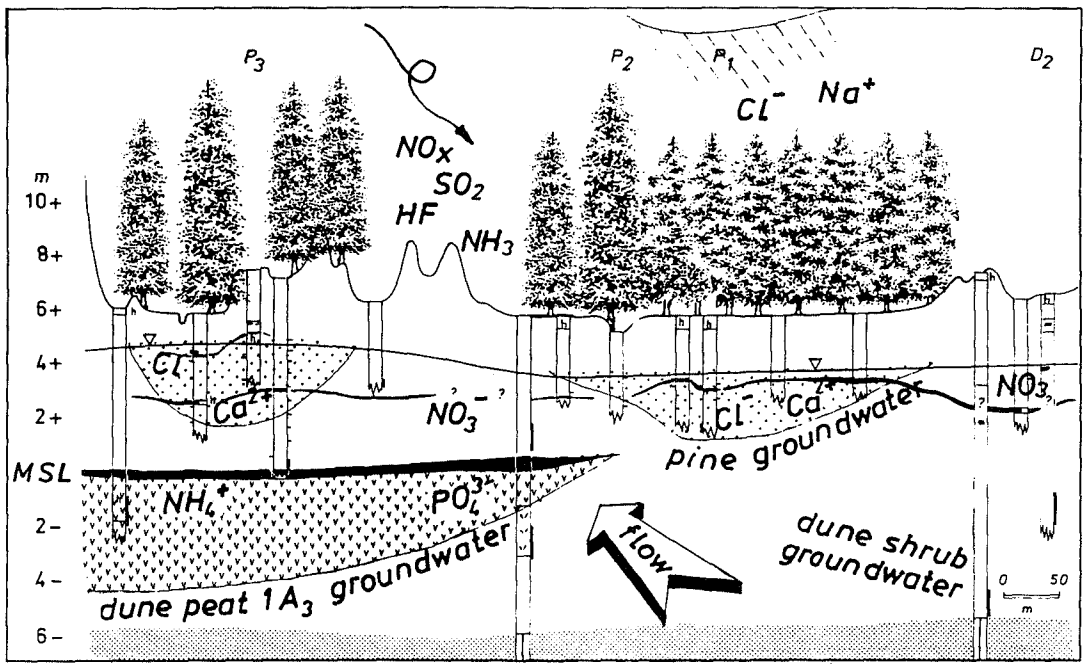

FIG. 6.6 Two pine-water lenses floating on dune shrub-water in coastal dunes south of Zandvoort aan Zee. Dissolved constituents with a diagnostic high concentration are indicated for each type. Groundwater flow is perpendicular to this cross section, which includes the monitoring plots dune shrub D_2 and pines P_{1-3}. Dune peat $1A_3$ groundwater is discussed in section 6.6.5.

When the slope of the water table (dH/dX) is approximated by a sloping plane, which is realistic enough within most, small-scale vegetation units, Eq.6.1 reduces to :

$$D_x = \frac{-N X \Delta X}{K_h \Delta H} \qquad (6.1A)$$

where $\Delta H/\Delta X$ = constant slope of the water table below the vegetation unit under consideration.
Under these conditions, it becomes surprisingly easy to calculate the transit time of groundwater from the water table to any position within the considered vegetation water lens (t_d):

$$t_d = \varepsilon \cdot \frac{d}{N} \qquad (6.2)$$

where : ε = porosity [-]; d = depth below water table [m], provided that $d \leq D_x$ and $d \ll D$ (D = thickness of aquifer).
This can be proved as follows. The transit time from the upgradient edge of the surrounding vegetation unit towards a point at distance X at depth D_x below the water table, is $t_d = -(\varepsilon X \Delta X)/(K_h \Delta H)$. This yields after combination with Eq.6.1A : $t_d = \varepsilon D_x/N$.

Conformity of the triangles ABC and EBF in Fig.6.7, compels Eq.6.2 to be valid as well, quod erat demonstrandum. Eq.6.2 is consistent with the general solution of t_d under the present conditions, being according to Vogel (1967) and de Vries (1974) :

$$t_d = -\frac{\varepsilon D}{N} \cdot \ln\left(1 - \frac{d}{D}\right) \qquad (6.2A)$$

where D = thickness of the aquifer [m]. If $d/D <$ 0.3, then $\ln(1-d/D)$ approaches to $-d/D$. In that case Eq.6.2A simplifies to Eq.6.2 indeed. Eqs.6.2 and 6.2A are not valid close to the groundwater discharge area.

The total transit time (t_t) in the subsoil to a depth d below the water table not exceeding the thickness of the vegetation water lens now becomes, by addition of Eq.3.1 to Eq.6.2 :

$$t_t = \frac{h V + \varepsilon (c + d)}{N} \qquad (6.3)$$

where : h = thickness of unsaturated zone [m]; V = mean moisture content of unsaturated zone (fraction by volume); c = thickness of capillary fringe [m].

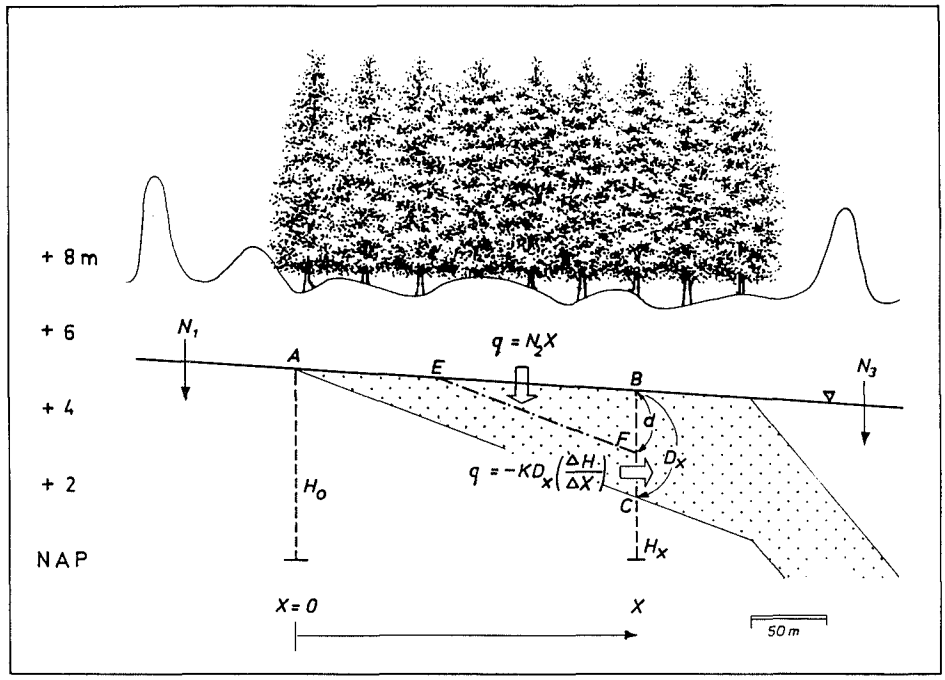

FIG. 6.7 Scheme of a vegetation water lens (stippled) on a sloping water table, with parameters and water balance for calculating its thickness. In this example : $H_o > H_x$, $N_2 = 0.37$ mm/d, $K_h = 12$ m/d and $\Delta H/\Delta X = 0.003$.

And the total distance travelled in the subsoil (s), at distance X and depth *d* below the water table is given then by :

$$s = h + c + X\left(\frac{d}{D_x}\right) \qquad (6.4)$$

The thickness of pure vegetation water (D_{80}) is calculated by subtracting the thickness of the zone with 50-20% admixing above the interface, which is calculated using Eq.3.16, from D_x. This yields:

$$D_{80} = D_x - 1.192\sqrt{\alpha_T X} \qquad (6.5)$$

where α_T = transversal dispersivity of the porous medium [m].

Results of calculation

The calculated thickness of the vegetation water lens, using Eq.6.1A, can be compared on 8 plots with observations on site (Table 6.2). In general there is quite an acceptable agreement.

Substituting 0.065 for V, 0.4 for ε, 0.25 m for *c* and appropriate values for h (= mean depth of the water table minus *c*) and *N* in Eq.3.1, yields the mean transit time in the vadose zone for each monitoring plot, as presented in Table 6.1. It can be concluded, that these transit times vary from 0.3 year for the bare lysimeter, mosses-1, grasses-1 and -2, to 2 years for pines-4.

The transit time from the mean water table to the upper and lowest miniscreen of those tapping (pure) vegetation water, has been calculated for each plot, using Eq.6.2. The variation of detention times within the groundwater reservoir of each lysimeter, which is inherent to the flow pattern in between the groundwater divide and drain (Fig.6.4), has been calculated as outlined in Stuyfzand (1986c). The results of these calculations are presented in Table 6.1 as well. They show that there is a large variation of transit times in the shallow, saturated zone as well, especially on the pine-plots equipped with miniscreens. There was no variation of course on the few plots, where only one miniscreen was installed.

Addition of the average of the travel time in the lens (t_d in Table 6.1) to the mean transit time in the vadose zone (t_v in Table 6.1), yields an average total transit time from the surface to the monitoring wells on each plot. This total transit time varies from 0.6 y for the bare lysimeter and bracken-2 to 5.5 y for pines-4. The total transit time as calculated with Eq.6.3, can be compared for selected miniscreens in Table 6.2 with the transit times as deduced from hydrochemical observations presented in section 6.7.4. The agreement is quite good, which raises the confidence in the constants used for calculation, and in the simple Eq.6.3 applied.

TABLE 6.2 The calculated and observed thickness of a vegetation groundwater lens (D_x) and the total transit time from the surface to the upper miniscreen (t_{upper}), on several plots. Hydrological data underlying the calculations and other calculated parameters are given as well. h = thickness unsaturated zone; X = horizontal distance of observation well to the upgradient edge of the surrounding vegetation unit; dH/dX = phreatic head gradient; N = natural recharge; D_{80} = thickness of pure vegetation water; t_u = transit time in unsaturated zone; t_c = ditto, in capillary fringe; t_l = total transit time up to 1 m below the water table.

	Basic hydrological data					calculated parameters				measured		
well	h (m)	X (m)	dH/dX	N mm/d	D_x (m)	D_{80} (m)	t_u (d)	t_c (d)	t_l (d)	t_{upper} (d)	D_x (m)	t_{upper} (d)
Mosses												
I	1.25	100	0.0004	1.35	28.1	27.5	60	74	430	240	>5	150
Oaks												
II	3.25	30	0.002	0.83	1.0	0.7	254	120	854	542	2-3	
IIC	3.35	45	0.002	0.83	1.6	1.2	262	120	862	478	>1.6	-
V	2.75	50	0.002	0.83	1.7	1.3	215	120	815	610	1.5	520
VII	3.65	45	0.0013	0.83	2.4	2.0	285	120	885	761	1.8	-
Pines												
VI&D	2.25	250	0.003	0.37	2.6	1.7	395	270	1745	900	>2.0	760
IV	2.35	200	0.0028	0.37	2.2	1.4	413	270	1763	530	2.0	480
Dune shrub												
C	2.4	110?	0.0027	1.04	3.5	2.9	134	96	615	420	>0.5	510
G	2.55	55	0.001	1.03	4.7	4.3	161	97	646	560	>1.0	880
III	2.1	-	-	1.12	-		107	89	554	720	2.5	850
IX	3.75	25	0.0025	1.19	1.0	0.7	218	84	625	413	0.6	?

6.3.4 Artificial dispersion by sampling

Groundwater is evacuated from a piezometer or miniscreen for (1) flushing the facility, sampling device and bottles, (2) measurements in the field and (3) the sampling. This leads to the mixing of water, that originally surrounded the screen at a certain distance, in the sample bottles. The more protracted the pumping, the longer is the distance travelled by the collected water particles outside the screen, and the greater is the chance of deleterious mixing. Twice the maximum travel distance to the screen, is defined here as the *mixing length (by sampling)*, either horizontally (M_{xy}) or vertically (M_z; Fig.6.8). A high mixing length stands for a strong mixing effect by the sampling itself, which may provoke an internal chemical inconsistency (section 2.3.3), fade away the original hydrochemical stratification and smooth natural quality fluctuations in the aquifer. Aquifer dispersivities deduced from observations on wells with a high mixing length, are to be examined critically.

In order to simplify our calculations, several assumptions have to be made. The total volume to be evacuated is fixed at three times the water volume of the riser and its screen, the so-called standing volume, plus 1 liter for the sample. The standing volume, however, was collected during the previous sampling from a groundwater parcel that has migrated in the meantime beyond the reach of the present sampling, and did not exchange with groundwater outside the facility. This reduces the total volume to be evacuated from the subsoil outside the facility (Q_s), to twice the standing volume plus 1 liter for the sample. The anisotropy of the sandy aquifer is fixed at $K_z = ½K_x = ½K_y$ (where $K_z = K_v$ and K_x, $K_y = K_h$) and its porosity ε at 0.38. Furthermore, it is assumed that the risers or support pipes of deeper samplers in the same well do not disturb the flow pattern around the well screen under consideration.

We then obtain for an approximately ellipsoidal flow pattern around a miniscreen (Fig.6.8A) of the type depicted in Fig.2.4, with screen length $L \leq 0.01$ m :

$$Q_s = \frac{4}{3}\pi R_x R_y R_z \varepsilon \qquad (6.6)$$

where R_x, R_y, R_z = half of the axis of the evacuated ellipsoidal groundwater body in the subsoil, which surrounded the miniscreen along its x-, y- or z-axis, respectively [m]; Q_s = the total volume to be evacuated from the subsoil outside the observation facility [m^3].

Substitution of $R_y = R_x$ and $R_z = ½R_x$ because of the assumed anisotropy, $\varepsilon = 0.38$ and $2R_x = M_{xy}$ in Eq. 6.6 yields for the horizontal (M_{xy}) and vertical (M_z) mixing length, respectively :

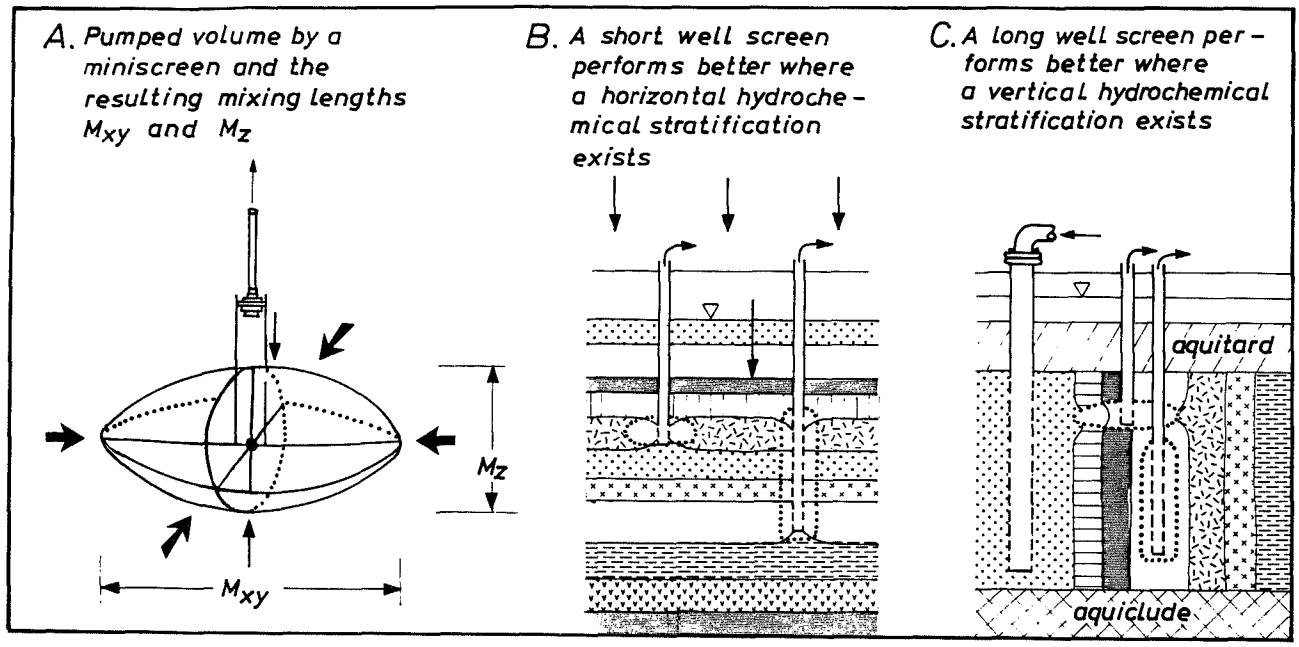

FIG. 6.8 Artificial mixing by sampling, quantified by the so-called horizontal and vertical mixing length, M_{xy} and M_z respectively (A). The ultimate water parcels entering the sample bottle, were originally situated at the circumference of the drawn ellipsoid or cylinder. In case of a subtle horizontal, hydrochemical stratification short screens are to be preferred (B). However, where this stratification is tilted to a vertical position, as in case of bank filtration and deep well infiltration, long screen lengths may reduce deleterious mixing (C).

$$M_{xy} = 2.16\ (Q_s)^{\frac{1}{3}} \qquad (6.7)$$

$$M_z = \tfrac{1}{2} M_{xy} \qquad (6.7A)$$

And we obtain for a piezometer with screen length L >> 0.01 m and with boundary conditions as above, in case of a cylindrical flow pattern with the cylinder length initially equal to L, untill M_z (as calculated above, assuming an ellipsoidal flow pattern around the heart of the screen) exceeds L :

$$M_{xy} = 1.83 \sqrt{\frac{Q_s}{L}} \qquad (6.8)$$

$$M_z = L \qquad (6.8A)$$

But when M_z (=½M_{xy} using Eq.6.7) starts to exceed the screen length L, then Eqs.6.7 and 6.7A are applied, for simplicity, to piezometers as well.

Thus calculated mixing lengths are listed in Table 6.3 for the miniscreens used in this study and for various types of common piezometers in the study area, as a function of the length of the water column in riser plus screen. The following conclusions are drawn :

- the shortest mixing length, which is very little dependent on the depth of the screen below the water level, applies to the miniscreens used in this study : about 11 cm vertically and about 22 cm horizontally;
- piezometers with a well screen in between 0.1 and 1.0 metre lead to much more mixing (mixing length 0.1-1.0 m, both horizontally and vertically), with a strong dependency on their diameter and depth below the water level;
- short well screens (≤0.1 m) are to be preferred where a subtle, vertical hydrochemical zonation (yielding a horizontal stratification) occurs, for instance close to the groundwater divide (Fig.6.8B). Longer well screens (>1.0 m) may perform better where the hydrochemical zonation is oriented in the horizontal plane (Fig.6.8C), like in case of lateral flow of highly variable surface water along deeply incised, influent rivers or around injection wells; and
- piezometers with a well screen 0.1 m long and with an internal diameter of 1.8 cm, form a good alternative for miniscreens.

TABLE 6.3 The required total water volume (Q_t) to be evacuated for flushing the observation facility three times and collecting a sample of 1 liter, and the so-called "mixing length by sampling" (M_{xy} or M_z), as a function of the inner diameter (d) of the riser, length of the well screen (L), and the depth of the heart of the screen below the water level in the riser. Calculated as outlined in text.

screen depth m-MPL[§]	mini-screen	PIEZOMETER WITH INDICATED DIAMETER d, AND SCREEN LENGTH L								
		d = 1.8cm			d = 2.5cm			d = 5.0cm		
		L = 0.1m	0.5m	1.0m	L = 0.1m	0.5m	1.0m	L = 0.1m	0.5m	1.0m
Required water volume Q (liters) for 3 times refreshing of standing volume and a sample of 1 liter:										
1m	1.04	1.8	1.8	1.8	2.5	2.5	2.5	6.9	6.9	6.9
2m	1.06	2.5	2.5	2.5	4.0	4.0	4.0	12.8	12.8	12.8
4m	1.10	4.0	4.0	4.0	6.9	6.9	6.9	24.6	24.6	24.6
8m	1.18	7.1	7.1	7.1	12.8	12.8	12.8	48.2	48.2	48.2
16m	1.35	13.2	13.2	13.2	24.6	24.6	24.6	95.3	95.3	95.3
32m	1.69	25.4	25.4	25.4	48.1	48.1	48.1	189.6	189.6	189.6
Horizontal mixing length M_{xy} (cm):										
1m	21.8	24.8	10.0	7.2	27.1	11.5	8.2	36.8	18.2	11.8
2m	21.9	27.2	11.6	8.1	31.0	14.1	10.0	44.7	24.4	17.3
4m	22.1	31.2	14.2	10.2	36.8	18.2	12.9	55.2	33.5	23.7
8m	22.4	37.0	18.4	13.0	44.7	24.4	17.3	68.9	46.7	33.0
16m	23.2	45.2	24.8	17.6	55.2	33.5	23.7	86.3	65.5	46.3
32m	24.5	55.8	34.0	24.0	68.9	46.7	33.0	108.5	108.5	65.3
Vertical mixing length M_z (cm):										
1m	10.9	12.4	50	100	13.6	50	100	18.4	50	100
2m	11.0	13.6	50	100	15.5	50	100	22.3	50	100
4m	11.1	15.6	50	100	18.4	50	100	27.6	50	100
8m	11.2	18.5	50	100	22.3	50	100	34.4	50	100
16m	11.6	22.6	50	100	27.6	50	100	43.2	50	100
32m	12.3	27.9	50	100	34.4	50	100	54.2	54.2	100

[§] = mean piezometric level.

6.4 Geochemistry of dune sand and dune peat

6.4.1 Dune sand as parent material

In this section dune sand unaffected by soil formation is considered, i.e. below the rooted and decalcified zones and without any admixing of buried soil horizons. This means, in the younger calcareous dunes, that only samples deeper than 0.3-1 m are considered. Attention is paid in succession to the overall mineralogical composition of two types of dune sand, the chemical composition of sea shells, being the most reactive constituent, the much more resistent primary silicates, several secundary phases and some further chemical characteristics.

Mineralogical composition of dune sand from the northern and southern dune district

As stated and discussed in section 3.2.4 and shown on Enclosure 1.1, an important geochemical transition zone is situated in between Egmond aan Zee and Bergen aan Zee. Calcareous, younger dune sands from the southern dune district and the primarily less calcareous, dune sands from the northern dune district meet there, in the former tidal inlet of Bergen.

The mineralogical composition of both dune sands is shown in Table 6.4. Both sands are largely composed of inert quartz grains and, to a lower degree, feldspars. They lack readily soluble minerals like gypsum and halite. The southern, calcareous dune sand contains more plagioclase, calcium carbonate and coatings of ferric hydroxide, whereas the northern dune sand contains a higher fraction of minerals that are very resistant to weathering, like quartz and tourmaline (concentrated in the heavy mineral fraction).

Calcium carbonate

The calcium carbonate is largely present as shells and shell debris. They derive, according to Van Straaten (1965) mainly from the following molluscs : several *Spicula* species, *Cardium edule* and *Macoma baltica*. The majority of the mollusc shells is composed of aragonite, which is corroborated by the chemical composition of cleaned, miscellaneous shell samples from the present beach, from younger dune sand and from underlying old beach sand

TABLE 6.4 Major mineralogical differences between primarily calcareous, yellow dune sands south of Egmond aan Zee, and fair dune sands primarily poor in lime, north of Bergen aan Zee. Data refer to parent material exclusively.

mineral phase (% dry weight)	calcareous dunes	decalcified dunes
quartz	80	91
plagioclase#	7.5	1
K-feldspar#	6.5	6
calciumcarbonate@	4.5	0.2
Σ heavy minerals#	0.3	2
clay minerals	<0.3	-
$Fe(OH)_3$-coatings#	0.34[A]	0.05[B]

= (calculated) from data in Eisma (1968); @ = based on data in Van der Sleen (1912), Bijhouwer (1926), Eisma (1968), Klijn (1981), Rozema et al. (1985); A : Mn/Fe on weight basis = 0.02 (Eisma et al., 1966); B : ditto = 0.01.

(samples 1-4 in Table 6.5) : the relatively high Na, high Sr and very low Mg and SO_4 contents closely correspond with an aragonite crystal lattice (Leutwein & Waskowiak, 1962; Ragland et al., 1979; Busenberg & Plummer, 1985).

The fine fraction of a sample from the present beach had an intermediate Mg content (Table 6.5). This may be connected with a contribution from calcitic foraminifera and echinoid detritus, which is very rich in Mg (1.9%, Leutwein & Waskowiak, 1962). In dune sand, this fraction can be highly reactive by virtue of a high surface to volume ratio. On the basis of the analytical results presented in Table 6.5, the average composition of calcium carbonate in dune sand is given by: $Sr_{0.002}Na_{0.024}Mg_{0.002}Ca(CO_3)_{1.016}(H_2PO_4)_{0.0004}$. It is to be expected that the shell fragments contain considerable amounts of fluoride, aragonite about 1075 ppm and calcite about 320 ppm, either dispersed, in fluoritic or fluoroapatitic parts (Carpenter, 1969). And finally there is some organic matter in the shell fragments, varying in between 0.5 to 4% for fresh shells and from 0.29-0.45% for shells in dune sand (Eisma, 1968). It is visibly released after dissolution experiments (Rijsdijk, pers. comm.). Taking 0.37% as an average amount, a carbon to organic matter ratio of 0.5 and 100% oxidability, would yield an oxygen consumption of 1.2 mg for each 100 mg Ca^{2+}/l dissolved from shell

TABLE 6.5 Chemical composition of (a) mixed samples of shells and shell debris in selected Holocene coastal barrier deposits and in underlying marine Eemian deposits; and (b) two contemporaneous molluscs along the German North Sea coast. The results are expressed for conveniency, in mg/l water in which 250 mg of shell debris was dissolved, leading to 100 mg Ca^{2+}/l. Conversion to mg/kg or µg/kg dry weight by multiplication of mg/l or µg/l with 4000.

n_0	sample description	Na^+	K^+	Ca^{2+}	Sr^{2+}	Mg^{2+}	Fe	Mn	Al	SiO_2	SO_4^{2-}	PO_4^{3-}	I
							mg/l						µg/l
Based on unpublished data from Appelo (Free Univ. Amsterdam)#													
1	fine fraction, present beach Zandvoort	1.3	-	100		0.28	0.28	<0.06	<0.04	<0.6			1.1[A]
2	coarse fraction, present beach Zandvoort	1.6		100		<0.05	0.12	<0.04	<0.03	0.4			-
Based on data in Rijsdijk (1984)##													
3	unsaturated zone Y dunes, mosses-2	2.0	0.10	100	0.58	<0.2	0.16	<0.03	<0.01	<0.3	<0.7	0.10	
4	upper sat zone NS dep, old beach sand	1.3	0.02	100	0.37	<0.02	0.07	0.05	-	0.1	≤0.1	0.15	
5	open marine silty sand, aquitard 1C	1.3	0.02	100	0.40	0.04	0.20	0.03		0.2	0.3	0.26	
6	sandy clay, aquitard 1D	1.0	0.02	100	0.44	0.36	0.25	0.08		0.1	0.5	0.23	-
7	*Ostrea edulis*, Eemian, aquifer II	0.9	0.02	100	0.42	0.21	0.38	0.12		0.3	3.3	0.11	0.1[A]

Based on data in Leutwein & Waskowiak (1962)

		B	Ba^{2+}	Ca^{2+}	Sr^{2+}	Mg^{2+}	Fe	Mn	Co	Cu	Ni	Pb	Zn
			µg/l			mg/l					µg/l		
8	*Cardium edule* (aragonite), Norderney	1	-	100	0.67	0.03	0.04	0.002	0.13	0.5	1.7	0.5	2[B]
9	*Ostrea edulis* (calcite), Sylt	5	8	100	0.38	0.42	0.06	0.007	-	0.6	0.6	0.3	1[B]
10	mean composition 155-378 Molluscs	1	9	100	0.56	0.26	-	0.004	0.50	0.4	0.8	0.2	1.4

= cleaned in aqua dest subject to ultra sone vibrations, dissolved in 0.25 N HNO_3 suprapure within 3 hours; ## = ditto, within 7 hours; A = Heymann, 1925; B = Ernst (1987) beach near Noordwijkerhout, Cd ≈ 1 and Pb ≈ 9 µg/l.

fragments. This makes shell fragments a very moderate yet significant redox buffer.

Significant contents of $MgCO_3$ as magnesite or as a solid solution with calcite (10-15% of $CaCO_3$) in dune sands, as reported by Van der Sleen (1912) and Eisma (1968), are very unlikely for the following reasons : (a) these minerals are preferentially leached with respect to calcite or aragonite in natural environments (Brand & Veizer, 1980) and would result in high Mg^* concentrations in the upper groundwater, which is definitely not the case (Table 6.15); (b) it can be concluded from data in Rijsdijk (1984a), that Mg leaching from dune sand in 0.25 N HNO_3 is very small even after 3 days (≤ 1% of $CaCO_3$); and (c) Van der Sleen and Eisma used warm 20% HCl to extract Mg from dune sand, which probably attacked the Mg contained in silicates.

Primary silicates

The general persistence order of primary minerals in sediments and their concentrations in fresh, calcareous dune sand (Table 6.6), indicate that the following silicates with > 100 mg/kg probably are the main targets of agressive rain water, in order of increasing resistance to chemical weathering : hornblende, anorthite, epidote, granate, albite and orthoclase (K-feldspar).

This coincides fairly well with the selective leaching of mineral assemblages in soils on Pleistocene sandy deposits in The Netherlands as observed by Van der Marel (1949), De Jong (1957) and Pons (1959).

A compilation of trace element analyses of selected silicates is given in Table 6.19. Especially ferromagnesian silicates like hornblende and biotite have a high trace element content.

Secundary phases

This category is composed of clay minerals and ill-crystallized to amorphous phases consisting of Fe- and Al-(hydr)oxides, in dune sand all together < 1% on a dry weight basis. They belong to the most reactive mineral phases by virtue of their presence as coatings, large surface area, porosity and instability. Contrary to most calcium carbonate and primary silicates, they are not only leached but also formed on site, in significant amounts. The majority of the clay minerals probably is allogenic (not formed on site), and therefore composed mainly of illite (30-40%), smectite (30-40%), kaolinite (5-10%) and chlorite (<5-10%), like most Pleistocene aquifers in The Netherlands (Breeuwsma & Zwijnen, 1984; Willemsen, 1984).

From the infinite number of possible, ill-crystallized and amorphous phases, Fe- and Al-hydroxides probably are the most common ones.

TABLE 6.6 Persistence order of identified, primary, mineral constituents of dune sands as deduced from literature, and their concentrations in fresh, calcareous dune sand. From top to bottom : an increasing persistence, which is equivalent to a decreasing sensitivity to chemical weathering.

mineral	chemical composition	PO* [-]	WPI** [-]	MLT@ [years]	conc# mg/kg
aragonite/calcite	$Sr_{.002}Na_{.024}Mg_{0.002}Ca(HCO_3)_{1.016}(H_2PO_4)_{.0004}$	>>21	>>39	$5 \cdot 10^{-3}$	45,000
actinolite	$Ca_2(Mg,Fe)_5Si_8O_{22}(OH)_2$	21	-	-	?
hypersthene	$(Fe,Mg)_2Si_2O_6$	19	-		<110
augite	$Ca(Mg,Fe)_3(Al,Fe)_4(SiO_3)_{10}$	17	39		80
andalusite	Al_2SiO_5	13	-		<110
hornblende	$Ca_3Na(Mg,Fe)_6(Al,Fe)_3(Si_4O_{11})_4(OH)_4$	12	36	-	480
anorthite	$CaAl_2Si_2O_8$	11	25	112	<75,000@
epidote	$Ca_2(Al,Fe)_3Si_3O_{12}(OH)$	11	23	-	450
kyanite	Al_2SiO_5	10	-		50
staurolite	$Al_2SiO_5Fe(OH)_2$	9			3
magnetite	Fe_3O_4	8	-		<3
biotite	$K(Fe,Mg)_3(AlSi_3O_{10})(OH)_2$	5	22		<110
granate	$(Fe,Mn,Ca,Mg)_3(Al,Fe,Cr)_2(SiO_4)_3$	4	-	-	150
albite	$NaAlSi_3O_8$	-	13	$8 \cdot 10^4$	<75,000@
K-feldspar	$KAlSi_3O_8$	-	12	$5 \cdot 10^5$	65,000
tourmaline	$NaFe_2Al_4B_2Si_4O_{19}(OH)$	2	-	-	50
zirkone	$ZrSiO_4$	1	-	-	<3
quartz	SiO_2	0	0	$34 \cdot 10^6$	800,000
rutile	TiO_2	-1	-	-	<3
muscovite	$KAl_3Si_3O_{10}(OH)_2$	-2	-10.7	$3 \cdot 10^6$	<110

* = Persistence Order, according to Pettijohn (1941); ** = Weathering Potential Index, according to Reiche (1943); @ = Mean Life Time of a 1-mm crystal (in years), according to Lasaga (1984), calcite according to Appelo (1988b); # = mean concentration in young dune sand without soil formation on a dry weight basis, compiled by Stuyfzand (1986d) from different sources; @ = all plagioclases together 7.5%.

The bulk of Fe-hydroxides is allogenic (Eisma, 1968). The Fe- and Al-hydroxides, which are well-known as excellent scavengers for many trace elements, may also contain significant amounts of major constituents, either (chemi)sorbed, randomly dispersed or incorporated on well defined positions in the crystal lattice. In the latter case more complex phases arise, of which the following have been recognized elsewhere (Nriagu, 1978; Nordstrom, 1982; Elrashidi & Lindsay, 1986; Bache, 1986) and might form in decalcified dune sand as well and dissolve upon further acidification : ferric-aluminosilicates ($Fe_{1-x}Al_{1-x}(SiO_2)_x(OH)_{6-6x}$), fluorophlogopite ($KMg_3AlSi_3O_{10}F_2$), alunite ($KAl_3(OH)_6(SO_4)_2$), basaluminite ($Al_4(OH)_{10}SO_4.5H_2O$) and jurbanite ($Al(OH)SO_4.5H_2O$).

The sulphate containing phases are supposed to form in primarily SO_4-deficient deposits, like dune sands, under the influence of air pollution and acidification, in soils with pH of 4.2-5, for instance according to reaction 8.24 in Table 8.3 (Ulrich, 1986; Nordstrom, 1982).

It is well-known from geochemistry (Wedepohl, 1978) and water technology (Reichert et al., 1972) that the following TEs are strongly associated with $Fe(OH)_3$ and $Al(OH)_3$: As, B, Co, Cr, Mn, Mo, Ni, Sb, Se, U, V, W and Zn.

Some further chemical characteristics

Total concentrations of the elements C, N, P and S are shown for calcareous dune sand in Table 6.8. They are very low, and in the less calcareous dune sand probably even lower. The cation exchange capacity (CEC) is about 6 - 10 meq/kg dry weight, with a base saturation of about 100%. Total concentrations of several trace elements are listed in Table 6.7. The contents observed in deep dune sand without soil formation, correspond well with the concentrations calculated on the basis of the sum of the individual constituents of dune sand, using data on trace elements for calcium carbonate from Table 6.5 and for silicates from Table 6.19. There is, however, a remarkable deviation for Ba and Cu, both being about 10 times too low in our observations. This might point at losses from dune sand by leaching. Concentrations of all 16 EPA-PAHs were below their individual detection limit of 0.01 mg/kg dry weight, at >0.7 m below the surface (Lüers & Stuyfzand, 1992).

6.4.2 *Dune sand in the soil zone*

The main soil forming processes in calcareous dunes consist of the accumulation of organic matter and decalcification (section 3.2.4). Their effects are illustrated in Fig.6.9 by measurements on samples from four borings perpendicular to the coastline, west of Hillegom. The first boring is situated at 0.8 km from the HWL in an about 200 y old landscape, and the ultimate boring was completed at 3.2 km inland, in the older dune area with an estimated age of about 3500 y. With increasing distance to the HWL, and thereby a more or less progressive age of the landscape, the depth of decalcification increases, while pH and the base saturation (=100 {CEC - Al - H}/CEC) decrease within the decalcified zone. With increasing depth below the surface there is a general decline in soil organic matter, CEC and the amount of adsorbed H^++Al^{3+}, and a rise in pH, lime content and base saturation.

The base saturation of the adsorption complex clearly depends on soil pH, the depth below the surface and the distance to the HWL (Fig.6.10). A low pH, shallow depth below the surface and a high distance to the HWL conduce to a low base saturation. The length of the leaching period is a

TABLE 6.7 Mean total concentrations of trace elements in dune sand, in younger dunes west of Hillegom in 1992, and in four dune areas in the period 1973-1991. The shallow samples are probably influenced by a significant atmospheric contribution of Cd, Hg, Pb and Zn. The calculated backgrounds correspond well with observations on deep samples, regarding As, Co, Mo, Ni, Pb, Sn and Zn. They also reveal a possible, natural leaching of Ba and Cu.

	$CaCO_3$ %	OM %	As	Ba	Cd	Co	Cr	Cu	Hg	Mo	Ni	Pb	Sn	Zn	n
							mg/kg d.w.								
5-20[1]	<0.1	7.7	5	7	0.21	0.9	9.1	2.0	0.043	0.23	2.6	25.9	0.4	311	11
75-185[1]	2.8	0.5	2	5	0.01	1.0	7.6	0.3	0.004	0.05	3.3	2.3	0.3	10	3
background[2]	4.5	0.1	2	4	<0.05	<1	2	0.8	<0.05	<1		2		6	10
calc. backgr.[3]	(4.5)	-	1.5	55	?	1.1	?	3.9	?	0.4	2.2	5	0.6	7	-

1 = dune sand at indicated depth (in cm below surface), in the Luchterduinen area, west of Hillegom (data derived from Lüers & Stuyfzand, 1992); 2 = natural background for dune sand without soil formation (parent material), mean value for 4 dune areas; 3 = calculated natural background (parent material), by summing up the individual contribution of the various silicates (Table 6.19) and $CaCO_3$ (Table 6.5) : 0.8 quartz + 0.075 plagioclase + 0.065 K-feldspar + 0.045 calcite/aragonite + 0.001 hornblende (as an exponent of ferromagnesian silicates).

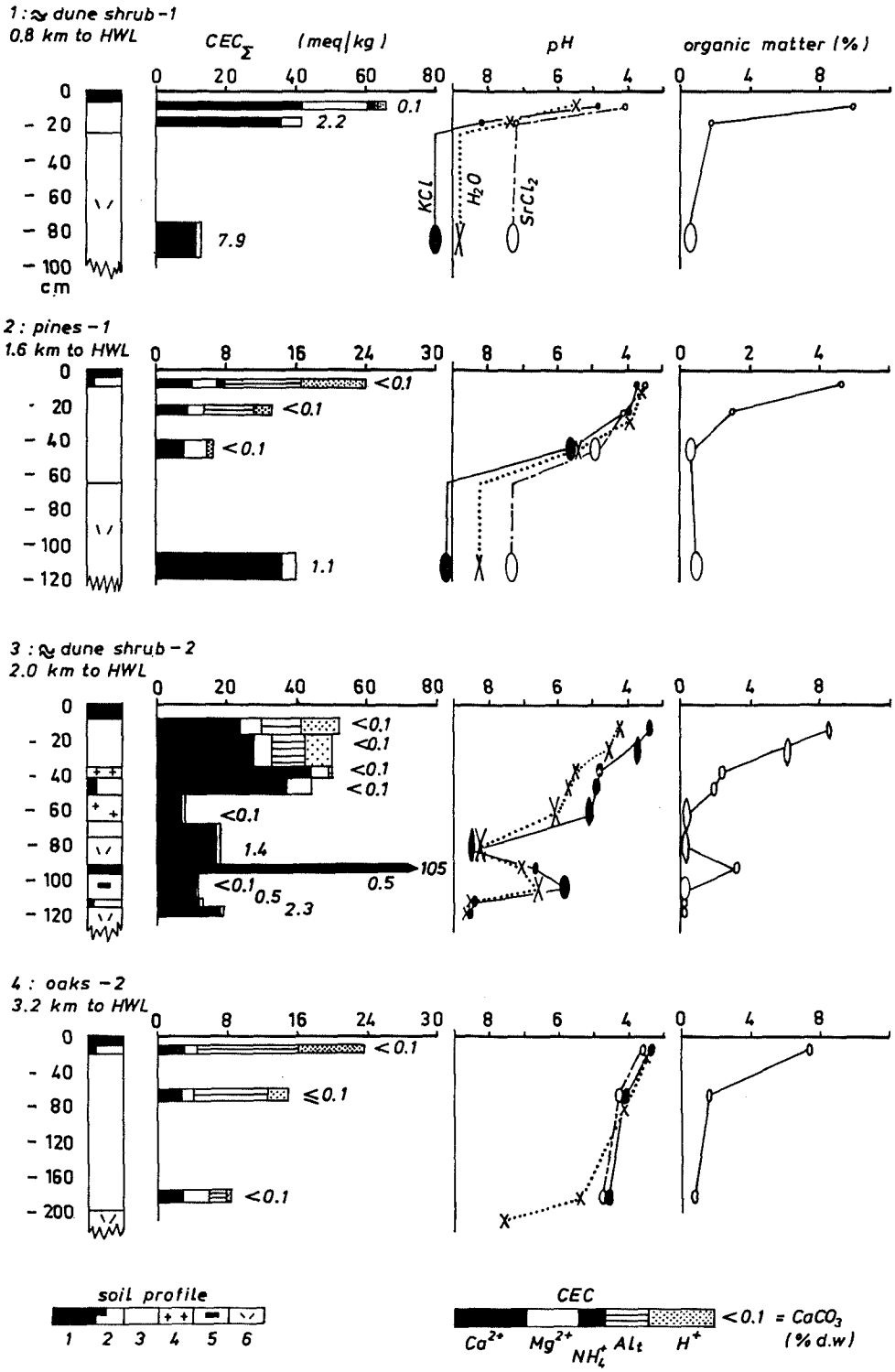

FIG. 6.9 Chemical profiles of dune soil and underlying parent material, on four locations at increasing distance to the HWL, in the dunes west of Hillegom in March 1992 (data of boring 3 derive from Perdijk, 1992). The increasing distance is accompanied by an increasing age of the landscape and, consequently, a deeper decalcification and lower base saturation of the adsorption complex. Also the amount of soil organic material increases inland, which can be inferred from the soil column description. CEC_Σ = sum of the individual ions adsorbed (extraction with 0.05 M $SrCl_2$ without pH regulation).

Soil column : 1 = litter, humus and sod, or buried soil; 2 = sand containing many roots and humus; 3 = decalcified sand (HCl field-test); 4 = sand with Fe mottling; 5 = sand with peat; 6 = calcareous sand.

very important factor, as shown by the pH relation : a pH-$SrCl_2$ of about 4.2 yields an average base saturation of 32, 80 and 97% for samples at 2-4, 1-2 and 0-1 km from the HWL, respectively (Fig.6.10). Further details on decalcification rates, the reduction of the base saturation of the adsorption complex and podzolization are given in section 6.8.4.

An interesting detail, which remained unnoticed as far as I know although there are clear but undiscussed indications in publications by Dahmke et al. (1986) and Hansen (1992), is formed by the behaviour of Mg^{2+} in the lower parts of the decalcified zone, where Al and H^+ are actively displacing Ca^{2+} and Mg^{2+} from the exchanger (Eq.8.22 in Table 8.3, with NH_4^+ low). The Mg^{2+} saturation of the adsorption complex shows an optimum in that exchange zone, where pH (both in H_2O and KCl or $SrCl_2$ solution) varies in between 4.3 and 6.2. The position of the Mg^{2+} peak is observed at pH-$SrCl_2$ = 4.8 (Fig.6.10), pH-KCl = 5.2 and pH-H_2O = 5.2 (Stuyfzand & Lüers, 1992b). An anomalously high Mg^{2+} adsorption in this zone was also inferred from column experiments, where five 20 cm slices of a decalcified dune soil profile were flushed individually with a $Ca(HCO_3)_2$ solution (Stuyfzand & Lüers, 1992b).

The phenomenon is thus localized close to the Al^{3+}+H^+ front and is tentatively explained by (a) a reduced mobility of Mg^{2+} in this zone, and (b) an increased mobilization above the Al^{3+}+H^+ front. To begin with the latter, after decalcification the most labile silicates become the target of the unbuffered, agressive soil solution. Ferromagnesian silicates belong to the most vulnerable category (Table 6.6), and may therefore supply the additional Mg^{2+}. This Mg^{2+} is then partly arrested (see also section 6.6.4) close to the Al^{3+}+H^+ front, probably by displacing Ca^{2+} from the exchanger. A reversal of the normal Mg^{2+}/Ca^{2+} selectivity (Ca^{2+} being preferred on the exchanger) would accentuate the Mg^{2+} adsorption.

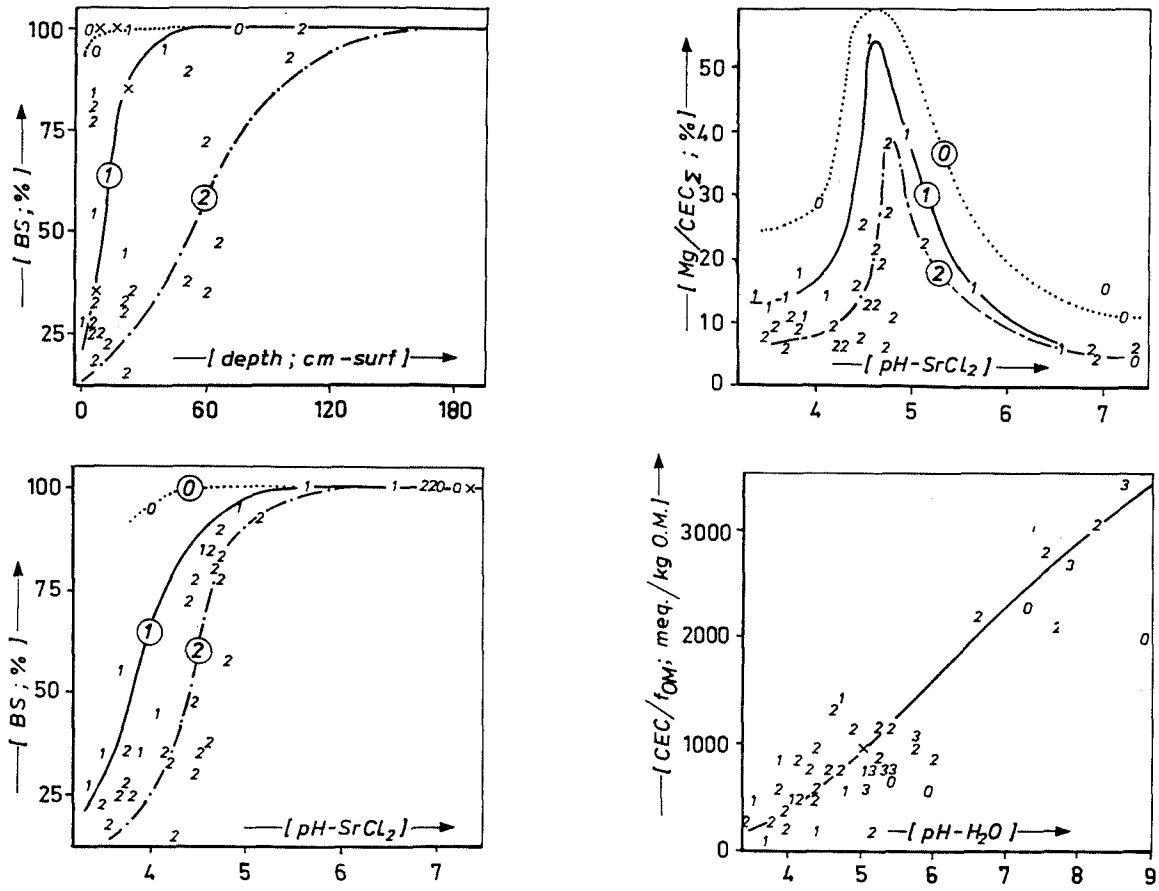

FIG. 6.10 Relations between the base saturation of the adsorption complex (BS) with depth below the surface and pH-$SrCl_2$, between the Mg^{2+} saturation of the adsorption complex (Mg^{2+}/CEC_Σ) and pH-$SrCl_2$, and between the computed CEC of the organic soil fraction ($CEC\Sigma/f_{OM}$) and pH-H_2O. The plotted digits indicate the distance of the sample locality to the HWL : 0 = 0-1 km; 1 = 1-2 km; 2 = 2-4 km; 3 = 4-8 km; x = >1 sample at this position. Based on 50 samples in the dunes west of Hillegom, taken in March 1992.

The higher, atmospheric Mg^{2+} input close to the HWL is reflected in an overall raised Mg^{2+} saturation of the adsorption complex (Fig.6.10).

The computed CEC of soil organic matter strongly depends on pH (Fig.6.10), roughly according to : $(CEC/f_{OM}) = 600\ pH - 2060$, in meq/kg OM. This approaches relations established elsewhere (Scheffer & Schachtschabel, 1970), and is explained by a pH variable charge of soil organic matter.

Mean total concentrations of heavy metals in the upper 5-20 cm of dune soils (litter, humus and sod excluded) are shown in Table 6.7. Compared with the contents in the parent material, there is a remarkable accumulation of Cd, Hg, Pb and Zn (>5 times higher). Atmospheric pollution probably constitutes their main source (section 5.3.5), which is corroborated by relatively high concentrations of several PAHs (mean sum of concentration of the 16 EPA-PAHs = 0.5 mg/kg; Lüers & Stuyfzand, 1992b).

6.4.3 Dune peat

Dune peat occurs as a discontinuous intercalation in dune sand, marking the former position of a primary dune valley, wet dune slack or forest floor. Dune peat is composed mainly of plant remains typical for meso- to eutrophic growth conditions (*Carex, Alnus, Phragmites*; Jelgersma et al., 1970). It constitutes aquitard 1A (Table 3.1). Little is known about the chemical composition of the meso- to eutrophic dune peats. Their concentration of organic matter (O.M.) is relatively low for peat (50%), due to aeolian admixing of sand (Rutgers Van Rozenburg et al., 1891). Concentrations of organic carbon (as humic substances mainly) and total nitrogen, phosphorus and sulphur were estimated from literature, accounting for the lower O.M. contents (Table 6.8). These levels are high as compared to dune sand and the upper A_1 horizon from dune soils. Inferred diagenetic changes of the O.M. in anoxic peat include losses of H_2O, N and P relative to organic carbon and relative gains in S (Table 6.8). The latter relates to sulphate reduction followed by the precipitation of iron sulphides (Shotyk, 1988). Mineral concretions of vivianite ($Fe_3(PO_4)_2 \cdot nH_2O$) in dune peat were noticed by Van der Sleen (1912), whereas the occurrence of siderite ($FeCO_3$) and rhodochrosite ($MnCO_3$) or a manganous siderite has been described in other peat deposits by Shotik, 1988.

Eutrophic peats are known to contain significantly higher concentrations of most TEs as compared to sandy soils (Edelman, 1983). This holds in particular for the chalcophile elements As, Cd, Cu, Hg, Pb and Sb, and the more hydrophile elements Br^- and I. It does absolutely not pertain to the lithophile TEs (see Table 1.1), like Ba, Cr, Ti, U and V.

TABLE 6.8 Chemical composition of dune sand without soil formation, present inceptisols in calcareous dune valleys, and dune peat.

		dune$^{\alpha}$ sand	dune$^{\beta}$ soils	dune$^{\gamma}$ peat
O.M.	% d.w.	0.2	10	50$^{\delta}$
$C_{organic}$	% d.w.	0.1$^{\varepsilon}$	4	28
N_{total}	mg/kg d.w.	20	4,000	14,000
P_{total}	mg/kg d.w.	82$^{\iota,\varepsilon}$	300	500$^{\pi}$
S_{total}	mg/kg d.w.	<10	240$^{\kappa}$	3000$^{\mu}$
C.E.C.	meq/kg d.w.	7	300$^{\lambda}$	1500$^{\lambda}$
C/N-molal	-	23	12	23
N/P-molal	-	0.5	30	62

α = parent material; β = upper 0.05 m from A_1 horizon (calculated from data in Nijssen (1989) and Louman (1989)); γ = based on data in Göttlich (1980) and Van Smeerdijk (1989); δ = Rutgers Van Rozenburg et al. (1891); ε = Stuyfzand et al. (1991), Stuyfzand & Lüers (1992b); ι = Oosterhout et al. (1982); κ = Fiedler & Thakur (1984), 85% organic; λ = calculated using CEC = %clay + 3·(%OM); μ = 90% organic, 10% bound to $FeS_{(2)}$; π = Sapek et al. (1984).

6.5 Changes "en route" from rain water to the upper dune waters

6.5.1 Review of processes

On its way to the groundwater table, rain water has to pass several important zones (Fig.6.1), where its chemical composition markedly changes. The most important processes, that effectuate the chemical metamorphosis of rain water into the upper groundwater, are :

(1) evapotranspiration, by interception, soil evaporation and plant transpiration (Table 3.3), which leads to a concentration increase for the remaining solution with a factor varying on the plots studied in between 1.3 (bare dune sand) and 5.8 (pines) on a mean annual basis (Table 6.1);

(2) interception deposition (ID), defined as the additional deposition compared with bulk precipitation (in the open), of marine and continental aerosols and gases such as SO_2, NO_x and HF (Mayer & Ulrich, 1974; Eaton et al., 1978; Ulrich, 1983). In other words, ID is the total dry deposition minus the dry deposition on a bulk precipitation collector;

(3) filtration of matter suspended in rain water;

(4) nitrification of ammonium, which is favoured among others by a lack of decalcification and soil temperatures above 5°C;

(5) preferential uptake of dissolved ions (mainly K^+, NH_4^+, NO_3^- and PO_4^{3-}) during the growing season, with storage as long as biomass is accumulating. This also holds to a less extent for Ca^{2+}, Mn, Mg^{2+}, Fe, SO_4^{2-} and SiO_2, but it strongly depends on soil chemistry. The uptake is postulated to be counteracted by a concentration increase for Al, Cl^- and Na^+ in soil moisture around the roots (Prenzel, 1979). The selectivity thus results in a relatively low biological (nonatmospherical) contribution of above ground vegetation and litter to the concentration of these ions in litter leachate (Ulrich et al., 1979). The exclusion of Cl^- and Na^+ from uptake is, however, not perfect (Ernst, 1990b). Selective retranslocation processes prevent nutrients to be lost and thereby lead to storage, whereas non-essential elements accumulate in senescent leaves and are eliminated upon leaf fall (Ernst, 1990a);

(6) production of inorganic carbon (CO_2, HCO_3^-; Witkamp & Frank, 1969; Reardon et al., 1979; Matthess, 1990) and organic carbon compounds (Smith, 1976; Pekdeger, 1979; Kuiters, 1987) through photosynthesis, respiration and decomposition;

(7) in specific cases an indirect production of nitrate through N_2 fixation by (symbiotic) bacteria, especially in the root nodules of sea buckthorn (*Hippophaë rhamnoides*) and legumes (*Torfelium* species, *Lotus corniculatus*), or by blue green algae, in bare dune sand for instance;

(8) release of nutrients during decomposition of organic matter in the litter layer (mainly PO_4^{3-}, NO_3^- and K^+, to a less extent Ca^{2+}, Mg^{2+} and Mn, and also some SO_4^{2-}), especially by the end of the growing season and after reaching the climax stage in growth. Oxygen and, depending on aeration, also NO_3^- and SO_4^{2-} are consumed during this mineralization and their concentration in soil moisture may thus decrease. However, during decomposition of organic matter poor in N and P, the microflora may temporarily also accumulate nutrients (W. Koerselman, pers. comm.);

(9) exchange reactions with vegetation, dead biomass and mineral soil, which among others lead to retardation in reaching the water table for those constituents of atmospheric deposition, that have been raised by pollution, like SO_4^{2-} (retained in acid soils only), F^-, Cd, Cu, Ni, Pb, Sb, V and Zn;

(10) dissolution of atmospheric aerosols, that were filtered in the upper soil layer, and of mineral constituents of the soil, like the primary minerals calcite, anorthite, hornblende, epidote, augite and biotite, and secundary minerals such as ferric and aluminium hydroxides, clay minerals and iron sulphides. The sulphides are generally oxidized after a drawdown of the water table;

(11) precipitation of minerals, for instance calcite upon desiccation of dune sand in summer, or aluminium hydroxisulphates like jurbanite in acid soil horizons with a high SO_4^{2-} load;

(12) mineralization of ancient organic matter, dispersed in dune sand or intercalated as a palaeosol or peat layer, especially after a drawdown of the water table;

(13) leaching of fertilizers, compost, animal manure or litter, added to natural dune soils in order to stimulate growth of pines and oaks or to cultivate potatoes; and

(14) dispersion and to a less extent diffusion, that lead to the smoothing of quality fluctuations.

6.5.2 The changes, in a bird's-eye view

The change in (weighted) mean composition of water "en route", from rain water (as bulk precipitation in the open) towards the upper groundwater, is shown for the plots mosses-1, dune shrub-1, oaks-2 and pines-3 in Table 6.9 and Fig.6.11. Comparison of the data presented for bulk precipitation, litter leachate, soil moisture and shallow groundwater, permits qualitative conclusions to be drawn mainly, on account of the following drawbacks : (a) the number of monitoring facilities for each compartment was too low to obtain a reliable estimate of annual means on each plot; (b) the sampling period for the relatively old, upper groundwater differs from that for the younger water in the compartments above; and (c) the sampling period was too short for soil moisture on all plots and for litter leachate on pines-1.

The materials and methods regarding the monitoring of throughfall, litter leachate and soil moisture, are described by Stuurman (1984a). Stemflow is not considered here by lack of data. However, the contribution of stemflow to the total flux of solutes to groundwater can be neglected for the vegetation types considered in Table 6.9 (Ivens et al., 1989; footnote in Table 3.3).

Nonetheless it can be concluded from the data presented, that concentrations of most ions in bulk precipitation increase upon passage of the vegetation canopy as throughfall or properly speaking crown-drip (mosses-1 not measured), and increase still further after percolation through the litter layer. The so-called litter leachate is depleted in most nutrients (K^+, PO_4^{3-}, NO_3^-, NH_4^+, Mn) by uptake upon passage of the intensively and extensively rooted and mycorrhized unsaturated zone. This uptake seems to keep pace fairly well with the release by the litter layer, thereby illustrating the concept of nutrient cycling. Nitrate, however, is leaking significantly down to the groundwater below mosses-1, dune shrub-2 and oaks-2, due to a raised atmospheric deposition.

Other changes in the unsaturated zone imply a further increase of : Al in the upper decalcified soil

TABLE 6.9 Weighted mean composition of bulk precipitation (open-field), throughfall, litter leachate and soil moisture, and arithmetic mean composition of shallow groundwater as measured in the upper miniscreen, at four monitoring plots with different vegetation cover. Based on own measurements regarding all groundwaters and bulk precipitation on mosses-1, on measurements regarding the lysimeter under pines-3 by Berhane & Van de Coevering (1987) and for the remaining part on observations reported by Stuurman (1984a).

period	depth cm + surface	sampling period yymm-yymm	n_o samples	water flux mm	EC 20°C µS/cm	pH	Cl^-	SO_4^{2-}	HCO_3^-	NO_3^-	PO_4^{3-}	Na^+	K^+	Ca^{2+}	Mg^{2+}	NH_4^+	Fe	Mn	SiO_2	Al	F^-	SI_c	TIN	water-type µmol/l
							mg/l													µg/l				
MOSSES-1																								
bulk precipitation	150	8101-8201	24	795	153	4.22	39	9	0	4.0	0.08	20.3	0.9	2.1	2.5	0.96	0.07	0.02	0.3	-	49	<-6.0	121	F.NaCl.
soil moisture, plate	-5	8210-8211	1	-	160	3.94	14	15	0	9.4	0.39	9.5	2.3	10.7	2.3	0.14	0.05	<0.01	0.7	73	57	<-6.0	159	F.$CaSO_4$.
soil moisture, plate	-10	8206-8210	3	-	246	7.24	30	23	58	16.9	0.61	17.9	2.8	33.4	3.1	0.30	0.08	0.01	1.5	77	-	-1.1	568	F_0CaMix.
groundwater α	-200	8009-8301	16	520	451	7.83	52	30	136	38.6	0.20	28.6	2.6	60.0	7.3	<0.10	<0.10	<0.10	4.0	<20	220	0.1	694	F_2CaMix.
DUNE SHRUB-1																								
bulk precipitation	30	8202-8302	12	790	95	4.23	19	9	0	3.9	0.04	10.7	0.7	2.1	1.8	0.79	0.05	0.02	0.2	72	32	<-6.0	105	f.NaCl.
throughfall	20	8202-8302	12	630	256	4.07	60	19	0	5.3	0.05	32.9	2.7	5.8	5.4	1.77	0.15	0.04	0.3	130	89	<-6.0	183	F.NaCl.
litter leachate	-5	8206-8210	4	-	524	6.73	41	41	43	91.5	2.03	38.2	22.1	56.7	7.6	0.32	0.16	0.02	5.1	98	144	-1.6	1494	$F_0$$CaNO_3$.
groundwater β	-200	7911-8301	23	380	744	7.77	121	55	162	52.4	0.09	68.1	1.5	89.0	6.3	0.09	<0.20	<0.08	7.6	<20	57	0.2	597	F_2CaMix.
OAKS-2																								
bulk precipitation	30	8202-8302	12	734	67	4.24	12	7	0	3.6	0.05	6.4	0.6	1.8	0.9	0.91	0.09	0.03	0.2	92	34	<-6.0	119	f.NaCl.
throughfall	20	8202-8302	12	526	132	4.40	23	19	3	7.0	1.76	12.1	4.8	2.7	2.6	2.85	0.09	0.19	0.3	89	78	<-6.0	271	f.NaCl.
litter leachate	-5	8203-8202	11	400	386	3.73	39	64	0	76.4	12.35	18.2	14.5	16.3	8.4	10.64	0.39	1.41	5.4	305	103	<-6.0	1822	F.$CaSO_4$+
soil moisture, plate	-10	8210-8211	3	-	245	3.87	24	50	0	39.0	3.10	12.4	10.0	11.7	6.6	2.24	0.91	2.97	6.0	740	96	<-6.0	753	f.$CaSO_4$+
soil moisture, cup	-100	8203-8206	4	-	515	<4.0	97	-	0	20.1	0.56	21.8	8.7	12.6	6.0	1.18	0.40	0.89	-	3700	231	<-6.0	390	F.CaCl-
groundwater γ	-410	8006-8301	12	310	571	7.59	66	63	193	13.2	0.05	31.9	2.1	83.0	12.2	0.06	0.40	<0.09	11.1	<20	215	0.1	215	F_2CaMix.
PINES-3																								
bulk precipitation	150	8202-8302	12	728	71	4.28	14	7	0	3.6	0.05	7.7	0.5	2.2	1.1	0.77	0.10	0.02	0.1	101	31	<-6.0	101	f.NaCl.
throughfall	20	8202-8302	12	351	252	4.27	48	36	0	14.0	1.76	23.3	8.8	4.8	4.7	7.13	0.08	0.14	0.4	159	163	<-6.0	621	F.NaCl.
litter leachate	-10	8203-8302	11	85	715	4.24	148	100	0	32.6	2.76	76.5	14.3	24.1	15.5	16.34	0.31	0.47	1.5	450	320	<-6.0	1432	F.NaCl.
soil moisture, lys	-19	8411-8504	7	70	598	7.23	41	65	271	70.4	0.04	-	-	-	-	1.20	-	-	-	-	-	-	1202	-
groundwater δ	-300	8004-8301	13	200	959	7.15	117	91	392	1.3	0.06	73.9	1.2	150.0	8.2	<0.05	0.50	<0.08	6.9	<20	192	0.2	95	F_3CaHCO_3

α = 24H.470+0.8; β = G+0.3; γ = V+0.2; δ = IV+4.0; yymm = year-month.

(especially on oaks-2), by dissolution of aluminium hydroxides and silicates; Ca^{2+} and HCO_3^- in calcareous dune sand below the $CaCO_3$ leaching zone, by dissolution of shell debris; and SiO_2 by dissolution of biogenic opal (phytoliths and diatom skeletons), aluminium silicates and probably some quartz as well. A decrease can be stated for F^- likely by adsorption, and for dissolved organic carbon (as deduced from oxygen consumption by $KMnO_4$ in Fig.6.30) by adsorption, precipitation and oxidation.

An increase for Na^+, Cl^- and SO_4^{2-} in the rooted parts under dune shrub, oaks and pines, by a selective exclusion from uptake and retranslocation processes, cannot be deduced unambiguously from the data presented, due to the high susceptibility of these constituents to the drawbacks mentioned above. More details about the composition and fluxes for throughfall, litter leachate and soil moisture are given in the next sections, together with further interpretations.

6.5.3 Throughfall

Mean composition

Throughfall consists of direct throughfall and canopy drip. Its composition is determined mainly by the composition of bulk precipitation, evaporation losses by interception, interception deposition (defined in section 6.5.1), and interactions with the canopy (Parker, 1983). These interactions are composed of : an excess of leaching of ions from the canopy over foliar uptake and binding during the growth season (Ca^{2+}, Mg^{2+}, K^+, Mn, PO_4^{3-}); leaching of senescent leaves before leaf fall (Na^+, K^+, Ca^{2+}, Mg^{2+}, Cl^- and SO_4^{2-}); precipitation of dissolved elements (Al, heavy metals) and their subsequent (partial) dissolution; foliar uptake into the metabolism of cells (principally NH_4^+); and detention of dust particles (Ulrich, 1983). Also the leaching of animal excretions on leaves and twigs should be important, for instance bird droppings (section 5.3.4) and the honey dew excreted by aphids (Van Hook et al., 1980).

The weighted mean composition of throughfall on the plots dune shrub-1, oaks-2 and pines-3, as measured by Stuurman (1984a), is shown in Table 6.9 and Fig.6.11. It can be concluded from the results presented, that throughfall on these plots exceeds bulk precipitation in the concentration of practically all ions. This cannot be attributed to evaporation alone, because there is a significant, positive difference in ion fluxes between throughfall and bulk-precipitation (Table 6.10).

The results in Table 6.10 reveal, that the canopy of pines-3 is most effective and the canopy of dune shrub-1 least effective in (a) the interception of water and gases (see SO_4^{2-} and NO_3^-), (b) release of K^+, Mn and PO_4^{3-}, and (c) uptake of H^+, Fe and Al.

Dune shrub-1 intercepts more sea spray than the plots oaks-2 and pines-3, which is explained by its proximity to the HWL and its shrub structure (Sloet van Oldruitenborgh, 1976). Fluxes of Fe, Al and Ca^{2+} in throughfall under dune shrub-1 exceed those in bulk precipitation and those in throughfall on the plots oaks-2 and pines-3 (Table 6.10). This may point at dissolution of intercepted dust particles, which is promoted by the reduced interception losses of water and a relatively low pH.

Seasonal fluctuations

Seasonal fluctuations in the composition of throughfall on the plot oaks-2 are shown in Fig.6.12, together with those for bulk precipitation, litter

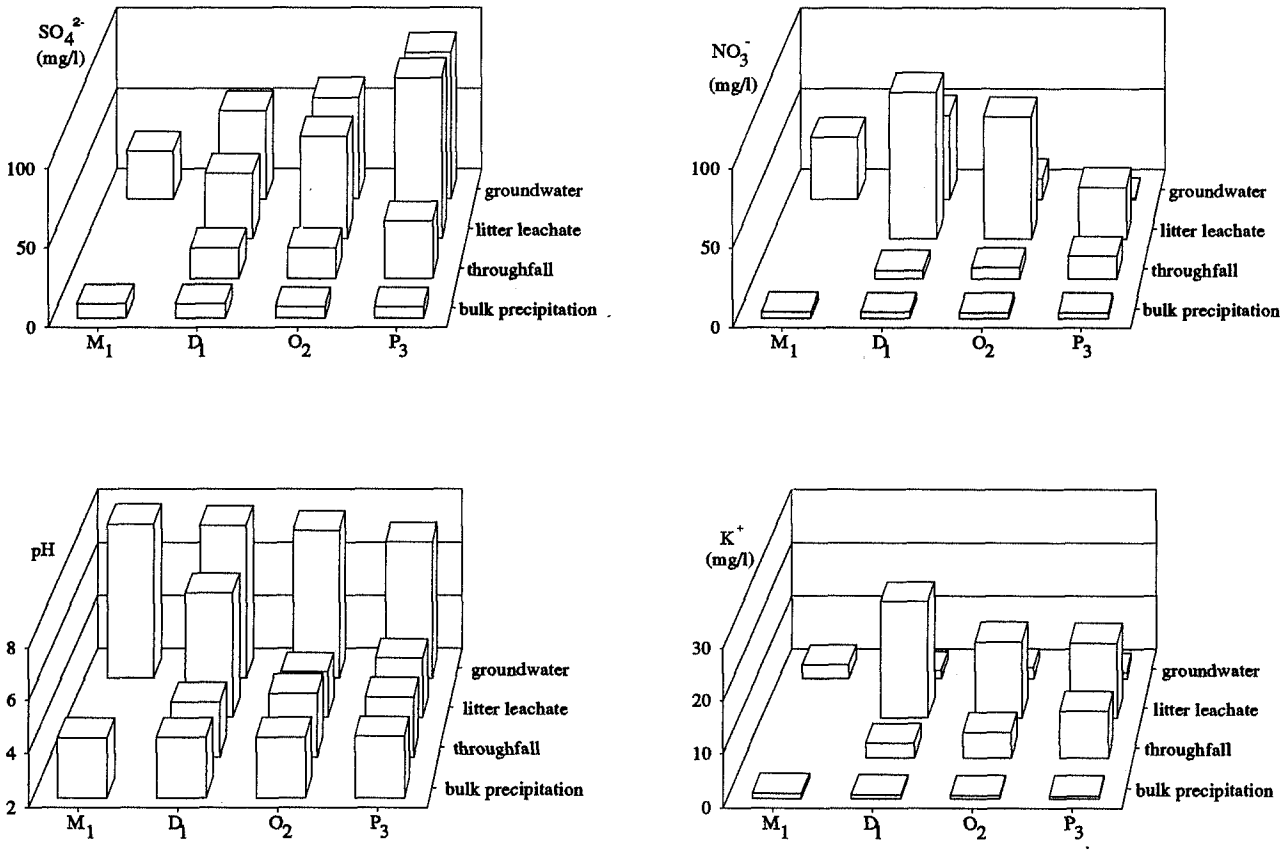

FIG. 6.11 An impression of the chemical changes of rain water on its way to shallow groundwater (<1 m below the water table), at the monitoring plots mosses-1 (M_1), dune shrub-1 composed mainly of Hippophaë rhamnoides (D_1), oaks-2 (O_2) and pines-3 (P_3). Based on data in Table 6.9. Passage of the vegetation canopy as throughfall and percolation through the litter layer yield a substantial increase of sulphate, nitrate and potassium by evaporation (all), interception deposition (SO_4^{2-} and NO_3^-) and leaching of leaves and mineralization of litter (NO_3^- and K^+). Hippophaë excells in the highest concentrations of NO_3^- in litter leachate and groundwater (related to N_2 fixation), and pines (Pinus nigra ssp. nigra) in the highest concentration of SO_4^{2-} (by evaporation and interception deposition) and lowest NO_3^- concentration in groundwater (by uptake). As the litter leachate passes through the rooted unsaturated zone, K^+ and NO_3^- are preferentially withdrawn from the water phase again. This nutrient cycling performs well with respect to K^+. NO_3^- is leaking to a much higher degree to the groundwater zone, because of a raised atmospheric deposition. Passage of the lower boundary of the $CaCO_3$ leaching zone above the water table and rapid equilibration with shell debris lead to a high pH in groundwater on all plots.

TABLE 6.10 The impact of canopy interception and canopy leaching as demonstrated by the difference in the ion fluxes between throughfall and bulk precipitation (in the open) on the plots dune shrub-1, oaks-2 and pines-3, during a one year period (February 1982 - February 1983), summer (11 May till 6 October 1982, 148 d) and winter (24 January till 14 April 1982 plus 23 November 1982 till 23 February 1983, 141 d). Calculated from data listed in Stuurman (1984a). Positive values indicate an addition from the canopy, negative values indicate storage or losses in the canopy. X^* = X corrected for a contribution of air-borne sea salts .

period	Cl^-	SO_4^{2-}	HCO_3^-	NO_3^-	PO_4^{3-}	H^+	Na^*	K^*	Ca^*	Mg^*	NH_4^+	Fe	Mn	SiO_2	Al	F^-	H_2O
	mg/m²/d														µg/m²/d		mm/d
DUNE SHRUB-1																	
summer	32.9	5.8	0	2.2	0.04	0.03	-1.3	4.5	6.6	0.8	1.68	0.24	0.03	0.2	72	60	-0.35
winter	87.7	3.3	1	0.4	-0.03	0.19	0.9	0.6	4.1	2.3	1.16	0.17	0.05	0.3	52	132	-0.20
year	62.4	4.6	0	0.7	0.00	0.02	-1.1	1.9	4.2	1.3	1.35	0.15	0.03	0.1	69	84	-0.44
OAKS-2																	
summer	2.1	18.9	8	6.1	3.35	-0.04	0.2	8.5	-1.6	1.5	3.21	-0.06	0.18	0.1	-24	49	-0.48
winter	2.0	9.4	2	-0.3	1.34	-0.04	0.1	2.4	0.9	1.0	1.70	-0.01	0.22	0.1	-160	27	-0.84
year	9.0	12.0	5	2.8	2.44	-0.06	-0.4	5.5	0.1	1.3	2.28	-0.05	0.21	0.1	-57	44	-0.57
PINES-3																	
summer	12.7	14.8	9	11.3	1.92	-0.04	-1.8	10.1	-3.8	1.1	6.29	-0.29	0.06	0.2	-63	85	-0.92
winter	9.1	18.1	-3	1.4	1.05	-0.03	-4.2	2.6	1.7	1.0	4.13	-0.01	0.12	0.0	-107	82	-1.51
year	18.2	18.1	-	6.3	1.59	-0.05	-3.1	7.1	-0.1	1.1	5.32	-0.12	0.09	0.1	-49	95	-1.08

leachate and the upper groundwater. Those for the air-borne sea salts Cl^-, Na^+ and Mg^{2+} (Cl^- shown only), and for SO_4^{2-} more or less parallell their fluctuation pattern in bulk precipitation. The major plant nutrients K^+, NO_3^-, NH_4^+ and PO_4^{3-} (K^+ and NO_3^- shown only) and SiO_2 (not shown; to be considered as a chemical element sustaining the leaf and shoot structure) deviate strongly in their fluctuation pattern from bulk precipitation, by a remarkable increase during the flourishing season and subsequent fall. This is related to exudation, foliar exchange and leaching. The fluctuation patterns described, also hold for the plots dune shrub-1 and pines-3, as can be deduced from the data listed in Stuurman (1984a).

Changes in the flux of dissolved compounds in throughfall on the plots dune shrub-1, oaks-2 and pines-3 as compared to bulk precipitation, are listed for summer and winter separately, in Table 6.10. The throughfall flux minus the bulk precipitation flux is called here for simplicity the "canopy's flux contribution". The summer period is defined in this context as the overall flourishing season (May till October) and the winter period as the season without leaves or with a strongly reduced growth (mid-November till mid-April).

The canopy's flux contribution evidently depends on the season : during summer it is remarkably higher (more positive) for the nutrients PO_4^{3-}, K^+, NH_4^+ and NO_3^-, and for SiO_2 (dune shrub excluded), in accordance with their concentration pattern discussed above. This pattern does not hold for Mn, contrary to observations by Verstraten et al. (1984) regarding forests on acid soils in the eastern Netherlands. A deciduous vegetation (dune shrub-1 and oaks-2) intercepts more continental sulphate (SO_4^*) during summer, mainly thanks to a higher reactive surface offered by its leaves. The evergreen pines, however, intercept more SO_4^* in winter, as expected from the seasonal SO_4^{2-} fluctuation in precipitation (Fig.5.8).

The canopy of oaks and pines behaved quite differently over the seasons as compared to the canopy of dune shrub, mainly regarding the air-borne sea salts, F^-, Ca^*, Mg^{2+}, Fe, SiO_2 and water. Most water was intercepted during winter by pines and surprisingly by oaks as well, which agrees with observations on the lysimetric plots by Dolman & Oosterbaan (1986). A relatively effective interception of snow and lower rainfall intensities in winter might explain the curious behaviour of oaks.

Another curiosity is offered by the low interception deposition of air-borne sea salts in winter by pines, when we consider the normal seasonal pattern of these sea salts in bulk precipitation (Fig.5.8). This can be explained by exclusion of the stormy months October and November in the winter period considered here. The last curiosity is the foliar retention of Ca^{2+} by oaks and pines in summer, which contrasts with observations by Verstraten et al. (1984) regarding forests on acid soils in the eastern Netherlands.

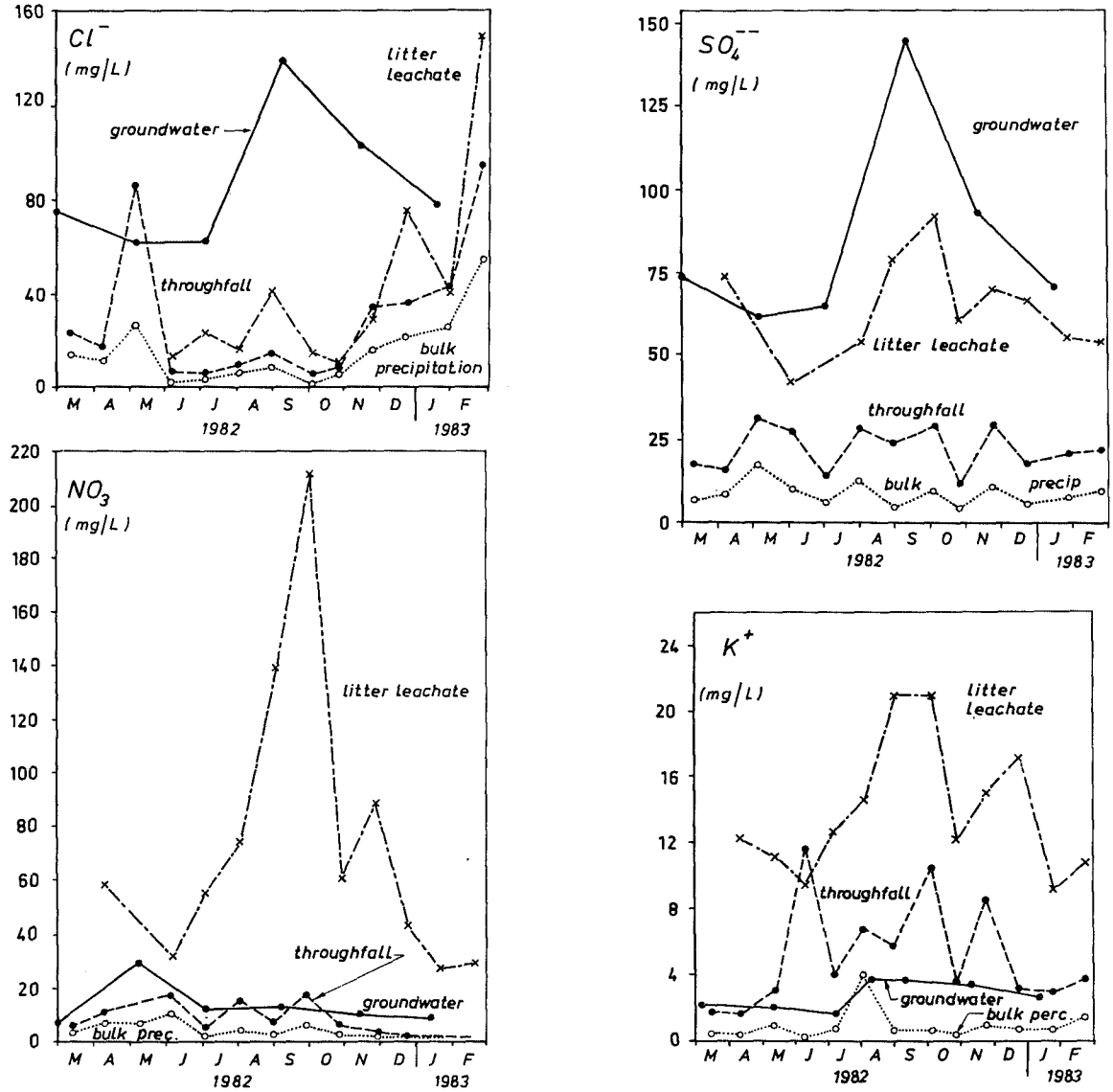

FIG. 6.12 Concentrations of Cl^-, SO_4^{2-}, NO_3^- and K^+ in bulk precipitation, throughfall, litter leachate and the upper groundwater on the plot oaks-2 during the period March 1982 till March 1983 (redrawn after Stuurman, 1984a).

Spatial variations

Concentrations of air-borne sea salts in throughfall under the canopy of a dune shrub or forest stand, generally increase with the approach of its west-southwestern edge (Fig.6.13 and Table 6.11), which is in agreement with Potts (1978). This edge faces the wind direction (N260°) with the highest storm frequency (wind speeds superior to 5 Beaufort) and thereby highest load of sea spray.

The chemical windward egde probably deviates from N260° for those constituents of throughfall, that are strongly raised by interception deposition and have their major sources in quite another direction. This might be the case for F^- on the plot pines-3, with a strong local source due north in the Hoogovens industrial area. The concentration of F^- in throughfall below the N260° facing edge of the forest was about twice that below the centre, which is a low figure compared with for instance sea salts and SO_4^{2-} (Table 6.11). The low edge/centre-ratio for PO_4^{3-}, K^+, NH_4^+ and NO_3^- (<2.5) is related to the fact that foliar leaching contributes most to their concentrations.

6.5.4 Litter leachate

The composition of litter leachate (Table 6.9, Figs. 6.11 and 6.12) is determined by: (a) the composition of throughfall, (b) mineralization of leaves and twigs, (c) soil evaporation (Table 3.3),

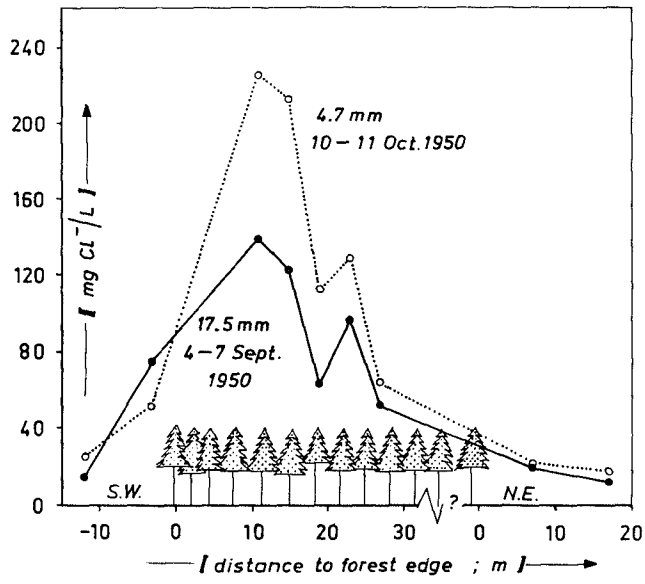

FIG. 6.13 Chloride concentration in throughfall below a 20 years old plantation of pines (Pinus maritima), in Meijendel at 1.5-2 km from the HWL along a SW-NE transect, and in bulk precipitation outside the forest. Based on data in Wind (1953). The windward edge in the SW part of the pine stand, intercepts much more airborne Cl^- than the central and leeward parts.

TABLE 6.11 Comparison of the weighted mean composition of throughfall in the centre (averaged over two gauges) and in the N260° facing windward edge (one gauge) of plot pines-3, for the period February 1982 till February 1983 (from Stuurman, 1984a).

mg/l	center C	edge E	E/C
P(mm)	351	368	1.0
EC[a]	252	775	3.1
SiO_2	0.4	1.2	2.8
pH	4.27	4.51	0.6
Na^+	23.3	79.1	3.4
K^+	8.8	17.7	2.0
Ca^{2+}	4.8	17.3	3.6
Mg^{2+}	4.7	14.9	3.2
NH_4^+	7.1	17.4	2.4
Fe	0.08	0.23	2.8
Mn	0.14	0.47	3.4
Al	0.16	0.48	3.0
Cl^-	47.7	151.4	3.2
SO_4^{2-}	35.5	103.8	2.9
NO_3^{2-}	14.0	28.8	2.1
PO_4^{3-}	1.76	2.45	1.4
F^-	0.16	0.32	2.0
SO_4^*	28.8	82.6	2.9

a = µS/cm at 20°C.

(d) soil interception deposition and (e) interaction with the mineral soil, that is intermixed by soil organisms, rabbits, wind, etc.

The following conclusions are drawn from Table 6.9 :

Litter leachate exhibits on the plots dune shrub-1, oaks-2 and pines-3 higher concentrations for practically all dissolved constituents as compared with throughfall. The concentrations of K^+, TIN (NO_3^- and/or NH_4^+), PO_4^{3-}, Mg^{2+}, Mn (not for dune shrub-1) and probably DOC (up to 200 mg C/l according to Pekdeger, 1979), reach their maximum levels within this compartment, obviously due to the decomposition of litter.

Below the litter of dune shrub-1 high pH values are found already, which is related to the intermixing of calcareous dune sand and a low age of the dune landscape (section 6.4.2). Most NH_4^+ is nitrified under these favourable pH conditions, whereas the mobility of Mn is clearly reduced.

The lowest pH occurred below the litter of oaks-2, in accordance with a deep decalcification on site. This probably favours the leaching of PO_4^{3-} and Mn. The litter leachate of pines is characterized by an exceptionally low SiO_2 and NO_3^- content and high NH_4^+ concentration. The low SiO_2 level might correspond with observations by Bartoli (1986), that pines accumulate relatively little SiO_2, generally as a gel, and therefore contribute little well-soluble SiO_2 to the forest floor, in combination with a lower dissolution rate of the opaline phytoliths produced by pines (Bartoli & Wilding, 1980). The relatively high NH_4^+ concentration of pine leachate as compared with oaks-2 can be explained by the presence of more ferulic acid, which is known (Kuiters, 1987) to inhibit nitrification processes in soils.

Concentrations and fluxes of nutrients reach their maximum values in the period August till mid-October running out to the end of November (see K^+ and NO_3^- in Fig.6.12). This coincides with the peak of leaching from fresh litter (Ellenberg et al., 1986; Kuiters, 1987), which is stimulated by a high temperature and humidity.

6.5.5 Soil moisture

The composition of soil moisture depends on the composition of litter leachate and interactions with roots and mineral phases in the soil. The vertical zonation of the unsaturated zone, with litter on top of the rooted zone, an upper decalcified zone and occasionally an unrooted zone at the bottom (Fig.6.1), leads to a strong dependency of the composition of soil moisture on the depth below the surface, as shown for oaks-2 in Fig.6.14.

The upper decimeter generally exhibits the

following changes : a fast decrease in concentration of NH_4^+ by nitrification and uptake; a decrease for PO_4^{3-}, Mg^{2+} and probably K^+ and NO_3^- as well (the raised level at 0.2 m below pines might represent a seasonal peak) by uptake; and either a rapid hardening and pH increase in calcareous soils (shown by pines-3 in Table 6.9) or a somewhat more sluggish increase of Al in decalcified soils (shown by oaks-2 in Table 6.9).

Below the intensively rooted zone, that extends down to about 0.25 m below the surface for pines-3 and somewhat deeper for oaks-2, nutrient concentrations gradually decrease to the low levels measured in the upper groundwaters. High concentrations of Al, Mg^{2+} and Mn probably persist down to several decimeters above the depth of decalcification, as can be deduced from the Al and Mg^{2+} saturation of the adsorption complex of soil samples from boring 3 in Fig.6.9. With increasing depth soil moisture loses a lot of dissolved organic compounds, by sorption, precipitation and oxidation. This can be deduced from the COD and colour data in Table 6.12. The DOC is composed, among others, of carboxylic acids, polyphenols, humic and fulvic acids, which are known to complex Fe^{3+} and Al^{3+} strongly (Schnitzer & Hansen, 1970; Matthess et al., 1992). Where podzolic soils develop, considerable losses are to be expected for Al, Fe, SiO_2, humic and fulvic acids in the illuvial B_2 horizon (Ugolini et al., 1977).

Effects of different vegetation types and the addition of black earth to the top dune soil, can be deduced from Table 6.12 and Fig.6.15, which are based on data from Wind (1952). Before discussing the results, some marginal notes have to be placed on the effects of the peculiar sampling method applied, on the composition of the soil moisture samples obtained. The unique, but protracted extraction of soil solution consisted of the displacement of soil moisture through poured-up, distilled water with fluorescein as indicator. It was applied to 1 m long soil cores, and probably led to problems in sample conservation. These conduced to : (1) an underestimation of HCO_3^- and total hardness by escape of CO_2 and subsequent precipitation of $CaCO_3$; (2) unreliable results for Fe by lack of filtration of the samples and by oxygenation and subsequent precipitation; and (3) too high pH values, that were on all six plots within the surprisingly narrow range of 8.0 to 8.2. Data of pH and total iron have therefore been discarded. Concentrations of SO_4^{2-} were calculated on the assumption of a square ionic balance after an estimate for Na^+ and K^+ as based on Cl^-.

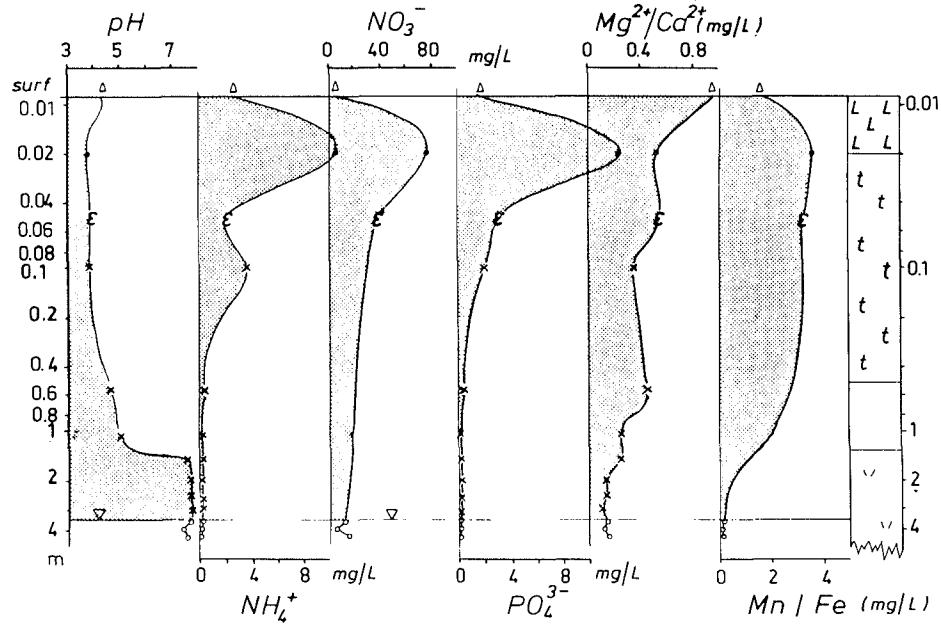

FIG. 6.14 Evolution of the composition of soil moisture and the upper groundwater with depth, on the plot oaks-2. Based on measurements with different sampling facilities during varying periods : Δ = throughfall (Febr.1982-Febr.1983; after Stuurman, 1984a); · = litter leachate (Febr.1982-Febr.1983; after Stuurman, 1984a); ε = plate (Oct.-Nov.1982; after Stuurman, 1984a); c = porous cup; x = centrifugation of a for 24 hours shaken 1:1 suspension of soil sample in de-aerated aqua dest. (Nov.1982, data derived from Stuurman, 1984a); o = groundwater (May 1980-Jan.1983; this study).
Soil column : l = litter; t = humic sand with gradual decrease in humus with depth; ˇ = calcareous sand (HCl-test).

TABLE 6.12 Arithmetic mean composition of soil moisture on the six dune plots indicated in Fig.6.2, each with different vegetation and/or geochemistry, north of The Hague (Meyendel, without soil amendments) and southeast of Zandvoort aan Zee (Leiduin, with soil amendments for oaks and pines). Based on data in Wind (1952). On each plot 25-32 samples were taken in the period April/July 1950 till October 1951.

plot	depth m-surf.	Cl^-	HCO_3^-	NO_3^-	SO_4^{2-}	TotH$^\beta$	COD$^\alpha$	colour
		mg/l				mmol/l	mg/l	γ
SCANTY								
Kijfhoek[1]	0-1	19	105	6.9	13	1.04	8.2	11.0
Kijfhoek[1]	1-2	19	109	3.8	16	1.07	5.3	8.2
Leiduin[4]	1-2	20	118	2.9	>6	1.04	6.9	9.7
OAKS								
Meijendel[2]	0-1	66	216	11.0	42	2.36	111	102
Meijendel[2]	1-2	61	172	8.1	32	1.86	58.3	48.5
Leiduin[5]	1-2	75	173	36.8	24	2.04	88.0	59.2
PINES								
Meijendel[3]	0-1	103	220	4.4	94	2.95	50.9	39.4
Meijendel[3]	1-2	105	138	4.6	93	2.27	26.7	18.9
Leiduin[6]	1-2	81	169	79.1	235	4.57	55.0	34.0

[4] = 15% bare, 50% mosses, 20% dune grasses, 15% low dune shrub, buried forest floor at 0.3-0.5 m depth, surface at 6½ m+MSL, groundwater table at <4½ m+MSL;
[1] = *Quercus robur*, 70 - 110 years old, 8 - 12 m tall with a variegated undergrowth, surface at 4 m + MSL, groundwater table < 2 m + MSL;
[2] = *Pinus maritima*, 20 years old plantation, surface at 4.3 m + MSL, groundwater table at < 2.3 m + MSL;
[5] = mainly mosses, dune grasses and creeping willow, surface at 10 m + MSL and groundwater table at 1½ m + MSL;
[3] = *Quercus robur* with an undergrowth composed of elder (*Sambucus nigra*), 40 years old plantation, surface at 12½ m + MSL, groundwater table at 1½ m + MSL;
[6] = *Pinus nigra ssp nigra*, 20 years old plantation, 5-7 m tall, surface at 8 m + MSL, groundwater table at 0.8 m + MSL; γ = mg Pt/l
α = chemical oxygen demand by and expressed as $KMnO_4$; β = total hardness.

With these drawbacks in mind, it can be concluded nonetheless that soil moisture beneath oak and pines exhibits much higher levels for the considered parameters, NO_3^- excluded, than soil moisture beneath sparsely vegetated dunes. The results also show that soil moisture beneath 40 years old oaks and 20 years old pines planted on dunes with a soil amended at about the same time by 20 cm of humus and peat, can still contain considerably more NO_3^- and organic substances, than soil moisture beneath oaks and pines planted on dunes without soil amendment.

6.6 Spatial variations in the composition of upper dune water

6.6.1 Presentation of results

In this section, spatial variations are largely deduced from the differences in mean composition of pure vegetation water, between the 28 plots. This means that a lot of horizontal and vertical variation within each plot has been levelled out completely, thus minimizing the influence of temporal variations, but narrowing the spectrum of natural spatial variation. The calculation of mean concentrations also implies that apparent chemical inconsistencies may arise, for instance when winter water with a high NO_3^- but very low Fe concentration is combined in that way with summer water rich in Fe and without NO_3^-.

About 1250 samples were included in averaging the composition of the upper dune groundwaters at the 28 monitoring plots. For an extensive listing reference is made to Stuyfzand (1991b).

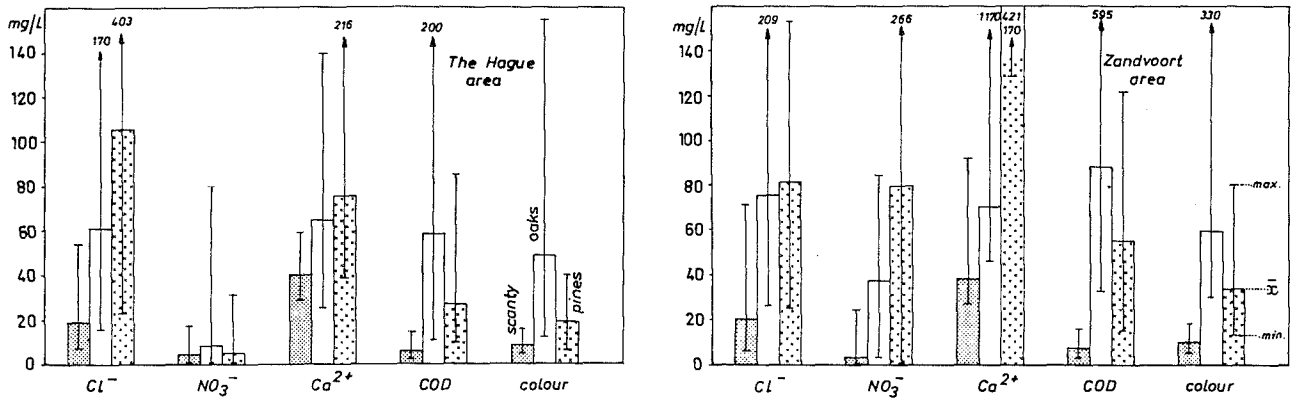

FIG. 6.15 Arithmetic mean composition of soil moisture on the six dune plots indicated in Fig.6.2, with different vegetation and/or geochemistry, north of The Hague (Meyendel, without soil amendments) and southeast of Zandvoort aan Zee (Leiduin, with soil amendments for oaks and pines). Based on data in Table 6.12 and in Wind (1952). Minima and maxima refer to the combined effect of temporal and spatial variations inherent to the 25-32 core samples taken in the period April/July 1950 till October 1951.

The analytical results pertaining to the lysimeters west of Castricum, were weighted according to the drainage quantity in the collection period. The arithmetic mean was calculated for samples obtained from miniscreens and piezometers.

The mean concentrations of major constituents are listed in Table 6.13, and those for trace elements and oxygen-18 in Table 6.14. These data were used to compute the derivative quality parameters listed in Table 6.15. And data on some organic microcontaminants are shown in Table 6.16. Mean values of SO_4^{2-}, NO_3^- and HCO_3^- for each plot are arranged in increasing order in bar diagrams (Fig.6.16), together with the minima and maxima observed. The extremes for the lysimeters refer to temporal fluctuations exclusively, but those for the other plots cover both temporal and spatial variations.

The collection period, number of observation facilities visited and number of samples involved in the analysis of major constituents, are indicated for each plot in Table 6.13. The number of samples analysed on trace elements, oxygen-18 and AOCl amounts to 5-50% of the indicated number.

The spatial variability of shallow dune groundwater is discussed in the next sections, by analysing the effects of : spatial variations in the composition of bulk precipitation, different vegetation covers, differences in geochemistry ($CaCO_3$ content and dune peat), and differences in thickness of the unsaturated zone. Differences between dune sands with and without soil amendments have been discussed previously (section 6.5.5) and follow below, where some marginal notes on the representativity of the lysimeters are made.

Representativity of the lysimeters

A comparison of the results obtained with the lysimeters west of Castricum with those from the other plots in calcareous dunes, with due consideration of differing boundary conditions (Table 6.1), leads to detection of several deviations. The drainage solute of each lysimeter is somewhat enriched in K^*, As, Li^+ and Rb^+. This may be due to a slow leaching of substances added to the upper soil (erroneously also to the bare lysimeter) in order to stimulate growth (see section 6.2).

Relatively high F^-, B and, to a lesser extent, SiO_2 levels are found in the drainage solute of the vegetated lysimeters. This may be related again to soil amendments, and partly to an about 20% higher atmospheric deposition of F^-, from emissions in the Hoogovens industrial zone, as compared to the dunes south of Zandvoort aan Zee.

Concentrations of air-borne sea salts (mainly Cl^-, Na^+, Mg^{2+}, Br^-) and SO_4^{2-} seem to be exceptionally high for the lysimeter covered with pines. Such levels are within normality for the windward edges of pine forests in the coastal dunes, but surely are exceptional for an extensive pine forest (>1km^2) as a whole. Results obtained with this lysimeter in the period 1955-1962 (Cl^- = 103, SO_4^{2-} = 87 mg/l), compare far better with observations south of Zandvoort aan Zee, probably because the top of the pines was less exposed to westerly winds at that time (Stuyfzand, 1984d).

The following deviations cannot be deduced from the results presented, because a correction has been included already on the basis of previous research. In the period 1988-1989 three shallow observation wells just outside, in terrain with similar vegetation cover, and one inside each lysimeter were sampled thrice, together with the drainage water as collected from the main drainage artery before entrance into the central collection tank. Comparison of thus obtained samples with simultaneous samples from each tank, revealed that water from the tank had gained considerably in Cu and to a lesser extent in Zn by contact with brass in between the drain and collection tank, and in PAHs delivered by a bituminous coating of the inner lysimeter wall. It revealed also that the long residence time (at least one week) of the water drained into the central collection tank, which is open to the atmosphere below a lid, leads to significant losses of Fe, As and PO_4^{3-} (about 50%). For the other constituents and quality parameters differences were ≤20% and have been neglected. The lysimetric results in Tables 6.14 and 6.16 have been corrected according to these findings, for Cu, Zn and PAHs.

Time effects

Differences in sampling period (up to 7 years apart, Table 6.13) or in mean detention times in both the vadose and saturated zone (5.5 years at most, Table 6.1), likely contribute to some of the differences in groundwater composition between the 28 plots, by introduction of variations in both the recharge and transit period. These in turn conduce to variations in atmospheric inputs, water losses by evapotranspiration, soil moisture content, temperature, etc. In the following discussion such time effects will be mentioned only when considered relevant.

6.6.2 *Effects of spatial variations in bulk precipitation chemistry*

The most obvious effect of spatial variations in the composition of bulk precipitation on shallow dune groundwater, is the increase of air-borne sea salts (Cl^-, Na^+, Mg^{2+}, Br^-) below identical vegetation types in the direction of the HWL (Figs. 6.17 and 6.18). The observed patterns closely follow the chloride curve of bulk precipitation (Fig.5.4), especially in groundwater under low vegetation types, like

TABLE 6.13 Survey of mean concentrations for main constituents of pure vegetation groundwater on 28 plots in the coastal dunes of the Western Netherlands.

monito-ring plot	dune peat m	dist. coast	MGL m-surf	EC µS/cm	pH	Cl^-	SO_4^{2-}	HCO_3^-	NO_3^-	PO_4^{3-}	Na^+	K^+	Ca^{2+}	Mg^{2+}	NH_4^+	Fe	Mn	SiO_2	COD[a]	DOC	sampling period yymm	n_F	n_S
						mg/L																n	n
MINISCREENS, DUNES POOR IN CALCITE, NORTH OF BERGEN																							
scanty	-	950	3.1	156	4.40	29.0	17.0	<1	10.5	0.24#	17.8	1.6	2.0	2.5	0.03	0.24	0.03	10.0	9.9	3.4	8709-8709	7	7
heather	h	1400	2.1	170	4.79	33.4	20.4	5	2.7	0.19#	20.1	2.1	6.3	3.0	0.09	2.05	0.04	13.1	27.1	9.8	8709-8709	8	8
pines-4		800	2.9	493	4.80	128	46	5	0.7	0.14#	74.8	2.2	9.5	10.8	0.04	0.42	0.09	16.2	30.4	10.4	8709-8709	6	6
pines-5		3000	3.7	286	5.31	63.4	36.3	7	1.0	0.31#	38.3	2.8	6.8	7.9	0.04	0.87	0.05	23.1	20.4	8.3	8709-8709	8	8
LYSIMETERS, CALCAREOUS DUNES, WEST OF CASTRICUM																							
bare-L	-	2000	2.2	272	7.96	16.1	16.5	116	16.7	0.05	9.2	2.33	47.4	2.4	0.03	0.03	<0.01	4.4	4.3	3.1	8003-8302	1	156
dune shrub-L	-	2040	2.3	692	7.42	63.3	50.8	270	35.3	0.04	33.4	3.28	119	6.4	0.04	0.04	0.03	8.7	18.7	7.8	8003-8302	1	114
oaks-L	-	2115	2.3	682	7.38	79.1	47.4	276	0.5	0.15	42.1	4.86	110	5.7	0.03	0.08	0.07	10.8	25.8	10.4	8003-8302	1	97
pines-L		2200	2.4	2161	7.41	435	304	388	0.6	0.27	242	15.4	252	24.7	0.04	0.04	<0.01	13.0	39.3	17.2	8003-8302	1	59
PIEZOMETERS, CALCAREOUS DUNES SOUTH OF EGMOND AAN ZEE																							
grasses-4	-	340	0.4	799	7.15	115	24.1	330	<0.1	0.15	67.5	3.56	103	13.8	0.10	2.23	0.16	6.5	-	20.6	8409-8509	2	18
grasses-5		360	1.1	573	7.58	76.5	32.2	202	9.4	0.16	48.3	2.25	73.3	7.4	0.02	0.05	0.01	4.6	-	-	8306-8309	3	6
MINISCREENS, CALCAREOUS DUNES, SOUTH OF ZANDVOORT AAN ZEE																							
mosses-1	-	325	1.5	492	7.77	58.1	34.3	152	36.1	0.10	33.9	1.75	66.7	6.3	<0.1	<0.2	<0.08	5.2	8.8	2.7	7903-8301	6	142
mosses-2		2500	1.7	340	7.86	22.9	22.9	141	25.6	0.07	15.7	1.19	56.2	4.1	0.16	0.11	<0.05	4.2	3.8	3.3	8103-8210	10	18
mosses-3		2725	2.5	473	7.74	39.5	37.1	176	34.2	<0.10	28.0	1.16	74.0	5.1	<0.10	0.28	<0.05	5.1	7.5	4.1	8103-8210	8	15
grasses-1		2100	0.7	571	7.36	34.9	28.7	315	8.5	0.21	19.1	0.98	109	7.4	0.45	2.44	0.26	4.8	15.1	6.3	8103-8210	8	15
grasses-2		2650	0.3	543	7.31	34.4	20.8	321	<0.2	0.64	21.2	1.40	104	6.1	0.59	14.21	1.78	9.6	-	20.8	8502-8605	7	19
grasses-3		3310	3.1	581	6.66	42.0	66.4	287	4.9	0.22	21.5	2.22	112	6.4	0.37	1.52	0.13	10.1	112.8	33.5	8009-8112	4	28
bracken-1	-	3485	4.1	352	7.76	21.8	30.5	158	14.7	0.05	12.5	2.06	61	5.2	0.07	<0.2	<0.10	7.3	6.4	1.8	7911-8301	1	22
bracken-2	+	3115	2.1	1214	7.20	34.6	128.1	282	381	0.05	19.8	0.41	266	3.6	0.05	<0.2	<0.10	5.4	93.8	27.9	8106-8301	1	8
dune shrub-1	-	625	2.7	744	7.77	121.1	54.6	162	52.4	0.09	68.1	1.54	89	6.3	0.09	<0.2	<0.08	7.6	6.2	1.6	7911-8301	1	23
dune shrub-2	-	1685	2.4	579	7.34	41.7	40.3	275	21.9	0.06	24.6	0.67	104	7.2	0.06	<0.2	0.09	5.4	20.0	5.5	7911-8301	1	22
dune shrub-3	S	3175	3.7	701	7.12	41.2	73.6	268	85.4	0.06	23.5	0.85	136	5.9	<0.05	<0.3	<0.08	3.6	42.7	13.6	8009-8112	1	9
dune shrub-4	+	1145	2.1	835	7.15	94.2	77.6	344	0.6	0.22	53.9	1.64	135	7.6	0.46	3.61	0.15	7.3	22.2	8.0	7903-8108	5	102
oaks-1	S	3260	3.5	887	7.12	86.7	167	298	18.3	0.07	48.4	2.28	162	8.0	0.22	3.33	0.10	10.4	100	32.7	7903-8301	6	115
oaks-2	-	3200	3.0	564	7.58	61.2	67.6	202	7.1	0.07	36.3	1.69	80.7	10.3	0.07	0.35	<0.09	6.8	16.4	5.0	8006-8301	5	54
oaks-3		3245	3.6	738	7.46	83.7	93.1	212	45.6	0.05	45.6	5.64	109	11.5	<0.05	0.45	<0.09	7.3	38.2	18.6	8106-8209	2	16
pines-1		1515	2.2	1265	6.90	146	78.1	638	1.4	0.25	91.0	1.17	220	13.5	0.29	4.04	0.33	6.9	107	37.6	7911-8301	5	58
pines-2	-	1635	1.6	860	7.47	107	86	352	<0.2	<0.1	57.6	0.75	130	13.4	<0.1	0.24	0.37	8.5	45.7	-	8006-8011	1	2
pines-3	S	1700	2.9	754	7.26	73.8	76.0	336	4.7	0.13	42.8	1.45	131	7.4	0.12	0.71	0.23	7.6	47.5	15.9	8004-8301	9	104

+ , S, - = peat clearly present, in traces and not present respectively, h = 0.1 m thick, humic top layer; n_F = number of sampled miniscreens cq lysimeters; n_S = number of samples analysed; a = Chemical Oxygen Demand by and expressed as $KMnO_4$; # = total PO_4.

TABLE 6.14 Survey of mean concentrations for trace elements and oxygen-18 in pure vegetation groundwater on 28 plots in the coastal dunes of the Western Netherlands. Not listed are concentrations of Hg (<0.2 µg/l), Mo (<0.5 µg/l), Sb (<0.5 µg/l), Se (<1 µg/l), Sn (<1 µg/l), Te (< 0.5 µg/l), Ti (<2 µg/l) and Tl (<2 µg/l).

monito-ring plot	Al	As	B	Ba^{2+}	Be	Br^-	Cd	Co	Cr	Cu	F^-	I	Li^+	Ni	Pb	Rb^+	Sr^{2+}	U	V	Zn	$\delta^{18}O$
	µg/L																				‰
MINISCREENS, DUNES POOR IN CALCITE, NORTH OF BERGEN																					
scanty	1920	1	<50	49	0.9	120	0.9	16	<1	2	67	1.9	7	16	2.5	5.8	<100	-	2	81	
heather	800	12	<50	9	≤0.1	97	0.4	6	<1	2	78	1.6	9	10	1.5	1.2	<100	-	≤1	20	
pines-4	900	1	<50	15	0.5	-	0.6	7	1	3	323	2.4	17	36	2.2	2.5	≤100	-	3	138	
pines-5	600	2	<50	17	1.0	-	1.4	15	[illegible]	2	409	2.5	26	70	0.9	2.0	120	-	5	270	
LYSIMETERS, CALCAREOUS DUNES, WEST OF CASTRICUM																					
bare-L	<5	1.3	<100	14	<0.05	47	<0.1	<1	<1	≤6	109	1.9	5	1.5	[illegible]	1	160		<2	12	
dune shrub-L	<10	1	135	10	<0.05	240	<0.1	<1	<1	<5	303	1.7	6	2.7	2	1.5	550		<2	16	
oaks-L	<1	4.3	200	13	<0.05	140	<0.1	<1	<1	<5	376	2.1	8	3.7	3	3.7	500		<1	13	
pines-L	<1	5.3	350	28	<0.05	1550	<0.1	<1	<1	≤5	780	1.8	10	3.7	3	4.1	1300		<2	10	
MINISCREENS, CALCAREOUS DUNES, SOUTH OF ZANDVOORT AAN ZEE																					
mosses-1	18	≤1	<50	11	<0.05	-	<0.1	0.2	0.8	7.4	148		1.7	2.2		2.0	275	0.19	0.2	23	-7.25#
mosses-2	<165	<1	70	<10	<0.05	-	-	0.3	0.5	2	179		0.5	1.9	1	0.1	210	0.12	0.1	6	-7.27
mosses-3	<469	<1	-	-	-			0.5	<1	1.8	143		-	<2	[illegible]	-	-	0.31	0.1	3	-7.55
grasses-1	<149	3.4	-	-				0.9	0.6	2.6	174			2		-	-	0.14	0.3	9	-7.45
grasses-2	-	33.1	80	46			-	-	-	-	240			[illegible]	-	0.2	335	-	-	-	-
grasses-3	<20	19.2	-	30			0.1			4.0	180				2	-	-			35	-
bracken-1	<20	0.1	-	20			<0.1			4.6	317				3					17	-7.54
bracken-2	<20	0.9	-	30			<0.1	-		3	87				1	-	-			33	-
duneshrub-1	<20	<1	148	9			0.1	-		3.0	57				1	<0.5	410			21	-7.50#
duneshrub-2	<20	0.5	-	20			<0.1	-		4.8	156				1	-	-			20	-
duneshrub-3	<20	0.2	-	20			<0.1	-	-	5	37			-	1		-	-	-	95	-
duneshrub-4	30	4.3	60	58			<0.1	0.2	0.5	3.7	71			<5	2	-	460	0.10	0.5	26	-7.17
oaks-1	<20	2.1	108	25			0.1	1.7	<1	6.8	95			<5	2	1.4	530	0.33	1.0	51	-7.50#
oaks-2	<20	<1	-	24			<0.1	-	-	3.4	191			-	3	-	340	-	-	25	-
oaks-3	<20	<1	-	25			<0.1	-		6.0	96				3	-	-			36	-
pines-1	<20	9.1	100	38			0.1			4.3	130				2	3.1	910			164	-6.85#
pines-2	<20	-	-	-	-	-	-	-	-	-	-	-	-	-	-	-	-	-	-	-	-
pines-3	<20	1.6	150	34	-	-	<0.1	-	-	6.8	165	-	-	-	2	<0.5	490	-	-	19	-

= sampled 7-18 times during the same 1-year period.

TABLE 6.15 Survey of derivative quality parameters for pure vegetation groundwater on 28 plots in the coastal dunes of the Western Netherlands, as calculated from data in Tables 6.13 and 6.14.

monito-ring plot	Na^*	K^*	Ca^*	Mg^*	SO_4^*	BEX[§]	TIC	TIN	DOC TIC	COD DOC	watertype	redox	polin	SI_c
			µmol/L			meq/L	mmol/L	mmol/L	mmol/L	mmol/L				
MINISCREENS, DUNES POOR IN CALCITE, NORTH OF BERGEN														
scanty	73	26	35	23	135	0.17	1.17	0.17	0.24	0.55	g_4NaCl	1-5	2.7	-6.52
heather	66	36	139	32	164	0.10	1.26	0.05	0.65	0.53	F_4NaCl	2-4	2.2	-5.25
pines-4	156	-11	169	93	292	0.33	1.72	0.01	0.50	0.56	F_4NaCl	2-4	3.7	-5.15
pines-5	131	38	136	151	285	0.47	1.44	0.02	0.48	0.47	F_4NaCl	2-4	3.2	-4.60
LYSIMETERS, CALCAREOUS DUNES, WEST OF CASTRICUM														
bare-L	17	51	1175	54	149	0.18	1.97	0.27	0.13	0.26	g_1CaHCO_3	1	1.7	0.04
dune shrub-L	-61	51	2944	91	436	0.17	4.89	0.57	0.13	0.46	F_3CaHCO_3	1	2.5	0.17
oaks-L	-61	84	2695	16	378	0.06	5.05	0.01	0.17	0.47	F_3CaHCO_3	2-3	2.2	0.10
pines-L	122	171	6215	-185	2530	-0.08	7.01	0.01	0.20	0.43	B_3CaMix	2-3	3.1	0.51
PIEZOMETERS, CALCAREOUS DUNES SOUTH OF EGMOND AAN ZEE														
grasses-4	197	36	2570	252	84	0.74	6.36	0.01	0.27		F_3CaHCO_3	4-5		0.01
grasses-5	249	17	1788	94	224	0.45	3.53	0.15	-		F_2CaHCO_3	1-2		0.04
MINISCREENS, CALCAREOUS DUNES, SOUTH OF ZANDVOORT AAN ZEE														
mosses-1	82	15	1633	100	272	0.30	2.61	0.59	0.09	0.62	F_2CaMix	1	2.4	0.07
mosses-2	130	19	1389	106	205	0.36	2.38	0.42	0.12	0.22	g_2CaHCO_3	1	2.0	0.08
mosses-3	223	8	1824	105	328	0.44	3.05	0.55	0.11	0.35	F_2CaHCO_3	1	2.0	0.15
grasses-1	-18	7	2706	207	248	0.40	5.78	0.16	0.09	0.46	F_3CaHCO_3	1-4	1.9	0.19
grasses-2	95	40	2566	150	166	0.44	6.25	0.03	0.28	-	F_3CaHCO_3	4-5	2.2	0.14
grasses-3	-69	35	2773	147	630	0.26	7.85	0.10	0.36	0.64	F_3CaHCO_3	2-5	2.6	-0.59
bracken-1	22	42	1511	154	286	0.37	2.71	0.24	0.06	0.68	g_2CaHCO_3	1-2	2.3	0.08
bracken-2	33	-7	6619	53	1283	0.13	5.44	6.15	0.43	0.64	F_3CaNO_3	1	3.2	0.29
duneshrub-1	65	-23	2157	-75	392	-0.11	2.76	0.85	0.05	0.74	F_2CaMix	1	2.8	0.19
duneshrub-2	72	-4	2573	181	359	0.43	5.05	0.36	0.09	0.69	F_3CaHCO_3	1	2.5	0.09
duneshrub-3	37	1	3372	129	706	0.30	5.28	1.38	0.21	0.60	F_3CaHCO_3	1	3.2	-0.04
duneshrub-4	92	-6	3309	52	670	0.19	6.70	0.04	0.10	0.53	F_3CaHCO_3	4	2.4	0.09
oaks-1	28	14	3991	90	1615	0.22	5.90	0.31	0.46	0.58	F_3CaMix	2-4	3.0	0.03
oaks-2	116	12	1981	253	614	0.63	3.55	0.12	0.12	0.62	F_2CaHCO_3	2-4	2.7	0.06
oaks-3	-19	102	2676	243	847	0.57	3.80	0.74	0.41	0.39	F_2CaMix	1-2	3.1	0.08
pines-1	476	-45	5404	153	601	0.74	13.93	0.04	0.22	0.54	F_4CaHCO_3	2-5	3.2	0.26
pines-2	-87	-38	3173	257	742	0.39	6.45	<0.01	-	-	F_3CaHCO_3	3	2.6	0.36
pines-3	95	-1	3232	102	683	0.30	6.37	0.08	0.21	0.57	F_3CaHCO_3	2-4	2.7	0.17

X^* = X corrected for sea salt according to Eq.5.7 and Table 5.5; § : BEX = 0.001 ($Na^* + K^* + 2Mg^*$); TIC = $HCO_3^- + CO_3^{2-} + CO_2$; TIN = $NO_3^- + NH_4^+ + NO_2^-$; $[COD/DOC]_{mmol/L}$ = 0.1899 $[KMnO_4$- consumption/$DOC]_{mg/L}$; Polin : calculated without tritium data, assuming Coli = 0 and missing AOCl estimated by interpolation of lys. data.

TABLE 6.16 Survey of organic microcontaminants in bulk precipitation and pure vegetation groundwater in the coastal dunes of the Western Netherlands.

compound	unit	bulk precip.	LYSIMETERS WEST OF CASTRICUM@ bare	dune shrub	oaks	pines	MINISCREENS NORTH OF BERGEN 14C41 +4	14C41 -1.3	19AL31 +0	19A326W +1.8	19A326 -4.9	19A326 -14.9
								scanty	pines		heather	
GROUP PARAMETERS												
AOCl	µg/l	13[A]	5	23	30	45	5.1	<5	39	67	9.3	7.4
VOCl	µg/l	<0.5[B]	0.2	0.3	0.3	0.2	1.1	0.8	0.5	1.1	0.9	2.5
THMs	µg/l	-	-	-	-	-	<2	<2	<2	<2	<2	<2
PAHs Borneff	ng/l	530[B]	<30	<30	30	<30	50	50	40	30	40	30
MONOCYCLIC AROMATICS												
benzene	ng/l	<20[B]	<100	<100	<100	<100						
toluene	ng/l	<40[B]	<100	<100	<100	<100						
xylenes	ng/l	<20[B]	<100	<100	<100	<100						
INDIVIDUAL PESTICIDES												
atrazine	ng/l	-	<50	<50	<50	<50						
bentazone	ng/l	-	<50	<50	<50	<50						
bromacil	ng/l	-	<50	<50	<50	<50						
pyrazon	ng/l	-	<50	<50	<50	<50						
simazin	ng/l	-	<50	<50	<50	<50						
INDIVIDUAL PAHs												
fluoreen	ng/l	-	<30	<10	10	<10	50	40	30	20	30	20
fluorantheen	ng/l	190[B]	<400	<10	<10	<10	20	20	10	<10	10	<10
phenanthreen	ng/l	130[B]	<450	<10	20	10	100	80	80	50	60	30
pyreen	ng/l	140[B]	<250	<10	<10	<10	10	<10	<10	<10	<10	<10
INDIVIDUAL CHLORINATED ALIPHATICS												
1,1,1-tri	µg/l	-	-	-	-	-	<0.1	<0.1	0.3	<0.1	0.2	0.3

@ = drainage water lysimeters (PAHs excluded) and observation-wells in (PAHs excluded) and outside lysimeters; A = Van der Neut, 1992; Ten Harkel, 1992a; B = De Bilt 1981 (KNMI, 1981).

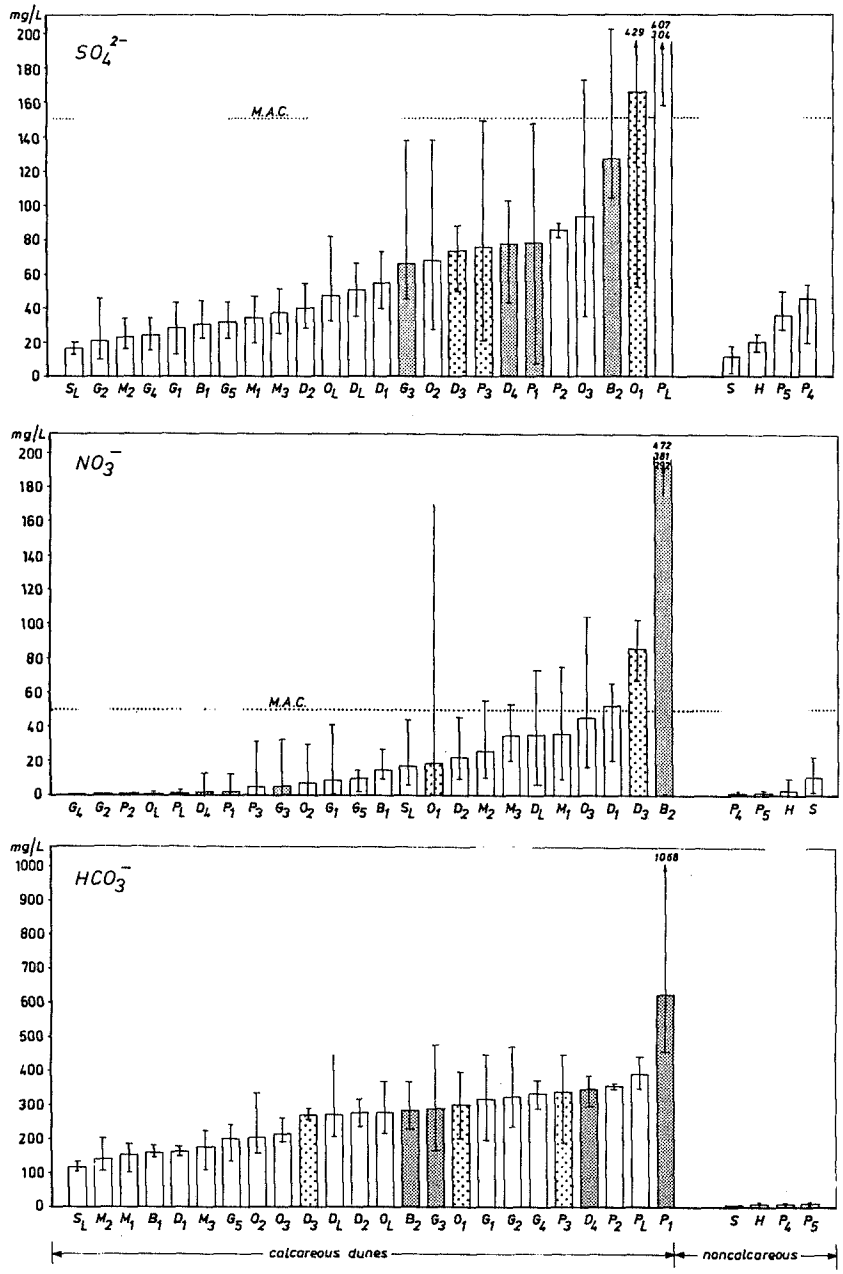

FIG. 6.16 Bar diagrams with the mean concentration of sulphate, nitrate and hydrogencarbonate (derived from Table 6.13), arranged in increasing order for the 28 plots, with separation of calcareous and decalcified plots and with indication of the minima and maxima observed. Interaction with intercalated dune peat is indicated by fine dots (strong) or crosses (weak, peat in traces).

High SO_4^{2-} concentrations are associated with : (1) the oxidation of iron sulphides where the water table dropped and dune peat is involved (B_2, O_1); and (2) dense and tall vegetation covers (oak and pines) by high evaporation losses and a high interception. High NO_3^- levels combine with oxidizing dune peat permanently above the water table (D_3, B_2), dune shrub (N_2 fixation by symbiontic bacteria), a low uptake (mosses), absence of peat below the water table and a deep water table. High alkalinities are generated in calcareous dunes only, under dense and tall vegetation covers (by high evaporation losses and a high CO_2 production) and after interaction with dune peat. The relatively low SO_4^{2-} concentrations in the decalcified dunes north of Bergen are caused by lower atmospheric pollution levels (there and at the later moment of sampling) and adsorption losses to the acidified soil.

M.A.C. = Maximum Acceptable Concentration for drinking water, according to the Dutch Drinking Water Act. B = bracken; D = dune shrub, composed mainly of Hippophaë; G = (dune) grasses; H = heather; M = mosses; O = oaks; P = pines; S = scanty or bare; D_3 = dune shrub-3 (see Table 6.1).

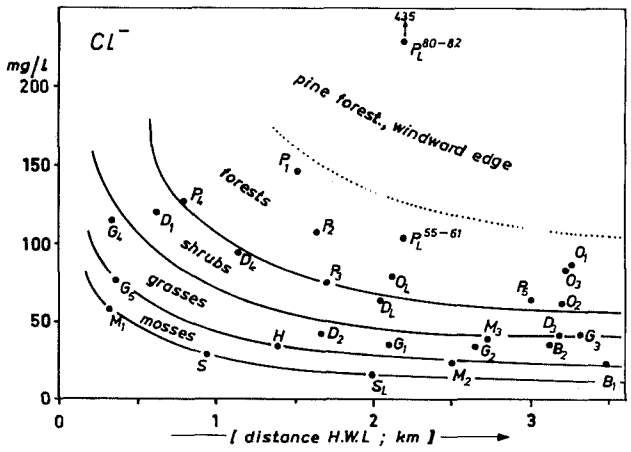

FIG. 6.17 Mean chloride concentration of the upper 0.3-3 metres of dune water at 28 monitoring plots, as a function of the distance to the mean High Water Line (HWL) of the North Sea. The pattern under each vegetation cover is dictated mainly by the exponential decrease in sea spray deposition inland (Fig.5.4). B = bracken; D = dune shrub, composed mainly of Hippophaë; G = (dune) grasses; H = heather; M = mosses; O = oaks; P = pines; S = scanty or bare.

mosses, grasses and low dune shrubs, not only in the upper 0.3-3 metres (Fig.6.17) but still at 5-9 m below the water table (Fig.6.18).

The simple relation is disrupted, however, for plots within pine or oak forests (Fig.6.17), largely by variations of their distance to the windward edge. Salt sieving by the first windward trees is in fact well-known (Fig.6.13), and indeed applies most to the outliers pines-L and pines-1 in Fig.6.17.

Another effect should be a northward gradient in SO_4^* levels with superimposed, subregional gradients around industrial zones and cities (Fig.5.3). This cannot be concluded from the presented data, however, for several reasons : the subregional gradient around the Hoogovens industrial complex approximately compensates for the northward gradient with regard to the lysimetric plots; SO_4^{2-} sorption to acid dune sand is probably responsible for the low SO_4^{2-} levels north of Bergen; and these low SO_4^{2-} concentrations are further explained by a relatively late sampling (1987 versus 1979-1983) in a period of declining SO_4^* concentrations in bulk precipitation (Fig.5.5).

And finally, there probably is a coastal gradient in SO_4^* levels in between the HWL and first km inland, for locations with a similar vegetation cover (Fig.6.19). This gradient is caused by the seaward increasing SO_2 deposition (as deduced from SO_4^* in

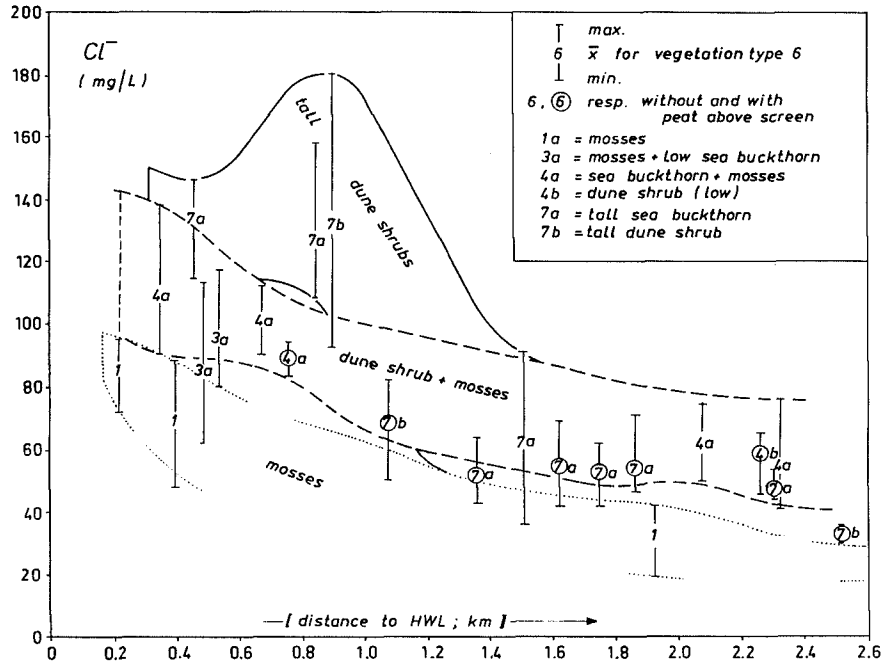

FIG. 6.18 Mean, minimum and maximum chloride concentration of dune water from piezometers 1 m long at 5-9 m below the water table in dunes south of Zandvoort aan Zee (Luchterduinen), as a function of (1) the distance to the mean High Water Line (HWL) of the North Sea, and (2) local vegetation. Based on 8-18 samples taken in the period May 1976 till June 1981. The presence of dune peat at approximately MSL, reduces the Cl^- variation.

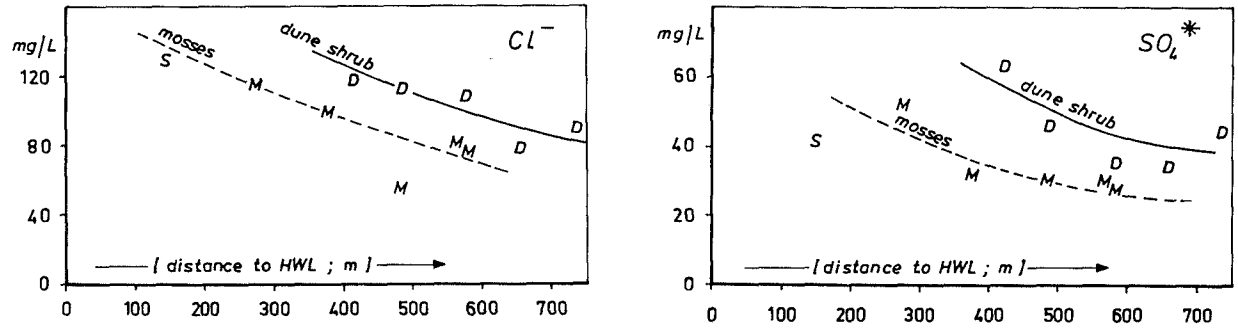

FIG. 6.19 Dependence of the concentrations of chloride and sea spray corrected sulphate (SO_4^*) in dune groundwater at 5 m-MSL, on the distance to the mean High Water Line (HWL) of the North Sea. Based on samples to the west of the Westerkanaal south of Zandvoort aan Zee, taken in the period December 1977 - March 1978. An increased SO_4^* deposition in the direction of the HWL is postulated and explained by an enhanced absorption of SO_2 gas to hygroscopic, reactive surfaces covered with sea spray and calcareous dust or sand. D = dune shrub, composed mainly of Hippophaë rhamnoides and Salix repens; M = mosses; S = scanty or bare.

Fig.5.4), due to a stimulated SO_2 absorption to surfaces covered with sea spray, calcareous dust and calcareous dune sand (section 5.4.2). Difficulties in proving this gradient also for groundwater, consist of the superimposed effects of : (a) an inland increasing depth of decalcification, which raises the chance of SO_4^{2-} losses due to the formation of jurbanite-like phases (section 6.6.4); (b) dune peat interference, which may cause either a mobilization or retention (section 6.6.5); (c) interference with iron sulphides that may be formed or oxidized; and (d) differences in age, which may have a strong impact on the atmospheric input at the time of infiltration (Figs. 5.5 and 5.8). The data used for constructing Fig.6.19 were carefully selected, however, by taking samples that were collected from piezometers at about the same time and same depth below the phreatic level in an area without dune peat, with the phreatic level uniformly at about 3-4 m below ground surface.

6.6.3 Effects of different vegetation covers

All data presented and those from the lysimetric plots in particular, as their environmental boundary conditions are about equal, reveal that different vegetation covers lead to quite different dune groundwaters. This can be specified in general terms, as follows. The amount of total dissolved solids increases for pure vegetation water in the following order, with all hydrological, geochemical and topographical boundary conditions equal : bare dune sand < mosses < {grasses ≈ heather ≈ bracken} < dune shrub (mainly *Hippophaë rhamnoides*) < oaks (*Quercus robur*) < pines (*Pinus nigra* ssp. *nigra*). This order is in general also valid for the main constituents Cl^-, SO_4^{2-}, HCO_3^-, Na^+, Ca^{2+}, SiO_2 and DOC, and for the trace constituents Br^-, F^-, Li^+, Ni, Sr^{2+} and AOCl, individually (Tables 6.13-6.16).

The sequence is explained by a more or less steady increase of : evapo(transpi)ration (Table 3.2), interception deposition of sea spray and atmospheric pollutants (also including halogenated hydrocarbons), production of CO_2, HCO_3^- and DOC, and agressivity towards various soil components. Their solubility is enhanced by (a) the production of CO_2 and organic acids, (b) the atmospheric deposition of acidic (SO_2, NO_x, HF) or acid-forming (NH_4^+) components, (c) the complexing abilities of for instance fulvic acids (the bulk of DOC probably), SO_4^{2-} and F^-, and (d) a reduction of activity coefficients in a more mineralized solution. The simultaneous increase of air-borne Na^+, K^+ and Mg^{2+} will, however, reduce the solubility of primary Al-silicates by raising the activity of these sea salts in solution before contacting the mineral soil. In that way Etherington (1967) explained the lack of biotite weathering in coastal dunes in Wales.

The sequence for nitrate in pure vegetation water, without dune peat interference and with its water table well below the surface (> 0.5 m), becomes from low to high concentrations (Fig.6.16) : {fast growing pines (*Pinus nigra* ssp. *nigra*) ≈ fast growing oaks (*Quercus robur*)} < heather < {scanty ≈ bracken ≈ bare dune sand with few mosses} < oaks beyond their climax stage < mosses < dune shrub (composed mainly of *Hippophaë rhamnoides*). On the low side we see a high uptake and storage in biomass in combination with denitrification in consequence of the oxidation of high DOC levels, and on the high side we see the effect of increasing N_2-fixation (see also section 6.8.3). Intermediately

high, but incidentally very high NO_3^- concentrations below oaks-1, -2 and -3 are probably related to the general stage of decay of this 80 years old plantation on decalcified dune sand, leading to an excess of NO_3^- and K^+ release over NO_3^- and K^+ storage.

Fast growing vegetations like most dune shrubs and pines south of Zandvoort aan Zee, on dune sand without any soil amendment (dune shrubs) or in case of pines with less amendments than on the lysimetric plot, lead to remarkably low levels for K^+ (and K^*), by uptake and storage in biomass (section 6.8.2). This K^+-uptake also has a measureable effect on the K content of the rooted soil, which was observed by Wright (1956) to decrease after plantation of Scotch pine on dune sand, until complete closure of the canopy (15-20 years later). For the major and trace constituents not mentioned so far, no general relations with vegetation could be found.

The effect of different vegetation covers on $\delta^{18}O$ in soil moisture has been given attention by Zimmerman et al. (1967) and Sauzay (1972). A bare soil (in Western Europe) yields a percolate enriched by 1‰ in $\delta^{18}O$ as compared to a soil covered by grass, probably by enrichment upon soil evaporation and due to a higher transmission of summer rains high in ^{18}O. Under forest cover a 0.6‰ higher ^{18}O concentration was observed than under a grass cover, which may be attributed to enrichment upon evaporation of water intercepted by the canopy. The results presented in Table 6.14 reveal a rather narrow range (-6.85 to -7.55‰) for the vegetation groundwaters studied (from mosses to pines). Relatively high ^{18}O concentrations are observed under pines. For the other vegetation types no significant difference can be deduced, also because differences in groundwater age and distance to the HWL have some impact on the data set, which covers a one year sampling only.

And finally, there is a significant effect of vegetation on the mean temperature of pure vegetation water. The drainage water from the lysimeters west of Castricum had a temperature of 9.9, 8.8, 8.3 and 8.2 °C in case of bare dune sand, dune shrub, oaks and pines, respectively (Stuyfzand, 1984d). The temperature decrease with increasing density and height of vegetation, is explained by an increasing evapotranspiration especially of the warm summer rains. This agrees with observations by Pluhowski & Kantrowitz (1963), who found lower groundwater temperatures under wooded areas than under cleared areas. The relatively low temperature below pines slightly favours the dissolution of calcite and reduces the dissolution of silicates (Table 2.13).

Measurable quantities of volatile organochlorine (VOCl), polycyclic hydrocarbons (PAHs) and 1,1,1-trichloroethylene apparantly vary at random (Table 6.16). The more hydrophobic PAHs (with an octanol-water distribution coefficient [K_{ow}] inferior to $10^{-5.5}$) were not detected. The individual monocyclic aromatics and pesticides studied and the total of trihalomethanes (THMs), were all below their analytical detection limit (<0.05 or <0.1 µg/l).

Spatial variations within pure vegetation water

Within pure vegetation water having uniform hydrological and geochemical boundary conditions, significant spatial variations are to be expected, on both a large and small scale.

Large scale variations are related mainly to (1) different degrees of exposition to winds carrying the bulk of sea spray or pollutants from local sources (section 6.5.3, under "spatial variations"), and (2) differences in age, leading to changes in uptake and release. In the so-called edge zone, about three times the tree or shrub height wide (Potts, 1978) the highest concentrations are generally found.

Small-scale variations arise from among others open spots in a forest stand, differences in distance to the tree boles (Krajenbrink et al., 1988), local anomalies in litter accumulation, vitality, crown height etc. (Boumans & Beltman, 1991).

Relation between $CaCO_3$ dissolution and evapotranspiration

Brook et al. (1983) presented a useful relationship between soil CO_2 pressure and evapotranspiration:

$$\log P_{CO_2} = -3.47 + 2.09 \cdot (1 - e^{-0.00172 \cdot E}) \qquad (6.9)$$

with : P_{CO2}= partial CO_2 pressure [100 kPa]; E = mean annual actual evapotranspiration [mm/y]. Although this relation was primarily used for large scale work as the production of a world map of soil CO_2 pressure, it also applies reasonably well to different vegetation covers within a single landscape as the coastal dunes. Thus calculated P_{CO2} values were used to compute the equilibrium Ca^{2+} concentration of several calcareous, pure vegetation groundwaters in the study area, assuming an open system (CO_2 pressure constant during dissolution) and using :

$$Ca^{2+} = \frac{8.2\ (P_{CO_2})^{0.333}}{\gamma_{Ca}} \qquad (6.10)$$

with : Ca^{2+} = equilibrium concentration at 10°C [mmol/l]; γ_{Ca} = activity coefficient for Ca^{2+} [-]. For derivation of Eq.6.10 see for instance Appelo (1988b). The term γ_{Ca} is accurately calculated with for instance WATEQX (Van Gaans, 1989) or approximated by :

$$\gamma_{Ca} = 10^{-2(\sqrt{i}/[1+\sqrt{i}] - 0.3i)} \qquad (6.11)$$

where i = ionic strength = $1.83 \cdot 10^{-5}$ EC_{20} (if $EC_{20} \leq$

700 µS/cm) and else i = $1.42 \cdot 10^{-5}$ EC_{20} (Stuyfzand, 1989b).

Results of calculation are shown for five plots with diverging evapotranspiration, in Table 6.17. They do not compare sufficiently well with the Ca^{2+} levels observed, especially at higher concentrations. The reason for the discrepancy consists of the fact, that significant amounts of Ca^{2+} are leached not only by H_2CO_3, but also by strong acids, mainly HNO_3 and H_2SO_4, either by direct dissolution of calcite or by base exchange (Ca^{2+} depletion by H^+ and Al^{3+} ions). The simple Eq.6.10 is only valid when HCO_3^- equals $2Ca^{2+}$ on a molar basis, so that the predicted Ca^{2+} levels need a correction for all other reactions mobilizing Ca^{2+}. This is achieved by deviding the result of Eq.6.10 by the relative H_2CO_3 contribution to the mobilization of Ca^{2+} ($\%Ca_{H2CO3}/100$). This term can be simply approximated by taking 50 (HCO_3^-/Ca^*), where HCO_3^- and Ca^* are the measured concentrations in mol/l (further details are given in section 8.4.3). Thus corrected values compare well with the Ca^{2+} concentrations observed (Table 6.17). This indicates that there is a good relation between $CaCO_3$ dissolution and evapotranspiration indeed, if complications are properly accounted for.

6.6.4 Effects of differences in decalcification

Decalcification and the acid buffer sequence

The leaching of calcium carbonate is the most prominent weathering reaction in coastal dunes. This is evidenced by the general predominance of Ca^{2+} and HCO_3^- in the charge balance and in the amount of total dissolved solids, for most shallow dune groundwaters. Decalcification is defined here for practical purposes as the moment, where this leaching has reached the critical level of 0.1% $CaCO_3$ on a dry weight basis for the porous medium.

Somewhat earlier, below 0.3%, Boerboom (1963), Rozema et al. (1985) and Grootjans et al. (1989) observed the pH of soil moisture to rapidly drop below 7 (Fig.6.20), indicating that calcium carbonate fails to completely buffer the acid inputs from above. Most shallow dune groundwaters with pH < 7, in fact exhibit negative values of the calcite saturation index SI_c (Fig.6.21).

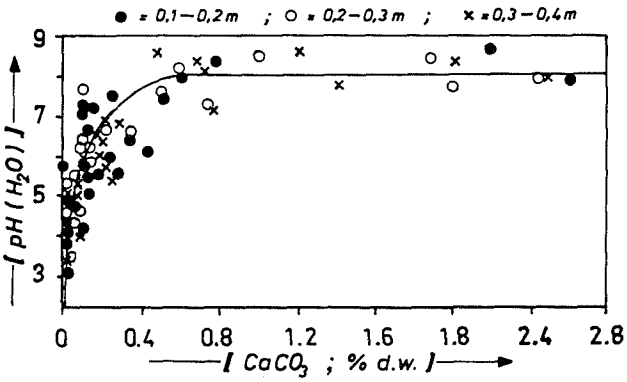

FIG. 6.20 Relation between mineral soil pH (pH-H_2O) and $CaCO_3$ content (% dry weight) at 0.1-0.4 m below the surface, in the transition zone between the primarily calcareous dunes and dunes primarily poor in lime, roughly in between Bergen aan Zee and Egmond aan Zee (synthesis of plots for three depth intervals, from Rozema et al., 1985).

When the $CaCO_3$ content of the soil drops below 0.1% , which approximately happens if pH < 6.2, calcium carbonate loses its dominant position as acid buffering phase (Fig.6.21). This agrees with the generally accepted acid buffer sequence for mineral soils (Table 6.18; Ulrich et al., 1979). The principle of this sequence corresponds with the redox buffer

TABLE 6.17 Comparison of calculated and measured Ca^{2+} concentrations in five calcareous, diverging vegetation groundwaters in the study area. Calculated values are based on the relation between soil CO_2 pressure and mean annual evapotranspiration (Eq.6.9), and open system dissolution of calcite as a function of P_{CO2} and the activity coefficient γ_{Ca} (Eq.6.10).

plot code	E mm/y 1	log P_{CO2} 100 kPa 2	EC_{20} µS/cm 3	γ_{Ca} [-] 4	Ca^{2+}_{calc} mg/l 5	$\%Ca_{H2CO3}$ [%] 6	Ca_{corr} mg/l 7	Ca^{2+}_{meas} mg/l 8
bare-L	200	-2.86	272	0.74	49.4	81	60.9	47.4
mosses-1	300	-2.63	492	0.68	64.2	76	84.5	66.7
dune shrub-L	480	-2.30	692	0.64	87.9	75	117	119
oaks-L	520	-2.23	682	0.64	92.7	84	110	110
pines-L	680	-2.03	2161	0.53	130	51	256	252

1 = evapotranspiration derived from Table 6.1; 2 = calculated using Eq.6.9; 3 = measured (Table 6.13); 4 = calculated (using Eq.6.11); 5 = first approximation using Eq.6.10; 6 = the relative contribution of H_2CO_3 to the mobilization of Ca^{2+}, being approximately 50(HCO_3/Ca^*) in mmol/l (Eq.8.63 in section 8.4.3); 7 = 100 $Ca_{calc}/\%Ca_{H2CO3}$; 8 = observed Ca^{2+} concentration (Table 6.13).

TABLE 6.18 General acid buffer sequence for multi-mineral soils, with the predominant weathering reactions in their specific pH-ranges, such that the most labile constituent is lost first before the next is attacked (adapted from Ulrich et al., 1979). The whole sequence can be traversed, from top to bottom by the soil upon progressive leaching, and from bottom to top by descending water. NB : this sequence holds for a homogeneous soil only (no mixing of different soil horizons, by bioturbation for instance).

pH range	dominating dissolution reaction	base saturation (BS)	CEC-pHX@ / CEC-pH8
6.2 - 8.0	$CaCO_3$ *aragonite* + H_2CO_3 <---> Ca^{2+} + 2 HCO_3^-	≥ 90%	1.0
5.0 - 6.2	cations-Al-silicate[1] + H_2CO_3 + H_2O --> H_4SiO_4 + x cations + HCO_3^- + cations $_{(1-x)}$-Al-silicate[2]	≥ 80%	0.7-1.0
4.2 - 5.0	Al^{3+} + H^+ + [Ca, Mg]· OM <--> Ca^{2+} + Mg^{2+} + [Al, H]· OM	20-90%	0.1-0.7
3.6 - 4.2	$Al(OH)_3$ *gibbsite* + 3 H^+ <--> Al^{3+} + 3 H_2O	≤ 20%	0.1
3.0 - 3.6	$Al(OH)_3$ + $Fe(OH)_3$ + 6 H^+ <--> Al^{3+} + Fe^{3+} + 6 H_2O	≤ 1%	<0.1
≤ 3.0	$Fe(OH)_3$ *ferrihydrite* + 3 H^+ <--> Fe^{3+} + 3 H_2O	~ 0%	<0.1

@ = at ambient pH; [1] = primary silicate; [2] = clay mineral.

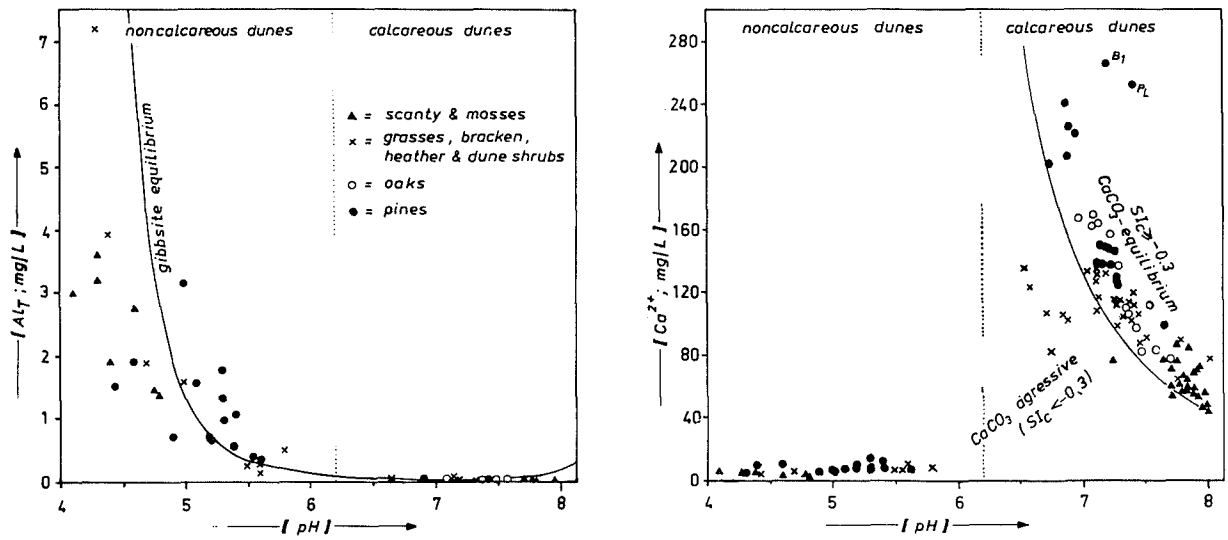

FIG. 6.21 The pH as a master variable in regulating Ca^{2+} and Al concentrations in the upper 0.3 - 3 metres of pure vegetation water, as based on the mean values for all sampling facilities on the 28 plots. The gibbsite ($Al(OH)_3$) equilibrium line was calculated with consideration of $Al(OH)^{2+}$, $Al(OH)_2^+$ and $Al(OH)_4^-$ complexes and a mean activity coefficient for Al^{3+} of 0.66. Samples above this line are not always supersaturated, however, due to neglect of Al-complexes with F^-, SO_4^{2-} and organic acids. The solid line in the Ca^{2+}-pH diagram represents the division between calcite equilibrated and supersaturated water (SI_c>-0.3) and calcite agressive waters.

sequence discussed in section 2.4.2 : the most labile constituent is consumed first before the next most labile constituent is attacked. The "dominant" role of $CaCO_3$ is thus first taken over by primary silicates (pH 5-6.2) and subsequently by the cation exchange complex (pH 4.2-5), amorphous Al-hydroxides (pH 3.8-4.2), Al- and Fe-hydroxides (pH 3.2-3.8) and Fe-hydroxides (pH <3.2). Aluminium phases increase in importance as acid buffering phases when pH<5.5 (Fig.6.21).

The pH-H_2O of soil samples in the dunes under consideration, varies within 2.9 and 8.5 (Figs. 6.10 and 6.20) and generally increases with depth (Fig.6.9; Boerboom, 1963; Rozema et al., 1985). This means that percolating acid rain may experience the whole buffer sequence in principle, starting with the dissolution of Fe-hydroxides near the surface and ending with the dissolution of calcium carbonate at the decalcification depth.

There are essentially two different situations : (a) decalcification proceeded to a certain depth above the phreatic level; and (b) decalcification reached a depth below the phreatic level. Both situations are briefly discussed below, after which the interaction with calcium carbonate, primary silicates and secundary phases is treated in more detail.

Depth of decalcification above the phreatic level
This situation predominates in the primarily calcareous dunes to the south of Egmond aan Zee and in the lime transition zone in between Egmond aan Zee and Bergen aan Zee. It holds for all 24 plots in the primarily calcareous dunes, where the upper parts of the calcareous zone are encountered at a depth varying from <0.1 to 2.7 m above the mean phreatic level (Table 6.1).

Even a short $CaCO_3$ contact above the groundwater table, suffices to transform acid soil moisture into calcareous groundwater in close equilibrium with calcite or aragonite (Figs. 6.9 and 6.14, Table 6.9). Although the whole buffer sequence may be encountered up to the depth of decalcification, generally within a short vertical distance (≤ 2 m on the monitoring plots), most species that dissolve in the acid upper zone, like Al, Fe, Mn, Be, Cd, Co, Ni and Zn, are immobilized before reaching the groundwater table. They precipitate or adsorb to precipitated $Fe(OH)_3$ or $Al(OH)_3$, or substitute for Ca^{2+} in the exchange complex above the decalcification boundary (Fig.6.9).

Somewhat higher soil pH values and relatively short transit times in a thin decalcified zone, as compared to the decalcified dunes north of Bergen aan Zee, probably explain the lower SiO_2 concentrations for the shallow, calcareous dune groundwaters (Fig.6.23). The $CaCO_3$ equilibrated waters exhibit a negative correlation of Ca^{2+} with pH (Fig.6.21) : a high pH means a low Ca^{2+} concentration. This is due to a low CO_2 production under a scanty vegetation cover without dune peat interaction.

Depth of decalcification below the phreatic level
This situation predominates in the dunes primarily poor in lime, to the north of Bergen aan Zee, and thus holds for the plots scanty, heather, pines-4 and pines-5 exclusively. Aluminium hydroxide, the cation exchange complex and primary silicates buffer the acid input down to several metres below the groundwater table. Concentrations are consequently high for SiO_2, Al, Be, Cd, Co, Cr, Li^+, Ni, Rb^+, V and Zn, and low for Ca^{2+}, HCO_3^- and Sr^{2+}, as compared to the calcareous counterparts (Tables 6.13-6.14). This is explained by (a) the lack of $CaCO_3$, (b) reactivity of Al-phases in decalcified dunes when pH drops below about 5.5 (Fig.6.21), (c) a raised mobility for many trace elements, which are partly atmogenic, in acid solutions (Benjamin & Leckie, 1981; Stumm & Morgan, 1981; Garrels & Christ, 1965), and (d) a lower pH and longer transit time in the decalcified zone.

Concentrations of Al rapidly increase when pH drops below 5.5 and thereby approximate equilibrium with gibbsite ($Al(OH)_3$; Fig.6.21). The gibbsite saturation line was calculated neglecting AlF^{2+}, AlF_2^+ and $AlSO_4^+$ complexes. This explains the apparant supersaturation for several samples, especially those below pines with high F^--levels resulting in a 30-85% complexing of Al (Stuyfzand, 1989a). In fact, most samples in Fig.6.21 are undersaturated with respect to gibbsite and (slightly) supersaturated with respect to Al-hydroxisulphate minerals like alunite and jurbanite, that may form as secundary phases.

Calcium carbonate
The geochemistry of the shell fragments (Table 6.5) reveals that their congruent dissolution would explain not only most of the Ca^{2+} and HCO_3^- concentrations of pure vegetation water in the calcareous dunes, but also most of its Sr^{2+} content and a significant portion of its Na^* , PO_4^{3-}, I, Ba^{2+}, Co, Fe, Mn, Ni and Pb concentration (Tables 6.13-6.15). No significant positive correlations were found at all, however, between Ca^{2+}, that indeed originates for >90% from the dissolution of calcium carbonate, and these constituents, Sr^{2+} excluded. The mean Sr^{2+}/Ca^{2+} ratio for all pure vegetation water samples (Fig.6.22), approximates the mean ratio for aragonitic and calcitic shells in dune sand, which suggests that Sr^{2+} dissolves about congruently indeed (reaction 8.30A/B in Table 8.3).
Especially Co, Fe, Mn, Ni and Pb probably dissolve incongruently and accumulate in secundary phases like $Fe(OH)_3$ and MnO_2. Congruent dissolution of

TABLE 6.19 Modal trace element content of important silicates (compilation of data dispersed in Wedepohl, 1978), their calculated concentration in water assuming congruent dissolution of these minerals to yield 6 mg/l SiO_2, and the concentration variation as observed for the pure vegetation groundwaters on the 28 plots studied. Concentrations were calculated using : $(TE)_{H2O,\ \mu g/l} = 6000 \cdot (TE/SiO_2)_{solid,\ mg/kg}$. For deviating dissolved SiO_2 concentrations, multiply the indicated concentrations with : (observed SiO_2 in mg/l)/6. In reality, silicates dissolve incongruently with most TEs accumulating in the weathering residues. The calculated release of TEs must therefore be considered as an upper limit in most cases.

trace element	solid phase (mg/kg)						solution (µg/l) with 6 mg/l SiO_2 from congruent dissolution						groundwater (µg/l)			
	K-feld-spar	plagio-clase	horn-blende	biotite	quartz	illite	K-feld-spar	plagio-clase	horn-blende	biotite	quartz	illite	calcareous dunes min.	calcareous dunes max.	noncalcareous min.	noncalcareous max.
Al	97,000	103,000	23,500	90,000		54,000	900	900	250	1,350		620	≤1	89	130	7,200
As	1.5	1.5	1.5	1.5	-	22	0.01	0.01	0.02	0.02	-	0.25	≤0.1	105	≤1	24
B	15	100	20?	15	0.3	270	0.1	0.9	0.2	0.2	<0.1	3.1	<50	260	<50	<50
Ba	500	150	1,200?	1,200	10	380	4.6	1.3	13	18	0.1	4.4	10	79	<5	87
Be	2.3	5.5	9	8	1.3	-	0.02	0.05	0.10	0.12	0.01	-	<0.05	<0.05	<0.05	5.2
Cd	-	0.15	-	1.5	-	-	-	0.001	-	0.02	-	-	<0.1	0.2	0.1	2.7
Co	0.1	15	50	55	0.5	19	<0.001	0.13	0.54	0.82	0.003	0.22	<0.1	3.6	0.5	62
Cr	-	-	40?	45?	-	167	-	-	0.43?	0.67?	-	1.9	<0.2	2.2	0.2	4
Cs	10	-	10?	10		21	0.1	-	0.11?	0.15	-	0.24	-	-	-	-
Cu	10	20	20	15		-	0.1	0.2	0.2	0.2	0.01	-	0.8	27	1.1	22
Eu	0.9	0.9	2.1	-			0.008	0.008	0.023	-	-		<0.02	<0.02	-	-
F	300	790	6,000	4,000		-			65	60		-	37	440	10	580
Fe	-	-	145,000	187,000		25,600	-	-	1,570	2,800		300	20	36,300	70	4,710
Hg	0.08?	0.08?	-	-	-	-	0.001	0.001	-	-		-	<0.1	<0.1	<0.2	<0.2
I	-	-	0.16	0.5	-		-	-	<0.01	0.001	-		<0.5	9	<1	16
Li	10	6	33	400	10		0.1	0.1	0.4	6.0	0.1		<0.5	10	4	30
Mn	9	15	1,550	1,400	-		0.1	0.1	17	21	-		<10	4,350	10	300
Mo	0.9	0.9	3.5	4.5	0.3		0.01	0.01	0.04	0.07	0.002		<1	<1	<0.1	<0.1
Ni	-	20	30	50	-	-	-	0.2	0.3	0.7	-	-	1	8	3.5	187
Pb	45	24	20	35		160	0.4	0.2	0.2	0.5		1.8	<0.5	9	0.1	3.8
Rb	250	20	-	500		220	2.3	0.2	-	7.5		7.5	<0.1	3.1	0.6	6.2
Sb		0.1	-	-		1.2		0.001	-	-		0.01	<1	<1	<0.5	<0.5
Sc	-	-	<30?	<30		24	-	-	<0.32	<0.45		0.27	<0.02	<0.02	-	-
Se	0.15	0.15	0.15	0.15	-	-	0.001	0.001	0.002	0.002	-	-	0.01	0.2	<1	<1
Sn	2	1.2	6	6	0.5		0.02	0.01	0.06	0.09	0.003		<2	4.3	<0.5	<0.5
Sr	140	170	15	20	-	-	1.0	1.5	0.2	0.3	-	-	240	1,000	<50	<100
Ti	100	120	-	24,000	50	3,450	0.9	1.0	-	359	0.3	40	<2	8	<2	4
U	2.7	2.7	7.9	8.1	1.7	-	0.025	0.024	0.085	0.121	0.01	-	<0.02	2.7	-	-
V	10	13	150	110	-	105	0.1	0.11	1.62	1.64	-	1.21	0.10	14	0.7	36
Zn	10	15	270?	400	6	120	0.1	0.1	3.0	6.0	0.04	1.4	<2	530	4	739

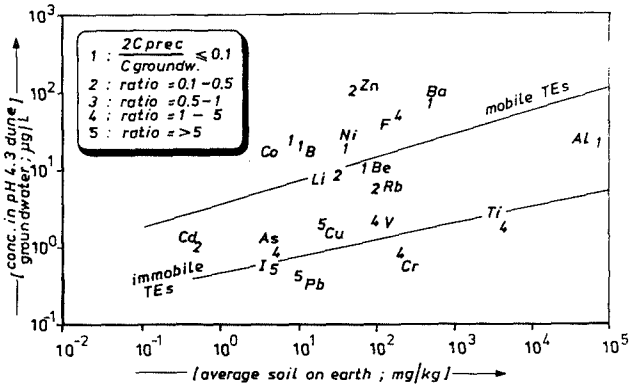

FIG. 6.24 Concentration of trace elements in pH 4.3 dune groundwater north of Bergen plotted against their average abundance in soil material (according to Rahn, 1975; Table 1.1), with indication of their mobility (1 = high, 5 = low). The latter is deduced from the ratio of 50% evaporated bulk precipitation ($2C_{prec}$) to shallow groundwater ($C_{groundwater}$), on a µg/l basis.

become positively charged and sorb oxy-anions like AsO_4^{3-}, CrO_4^{2-}, MoO_4^{2-}, $Sb(OH)_6^-$, SeO_4^{2-}, VO_4^{3-} and WO_4^{2-}, thus explaining their positive correlation with pH (Arends et al., 1987; Tanji & Valoppi, 1989; Stuyfzand & Reiniers, 1990).

A negative correlation with pH or positive correlation with Al should remain in this case for B, Co, Mn, Ni, U and Zn. But also now complications arise, as shown for Co and Ni in Fig.7.4. Their maximum levels do not coincide with pH minima or Al maxima, but are encountered in the downward migrating transition zone between the upper groundwater with Al > 1 mg/l and pH < 5 and groundwater several metres deeper with Al ≤ 0.3 mg/l and pH ≥ 5.5 (section 7.3). This can be explained in a similar way as uranium roll-front deposits are known to originate (section 7.3.4 under "acidified zone, 2-5 m").

Most iron in groundwater is mobilized from $Fe(OH)_3$ by reduction and complexation to organic acids. The highest levels of Fe-total are in fact

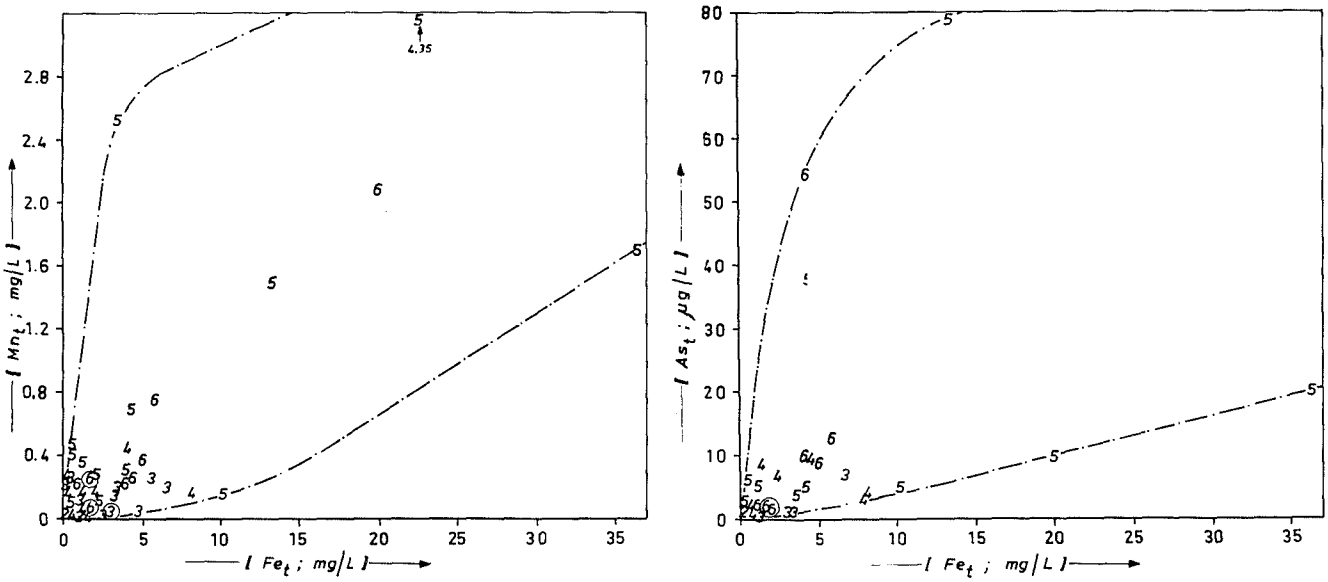

FIG. 6.25 Scatter diagram of the mean concentrations of As-total and Mn-total against the mean total Fe concentration, for each observation facility involved in sampling the vegetation waters studied. The DOC content (1 = 0-2; 2 = 2-4; 3 = 4-8; 4 = 8-16; 5 = 16-32; and 6 = 32-64 mg/l), and redox level (encircled = (sub)oxic; not-encircled = anoxic) are indicated.

encountered in anoxic, sulphate-stable environments and are associated with DOC-levels superior to 16 mg/l (Fig.6.25). Correlations of the above mentioned TEs with Fe are very poor, even Mn and As do not correlate well with Fe (Fig.6.25). This is probably connected with complications like : a selective leaching of Co, U and Mn, just before reduction of $Fe(OH)_3$ (section 7.4.4); other sources of TEs (organic matter, calcium carbonate, pyrite); retention of Fe by formation of anoxic secundary minerals (like pyrite or hydrotroillite, vivianite or siderite) or by sorption.

The present formation of aluminium hydroxi-sulphates, like ill-crystallized jurbanite ($Al(OH)SO_4 \cdot 5H_2O$), helps to explain the relatively low SO_4^{2-} levels encountered in (sub)oxic and sulphate-(meta)stable groundwater in the decalcified dunes, as compared to the calcareous dunes.

6.6.5 *Effects of different kinds of dune peat interaction*

The hydraulic resistance and hydrochemical changes largely depend on the type of dune peat involved and the position of the peat with respect to the groundwater table (Fig.6.26). The passage of the generally eutrophic dune peats is influencing the upper groundwater considered, on the plots grasses-3, bracken-2, dune shrub-3, dune shrub-4, oaks-1, pines-1 and pines-3 (Table 6.1), all situated in the area to the south of Zandvoort aan Zee. More detailed information on the effects of different kinds of dune peat interaction in this area, using additional piezometer nests (Stuyfzand & Lüers, 1991), has been included in the following.

Dune waters that passed through dune peat, generally rank amongst the highest in HCO_3^-, Ca^{2+}, DOC, COD and Ba^{2+}, amongst both the highest and the lowest in NO_3^-, SO_4^{2-}, NH_4^+, PO_4^{3-}, Fe, Mn, SiO_2 and As, and amongst the lowest in pH (of the calcareous dune waters) and Mg^* (Tables 6.13-6.15).

Types of dune peat

Three types of dune peat are involved, in order of increasing depth below the surface (Fig.6.26) : type $1A_1$, about 800 years old, humic sand to sandy peat at 4.5 to 6 m+MSL and 0.01-0.1 m thick (observed on plot pines-3); type $1A_2$, 1100-2000 years old sandy peat at 3-4 m+MSL with a median thickness of 0.2 m (found on plot pines-1); and type $1A_3$, 2000-3000 years old, strongly compacted dune peat at 2 m ± MSL and 0.05-1.0 m thick (encountered on the plots bracken-2, 0.4 m thick; grasses-3, 0.4 m thick; dune shrub-3, 0.05 m thick; dune shrub-4, 0.1 m thick; and oaks-1, 0.4 m thick).

Dune peat permanently or periodically above the groundwater table

The composition of the upper groundwater in areas, where dune peats $1A_1$ or $1A_2$ have been permanently situated above the phreatic level for decennia,

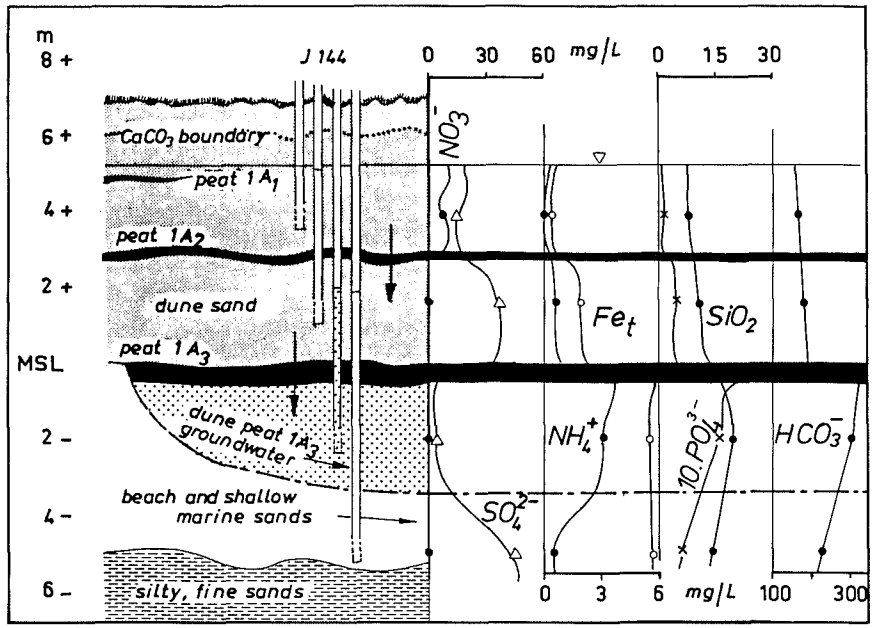

FIG. 6.26 Schematized cross section over the central younger dune area 6.5 km to the south of Zandvoort aan Zee (100 m east of the plot pines-3), with the position of three types of dune peat ($1A_1$- $1A_3$) and some hydrochemical effects. Passage of $1A_2$ peat leads to complete denitrification and some mobilization of PO_4^{3-}, NH_4^+ and Fe. Passage of $1A_3$ peat conduces to more spectacular changes including methanogenesis. Groundwater deeper than 3.5 m-MSL did not contact $1A_3$ peat and consequently contains sulphate and low concentrations of nutrients.

does not deviate much from that in areas without dune peat interference (Table 6.20; Fig.6.27). The prolonged leaching in an oxic environment open to the atmosphere, left only the most stabilized organic matter, which does not decompose or decomposes very slowly.

Quite a different picture arises, however, for dune peat $1A_3$ as observed on the plot bracken-2. Larger reserves of unstabilized O.M. due to a greater thickness and much higher degree of compaction probably still lead to the observed high-rate transformation of organic nitrogen into NO_3^- and of sulphur (organic and bound to Fe^{2+}) into SO_4^{2-}. These acid-forming reactions (see Table 8.2) are completely buffered by the dissolution of shell debris, which leads to the formation of the $CaNO_3$ water type. Ferric hydroxides, that remain stable in this (sub)oxic environment and are formed upon oxidation of iron sulphides, effectively sorb the mineralized phosphorus and arsenic.

Dune peat type $1A_3$ was observed to be periodically drowned by groundwater on the plots grasses-3 and oaks-1. This situation leads to very strong quality fluctuations in the underlying groundwater (section 6.7.4). The mean composition does not testify of large changes in NO_3^- and shows mild increases for SO_4^{2-}, PO_4^{3-}, As, Fe, Mn and SiO_2.

Permanently submerged dune peat

The passage of permanently submerged dune peat leads to a significant increase of NH_4^+, Fe, Mn, SiO_2, HCO_3^-, DOC and PO_4 (both ortho and total), a slight increase of Ca^{2+}, and a strong decrease for pH, Mg^{2+}, O_2, NO_3^- and possibly SO_4^{2-}. These changes become more pronounced and roughly follow the redox sequence depicted in Fig.2.11, as the groundwater passes through the peat types $1A_1$, $1A_2$ and $1A_3$ successively (Figs. 6.26 and 6.27, Table 6.20). Peat type $1A_1$ leads to a partial denitrification, peat type $1A_2$ at least to a nearly complete denitrification and peat type $1A_3$ generally to sulphate reduction. A strong uptake of nitrate by pines and the oxidation of dissolved organic carbon in the unsaturated zone, probably explain the partial SO_4^{2-} reduction also upon passage of dune peat $1A_2$ on the plot pines-1 (Fig.6.45).

The NH_4^+ and PO_4^{3-} produced by oxidation of O.M., remain mobile in the anoxic environment below peat type $1A_2$. Ammonium was preferred to HCO_3^- and PO_4^{3-} as an indicator of the extent of anoxic interaction with dune peat. It is, contrary to HCO_3^-, relatively independent of the local vegetation cover and explained most quality variations below the anoxic dune peats best, as evidenced by excellent positive correlations with HCO_3^-, PO_4^{3-}, DOC, Fe, Mn and SiO_2 concentrations (r^2 >0.8).

TABLE 6.20 Mean composition of dune groundwater (2-48 samples), that passed one or several distinct dune peat layers (types $1A_{1-3}$ depicted in Fig.6.26) either permanently above or below the phreatic level. Based on a survey in the Luchterduinen south of Zandvoort aan Zee (mosses, dune grasses and dune shrub), in March 1990 - February 1991, and including data from the plot bracken-2. TEs were analysed in 0.45 µm filtered samples. The concentration of TEs in water that passed through $1A_3$ peat was calculated under the assumption of congruent dissolution.

n_o samples	depth m+MSL	peat passed	EC_{20} µS/cm	pH	Cl^-	SO_4^{2-}	HCO_3^-	NO_3^-	PO_4-t	Na^+	K^+	Ca^{2+}	Mg^{2+}	NH_4^+	Fe-t	Mn-t	SiO_2	DOC	O_2	SI_c
												mg/l								
PEAT PERMANENTLY IN UNSATURATED ZONE																				
2	3.7	$1A_1$	515	7.55	47.5	21.0	196	26.6	0.13	21.0	1.3	86	4.4	0.04	0.05	0.01	4.8	2.0	6.5	0.13
5	1.5	$1A_2$	708	7.42	81.6	38.8	266	30.0	0.06	38.6	1.4	110	7.9	0.03	0.10	0.03	5.2	6.5	1.5	0.19
8	0.5	$1A_3$	1214	7.20	34.6	128	282	381	0.05	19.8	0.4	266	3.6	0.05	<0.2	<0.1	5.4	27.9	-	0.29
NO PEAT INTERACTION																				
48	3.8	-	569	7.42	49.9	32.3	231	27.0	0.09	23.0	1.2	97	6.5	0.05	0.17	0.05	5.2	4.8	1.8	0.05
PEAT PERMANENTLY IN SATURATED ZONE																				
12	3.7	$1A_1$	568	7.40	55.8	38.6	231	7.0	0.22	27.5	2.4	92	6.2	0.15	1.24	0.06	5.3	5.9	1.1	0.02
18	1.5	$1A_{1-2}$	538	7.39	41.0	29.2	266	1.9	0.56	22.3	1.1	95	5.2	0.43	2.62	0.14	7.5	5.3	<1	0.10
14	-1.7	$1A_{1-3}$	556	7.12	41.1	3.7	321	<0.5	1.85	21.2	1.5	98	3.9	4.3	6.24	0.44	21.0	5.9	<0.5	-0.03

TRACE ELEMENTS

n_o samples	depth m+MSL	peat passed	Al	As	B	Ba^{2+}	Br^*	Cd	Co	Cr	Cu	F^-	I	Li^+	Ni	Pb	Rb^+	Sr^{2+}	V	Zn
												µg/l								
PEAT PERMANENTLY IN UNSATURATED ZONE																				
2	0.5	$1A_3$	<20	0.9	-	30		<0.1				87								33
NO PEAT INTERACTION																				
4	3.8	-		1.7	<50	10	36	<0.1	<1	<0.5	1.6	165	1.6	1.3	2.1		0.4	475	<1	<10
PEAT PERMANENTLY IN SATURATED ZONE																				
2	3.7	$1A_1$	3	0.9	<50	12	159	0.1	<1	0.9	1.0	160	2.8	0.9	4.2	<1	0.4	385	<1	<10
2	1.5	$1A_{1-2}$	5	<1	<50	12	51	≤0.1	<1	1.0	0.8	130	2.8	1.5	1.2	<1	0.4	390	<1	<10
2	-1.7	$1A_{1-3}$	7	<1	<50	15	61	≤0.1	<1	0.8	<1	140	7.4	2.9	1.3	<1	1.2	455	<1	<10
CALCULATED FOR $1A_3$			573	0.7	-	3	4	0.07	0.2	1.4	0.8	-	0.9	-	0.4	4	0.5	-	1.1	4

The molal N/P ratio of groundwater below the peats $1A_1$, $1A_2$ and $1A_3$ increases from 3.6 to 4.0 and 12.2, respectively. This corresponds with a preferential leaching of phosphate as compared to NH_4^+ and concomitant PO_4 depletion of the older peat (Table 6.8). The high ratio below peat $1A_3$ may also point at the formation of vivianite, as the groundwater below that peat is supersaturated.

The low Ca^{2+} production as compared to HCO_3^-, is explained by the minor CO_2 increase upon denitrification and the reduction of sulphate, Fe- and Mn-oxides (Table 8.2). Only where also methane (and concomitantly CO_2) is formed, Ca^{2+} is expected to increase significantly.

Strong increases of SiO_2 below $1A_3$ peat can be explained by a combination of processes : (1) the dissolution of ferric hydroxide coatings, which protect reactive phases; (2) the dissolution of amorphous ferric hydroxide phases containing significant amounts of sorbed or coprecipitated SiO_2 (reaction 8.20 in Table 8.2), for instance in buried B_2-illuvial horizons; (3) the dissolution of phytoliths (opaline grains excreted by plants), which possess a high solubility (Bartoli & Wilding, 1980); and (4) complexation of SiO_2 to fulvic acids (Huang & Kiang, 1972; Pekdeger, 1979).

Above dune peat, Mg^* concentrations in the upper groundwaters generally exceed the levels expected from the dissolution of shells (Table 6.5 and 6.15) and silicates (Fig.6.23). The exchange complex in the acidifying upper soil is postulated as the Mg-donor (sections 6.4.2 and 6.6.4), whereas the Mg^{2+}-decrease upon peat passage may relate to cation exchange, probably for Ca^{2+}, NH_4^+ or Fe.

Trace elements

The oxidation of peat does not lead to significant mobilizations of TEs (Tables 6.14 and 6.20), notwithstanding its high contents (section 6.4.3). Using the mean composition of peat given by Edelman (1983, annex 75) and a mineralization of 20 mg C/l water that passed through peat $1A_3$ (90 mg HCO_3^-/l + 2 mg DOC/l), would indeed yield, upon congruent decomposition of peat and

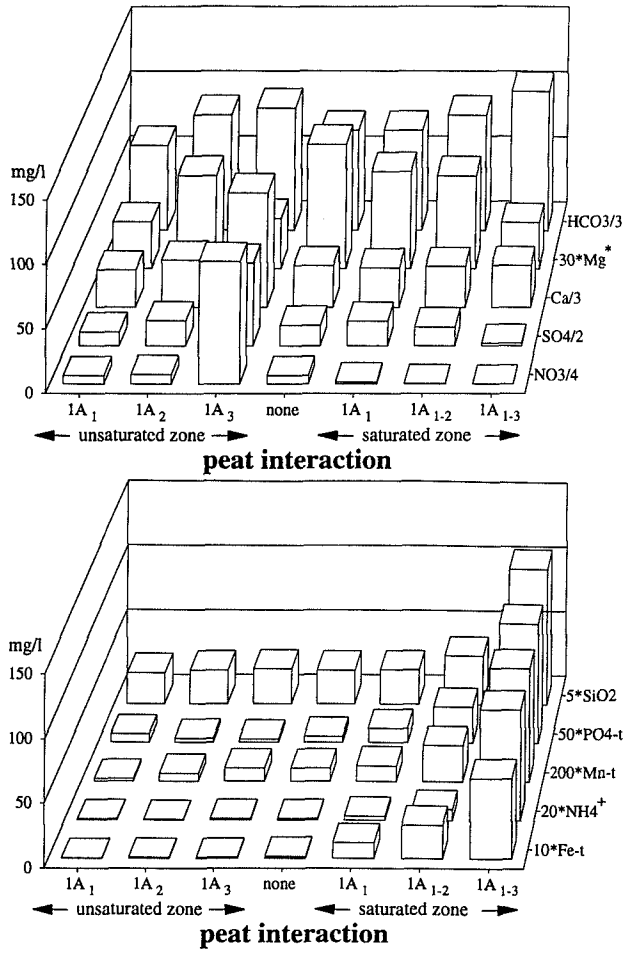

FIG. 6.27 Effects of different kinds of dune peat interaction on the mean composition of the upper groundwater in the dunes about 6.5 km to the south of Zandvoort aan Zee, mainly in the period March 1990 - February 1991 (based on data in Table 6.20). Peat types $1A_{1-3}$ are explained in Fig.6.26. - = without peat interaction.

dissolution of all other included phases, the low concentration increments listed in Table 6.20. Despite many drawbacks, these calculations roughly agree with observations on dune water below $1A_3$ peat, regarding As, Ba^{2+}, Cd, Co, Cr, Rb^+ and Zn (Table 6.20). The release of Al is much smaller, as expected from the pH attained, and higher for I, perhaps due to preferential leaching. The concentrations of Cu, Ni, Pb and V do not increase but decrease, probably by adsorption or coprecipitation with iron sulphides. The increases for Li^+ and Rb^+ may relate to the dissolution of silicates, the Sr^{2+} increase to the dissolution of shell fragments, and the F^- decrease to adsorption.

Areal extent of dune peat $1A_3$ groundwater

Passage of the most reactive dune peat $1A_3$ labelled the groundwater downgradient in such a way, that this water could be recognized easily amidst groundwater without this interaction (Fig.6.28). The boundary between ≥80% dune peat $1A_3$ water and <20% surrounding groundwater was set at $NH_4^+ \geq 2$, PO_4-total ≥ 1.5 and $HCO_3^- \geq 300$ mg/l, the boundary between <20% dune peat $1A_3$ water and ≥80% surrounding water at $NH_4^+ \leq 0.7$, PO_4-total ≤ 0.7 and $HCO_3^- \leq 260$ mg/l, and the 50% mixing divide in between. A predominantly horizontal flow below the peat, due to strong draining effects of the Oosterkanaal, permitted to calculate the hydraulic resistance of the peat layer from the observed thickness of the peat water lens. Approximately the same approach as applied to vegetation groundwater lenses (section 6.3.3) could be used (Stuyfzand & Lüers, 1991).

6.6.6 *Effects of differences and changes in thickness of the unsaturated zone*

Variations in thickness of the unsaturated zone between dune tops and valleys, may amount to 20-40 metres. The maximum difference between the plots studied, is only 3.8 m, and between plots with a comparable vegetation cover and distance to the HWL, it is not more than 0.4 m (grasses-1 and -2) or 0.7 m (grasses-4 and -5). These small differences are nevertheless sufficient to indicate the direction of the hydrochemical effects, even though they are also accompanied by small (grasses-2) and significant (grasses-4) increases of density and height of the vegetation (Table 6.1).

The data presented in Fig.6.29, reveal that a mean position of the water table within 0.5 m below the surface causes anoxic conditions by waterlogging. The upper soil is drowned in winter then, because of a mean amplitude of fluctuation of 0.3 m and a 0.25 m thick capillary fringe. This leads to raised concentrations of HCO_3^-, DOC, NH_4^+, Fe, Mn, PO_4^{3-} (Fig.6.29), As and SiO_2, and low concentrations of O_2, NO_3^- (Fig.6.29) and occasionally SO_4^{2-} (Table 6.13) by (complete) reduction. Complete sulphate reduction and methanogenesis are observed in dune slacks with a prolonged or permanent inundation, like the Kapenglop valley on the island of Schiermonnikoog (Stuyfzand et al., 1993) and the Zwanenwater (Stuyfzand & Lüers, 1992a), respectively. The phosphate increase in the upper groundwater, with decreasing depth to the water table (Fig.6.29), is explained by :

(1) a raised mobility in anoxic environments due to dissolution of the sorbent ferric hydroxide, and by increased concentrations of humic substances that compete for sorption sites and may complex PO_4^{3-} (Sanyal & De Datta, 1991); and

(2) the recycling of PO_4^{3-} in the root zone, i.e. within the upper 1 m. The high phosphate levels arise from decomposing litter or soil humus (Section 6.5).

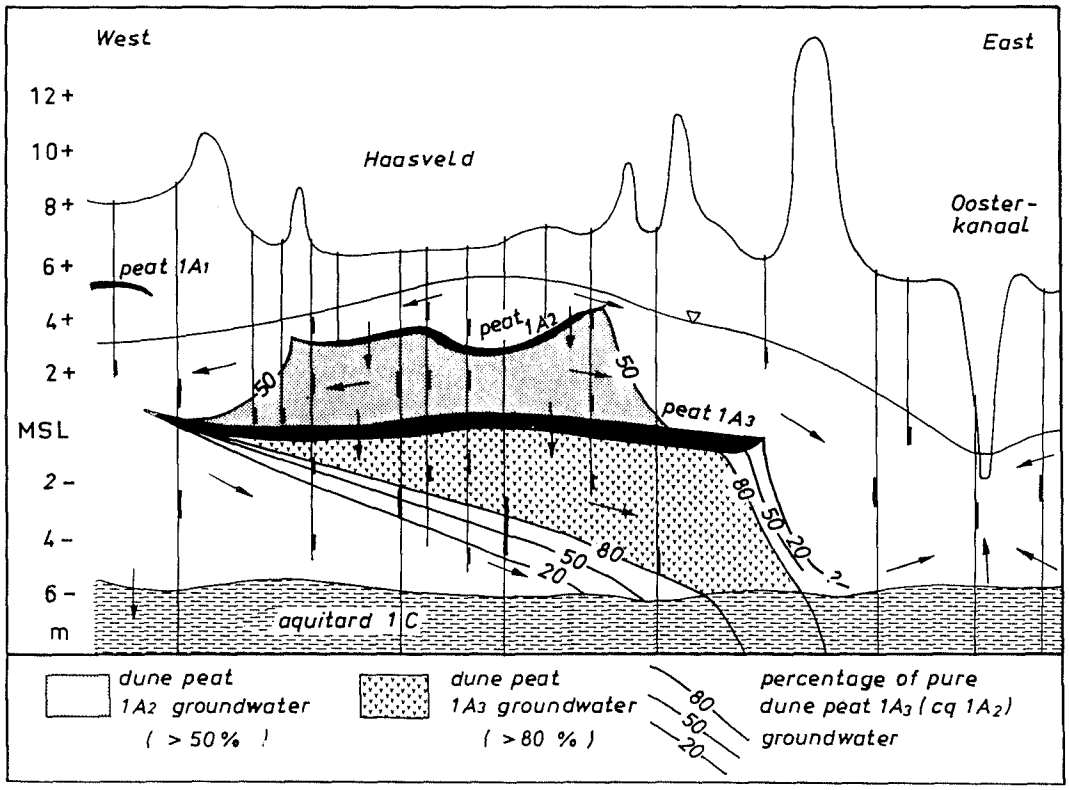

FIG. 6.28 Areal extent of dune peat $1A_3$ groundwater about 6.5 km to the south of Zandvoort aan Zee (close to the plot pines-3) in 1990-1991, as visualized using the geochemical labels NH_4^+, PO_4-total and HCO_3^-.

When the mean water table is situated deeper than 0.5 m below the surface, (sub)oxic conditions prevail throughout the upper soil and in the upper groundwater. Relations between the depth of the groundwater table and concentrations of nitrate were also established, but for other areas (Van Duijvenbooden, 1989; Boumans & Beltman, 1991).

Some effects of still deeper water tables can be deduced from Fig.6.30, where a prolonged detention in the (sub)oxic unsaturated zone clearly promotes (a) the removal of DOC (as deduced from COD by $KMnO_4$), by sorption, precipitation and subsequent partial oxidation, and (b) the smoothing of quality fluctuations by dispersion (Cl^-) and physico-chemical processses as well (COD). The significance of the partial DOC removal in this system open to the atmosphere, reaches very far. It means that the dissolved oxidants O_2, NO_3^- and SO_4^{2-}, as well as substances that are not broken down in (sub)oxic environments like many halogenated hydrocarbons, can penetrate into the water table domain and reach the deeper parts of aquifers poor in OM and pyrite. The increased oxic mineralization of OM (reaction 8.11), the lack of reduction of SO_4^{2-}, Mn- and Fe-oxides (reactions 8.13-8.15) in an extended unsaturated zone and perhaps the higher flow velocity (about

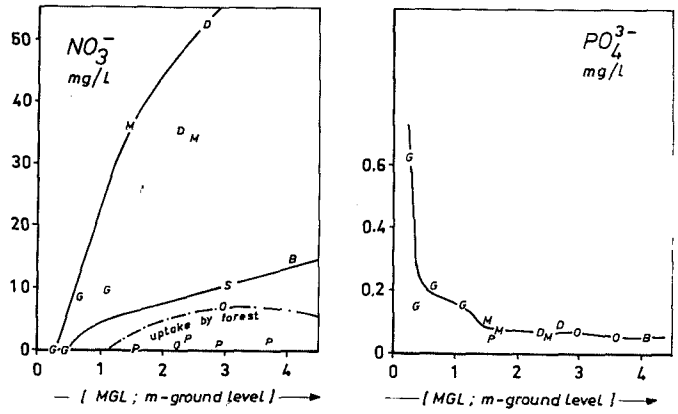

FIG. 6.29 The mean depth to the groundwater table (MGL) as a master variable in regulating nitrate and orthophosphate concentrations in the upper 0.3 - 3 metres of pure vegetation water. Based on the mean values for all plots that lacked any dune peat interference (NO_3^-), and ditto excluding the lysimeters and decalcified dunes (PO_4^{3-}). Plotted characters indicate the vegetation cover : B = bracken; D = dune shrub; G = dune grasses; M = mosses; O = oaks; P = pines; S = scanty or bare.

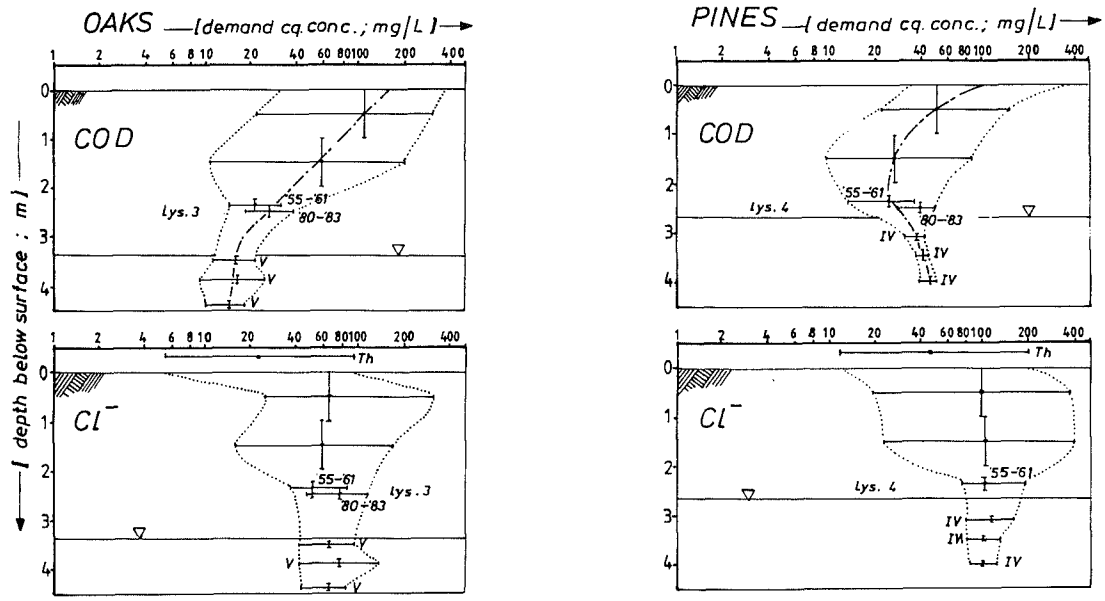

FIG. 6.30 Changes in the mean, minimum and maximum COD (Chemical Oxygen Demand by and expressed as $KMnO_4$) and Cl^- concentration of soil moisture and the upper groundwater, as a function of the depth below ground level, covered by either oaks or pines. Synthesis of data from various sources and sampling periods : soil moisture from Wind (1952), lysimeters from Stuyfzand (1984d), throughfall (=Th) from Stuurman (1984a) and groundwater from this study. A deep water table promotes the aerobic decomposition of dissolved organics in a system open to the atmosphere, and thereby raises the downward flux of oxidants towards the water table, leading to an accelerated acidification and persistence of various xenobiotics.

six-fold in connection with the lower water content) are expected to accellerate acidification (the leaching of acid buffering minerals). The higher flow velocity and variable moisture content in the unsaturated zone as compared to the saturated zone, probably conduce to a more effective discharge of the weathering products.

Micro-scale variations in a wet dune slack

Investigations in the wet dune slack "Kapenglop" on the island of Schiermonnikoog (Fig. 1.1), yielded information on micro-scale variations of hydrochemistry and geochemistry in consequence of local differences in the dominant, vertical flow direction and the mean depth to the groundwater table (Esselink et al., 1989; Stuyfzand et al., 1993). The situation along a transect in the eastern part of the dune slack in July 1987 (Fig.6.31) revealed the strong influence of micro-scale relief on the redox level and degree of decalcification : under the small dune hummocks within the dune slack, more acid and less anoxic groundwater (SI_c <-2, SO_4^{2-}>10 mg/l) is observed, in dune sand that is more depleted in $CaCO_3$. This corresponds with a mean depth to the water table superior to 0.5 m, a longer period of downward water movement and less interaction with decomposing organic matter.

Only in the east-southeast corner an upward flow of groundwater is deduced from the diagnostic combination of a calcareous and (sub)oxic to reduced facies (SI_c >-0.3; SO_4^{2-}>10 mg/l). Piezometric heads showed insufficient vertical differentiation for conclusions on the vertical flow direction (Fig.3.51).

Shallow groundwater in the lower parts of the dune slack, the ESE-corner excluded, exhibits a typical acid, deep anoxic facies. Sulphate is (nearly) completely reduced by interaction with decomposing biomass, that is partly composed of algal mats. This sulphate depleted water formed a well recognizable plume downgradient, demonstrating the large-scale dominance of downward over upward groundwater flow in the western part of the Kapenglop valley (Stuyfzand et al., 1993).

Changes after a drawdown or rise of the water table

A drawdown of the mean water table from <0.5 to >>0.5 m below the surface, as happened in the dunes (section 3.8) and elsewhere, is thus accompanied by an increased flux of dissolved oxidants towards the water table, a change from anoxic into (sub)oxic conditions with all inherent consequences for redox sensitive constituents of water and soil (see above), and an increased acidification. Of

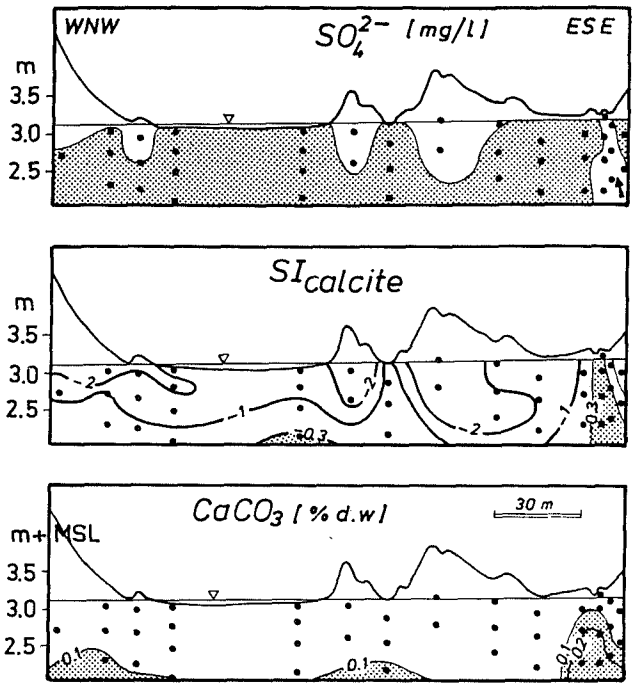

FIG. 6.31 Micro-scale hydrochemical and geochemical variations in the wet dune slack "Kapenglop" on the island of Schiermonnikoog (Northern Netherlands) in July 1987, due to differences in dominant, vertical flow direction and the mean depth to the groundwater table. Only on the right hand side and in between both small dune hummocks groundwater flows predominantly in an upward direction. Reduced, calcareous dune-top groundwater (SO_4^{2-} >10 mg/l; SI_c >-1) exfiltrates there in a zone with a relatively weak decalcification. Elsewhere the predominant vertical flow is directed downwards, and either acid, deep anoxic dune valley water develops or acid, (sub)oxic to reduced dune-top groundwater. Elaboration of data supplied by A.P. Grootjans (RUG). The heavy dots represent the sampled mini-piezometers.

course, many complications will arise due to the more subtle reactions of vegetation which also strongly depend on the extent of the drawdown.

A rise of the water table has been observed in and close to the spreading areas, and is expected in dune areas where groundwater withdrawal is to be reduced or stopped. The chemical consequences are about contrary to the changes after a drawdown. However, only when periodical or (semi)permanent flow-through lakes reappear on the scenery, the effects of acidification can be reversed by a substantial upward flow of relatively deep, calcareous groundwater. The base saturation is slowly restored then after displacement of Al and H^+ from the exchange complex, by Ca^{2+} and Mg^{2+}. This process may require several years (Stuyfzand & Lüers, 1992b).

6.7 Fluctuations in the composition of upper dune water

6.7.1 Main causes

Quality fluctuations of groundwater can be classified as natural or anthropogenic, as real or apparent, as periodical or accidental and as long-term or seasonal or diurnal. The real fluctuations are generated in various ways, for instance : in the atmosphere by the annual temperature cycle and by variations of the composition of bulk precipitation, aerosols and gases; in the biosphere by the seasonal life cycle of plants, long-term successions and afforestation; in the lithosphere by seasonal changes in solubility or mineralization due to variations in temperature (Table 2.13) and agressivity of recharged water, and by long-term leaching or soil amendments; and in the hydrosphere by fluctuations in the position of the water table and flow lines.

The driving force behind seasonal fluctuations in the chemistry of the upper groundwater generally is the seasonal course of air temperature, which approaches a sine with a maximum of 17°C in mid-July (daily mean for 10 days) and minimum of 2°C in mid-February (daily mean for 10 days), in the study area (Fig.6.32). The fluctuations in temperature and in the composition of groundwater are not necessarily in phase, however, not even after a correction for the transit time of water in the vadose zone. This can be predicted already from the deviating phases of the seasonal fluctuations in : temperature, the chemistry of bulk precipitation, groundwater recharge and the elevation of the groundwater table (Fig.6.32).

Other complicating factors are the amplitude reduction and retardation of the annual temperature cycle with increasing depth below the surface, by heat transfer. The amplitude of the temperature wave at depth z (A_z) below the surface is calculated, according to Sellers (1965), by :

$$A_z = A_o \cdot e^{\left(-z \cdot \sqrt{\frac{\omega}{2\kappa}}\right)} \qquad (6.12)$$

and the phase delay Δt, in s, by :

$$\Delta t = z \cdot \sqrt{\frac{1}{2\omega\kappa}} \qquad (6.13)$$

where : A_o = amplitude of the temperature wave [°C] at z = 0 m; z = depth below surface [m]; ω =

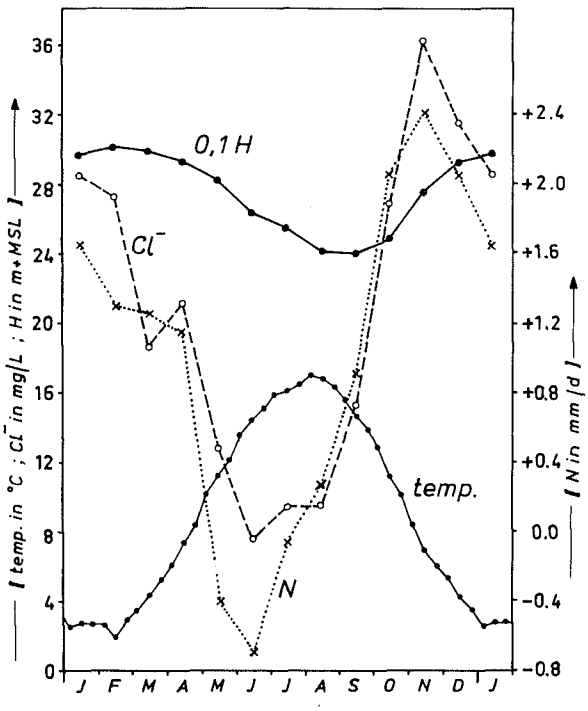

FIG. 6.32 The sinusoidal course of seasonal fluctuations in daily mean temperature (temp), groundwater recharge (N), elevation of the groundwater table (H) and chemistry of bulk precipitation (Cl^-), together responsible for a complicated pattern of seasonal fluctuations in the composition of the upper groundwater.

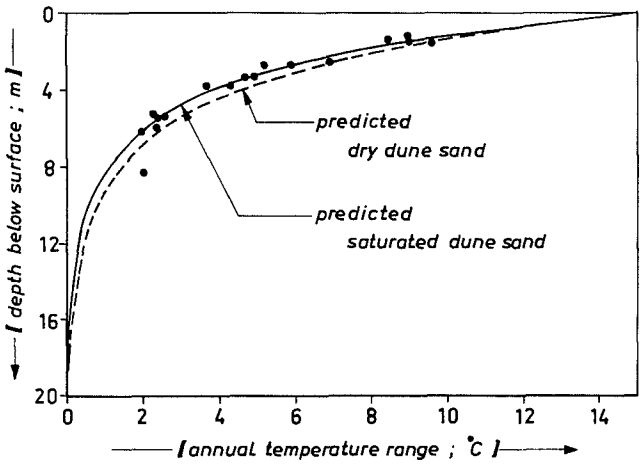

FIG. 6.33 Reduction of the annual temperature range at the surface, with increasing depth in water saturated sand, as observed on the plot grasses-4 and as calculated using Eq.6.12. The water content of sand has a negligible effect on the annual temperature range, just like the predominantly downward flow of groundwater, which is ignored in Eq.6.12.

angular frequency of oscillation, equal to 2π/wave period [rad/s]; κ = thermal diffusivity [m^2/s].

Applying both equations with thermal diffusivities of 1.15 10^{-6} m^2/s for unsaturated sand (ε = 0.43, V = 0.065) and 9.5 10^{-7} m^2/s for saturated sand (ε = 0.34), yields the reduction of the annual temperature range (twice the amplitude and ω = 1.99 10^{-7} rad/s) with increasing depth, as depicted in Fig.6.33, and a propagation velocity of about 20 m/y for the wave. At 4, 8 and 16 metres below the surface the temperature range is reduced then from 15°C at the surface to 4, 1 and 0.1 °C, respectively, with little dependence on the depth to the water table. Daily temperature fluctuations penetrate not deeper than about 0.8 m.

Although the calculated amplitude reduction does not account for convective transport in the water-phase, it still corresponds well with observations on the monitoring plot grasses-4 (Fig.6.33) and with the maximum depth of seasonal fluctuations as observed by Chang (1957) and Boyle & Saleem (1979). The phase delay implies that the temperature wave at the surface is retarded at a depth of 4, 8 and 16 m by about 2.5, 5 and 8 months, respectively.

Fluctuations in the position of the groundwater table may have a strong impact on the flow pattern. They can lead to strong hydrochemical fluctuations as measured on a fixed site, especially in a heterogeneous area regarding either geochemistry or vegetation and in case of an oscillation occupying several years (Fig.6.34).

Apparent fluctuations are due to all kinds of errors in observation, introduced either by sampling, pretreatment, analysis or data handling. It is considered of paramount importance to extract during each sampling equal water volumes from the facility, for either flushing, measurements on site or ultimately, the samples. Changes in this respect may have a profound impact on the mixing length introduced by sampling (see section 6.3.4). Consideration of the analytical standard deviation for each compound may assist in the separation of analytical noise from real fluctuations. This noise can be relatively large for certain compounds or parameters, like DOC, COD, most TEs and organic microcontaminants.

6.7.2 Trends

Natural and anthropogenic long-term fluctuations are connected mainly with changes in vegetation cover, phreatic level, leaching and atmospheric pollution.

An example of the effects of changes in vegetation cover is offered by lysimeter 4 west of Castricum (plot pines-L) : about 700 pines less than 0.1 m high were planted on bare dune sand in 1941 and

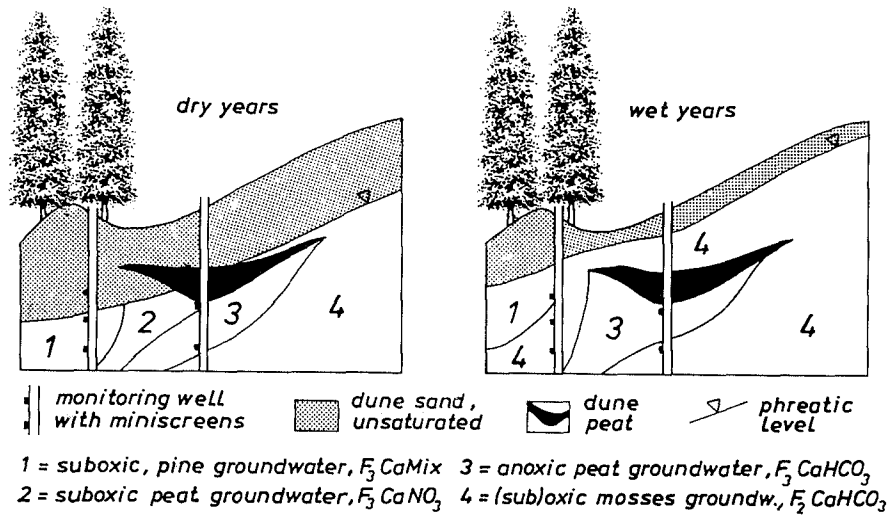

FIG. 6.34 Link between fluctuations in the position of the groundwater table and induced changes in the flow pattern on the one hand, and hydrochemical fluctuations as measured on a fixed site with a piezometer or miniscreen on the other.

about 50 years later 35 trees with a height of 15 m survived the necessary thinnings. Although this tree stand is considered hydrologically mature since 1953, as the continuous growth and periodical thinnings offset each others effects on the water balance, further tree growth clearly continued to influence the chemical composition of the drainage solute (Fig.6.35). A steady decline is observed for TIN (mainly as NO_3^-) until 1960, whereas most dissolved major constituents, like Cl^- and SO_4^{2-}, steadily increased, probably until 1978. During the initial 13 years the effects of increasing evapotranspiration and the application of fertilizers rich in nitrogen and sulphate can be noticed. Since 1953 the increasing salinity of the drainage solute is related mainly to the enhanced interception deposition in consequence of continued tree growth. After about 30 years of growth the tree stand seems to reach chemical maturity, for the drainage water. The exceptionally dry and stormy years in the period 1967-1977 (Fig.6.40) were not monitored, but probably yielded the indicated maximum concentration of air-borne ions and Ca^{2+}. The return of significant TIN-levels (mainly as NO_3^-) in the drainage solute since 1984, is probably related to a reduced uptake in consequence of biological maturity (a reduced tree growth and reduced number of trees; Fig.6.35). The order of the different maturities thus becomes : first the hydrological, then the hydrochemical and ultimately the biological maturity.

Another example is offered by the more or less steady increase of the mean Cl^- concentration of shallow dune groundwater in between Wijk aan Zee and Egmond aan Zee, in the catchment area of PWN (Fig.6.36A). This increase is partly explained by a steady growth of pines planted on about half of the locations involved, quite comparable to lysimeter P_L (Fig.6.35), and the expansion of dune shrubs. In non-afforested dune terrains significantly higher Cl^- concentrations were observed in the 1970s as compared to the 1940s (Fig.6.36B). This is explained by (1) the rather exceptional period 1967-1977 regarding both sea spray deposition (Fig.5.5) and evaporation losses (Fig.6.40A) and (2) an increase of dune shrubs.

Effects of leaching and increased atmospheric pollution are well illustrated by changes in composition of the drainage solute from the bare lysimeter (bare-L), from 1946 till 1990 (Fig.6.37). The decreasing concentrations of HCO_3^-, COD, SiO_2 and K^* probably relate to a noticeable leaching of both black earth, that was erroneously deposited in 1942, and bare twigs and tree branches, that were spread over the surface to prevent aeolian erosion. The increased NO_3^- concentrations in the 1980s as compared to the period before 1961, on the other hand, are probably connected with the increase of atmospheric deposition of NO_3^- and NH_4^+ (Fig.5.5).

The general rise of Cl^-, SO_4^{2-}, NO_3^- and Ca^{2+} concentrations in both the calcareous and decalcified dunes around 1980 as compared to 1910 (Fig.6.38), is explained by the combined effects of : (a) an increased atmospheric deposition of NO_x, NH_y and SO_2; (b) an expansion of vegetation units with a raised capability to evaporate water, intercept aerosols and gases, and fix N_2 (Table 3.5); and (c) a drawdown of the groundwater table, thereby expanding the (sub)oxic zone with the breakthrough

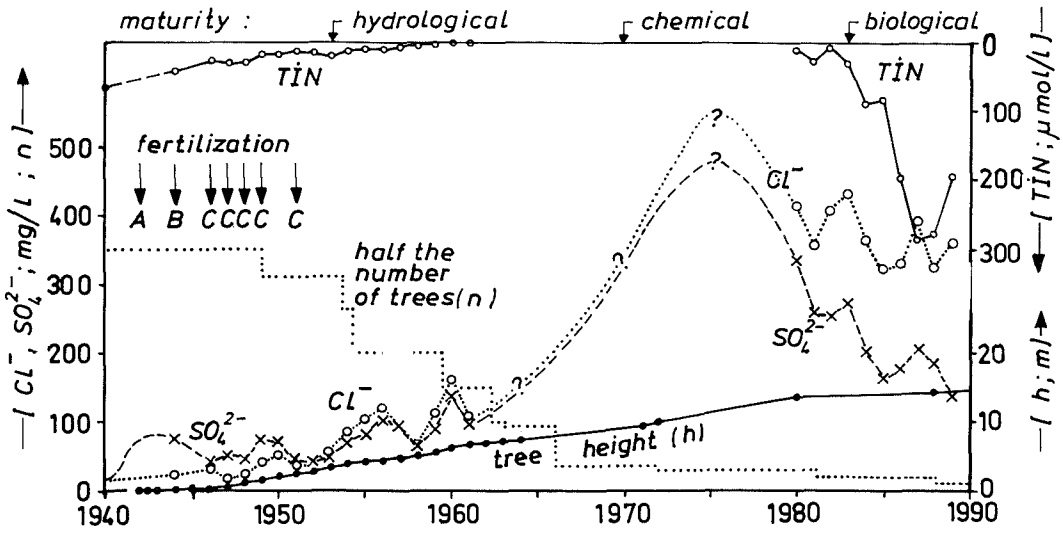

FIG. 6.35 Fluctuations in annual mean composition of the drainage water and its fluxes from the lysimeter planted with pines (plot pines-L) west of Castricum, from the initial stage after plantation in 1940 (tree length <0.1 m) until 1990 (tree length 15 m). Solute fluxes are strongly correlated with discharge, tree growth and the application of fertilizers during the first decade (A = black soil; B = straw; C = fertilizers). Hydrological maturity (Q constant) is reached after about 13 years, hydrochemical maturity (Cl^-, SO_4^{2-}, Ca^{2+} etc. constant) after 30 years and biological maturity (growth slowing down and NO_3^- reappearing in drainage solute) after 43 years.

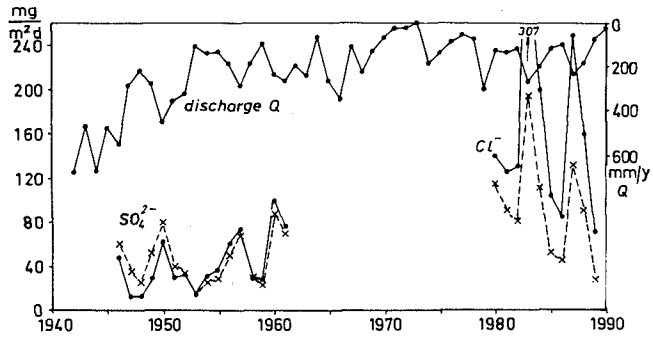

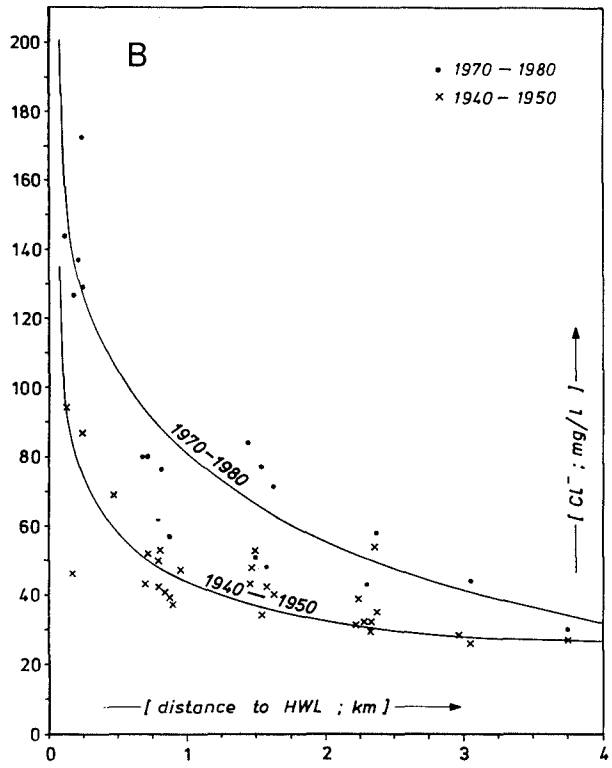

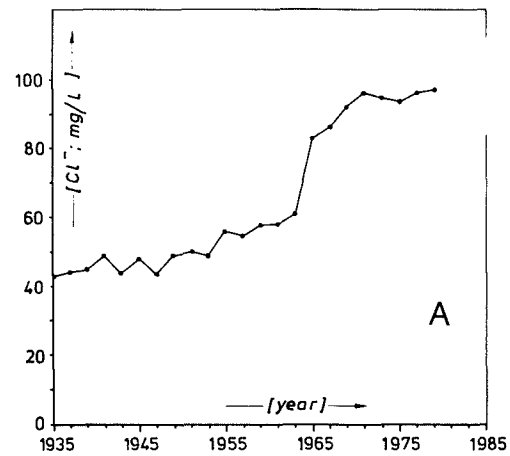

FIG. 6.36 Long-term development of the mean Cl^- concentration in shallow dune groundwater (0-7 m-MSL) in the dune area between Wijk aan Zee and Egmond aan Zee, where influences of salt water intrusion or mixing with recharged river Rhine water can be excluded. A : on 22 locations of which 50% was planted with pines, from 1935 till 1981; and B : on about 25 locations, pine forests excluded, for the 1940s and the 1970s.

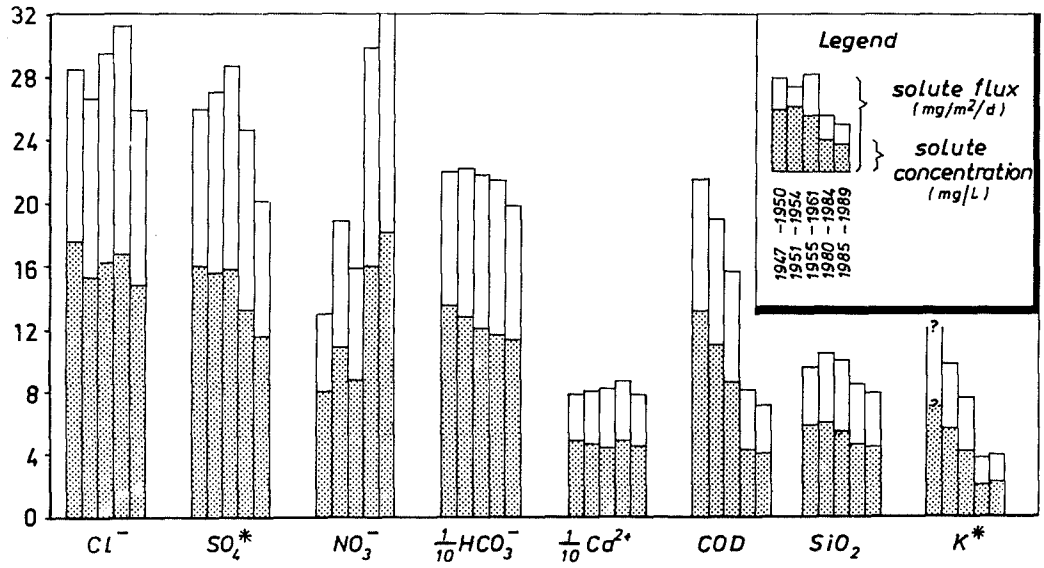

FIG. 6.37 Long-term changes in the mean composition of the drainage water and its fluxes from the bare lysimeter (plot bare-L) west of Castricum, from 1946 till 1990 in selected periods. There is a significant decrease in SO_4^* and rise of NO_3^- caused by changes in atmospheric deposition, and a decrease in HCO_3^-, COD (=Chemical Oxygen Demand by and expressed as $KMnO_4$), SiO_2 and K^*, due to the leaching of black earth and litter deposited on the bare dune sand in 1942.

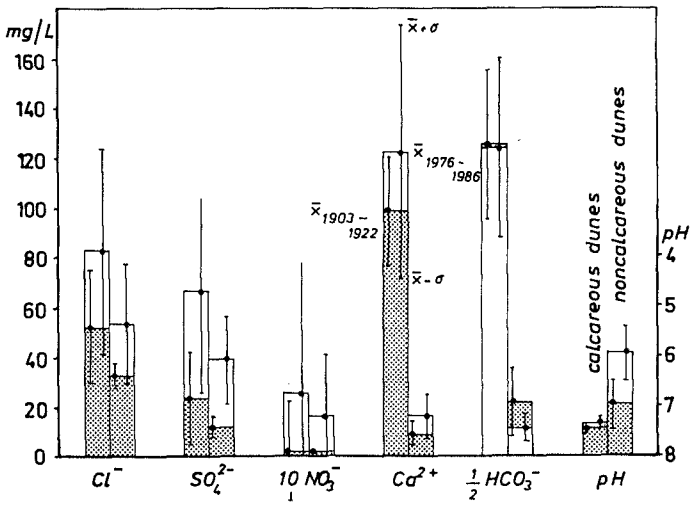

FIG. 6.38 Comparison of the mean composition of shallow dune groundwater around 1980 and 1910, for both the calcareous (number of measurements n=35) and decalcified dunes (n=4). The increase of Cl^-, SO_4^{2-}, NO_3^- and Ca^{2+} concentrations proved statistically significant (>95%) for both dune systems, and the decrease in pH and HCO_3^- for the decalcified dunes only. $\bar{x}$ = mean value; σ = standard deviation.

of NO_3^- in a formerly anoxic environment, which temperates a HCO_3^- increase parallel to Ca^{2+}. The significant decrease in pH and hydrogencarbonate in the decalcified dunes testifies of a progressive leaching of the acid neutralizing buffer.

The impact of the annual mean level of atmospheric pollution is demonstrated for sulphur in Fig.6.39. The lower atmospheric SO_2 levels in the late 1980s (Fig.5.5, inset SO_4^*) are reflected in lower SO_4^* concentrations in both bulk precipitation and the upper dune waters. Their relation is approximately linearly positive, with a rising intercept and angle for increasing vegetation covers. The intercept for the plots bare-L and oaks-L was calculated from the extrapolated linear intercept for bulk precipitation and the respective concentration factors (1.3 and 2.7) to correct for evaporation losses. The dotted curves connect the linear relations to the natural SO_4^* background of bulk precipitation (0.3 mg/l; Table 5.3), which probably is more realistic. The trend of decreasing SO_4^* concentrations in bulk precipitation in the 1980s is also encountered in the drainage solute from the lysimeter planted with pines (Fig.6.35).

6.7.3 Fluctuations in annual means

Erratic fluctuations in the annual mean composition of the upper dune groundwater are considerable (Fig.6.35). Their size necessitates a prolonged monitoring over several years in order to obtain

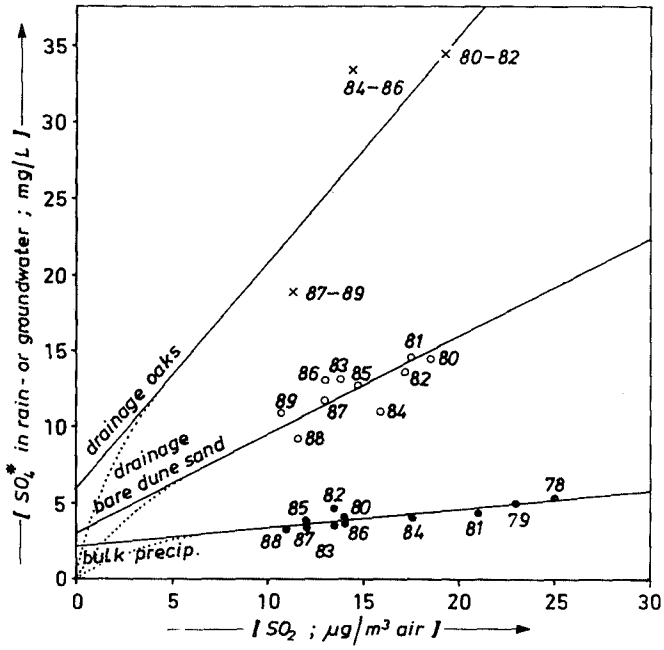

FIG. 6.39 Plot of dated, annual mean SO_4^* concentrations in bulk precipitation and in pure vegetation groundwaters, where SO_4^{2-} is assumed to behave conservatively, versus annual mean atmospheric SO_2 concentrations as derived from PWS (1973-1988) and RIVM (1974-1988). Bulk precipitation = Leiduin (station 3 in Fig.5.3); SO_2 = dunes west of Castricum; bare dune sand = lysimeter S_L; oaks = lysimeter O_L.

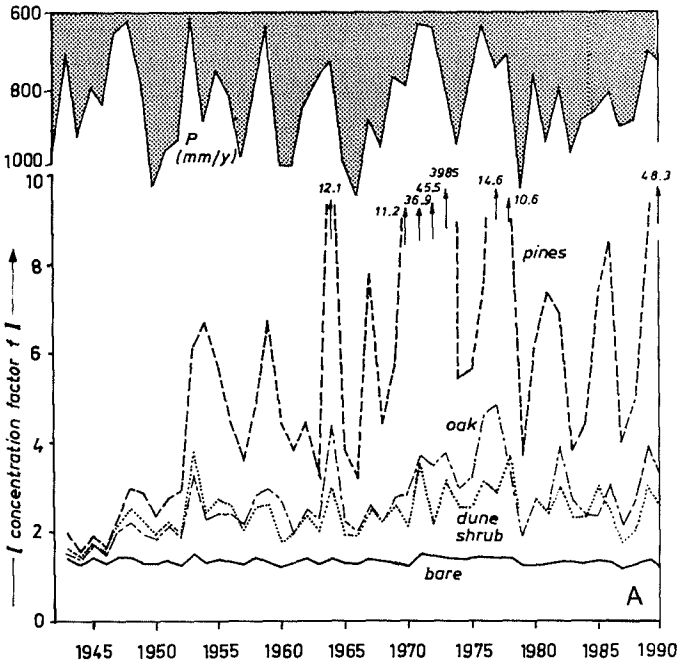

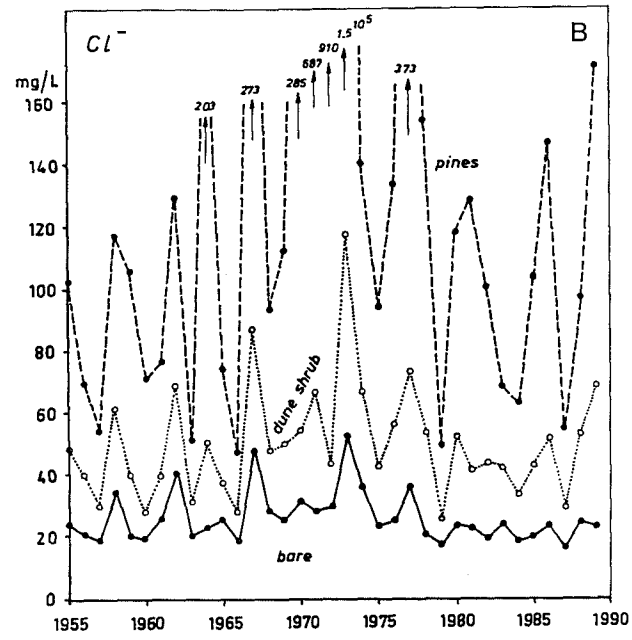

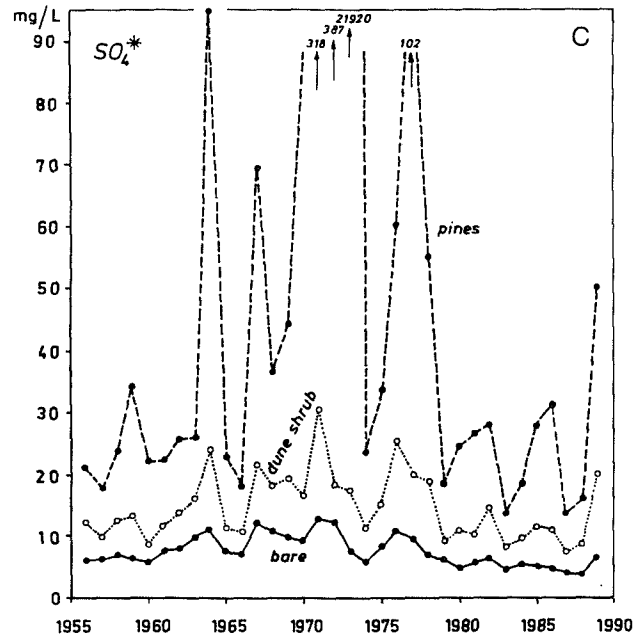

FIG. 6.40 Fluctuations in the weighted annual means of : (A) gross precipitation (P) and the solute concentration factor (f) to correct concentrations in bulk precipitation for evaporation losses (f = P/N); (B) the Cl^- concentration in the natural groundwater recharge; and (C) the SO_4^* concentration in the natural groundwater recharge. A, B and C for bare dunes and dunes with a vegetation cover of either dune shrub, oaks (only A) or pines. Calculated from lysimetric data with the reconstructed Cl^- and SO_4^* logs for bulk precipitation at 2 km from the HWL at a coastal background station in the Western Netherlands (Fig.5.5).

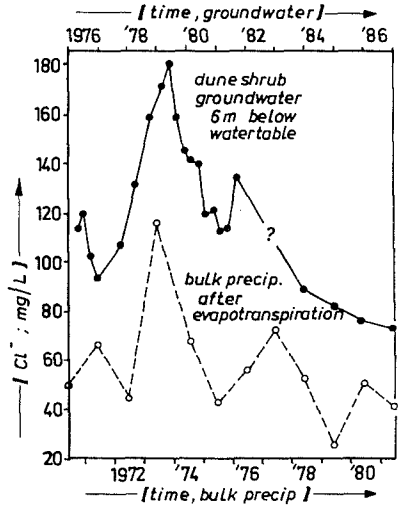

FIG. 6.41 Sequential history matching using natural fluctuations of the Cl^- concentration in dune shrub water about 1 km from the high water line at 6 metre below the groundwater table, and those in the weighted annual means for recharge water. The time shift applied for overlap, yields a groundwater age of 5.5 y. Measurements in well 24H.94 at 5 m-MSL, south of Zandvoort aan Zee, with a screen length of 1 m. The chlorinity of recharge water at 2 km from the HWL derives from Fig.6.40B. The shorter distance of the well to the HWL explains its overall higher chlorinity.

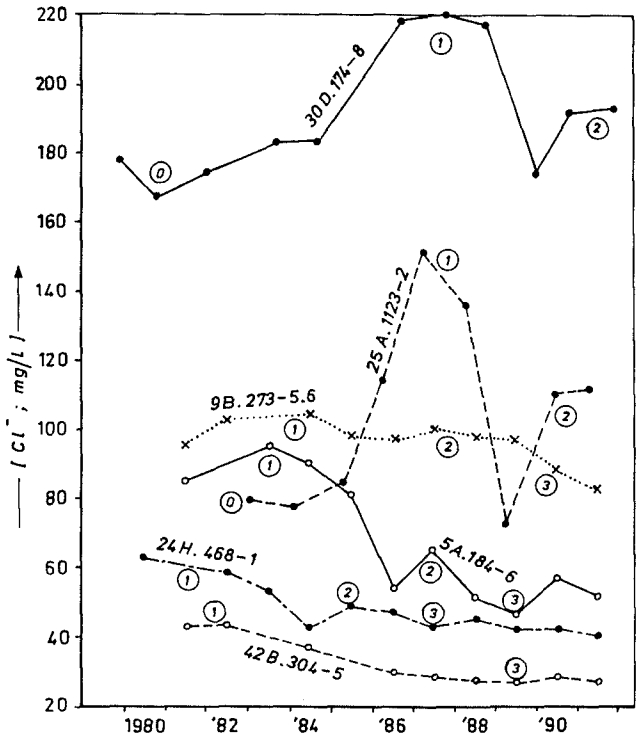

FIG. 6.42 Results of sequential history matching using Cl^-, by recognition of 4 well-known years with anomalous sea spray deposition : 0 = 1968-1969 (low); 1 = 1973 (absolute maximum in period 1956-1989); 2 = 1976-1977 (high, preceded by the low 1975-1976); 3 = 1979 (low). Each well (screen length = 2 m) belongs to the national groundwater monitoring network of RIVM : 5A.186 = island of Terschelling; 9B.273 = island of Texel; 24H.468 = Luchterduinen, south of Zandvoort aan Zee; 25A.1123 = IJmuiden; 30D.174 = NW of Monster; 42B.304 = island of Schouwen. Screen depth is indicated behind well code (m+MSL). Variations in amplitude of fluctuations relate to differences in vegetation cover, distance to the HWL and hydrodynamic dispersion. Based on data supplied by RIVM.

representative annual means, and also requires consideration of preceding years in order to understand anomalous concentrations of nonconservative atmospheric ions, like Na^+, K^+ and Mg^{2+}.

These fluctuations are caused mainly by yearly variations of (1) the composition of bulk precipitation (Fig.5.5) and (2) the solute concentration factor by evaporation losses (Fig.6.40A), together leading to a highly variable input signal for groundwater with regard to for instance Cl^- (Fig.6.40B) and SO_4^* (Fig.6.40C). The input signal of conservative environmental tracers can be recognized in shallow dune groundwater, with a phase delay that matches the total transit time in the subsoil to the sampled monitoring screen, thus offering an excellent groundwater dating (Figs. 6.41-6.43). The recharge history is traced back by either sequential sampling of one well (Figs. 6.41 and 6.42), detailed hydrochemical well-logging at one site (Fig.6.43; Fig.7.8) or a combination of both (Fig.6.43). The results obtained, indicate piston flow with a downgradient smoothing by hydrodynamic dispersion. The interpretation of the hydrochemical well-log (Fig.6.43) is hampered by complications connected with heterogeneities of the surrounding vegetation cover (from scanty near the well [zone I] to low dune grasses further away [zone III]).

The presented kind of history matching is not new, but examples from literature relate to either the unsaturated zone using Cl^- and isotopes (for instance Andersen & Sevel, 1974; Eichinger & Schulz, 1984; Cook et al., 1992) or the groundwater zone using isotopes (Van Duijvenbooden, 1979; Meinardi, 1983b,c; Robertson & Cherry, 1989). Chloride history matching has not been applied to groundwater earlier. This dating technique has the best perspectives in coastal, homogeneous, sandy aquifers with predominant onshore winds, a precipitation excess and a well documented Cl^- record of bulk precipitation. The denser and taller the vegetation cover and the more remote the area from the HWL, the larger

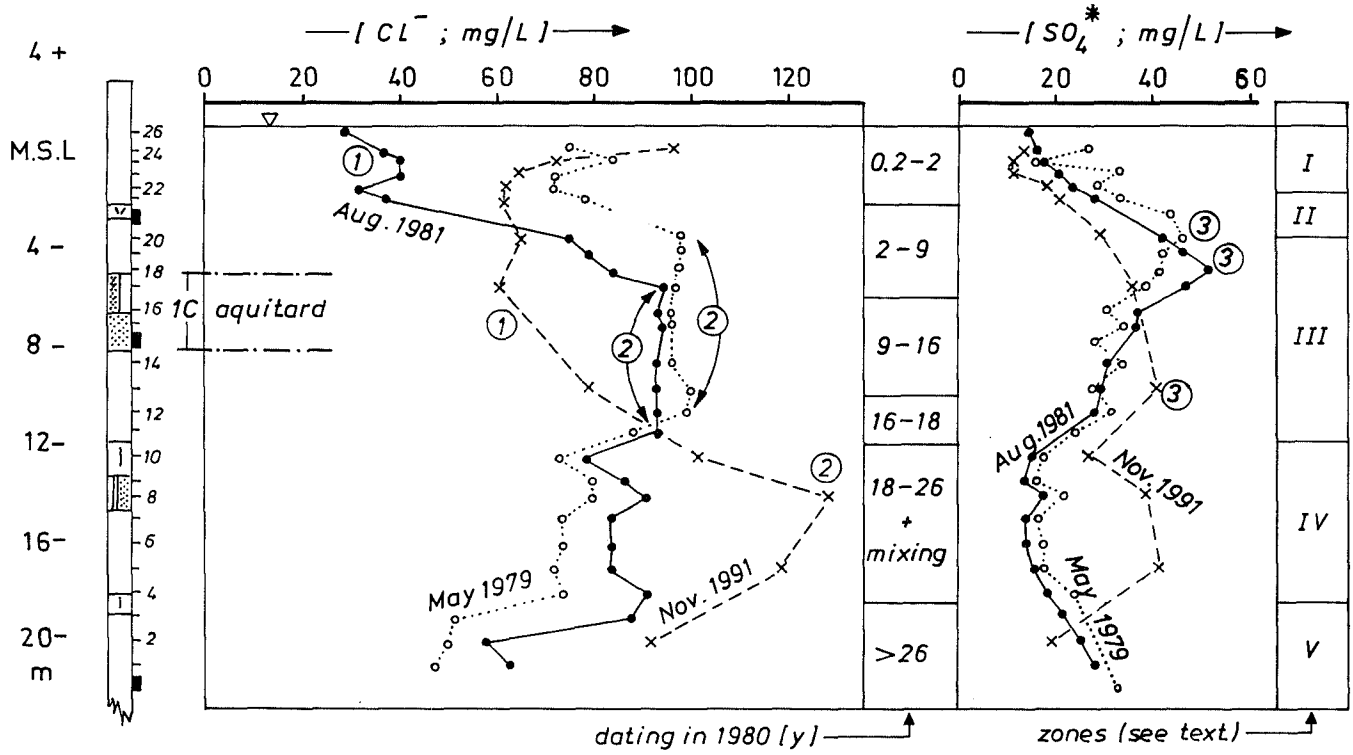

FIG. 6.43 Results of a complicated case of combined sequential and spatial history matching : multilevel well 24H.470 south of Zandvoort aan Zee, using Cl^- and sea-salt-corrected SO_4^{2-}. Three well-known years or periods with anomalous sea spray deposition or SO_4^* concentration are indicated : 1 = 1979 (low Cl^-); 2 = 1967-1977 (high Cl^-); and 3 = 1976-1978 (high SO_4^*). The independent dating in 1980 was based on tritium and $\delta^{18}O$ (discussed in section 7.4.5). The descent of the labelled water during a period of 10 years (in between the sampling of August 1981 and November 1991) corresponds with groundwater ages based on the isotope datings. There are, however, complications by significant dispersion, heterogeneities in vegetation cover around the well, and sulphate reduction. Zones : I = scanty vegetation cover of recharge area (mosses and bare dune sand), SO_4^{2-} conservative; II = transition from I to III, SO_4^{2-} conservative; III = low dune grasses, little SO_4^{2-} reduction; IV = tall dune grasses and clear sulphate reduction; V = gradual transition to groundwater with recharge more inland and less SO_4^{2-} reduction.

is the impact of variations of the precipitation excess as compared to fluctuations in the atmospheric Cl^- input (Fig.6.47). The high concentrations of Cl^- and SO_4^{2-} in the drainage water from the lysimeter planted with pines, therefore combine mainly with a low discharge (Fig.6.35).

Fluctuations in the input signal for the non-conservative sea spray components Na^+, K^+ and Mg^{2+} are retarded and smoothed by sorption, which is clearly demonstrated for seasonal fluctuations in the next section.

6.7.4 *Seasonal fluctuations*

Presentation

Seasonal fluctuations in the composition of the upper vegetation groundwaters are deduced from the monthly or bimonthly observations on a single miniscreen during several years, as shown in Figs. 6.44-6.45, and from the monthly or weekly observations on the drainage solute from the bare lysimeter and the lysimeter covered with dune shrub in Fig.6.46. A brief description of the fluctuations is given below, explanations follow where different types of fluctuation patterns are introduced.

As a general rule, quality fluctuations appear to be most pronounced a below dense and tall vegetations (compare oaks and pines in Fig.6.45 with mosses and dune shrub in Fig.6.44), (b) close to the HWL (compare Cl^- for dune shrub-1 and -4 with dune shrub-2 in Fig.6.44), (c) close to the water table (see Fig.6.54) and (d) near dune peat, provided that its position oscillates above and below the groundwater table (compare SO_4^{2-} and NO_3^- for oaks-1 with -2 in Fig.6.45). This rule does not hold for each constituent separately, however. Potassium for instance shows negligible fluctuations under oaks where peat is situated alternatingly below and above the groundwater table (oaks-1 in Fig.6.45).

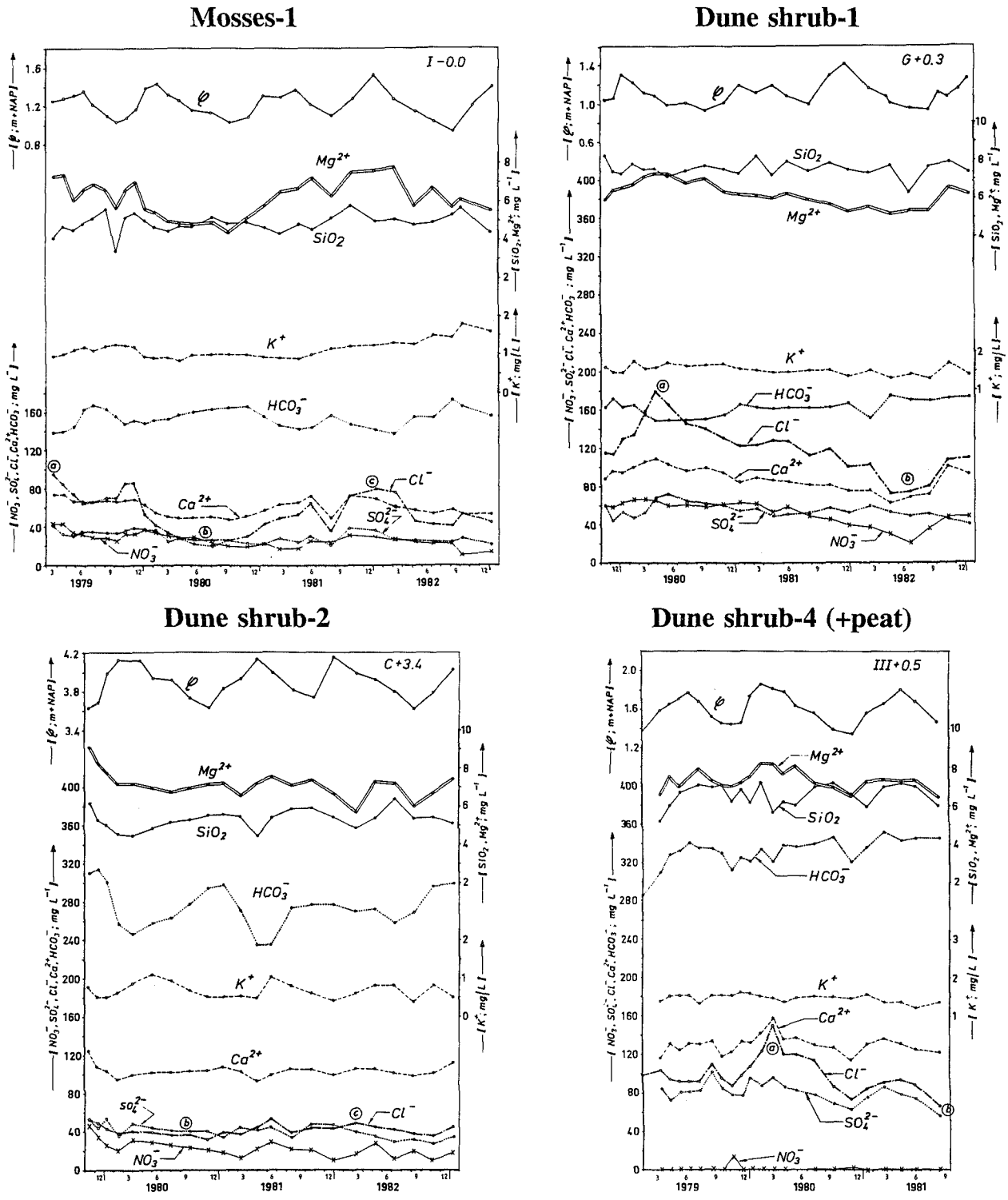

FIG. 6.44 Seasonal fluctuations of the atmospherical type, in the composition of pure vegetation groundwater below mosses (miniscreen I-0.0 on plot M_1), and below seabuck thorn either close to the HWL (miniscreen G+0.3 on plot D_1), more inland (miniscreen C+3.4 on plot D_2) or with peat interference (miniscreen III+0.5 on plot D_4). The atmospherical fluctuation pattern is dominated by the Cl^- peak deriving from winter storms, with the resulting cation exchange and reduced HCO_3^- fluctuations often in counterphase with Ca^{2+}. The fluctuations on the plot dune shrub-2, which is situated most inland and consists of the highest Hippophaë cover, exhibit also a biological character. a,b,c = episodes with anomalous Cl^- concentration in bulk precipitation, that can be recognized in shallow dune water : a = November-December 1977; b = January-July 1979; c = October 1980-Januari 1981. φ = phreatic level.

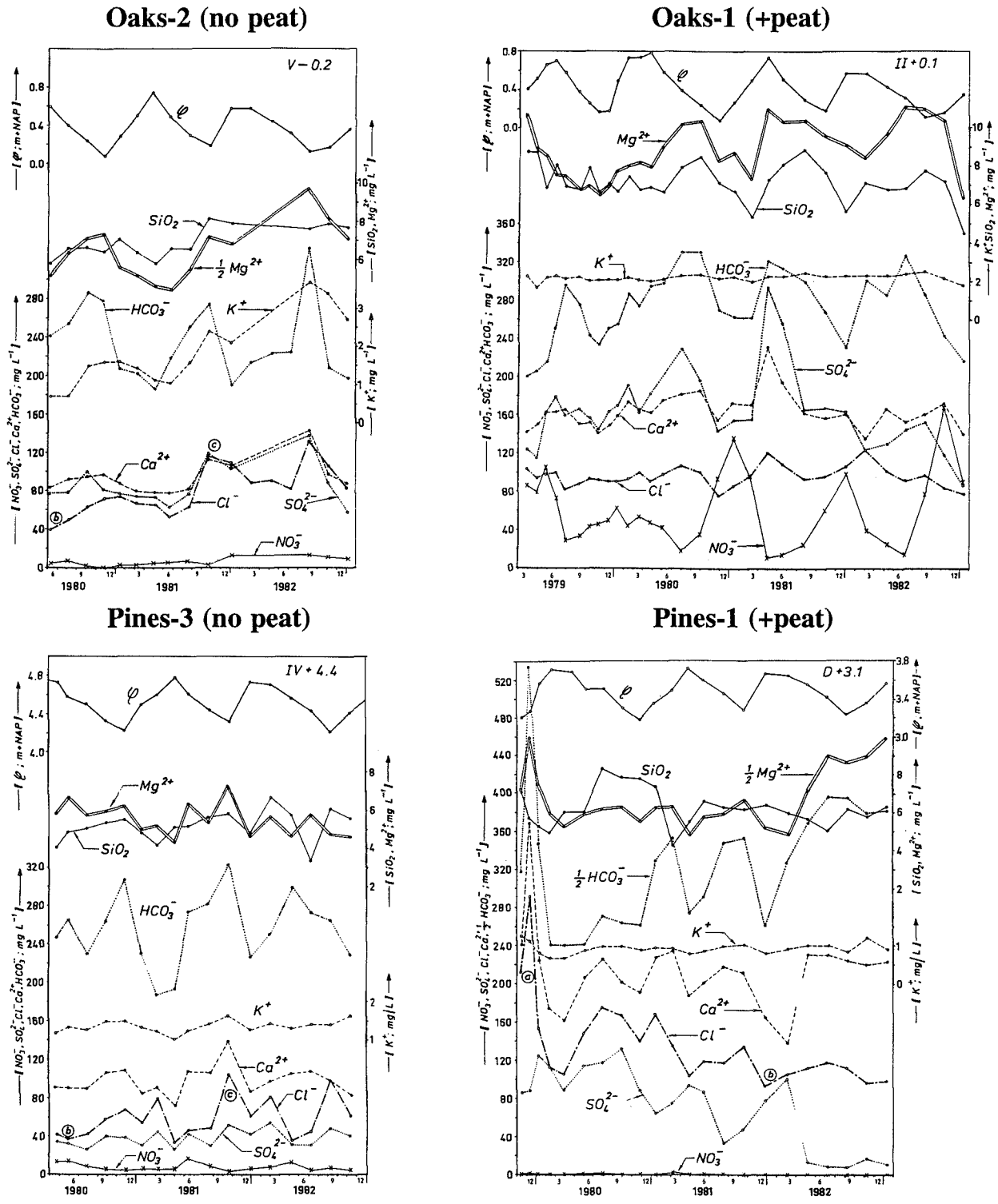

FIG. 6.45 Seasonal fluctuations, of the biological type mainly, in composition of pure vegetation groundwater below oaks without (miniscreen V-0.2 on plot O_2) and with peat interference (miniscreen II+0.1 on plot O_1), and below pines without (miniscreen IV+4.4 on plot P_3) and with peat interference (miniscreen D+3.1 on plot P_1). The biological fluctuation type is characterized by a dominant effect of summer evapotranspiration, leading to synchronous peaks of Na^+, Cl^-, Ca^{2+} and HCO_3^- and rather strong HCO_3^- fluctuations. a,b,c = episodes with anomalous Cl^- concentration in bulk precipitation, that can be recognized in shallow dune water : a = November-December 1977; b = January-July 1979; c = October 1980-Januari 1981. φ = phreatic level.

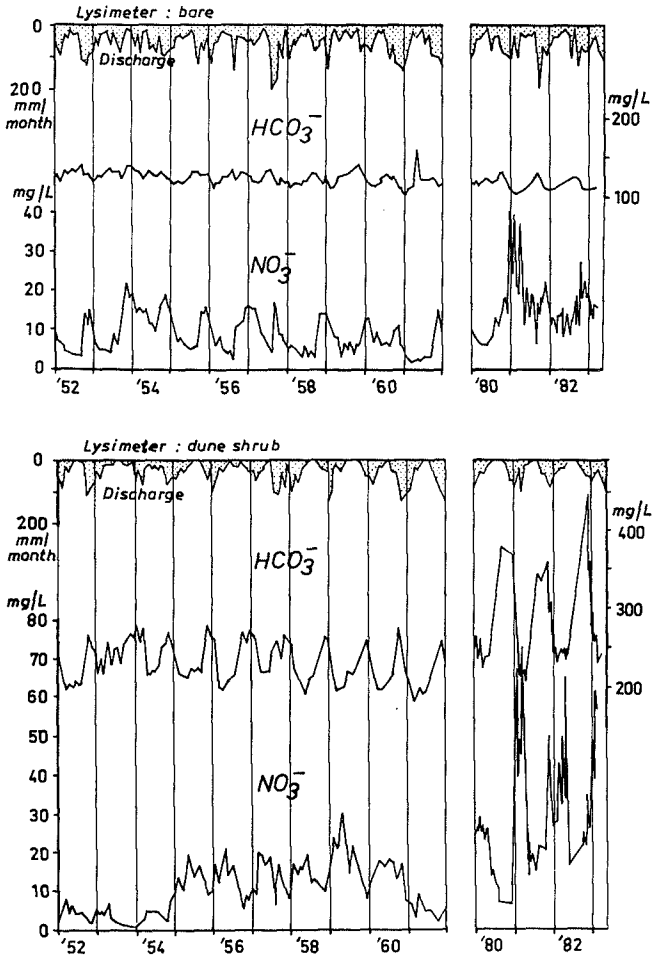

FIG. 6.46 Seasonal fluctuations of HCO_3^- and NO_3^- concentrations in two pure vegetation groundwaters, as measured in the drainage from the bare lysimeter (plot S_L) and the lysimeter covered with dune shrub (mainly seabuck thorn, plot D_L). The time axis shows real sampling time. The seasonal nitrate peak coincides in both cases with maximum discharge, and the HCO_3^- pattern is in counterphase with NO_3^-. The HCO_3^- peaks therefore represent summer percolate and the NO_3^- peaks autumnal percolate.

Dating the groundwater by its fluctuations

In order to relate peaks and minima to processes at the surface, the time axis for sampling has to be shifted back in accordance with the (mean) transit time in the subsoil. This problem of groundwater dating was tackled as follows :

First, the annual Cl^- cycle for groundwater under various vegetation covers was calculated from the annual cycles of Cl^- in bulk precipitation (Fig.5.8) and the various terms of the water balance (Fig.3.14). The annual groundwater stratum was subdivided, for practical reasons, into groundwater layers 0.1 m thick. This thickness corresponds with the vertical mixing length by sampling via mini-screens (section 6.3.4). The calculation method is elucidated in Table 6.21 and the results are shown in Fig.6.47. It follows that the November Cl^- peak in bulk precipitation should be retraceable in groundwater only under mosses or other scanty vegetation covers, where groundwater is recharged also during summer. The solute concentrating effect of high evaporation losses by denser and taller vegetations during the growing season, clearly overcompensates for the low Cl^- concentrations in summer bulk precipitation.

Second, the Cl^- record of bulk precipitation was compared with the Cl^- record of shallow groundwater on the plot mosses-1 (Fig.6.48), where Cl^- fluctuations in bulk precipitation are expected to be preserved in groundwater with least disturbance. The Cl^- fluctuations in groundwater are shown for three depths, each with a shift to get the best overlap with the Cl^- graph of bulk precipitation. The shift needed, is considered equal to the indicated modal transit time in the subsoil. The seasonal Cl^- fluctuations in bulk precipitation are indeed still recognizable to a depth of 2 m-MSL, i.e. 3.2 m below the phreatic level, although a clear smoothing occurs with depth (treated further in section 6.7.5). The hydrochemically deduced transit times (150, 410 and 840 days) are only slightly lower than the ages calculated with Eq.6.3 using the hydrological data in Table 6.1 (240, 460 and 900 days, respectively).

Although the Cl^- graphs for the more vegetated plots (Figs. 6.44 and 6.45) could not be matched so easily with bulk precipitation, three important points of contact show up in Fig.6.48 : (a) the extremely salty and wet November and December months of 1977; (b) the extremely Cl^--poor, continental period with high rainfall, from January till July 1979; and (c) the less extreme salty period from September 1980 through January 1981. They are easily retraceable on the plots dune shrub-1 and -4 (Fig.6.44), and with some more scrutiny also on the other plots in Figs. 6.44 and 6.45. Only oaks-1 remained obscure. Thus determined transit times correspond reasonably well with calculated values (see Table 6.2). The deviations can be explained by deviations from the assumed, mean groundwater recharge (N in Table 6.1).

Types of fluctuation patterns

Most peaks and minima in the chemical records of the studied vegetation groundwaters can be correlated now with events near the surface. The following types of fluctuation patterns are discerned on the basis of their main origin : the biological, atmospherical, hydrological and lithological type, of which the latter was not encountered here.

TABLE 6.21 Calculation scheme for the annual cycle of Cl^- concentrations in 0.1 m thick layers of groundwater, using mean monthly Cl^- data for bulk precipitation (Monster 1958-1977, Fig.5.8) and mean monthly terms of the water balance for dune shrub (plot D_L 1957-1981, Fig.3.14). The results are depicted in Fig.6.47.

MEAN MONTHLY DATA

month month i		Jan 1	Febr 2	March 3	April 4	May 5	June 6	July 7	August 8	Sept 9	Oct 10	Nov 11	Dec 12	year Σi
P_i= gross precip	mm	73.5	53.0	55.6	48.7	48.1	46.0	71.6	76.3	81.6	91.4	103.5	91.6	841
Q_i= discharge lys	mm	53.8	44.0	39.4	32.7	20.6	6.8	7.5	8.3	14.0	23.7	48.1	63.0	361
S_i= precipit. excess##	mm	51.5	37.0	38.8	34.2	-12.4	-20.7	-1.9	8.4	25.5	63.9	72.3	64.2	361
E_{Si}= evap. from S_i	mm	0	0	0.8	34.2	0	0	0	0	0	0	0	0	35.0
$N_i = S_i - E_{Si}$	mm	51.5	37.0	38.0	0	0	0	0	8.4	25.5	63.9	72.3	64.2	361
$N_i/40$ = number of layers§		1.29	0.93	0.95					0.21	0.64	1.60	1.81	1.61	9.03
$f_i = P_i/S_i$		1.4	1.4	1.4	1.4	∞	∞	∞	9.1	3.2	1.4	1.4	1.4	2.3
Cl_i= Cl bulk precipit.	mg/l	28.5	27.2	18.7	21.1	12.8	7.6	9.4	9.5	15.3	26.8	36.2	31.5	20.9
f_iCl_i	mg/l	40.8	39.2	26.7	30.0	∞	∞	∞	86.6	49.0	38.3	51.8	45.1	48.7
P_iCl_i	mg/m²	2095	1442	1040	1028	616	350	673	725	1248	2450	3747	2885	17577

CALCULATION MEAN Cl^- CONTENT FOR 0.1 m THICK GROUNDWATER LAYER, WITH STARTING DATUM = 1 JANUARY AND WITH POROSITY = 0.4.

layer	Calculation of Cl^- content	Cl^- (mg/l)	calculation end of period	
a	f_1Cl_1	40.8	(1/1.29)*31	= 24 Jan
b	$0.29f_1Cl_1 + 0.71f_2Cl_2$	39.7	(0.71/0.93)*28¼	= 22 Feb
c	$0.22f_2Cl_2 + 0.78f_3Cl_3$	29.5	(0.78/0.95)*31	= 25 Mar
d	$0.17f_3Cl_3 + 0.21f_8Cl_8 + 0.62f_9Cl_9 + (E_{S3}f_3Cl_3 + E_{S4}f_4Cl_4 + P_5Cl_5 + P_6Cl_6 + P_7Cl_7)/40$	120.3	(0.62/0.64)*30	= 29 Sep
e	$0.02f_9Cl_9 + 0.98f_{10}Cl_{10}$	38.5	(0.98/1.60)*31	= 19 Oct
f	$0.62f_{10}Cl_{10} + 0.38f_{11}Cl_{11}$	43.4	(0.38/1.81)*30	= 6 Nov
g	$f_{11}Cl_{11}$	51.8	(1.38/1.81)*30	= 23 Nov
h	$0.43f_{11}Cl_{11} + 0.57f_{12}Cl_{12}$	48.0	(0.57/1.61)*31	= 11 Dec
i	$f_{12}Cl_{12}$	45.1	(1.57/1.61)*31	= 30 Dec

= for calculation reference is made to Stuyfzand (1986c); § = layers 100 mm thick, with porosity = 0.4.

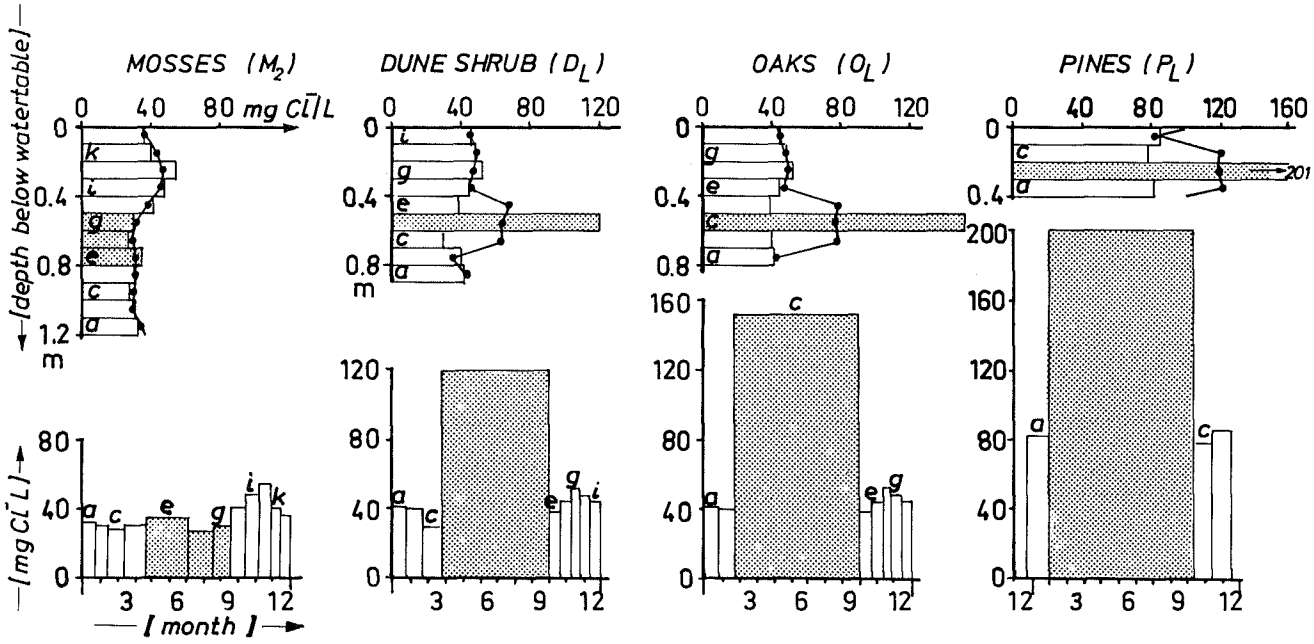

FIG. 6.47 Calculated, mean annual cycle of the Cl^- concentration in 0.1 m thick layers of bulk precipitation after correction for evaporation losses (lower side), and the position of these layers in an annual groundwater stratum (upper side), below selected vegetation covers at 2 kms from the HWL. Summer water (period April-September) is stippled. The 3 months moving average of Cl^- concentrations is shown as a curve in the depth graphs. The fluctuations under mosses-1 are dominated by the winter storms, they belong to the atmospherical type. The other fluctuations are controlled by summer evapotranspiration, which overrules the effects of winter storms, and therefore belong to the biological type.

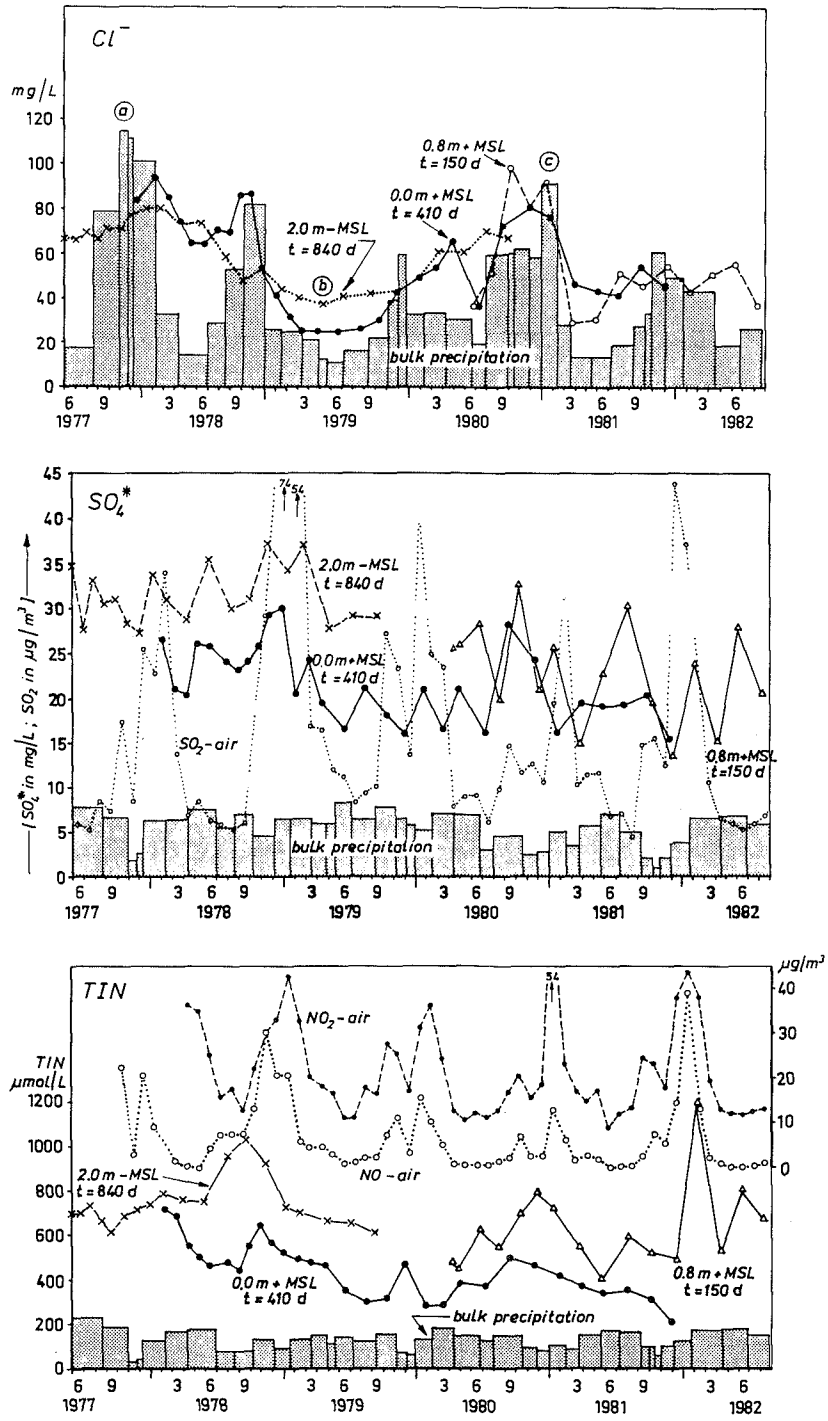

FIG. 6.48 Seasonal fluctuations in concentration of Cl^-, SO_4^* and TIN (mainly as NO_3^-) in the upper groundwater below mosses at 3 depths (plot M_1, well I = 24H.470) and bulk precipitation on site. Also presented are the fluctuations of SO_2, NO_2 and NO in air, as measured on the coastal background station Castricum. The patterns of (potential) atmospheric input and concentration in groundwater coincide regarding Cl^- and TIN/NO_x-air, but they do not in respect of SO_4^*/SO_2. The horizontal axis shows real time for bulk precipitation and atmospheric gases, and the time of infiltration for groundwater, as deduced from the horizontal shift to get the best overlap with the Cl^- graph of bulk precipitation. Each bar represents a 0.1 m thick layer of bulk precipitation. The record of bulk precipitation was reconstructed by measurements on site during the period December 1980 till January 1982 and by regression with measurements on three coastal stations in the vicinity. a,b,c = episodes with anomalous Cl^- concentration in bulk precipitation, that could be recognized in shallow dune water on other locations as well : a = November-December 1977; b = January-July 1979; c = October 1980-Januari 1981. φ = phreatic level. t = travel time from surface (2.8 m+MSL) to indicated depth.

The biological type

This pattern is dominated by the seasonal life cycle of plants and soil organisms, in particular by the resulting evapotranspiration cycle. During the growing season, here from about April till October, the maximum evaporation losses raise the concentrations in the remaining solute or, upon drying, for the subsequent flushing solute (Fig.6.47 and Table 6.21). A clear annual course of CO_2-production was observed in forests by Dörr et al. (1992), with a maximum during summer and a major contribution of microbial decomposition to the total soil CO_2 production.

Most constituents have their maximum concentrations together in the same period (see for instance oaks-2 and pines-3 in Fig.6.45). The peaks of both Na^+-Cl^- and Ca^{2+}-HCO_3^- typically coincide, although cation exchange buffers the peaks of Na^+ (Table 6.22) and Ca^{2+} to some extent. Atmospherical fluctuations of K^+ and Mg^{2+} are considerably smoothed where the forest is growing fast (P_1 and P_3 in Table 6.22) and are accentuated where the forest is degrading (O_1-O_3 in Table 6.22). Although these differences can be noted in Fig.6.45 (compare oaks-2 with pines-3) directly, a better diagnosis is obtained after correction for differences in size of the Cl^- signal, using Eq.6.15 (Table 6.22).

The biological type is observed in the coastal dunes, below oaks and pines, that is below dense and tall vegetation covers at least 1.5 km from the HWL. A mixed fluctuation pattern of the biological-atmospherical type is found along forest edges exposed to the sea winds, in forest stands closer to the HWL and on relatively open spots in forests. Miniscreen IV+4.4 on the plot pines-3 (Fig.6.45) is an example, showing two adjacent Cl^- peaks in an annual cycle, the first probably coinciding with the growing season (maximum evapotranspiration losses) and the second representing the maximum sea spray deposition around November.

A mixed fluctuation pattern of the biological-hydrological type is found in forests with dune peat alternatingly above and below the phreatic level. Fluctuations of the water table, which are related to both hydrological and biological processes, induce alternating (sub)oxic and anoxic, or anoxic and deep anoxic episodes in and below the peat. This leads to counterphase fluctuations of HCO_3^- and NO_3^- (oaks-1 in Fig.6.45) or HCO_3^- and SO_4^{2-} (pines-1 in Fig.6.45), respectively.

The atmospherical type

This fluctuation pattern is predominantly induced by seasonal changes in the atmospheric chemistry, here specifically the maximum sea spray concentrations in the atmosphere around November (Fig.5.8), leading to a pronounced Cl^- maximum in groundwater. It is encountered below scanty and low vegetation covers, like mosses-1 (Figs. 6.44, 6.48, 6.49) and bare dune sand (Fig.6.46), below bracken and dune grasses (notably B_1 and G_4; Table 6.22), and below dune shrub relatively close to the HWL, like D_1 and D_4 (Fig.6.44).

Other characteristics of this fluctuation type are: a HCO_3^- maximum in summer (Figs. 6.44 and 6.49), a NO_3^- peak in the period September-December (Figs. 6.46 and 6.48) for the (sub)oxic waters, and very pronounced cation exchange phenomena (Figs. 6.49-6.51), in many respects similar to those observed during and after fresh or salt water intrusion (section 7.7).

Cation exchange is clearly demonstrated on the plot mosses-1 (Fig.6.49) and dune shrub-1 (Fig.6.50). The autumnal Cl^- peaks are accompanied by a strong Na^+ sorption (negative Na^* values), moderate K^+ and Mg^{2+} sorption and strong Ca^{2+} desorption (high Ca^* values). The reverse is seen in summer, when the Ca^{2+}/Na^+-ratio increases in the upper soil moisture by low sea spray concentrations in bulk precipitation and perhaps by a raised $CaCO_3$ dissolution due to CO_2 development. As a result, fluctuations of Na^* and TIC are more or less synchronous and in counterphase with those of Cl^- and Ca^{2+}, being synchronous as well (Figs. 6.49 and 6.50). The behaviour for TIC (mainly as HCO_3^-) is probably influenced by the precipitation of calcite during Ca^{2+}-desorption and by calcite dissolution during Ca^{2+}-adsorption (Foster, 1950). The overall exchange reaction, in which no Al, Fe, Mn nor NH_4^+ are involved, can be schematized as follows :

$$aCa^{2+} + [bNa, cK, dMg]\cdot Exch + eCaCO_3 + eH_2CO_3 \leftrightarrows bNa^+ + cK^+ + dMg^{2+} + [aCa]\cdot Exch + eCa^{2+} + 2eHCO_3^- \quad (6.14)$$

with : Exch = exchanger, composed mainly of organic material; a >> e; and the meq-balance : 2a = b+c+2d.

The ratio b : c : d is equal to Na^* : K^* : Mg^* on a mol basis, and Na^* : K^* : $2Mg^*$ on a meq basis. The latter amounts to 1 : 0.02 : 0.15 meq/l on average. The maximum reaction coefficients for miniscreen I-0.0 (plot M_1) can be read from Fig.6.49 : b = 0.7, c = 0.01 and d = 0.1 meq/l; and those for miniscreen G+0.3 (plot D_1) from Fig.6.50: b = 1.13, c = 0.025 and d = 0.2 meq/l. The observed extremes for $|Ca^*-\overline{Ca}^*|$ are 0.65 and 1.1 meq/l for miniscreens I-0.0 and G+0.3, respectively. This means that the maximum reaction coefficient e, which is equal to the maximum of $(b+c+d-[Ca^*-\overline{Ca}^*])$, should be about 0.15 and 0.25 meq/l, respectively. It is noteworthy that the groundwater remained in equilibrium with calcite/aragonite (SI = 0 ± 0.2) during

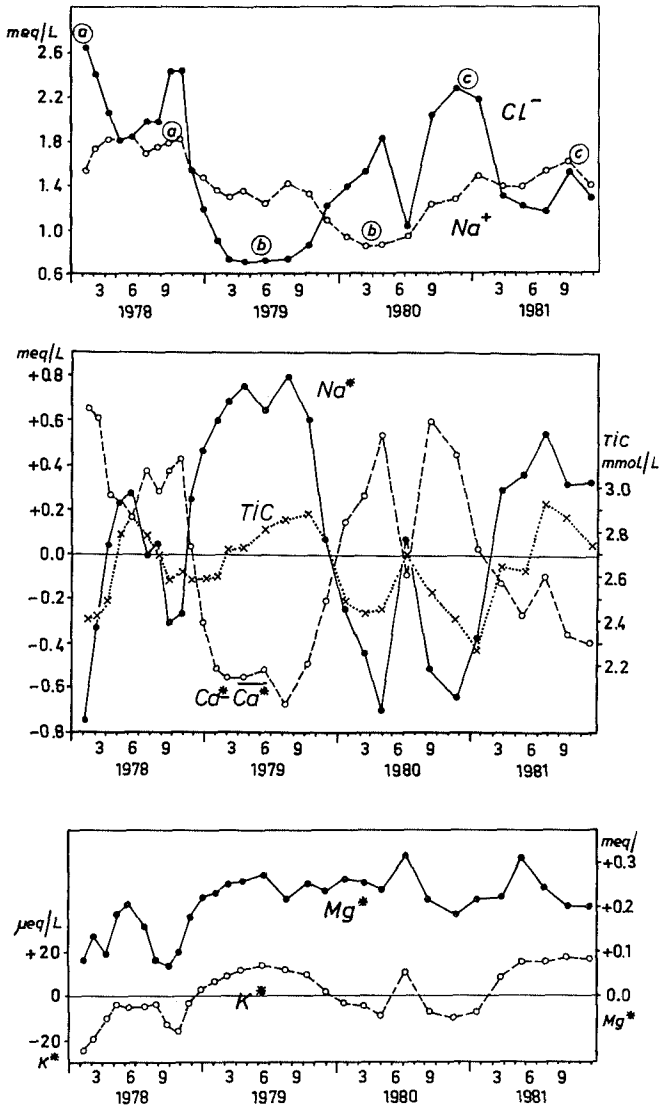

FIG. 6.49 Seasonal fluctuations in concentrations of the major cations and TIC (mainly HCO_3^-) in the upper groundwater below mosses (plot M_1, well I-0.0), with the time axis corresponding with infiltration time of recharging precipitation (as in Fig.6.48). a,b,c = episodes with anomalous Cl^- concentration in bulk precipitation (see Fig.6.48). These Cl^- anomalies are accompanied by a strong cation exchange of Na^+ for Ca^{2+} as evidenced by the strong counterphase fluctuations of sea-salt-corrected Na^+ (Na^*) and non-marine Ca^{2+} (Ca^*, expressed as the deviation from its mean level). As a result of this exchange, Na^+ concentrations are smoothed.

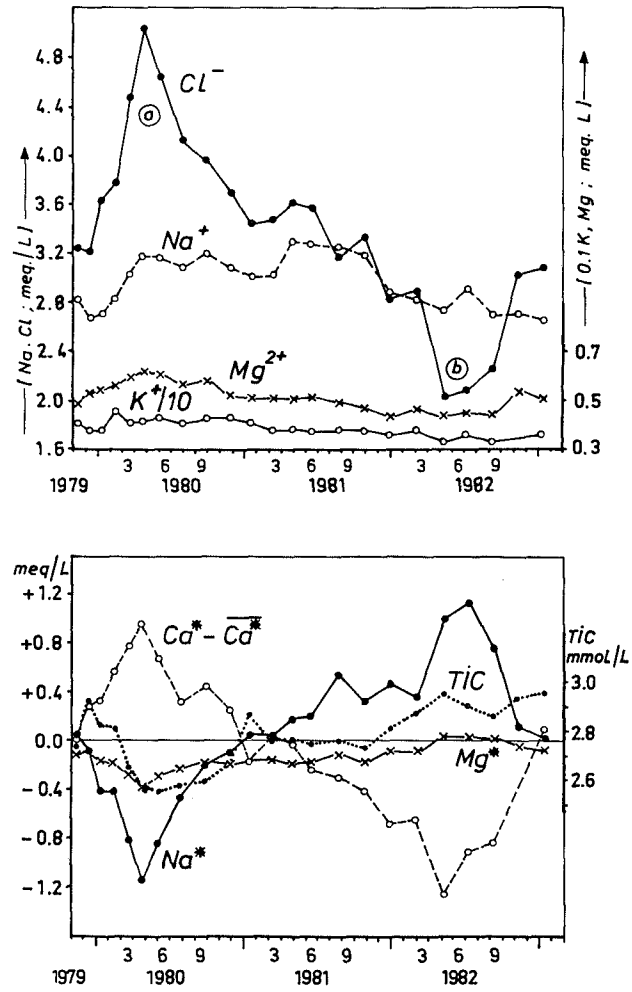

FIG. 6.50 Fluctuations in concentrations of the major cations and TIC (mainly HCO_3^-) for the upper groundwater below dune shrub close to the HWL (miniscreen G+0.3 on plot D_1), showing real time (time of sampling). The Cl^- extremes a and b are accompanied by a strong cation exchange of Na^+ (and Mg^{2+}) for Ca^{2+}, as evidenced by the strong counterphase fluctuations of sea-salt-corrected Na^* and non-marine Ca^* (expressed as the deviation from its mean level). As a result of this exchange, Na^+ concentrations are smoothed, and TIC is depressed during Ca^{2+} desorption and raised during Ca^{2+} adsorption according to Eq.6.14. a = November-December 1977 peak in bulk precipitation; b = January-July 1979 Cl^- minimum in bulk precipitation.

the whole monitoring period, without significant changes between each exchange cycle. Neither did the pH (7.75±0.15 for both wells) show systematic changes between each exchange cycle, which testifies of open system conditions during Ca^{2+} exchange and $CaCO_3$ dissolution in the unsaturated zone.

The most consistent and important consequence of the exchange reaction is the smoothing of fluctuations in HCO_3^- and the major cations Na^+, K^+, Ca^{2+} and Mg^{2+} (Table 6.22). This damping (%d) can be quantified for Na^+, K^+ and Mg^{2+}, that derive mainly from air-borne sea salts, as follows [in %] :

TABLE 6.22 Quantitative characterization of the fluctuations for the main sea spray ions Cl^-, Na^+, K^+ and Mg^{2+} in several shallow vegetation groundwaters, as observed in a single miniscreen. The atmospheric fluctuation type is characterized by a relatively strong smoothing and retardation of Na^+, K^+ and Mg^{2+} oscillations, that derive mainly from Cl^- variations in atmospheric deposition.

Monit. plot	screen	sampling period	Amplitude$^{\alpha}$ (µmol/L) Cl^-	Na^+	K^+	Mg^{2+}	% damping by exchange$^{\beta}$ Na^+	K^+	Mg^{2+}	Phase lag$^{\gamma}$ (month) Na^+	K^+	Mg^{2+}	Periodicity of fluctuation
ATMOSPHERICAL FLUCTUATION TYPE :													
M_1	24H470-0	7903-8101	973	498	12	70	40	37	26	10	8	0	2½ y
	24H470-2	8004-8201	606	>350	>15	44	>34	-36	44	4	4	2	2½ y
	24H470+1	8009-8201	973	254	15	78	70	21	18	4	2	0	1 y
	24H470-0	8106-8301	621	374	10	47	30	17	22	10	8	0	1 y
B_1	J	7911-8301	508	228	8	72	48	16	-46	3	n.v	10	2½ y
B_2	XII$^{\delta}$	8106-8301	155	50	3	21	62	0	-39	n.v	n.v	n.v	1 y
G_4	6,4+2.5	8409-8509	1072	478	9	136	48	55	-30	2.5	1	0	1 y
D_1	G	7911-8301	1509	316	7	45	76	75	69	13	1	0	2½ y
D_2	C	7911-8301	296	168	9	39	34	-63	-35	2.5	0?	0?	1 y
D_4	24H472+1$^{\delta}$	7903-8108	1156	424	4	35	57	81	69	1	n.v	n.v	2½ y
BIOLOGICAL FLUCTUATION TYPE :													
O_1	24H471+0	7903-8301	677	579	10	95	0	21	-44	1	0?	0	1 y
O_2	IIC+0	8106-8209	367	228	15	72	27	-114	-100	4?	0?	0?	1 y
O_3	V+0.2	8006-8207	733	320	15	111	49	-9	-55	0	0?	5	1 y
	V-0.2	8006-8301	1269	666	36	216	39	-52	-75	0	0?	0?	1 y
P_1	D	7911-8301	2792	2555	9	208	-7	83	23	0	0?	0?	2½ y
P_3	IV+4.4	8004-8211	987	750	8	60	11	57	38	0	0	0?	1 y
	IV+4.0$^{\delta}$	8004-8301	1100	705	5	51	25	76	52	1	0	0	1 y
	L+4.2	8006-8301	649	520	12	51	7	0	19	1	1?	0?	1 y

α = (max - min)/2; β = calculated using Eq.6.15, with negative values indicating accentuation of fluctuations; γ = retardation of peaks and minima with respect to Cl^- (see for instance Na^+ in Fig.6.49); δ = below dune peat; n.v. = not visible; B = bracken; D = dune shrub; G = tall grasses and herbs; M = mosses; O = oaks; P = pines.

$$\%d = 100\,[1 - \frac{A_x}{(\alpha_x A_{Cl})}] \qquad (6.15)$$

where A_x = the observed amplitude for constituent x [µmol/l]; A_{Cl} = ditto, Cl^-; α_x = x/Cl^- in sea water (see Table 5.5).

The thus quantified smoothing is listed for several vegetation groundwaters, sampled through miniscreens, in Table 6.22. Fluctuations that have a wave period of 1 year or 2.5 years (the wave comprising the extremes of November 1977 and May 1979), and fluctuations of the atmospherical and biological type are discerned in that table. The plots with an atmospherical fluctuation pattern exhibit on average a significantly stronger smoothing and retardation of Na^+, K^+ and Mg^{2+} oscillations than the plots with a biological fluctuation pattern. This is explained by (1) a higher share of Na^+ in the ionic balance of vadose water on the plots with an atmospheric fluctuation pattern, and (2) less interference with biological processes that may accentuate especially K^+ and Mg^{2+} fluctuations. A deep decalcification of the upper dune sand (B_1, B_2, D_2, $O_{1,3}$) seems to promote fluctuations in K^+ and Mg^{2+}, perhaps by lability of the biological system under stress or by seasonality of exchange reactions with Al or NH_4^+.

The exchange reaction is postulated to take place in the upper soil horizons mainly, with mosses, well-humified organic material and plant roots as the major exchanging phases. Litter does not sorb measurable amounts of Na^+, as evidenced by rather constant Na^+/Cl^- ratios for litter leachate from sea buckthorn, oaks and pines over the seasons (deduced from data in Stuurman, 1984a). And the dune sand does not contribute much either, because an increase of the flow length is not accompanied by a clear rise in damping or phase lag. This can be deduced from Fig.6.51, where the Na^* wave is seen to migrate rather conservatively with depth on the plot mosses-1. Calculations with the PHREEQM-model of Nienhuis et al. (1987) confirmed, that exchange with the dune sand alone was quite insufficient to explain the strong sorption phenomena observed (C.A.J. Appelo, pers. communication).

The NO_3^- peaks generally coincide with an infiltration period from September till December, and relate to the combination of a maximum decomposition (Fig.6.12), little uptake and high atmospheric NO_x levels in the period October till March (Fig.6.48). Fluctuations in SO_4^* have quite an irregular appearance (Fig.6.48). This is probably caused by : (1) the interfering effects of fluctuations in atmospheric SO_2 concentrations (Fig.6.48), gross

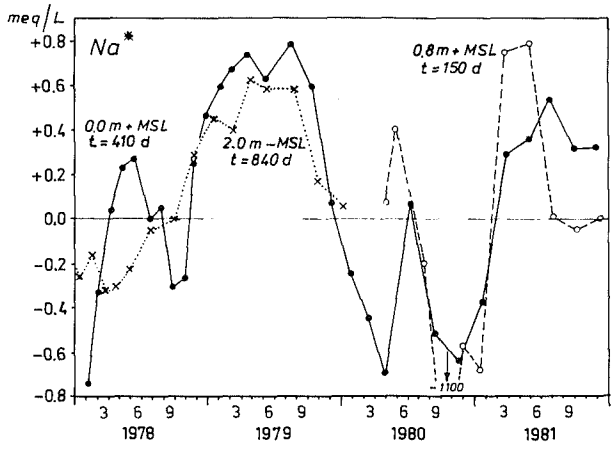

FIG. 6.51 Propagation of the cyclic Na^* wave in the upper groundwater below mosses (plot M_1), from 0.8 m above to 2.0 m below MSL. The time axis corresponds with infiltration time, each curve has been shifted back according to its total transit time in the subsoil (surface at 2.8 m+MSL). The relatively small smoothing of the peaks in the downward direction, indicates that the cation exchange responsible for the peaks takes place in the upper soil horizons. $Na^* = Na^+$ corrected for sea spray.

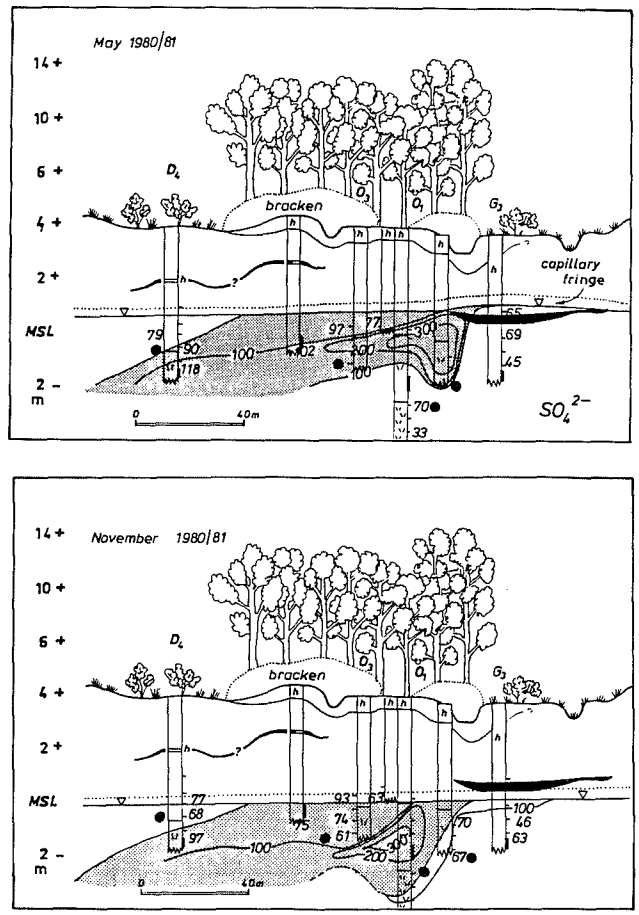

FIG. 6.52 The mean position of oak-groundwater (stippled) and mean spatial patterns of SO_4^{2-} concentrations (in mg/l), during the maximum and minimum phreatic level (mean for indicated month over 1980 and 1981). Interference with the geohydrochemically active dune peat aquitard $1A_3$, can be deduced from the raised SO_4^{2-} concentrations. Vertical hydrochemical zones, due to heterogeneities in vegetation cover (here a small oak stand amidst grasses and low dune shrub) and geochemistry (a dune peat lens), pendulate up and down with changes in the water table, leading to strong hydrochemical fluctuations of the hydrological type in, among others, the miniscreens marked with a heavy dot.

precipitation, evaporation losses, biological processes and sorption of peaks to the moss layer and decalcified dune sand; and (2) a relatively low analytical precision of ± 2 mg/l.

The hydrological type

This fluctuation pattern is dominated by the seasonal change in the position of the water table and flow lines. Nice examples are encountered along the interface between one vegetation groundwater lens and another. During a low phreatic level in autumn, the local vegetation lens may reach the deeper miniscreens, which are flushed by the underlying vegetation water lens in early spring, when the water table is high (Fig.6.52).

Within vegetation groundwater, a vertical zonation due to horizontal differences in for instance geochemistry, may pendulate up and down with the phreatic level as well, and thus show up in a fixed miniscreen as a hydrochemical fluctuation of the hydrological type. This is shown for oak water with a relatively low and high SO_4^{2-} concentration in Fig.6.52. The high sulphate oak-water is associated with dune peat, that is periodically drowned by groundwater. The resulting, very strong hydrochemical fluctuations are shown in Fig.6.45 (oaks-1).

6.7.5 *Effects of dispersion*

Quality fluctuations of soil moisture and shallow groundwater are generally smoothed upon progressive subsoil passage, by hydrodynamic dispersion and, depending on the constituent of water and soil type, exchange reactions (Table 6.22), filtration, precipitation, breakdown or transformation. The mechanism of damping of seasonal quality fluctuations by dispersion is visualized in Fig.6.53. For the nonconservative parameters HCO_3^- and NO_3^-

a stronger smoothing downgradient can be observed than for Cl^- (Fig.6.54).

In this section we focus on the conservative chloride, the fluctuations of which are only subjected to dispersive and diffusive mixing in the subsoil. For simplicity we assume one-dimensional flow and initially neglect the effects of mixing within the active plant root zone. Preferential flow through root channels, lateral flow to roots, upward flow in response to evapotranspiration and bioturbation conduce to a considerable mixing within this upper soil layer (Cook et al., 1992). However, the thickness of this layer rarely exceeds 0.3-0.5 m and with a mean moisture content of 6.5% by volume, a short residence time of 11-85 days can be calculated for water under bare dune sand and a pine stand, respectively. Complete mixing within this layer does not transform the essence of variable input signals with a mean wave period superior to about 1-8 months, respectively.

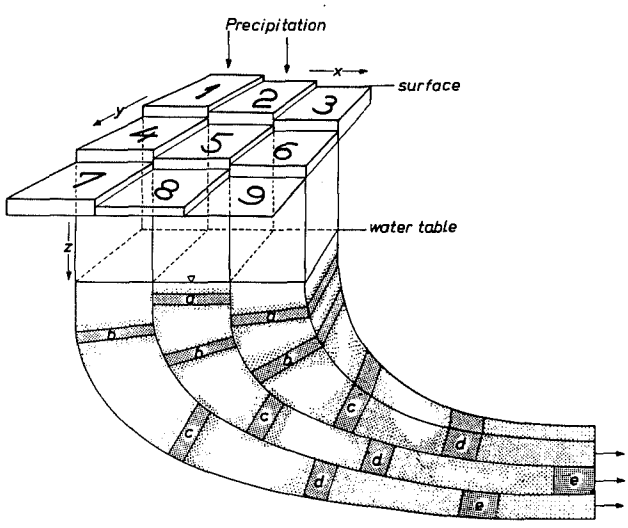

FIG. 6.53 Longitudinal and transversal dispersion, leading to the smoothing of the dotted and alphabetically numbered concentration maxima each year in groundwater below a scanty vegetation cover, for instance the winter maxima in Cl^- concentration close to the HWL. The larger the difference in thickness of the unsaturated zone between adjacent blocks, and the smaller the size of each block, the more transversal dispersion will have a smoothing effect on fluctuations in the chemical composition along each homogeneous flow tube.
A two times higher precipitation excess for one block due to a different vegetation cover, leads to a groundwater flow tube with a two times larger cross section. This reduces the chance of transversal dispersion with adjacent flow tubes for the interior flow lines within the tube.

The effects of artificial dispersion by sampling with miniscreens are significant but not deleterious. The vertical mixing length of about 0.1 m (section 6.3.4), contributes significantly to the dispersion within the annual stratum of new groundwater below pines (0.35-0.5 m thick) and relatively little below bare dune sand (1.55 m thick). This contribution is practically independent of the depth below the water table (Table 6.3) and therefore does not explain the observed damping with depth in Fig.6.54.

An analytical solution for longitudinal dispersion of a sinusoidal wave
Many quality fluctuations in shallow dune groundwater, especially those on a seasonal basis, approximate a sine (Figs. 6.44-6.51) thanks to a sinusoidal input signal (Fig.6.32). In case of one-dimensional flow and a sinusoidal input signal for dissolved constituents at distance x = 0 with amplitude A_o [mg/l], a wave period T' [d] and phase ωt [rad], we obtain, in analogy with the propagation of a temperature wave, according to Maas (1991) :

$$c_{(x,t)} = A_o \cdot e^{-aX} \cdot \sin(\omega t - BX) \qquad (6.16)$$

with : $a = \ln \{A_o/A_x\}/x$ [m^{-1}]; $B = \omega/v_w$ [rad/m]; ω = angular frequency of oscillation = $2\pi/T'$ [rad/d]; v_w = migration velocity of water or conservative tracer [m/d]; X = travel distance [m]; t = time [d].
The hydrodynamical dispersion coefficient equals in this one-dimensional flow case, the longitudinal dispersion coefficient D_L [m^2/d] :

$$D_L = \frac{a\,v}{a^2+B^2} = \alpha_L v_w + D_d \qquad (6.17)$$

with : D_d = molecular diffusion coefficient [m^2/d]; α_L = longitudinal dispersivity [m].
The order of magnitude of α_L for dune sand amounts to 0.01 - 0.1 m, as the longitudinal dispersivity of sandy deposits generally is about ten times the transversal dispersivity (Verruijt, 1971; De Jonge, 1981; Uffink, 1990). Defining damping (%d, in %), in analogy with Eq.6.15, as :

$$\%d = 100 \cdot (1 - \frac{A_x}{A_o}) \qquad (6.18)$$

gives after combination of the Eqs. 6.16-6.18 :

$$\%d = 100 \cdot (1 - e^{-X\{\frac{v_w - \sqrt{v_w^2 - (\frac{2D_L\omega}{v_w})^2}}{2D_L}\}}) \qquad (6.19)$$

Calculations compared with observations
The smoothing has been calculated with Eq.6.19 as a function of the total travel distance in the subsoil,

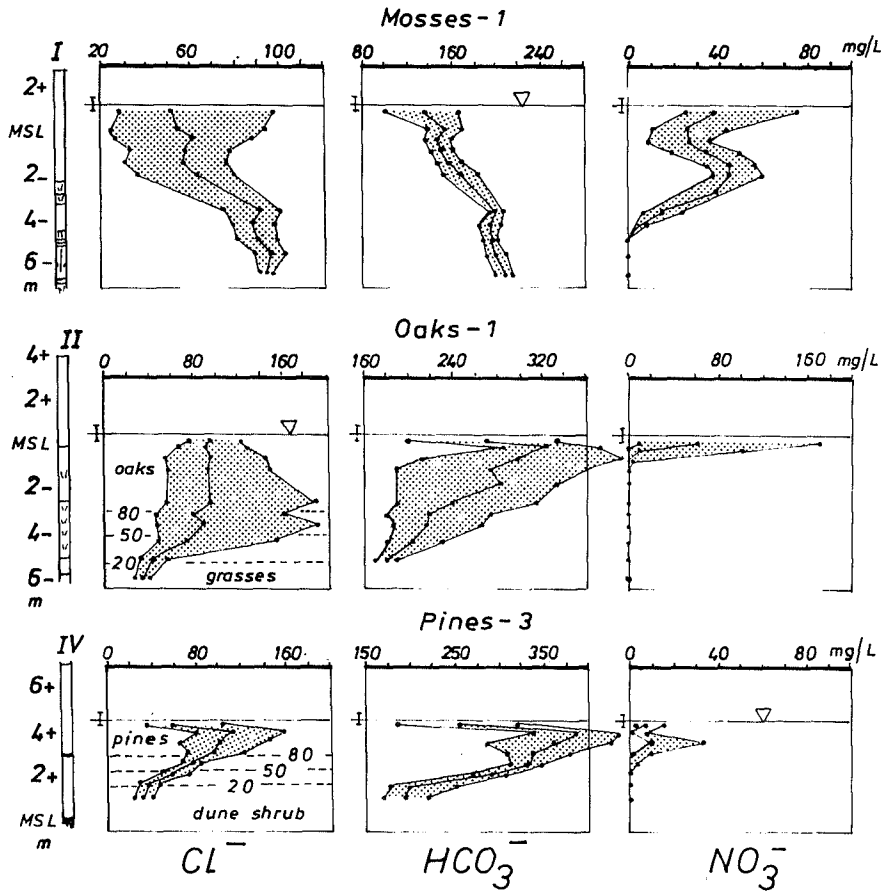

FIG. 6.54 The smoothing of fluctuations in Cl^-, HCO_3^- and NO_3^- with depth, for multilevel wells equipped with miniscreens, on the plots mosses-1, oaks-1 and pines-3. The presented lines connect the minima, maxima and mean values for 2-4 years of intensive monitoring. Forest water is floating on grasses and dune shrub water on the plots oaks-1 and pines-3, respectively. The position of 20, 50 and 80% mixing of both waters is indicated. The smooting of HCO_3^- and NO_3^- fluctuations is more effective than the smoothing of Cl^-, due to chemical processes.

for four typical flow velocities of water, three longitudinal dispersivities and three wave periods (Table 6.23; Fig.6.55). The chosen flow velocities correspond with those on the groundwater divide below pines in the saturated zone or in the capillary fringe (v_w = 0.001 m/d, vertical), those in the unsaturated zone below a wet dune shrub or wet deciduous forest (v_w = 0.01 m/d), those in the saturated zone with predominantly horizontal flow in dunes with natural recharge (v_w = 0.1 m/d) and artificial recharge (v_w = 1.0 m/d, see section 7.5).

The longitudinal dispersivities chosen, are within the natural range for homogeneous, (fine) sandy, porous media (De Jonge, 1981), with a value of 0.01-0.1 metre as most probable for dune sand. The wave periods are such that 0.1 year approximately corresponds with monthly vagaries, 1.0 year with the summer-winter cycle and 10 years with long-term fluctuations in either the precipitation excess or the chemical composition of bulk precipitation.

The results of calculation are presented in Table 6.23 and Fig.6.55, and lead to the following expectations and confrontations with our observations :

- high values for α_L and low values for v_w and T' enhance the smoothing of quality fluctuations;
- vagaries (T' = 0.1 y) are largely smoothed, also with low values for α_L (0.01 m), in the unsaturated zone (v_w = 0.01 m/d) and still further in the capillary fringe (v_w = 0.001 m/d). They do not reach therefore the upper dune groundwater, also because of additional mixing in the upper soil horizons and mixing by sampling. This corresponds well with the observed lack of vagaries in the composition of the upper dune groundwater (Figs. 6.44 and 6.45);
- seasonal fluctuations (T' = 1 y) do not survive the capillary fringe below pines (v_w = 0.001 m/d), not even with low values of α_L (0.01 m). This contrasts with our observations (Fig.6.45) and leads to the conclusion that the strong fluctuations observed, must relate to shifts in the position of flow lines (as

TABLE 6.23 Calculated damping (in %) by hydrodynamic dispersion (including diffusion), of the amplitude of a sinusoidal input signal for a conservative tracer under various flow velocities of water (v_w), longitudinal dispersivities (α_L) and wave periods (T'). 100 = complete smoothing. Calculated using Eq.6.19.

	α_L= 0.01m				α_L= 0.1m				α_L= 1.0m			
X	v_w (m/d)				v_w (m/d)				v_w (m/d)			
(m)	0.001	0.01	0.1	1.0	0.001	0.01	0.1	1.0	0.001	0.01	0.1	1.0
T' = 0.1 year												
1	100	99	3	0	100	100	26	0	100	100	95	3
2	100	100	6	0	100	100	46	1	100	100	100	6
4	100	100	12	0	100	100	71	1	100	100	100	11
8	100	100	22	0	100	100	91	2	100	100	100	22
16	100	100	39	0	100	100	99	5	100	100	100	39
32	100	100	63	1	100	100	100	9	100	100	100	62
64	100	100	87	2	100	100	100	17	100	100	100	86
128	100	100	98	4	100	100	100	32	100	100	100	98
256	100	100	100	7	100	100	100	53	100	100	100	100
T' = 1.0 year												
1	100	5	0	0	100	28	0	0	100	100	3	0
2	100	9	0	0	100	48	1	0	100	100	6	0
4	100	17	0	0	100	73	1	0	100	100	11	0
8	100	32	0	0	100	93	2	0	100	100	22	0
16	100	53	1	0	100	99	5	0	100	100	39	0
32	100	78	1	0	100	100	9	0	100	100	62	1
64	100	95	2	0	100	100	17	0	100	100	86	2
128	100	100	4	0	100	100	32	0	100	100	98	4
256	100	100	8	0	100	100	53	1	100	100	100	7
T' = 10 years												
1	19	0	0	0	40	0	0	0	100	3	0	0
2	34	0	0	0	64	1	0	0	100	6	0	0
4	57	0	0	0	87	1	0	0	100	12	0	0
8	81	0	0	0	98	2	0	0	100	22	0	0
16	97	1	0	0	100	5	0	0	100	39	0	0
32	100	2	0	0	100	10	0	0	100	63	1	0
64	100	3	0	0	100	18	0	0	100	86	2	0
128	100	6	0	0	100	33	0	0	100	98	4	0
256	100	11	0	0	100	55	1	0	100	100	7	0

in Fig.6.52), in combination with higher recharge rates along zones with preferential flow (for instance open spots in the pine stand);

· seasonal fluctuations are predicted to reach, however, the upper groundwater below oaks, dune shrub and scantier vegetation covers, if α_L is low enough (≤0.1 m). The deepest observable propagation of seasonal fluctuations is theoretically expected below bare dune sand. Seasonal fluctuations could indeed be clearly followed up to about 3 m below the phreatic level on the plot mosses-1 only (Fig.6.48). The smoothing observed between the upper and middle miniscreen yields an α_L of 0.01 m, and that between the middle and lower miniscreen an α_L of 0.1 m; and finally

· long-term fluctuations (T' = 10 y) can easily penetrate into the upper groundwaters without considerable smoothing and remain manifest up to a depth of 20-30 meters. This corresponds well with observations discussed in sections 7.3 and 7.4.

6.8 Important fluxes

So far, we focused mainly on concentrations in the water phase. By multiplication of concentrations in mg/l with precipitation, throughfall or recharge in mm/d, we obtain the flux of dissolved constituents in mg m^{-2} d^{-1} (for conversion to kg ha^{-1} y^{-1} multiply this flux with 3.65). Four important fluxes are considered here, in order : interception deposition, storage in biomass, fixation of atmospheric N_2 and the rate of decalcification. Chemical mass balances are presented for selected vegetation groundwaters in contrasting dune areas, in section 8.4.

6.8.1 Interception deposition

Methods of calculation

Interception deposition (ID_x) was defined as the additional atmospheric deposition on the land

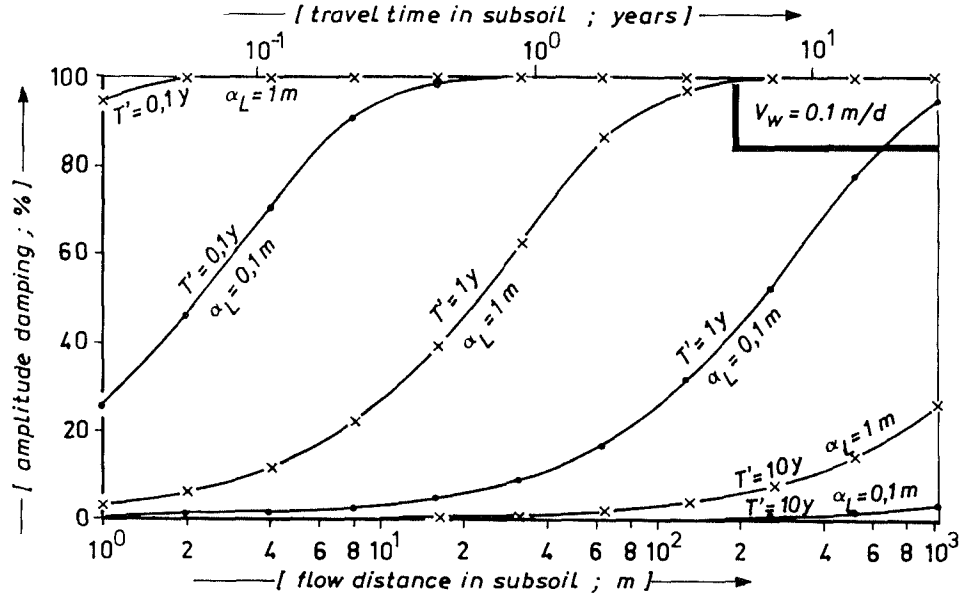

FIG. 6.55 The smoothing [expressed as % damping] of sinusoidal fluctuations in water quality by hydrodynamic dispersion (including diffusion), during flow through the unsaturated or saturated zone, as a function of the wave period T' and longitudinal dispersivity α_L of the porous medium. In this example the flow velocity v_w (migration velocity of water) was set at 0.1 m/d. For a tenfold higher or lower flow velocity read the curve of 10T' and T'/10, respectively. Based on data in Table 6.23.

surface as compared to a collector of bulk precipitation (section 6.5.1). Its magnitude is calculated here for various elements and compounds, using data of bulk precipitation and either throughfall, the drainage solute of lysimeters or the upper groundwater in the following ways.

For constituents with conservative behaviour (no geochemical nor biological sources and sinks), calculation reduces to :

$$ID_x = TD_x - BD_x \qquad (6.20)$$

where : ID_x = interception deposition [mg m^{-2} d^{-1}]; TD_x = Total atmospheric Deposition of x, as measured in either throughfall, lysimeter or groundwater (mg/l * mm/d); and BD_x = Bulk Deposition of x (mg/l * mm/d).

Conservative behaviour is assumed for Cl^- in all environments, for SO_4^{2-} (and SO_4^*) only in calcareous environments without iron sulphides and with a shallow decalcified upper zone, and for F^- solely in throughfall. Geochemical sources of Cl^- and SO_4^{2-} in the (sub)oxic dune sands considered, can indeed be excluded (Van der Sleen, 1912; Rijsdijk, 1984a). Their sensitivity to sorption upon soil passage is very low in the near neutral pH domain (Scheffer & Schachtschabel, 1970). Internal uptake and release of Cl^- and SO_4^{2-} by vegetation can be ignored against high external fluxes in this coastal area (Ulrich et al., 1979; Garten et al., 1988). A significant SO_4^{2-} supply from decomposing litter and humus, cannot be expected (Jansen, 1989). Fiedler & Thakur (1984) estimate this supply at 1.1-3.3 mg m^{-2} d^{-1}, which is indeed low compared to the fluxes in shallow groundwater and the drainage solute of the lysimeters near Castricum (14-84 mg m^{-2} d^{-1}; Table 6.24).

The interception deposition of aerosols containing for instance Na, K, Ca, Mg, Mn and Al, in mg m^{-2} d^{-1}, is calculated according to Bredemeier et al. (1988) :

$$ID_x = \frac{ID_{Cl}}{BD_{Cl}} \cdot BD_x \qquad (6.21)$$

which implies a constant ID/BD ratio, notwithstanding differences in median mass diameter of the particles involved. And the interception deposition of NH_y (= NH_3 + NH_4^+), NO_x (= NO + NO_2^- + NO_3^-) and F_t (=HF^- + CaF_2 etc.) was estimated in µmol m^{-2} d^{-1}, for the 1980s exclusively, as follows :

$$ID_{NHy} \approx 1.5 \cdot ID_{SO_4^*} \qquad (6.22)$$

$$ID_{NOx} \approx 0.5 \cdot ID_{SO_4^*} \qquad (6.23)$$

$$ID_{HF} = 0.05 \cdot ID_{SO_4^*} \qquad (6.24)$$

These estimates are based on mean NH_4^+/SO_4^*, NO_3^-/SO_4^* and F^-/SO_4^* molar ratios in the canopy's flux contribution (throughfall minus bulk deposition) by dune shrub-1, oaks-2, pines-3 centre and pines-3

TABLE 6.24 Calculated interception deposition (ID) for several plots, as deduced from fluxes in either throughfall, the drainage solute of lysimeters or the upper groundwater, each minus bulk deposition. The contribution of ID to the total atmospheric deposition (TD) of x is indicated as a percentage (%TD). Bulk precipitation on the lysimetric plots in 1955-1961 was assumed equal to that in 1980-1982.

ID as deduced from :	crown height m + surf	distance HWL m	Cl^- ID α	Cl^- %TD	SO_4^{2-} ID α	SO_4^{2-} %TD	SO_4^* ID α	SO_4^* %TD	F^- ID β	F^- %TD	TIN ID γ	TIN %TD
THROUGHFALL, 1982												
Dune shrub-1	1.5	625	62	60	13	41	5	25	84	55	86	27
Oaks-2	6	3200	9	27	13	49	12	53	44	39	171	44
Pines-3, center	8	1700	18	39	21	60	18	64	95	61	397	66
Pines-3, edge	8	1680	125	82	91	87	73	88	261	81	1239	86
Pines-5##	15	3000	24	75	38	76	32	75	-	-	690	72
UPPER GROUNDWATER, 1980-1982												
Mosses-1	<0.1	325	≤7	≤10	28	58	26	70	97?	46?	520[c]	70
Dune shrub-1	1.5	625	83	66	37	65	25	64	-13?	-22?	500[c]	64
Oaks-2	6	3200	25	48	42	73	38	76	86?	53?	760[c]	76
Pines-3, center	8	1700	33	51	34	68	30	72	36?	34?	600[c]	72
DRAINAGE SOLUTE LYSIMETERS, 1955-1961												
Bare-L	<0.1	2000	3	12	17	52	16	57	56?	27?	-[d]	
Dune shrub-L	1.5	2040	25	49	21	57	18	59	37?	20?	-[d]	
Oaks-L	3	2115	24	48	21	56	17	58	32?	18?	-[d]	
Pines-L	5	2200	29	52	30	65	26	68	-60?	-67?	-[d]	
DRAINAGE SOLUTE LYSIMETERS, 1980-1982												
Bare-L	<0.1	2000	3	9	14	46	13	52	45?	23?	260[c]	52
Dune shrub-L	2.5	2040	28	51	27	63	23	65	108?	42?	460[c]	65
Oaks-L	8	2115	36	58	22	58	16	57	147?	49?	320[c]	57
Pines-L	14	2200	118	82	84	84	68	85	107?	42?	1360[c]	85

α = mg $m^{-2}d^{-1}$; β = µg $m^{-2}d^{-1}$; γ = µmol m^{-2} d^{-1}; ## = Nov. 1986 - Nov. 1987, calculated from data in Houdijk (1990); ? = uncertain due to nonconservative behaviour of F^- (negative values indicate F-sorption); c = calculated using Eq. 6.22 + 6.23; d = cannot be calculated using the Eqs.6.22 + 6.23, which apply to the 1980s exclusively.

edge (Tables 6.10 and 6.11), and their ratio in the interception deposition of a bulk collector as compared to a wet-only sampler (Table 5.3). The canopy's flux contribution probably does not contain any inorganic nitrogen leached from foliage, but is depressed to some extent by foliar uptake (Ivens et al., 1989) or foliar adsorption in the cuticula (Kisser-Priesack et al., 1990). The estimates are therefore to be considered as approximations on the low side.

The data on throughfall (Table 6.24) refer to the canopy's interception deposition exclusively, whereas those on the lysimetric drainage and upper groundwater encompass the total interception deposition by both the canopy and upper soil.

Results

The interception deposition of Cl^-, SO_4^{2-}, SO_4^*, F_t and TIN has been quantified for various dune plots in Table 6.24, by application of Eq.6.20 to the data on bulk precipitation and either throughfall, the drainage solute of the lysimeters west of Castricum or the upper groundwater. Values for PO_4^{3-}, Na^+, K^+, Ca^{2+}, Mg^{2+}, Mn, Al and SiO_2 were calculated using Eq.6.21 and can be deduced from Table 6.25, where both the total atmospheric deposition and bulk deposition are listed. The following conclusions are drawn from the results in Table 6.24.

Although throughfall and the upper groundwater are to be compared in a qualitative sense mainly (section 6.5.2), soil interception appears important especially regarding SO_4^* on dunes with a deciduous vegetation (D_1 and O_2). Soil retention of fluoride may be important on the calcareous plots dune shrub-1 and pines-3, and much less pronounced or even lacking on the deeper decalcified plot oaks-2. The increase of the F^- drainage from all vegetated lysimeters in 1980-1982 as compared to 1955-1962, points at F^- breakthrough, because the atmospheric F^- deposition was not higher in 1980-1982 in comparison with 1955-1962.

Bare dune sand with few mosses (S_L) and a low vegetation composed mainly of mosses (M_1), intercept little more (5-15%) Cl^- than a bulk precipitation collector in this coastal area, but considerably more SO_4^* : about twice and thrice as much for S_L and M_1, respectively. An interception deposition of about

TABLE 6.25 Storage in living biomass of heather, oak and pine (including thinnings and excluding the forest floor) and storage in soil humus, as compared with atmospheric deposition (bulk and total) and with drainage losses from the unsaturated zone as deduced from the upper vegetation groundwater on selected monitoring plots. Data on storage in biomass derive from various sources, see footnotes below.

mg m^{-2} d^{-1}	Cl^-	SO_4^{2-}	TIN$^{\alpha}$	PO_4^{3-}	Na^+	K^+	Ca^{2+}	Mg^{2+}	Mn	Al	SiO_2
IN- AND OUTPUT CALCAREOUS DUNES, 2000 m FROM HWL, 1980-1982											
bulk precipitation	26	16	270	0.12	15	0.8	2.7	2.0	0.07	0.16	0.5
total atm. dep., bare$^{@}$	29	30	540	0.13	17	0.9	3.0	2.2	0.08	0.18	0.6
total atm. dep., pines-edge$^{@}$	144	100	1690	0.67	83	4.4	15.1	11.1	0.39	0.89	2.8
drainage losses, bare	29	30	485	0.09	17	4.2	84.9	4.3	<0.02	<0.04	7.9
drainage losses, shrub	54	43	486	0.03	28	2.8	101	5.4	0.03	<0.04	7.4
drainage losses, oaks	63	38	8	0.12	33	3.8	86.9	4.5	0.06	<0.01	8.5
drainage losses, pines-edge	144	100	4	0.09	80	5.1	83.2	8.2	<0.01	<0.01	4.3
IN- AND OUTPUT DECALCIFIED DUNES, 800-1400 m FROM HWL, 1985-1987											
bulk precipitation**	29	14	284	0.12	16	0.9	2.0	2.2	0.07	0.16	0.5
total atm. dep, pines-center	51$^{\#}$	50$^{\#}$	959$^{\#}$	0.20$^{@}$	$^{\#}$26	1.5$^{@}$	3.4$^{@}$	3.7$^{@}$	0.12$^{@}$	0.39$^{\#}$	0.9$^{@}$
drainage losses, scanty	40	17	235	0.33	24	2.2	2.7	3.4	0.04	2.62	13.7
drainage losses, heather	34	21	49	0.19	20	2.1	6.4	3.0	0.04	0.81	13.3
drainage losses, pines-cent	35	20	10	0.17	21	1.5	3.7	4.3	0.03	0.33	12.6
STORAGE IN LIVING BIOMASS											
heather (Calluna vulgaris)$^{\beta}$	-		79§	0.42		0.95	1.0	0.3	0.10	0.02	-
oaks (Quercus robur)$^{\gamma}$	-	1	222§	0.67	-	1.53	6.1	0.7	-	-	3$^{\lambda}$
pines (Pinus nigra)$^{\delta}$	0.3	2	286§	1.12	0.2	1.8	2.5	0.6	0.14		2$^{\lambda}$
STORAGE IN SOIL HUMUS											
heather (Calluna vulgaris)$^{\beta}$	0	1.1	262§	0.13	-0.3	-0.74	1.0	0.2	0	-0.37	
calcareous dune soil$^{\varepsilon}$	-	-	200§	0.51	-	-	-	-	-	-	-

α = NO_3^- + NO_2^- + NH_4^+ in µmol m^{-2} d^{-1}; β = Matzner & Ulrich (1980); γ = Duvignaud & Denaeyer-De Smet (1970); δ = synthesis of data in Minderman (1967), Miller et al. (1980) and Ovington (1959); ε = calculated from soil analyses in Boerboom (1963), Nijssen (1989) and Louman (1989) and an estimated soil age of 200-500 years ; λ = Bartoli (1983). @ = calculated using Eq.6.21; # = measured in throughfall by Houdijk (1990); ** = estimated from data in Ch.5 and Houdijk (1990); § = organic N.

15 mg SO_4^* m^{-2} d^{-1} for dune sand with few mosses, compares well with observations by Kühn & Weller (1977) for bare sand in West Germany, under similar conditions (9 mg m^{-2} d^{-1}).

The negligible amount of Cl^- interception by low vegetation types, allows to calculate the natural recharge (N) or total evaporation losses (E_t) from the weighted mean Cl^- content of bulk precipitation ($\overline{Cl}_{BD}$) and from either the mean Cl^- concentration of the upper groundwater or the weighted mean of the drainage solute of a lysimeter (both : $\overline{Cl}_G$), after a time shift to correct for the transit time in the subsoil :

$$N = 1.1 \cdot \frac{\overline{Cl}_{BD}}{\overline{Cl}_G} \cdot P \qquad (6.25)$$

where : N in m/y; and the factor 1.1 corrects for an interception deposition of 10%.

Already in 1927, Heymann demonstrated the excellent agreement between a thus calculated natural recharge (neglecting the factor 1.1) and the drainage quantity measured with a lysimeter (see section 1.4 for further details).

The about equal rates of calculated interception deposition of SO_4^* for all upper groundwaters (M_1, D_1, O_2 ,P_3), notwithstanding large differences in vegetation cover, are very surprising indeed, especially when we consider the significantly higher values for pines in throughfall measurements (Table 6.24, Verstraten et al., 1984; Ulrich, 1983). The relatively high interception deposition on mosses-1, dune shrub-1 and oaks-2 as compared to the lysimeters S_L, D_L and O_L respectively, is probably caused by : (a) a more effective sorption of SO_2 gas to mosses as compared to bare dune sand, which is further enhanced by a more reactive surface in the direction of the HWL in consequence of a raised deposition of hygroscopic sea salts and calcareous dust (Fig.6.19); (b) a more effective sorption of SO_2 gas to dune shrub receiving a higher deposition of sea spray (as above); and (c) the isolated, highly exposed position of the oak stand comprising

oaks-2, contrary to O_L, in combination with a possible desorption of SO_4^{2-} from the acid soil on oaks-2, in consequence of a declining atmospheric deposition of SO_x in the previous period (Fig.5.5).

The interception deposition by the central parts of pines-3 agrees with that by pines on the lysimetric plot in the period 1955-1961, probably by a similar exposition to winds. In the period 1980-1982 the crown of the pines on plot P_L dominated the surroundings and thereby intercepted much more sea spray and air pollutants in amounts about equal to the windward edge of pines-3.

In conclusion

It can be concluded that interception deposition as defined here, contributed in the early 1980s for 50-75% to the total atmospheric deposition of SO_4^*, probably for at least 40-60% regarding F^-, for 50-75% regarding TIN, and for 10-65% regarding Cl^-. Their contribution can reach 90% in the edge zone of shrubs and forests.

The 50-75% for both SO_4^* and TIN is somewhat lower than the mean contribution of dry deposition during those years to the mean total deposition on The Netherlands as a whole, according to Erisman (1992) 80 and 70%, respectively. The difference is explained mainly by the inclusion of a significant portion of dry deposition, in bulk precipitation samples (section 5.3.1), so that the interception deposition as defined here underestimates dry deposition. The 50-75% for SO_4^* and TIN also overlaps with the range for Calluna heathland (60-65%; Bobbink et al., 1992). However, the 57-70% for SO_4^* and TIN on scanty and low vegetation covers (mosses and bare plus some mosses) are relatively high as compared to data given by Van Dam et al. (1990) for grassland (48% for S and 43% for N). These low values are explained by the significantly lower Cl^- deposition, which mediates gas absorption (Fig.6.19), on their plots and by their use of an inert quartz top soil. The absolute levels for the coastal area are relatively low for The Netherlands, which is in harmony with conclusions by Houdijk (1990).

6.8.2 *Storage in biomass*

During the first 6-10 centuries after fixation of dunes by vegetation, biomass is accumulating both in standing crops and soil humus (Olson, 1958; Gerlach et al., 1989). The order of magnitude of the storage in heather, oaks and pines, as well as in soil humus could be estimated with suitable data from literature (Table 6.25). In the same table, data are listed on atmospheric deposition and the drainage losses from an unsaturated zone without interferences by peat or soil amendments, as deduced from the upper groundwater on selected monitoring plots.

Intercomparison leads to the following conclusions. Compared with atmospheric deposition today, storage in biomass is negligible (≤1%) for Na^+ and Cl^-, very small (5-10%) for SO_4^{2-}, small (10-20%) for Mg^{2+}, of about equal magnitude regarding K^+, Ca^{2+} (in decalcified dunes only) and NO_3^-+NO_2^- +NH_4^+ (TIN), and significantly higher for PO_4^{3-} and Mn. The relatively low drainage losses of K^+, TIN and PO_4^{3-} from the unsaturated zone below oaks and pines can therefore be explained at least partly by uptake and storage in biomass.

Growth of oaks and pines clearly requires additional sources of phosphate and possibly Mn, such as weathering (PO_4^{3-} from shell fragments and possibly apatites, Mn from ferric hydroxide coatings and primary silicates), bird droppings (PO_4^{3-}) and fertilizers. Calcium requirements by oak exceed atmospheric deposition and are satisfied in calcareous dunes by the weathering of calcite and in decalcified dunes possibly by the weathering of anorthite.

6.8.3 *N_2-fixation*

An important source of nitrate in dune water, besides bulk and interception deposition, is the fixation of atmospheric N_2 gas by specific bacteria and algae in dune sand (Table 6.26). Quantitatively most important is the fixation by symbiontic bacteria in the root nodules of sea buckthorn, regarding both the areal extent and the level achieved. The effect is indeed, that the highest nitrate concentrations in groundwater without peat interferences, are observed below dune shrub that is composed mainly of sea buckthorn (Table 6.13, Fig.6.16).

An important question is : Are the high drainage losses of nitrate below bare dune sand with few mosses (485 µmol N m^{-2} d^{-1} for S_L, Table 6.25) and below extensive moss carpets (about 690 µmol N m^{-2} d^{-1}, average for M_1 and M_2), attributable solely to atmospheric deposition including a high contribution from interception deposition, or to a combination with N_2-fixation by blue-green algae? The data on total atmospheric deposition (Table 6.25) reveal that atmospheric deposition alone could account for such elevated drainage losses indeed.

The lysimetric data suggest that the amount of N_2 fixed by sea buckthorn, is more or less entirely taken up and stored in living biomass, litter and the soil. This leaves an amount equal to the total atmospheric deposition, to be leached to the upper groundwater. The data on storage in living biomass and soil humus in the dunes (Table 6.25), indicate that the amount of N_2 fixed by *Hippophaë rhamnoides* probably is 300-500 µmol N m^{-2} d^{-1}. This figure is closer to the conservative estimates by Akkermans (1971) than to the data presented by Stewart & Pearson (1967).

TABLE 6.26 N_2-fixation by various organisms in coastal dune sand, according to several authors.

N_2-fixing organism	location c.q. vegetation type		µmol N m^{-2} d^{-1}	reference
Azotobacter chroöcoccum	marram in young dunes		2	Akkermans, 1971
cyano-bacteria: genera#	bare dune sand in blow-outs		-	Pluis & De Winder, 1990
genera§	wet dune slack		130-260	Stewart, 1965; Reynaud & Roger, 1980
symbiontic bacteria, genus	root nodules of sea buckthorn		350	Akkermans, 1971
Frankenia (Actinomycetes)	*(Hippophaë rhamnoides),*	0- 3 y	530	Stewart & Pearson, 1967
		3-11 y	1335	Stewart & Pearson, 1967
		11-13 y	2605	Stewart & Pearson, 1967
		13-16 y	3520	Stewart & Pearson, 1967
symbiontic bacteria, ditto	ditto of alder *(Alnus glutinosa)*		1145	Akkermans, 1971

= *Microcoleus, Oscillatoria & Tychonema*; § = *Anabaena* and *Nostoc.*

6.8.4 Decalcification rates

The most prominent weathering reaction in calcareous dunes with a precipitation excess, both quantitatively and ecologically, is the leaching of calcium carbonate, leading to a progressive decalcification with time and depth. This process was studied or noticed in dune areas through soil chemical analysis, in the UK by Salisbury (1925, 1952), Wilson (1960), Ball & Williams (1974), James & Wharfe (1989) and Wilson (1992), in France by Gehu-Franck (1971), in Australia by Burges & Drover (1953), in the US Great Lakes district by Olson (1958), in the Hudson Bay, Canada (beach barriers : Protz et al., 1984, 1988) and in The Netherlands by Boerboom (1963), Klijn (1981), Rozema et al. (1985), Grootjans et al. (1990) and (Stuyfzand & Lüers, 1992b).

Here, we first focus on the amounts of dissolved calcium carbonate leaving the leaching zone, by consideration of the hydrochemical and hydrological data pertaining to the calcareous plots, where the upper groundwater was observed to be in close equilibrium with calcite/aragonite. Subsequently the rate of decalcification is considered by including geochemical data, and finally some consequences of decalcification are discussed.

$CaCO_3$ fluxes in solution below the leaching zone
The majority of Ca^{2+} in the studied, calcareous vegetation groundwaters, derives from the dissolution of calcium carbonate. Other sources of Ca^{2+} are sea spray, the weathering of silicate minerals and cation-exchange. The sea spray contribution is equal to $\{Ca^{2+} - Ca^*\}$ and generally < 5% . The dissolution of silicates containing Ca, may contribute at most 2 mg Ca^{2+}/l for each dissolved 6 mg SiO_2/l, by congruent dissolution of anorthite (Eq.8.26B in Table 8.3). We take half this amount as most probable, which is also < 5%. Desorbed Ca^{2+} is principally derived from earlier carbonate dissolution, and as such treated here. We then obtain for the mean decalcification flux (Q_{CaCO3}), in mg $CaCO_3$ m^{-2} d^{-1} :

$$Q_{CaCO_3} = 2.5 \cdot Ca^{\#} \cdot N \qquad (6.26)$$

where : N = mean diurnal groundwater recharge [mm/d]; $Ca^{\#} = Ca^* - SiO_2/6$ = the mean Ca^{2+} concentration (mg/l) of the upper groundwater, as derived exclusively from $CaCO_3$ dissolution; and 2.5 = conversion factor of Ca^{2+} to $CaCO_3$.

Thus, the main leaching zone is considered to reside above the water table, which is consistent with geochemical observations in the calcareous dunes. Results of calculation using Eq.6.26, are presented as bar diagrams for the 24 calcareous plots, arranged in increasing order (Fig.6.56). It can be concluded that $CaCO_3$ leaching is favoured by (1) passage through dune peat above or close to the water table (B_2, O_1), due to CO_2 release upon oxic decomposition, and (2) sea buckthorn (all D-plots). Intercepted atmospheric acids (H_2SO_4 and HNO_3) and acid precursors (NH_4^+), and biogenic acids (H_2CO_3 and organic acids) are evidently consumed most effectively below *Hippophaë rhamnoides*, by dissolution of $CaCO_3$ in the root zone. Although the strong N_2-fixation in its root nodules is a H^+-indifferent process (Eq.8.10 in Table 8.1), this probably prevents the uptake of $H^+ + NO_3^-$ (Eq.8.6 in Table 8.1), and thereby helps to explain the high decalcification rate.

Although pines intercept larger quantities of atmospheric acids and acid precursors than all other vegetation types studied (Table 6.24), and probably produce more CO_2 and biogenic acids than sea

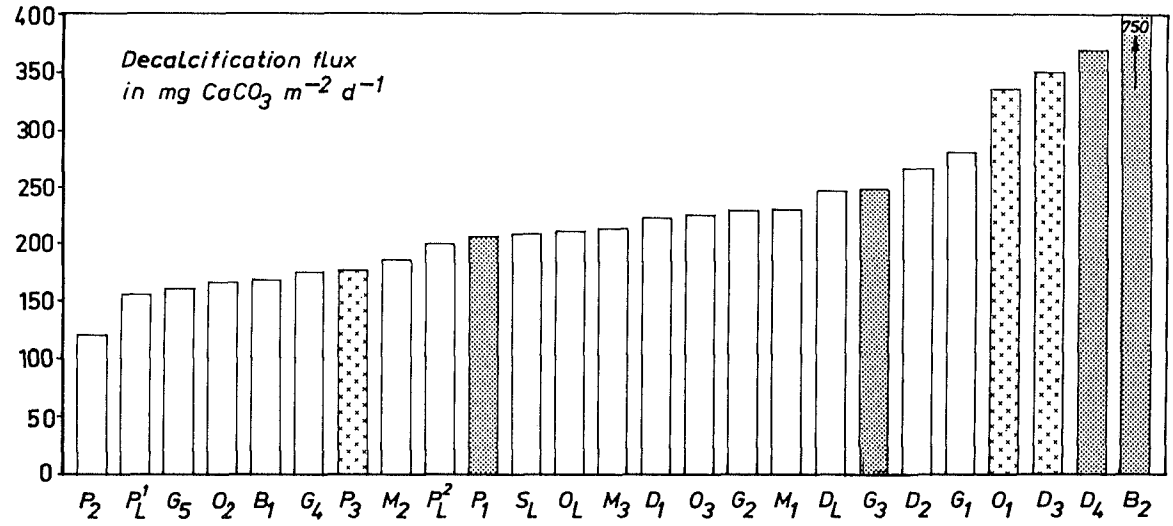

FIG. 6.56 Bar diagrams with the daily calcium carbonate flux from the zone of decalcification in the primarily calcareous dunes, arranged in increasing order. Interaction with intercalated dune peat is indicated by fine dots (strong) or crosses (weak, peat in traces). The maximum values are encountered where dune peat oxidizes above the water table, and under Hippophaë (due to N_2-fixation). Pines rank amongst the vegetation covers with the lowest decalcification flux. B = bracken; D = dune shrub, composed mainly of Hippophaë; G = grasses; M = mosses; O = oaks; P = pines; S = scanty; P^1_L = pines lysimeter, 1955-1961; P^2_L = ditto, 1980-1983.

buckthorn, they rank among the vegetation types with the lowest decalcification rate (Fig.6.56). This is probably caused by : (a) CO_2 losses to the atmosphere through diffusion, after precipitation of calcite upon drying of the intensively rooted soil horizons, and in consequence of shortage of water to take up the CO_2 produced; (b) denitrification (Eq.8.12 in Table 8.2), yielding bicarbonate, which buffers H^+ by formation of volatile H_2CO_3; and (c) acid buffering by the tree canopy (Table 6.10), NO_3^- uptake (Table 6.25) and the soil organic matter formed.

Decalcification rates and soil analyses

It is generally recognized that the dissolution of calcium carbonate, if omnipresent, is a very fast process, requiring only a few days to reach equilibrium (White, 1984). The sharp lime boundary in decalcifying calcareous dune sands in the Western Netherlands (Pons & Van Oosten, 1974; Van der Meer, 1952) also testifies of a high reaction rate. The width of the transition zone between completely decalcified dune sand and practically unleached calcareous dune sand generally ranges from 0.05-0.5 m, which compares well with observations elsewhere in sandy areas with a precipitation surplus : 0.2-0.6 m below a 0.2-0.5 m thick decalcified zone in the Hudson Bay (Protz et al., 1984, 1988), and 1 m below a 15 m thick decalcified zone in Northern Germany (Dahmke et al., 1986). The rate of decalcification (v_{CaCO3}), i.e. the velocity with which the schematized sharp lime boundary migrates downwards, then simply becomes, in mm/d :

$$v_{CaCO_3} = \frac{Q_{CaCO_3}}{(1-\epsilon)\cdot\rho_s\cdot(CaCO_3)_{solid}} \qquad (6.27)$$

where : ϵ = porosity [-]; ρ_s = density of solids [kg/dm^3]; $(CaCO_3)_{solid}$ = lime content [mg/kg dry weight]; Q_{CaCO3} = mean daily $CaCO_3$ flux, calculated using Eq.6.26 [mg $CaCO_3$ m^{-2} d^{-1}].

Application of Eq.6.27 to the calcareous dunes, which contain in between 2 and 10 % $CaCO_3$ by dry weight (Klijn, 1981; Depuyt, 1972), with ϵ = 0.4, ρ_s = 2.65 kg/l and the median value for Q_{CaCO3}= 200 mg $CaCO_3$ m^{-2} d^{-1} (Fig.6.56), yields a decalcification rate of 6 and 1 µm/d, or 23 and 5 cm/century, respectively. Taking 5% as the average lime content for the dune plots south of Zandvoort aan Zee, would give a decalcification rate of 9 cm/century. This rate compares reasonably well with field data collected in the younger and older dunes to the south of Zandvoort aan Zee (Fig.6.57).

Application to the dunes primarily poor in lime, with a Q_{CaCO3} = 100 mg $CaCO_3$ m^{-2} d^{-1} (derived from data in section 7.3) and a primary lime content of 0.2% (Van der Sleen, 1912; Doing, 1966), yields a decalcification rate of 115 cm/century. With an age of the central comb dunes area (Fig.3.7) of 400-700 years, a complete decalcification becomes possible to a depth of 4-8 m below ground level, which is well below the present groundwater table. The observed occurrence of strongly acidified groundwater in the upper 3 m (Fig.7.2), with Al above 1

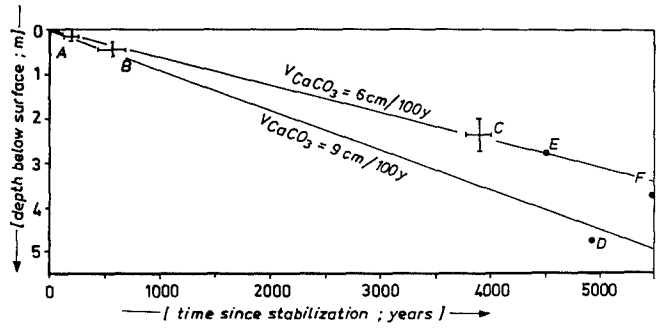

FIG. 6.57 The decalcification depth of dune sand in relation to the time elapsed since stabilization (younger dunes) or dune formation (older dunes), for the primarily calcareous dunes south of Zandvoort aan Zee. A, B and C : observations in dunes west of Hillegom by Stuyfzand & Lüers (1992b) and Blokzijl & Pruissers (1989); D : in the Keukenhof near Lisse, from Jelgersma et al. (1970); E and F : near Oranjekom (Leiduin) and Groenendaal, respectively, data obtained from L. van der Valk (RGD).

mg/l, confirms this natural decalcification to be completed.

The above calculations are only approximative and heavily rely on the following conditions : (1) decalcification started when the landscape remained fixed and was not disturbed by (a) any aeolian deposition of fresh calcareous dune sand, (b) any erosion or mining of decalcified parts, and (c) any mixing through bioturbation for instance by rabbits and the redistributing effects of vegetation by uptake and litter production;
(2) leaching of $CaCO_3$ is a steady process, i.e. the flux of Ca^{2+} as derived from $CaCO_3$ leaching remains constant for the solution below the descending leaching front; and
(3) the leaching front is composed of a sharp interface between completely decalcified sand and unleached parent material.
Especially the conditions 1 and 2 are very critical and rarely fully satisfied. A high variability of Q_{CaCO3} both in time and space should prevail : in time, through fluctuations in the acid input, in consequence of changes in atmospheric pollution, vegetation cover, groundwater recharge, redox conditions etc.; and in space, for the same reasons and due to heterogeneities in dune sand composition (primary lime content, dune peat lenses, iron sulphides).

Nevertheless a linear depletion of the $CaCO_3$ stock is evidenced by the data in Fig.6.57, and confirmed by data in Fig.6.58, from the island of Schiermonnikoog (Rozema et al., 1985), Blakeney Point (UK; Salisbury, 1925), Lake Michigan (USA; Olson, 1958), and Hudson Bay (Van Breemen & Protz, 1988; not shown). The data from Schiermonnikoog and Lake Michigan reveal, however, a higher decalcification rate during the initial 20 and 50-100

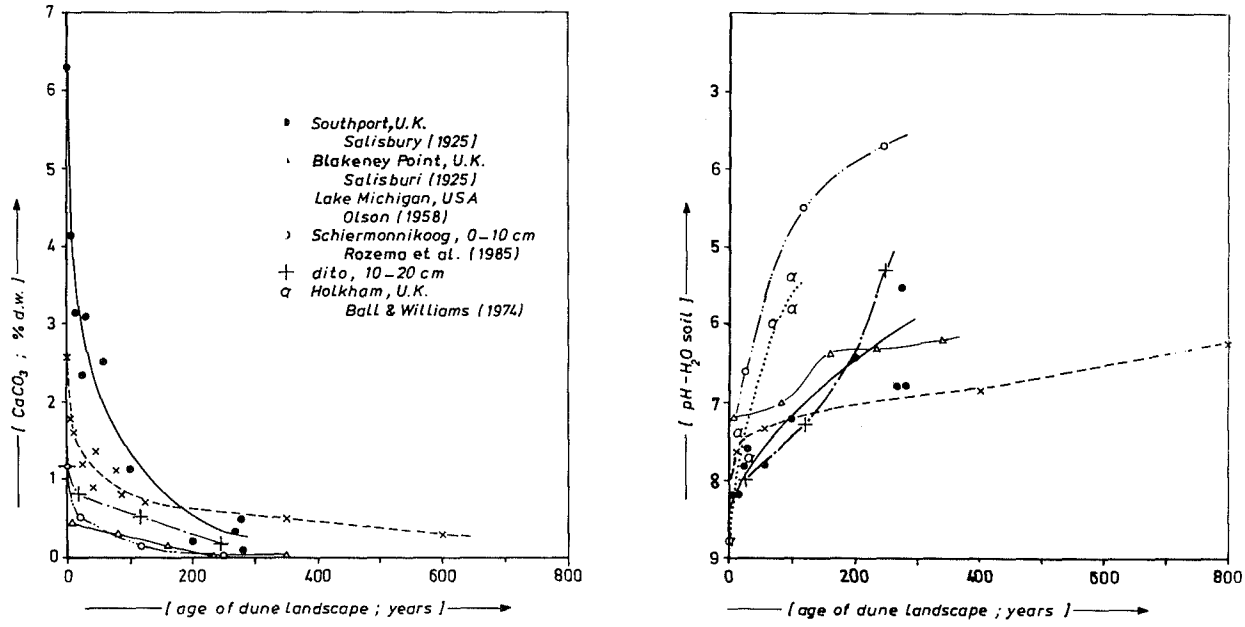

FIG. 6.58 The progress in decalcification and acidification of the upper 10-20 cm mineral soil, for calcareous sand dunes in selected humid areas of the world (P = 700-900 mm/y). The exponential $CaCO_3$ decrease for Southport (UK) and Lake Michigan (USA) contrast with observations elsewhere, which show a linear decrease in accordance with Eq.6.27. Decalcification is accompanied by a rising pH, the shape of which depends on many factors.

years, respectively. This appears to be the general picture, because : (1) also the curve for Southport (UK; Salisbury, 1925) can be divided into a high rate during the initial 100 y and a slow constant rate afterwards; and (2) there is other evidence from Burges and Drover (1953) who noticed that 50% was leached in a coastal dune system of New South Wales (Australia) in 50 y and the remaining part required an additional 150 y.

It appears that the duration of this initial phase of accelerated decalcification depends mainly on the original lime content (Fig.6.58), when gross precipitation does not deviate much : 100 y for Southport (6.3% $CaCO_3$), 50-100 y for Lake Michigan (2.6%), 20 y for Schiermonnikoog (1.2%) and probably 5 y for Blakeney Point (0.6%?). The duration of accelerated leaching thereby becomes about 20 y for each 1.2 % $CaCO_3$ originally present. There is, however, no question of the rate of $CaCO_3$ loss from the soil being proportional to the carbonate left at any time, as stated by Olson (1958) and explained by Klijn (1981) by an increasingly less efficient contact between the percolating water and the remaining, relatively large shell fragments upon progressive leaching (Fig. 6.59). Close inspection of Fig.6.58 yields a surprisingly uniform half-life for the original lime content, being about 20-25 y, and a much longer period is required to arrive at 25% of the original content. Thus the following intuitive relationship describing the exponential decrease in $CaCO_3$ content of the upper solum (Minderman & Leeflang, 1968; Stuyfzand, 1984d; Rozema et al., 1985), has to be rejected :

$$C_t = C_o \cdot e^{-\lambda t} \qquad (6.28)$$

where : C_o = original content [kg $CaCO_3$/kg oven-dry soil]; C_t = ditto after t years; t = time interval [y]; λ = -(dC/dt)/C = dissolution constant [y^{-1}], being equal to $\ln 2/T_{½}$ with $T_{½}$ = leaching time to obtain half the previous content.

The initial, high leaching rate is explained by : (1) the specific characteristics of pioneer vegetations, with their N_2-fixation (reducing the uptake of atmospheric $H^+ + NO_3^-$) and low evapotranspiration losses (which reduces CO_2 losses to the atmosphere); (2) an initial optimal contact of CO_2 and organic acids with $CaCO_3$ in a calcareous root zone; and (3) a relatively high uptake and redistribution of Ca^{2+} by calciphilous vegetation.

After decalcification

When the $CaCO_3$ content drops below about 0.1% at pH 6.2 (Fig.6.20), other acid buffers take over the dominant role of $CaCO_3$ (section 6.6.4). The pH then rapidly declines to, or stabilizes at values in between 3 and 6.2 at Schiermonnikoog and Blakeney Point, respectively (Fig.6.58). The pH level attained by decalcified dune sand at Blakeney in 1925 (6.2) is high as compared to Schiermonnikoog in 1985 (3.7-5.3) and Holkham in 1970 (5.4), which is situated in the vicinity of Blakeney. A relatively short period of exposure to high atmospheric acidity inputs may explain the Blakeney data.

Decalcification is an essential part of the general soil succession in dunes. It is followed by podzolization, which may take about 600-2000 y in background areas (Burges & Drover, 1953; Wilson, 1992). In how far the raised acidity of atmospheric deposition during the past century accellerates this process, is an important question.

6.9 Concluding remarks

The upper metres of the coastal dune hydrosome exhibit an extremely large hydrochemical variety, both in space and time and applying to all major and many minor constituents. These variations are largely natural but they also contain the effects of diffuse atmospheric pollution, lowered phreatic levels and man-made changes in vegetation (pine plantations). They have to be taken into account in the set-up of groundwater monitoring programs for drinking water supply, environmental protection and nature conservation, by carefully selecting (a) strategical positions for monitoring wells (preferentially safely within a vegetation groundwater lens), (b) the right screen length (miniscreens if seasonal fluctuations are to be measured), and (c) the right analytical program (specific trace elements in acidified systems only). The enormous variation also explains that the distinction between dune water and waters belonging to other hydrosomes can be difficult.

On the other hand, the hydrochemical variability offers a unique opportunity to date shallow groundwater by its seasonal and annual fluctuations. And flow paths can be visualized by the natural labelling of, for instance, nested vegetation groundwaters, groundwater with a clear peat interference or groundwater with more or less sea spray influences in topographically well-defined recharge areas.

The mean composition of shallow dune groundwater is dictated mainly by the local atmospheric deposition record, vegetation cover, geochemistry (depth of decalcification and peat interference) and thickness of the unsaturated zone. Probably very specific for coastal dunes, are : (1) the gradients in air-borne sea salts and, within the first km behind the foredune ridge, gradients in sea-spray-corrected sulphate; (2) the very pronounced interception deposition of sea spray as a function of vegetation cover and the distance to the North Sea High Water Line; and (3) the large-scale N_2-fixation.

Monitoring of the upper decimeters to metres of dune groundwater offers a promising alternative or

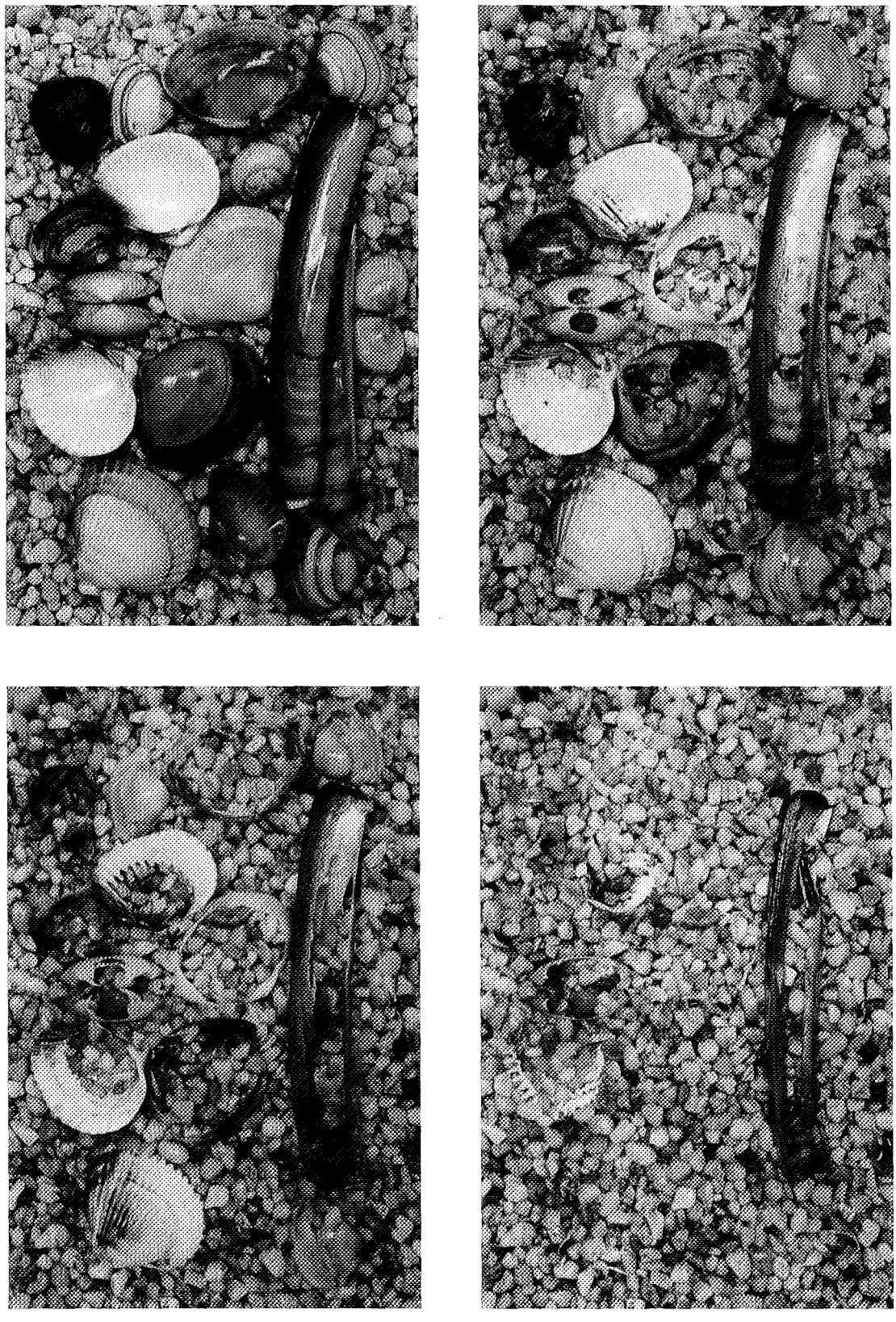

FIG. 6.59 The long-term fate of sea shells from the North Sea beach. Acid rain dissolves the more delicate shells first, and the shells with an organic coating constitute a significant redox buffer (photo F. Lüers).

even the best method for the otherwise complex monitoring of total atmospheric deposition of nitrogen and sulphur compounds, provided that (a) its water table stands >0.5 metre below a scanty vegetation cover (bare dune sand, marram or mosses), (b) interferences with peat and iron sulphides can be excluded, (c) decalcification of primarily calcareous dune sands is negligible, (d) measurements are continued for several years, and (e) vegetation cover does not change. The monitoring of throughfall below forest stands and dune shrub in particular, probably yields a significant underestimation of the total atmospheric deposition by neglect of soil interception. This is demonstrated by comparison of measurements on throughfall, litter leachate, soil moisture and groundwater.

The interception deposition of Cl^- amounted to only 5-15% of the total atmospheric deposition for plants less than circa 0.1 m high in this coastal area, so that the total evaporation losses or natural recharge can be estimated using the weighted mean Cl^- concentration of bulk precipitation multiplied with 1.1, and the mean Cl^- concentration of shallow groundwater, after a time shift to correct for the transit time in the subsoil. This time shift is essential, due to the high temporal variabilty of the atmospheric input signal.

The major long-term changes in the composition of shallow dune groundwater during the past century are : a rise of NO_3^- levels especially below scanty vegetation types without peat interference, in analogy with the increased atmospheric deposition of NO_x and NH_y; a rise of NO_3^- levels in dune terrains where sea buckthorn expanded or where the groundwater dropped below the critical mean level of 0.5 m below the surface, thereby changing the redox environment drastically from anoxic to (sub)oxic; first an increase of SO_4^{2-} and since the early 1980s a remarkable decline, in harmony with the atmospheric emission record of SO_2; a general increase of the salt concentration in consequence of expansion and growth of tall vegetation types with concomitantly a higher interception deposition, evapotranspiration and CO_2-production; and a Ca^{2+} increase, mainly due to (1) the above mentioned changes in vegetation, (2) the lack of the acid buffering reduction of Mn- and Fe-oxides and SO_4^{2-}, in consequence of an expansion of the (sub)oxic zone, and (3) an increased atmospheric input of acids. Decalcified dunes behaved differently through a significant decline in pH and HCO_3^- as a sign of a critical reduction of the acid neutralizing capacity.

The persistence of strong seasonal quality fluctuations in the upper metres, as measured with miniscreens, demonstrates that the transversal and longitudinal dispersivities of dune sand are in the order of 0.001-0.01 and 0.01-0.1 metre, respectively. The preservation of seasonal fluctuations corresponds with model predictions, using an analytical formula for the propagation of a one-dimensional sinusoidal input signal, at least regarding oaks and all scantier vegetation covers. Seasonal fluctuations were predicted to extinct completely in the capillary fringe below pines. This contrasts with our observations, that demonstrate strong fluctuations, and is explained by preferential flow paths and seasonal shifts in the position of flow lines.

The upper few metres of dune groundwater rather frequently do not satisfy the drinking water standards as embedded in the Drinking Water Act for the European Community (Table 1.1; EC, 1984). This holds for practically all main constituents, as well as Al, As and Zn. There is no question of a general problem, however, because (a) the drinking water supply companies abstract for the larger part deeper groundwater of better quality, and (b) shallow private wells are used largely for irrigation purposes. The ions Na^+, Cl^- and NO_3^- may pose some problems, where dune water is deliberately admixed to dilute recovered river Rhine or Meuse water.

The upper dune groundwaters systematically exceed the upper background levels for natural groundwater in The Netherlands (Table 1.1), as proposed by LBS (1988) and adopted by MILBOWA (1991). This does not testify of a large-scale pollution, but pleads for specific baseline conditions for the coastal dunes as presented by Stuyfzand (1991b), in connection with their particular hydrochemical environments.

Chapter 7

CHEMICAL EVOLUTION OF INTRUDING DUNE, RHINE AND NORTH SEA WATER DOWNGRADIENT

Abstract

Changes in concentration of major constituents, trace elements and the isotopes ^{3}H, ^{13}C and ^{18}O are presented for dune, Rhine and North Sea water, from recharge towards their intrusion front. They are shown in detailed well logs, in specific cross sections and along a generalized flow path down the hydraulic gradient at specific locations. The flow paths selected, vary in length from 0.8 km for Rhine water which escaped from direct recovery, to 6-10 km for dune and North Sea water flowing towards reclaimed lakes.

Evolution lines, which the three hydrosomes have in common, are made up of several fronts downgradient due to redox reactions, cation exchange and displacement. Fronts in connection with environmental pollution could be traced back in dune and Rhine water only, as North Sea groundwater was not examined in detail at shallow depth. An acidification front in shallow groundwater was exclusively found in the decalcified dunes north of Bergen.

The position of redox fronts is related mainly to the geochemical zonation (availability of organic matter), flux of the mobile oxidants O_2, NO_3^- and SO_4^{2-}, and antecedent water table fluctuations (leaching). Oxygen and nitrate generally survive the dune sands, but are completely consumed in the sandy North Sea deposits at 1-5 m-MSL (dune and Rhine water) or deeper where the present sea floor cut through these deposits. Sulphate reduction and methanogenesis are quantitatively important for dune water only, in connection with its relatively low flux of oxidants. It occurs where well developed dune or basal peat or specific Holocene clastic aquitards are passed. The highest Fe and As levels are encountered in the anoxic sulphate (meta)stable zone. Uranium is strongly mobilized in the lower parts of the suboxic zone, where U roll front deposits are dissolved, and it probably precipitates as UO_2 where Fe is mobilized.

Specific exchange zones develop behind each intrusion front in analogy with the ion chromatographic effects demonstrated with column experiments by Beekman (1991). A fresh dune water intrusion into brackish Holocene transgression water results in (a) a broad exchange zone with specific patterns for Na^+, K^+, Li^+, Rb^+, Ca^{2+}, Mg^{2+}, Sr^{2+}, NH_4^+ and SiO_2, and (b) several secundary reactions in consequence of strongly reduced Ca^{2+} concentrations (dissolution of fluorapatite-like phases), raised HCO_3^- levels and increased pH (dissolution of gibbsite and precipitation of a manganous siderite). The intrusion of North Sea water at 60-100 m-MSL into dune water leads to a very narrow exchange zone with opposite reactions and a clear mobilization of Fe, Mn and Ba^{2+}. The displacement of dune water by recharged Rhine water is to be considered as a salinization as well, with similar reactions in many respects. The exchange zone is wider due to the lower displacing capacity of Rhine water (Σcations = 8.6 instead of 515 meq/l for coastal North Sea water).

The environmental pollution record of precipitation is reflected in dune water by decreasing levels downgradient for the mainly atmogenic trace elements Se, Cu, F^-, Zn, Pb, Sb and V (in decreasing order of depth of penetration) and organohalogens adsorbable to activated carbon, and by the tritium and sea-spray-corrected SO_4^{2-} patterns.

Recharged Rhine water shows well conserved patterns for Cl^-, SO_4^{2-} and tritium, a smoothed pattern for dissolved organic matter, and breakthrough of Na^+, Mg^{2+}, K^+, F^- and PO_4^{3-} in dune sand after about 1.2, 3, 5, 5 and 30 pore flushes, respectively.

An acidification front was observed in dune groundwater north of Bergen exclusively, at about 5 m below ground level, i.e. 3 m below the phreatic level. The pH rapidly increases in the front from about 4.5 to 6, with a concomitant decline of Al concentrations and a remarkable mobilization of Be, Cd, Co, Li^+, Ni, Rb^+ and Zn. These trace ions probably reach the extreme levels observed by dissolution of "roll-deposits", which form downgradient of the advancing acid front. Concentration peaks of the trace cations are separated probably by ion chromatographic effects, in order of increasing distance down the hydraulic gradient, and concomitantly increasing pH : Pb < Cu < Al < {Be $\cong$ Rb $\cong$ Zn $\cong$ Cd} < {Co $\cong$ Ni} < Li. The position of the acid front coincides with the redox cline, and it is calculated that denitrification and the reduction of $Fe(OH)_3$ contribute in this case for about 60% to the acid buffering.

Dune water that formed after 1953, was dated using the technique of history matching. Years with an anomalous atmospheric input of tritium, $\delta^{18}O$ and Cl^- could be traced back in detailed vertical hydrochemical logs. Dune water older than 70 years

could be dated using (1) a $\delta^{18}O$ front, which matched a strong drawdown of the water table in the area in the period 1880-1920, and (2) ^{14}C radiometry, with the approach of Pearson & Hanshaw (1970). A maximum age of 800 years was deduced. Rhine water, that was recharged since 1957, could be dated in more detail in a cross section, by matching the combined chloride and tritium input record.

7.1 General

After the transformation of rain water into groundwater in an initially open system, further important changes occur downgradient in a system more or less closed from the atmosphere, by interaction with various reactive phases. These changes generally contain many of the 6 systematic quality evolution lines, described in section 2.7. Such evolution lines were briefly described for hydrosomes in the study area, in sections 4.4 and 4.5. They are presented and explained here in more detail, including the results of calculation of mineral saturation indices and groundwater dating, for three important hydrosome types towards their intrusion front : fresh dune water invading a brackish aquifer, pretreated river Rhine water displacing dune water, and North Sea water intruding into less salty aquifers. This chapter thereby constitutes the sixth step in regional hydrochemical surveys (Fig.1.7).

Notwithstanding a copious data base, it still was a problem in each case to find sufficient or the right observation wells along a representative flow path, in order to depict a prograde quality evolution without introduction of anomalies due to local heterogeneities and deviations from the assumed flow path. These anomalies are posed, in case of dune water, by among others : (a) small scale spatial changes in vegetation; (b) intercalated clay lenses that slow down freshening by low permeability and high CEC; and (c) recent salt water upconings due to large scale pumping, which cut off dune water downgradient from its recharge upgradient.

In order to circumvent these problems, several observation wells had to be projected on the flow path chosen, after preselection on the basis of a fitting alkalinity and salinity. By doing so, generalised quality trends are offered instead of a specific one. Such an approach is not required where the aquifer system is more homogeneous and not disturbed by discontinuities, like in case of the Chalk aquifer in the London basin (Edmunds et al., 1987), the Lincolnshire limestone in the East Midland of England (Bishop & Lloyd, 1990) or the Tertiary Ledo-Paniselian aquifer in Northwest Belgium (Walraevens, 1987).

Two freshening dune chains are considered, the initially low alkalinity type (Bergen dune hydrosome, section 7.3) and medium alkalinity type (Zandvoort dune hydrosome, section 7.4), because of the strong impact of a deep decalcification on the quality evolution, not only in the upper zone but also further down the hydraulic gradient. A salinizing Rhine chain is studied, in the upper aquifer and the Holocene aquitards in the Leiduin artificial recharge area, situated to the south of Zandvoort aan Zee (section 7.5). And two North Sea flow branches are examined, both in the area south of Zandvoort aan Zee : a 10 km long one intruding into relict Holocene transgression water at about 120-200 m-MSL without clear salinization phenomena (section 7.6.2); and a 2 km long one intruding into dune water at 60-100 m-MSL with pronounced salinization phenomena (section 7.6.3).

Before presenting and discussing the chemical evolution of these waters downgradient, some chemical characteristics of the contacted marine Holocene and selected Pleistocene deposits are given in section 7.2. The geochemistry of dune sand and dune peat was treated in section 6.4. For detailed information on the Bergen and Zandvoort area, including an extensive listing of groundwater analyses, reference is made to Stuyfzand (1989a and 1988b, respectively).

7.2 Geochemistry of marine Holocene and selected Pleistocene deposits

Some geochemical characteristics of the marine Holocene and selected Pleistocene aquifer and aquitard materials in the coastal dunes are listed in Table 7.1. The presented data refer to soil samples, that were obtained from bailer drilled wells in the study area. The samples were analysed for the greater part in the laboratory of the Institute of Earth Sciences of the Free University of Amsterdam.

The following conclusions are drawn. The marine Holocene and Eemian deposits and the fluvial Rhine deposits (Urk, Sterksel and Kedichem Formations) are calcareous, whereas the fluvial deposits from North-German rivers (Harderwijk and Enschede Formations) are practically devoid of $CaCO_3$. The CEC ranges from 5 to 20 meq/kg (dry weight) for most aquifers and from 20 to 265 meq/kg for most clastic aquitards. The adsorption complex is for >85% occupied by Ca^{2+}, only in well-flushed fresh dune water systems without base exchange. In freshened dune water systems, Mg^{2+}, K^+ and occasionally Na^+ occupy a significant part of the adsorption complex (in the deep Enschede Formation up to 67%). The concentration of iron sulphides is generally low in the aquifers (<10 mg/kg in the upper, (sub)oxic sands, and about 220 mg/kg was observed in anoxic Eemian sands), and

TABLE 7.1 Some geochemical characteristics of selected Holocene and Pleistocene aquifer and aquitard materials in the coastal dunes. These materials are contacted during groundwater flow within the hydrosomes discussed in this chapter.

Sample no. §	Hydro-geol. unit *	Geological formation #	Type of sediment	Hydro-chem. envir. **	clay (<2 μm) %	$CaCO_3$ %	CEC_Σ meq/kg	Na^+ % of CEC_Σ	K^+ % of CEC_Σ	Ca^{2+} % of CEC_Σ	Mg^{2+} % of CEC_Σ	FeS + FeS_2 mg/kg	C_{org} %	
AQUIFERS														
1	I	WF (YD)	dune sand	F	≤0.3	2-4.5	7-10	7	2	88	3	<10	0.1	3-19
2	I	WF (NS II)	marine sand	F	<1	6	17	8	2	87	3	<10	0.2	2-16
3	II	Eemian	marine sand	F+	1.2	3-15	18	6	2	64	28	220	0.2	1
4	II	Urk & Sterksel	fluvial sand	F+	<1	1.5	8	8	5	57	30	-	-	7
5	IIIB	Harderwijk	fluvial sand	F+	<1	≤0.1	5-10	-		-	-			3
AQUITARDS														
6	1C	WF (NS I/II)	silty, sand	F	-	10	18-70	2	2	91	5	++$^\alpha$		5
7	1E	WF (Bergen clay)	sandy clay	F+	36	10-20	160	1	12	67	20	++$^\alpha$		2
8	1G	WF (Velsen clay)	lag. clay	F/F+	42	++	265	3	4	63	30	++$^\alpha$		3
9	2A	Eemian	marine clay	F+	33	++	136	2	6	73	18	++		5
10	2D	Drente	boulder clay	F+	-	++	85	6	6	67	22	-		2
11	2E	Kedichem	fluv. loam	F+		12$^@$	-	-	-	-	-	++		3
12	3A	Enschede	fluv. loam	F+		-	138	22	8	37	33	-		3

@ = containing many siderite nodules with composition $Fe_{0.85}Ca_{0.1}Mn_{0.05}CO_3$ (Van der Sleen, 1912); * = numbering according to Table 3.1; ** : F = fresh dune water without base exchange (BEX = 0); F+ = fresh dune water with freshened facies (BEX > 0); # : NS = North Sea; WF = Westland Formation; YD = Younger Dunes; α = up to 3% in clay lenses; ++ = visually present; - = not analysed; § : 1 = from 24H.471, 472, 482 and 483; 2 = from 24H.484 and 30E.b01-b14; 3 = from 30G.WA+WD (Rijsdijk, 1984b); 4 = from 24H.70 (after Van der Sleen, 1912) and 30E.144-146; 5 = from 24H.70 (after Van der Sleen, 1912); 6 = from 24H.471 and 472; 7 = from 19A.181; 8 = from 19C.101, 105, 109; 9 = from 19A.160 and 19C.105; 10 = from 19C.101 and 109; 11 = from 24H.70 (after Van der Sleen, 1912); 12 = from 19C.101.

much higher (probably up to a few percent) in the marine aquitards. Van der Sleen (1912) observed numerous siderite ($FeCO_3$) concretions in the fluvial Kedichem Formation (aquitard 2E), and tiny siderite crystals in the marine Holocene sediments.

Table 6.5 contains information on the chemical composition of shell debris in various Holocene aquitards and the Eemian aquifer. It can be concluded that this shell debris contains less Na and little more Mg, Fe, Mn and SO_4 than the debris in the dune and beach sands, probably because of a higher calcite/aragonite ratio (section 6.4.1).

Additional data may be obtained by extrapolation of data on recent, marine sediments (among others : Van Straaten, 1954; Verhoeven, 1962; Vosjan & Olanczuk-Neyman, 1977; Salomons & De Groot, 1978; Oenema, 1990), marine Holocene sediments in the polder areas (among others : Van Bemmelen, 1864; Harmsen, 1954; Van der Molen, 1958), and aquifer and aquitard materials from other parts of The Netherlands (Willemsen, 1984; Breeuwsma & Zwijnen, 1984). These studies reveal a general positive correlation, within a single sedimentary unit, between organic carbon, calcium carbonate and iron sulphides on the one side, and the clay content (fraction <2 μm) on the other. Well-soluble, biogenic opal is especially present in the marine Holocene (and probably Eemian) clastic aquitards. Van Straaten (1954) observed skeleton remains of silica organisms (mainly diatoms, spicules of sponges and radiolarians) and silica-elements of primary or replacement origin from higher plants (notably reeds), in recent tidal flat deposits. Van der Valk (1992) noticed that the Holocene North Sea deposits are practically devoid of diatoms, and that diatoms abound in the Holocene tidal flat deposits. The clay minerals in the Holocene and Pleistocene formations are composed, according to Breeuwsma & Zwijnen (1984), mainly of illite (30-40%), smectite (30-40%), kaolinite (5-10%) and chlorite (<5-10%).

7.3 Bergen dune water towards the Geestmerambacht polder

7.3.1 Situation and collection of hydrochemical data

The flow path studied, starts in the centre of the decalcified dune area with a rather scanty vegetation cover, in the recharge focus area of the second aquifer, and terminates in the Geestmerambacht polder, where several reclaimed lakes drain deep groundwater since about 1550 AD (Fig.7.1).

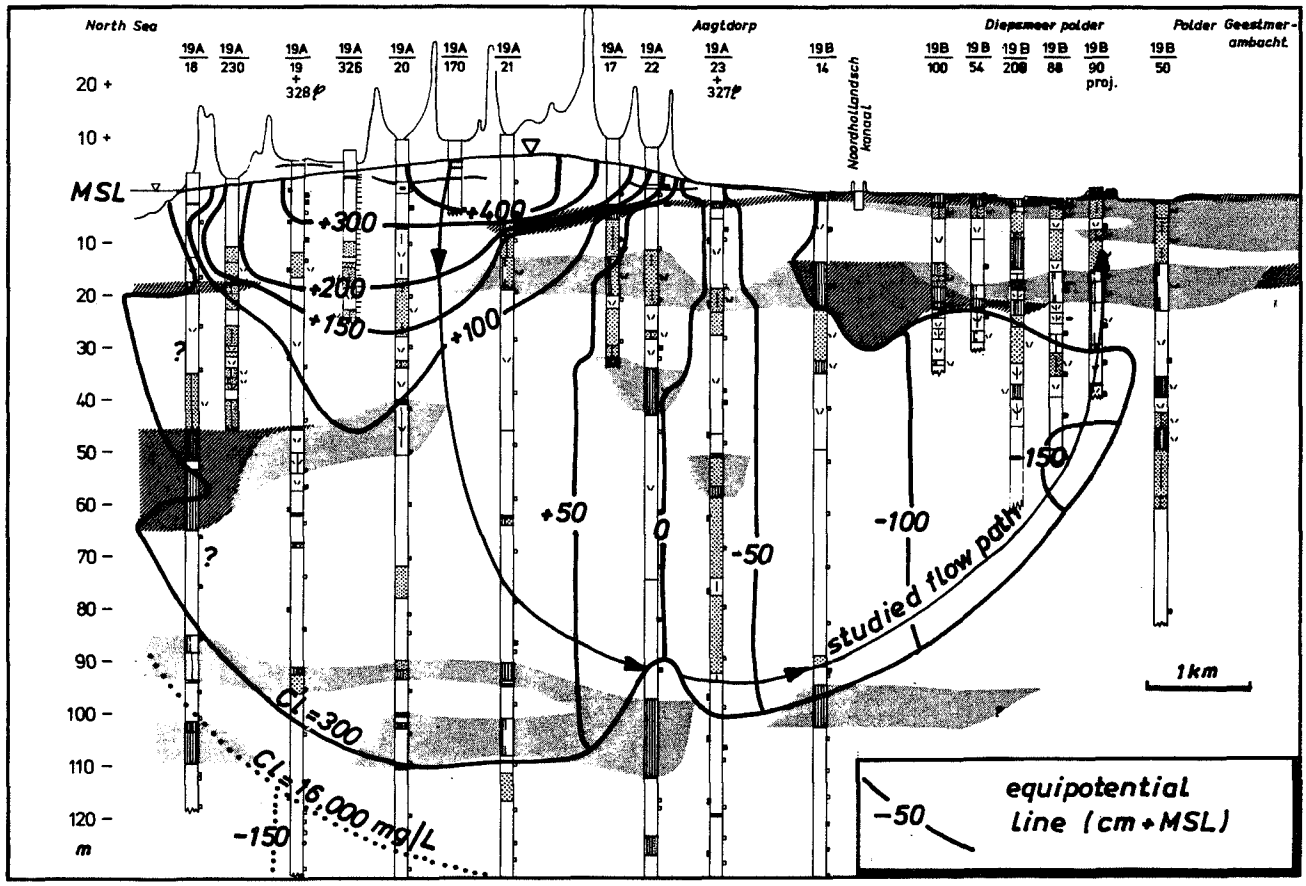

FIG. 7.1 Position of the flow path within the Bergen dune hydrosome in cross section C, along which the chemical evolution was studied. The situation of those observation wells is indicated, for which either chemical analyses are listed in Table 7.2 or a detailed hydrochemical log is shown in Fig.7.2. The recent brackish upconing near well 19A.22 has been ignored in constructing the generalized quality evolution downgradient.
To the right: location map.

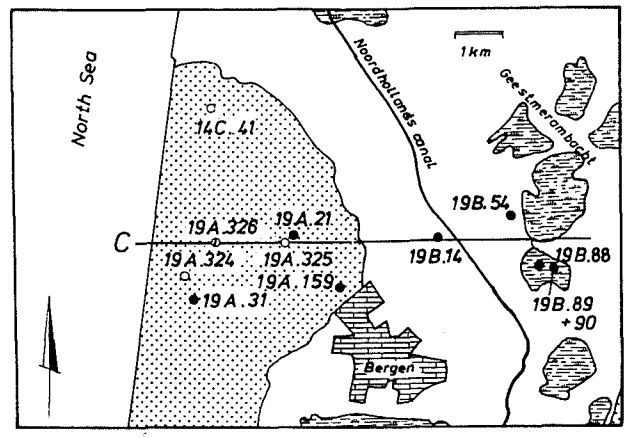

The acquisition and screening of hydrochemical data was elucidated in general terms in section 4.2. This applies to about 300 complete analyses in a 2 km broad band along the section shown in Fig.7.1. In February 1990 and November 1991 a selection of observation wells was sampled again for closer examination, including the quantitative analysis of :
· about 20 trace elements by KIWA with AAS - graphite furnace, using an element specific receipt of matrix modifiers, background correction by deuterium and/or Zeeman, and reduction in order to convert all redox dependent species into a single reduced one (Van der Jagt & Stuyfzand, 1991);
· methane by KIWA, using (a) a special sampling pipette, that can be closed at the depth of the well screen and maintains the original pressure (Hettinga, 1988), (b) head space technique and (c) gas chromatographic analysis;
· nonvolatile AOCl (see section 4.2.3) by KIWA using adsorption-microcoulometry;
· 16 PAHs by PWN, using HPLC (high-pressure liquid chromatography) with fluorescence and UV detection after extraction with dichloromethane; and
· 13 chlorinated aliphatics by PWN, using GC (gas chromatography) with ECD (electron capture detection) after extraction with pentane.

7.3.2 Heterogeneities in the upper 30 metres.

Hydrochemical logs representative of the upper 10-30 metres of the main recharge area in decalcified dunes northwest of Bergen, are shown in Fig.7.2. The chosen multilevel wells equipped with mini-screens (14C.41, 19A.324, 19A.325 and 19A.326), are situated on the plots S (scanty vegetation), P_4 (pines 800 m from the HWL), P_5 (ditto 3000 m from the HWL) and H (heather), respectively. These plots were discussed in detail in chapter 6.

The logs are based on a sampling without filtration in October 1987, and on a second survey, including 0.45 µm filtration on site, in November 1991. Where the latter sampling yielded more reliable results (section 6.2), those data were used. The results confirm the image created in sections 6.6 and 6.7, of an extreme variability of the composition of dune groundwater both in space and time. The overall difference between the four logs can be attributed to the diverging vegetation and distance to the HWL, the effects of which were discussed in section 6.6.3 and 6.6.2, respectively.

Changes with depth are associated on each location with variations in recharge, spatial heterogeneities above the groundwater table and geochemical heterogeneities :
Variations in recharge include temporal changes in: (1) the precipitation excess (Figs. 3.13 and 3.14) leading to more or less dilution of dry deposited aerosols and gases; (2) evapotranspiration losses, which cause a highly variable concentration increase for the remaining solute (Fig.6.40); and (3) the amount and composition of atmospheric deposition (Figs. 5.5 and 5.8). The Cl^- peaks in 19A.324 and 19A.326 at resp. 2-3.5 and 4-9.5 m-MSL are probably associated with the period 1970-1978, which is characterized by stormy years and a high evapotranspiration (Fig.6.40). The hydrological boundary conditions on both sites (Table 6.1), a porosity of 0.38 and the assumption of vertical flow, would yield raised Cl^- concentrations at these depths around the year of sampling (1987) indeed.
A horizontal flow component causes heterogeneities in vegetation, thickness of the unsaturated zone or distance to the windward edge of the vegetation unit to become hydrochemically manifest in a vertical direction (section 6.6). And a relatively thick organic upper soil horizon around well 19A.326, seems responsible for complete denitrification, retention of many trace elements and, either directly or indirectly, the supply of As. Intercalated thin dune peat bands on the sites 14C.41 and 19A.324 have minor hydrochemical effects, probably by old age. The rather high Ca^{2+} and HCO_3^- concentrations at relatively shallow depth for 19A.324 (below 2 m-MSL) and 19A.326 (4-10 m-MSL) may be related to lateral flow and the passage of strata not yet completely decalcified.

Notwithstanding large differences there are enough similarities, which justify the derivation of a generalized evolution pattern in section 7.3.4. But first, heterogeneities further downgradient in the (semi)confined aquifers are considered.

7.3.3 Heterogeneities further downgradient

The scale of hydrochemical heterogeneities generally increases further downgradient, for 2 main reasons: (1) variations that arise in the upper zone, are smoothed by hydrodynamic dispersion and physico-chemical processes; and (2) the tendency of the groundwater to react with various deposits is strongly reduced, due to the high acid and redox buffer capacity, which it acquired in the Holocene deposits above.

For the cross section shown in Fig.7.1 the areal distribution of hydrosomes and their facies is presented in Enclosure 5.1, the distribution of chemical water types in Enclosure 6.1, and the concentration patterns of Ca^{2+} and NH_4^+ in Fig.7.3. Heterogeneities obviously continue below 20 m-MSL in the Pleistocene deposits. They are connected mainly with the occurrence of aquitards and isolated clay lenses, which delay the process of freshening and yield among others NH_4^+ by decomposition of organic matter. The flow path chosen, was hardly affected by these lithological anomalies, but did suffer from a local brackish upconing in well 19A.22 at about 90 m-MSL. Well 19A.159 in the vicinity was therefore selected to circumvent this interruption of the normal evolution.

7.3.4 The generalized evolution over 7 km

The generalized changes in concentration downgradient are depicted for all major ions, about 15 trace elements, pH and AOCl in Fig.7.4. The chemical water type and hydrochemical facies (with associations conform section 4.3.1) are shown as well. The position of aquitard 1C', the top of which approximately coincides with the decalcification boundary, is indicated.

Results of chemical analysis are listed in Table 7.2, for 16 well distributed samples along the flow path. Also the saturation index SI, as defined in Eq.2.13 and calculated using WATEQX (Van Gaans, 1989), is given for potentially relevant minerals. Chemical mass balances along the flow path are presented in section 8.5.

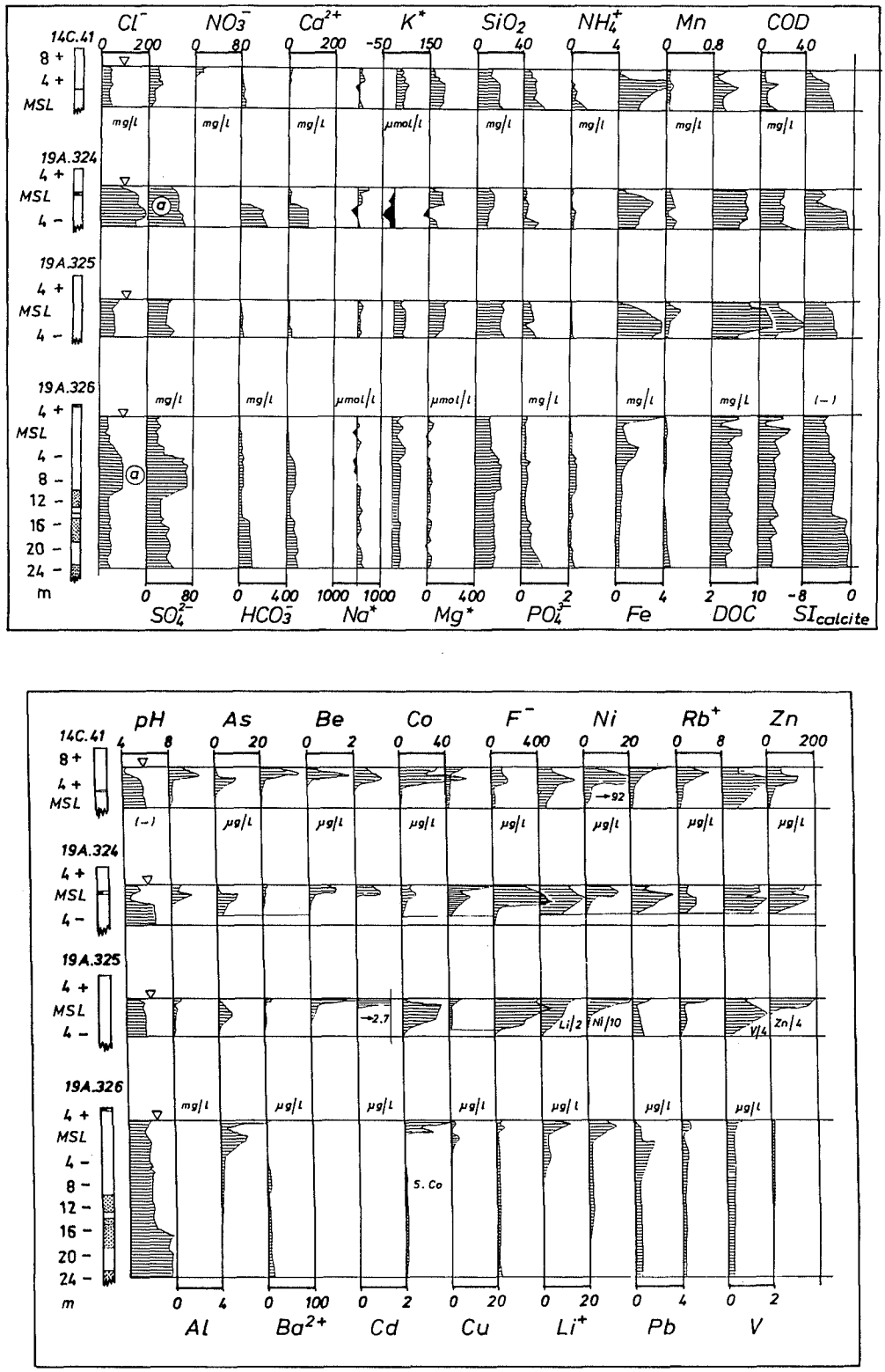

FIG. 7.2 Hydrochemical log of four shallow, multilevel wells equipped with miniscreens, in decalcified dunes northwest of Bergen, in October 1987 - November 1991. The peak marked "a" in the Cl⁻ logs, corresponds with the exceptional recharge period 1970-1978 with a high sea spray deposition and high evapotranspiration. Well 14C.41 is situated on plot scanty (S), 19A.324 on pines-4, 19A.325 on pines-5 and 19A.326 on heather (H). The legend to the lithological log is given in Enclosure 9. X^* = X corrected for a sea spray contribution.

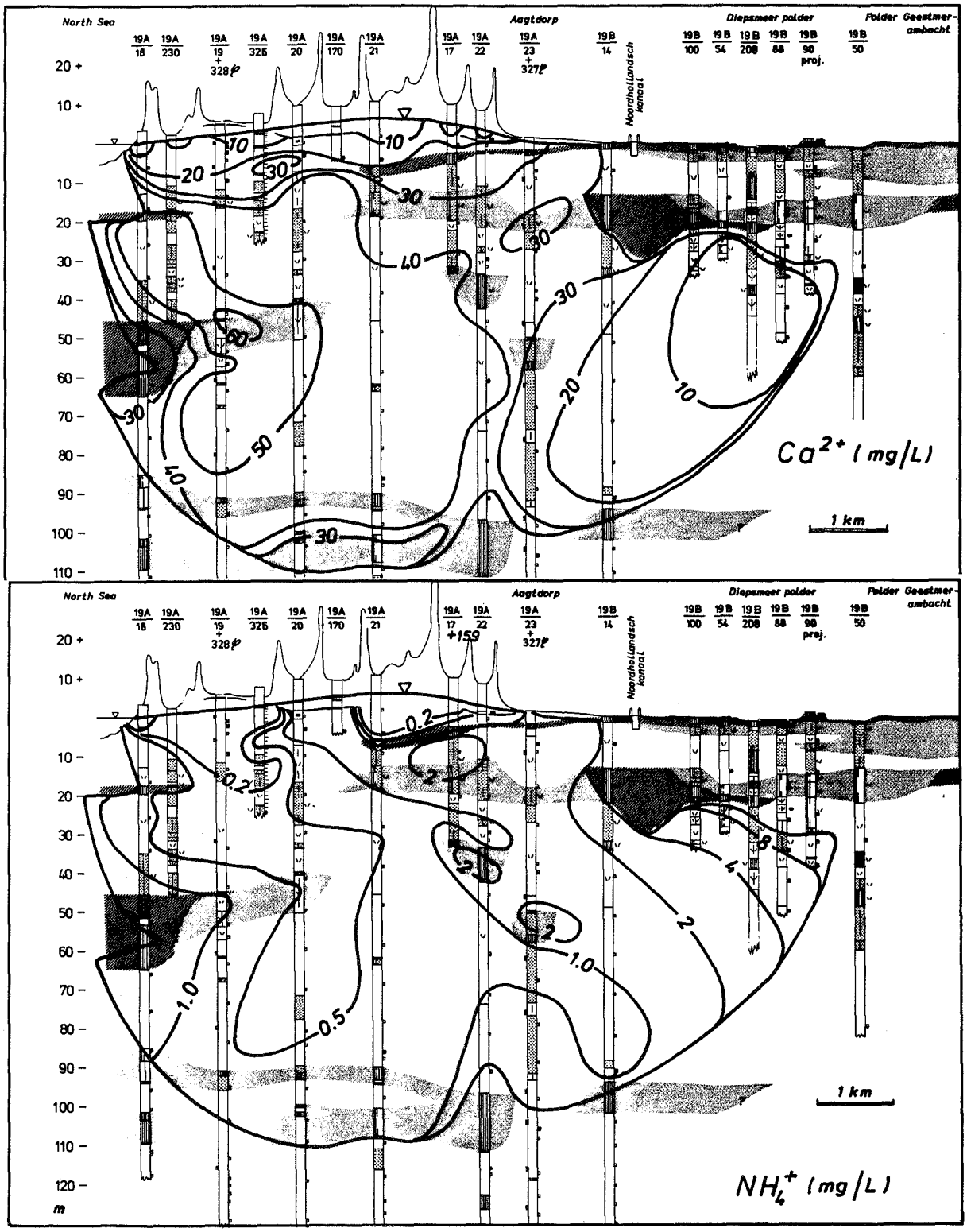

FIG. 7.3 Cross section C over decalcified dunes near Bergen, showing the areal distribution of Ca^{2+} and NH_4^+ concentrations in fresh dune groundwater, for the period 1977-1991. The patterns are related to : (1) the lithology (Ca^{2+} increases below the depth of decalcification at 10 m-MSL, and NH_4^+ increases in clay and peat layers); (2) cation exchange due to freshening (Ca^{2+} decreases in Eemian clay in the west, at the base of the fresh water lens and in its eastern parts); and (3) desorption of NH_4^+ after displacement of relict Holocene transgression water with extreme NH_4^+ levels, in the eastern parts.

The first 30 metres of flow are directed predominantly downwards in the Holocene, Westland Formation, the subsequent 170 metres still contain a significant downward component, and beyond 200 metres flow attains a (sub)horizontal direction (Fig.7.1). The (sub)horizontal flow velocity (in the pores) approximates 1 km/century since the reclamation of the Geestmerambacht lakes in 1550 AD. Downgradient, the following 10 zones (indicated in Fig.7.4), are discerned :

I. The acidified vadose zone (0-2 m.)

From the differences in composition of 50% evaporated bulk precipitation and the upper groundwater (Fig.7.4), a significant, progressive mobilization can be deduced for Al, SiO_2, Be, Co, Li^+, Ni, Rb^+ and Zn. Also Edmunds et al. (1992) noticed a strong mobilization of trace cations (Al, Ba, Be, Cu, Fe, Mn, Ni and Zn) in the vadose zone of sandy aquifer materials, in the UK. Various Al-silicates (notably albite, illite, hornblende, biotite), gibbsite and atmospheric dust particles rich in trace elements, likely dissolve in soil moisture (see also section 6.6.4), which has a pH as low as 3-4 according to Rozema et al. (1985). The negative SIs for silicates and gibbsite (Table 7.2) confirm their dissolution, whereas the very negative SIs for the much faster reacting carbonates correspond with their observed absence. Various sources of the trace elements were discussed in sections 6.4.1 and 6.6.4. The nitrification of ammonium, oxidation of deposited NO_x and SO_2, the low pH of precipitation itself, evapotranspiration and organic acids introduced in the upper soil, contribute to the observed low pH values in soil moisture.

Organic Carbon dissolves in the upper soil horizons by exudation and decomposition of organic matter. Below 1 m the DOC is probably composed mainly of humic and fulvic acids, and is adsorbed and broken down upon further soil passage (Fig.6.30). The behaviour of Fe and Mn probably resembles that of DOC, to which they are strongly complexed. Whether also Al, SiO_2 and various TEs initially follow the DOC pattern, is unknown and has been ignored in Fig.7.4. An initial mobilization and subsequent uptake is assumed for the nutrients PO_4^{3-}, NH_4^+, NO_3^-, K^+ and Mn in analogy with results presented in section 6.5.2.

Cu, Pb and probably SO_4^{2-} are progressively retained. Cu and Pb derive mainly from atmospheric pollution (section 6.6.4), but the mobility of Cu is clearly superior to that of Pb. This corresponds with the stronger adsorption of Pb to ferric hydroxides and clay minerals (Benjamin & Leckie, 1982; Harmsen, 1977) and the stronger complexation of Cu to organic acids at low pH (Schnitzer & Hansen, 1970). Sulphate retention may be important and is corroborated by positive SIs for aluminium hydroxisulphate minerals like alunite (Table 7.2).

II. The acidified upper groundwater zone (2-5 m.)

Most patterns and processes discussed above, continue in this completely decalcified zone with pH in between 4 and 5.5 (Fig.7.4). However, Al attains its peak at 3 m below ground level, after which it decreases in analogy with the increasing pH and SI for gibbsite.

The decrease in Al and H^+ concentration is explained by a combination of : (1) cation exchange for Ca^{2+} and Mg^{2+} (Eq.8.22 to the right), (2) dissolution of silicate minerals (Eqs.8.19, 8.25-8.27), (3) denitrification (Eq.8.12A) and (4) reduction of ferric hydroxides (Eq.8.14). The removal of 0.195 meq Al^{3+}/l and 0.04 meq H^+/l from 5.5 to 4.5 m+MSL in piezometer 14C.041 (Table 7.2), is indeed neatly balanced by the production of 0.085 meq $\{Na^* + K^* + Ca^* + Mg^*\}$/l and 0.079 meq Fe^{2+}/l, and the conversion of 0.19 meq NO_3^-/l into 0.11 meq HCO_3^-/l (which means a conversion of 0.19 - 0.11 = 0.08 meq HCO_3^- into H_2CO_3). The concomitant increase in TEs is negligible (about 0.01 meq/l). This calculation indicates the importance of anoxic redox reactions in acid buffering (here 63%). It should be noted that in this example 0.029 meq Na^+/l were lost due to exchange in connection with the variability of sea spray deposition (see section 6.7.4), and that the dissolution of silicate minerals has been accounted for by simply collecting its effects in the term $\{Na^* + K^* + Ca^* + Mg^*\}$.

The trace elements (TEs) Ba^{2+}, Be, Cd, Co, Cr, Li^+, Ni, Rb^+, V and Zn attain their absolute maximum concentrations in between 3 and 5 metres, where Al concentrations are sharply decreasing with depth. This behaviour is explained in a similar way as Drever (1982) described the genesis of uranium roll-deposits in terms of an advancing oxidation front. Here, an acid front is advancing and the TEs, that were concentrated in weathering residues after millennia of leaching, are now dissolved. Vadose and groundwater carry them through the front into an environment with higher pH (about 6) and a higher redox level (anoxic, sulphate-stable), where they (co)precipitate or become adsorbed. The zone of accumulation is, however, slowly pushed down by the advancing front and the highest concentrations in the water phase are observed where the enriched zone of accumulation is dissolved.

The exact mechanism of immobilization is unknown. The most probable one is the adsorption to $Fe(OH)_3$ and $Al(OH)_3$ when the pH is sufficiently above the zero point of charge (zpc) : for α-$Al(OH)_3$ pH_{zpc} = 5.0 (Stumm & Morgan, 1981); for ferrihydrite containing >3% Si, pH_{zpc} is below 6.3 (Schwertmann & Fechter, 1982); and various Al- and Fe(III)-oxides with Si/(Si+Al) >40%, exhibit a pH_{zpc} below 6.3 (Parks, 1967). But also the removal of ferric hydroxide coatings may increase the sorptive capacity of the porous medium for TEs,

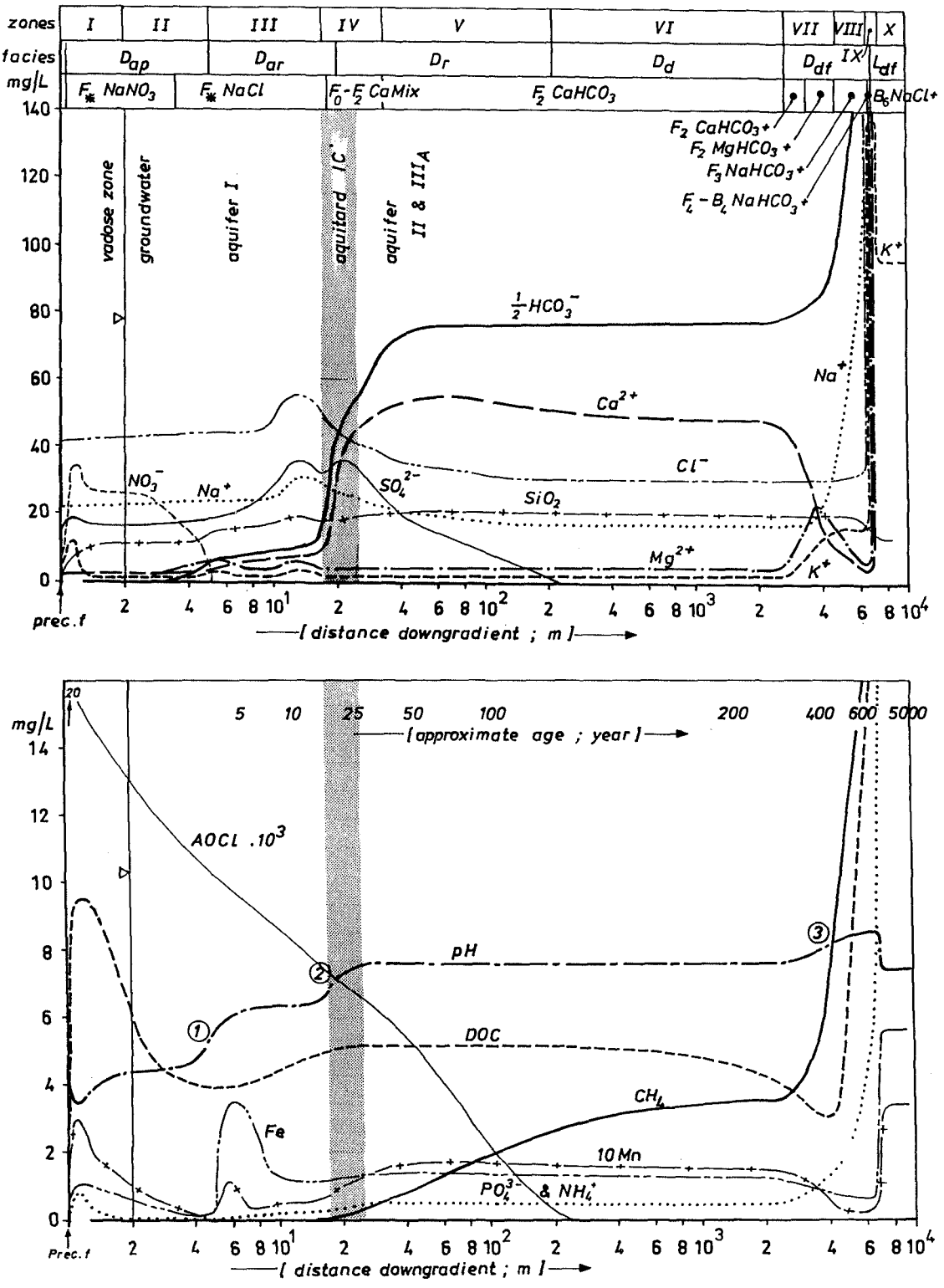

FIG. 7.4 Generalized chemical evolution of dune water along a flow path from the surface in decalcified dunes northwest of Bergen, towards its intrusion front in the Geestmerambacht Polder, in the period 1987-1991 : Main constituents, AOCl (= halogenated hydrocarbons adsorbable to activated carbon), HYFA (for codes see Enclosure 8) and zones I-X (discussed in text). The evolution lines closely follow the data in Table 7.2. The changes of 50% evaporated bulk precipitation (prec·f) in the vadose zone were extrapolated from observations on monitoring plot oaks-2 (Table 6.9). 1 = acidification front; 2 = decalcification front; 3 = base exchange front. Continued on next page.

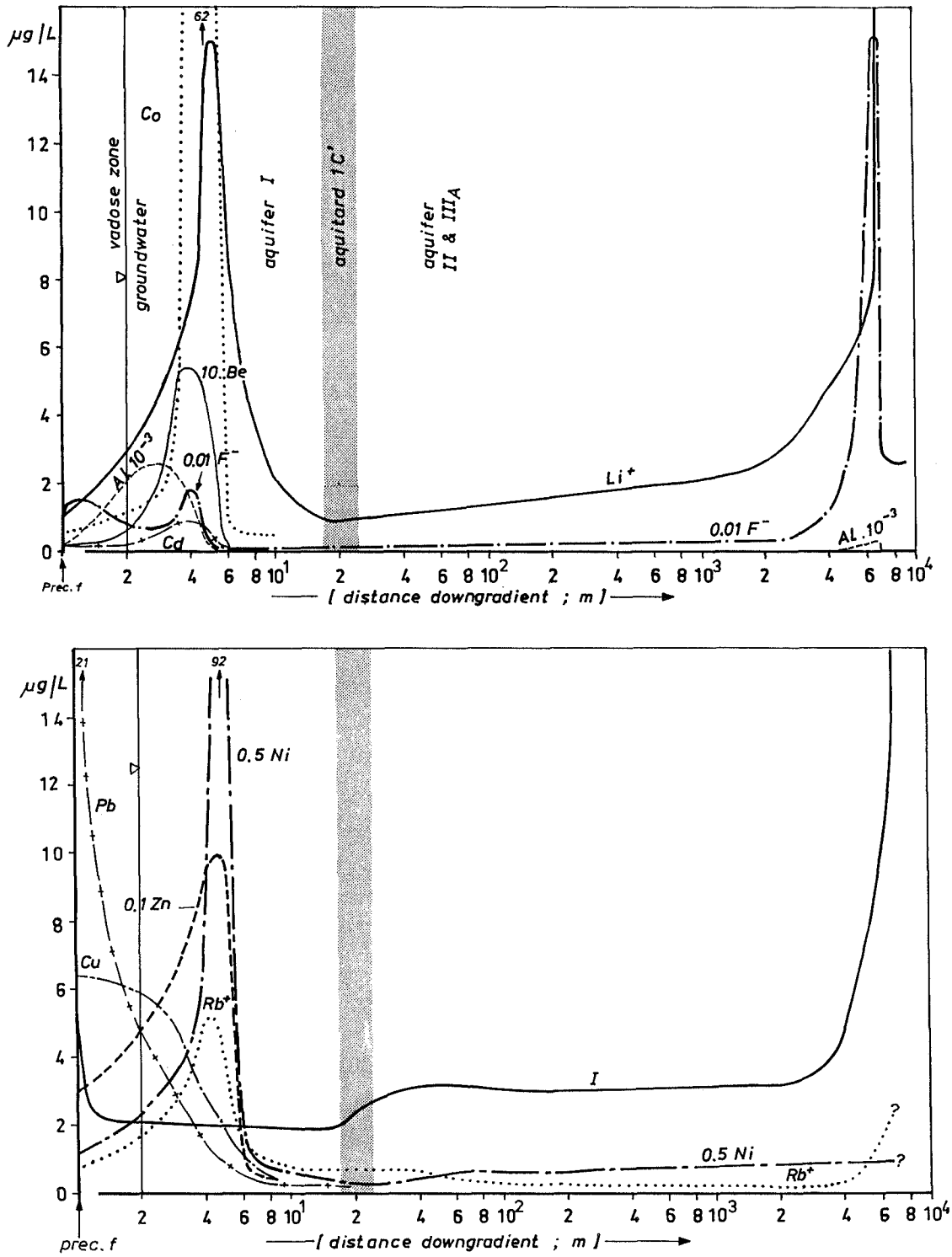

FIG. 7.4 Continued. Generalized chemical evolution of dune water along a flow path from the surface in decalcified dunes northwest of Bergen, towards its intrusion front in the Geestmerambacht Polder, in the period 1987-1991 : Trace elements. prec·f = 50% evaporated bulk precipitation.

TABLE 7.2 Major and trace components of precipitation, dune water downgradient and the expelled, relict Holocene transgression water, in the period 1987-1991. The selected wells, along a 8 km long flow path from decalcified dunes northwest of Bergen towards the Geestmerambacht Polder, are indicated in Fig.7.1. Not shown are concentrations of NO_2^- (<50), Hg (<0.2), Mo (<0.5), Sb (<0.5), Se (<1), Sn (<0.5) and Te (<0.5), all in µg/l. Prec. = bulk precipitation.

piezo-meter no.	sample depth m+MSL	subsoil flow m	subsoil age§ y	temp 20°C C	EC µS/cm	pH	Cl^- mg/l	SO_4^{2-} mg/l	HCO_3^- mg/l	NO_3^- mg/l	PO_4T mg/l	Na^+ mg/l	K^+ mg/l	Ca^{2+} mg/l	Mg^{2+} mg/l	Fe mg/l	Mn mg/l	NH_4^+ mg/l	SiO_2 mg/l	DOC mg/l	COD mg/l	O_2 mg/l	CH_4 mg/l	watertype	code
Prec. 1987	8	0	0	10	65	4.5	16	7	0	3.4	0.04	9	0.4	1	1.1	0.10	0.02	1.29	0.2	1.5	5.2	11.0	<0.05	F_sNaCl	-
14C.041	6.5	3_v	1	10	140	4.3	19	16	0	22.6	0.04	15	1.1	2	1.6	0.29	0.05	0.05	11.2	4.4	17.4	2.0	<0.05	F_sNaNO_3	D_{ap}
14C.041	5.5	4_v	2	10	161	4.4	31	18	0	12.0	0.24	19	1.8	2	3.0	0.12	0.03	0.05	10.6	2.3	3.0	1.0	<0.05	F_sNaCl	D_{ap}
14C.041	4.5	5_v	3	10	157	5.5	34	19	7	0.1	0.46	20	2.1	3	3.9	2.33	0.06	0.08	15.4	3.9	5.3	<0.2	<0.01	F_sNaCl	D_{apr}
14C.041	3.5	6_v	5	10	180	5.7	41	20	13	<0.1	0.43	21	2.8	5	5.4	3.43	0.13	0.19	18.6	5.8	7.3	<0.2	-	F_sNaCl	D_{ar}
19A.326	-12.5	18	16	10	209	6.2	41	24	23	<0.1	0.15	24	1.8	13	2.7	0.70	0.03	0.23	15.1	5.1	13.9	<0.2	-	F_sNaCl	D_{ar}
19A.326	-17.5	21_v	20	10	332	7.4	44	36	92	<0.2	0.34	29	1.9	38	2.8	0.30	0.09	0.24	15.6	5.8	16.8	<0.2	0.14	F_1CaMix	D_r
19A.326	-23.5	29	30	10.0	388	7.6	50	35	121	<0.2	0.36	31	2.0	47	3.3	0.40	0.13	0.34	13.3	4.8	11.9	<0.2	-	F_1CaMix	D_r
19A.031	-30	35	40	10.1	390	7.7	45	22	146	>0.5	0.43	29	2.0	51	3.4	0.51	0.13	0.44	20.0	6.9	-	<0.2		F_2CaHCO_3	D_r
19A.021	-87	1000	100	10.2	300	7.7	33	0	151	<0.1	0.43	15	1.4	48	3.1	3.40	0.18	0.68	16.0	4.7	-	<0.2	-	F_2CaHCO_3	D_d
19A.159	-93	2500	250	10.5	303	7.6	29	0	156	<0.2	0.43	15	1.2	48	2.5	1.22	0.13	0.45	17.6	4.7	16.6	<0.2	5.0	F_2CaHCO_3	D_d
19B.014	-92	4000	350	10.7	323	8.1	33	0	169	<0.5	0.83	24	9.5	13	21	0.69	0.04	0.83	22.9	2.9	11.5	<0.2	9.1	F_2MgHCO_3+	D_{df}
19B.088	-44	6500	600	10.8	696	8.5	35	0	398@	<0.5	10.56	155	11.5	3	3.1	0.62	0.04	6.19	17.4	20.0	84.9	<0.2	18.2	F_3NaHCO_3+	D_{df}
19B.054	-25	6500	600	10.7	879	8.2	60	0	525	<0.5	9.18	190	16.8	9	9.5	0.17	0.12	8.26	45.0	34.0	132	<0.2	-	F_4NaHCO_3+	D_{df}
19B.088	-20	6550	625	10.8	2040	7.7	390	9	801	<0.2	20.9	445	58	27	19.9	1.6	0.12	20.0	83.2	-	470	<0.2		B_4NaHCO_3+	D_{df}
19B.089	-19	6600	650	10.8	4730	8.5	1320	15	903	<0.2	21.2	910	134	66	71	5.4	0.30	49.0	71.6	-	130	<0.2		B_4NaCl+	$D+L_{df}$
19B.090	-15	?	6000_L	11.0	14950	7.8	5285	4	2635	<0.2	60	3380	95	160	390	2.3	0.03	49.0	71.6	40	160	<0.2	-	B_6NaCl+	L_{df}

piezo-meter no	sample depth m+MSL	Al µg/l	As µg/l	B µg/l	Ba^{2+} µg/l	Be µg/l	Br^- µg/l	Cd µg/l	Co µg/l	Cr µg/l	Cu µg/l	F^- µg/l	I^- µg/l	Li^+ µg/l	Ni µg/l	Pb µg/l	Rb^+ µg/l	Sr^{2+} µg/l	V µg/l	Zn µg/l	AOCl µg/l	$\delta^{13}C$ ‰	$\delta^{18}O$ ‰	redox index	polin
Prec. 1987	8	99	0.8	<5	3	<0.02	56	0.11	0.3	0.7	3.2	27	4	0.6	0.6	10.4	0.4	7	2	15	10	-8	-7.8	0	2.5
14C.041	6.5	2600	<1	<50	44	0.26	-	0.6	1.2	<1	4.0	80	1.9	5	7	2.7	2.8	<100	1	60	-	-	-	1	3.2
14C.041	5.5	1900	<1	<50	54	0.54	-	0.8	30	<1	2.2	70	<1	6	17	1.5	4.0	<100	3	59	-			1	3.0
14C.041	4.5	150	8	<50	10	0.41	110	<0.1	62	1	1.6	120	1.9	15	92	0.9	3.4	<50	<1	100	10			2	2.5
14C.041	3.5	68	6	<50	<10	<0.05	-	0.2	<1	2	1.8	≤10	2	9	4	0.5	1.8	60	<1	26	-	-	-	4	1.9
19A.326	-12.5	45	1	<100	<10	<0.05	-	<0.1	<1	<1	<1	≤10	0.6	1	<0.5	≤1	0.5	100	<1	7		-22.2	-7.2	4	1.2
19A.326	-17.5	60	1	<100	<10	<0.05	160	<0.1	<1	<1	<1	≤10	3	1	<0.5	≤1	0.6	160	<1	7	-	-	-	4	1.3
19A.326	-23.5	<50	1	<100	11	<0.05	-	<0.1	<1	<1	<1	≤10	0.6	1	<0.5	≤1	0.8	170	<1	7			-	4	1.4
19A.031#	-30	4	1	<100	10	<0.05	-	<0.1	<0.5	<0.5	<0.5	10	3	2	<1	<0.5	<1	170	<0.5	<5			-7.3	5	0.7
19A.021#	-87	5	1	<100	10	<0.05	-	<0.1	<0.5	0.2	<0.5	10	3	2	<1	<0.5	<1	180	<0.5	<5	-	-	-	6	0.2
19A.159	-93	9	1	<100	21	0.06	90	<0.1	<1	<0.5	-	30	1.5	3	≤1	≤1	<0.3	190	<0.5	15	<4	-8.82#	-6.6#	6	0.5
19B.014	-92	17	1	-	31	<0.05	120	<0.1	<1	0.2	<5	100	4.9	5	≤1	≤1	<0.3	160	<0.5	5	<4	-	-	6	0.4
19B.088	-44	240	1	<100	<5	0.10	120	<0.1	<1	6.9?	<5	1500	-	6	≤1	≤1	2.2	<50	15?	3	<4			6	0.7
19B.054	-25	31		1400	<5	0.12	260	≤0.1	<1	7.1?	<5	1100	13	11	≤1	≤1	0.7	140	14?	3	6			6	0.6
19B.088	-20	-		-	-	-	-	-	-	-	-	-	-	-	-	-	-	-	-		-			6	0.3
19B.089	-19																							6	0.3
19B.090	-15	-	-	-	-	-	-	-	-	-	-	-	-	-	-	-	-	-	-	-	-	-	-	6	0.3

piezo-meter no.	sample depth m+MSL	sea salt corrected (µmol/l) Na^*	K^*	Ca^*	Mg^*	SO_4^*	BEX meq/l ##	SATURATION INDEX log(IAP/K_s)† Hydroxides & sulphates gibbsite	alunite	barite	Silicates SiO_2-am	albite	chlorite	illite	kaol	K-mica	Carbonates calcite	dolom	sider	rhodo	Phosphates & fluorides apatO	apatF	vivian	fluo
Prec 1987	8	4	2	16	1	50	<0.1	-1.98	-4.54	-1.7	-2.60	-13.4	-50.9	-15.1	-6.2	-16.3	-6.8	-13.4	-11.6	-6.7	-30.7	-27.5	-32.6	-7.7
14C.041	6.5	193	18	40	14	139	0.2	-1.02	0.01	-0.2	-0.82	-7.2	-45.1	-6.7	-0.79	-8.0	-6.6	-13.1	-10.3	-6.4	-30.7	-28.4	-29.3	-9.6
14C.041	5.5	76	30	33	38	142	0.2	-0.88	0.43	-0.1	-0.84	-6.9	-42.5	-6.2	-0.56	-7.3	-6.6	-12.9	-10.6	-6.6	-27.7	-25.4	-28.0	-9.4
14C.041	4.5	47	36	57	67	148	0.2	0.03	-0.00	-0.8	-0.68	-4.4	-28.6	-2.2	1.59	-2.9	-4.8	-9.6	-3.1	-4.7	-18.4	-14.8	-5.6	-4.6
14C.041	3.5	-79	50	103	110	148	0.2	0.40	0.66	-1.1	-0.60	-3.5	-25.0	-0.8	2.5	-1.2	-4.1	-8.1	-2.5	-3.9	-16.0	-13.6	-4.4	-6.1
19A.326	-12.5	52	24	303	-2	190	0.1	0.81	0.34	-1.0	-0.69	-2.8	-21.0	0.2	3.1	0.05	-2.9	-6.5	-2.1	-3.8	-11.9	-9.7	-4.4	-5.1
19A.326	-17.5	196	25	925	-6	311	0.2	1.75	-0.16	-0.9	-0.68	-0.58	-7.1	3.8	5.1	4.1	-0.71	-2.5	-0.27	-1.6	-1.8	-0.66	0.14	-4.6
19A.326	-23.5	138	22	1221	-2	291	0.2	1.63	-1.2	-0.6	-0.76	-0.70	-5.0	3.5	4.7	3.8	-0.29	-1.6	-0.24	-1.1	-0.18	0.67	-0.19	-4.6
19A.031	-30	172	27	1249	16	163	0.2	0.42	-5.5	-0.8	-0.57	-1.29	-6.1	1.4	2.6	0.78	-0.08	-1.3	-0.29	-0.90	0.54	1.3	-0.5	-4.5
19A.021	-87	-146	18	1180	37	-48	-0.1	0.52	<-6.0	-30.0	-0.67	-1.77	-6.3	1.2	2.6	0.62	-0.08	-1.26	0.57	-0.72	0.43	1.2	2.0	-4.5
19A.159	-93	-49	15	1182	23	-42	0.0	0.83	-60.9	-28.9	-0.63	-1.44	-6.9	1.9	3.3	1.5	-0.15	-1.5	0.05	-0.94	0.09	1.4	0.47	-3.6
19B.014	-92	245	226	307	773	-48	2.0	0.67	-62.0	-28.8	-0.52	-0.56	2.8	3.3	3.2	2.8	-0.20	-0.09	0.33	-0.93	0.24	1.6	1.4	-3.1
19B.088	-44	5895	276	56	31	-51	6.2	1.42	-60.9	-29.8	-0.64	1.01	3.4	4.8	4.5	5.1	-0.12	-0.13	0.96	-0.19	2.0	4.1	4.1	-1.5
19B.054	-25	6812	398	193	226	-87	7.7	0.83	-63.7	-30.9	-0.23	1.46	2.8	4.8	4.1	4.4	0.14	0.39	0.19	0.04	2.7	5.0	1.6	-1.3
19B.088	-20	9917	1278	467	-253	-475	10.7	-	-	-	0.04	-	-	-	-	-	0.21	0.37	0.73	-0.38	3.4	-	3.6	-
19B.089	-19	7633	2731	947	-705	-1769	9.0				-0.02						1.3	2.7	2.0	0.72	7.5		6.2	
19B.090	-15	19103	-358	1189	1527	-7665	21.8	-	-	-	0.00	-	-	-	-	-	1.3	3.0	1.1	-0.80	6.5	-	3.5	-

= extrapolated; ## : BEX = $Na^* + K^* + 2Mg^*$; @ = not included CO_3 = 17 mg/l; v = vertical distance; § = calculated; † = calculated using WATEQX (Van Gaans, 1989);

as this removal results in a lowering of the pH of zero point of charge. Besides, Cr and V may change at the redox boundary from oxy-anions into cations and then become adsorbed.

The position of the concentration peaks and the top of the immobilization zone are slightly different for the TEs considered (Fig.7.4). This is also to be expected for elements with contrasting electronegativities, ionic radii and hydration tendency. The position of the peaks is, in order of increasing distance down the hydraulic gradient, and concomitantly increasing pH : Pb < Cu < Al < {Be ≅ Rb ≅ Zn ≅ Cd} < {Co ≅ Ni} < Li. This sequence approximates the sequence of the retention against pH curves for Pb, Cu, Zn, Ni, Cd and Co, with freshly precipitated Fe and Al gels (Kinniburgh et al., 1976) or oxides of manganese and iron as adsorbents (McKenzie, 1980). The field data of Pb and Cu are consistent with the low pH (3-5) at which they adsorb to hydrous Fe oxide gels (Kinniburgh et al., 1976) and hematite (McKenzie, 1980). And the field data of Zn, Cd, Ni and Co also correspond with their laboratory experiments, showing a strong adsorption at a pH in between 5 and 6.5, also regarding hydrous Al oxide gel.

In zone II with its clear impact of acid atmospheric deposition superimposed on a natural decalcification, the water type is predominantly F_*NaCl and incidentally F_*NaNO_3, the facies is acid, (sub)oxic, without base exchange and polluted.

III. The naturally decalcified zone (5-17 m.)

The pH typically is about 6.2 and locally (also in Fig.7.4) the top coincides with the redoxcline (boundary between the (sub)oxic and anoxic facies). The upper metre of this zone includes the lower part of the mobilization zone for TEs discussed above.

Coinciding peaks were observed here in 1987 for all major constituents (well 19A.326 in Fig.7.2), and are partly attributed to the exceptional recharge period 1970-1978 (section 7.3.2), which is characterized by high evapotranspiration rates, stormy years and a high atmospheric SO_x input. Comparison with groundwater of the same period in other wells (Fig.7.8) leads to the conclusion that also a local anomaly in vegetation cover (taller and denser) and perhaps lime content (higher) adds to the chemical anomaly, so that the patterns in well 19A.326 were strongly temperated in the generalized trends depicted in Fig.7.4.

Apart from this anomaly, a minor increase is observed with depth for pH, HCO_3^-, PO_4, NH_4^+ and DOC (Fig.7.4). This corresponds with the decomposition of organic material in an anoxic environment, probably through sulphate reduction, the size of which is so small that it cannot be deduced from the SO_4^{2-} data. The decrease in Fe concentration in between 6 and 9 m can be related to this sulphate reduction and the formation of $FeS_{(2)}$. The whole decrease (about 2.5 mg Fe^{2+}/l), consumes only 4.3 mg SO_4^{2-}/l (Eq.8.15), an amount that is easily overshadowed by changes in the atmospheric input record and changes in evapotranspiration. The Fe peak also coincides with a notable As peak (Table 7.2). The As derives from the $Fe(OH)_3$ dissolved, to which it was adsorbed, and may coprecipitate with $FeS_{(2)}$.

Apart from the above mentioned anomaly, Ca^{2+} increases by about 0.2 mmol/l in this zone. This can be accounted for by : (a) displacement from the adsorption complex by Mg^{2+}, which was mobilized earlier by exchange for Al and H^+ (section 6.4.2); (b) Ca-Fe exchange; and (c) the dissolution of some last calcium carbonate remains in water with a $SI_{calcite}$ below -2. Calcite dissolution cannot be the main cause, however, as the rise of the HCO_3^- concentration is too low (0.16 instead of 0.4 mmol/l) and the formation of other carbonates can be excluded by their negative SIs (Table 7.2).

Again setting aside the anomaly mentioned earlier, no significant changes are observed for SiO_2 and Al. This agrees with the slightly positive SIs for most silicate minerals and other Al-phases (Table 7.2). Li^+ shows a significant decrease (Fig.7.4), which is explained in terms of its breakthrough in zone III, from the zone above where TEs are mobilized. Of the TEs considered lithium is least affected by retardation, due to its relatively low selectivity coefficient in exchange reactions.

The concentration of most TEs (As, Ba^{2+}, Be, Co, Cr, Cu, Mo, Ni, Pb, Sb, Se, Ti, U and Zn) is very low, generally below detection for AAS-graphite furnace without preconcentration, by lack of mobilizing factors, lack of sources and retention of atmospheric supplies in the zones above. The water type changes with depth from F_*NaCl to F_oNaCl, the facies is acid, anoxic (sulphate metastable), without base exchange and nonpolluted.

IV. The $CaCO_3$ dissolution zone (17-30 m.)

The upper 8 metres of this zone coincide with aquitard 1C', which is composed of marine, silty fine sands with visible shell debris. The dissolution of the shell fragments leads to the sharp rise in Ca^{2+}, HCO_3^- and Sr^{2+} concentrations (conform Eq.8.30A/B in Table 8.3), and near-equilibrium is reached, in well 19A.326, after about 3-5 metres ($SI_{calcite}$ > -1.0). This relatively slow equilibration with calcite as compared to the unsaturated zone in calcareous dunes (within 1 meter; section 6.8.4), may be explained by the overall lower lime content, a more isolated position of the shell fragments and the dissolution in a system closed to CO_2.

Equilibration of sample 19A.326-12.5 (Table 7.2), which represents groundwater just before entrance into the $CaCO_3$ dissolution zone, with

calcite in a closed system would add about 0.6 mmol Ca^{2+}/l and 1.2 mmol HCO_3^-/l to its composition. This leaves 0.3 and 0.4 mmol/l, respectively, unexplained for sample 19A.326-23.5 (Table 7.2), forming the ultimate composition attained in this zone. About 0.3 mmol/l of an additional strong acid is required to acquire a practically square balance for both ions. The oxidation of 0.15 mmol FeS according to Eq.8.17B would suffice. This requires a critical drawdown of the groundwater table about 30 years before sampling in 1987. Data in Krul (1946) and Stuyfzand (1989a) reveal a gradual drawdown by 1 m in the area from 1880 till the late 1950s, due to afforestation and groundwater abstraction by pumping station Bergen. This may have been sufficient.

For the remainder no significant changes occur. The water type changes downgradient from F_0NaCl. via F_1CaMix. to F_2CaMix., the facies changes from acid to calcareous, and is throughout anoxic (sulphate metastable), without base exchange and nonpolluted.

V. The sulphate reducing zone (30-200 m.)

This zone, with 3-30 mg SO_4^{2-}/l and 0.5-2 mg CH_4/l, is situated largely in marine sandy deposits of Eemian age, rich in shell debris and with intercalations of fine silty sand and some clay. All sulphate is gradually reduced and some methane produced, which leads to significant increases of HCO_3^- and minor increases of Ca^{2+}. The Ca^{2+} rise should approximate the quantity of methane produced (Eq.4.3), but beyond 60 m its increase is probably counteracted by decreasing effects of (a) atmospheric pollution, (b) oxidation of iron sulphides and (c) an increasing vegetation cover, all due to an increasing age.

The SO_4^{2-} levels in this zone doubled in the period 1915 - 1990, which probably relates to the increased atmospheric deposition of SO_x (Fig.5.5) and, in the upper parts, to the oxidation of iron sulphides close to the water table about 40 years ago (see previous zone).

A decrease can be noted for Na^+, Cl^- and AOCl. The pattern for the air-borne sea salts in zone V is connected mainly with developments in vegetation cover, in combination with coastal erosion that reduced the distance to the HWL of the North Sea. The evolution of AOCl probably reflects the atmospheric pollution record, with the superimposed effects of sorption and a reductive dehalogenation in this anoxic environment.

The Li^+ concentration exhibits a slow increase, which may relate to a very slow dissolution of silicate minerals or cation exchange. The other constituents do not notably change. The water type is F_2CaHCO_3, the facies is calcareous, anoxic to deep anoxic, without base exchange and nonpolluted. PAHs, pesticides and chlorinated aliphatics were indeed, all of them, below analytical detection (resp. <3, <10 and <{10-100} ng/l; Stuyfzand, 1989a p.110).

VI. The deep anoxic zone without base exchange (200-2500 m.)

This methanogenic zone, with 2-5 mg CH_4/l and SO_4^{2-} ≤3 mg/l, is found in coarse sandy, continental deposits of Middle Pleistocene age. It is characterized by a very stable groundwater composition of excellent quality. The water type is F_2CaHCO_3. The lack of any sign of pollution is largely connected with an age superior to about 100 years. The maximum age of water at the point of exit from zone VI was calculated at 300 years.

Yet, the base exchange reaction due to fresh dune water intrusion was already completed downgradient of this zone, notwithstanding the relatively low displacing power of its low-hardness dune groundwater (Σcations = 3.5 meq/l; sample 19A.159 in Table 7.2). Simplifying the exchange process into the displacement of all sorbed ions (mean CEC estimated at 6 meq/kg; Table 7.1), would result in a retardation factor for complete Ca^{2+} breakthrough in a system with piston flow, of 9.3 (see Eqs.7.5-7.6). This means that the system up to this point must have been flushed with fresh dune water for about 2800 years (300*9.3). This corresponds reasonably well with the formation and accretion of the Bergen beach barrier in the period 4850-3000 BP (De Mulder & Bosch, 1982), and a time of formation of the fresh water lens being 300-600 y.

VII. The inner freshened zone (2500-4000 m)

In about the same deposits as upgradient, quite stable Na^+ and Cl^- concentrations are typically traversed by a sharp increase of Mg^{2+} and K^+, which exchanged for Ca^{2+}. In this ultimate stage of cation exchange lagging behind a remote fresh dune water intrusion front, the easily exchangeable Na^+ has already been depleted from the adsorption complex and the less easily desorbing K^+ and Mg^{2+} follow now. The exchange is accompanied by mild increases for CH_4, HCO_3^-, pH, PO_4, NH_4^+, Al, I, Li^+ and F^-, and a decline in concentrations of Fe and Mn. These changes are further commented upon in the next zone. Concentrations of all chalcophile and siderophile TEs (see Table 1.1) remain low. The water type changes downgradient from F_2CaHCO_3+ to F_2MgHCO_3+, the facies is calcareous, deep anoxic, freshened (positive BEX) and nonpolluted.

VIII. The outer freshened zone (4000-6500 m)

This zone consists of fresh dune water with about 33 ± 3 mg Cl^-/l, and therefore does not contain any

admixed Holocene transgression water. It is situated immediately behind the dune water intrusion front, mainly in the marine Eemian deposits described before. It shows characteristic increases regarding Na^+, HCO_3^-, DOC, CH_4, PO_4, NH_4^+, I, Li^+ and Rb^+, a further decline for Ca^{2+}, Sr^{2+}, Fe and Mn, and a rise in pH and Al. Concentrations of the chalcophile and siderophile TEs remain very low.

The cation exchange

Na^+, Li^+ and Rb^+ are obviously exchanged for Ca^{2+} and Sr^{2+} during this phase of cation exchange, where the monovalent marine cations with the lowest selectivity coefficient desorb first. The Na^+ increase is not simply paralleled by K^+ and Mg^{2+} (Fig.7.4). As a matter of fact, where Na^+ steadily increases, Mg^{2+} is adsorbed as evidenced by its decreasing concentration together with Ca^{2+}. Potassium shows only a minor increase in this zone, which is practically neglible as compared to the Na^+ change. The paradoxal sorption of the sea salt cation Mg^{2+} during the initial stage of freshening, can be easily explained by : (1) its desorption upgradient (exchange for Ca^{2+}) yielding a $MgHCO_3$ water type, (2) lack of sufficient Ca^{2+} to drive Na^+ from the adsorption complex; and (3) passage of $MgHCO_3$+ water through an exchanger loaded with Na^+. Further details on the ion-chromatographic separation of Na^+ and Mg^{2+} in salt water displacement by calcareous fresh water, are given by Appelo (1990) and Beekman (1991).

The Na^+ increase (5.6 meq/l between wells 19B.014-92 and 19B.088-44; Table 7.2) cannot be accounted for by the observed Ca^{2+} and Mg^{2+} decrease alone (together 2.0 meq/l). The most plausible explanantion is an additional Ca^{2+} supply through the dissolution of Eemian shell debris upon methanogenesis (Eq.4.3). This is further corroborated by chemical mass balance calculations in section 8.5. A secundary source of calcite dissolution is formed by the adsorption of Ca^{2+}, whereby the solute becomes undersaturated and part of its now superfluous equilibrium CO_2 is consumed. This explains the observed pH increase, which yields the pH-record (8.5) for groundwater in the whole coastal area. The extreme pH and high DOC in turn, explain the raised mobility of Al, which is probably released by dissolution of gibbsite.

Decomposition of organic material

The quantities of NH_4^+, PO_4, CH_4, DOC and I produced in this zone, partly derive from decomposing organic matter, contained in the silty-clayey intercalations of the sandy Eemian Formation. The so-called Redfield equation for marine plankton ($CH_2O(NH_3)_{0.151}(H_3PO_4)_{0.0094}$), which is generally assumed for organic matter in anoxic marine sediments (Froelich et al., 1979), and its congruent decomposition in a methanogenic environment under equilibrium with calcite, result in the following reaction :

$$2\ CH_2O(NH_3)_{0.151}(H_3PO_4)_{0.0094} + 0.736\ CaCO_3 + H_2O \rightarrow CH_4 + 0.736\ Ca^{2+} + 0.3\ NH_4^+ + 0.0188\ HPO_4^{2-} + 1.736\ HCO_3^- \quad (7.1)$$

The observed HCO_3^- increase (4.3 mmol/l between wells 19B.014-92 and 19B.088-44; Table 7.2) then should yield 0.74 mmol NH_4^+/l and 0.047 mmol PO_4/l. This is about twice too much NH_4^+ and half the PO_4 observed (Fig.7.5).

The discrepancy can be explained in various ways : (1) a different composition of the organic substances, containing less NH_3. Hartmann et al. (1973) suggested $CH_2O(NH_3)_{0.075}(H_3PO_4)_{0.0045}$ as a more probable average composition of organics in anoxic marine sediments; (2) incongruent decomposition, with conservation of organic N-compounds and preferential leaching of PO_4, as deduced for peat deposits (section 6.6.5); (3) the conservation of NH_4^+ by adsorption (Eq.8.34) and additional sources for phosphate (see below); and (4) combinations of 1-3.

The Bergen clay as an indirect source

There are three reasons to assume that the Bergen clay, which confines the upper face of this hydrochemical zone in its eastern and southern parts (Enclosures 1.3 and 4.2), constitutes an important, indirect source of NH_4^+, PO_4 and possibly DOC and I, in addition to the local organic matter in the Eemian Formation :

(a) dune water samples from the Eemian Formation with similar sedimentological characteristics but situated outside the areal distribution area of the Bergen clay, contain considerably less NH_4^+ and PO_4 than those situated below Bergen clay (Fig.7.5);

(2) dune waters that intrude laterally into the area covered by Bergen clay, in coarse grained sandy deposits also exhibit rather extreme NH_4^+ and PO_4 concentrations; and (3) it seems unlikely that the about 90,000 years old, sandy Eemian deposits, although containing finegrained intercalations, would still contain so much reactive organic matter.

The thick, heavy Bergen clay contains a lot of unstabilized organic matter, which is also evidenced by the exceptional composition of connate water in well 19B.109-16 (Table 4.3). Groundwaters under the Bergen aquitard acquired their exceptional composition upon its passage during Holocene transgressions or after the formation of dunes on top of it, upon compaction and through diffusion. And these groundwaters subsequently transferred part of their load to the subsoil, thereby causing a sort of convective, anoxic aquifer fouling.

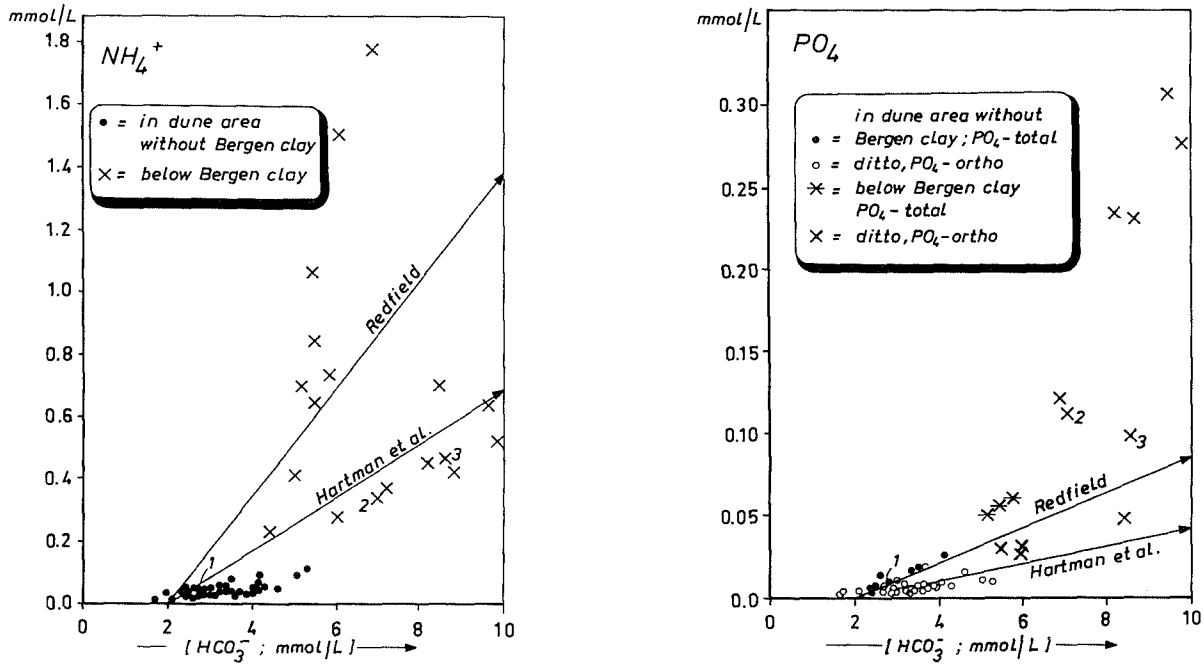

FIG. 7.5 Plot of NH_4^+ and PO_4 concentrations in anoxic Bergen dune groundwater with partial or complete sulphate reduction, versus HCO_3^- as an indicator of the interaction with decomposing organic matter. The samples 1, 2 and 3 correspond with 19B.014-92, 19B.088-44 and 19B.054-25 in Table 7.2, respectively. The arrows indicate the relations under the assumption of congruent decomposition of organic matter as described by either the so-called Redfield equation (Eq.7.1) or the equation of Hartmann et al. (1973; see text).

The retained PO_4, NH_4^+ and possibly DOC and I are now released to the invading dune water.

Phosphate and fluoride mineral phases

The phosphate and fluoride levels are negatively related to the Ca^{2+} concentration (Fig.7.6), which pleads for a contribution of a Ca-PO_4, a Ca-F or a Ca-PO_4-F solid phase, for instance fluorapatite. The dune water in this zone is strongly supersaturated with respect to apatite phases (Table 7.2). This could signify that they are not contributing at all or even formed, that fulvic acids raise their solubility (Inskeep & Silvertooth, 1988) or that impure or cryptocrystalline apatite-like minerals with a much higher solubity are involved, for instance β-tricalcium phosphate or whitlockite ($Ca_{18}(Fe,Mg)_2H_2(PO_4)_{14}$; Moore et al., 1991). Vivianite (see Eq.8.33 in Table 8.3) is not considered a likely source of phosphate in marine Eemian deposits. Instead, it could be formed in the fresh, sulphate depleted dune water, which is in fact supersaturated (Table 7.2). The presence of fluorite is unlikely, due to its high solubility in these environments, where all waters are highly undersaturated (Table 7.2). Anyhow, geochemical evidence should provide the clue to the exact source(s) of PO_4 and F^-, as there are too many theoretical candidates for this difficult solution matrix with high DOC.

Miscellania

The decreasing Fe and Mn concentrations can be explained by the precipitation of a manganous siderite (Eq.8.32), triggered by the HCO_3^- and pH increase. The water is indeed supersaturated with respect to siderite, but remains agressive towards pure rhodochrosite (Table 7.2). The formation of siderite gains in probability as Van der Sleen (1912) observed siderite nodules in the Kedichem Formation south of Zandvoort aan Zee (Table 7.1), and authigenic siderite coatings have been observed in both a coastal dune aquifer system in Oregon, U.S.A. (Magaritz & Luzier, 1985), and Pleistocene aquifers in W-Germany (Leuchs & Obermann, 1992). The siderite nodules analysed by Van der Sleen, are composed of a manganous siderite ($Fe_{0.85}Ca_{0.1}Mn_{0.05}CO_3$) indeed.

The strange behaviour of Cr and V, that reach quite high levels in the outer freshening zone (Table 7.2), is attributed to dissolution from either the piezometer or centrifugal pump. Part of the vanadium could, however, be also natural, as anoxic, high DOC groundwaters scored high in a national inventory as well (Stuyfzand, 1991e). The water type changes downgradient from F_2MgHCO_3+ via F_3NaHCO_3+ to F_4NaHCO_3+, the facies is calcareous, deep anoxic, freshened (positive BEX) and nonpolluted.

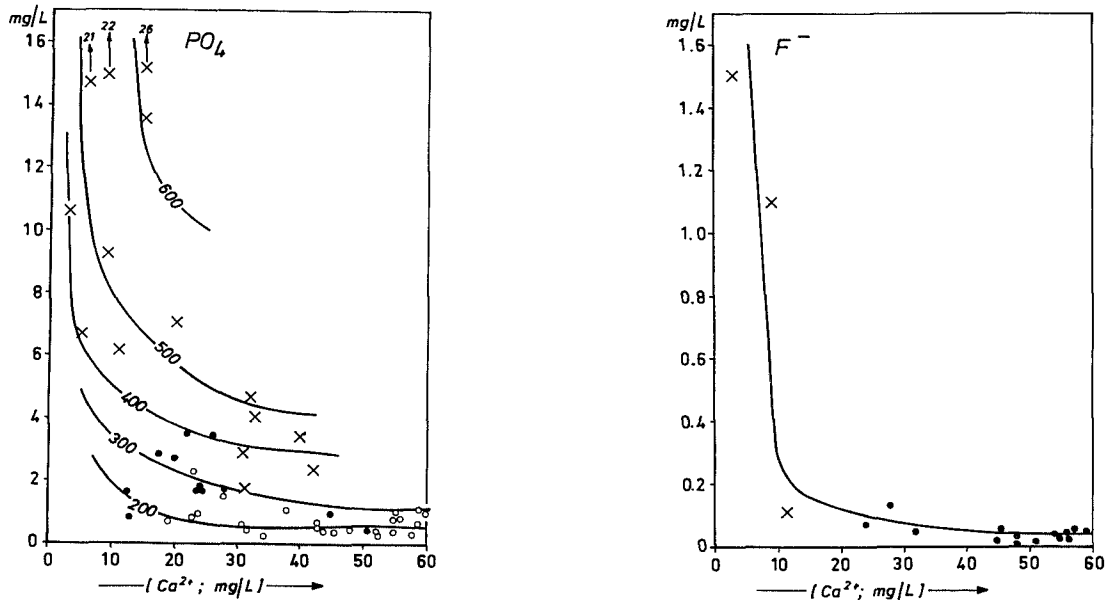

FIG. 7.6 Plot of F^- and PO_4 concentrations in anoxic Bergen dune groundwater with partial or complete sulphate reduction in the second aquifer, versus the Ca^{2+} concentration. The low Ca^{2+} levels are caused by cation exchange and believed to provoke a further dissolution of F^- and PO_4 containing solid phases, for instance fluorapatite. Part of the phosphate is also generated by decomposition of organic matter, as suggested by the strong correlation with HCO_3^-. The legend to the plotted symbols, is given in Fig.7.5.

IX. The freshening breakthrough zone (6500-6600 m)

In this downgradient migrating mixing zone between fresh dune and brackish Holocene transgression water, the chloride concentration steadily increases down the hydraulic gradient. Many of the processes described for the previous zone, continue here in initially the same geological formation and sedimentary facies and subsequently in the Bergen clay. The discussion is limited to deviations.

The concentration of SiO_2 is raised, probably through dissolution of biogenic opal (diatom skeletons and silicified reeds in tidal flat deposits; section 7.2) and desorption from the naturally fouled aquifer (see previous zone). The SiO_2 levels attained, indeed constitute the record for the whole study area. They approach equilibrium with amorphous SiO_2 (Table 7.2), the dissolution rate of which approaches that for clean diatoms (Kamatani & Riley (1979).

The increases in concentration of Fe and Mn remain puzzling, as the water is even more supersaturated with respect to siderite and vivianite than before. Their complexation to raised concentrations of dissolved humic substances may form the explanation. The concentration of Ca^{2+} and Mg^{2+} rises due to an increasing share of relict Holocene transgression water in the mixture. It should be noted, that the Mg^{2+} concentrations corrected for sea spray and the admixing of sea water (Mg^* in Table 7.2) become even negative. This indicates that Mg^{2+} is still transferred from the liquid to the solid phase, probably by exchange for Na^+. However, the precipitation of dolomite or conversion of calcite into dolomite is thermodynamically possible with SIs above 2 (Table 7.2). The extreme PO_4 and DOC concentrations may inhibit the formation of dolomite and also explain the supersaturation with respect to calcite (SI > 0.8; Table 7.2). The dissolution of calcite in this methanogenic environment actually sustains the Na^+ exchange. The formation of dolomitic cement in an environment where sulphate is reduced by methane, has been reported by several authors (Hovland et al. 1987; Jorgensen, 1989) and cannot be easily excluded without evidence. Other explanations for the Mg^{2+} removal are an enhanced adsorption by reduction of ferric hydroxide coatings (Bischoff et al., 1975), and the formation of chlorite-like phases (the water is strongly supersaturated; Table 7.2).

X. The zone of relict Holocene transgression water (>6600 m.)

This water surrounds the inland parts of the deformed dune hydrosome (Fig.4.3). Along the flow path selected here, it is found in the Bergen clay exclusively. The brackish water is probably already subject to dilution with intruding dune water, as evidenced by the high positive base exchange.

It contains extreme amounts of organic and inorganic carbon, ammonium, phosphate and probably methane, by interaction with the Holocene Bergen clay (aquitard 1E). The water type is B_6 to S_6NaCl+ and the facies is calcareous, deep anoxic, freshened and nonpolluted. Further characteristics are discussed in section 4.4.2, and largely agree with comments on the previous zone.

7.4 Zandvoort dune water towards the Haarlemmermeer polder

7.4.1 Situation and collection of hydrochemical data

The flow path studied, starts in the centre of the calcareous dune area about 7 km south of Zandvoort aan Zee, in the recharge focus area of the second aquifer, and terminates in the reclaimed lake Haarlemmermeer (Fig.7.7). Dune shrub covers the recharge area. The acquisition and screening of hydrochemical data was elucidated in general terms in section 4.2.3. This applies to about 300 complete analyses in a 1 km broad band along the section shown in Fig.7.7.

In the period November 1977 through November 1991 several observation wells were resampled for the additional analysis of :

- the isotopes ^{3}H, ^{13}C, ^{14}C and ^{18}O, by the Centre for Isotope Research Groningen in the period November 1977 - March 1981;
- many TEs using neutron activation analysis after preconcentration on activated carbon (see section 4.2.3), by ECN in May 1980; and
- about 20 trace elements, by KIWA with AAS-graphite furnace (see section 4.2.3) in June-August 1987, January-February 1991 and in November 1991.

7.4.2 Heterogeneities in the upper 30 metres

Hydrochemical logs of four multilevel wells, 25-30 metres deep and equipped with miniscreens, are presented in Fig.7.8. They are based largely on a sampling without filtration in 1980-1981, and partly on a second sampling, including 0.45µm filtration in the field, in November 1991. The latter sampling yielded similar results and additional information on B, Be, Hg, Li^+ and Rb^+.

The wells 24H.470, 24H.471 and 24H.472 are situated south of Zandvoort aan Zee on the plots M_1 (mosses), O_1 (oaks) and D_4 (dune shrub) respectively, plots that were discussed in detail in chapter 6. Well 30G.VUX is situated to the north of The Hague, on a plot 4000 m from the HWL and very close to a local groundwater divide near Waalsdorp, where bare dune sand was covered for 50% with low dune grasses. The log of this well has been included in order to substantiate the detailed evidence for TEs and isotopes, and to validate that the logs south of Zandvoort aan Zee contain representative patterns for the calcareous dunes of the Western Netherlands as a whole.

Once more, these four hydrochemical logs confirm the extreme variability of the composition of dune groundwater both in space and time. The uniqueness of each log is attributed to an unparalleled combination of site specific factors, like vegetation, distance to the HWL and lithology.

Changes with depth on each location are, in analogy with those in the Bergen dune area (section 7.3.2), associated with variations in recharge, spatial and geochemical heterogeneities.

Variations in recharge lead to the distinct patterns for tritium, chloride and oxygen-18, that are discussed and used in section 7.4.5 to date the groundwater. Spatial heterogeneities on the land surface are expressed by : (a) relatively low Cl^- concentrations below 18 m-MSL in well 24H.470 due to a further inland position of the recharge area; (b) the occurrence of local oak-groundwater above 4 m-MSL in well 24H.471, on top of laterally migrating grasses-and mosses-groundwater (see also Fig.6.52); and (c) the presence of local dune shrub-groundwater above 1 m-MSL in well 24H.472, on top of laterally migrating groundwater that originated under a somewhat scantier vegetation cover. And the geochemical heterogeneities are clearly reflected in: (1) the complete absence of nitrate in well 24H.472 below dune shrub, due to denitrification in dune peat; (2) more rapid increases for SiO_2, PO_4 and NH_4^+ upon the passage of strata rich in fines; and (3) the anomalous increases for SiO_2, PO_4, NH_4^+, K^* and Mg^* below 19 m-MSL in well 30G.VUX, due to eastward flow of groundwater that passed a more substantial Holocene aquitard 1D (more interaction with organic material).

Notwithstanding the unique hydrochemical fingerprint shown by each log, many similarities that were also noted in other logs not presented here, justify the derivation of a generalized evolution pattern in section 7.4.4.

7.4.3 Heterogeneities and discontinuities further downgradient

Concentration patterns of Ca^{2+}, NH_4^+ and SiO_2 in the relevant cross section (Fig.7.9), reveal that lithological heterogeneities continue below 20 m-MSL in the Pleistocene deposits, and that there are two important hydrological discontinuities.

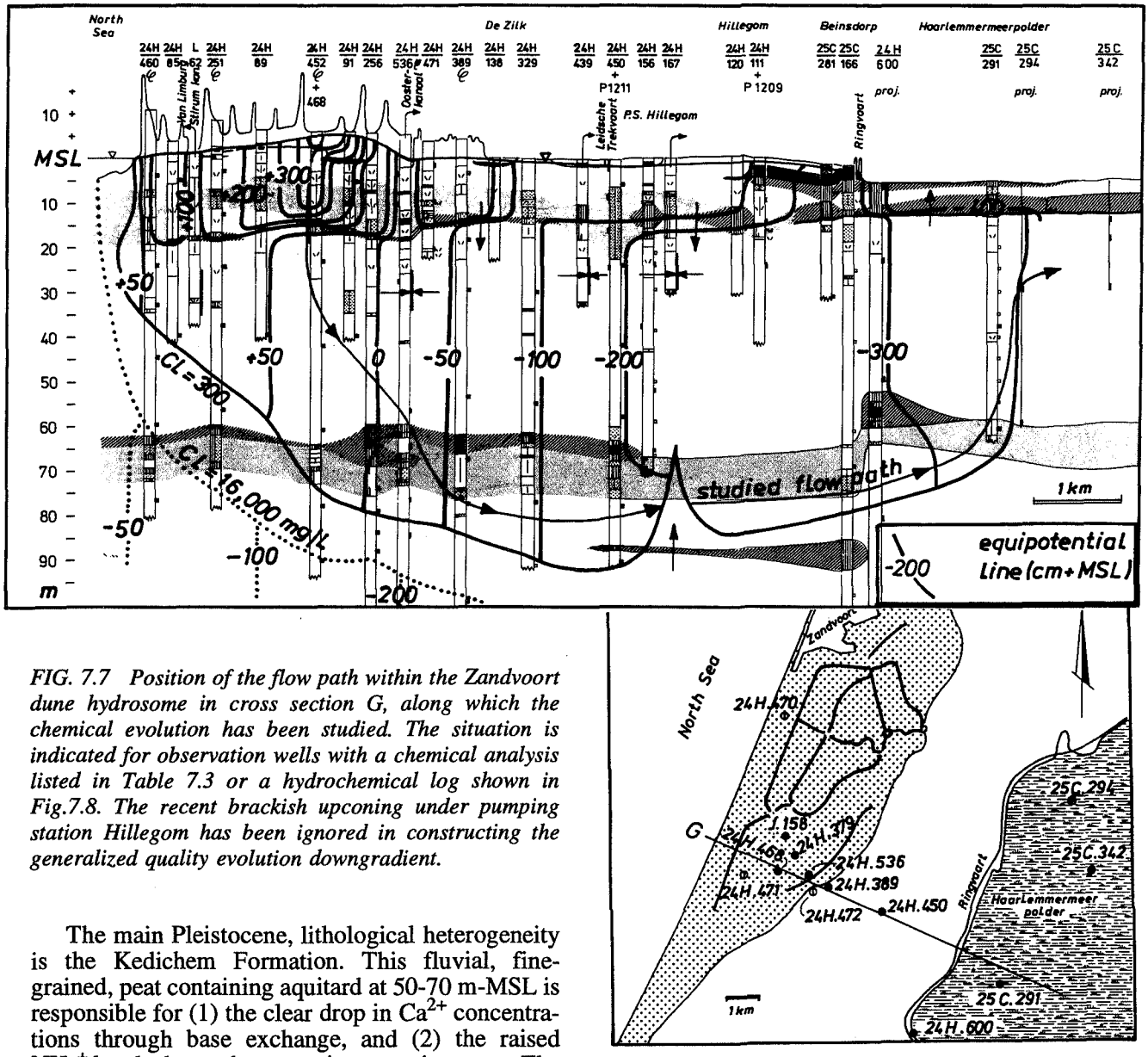

FIG. 7.7 Position of the flow path within the Zandvoort dune hydrosome in cross section G, along which the chemical evolution has been studied. The situation is indicated for observation wells with a chemical analysis listed in Table 7.3 or a hydrochemical log shown in Fig.7.8. The recent brackish upconing under pumping station Hillegom has been ignored in constructing the generalized quality evolution downgradient.

The main Pleistocene, lithological heterogeneity is the Kedichem Formation. This fluvial, fine-grained, peat containing aquitard at 50-70 m-MSL is responsible for (1) the clear drop in Ca^{2+} concentrations through base exchange, and (2) the raised NH_4^+ levels due to decomposing organic matter. The most important hydrological discontinuity is formed by the regional rise of the fresh-salt water interface in the period 1910-1981 (Enclosure 3.4; Fig.3.41), amounting to 18-30 m in the younger dune area. The relatively high NH_4^+ concentrations for the deep parts of the second aquifer, just above the Kedichem Formation, probably resulted from this upward flow through the Kedichem aquitard. A more local upconing below the well field of pumping station Hillegom (abandoned in 1982), constitutes the second discontinuity. Its effects on the flow path chosen have been neglected, in order to present a prograde, generalized, quality evolution downgradient.

An interesting facet in the SiO_2 pattern (Fig.7.9) is, that the passage of well-developed, marine, Holocene aquitards at 10-20 m-MSL, outside the recharge focus area, yields much higher concentrations of SiO_2 and NH_4^+. But the areal extent of high SiO_2 and NH_4^+ groundwaters thus generated, is limited to the upper 10-20 m of the second aquifer. This is explained by a predominantly lateral flow (Fig.7.7), but could also be due to losses by adsorption. Such losses are evidenced by an initial, significant SiO_2 mobilization when river Rhine water low in SiO_2 is infiltrated by deep wells in the upper 10-20 m of aquifer II (Stuyfzand, 1977, 1989i).

The relatively deep penetration of dune water with high Ca^{2+} concentrations only in the recharge focus area (Fig.7.9), is explained by an increase in vegetation cover (from scanty towards more dune shrub) and the oxidation of iron sulphides and dune peat (type $1A_1$ and $1A_2$) in connection with a drawdown of the groundwater table in the 1920s, when the exploitation of dune water began in this area.

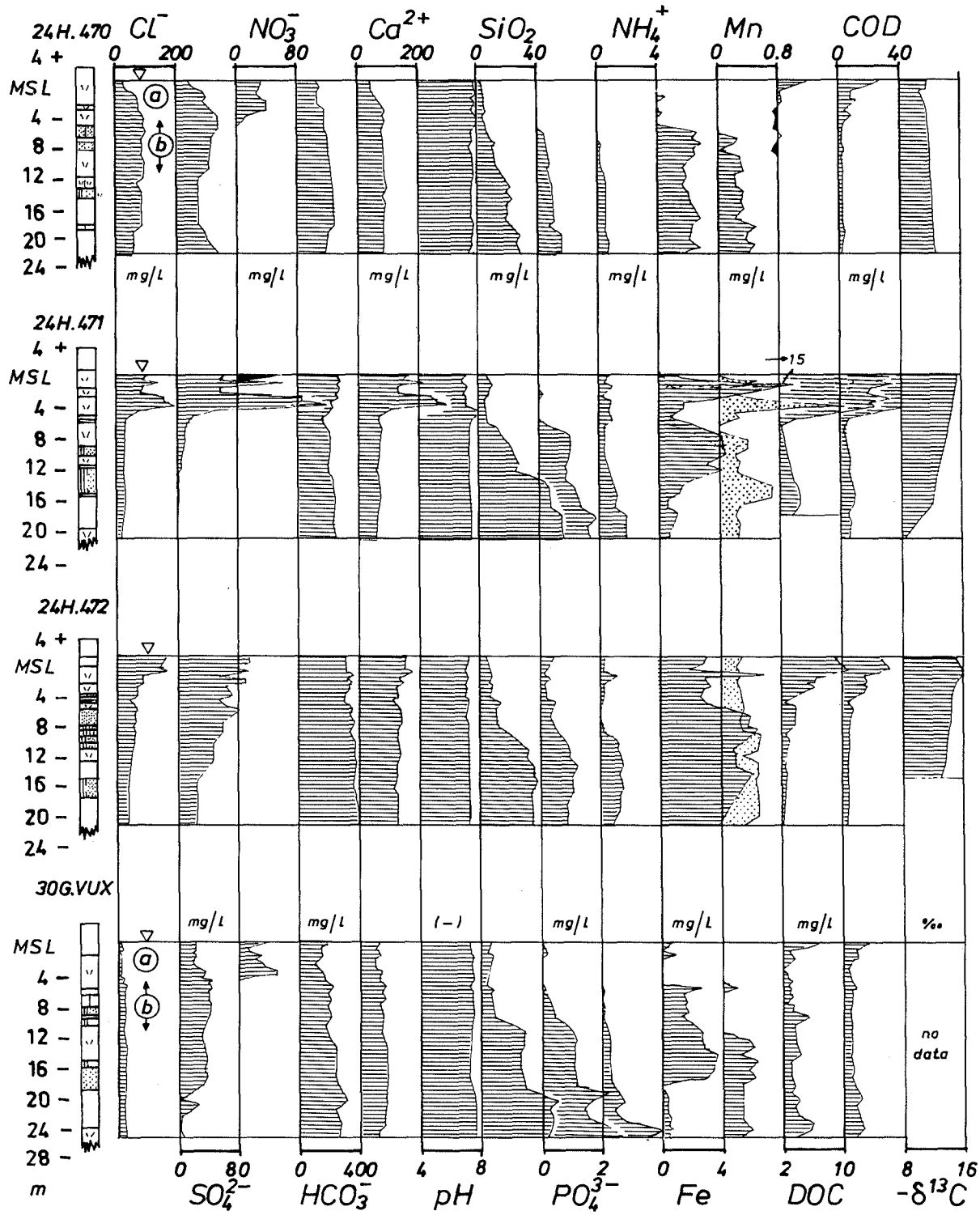

FIG. 7.8 Hydrochemical log of three multilevel wells equipped with miniscreens in calcareous dunes south of Zandvoort aan Zee (24H.470-472), and one to the north of The Hague (30G.VU X), in 1980 and September 1981, respectively. The encircled alphabethical characters in the Cl⁻ logs, correspond with exceptional recharge periods : a = 1979 (continental year low in Cl⁻); and b = 1970-1978 (high sea spray deposition and high evapotranspiration). Well 24H.470 is situated on the plot mosses-1, 24H.471 on oaks-2, and 24H.472 on dune shrub-4 (see Fig.3.1). The lower boundary of oak- and dune shrub-groundwater is situated at 2-4 m below the water table in the wells 24H.471 and 472. Below this interface groundwater occurs, that infiltrated in dunes with a sparse vegetation cover. The legend to the lithological logs is given in Enclosure 9.

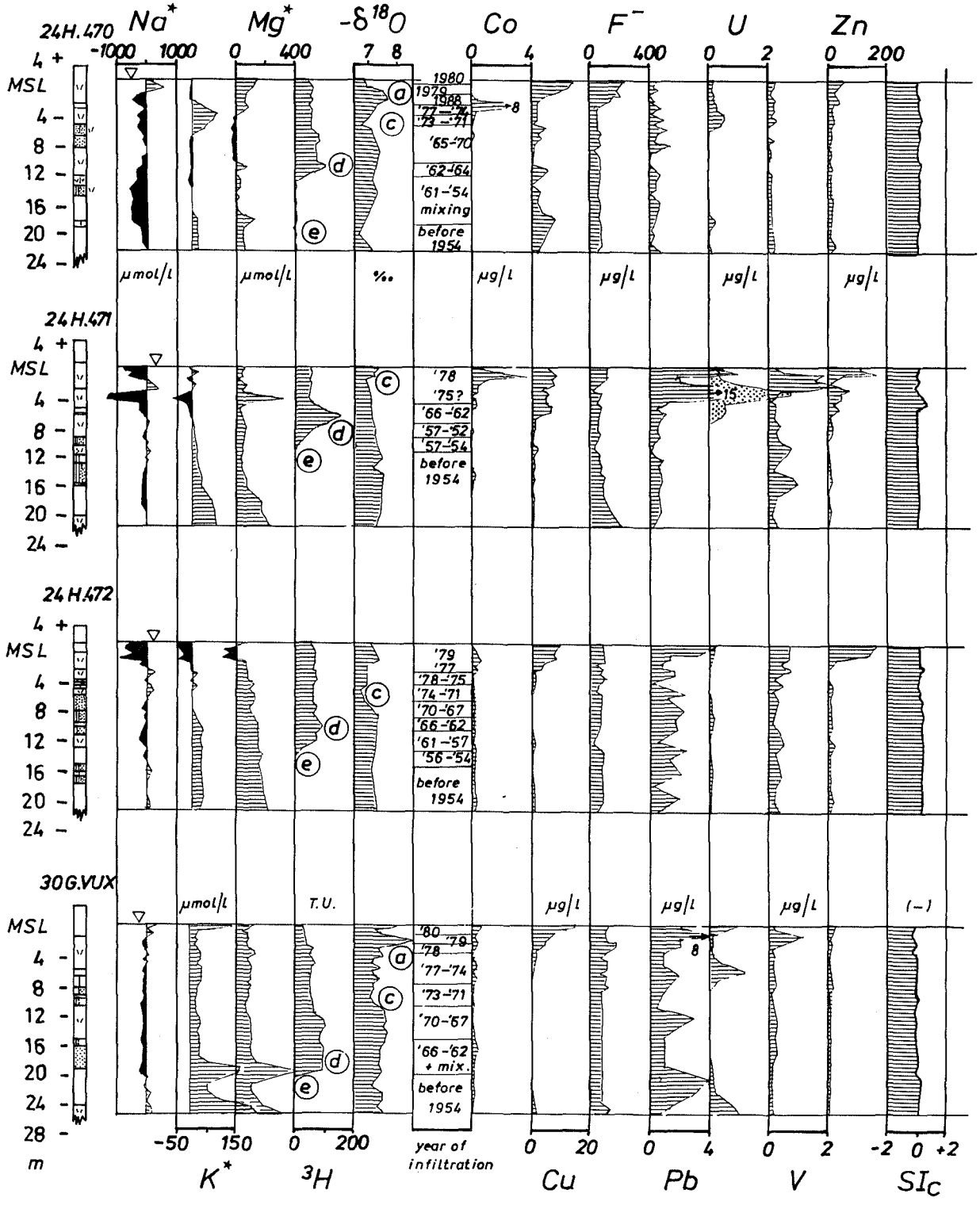

FIG. 7.8 Continued. The encircled alphabethical characters in the ^{3}H and $\delta^{18}O$ logs, correspond with the following exceptional recharge periods : a = 1979 (continental year low in ^{18}O); c = 1971-1973 (high in ^{18}O); d = 1962-1966 (tritium peak by culmination of nuclear weapon tests above ground); and e = before 1953 (tritium now <1 TU, by decay). The groundwater dating (indicated by year of infiltration) was based on these labels and the Cl^- labels. Note that $-\delta^{18}O$ is plotted (7 being relatively high). X = X corrected for a sea spray contribution.*

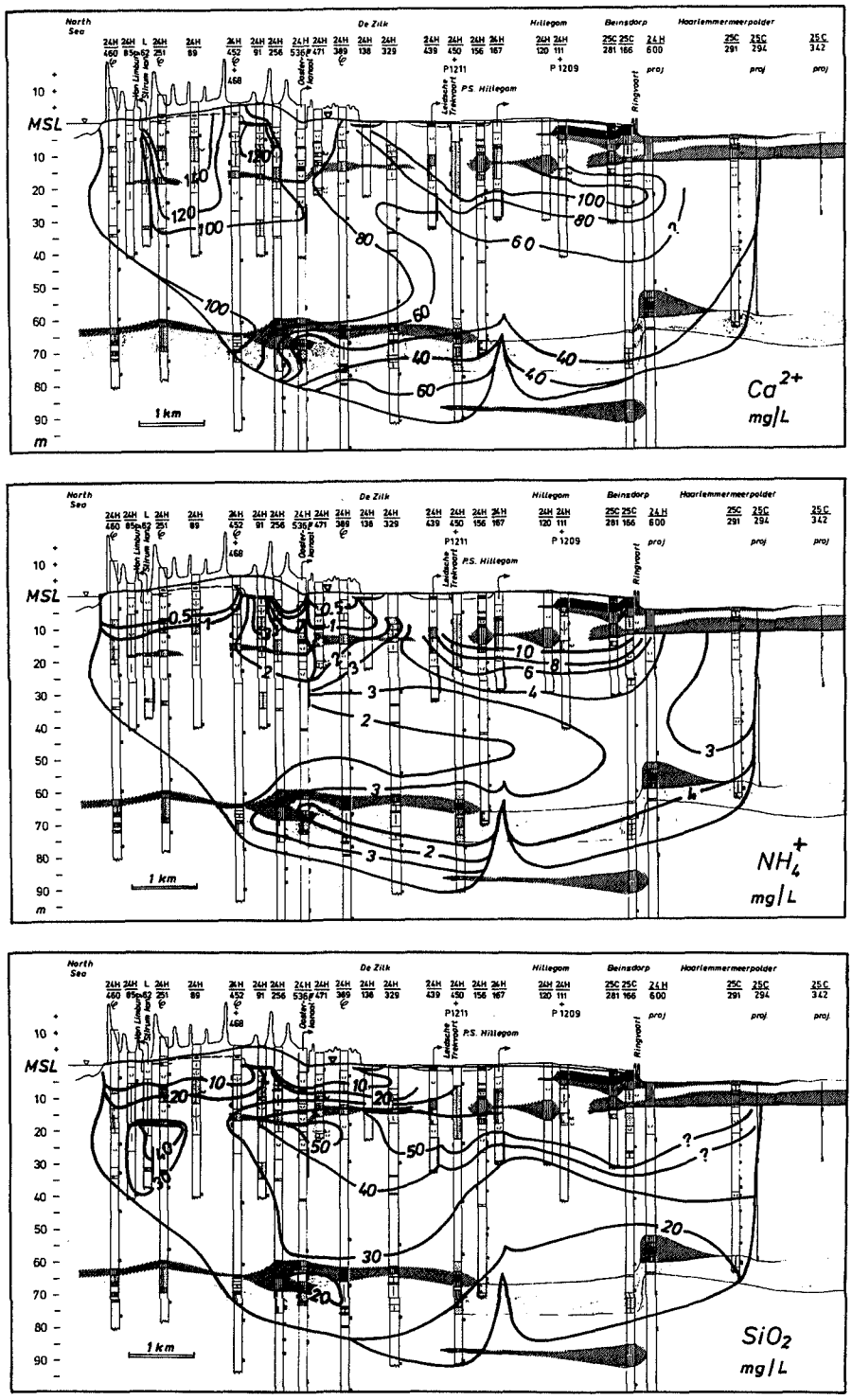

FIG. 7.9 Cross section G over the calcareous dunes 7 km to the south of Zandvoort aan Zee, showing the areal distribution patterns of Ca^{2+}, NH_4^+ and SiO_2 in fresh dune groundwater in the period 1977-1991. Lithology dictates the SiO_2 increase in Holocene aquitards in between 5 and 20 m-MSL, and NH_4^+ increase in clay and peat layers. Base exchange due to freshening is responsible for the Ca^{2+} decrease in the Kedichem Formation at 55-70 m-MSL, and downgradient of this formation in the eastern parts of the second aquifer. An increased vegetation cover and dune peat oxidation led to the raised Ca^{2+} levels in the central younger dune area. The recharge focus area of the second aquifer is situated in between the wells 24H.251 and 24H.452.

7.4.4 The generalized evolution over 9 km

The generalized trends downgradient are depicted for all major ions, about 8 trace elements, pH, tritium and oxygen-18 in Fig.7.10. The chemical water type and hydrochemical facies (option II in Table 2.15) are shown as well. The position of the Holocene aquitard complex 1C+1D and the Pleistocene Kedichem aquitard 2E, is indicated. Results of chemical analysis and calculation of mineral equilibria using WATEQX (Van Gaans, 1989), are listed in Table 7.3 for 13 samples along the flow path.

The flow path chosen, starts in the recharge focus area, where marine Holocene aquitards are weakly developed. The first 30 metres of flow are therefore directed downwards. The eastward flow velocity in the second and third aquifer approximates 2-3 km/century since the reclamation of the Haarlemmermeer in 1852. Downgradient 10 zones are discerned. These are briefly discussed below, as there is a lot of overlap with the description of the Bergen dune water in section 7.3. The $\delta^{18}O$ and ^{3}H patterns are discussed in section 7.4.5.

I. An upper decalcified, vadose zone (0-0.4 m)
Changes in this zone parallel those observed in zone I of the Bergen dune hydrosome (section 7.3.4). However, the mobilization of Al, SiO_2, Be, Co, Li^+, Ni, Rb^+ and Zn is probably less pronounced, due to (a) higher pH values, 3.5-5 (Veer, 1991; Stuyfzand & Lüers, 1992b) as compared to 2.9-5 (Rozema et al., 1985); (b) a shorter residence time, roughly one fifth of that in the Bergen area due to the smaller thickness of the decalcified zone; and (c) a shorter distance over which the advancing acid front concentrates the trace elements leached (section 7.3.4, zone II). Aluminium concentrations are strongly reduced in the lower parts of this zone by exchange for Ca^{2+} (section 6.4.2) and precipitation. The shorter transit time and smaller volume of the sorbent should also lead to a reduced size of the sulphate retention.

II. The calcareous, vadose zone (0.4-2 m)
The most prominent changes consist of a strong rise in pH and concentrations of Ca^{2+}, Sr^{2+} and HCO_3^-, due to the dissolution of calcium carbonate (section 6.6.4). This leads to an estimated decalcification rate of 9 cm/century (section 6.8.4). The contribution of strong atmogenic acids (HNO_3, H_2SO_4 and HF) and soil CO_2 to the dissolution process is calculated at about 10 and 90%, respectively (section 8.4.3). The significant drop in DOC concentrations is probably effectuated by adsorption, precipitation and oxidation with atmospheric oxygen as the oxidant.

The atmospheric trace elements As, Cd, Cr, Cu, Pb, Sb, Se, V and Zn are partly retained in the vadose zone, as can be deduced from the positive difference between 50% evaporated bulk precipitation and the upper dune groundwater (Table 7.3 and Fig.7.10). The true retention should exceed this difference, as the contributions of interception deposition on the one hand and soil constituents on the other are thus ignored. For elements with a presumably negligible dune sand contribution (section 6.6.4), the relative mobilities in the vadose zone as inferred from Fig.7.10, decrease in the following order : Se > Cu > Zn >> V > Pb ≅ Sb. The higher mobility of Cu as compared to Zn and Pb corresponds with the much stronger accumulation of Zn and Pb in the upper dune soils (Table 6.7). Sulphate retention can be ignored in this high pH zone (Scheffer & Schachtschabel, 1970).

III. The (sub)oxic upper zone (2-8 m)
This zone is contained in, from above to below, dune sand, beach sand rich in shell debris and shallow North Sea sand. The main changes affect trace elements and DOC (Fig.7.10). The more mobile, mainly atmogenic elements Cu, Se, Zn and F^- continue to decrease, whereas Co and U show a peak at about 5-6 and 6-8 m, respectively. The Co peak is somehow related to the beach sand deposits, where it is generally observed (Fig.7.8).

The U peak is attributed to the genesis of U roll-front deposits in the transition zone of (sub)oxic to anoxic conditions (Drever, 1982). Behind the advancing oxidation front U is slowly dissolved and carried by vadose and groundwater through the front into an environment with a higher redox level (anoxic, sulphate-stable), where it is immobilized. The zone of accumulation is slowly pushed down by the advancing front and the highest concentrations in the water phase are observed where U is dissolved from the enriched zone of accumulation. The mechanism of immobilization could be the reduction of UO_2^{2+}, which forms stable, soluble complexes with carbonate and sulphate, to the much less soluble UO_2. The field data suggest that this reduction of U-species occurs just before the onset of the reduction of ferric hydroxides (Fig.7.10). The U-peak at 24 m-MSL in deep anoxic dune water from well 30G.VUX (Fig.7.8) is probably an artefact and surely an exception.

The slight increases of Ca^{2+} and Sr^{2+} concentrations with depth are connected with the oxidation of dissolved organic matter by dissolved oxygen (Eq.8.11). This yields the necessary CO_2 to dissolve the aragonitic and calcitic shell fragments according to reaction 8.30B. The more pronounced HCO_3^- increase at about 6-8 m coincides with complete denitrification (Eq.8.12A). This reaction yields about just enough CO_2 to maintain internal equilibrium with the much larger quantity of HCO_3^- produced, and therefore does not lead to a significant Ca^{2+}

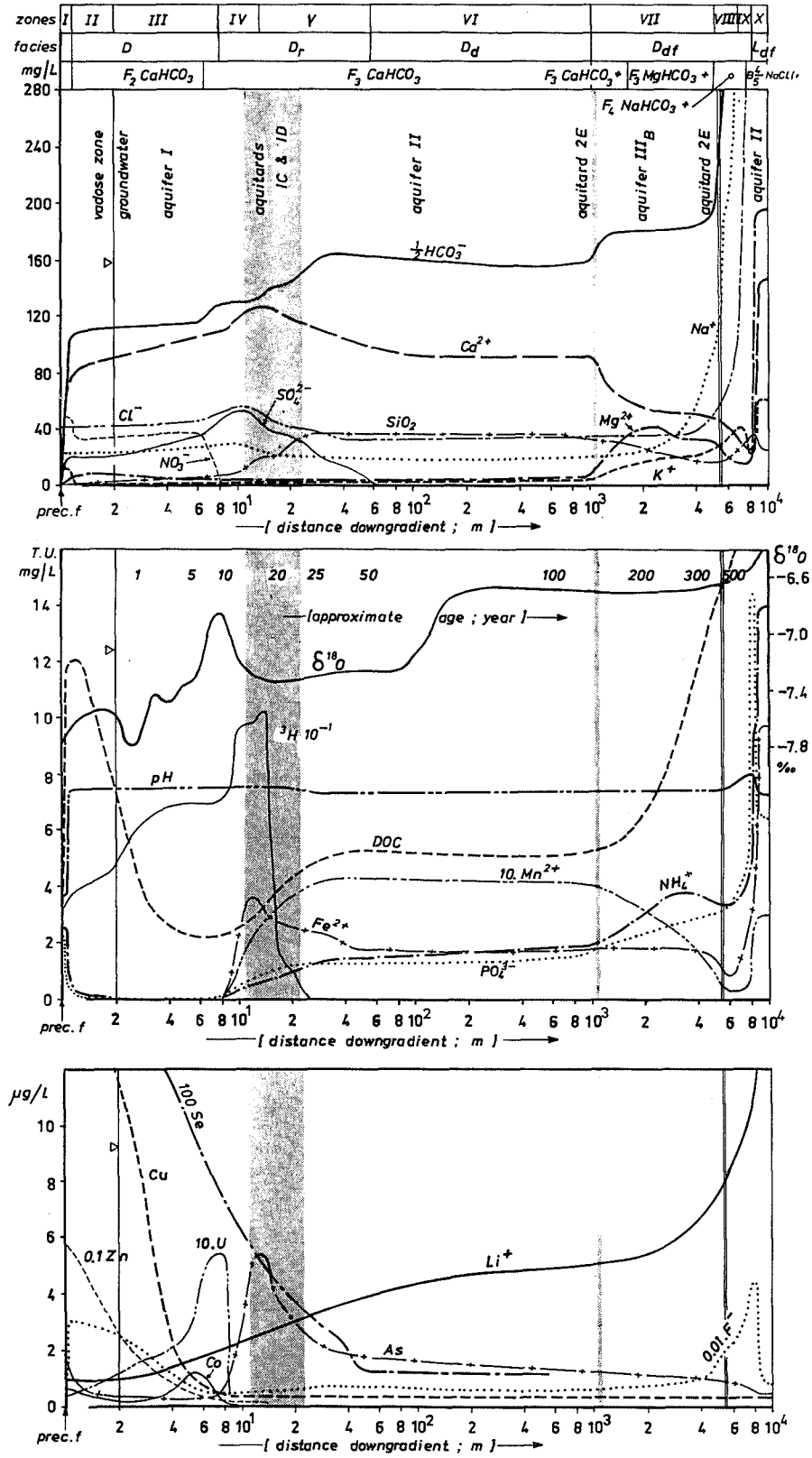

FIG. 7.10 Generalized chemical evolution of dune water along a flow path from the surface in calcareous dunes south of Zandvoort aan Zee, towards its intrusion front in the reclaimed lake Haarlemmermeer, in the period 1980-1991 (^3H around 1981). The evolution lines closely follow the data in Table 7.3. The changes of 50% evaporated bulk precipitation (prec·f) in the vadose zone were extrapolated from observations on monitoring plot dune shrub-1 (Table 6.9). The zones I-X are discussed in the text, the facies symbols are explained in Enclosure 8.

TABLE 7.3 Major and trace components of precipitation, dune water downgradient and the expelled, relict Holocene transgression water, in the period 1980-1991. The selected wells along a 9 km long flow path from the centre of the calcareous younger dunes south of Zandvoort aan Zee towards the Haarlemmermeer polder, are indicated in Fig.7.7. Not shown are concentrations of NO_2^- (<50), Hg (<0.2), Mo (<0.5), Sb (<0.5), Sn (<0.5) and Te (<0.5), all in µg/l. Prec. = bulk precipitation.

piezo-meter no.	sample depth m+MSL	subsoil flow m	subsoil age y	temp °C	EC 20°C µS/cm	pH	Cl^- mg/l	SO_4^{2-} mg/l	HCO_3^- mg/l	NO_3^- mg/l	PO_4T mg/l	Na^+ mg/l	K^+ mg/l	Ca^{2+} mg/l	Mg^{2+} mg/l	Fe mg/l	Mn mg/l	NH_4^+ mg/l	SiO_2 mg/l	DOC mg/l	COD mg/l	O_2 mg/l	watertype	redox index	polin	code
Prec. 1981	7	0	0	10.0	68	4.4	15	8	0	3.5	0.15	8	0.6	2	1.0	0.05	0.03	1.21	<0.5	1.5	4.9	11.0	F_aNaCl	0	2.8	D_{ap}
24H.J158	4.3	3	1	10	570	7.4	43	27	232	46.5	0.05	19	1.2	96	7.2	0.03	<0.02	<0.05	4.6	3.4	-	0.9	F_2CaHCO_3	1	1.8	D
24H.468	-4.6	11	13	10	630	7.5	62	70	259	<0.5	0.55	31	1.2	110	5.2	2.77	0.10	0.20	8.6	6.0	16.8	<0.2	F_2CaHCO_3	4	1.8	D_r
24H.468	-12.6	19	20	10	590	7.4	45	66	279	0.1	0.70	21	1.0	110	4.6	3.5	0.20	0.50	26.5	7.0	28.0	<0.2	F_3CaHCO_3	4	1.5	D_r
24H.468	-18.9	25	23	10	570	7.5	44	41	314	0.1	0.95	23	2.0	118	5.4	6.25	0.40	0.97	33.2	8.0	24.0	<0.2	F_3CaHCO_3	4	0.8	D_r
24H.379	-21.0	28	25	10	543	7.3	31	12	325	<0.1	1.32	19	1.8	103	4.2	6.87	0.50	1.7	32.6	-	-	<0.2	F_3CaHCO_3	5	0.2	D_d
24H.536	-57	1000	120	10.8	570	7.3	41	0	312	<0.2	1.40	22	4.4	90	6.2	2.3	0.42	2.8	30.8	6.0		<0.2	F_3CaHCO_3	6	0.1	D_d
24H.389	-77	1500	250	11.0	525	7.3	36	0	389	<0.5	1.82	51	10.2	69	19.8	2.2	0.18	2.8	28.4	5.2	-	<0.2	F_3CaHCO_3+	6	0.1	D_{df}
24H.450	-77	3500	400	11.3	580	7.2	33	0	365	<0.5	2.60	43	19.8	60	20.6	2.31	0.22	1.5	18.6	6.5	12.0	<0.2	F_3CaHCO_3+	6	0.1	D_{df}
24H.600	-69	5480	600	11.4	905	7.3	68	0	540	<0.1	4.07	97	27.6	45	44.5	1.61	0.1	4.6	14.7	10.8	-	<0.2	F_4MgHCO_3+		6	0.1
D_{df}																										
24H.600	-49	5500	650	11.5	1014	7.4	58	0	639	<0.5	3.03	180	23.1	44	22.2	0.84	0.05	3.3	15.9	15.2	-	<0.2	F_4NaHCO_3+	6	0.1	D_{df}
25C.291	-60	7000	800	11.6	1750	7.3	225	6	927	<0.5	5.1	400	40.0	34	13.8	1.80	0.03	4.6	26.0	(80)	280	<0.2	F_4NaHCO_3+	6	0.1	D_{df}
25C.294	-30	8000	900	11.7	2274	7.9	515	81	533	<0.5	15.9	520	21.0	13	14.0	3.15	0.25	2.2	36.4	47.0	-	<0.2	B_4NaCl+	5	0.3	$(D+L)_{df}$
25C.342	-28	?	?	11.3	10250	7.3	3200	3	1200	<0.2	6.43	1950	61.0	145	195	9.7	0.30	14.2	25.3	18.0	46.2	<0.2	B_5NaCl	6	0.1	L_d

piezo-meter no	sample depth m+MSL	Al µg/l	As µg/l	B µg/l	Ba^{2+} µg/l	Be µg/l	Br^- µg/l	Cd µg/l	Co µg/l	Cu µg/l	Cr µg/l	F^- µg/l	I^- µg/l	Li^+ µg/l	Mo µg/l	Ni µg/l	Pb µg/l	Rb^+ µg/l	Sb ng/l	Se ng/l	Sr^{2+} µg/l	U µg/l	V µg/l	Zn µg/l	^3H TU	$\delta^{13}C$ ‰	$\delta^{18}O$ ‰
Prec. 1981	7	72	0.8	5	4	<0.02	50	0.22	0.3	8	0.7	56	3.0	<1	<0.6	0.6	15.0	0.4?	890	<160	3	0.02	3.5	29	25	-24.0	-7.8
24H.J158	4.3	5	1	<50	10	<0.05	224	<0.1	<1	3.8	<0.5	170	1.4	<1	<0.5	3.1	1.6	0.4	85	130	325	0.16	<1	10	30	-11.5	-
24H.468	-4.6	<13	2	<50	20	<0.05	340	<0.02	<0.1	<0.6	<0.5	50	1	3	0.3	0.6	1.6	-	52	24	350	0.20	1.2	9	81	-	
24H.468	-12.6	<13	<2	<50	15	<0.05	160	<0.02	<0.5	<0.6	<0.5	50	1	4	<0.5	<0.6	<0.5	-	42	15	400	<0.05	-	-	95	-	
24H.468	-18.9	<13	0.2	<50	10	<0.05	160	<0.02	0.1	<0.6	<0.5	<50	1	4	<0.1	<0.6	0.1	<1	37	5	455	0.03	0.7	<2	20	-12	-
24H.379	-21.0	<20	0.3	50	20	<0.05	110	<0.1	0.1	<1	0.3	40	4	5	<0.1	0.6	0.1	-	-	-	450	<0.05	<0.5	<5	11	-	-7.2
24H.536	-57	3	1	-	40	<0.05	150	<0.05	<0.5	<1	<1	60	4	6	<0.5	<0.5	<0.5	<1	30	13	400	<0.05	<0.5	<10	<2	-9.8	-7.1
24H.389	-77	3	1		30	<0.05	140	<0.05	<0.5	<1	<1	40	4	6	<0.5	<0.5	<0.5	<2	30	10	400	<0.05	<0.5	<10	<2	-8.4	-
24H.450	-77	3	1.2		72	<0.05	115	<0.05	0.2	<1	<1	70	3	6	<0.5	<0.5	<1	-	-	11	320	<0.01	0.2	9	<2	-7.9	-6.8
24H.600	-69	3	1		40	<0.05	240	<0.05	<0.5	<1	<1	100	-	7	<0.5	<0.5	<0.5	<2	30	5	300	<0.05	<0.5	<10	<2	-	-
24H.600	-49	3	1		50	<0.05	200	<0.05	<0.5	<1	<1	120	-	8	<0.5	<0.5	<0.5	<2	30	5	300	<0.05	<0.5	<10	<2	-	
25C.291	-60	3	1		60	<0.05	740	<0.05	<0.5	<1	<1	300	-	9	<0.5	<0.5	<0.5	<2	30	5	200	<0.05	<0.5	<10	<2	-	
25C.294	-30	3	0.7		74	<0.05	1750	-	-	-	-	470	13	10	<0.5	0.6	<1	5	26	-	250	-	2.5	-	<2		
25C.342	-28	<20	0.4	-	520	<0.05	10800	<0.1	0.1	<0.6	1.5	(80)	-	-	<0.1	<0.6	<2	<2	5	5	1570	0.01	2.8	<2	<2	-	-

piezo-meter no.	sample depth m+MSL	sea salt corrected (µmol/l) Na^*	K^*	Ca^*	Mg^*	SO_4^*	BEX meq/l ##	SATURATION INDEX log(IAP/K)† Hydroxides & sulphates $Fe(OH)_3$	gibbsite	alunite	barite	Silicates SiO_2-am	albite	chlorite	illite	kaol	K-mica	Carbonates calcite	dolom	sider	rhodo	Phosphates & fluorides apatO	apatF	vivian	fluo
Prec 1981	7	-15	7	42	0	61	-0.0	-0.9	-3.0	-6.9	-1.5	-2.6	-14.5	-54.1	-17.4	-8.2	-19.2	-6.5	-13.2	-10.7	-6.5	-28.2	-24.0	-29.2	-5.7
24H.J158	4.3	-214	8	2372	178	218	0.2	1.7	0.67	-4.0	-0.88	-1.2	-3.5	-9.1	-0.63	1.8	-0.94	0.05	-0.94	-11.1	-2.2	-2.7	-0.36	-35.2	-1.9
24H.468	-4.6	-152	-2	2712	44	638	-0.1	1.5	0.71	-3.4	-0.19	-0.93	-2.3	-8.0	0.49	2.5	0.11	0.23	-0.78	0.43	-1.0	1.0	2.7	1.1	-2.9
24H.468	-12.6	-176	2	2721	66	621	-0.0	-0.5	0.74	-3.1	-0.34	-0.44	-1.1	-7.7	2.1	3.5	1.5	0.17	-0.96	0.47	-0.80	0.87	2.6	1.4	-2.9
24H.468	-18.9	-65	28	2921	101	363	0.2	-0.1	0.71	-3.7	-0.74	-0.35	-0.65	-6.1	2.7	3.6	2.1	0.35	-0.56	0.88	-0.35	1.8	3.5	2.6	-2.9
24H.379	-21.0	76	30	2553	88	80	0.3	-3.2	0.58	-4.6	-0.94	-0.35	-1.1	-8.9	2.1	3.3	1.4	0.13	-1.1	0.75	-0.42	1.1	2.9	2.6	-3.1
24H.536	-57	-35	91	2224	142	-60	0.3	-4.5	0.45	<-99	-	-0.39	-1.2	-8.1	2.0	3.0	1.4	0.07	-0.93	0.29	-0.49	1.1	3.1	1.3	-2.8
24H.389	-77	1347	242	1702	716	-52	3.0	-5.2	0.45	<-99	-	-0.43	-0.98	-5.7	2.2	3.0	1.6	0.04	-0.37	0.35	-0.77	0.83	2.6	1.4	-3.3
24H.450	-77	1072	489	1480	757	-48	3.1	-5.6	0.45	<-99	-	-0.61	-1.7	-7.1	1.6	2.6	1.3	-0.14	-0.64	0.26	-0.80	0.58	2.6	1.6	-2.9
24H.600	-69	2573	670	1087	1644	-99	6.5	-5.7	0.44	-262	-130	-0.72	-1.6	-4.9	1.5	2.4	1.1	-0.04	0.02	0.33	-1.9	0.77	2.9	1.6	-2.7
24H.600	-49	6426	560	1067	754	-85	8.5	-5.9	0.41	-264	-130	-0.68	-1.1	-5.4	1.5	2.4	1.2	0.12	0.05	0.23	-1.1	0.94	3.0	0.81	-2.6
25C.291	-60	11953	904	729	-50	-266	12.8	-5.9	0.43	-23.2	-10.3	-0.47	-0.25	-6.9	2.3	2.8	2.0	0.01	-0.26	0.56	-1.3	0.36	2.9	1.9	-2.0
25C.294	-30	10154	265	51	-839	92	8.7	-3.4	0.02	-6.4	-0.17	-0.33	0.5	-1.3	2.3	2.3	1.5	-0.13	-0.13	1.0	-0.07	2.4	4.6	4.8	-2.0
25C.342	-28	7367	-128	1921	-768	-4635	5.7	-3.4	0.38	-24.3	-10.1	-0.45	0.36	-2.1	2.5	2.7	2.0	0.51	1.3	1.1	-0.46	2.0	3.9	2.9	-2.9

: BEX = (Na^* + K^* + $2Mg^*$); † = calculated using WATEQX (Van Gaans, 1989).

increase by dissolution of $CaCO_3$. The water type consequently changes from F_2CaHCO_3 or F_2CaMix to F_3CaHCO_3. The facies is calcareous, (sub)oxic, nonpolluted and without base exchange.

IV. The anoxic sulphate-stable zone (8-13 m)

The upper parts of this zone occupy shallow marine, fine sand, and the lower parts are contained in the Holocene aquitard 1C, which is composed of shallow marine, very fine sand with clay intercalations. The most important changes consist of concentration peaks for Fe, As, Cl^-, SO_4^{2-} and Ca^{2+}. The mobilization of Fe^{2+} is neatly preceded by a complete denitrification, and is accompanied by the mobilization of AsO_2^-. Ferric hydroxide coatings, that are reduced by decomposing marine organic matter, probably form the source of Fe and As. Their mobility is high in this zone, because sulphate is not yet reduced to a significant degree to sulphide. The oxidation of marine organic matter is also reflected in increases

for NH_4^+, PO_4, HCO_3^- and probably I. The presence of more diatom sceletons in the finer-grained deposits (Van Straaten, 1954; Van der Werff, 1957), and the removal of protective $Fe(OH)_3$ coatings lead to the significant SiO_2 gains, especially in aquitard 1C. The strongest Mn increase generally occurs in aquitard 1C as well. Obviously these fine-grained deposits also contain much more Mn than the sandy deposits above. There could be a relation between this Mn and the relatively high amount of diatoms, as stated for various sediments by De Groot (1963).

The peaks for Ca^{2+}, Cl^- and SO_4^{2-} coincide with the period 1970-1978, which is characterized by high evapotranspiration losses and a high atmospheric deposition of sea spray and SO_x (section 6.7). The water type remains F_3CaHCO_3 and only the redox aspect changed from (sub)oxic into anoxic (sulphate-(meta)stable).

V. The sulphate-reducing zone (13-55 m)

This hydrochemical zone is contained in marine sands below aquitard 1C, in aquitard 1D (18-23 m) at the base of the Holocene deposits, and in aquifer II. This aquifer is composed of coarse, marine Eemian sands and coarse sands belonging to the Formations of Urk and Sterksel. The bulk of the sulphate-reduction occurs within aquitard 1D, and the SO_4^{2-} pattern further downgradient is probably dominated by two anthropogenic effects. The first is the oxidation of iron sulphides upon the rapid drawdown of the phreatic level in the period 1923-1925 AD, after completion of the abstraction canal "Oosterkanaal", about 1 km to the east. In 1914 the sulphate concentrations in the area generally were below detection (<4 mg/l) at a depth exceeding 13 m-MSL, which means that the sulphate reduction took place above aquitard 1D! And the second effect consists of the increased atmospheric SO_x input till the late 1960s (Figs. 5.5 and 5.6).

The sulphate reduction is accompanied by a significant decline in concentrations of Fe and As, through the precipitation of iron sulphides, that range from the least stable hydrotroillite to the most stable pyrite (Van der Sleen, 1912). The data in Table 7.3 do not reveal this clearly, as there are several complications posed by the samples 24H.468 and 24H.379, perhaps due to interference with siderite (note the high SIs in Table 7.3). But the generalized pattern depicted here, does follow from the detailed Fe-logs in Fig.7.8 and many other data. Coprecipitation with iron sulphides may explain the further decrease in Se concentration, but does not affect the Mn levels. A smaller tendency of Mn to form sulphides in this environment is therefore inferred.

On the other hand, the concentrations of HCO_3^-, NH_4^+ and PO_4 increase by decomposition of organic matter. For practically all Zandvoort dune groundwaters at 0-10 m below anoxic Holocene aquitards in the recharge areas of the second aquifer, the congruent oxidation of organic matter as represented by the Redfield equation seems to explain the observed NH_4^+/HCO_3^- and PO_4/HCO_3^- ratios fairly well (Fig.7.11).

The passage of aquitard 1D yields the strongest increase in SiO_2 concentration for the whole flow path, probably through the dissolution of diatom sceletons and silicified reeds, which consist of well-soluble opal. This strong, localized SiO_2 supply explains the similarity in the pattern of the thickness of aquitard 1D and the SiO_2 pattern for dune groundwater below this aquitard (Stuyfzand, 1988b).

Concentrations of Ca^{2+} and Cl^- decrease downgradient due to an increasing age of the water, with the traces of changes in vegetation cover and phreatic level (section 7.4.3). The water type and hydrochemical facies do not change with respect to the previous zone.

The zones VI - X (55-9000 m)

About 99% of the total flow path considered, is covered in the following five zones : the deep anoxic zone (VI), the inner freshened zone (VII), the outer freshened zone (VIII), the freshening breakthrough zone (IX) and the zone of relict Holocene transgression water (X). The changes in these zones are very similar to those described for the Bergen dune hydrosome, so that reference is made to section 7.3.4 for details.

The passage of aquitard 2E in the Zandvoort area, results in an earlier start of base exchange reactions due to freshening, namely beyond 1000 instead of 2500 m. The decomposition of organic matter in this fluvial, about one million years old Kedichem Formation yields considerably less NH_4^+ and PO_4 than the decomposition in the marine, >100 times younger Holocene aquitards (Fig.7.11). The NH_4^+ and PO_4 concentrations in dune water in the Haarlemmermeer polder correspond with those in and below the Kedichem Formation (Fig.7.11). This means that there are practically no signs of the anoxic aquifer fouling as observed in the Geestmerambacht area (section 7.3.4, zone VIII).

Contrary to the Bergen area, there is a significant SiO_2 decline downgradient within the inner freshened zone (VII). This is probably caused by adsorption (section 7.4.3), in connection with a much higher release of SiO_2 from the Holocene aquitards and a relatively high exchange capacity of the Kedichem Formation. Within the intrusion front (zone IX) a more temperate SiO_2 increase is observed in the marine Eemian Formation as compared to the Bergen area, probably due to its lack of fine-grained intercalations rich in diatoms.

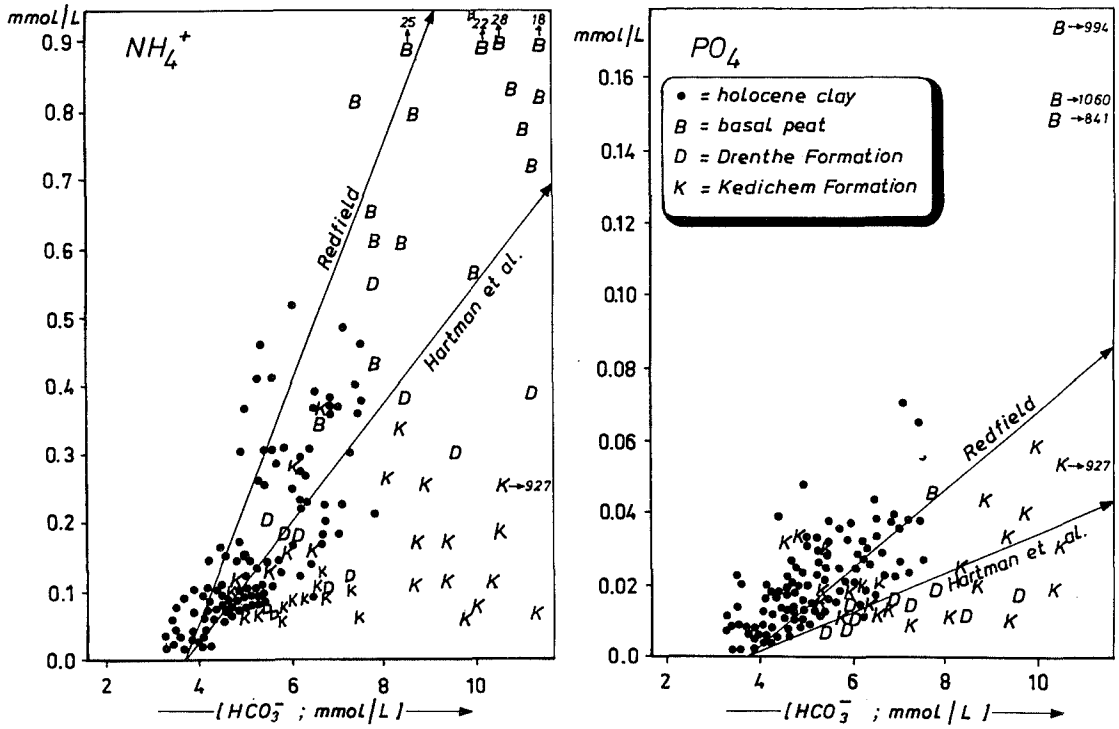

FIG. 7.11 Plot of NH_4^+ and PO_4 concentrations in anoxic Zandvoort dune groundwater with partial or complete sulphate reduction, versus HCO_3^- as an indicator of the interaction with decomposing organic matter. The arrows indicate the relations under the assumption of congruent decomposition of organic matter as described by either the so-called Redfield equation (Eq.7.1) or the equation of Hartmann et al. (1973; see section 7.3.4).

Relations with the Base EXchange index (BEX)
The relation between the sea-salt-corrected bases (Na^*, K^*, Ca^*, Mg^*), total inorganic carbon (TIC) and pH on the one hand, and BEX as a parameter indicating the direction and approximate extent of base exchange on the other (see section 2.4.1), is shown in Fig.7.12 for 36 samples of anoxic, pure dune water with a freshened facies. These plots confirm and quantify, more or less, the base exchange processes that are described in section 7.3.4.

A positive BEX generally implies positive values for Na^*, K^* and Mg^* individually, but the relation certainly is not linear (Fig.7.12). There are two distinct zones : (a) the zone with BEX ≤ 3.5 meq/l, where $Na^* \approx 0$ meq/l, $K^* \approx 0.1$BEX and $Mg^* \approx 0.9$BEX. It corresponds with the inner freshened zone, where the more easily desorbing Na^+ had been driven from the exchange complex already; and (b) the zone with BEX > 3.5 meq/l, where $Na^* \approx 1.77$[BEX-3.5] meq/l, $K^* \approx 0.55 - 0.1$[BEX-3.5] meq/l, and $Mg^* \approx 4.5 - 1.3$[BEX-3.5] meq/l. It forms the outer freshened zone, where the Mg^{2+} and K^+ that were acquired in the inner zone are exchanged, together with Ca^{2+}, for Na^+. Magnesium is thus involved in the cation exchange reaction about 10 times more than potassium on a meq-basis. And negative Mg^* and K^* levels only occur (here) when BEX surpasses about 7 and 9 meq/l, respectively.

The Ca^* decrease (on a meq-basis) approaches half the BEX increase. This signifies that exchange reaction 8.31 is accompanied by a simultaneous dissolution of $CaCO_3$, on average about equal to ½BEX. This dissolution cannot be sustained by the Ca^{2+} losses alone, because equilibration of Ca^{2+} depleted, deep anoxic dune water without base exchange, would yield in a closed system only about 10-20% of the amount required. When also supersaturation is allowed (due to raised levels of PO_4^{3-}, DOC and Mg^{2+}), then this share may double. The necessary, additional acidity is likely supplied by methanogenesis. This fermentation yields after equilibration with $CaCO_3$ about twice as much HCO_3^- as Ca^{2+} according to reaction 7.1, after correction for a strongly reduced NH_4^+ production (Fig.7.11). This agrees with the TIC increase, which approaches the increase in BEX (Fig.7.12). However, where methanogenesis does not occur or only sparingly, the internal driving force should predominate and the pH should rise significantly. Relatively low methane waters as deduced from HCO_3^- and DOC concentrations, indeed establish higher pH values and a more significant positive relationship with BEX than high methane waters (Fig.7.12).

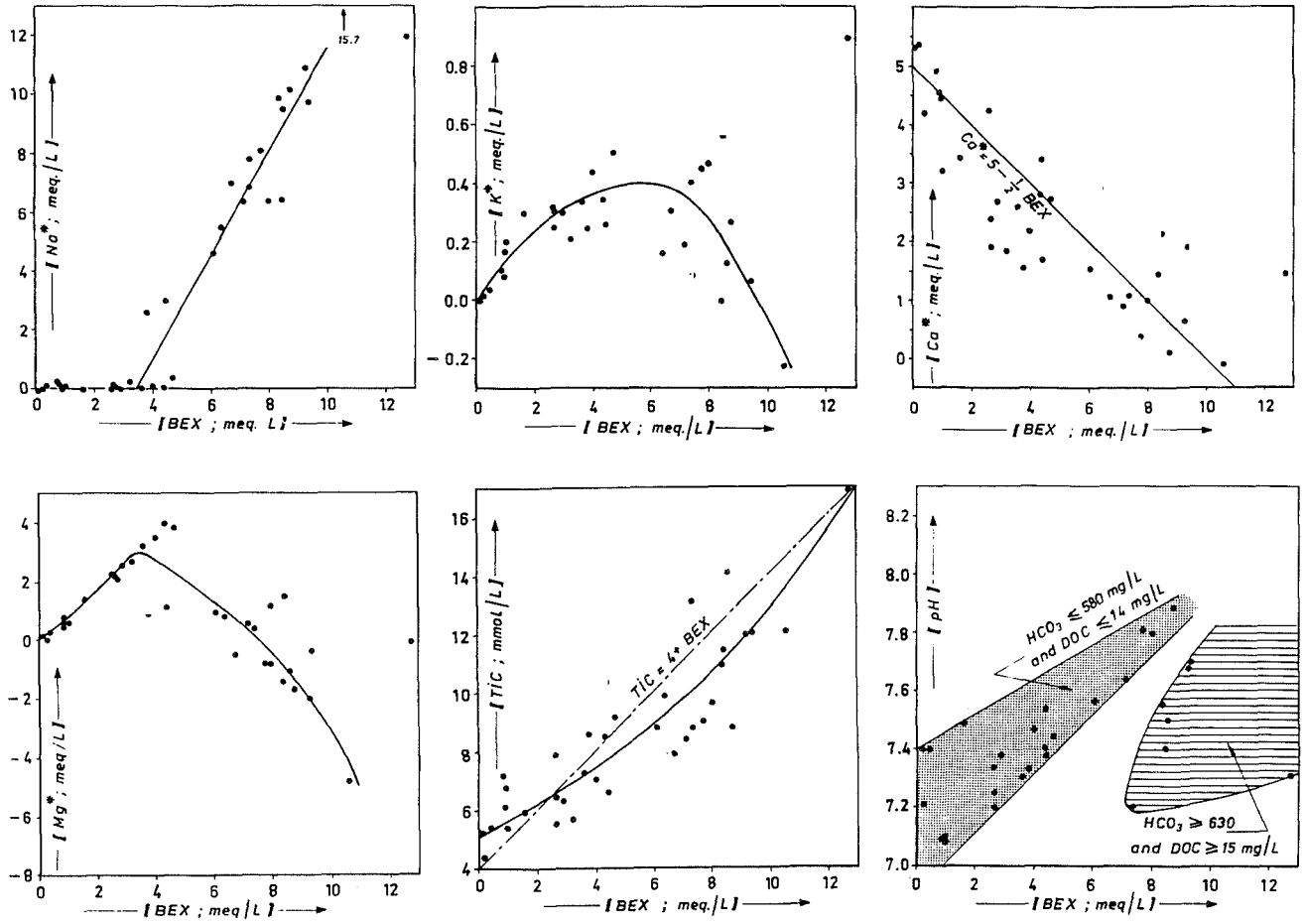

FIG. 7.12 Plot of sea-salt-corrected, main cations (Na^*, K^*, Ca^*, Mg^*), total inorganic carbon (TIC) and pH in 36 anoxic, Zandvoort dune groundwater samples with complete sulphate reduction and a freshened facies, versus BEX ($=Na^* + K^* + Mg^*$ in meq/l). BEX is a parameter of the direction and approximate extent of base exchange due to fresh or salt water intrusion.

7.4.5 Groundwater dating

Dune groundwater could be dated in detail, using three techniques : (1) spatial history matching, where in a snapshot either the hydrochemical consequences of a dated event in the atmosphere or close to ground level are searched for, or a copy of the whole input signal for a certain period has to be traced back in the groundwater along a flow path; (2) sequential history matching, where the above mentioned events or input record are followed in one observation well; and (3) radiometry, which implies measurement of the activity of radioactive tracers with a well-known input activity and decay constant.

The tracers used, are chloride (technique 1 and 2), tritium (technique 1 and 3), oxygen-18 (technique 1) and carbon-14 (technique 3). The generalized patterns of Cl^-, ^3H and $\delta^{18}O$ downgradient and the inferred groundwater ages are shown in Fig.7.10. Isochrones for cross section F in Fig.3.1 (about 6 km to the north of the flow path considered here), are shown in Fig.7.13.

Chloride

The highly variable Cl^- input record for coastal dune groundwater has been discussed in section 6.7. Variations in annual means are shown in Fig.6.40, and mean seasonal fluctuations are presented in Fig.6.47. The best points of reference for history matching on samples collected in the 1980s were (a) the Cl^--deficient, continental year 1979, and (b) the salty period 1967-1978 (with culmination in 1971-1977), by virtue of a high sea spray deposition and high evapotranspiration losses.

Examples of sequential history matching are shown in : Fig.6.41 (variations in annual means at 6 m below the water table), Fig.6.42 (10 years of monitoring in 6 wells scattered over the coastal dunes and belonging to the national groundwater

monitoring network of RIVM), Fig.6.43 (a detailed depth-log repeated after 10 y), and Fig.6.48 (seasonal fluctuations in the upper 3 metres). Examples of spatial history matching are presented in the Figs. 6.43 and 7.8, where detailed vertical logs using miniscreens revealed the position of the above mentioned extremes.

Changes in vegetation with time (Fig.6.35) may spoil the sequential history matching technique. Spatial heterogeneities in vegetation cover may trouble the spatial history matching technique, especially when not a flow path but vertical logs are investigated (wells 24H.471 and 472 in Fig.7.8 for instance).

Tritium

The tritium-logs with depth (Fig.7.8) roughly correspond with the tritium input-signal in precipitation after correction for radioactive decay (Fig.5.7). Water without tritium, which infiltrated before 1953 and therefore must be older than 1980 (sampling in this case) - 1953 = 27 year, is observed below 18, 10, 13 and 20 m-MSL in well 24H.470, 471, 472 and 30G.VUX, respectively (Fig.7.8). The difference between these depths can be explained by disparities in natural recharge for the close surroundings of the wells, being 0.52 (plot mosses-1), 0.31 (plot oaks-1), 0.41 (plot dune shrub-4) and 0.52 m/y (bare with some short grasses). It is concluded from these data, that on average 50% of groundwater containing tritium migrates laterally, as 100% vertical transport would double the depth of the upper water without tritium when a porosity of 0.38 is taken.

The tritium peak in rain water during the years 1962 through 1966 (Fig.5.7), can be traced back in the logs at resp. 11, 6, 9 and 16 m-MSL, which roughly corresponds again with differences in natural recharge. The 1962-1966 tritium peak in groundwater is much less pronounced as compared to that in rainwater, for three reasons : (a) evapotranspiration losses of summer precipitation with high tritium activities (Fig.5.9) are much larger than those of the relatively tritium-poor winter rains; (b) smoothing by hydrodynamic dispersion; and (c) an (apparent) hiatus in the vertical tritium-log may occur where flow abruptly changes from a predominantly vertical to a horizontal direction, so that the peak may be downgradient of the sampler. This may explain the lack of a clear peak in well 30G.VUX.

Hydrodynamic dispersion leads to a significant mixing, indeed. As a first approximation Eq.6.19 can be used to calculate the smoothing of the amplitude. An α_L= 0.1 m, a wave period of 10 years (comprising the period 1962-1971), groundwater flow velocities of 10-20 m in 16 years (the vertical distance migrated by the tritium peak), a vertical flow distance of 10-20 m, and a median horizontal flow velocity of 0.01-0.05 m/d for 50% of the time in 16 years, would yield a damping of 7-43%, of a wave with a maximum of 600 and a minimum of 60 TU (Fig.5.7). Thus, the peak reduces to 490-580 TU in 1964 and the minimum rises to 80-170 TU in 1969. This strongly contrasts with our measurements (Fig.7.8) and observations near Monster by RIVM (Stuyfzand, 1991b p.82), showing in 1979-1981 a peak of 100-185 TU and a minimum of 55-65 TU for groundwater with a postulated recharge in 1962-1971. The calculated minimum of 80 TU approaches the field data, but the calculated maximum of 490 TU strongly exceeds them. This pleads for a much lower tritium input in the years 1962-1966, which can be achieved for a large part by taking into account the large evapotranspiration losses of summer precipitation. Raising α_L to 1 m, which probably is a more realistic value for the traversed Holocene aquitards, in our calculations does not reduce the gap between the calculated and observed tritium-logs!

Oxygen-18

The ^{18}O logs in Fig.7.8 reveal a peak (coded c) at about 5 m-MSL in the wells 24H.470 and 472, and at 9 m-MSL in well 30G.VUX, above the 1962-1966 tritium maximum. This ^{18}O peak probably corresponds with that in rainwater during the years 1971 through 1973 (Fig.5.7), and was observed also in multilevel wells near Monster (Stuyfzand, 1991b). A clear $\delta^{18}O$ drop is visible close to the phreatic level in the wells 24H.470 and 30G.VUX (Fig.7.8), which reflects the exceptional continental year 1979 (precipitation low in both Cl^- and $\delta^{18}O$).

At greater depth, in the second aquifer a very consistent increase is observed from -7.2 ± 0.2 to -6.5 ± 0.2 ‰ (Fig.7.13). These higher values continue downgradient of the transition zone and hold for all coastal dune hydrosomes in the study area. This change is probably connected with the general drawdown of the groundwater table in the study area (Enclosure 3.2). This happened in the northern parts of the dune catchment area of GW, which is traversed by the section shown in Fig.7.13, around 1880 AD (Fig.3.32). And in the southern part of that catchment area, which is considered in Fig.7.10, the major drawdown took place in the 1920s.

Two factors explain the drop in ^{18}O concentrations after the major drawdown of the water table in the dunes : (1) open water evaporation, which concentrates the heavier oxygen-18 water molecules in the remaining liquid, was strongly reduced as the majority of (periodical) dune lakes dried up completely; and (2) also the dune brooks that drained mainly the winter rains low in $\delta^{18}O$, dried up. The effect of the general increase in vegetation cover since the 1920s (Table 3.5), remains obscure, as no significant differences could be derived from recent observations on different

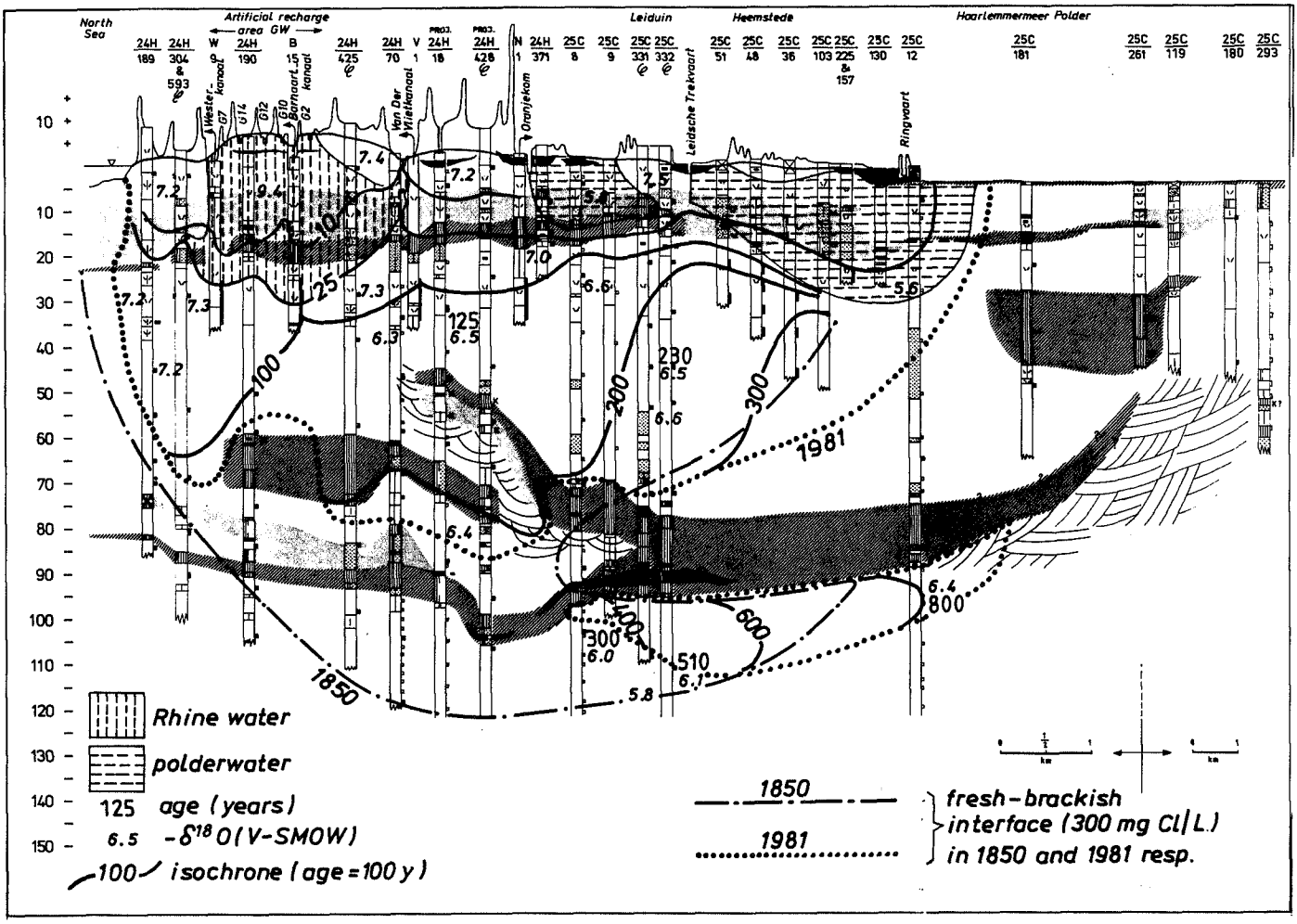

FIG. 7.13 Age distribution in cross section F over the fresh dune water lens south of Zandvoort aan Zee in 1981, based on Cl^-, ^3H, ^{14}C and ^{18}O analyses, and on the breakthrough of Rhine water recharged since 1957. The fresh-brackish interface around 1850 AD, indicates a general salinization along the seaward face and a freshening inland.

vegetation groundwaters (section 6.6.3). Anyhow, the transition zone between the younger dune groundwater low in ^{18}O and the older dune water with higher ^{18}O concentrations, can be assumed to represent the onset of the drawdown and thus form an isochrone by interpolation of measurements. In that way the 100 year isochrone was drawn in Fig.7.13.

Radiocarbon

The dating by means of ^{14}C (T½ = 5730 years) is troubled by many geochemical complications (Mook, 1989). These can be circumvented, however, under certain conditions with the approach of Pearson & Hanshaw (1970), here below 25 m-MSL in aquifer II. In the upper parts of this aquifer ^{14}C levels of 88±2 pmc prevail, the water does not contain tritium and hydrological calculations yield an age of approximately 70 years. The concentration of total inorganic carbon (TIC) amounts to 5-7 mmol/l, depending mainly on the thickness of aquitard 1D (Stuyfzand, 1988b). Higher TIC levels downgradient originate from interaction with sediments older than 80,000 years and can therefore be judged to dilute ^{14}C activities, so that

$$Age = 70 - 8270 \ln\left(\frac{^{14}C_m}{88} \cdot \frac{TIC_m}{TIC_o}\right) \qquad (7.2)$$

where : Age = time elapsed since infiltration [y]; $^{14}C_m$ = carbon-14 activity measured [pmc]; TIC_m = $CO_2 + H_2CO_3 + HCO_3^- + CO_3^{2-}$ measured [mmol/l]; TIC_o = ditto, in upper part of aquifer II (5-7 mmol/l depending on location).

Results of thus calculated ^{14}C ages from activi-

ties varying in between 88 and 53 pmc, are plotted in Fig.7.13. The highest age was calculated for dune water in aquifer IIIB, below glacio-lacustrine clay, at the border of the Haarlemmermeerpolder (25C.12) : about 800 years. This deep dune water was cut-off from the fresh water lens probably in the period 1905-1935, by salt water intrusion.

7.5 Rhine water intruding into dune water

7.5.1 Situation and collection of hydrochemical data

The intrusion of pretreated river Rhine water in the dunes can be considered as a mild form of salinization (section 4.4.6). The focus is directed here on pretreated Rhine water after spreading in the dunes south of Zandvoort aan Zee. It infiltrated into dune sand and migrated about 800 m laterally in the upper aquifer and Holocene aquitards, in 27 years. No attention has been paid in this investigation to the behaviour of organic microcontaminants. For information on quality changes during (1) pretreatment, (2) detention in spreading basins, (3) the relatively short detention in the subsoil in between recharge basins and recollection, and (4) deep well infiltration, reference is made to the literature cited in section 1.4. Some concise information regarding the quality changes in spreading basins and upon a short subsoil passage is also given in section 4.4.6.

Situation
Upon arrival by pipeline in the dune catchment area of the Municipal Water Supply Co. of Amsterdam (GW) south of Zandvoort, the pretreated water feeds an extensive system of spreading basins. The bulk of water is recollected by a combination of drains, drainage canals and wells, which are situated at 70-140 m from the infiltration ponds and permit underground detention times of 60-110 days. However, drainage canals in the eastern parts of the recharge area are often ≥1 km away from the spreading basins, and lead to an extremely long flow path. This situation was studied in the eastern part of the area in between the Barnaart and Van der Vliet canal (see Figs. 3.1 and 3.47A), using the same row of multilevel wells equipped with miniscreens, as employed in the survey of rain water lenses (Fig.3.47B).

Hydrological backgrounds for the section to be discussed here, are presented in section 3.10.2. The high flow velocity in the supply canal prevents the accumulation of bottom sludge, so that anoxic conditions in the immediate vicinity of this strongly recharging artery do not develop. The short transit time in the supply canal means that its quality does not deviate significantly from the pipeline discharge of the pretreated Rhine water (Stuyfzand, 1984a), the composition of which was monitored since the start of artificial recharge in 1957.

The section of observation wells had to be oriented in a direction oblique to the general groundwater flow direction (Fig.3.47), in order to obtain easy access. The distance of the flow path to each of the eight multilevel wells therefore differs from the position in the section. Transit times in the subsoil and lengths of the flow path for the wells 477 - 484 are specified in Table 7.4. They increase for these wells from 2.5 to 16.5 years (section 7.5.5) and from 50 to 790 m, respectively.

Data collection
After bailer drilling and well completion in May 1980, all 170 screens were sampled in March 1981 for analysis on major constituents, trace elements (most by neutron activation analysis, As, Cr, Cu, Pb and Zn by AAS), and the isotopes ^{3}H and ^{18}O. Most samples were not filtered, which led to a significant contribution of suspended fines to the concentrations of trace elements. The relations between Al (as an indicator of interference by suspended fines) and several trace elements that are given in Table 2.3, stem as a matter of fact from this data set. Major constituents were not influenced significantly, as evidenced by several filtered samples and by a resampling in the period March 1982 - March 1983 by Stuurman (1984) for the analysis of main components. The results of Ce, Cr, Hf, Lu, Pb, Sc, Ti, Th, V and Zn were corrected according to Eq.2.1.

7.5.2 Some calculations

Changes in the concentration of Na^+, K^+, Ca^{2+}, Mg^{2+} and SO_4^{2-} upon subsoil passage (ΔX) can be calculated by using their strong positive correlation with Cl^- in pretreated river Rhine water and by assuming conservative behaviour of Cl^- :

$$\Delta X = X_m - X_o \qquad (7.3)$$

where : ΔX = concentration of X corrected for a contribution of river Rhine water [µmol/l]; X_m = measured concentration of X [µmol/l]; X_o = original concentration of X in pretreated Rhine water, as calculated from the measured Cl^- concentration according to : $Na_o = 0.836Cl_m - 26$ (R=0.98); $K_o = 0.026Cl_m + 64$ (R=0.93); $Ca_o = 0.185Cl_m + 1208$ (R=0.93); $Mg_o = 0.037Cl_m + 276$ (R=0.60); $(SO_4)_o = 108Cl_m + 372$ till 1974, since then $(SO_4)_o = 108Cl_m + 259$ (R=0.83); all in µmol/l. The calculation of $(SO_4)_o$ requires a division into the period before and since 1974, due to extension of the pretreatment

with a coagulation step by addition of $FeCl_3$, in 1974. The other elements were less affected.

These relations are based on annual means in the period 1957-1980 and individual analyses in the period 1969-1975 (N = 52/y). The rather low correlation coefficient R for Mg^{2+} is compensated for by a relatively small impact of Cl^- and an overall constancy of Mg^{2+}. The calculation of ΔNa and ΔK approximates that of Na^* and K^* (Eq.5.7 and Table 5.5), the discrepancy between both correction types is large for the other ions.

The change in concentration of total inorganic carbon (ΔTIC) can be calculated even more easily, as fluctuations of its concentration in pretreated Rhine water can be neglected, especially on an annual basis:

$$\Delta TIC = TIC_m - 2.75 \qquad (7.4)$$

Calculation of ΔHCO_3 requires a division into the period preceding coagulation (before August 1974 : lower pH, more CO_2 and less HCO_3^-) with $\Delta HCO_3 = HCO_{3m} - 146$, and the period since then, with $\Delta HCO_3 = HCO_{3m} - 162$ (mg/l). The coagulation is followed by a pH-correction.

Retardation

Many substances dissolved in the polluted Rhine water, are retarded upon subsoil passage with respect to the water phase, by adsorption. And when their concentrations decrease due to sanitation measures in the Rhine basin or an intensified pretreatment (Fig.4.25), desorption occurs, which again leads to retardation, this time of a positive effect. A simple parameter for delay, of any kind, is the well-known, dimensionless retardation factor R_i for constituent "i" :

$$R_i = \frac{v_i}{v_w} \qquad (7.5)$$

where : v_i = migration velocity of constituent i, to be calculated from the 50% breakthrough of the front and the distance covered [m/d]; and v_w= migration velocity of the water phase or a conservative tracer like Cl^- [m/d].

The well-known equation to calculate R_i of sorbing chemicals in aqueous solution from the distribution coefficient and aquifer properties (for a review see Bouwer, 1991), is :

$$R_i = 1 + \frac{\rho_b}{\varepsilon} K_d = 1 + \frac{\rho_b CEC}{\varepsilon \Sigma k} \qquad (7.6)$$

where : ρ_b = dry bulk density [kg/l]; ε = porosity [fraction by volume]; K_d = the slope of the linear portion of the adsorption isotherm, where K_d = C_s/C_w [l/kg] with C_s = the amount adsorbed to the solid phase(s) in kg/kg, and C_w = concentration in the water phase at equilibrium in kg/l; CEC = cation exchange capacity [meq/kg dry weight]; Σk = sum of cations in displacing fluid [meq/l].

This formula applies to one-dimensional, single-phase, nondispersive flow in saturated, unconsolidated, homogeneous porous media with a low enough water velocity for sorption to be at equilibrium.

7.5.3 Areal patterns in cross section

Results of analysis of main constituents are plotted for the Rhine hydrosome in cross section in Fig.7.14 (HCO_3^-, NO_3^-, PO_4^{3-}, Fe, Mn, SiO_2 and chemical oxygen demand by $KMnO_4$) and Fig.7.15 (Cl^-, ^3H, ΔNa, ΔK, ΔCa and ΔMg). The hydrochemical patterns can be explained in terms of the pollution record of the Rhine water recharged, sorption phenomena, biodegradation, geochemical anomalies for specific aquifer strata and aquitards, mixing with dune water along the borders of the Rhine hydrosome and historical changes in groundwater level and flow pattern.

The pollution record

The pollution record of pretreated Rhine water (Fig.4.25) and the groundwater flow pattern (Figs. 3.47 and 3.48), explain the position of zones with high concentrations of Cl^- (Fig.7.15), SO_4^{2-} (not shown, pattern similar to that of Cl^-) and tritium (Fig.7.15). Chloride and tritium behave conservatively in this system and therefore are excellent tracers for dating purposes (section 7.5.5). Sulphate concentrations deviate less than 5-10% from the SO_4^{2-} levels calculated with Eq.7.3. This indicates that SO_4^{2-} approximates conservative behaviour as well. The rather low HCO_3^- concentrations (Fig.7.14) and ΔCa values (Fig.7.15) close to the supply canal, are related to a practically calcite indifferent influent since 1975 and a calcite-agressive composition of the influent before 1975 (Fig.4.26).

Sorption and biodegradation

Sorption leads to the generally negative ΔNa, ΔK and ΔMg values especially in the aquitards with their raised CEC, and close to the intrusion front (Fig.7.15). The extreme ΔCa values in aquitard 1D and aquifer II (close to the intrusion front), are caused mainly by exchange for Na^+. The zone with a high chemical oxygen demand (COD by $KMnO_4$) in the middle of the section, probably results from losses downgradient due to biodegradation and some sorption, and quality improvements in infiltrated Rhine water upgradient.

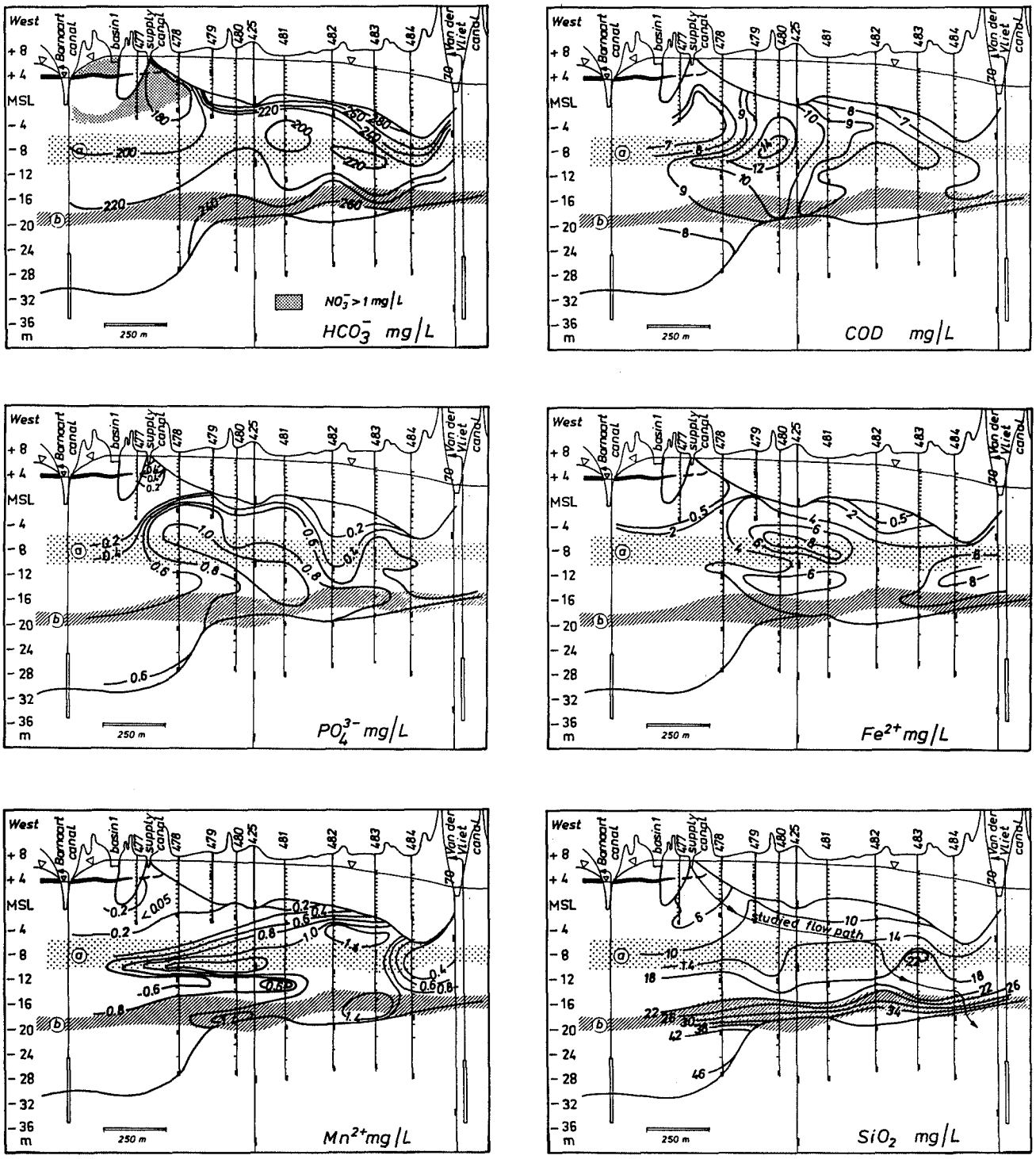

Fig. 7.14 Areal distribution pattern of HCO_3^-, NO_3^-, PO_4^{3-}, Fe, Mn, SiO_2 and chemical oxygen demand by $KMnO_4$ (COD) exclusively within the Rhine hydrosome, in the cross section over the Barnaart and Van der Vliet kanaal, in March 1981. The area is situated in the artificial recharge area of the Municipal Water Supply Co. of Amsterdam, south of Zandvoort aan Zee (see Fig.3.1 and 3.47A). The flow path studied in section 7.5.4, is indicated in the distribution pattern of SiO_2. a = aquitard 1C (very fine North Sea sand with some clay lenses); b = aquitard 1D (clay lenses alternating with very fine sand).

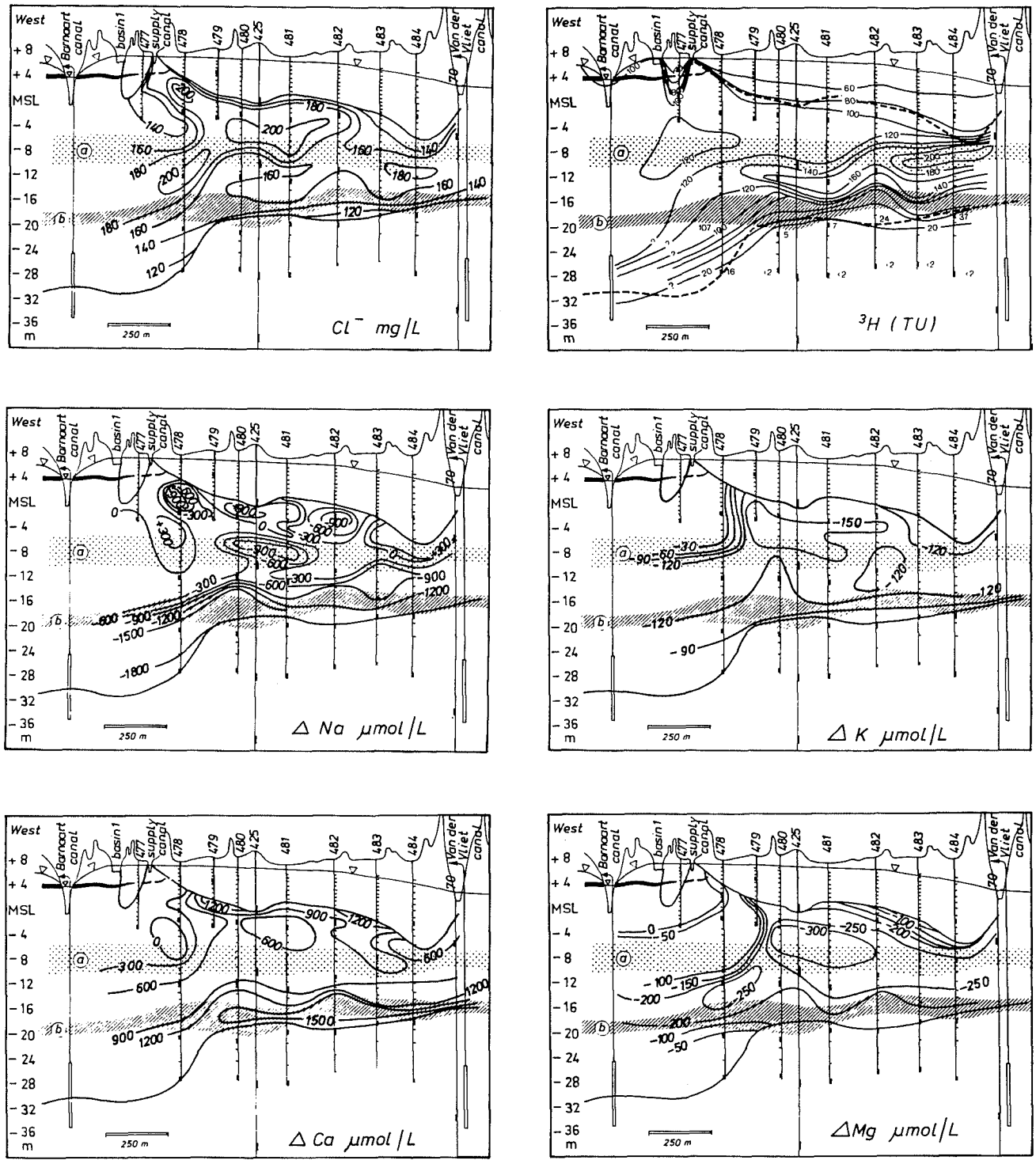

Fig. 7.15 Areal distribution pattern of Cl^-, ^3H, ΔNa, ΔK, ΔCa and ΔMg exclusively within the Rhine hydrosome, in the cross section over the Barnaart and Van der Vliet kanaal, in March 1981. The area is situated in the artificial recharge area of the Municipal Water Supply Co. of Amsterdam, south of Zandvoort aan Zee. ΔX = concentration of X corrected for a contribution of Rhine salt. a = aquitard 1C (very fine North Sea sand with some clay lenses); b = aquitard 1D (clay lenses alternating with very fine sand).

Sorption of orthophosphate leads to the low natural concentrations in the (sub)oxic zone around wells 477 and 478 (Fig.7.14), with the Rhine phosphate peak of 1969-1974 (Fig.4.25) probably upgradient (Fig.7.14 and 7.17; section 7.5.4 under zone I). The remaining part of the PO_4 distribution can be explained by geochemical supplies (see below).

Geochemical stratification

Dune peat $1A_2$ at about 3.5 m+MSL leads to complete denitrification of the influent of spreading basin G1 (Fig.7.14), which is deduced from a row of 6 observation wells in between this basin and the Barnaart kanaal (not shown). This peat layer is wedging out in the vicinity of the supply canal, and obviously has no denitrification capacity there, as evidenced by the breakthrough of nitrate in well 477 and the upper parts of well 478 (Fig.7.14).

The beach and shallow marine sands (Fig.7.16) yield high phosphate levels, which cannot be supplied by decomposing organic matter alone, and high Mn and As concentrations as well. The most plausible explanation is the protracted flow in these deposits as the flow field changed in 1957 from predominantly vertical into horizontal. This leads to a continuous leaching up to the point where such a peak develops, that the front is retarded downgradient (see further under "Historical changes etc.", this section).

The aquitards 1C and especially 1D clearly yield the bulk of SiO_2 (Fig.7.14) by dissolution of biogenic opal, which was observed for dune water as well (section 7.4). The highest concentrations of Fe, Mn, HCO_3^-, NH_4^+ and PO_4^{3-} are also generated in these aquitards (Fig.7.14), probably because they contain more unstabilized organic matter which reduces ferric hydroxides in the close vicinity. Another, more spectacular explanation, which requires further geochemical validation, is the dissolution of a manganous siderite, that formed on site before the passage of infiltrated Rhine water, in a deep anoxic environment with much higher HCO_3^- concentrations than at present. The introduction of low HCO_3^- Rhine water, which does not exhibit sulphate reduction, indeed yields water initially undersaturated with respect to siderite and rhodochrosite (calculated using the WATEQX program of Van Gaans, 1989), and after passage of aquitard 1C, supersaturated water.

Concentrations of Fe do not exceed those observed in dune groundwater from the same hydrogeological formations (well 24H.472 in Fig.7.8), although they surpass the average. The Mn concentrations, however, exceed those in dune water by a factor of 2-4. This corresponds with the diagnostic high Mn/Fe ratio, for Rhine bank groundwater in The Netherlands, that passed Holocene aquitards (Stuyfzand, 1985b).

Within transition zones

Relatively high concentrations of HCO_3^- and ΔCa values occur in the transition zone of Rhine to dune water in the upper aquifer (Fig.7.14 and 7.15). These are connected with the vegetation cover of the area close to the supply canal : tall grasses and some reeds in an area with a relatively high phreatic level (plot G_1 in Table 6.13). Effects of Mischungscorrosion (agressivity towards calcite due to mixing of two saturated waters) are quite negligible, also because the redox state of both end members is about equal near the transition zone.

Relatively low SO_4^{2-} and high HCO_3^- concentrations are found in the transition zone of Rhine to deep dune water in the upper parts of the second aquifer. This is explained by the mixing of both water types.

Historical changes in phreatic level and flow patterns

Before the start of dune water abstraction from the area in 1853, the groundwater table was situated close to ground level. Downward flow strongly dominated over lateral flow, due to the position of this area close to the regional groundwater divide (Fig.7.16). The upper boundary of iron sulphides probably coincided with the top of the beach deposits at about MSL. This is deduced from the undisturbed dune area Zwanenwater (about 16 km north of Bergen; Stuyfzand & Lüers, 1992a), and from statements by Van der Sleen (1912).

The period 1853-1957

The strong drawdown of the phreatic level due to abstraction, first through draining canals only and since 1915 also by deep wells, led to a strong expansion of the (sub)oxic and anoxic, sulphate-stable zones and to oxidation of iron sulphides (Fig.7.16). Measurements at 1-5 m-MSL in the upper aquifer in the period 1903-1915 (Stuyfzand, 1988b) confirm this oxidation, yielding about 20 mg SO_4^{2-}/l in addition to atmogenic SO_4^{2-}, and reveal that sulphate was still largely reduced in aquitard 1C. Groundwater flow continued to be directed mainly downwards, except for the areas bordering the Barnaart and Van der Vliet Canal (Fig.7.16). Dune peat $1A_2$ in the western parts, emerged above the receding water table. This must have led to an enhanced oxidation of iron sulphides, because the large NO_3^- amounts formed upon oxidation of peat (see plot bracken-2 in Table 6.13), can tresspass the capillary fringe whereas oxygen has to obey its solubility in water. In this way more oxidant, which is quite capable to oxidize iron sulphides according to Kölle & Schreek (1982), enters the vulnerable, saturated zone than when only atmospheric oxygen is involved.

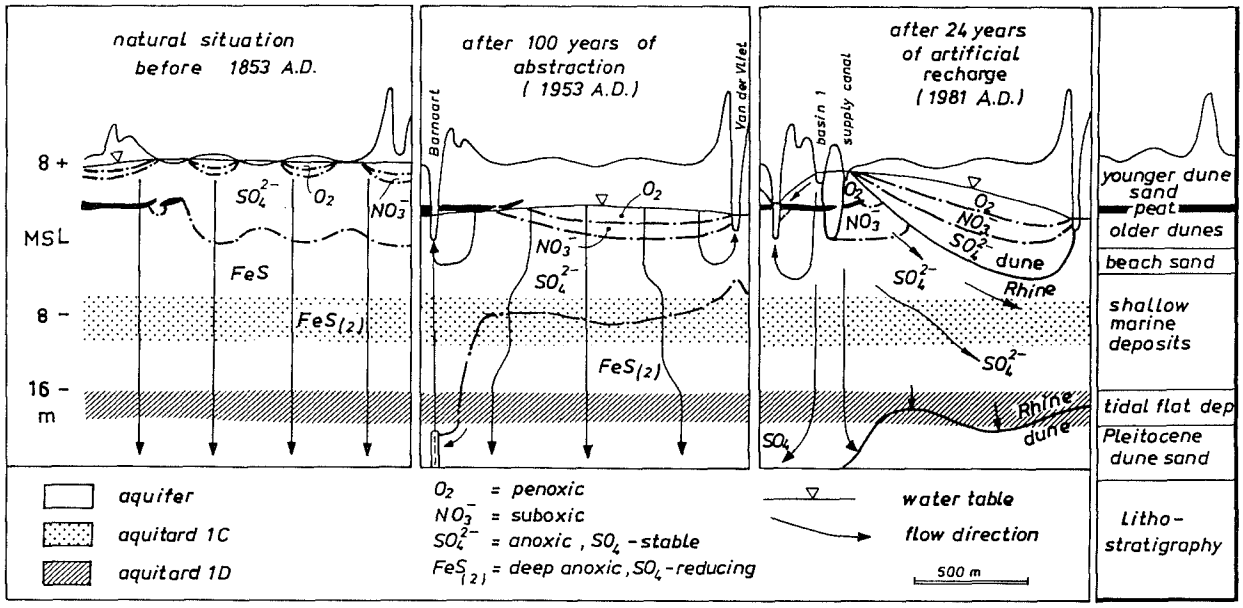

FIG. 7.16 Historical changes in phreatic level and groundwater flow pattern in the area in between the Barnaart Canal and Van der Vliet Canal, south of Zandvoort aan Zee, with geohydrochemical consequences. The drawdown of the water table in the period 1853-1957 led to the expansion of the (sub)oxic and sulphate-stable redox environments. The introduction of river Rhine water in 1957 by spreading, conduced to a further expansion of the sulphate-stable zone and, due to the tilting of groundwater flow from predominantly vertical to (sub)horizontal, relatively high concentrations of PO_4^{3-}, As and Mn are attained in the aquitards by a prolonged leaching. The situation before 1853 is extrapolated from data pertaining to 1905-1910, the situations anno 1953 and 1981 are based on observations.

The period since 1957

Artificial recharge since April 1957 led to a fast rise of the groundwater table (Fig.3.32), and to a drastic change from mainly vertical to mainly horizontal flow (Fig.7.16). This change signifies that the contact time and, much more, the flow distance in the upper aquifer strongly increased, with very significant hydrochemical consequences for the infiltrated Rhine water indeed, especially regarding NO_3^-, PO_4, Mn and As.

The nitrate front of Rhine water probably received little delay in the dune sands, which have a very low denitrifying capacity (if any), due to a low content of organic matter (about 0.1% dry weight) and prolonged leaching. The underlying beach and shallow marine sands at 0-6 m-MSL, evidently constitute a powerful anoxic redox buffer, by presence of both reactive organic matter and iron sulphides. The ΔSO_4 values in and downgradient of the Rhine nitrate front do not deviate significantly from zero, which indicates that nitrate is predominantly consumed by oxidation of organic matter. This can be explained by the position of the NO_3^- front still in the upper parts of these sands, where iron sulphides, if formerly present, were oxidized in the period 1853-1957 AD (see above). Anyhow, where denitrification is complete, ferric hydroxides that contain PO_4^{3-}, As and Mn as an impurity, and MnO_2 are unstable and dissolve. Phosphate may also derive from apatites or calcite to which it was adsorbed during decomposition of organic matter in earlier times. Due to their limited supply or availability, PO_4^{3-}, Mn and As ions steadily increase downgradient by progressive leaching, as shown in Fig.7.14 for PO_4^{3-} and Mn, and in Fig.7.17 for As. At a certain distance a peak is formed, Mn farthest downgradient and PO_4^{3-} most upgradient, due to adsorption of the swollen wave.

The major changes for aquitards 1C and 1D and the intercalated sandy aquifer (Fig.7.14), are connected with a redox change from deep anoxic (sulphate reducing or methanogenic) into anoxic (sulphate-metastable), about 40 years before or since the introduction of Rhine water. This change is inferred from sulphate logs in 1903-1915 with temporary piezometers (for a listing see Stuyfzand, 1988b), showing a nearly complete SO_4^{2-} reduction in aquitard 1C, and the present overall penetration of Rhine sulphate, on most locations without clear signs of reduction ($\Delta SO_4 \approx 0$, no H_2S smell). Only aquitard 1D shows a rather consistent, small sulphate reduction of about 0.1 mmol/l.

The main reason for the redox change could be the strongly increased SO_4^{2-} flux by combination of

increased flow velocities and SO_4^{2-} concentrations (Rhine water contains about 2-4 times more than the upper dune water in the rain water lens). This requires that the sulphate reducing capacity of aquitards 1C and 1D originally was low, and that the rate of sulphate reduction is too slow to yield perceptible changes against the relatively high backgrounds. A change from 13 to 0 mg SO_4^{2-}/l is noticed much easier than the change from 85 to 72 mg/l with further uncertainties due to strong fluctuations in the SO_4^{2-} input of Rhine water. A relatively low sulphate reducing capacity for these anoxic aquitards may result from a high content of ferric hydroxides. If sufficient Fe(III) is available, Fe(III)-reducing bacteria outcompete sulphate reducers and maintain concentrations of dissolved hydrogen, formate and acetate at levels lower than thresholds required by sulphate-reducing bacteria (Lovley & Phillips, 1987).

Anyhow, the redox environment in aquitard 1C and aquifer I_b in between aquitard 1C and 1D thus became favourable to high Fe and As concentrations. In sulphate reducing environments their concentration would drop by formation of iron sulphides with coprecipitation of As.

7.5.4 The generalized quality evolution downgradient

Generalized changes down the hydraulic gradient are depicted in Fig.7.17 for the same parameters as shown in the cross sections and, in addition, for SO_4^{2-}, NH_4^+, As, Co, F^-, Zn, the chemical water type and hydrochemical facies. The flow path is indicated in Fig.7.14 (SiO_2), the position of the aquitards 1C and 1D in Fig.7.17 as well.

Concentrations were extremely low along the whole flow path for the following TEs : Al (<20), Ce (<0.024), Cr (0.1-0.5), Cu (<1-3), Eu (<0.015), Hf (<0.01), Lu (<0.002), Nd (<0.0005), Ni (≤4), Pb (0.2-2), Sb (<0.5), Sc (≤0.05), Se (<0.5), Tb (<0.01), Th (<0.01), Ti (<2), V (<0.3) and U (<1.2), all in µg/l. This corresponds with calcareous dune water several metres below the phreatic level in the upper aquifer and in the Holocene aquitards. Low concentrations of the lanthanides and actinides in pretreated Rhine water and a low mobility for Cr, Cu, Ni, Pb and V are postulated. The following 6 zones are discerned downgradient (Fig.7.17) :

I. The (sub)oxic zone (0-140 m)

Relatively few changes occur in this environment, with respect to the major constituents of pretreated Rhine water in the supply canal. Water at the downgradient end is about 3 years old, which means that the subsoil has been flushed there with Rhine water 8 times ([1981-1957]/3). Breakthrough should therefore be complete for substances with an $R_i < 8$.

Simplifying the cation exchange into a displacement process of all sorbed cations (CEC = 6 meq/kg for dune sand) by the cations in pretreated Rhine water (Σcations = 8.6 meq/l), yields a R_i of 4 calculated with Eq.7.6. This corresponds with the general lack of negative ΔNa, ΔK and ΔMg values in this zone. Beyond about 90 metres of flow slightly negative values for ΔNa are found, however, which probably correspond with a renewed sorption due to the extreme salt input in the years 1971-1976 (Fig.7.19). Vagaries in the ΔNa pattern may occur within zone I as the result of sorption phenomena accompanying the passage of seasonal and irregular NaCl peaks and dips in the Rhine input. This can be observed in the hydrochemical log of well 24H.478 in Fig.7.18, where the passage of high Cl^- water of August through December 1978 and low Cl^- water of February 1978 through July 1978 in between 2 m+MSL and 4 m-MSL is clearly accompanied by exchange of Na^+ for Ca^{2+}.

The complete breakthrough of fluoride in this zone is consistent with a R_i of about 5 for dune sand, as observed south of Katwijk (Stuyfzand, 1991d). The Co decrease beyond 90 m. may reflect the breakthrough of the Rhine input, but could also be the result of a natural mobilization as observed in calcareous dune water in the same (sub)oxic beach sand (Fig.7.8).

Phosphate did not break through yet in the wells 477 and 478, which are closest to the supply canal. This is consistent with the observed retardation factor for PO_4^{3-} in dune sand ranging from 10-55, for both an adsorption (Stuyfzand, 1986d p.226) and desorption front (Stuyfzand et al., 1991). Schematizing the phosphate input signal as a three-step function (0.20 mg PO_4^{3-}/l for the period 1957-1969, 0.55 for 1970-1974 and 0.10 since 1975), yields with a median R_i of 30 the following front positions: 30 m for the 0.20 mg front, 13 m for the 0.55 front and 7 m for the 0.10 front.

The concentration of dissolved organic carbon is somewhat reduced by sorption and biodegradation, especially in the first metres. Close to the next zone Zn and As are mobilized and Co immobilized.

II. The anoxic zone (140-290 m)

The interface between zone I and II approximately coincides with the transition from dune into beach sand. It is characterized by complete denitrification, probably through decomposing organic matter in the richer beach sands (section 7.5.3 under "Historical changes etc."). The change in redox environment is reflected as usual, in increases for HCO_3^-, Fe, Mn, As, PO_4^{3-} and SiO_2 (see zone IV in section 7.4.4).

The first HCO_3^- increase (Fig.7.17) is related to

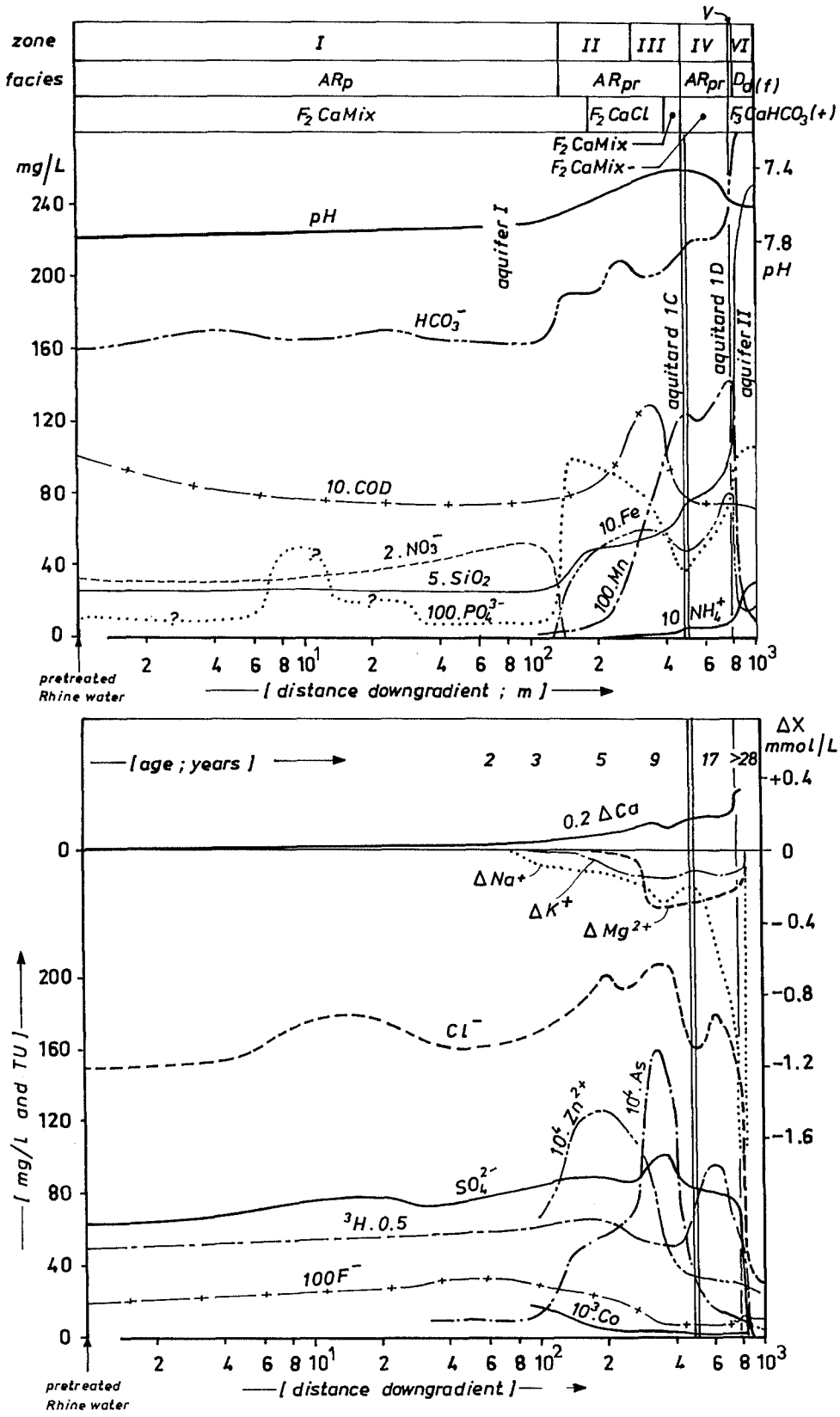

FIG. 7.17 Generalized chemical evolution of pretreated Rhine water along a flow path from the recharging supply canal towards its intrusion front about 800 m downgradient in the upper parts of the second aquifer, in March 1981. The zones are discussed in the text, the facies symbols are explained on Enclosure 8.

the NO_3^- decrease (Eq.8.12A). This cannot be deduced from well log 478 in Fig.7.18, partly because of seasonal effects : Rhine water, that infiltrated in May-August with a much lower NO_3^- concentration and therefore with a lower HCO_3^- production upon denitrification, occupied the denitrification zone at that moment.

The high PO_4^{3-} levels strongly exceed any possible supply from decomposing organic matter. This is further evidenced by the diverging behaviour of NH_4^+ and PO_4 in zone II in the hydrochemical log of well 24H.478 (Fig.7.18), whereas decomposing organic matter as a unique source would yield a more parallel behaviour (Fig.7.11). The bulk of the phosphate peak within this zone, must therefore stem from inorganic phases, either adsorbed to for instance calcite and $Fe(OH)_3$ or contained in for instance apatite. The PO_4^{3-} and As levels attained in the beach and shallow marine sands (resp. 1 mg/l and 14 µg/l or even more) at a certain point downgradient exceed the normal levels for dune groundwater in this zone (resp. 0.5 mg/l and 2-6 µg/l), probably because of protracted lateral flow (section 7.5.3 under "Historical changes etc."). The diverging behaviour of PO_4^{3-} and NH_4^+ can also be observed in dune groundwater (Fig.7.8), although less clearly.

The relatively sluggish increase of Mn as compared to Fe (Fig.7.14 and 7.18) probably reflects the geochemical availability of Mn, which is low in dune and beach sands and becomes higher in the underlying shallow marine, finer-grained sands (see zone III).

The second HCO_3^- increase at 200-250 metre (Fig.7.17) should relate to the decrease in calcite saturation index of the pretreated Rhine water and the increase in potential acidity through NH_4^+, in 1974 (section 7.5.3). The Zn peak can be connected with adsorption on its downgradient front and desorption in connection with lower concentrations in the input since about 1965 (similar to the Pb pattern in Fig.4.25). Both F^- and Co decrease to natural concentrations near the exit from this zone.

The sum of ΔNa, ΔK and 2ΔMg decreases further in zone II, from -0.12 meq/l to -0.52 meq/l, with Na^+ as the dominant ion adsorbed. The changes in ΔNa relate to the raised Cl^- concentrations in the Rhine input during the period 1971-1976, and do not reject the general conclusion that the principal Na^+ front is further downgradient (in zone IV). However, for K^+ the principal front occurs within this zone, at about 200 m and yields a R_K of 5.

The water type changes from F_2CaMix to F_2CaCl, in connection with the raised Cl^- concentrations in the period 1971-1976. The facies is calcareous, anoxic sulphate-(meta)stable, without significant base exchange (notwithstanding small negative values for ΔNa and ΔK), and polluted.

III. The anoxic, inner salinized zone (290-480 m)
This zone starts, along the flow path, in the shallow marine sands. Closer to the supply canal the upper parts of zone III are situated deeper, just below the top of aquitard 1C (Fig.7.18). The ΔNa, ΔK and ΔMg values are typically negative, together not yet sufficient to score a significantly negative BEX according to the criteria in Table 2.7, also because the latter refers to sea salt from which Rhine salt differs. Their values are sufficient, however, to indicate effects of salinization. The sum of ΔNa, ΔK and 2ΔMg values changes within zone III from -0.52 to -1.04 meq/l, whereas the main counter-ion in the exchange reaction, Ca^{2+}, shows an increase of ΔCa from +1.2 to +1.6 meq/l (Fig.7.15). Its increase is slightly suppressed by precipitation of about 0.06 mmol $CaCO_3$/l (½[1.6-1.2] - ½[1.04-0.52]), as evidenced by a double as high decrease for HCO_3^- (about 10 mg/l : Fig.7.17). The dominant cation adsorbed is Mg^{2+} : ΔMg ≈ -0.6 meq/l, ΔNa ≈ -0.24 meq/l and ΔK ≈ -0.15 meq/l. This corresponds with its higher selectivity as compared to Na^+. The principal Mg^{2+} front is situated at the entrance of zone III at 300 m, and yields a R_{Mg} of 3.

Other important changes already discussed in section 7.5.3, are : (a) a further, strong Mn increase whereas Fe decreases somewhat, (b) a further increase in SiO_2 concentration, (c) a COD peak, and (d) a strong As peak. The water type changes within zone III from F_2CaCl back to F_2CaMix, in consequence of a decreasing chlorinity conform the Rhine input record. Notwithstanding a notable decrease of BEX below zero, the facies remains equal to that in zone II.

IV. The anoxic, outer salinized zone (480-800 m)
Along the flow path studied, this zone starts in aquitard 1C and terminates at the lower face of aquitard 1D, immediately behind the Rhine intrusion front. The main reaction here is the cation exchange of Na^+ for Ca^{2+}, which constitutes the initial phase of cation exchange (see section 7.3.4). The value of ΔNa decreases from -0.2 meq/l to -1.7 meq/l, whereas ΔCa changes from +1.6 to +3.2 meq/l (Fig.7.15). The about 0.1 meq higher change in ΔCa as compared to the change in ΔNa, can be attributed to $CaCO_3$ dissolution in connection with the extreme agressivity towards calcite (SI_c ≈ -0.55) and high NH_4^+ concentrations, yielding additional acidity upon nitrification, of the Rhine input in the early 1960s (Fig.4.26 and 4.25, resp.).

The 0.5 mmoles HCO_3^-/l gained in zone IV, can be largely accounted for by (a) this $CaCO_3$ dissolution (0.1 mmol), (b) $Fe(OH)_3$ reduction (0.14 mmol) and (c) sulphate reduction in aquitard 1D (0.1 mmol yielding 0.2 mmol HCO_3^-/l). The values of ΔK and ΔMg slighlty increase (Fig.7.15), probably in

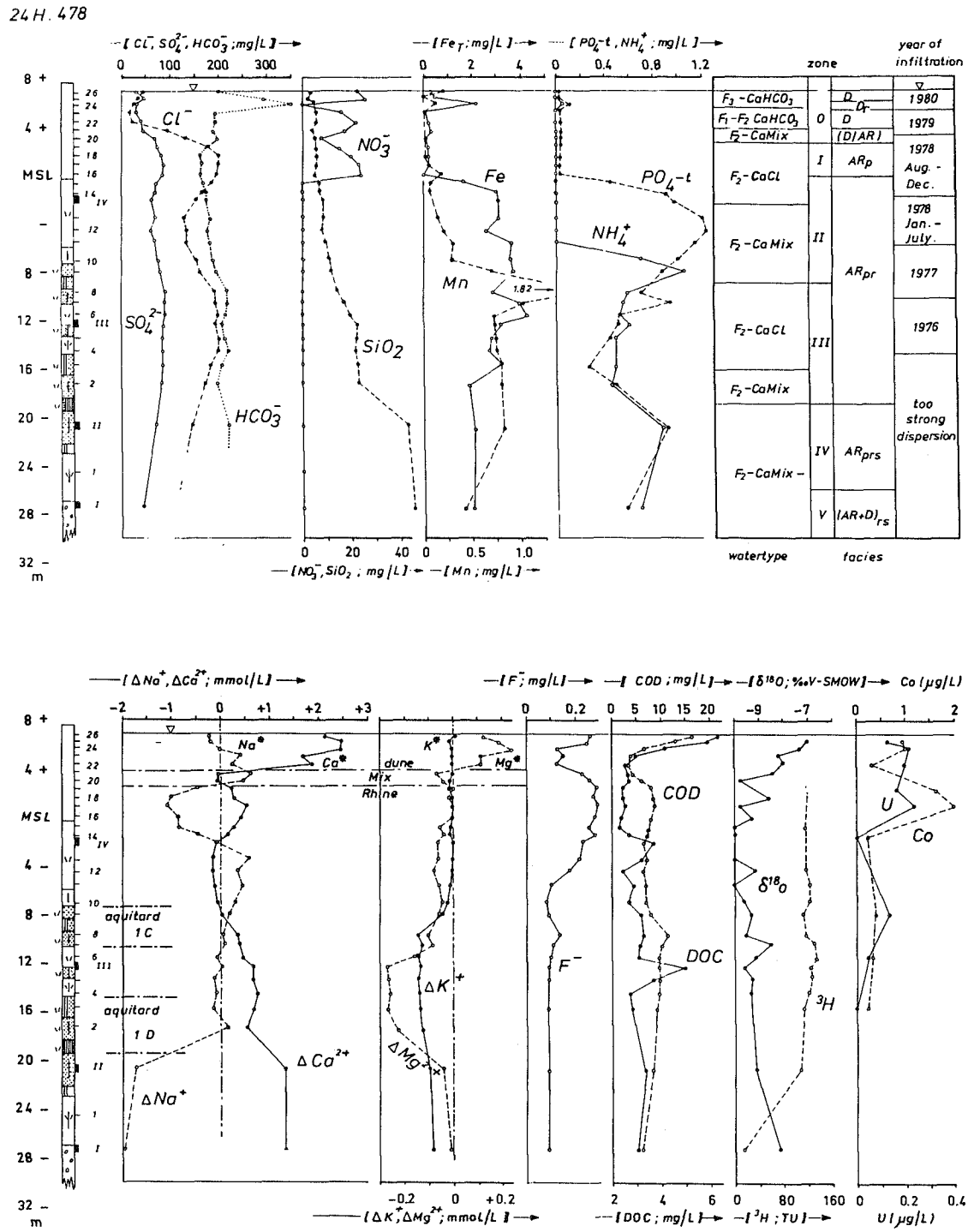

FIG. 7.18 Hydrochemical log of multilevel well 24H.478 at 95 m from the recharging supply canal, in the Barnaart-Van der Vliet dune area south of Zandvoort aan Zee, in March 1981.

relation to the lower chlorinity of the Rhine water. The retardation factor for Na^+ as derived from the breakthrough curve, is about 1.2.

Other changes consist of earlier discussed increases in concentration of SiO_2, Fe, Mn and PO_4^{3-}. There is a significant NH_4^+ increase of 0.5 mg/l, due to the decomposition of organic matter by $Fe(OH)_3$ reduction, desorption or both. The water type is F_2CaMix- and the facies consequently changed into one with a significantly negative BEX.

V. The breakthrough zone (800-810 m)

The intrusion front of Rhine water is found just below aquitard 1D, in the upper zone of aquifer II, which is composed of aeolian sand belonging to the Twente Formation. The changes are the result of linear mixing with deep anoxic dune water from zone VI, and cation exchange. The water type changes within this zone from F_2CaMix- to F_3CaHCO_3, and the facies from calcareous, anoxic, salinized and polluted Rhine water to calcareous, deep anoxic and nonpolluted dune water without base exchange.

VI. Deep anoxic dune water (>810 m)

The quality of this calcareous, deep anoxic and nonpolluted dune water without base exchange is discussed in general terms in section 4.4.4. Tritium is below detection, which indicates an age superior to 27 years. The layer of dune water without base exchange, below the intruding Rhine water, may be less than 1 m thick. In that case F_3CaHCO_3+ dune water is found very close to the intruding Rhine water. The shallow position of this freshened dune water probably represents the upconing of deep dune water with an originally more pronounced freshened facies, from aquitards 2D and 2E (end of section 4.5.2).

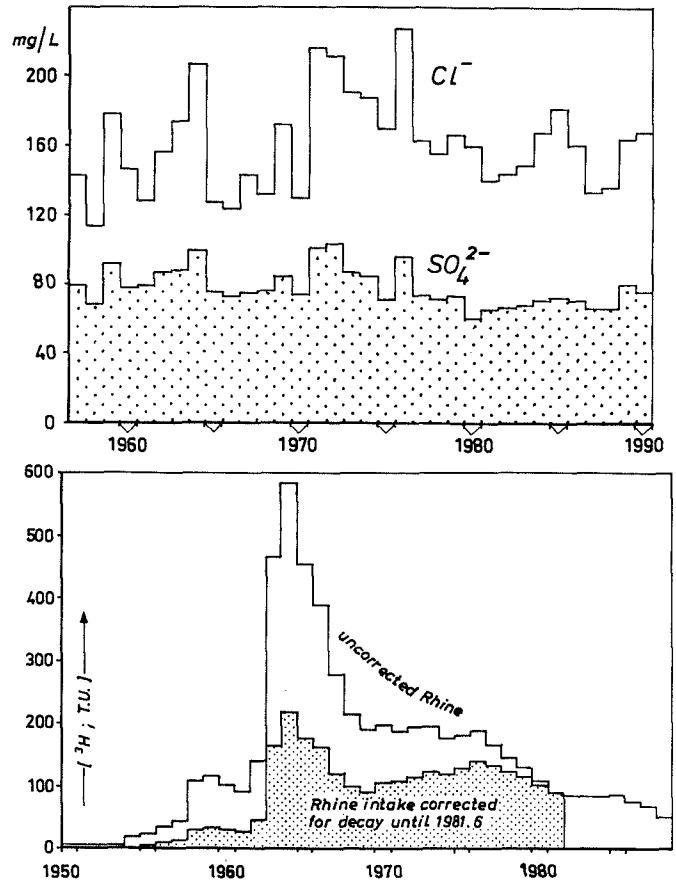

FIG. 7.19 Input signal of tritium, chloride and sulphate in pretreated Rhine water, recharged in dunes south of Zandvoort aan Zee. Anomalous years are used for groundwater dating.

7.5.5 Dating

Infiltrated Rhine water in the dunes can be dated in detail using the technique of both spatial and sequential history matching (see section 7.4.5). An example of sequential history matching is given in Fig.1.4. The spatial variant is applied to the cross section under focus here, using the environmental tracers chloride and tritium.

Anomalous years in the input signal of these semi-natural labels (Fig.7.19) can be easily traced back in the areal distribution of Cl^- and tritium (Fig.7.15). These are in order of increasing age : 1976 with Cl^- = 200 mg/l and ^3H = 128 TU; 1971-1972 with Cl^- = 212 mg/l and ^3H = 110 TU; 1968-1969 with Cl^- = 150 mg/l and ^3H = 100 TU; 1964 with Cl^- = 180 mg/l and ^3H = 200 TU; 1961-1962 with Cl^- = 145 mg/l and ^3H = 60 TU; and dune water before 1953 with ^3H < 1 TU. With these key years, the 24 years old interface between Rhine and displaced, deep dune water, and additional information in the input record, years of infiltration were determined for Rhine groundwater samples where possible. The results are shown together with the derived isochrones in Fig.7.20. The age distribution obtained, reveals the expected high flow velocity in the upper aquifer and a strong delay in the aquitards 1C and especially 1D. It should be noted that this pattern is distorted by vertical exaggeration and by a very close hydrological position of the wells 480 through 482 (in section remote from each other). The latter is related to the oblique position of the cross section and complications in the groundwater flow pattern (Fig.3.47).

It is quite remarkable that the 1964 peak of 218 TU is traced back at a distance of 610-790 m, without significant smoothing (206 TU), whereas it is levelled off in other parts of the section (Fig.7.15 and 7.18). This is explained by the low longitudinal dispersivity of the homogeneous, well sorted dune, beach and shallow marine sands, and a much higher

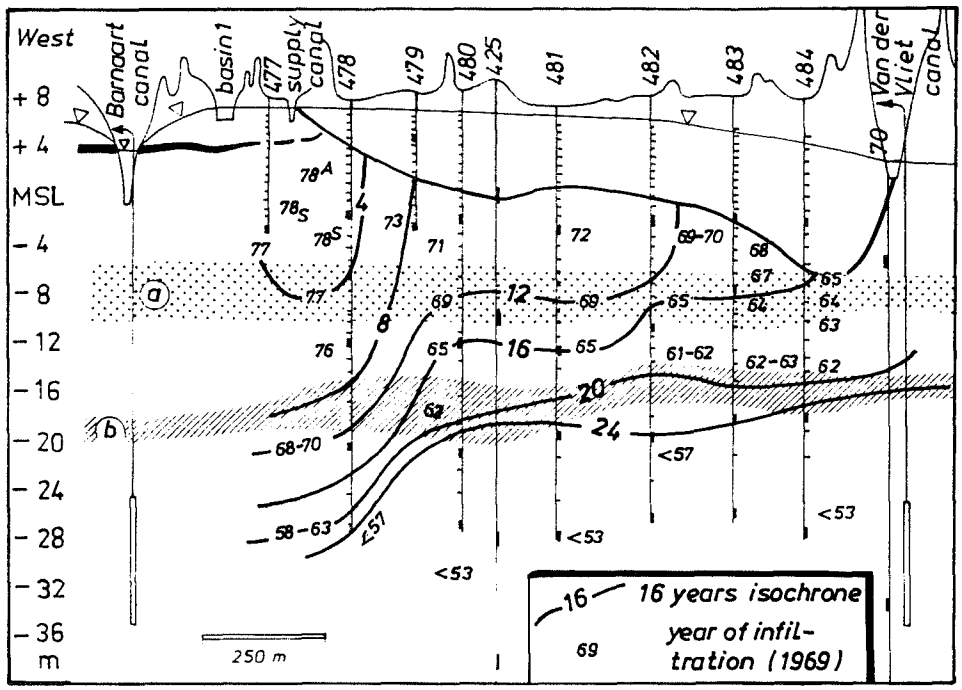

Fig. 7.20 Age distribution of recharged Rhine water in the cross section over the Barnaart - Van der Vliet area, south of Zandvoort aan Zee, in March 1981. 78^A, 78^S = autumn and summer 1978, resp. a,b = aquitard 1C and 1D, resp.

dispersivity of the very heterogeneous aquitards 1C and 1D. When the 1964 tritium peak is roughly approximated as part of a sinus with a period of 10 years (see also section 7.4.5), Eq.6.19 would yield a damping of only 1% after insertion of the following data : α_L = 0.1 m, a flow velocity of 0.13 m/d (17 years to reach well 484) and X = 790 m. This corresponds well with the damping observed.

Comparison with hydrological calculations

The travel time of water (dt) in the saturated subsoil over a distance dX can be calculated from the hydraulic properties of the subsurface and the hydraulic gradient with Darcy's law, in days :

$$dt = \frac{-\varepsilon}{K_h} \cdot \frac{dX}{dH} \cdot dX \qquad (7.7)$$

with : ε = porosity (fraction by volume; K_h = horizontal permeability [m/d]; dH/dX = slope of the phreatic head [-].

Integration of dH/dX (={ } in Eq.3.23), under the general boundary conditions mentioned in section 3.10.2 and with initial condition t = 0 for X = 0, yields :

$$t_x = \frac{-\varepsilon\lambda^2}{K_h\sqrt{A}} \cdot \ln\left[\left\{\frac{2C_2e^{\frac{X}{\lambda}} + B\lambda - \sqrt{A}}{2C_2e^{\frac{X}{\lambda}} + B\lambda + \sqrt{A}}\right\} \cdot \left\{\frac{2C_2 + B\lambda + \sqrt{A}}{2C_2 + B\lambda - \sqrt{A}}\right\}\right] \qquad (7.8)$$

if A > 0, and

$$t_x = \frac{-2\varepsilon\lambda^2}{K_h\sqrt{-A}} \cdot \left[\arctan\left\{\frac{2C_2e^{\frac{X}{\lambda}} + B\lambda}{\sqrt{-A}}\right\} - \arctan\left\{\frac{2C_2 + B\lambda}{\sqrt{-A}}\right\}\right] \qquad (7.9)$$

if A < 0, and

$$t_x = \frac{-2}{2C_2e^{\frac{X}{\lambda}} + B\lambda} \qquad (7.10)$$

if A = 0, with : $A = B^2\lambda^2 + 4C_1C_2$; and $B = (\varphi_m - \varphi_o)/M$,

where : t_x = travel time in the subsoil from the recharge canal to X [d]; X = horizontal distance from the supply canal along the flow path [m]; ε = porosity [-]; K_h = horizontal permeability [m/d]; $\lambda = \sqrt{(K_h D c_v)}$ = leakage factor [m]; C_1 = integration constant (Eq.3.22C); C_2 = integration constant (Eq.3.22D); c_v = vertical flow resistance [d]; D = mean thickness upper aquifer [m]; φ_m = piezometric head in second aquifer at distance M to supply canal [m+MSL]; φ_o = ditto at X = 0 [m+MSL]; M = distance from point M to supply canal along X-axis [m]. Note that observation point M may

TABLE 7.4 Basic data for observation wells 24H.477-484 in the Barnaart - Van der Vliet area south of Zandvoort aan Zee, with the observed and calculated travel time in the subsoil (t_x), thickness of the rainwater lens (D_x) and transition zone of 10 to 90% rainwater (D_{10-90}). The following soil constants apply : K_h = 12 m/d, ε = 0.38, c_v = 14,600 d, $D = 0.5(H_o+H_x) + 16$ [m], λ_T = 0.0025 m. The position of the wells is shown in Fig.3.47 and 7.20.

Well no	X	N	H_o	H_x	φ_o	φ_x	D_x	D_{10-90}	t_x	D_x	D_{10-90}	t_x
								observed			calculated#	
	(m)	(mm/y)	(m+MSL)				(m)	(m)	(y)	(m)	(m)	(y)
477	50	450	6.97	6.92	0.60	0.63	5.1	1.4	3	4.8	1.3	4.3
478	95	480	6.97	6.67	0.68	0.64	3.1	2.0	2.5	3.1	1.8	2.6
479	235	295	6.85	6.29	0.32	0.18	6.1	2.4	8	6.2	2.8	8.6
480	345	300	6.81	5.91	0.16	-0.05	6.6	2.6	10	8.2	3.4	11.5
481	375	290	6.80	5.65	0.34	0.07	5.8	2.8	9	7.4	3.5	10.6
482	500	305	6.78	5.15	0.25	-0.07	6.7	2.8	11.5	9.4	4.1	13.4
483	610	290	6.76	4.48	0.21	-0.19	7.1	4.6	13.5	7.9	4.3	14.2
484	790	330	6.74	3.57	0.27	-0.21	10.4	5.6	16.5	12.1	5.1	17.3

: D_x using Eq.3.23, D_{10-90} using Eq.3.24 with α_T = 0.0025 m, and t_x using Eq.7.8.

coincide with X, but this is not necessary.

A simplified calculation of t_x, which derives from Eq.7.7 directly in case of a steady flow velocity downgradient, reads :

$$t_x = \frac{-\varepsilon X^2}{K_h(H_x - H_o)} \qquad (7.11)$$

Application of Eqs.7.8-7.10 to the upper aquifer, with K_h = 12 m/d, ε = 0.38, D = 21-23 m and c_v of the underlying aquitard 1D being 14,600 d, yields the calculated travel times to the observation wells 477-484 that are given in Table 7.4. Changes in the position of the water table during the respective transit period for each well, as observed in old piezometer nests in the area, were included in the calculation. This explains the slight differences in H_o and somewhat larger differences in φ_o. The calculated travel times correspond very well with the hydrochemically determined ages (Table 7.4).

7.6 Intruding North Sea water

7.6.1 Situation and collection of hydrochemical data

The densest observation network for deep seated North Sea water intruding inland, is found about 2 km south of Zandvoort aan Zee, across the artificial recharge area discussed in the previous section towards the Haarlemmermeer polder. Most of the piezometer nests examined here, plot in cross section F (Fig.7.21). Two intruding flow branches are examined, a 10 km long flow branch, still intruding at 120-200 m-MSL into relict Holocene transgression water of the coastal type in the Haarlemmermeer polder (section 7.6.2), and a 2 km long one, which intruded into dune water mainly before 1957, at 60-100 m-MSL (section 7.6.3).

The acquisition and screening of hydrochemical data is elucidated in general terms in section 4.2.3. This applies to about 200 brackish to salt groundwater samples in a 2 km broad band along section F, collected in the period 1939-1987. Inspection of these data led to a selection of 20 piezometers for resampling in June 1987. The samples were analysed on major constituents by PWN using conventional analytical techniques, and on several trace elements by KIWA, using the techniques specified in section 4.2.3.

7.6.2 Intrusion into relict Holocene transgression water

North Sea water at 120-200 m-MSL intrudes into relict Holocene transgression water in the Haarlemmermeer polder. Its quality changes downgradient over 10 km, can be deduced from the analyses in Table 7.5, where the wells are listed in order of increasing distance to the present HWL, and from Fig.7.22, where the most evident long-distance changes are depicted. All piezometers involved in this survey are positioned in aquifer III_B, which is composed of very coarse sands poor in reactive solid phases, belonging to the Harderwijk Formation.

The exact length of the flow path chosen, is unknown because of a strong reduction of the fresh water tongue below the sea in the period 1853-1957 (Fig.3.35). The length of this tongue diminished from about 800 m in 1850 (Stuyfzand, 1988b) to about 100-200 m in 1981. The present position of

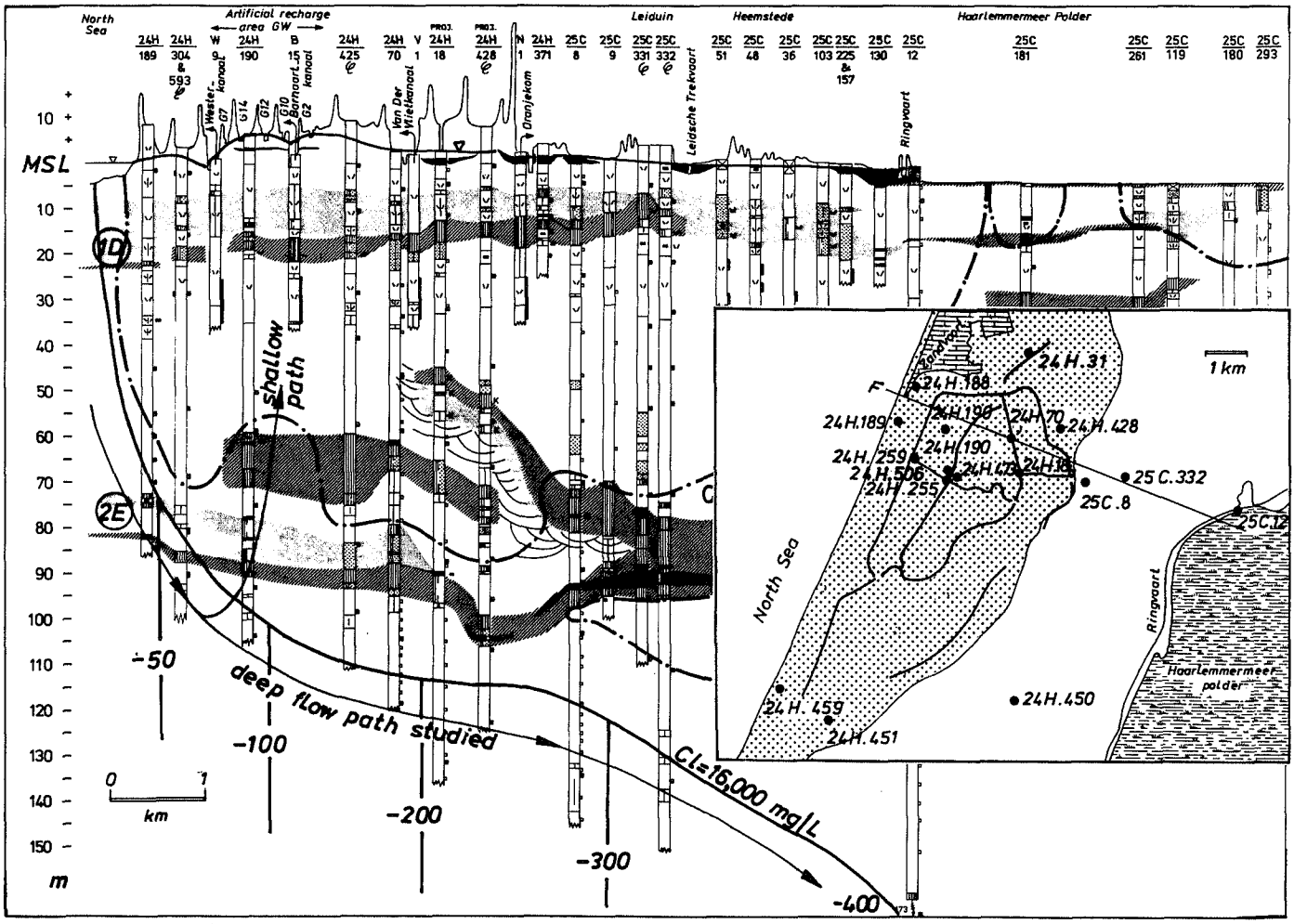

FIG. 7.21 Position of the North Sea flow branches studied. The situation of those piezometers is indicated, for which chemical analyses are listed in Table 7.5 or 7.6.

the HWL has been taken therefore as a measure of the distance travelled in the subsurface. The exact position of the intrusion front cannot be easily determined either, because the relict Holocene transgression water probably consists of the coastal type (section 4.4.2), which is essentially about the same as the coastal North Sea water considered here. However, its chlorinity probably was slightly lower (12,000-15,000 versus 16,000-17,000 mg Cl^-/l) due to the admixing of fresh Rhine water, that was discharged by the Old Rhine outlet near Katwijk till about 850 AD. The front could therefore be close to the western border of the Haarlemmermeer polder (well 25C.12), which is corroborated by hydrological calculations in Fig.4.7 and section 4.4.3.

The data presented, indicate relatively strong quality changes in between the North Sea and first observation well. They consist of the complete elimination of O_2 and NO_3^-, a decrease in pH, F^- and K^*, an increase of HCO_3^-, PO_4, Ca^{2+} (and Ca^*), NH_4^+, Fe, Mn, SiO_2 and Ba^{2+}. These changes largely correspond with the meanwhile well-known effects of decomposing organic matter in the aquitards 1D and 2E, dissolution of ferric hydroxides, biogenic opal and shell fragments, and sorption of F^- and K^+ (section 7.5). Barium is probably mobilized by desorption, because North Sea water is supersaturated with respect to barite already (Table 7.5) and no complexing organics seem to have joined the solution. Changes in Na^*, Mg^* and SO_4^* are considered insignificant, also because they appear erratic due to small analytical errors.

Further downgradient relatively few changes occur. Sulphate behaves conservatively in the coarse grained Harderwijk Formation, so that effects of further redox reactions are limited to an increase of the Fe concentration from circa 8 to 12 mg/l. Exchange of Na^+ and Mg^{2+} does not occur, which

TABLE 7.5 Inorganic composition of coastal North Sea water near Zandvoort aan Zee and intruded North Sea water in aquifer III_B along section F (Fig.7.21) towards the Haarlemmermeer polder, in 1987.

piezo-meter no.	sample depth m+MSL	dist. HWL m	estim age y	temp °C	EC 20°C µS/cm	pH	Cl^- mg/l	SO_4^{2-} mg/l	HCO_3^- mg/l	NO_3^- mg/l	PO_4T mg/l	Na^+ mg/l	K^+ mg/l	Ca^{2+} mg/l	Mg^{2+} mg/l	Fe mg/l	Mn mg/l	NH_4^+ mg/l	SiO_2 mg/l	DOC mg/l	O_2 mg/l	watertype	code
North Sea	0	0	0	10.5	39000	8.1	16800	2355	160	3	0.51	9350	346	350	1122	<0.1	<0.1	0.4	0.9	2.4	9.4	S_2NaCl	S
24H.459	-110	150	60	11.5	39400	7.1	17200	2400	205	<1	1.90	9400	350	425	1255	8.6	0.71	4.2	10.5	2.4	<0.2	S_2NaCl	S_r
24H.259	-105	800	80	11.5	40700	7.2	16300	2294	253	<1	2.78	9208	330	357	1080	6.4	0.46	6.1	10.5	4.9	<0.2	S_3NaCl	S_r
24H.190	-103	1280	100	12.5	40500	7.2	16320	2129	438	<1	3.79	9300	303	375	1090	8.7	0.41	8.1	-	7.4	<0.2	S_3NaCl	S_r
24H.451	-97	1600	110	12.0	39200	7.3	16700	2400	240	<0.2	3.20	9200	315	400	1095	8.6	1.24	5.1	9.7	4.8	<0.2	S_3NaCl	S_r
24H.506	-132	1840	115	11.0	38900	7.2	16900	2400	220	<0.2	3.10	9300	335	420	1225	6.5	0.69	4.0	11.0	2.2	<0.2	S_2NaCl	S_r
24H.473	-171	1920	120	11.5	38900	7.0	16900	2300	220	<1	2.60	9300	345	435	1210	10.0	0.74	4.4	13.0	2.4	<0.2	S_2NaCl	S_r
24H.031	-134	2530	140	12.5	36800	7.3	16800	2260	230	<1	-	9500	340	305	1100	13.2	0.74	4.6	13.2	-	<0.2	S_2NaCl	S_r
24H.070	-118	2830	150	12.0	39300	7.4	16185	2300	253	<0.2	2.11	9300	313	425	1100	13.8	0.65	6.8	-	4.5	<0.2	S_3NaCl	S_r
24H.018	-132	3370	165	11.0	36750	7.6	16800	2120	260	<0.2	-	9500	310	310	1080	12.5	0.56	5.8	10.2	-	<0.2	S_3NaCl	S_r
24H.428	-123	3850	180	11.5	38150	7.2	17000	2250	247	<1	-	9400	300	400	1210	10.0	0.99	7.2	12.8	-	<0.2	S_3NaCl	S_r
25C.008	-134	4840	400	12.5	37500	7.3	15410	2198	238	<1	1.04	8515	267	429	1025	11.0	0.63	8.9	-	4.0	<0.2	S_2NaCl	S_r
25C.332	-136	5760	960	12.0	36700	7.0	15800	2200	225	<0.2	1.00	8400	265	480	1155	11.0	0.76	8.1	12.0	2.5	<0.2	S_2NaCl	S_r
25C.012	-165	8600	>2000	11.0	36000	7.1	14752	2132	290	<0.2	0.92	8218	249	459	990	12.8	0.56	10.6	-	5.8	<0.2	S_3NaCl	S_r

piezo-meter no	sample depth m+MSL	Al µg/l	As µg/l	B µg/l	Ba^{2+} µg/l	Be ng/l	Br^- µg/l	Co µg/l	Cu µg/l	F^- µg/l	I µg/l	Li^+ µg/l	Mo µg/l	Ni µg/l	Pb µg/l	Rb^+ µg/l	Se ng/l	Sr^{2+} ng/l	U µg/l	V µg/l	Zn µg/l	$\delta^{13}C$ ‰	$\delta^{18}O$ ‰
North Sea	0	5	2.5	3900	40	<10	56000	0.2	1.4	1200	55	160	10.7	0.9	0.7	103	90	7100	2.6	1.9	5	-	-1.3
24H.459	-110	-	-	-	140	-	-	-	-	160	-	-	10.0	-	-	-	-	-	-	-	-	-	-
24H.259	-105	25	-		120	<10	58000	1.1	≤5.8	240	73	175	6.2	-	<3	9.6		7000	<0.05	1.3	26	-11.1	-1.3
24H.190	-103	-	-		250	-	-	-	-	40	-	-	2.4		-	-		-	-	-	-	-	-
24H.451	-97				370		56000	-		130			7.0										
24H.506	-132				-		-	-		-			-										
24H.473	-171				120					170			8.8										
24H.031	-134				-					-			-										
24H.070	-118	-	-		130		-	-		50	-	-	5.6		-	-	-	-	-		-		-
24H.018	-132	<5	8		140		55000	0.1		40	137	165	5.6		<3	10.0	13	7000	<0.05		25		-1.3
24H.428	-123	-			-		-	-		-	-	-	-		-	-	-	-	-		-		-
25C.008	-134				150					30			3.7										
25C.332	-136				200		-	-		60	-	-	9.5			-		-			-		
25C.012	-165	-	-	-	120	-	55000	-	-	10	120	170	3.8	-	-	10.0	-	7000	-	-	<4	-	-

piezo-meter no.	sample depth m+MSL	sea salt corrected (µmol/l) Na^*	K^*	Ca^*	Mg^*	SO_4^*	BEX meq/l ##	SATURATION INDEX log(IAP/K_s)† Hydroxides & sulphates gibbsite #	alunite #	barite	Silicates SiO_2	albite #	illite #	kaol #	Carbonates calcite	dolom	magn	sider	rhodo	Phosphates & fluorides apatO	apatF	vivian
North Sea	0	0	0	0	0	0	0	0.03	-3.5	0.33	-1.84	-2.7	-1.7	-0.72	0.50	1.66	0.67	-13.5	-5.2	1.9	4.0	-41.5
24H.459	-110	-7381	-120	1483	4396	-107	1.3	0.32	0.30	0.85	-0.78	-0.19	1.7	2.0	-0.28	0.08	-0.13	-0.43	-1.5	-0.03	2.1	-0.65
24H.259	-105	6532	-147	274	-277	132	5.8	1.3	2.8	0.79	-0.78	0.82	3.9	3.9	-0.15	0.34	0.00	-0.35	-1.4	0.66	2.9	-0.35
24H.190	-103	9566	-871	702	25	-1644	8.7	0.34	-0.12	1.1	-0.81	-0.16	1.7	2.0	0.12	0.88	0.27	0.05	-1.2	1.2	2.7	0.32
24H.451	-97	-3980	-752	1124	-813	623	-6.4	0.33	-0.31	1.3	-0.82	-0.11	1.7	1.9	-0.02	0.56	0.09	-0.14	-0.93	1.5	3.4	0.35
24H.506	-132	-4471	-346	1517	3986	331	3.2	0.33	0.06	1.1	-0.75	-0.02	1.9	2.1	-0.21	0.39	-0.03	-0.56	-1.3	1.3	3.8	-0.44
24H.473	-171	-4471	-90	1892	3369	-710	2.2	0.28	0.45	0.77	-0.69	-0.06	1.8	2.1	-0.33	-0.07	-0.21	-0.43	-1.5	0.00	2.3	-0.39
24H.031	-134	6649	-165	-1299	-882	-981	4.7	0.32	-0.39	0.75	-0.69	0.29	2.2	2.2	-0.15	0.43	0.09	0.04	-1.2	0.63	2.2	0.67
24H.070	-118	12809	-545	2021	804	331	13.9	0.29	-0.76	0.81	-0.73	0.23	2.1	2.0	0.13	0.83	0.22	0.20	-1.1	1.5	2.9	0.83
24H.018	-132	6649	-933	-1174	-1705	-2438	2.3	-1.6	-1.6	0.82	-0.79	0.16	1.9	1.8	0.19	1.1	0.40	-	-0.95	1.2	2.3	1.7
24H.428	-123	-2541	-1294	965	3094	-1377	2.4	-1.4	-0.06	0.79	-0.69	0.18	2.1	2.2	-0.12	0.41	0.04	-0.18	-1.1	-0.18	1.3	-0.52
25C.008	-134	-2557	-1294	2532	-155	401	-4.2	0.32	-0.44	0.88	-0.74	0.10	1.9	2.1	0.02	0.60	0.09	0.01	-1.2	0.31	1.5	-0.22
25C.332	-136	-16997	-1556	3598	4127	-147	-10.3	-1.5	0.40	1.0	-0.73	-0.21	1.6	2.0	-0.26	0.02	-0.20	-0.34	-1.4	-0.96	0.85	-1.0
25C.012	-165	449	-1420	3629	217	674	-0.5	-1.5	0.18	0.82	-0.73	-0.11	1.7	2.1	-0.07	0.33	-0.08	-0.06	-1.4	-0.68	0.32	-0.55

= where Al was not analysed, a concentration of 3 µg/l was assumed; ## : BEX = (Na^* + K^* + 2Mg^*); † = calculated using WATEQX (Van Gaans, 1989).

can be explained by the high displacing power of sea water (Σcations = 515 meq/l) as compared to the low CEC of the Harderwijk Formation (about 0.5-1 meq/l according to Willemsen, 1984). The retardation factor approaches 1, and exchange should be completed for these ions within a maximum of respectively 2 and 2.5 pore flushes (Fig.7.25). About two pore flushes seem reasonable for a system that was previously flushed with coastal Holocene transgression water of high salinity.

Potassium, however, exhibits a clear progressive sorption (Fig.7.22). This is consistent with the behaviour of K^+ in intruding Rhine water (section 7.5) and the late breakthrough in column experiments (Fig.7.25; Beekman, 1991). Calcium and ammonium probably constitute the counter-ions in the exchange of K^+, as can be deduced from the field data (Fig.7.22) and laboratory experiments (Fig.7.25). The amount of Ca^{2+} released, exceeds the amount of K^+ sorbed minus the amount of NH_4^+ mobilized, so that an additional source is required. Dissolution of $CaCO_3$ has to be excluded as there is no HCO_3^- trend consistent with this reaction. Perhaps there is a slight adsorption of Mg^{2+} and Na^+

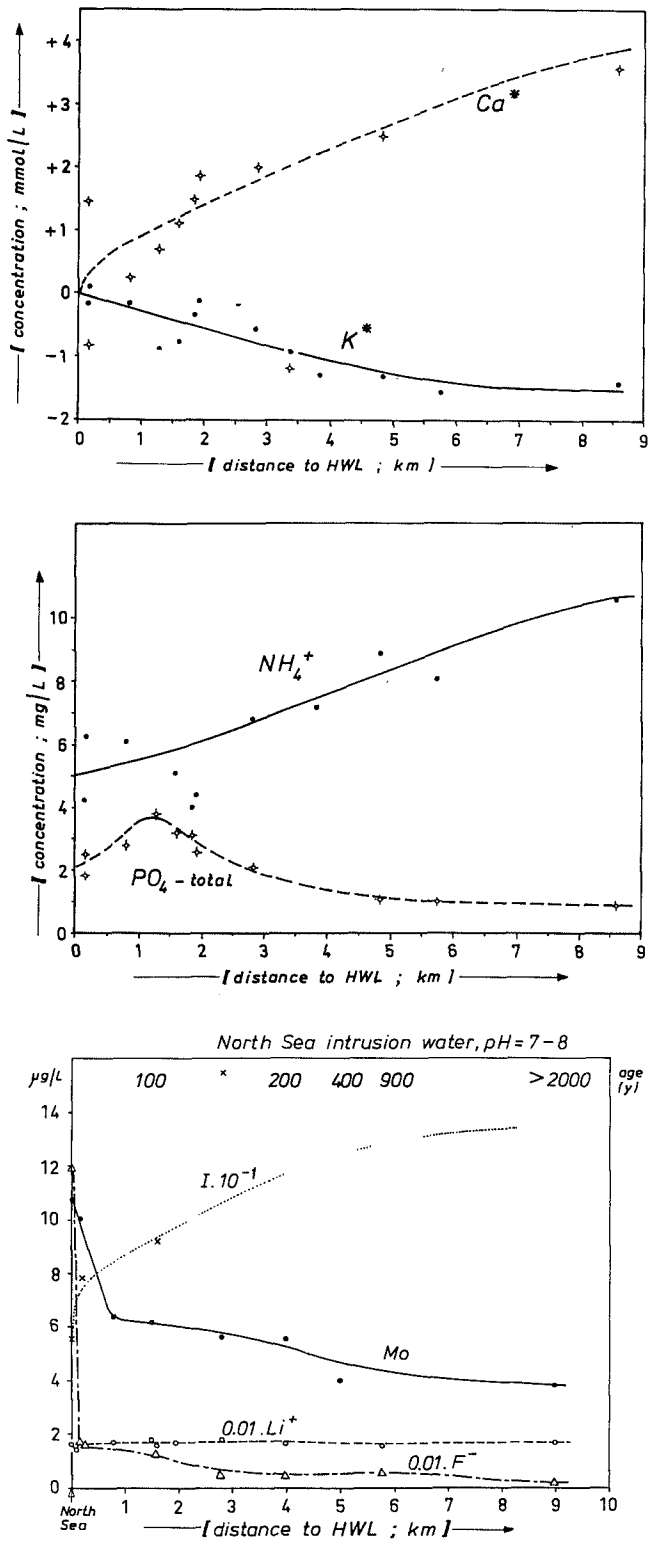

FIG. 7.22 Changes of North Sea water down the hydraulic gradient, at 100-170 m-MSL in aquifer III_B, intruding into relict Holocene transgression water in the Haarlemmermeerpolder. Based on data in Table 7.5.

downgradient, which is now obscured by analytical inaccurracies.

Phosphate exhibits a peculiar behaviour with a peak at a distance of 1-1.5 km from the HWL. The peak could be the result of more interaction with organic matter contained in aquitard 2E (at 70-90 m-MSL, Fig.7.21). Most of the wells involved, indeed have their screens relatively close to a well developed aquitard 2E. The decrease in PO_4 concentration further downgradient is probably caused by sorption. The trace elements F^-, Mo, Rb^+, V and U are likely adsorbed as well, whereas Li^+ and Sr^{2+} are not retarded, in a similar way as Na^+ and Ca^{2+}, respectively (Table 7.5 and Fig.7.22). The mobilization of iodide is not understood.

7.6.3 Intrusion into dune water

North Sea water intruded into dune water south of Zandvoort aan Zee, mainly in the period 1853-1957 (section 3.7). The most impressive hydrochemical logs displaying hydrochemical effects of salt water intrusion, were obtained with temporary piezometers during the drilling of new observation wells in 1939.

Piezometer nest 24H.255

The log of this observation well, drilled in 1939, is shown in Fig.7.23. The interface between fresh dune and salt North Sea water was drawn up there by about 30 m in the period 1905-1939. Cation exchange was the most prominent reaction accompanying the upconing of North Sea water. The meqs of Ca^{2+} released are about equal to the meqs of (Na^+ + Mg^{2+}) adsorbed (Fig.7.23) as expected from Eq.8.31. However, in the intrusion front a slight desorption of Mg^{2+} can be inferred, which is observed in the initial phase of salinization on many other locations as well. The phenomenon was noticed for the first time in model simulations by Appelo & Willemsen (1987), and subsequently demonstrated in column studies by Beekman & Appelo (1989). It can be explained as the result of Ca-Mg exchange when Na^+-depleted CaCl water enters an exchanger loaded mainly with Ca^{2+} and Mg^{2+}.

The more Mg^{2+} the exchanger contains the more prominent the Mg^{2+} release will be. A strong Mg^{2+} mobilization is therefore to be expected where salt water intrudes into a system which previously was in an intermediate stage of freshening, in the transition zone of F_3MgHCO_3+ to F_3NaHCO_3+ water. These conditions are satisfied near pumping station Bergen, where below freshening water types the relatively rare, salinizing water types F_2MgCl- and B_3MgCl- were found (Stuyfzand, 1989a).

NH_4^+, Fe and Mn are clearly mobilized in the intrusion front (Fig.7.23). Desorption is the most

TABLE 7.6 Inorganic composition of North Sea water intruding into dune water, with both end members (24H.259-103 and 24H.189-45) and their mixture in order of decreasing chlorinity.

piezo-meter no.	sample depth m+MSL	subsoil flow m	subsoil age§ y	temp °C	EC 20°C µS/cm	pH	Cl^- mg/l	SO_4^{2-} mg/l	HCO_3^- mg/l	NO_3^- mg/l	PO_4T mg/l	Na^+ mg/l	K^+ mg/l	Ca^{2+} mg/l	Mg^{2+} mg/l	Fe mg/l	Mn mg/l	NH_4^+ mg/l	SiO_2 mg/l	DOC mg/l	O_2 mg/l	watertype	code
24H.259	-105	800	80	11.5	40700	7.2	16300	2294	253	<1	2.78	9208	330	357	1080	6.4	0.46	6.1	10.5	4.9	<0.2	S_3NaCl	S_r
24H.190	-75	1300	130	12.0	27000	6.8	10865	1534	334	<0.2	0.61	5500	70	1150	613	14.9	1.57	13.0	30.0	4.6	<0.2	S_3NaCl-	$(S+D)_{rs}$
24H.259	-70	830	120	11.3	21450	7.1	8400	1044	367	<0.5	0.86	3800	140	770	750	8.2	1.24	11.0	14.2	-	<0.2	B_3NaCl-	$(S/D)_{rs}$
24H.189	-60	500	90	11.0	17970	6.8	7873	1032	293	<0.5	0.7	3593	21	1314	222	27.2	1.30	7.5	17.4		<0.2	B_3NaCl-	$(S/D)_{rs}$
24H.255	-78	1900	160	11.0	15690	6.9	6000	456	242	<0.5	-	834	-	2199	454	13.1	1.28	3.6	-	-	-	B_2CaCl-	$(D+S)_{rs}$
24H.451	-60	1600	150	11.0	2330	7.3	810	42	175	<0.5	0.70	200	10	290	36	4.8	0.39	3.0	27.0	1.8	<0.2	B_2CaCl-	$(D+S)_{rs}$
24H.450	-90	5500	450	11.8	2450	7.0	690	2	385	<0.1	2.10	205	12	280	27	5.5	0.36	5.4	20.0	6.1	<0.2	B_3CaCl-	$(D+S)_{ds}$
24H.189	-55	520	100	11.0	930	7.4	243	3	313	<0.2	0.48	66	3	154	7	5.0	0.33	1.1	22.2	-	<0.2	F_3CaCl-	D_{ds}
24H.189	-45	570	70	10.8	470	7.4	36	11	264	<0.2	0.51	24	2	79	6	0.6	0.58	0.3	19.9	-	<0.2	F_3CaHCO_3	D_r

piezo-meter no	sample depth m+MSL	Al µg/l	As µg/l	Ba^{2+} µg/l	Be ng/l	Br- µg/l	Cd µg/l	Co µg/l	Cu µg/l	Eu ng/l	µg/l	µg/l	Li^+ µg/l	Mo µg/l	Ni µg/l	Pb µg/l	Rb^+ µg/l	Sb ng/l	Se ng/l	Sr^{2+} µg/l	µg/l	µg/l	Zn µg/l
24H.259	-105	25	8	120	<10	58000	-	1.1	<5.8	-	240	73	175	6.2	4	<3	9.6	-	-	7000	<0.05	1.3	26
24H.190	-75	-	-	150	-	35000	-	-	-		70	312	175	<0.1		-	-			12000	-	-	-
24H.259	-70		-	-		-	-	-		-	-	-	-	-		-	-	-		-	-	-	
24H.189	-60		<1.3	41		18700	-	0.3		16	<100	24		<1.5		<3	<0.5	<10		6124	<0.05	<0.1	
24H.255	-78		-	-		-	-	-		-	-	-		-		-	-	-		-	-	-	
24H.451	-60		-	-		-					-	-	-	-			-			-	-	-	-
24H.450	-90	5	0.9	310		2955	-		2	-	50	17	28	1.3			3.1	-	-	2000	<0.01	0.2	28
24H.189	-55	<100	-	300	-	860	<0.05	-	<5.4	<3	<100	12	-	<0.1	-	-	<0.5	50	13	-	-	-	-
24H.189	-45	3	1	30	<50	110	<0.05	<0.5	<1	4	100	<1	4	0.2	<0.6	<0.5	0.3	30	10	-	<0.05	<0.5	<7

piezo-meter no.	sample depth m+MSL	sea salt corrected (mmol/l) Na^*	K^*	Ca^*	Mg^*	SO_4^*	BEX ## meq/l	SATURATION INDEX log(IAP/K_s)† Hydroxides and sulphates gibbs #	alun #	barite	Silicates SiO_2	albite #	illite #	kaol #	Carbonates calcite	dolom	magn	sider	rhodo	Phosphates and fluorides apat-OH	apat-F	vivian
24H.259	-105	6.53	-0.1	0.3	-0.3	0.1	5.8	1.3	2.8	0.79	-0.78	0.82	3.9	3.9	-0.15	0.34	0.00	-0.35	-1.4	0.66	2.9	-0.35
24H.190	-75	-23.7	-3.9	22.9	-4.6	0.1	-36.9	0.01	-0.54	0.88	-0.36	0.24	1.6	2.2	0.14	0.16	-0.46	-0.11	-1.1	-0.41	1.7	-1.2
24H.259	-70	-38.0	-0.9	14.8	7.8	-1.4	-23.3	0.34	-0.31	-	-0.69	-0.29	1.7	2.2	0.33	0.79	-0.03	0.02	-0.78	0.65	-	-0.73
24H.189	-60	-34.2	-3.6	28.6	-12.5	-0.7	-62.9	-1.8	-1.3	0.31	-0.60	-0.72	0.24	1.7	0.19	-0.26	-0.93	0.17	-1.1	0.31	2.4	0.07
24H.255	-78	-109.0	-	51.7	2.2	-4.0	-104.6	0.23	-	-	-	-	-	-	0.44	0.33	-0.60	-0.09	-1.1	-	-	-
24H.451	-60	-10.9	-0.2	6.8	-0.7	-0.7	-12.6	0.42	-3.6	-	-0.44	-0.50	2.1	2.9	0.17	-0.46	-1.1	0.17	-0.93	1.6	-	0.81
24H.450	-90	-7.8	-0.1	6.6	-0.8	-1.0	-9.4	0.6	-19.6	-8.3	-0.58	-1.0	1.7	2.9	0.28	-0.47	-1.2	0.31	-0.91	1.6	3.7	1.2
24H.189	-55	-3.0	-0.1	3.7	-0.4	-0.3	-3.8	0.24	-13.0	-3.5	-0.53	-1.3	1.0	2.3	0.35	-0.55	-1.4	0.66	-0.55	0.9	2.6	1.3
24H.189	-45	0.2	0.0	2.0	0.1	0.1	0.5	0.43	-4.3	-0.78	-0.58	-1.7	1.8	2.6	0.05	-0.93	-1.5	-0.26	-0.31	0.13	2.2	-1.0

§ = calculated; # = where Al was not analysed, a concentration of 3 µg/l was assumed; ## : bex = (Na^* + K^* + 2Mg^*); † = calculated using WATEQX (Van Gaans, 1989).

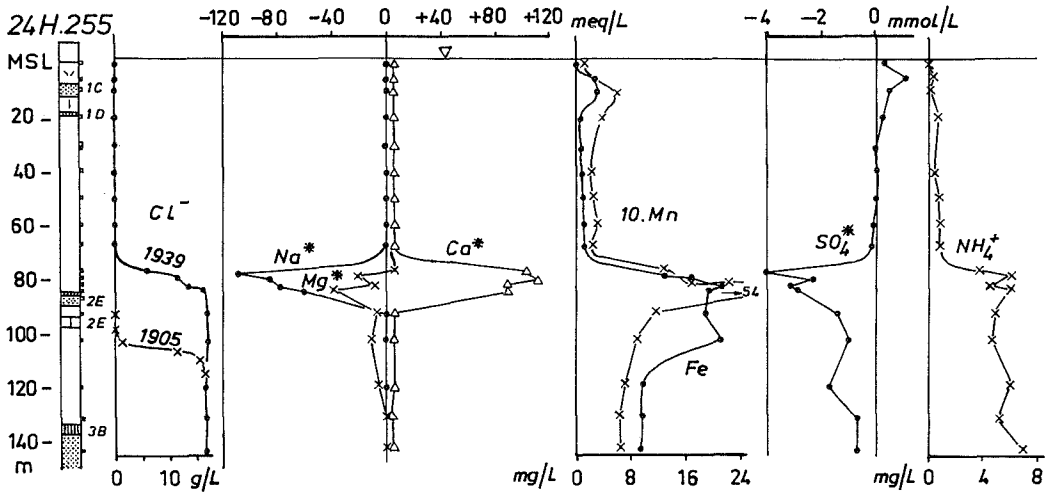

FIG. 7.23 Hydrochemical log of observation well 24H.255 in 1939, showing salinization and the resulting cation exchange of Na^++Mg^{2+} for Ca^{2+}, a mobilization for NH_4^+, Fe and Mn, and some SO_4^{2-} reduction. The position of 5 aquitards is indicated. Data at 132 and 144 m-MSL derive from the nearby well 24H.473.

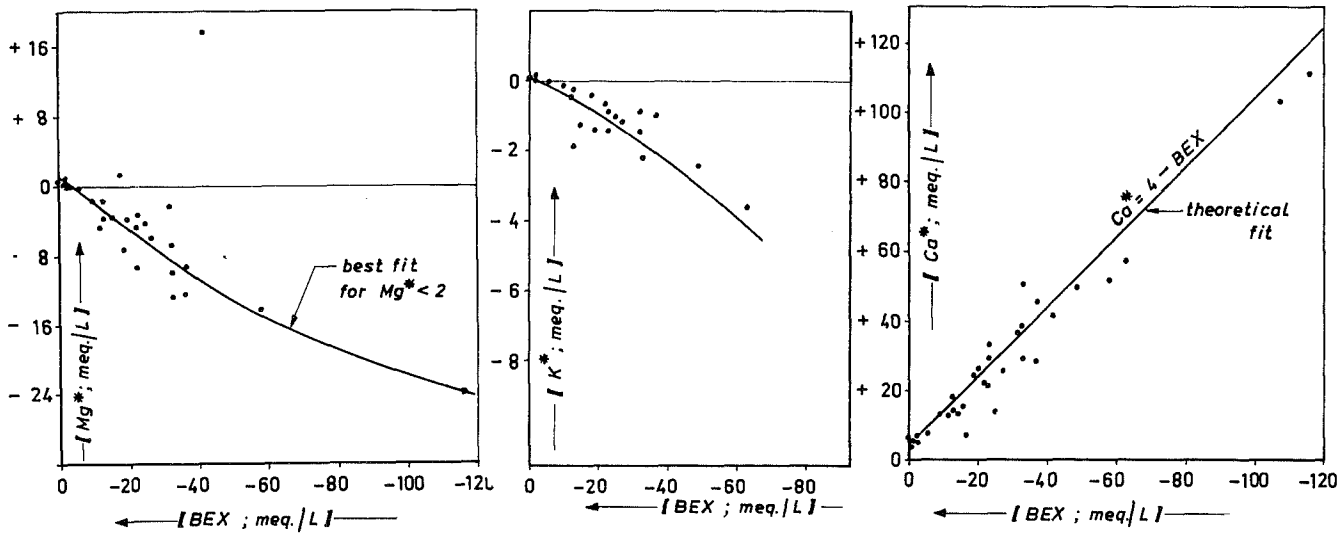

FIG. 7.24 Plot of sea-salt-corrected, main cations (Na^*, K^*, Ca^*, Mg^*) in 31 brackish to salt, salinized groundwater samples south of Zandvoort aan Zee, versus BEX (=$Na^* + K^* + Mg^*$ in meq/l). BEX is a parameter of the direction and approximate extent of cation exchange. All samples are composed of a mixture of intruding North Sea water and dune water being displaced.

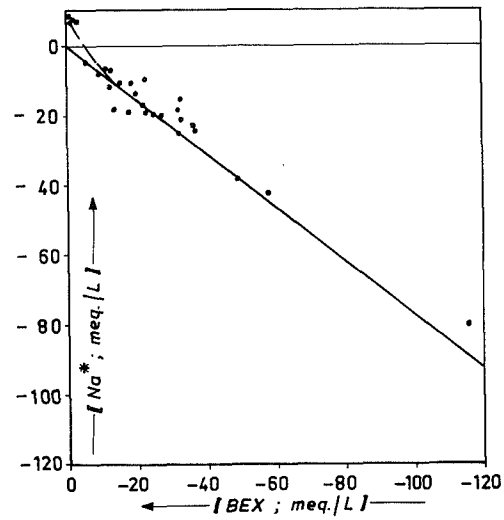

plausible explanation, but also the dissolution of a manganous siderite may contribute to the Fe and Mn mobilization, because Van der Sleen (1912) diagnosed the presence of such a siderite in the Kedichem Formation (aquitard 2E; Table 7.1) and the salinized water is often undersaturated with respect to siderite and rhodochrosite (Table 7.6). Little sulphate is reduced in the North Sea water behind the front, somewhat more was reduced in the front as it passed aquitard 2E.

Comparison of both end members and their mixture
Further changes can be deduced from Table 7.6, where several analyses on North Sea water intruding into dune water are ordered from low to high chlorinity, including both end members (24H.259-105 and 24H.189-45). Changes not mentioned so far, are : (1) the adsorption of K^+ (see K^*), F^-, Mo, Rb^+, U and V, conform the trend for the deep North Sea flow branch (section 7.6.2); (2) retention of PO_4 and F^-, possibly in connection with the raised Ca^{2+} levels, which could lead to the precipitation of apatite-like phases (the water is supersaturated indeed; Table 7.6); (3) a decrease in pH, possibly due to precipitation of calcite as the Ca^{2+} exchange creates supersaturation (Table 7.6); and (4) a mobilization of Sr^{2+}, conform Ca^{2+}, and of I, probably due to decomposition of organic matter, which is manifest in the raised HCO_3^- concentrations.

Relations with the parameter BEX.
The relation between Na^*, K^*, Ca^* and Mg^* on the one hand and BEX as a parameter of the direction and approximate extent of base exchange on the other, is shown for 31 diverging, salinized samples in Fig.7.24. Negative values of BEX, indicating salinization, are generally accompanied by negative values for Na^*, K^* and Mg^* individually as well, with a contribution to BEX of roughly 75% by Na^*, 20% by Mg^* and 5% by K^*. The main exception is formed by Mg^* that may become positive during the initial phase of salinization, as discussed before.

The negative BEX is compensated for by an equal amount of Ca^* on a meq basis : (Ca^*-4) ≡ -BEX (Fig.7.24). This corresponds with exchange reaction 8.31 (to the left) and a Ca^* concentration in deep dune and North Sea water in aquifer III_B of 4 ± 1 meq/l.

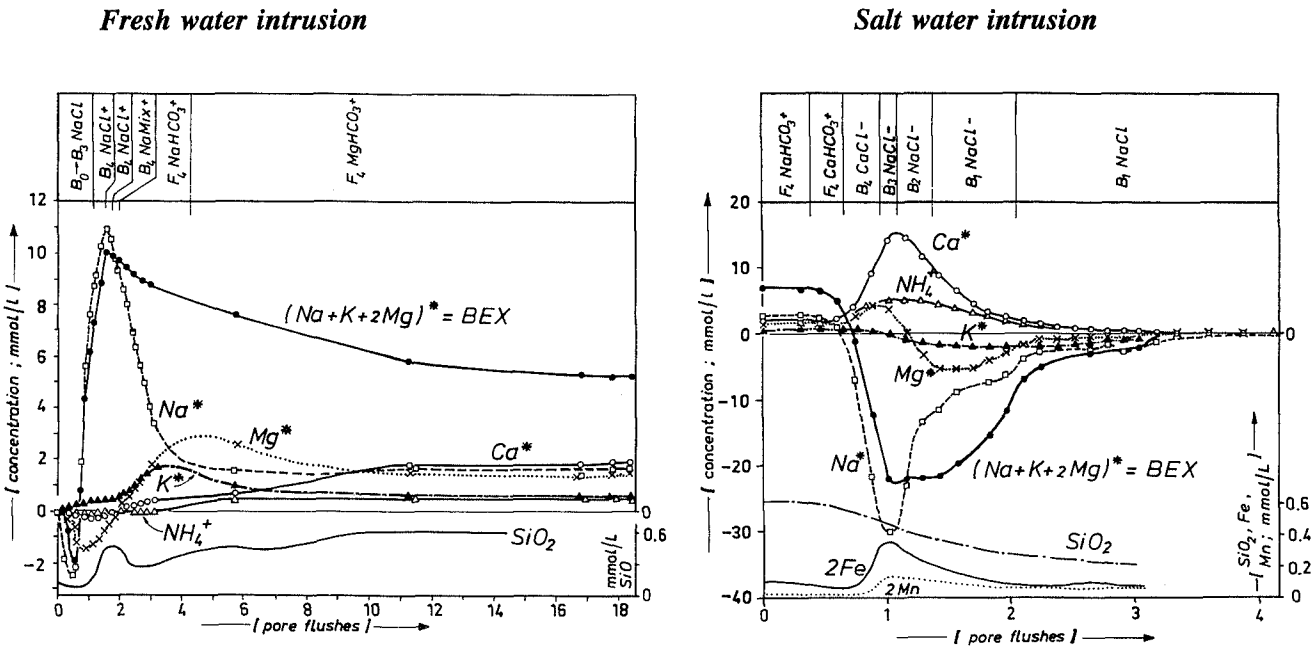

FIG. 7.25 Quality changes in the discharge of both a fresh and salt equilibrated soil column upon flushing with salt and fresh water, respectively. The time or volume axis is replaced by the amount of pore flushes, and the resulting water types are indicated. The water type on the right side is the displacing fluid after equilibrium has been attained. X = concentration of X corrected for a contribution of sea salt, positive values indicating desorption, and negative values adsorption. Based on data from Beekman (1991).*

7.7 Comparison of field data with column experiments by Beekman

General comments

Beekman (1991) simulated fresh water and sea water intrusions by flushing a column containing natural, anoxic, Holocene tidal channel sand (CEC = 12 meq/kg dry weight), with oxic coastal North sea water type B_1NaCl (diluted with demineralized water in a ratio of 1:1) and deep anoxic groundwater type F_4NaHCO$_3$+. These experiments therefore deviate from the natural situation in the coastal dune area, by the following : (a) a reduced displacing power of the diluted North Sea water. With Σcations being 235 meq/l it is 46% of the value pertaining to the coastal dune area (Σcations = 515 meq/l); and (b) the lack of an effective redox barrier before displacement of fresh water yields an oxic facies for the diluted North Sea water. This contrasts with the anoxic, sulphate-stable redox state of infiltrated North Sea water in the coastal area.

The salt water intrusion experiment is representative of the particular situation of displacement of a fresh end-member composed of freshened NaHCO$_3$ water. This situation occurs in the dunes, especially where deep aquitards were still in the stage of freshening prior to salinization. The fresh water intrusion experiment with NaHCO$_3$ water as displacing fluid, represents an uncompleted freshening process, as the MgHCO$_3$ and CaHCO$_3$ stages are lacking.

Beekman's results

Results of the displacement simulations were kindly elaborated by dr. H.E. Beekman on request, to yield sea-salt-corrected concentrations of the main cations and the parameter BEX. Changes in their value and in concentration of NH_4^+, Fe, Mn and SiO_2 are shown in Fig.7.25 for both the fresh and salt water intrusion.

About 11 pore flushes were required during freshening, in order to attain equilibrium for all main cations (Na^+, K^+, Ca^{2+}, Mg^{2+} and NH_4^+). This is about 2.5 times more than when the exchange process is simplified to the complete displacement of all adsorbed cations (CEC = 12 meq/kg) by the cations in the displacing fresh water (Σcations = 16.7 meq/l). Complete equilibrium was reached for Na^+, NH_4^+, K^+, Mg^{2+} and Ca^{2+} after resp. 5, 7, 8, 11 and 11 pore flushes. The behaviour of Fe, Mn and SiO_2 was influenced by oxidation of the displacing, anoxic NaHCO$_3$ water (Beekman, 1991). The dip in SiO_2 after an initial fast breakthrough could, however, also be related to the strong concomitant increases of K^+ and Mg^{2+}. The

maximum amount of exchanged bases relative to the displacing fluid is 4 meq/l (10-6).

Salinization required only 3.3 flushes for complete equilibrium of Na^+, K^+, Ca^{2+}, Mg^{2+} and NH_4^+. This is also about 2.5 times more than when the exchange process is simplified to a displacement reaction. Complete equilibrium was attained for these constituents at about the same time, after 3.3 pore flushes, although Na^+ approached equilibrium much faster than the others. This means that there is a less spectacular chromatographic separation of ions than during fresh water intrusion, as expected. Iron, manganese and siliciumdioxide required more than 3.3 flushes. The behaviour of SiO_2 is probably governed by desorption as demonstrated in other systems by Bassett (1973, cited in Wood & Signor, 1975) and Stuyfzand (1986d), but may have been also influenced by the dissolution of diatom skeletons. The maximum quantity of adsorbed (Na+K+Mg), relative to the displacing fluid, was 22 meq/l, that is about five times more than during fresh water intrusion.

Comparison with field data

Most of the patterns revealed by the experiments of Beekman (1991), are consistent with the field data collected in the coastal dune area. The chromatographic effects of cation exchange, as far as the separation of Na^+, K^+, Ca^{2+}, Mg^{2+} and NH_4^+ peaks or fronts is concerned, correspond well with those observed in freshening dune water (Fig.7.4 and 7.10), salinizing Rhine water (Fig.7.17), weakly and strongly salinizing North Sea water (Fig.7.22 and 7.23, respectively). Even the, at first sight, more enigmatic Mg^{2+} sorption and Mg^{2+} desorption in the initial phase of freshening and salinization, respectively, can be nicely traced back in field data, although the relatively narrow zones of occurrence require a dense sampling network.

The mobilization of Fe, Mn and SiO_2 upon salinization is very consistent with the field data (Fig.7.23 and Table 7.6), notwithstanding the oxic character of the diluted North Sea water used by Beekman.

7.8 Conclusions

The presentation and evaluation of (generalized) quality changes downgradient are to be considered as the crown on both the descriptive and analytical phase of a regional hydrochemical survey. A couple of diagrams may suffice to show hydrochemical trends versus the distance of flow, with indication of the main aquitards or geological formations that constitute geochemical anomalies. A log-scale for the X-axis is advised as the strongest changes over short distances normally occur in the recharge proximal zone.

One of the main problems encountered, was the selection of the flow path and observation wells, due to uncertainties in (a) the exact position of the flow lines, (b) heterogeneities composed of differences in vegetation cover, thickness of the unsaturated zone and interaction with local peat and clay beds, and (c) discontinuities like recently induced, brackish upconings. These problems necessitated the presentation of generalized quality trends downgradient that, still, closely followed the observations. The advantage of this approach is that the trends are representative of similar flow domains within the studied hydrosome. The exact concentration levels and the length and position of the various hydrochemical zones along other flow paths are, however, likely to deviate in one or other way from the presented results. It is also stressed that the trends presented in this chapter, do not cover all the general hydrochemical facies chains encountered in the study area (see Fig.4.20).
Specific local circumstances, like dune water in urban and industrial areas, remained unexplored.

Fresh as well as salt water intrusions generally yield characteristic concentration patterns upgradient of the front, both in space and time. This is evidenced by the world-wide recognition of freshened $NaHCO_3$ and salinized $CaCl_2$ water. However, reactions accompanying the universal cation exchange probably depend much more on local circumstances, as observed even within the study area. For instance, fresh water intrusion may lead to the adsorption of NH_4^+ and SiO_2, as observed in column experiments by Beekman (1991) and in the Zandvoort aan Zee area, but in the Bergen area below the Bergen clay NH_4^+ desorbed and SiO_2 dissolved from diatom sceletons in the marine Eemian Formation. Here the second law in geohydrochemistry (section 1.1) may serve as a compass in assessing the overall direction of quality changes upon displacement : reactions will tend to minimize the chemical difference between the original and invading groundwater.

Changes in the groundwater flow pattern, the flux of oxidants and the position of the phreatic level influenced the hydrochemical patterns significantly. The change from vertical to subhorizontal flow in the upper aquifer after the start of artificial recharge and recollection in 1957, increased the contact time and the length of the flow path within the upper sandy North Sea deposits. This probably meant, in an anoxic environment, that PO_4, Mn and As, with otherwise low concentrations due to a limited availability and short contact, now steadily increase by progressive leaching downgradient, to yield at a certain distance the rather extreme concentration peaks observed.

The introduction of Rhine water changed the redox environment in the Holocene deposits below circa 7 m-MSL, from sulphate-reducing or methanogenic to sulphate-(meta)stable. This is probably connected with an a priori low, sulphate-reducing capacity of the aquitards 1C and 1D, and an about tenfold increase of the sulphate flux.

A drawdown of the phreatic level with concomitant oxidation of iron sulphides, can be traced back in several cases, with some difficulty, in raised SO_4^{2-} levels at a certain depth. The depth should correspond with the period of the lowest phreatic level attained for several years, which strongly depends on local conditions in the studied dune area. In the Bergen dune area this happened around 1950, west of Hillegom in 1925 and south of Zandvoort aan Zee in the 1880s. Complications arise where also the sulphate flux increased (see above). Positive evidence of the penetration of solid phase derived sulphate can only be obtained with $\delta^{34}S$ analysis (Robertson et al., 1989). This is therefore recommended in future research.

Dune groundwater with the best quality for drinking water supply, is either deep anoxic F_2-F_3CaHCO_3 water without base exchange, deep anoxic F_2-F_3CaHCO_3+ water or F_2-F_3MgHCO_3+ water. These waters generally exhibit extremely low concentrations of most trace elements and organic micropollutants and low Na^+ concentrations. Deep anoxic F_3-F_4NaHCO_3+ water has a problematic high Na^+ concentration often exceeding drinking water standards, a strong colour and raised DOC, CH_4, NH_4^+ and PO_4^{3-} concentrations, which conduce to high demands upon the treatment.

Chapter 8

CHEMICAL MASS BALANCES FOR DUNE GROUNDWATER

Abstract

Chemical mass balances are composed here of a set of 25-50 reaction equations in appropriate order and the sum of all resulting mass transfers between bulk precipitation and dune groundwater. A general set-up of the balance approach is presented, consisting in this complicated case of 31 consecutive steps. In addition to water-rock interaction, also reactions at the interface of the upper soil with the atmosphere (like interception deposition) and vegetation (for instance uptake) are considered.

Mass balances for 4 shallow vegetation groundwaters in contrasting dune areas revealed the main sources and sinks of the strong acids H_2SO_4, HNO_3 and HF on the one hand, and carbonic acid on the other. Interception deposition constitutes the main source of the strong acids, and is generally followed in second position by nitrification and, in case of fast growing pines, by the uptake of cations. Respiration generally yields the bulk of carbonic acid, except for pines in decalcified dunes where dry soil conditions and the lack of reactive $CaCO_3$ hamper an effective transfer of CO_2 gas to the water phase. Reaction with $CaCO_3$ explains the higher contribution of CO_2 produced by respiration in calcareous dunes as compared to decalcified dunes.

Strong acids are neutralized in the calcareous dunes, mainly by reduction of the base saturation of the exchange complex in the upper unsaturated zone. In decalcified dunes, various sinks of strong acids can be assigned, the most important being : the uptake of anions under fast growing pines, SO_4^{2-} adsorption (or the formation of jurbanite-like phases), the dissolution of gibbsite and the HCO_3^- buffer, which is mainly formed by interaction with decomposing organic matter. The dissolution of $CaCO_3$ and free drainage constitute the main sink of carbonic acid in calcareous and decalcified dunes, respectively.

Mass balances were also drawn up for 5 samples of Bergen dune groundwater down the hydraulic gradient, from close to the water table in the younger dunes towards exfiltration in the polder area. They revealed the strong impact of atmospheric pollution in the upper zone, and further downgradient the increasing effects of methanogenesis, cation exchange due to freshening and dissolution of apatites, including the conversion of fluor- into hydroxyapatite. The present supply of strong acids to dune water (waters <50 y old) is about 13 times higher than the natural background supply to dune water (waters >150-200 y old).

Carbon-13 data assisted in the distinction between $CaCO_3$ dissolution by strong atmospheric acids and the dissolution by carbonic acid, regarding shallow dune groundwater without interference of dune peat. Interaction with dune peat results in a rather uniform $\delta^{13}C$ value of -16‰, by the overwhelming effect of isotopic exchange between the relatively small quantity of dissolved HCO_3^- and the huge reservoir of CO_2 in soil air and organic matter in the peat. The mass balance for ^{13}C in deep dune waters containing high methane concentrations, corresponded well with observations if a $\delta^{13}C$ value of +30‰ is assumed for the CO_2 originating from methanogenesis.

8.1 Definition, purpose and limitations

All previous field data and the many explanations proposed, should ideally combine to yield a model, which perfectly simulates the quality evolution from rainfall down the hydraulic gradient, along a well-defined subterranean flow path to the exfiltration area. Chemical mass balances constitute the first step in this direction by offering a general set-up for modelling, with indication of the most plausible reactions and their respective contribution to the observed water quality. They also form the last step in the regional hydrochemical survey presented in this thesis, step 7 according to Fig.1.7.

Chemical mass balances are drawn up by using a set of reaction equations in appropriate order and summing up all resulting mass transfers between an arbitrary starting and ending point in a flow system (Garrels & Mackenzie, 1967; Plummer & Back, 1980; Plummer et al., 1991). The groundwater composition is actually simulated by calculations on the basis of all relevant processes and concentration levels attained in specific compartments, stepwise following the hydrological and hydrochemical

pathways. If such a simulated transformation of rain water into the observed groundwater succeeds well, we may have confidence in the model applied and we obtain insight into the relative contribution of each process. Such a simulation approach is, however, never unequivocal and requires further independent evidence from geochemical inspection and laboratory experiments. Several of the reactions proposed, should therefore be checked in future studies, as part of the final step in regional hydrochemical surveys (Fig.1.7).

Balances for the main constituents can be validated by separate balances for natural isotopes like ^{13}C, ^{15}N and ^{34}S, because if the reaction model is correct, it will describe both the observed chemical and isotopic composition of aqueous and solid phases (Plummer et al., 1990). In this study only some data on ^{13}C in groundwater are available for this purpose.

General limitations to the mass balance approach consist of : (1) the necessity to consider idealized mineral compositions, that represent the known range of mineral stoichiometry in the system; (2) the assumption of a steady state; (3) analytical inaccuracies and errors introduced during sampling (for instance methane losses); and (4) the occurrence of reactions, which either remain unnoticed in the water sample, or are underestimated, because of masking by other reactions. For instance, the weathering rate of silicates may be higher than deduced from SiO_2 concentrations alone, as vegetation may store significant amounts of SiO_2 (Bartoli, 1983). And the precipitation of siderite can be obscured by the simultaneous reduction of ferric hydroxides by organic matter in anoxic sediments.

8.2 General set-up

8.2.1 Principles

The composition of bulk precipitation constitutes the starting point for each mass balance calculation and the composition of groundwater sampled from a specific observation well along the flow path considered, forms the ending point. The reason to start each time with bulk precipitation and not with groundwater upgradient, consists of the high variability in the composition of bulk deposition, both in space and time (chapter 5).

Mass balances are drawn up here on the basis of three to four sets of reaction equations :
(1) those at the interface of the upper soil with the atmosphere and the vegetation (Table 8.1);
(2) the main redox reactions, involving the oxidation of organic matter in a closed system, the oxidation of iron sulphides and oxidation cq reduction of silicate minerals (Table 8.2);
(3) the main water-rock interactions without redox component, more or less ordered according to the prograde quality evolution of (sub)oxic acid to (sub)oxic calcareous to deep anoxic calcareous dune water (Table 8.3); and, if necessary
(4) reactions upon the mixing of groundwaters with a different redox facies (Table 8.4).

Many of these reactions are strongly schematized by neglect of the exact mechanistic steps, the trace constituents (for instance sulphur in organic matter) and the different speciation forms (for instance regarding phosphate derived from organic matter and apatite).

Idealized silicate, sulphide and hydroxide

TABLE 8.1 Principal reactions at the interface of the soil with the atmosphere and biota, including the resulting changes in acidity (mmol/l), alkalinity (meq/l) and Total Inorganic Carbon (TIC; mmol/l).

Process from left to right	REACTION EQUATION	Eq N_o	change in Acidity	Alk.	TIC
ATMOSPHERIC INTERFACE					
gas absorption and oxidation	$SO_2 + 0.5\ O_2 + H_2O \rightarrow SO_4^{2-} + 2H^+$	8.1	+2	-2	0
ditto	$H_2S + 2O_2 \rightarrow SO_4^{2-} + 2H^+$	8.2	+2	-2	0
ditto	$NO_x + 0.25\ (5\text{-}2x)O_2 + 0.5\ H_2O \rightarrow NO_3^- + H^+$	8.3	+1	-1	0
ditto	$NH_3 + 2O_2 \rightarrow NO_3^- + H_2O + H^+$	8.4	+1	-1	0
nitrification	$NH_4^+ + 2O_2 \rightarrow NO_3^- + H_2O + 2H^+$	8.5	+2	-2	0
GROWING BIOMASS					
uptake anions	$a\ NO_3^- + b\ H_2PO_4^- + c\ SO_4^{2-} + (a+b+2c)\ H^+ + (a+b+c)\ R\cdot OH \rightarrow a\ R\cdot NH_2 + b\ R\cdot H_2PO_4^- + c\ R\cdot SH + (2a + 7c/4)\ O_2 + (b + 1.5c)\ H_2O$	8.6	-a-b-2c	a+b+2c	0
uptake cations	$M^+ + R\cdot OOH \rightarrow R\cdot OOM + H^+$	8.7	+1	-1	0
uptake NH_4	$NH_4^+ + R\cdot OH \rightarrow R\cdot NH_2 + H_2O + H^+$	8.8	+1	-1	0
respiration	$O_2 + CH_2O \rightarrow CO_2 + H_2O$	8.9	+1	0	+1
N_2-fixation	$N_2 + 2\ R\cdot OH + H_2O \rightarrow 2\ R\cdot NH_2 + 1.5\ O_2$	8.10	0	0	0

TABLE 8.2 Principal redox reactions in natural groundwater systems, between dissolved and solid phases, or between solid phases (Eqs.8.13 and 8.14). The resulting changes in acidity (mmol/l), alkalinity (meq/l) and Total Inorganic Carbon (TIC; mmol/l), with the reaction proceeding from left to right, are indicated. The clay mineral formed in reaction 8.19, is a Mg-beidellite.

Process from left to right	REACTION EQUATION	Eq N_o	change in Acidity	change in Alk.	change in TIC
REDOX SEQUENCE					
aerobic oxidation	$O_2 + \frac{1}{(1+2y)}\{CH_2O(NH_3)_y(H_3PO_4)_z\} + \frac{y}{(1+2y)} HCO_3^- \rightarrow \frac{(1+y)}{(1+2y)} H_2CO_3^* + \frac{y}{(1+2y)} NO_3^- + \frac{z}{(1+2y)} H_3PO_4 + \frac{2+3y}{(1+2y)} H_2O$	8.11	$+\frac{2+y}{(1+2y)}$	$-\frac{y}{(1+2y)}$	$+\frac{1}{(1+2y)}$
denitrification	$NO_3^- + \frac{5}{(4+3y)}\{CH_2O(NH_3)_y(H_3PO_4)_z\} \rightarrow \frac{2+4y}{(4+3y)} N_2 + \frac{1-3y}{(4+3y)} H_2CO_3^* + HCO_3^- + \frac{5z}{(4+3y)} H_3PO_4 + \frac{2+9y}{(4+3y)} H_2O$	8.12A	$+\frac{6-3y}{(4+3y)}$	$+\frac{6-3y}{(4+3y)}$	$+\frac{5}{(4+3y)}$
ditto	$NO_3^- + 1¼\{CH_2O(NH_3)_y(H_3PO_4)_z\} \rightarrow 0.5\ N_2 + 1¼y\ NH_4^+ + \frac{1-5y}{4} H_2CO_3^* + \frac{4+5y}{4} HCO_3^- + 1¼z\ H_3PO_4 + 0.5\ H_2O$	8.12B	$+\frac{6-5y}{4}$	$+\frac{4+5y}{4}$	$+1¼$
reduction Mn^{4+}	$MnO_2 + \frac{2}{(4+3y)}\{CH_2O(NH_3)_y(H_3PO_4)_z\} + \frac{6+6y}{(4+3y)} H_2CO_3^* + 2\ H_2O \rightarrow Mn^{2+} + 2\ HCO_3^- + \frac{y}{(4+3y)} N_2 + \frac{2z}{(4+3y)} H_3PO_4$	8.13	$-\frac{(4+6y)}{(4+3y)}$	+2	$+\frac{2}{(4+3y)}$
reduction Fe^{3+}	$Fe(OH)_3 + 0.25\{CH_2O(NH_3)_y(H_3PO_4)_z\} + \frac{7+y}{4} H_2CO_3^* \rightarrow Fe^{2+} + \frac{8+y}{4} HCO_3^- + 0.25y\ NH_4^+ + 0.25z\ H_3PO_4 + 2.5\ H_2O$	8.14	$-\frac{(6+y)}{4}$	$+\frac{8+y}{4}$	$+¼$
reduction SO_4^{2-}	$SO_4^{2-} + 2\{CH_2O(NH_3)_y(H_3PO_4)_z\} + Fe^{2+} + (n+1)\ H_2O \rightarrow FeS{\cdot}nH_2O + 2y\ HCO_3^- + (2-2y)\ H_2CO_3^* + 2y\ NH_4^+ + 2z\ H_3PO_4$	8.15	+ (4-2y)	+ 2y	+ 2
methanogenesis	$CO_2 + 2\{CH_2O(NH_3)_y(H_3PO_4)_z\} + 2\ H_2O \rightarrow CH_4 + (2-2y)\ H_2CO_3^* + 2y\ HCO_3^- + 2y\ NH_4^+ + 2z\ H_3PO_4$	8.16	+ (2-2y)	+ 2y	+ 1
OXIDATION OF IRON SULPHIDES					
oxic oxidation hydrotroillite	$FeS{\cdot}nH_2O + 2\ O_2 \rightarrow Fe^{2+} + SO_4^{2-} + n\ H_2O$	8.17A	0	0	0
oxic, ditto	$FeS{\cdot}nH_2O + 2.25\ O_2 + 2\ HCO_3^- \rightarrow Fe(OH)_3 + SO_4^{2-} + 2\ H_2CO_3^* + (n-2.5)\ H_2O$	8.17B	+2	-2	0
suboxic, ditto	$FeS{\cdot}nH_2O + 1.6\ NO_3^- + 1.6\ H_2CO_3^* \rightarrow Fe^{2+} + SO_4^{2-} + 1.6\ HCO_3^- + 0.8\ N_2 + (n-2.4)\ H_2O$	8.17C	-1.6	+1.6	0
suboxic, ditto	$FeS{\cdot}nH_2O + 1.8\ NO_3^- + 0.2\ HCO_3^- \rightarrow Fe(OH)_3 + SO_4^{2-} + 0.2\ H_2CO_3^* + 0.9\ N_2 + (n-1.6)\ H_2O$	8.17D	+0.2	-0.2	0
oxic oxidation pyrite	$FeS_2 + 3.5\ O_2 + 2\ HCO_3^- + H_2O \rightarrow Fe^{2+} + 2\ SO_4^{2-} + 2\ H_2CO_3^*$	8.18A	+2	-2	0
oxic, ditto	$FeS_2 + 3.75\ O_2 + 4\ HCO_3^- + 3.5\ H_2O \rightarrow Fe(OH)_3 + 2\ SO_4^{2-} + 4\ H_2CO_3^*$	8.18B	+4	-4	0
suboxic, ditto	$FeS_2 + 2.8\ NO_3^- + 0.8\ H_2CO_3^* \rightarrow Fe^{2+} + 2\ SO_4^{2-} + 0.8\ HCO_3^- + 1.4\ N_2 + 0.4\ H_2O$	8.18C	-0.8	+0.8	0
suboxic, ditto	$FeS_2 + 3\ NO_3^- + HCO_3^- + 2\ H_2O \rightarrow Fe(OH)_3 + 2\ SO_4^{2-} + H_2CO_3^* + 1.5\ N_2$	8.18D	+1	-1	0
OXIDATION AND REDUCTION OF SILICATES					
hornblende	$7\ Ca_3NaMg_3Fe^{II}{}_3\ Al_2Fe^{III}\ (Si_4O_{11})_4(OH)_4 + 103\ H^+ + 5.25\ O_2 + 169.5\ H_2O \rightarrow 21\ Ca^{2+} + 7\ Na^+ + 20\ Mg^{2+} + 28\ Fe(OH)_3 + 90\ H_4SiO_4 + 6\ Mg_{1.67}Al_{2.33}Si_{3.67}O_{10}(OH)_2$	8.19	-103	0	0
ferrialuminosilicate	$Fe^{III}{}_{1-x}Al_{1-x}(SiO_2)_x(OH)_{6-6x} + \frac{1-x}{4} CH_2O + \frac{7(1-x)}{4} H_2CO_3^* \rightarrow (1-x)\ Fe^{2+} + (1-x)\ Al(OH)_3 + x\ H_4SiO_4 + (2-2x)\ HCO_3^- + \frac{10-18x}{4} H_2O$	8.20	-1½+1½x	2-2x	¼+5x

minerals are taken as the reactive solid phases in these reactions. Calcium carbonate is represented by the mean composition of the marine shell samples 1-7 in Table 6.5. Organic matter is simplified as $CH_2O(NH_3)_y(H_3PO_4)_z$, with y and z depending on the type of organic matter : for terrestrial organic matter in the upper dune soils and in dune peat the choice was y = 0.04 and z = 0.002 (Table 6.8). For organic matter in the marine Westland and Eemian Formations, y was set at 0.075 and z at 0.0045, which agrees with the suggestion of Hartmann et al. (1973) and yields a better explanation for the NH_4^+ and PO_4 plots against HCO_3^- of anoxic Bergen dune water (Fig.7.5). The formation of iron monosulphides was chosen in reaction 8.15 instead of the formation of pyrite or H_2S, because of (a) the relative abundance of Fe in the aquifer system, (b) low SO_4^{2-} concentrations in dune water, and (c) low H_2S levels generally encountered (<0.1 mg/l).

Complications due to the mixing of two end-member waters, for instance dune and relict Holocene transgression water, do not need consideration here. The focus is directed on dune groundwater without admixing of any other end-member water.

The procedure presented below and subsequently followed to calculate the mass balance for selected dune water samples, can be considered an intelligible, first blueprint for a computerized solution of all the given equations, as offered by models like BALANCE (Parkhurst et al., 1982) and NETPATH (Plummer et al., 1991). Before applying these models, it should be verified that the number of phases (mineral solids, gases and ion exchangers) equals the number of elements, in order to be able to solve the set of equations. This restriction was not considered in the approach followed in this chapter. This leads to a more laborious calcalution and, in several cases, loss of specific information.

TABLE 8.3 Principal dissolution, neoformation and exchange reactions in the coastal dune aquifer system, more or less in order of subsequent contact or formation downgradient. The clay mineral formed in Eq.8.27, is kaolinite, and in Eq.8.36 (from left to right) the clay mineral Na-montmorillonite is formed.

Process from left to right	REACTION EQUATION	Eq N_o	change in Acidity	Alk.	TIC
ferrihydrite dissolution	$Fe(OH)_3 + 3\ H^+ \leftrightarrows Fe^{3+} + 3\ H_2O$	8.21A	-3	+3	0
ditto, by complexation	$Fe(OH)_3 + R{\cdot}[COOH]_3 \leftrightarrows R{\cdot}[COO]_3Fe + 3\ H_2O$	8.21B	-3	+3	0
reduction base saturation	$a\ Al^{3+} + b\ H^+ + c\ NH_4^+ + [dCa,eMg]{\cdot}EXCH \leftrightarrows d\ Ca^{2+} + e\ Mg^{2+} + [aAl,bH,cNH_4]{\cdot}EXCH$ (with $3a + b + c = 2d + 2e$)	8.22	-b	+b	0
gibbsite dissolution	$Al(OH)_3 + 3\ H^+ \leftrightarrows Al^{3+} + 3\ H_2O$	8.23A	-3	+3	0
ditto at high pH	$Al(OH)_3 + OH^- \leftrightarrows Al(OH)_4^-$	8.23B	+1	-1	0
jurbanite formation	$Al(OH)_3 + SO_4^{2-} + 2\ H^+ + 3\ H_2O \leftrightarrows Al(OH)SO_4{\cdot}5H_2O$	8.24	-2	+2	0
illite dissolution	$K_{0.6}Mg_{0.25}Al_{2.3}Si_{3.5}O_{10}(OH)_2 + 1.1\ H^+ + 8.9\ H_2O \rightarrow 0.6\ K^+ + 0.25\ Mg^{2+} + 3.5\ H_4SiO_4 + 2.3\ Al(OH)_3$	8.25	-1.1	+1.1	0
albite dissolution	$NaAlSi_3O_8 + H^+ + 7\ H_2O \leftrightarrows Na^+ + 3\ H_4SiO_4 + Al(OH)_3$	8.26A	-1	+1	0
anorthite dissolution	$CaAl_2Si_2O_8 + 2H^+ + 6\ H_2O \leftrightarrows Ca^{2+} + 2\ H_4SiO_4 + 2\ Al(OH)_3$	8.26B	-2	+2	0
orthoclase dissolution	$KAlSi_3O_8 + H_2CO_3^* + 4.5\ H_2O \rightarrow K^+ + 2\ H_4SiO_4 + HCO_3^- + 0.5\ Al_2Si_2O_5(OH)_4$	8.27	-1	+1	0
quartz dissolution	$SiO_2 + 2\ H_2O \leftrightarrows H_4SiO_4$	8.28A	0	0	0
opal dissolution	$SiO_2{\cdot}nH_2O \leftrightarrows H_4SiO_4 + (n-2)\ H_2O$	8.28B	0	0	0
hydroxi-apatite dissolution	$Ca_5(PO_4)_3OH + 7\ H^+ \leftrightarrows 5\ Ca^{2+} + 3\ H_2PO_4^- + H_2O$	8.29A	-7	+7	0
fluoroapatite dissolution	$Ca_5(PO_4)_3F + 6\ H_2CO_3^* \leftrightarrows 5\ Ca^{2+} + 3\ H_2PO_4^- + 6\ HCO_3^- + F^-$	8.29B	-6	+6	0
conversion to fluorapatite	$Ca_5(PO_4)_3OH + F^- + H_2CO_3^* \leftrightarrows Ca_5(PO_4)_3F + HCO_3^- + H_2O$	8.29C	-1	+1	0
shell dissolution by strong acid	$Sr_{0.002}Na_{0.024}Mg_{0.002}Ca(CO_3)_{1.016}(H_2PO_4)_{0.0004} + 1.016\ H^+ \leftrightarrows 0.002\ Sr^{2+} + 0.024\ Na^+ + 0.002\ Mg^{2+} + Ca^{2+} + 1.016\ HCO_3^- + 0.0004\ H_2PO_4^-$	8.30A	0	+2	+1
ditto by CO_2	$Sr_{0.002}Na_{0.024}Mg_{0.002}Ca(CO_3)_{1.016}(H_2PO_4)_{0.0004} + 1.016\ H_2CO_3^* \leftrightarrows 0.002\ Sr^{2+} + 0.024\ Na^+ + 0.002\ Mg^{2+} + Ca^{2+} + 2.032\ HCO_3^- + 0.0004\ H_2PO_4^-$	8.30B	0	+2	+1
ditto by organic acids	$2\ CaCO_3 + 2\ H(hum) \leftrightarrows 2\ HCO_3^- + Ca(hum)_2$	8.30C	-2	+2	+2
base exchange (freshening)	$a\ Ca^{2+} + [bNa,cK,dMg]{\cdot}EXCH \leftrightarrows [aCa]{\cdot}EXCH + b\ Na + c\ K + d\ Mg^{2+}$ $(2a = b+c+2d)$	8.31	0	0	0
manganous siderite formation	$x\ Fe^{2+} + (1-x)\ Mn^{2+} + 2\ HCO_3^- \leftrightarrows Fe_xMn_{1-x}CO_3 + H_2CO_3^*$	8.32	0	-2	-1
vivianite formation	$3\ Fe^{2+} + 2\ H_2PO_4^- + 4\ HCO_3^- + 8\ H_2O \leftrightarrows Fe_3(PO_4)_2{\cdot}8H_2O + 4\ H_2CO_3^*$	8.33	+4	-4	0
anoxic ammonium exchange	$a\ NH_4^+ + [bNa, cK, dMg]{\cdot}EXCH \leftrightarrows [aNH_4]{\cdot}EXCH + b\ Na^+ + c\ K^+ + d\ Mg^{2+}$ (with $a = b + c + 2d$)	8.34A	0	0	0
ditto for Ca^{2+}	$2\ NH_4^+ + [Ca]{\cdot}EXCH \leftrightarrows [2NH_4]{\cdot}EXCH + Ca^{2+}$	8.34B	0	0	0
sorption of silica	$H_4SiO_4 + SURF{\cdot} \leftrightarrows H_4SiO_4{\cdot}SURF$	8.35	0	0	0
transformation of kaolinite	$H_4SiO_4 + 0.2\ Na^+ + 0.2\ Mg^{2+} + 0.6\ HCO_3^- + 0.3\ Al_2Si_2O_5(OH)_4 \leftrightarrows 0.4\ Na_{0.5}Al_{1.5}Mg_{0.5}Si_4O_{10}(OH)_2 + 0.6\ H_2CO_3^* + 1.9\ H_2O$	8.36	+0.6	-0.6	0

dissolved SiO_2 is represented by H_4SiO_4;

TABLE 8.4 The main redox reactions due to the mixing of two fluids with a different redox facies (Eqs.8.37-8.47), and due to the contact of deep anoxic gases with solid phases stable in (sub)oxic environments only (Eqs.8.48-8.49). The reactions are given in approximate order of increasing redox level.

Process from left to right	REACTION EQUATION	Eq N_o	change in Acidity	Alk.	TIC
oxic with anoxic water	$Mn^{2+} + 0.5\ O_2 + 2\ HCO_3^- + 2\ H_2O \rightarrow MnO_2 + 2\ H_2CO_3^*$	8.37	+2	-2	0
ditto	$NH_4^+ + 2\ O_2 + 2\ HCO_3^- \rightarrow NO_3^- + 2\ H_2CO_3^* + H_2O$	8.38	+2	-2	0
ditto	$Fe^{2+} + 0.25\ O_2 + 2\ HCO_3^- + 2.5\ H_2O \rightarrow Fe(OH)_3 + 2\ H_2CO_3^*$	8.39	+2	-2	0
ditto	$HS^- + 2\ O_2 + HCO_3^- \rightarrow SO_4^{2-} + H_2CO_3^*$	8.40	+1	-1	0
ditto	$CH_4 + 2\ O_2 \rightarrow H_2CO_3^* + H_2O$	8.41	+1	0	+1
suboxic with anoxic water	$Mn^{2+} + 0.4\ NO_3^- + 1.6\ HCO_3^- + 0.8\ H_2O \rightarrow MnO_2 + 1.6\ H_2CO_3^* + 0.2\ N_2$	8.42	+1.6	-1.6	0
ditto	$NH_4^+ + 0.6\ NO_3^- + 0.4\ HCO_3^- \rightarrow 0.8\ N_2 + 0.4\ H_2CO_3^* + 2.6\ H_2O$	8.43	+0.4	-0.4	0
ditto	$Fe^{2+} + 0.2\ NO_3^- + 1.8\ HCO_3^- + 2.4\ H_2O \rightarrow Fe(OH)_3 + 0.1\ N_2 + 1.8\ H_2CO_3^*$	8.44	+1.8	-1.8	0
ditto	$HS^- + 1.6\ NO_3^- + 0.6\ HCO_3^- \rightarrow SO_4^{2-} + 0.8\ N_2 + 0.6\ H_2CO_3^* + 0.8\ H_2O$	8.45	+0.6	-0.6	0
ditto	$CH_4 + 1.6\ NO_3^- + 0.6\ H_2CO_3^* \rightarrow 1.6\ HCO_3^- + 0.8\ N_2 + 1.8\ H_2O$	8.46	+0.4	+1.6	+1
anoxic with deep anoxic water	$CH_4 + SO_4^{2-} + Fe^{2+} + (n-1)\ H_2O \rightarrow FeS{\cdot}nH_2O + H_2CO_3^*$	8.47	+2	0	+1
anoxic gas with $Fe(OH)_3$	$H_2S + 8\ Fe(OH)_3 + 14\ H_2CO_3^* \rightarrow 8\ Fe^{2+} + SO_4^{2-} + 14\ HCO_3^- + 20\ H_2O$	8.48	-14	+14	0
ditto, deep anoxic	$CH_4 + 8\ Fe(OH)_3 + 15\ H_2CO_3^* \rightarrow 8\ Fe^{2+} + 16\ HCO_3^- + 21\ H_2O$	8.49	-14	+16	+1

8.2.2 Normal sequence in the procedure

Chemical mass balances are drawn up here in four consecutive phases, involving all together about 31 steps.

Phase I : bulk precipitation and precalculations
This is the preparative phase consisting of 6 steps, with the selection of the composition of bulk precipitation that formed the recharge of the groundwater sample, and with all necessary precalculations :
(1) assess the age of the groundwater sample, by combination of the chemical techniques discussed in section 7.4.5, with hydrological calculations.
(2) determine the weighted mean composition of bulk precipitation that formed the input for the groundwater composition to be simulated. When this cannot be obtained from measurements on site, an estimate may be made for the specific time period and location, using all the data presented in chapter 5. Bulk precipitation before 1800 AD is approximated by taking the natural backgrounds for coastal areas presented in Table 5.3, with adaptation of sea spray dominated ions in dependence of the distance to the HWL. Chloride constitutes a key parameter here, because the following condition must be satisfied :

$$Cl_g = \frac{Cl_{BD} + Cl_{ID}}{N} \qquad (8.50)$$

where : Cl_g = Cl^- concentration in groundwater [mg/l]; Cl_{BD} = Cl^- flux in bulk deposition [mg m^{-2} d^{-1}]; Cl_{ID} = ditto, in interception deposition [mg m^{-2} d^{-1}]; N = excess precipitation [mm/d], see step 6.
The interception deposition of Cl^- can be estimated from data in Table 6.24, after interpolation of the relevant vegetation cover. The latter refers to the recharge site for the groundwater sample at the time that groundwater was formed.
(3) calculate the ionic balance for both bulk precipitation and the groundwater sample, preferably by using a program like WATEQX (Van Gaans, 1989) or the scheme in Fig.2.7, convert the measured alkalinity into total HCO_3^- and CO_3^{2-}, and calculate, if not measured, the $H_2CO_3^*$ (=CO_2 + H_2CO_3) concentration. Subsequently square the ionic balances completely, either by adapting the concentration of the most doubtful ion, or by a proportional change for each cation or anion or both, after determining what needs to be done by comparison of the measured with the calculated electrical conductivity (section 2.3.4 under "Case 2"). Recalculate if necessary, inorganic carbon speciation.
(4) convert all concentrations in bulk precipitation and groundwater into micromoles per liter.
(5) Correct Na^+, K^+, Ca^{2+}, Sr^{2+}, Mg^{2+} and SO_4^{2-} for a contribution of sea spray according to Eq.5.7 with the constants listed in Table 5.5.
(6) if only the very upper groundwater in a recharge area is considered and flow is directed predominantly downwards, then the balance is preferably drawn up in fluxes. In that case multiply the concentrations in bulk precipitation and in the upper groundwater with gross precipitation (P) and the groundwater recharge rate (N), respectively. Dissolved gases in bulk precipitation should be multiplied with N, as they are assumed to disappear in the fraction lost by evapotranspiration. In case of deeper groundwater and a substantial horizontal flow component, the balance is drawn up in terms of concentrations. Concentrations in bulk precipitation must be multiplied with the evaporation factor f (=P/N). The necessary data on P and N can be obtained from the lysimeters west of Castricum, either directly or by interpolation to correct for differences in vegetation cover. Data in Table 3.2 can be used as a first approximation.

Phase II : reactions at the interface of the upper soil with the atmosphere
The interception deposition of nongaseous and gaseous compounds, filtration of suspended solids in bulk precipitation, nitrification and uptake in biomass constitute the second phase, in 5 steps :
(7) estimate the contribution of interception deposition for the nongaseous substances Na^*, K^*, Ca^*, Sr^*, Mg^*, Fe, Mn, Al and SiO_2, by application of Eq.6.21. Add these to the values for bulk deposition obtained under step 6 directly, or divide them by the natural recharge prior to addition to bulk precipitation, that was concentrated by evaporation losses under step 6.
(8) estimate the contribution of interception deposition for the gaseous substances SO_2, NO_x, NH_3 and HF. For simplicity the interception deposition of for instance $(NH_4)_2SO_4$ aerosols has been included in the terms SO_2 and NH_3. This does not change the deposition of potential acidity nor the deposition of sulphur and nitrogen ions.

In the easiest case, on the condition that SO_4^{2-}-sinks and other SO_4^{2-}-sources can be neglected, the contribution of SO_2 is calculated by balancing SO_4^* directly, i.e by complete assignment of the difference between the groundwater and bulk input to SO_2 absorption. Subsequently Eqs.6.22 - 6.24 are applied, if the 1980s are involved, to arrive at the contribution of intercepted NH_3, NO_x and HF, respectively. For periods prior to 1980 the contribution of HF is estimated using Eq.6.24 as well, whereas the contributions of NO_x and NH_3 are approximated using respectively :

$$ID_{NO_x} = 0.5 ID_{SO_4^*} \frac{(NO_x\text{-}emission)_t}{(NO_x\text{-}emission)_{1980s}} \quad (8.51)$$

$$ID_{NH_3} = 1.5 ID_{SO_4^*} \frac{(NH_3\text{-}emission)_t}{(NH_3\text{-}emission)_{1980s}} \quad (8.52)$$

with ID = Interception Deposition [μmol m^{-2} d^{-1}]; and where the emissions refer to the national emissions shown in Fig.5.6, assuming a general validity for Western Europe, and the suffix t indicates the year.
The interception deposition of SO_2, NO_x and NH_y before 1800 AD is assumed to equal the bulk deposition of SO_4^*, NO_3^- and NH_4^+, respectively. This yields estimates very close to those given by Locht & Van Aalst (1988) and Erisman (1992). The absorbed atmospheric gases SO_2, NO_x and NH_3 are subsequently oxidized to yield SO_4^{2-}, NO_3^- and equivalent amounts of hydrogen ions, according to Eqs.8.1, 8.3 and 8.4, respectively.

However, there should be a rigorous check on SO_4^*-sinks (the formation of iron sulphides and jurbanite-like minerals) and other SO_4^*-sources (the oxidation of iron sulphides and peat, and dissolution of jurbanite-like minerals). This should be done by consideration of : (a) $\delta^{34}S$ analysis of dissolved sulphate (see e.g. Robertson et al., 1989). In this study no data on ^{34}S were available, however; (b) analysis of soil samples on solid phase sulphur. Calcareous dune sand and underlying beach sand generally are devoid of sulphur, whereas the aquitards 1C and 1D and the upper parts of the second aquifer contain significant amounts of iron sulphides (Van der Sleen, 1912; Rijsdijk, 1984a; Stuyfzand, 1989i); (c) the redox state both up- and downgradient of the sample, including H_2S observations on site; (d) changes in the position of the water table (section 7.5.3 under "Historical changes in phreatic level and flow patterns"); (e) the colour of the porous medium from which the groundwater was sampled. Yellow indicates (sub)oxic conditions, sulphate reduction or oxidation is not probable. Grey or black signifies that sulphate may be reduced. At the interface of yellow to grey/black both oxidation and reduction of SO_4^{2-} may occur; and (f) the passage of aquitards. Conservative behaviour of atmospheric SO_4^{2-} is guaranteed most where no aquitards are passed. Aquitards with a low SO_4^{2-} reduction capacity are dune peat $1A_1$ and $1A_2$, and the Holocene aquitards 1C and 1C'.

SO_4^* concentrations in groundwater which formed in the late 1950s or after 1979, can be compared with those in the drainage solute from the lysimeters west of Castricum, where complications due to SO_4^{2-} sorption in a decalcified upper soil or due to interference with dune peat or iron sulphides can be excluded (Table 6.15, Fig.6.35 and 6.37). In case of nonconservative SO_4^{2-} behaviour, the interception deposition of SO_4^* can be estimated using these lysimetric results by interpolation of the vegetation cover, or using throughfall data. Another approach is to use the relations between mean annual SO_2 concentrations in air and the SO_4^* concentrations in bulk precipitation and shallow groundwater with conservative SO_4^{2-} behaviour (Fig.6.39). Or estimate first the SO_4^* losses by jurbanite formation (see step 14) and subsequently start with step 8.
(9) remove atmospheric Fe^{3+} by filtration, assuming its presence as $Fe(OH)_3$ particles.
(10) nitrify all atmospheric NH_4^+ according to Eq.8.5, unless output NH_4^+ of shallow dune groundwater exceeds NH_4^+ production by anoxic mineralization. In that case balance NH_4^+ by nitrification. Or, in case of acid soils, nitrify 50%.
(11) estimate losses through uptake by vegetation and storage in soil humus, from data in Table 6.25. The net N-uptake by sea buckthorn is assumed to be completely covered by N_2-fixation according to Eq.8.10. In relatively rare cases there is a net release of elements from decaying biomass. This situation was not encountered in the samples for which a mass balance was drawn up.

Phase III : Interactions with the porous medium
The third phase consists of 16 steps. The steps 18-24 generally require several iterations, as they influence one another.
(12) balance SiO_2 arbitrarily for 50% by the dissolution of hornblende (as an exponent of the ferromagnesian minerals) according to Eq.8.19, and in case of a thin decalcified zone for 25% by the dissolution of orthoclase according to Eq.8.27 and for 25% by the dissolution of quartz or biogenic opal according to Eq.8.28A/B. In case of a thick decalcified zone the other 50% is balanced completely by the dissolution of anorthite, albite or orthoclase according to Eqs.8.26A, 8.26B and 8.27, respectively.
(13) balance Al by the dissolution or formation of gibbsite according to Eq.8.23A or B, depending on the pH of the sample.
(14) balance SO_4^* if still necessary, either by the oxidation of hydrotroillite according to Eq.8.17B or 8.17D (depending on changes in the position of the water table), by jurbanite formation in acid environments (pH<6) according to Eq.8.24, by reduction through organic matter according to Eq.8.15, or by a combination of these reactions. In calcareous dunes with a decalcified upper horizon, SO_4^{2-}-losses by jurbanite formation are estimated for the 1980s at 60 μmol m^{-2} d^{-1} for each decalcified meter, a figure derived from data in Ulrich et al. (1979) and corresponding with data deduced for the decalcified dunes. Jurbanite formation is neglected in water

older than 100 years.
(15) balance oxygen by oxidation of organic matter according to Eq.8.11;
(16) balance NO_3^-, if still necessary, either by oxidation of hydrotroillite according to Eq.8.17D or by denitrification through organic matter according to Eq.8.12A.
(17) balance Mn^{2+} (in anoxic environment assumed to correspond with total manganese) by reduction of MnO_2 through organic matter according to Eq.8.13;
(18) balance ferrous iron (in anoxic environment assumed to correspond with total iron) by reduction of ferric hydroxides through organic matter according to Eq.8.14. In case of (sub)oxic water ferric iron is balanced either by complexation according to Eq.8.21B or, in low pH (<3.4) water by dissolution according to Eq.8.21A.
(19) balance CH_4 by methanogenesis according to Eq.8.16.
(20) balance PO_4^{3-} and F^- by the dissolution or (trans)formation of apatite according to the Eqs.8.29A-C;
(21) balance HCO_3^- by the dissolution of shells according to both Eq.8.30A and Eq.8.30B. The distribution over both is estimated on the basis of carbon-13 isotope analysis, if significantly superior to -16‰ (section 8.4.3), or on the basis of the HCO_3^-/Ca^* ratio (section 8.4.3). In samples with an age superior to 100-200 years reaction 8.30A is neglected, because the input of strong acids was very low. The complexation-dissolution reaction 8.30C can be ignored in low-DOC waters. The Ca-complexation capacity of dissolved humic substances is inferior to 40-130 µg Ca^{2+}/mg DOC (extrapolated from data in Frimmel, 1992, assuming a lower capacity for Ca^{2+} as compared to Cu^{2+}).
(22) balance Na^* by sea salt (base) exchange according to Eq.8.31. For shallow dune groundwater the coefficients b : c : d (for Na^*, K^* and Mg^*, respectively) can be taken equal to 1 : 0.02 : 0.1 (on a mol-basis), as generally observed in the field (section 6.7.4 close to Eq.6.14). In deep, freshened dune water these coefficient may vary more at random, even with negative values for K^* and Mg^* in $NaHCO_3$ water (Fig.7.12).
(23) balance NH_4^+ in deep dune water by anoxic cation exchange either for Ca^* (Eq.8.34B) or for Na^*, K^* and/or Mg^* (Eq.8.34A).
(24) balance Ca^* and Mg^* by exchange for H^+ according to Eq.8.22 (reduction of base saturation). For simplicity, the amount of Mg^* is taken proportional to the Mg^*/Ca^* ratio in groundwater, as their selectivity coefficient in exchange reactions generally approaches 1. The effect of $Al(OH)_3$ dissolution and subsequent Al-sorption has not been treated separately, but is incorporated in our consideration of H^+ exclusively. Reaction 8.22 is neglected in dune water >100-200 years old.
(25) balance CO_3^{2-} included in the alkalinity as HCO_3^-, by addition of an equal amount of H^+ and subtraction of an equal amount of HCO_3^-, using :

$$HCO_3^- \leftrightarrows H^+ + CO_3^{2-} \qquad (8.53)$$

(26) balance H^+ by using the CO_2/HCO_3^- buffer :

$$HCO_3^- + H^+ \leftrightarrows H_2CO_3 \qquad (8.54)$$

(27) balance CO_2 by respiration according to Eq.8.9. This term covers both true respiration and the oxidation of organic matter in the unsaturated zone. These reactions cannot be separated.

Phase IV : evaluation
The final phase consists of an evaluation of the balance after the following checks :
(28) compare the calculated concentration of HCO_3^-, which was balanced under step 21 but subsequently altered by steps 25-26, with the level observed in groundwater. Hydrogencarbonate is indeed the most important reaction progress variable and as such the best parameter to check a balance on.
(29) compare the respiration term, which also constitutes a quantitatively important balance element, for several diverging samples, either shallow under different vegetation covers, or down-gradient, and check for logic. For instance, dune shrub-groundwater in calcareous dunes should have a higher CO_2 production by respiration than mosses-groundwater, and down the hydraulic gradient respiration should not change much, unless a plausible explanation can be given.
(30) calculate the $\delta^{13}C$ value for the groundwater sample using the reaction scheme inherent to the mass balance, and compare this value with the $\delta^{13}C$ analysis.
(31) if all simulated and observed levels are sufficiently close to each other and logic is warranted, one may feel satisfied with the results. Otherwise, crucial steps like 2, 8, 11, 12, 14 and 16 which heavily rely on assumptions or estimates, need to be reconsidered. Or the composition of the solid phases (organic matter, calcium carbonate or silicates) requires adjustment. Or other reactions must be added, for instance the dissolution or formation of vivianite (Eq.8.33) and siderite (Eq.8.32), the transformation of clay minerals (Eq.8.36), or the mixing of methane with water containing sulphate (Eq.8.47), or ascending CH_4 bubbles that reduce $Fe(OH)_3$ (Eq.8.49).

8.3 Carbon-13

General information
The heaviest, stable isotope of carbon is ^{13}C, with an abundance of about 1.1% and concentrations expressed according to Eq.1.2. Fractionation during natural physical and chemical processes, yields well-measurable variations in the ^{13}C concentration of environmental water (here up to 40‰; Fig.8.1), which may give clues about the fate of acids and sources of TIC in groundwater.

Results of analysis refer to Total Inorganic Carbon ($\delta^{13}C_{TIC}$), which in dune groundwaters is about completely made up of H_2CO_3 and HCO_3^-. For the equilibrium system CO_2-H_2O we may assume, according to Mook (1989), that :

$$\delta^{13}C_{CO_2} \simeq \delta^{13}C_{HCO_3} + \varepsilon_b^a \qquad (8.55)$$

where the fractionation factor $\varepsilon_b{}^a$ (the acid relative to hydrogencarbonate) amounts to -10.72‰ at 10°C. For hydrogencarbonate we then obtain :

$$\delta^{13}C_{HCO_3} \simeq \delta^{13}C_{TIC} + 10.72\frac{CO_2}{TIC} \qquad (8.56)$$

where $CO_2 = H_2CO_3{}^*$, and both CO_2 and TIC expressed as mmol/l.

Major sources of TIC in dune groundwater are : CO_2 generated in the soil by respiration and mineralization of biomass ($\delta^{13}C$ = -25‰; Mook, 1989), HCO_3^- from marine shell fragments ($\delta^{13}C$ = +1‰; Mook, 1989), and CO_2 produced during methanogenesis ($\delta^{13}C$ = >+10‰; see below, under "Deep dune water"). Other sources like atmospheric CO_2 ($\delta^{13}C$ = -8‰), other carbonates like siderite, and CO_2 that formed by oxidation of methane ($\delta^{13}C$ = <-60‰; Barker & Fritz, 1981) can probably be neglected.

Shallow dune groundwaters
If the dissolution of shells by soil CO_2 (Eq.8.30B) would be the only process, the resulting HCO_3^- ions would possess a $\delta^{13}C_{HCO3}$ of -12‰ (= [+1-25]/2). Most shallow dune groundwaters with a CO_2/TIC molar ratio in between 0.05 (TIC = 2-4 mmol/l) and 0.16 (TIC = 4-15 mmol/l), then yield according to Eq.8.56 a $\delta^{13}C_{TIC}$ in between -12.5 and -13.7‰, respectively. This agrees fairly well with the results of analysis on shallow dune groundwaters without peat interference (Fig.8.2).

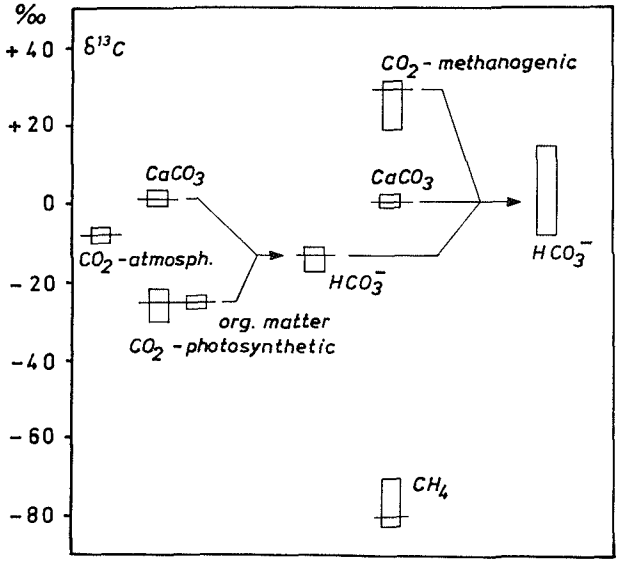

FIG. 8.1 Schematic survey of $\delta^{13}C$ variations relative to PDB in the coastal dune environment.

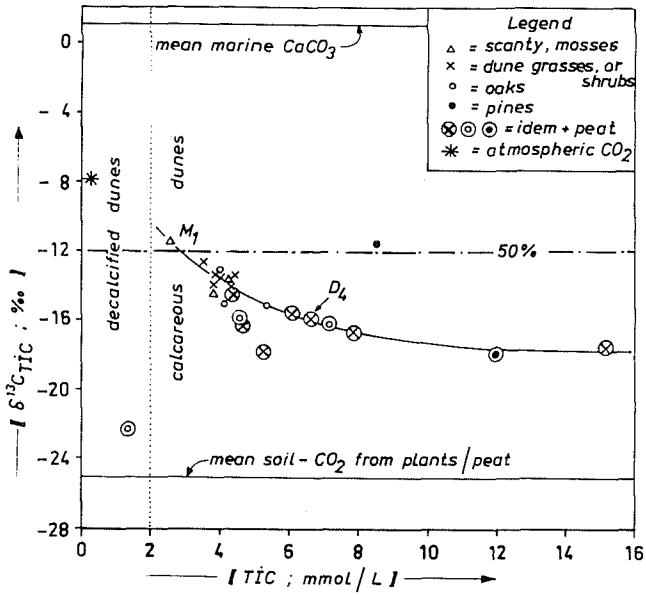

FIG. 8.2 Plot of $\delta^{13}C_{TIC}$ versus Total Inorganic Carbon (TIC) for 24 shallow dune groundwaters (upper aquifer), with indication of the vegetation cover and interaction with dune peat. The ^{13}C concentration in decalcified dunes is dictated by soil CO_2 (without $CaCO_3$ dissolution). In calcareous environments without dune peat interaction, ^{13}C approaches a level in between soil CO_2 and marine calcium carbonate (the indicated 50%-line), by reaction of 1 mmol CO_2 ($\delta^{13}C$ = +1‰) yielding 2 mmoles HCO_3^- ($\delta^{13}C$ = [-25 +1]/2 = -12‰). The interaction with dune peat, the intensity of which is positively related to TIC, conduces to lower ^{13}C concentrations by exchange of carbon isotopes from dissolved hydrogencarbonate with an excess of carbon dioxide and organic matter with $\delta^{13}C$=-25‰.

This is quite surprising though, as we know that there is also a strong input of the atmospheric acids H_2SO_4 and HNO_3, which by reaction with $CaCO_3$ yield $\delta^{13}C_{HCO3}$ values of +1‰. Evidently, these strong acids contribute little to the dissolution of calcium carbonate, because they are largely neutralized in other reactions above the $CaCO_3$-leaching zone, like in the reduction of the base saturation of the exchange complex in the decalcified zone. This contribution is quantified for the plot mosses-1 in section 8.4.3.

Other complications appear negligible as well, like : (a) $CaCO_3$ dissolution by humic acids yielding a $\delta^{13}C_{HCO3}$ of +1‰; (b) $CaCO_3$ dissolution upon Ca^{2+} adsorption by sea salt (base) exchange (reaction 6.14 from left to right), yielding a $\delta^{13}C_{HCO3}$ in between +1‰ (without CO_2 consumption) and -10.9‰ (dissolution by CO_2 consumption; [-22.72 + 1]/2). In the latter case the losses of the light CO_2 will result in an additional rise of $\delta^{13}C_{TIC}$; (c) $CaCO_3$ dissolution by the heavy CO_2 formed during methanogenesis, ultimately yielding a $\delta^{13}C_{TIC}$ of +20‰ (see below under "Deep dune water"); and (d) the consumption of CO_2 in reactions with solid phases devoid of carbonate, like the dissolution of silicates, yielding a $\delta^{13}C_{TIC}$ of -25‰. This reaction explains the very low $\delta^{13}C_{TIC}$ values in the upper dune groundwaters in the noncalcareous dunes (Fig.8.2).

Shallow dune groundwaters with a clear dune peat interference generally possess lower $\delta^{13}C$ values than those lacking such interferences (Fig.8.2). There is also a negative relationship with TIC : the higher TIC, the lower is $\delta^{13}C_{TIC}$. This is explained in two ways :

(1) by the exchange of carbon isotopes from dissolved hydrogencarbonate with an excess of carbon dioxide and organic matter with $\delta^{13}C$=-25‰, ultimately yielding a $\delta^{13}C_{HCO3}$ of -14.4‰ according to Eq.8.55. This leads in high CO_2 and TIC water (CO_2/TIC = 0.16) to a $\delta^{13}C_{TIC}$ of about -16‰ according to Eq.8.56, which approaches the values observed (Fig.8.2); and

(2) by slightly reduced $\delta^{13}C$ levels for the solid calcium carbonate (from +1 down to about -2‰) by isotopic exchange with more abundant soil CO_2, which is enhanced by frequent precipitation upon for instance drying and heating (Mook, 1989).

Deep dune groundwaters

The general evolution pattern downgradient consists of an increase in both $\delta^{13}C$ and TIC (Fig.8.3). The increase in TIC (HCO_3^- mainly) is the result of both the continued decomposition of organic matter and

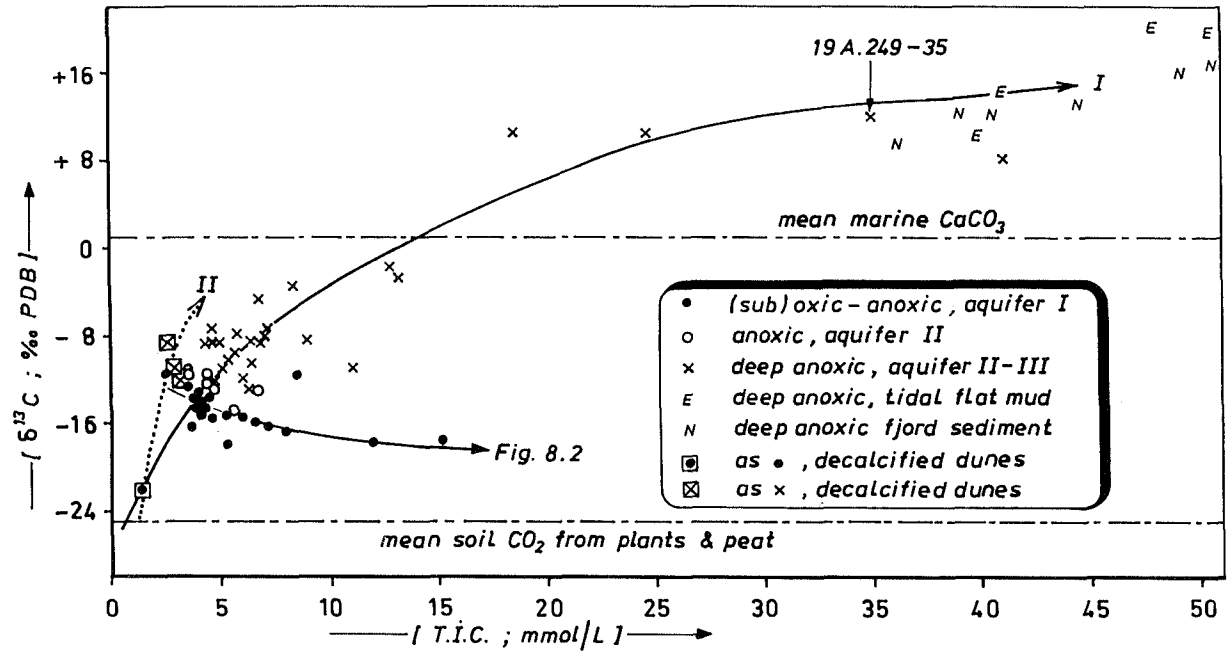

FIG. 8.3 Relation between $\delta^{13}C_{TIC}$ and total inorganic carbon (TIC) in various dune groundwaters, from calcareous and decalcified dunes, the upper and second aquifer and selected redox levels. The general evolution in the calcareous and decalcified dunes follows resp. curve I and II. Samples coded E refer to aqua dest equilibrated with deep anoxic tidal flat mud at 25°C (data obtained from H.J. Streurman) and those coded N represent salt pore water in deep anoxic fjord sediment (Nissenbaum et al., 1972). Dune water with TIC exceeding 15 mmol/l is slighly brackish (300-600 mg Cl⁻/l) due to minor admixing of connate salt water from the Bergen clay.

dissolution of $CaCO_3$. The latter is mainly driven, in deep dune water, by (a) methanogenesis, which produces CO_2 and, to a smaller degree, organic acids; and (b) Ca^{2+} depletion by exchange for Na^+, K^+ and Mg^{2+} (sections 7.3 and 7.4). Both processes also lead to a strong increase in $\delta^{13}C$, which qualitatively explains the relation of $\delta^{13}C$ with TIC.

Decomposition of organic matter in less anoxic environments cannot contribute to high ^{13}C concentrations, as it yields $\delta^{13}C$ values in between -12 (only in case of the aerobic oxidation with complete CO_2 consumption by dissolution of $CaCO_3$) and -25‰. The difference between (sub)oxic to anoxic dune water from the upper aquifer and anoxic deep dune water (both without sulphate reduction!) is indeed small (Fig.8.3; see also the $\delta^{13}C$ log of well 24H.470 in Fig.7.8).

Extreme $\delta^{13}C_{TIC}$ values in dune water with extremely high concentrations of TIC, for instance +12‰ and 35 mmol TIC/l in sample 19A.249-35 in Fig.8.3, can be explained in a simplified way, as follows. Biogenic methane is strongly depleted in ^{13}C, which may yield a $\delta^{13}C$ value as low as -80‰ (Barker & Fritz, 1981). This leaves, under ideal circumstances with a $\delta^{13}C$ for decomposing organic matter equal to -25‰, and simplifying the reaction as $2CH_2O$ --> $CH_4 + CO_2$, a $\delta^{13}C$ value of +30‰ (= 2[-25] + 80) for the other reaction product, CO_2. Reaction of this CO_2 with calcite yields a $\delta^{13}C_{TIC}$ of +15.5‰ (= [30 + 1]/2). Sample 19A.249-35 contains 4.2 mmol CO_2/l and 30.8 mmol HCO_3^-/l, no sulphate with an estimated reduction of 2.3 mmol SO_4^{2-}/l and, before entrance into the deep anoxic environment composed of the Bergen clay, an initial TIC equal to 4 mmol/l with $\delta^{13}C_{TIC}$ = -14‰. A simple balance then yields a calculated $\delta^{13}C_{TIC}$ of {4*[-14] + 2.3*[-25] + 4.2*[+30] + 24.5*[+15.5]}/35 = +11.2‰. This compares well with the measured +12‰.

8.4 Shallow groundwater in contrasting dune areas

8.4.1 Presentation of balances

Tentative mass balances were drawn up following the general set-up presented in section 8.2, for 4 shallow vegetation-groundwaters in contrasting dune areas : in calcareous dunes on the plots mosses-1 (penoxic, without peat) and dune shrub-4 (anoxic sulphate-(meta)stable, with peat), and in decalcified dunes without dune peat interference on the plots scanty-1 (suboxic) and pines-5 (transition from suboxic to anoxic). Background information on these plots is presented in Table 6.1 and results of chemical analysis of the upper 1-3 metres of groundwater are given in Tables 6.13-6.15. The elaborate chemical mass balance is shown for the plots in calcareous dunes in Table 8.5, and those for the plots in decalcified dunes in Table 8.6.

The calculated HCO_3^- concentrations deviate less than 0.2 mmol/l from the measured concentrations. This is a negligible fraction of each ionic balance and means that each balance could be squared with the balance terms 1-27 declared in section 8.2.2. Other checks of the balance, the comparison of respiration rates and the $\delta^{13}C$ balance, are discussed in sections 8.4.2 and 8.4.3, respectively.

The most important outcome, the H^+ budget, is presented for the four plots in Fig.8.4. Sources and sinks are shown there, both for the strong, mainly atmogenic acids H_2SO_4, HNO_3 and HF, and for the weak carbonic acid H_2CO_3. First, these budgets are intercompared (section 8.4.2) and then the dissolution of calcium carbonate by strong acids on the one hand and by the weak carbonic acid on the other hand is specified (section 8.4.3).

8.4.2 Intercomparison of H^+ budgets

The size of reactions which produce or neutralize the strong acids H_2SO_4, HNO_3 and HF on the one hand and the weak carbonic acid H_2CO_3 on the other, is depicted in cumulative bar diagrams for each plot (Fig.8.4). The most relevant sources of strong acids are composed of the free acidity of bulk deposition, interception deposition of SO_2, NO_x and NH_3, nitrification of NH_4^+ in bulk deposition, the oxidation of iron sulphides with immobilization of Fe by formation of $Fe(OH)_3$, and the uptake of cations by vegetation. The position of the latter in this group is questionable, but was also dictated by the desire to separate carbonic acid from all other sources of acidity. Carbonic acid is mainly generated in vadose water and shallow dune groundwater during respiration, aerobic decomposition of organic matter, denitrification and upon the buffering of strong acids by HCO_3^- (reaction 8.54). Organic acids of various strength can be generally neglected in dune groundwater (section 8.4.3) or have been largely included in the determination of alkalinity.

The results presented in Fig.8.4, lead to the following conclusions. The total input of strong acids is highest on the plot pines-5, followed by mosses-1 and dune shrub-4 (both with a nearly equal input), and is lowest on the scanty plot. These differences are dictated mainly by disparities in interception deposition, which constitutes the main source of the strong acids H_2SO_4, HNO_3 and HF. The 1.8 times higher interception deposition by mosses south of Zandvoort aan Zee as compared to the scanty vegetation cover north of Bergen is attributed to : (a) the generally higher SO_2

TABLE 8.5 A tentative chemical mass balance for the upper dune groundwater on the plots mosses-1 and dune shrub-4 in calcareous dunes south of Zandvoort aan Zee, in the period 1979-1982. The numbers within brackets refer to the reaction equations in Tables 8.1-8.3 and section 8.2.2.

MOSSES-1

balance term µmol m^{-2} d^{-1}		O_2	CO_2	CH_4	H^+	Cl^-	SO_4^*	NO_3^-	F^-	HCO_3^-	PO_4^{3-}	Na^*	K^*	Ca^*	Sr^*	Mg^*	NH_4^+	Fe	Mn	Al	SiO_2
INPUT																					
bulk precipitation		490γ	26	<2	112	2059	117	146	3.6	0	1.0	0		72	0.04	0	123	4	0.9	6	
nongaseous ID		-	-	-	-	274	-	-	-	-	0.1	0	1	10	0	0	-	0.5	0.1	1	1
SO_2-deposition	(8.1)	Ω			564	-	282	-			-	-		-	-	-		-	-		
NO_x-deposition	(8.3)	Ω			141		-	141													
NH_3-deposition	(8.4)	Ω			423			423	-												
HF -deposition		Ω	-		14			-	14												
respiration	(8.9)	Ω	1345		-				-								-				
N_2-fixation	(8.10)	Ω	-	-	-	-	-	-	-	-	-	-	-	-	-	-	200[α]	-	-	-	-
Σin		490γ	1371	<2	1254	2333	399	710	18	0	1.1	0	0	82	0.04	0	123	4.5	1.0	7	0
REACTIONS																					
filtration		-			-			-									-	-4.5			
nitrification	(8.5)	Ω			238		-	119			-						-119	-			
storage-anion	(8.6)	-			-27		-6	-			-5			-		-	-				
storage-cation	(8.7)	-			27		-				-			-6		-5					-
hornblende	(8.19)	Ω	-		-65					-			-	13		13					58
orthoclase	(8.27)	-	-10		-					10			13	-		-1					29
SiO_2	(8.28)		-		-					-			-							-	29
gibbsite	(8.23)	-			18						-									-6	-
apatite	(8.29A)	-			-9					-	3.9									-	
conv. apatite	(8.29C)	-	,		-		-			+7	-										
jurbanite	(8.24)	-	-		-12		-6	-		-	-										
O_2+O.M	(8.11)	312	301		-		-	11		-11	0.6										
NO_3+O.M	(8.12A)	-	3		-			-11		11	0.1			-	-	-					
reduction BS	(8.22)	-			-985			-		-	-			365	0.7	125					
$H^+ + CaCO_3$	(8.30A)	-	-		-314					314[β]	0.1	7		309	0.6	1					
CO_2+$CaCO_3$	(8.30B)	-	-1622	-	-					3244[β]	0.6	38		1596	3.2	3					
Base-exchange	(8.31)	-	-	-	-					-	-	68		-41	-0.1	7					
HCO_3^--buffer	(8.53)	-	123	-	-123	-	-	-	-	-123	-	-	-	-	-	-	-	-	-	-	-
OUTPUT[δ]																					
calculated		178	159	<2	0	2333	387	829	11	**3452**	1.4	117	21	2325	4.4	143	4	≤1	1	1	124
measured		178	159	<2	0	2333	387	829	11	**3594**	1.4	117	21	2325	4.1	143	4	≤1	≤1	.	124

DUNE SHRUB-4

balance term µmol m^{-2} d^{-1}		O_2	CO_2	CH_4	H^+	Cl^-	SO_4^*	NO_3^-	F^-	HCO_3^-	PO_4^{3-}	Na^*	K^*	Ca^*	Sr^*	Mg^*	NH_4^+	Fe	Mn	Al	SiO_2
INPUT																					
bulk precipitation		386γ	20	<2	107	1203	106	146	3.6		1.1	0	7	55	0.04	0	112	4	0.9	6	7
nongaseous ID		-	-	-	-	1780	-	-	-	-	1.6	0	10.4	80	0.06	0	-	6	1.3	9	10
SO_2-deposition	(8.1)	Ω			500	-	250	-			-		-	-	-	-			-		-
NO_x-deposition	(8.3)	Ω			125		-	125													
NH_3-deposition	(8.4)	Ω			375			375	-												
HF -deposition		Ω	-		12			-	12.5												
respiration	(8.9)	Ω	3666		-				-								-				
N_2-fixation	(8.10)	Ω	-	-	-	-	-	-	-	-	-	-	-	-	-	-	350[α]	-	-	-	-
Σin		386γ	3686	<2	1119	2983	356	646	16	0	2.7	0	17	135	0.1	0	112	10	2	15	17
REACTIONS																					
filtration		-			-			-									-	-10			
nitrification	(8.5)	Ω			168		-	84			-						-84	-			
storage-anion	(8.6)	-			-69		-15	-			-13		-	-		-	-				
storage-cation	(8.7)	-			115		-				-		-39	-25		-12					-
hornblende	(8.19)	Ω	-		-67					-			-	13		13					60
orthoclase	(8.27)	-	-11		-					11			14	-		-1					30
SiO_2	(8.28)		-		-					-			-							-	30
gibbsite	(8.23)				42						-			-						-14	-
apatite	(8.29A)	-			-25				-		10.8			18						-	
conv. apatite	(8.29C)	-			-12		-		-12		-			-							
jurbanite	(8.24)	-	-		-36		-18	-	-	-											
SO_4^{2-} mobil	(8.17D)	-	86		-		429	-772		-86								-			
Fe-mobil	(8.14)	-	-128				-	-		147								73			
Mn-mobil	(8.13)	-	-5					-		6	-							-			
O_2+O.M	(8.11)	-386	372		-			14		-14	0.7			-	-	-					
reduction BS	(8.22)	-	-		-722			-		-	-			311	0.6	49					
$H^+ + CaCO_3$	(8.30A)	-	-		-377					377[#]	0.1	9		371	0.7	1					
CO_2+$CaCO_3$	(8.30B)	-	-2951		-					5902[#]	1.2	70		2904	5.8	6					
Base-exchange	(8.31)	-	-		-					-	-	21		-13	-	2					
HCO_3^--buffer	(8.53)	-	136	-	-136	-	-	-	-	-136	-	-	-	-	-	-	-	-	-	-	-
OUTPUT[δ]																					
calculated		0	1193	<2	0	2983	752	**-28**	4	**6192**	2.6	103	-7	3714	7.2	58	29	73	3	1	137
measured		0	1193	<2	0	2983	752	**≤10**	4	**6328**	2.6	103	-7	3714	4.8	58	29	73	3	1	137

Ω = system open to atmosphere (infinite supply); α = as N_2 and therefore excluded from the balance; β = distribution calculated using carbon-13 (see text); γ = $(O_2)_{eq}$·N with N = natural recharge; δ : Output = Σin + Σreactions; # = distribution calculated using Eqs.8.61-8.66.

TABLE 8.6 A tentative chemical mass balance for the upper dune groundwater on the plots scanty-1 and pines-5 in decalcified dunes north of Bergen, in 1987. The numbers within brackets refer to the reaction equations in Tables 8.1-8.3 and section 8.2.2.

SCANTY-1

balance term µmol m^{-2} d^{-1}		O_2	CO_2	CH_4	H^+	Cl^-	SO_4^*	NO_3^-	F^-	HCO_3^-	PO_4^{3-}	Na^*	K^*	Ca^*	Sr^*	Mg^*	NH_4^+	Fe	Mn	Al	SiO_2
INPUT																					
bulk precipitation		471[γ]	25	<2	76	1008	105	123	3.8		1.0	0	4	36	0.04	0	160	4	0.9	6	
nongaseous ID		-	-	-	-	112	-	-	-	-	0.1	0	0.4	3.6	0	0	-	0.4	0.1	1	1
SO_2-deposition	(8.1)	Ω			316	-	158	-			-	-	-	-				-	-		
NO_x-deposition	(8.3)	Ω			79		-	79													
NH_3-deposition	(8.4)	Ω			237			237	-												
HF -deposition		Ω	-		8			-	7.9												
respiration	(8.9)	Ω	711						-								-				
N_2-fixation	(8.10)	Ω	-	-	-	-	-	-	-	-	-	-	-	-	-	-	200[α]	-	-	-	-
Σin		471[γ]	736	[illegible]	716	1120	263	439	11.7	0	[illegible]	0	4	40	0.04	0	160	4.4	1.0	7	9
REACTIONS																					
filtration		-			-			-									-	-4.4			
nitrification	(8.5)	Ω			316			158									-158	-			
storage-anion	(8.6)	-			-27			-						-			-				
storage-cation	(8.7)	-			27							-	-	-6		-5					-
hornblende	(8.19)	Ω	-		-127					-		9	-	26		25					110
orthoclase	(8.27)	-	-28		-					28		-	28	-		-					55
albite	(8.26)		-		-18					-		18	-							-	55
gibbsite	(8.23)				-270						-	-		-						90	-
apatite	(8.29A)	-			-11				-		4.7			8						-	
conv apatite	(8.29C)	-			-8		-		-8.2		-			-							
jurbanite	(8.24)				-144		-72		-												
Fe-mobil	(8.14)				-18		-												-		
Mn-mobil	(8.13)	-	-1		-			-		1	-							-	0.7		
O_2+O.M	(8.11)	-385	370					15		-15	0.7								-		
NO_3^-+O.M	(8.12A)	-	70		-			-380		380	2.0			-							
reduction BS	(8.22)	-	-		-61			-		-	-	-	5	24		4					
Base-exch.	(8.31)		-		-					-		73	1	-44		7					
HCO_3^--buffer	(8.53)	-	318	-	-318	-	-	-	-	-318	-	-	-	-	-	-	-	-	-	-	-
OUTPUT[δ]																					
calculated		86	1465	<2	57	1120	185	232	3.5	76	3.5	100	35	48	<1	31	2	6	0.7	97	228
measured		86	1465	<2	57	1120	185	232	3.5	<1	3.5	100	35	48	<1	31	2	6	0.7	97	228

PINES-5

balance term µmol m^{-2} d^{-1}		O_2	CO_2	CH_4	H^+	Cl^-	SO_4^*	NO_3^-	F^-	HCO_3^-	PO_4^{3-}	Na^*	K^*	Ca^*	Sr^*	Mg^*	NH_4^+	Fe	Mn	Al	SiO_2
INPUT																					
bulk precipitation		189[γ]	10	<2	76	361	105	123	3.8		1.0	0	4	37	0.04	0	160	4	1	6	7
nongaseous ID		-	-	-	-	618	-	-	-		2.0	0	7	63	0.07	0	-	8	2	10	12
SO_2-deposition	(8.1)	Ω			630	-	315	-			-	-		-	-	-		-		-	-
NO_x-deposition	(8.3)	Ω			158		-	158													
NH_3-deposition	(8.4)	Ω			473			473	-												
HF -deposition		Ω	-		16			-	15.8												
respiration	(8.9)	Ω	74		-				-												
N_2-fixation	(8.10)	Ω	-	-	-	-	-	-	-	-	-	-	-	-	-	-	-	-	-	-	-
Σin		189[γ]	84	<2	1353	979	420	754	20	0	2	0	11	100	0.1	0	160	12	2	16	19
REACTIONS																					
filtration		-			-			-									-	-12		-10	
nitrification	(8.5)	Ω			158		-	79			-						-79	-	-	-	
storage-anion	(8.6)	-			-503		-25	-406			-18		-	-		-	-				-
storage-cation	(8.7)	-			300		-	-			-	-	-46	-62		-25	-80				-33
hornblende	(8.19)	Ω			-129							8	-	26		25	-				112
orthoclase	(8.27)	-			-37							-	37	-		-					74
albite	(8.26)				-13							13	-								38
SiO_2	(8.28)				-							-								-	139
gibbsite	(8.23)				-18						-			-						6	-
apatite	(8.29A)	-			-36				-		5.5			26						-	
conv apatite	(8.29C)	-			-9		-		-9		-			-							
jurbanite	(8.24)	-			-478		-239		-									-			
Fe-mobil	(8.21A)	-	-		-51		-	-			-							-17			
O_2+O.M	(8.11)	-189	181		-			7		-7	0.4							-			
NO_3+O.M	(8.12A)	-	91		-			-425		425	1.0		-			-					
reduction BS	(8.22)	-	-		-164			-		-	-	-	18	-		73					
Base-exch.	(8.31)		-		-					-		50	1	-16		10					
HCO_3^--buffer	(8.53)	-	370	-	-370	-	-	-	-	-370	-	-	-	-	-	-	-	-	-	-	-
OUTPUT[δ]																					
calculated		0	726	<2	3	979	156	9	11	48	1.9	71	21	74	<1	83	1	17	1	12	210
measured		0	726	<2	3	979	156	9	11	63	1.9	71	21	74	<1	83	.	17	.	12	210

Ω = system open to atmosphere; α = as N_2 and therefore excluded from balance; β = distribution calculated using carbon-13 (see text); γ = $(O_2)_{eq}$**N*, with *N* = natural recharge.
δ = Σin + Σreactions

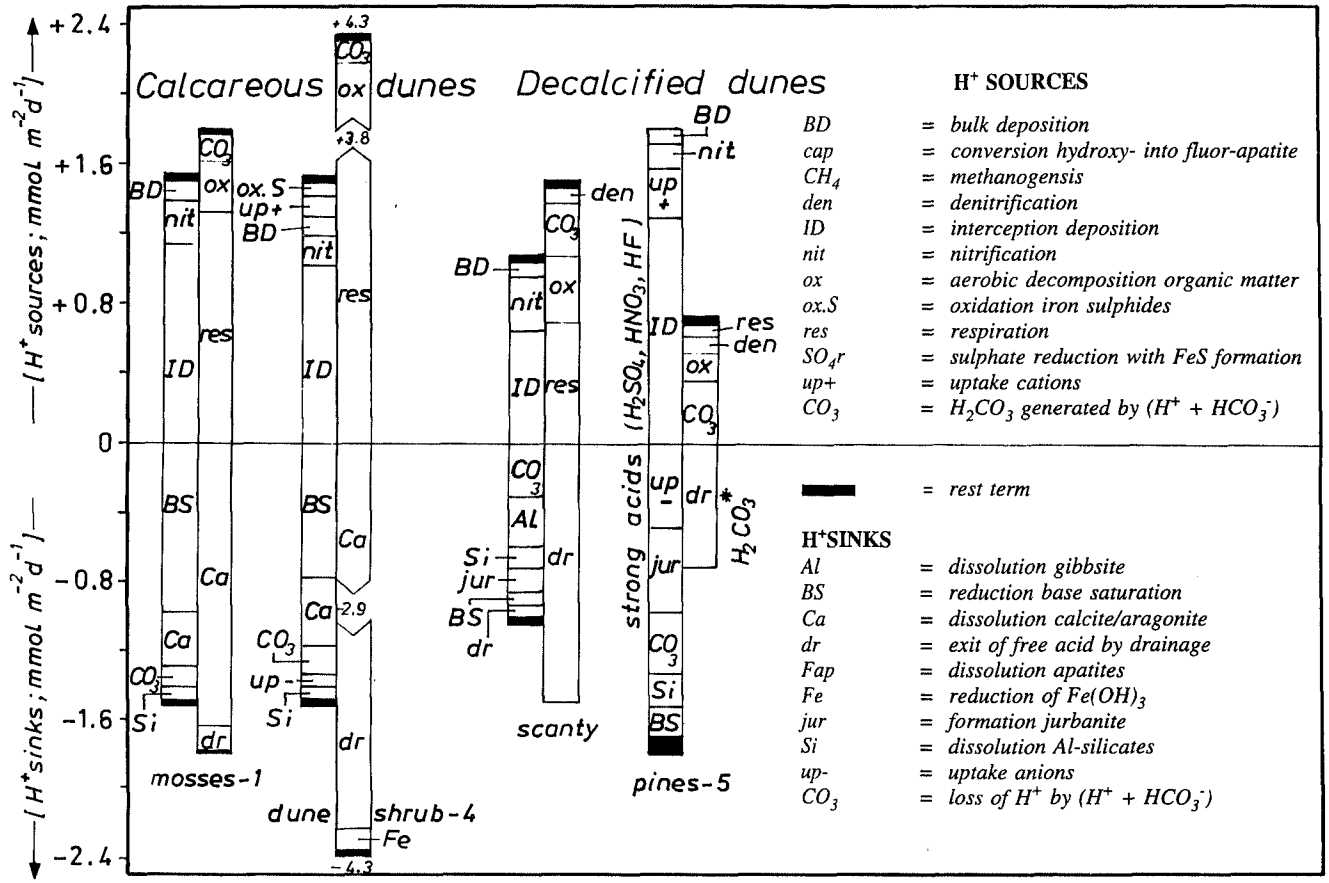

FIG. 8.4 The major H^+ sources and sinks, with distinction between strong (left hand bar) and weak acids (right hand bar), for shallow groundwater on the calcareous plots mosses-1 and dune shrub-4 (with dune peat interaction), and the decalcified plots scanty-1 and pines-5.

concentrations in air south of Zandvoort aan Zee (Fig.5.3); (b) the difference in period of measurement, yielding a somewhat more polluted episode for mosses-1 (1979-1983) than for scanty-1 (1987; Fig.5.5); and (c) an enhanced absorption of atmospheric gases on the plot mosses-1, by virtue of a higher sea spray deposition with a hygroscopic effect and a higher consumption of these gases by reaction with calcareous dust and calcareous dune sand (section 6.6.2).

Nitrification in case of shrubs and scantier vegetation covers, and the uptake of cations under forest stands, form the second most powerful source of strong acids.

Respiration generally constitutes the main source of H_2CO_3, except for pines in decalcified dunes, where the hydrogencarbonate buffer generates most. Respiration, which includes the unseparable aerobic decomposition in the unsaturated zone, yields 2-50 times more H_2CO_3 in calcareous dunes than in decalcified dunes, at least in this restricted comparison of four cases. This was expected, because the acid is rapidly consumed by $CaCO_3$ dissolution, which in an open system leads to further uptake of CO_2 by the water phase etc. The production below dune shrub superates that below mosses by a factor of 2.7. This is more than expected on the basis of Eq.6.9, relating soil CO_2 pressure to evapotranspiration, and the following relation (Stumm & Morgan, 1981) between the $H_2CO_3^*$ concentration in water [mol/l] and partial CO_2 pressure in soil air [10^5 Pa], at 10°C :

$$H_2CO_3^* = 10^{-1.27} \cdot P_{CO_2} \qquad (8.57)$$

For mosses-1 with E = 300 mm/y and dune shrub-4 with 410 mm/y, we thus obtain 126 and 209 µmol $H_2CO_3^*$/l, which gives 179 and 235 µmol m^{-2} d^{-1}, respectively. The ratio of dune shrub-4 to mosses-1 thereby becomes 1.3, which is only half of their calculated respiration ratio. The difference can be attributed to : (1) the aerobic decomposition of dune peat, which is episodically situated in the unsaturated zone, and the effects of which are included in

the respiration term; and (2) a raised root biomass of *Hippophaë*, which in the presence of N_2-fixing microorganisms conduces to an increased respiration.

The respiration rates at the four plots so far relate to each other in a logic way, and thereby constitute a validation of the underlying mass balances. However, the respiration term is extremely low for the plot pines-5 as compared to the scanty plot, which is also situated in decalcified dunes. With Eq.6.9 and 8.57 the predicted $H_2CO_3^*$ fluxes for pines-5 and scanty-1 become 234 and 192 μmol m^{-2} d^{-1}, respectively. This yields a ratio of 1.2, whereas the calculated respiration ratio reads 74/711 = 0.1 in the mass balance! The discrepancy is explained mainly by the dry soil conditions under pines, which lead to the lack of water to pick up the CO_2 respired, especially in the summer semester. The escape of more CO_2 gas during vacuum sampling of groundwater at pines-5 than at scanty-1 contributes relatively little to the difference. With the assumption that these losses are proportional to the measured concentration of dissolved CO_2 (1325 μmol/l for pines-5 and 1070 μmol/l for scanty-1) and the depth to the phreatic level (3.7 m for pines-5 and 3.1 m for scanty-1), we obtain a ratio of 1.5 for the losses on pines-5 and scanty-1. With an estimate of 20% lost on scanty-1 (268 μmol/l) and thereby 402 μmol/l on pines-5, we obtain a corrected respiration ratio (pines/scanty) of 294/1078 = 0.3, which still is much lower than 1.2.

The main process neutralizing strong acids in calcareous dunes, is the reduction of the base saturation of the exchange complex in the upper unsaturated zone, followed by the dissolution of calcium carbonate. In decalcified dunes, no uniform main consumer of strong acids can be assigned. The hydrogencarbonate buffer and dissolution of gibbsite preponderate on the plot scanty-1, whereas the uptake of anions, jurbanite formation and the hydrogencarbonate buffer consume the majority of strong acids on the plot pines-5. In decalcified dunes the already low base saturation of the exchange complex is hardly reduced any more, at least down to the upper metres of acid groundwater.

The dissolution of calcium carbonate consumes practically all $H_2CO_3^*$ in the calcareous dunes. The higher this consumption, the higher is the fraction of carbonic acid drained (compare mosses-1 with dune shrub-4), which is required to maintain internal equilibrium with HCO_3^-. The negligible H_2CO_3 consumption in decalcified dunes is explained by the low dissociation of carbonic acid in acid environments.

8.4.3 Dissolution of calcium carbonate by strong and weak acids

Calcium carbonate can be dissolved by the strong atmogenic acids H_2SO_4, HNO_3, HF and HCl (of which the latter two are ignored), by organic acids like oxalic and fulvic acid, and by the weak carbonic acid. The relatively low DOC-concentrations in the calcareous vegetation-groundwaters studied, as compared to TIC (Table 6.15), and the close equilibrium with calcite/aragonite, as calculated on the basis of inorganic species exclusively (Table 6.15), justify the assumption that the contribution of organic acids can be properly ignored.

The contribution from the strong atmogenic acids can be estimated either by an iterative approach of the mass balance, which is not considered here, or from the composition of the groundwater directly. In the latter case there are two different ways : by unravelling the main sources of either HCO_3^- using carbon-13 isotope analysis, or Ca^*. This is illustrated below, using the mean composition of pure vegetation groundwater on the plot mosses-1.

Assumptions

It is assumed that : (1) the dissolution of calcium carbonate according to the reactions 8.30A (strong acids) and 8.30B (carbonic acid), contributes for 100% to the dissolved HCO_3^- concentration in this groundwater; and (2) Ca^* is supplied exclusively by the dissolution of calcium carbonate and the ion exchange according to either Eq.8.22 (reduction of base saturation of the exchange complex) or Eq.8.31 (sea salt exchange, salinization). The $CaCO_3$ dissolution also includes the reaction :

$$CaCO_3 + 2\ H^+ \leftrightarrows Ca^{2+} + CO_2 + H_2O \quad (8.58)$$

where the carbondioxide is lost to the atmosphere, as happens in acid rain scavenging calcareous dust. Thereby, we ignore many sources and sinks for HCO_3^- and Ca^{2+} (Tables 8.2-8.4), among which the potentially strong HCO_3^- contributions from denitrification (Eq.8.12) and the reduction of $Fe(OH)_3$ (Eq.8.14). The high NO_3^- levels and negligible Fe concentrations on the plot mosses-1 justify this.

HCO_3^- with carbon-13

The upper groundwater on the plot mosses-1 has a $\delta^{13}C_{TIC}$ of -11.4‰. This is well above -16‰, which indicates that there has been a negligible exchange with excess carbondioxide (section 8.3). We therefore can use carbon-13 to arrive at the relative contribution of strong acids (Eq.8.30A) and carbonic

acid (Eq.8.30B) to the dissolution of calcite. Application of Eq.8.56 with CO_2 being 0.119 and TIC equal to 2.61 mmol/l, yields a $\delta^{13}C_{HCO3}$ of -10.9‰. Carbonic acid (reaction 8.30B) would give a $\delta^{13}C_{HCO3}$ of -12‰ (= [1 - 25]/2), whereas strong acids (reaction 8.30A) would result in a $\delta^{13}C_{HCO3}$ of +1‰. Using both reactions as the end-members in a binary mixture, gives : $\alpha \cdot (-12) + [1-\alpha] \cdot (+1) =$ -10.9‰.
This yields a relative contribution by carbonic acid of 91% (=100α) and by strong (mainly atmogenic) acids of 9% to the dissolved HCO_3^- on the plot mosses-1.

Ca^* and major constituents
Electroneutrality is required both for the groundwater as a whole, and for its dissolved sea salts, yielding respectively :

$$Cl^- + 2\ SO_4^{2-} + HCO_3^- + NO_3^- = Na^+ + K^+ + 2\ Ca^{2+} + 2\ Mg^{2+} \quad (8.59)$$

$$Cl_m^- + 2\ SO_{4m}^{2-} = Na_m^+ + K_m^+ + 2\ Ca_m^+ + 2\ Mg_m^{2+} \quad (5.2)$$

where all concentrations in mmol/l; X_m = concentration of X in dissolved air-borne sea salts; and NH_4^+, Fe, Mn, CO_3^{2-}, F^- etc. are neglected.
Subtraction of Eq.5.2 from Eq.8.59, assuming all Cl^- to derive from sea spray ($Cl^- = Cl_m^-$) and substituting X^* for $X - X_m$, yields after rearrangement :

$$Ca^* = SO_4^* + \tfrac{1}{2}(HCO_3^- + NO_3^-) - \tfrac{1}{2}(Na^* + K^* + 2\ Mg^*) \quad (8.60)$$

Expressed in words, Ca^* is equal to the amount of calcium carbonate (in mmoles) dissolved by sulphuric, nitric and carbonic acid, minus the Ca^{2+} lost by exchange for $\{\tfrac{1}{2}Na^* + \tfrac{1}{2}K^* + Mg^*\}$, in which case this sum is positive (section 2.4.1), or minus the acids lost for mobilizing $\{\tfrac{1}{2}Na^* + \tfrac{1}{2}K^* + Mg^*\}$ from Al-silicates, or plus the Ca^{2+} gained by exchange for $\{\tfrac{1}{2}Na^* + \tfrac{1}{2}K^* + Mg^*\}$, this sum being negative then. In this expression we assume that all Ca^{2+}, that was mobilized by any chance in the upper decalcified soil through exchange for H^+, Al^{3+} and NH_4^+ (reduction of the base saturation of the exchange complex according to reaction 8.22), originally derived from the dissolution of calcium carbonate.

If the conjugate bases of the three acids behave conservatively, then the relative contribution of H_2SO_4, HNO_3 and H_2CO_3 to the mobilization of Ca^{2+} through the combined effect of the dissolution of $CaCO_3$ and displacement of Ca^{2+} from the exchanger by H^+, Al^{3+} and NH_4^+, can be easily calculated :

$$\%Ca_{H2SO4} = 100\beta(SO_4^*/Ca^*) \quad (8.61)$$
$$\%Ca_{HNO3} = 50\beta(NO_3/Ca^*) \quad (8.62)$$
$$\%Ca_{H2CO3} = 50\beta(HCO_3/Ca^*) \quad (8.63)$$

with $\%Ca_X$ in %, concentrations in mmol/l, and where the dimensionless correction factor β is calculated according to :

$$\beta = Ca^*/\{SO_4^* + \tfrac{1}{2}NO_3^- + \tfrac{1}{2}HCO_3^-\} \quad (8.64)$$

Values of β exceeding 1, may relate to an ionic imbalance ($\Sigma k > \Sigma a$) or indicate that as much Ca^* was mobilized as $\{\tfrac{1}{2}Na^* + \tfrac{1}{2}K^* + Mg^*\}$ disappeared, for instance through adsorption, precipitation or storage in biomass. Values of β inferior to 1, may relate to an ionic imbalance as well ($\Sigma a > \Sigma k$) or indicate that as much Ca^* disappeared from the solution as $\{\tfrac{1}{2}Na^* + \tfrac{1}{2}K^* + Mg^*\}$ was mobilized, for instance through desorption, weathering of Al-silicates or decomposition of organic matter.

Application of the Eqs.8.60-8.64 to the data for the upper groundwater on mosses-1 (Tables 6.13 and 6.15), yields a relative contribution by H_2SO_4, HNO_3 and H_2CO_3 to the mobilization of Ca^* of 15, 16 and 69%, respectively.

We now assume that the contribution of strong acids to the mobilization of Ca^* is equally distributed over the dissolution of $CaCO_3$ and Ca displacement from the exchanger by H^+. Statistically this is the safest assumption. In the exchange reaction (Eq.8.22) NH_4^+ is thus neglected and Al^{3+} is substituted for by 3 H^+, as these protons were required to dissolve the Al from gibbsite according to Eq.8.23A. We then obtain the following equations for the contributions of H_2CO_3 and strong acids to the HCO_3^- dissolved :

$$\%(HCO_3^-)_{H_2CO_3} = \frac{2 \cdot \%Ca^*_{H_2CO_3}}{2 \cdot \%Ca^*_{H_2CO_3} + 0.5 \cdot (\%Ca^*_{H_2SO_4} + \%Ca^*_{HNO_3})} \quad (8.65)$$

$$\%(HCO_3^-)_{H_2SO_4+HNO_3} = 100 - \%(HCO_3^-)_{H_2CO_3} \quad (8.66)$$

Substituting the calculated values 15, 16 and 69 for $\%Ca_{H2SO4}$, $\%Ca_{HNO3}$ and $\%Ca_{H2CO3}$ respectively, yields a contribution of H_2CO_3 and the combined sulphuric and nitric acids to the dissolved hydrogencarbonate for mosses-1, of 90 and 10% respectively. These figures correspond very well with the previous calculation as based on carbon-13, yielding 91 and 9% respectively.

8.5 Bergen dune water downgradient

8.5.1 Presentation of balances

Tentative mass balances were drawn up following the general set-up presented in section 8.2, for 5 samples of Bergen dune groundwater down the hydraulic gradient, along the same flow path as studied in section 7.3.4. The samples considered, vary from acid, (sub)oxic groundwater 1-2 years old on the plot scanty-1 in the centre of the younger dunes (14C.41+6), to deep anoxic, freshened groundwater about 600 years old and 6.5 km downgradient, in the Geestmerambacht polder (19B.88-44). Results of their chemical analysis are given in Table 7.2. An elaborate chemical mass balance is shown for 19B.88-44 in Table 8.7, and the most important terms of the 5 chemical mass balances are listed in Table 8.8.

The calculated HCO_3^- concentrations deviate less than 0.18 mmol/l from the measured concentrations (Table 8.8). This is a negligible fraction of each ionic balance and means that each balance could be squared with the balance terms 1-27 declared in section 8.2.2. Other checks of the balance, the comparison of respiration rates and the $\delta^{13}C$ balance, are discussed in sections 8.5.2 and 8.5.3, respectively.

The most important outcome, the H^+ budget, is presented for the five samples in Fig.8.5. Sources and sinks are shown there, both for the strong, mainly atmogenic acids H_2SO_4, HNO_3 and HF, and

TABLE 8.7 Tentative chemical mass balance for deep anoxic, freshened dune groundwater from observation well 19B.88-44 in the Geestmerambacht polder, about 6.5 km downgradient and with a calculated age of about 600 years. The numbers within brackets refer to the reaction equations in Tables 8.1-8.3 and section 8.2.2.

balance term µmol l^{-1}		O_2	CO_2	CH_4	H^+	Cl^-	SO_4^*	NO_3^-	F^-	$HCO_3^- + CO_3^{2-}$	PO_4^{3-}	Na^*	K^*	Ca^*	Sr^*	Mg^*	NH_4^+	Fe	Mn	Al	SiO_2
INPUT																					
bulk precipitation		344	18	<2		444		2	0.5	0	0.25	0	0	4	0.01	0	2	≤0.4	≤0.15	≤1.5	3
nongaseous ID		-	-	-	-	49	-	-	-	-	0.03	0	0	0.4	0	0	-	≤0.04	≤0.05	≤0.2	0.3
SO_2-deposition	(8.1)	Ω			6	-	3	-			-	-	-	-	-	-		-	-	-	-
NO_x-deposition	(8.3)	Ω			2		-	2													
NH_3-deposition	(8.4)	Ω			2			2	-												
HF -deposition		Ω	-		0				0.1												
respiration	(8.9)	Ω	1932		-				-							-	-				
N_2-fixation	(8.10)	Ω	-	-	-	-	-	-	-	-	-	-	-	-	-	-	200[α]	-	-	-	-
Σin* 2.0[@]		344	1950	<2	30	987	12	12	1	0	0.6	0	0	9	0.02	0	4	1	0.3	≤3	7
REACTIONS																					
filtration		-			-			-									-		-0.3	-3	
nitrification	(8.5)	Ω			8		-	4			-						-4	-	-	-	
storage-anion	(8.6)	-			-27		-6	-			-5		-	-		-	-				
storage-cation	(8.7)	-	-		27		-	-		-	-		-5	-6		-5					
O_2+O.M	(8.11)	-344	322		-			23		-23	1.4		-	-		-					
denitrification	(8.12A)	-	8					-39		39	0.2										
Mn-mobil	(8.13)		-2					-		2	-						-	-			
Fe-mobil	(8.14)		-120				-			137	0.1						1.3	68			
SO_4-reduction	(8.15)		105	-			-57			9	0.5						9	-57			
CH_4-production	(8.16)	-	967	1138	-		-			171	10.2	-		-		-	171	-			-
hornblende	(8.19)	Ω	-	-	-82					-	-	6		17		16	-			-	72
gibbsite	(8.23B)	-			9							-		-		-				9	-
albite	(8.26)		-		-12					-		12	-			-				-	36
orthoclase	(8.27)		-13		-					13		-	18			-3					36
SiO_2	(8.28)		-						-	-	-		-	-		-					48[#]
F-apatite	(8.29B)		-204						34	204	102			170							-
conv apatite	(8.29C)		44						44	-44	-	-		-	-	-					
CO_2+$CaCO_3$	(8.30B)		-3042						-	6084	1.2	71	-	2994	6.0	6					
Base-exch.	(8.31)		-							-	-	5806	264	-3047	-6.0	17	-				
anoxic-exch.	(8.34)				-							-	-	-81	-	-	162				
CO_3buffer	(8.53)		-		86					-				-			-				
H_2CO_3buffer	(8.54)	-	39	-	-39	-	-	-	-	-39								-	-	-	-
OUTPUT																					
calculated		0	54	1138	0	987	-51	0	79	**6553**	111	5895	276	56	0	31	343	11	1	9	290
measured		0	54	1138	0	987	-51	0	79	**6376**	111	5895	276	56	≤0.6	31	343	11	1	9	290

Ω = system open to atmosphere; α = as N_2 and therefore excluded from the balance; @ = O_2 and CO_2 excluded; # about 91 µmol/l probably lost by sorption.

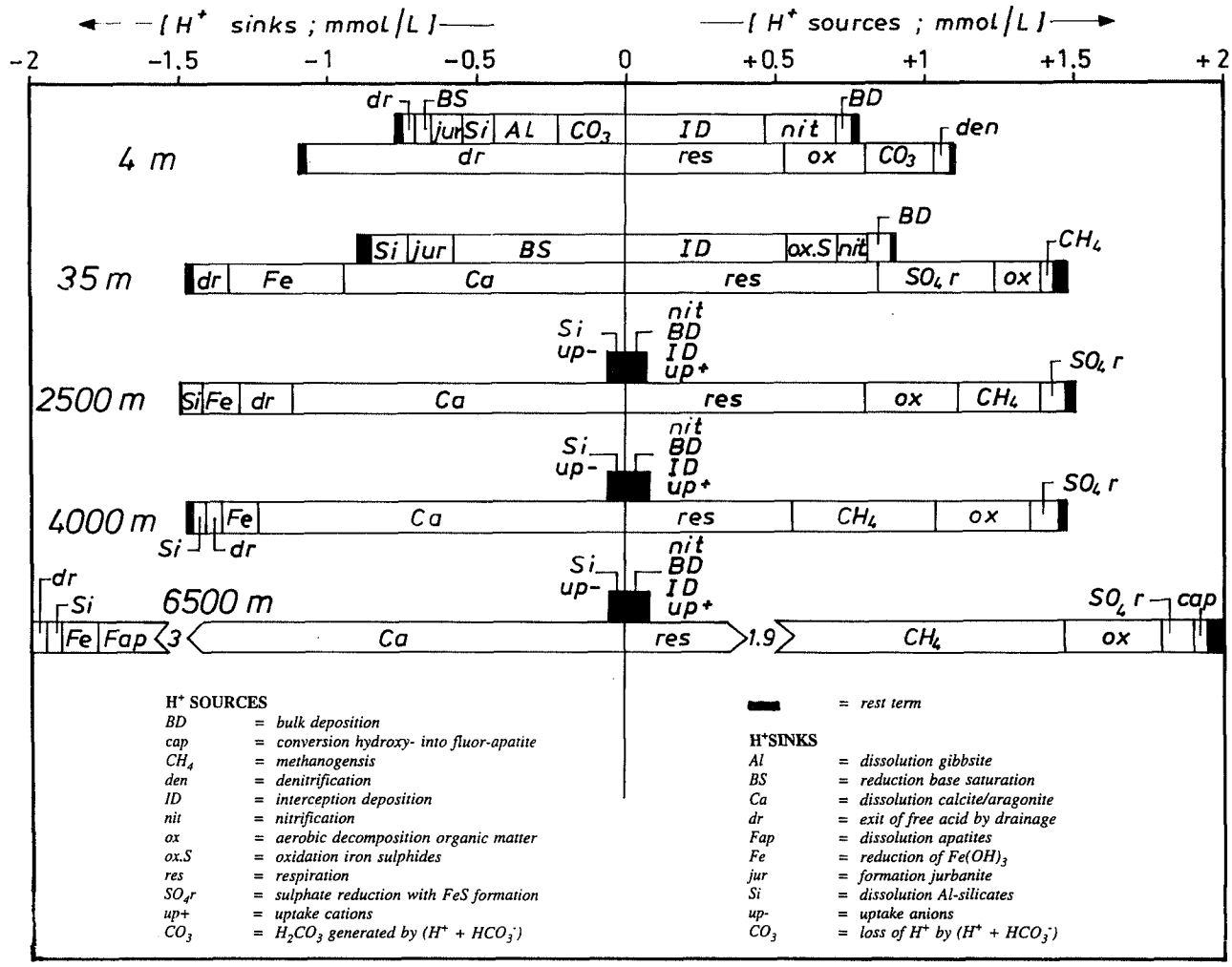

FIG. 8.5 The major H^+ sources and sinks, with distinction between strong (upper bar) and weak acids (lower bar), for five samples of Bergen dune groundwater down the hydraulic gradient, from close to the water table in the younger dunes (4 m = 14C.41+6) towards exfiltration in the Geestmerambacht polder (6500 m = 19B.88-44).

for the weak carbonic acid H_2CO_3. First, these budgets are intercompared (section 8.5.2) and then the balance is checked for one of the samples by Carbon-13 analysis (section 8.5.3).

8.5.2 *Intercomparison of H^+ budgets*

Sources and sinks of the strong acids H_2SO_4, HNO_3 and HF on the one hand, and the weak carbonic acid on the other, are depicted in cumulative bar diagrams for each sample (Fig.8.5). They reveal the following important sources and sinks of H^+ ions for deep dune groundwater, in addition to those applying to shallow groundwater (section 8.4.2) : the conversion of fluor- into hydroxy-apatite, acting as a source of strong acid (HF; Eq.8.29C to the left); sulphate reduction (in combination with the precipitation of iron sulphides; Eq.8.15) and methanogenesis (Eq.8.16), both constituting a source of carbonic acid; and the dissolution of fluor- or hydroxy-apatites, forming a sink of acid, that in anoxic environment is mainly composed of carbonic acid.

The results presented in Fig.8.5, lead to the following conclusions. The supply of strong acids to dune water less than 50 years old (samples 14C.41 +6 and 19A.31-30, at 4 and 35 m resp.) is about 13 times higher than the supply to dune groundwater older than approximately 150-200 years (the other 3 samples). The difference is dictated mainly by the strong increase in atmospheric pollution and interception deposition of the strong acids H_2SO_4,

TABLE 8.8 Concise presentation of the tentative, chemical mass balances for five samples of Bergen dune groundwater along a 6.5 km long flow path, from close to the water table in the centre of the younger dunes towards exfiltration in the Geestmerambacht polder. The flow path is indicated in Fig.7.1.

observation well	reaction	expressed	14C.41	19A.31	19A.159	19B.14	19B.88
screen depth (m+MSL)		as	6	-30	-90	-90	-44
age (year)			1-3	40	250	350	600
INPUT							
H^+ bulk precipitation		µmol/l	34	37	5	5	5
Cl^- bulk precipitation		µmol/l	449	404	368	419	444
SO_4^* bulk precipitation		µmol/l	47	45	3	3	3
NO_3^- bulk precipitation		µmol/l	55	18	2	2	2
Ca^* bulk precipitation		µmol/l	16	16	4	4	4
NH_4^+ bulk precipitation		µmol/l	71	24	2	2	2
Cl^--interception/precip.		µmol/l	50	173	41	47	49
SO_2-deposition/precip.	(8.1)	µmol SO_4^{2-}/l	70	90	3	3	3
NO_x-deposition/precip.	(8.3)	µmol NO_3^-/l	35	15	2	2	2
NH_3-deposition/precip.	(8.4)	µmol NO_3^-/l	105	45	2	2	2
respiration	(8.9)	µmol CO_2/l	525	845	790	549	1932
evap.factor (f=P/N)@			1.64	2.2	2.0	2.0	2.0
MASS TRANSFER BY SOIL REACTIONS							
nitrification	(8.5)	µmol NO_3^-/l	83	53	4	4	4
storage-anions	(8.6)	µmol PO_4^{3-}/l#	-4	-4	-4	-4	-4
storage-cations	(8.7)	µmol K^+/l#	-4	-4	-4	-4	-4
O_2+O.M	(8.11)	µmol O_2/l	-281	-161	-344	-344	-344
denitrification	(8.12B)	µmol NO_3^-/l	-278	-99	-39	-39	-39
Mn-mobilisation	(8.13)	µmol Mn^{2+}/l	1	2	2	1	1
Fe-mobilisation	(8.14)	µmol Fe^{2+}/l	0	217	70	66	68
SO_4^{2-}-reduction	(8.15)	µmol SO_4^{2-}/l	0	-208	-48	-54	-57
CH_4-production	(8.16)	µmol CH_4/l	0	45	310	560	1138
FeS + O_2 -> SO_4^{2-}	(8.17B)	µmol SO_4^{2-}/l	0	76	0	0	0
FeS + NO_3^- -> SO_4^{2-}	(8.17D)	µmol SO_4^{2-}/l	0	76	0	0	0
hornblende dissolution	(8.19)	µmol SiO_2/l	80	91	72	72	72
$Fe(OH)_3$ dissolution	(8.21A)	µmol Fe^{3+}/l	4	0	0	0	0
reduction base satur.	(8.22)	µmol H^+/l	-45	-580	0	0	0
gibbsite dissolution	(8.23A)	µmol Al/l	66	0	0	0	0
gibbsite dissolution	(8.23B)	µmol Al/l	0	0	0	1	9
jurbanite formation	(8.24)	µmol SO_4^{2-}/l	-53	-72	0	0	0
albite dissolution	(8.26)	µmol SiO_2/l	40	46	36	36	36
orthoclase dissol.	(8.27)	µmol SiO_2/l	40	46	36	36	36
SiO_2-opal. dissolution	(8.28)	µmol SiO_2/l	0	142	142	230	48
OH-apatite dissolution	(8.29A)	µmol PO_4^{3-}/l	3	5	4	0	0
F-apatite dissolution	(8.29B)	µmol F/l	0	0	0.5	2	34
conv OH- to F-apatite	(8.29C)	µmol F/l	-6	-10	0	2	44
H^+ +$CaCO_3$	(8.30A)	µmol Ca^{2+}/l	0	19	0	0	0
CO_2+$CaCO_3$	(8.30B)	µmol Ca^{2+}/l	0	932	1107	1221	2994
Base-exchange	(8.31)	µmol Ca^{2+}/l	-32	-67	+33	-920	-3042
NH_4^+-exchange	(8.34)	µmol NH_4^+/l	0	-18	-30	-47	162
HCO_3^-->H^++CO_3^{2-}	(8.53)	µmol H^+/l	0	9	7	22	86
H^+ + HCO_3^--> H_2CO_3	(8.54)	µmol CO_2/l	232	-147	-58	-34	39
CHECKS							
(HCO_3^-+CO_3^{2-})-measured		µmol C/l	≤20	2450	2539	2760	6376
(HCO_3^-+CO_3^{2-})-calculated		µmol C/l	56	2480	2534	2780	6553

@ = dissolved gasses excluded; # = other nutrients in proportion to PO_4^{3-} and K^+ resp. , with N-supply covered by N_2-fixation.

HNO_3 and HF during the past 100-150 years.

Oxidation of iron sulphides, however, also contributes significantly to the acid input for sample 19A.31-30 in the upper part of the second aquifer. This is connected with a critical drawdown of the water table several decades ago (see section 7.3.4 under zone IV). Reduction of the base saturation of the adsorption complex forms the most important sink of strong acids for $CaCO_3$-equilibrated dune groundwater probably not more than 50-150 years old (sample 19A.31-30). This is consistent with observations on shallow calcareous dune groundwater (section 8.4.2).

Respiration, which includes the unseparable aerobic decomposition in the unsaturated zone, is calculated to be the main source of H_2CO_3 along the flow path studied. The somewhat higher respiration rates for sample 19A.31-30 can be attributed to a denser vegetation cover on that particular location. Downgradient of this well the respiration term decreases, which is consistent with a decreasing vegetation cover of the dunes back in time (section 3.2.5). Sample 19B.88-44, however, constitutes an abrupt end to this pattern. A rather extreme production of carbonic acid by respiration resulted from its mass balance, which is hard to explain. The most plausible explanation is that the concentration of methane analysed, was underestimated by losses either during sampling or during transfer from the sampling pipette to the headspace or from the headspace to the mass chromatograph. With a methane production 2.4 times the methane concentration analysed, a more fitting respiration would be obtained (549 µmol CO_2/l), as the additional CO_2 production accompanying methanogenesis would fill up the gap. In that case, however, also more HCO_3^- would be generated (about 180 µmol/l, taking all other changes into account). This would disrupt the HCO_3^- balance, which already has a surplus. A more audacious hypothesis is, that the desired additional CO_2 stems from ascending gas bubbles, with or without methane. Carbon-13 analysis would certainly help to solve the enigma, a must for future research!

Aerobic decomposition of organic matter constitutes a rather stable H_2CO_3 source, with a small dip in well 19A.31-30, due to oxygen consumption in the oxidation of $FeS_{(2)}$. Sulphate reduction appears as the second most important H_2CO_3 source in this well only, and forms a rather constant but small H_2CO_3 source in dune water older than circa 150 years.

Methanogenesis strongly increases downgradient and occupies the second position as a H_2CO_3 donor in and downgradient of well 19B.14-90. In well 19B.88-44 it may even form the principal supply of carbonic acid (see above).

The dissolution of $CaCO_3$ consumes the bulk of carbonic acid, at least downgradient of the decalcification boundary. In and downgradient of well 19B.14-90 the Ca^{2+} produced, is immediately exchanged for Na^+, K^+ and/or Mg^{2+} (Table 8.8; section 7.3.4). The reduction of ferric hydroxides loses its second place as a H_2CO_3 sink in well 19B.88-44, to the dissolution of apatite minerals.

8.5.3 Check by carbon-13

None of the five wells was sampled for ^{13}C analysis, unfortunately. However, the $\delta^{13}C$ analysis of water from the nearby observation well 19A.23-41 (-8.8‰) can be assumed to pertain to water from observation well 19A.159-90, because of the identical chemical composition and similar hydrological position of both samples.

The balance terms of inorganic carbon, and the resulting $\delta^{13}C$ value for each contribution are shown for well 19A.159-90 in Table 8.9. With a mean $\delta^{13}C$ level of the CO_2 input equal to -15.1‰, the $\delta^{13}C$ of sample 19A.159-90 is calculated at -8.2‰, which compares well with the -8.8‰ measured.

TABLE 8.9 The inorganic carbon and ^{13}C balance for observation well 19A.159-90 in the Bergen dune area. The calculated $\delta^{13}C$ of -8.2‰ compares well with the -8.8‰ measured.

Process	reaction Eq.	CO_2 µmol/l	HCO_3^- µmol/l	$\delta^{13}C$ ‰
SOURCES OF CARBONIC ACID				
respiration	8.9	790	0	-25
aerobic decomposition	8.11	331	0	-25
SO_4^{2-} reduction	8.15	92	0	-25
methanogenesis	8.16	264	0	+30
atmospheric CO_2	-	18	0	-8
Combined CO_2 mixture		Σ = 1495	Σ = 0	$\Sigma^{\#}$ = -15.08
SINKS OF CARBONIC ACID				
$CaCO_3$ dissolution§	8.30B	-1127	+2254	[-15.08+1]/2
dissolution of silicates	8.27	-71	71	-15.08
dissolution of apatite	8.29B	-6	6	-15.08
$Fe(OH)_3$ reduction	8.14	-126	126	-15.08
CO_2 drainage (no reaction)	-	170	0	-15.08
Final composition		Σ = 170	Σ = 2457	$\Sigma^{@}$ = -8.18

= $\Sigma(CO_2)_i\delta^{13}C_i$; @ = $CO_2\delta^{13}C + \Sigma(HCO_3)_i\delta^{13}C_i$; § = with $\delta^{13}C$ = +1.

8.6 Concluding remarks

Drawing up a chemical mass balance for dune groundwater in the coastal aquifer system of the Western Netherlands requires about 31 steps, the use of 25-50 reaction equations and usually several iterations. This is a lot of work, to be done by a computer program like BALANCE, developed by Parkhurst et al. (1982), or the recently released model NETPATH (Plummer et al., 1991). To this purpose reactions at the interface of the upper soil with the atmosphere and vegetation need to be incorporated in those models, as they were observed to have a strong impact on the composition of dune groundwater. The preliminary balances presented here, yield the ingredients for a more advanced simulation, and show where gaps in knowledge need to be filled up.

Accurate balances require accurate chemical analyses, also of the crucial gases CO_2 and CH_4, which can be easily underestimated by losses during sampling, sample conservation and sample transfer to the detector. The balances presented, require further checks by analysis of $\delta^{13}C$ and $\delta^{34}S$ and by solid phase research. The latter should focus on : sulphate adsorption or precipitation as alunite- and jurbanite-like phases in acid dune soils; siderite formation; the reaction products of decomposing organic matter; and the identification of reactive phosphate and fluoride minerals.

CONCLUSIONS

The main conclusions or issues presented here, have been grouped together in specific subjects. These are given in alphabethical order :

Acidification and atmospheric deposition

Where dune sand has been completely decalcified, soil moisture and groundwater may acidify. Acidifying groundwater is encountered in the decalcified dunes to the north of the village of Bergen aan Zee.

· The deposition of air-borne sea salt and calcareous dust, and a calcareous dune soil promote the atmospheric deposition of acid gases like SO_2, NO_x and HF (Figs.5.4 and 6.19).

· The monitoring of throughfall below forest stands and dune shrub in particular, probably yields a significant underestimation of the total atmospheric deposition by neglect of soil interception (section 6.8.1).

· The expansion of acidified groundwater (in the Bergen dune area) may lead to the development of a pH front (pH4-6), where in the downgradient direction Al is arrested and the trace elements Be, Cd, Co, Li^+, Ni, Rb^+ and Zn are mobilized (Figs.7.2 and 7.4). These trace ions probably reach the rather extreme levels observed by the dissolution of "roll-front deposits", which form downgradient of the advancing acidification front. The concentration peaks do not coincide; they are separated probably by ion-chromatographic effects (governed by a pH gradient), in order of increasing distance downgradient : Pb < Cu < Al < {Be ≅ Rb ≅ Zn ≅ Cd} < {Co ≅ Ni} < Li.

Artificial recharge

The dunes are recharged by large-scale spreading of polder, Rhine and Meuse water since the 1950s.

· The areal extent of these surface waters in the subsoil is shown on maps in Enclosures 4-7.

· Analytical solutions are presented for the calculation of the thickness of rain water lenses adjacent to recharge basins (Eq.3.23), the shape of the lower transition zone (Eq.3.24) and the transit time in the lens or recharged surface water beneath the lens (Eqs.7.8-7.10).

· The local change from vertical to subhorizontal flow in the upper aquifer after the start of artificial recharge, increased the contact time and the length of the flow path within the upper sandy North Sea deposits (0-7 m-MSL). This probably meant, in an anoxic environment, that PO_4, Mn and As, with otherwise low concentrations due to a limited availability and short contact, now steadily increase by progressive leaching downgradient, to yield at a certain distance the rather extreme concentration peaks observed.

· The introduction of Rhine water changed the redox environment in the Holocene deposits below circa 7 m-MSL, from sulphate-reducing or methanogenic to sulphate-(meta)stable. This is probably connected with an a priori low, sulphate-reducing capacity of the aquitards 1C and 1D, and an about tenfold increase of the sulphate flux.

· Wet dune slacks in areas affected by artificial recharge probably cannot return to their original mesotrophic or slightly eutrophic state, solely by further pretreatment of surface waters to be infiltrated and the removal of sludges from spreading ponds and flow-through lakes. The hydraulic gradient should be reduced as well. This will decrease the flux of nutrients and the depth of the deepest flow lines. The deepest flow lines exfiltrating into the lake may contact strata where nutrients are dissolved (section 4.6).

Decalcification

The leaching of calcium carbonate (shell debris) constitutes the main weathering reaction of dune sand prior to acidification of soil moisture and groundwater.

· The leaching of calcium carbonate in dune sand is favoured by interaction of water with dune peat which, after a drawdown of the water table, remains permanently situated in the unsaturated zone.

· From the 7 vegetation covers studied, dune shrub (*Hippophaë rhamnoides*) gave the highest and pine (*Pinus nigra* ssp *nigra*) the lowest decalcification rate (section 6.8.4; Fig.6.56).

· Decalcification can be described using a linear

equation (Eq.6.27), if the decalcification front is situated below the root zone (Fig.6.57). Field data from several dune areas with a precipitation surplus, suggest an accelerated $CaCO_3$ leaching during the initial period with calcium carbonate still present in the root zone. This period lasts about 17 years per weight percent $CaCO_3$ in the parent material (section 6.8.4).

Drawdown of groundwater tables

· In the younger dunes, water tables declined in the period 1853-1957 for the following reasons, in approximate order of decreasing impact : abstraction of groundwater for drinking water supply, drainage by the North Sea Canal and sea port of IJmuiden, abstraction for industrial water supply, increased evapotranspiration by man-induced changes in vegetation, the export of rain water by sewers in urbanized dune areas, coastal erosion to the north of Egmond and south of Scheveningen, and intensified drainage along the landward limit of the younger dunes (section 3.7).

· A map showing the drawdown of the water table in the area to the north of the Old Rhine in the period 1850-1981, is given in Enclosure 3.2.

· The actual position of the surface of dune valleys can be used to reconstruct palaeo-isohypses of the mean groundwater table before the onset of a drastic drawdown, on the condition that the dunes were simultaneously fixed by vegetation or man (section 3.2.3 and 3.6.4).

· A strong drawdown of the groundwater table can be accompanied by an increased flux of oxidants towards the water table, a change from anoxic into (sub)oxic conditions with all inherent consequences for redox sensitive constituents of water (including the persistence of for instance many chlorinated hydrocarbons), and an increased acidification (section 6.6.6).

· A drawdown of the phreatic level with concomitant oxidation of iron sulphides, can be traced back in several cases, with some difficulty, in raised SO_4^{2-} levels at a certain depth. The depth should correspond with the period of (or shortly after) the lowest phreatic level attained for several years, which strongly depends on local conditions in the studied dune area. In the Bergen dune area this happened around 1950, west of Hillegom in 1925 and south of Zandvoort aan Zee in the 1880s.

Eco-hydrology

· Analytical solutions are given for the shape of, and transit time to or within, vegetation water lenses. These are defined as groundwater bodies receiving their recharge for > 50% from precipitation on a specific vegetation unit (Eqs.6.1-6.5).

· The high biological productivity of flow-through lakes in dunes is explained by the focusing of both (sub)regional groundwater flow (Figs.3.50-3.52) and nutrient transport towards the lake (section 4.6), and the biological and chemical capture of these nutrients.

· Pine stands (*Pinus nigra* ssp *nigra*) in coastal dunes may display the following maturity sequence : hydrological maturity after about 15 years, hydrochemical maturity after 30 years and biological maturity after 45 years (Fig.6.35).

Freshening of groundwater

Growth of fresh dune and polder water bodies occurred (locally) since about 3800 BC, with various interruptions and even reversals. When a growing fresh water lens reaches its equilibrium (stable) position, processes like cation exchange, accompanying fresh water intrusion, generally continue.

· The map showing the change in the position of the fresh-brackish water interface in the area to the north of the Old Rhine in the period 1910-1981 (Enclosure 3.4), reveals that fresh water is expanding mainly in the western parts of the polder area.

· An interesting fresh dune water reserve is presently accumulating in the south-west corner of the Haarlemmermeer polder near Nieuw-Vennep. It is composed of old dune water of excellent quality, well-protected under aquitards and constitutes a strategic groundwater reserve for drinking water supply.

· The analytical solution for the time of formation of a fresh groundwater lens on salt groundwater, given by Braak (1968), is extended to account for anisotropy (Eqs.3.11-3.13). The resulting correction factor varies from 1.2 to 4.3.

· Maps showing the areal extent of freshened groundwater types are given in Enclosures 4-7.

· The observation of freshened watertypes like F_3NaHCO_3+, cannot be translated straight away into an actual fresh water intrusion, because the flow system may be in a steady state already whereas the hydrochemical equilibrium system is lagging behind. The flow system may even be contracting, and in extreme cases the appearance of a freshened watertype in a well can be the precursor of salinization (section 4.5.2).

· Fresh-water intrusion is not only accompanied by the well-known base exchange and dissolution of calcium carbonate, but may also conduce to several side reactions in consequence of strongly reduced Ca^{2+} concentrations, raised HCO_3^- levels and an increased pH. These reactions probably consist, in the study area, of the dissolution of fluorapatite-like phases (mobilization of F^- and PO_4^{3-}) and gibbsite (increase of Al), the precipitation of a manganous siderite (Fe^{2+} and Mn^{2+} drop to very low concentrations) and mobilization of DOC (section 7.3.4).

Mapping of groundwater chemistry

· A new, sophisticated hydrochemical mapping system for areas with a high complexity and abundant data is presented. The details of the evolved "HYdrochemical Facies Analysis (HYFA)" are given in chapter 2.

· Various hydrochemical maps of the study area are shown in Enclosures 4-7. They reveal the spatial distribution of the various water bodies having a specific origin (like Rhine, dune and North Sea water), the chemical zones within these water bodies (acid, calcareous, polluted, unpolluted, freshened, salinized, without base exchange, (sub)oxic, reduced and deep anoxic waters), and the chemical watertype (containing information on the salinity, alkalinity, dominating cation and anion, and base exchange).

Monitoring and protection

· Groundwater monitoring programs for drinking water supply, environmental protection and nature conservation benefit from a HYdrochemical Facies Analysis (chapter 2) and the concept of vegetation water lenses (section 6.3.3), by selection of : the strategical positions for monitoring wells (safely within a vegetation water lens or downgradient of expanding hydrosomes [water bodies with a specific origin] and downgradient of facies [hydrochemical zone] boundaries); and the right analytical program (specific trace elements in acidified systems only, and specific organic microcontaminants exclusively in young, (sub)oxic dune water or recharged Rhine water).

· Effects of hydrodynamic dispersion (in the porous medium) and artificial dispersion by various sampling facilities can be calculated using Eqs.6.19 and 6.7-6.8, respectively. These effects on groundwater samples must be considered in selecting the right type of observation well in dependence on the purpose of the monitoring and the position of the well in the flow system.

· The indicated recharge focus areas of deep aquifers in the younger dune area (Figs. 4.10 and 4.22), are to be considered as the most vulnerable groundwater protection areas, requiring "superprotection".

Natural backgrounds for groundwater in dunes

· The natural background composition of the various "natural" groundwater bodies (dune, North Sea, relict Holocene transgression and connate Maassluis water) is specified for various environments (chapters 4, 6 and 7). True natural backgrounds refer to water samples more than 100 years old. Younger, unpolluted samples of dune water contain an overprint from the effects of diffuse atmospheric pollution, lowered water tables and man-made changes in vegetation.

· Coastal dune groundwater is unique by virtue of : strong gradients, within the first km behind the foredune ridge, in sea-spray-corrected sulphate (Fig.6.19); the very pronounced interception deposition of sea spray as a function of the vegetation cover and the distance to the high water line on the beach (Figs.6.17-6.18); and the large-scale N_2-fixation, especially by sea buckthorn (*Hippophaë rhamnoides*; Tables 6.13 and 6.26).

· The chemical composition of natural dune groundwater in the water table domain, is governed mainly by the distance to the coast, vegetation cover, depth of decalcification of dune sand, and thickness of the unsaturated zone (section 6.6).

· Annual and seasonal fluctuations in the chemistry of pure dune vegetation groundwaters are extremely high, which appears characteristic for a dynamic coastal environment. Seasonal fluctuations of the biological, atmospherical and hydrological type are discerned (section 6.7).

· The upper dune groundwaters systematically exceed the upper background or target levels for groundwater in The Netherlands as proposed by LBS (1988) and adopted by MILBOWA (1991). This does not indicate a large-scale pollution in these nature reserves, but pleads for specific background or target levels for groundwater in coastal dunes, in connection with their particular hydrochemical setting.

Pollution of groundwaters

· Maps showing the areal extent of polluted groundwaters in the area are depicted in Enclosures 4-7.

· The environmental pollution record of precipitation is reflected in dune water by decreasing levels downgradient for the mainly atmospheric trace elements Se, Cu, F^-, Zn, Pb, Sb and V (in decreasing order of depth of penetration) and organohalogens adsorbable to activated carbon, and by the tritium and sea-spray-corrected SO_4^{2-} patterns.

· Long-term changes in the composition of shallow dune groundwater are composed of an overall increase in total dissolved solids, a specific rise of NO_3^- and Ca^{2+}, and a rise followed by a decrease, in SO_4^{2-}. These are largely connected with changes in vegetation cover, atmospheric deposition and a drawdown of the water table.

· Recharged Rhine water shows well conserved patterns for Cl^-, SO_4^{2-} and tritium, a smoothed pattern for dissolved organic matter, and breakthrough of Na^+, Mg^{2+}, K^+, F^- and PO_4^{3-} in dune sand after about 1.2, 3, 5, 5 and 30 pore flushes, respectively.

· Also the anthropogenic oxidation of iron sulphides and peat, and widening of the fresh-salt water interface are to be considered as a kind of

environmental pollution.
· Aquifers surrounding thick aquitards rich in organic matter, may be subject to a significant natural, anoxic fouling by sorption of NH_4^+, PO_4^{3-} and possibly DOC and I, which derive from this aquitard, either by diffusion, compaction driven flow or the passage of another fluid. An example is offered by the Bergen clay (section 7.3.4, below Eq.7.1).

Salinization of groundwater
Growth of salt and brackish water bodies occurred (locally) since about 6000 BC, with various interruptions and reversals. When a growing saline water body reaches its equilibrium (stable) position, chemical processes like cation exchange, accompanying the intrusion, generally continue.
· A map showing the change in the position of the fresh-brackish water interface in the area to the north of the Old Rhine in the period 1910-1981 (Enclosure 3.4), reveals that the intrusion of North Sea water into dune water occurred mainly in the western parts of the dune area in this period.
· Maps showing the areal extent of salinized groundwater types are given in Enclosures 4-7.
· A further salinization of the drainage water in deep polders is expected to occur especially to the south of the North Sea Canal, where the relict, Holocene transgression waters are less saline and will be displaced by actual North Sea water of much higher salinity. This salt front is advancing with a calculated velocity of 5-30 m/y, and will therefore manifest itself within several centuries.
· Salt-water intrusion can be accompanied by a significant mobilization of Fe^{2+} and Mn^{2+}, probably by dissolution of a manganous siderite and desorption, the mobilization of Ba^{2+} probably by desorption, the precipitation of F^- and PO_4^{3-} in apatite-like phases, and sorption of Mo, Rb and V (section 7.6.3).
· The displacement of dune water by recharged Rhine water is to be considered as a salinization, with similar reactions as observed on intruding North Sea water. The exchange zone is wider, however, due to the lower displacing capacity of Rhine water (in consequence of its much lower sum of dissolved cations).

Tracing : hydrochemistry as an aid in hydrology
Hydrochemistry may assist in solving hydrological problems or yielding independent evidence with which hydrological models are to be validated.
· The spatial patterns of water bodies and chemical zones often display the true flow patterns. This is demonstrated for instance by the so-called rain water lenses (Fig.3.48), vegetation water lenses (Fig. 6.52), lenses of dune peat water (Fig.6.28), the chemical patterns around flow-through dune lakes (Fig.3.49 and 4.30), and the chemical anomalies indicating the position of the recharge focus areas of deep aquifers (Figs.4.10 and 4.22).
· The determination of the degree of mixing between flow systems, yielded transversal dispersivities of dune sand and Pleistocene sands of 0.25-1 cm (sections 3.5.5 and 3.10.2).
· The best environmental tracers for the recognition of various, artificially recharged surface waters, polder waters, dune water, North Sea water, relict Holocene transgression waters and connate Maassluis water, are indicated in Table 4.1.
· Chloride-history matching can be successfully applied to date shallow groundwater in coastal dune sands, on the condition that the Cl^- record of bulk precipitation is well documented. Examples of sequential history matching are shown in Figs.6.41-6.43, and examples of the spatial variant in Figs.6.43 and 7.8. Both annual and seasonal Cl^- fluctuations, with the years 1974, 1977 and 1979 and the month November as recognizable extremes, proved useful in shallow groundwater dating in the study area, notwithstanding smoothing by dispersion.
· A sharp $\delta^{18}O$ discontinuity in a groundwater body may point at an abrupt change in the position of the water table, for instance by pumping, and offer a point of reference for dating. In the study area a discontinuity from $\delta^{18}O$ = -7.2 ± 0.2‰ to -6.5 ± 0.2‰ is observed in deep dune water, and related to a drawdown of the groundwater table in the 1880s in the Zandvoort area (Fig.7.13) and in the 1920s in the dunes 7 km to the south of Zandvoort aan Zee (Fig.7.9).

Various hydrochemical processes
· The expansion of (sub)oxic, calcareous groundwater may conduce to the development of a redox front (from suboxic to anoxic), where nitrate is reduced, uranium mobilized (somewhat prior to complete denitrification) and Fe^{2+} mobilized (after complete denitrification) and subsequently U precipitated (probably as UO_2). This is demonstrated in Figs.7.8 and 7.10, and corresponds with the concept of the genesis of U "roll-front deposits".
· The chemical composition of dune groundwater can be simulated with mass balances requiring about 25-50 reaction equations (chapter 8).

CONCLUSIES

De hier gepresenteerde conclusies zijn op thema gegroepeerd en vervolgens alfabetisch gesorteerd :

Bewaking en bescherming

· Meetnetten voor kwaliteitsbewaking van grondwater zijn gebaat met een HYdrochemische Facies Analyse (hoofdstuk 2) en het concept "vegetatie-waterlens (par.6.3.3) door de mogelijkheid om : (1) strategische posities voor waarnemingsputten aan te wijzen, n.l. binnen een vegetatie-waterlens of stroomafwaarts van expanderende hydrosomen (waterlichamen met een specifieke herkomst) en stroomafwaarts van facies grenzen (randen van hydrochemische zones); en (2) het juiste meetprogramma te kiezen, b.v. specifieke sporenelementen alleen in zure systemen, en bepaalde organische microverontreinigingen alleen in jong, (sub)oxisch duin- of Rijnwater.

· Effecten van hydrodynamische dispersie (in het poreuze medium) en kunstmatige dispersie door diverse systemen van bemonstering kunnen berekend worden met behulp van resp. Eq. 6.19 en 6.7-6.8. De effecten hiervan op grondwatermonsters dienen in beschouwing genomen te worden bij de keuze van het juiste type waarnemingsput, in afhankelijkheid van de vraagstelling en de positie van de put in het stromingsstelsel.

· De chemisch vastgestelde hoofdvoedingsgebieden van de diepere watervoerende pakketten in het jonge duingebied (Fig. 4.10 en 4.22), zijn te beschouwen als de meest kwetsbare grondwaterbeschermingsgebieden, die "superbescherming" verdienen.

Eco-hydrologie

· Analytische oplossingen worden gegeven voor de berekening van de vorm van en reistijd naar of binnen vegetatie-waterlenzen. Deze lenzen zijn gedefinieerd als grondwaterlichamen met > 50% van hun voeding uit regenwater op een specifiek begroeiingstype (Eq. 6.1-6.5).

· De hoge biologische productiviteit van kwelplassen in duinen wordt verklaard door de optredende convergentie van stroombanen aan de kwelzijde (Fig. 3.50-3.52), de daardoor verhoogde nutriëntentoevoer en de chemische en biologische vastlegging van nutriënten in het meer (par.4.6).

· Dennenopstanden (*Pinus nigra* ssp *nigra*) kunnen in kustduinen de volgende maturiteitsreeks etaleren : hydrologisch volwassen na ongeveer 15 jaar, hydrochemisch na 30 jaar en biologisch na 45 jaar (Fig.6.35).

Hydrochemische processen (diverse)

· De expansie van (sub)oxisch, kalkrijk grondwater kan leiden tot de ontwikkeling van een redox front (van suboxisch tot anoxisch), waar nitraat gereduceerd wordt, eerst uranium (iets vóór complete denitrificatie) en dan Fe^{2+} oplost (na volledige denitrificatie) en vervolgens U weer neerslaat (waarschijnlijk als UO_2). Dit volgt uit Fig. 7.8 en 7.10, en leidt via een soort chemisch bezem-effect tot de genese van U "roll-front afzettingen".

· De chemische samenstelling van duingrondwater kan gesimuleerd worden met massabalansen opgebouwd uit 25-50 reactievergelijkingen (hfdstuk 8).

Kartering van grondwaterchemie

· Een algemeen toepasbare, nieuwe methode voor het in kaart brengen van de grondwaterchemie in ingewikkelde gebieden met veel gegevens (hoofdstuk 2).

· Een aantal hydrochemische kaarten van het studiegebied is weergegeven in de Bijlagen 4-7. Zij onthullen de ruimtelijke verdeling van verschillende waterlichamen met een specifieke herkomst (zoals Rijn-, duin- en Noordzeewater), de chemische zones binnen deze waterlichamen (zuur, kalkrijk, verontreinigd, onverontreinigd, verzoet, verzilt, zonder basenuitwisseling, (sub)oxisch, gereduceerd en diep anoxisch), en het chemische watertype (met informatie over de chloride concentratie, alkaliteit, het dominante kation en anion, en basenuitwisseling).

Kunstmatige infiltratie

De duinen worden op grote schaal kunstmatig aangevuld met polder-, Rijn- and Maaswater sinds of na 1955.

· De ruimtelijke verbreiding van deze oppervlaktewateren in de ondergrond wordt op kaarten in de Bijlagen 4-7 getoond.

· Analytische oplossingen worden gepresenteerd voor berekening van de dikte van regenwaterlenzen grenzend aan infiltratievijvers (Eq.3.23), de vorm van de mengzone aan de onderzijde (Eq.3.24) en de verblijftijd in de lens en het eronder stromende, geïnfiltreerde water (Eq. 7.8-7.10).

· Kunstmatige infiltratie veranderde de locale grondwaterstroming in het bovenste watervoerende pakket van veelal verticaal in subhorizontaal, waardoor de locale contacttijd en stroombaanlengte in de zandige Noordzee-afzettingen (0-7 m-NAP) toenamen. Dit had waarschijnlijk tot gevolg, in het heersende anoxische milieu, dat de PO_4, Mn en As concentraties tot de waargenomen piek-

niveaus aanzwellen, door langzame opname van beperkt voorradig, reactief fosfaat, arseen en mangaan uit de bodem.
· De introductie van gebiedsvreemd Rijnwater veranderde de redox toestand in de Holocene afzettingen beneden ongeveer 7 m-NAP, van sulfaat-reducerend of methanogeen in sulfaat-(meta)stabliel. Deze wijziging houdt waarschijnlijk verband met een toch al lage, sulfaatreducerende capaciteit van de slecht-doorlatende pakketten 1C en 1D, en een ongeveer tienvoudige toename van de sulfaatflux.
· Natte duinvalleien in door kunstmatige infiltratie beïnvloede gebieden zullen waarschijnlijk niet tot hun oorspronkelijke mesotrofe of licht-eutrofe toestand van veeleer terugkeren door louter verdere voorzuivering van het infiltratiewater en het ruimen van bodemslib uit infiltratie- en kwelplassen. Ook het grondwaterverhang dient verkleind te worden ter vermindering van de flux van voedingsstoffen en de diepte van de kwelstroom. Een grote diepte van de kwelstroom brengt namelijk hoge concentraties nutriënten, die uit diepere grondlagen oplossen, met zich mee (section 4.6).

Natuurlijke achtergronden voor grondwater in duinen

· Een gedetailleerde specificatie van de natuurlijke achtergrondsamenstelling van de verschillende "natuurlijke" grondwaterlichamen (duin-, Noordzee-, relict Holocene transgressie- en ingesloten Maassluis water) in de onderscheiden milieus, wordt in de hoofdstukken 4, 6 en 7 gegeven. Werkelijke achtergrondniveaus hebben betrekking op meer dan 100 jaar oude watermonsters. Jongere, onverontreinigde duinwatermonsters bevatten een zekere invloed van diffuse luchtverontreiniging, grondwaterstandsdalingen en antropogene veranderingen in de begroeiing.
· Grondwater in kustduinen is uniek door toedoen van : een sterke gradiënt, binnen de eerste km achter zeereep, in voor-zeezout-gecorrigeerd sulfaat (Fig.6.19); de zeer geprononceerde droge depositie van zeezout als functie van het type begroeiing en de afstand tot de hoogwaterlijn op het strand (Fig. 6.17-6.18); en de grootschalige N_2-binding, vooral door duindoorn (*Hippophaë rhamnoides* (Tabellen 6.13 en 6.26).
· De chemische samenstelling van natuurlijk duingrondwater nabij de grondwaterspiegel, wordt hoofdzakelijk gedicteerd door de afstand tot de kust, het type begroeiing, de ontkalkingsdiepte van duinzand, en de dikte van de onverzadigde zone.
· Jaarlijkse schommelingen en seizoensfluctuaties in de chemische samenstelling van pure vegetatiegrondwateren zijn in de duinen bijzonder sterk, hetgeen kenmerkend lijkt voor een dynamisch systeem als kustduinen. Seizoensfluctuaties van het biologische, atmosferische en hydrologishe type zijn onderscheiden (par.6.7).
· Het ondiepe duingrondwater overschrijdt systematisch de natuurlijk achtergrondwaarden of streefwaarden voor grondwater in Nederland volgens LBS (1988) en aangepast door MILBOWA (1991). Dit wijst niet op een grootschalige verontreiniging in de onderzochte natuurgebieden, maar pleit voor opstelling van specifieke achtergrondniveaus voor kustduinen, die verband houden met het bijzondere hydrochemishe milieu.

Ontkalking

De uitloging van schelpkalk vormt de belangrijkste verweringsreactie van duinzand voordat bodemvocht en grondwater kunnen verzuren.
· De ontkalkingssnelheid van duinzand is het hoogst onder duindoorn (*Hippophaë rhamnoides*) en het laagst onder Corsicaanse den (*Pinus nigra* ssp *nigra*), van de 7 onderzochte vegetatietypen.
· De ontkalkingssnelheid van duinzand wordt bevorderd door interactie van water met duinveen dat, na een daling van de grondwaterspiegel, permanent boven het grondwater gesitueerd is.
· De ontkalking kan beschreven worden met een lineare vergelijking (Eq.6.27), indien het ontkalkingsfront beneden de wortelzone gesitueerd is (Fig.6.57). Veldwaarnemingen in verschillende duingebieden in de wereld met een neerslagoverschot, suggereren een versnelde $CaCO_3$ uitloging tijdens de beginperiode (wanneer er nog kalk in de wortelzone aanwezig is). Deze periode duurt ongeveer 17 jaar per gewichtsprocent oorspronkelijk $CaCO_3$ (par.6.8.4).

Tracers : hydrochemie als hydrologische detective

De hydrochemie kan helpen bij het oplossen van hydrologische problemen of kan onafhankelijk bewijsmateriaal aanrijken waarmee hydrologische modellen geijkt kunnen (zouden moeten) worden.
· De contouren van waterlichamen en chemische zones vertolken dikwijls de ware stromingspatronen. Dit is b.v. het geval bij de zogenaamde regenwaterlenzen (Fig.3.48), vegetatie-waterlenzen (Fig.6.52), duinveen-waterlenzen (Fig.6.28), de chemische patronen rond kwelplassen (Fig.3.49 en 4.30), en chemische afwijkingen die de positie van de hoofdvoedingsgebieden van diepe watervoerende pakketten aanwijzen (Fig. 4.10 en 4.22).
· De bepaling van de graad van menging binnen stromingsstelsels leverde dispersiviteiten van duinzand en Pleistocene zanden van 0.25-1 cm op (par.3.5.5 en 3.10.2).
· De beste gidsparameters (tracers) voor herkenning van verschillende waterlichamen (diverse kunstmatig geïnfiltreerde oppervlaktewateren, polderwater, duinwater, Noordzeewater, relict Holoceen transgressiewater en ingesloten Maas-

sluis water), zijn in Tabel 4.1 bijeengezet.
· Vergelijking van het Cl^- verloop van regenwater met dat in grondwater kan succesvol worden aangewend als dateringsmethode voor ondiep grondwater in kustduinen. Voorbeelden van waarnemen aan één put in de tijd staan in de Fig. 6.41-6.43, en voorbeelden van opnames met de diepte staan in de Fig. 6.43 en 7.8. Zowel jaarlijkse schommelingen als seizoensfluctuaties in Cl^- concentratie, met de jaren 1974, 1977 en 1979 en de maand november als herkenbare extremen, bleken goede aanknopingspunten in dit onderzoek voor de datering van zeer ondiep duingrondwater, ondanks afvlakking door dispersie.
· Een scherpe $\delta^{18}O$ discontinuiteit in een grondwaterlichaam kan wijzen een abrupte verandering in de positie van de waterspiegel, b.v. door grondwaterwinning, en daardoor een aanknopingspunt voor datering vormen. In het studiegebied is een discontinuiteit van $\delta^{18}O$ = -7.2 ± 0.2‰ tot -6.5 ± 0.2‰ waargenomen in diep duinwater, en gerelateerd aan een daling van de grondwaterstand omstreeks 1880 in de duinen bij Zandvoort aan Zee (Fig.7.13) en in 1925 in de duinen 7 km ten zuiden van Zandvoort aan Zee (Fig.7.9).

Verdroging

· In de jonge duinen daalde de grondwaterstand in de periode 1853-1957 om de volgende redenen, bij benadering in volgorde van afnemende gemiddelde bijdrage : grondwateronttrekking voor de drinkwatervoorziening, de aanleg en aanwezigheid van het Noordzeekanaal en de zeehaven van IJmuiden, grondwateronttrekking voor industrieel gebruik, een toegenomen verdamping door antropogene veranderingen in duinbegroeiing, de afvoer van hemelwater door het riool in stedelijke duingebieden, kusterosie ten noorden Egmond en zuiden van Scheveningen, en geïntensiveerde drainage langs de binnenduinrand (par.3.7).
· Een kaart met de grondwaterstandsdaling voor het gebied ten noorden van de Oude Rijn in de periode 1850-1981, is weergegeven in Bijlage 3.2.
· De actuele positie van het maaiveld van duinvalleien kan gebruikt worden bij de reconstructie van paleo-isohypsen van de gemiddelde grondwaterstand vóór de start van een drastische daling van de grondwaterstand, op voorwaarde dat het maaiveld gelijktijdig werd vastgelegd door de begroeiing of door de mens (par.3.2.3 en 3.6.4).
· Een sterke daling van de grondwaterspiegel kan een toename inhouden van de flux van oxydatoren richting grondwaterspiegel, een wijziging van anoxische in (sub)oxische omstandigheden met alle gevolgen van dien voor redoxgevoelige bestanddelen van water (b.v. leidend tot doorbraak van persistente gechloreerde koolwaterstoffen), en een versnelde verzuring (par.6.6.6).
· Een daling van de grondwaterstand met de daardoor veroorzaakte oxydatie van ijzersulfiden, kan in enkele gevallen, zij het met enige moeite, worden teruggevonden in toegenomen SO_4^{2-} concentraties op zekere diepte. Die diepte zou overeen moeten komen met de periode (of kort daaropvolgende periode) van de laagst waargenomen grondwaterstand gedurende enkele jaren. Die periode is voor de diverse duingebieden sterk verschillend : rond 1950 bij Bergen, ongeveer 1925 ten westen van Hillegom en omstreeks 1880 voor het gebied ten zuiden van Zandvoort aan Zee.

Verontreiniging van grondwater

· Kaarten met de ruimtelijke verbreiding van verontreinigd grondwaters in het studiegebied zijn in de Bijlagen 4-7 weergegeven.
· De historische ontwikkeling van de luchtverontreiniging manifesteert zich in duinwater door middel van in stroomafwaartse richting afnemende concentraties van de voornamelijk atmosferisch gedeponeerde sporenelementen Se, Cu, F^-, Zn, Pb, Sb en V (in volgorde van afnemende penetratiediepte) en aan actieve kool adsorbeerbare organohalogenen, en door de tritium en zee-zout-gecorrigeerde SO_4^{2-} patronen.
· Gemiddelde veranderingen in de samenstelling van ondiep duingrondwater op de lange termijn (1910-1990) bestaan uit een algehele toename van de totale hoeveelheid opgeloste stoffen, een specifieke stijging van NO_3^- en Ca^{2+}, en een toename gevolgd door een afname voor SO_4^{2-}. Deze wijzigingen houden verband met veranderingen in begroeiing, atmosferische depositie en een gemiddelde daling van de grondwaterspiegel.
· Geïnfiltreerd Rijnwater vertoont goed bewaard gebleven patronen voor Cl^-, SO_4^{2-} en tritium, een afgevlakt patroon voor opgeloste organische stof, en de doorbraak van Na^+, Mg^{2+}, K^+, F^- en PO_4^{3-} in duinzand na resp. ongeveer 1,2, 3, 5, 5 en 30 poriedoorspoelingen.
· Ook de door de mens veroorzaakte oxydatie van ijzersulfiden en veen, en de verbreding van het zoet-zout grensvlak dienen als een soort milieuverontreiniging beschouwd te worden.
· Watervoerende pakketten rondom dikke slechtdoorlatende lagen met een hoog gehalte aan organische stof, kunnen onderworpen zijn (geweest) aan een aanzienlijke anoxische vervuiling door sorptie van NH_4^+, PO_4^{3-} en mogelijk DOC en I, alle afkomstig van dit slecht-doorlatende pakket, hetzij via diffusie, door compactie ontstane stroming of gewoon de passage van een andere watersoort. De Eem formatie onder de Bergen klei vormt een voorbeeld (par.7.3.4, onder Eq.7.1).

Verzilting van grondwater

In de periode van ongeveer 6000 - 3800 v.Chr. trad een grootschalige verzilting van de ondergrond van het studiegebied op. Na het bereiken van een stabiele positie van zout grondwater kunnen daarbinnen nog geruime tijd processen als kationuitwisseling, die de verzilting normaliter begeleiden, werkzaam zijn.

· De kaart met de verandering in de ligging van het zoet-brak grensvlak ten noorden van de Oude Rijn in de periode 1910-1981 (Bijlage 3.4), onthult dat Noordzeewater in die periode vooral in de westelijke regionen van de jonge duinen tot verdringing van duinwater leidde.

· Kaarten met de ruimtelijke verbreiding van grondwater met basenuitwisseling door verzilting zijn weergegeven in de Bijlagen 4-7.

· Verdere verzilting van het drainagewater in de diepe polders is te verwachten vooral ten zuiden van het Noordzeekanaal, waar de relicte, Holocene transgressiewateren minder zout zijn en verdrongen zullen worden door het huidige, veel zoutere Noordzeewater. Dit zoutfront rukt ondergronds met een berekende snelheid van 5-30 m/j op, en zal zich binnen enkele eeuwen manifesteren.

· Zoutwaterintrusie kan leiden tot een aanzienlijke mobilisatie van Fe^{2+} en Mn^{2+}, waarschijnlijk door oplossing van mangaanhoudende sideriet en desorptie, de mobilisatie van Ba^{2+} waarschijnlijk door desorptie, het neerslaan van F^- en PO_4^{3-} in apatiet, en sorptie van Mo, Rb en V (par.7.6.3).

· De verdringing van duinwater door geïnfiltreerd Rijnwater dient eveneens als een verzilting te worden opgevat, met reacties die in veel opzichten lijken op die tijdens Noordzeewaterindringing. De uitwisselzone is echter breder door de geringere verdringingscapaciteit van Rijnwater (vanwege de lagere som der kationen).

Verzoeting van grondwater

De uit zoetwater bestaande duin- en polderwaterlichamen vormden zich na 3800 v.Chr. Wanneer een zoetwaterlens zijn evenwichtsvorm bereikt heeft, lopen processen als kationuitwisseling, die de zoetwaterindringing normaliter begeleiden, nog geruime tijd door.

· De kaart met de verandering in de ligging van het zoet-brak grensvlak ten noorden van de Oude Rijn in de periode 1910-1981 (Bijlage 3.4), onthult dat zoetwater de westelijke regionen van de droogmakerijen aan het binnendringen is.

· Er is een interessante zoetwater-reserve ontstaan in de zuidwest hoek van de Haarlemmermeer polder nabij Nieuw-Vennep. Zij bestaat uit oud duinwater van uitstekende kwaliteit, ligt goed beschermd onder basisveen en Velsenklei met zeer hoge weerstand, en vormt een strategische watervoorraad voor de drinkwatervoorziening.

· Aan de analytische oplossing van Braak (1968), voor berekening van de tijd nodig voor de vorming van een zoetwaterlens op zout grondwater, is de mogelijkheid van verdiscontering van anisotropie toegevoegd (Eq. 3.11-3.13). De resulterende correctiefactor varieert van 1,2 tot 4.3.

· Kaarten met de ruimtelijke verbreiding van grondwater met basenuitwisseling door verzoeting zijn weergegeven in de Bijlagen 4-7.

· De aanwezigheid van verzoete watertypes als F_3NaHCO_3+, kan niet zonder meer vertaald worden in een actuele zoetwater intrusie, omdat het stromingsstelsel al wel in een stationaire toestand kan verkeren terwijl het hydrochemisch nog streeft naar evenwicht. Het stromingstelsel kan zelfs aan het inkrimpen zijn, en in extreme gevallen kan de verschijning van een verzoet watertype in een put de voorbode van verzilting vormen (par.4.5.2).

· Zoetwaterindringing gaat niet alleen vergezeld van de welbekende basenuitwisseling en oplossing van calciumcarbonaat, maar kan ook leiden tot enkele nevenreacties tengevolge van sterk verlaagde Ca^{2+} concentraties, verhoogde HCO_3^- niveaus en een pH-toename. Deze reacties bestaan waarschijnlijk, in het studiegebied, uit de oplossing van fluorapatiet (met mobilisatie van F^- en PO_4^{3-}) en gibbsiet (toename van Al), het neerslaan van mangaanhoudende sideriet (Fe^{2+} en Mn^{2+} nemen sterk in concentratie af) en de mobilisatie van DOC (par.7.3.4).

Verzuring en atmosferische depositie

Waar duinzand volledig ontkalkt is, kan grondwater verzuren. Zuur grondwater (pH<6) wordt aangetroffen in de ontkalkte duinen ten noorden van Bergen aan Zee.

· De depositie van zoutspray en kalkhoudend stof, en een kalkrijke duinbodem bevorderen de atmosferische depositie van zuurvormende gassen als SO_2, NO_x en HF (Fig. 5.4 en 6.19).

· De monitoring van doorval in bos en vooral duindoorns, levert een onderschatting op van de totale atmosferische depositie door verwaarlozing van de droge depositie op de bodem (par.6.8.1).

· De opdringing van zuur grondwater (in de duinen van Bergen) kan leiden tot de ontwikkeling van een pH front (pH4-6), waar Al wordt vastgelegd en de sporenelementen Be, Cd, Co, Li^+, Ni, Rb^+ en Zn gemobiliseerd worden (Fig. 7.2 en 7.4). Deze sporenelementen vertonen de waargenomen piekconcentraties waarschijnlijk door oplossing van "roll-front afzettingen", die zich stroomafwaarts van het oprukkende zuurfront vormen. Hun pieken vallen niet samen, zij worden waarschijnlijk gescheiden door ion-chromatographische effecten, in volgorde van toenemende afstand ondergronds langs de stroombaan : $Pb < Cu < Al < \{Be \cong Rb^+ \cong Zn \cong Cd\} < \{Co \cong Ni\} < Li^+$.

REFERENCES

ABRAMOWITZ, M. & I.A. STEGUN 1965. Handbook of mathematical functions. Dover, New York.

ADRIANI, M.J. & E. VAN DER MAREL 1968. Voorne in de branding. Brochure Stichting Wetenschappelijk Duinonderzoek, De Volharding Amsterdam.

ADRIANI, M.J., G.P. GONGGRIJP, J.A. NIJKAMP & J.F. VAN REGTEREN-ALTENA 1980. Ontdek de duinen. Serie Nederlandse landschappen, Uitgave I.V.N. (Amsterdam) & VARA (Hilversum), 288p.

AKKERMANS, A.D.L. 1971. Nitrogen fixation and nodulation of Alnus and Hippophaë under natural conditions. Ph.D Thesis, Univ. Leiden, The Netherlands.

ALBERTSEN, M. 1977. Labor- und Felduntersuchungen zum Gasaustausch zwischen Grundwasser und Atmosphäre über natürlichen und verunreinigten Grundwässern. Ph.D. Thesis Univ. Kiel, W-Germany.

ALEKIN, O.A. 1953. Principles of Hydrochemistry. Leningrad, 296 p. in russian.

ANDERSEN, L.J. & T. SEVEL 1974. Six years environmental tritium profiles in the unsaturated and saturated zones, Grønhøj, Denmark. Isot. Techn. in Groundw. Hydrol., Proc. Symp. Vienna, Vol I, IAEA, 3-20.

ANONYMOUS 1959. Final resolution, the Venice system. Symp. Classification of Brackish Waters, Archo Oceanogr. Limnol 11, 243-245.

APPELO, C.A.J. 1982. Verzuring van het grondwater op de Veluwe. H_2O 15, 464-468.

APPELO, C.A.J. 1988a. Beïnvloeding van de waterkwaliteit in het Hierdensche Beek gebied. Rapport Instit. Aardwetenschappen, Vrije Univ. Amsterdam, 100p.

APPELO, C.A.J. 1988b. Hydrochemistry for hydrologists, application of chemical theory. Instit. Earth Sci, Free Univ. Amsterdam.

APPELO, C.A.J. 1990. Eenvoudige rekenmethoden voor uitwisselfronten bij kunstmatige infiltratie. H_2O 23, 164-166.

APPELO, C.A.J. & GEIRNAERT, W. 1983. Processes accompanying the intrusion of salt water. Geol. Appl. Idrogeol. 18(II), 29-40.

APPELO, C.A.J. & D. POSTMA 1992. Geochemistry, groundwater and pollution. Balkema, 500p.

APPELO, C.A.J., P.J. STUYFZAND & G.B. ENGELEN 1979. Reacties van Rijnwater in de Veluwe en duinen: een experimentele studie en een infiltratie proef. H_2O 12, 328-332.

APPELO, C.A.J. & A. WILLEMSEN 1987. Geochemical calculations and observations on salt water intrusions, I. A combined geochemical/mixing cell model. J. Hydrol. 94, 313-330.

APPELO, C.A.J., A. WILLEMSEN, H.E. BEEKMAN & J. GRIFFIOEN 1990. Calculations and observations on salt water intrusions, II. Validation of a geochemical model with laboratory experiments. J. Hydrol. 120, 225-250.

ARENDS, B.G., H.A. VAN DER SLOOT & W. VAN DUYVENBOODEN 1987. Influence of acidification on the concentration of less common trace elements in Dutch groundwater. CHO-TNO Verslagen & Meded 38, 527-543.

ARIMOTO, R. & R.A. DUCE 1987. Air-sea transfer of trace elements. Adv. in Chem. Series 216, Am. Chem. Soc. Wash.D.C., 131-150.

ASMAN, W.A.H., J. SLANINA & J.H. BAARD 1981. Meteorological interpretation of the chemical composition of rain water at one measuring site. Water, Air & Soil Pollution 16, 159-175.

ASMAN, W.A.H., T.B. RIDDER, H.F.R. REIJNDERS & J. SLANINA 1982. Influence and prevention of bird droppings in precipitation chemistry experiments. Water, Air & Soil Pollution 17, 415-420.

ATAKAN, Y., W. ROETHER, G. MATTHESS & K-O. MÜNNICH 1974. Felduntersuchungen von Fliessvorgängen in einem Porengrundwasserleiter mittels Farbstoffindicatoren. GWF-Wasser/Abwasser 115, 159-164.

BAAN, P.J.A., M.J.P.H. WALTMANS, G.G.C. VERSTAPPEN & J.W. PULLES 1991. Bronnen van belasting van de Noordzee met stoffen. H_2O 24, 582-586.

BAARS, J.K. 1957. Travel of pollution, and purification en route, in sandy soils. Bull. World Health Org. 16, 727-747.

BAARS, J.K. & I.J. LE COSQUINO DE BUSSY, 1960. Infiltration of river water in dune areas. Schweiz. Z. f. Hydrologie 22, in german, 380-395.

BACHE, B.W. 1986. Aluminium mobilization in soils and waters. Journal of the Geological Society, London 143, 699-706.

BACK, W. 1960. Origin of hydrochemical facies of ground water in the Atlantic Coastal plain. Internat. Geol. Cong. 21st, Copenhagen 1960, Rept.pt.1, 87-95.

BACK, W. 1966. Hydrochemical facies and ground water flow patterns in northern part of Atlantic Coastal Plain. U.S. Geol. Surv. Profess. Papers 498-A, 42p.

BACK, W., B.B. HANSHAW, T.E. PYLE, L.N. PLUMMER & A.E. WEIDIE. 1979. Geochemical significance of groundwater discharge and carbonate solution to the formation of Caleta Xel Ha, Quintana Roo, Mexico. Water Res. Res. 15, 1521-1535.

BADON GHYBEN, W. 1889. Nota in verband met de voorgenomen putboring nabij Amsterdam. Tijdschrift Kon. Instit. Ingenieurs, The Hague, 1888/1889, 209-223.

BAKKER, T.W.M. 1981. Nederlandse kustduinen geohydrologie. Ph.D. Thesis, PUDOC Wageningen, 189p.

BAKKER, T.W.M., J.A. KLIJN & F.J. VAN ZADELHOFF 1979. Basisrapport TNO Duinvalleien, algemene hoofdstukken (644p) + deelrapporten Camperduin-Egmond, Egmond-IJmuiden, Noordwijk-IJmuiden, Monster-Noordwijk, Stud. & Inf. centrum TNO voor Milieu-onderzoek.

BAKKER, T.W.M & P.J. STUYFZAND, 1993. Nature conservation and extraction of drinking water in coastal dunes : the Meijendel dunes. In : "Landscape ecology of a stressed environment", C.C. Vos & P. Opdam (eds), IALE-Studies in Landscape Ecology 1, Chapman & Hall, London, 244-262.

BALL, D.F. & W.M. WILLIAMS 1974. Soil development on coastal dunes at Holkham, Norfolk, England. Proc. 10th Intern. Congress of Soil Science (Moscow) VI, 380-386.

BARCELONA, M.J., J.A. HELFRICH, E.E. GARSKE & J.P. GIBB 1984. A laboratory evaluation of ground water sampling mechanisms. Ground Water Monit. Review, spring 1984, 32-41.

BARCELONA, M.J., T.R. HOLM, M.R. SCHOCK & G.K. GEORGE 1989. Spatial and temporal gradients in aquifer oxidation- reduction conditions. Water Res. Res. 25, 991-1003.

BARKER, J.F. & P. FRITZ 1981. The occurrence and origin of methane in some groundwater flow systems. Can. J. Earth Sci. 18, 1802-1816.

BARTOLI, F. 1983. The biogeochemical cycle of silicon in two temperate forest ecosystems. In "Environmental biogeochemistry", R. Hallberg (ed), Ecol. Bull. 35, 469-476.

BARTOLI, F. 1986. Les cycles biogeochimiques dans les ecosystemes forestiers temperes. Sci. Geol. Bull. 39, 195-209.

BARTOLI, F. & L.P. WILDING 1980. Dissolution of biogenic opal as a function of its physical and chemical properties. Soil Sci. Soc. Am. J. 44, 873-878.

BÄTJER, D. & H. KUNTZE 1963. Untersuchungen des Niederschlagswassers im Küstengebiet Ostfrieslands und Oldenburgs. Küste 11, 34-51.

BEAR, J. & D.K. TODD 1960. The transition zone between fresh and salt water. Water Resor. Centre Contr. 29, Berkeley, Calif.

BEEKMAN, H.E. 1991. Ion chromatography of fresh- and seawater intrusion; multicomponent dispersive and diffusive transport in groundwater. Ph.D. Thesis Vrije Univ. Amsterdam, 198p.

BEEKMAN, H.E. & C.A.J. APPELO 1989. Fresh- and saltwater intrusion : laboratory experiments and geochemical transport modelling. (Vlaams) Natuurwetensch. Tijdschr. 70, 247-255.

BEIJERINCK, M.W., H.E. DE BRUYN, P. HUFFNAGEL & C.P.E. RIBBIUS 1909. Rapport van de commissie van advies, inzake de watervoorziening van de Gemeente Delft. Delft, 141 p.

BEILKE, S. & H.W. GEORGII, 1968. Investigation on the incorporation of sulfurdioxide into fog and rain droplets. Tellus 20, 435-442.

BELOUSOVA, N.I. 1974. Role of the migration of water-soluble substances in the formation of podzolic Al-Fe-humic soils (based on lysimetric data). Pochvovedeniye (translated) 12, 55-69.

BENJAMIN, M.M. & J.O. LECKIE 1982. Multiple-site adsorption of Cd, Cu, Zn and Pb on amorphous iron oxyhydroxyde. J. Colloid Interf. Sc. 79, 209-221.

BERHANE, D. & F.P.T. VAN DE COEVERING 1987. Estimation of the waterbalance of a small coniferous forest in the coastal dunes near Znadvoort, The Netherlands. Doktoraal onderzoek IvA Vrije Universiteit, 47 p + 10 bijlagen.

BERNATOWICZ, S., S. LESZCZYNSKI & S. TYCZYNSKA 1976. The influence of transpiration by emergent plants on the water balance in lakes. Aquatic Botany 2, 275-288.

BERNER, R.A. 1971. Principles of chemical sedimentology. Mc Graw Hill, New York.

BERNER, R.A. 1981. A new geochemical classification of sedimentary environments. J. Sediment. Petrol. 51, 359-365.

BEUKEBOOM, Th.J. 1976. The hydrology of the Frisian islands. Ph.D. Thesis Vrije Univ. Amsterdam, Rodopi, 121p.

BIESHEUVEL, A., J.L. VAN DE MEY & R.J. STUURMAN 1987. Storage and elaboration of ground and surface waters with CHEMPROC. DGV-TNO rapport OS 87-28, 22pp.

BIJHOUWER, J.T.P 1926. Geobotanische Studie van de Berger Duinen. Ph.D. Thesis, 202 p.

BIJL, J.G. 1933. Polderproblemen in de loop van drie eeuwen. De Ingenieur 48, B.103-B.109.

BIJVOET, L. & M. TAAL 1991. Zee, zand en zorgen : Knelpuntennota Nederlandse duinen. Uitgave Stichting Duinbehoud Leiden, 57p.

BISCHOFF, J.L., S.J. CLANCY & J.S. BOOTH 1975. Magnesium removal in reducing marine sediments by cation exchange. Geochim. Cosmochim. Acta 39, 559-568.

BISHOP, P.K. & J.W. LLOYD 1990. Chemical and isotopic evidence for hydrogeochemical processes occurring in the Lincolnshire limestone. J. Hydrol. 121, 293-320.

BLANQUET, P. 1946. Détermination de parameters permettant le calcul de la conductivité de certaines solutions salines complexes : application à la vérification de l'analyse chimique d'une eau minerale. Annales Instit. Hydrol. 62, 131-143.

BLASZYK, T. & J. GORSKI 1981. Groundwater quality changes during exploitation. Ground Water 19, 28-33.

BLOKZIJL, J. & A.P. PRUISSERS 1989. Het voorkomen van veen- en humeuze lagen in en rondom het infiltratiegebied van Gemeentewaterleidingen Amsterdam. Rapport Bp 10815, Rijks Geol. Dienst, 7p + 13 bijlagen.

BOBBINK, R., G.W. HEIL & M.B.A.G. RAESSEN 1992. Atmospheric deposition and canopy exchange processes in heathland ecosystems. Env. Pollution 75, 29-37.

BOELENS, A.H.M. 1959. Loodafgifte door buizen uit hard PVC. Water 43, 182 en Water 44, 350.

BOERBOOM, J.H.A. 1963. Het verband tussen bodem en vegetatie in de Wassenaarse duinen. Boor & Spade 13, 120-155 (in dutch).

BOL, J. 1991. Moeras- of brongas. Grondboor & Hamer 45, 150-153.

BOORMAN, L.A. 1977. Sand-dunes. Ch.9 in "The coastline", R.S.K. Barnes (ed), J. Wiley & Sons, 161-197.

BORN, S.M., S.A. SMITH & D.A. STEPHENSON 1979. Hydrogeology of glacial-terrain lakes, with management and planning applications. J. Hydrol. 43, 7-43.

BOSTRÖM, K., B. BOSTRÖM & P. ANDERSSON 1989. Natural and anthropogenic components in bulk precipitation at Blidö (Archipelago of Stockholm). Water Res. Research 25, 1291-1301.

BOUMANS, L.J.M. & W. VAN DUIJVENBOODEN 1985. Grondwaterkwaliteitsvariaties naar de diepte en in de tijd. RIVM-report 840381001, 53pp + 167 annexes (in dutch).

BOUMANS, L.J.M. & W.H.J. BELTMAN 1991. Kwaliteit van het bovenste freatische grondwater in de zandgebieden van Nederland, onder bos en heidevelden. RIVM-rapport 724901001, 66p.

BOUWER, H. 1991. Simple derivation of the retardation equation and application to preferential flow and macrodispersion. Ground Water 29, 41-46.

BOYCE, S.G. 1954. The salt spray community. Ecol. Monographs 24, 29-67.

BOYLE, J.M. & Z.A. SALEEM 1979. Determination of recharge rates using temperature-depth profiles in wells. Water Resources Res. 15, 1616-1622.

BRAAK, C. 1945. Invloed van den wind op regenwaarnemingen. Meded. & Verh. Kon. Ned. Meteor. Inst. 48, 74p.

BRAKEL, J. 1968. De vorming van een zoetwaterlens in een duingebied t.g.v. de nuttige neerslag als functie van de tijd. Doctoraalstudie TH Delft.

BRAND, U. & J. VEIZER 1980. Chemical diagenesis of a multicomponent carbonate system, I. trace elements. J. Sedim. Petrol. 50, 1219-1236.

BRANDES, M.C. 1985. Gases in groundwater. In "Groundwater infiltration with bored wells", Communications Rijkswaterstaat 39, The Hague, 67-71.

BRASSER, L.J. 1980. Polycyclic aromatic hydrocarbon concentrations in the Netherlands. VDI-Berichte 358, 171-180.

BRAY, J.T., O.P. BRICKER & B.N. TROUP 1973. Phosphate in interstitial waters of anoxic sediments : oxidation effects during sampling procedure. Science 180, 1362-1364.

BREDEMEIER, M., E. MATZNER & B. ULRICH 1988. A simple and appropriate method for the assessment of total atmospheric deposition in forest ecosystem monitoring. In : Acid deposition at high elevation sites, M.H. Unsworth & D. Fowler (eds), Kluwer Acad. Publ, 607-614.

BREEUWER, J.B., S. JELGERSMA & E.F.J. DE MULDER 1979. Geologie van de provincie Noord-Holland. Rapport R.G.D. Haarlem, no. 0.7106, 12 p, 16 bijlagen.

BREEUWSMA, A. & R. ZWIJNEN 1984. Kleimineralogische samenstelling van Nederlandse aquifers. StiBoKa rapport 1816, 11p.

BROERS, H.P. & J. GRIFFIOEN 1992. Het grondwaterkwaliteitsmeetnet van de provincie Noord-Brabant : opzet en eerste resultaten. H_2O 25, 728-735.

BROOK, G.A. et al. 1983. A world model of soil carbon dioxide. Earth Surf. Proc. 8, 79-88.

BROWN, R.M., N.I. McCLELLAND, R.A. DEINIGER & R.G. TOZER 1970. A water quality index, do we dare? Water & Sewage Works 117, 339-343.

BUIJSMAN, E. 1989a. Onderbouwende informatie over het Landelijk Meetnet Luchtkwaliteit; I. Het Landelijk Meetnet Regenwatersamenstelling. RIVM-rapport 228703006, 50 p.

BUIJSMAN, E. 1989b. De relevantie van metingen van orthofosfaat en totaal fosfaat in het Landelijk Meetnet Regenwatersamenstelling. RIVM-rapport 228703010, 13 p.

BULL,J. & KOPFLER, F.C. 1991. Health effects of desinfectants and desinfection by-products. AWWA, Research Foundation, Denver.

BURGES, A. & D.P. DROVER 1953. The rate of podzol development in sands of the Woy Woy district, N.S.W. Australian J. Botany 1, 83-94.

BURIAN, K. 1971. Primary production, carbondioxide exchange and transpiration in Phragmites communis trin. on the lake Neusiedler See, Austria. Hydrobiol. 12, 203-218.

BUSENBERG, E. & L.N. PLUMMER 1985. Kinetic and thermodynamic factors controlling the distribution of SO_4^- and Na^+ in calcites and selected aragonites. Geochim. et Cosmochim. Acta 49, 713-725.

CAMBRAY, R.S., D.F. JEFFERIES & G. TOPPING 1979. The atmospheric input of trace elements to the North Sea. Mar.Sci.Commun. 5, 175-194.

CAMPBELL, E.E. & G.C. BATE 1991. Ground water in the Alexandria dune field and its potential influence on the adjacent surf- zone. Water SA 17, 155-160.

CARPENTER, R. 1969. Factors controlling the marine geochemistry of fluorine. Geochim. Cosmochim. Acta 33, 1153-1167.

CARRIERE, J.E. 1929. De waterleidingen in vele gevallen het behoud van onze duinen. De Levende Natuur 34, 126-134 + 161-172.

CBS, 1979-1988. Luchtverontreiniging, metingen buitenlucht april 1978-maart 1979, idem volgende jaren. Rapport Centraal Bureau voor de Statistiek, Afd. Milieuhygiene, Voorburg.

CEDERSTROM, D.J. 1946. Genesis of ground waters in the coastal plain of Virginia. Econ. Geol. 41, 218-245.

CHAKRABARTI, C.L., K.S. SUBRAMANIAN, J.E. SUEIRAS & D.J. YOUNG 1978. Preservation of some anions in natural waters. JAWWA 70, 560-565.

CHAMP, D.R., J. GULENS & R.E. JACKSON 1979. Oxidation reduction sequences in groundwater flow systems. Canad. J. Earth Sci. 16, 12-23.

CHANG, J.H. 1957. Global distribution of the annual range in soil temperature. Trans. Am. Geophys. Union 38, 718-723.

CHAPELLE, F.H. & L.L. KNOBEL 1983. Aqueous geochemistry and the exchangeable cation composition of glauconite in the Aquia aquifer, Maryland. Ground water 21, 343-352.

CHEBOTAREV, I.I. 1955. Metamorphism of natural waters on the crust of weathering. Geochim. et Cosmochim. Acta 8, 22-48, 137- 170, 198-212.

CIAVATTA, C., L.V. ANTISARI & P. SEQUI 1990. Interference of soluble silica in the determination of orthophosphate-phosphorus. J. Environ. Qual. 19, 761-764.

COLLINS, W.D. 1923. Graphic representation of analyses. Indus. & Eng. Chemistry 15, 394.

COOK, J.M., W.M. EDMUNDS & N.S. ROBINS 1991. Groundwater contribution to an acid upland lake (Loch Fleet, Scotland) and the possibilities for amelioration. J. Hydrol. 125, 111-128.

COOK, P.G., W.M. EDMUNDS & C.B. GAYE 1992. Estimating paleorecharge and paleoclimate from unsaturated zone profiles. Water Resources Res. 28, 2721-2731.

COOPER, H.H., F.A. KOHOUT, H.R. HENRY & R.E. GLOVER (1964) : Sea water in coastal aquifers. Geol. Survey Water-supply Paper 1613-C, 84p.

CORNELISSEN, C.M.L. 1980. Geo-elektrisch onderzoek 's-Gravenhage/Utrecht; kaartbladen 30D, 30 Oost en 31 West. DGV-TNO rapport GF-125, 41p + 11 bijlagen.

CROIN MICHIELSEN, N. [ed.] 1974. Meijendel, duin-waterleven. Meded. Meijendel-comité, Nieuwe Serie 28, 271p.

DAHMKE, A., G. MATTHESS, A. PEKDEGER, D. SCHENK & H.D. SCHULZ 1986. Near-surface geochemical processes in Quarternary sediments. J. Geol. Soc. London 143, 667-672.

DANSGAARD, W. 1964. Stable isotopes in precipitation. Tellus 16, 436-468.

DE GANS, W. 1991. Kwartairgeologie van West-Nederland. Grondboor & Hamer 45, 103-114.

DE GROOT, A.J. 1963. Mangaantoestand van Nederlandse en Duitse Holocene sedimenten in verband met slibtransport en bodemgenese. Versl. Landbk. Onderz. 69.7, PUDOC, 164p.

DE GROOT, W.T. 1981. Het gedrag van fosfaat bij duininfiltratie. H_2O 14, 152-158.

DE GRUYTER, P. & E.L. MOLT 1950. Rijnlands boezemwater, deel III : De hoedanigheid van het boezemwater. Herziene uitgave Hoogheemraadschap Rijnland, 332 pp + 47 annexes.

DE JONG, J.D. 1957. Heavy mineral composition of the podsol profile at the top of the Pleistocene. Verh. Kon. Ned. Geol. Mijnbk. Gen., Geol. Serie 17, 146-147.

DE JONGE, H.G. 1981. Onderzoek naar de invloed van inhomogeniteiten op de verblijftijden van het grondwater. KIWA-rapport SWO-326, 191p + 48p. annex.

DEKKER, L.W. & P.D. JUNGERIUS 1990. Water repellency in the dunes with special reference to the Netherlands. Catena Supplement 18, 173-183.

DELECOURT, J. 1941. Le Titre natronique (1re note). Bull. Soc. belge de Géol., Paléont. et Hydrol. 50, 152-166.

DE MULDER, E.F.J. & J.H.A. BOSCH 1982. Holocene stratigraphy, radiocarbon datings and paleogeography of central and northern North-Holland (The Netherlands). Meded. Rijks Geol. Dienst 36-3, 111-160.

DE MULDER, E.F.J., A.P. PRUISSERS & H. ZWAAN 1983. Kwartairgeologie van 's-Gravenhage. Meded. Rijks Geol. Dienst 37-1, 12-43.

DEN HOED, M.A., F.M.L. MOBERTS & P.J. STUYFZAND 1987. Mogelijkheden voor een verschralend maaibeheer in twee (ver)natte duinterreinen. KIWA-rapport SWE 86.007.

DEPUYT, F. 1972. De Belgische strand- en duinformaties in het kader van de geomorfologie der zuidoostelijke Noordzeekust. Verh. Kon. Acad. voor Wetenschappen, Letteren en Schone Kunsten van België 34, 228p.

DE ROO, H.C. 1953. De bodemkartering van Noord-Kennemerland. Diss. Wageningen, Versl. Landbouwk. Onderz. 59.

DE RUITER, J.C. 1990. Some aspects of a hydrological systems analysis in the province of South Holland. Proc. 11th Salt Water Intrusion Meeting, Gdansk 1990, B. Kozerski & A. Sadurski (eds), Techn. Univ. Gdansk, Poland, 56-71.

DE VOOGD, J.G. 1941. Brongas. Tijdschrift Het Gas, 213-218 + 225-230.

DE VRIES, J.J. 1974. Groundwater flow systems and stream nets in The Netherlands. Ph.D. Thesis Free Univ. Amsterdam, RODOPI, Amsterdam, 226p.

DE VRIES, J.J. 1977. The stream network in The Netherlands as a groundwater discharge phenomenon Geol. & Mijnbouw 56, 103-122.

DE VRIES, J.J. 1981. Fresh and salt groundwater in the Dutch coastal area in relation to geomorphological evolution." Geol. & Mijnb. 60, 363-368.

DE VRIES, J.J. 1982. Anderhalve eeuw hydrologisch onderzoek in Nederland. Rodopi, Amsterdam, 195p.

DE WINDER, G.B.M. 1990. Ecophysiological strategies of drought-tolerant phototrophic micro-organisms. Ph.D. Thesis Univ. Amsterdam, 94p.

DIEDEREN, H.S.M.A. & R. GUICHERIT 1981. Bronherkenning van aerosolen door middel van concentratiemetingen van elementen in de buitenlucht. IMG-TNO- rapport G799, 15p.

DOING, M. 1966. Beschrijving van de vegetatie der duinen tussen IJmuiden en Camperduin. Meded. LH Wageningen. 66-13, 63 p.

DOING, H. 1988. Landschapsoecologie van de Nederlandse kust. Stichting Publicatiefonds Duinen, Leiden, 217p, in dutch.

DOLMAN, A.J. 1987. Predicting evaporation from an oak forest. Ph.D. Thesis Rijksuniversiteit Groningen, 91p.

DOLMAN, A.J. & W.E. OOSTERBAAN 1986. Grondwatervoeding, interceptie en transpiratie van de Castricumse boslysimeters. H_2O (19), 174-175.

DÖRR, H., W. LEUCHS, P. OBERMANN, W. REGENBERG & C. SONNTAG 1992. Isotope geochemistry of the subsurface carbonate system in Sandhausen and Bocholt. In "Progress in hydrogeochemistry", G. Matthess, F. Frimmel, P. Hirsch, H.D. Schulz & H.-E. Usdowski (Eds), Springer Verlag, Berlin, 149-157.

DRESSCHER, Th.G.N. & H. VAN DER MARK 1976. A simplified method for the biological assessment of the quality of fresh and slightly brackish water. Hydrobiologia 48, 199-201.

DREVER, J. 1982. The geochemistry of natural waters. Prentice-Hall, NJ, 388p.

DUBOIS, E. 1909. De prise d'eau der Haarlemsche Waterleiding. Rapport uitgebracht aan gemeente Bloemendaal. 30 p.

DUCE, R.A. & E.J. HOFFMAN 1976. Chemical fractionation at the air/sea interface. Ann. Rev. Earth Planet. Sci. 4, 187-228.

DU COMMUN, J. 1828. On the causes of fresh water springs, fountains etc. Am. J. Sci (1st ser.) 14, 174-176.

DUNLAP, H.F. & R.R. HAWTHORNE 1951. The calculation of water resistivities from chemical analyses. J. Petr. Techn. 3, Section 1 p.17, section 2, p.7.

DUROV, S.A. 1948. Natural waters and graphic representation of their composition. Akad. Nauk. SSSR Doklady 59, 87-90.

DUVIGNEAUD, P. & S. DENAEYER-DE-SMET 1970. Biological cycling of minerals in temperate deciduous forests. In "Analysis of temperate deciduous forest ecosystems", D.E. Reichle (ed), Ecol. Studies 1, Springer Verlag NY, 199-225.

DUYVE, J. & B. STIJGER 1957. De nieuwe werken in de duinwaterwinplaats. De Overstort 10, 1-11.

EATON, J.S., G.E. LIKENS & F.H. BORMANN 1978. The input of gaseous and particulate sulfur to a forest ecosystem. Tellus 30, 546-551.

EC 1980. Richtlijn 80/778/EEG, Richtlijn van de Raad betreffende de kwaliteit van voor menselijke consumptie bestemd water. Publicatieblad Europese Gemeenschappen L229, 11-29.

EDELMAN, Th. 1983. Achtergrondgehalten van een aantal anorganische en organische stoffen in de bodem van Nederland; een eerste verkenning. RIN-rapport 83/8, 49p + 79 bijlagen.

EDGE, R.W. & K. CORDRY 1989. The hydropunch : an in situ sampling tool for collecting ground water from unconsolidated sediments. Ground Water Monit. Review, Summer 1989, 177-183.

EDMUNDS, W.M. 1981. Hydrogeochemical investigations. Ch.6 in "Case studies in groundwater resources evaluation" Lloyd, J.W. (ed), Clarendon Press Oxford, 87-112.

EDMUNDS, W.M., A.H. BATH & D.L. MILES 1982. Hydrochemical evolution of the East Midlands Triassic sandstone aquifer, England. Geochimica et Cosmochimica Acta 46, 407-424.

EDMUNDS, W.M. & D.G. KINNIBURGH 1986. The susceptibility of UK groundwaters to acidic deposition. J. Geol. Soc. London 143, 707-720.

EDMUNDS, W.M., D.G. KINNIBURGH & P.D. MOSS 1992. Trace metals in interstitial waters from sandstones : acidic inputs to shallow groundwaters. Envir. Pollution 77, 129-141.

EDMUNDS, W.M., D.L. MILES & J.M. COOK 1984. A comparative study of sequential redox processes in three British aquifers. IAHS Publ. 150, 55-70.

EDMUNDS, W.M., J.M. COOK, W.G. DARLING, D.G. KINNIBURGH, D.L. MILES, A.H. BATH, M. MORGAN-JONES & J.N. ANDREWS 1987. Baseline geochemical conditions in the Chalk aquifer, Berkshire, U.K. : a basis for groundwater quality management. Appl. Geochem. 2, 251-274.

EDWARDS, R.S. & S.M. CLAXTON 1964. The distribution of air-borne salt of marine origin in the Aberystwyth area. J. Applied Ecol. 1, 253-263.

EDWARDS, A.C., R.C. FERRIER & J.D. MILLER 1992. The contribution of sulphate to total sulphur in a range of natural water samples. Hydrol. Sci. J. 37, 277-283.

EGMOND, N.D. VAN: 1984. Herkomst van SO_x en NO_x-deposities. In: "Zure regen; oorzaken, effecten en beleid, PUDOC- Wageningen, p. 59- 65.

EICHINGER, L. & H.D. SCHULZ 1984. Bestimmung der Sickerrate in einem Sandr Norddeutschlands durch Messungen der Umweltisotopen und Chlorid-Konzentrationen des Sickerwassers. In : Udluft, P., B. Merkel & K.H. Prösl (eds), Proc. RIZA-Symp., Dept. Hydrogeol. Hydrochem., Techn. Univ. München, Vol II, 547-558.

EISMA, D., H.A. DAS, D. HOEDE, J.G. VAN RAAPHORST & J. ZONDERHUIS 1966. Iron and trace elements in Dutch coastal sands. Neth. Instit. for Sea Research 3, 68-94.

EISMA, D. 1968. Composition, origin and distribution of Dutch coastal sands between Hoek van Holland and the island of Vlieland. Neth. J. Sea Research 4, 123-267.

ELRASHIDI, M.A. & W.L. LINDSAY 1986. Chemical equilibria of fluorine in soils : a theoretical development. Soil Sci. 141, 274-280.

ELLENBERG, H., R. MAYER & J. SCHAUERMANN 1986. Ökosystemforschung; Ergebnisse des Sollingsprojekts 1966-1986. E. Ulmer Verlag Stuttgart.

EMERSON, S. 1976. Early diagenesis in anaerobic lake sediments : chemical equilibria in interstitial waters. Geochim. et Cosmochim. Acta 40, 925-934.

ENGELEN, G.B. 1981. A systems approach to groundwater quality-methodological aspects. Sci. Tot. Envir. 21, 1-15.

ENGELEN, G.B.: 1984. "Hydrological systems analysis a regional case study" Rapport DGV-TNO, nr. OS84-20, 43 p. + 23 kaarten.

ENGELEN, G.B. 1986. The Quarternary sequence of water systems in the Western part of the Netherlands. IAHS Publ. 163, 181-195.

ENGELEN, G.B. & A.J ROEBERT 1974. Chemical watertypes and their distribution in space and time in the Amsterdam dunewater catchment area with artificial recharge. J. Hydrol. 21, 339-356.

ENGELEN, G.B. & J.C. DE RUITER-PELTZER 1986. A case study of regional hydrological systems and fresh-salt water interaction in the western part of the Netherlands. Proc. 9th Salt Water Intrusion Meeting, Univ. Delft, R.H. Boekelman et al. (eds), 177-191.

ENGELEN, G.B. & G.P. JONES 1986. Developments in the analysis of ground water flow systems. IAHS Publ. 163, 356 pp.

ENGELEN, G.B., J.M.J. GIESKE & S.O. LOS 1988. Grondwater stromingsstelsels in Nederland Werkdocument. Rapport Staatsbosbeheer 1988-36, 166 p.

ERIKSSON, E. 1952. Composition of atmospheric precipitation; II. Sulfur, chloride, iodine compounds , Bibliography. Tellus 4, 280-303.

ERIKSSON, E. 1987. Alkalinity production in soil and rock : a useful concept for understanding acidification of soil and fresh water. In : "Acidification and Water Pathways" Proc. Int. Symp. Bolkesjo Norway 4-8 may 1987, Norw. Nat. Comm. for Hydrol., Vol.1 , 29-35.

ERISMAN, J.W. 1992. Atmospheric deposition of acidifying compounds in the Netherlands. Ph.D. Thesis, Rijksuniv. Utrecht, 155 p.

ERNST, W.H.O. 1984. De begroeiing als onderdeel van het duinecosysteem : haalt het duin het jaar 2000? In "Van duingebruik naar duinbeheer; 50 jaar onderzoek en beheer Noordhollands Duinreservaat", uitgave PWN, 30-39.

ERNST, W.H.O. 1987. Metal fluxes to coastal ecosystems and the response of coastal vegetation. Ch.24 in "Vegetation between land and sea", A.H.L. Huiskes, C.W.P.M. Blom & J. Rozema (eds), W. Junk Publ, Dordrecht, 302-310.

ERNST, W.H.O. 1990a. Element allocation and (re)translocation in plants and its impact on representative sampling. In : H. Lieth & B. Markert (eds), Element concentration cadasters in ecosystems, VCH Verlagsgesellschaft, Weinheim, 17-40.

ERNST, W.H.O. 1990b. Ecological aspects of sulfur metabolism. In : H. Rennenberg, C. Brunold, L.J. de Kok & J. Stulen (eds) Sulfur nutrition and sulfur assimilation in higher plants, SPB Acad. Publ., The Hague, 131-144.

ESSELINK, H., A.P. GROOTJANS, P. HARTOG & T. JAGER 1989. Kalkrijke vegetaties in een duinvallei op Schiermonnikoog. Duin 2, 75-79.

ETHERINGTON, J.R. 1967. Studies of nutrient cycling and productivity in oligotrophic ecosystems, I. Soil potassium and wind- blown sea-spray in a South Wales dune grassland. J. Ecol. 55, 743-752.

FAY, P.J. & D.W. JEFFREY 1992. The foreshore as a nitrogen source for marram grass. In "Coastal dunes", Carter, Curtis & Sheehy-Skeffington (eds), Balkema, Rotterdam, 177-188.

FEENSTRA, S. 1987. Screening/indicator parameters for organic contaminants in ground water. Water Poll. Res. J. Can. 22, 73-84.

FIEDLER, H.J. & S. dev TAKUR 1984. Gehalt und transformation des Schwefels in Böden von Waldökosystemen. Arch. Naturschutz u. Landschaftsforsch. 24, 17-35.

FOSTER, M.D. 1942. Base exchange and sulphate reduction in salty groundwaters along Atlantic and Gulf Coast. Am. Assoc. Petl. Geol. Bull. 26, 838-851.

FOSTER, M.D. 1950. The origin of high sodium bicarbonate waters in the Atlantic and Gulf Coastal Plains. Geochim. et Cosmochim. Acta 1, 33-48.

FOURNIER, R.O. & R.W. POTTER 1982. A revised and expanded silica (quartz) geothermometer. Geotherm. Resour. Counc. Bull. nov., 3-9.

FOWLER, D. 1978. Wet and dry deposition of sulphur and nitrogen compounds from the atmosphere. In NATO Conf. on " Effects of acid precipitation on terrestrial ecosystems", Toronto 1978, T.C. Hutchinson & M. Havas (eds), Plenum Press, NY, 9-27.

FOWLER, D. 1984. Transfer to terrestrial surfaces. In : Ecological effects of deposited sulphur and nitrogen compounds. Phil. Trans. Soc. London, B 305, 281-297.

FRAKES, R.A. 1988. Drinking water guideline for ethylene thiourea, a metabolite of ethylene bisdithiocarbamate fungicides. Regulatory Toxic. & Pharmacol. 8, 207-218.

FRAPPORTI, G., S.P. VRIEND & W. VAN DUIJVENBOODEN 1990. Hydrogeochemistry of the dutch groundwater-classification into homogeneous groupings with fuzzy c-means clustering. Applied Geochem. Special Issue Uppsala.

FREEZE, R.A. & J.A. CHERRY 1979. Chemical evolution of natural groundwater. Ch.7 in "Groundwater", Prentice Hall Englewood Cliffs, N.Y. ,237-302.

FRIMMEL, F.H. 1992. Investigation of metal complexation by polarography and fluorescence spectroscopy. In "Progress in hydrogeochemistry", G. Matthess, F. Frimmel, P. Hirsch, H.D. Schulz & H.-E. Usdowski (Eds), Springer Verlag, Berlin, 61-65.

FRITZ, P. 1983. Geochemical parameters as indicators for groundwater flow. IAHS Publ. 146, 229-239.

FROELICH, P.N. & MANY OTHERS 1979. Early oxidation of organic matter in pelagic sediments of the eastern equatorial Atlantic : suboxic diagenesis. Geochim.et Cosmochim. Acta 43, 1075-1090.

FUNK, W. 1977. Konservierung von Proben zur späteren Analytik im Laboratorium. Vom Wasser 48, 75-87.

GALLOWAY, J.N. & G.E. LIKENS 1978. The collection of precipitation for chemical analysis. Tellus 30, 71-82.

GALLOWAY, J.N., G.E. LIKENS, W.C. KEENE & J.M. MILLER 1982. The composition of precipitation in remote areas of the world. J. Geophys. Research 87, 8771-8786.

GARTEN, C.T., E.A. BONDIETTI & R.D. LOMAX 1988. The contribution of foliar leaching and dry deposition to sulphate in net throughfall below deciduous trees. Atmospheric Environment 22, 1425-1432.

GEHU-FRANCK, J. & J.M. GEHU 1971. Données écosystémiques et évaluation de la phytomasse dans le transect dunaire de Wimereux-Ambleteuse (Pas-de-Calais, France). Colloques Phytosociologiques, I Dunes, Paris, 253-280.

GEIRNAERT, W. 1973. The hydrogeology and hydrochemistry of the lower Rhine fluvial plain. Ph.D. Thesis, Leiden, Leidse Geol. Med 49, 59-84.

GERLACH, A., E. ALBERS & W. BROEDLIN 1989. Nitrogen content and turnover in coastal dune succession on Spiekeroog, East Frisian Islands. EUCD-Congress Sevilla March 1989, Congress-Book in press.

GERRITSE, R.G. & R.J. GEORGE 1988. The role of soil organic matter in the geochemical cycling of chloride and bromide. J. Hydrol. 101, 83-95.

GEVERS, D.T. 1826. Verhandelingen over het toegangbaar maken van de duinvalleien langs de kust van Holland. Min. v. Landbouw.

GEZONDHEIDSRAAD 1932. Het krop-probleem in Nederland. Staatsuitgeverij, Den Haag.

GIESKE, J.M.J. 1991. De oorsprong van het brakke grondwater in het IJsselmeergebied : diffusie, dispersie of dichtheidsstroming? H_2O 24, 188-193.

GLASBERGEN, P.: 1981. "Extreme salt concentrations in deep aquifers in The Netherlands." Sci. Tot. Envir. (21), p. 251-259.

GLASS, R.J., G.H. OOSTING & T.S. STEENHUIS 1989. Preferential solute transport in layered homogeneous sands as a consequence of wetting front instability. J. Hydrology (110), 87-105.

GOLDENBERG, L.C., M. MAGARITZ & S. MANDEL 1983. Experimental investigation on irreversible changes of hydraulic conductivity on the seawater-freshwater interface in coastal aquifers. Water Res. Res. 19, 77-85.

GOLTERMAN, H.L. 1975. Physiological limnology; an approach to the physiology of lake ecosystems. Developments in water science 2, Elsevier Sci. Publ. Comp. Amsterdam, 489p.

GOLTERMAN, H.L., R.S. CLYMO & M.A.M. OHNSTAD 1978. Methods for physical and chemical analysis of fresh waters. IBP Handbook 8, Blackwell Sci. Publ., London, 2nd

ed., 213pp.
GORHAM, E. 1958. Soluble salts in dune sands from Blakeney point in Norfolk. J. Ecol. 46, 373-379.
GÖTTLICH, K. 1980. Moor- und Torfkunde. E. Schweizerbartsche Verlagsbuchhandlung Stuttgart, 338p.
GRIFFIOEN, J. 1992. Cation-exchange and carbonate chemistry in aquifers following groundwater flow. Ph.D. Thesis Free Univ. Amsterdam, 182p.
GROENEVELD, D.J. 1977. Tritium analysis of environmental water. Ph.D Thesis Rijksuniv. Groningen, 131p.
GRON, C., 1990. Organic halogen group parameters in groundwater investigations; part III. Chemosphere 21, 135-152.
GROOTJANS, A.P., H. ESSELINK, R. VAN DIGGELEN, P.HARTOG, T.D. JAGER, B. VAN HEES & J. OUDE MUNNINCK in press. Decline of rare calciphilous dune slack species in relation to decalcification and changes in local hydrological systems. Proc. Coastal Dune Congress, 1989 Sevilla, in press.
GROOTJANS, A.P., P. HENDRIKSMA, M. ENGELMOER & V. WESTHOF 1988. Vegetation dynamics in a wet dune slack I : rare species decline on the Waddenisland of Schiermonnikoog in the Netherlands. Acta Botan. Neerl. 37, 265-278.
GUILLERD, A. 1941. Contrôle de l'analyse, d'une eau minerale par sa resistivité electrique. Ann. Inst. Hydrol. et Climat. 48, 131-141.
HAASNOOT, J. & K.W.H. LEEFLANG 1971. Methods of sustaining good infiltration results. In: Proc. Artifical Groundwater recharge conference, 21-24 sept. 1970 Univ. Reading, Eng., Water Res. Ass. Engl. vol. 1, 133-168.
HAGEMAN, B.P. 1969. Development of the western part of the Netherlands during the Holocene. Geol. Mijnb. 48, 373-388.
HALLEWAS, D.P. 1984. The interaction between man and its physical environment in the county of Holland between circa 1000 and 1300 AD : a dynamic relationship. Geol & Mijnb. 63, 299-307.
HANSEN, B.K. 1992. Groundwater acidification by acid rain : mineral buffering and ion exchange. KNCV Symposia-reeks 4, 5-15.
HANSHAW, B.B. & W. BACK 1985. Deciphering hydrological systems by means of geochemical processes. Hydrol. Sci. J. 30, 257-271.
HANSHAW, B.B., W. BACK & R.G. DEIKE 1971. A geochemical hypothesis for dolomitization by ground water. Econ. Geol. 66, 710-724.
HARDIE, L.A. & H.P. EUGSTER 1978. The evolution of closed-basin brines. Miner. Soc. Am. Spec. Publ. 3, 273-290.
HARMSEN, G.W. 1954. Observations on the formation and oxidation of pyrite in the soil. Plant & Soil V, 324-347.
HARMSEN, K. 1977. Behaviour of heavy metals in soils. Agric. Research Report 866, Agric. Univ. Wageningen, Ph.D Thesis, 171p.
HARNED, H.S. & B.B. OWEN 1958. The physical chemistry of electrolytic solutions. 3rd ed. Reinhold, NY.
HARTMANN, M., P. MÜLLER, E. SUESS & C.H. VAN DER WEIJDEN 1973. Oxidation of organic matter in recent marine sediments. Meteor Forsch.-Ergebnisse, Reihe C, 12, 74-86.
HEEREBOUT, G.R. 1970. A classification system for isolated brackish inland waters, based on median chlorinity and chlorinity fluctuations. Neth. J. Sea Res. 4, 494-503.
HEINONEN, P. & S. HERVE 1987. Water quality classification of inland waters in Finland. Aqua Fennica 17, 147-156.
HEIJ, G.J. & T. SCHNEIDER 1991. Acidification research in the Netherlands. Studies in Environmental Science 46, Elsevier, Amsterdam.
HEM, J.D. 1970. Study and interpretation of the chemical characteristics of natural waters. Geol. Surv. Water-Supply Paper 1473, 363pp.
HEM, J.D. 1982. Conductance : a collective measure of dissolved ions. Ch.4 in "Water analysis", Vol. 1, Acad. Press Inc., 137-161.
HERZBERG, B. 1901. Die Wasserversorgung einiger Nordseebäder. J. Gasbeleuchtung & Wasserversorgung 44, 815-819 & 842-844.
HERZOG, B., J. PENNINO & G. NIELSEN 1991. Groundwater sampling. Ch.11 in "Practical handbook of groundwater monitoring", D.M. Nielsen (ed), Lewis Publ. Inc., 449-499.
HETTINGA, F.A.M. 1988. De invloed van vermesting en verzuring op de kwaliteit van het grondwater bij pompstation Vierlingsbeek. KIWA-rapport SWI 88.118, 130p.
HETTINGA, F.A.M. & P.J. STUYFZAND 1991. Problemen voorafgaande aan de analyse van sporenelementen. Ch.3 in KIWA- Meded. 118, 35-52.
HEYMANN, J.A. 1925. Het jodium in het waterleidingbedrijf. Water en Gas 9, 39-54.
HEYMANN, J.A. 1927. Het jodiumgehalte van duin- en regenwater. Water en Gas 11, 91-94.
HICKS, B.B. & R.S. ARTZ 1992. Estimating background precipitation quality from network data. Envir. Pollution 75, 137-143.
HIEGE, W. 1987. Inventarisatie van de gegevens van het lysimeterstation Castricum 1941-1985. Rapport 23, Vakgroep Fys. Geogr & Bodemk, Rijksuniv. Groningen, 111 p.
HOEKSTRA, A.C. 1984. Microbiologische aspecten van kunstmatige infiltratie. Ch.5 in KIWA-Meded 81, 220-259.
HOLDREN, G.R. & P.M. SPEYER 1986. Stoichiometry of alkali feldspar dissolution at room temperature and various pH values. Ch.4 in "Rates of chemical weathering of rocks and minerals", T.M. Colman & D.P. Dethier (eds), Acad. Press, Inc., Harcourt Brace Jovanovich, Orlando, 61-81.
HOOGESTEEGER, G.J. 1905. Rapport van de resultaten van het geologisch, hydrologisch, meteorologisch en water onderzoek, verricht in de Amsterdamse Duin-Prise d'eau, gedurende de jaren 1903, 1904 en 1905. GW rapport, Amsterdam.
HOPMAN, R., C.G.E.M. VAN BEEK, H.M.J. JANSSEN & L.M. PUIJKER 1990. Bestrijdingsmiddelen en de drinkwatervoorziening in Nederland. KIWA-Meded. 113, 251p.
HORTON, R.K. 1965. An index number system for rating water quality. J. Water Pollution Control Fed. 37, 300-306.
HOUDIJK, A.L.F.M. 1990. Effecten van zwavel- en stikstofdepositie op bos- en heidevegetaties. Rapport Vakgroep Aquat. Oecol. & Biogeol. Kath. Univ. Nijmegen, 124p.
HOVLAND, M., M.R. TALBOT, H.QVALE, S. OLAUSSEN & L. AASBERG 1987. Methane-related carbonate cements in pockmarks of the North Sea. J. Sed. Petrol. 57, 881-892.
HOWARD, K.W.F. & J.W. LLOYD 1983. Major ion characterization of coastal saline ground waters. Ground Water 21, 429-437.
HRUBEC, J., A.C. DEN BOER, W.C.M.M. LUIJTEN, J.A.M. VAN OERS & G.J. PIET 1984. Modelonderzoek betreffende het gedrag van verontreinigingen tijdens percolatie van voorgezuiverd oppervlaktewater door de zandbodem. RIVM-rapport Lab. Ecol. Water en Drinkwater 83-395A/HRU/mk, 50p.
HRUBEC, J., A. LUIJTEN, W.C.M.M. LUIJTEN & G.J. PIET 1986. A pilot plant study on water quality changes during groundwater recharge. Water Research 20, 1119-1127.
HRUBEC, J., A.C. DEN BOER & M.J. 't HART 1988. Onderzoek in een proefinstallatie naar het gedrag van organische microverontreinigingen tijdens infiltratie van voorgezuiverd rivierwater. RIVM-rapport 840803001, 172p.
HUANG, W.H. & W.C. KIANG 1972. Laboratory dissolution of plagioklase feldspars in water and organic acids at room temperature. Amer. Mineralogist 57, 1849-1859.
HUIBREGTSE, K.R. & J.H. MOSER 1976. Handbook for

sampling and sample preservation of water and waste water. US Dep. Commerce, Nat. Techn. Inf. Serv. PB-259946, 257 pp.

HUISMAN, L. & F.W.J. VAN HAAREN 1966. Treatment of water before infiltration and modification of its quality during its passage underground. Internat. Water Supply Assoc., 7th Congress, Barcelona, special subject no. 3, G1-26.

HUISMAN, L. & T.N. OLSTHOORN 1983. Artificial groundwater recharge. Pitman Adv. Publ. Program, London, 320 p.

HURLEY, J.P., D.E. ARMSTRONG, G.J. KENOYER & C.J. BOWSER 1985. Ground water as a silica source for diatom production in a precipitation-dominated lake. Science 227, 1576-1578.

ICW 1976. Hydrologie en waterkwaliteit van Midden West-Nederland. ICW Regionale Studies 9, 101 p.

ICW 1982. Kwantiteit en kwaliteit van grond- en oppervlaktewater in Noord-Holland benoorden het IJ. ICW Regionale Studies 16, 185 p.

IG-TNO 1959-1978. Verontreiniging buitenlucht Nieuwe Waterweg. Jaarverslagen Instit. Milieuhygiene en Gezondheidstechniek TNO, Delft, over de jaren 1958 t/m 1978. Periode 1959-1967 = Verontreiniging buitenlucht Westland.

INSKEEP, W.P. & P.R. BLOOM 1986. Kinetics of calcite precipitation in the presence of water-soluble organic ligands. Soil Sci. Soc. Am. J. 50, 1168-1172.

INSKEEP, W.P. & J.C. SILVERTOOTH 1988. Inhibition of apatite precipitation in the presence of fulvic, humic and tannic acids. Soil Sci. Soc. Am. J. 52, 941-946.

IVENS, W.P.M.F., G.P.J. DRAAIJERS, W. BLEUTEN & M.M. BOS 1989. The impact of air-borne ammonia from agricultural sources on fluxes of nitrogen and sulfur towards forest soils. Catena 16, 535-544.

JAMES, P.A. & A.J. WHARFE 1989. Timescales of soil development in a coastal sand dune system, Ainsdale, North-West England. Perspectives in coastal dune management, F. Van der Meulen, P.D. Jungerius & J.H. Visser (eds), SPB Acad. Publ. B.V., The Hague, The Netherlands, 287-295.

JANKOWSKI, J. & G. JACOBSON 1989. Hydrochemical evolution of regional groundwaters to playa brines in Central Australia. J. Hydrol. 108, 123-173.

JANSEN, P.C. 1989. Belang van de strooisellaag voor de totale depositie in een dennenbos. Landschap (6)2, 147-161.

JELGERSMA, S. 1976. De geologische grondslag van het geohydrologisch onderzoek in Nederland. H_2O 9, 543-550.

JELGERSMA, S. 1983. The Bergen inlet, transgressive and regressive Holocene shoreline deposits in the northwestern Netherlands. Geologie en Mijnbouw 62, 471-486.

JELGERSMA, S., J. DE JONG, W.H. ZAGWIJN en J.F. VAN REGTEREN ALTENA 1970. The coastal dunes of the western Netherlands; geology, vegetational history and archeology. Meded. Rijks Geol. Dienst, NS. 21, 93-167.

JORGENSEN, N.O. 1989. Holocene methane-derived, dolomite-cemented sandstone pillars from the Kattegat, Denmark. Marine Geol. 88, 71-81.

JUNGERIUS, P.D. 1990. The characteristics of dune soils. Catena Supplement 18, 155-162.

JUNGERIUS, P.D. & J.H. DE JONG 1989. Variability of water repellence in the dunes along the Dutch coast. Catena (16), 491-497.

KAMATANI, A. & J.P. RILEY 1979. Rate of dissolution of diatom silica walls in seawater. Mar. Biol. 55, 29-35.

KENNEDY, V.C., G.W. ZELLWEGER & B.F. JONES 1974. Filter pore-size effects on the analysis of Al, Fe, Mn, and Ti in water. Water Res. Res. 10, 785-790.

KENOYER, G.J. & M.P. ANDERSON 1989. Groundwater's dynamic role in regulating acidity and chemistry in a precipitation- dominated lake. J. Hydrol. 109, 287-306.

KERFOOT, W.B. 1984. A portable well point sampler for plume tracking. Ground Water Monit. Review, fall 1984, 38-42.

KINNIBURGH, D.G., M.L. JACKSON & J.K. SYERS 1976. Adsorption of alkaline earth, transition and heavy metal cations by hydrous oxide gels of iron and aluminum. Soil Sci. Soc. Am. J. 40, 796-799.

KIRCHMER, C.L. 1983. Quality control in water analyses. Envir. Sci. Technol. 17, 174A-181A.

KISSER-PRIESACK, G.M., D. BIENIEK & H. ZIEGLER 1990. NO_2 binding to defined phenolics in the plant cuticle. Naturwissenschaften 77, 492-493.

KLIJN, J.A. 1981. Coastal dunes of the Netherlands : Geomorphology and soils. Ph. D. Thesis LU Wageningen, Pudoc, 188 p.

KLOOSTERMAN, F.H. 1989. Groundwater flow systems in the nortern coastal lowlands of West- and Central Java, Indonesia; an earth-scientific approach. Ph.D. Thesis Free Univ. Amsterdam, 298p.

KNMI 1972. Klimaatsatlas van Nederland. 's-Gravenhage.

KNMI 1983. Klimatologische gegevens van Nederlandse stations, normalen en standaardafwijkingen 1951-1980. KNMI-rapport 150-10.

KNMI-RIVM 1978-1988. Chemische samenstelling van de neerslag over Nederland, cq Landelijk meetnet regenwatersamenstelling. Jaarrapporten 1978-1988, Kon. Ned. Meteo. Instit., De Bilt, KNMI-publ. 156-1 t/m 156-11.

KOERSELMAN, W. & B. BELTMAN 1988. Evapotranspiration from fens in relation to Penman's potential free water evaporation (E_0) and pan evaporation. Aquatic Botany 31, 307-320.

KOERSELMAN, W., M.A. DEN HOED, A.J.M. JANSEN & W.H.O. ERNST (Eds) 1990. Natuurwaarden en waterwinning in de duinen; mogelijkheden voor behoud, herstel en ontwikkeling van natuurwaarden. KIWA-Meded. 114, 264p.

KÖLLE, W. & D. SCHREECK 1982. Effect of agricultural activity on the quality of groundwater in a reducing underground. Int. Symp. IAH "Impact of agricultural activities on groundwater", Prague, vol. XVI, part 2, 191-202.

KÖLLING, M. 1986. Vergleich verschiedener Methoden zur Bestimmung des Redoxpotentials natürlicher Wässer. Meyniania 38, 1-19.

KOOISTRA, M.J. 1978. Soil development in recent marine sediments of the intertidal zone in the Oosterschelde, The Netherlands; a soil micromorphological approach. Soil Survey Instit. Wageningen, The Neth., Soil Survey Paper 14, 183p.

KONZEWITSCH, N. 1967. Estudio de las clasificaciones propuestas para aguas naturales segun su composicion quimica. Contribucion al decenio hidrologico international 1965-74, Aqua y Energia Electrica empresa del estado, division recursos hidricos, Buenos Aires, Arg., 108p.

KRABBENHOFT, D.P., M.P. ANDERSON & C.J. BOWSER 1990. Estimating groundwater exchange with lakes; 2. Calibration of a three-dimensional, solute transport model to a stable isotope plume. Water Res. Res. 26, 2455-2462.

KRAJENBRINK, G.J.W., D. RONEN, W. VAN DUIJVENBOODEN, M. MAGARITZ & D. WEVER 1988. Monitoring of recharge water quality under woodland. J. Hydrol. 98, 83-102.

KRAUSKOPF, K.B. 1967. Introduction to geochemistry. McGraw-Hill Book Co., New York, 721p.

KRUIJSEN, B.W.J.M., Q.L. SLINGS & H. SNATER 1992. Vegetatiekartering Noordhollands Duinreservaat 1982-1989. Rapport N.V. PWN, Bloemendaal, 191 p.

KRUL, W.F.J.M. 1946. Over een lange reeks waarnemingen van grondwaterstanden in het duingebied bij Schoorl. Water 30, 31-35.

KRUMBEIN, W.C. & L.L. SLOSS 1963. Stratigraphy and sedimentation. Freeman & Comp. San Francisco, 2nd ed, 660p.

KÜHN, H. & H. WELLER 1977. 6jahrige Untersuchungen über

Schwefelzufuhr durch Niederschläge und Schwefelverluste durch Auswaschung (in Lysimetern). Z. Pflanzenernähr. Bodenkd. 140, 431-440 (in german).

KUITERS, A.Th. 1987. Phenolic acids and plant growth in forest ecosystems. Ph.D. Thesis Free Univ. Amsterdam, 150p.

KURLOV, M.G. 1928. Classification of mineral medicinal waters of Siberia. Tomsk, in russian, discussed in Konzewitsch, opus cited.

LABRIJN, A. 1945. Het klimaat van Nederland gedurende de laatste twee en halve eeuw. KNMI, De Bilt, Meded. & Verh. 49, ca. 130p.

LAGAS, P., H.L.J. VAN MAAREN, P. VAN ZOONEN, R.A. BAUMANN, H.A.G. HEUSINKVELD, W.N. VAN DER HEEDEN & M. KOELEMAN 1990. Onderzoek naar het vóórkomen van bestrijdingsmiddelen in het grondwater in de provincie Zuid-Holland. RIVM-rapport 725803001, 42p.

LAGEMAN, R. 1979. Geo-elektrisch onderzoek Alkmaar, kaartbladen 19 West, 19 OOst en 20A. Dienst Grondwaterverkenning TNO, rapport nr. 115, 38 p. + 15 bijlagen.

LAGEMAN, R. & M. HOMAN 1979. Grondwaterkaart van Nederland 1:50.000, kaartbladen 19 West, 19 Oost en 20A. Dienst Grondwaterverkenning TNO, 70 p. + 22 bijlagen.

LANGEWEG, F. (ed) 1988. Zorgen voor morgen, nationale milieuverkenning 1985-2010. RIVM, Samson H.D. Tjeenk Willink, Alphen a/d Rijn, 456 p.

LASAGA, A.C. 1984. Chemical kinetics of water-rock interactions. J. Geophys. Research 89, 4009-4025.

LBS, 1988. Leidraad bodemsanering. Afl.4, Ministerie VROM., The Hague, in dutch.

LEBBE, L. (1981) : The subterrenean flow of fresh and salt water underneath the western Belgian beach. Proc. 7th Salt Water Intrusion Meeting Uppsala, Sver. Geol. Unders. Rap. Meddel. (27), 193-219.

LEBBE, L.C. 1983 Mathematical model of the evolution of the fresh water lens under the dunes and beach with semi-diurnal tides. Geologia Applicata e Idrogeologia (Italiana) 18, 211-226.

LEBBE, L.C. & W. DE BREUCK 1979? Hydrochemie van de freatische aquifer ten westen van De Panne (SW Belgium). Tijdschr. BECEWA 58, 124-138 (in dutch).

LEBBE, L.C. & K. WALRAEVENS 1989. Hydrochemical study of a cross-section through the coastal plain and its surroundings near the French-Belgian border. (Flemish) Natuurwetenschappelijk Tijdschr. 70, 56-64.

LEBBE, L., K. WALRAEVENS & K. PEDE 1989. Het probleem der lekkende peilbuizen in een hydrogeologisch onderzoek van de Zwarte Sluispolder. Water 46, 102-106, in dutch.

LEBBE, L.C., K. WALRAEVENS & W. DE BREUCK 1990. The evolution of the fresh and salt water flow and distribution in two cross sections through the dune area of De Haas. Proc. 11th Salt Water Intrusion Meeting, 14-17 may 1990 Gdansk, Kozerski, B. & A. Sadurski (eds), Techn. Univ. Gdansk Poland, 72-97.

LEEFLANG, K.W.H. 1938. De chemische samenstelling van den neerslag in Nederland. Chem. Weekblad (35), 658-664.

LEEFLANG, K.W.H. 1940. Infiltratie van rivierwater in de duinen. Bijlage 12 bij "Rapport 1940 inzake de watervoorziening van Amsterdam". Gemeentewaterleidingen Amsterdam, 188-199.

LEEFLANG, K.W.H. 1965. Kwaliteitsverandering door infiltratie. Water 49, 167-170 + 177-183.

LEEFLANG, K.W.H. 1974. Ons drinkwater in de stroom van de tijd. VEWIN, Rijswijk, 228p.

LEUCHS, W. & P. OBERMANN 1992. Anoxic reaction zones in an aquifer influenced by increasing nitrate and sulfate contents. In "Progress in hydrogeochemistry", G. Matthess, F. Frimmel, P. Hirsch, H.D. Schulz & H.-E. Usdowski (Eds), Springer Verlag, Berlin, 201-212.

LEUTWEIN, F. & R. WASKOWIAK 1962. Geochemische Untersuchungen an rezenten marinen Molluskenschalen. N. Jb. Miner. Abh. 99, 45-78

LI, Y.H.& GREGORY, S. 1974. Diffusion of ions in sea water and in deep-sea sediments. Geochim. Cosmochim. Acta 38, 703-714.

LIEBSCHER, H.J. 1970. Grundwasserneubildung und Verdunstung unter verschiedenen Niederschlags-, Boden- und Bewuchsverhaltnissen. Die Wasserwirtschaft (5), 168-173.

LINDBERG, R.D. & D.D. RUNNELLS 1984. Ground water redox reactions : an analysis of equilibrium state applied to Eh measurements and geochemical modelling. Science 225, 925-927.

LINDENBERGH, P.C. 1941. Bijdrage tot oordeelkundig beheer van het duinwaterkapitaal. Proefschrift Delft, 181p.

LIPS, H.J.M., B. BULTEN & J. VAN PUFFELEN 1969. Kwaliteitsverandering bij infiltratie in de duinen. Rapport Werkgroep Infiltratie Rivierwater in de DUinen, 60p.

LITAOR, M.I. 1988. Review of soil solution samplers. Water Res. Res. 24, 727-733.

LLOYD, J.W., K.W.F HOWARD, N.R. PACEY & J.H. TELLAM 1982. The value of iodide as a parameter in the chemical characterization of ground waters. J. Hydrol. 57, 247-266.

LOGAN, J. 1961. Estimation of electrical conductivity from chemical analyses of natural waters. J. Geophys. Res. 66, 2479-2483.

LONDO, G. 1966. Veranderingen in flora en vegetatie van het Lekwater-infiltratiegebied in de duinen bij Zandvoort. De Levende Natuur 69, 121-129.

LONDO, G. 1971. Patroon en proces in duinvalleivegetaties langs een gegraven meer in de Kennemerduinen. Ph.D. Nijmegen, Cuyk, 279p.

LOUGHNAN, F.C. 1969. Chemical weathering of the silicate minerals. Am. Elsevier Publ. Comp. Inc., NY, 137p.

LOUMAN, E.G.M. 1989. Effecten van vernatting op de vegetatie in het duingebied van Zuid-Kennemerland. KIWA-rapport SWE 88.005, 240 p.

LOVLEY, D.R. & E.J.P. PHILLIPS 1987. Competitive mechanisms for inhibition of sulfate reduction and methane production in the zone of ferric iron reduction in sediments. Appl. Environ. Micro. 53, 2636-2641.

LÜERS, F. & P.J. STUYFZAND 1992. Sporenelementen en organische microverontreinigingen in natuurlijke duinbodems van Gemeentewaterleidingen. KIWA-rapport SWO-92.305, 31p.

LUTEN, J.B. 1977. Neutron activation analysis of trace elements in rain water. Rapport Netherlands Energy Research Foundation, Petten, ECN-20, 98p.

MAAS, C. 1991. Afleiding van een formule voor hydrodynamische dispersie bij een sinusoïdaal ingangssignaal. Bijlage 9 in KIWA- rapport SWE 91.008, 171-172.

MAGARITZ, M. & J.E. LUZIER 1985. Water-rock interactions and seawater-freshwater mixing effects in the coastal dunes aquifer, Coos Bay, Oregon. Geochim. et Cosmochim. Acta 49, 2515-2525.

MAGARITZ, M., L. GOLDENBERG, U. KAFRI & A. ARAD 1980. Dolomite formation in the seawater-freshwater interface. Nature 287, 622-624.

MAGARITZ, M., A.J. AMIEL, D. RONEN & M.C. WELLS 1990. Distribution of metals in a polluted aquifer : a comparison of aquifer suspended material to fine sediments of the adjacent environment. J. Contaminant Hydrol. 5, 333-347.

MARKUS, W.C. & C. VAN WALLENBURG 1982. Bodemkaart van Nederland 1:50.000 : Bladen 30 West en Oost ('s-Gravenhage). STIBOKA, 130 p.

MARTENS, C.S. & R.A. BERNER 1974. Methane production in the interstitial waters of sulfate depleted marine sediments.

Science 185, 1167-1169.
MASCHHAUPT, J.G. 1941. Lysimeteronderzoekingen aan het Rijkslandbouw- proefstation te Groningen en elders; 2. De scheikundige samenstelling van het drainwater. Versl.Landbouwk.Onderz.47 (4a).
MATTERN, F.C.M. & L. STRACKEE 1973. Tritium in drinkwater, oppervlaktewater en neerslag in de periode 1970-1973. RIV- rapport 183/73, 30p.
MATTHESS, G. 1982. The properties of groundwater. J. Wiley & Sons, NY, 406p.
MATTHESS, G. 1990. Die Beschaffenheit des Grundwassers. Band 2, Zweite Auflage, Gebrüder Borntraeger, Berlin, 498p.
MATTHESS, G., F.H. FRIMMEL, P. HIRSCH, H.D. SCHULZ & E. USDOWSKI 1992. Progress in hydrogeochemistry. Springer-Verlag, Berlin, 544p.
MATZNER, E. & B. ULRICH 1980. The transfer of chemical elements within a heath-ecosystem (Calluna vulgaris) in Northwest Germany. Z. Pflanzenernähr. Bodenkd. 143, 666-678.
MAYER, R. & B. ULRICH 1974. Conclusions on the filtering action of forests from ecosystem analysis. Ecol. PLant 9, 157-168.
MAZOR, E. 1976. Multitracing and multisampling in hydrological studies. In : "Interpretation of environmental isotope and hydrochemical data in groundwater hydrology", IAEA Vienna, 7-36.
MAZOR, E. & R. GEORGE 1992. Marine airborne salts applied to trace evapotranspiration, local recharge and lateral groundwater flow in Western Australia. J. Hydrol. 139, 63-77.
McCORD, J.T. & D.B. STEPHENS 1987. Effect of groundwater recharge on configuration of the water able beneath sand dunes and on seepage in lakes in the sandhills of Nebraska, USA - Comment. j. hYDROL. 95, 365-367.
McKENZIE, R.M. 1980. The adsorption of lead and other heavy metals on oxides of manganese and iron. Aust. J. Soil Res. 18, 61-73.
McNEAL, B.L., J.D. OSTER & J.T. HATCHER 1970. Calculation of electrical conductivity from solution composition data as an aid to in-situ estimation of soil salinity. Soil Sci 110, 405-414.
MEERBURG, P.A. & A. MASSINK 1934. Methodieken voor chemisch en bacteriologisch drinkwateronderzoek. P. Noordhoff, Groningen.
MEINARDI, C.R. 1973. Het zoutwatervoorkomen in de ondergrond van de lage gedeelten van Nederland. H_2O 6, 454-460.
MEINARDI, C.R. 1976. Characteristic examples of the natural groundwater composition in The Netherlands. Verls. & Meded Comm. Hydrol. Onderz. TNO 21, Den Haag, 12-33.
MEINARDI, C.R. 1983a. Fresh and brackish groundwater under coastal areas and islands. Geojournal 7.5, 413-425.
MEINARDI, C.R. 1983b. De gehalten aan natuurlijke isotopen gemeten in het project "kwaliteitsvariaties grondwater". RID-rapport hy.h. 83-29, 73p.
MEINARDI, C.R. 1983c. Groundwater recharge in the Rhine fluvial plain. Z. dt. geo. Ges. 134, 581-611.
MERKEL, B. & J. GROSSMANN 1992. Pore water sampling in carbonate terrains. In "Progress in hydrogeochemistry", G. Matthess, F. Frimmel, P. Hirsch, H.D. Schulz & H.-E. Usdowski (Eds), Springer Verlag, Berlin, 129-138.
MILBOWA, 1991. Notitie milieukwaliteitsdoelstellingen bodem en water. Min. VROM, Tweede Kamer vergaderjaar 1990-1991, 21990 (1), 38p. + addendum 1992.
MILLER, H.G., J.D. MILLER & J.M. COOPER 1980. Biomass and nutrient accumulation at different growth rates in thinned plantations of Corsican pine. Forestry 53, 23-39.
MINDERMAN, G. 1967. The production of organic matter and the utilisation of solar energy by a forest plantation of Pinus nigra var. austriaca. Pedobiol. 7, 11-22.
MINDERMAN, G. & K.W.F. LEEFLANG 1968. The amount of drainage water and solutes from lysimeters planted with either oak, pine or natural dune vegetation or without any vegetation cover. Plant and Soil 28, 61-80.
MöLLER, D. 1990. The Na/Cl ratio in rainwater and the seasalt chloride cycle. Tellus 42B, 254-262.
MOLT, E.L. 1961. Verontreiniging van het Rijnwater. 13e Vakantiecursus Drinkwatervoorziening, Rijks Instit. Drinkwatervoorziening, Leidschendam, 46-71.
MOOK, W.G. 1989. Principles of isotope hydrology. Collegedictaat, Centre of Isotope Research, Univ. Groningen, 153p.
MOORE, P.A., K.R. REDDY & D.A. GRAETZ 1991. Phosphorus geochemistry in the sediment-water column of a hypereutrophic lake. J. Environ. Qual. 20, 869-875.
MORGAN-JONES, M. & M.D. EGGBORO 1981. The hydrogeochemistry of the Jurassic limestones in Gloucestershire, England. Q.J. eng. Geol. London 14, 25-39.
MORRISON, R.D. & P.E. BREWER 1981. Air-lift samplers for zone-of-saturation monitoring. Ground Water Monit. Review, Spring 1981, 52-55.
MULDER, J. 1988. Impact of acid atmospheric deposition on soils : Field monitoring and aluminum chemistry. Ph.D. Thesis LU- Wageningen, 163 p.
MULDER, J.P.M. 1983. A simulation of rainfall interception in a pine forest. Ph.D. Thesis Univ. Groningen, 109 p.
MULLER, G. 1967. Diagenesis in argillaceous sediments. Ch. 4 in "Diagenesis in sediments", Larsen, G. & G.V. Chilingar (eds), Vol. 8 Developments in sedimentology, Elsevier, Amsterdam, 127-177.
NIELSEN, D.M. & G.L. YEATES 1985. A comparison of sampling mechanisms available for small-diameter ground water monitoring wells. Ground Water Monit. Rev., Spring 1985, 83-99.
NIENHUIS, P.R., C.A.J. APPELO & A. WILLEMSEN 1987. PHREEQM, a geochemical model in a mixing cell flowtube. Vrije Universiteit Amsterdam.
NIGHTINGALE, H.I. & W.C. BIANCHI 1980. Wellwater quality changes correlated with well pumping time and aquifer parameters, Fresno, California. Ground Water 18, 274-280.
NIJSSEN, E.M. 1989. Bodemkenmerken in verdroogde en vernatte valleien in het Noord-Hollands Duinreservaat. KIWA-rapport SWE 88.022.
NIJSSEN, E.M. 1990. Een vegetatiekundige en floristische blik op Berkheide. KIWA-Meded 114, 15-42.
NISSENBAUM, A., B.J. PRESLEY & I.R. KAPLAN 1972. Early diagenesis in a reducing fjord, Saanich Inlet, British Columbia. I. Chemical and isotopic changes in major components of interstitial water. Geochim. et Cosmochim. Acta 36, 1007-1027.
NOIJ, Th.H.M., A. NOORDSIJ & J. VAN GENDEREN 1989. Drinkwater uit oppervlaktewater. KIWA-Meded. 107, 179p.
NOORDSIJ, A., L.M. PUIJKER & M.A. VAN DER GAAG 1985. The quality of drinking water prepared from bank-filtered river water in the Netherlands. Sci. Total Environ. 47, 273-292.
NORDSTROM, D.K. 1982. The effect of sulfate on aluminum concentrations in natural waters : some stability relations in the system Al_2O_3-SO_3-H_2O at 298K. Geochimica et Cosmochimica Acta 46, 681-692.
NRIAGU, J.O. 1978. Dissolved silica in pore waters of Lakes Ontario, Erie and Superior sediments. Limnol. & Oceanogr. 23, 53-67.
OENEMA, O. 1990. Pyrite accumulation in salt marshes in the Eastern Scheldt, southwest Netherlands. Biogeochemistry 9, 75-98.
OLIVER, B.G., E.M. THURMAN & R.L. MALCOLM 1983. The contribution of humic substances to the acidity of colored natural waters. Geochim. Cosmochim. Acta 47, 2031-2035.

OLSON, J.S. 1958. Rates of succession and soil changes on Southern Lake Michigan sand dunes. Bot. Gazette 119, 125-170.

OLSON, J.S. & E. VAN DER MAAREL 1989. Coastal dunes in Europe : a global view. In "Perspectives in coastal dune management", F. Van der Meulen, P.D. Jungerius & J.H. Visser (eds), SPB Acad. Publ. B.V., The Hague, The Netherlands, 3-32.

OLSTHOORN, T.N. 1982. Verstopping van persputten. KIWA-Meded. 71.

OLSTHOORN, T.N. 1989. Modellering met behulp van een spreadsheet...simultane stroming van zoet en zout grondwater. H_2O 22, 595-601.

OLSTHOORN, T.N., H. TUINZAAD, C.G.E.M. VAN BEEK & J. VAN PUFFELEN 1975. Putinfiltratie met drinkwater te 's-Gravenhage. KIWA-Meded. 41.

OREMUS, P.A.I. 1982. Growth and nodulation of Hippophaë Rhamnoides L. in the coastal sandnunes of The Netherlands. Ph.D. Thesis Univ. Utrecht, 116p.

OVINGTON, J.D. 1959. Mineral content of plantations of Pinus sylvestris L. Annals of Botany NS 23, 75-88.

PALMER, Ch. 1911. The geochemical interpretation of water analyses. U.S. Geol. Surv. Bull. 479, 31p.

PALMER, C.D. & J.A. CHERRY 1985. Geochemical evolution of groundwaters in sequences of sedimentary rocks. J. Hydrol. 75, 27-65.

PARKER, G.G. 1983. Throughfall and stemflow in the forest nutrient cycle. Advances in Ecol. Research 13, 58-120.

PARKER, L.V., A.D. HEWITT & T.F. JENKINS 1990. Influence of casing materials on trace-level chemicals in well water. Groundwater Monitoring Review (Spring).

PARKHURST, D.L., D.C. THORSTENSON & L.N. PLUMMER 1980. PHREEQE - a computer program for geochemical calculations. U.S. Geol. Surv., Water Resour. Invest. 80-96, 210p.

PARKHURST, D.L., L.N. PLUMMER & D.C. THORSTENSON 1982. BALANCE - a computer program for calculating mass transfer for geochemical reactions in ground water. U.S. Geol. Surv., Water Resour. Invest. 82-14, 29p.

PARKS, G.A. 1967. Aqueous surface chemistry of oxides and complex oxide minerals. In "Advances in Chem. Series", R.F. Gould (ed), Am. Chem. Soc. Publ., 121-160.

PAUL, E.A. & F.E. CLARK 1987. Soil microbiology and biochemistry. Acad. Press, Inc., Harcourt Brace Javanovich Publ, San Diego USA.

PEARSON, F.J. & B.B. HANSHAW 1970. Sources of dissolved carbonate species in groundwater and their effect on carbon-14 dating. Isotope Hydrology 1970, IAEA Vienna, 271-286.

PEDROLI, G.B.M. 1989. The nature of landscape. Ph.D. Thesis Univ. Amsterdam, 156p.

PEDROLI, G.B.M. 1990. Ecohydrological parameters indicating different types of shallow groundwater. J. Hydrol. 120, 381-404.

PEIFFER, S., O. KLEMM, K. PECHER & R. HOLLERUNG 1992. Redox measurements in aqueous solutions — A theoretical approach to data interpretation, based on electrode kinetics. J. Contam. Hydrol. 10, 1-18.

PEKDEGER, A. 1979. Labor- und Felduntersuchungen zur Genese der Sicker- und Grundwasserbeschaffenheit. Meyniana (31), 25-57.

PENNINK, J.M.K. 1914. Verzoutingsrapport. Stadsdrukkerij Amsterdam, 66 p. + 25 bijlagen.

PERDIJK, K. 1992. Vernatting van droge duinvalleien; 2. De invloed van kalkhoudende kwel op verzuurde bodems. Student report LU Wageningen, 44p.

PERELMAN, A.I. 1972. Die Geochemie der epigenetischen Prozesse; die hypergene Zone. Neuaflage, Akademie-Verlag Berlin.

PETERS, H. 1984. Pocket calculators and the oxygen saturation of water. H_2O 17, 73 (in dutch).

PETERS, J.H. 1985. State of the art of borehole recharge. Water Supply 3, 51-58.

PETERS, J.H., Q.L. SLINGS & A. STAKELBEEK 1992. Open infiltratie nieuwe stijl. H_2O 25, 532-537.

PETERS, R.J.B., J.F.M. VERSTEEGH & E.W.B. DE LEER 1989. Dihaloacetonitrillen in Nederlands drinkwater. H_2O 22, 800-804.

PETTIJOHN, F.J. 1941. Persistence of heavy minerals in geologic age. J. Geol. 49, 610-625.

PICKENS, J.F., J.A. CHERRY, G.E. GRISAK, W.F. MERRITT & B.A. RISTO 1978. A multilevel device for ground water sampling and piezometric monitoring. Ground Water 16, 322-327.

PIET, G.J. & J.G.M.M. SMEENK 1985. Behaviour of organic pollutants in pretreated Rhine water during dune infiltration. In "Ground water quality", C.H. Ward, W. Giger & P.L. McCarthy (eds), J. Wiley & Sons, NY, 122-144.

PIET, G.J. & B.C.J. Zoeteman 1980. Organic water quality changes during sand bank and dune filtration of surface waters in The Netherlands. J. AWWA, July 1980, 400-404.

PIPER, A.M. 1944. A graphic procedure in the geochemical interpretation of water analyses. Am. Geophys. Union Trans. 25, 914-923.

PLUHOWSKI, E.J. & I.H. KANTROWITZ 1963. Influence of land-surface conditions on ground-water temperatures in southwestern Suffolk County, Long Island, New York. US Geol. Survey Prof. Paper 475-B, B186-B188.

PLUIS, J.L.A. & B. DE WINDER 1990. Natural stabilization. Catena Supplement 18, 195-208.

PLUMMER, L.N., B.F. JONES & A.H. TRUESDELL 1976. WATEQF, a Fortran IV version of Wateq, a computer program for calculating chemical equilibrium of natural waters. U.S. Geol. Surv. Water Res. Invest. 76-13, 61pp.

PLUMMER, L.N. & W. BACK 1980. The mass balance approach : application to interpreting the chemical evolution of hydrologic systems. [Am] J. Science 280, 130-142.

PLUMMER, L.N., J.F. BUSBY, R.W. LEE & B.B. HANSHAW 1990. Geochemical modelling of the Madison aquifer in parts of Montana, Wyoming, and South Dakota. Water Res. Research 26, 1981-2014.

PLUMMER, L.N., E.C. PRESTEMON & D.L. PARKHURST 1991. An interactive code (NETPATH) for modeling net geochemical reactions along a flow path. US Geol. Surv. Water Resour. Invest. Rep., 91-4078.

POELS, C.L.M. & G. DIBBETS 1982. De initiële migratie van lood uit waterleidingbuizen van ongeplastificeerd Polyvinylchloride. H_2O 15, 588-590.

POHLMANN, K.F. & J.W. HESS 1988. Generalized ground water sampling device matrix. Ground Water Monit. Rev., Fall 1988, 82-83.

POMPER, A.B. 1977. An estimation of the chloride intrusion in the midwest Netherlands during the Pleistocene epoch. Proc 5th Salt Water Intrusion Meeting, Medmenham, 114-125.

PONS, L.J. & M.F. VAN OOSTEN 1974. De bodem van Noord-Holland. Toelichting bij blad 5 van de bodemkaart van Nederland 1:200.000, STIBOKA, 193 p.

PONS, L.J. 1959. Fossiele bodemprofielen in het dekzand in de tunnelput van Velsen. Boor & Spade X, 170-209.

POSTMA, D., C. BOESEN, H. KRISTIANSEN & F. LARSEN 1991. Nitrate reduction in an unconfined sandy aquifer; water chemistry, reduction processes and geochemical modeling. Water Resources Research 27, 2027-2045.

POTTS, M.J. 1978. The pattern of deposition of air-borne salt of marine origin under a forest canopy. Plant & Soil 50, 233-

236.
PRATI, L., R. PAVENELLO & F. PESARIN 1971. Assessment of surface water quality by a single index of pollution. Water Research 5, 741-751
PRENZEL, J. 1979. Mass flow to the root system and mineral uptake of a beech stand calculated from 3-year field data. Plant & Soil 51, 39-49.
PROTZ, R., G.J. ROSS, I.P. MARTINI & J. TERASMAE 1984. Rate of pozolic soil formation near Hudson Bay, Ontario. Can. J. Soil Sci. 64, 31-49.
PROTZ, R., G.J. ROSS, M.J. SHIPITALO & J. TERASMAE 1988. Podzolic soil development in the Southern James Bay lowlands, Ontario. Can. J. Soil Sci. 68, 287-305.
PRUIJT, M.J. 1984. Vegetatie, waterhuishouding en bodem in twee vochtige duinvalleien in het Noordhollands Duinreservaat. Rapport Prov. Waterl. Bedrijf Noord-Holland, project 1.2-38, 101p.
PRUISSERS, A.P., H.H. VOS & L. VAN DER VALK 1991. De geologische en landschappelijke ontwikkeling van het Breesaapduingebied. Regionaal-historisch tijdschrift Holland 23, 117-138.
PWN 1924-1928. Jaarverslagen van het Provinciaal Waterleidingbedrijf Noord-Holland.
PWN 1972. Het lysimeterwaarnemingsstation te Castricum, eindrapport (periode 1941-1971). Rapport Prov. Waterl. Bedrijf N- Holland, 11p + 6 bijlagen.
PWS 1973-1988. Metingen luchtverontreiniging in Noord-Holland. Halfjaarlijkse rapporten tot april 1981, daarna jaarrapporten, Dienst voor Milieuhygiëne Prov. Waterstaat Noord-Holland.
PWS 1981. Verzilting in boezem- en polderwateren in Noord-Holland, periode 1-1-1978 t/m 31-3-1979. Rapport Prov. Waterstaat N-Holland, 55 p.
RAGLAND, P.C., O.H. PILKEY & B.W. BLACKWELDER 1979. Diagenetic changes in the elemental composition of unrecrystallized mollusk shells. Chem. Geol. 25, 123-134.
RAHN, K.A. 1975. Chemical composition of the atmospheric aerosol : Compilation I. Extern 5, 286-313.
RAKHORST, H.D. 1991. De kust van Noord-Holland; verrassend en leuk. Grondboor & Hamer 45, 135-141.
RANDALL, R.E. 1970. Salt measurement on the coast of Barbados, West Indies. Oikos 21, 65-70.
RANWELL, D.S. 1959. Newborough Warren, Anglesey; I. the dune system and dune slack habitat. J. Ecol. 47, 571-601.
RANWELL, D.S. 1972. Ecology of salt marshes and sand dunes. Chapman & Hall, London, 258p.
REARDON, E.J., G.B. ALLISON & P. FRITZ 1979. Seasonal chemical and isotopic variations of soil CO_2 at Trout Creek, Ontario. J. Hydrol. 43, 355-371.
REDDY, M.M. 1977. Crystallization of calcium carbonate in the presence of trace concentrations of phosphorus-containing anions. J. Cryst. Growth 41, 287-295.
REDDY, M.M. & K.K. WANG 1980. Crystallization of calcium carbonate in the presence of metal ions, I. Inhibition by magnesium ion at pH 8.8 and 25°C. J. Cryst. Growth 50, 470-480.
REDEKE, H.C. 1922. Zur Biologie der niederlandischen Brackwassertypen. Bijdrage Dierkunde 22, 329-335.
REEBURGH, W.S. 1982. A major sink and flux control for methane in marine sediments : anaerobic consumption. In "The dynamic environment of the ocean floor", K. Fanning & F. Mannheim (eds), Heath, 203-217.
REICHE, P. 1943. Graphic representation of chemical weathering. J. Sed. Petrol. 13, 58-68.
REICHERT, J., K. HABERER & S. NORMANN 1972. Untersuchungen über das Verhalten von Spurenelementen bei der Trinkwasseraufbereitung. Vom Wasser 39, 137-146.
REILLY, T.E. & A.S. GOODMAN 1985. Quantitative analysis of saltwater-freshwater relationships in groundwater systems - a historical perspective. J. Hydrol. 80, 125-160.
RENICK, B.C. 1924. Base exchange in ground water by silicates as illustrated in Montana. U.S. Geol. Surv. Water Supply Paper 520-D, 53-72.
REYNAUD, P.A. & P.A. ROGER 1981. Variations saisonnières de la flore algale et de l'activité fixatrice d'azote dans un sol engorgé de bas de dune. Rev. Écol. Biol. Sol 18, 9-27.
RIBBIUS, C.P.E. 1898. Over de samenstelling en de waarde van het brongas. Het Gas XVIII, 17-20, 85-92, 151-163.
RIBBIUS, F.J. 1925. Bijdrage tot de chemie in dienst der hydrologie : onderlinge en afwisselende verdringing van zoet en zout water in den bodem van Nederland. Rapport 's-Gravenhage, 54 p. + 5 bijlagen.
RICHARDS, L.A. 1954. Diagnosis and improvement of saline and alkali soils. US. Dept. Agriculture Handbook (60), Washington, 160p.
RIDDER, T.B. 1978. Over de chemie van de neerslag; vergelijking van meetresultaten. KNMI-rapport WR 78-4, 45p.
RIDDER, T.B., J.H. BAARD & T.A. BUISHAND 1984. De invloed van monstermethoden en analysetechnieken op gemeten chemische concentraties in regenwater. KNMI rapport TR-55, 42 p.
RIJSDIJK, A. 1983. Het gedrag van enkele belangrijke elementen in het poriënwater tijdens vroege diagenese van anaerobe mariene sedimenten. M.Sc. report, Instit. v. Aardwetensch. Vrije Univ. Amsterdam, 91 p (in dutch).
RIJSDIJK, A. 1984a. Geochemisch laboratoriumonderzoek naar de invloed van sedimenten uit het duingebied ten zuiden van Zandvoort op de grondwatersamenstelling. M.Sc. report, Instit. voor Aardwetenschappen, Vrije Univ. Amsterdam, 54 p. (in dutch).
RIJSDIJK, A. 1984b. Geochemisch onderzoek van zandmonsters uit een diep te infiltreren watervoerend pakket ten behoeve van het FLIP/FLOP-project. Rapport DWL 's-Gravenhage, 48p.
RILEY, J.P. & G. SKIRROW (Eds) 1975. Chemical oceanography. Acad. Press, London & NY.
RIVM 1974-1988. Nationaal meetnet voor luchtverontreiniging, cq Landelijk meetnet luchtkwaliteit. Jaarverslagen van meetresultaten, eerst landelijk daarna gedifferentieerd naar diverse regios.
RIVM 1984-1989. Luchtkwaliteit, jaarverslagen 1984-1989, Rijksinstit. Volksgezondheid & Milieuhygiëne, Bilthoven.
RIWA 1980-1983. Annual reports, regarding the rivers Rhine and Meuse (separately). Samenwerkende Rijn- en Maaswaterleidingbedrijven, Amsterdam.
ROBAS, 1990. Historische atlas Noord- en Zuid-Holland; chromotopografische kaart des Rijks 1 : 25.000. Uitgeverij Robas Producties.
ROBERTSON, W.D. & J.A. CHERRY 1989. Tritium as an indicator of recharge and dispersion in a groundwater system in Central Ontario. Water Res. Research 25, 1097-1109.
ROBERTSON, W.D., J.A. CHERRY & S.L. SCHIFF 1989. Atmospheric sulfur deposition 1950-1985 inferred from sulfate in groundwater. Water Resources Res. 25, 1111-1123.
ROBINSON, R.A. & R.H. STOKES 1965. Electrolyte solutions. 2nd ed., Butterworths, London.
ROEBERT, A.J. 1972. Fresh water winning and salt water encroachment in the Amsterdam dune water catchment area. Geol. en Mijnbouw 51, 35-44.
ROELEVELD, W. 1974. The Groningen coastal area. Ph.D. Thesis Vrije Univ. Amsterdam, 252p.
ROEP, TH.B. 1984. Progradation, erosion and changing coastal gradient in the castal barrier deposits of the western Netherlands. Geologie en Mijnbouw 63, 249-258.
ROEP, TH.B., L. VAN DER VALK & D.J. BEETS 1991. Strandwallen en zeegaten langs de Hollandse kust. Grondboor

& Hamer 45, 115-124.
ROGERS, G.S. 1917. Chemical relations of the oil-field waters in San Joaquin Valley, California. US. Geol. Surv. Bull. 653, 110p.
RONEN, D., M. Magaritz & I. Levy 1987. An in situ multilevel sampler for preventive monitoring and study of hydrochemical profiles in aquifers. Ground Water Monit. Rev., Fall 1987, 69-74.
ROOK, J.J. 1974. Formation of haloforms during chlorination of natural waters. Water Treatment Exam. 23, 234-243.
ROSS, D.S. & R.J. BARTLETT 1990. Effects of extraction methods and sample storage on properties of solutions obtained from forested spodosols. J. Envir. Qual. 19, 108-113.
ROSSKNECHT, G.F., W.P. ELLIOTT & F.L. RAMSEY 1973. The size distribution and inland penetration of sea-salt particles. J. Appl. Meteorol. 12, 825-830.
ROSSUM, J.R. 1949. Conductance method for checking accuracy of water analyses. Anal. Chem. 21, 631.
ROSSUM, J.R. 1975. Checking the accuracy of water analyses through the use of conductivity. JAWWA 67, 204-205.
ROZEMA, J., P. LAAN, R. BROEKMAN, W.H.O. ERNST & C.A.J. APPELO 1985. On the lime transition and decalcification in the coastal dunes of the province of north Holland and the island of Schiermonnikoog". Acta Bot. Neerl. 34, 393-411.
RUDD, J.W.M. & C.D. TAYLOR 1980. Methane cycling in aquatic environments. Adv. Aquat. Microbiol. 2, 77-150.
RUIZ, F., V. GOMIS & P. BLASCO 1990. Application of factor analysis to the hydrogeochemical study of a coastal aquifer. J. Hydrol. 119, 169-177.
RUNNELLS, D.D., T.A. SHEPERD & E.E. ANGINO 1992. Metals in water determining natural background concentrations in mineralized areas. Envir. Sci. & Technol. 26, 2316-2323.
RUTGERS VAN ROZENBURG, J.W.H., J. FORSTER, H.S. VAN LENNEP, H. DE VRIES, N.H. HENKET, & A.W. MEES 1891. Rapport der Commissie van Onderzoek inzake de Duinwaterleiding van Amsterdam. Stadsdrukkerij Amsterdam, 121 p + 120 p. bijlagen + tekeningen.
RUTIN, J. 1983. Erosional processes on a coastal sand dune, De Blink, Noordwijkerhout. Ph.D. Thesis, Publ. (35) Lab. Phys. Geography and Soil Science, Amsterdam.
RUTTE, M. 1990. Speelt zuivering in de bodem bij diepinfiltratie een rol? H_2O 23, 241-245.
RvD 1933. Rapport inzake een geo-hydrologisch onderzoek van de waterwinplaats der N.V. Leidsche Duinwater Maatschappij. Rapport Rijksinstituut Voor Drinkwatervoorziening, 31 p + 8 bijlagen.
RWS 1979. Quality survey in the North Sea. Report with results for 1977 and 1978. Rijkswaterstaat, 256 pp.
RWS 1983-1985. "Kwaliteitsonderzoek in de Rijkswateren" Kwartaalverslagen Rijkswaterstaat, samengesteld door Rijksinstit. Zuiv. Afvalwater in de jaren 1983 t/m 1985.
RYAN, J.N. & P.M. GSCHWEND 1990. Colloid mobilization in two Atlantic coastal plain aquifers : field studies. Water Res. Res. 26, 307-322.
SALISBURY, E.J. 1925. Note on the edaphic succession in some dune soils with special reference to the time factor. J. Ecol. 13, 322-328.
SALISBURY, E.J. 1952. Downs and dunes, their plant life and its environment. London, Bell & Sons Ltd, 328p.
SALMAN, A.H.P.M. 1989. The role of the Stichting Duinbehoud in dutch coastal dune conservation. In "Perspectives in coastal dune management", F. Van der Meulen, P.D. Jungerius & J.H. Visser (eds), SPB Academic Publ. BV, The Hague, 239-247.
SALOMONS, W. & A.J. DE GROOT 1978. Pollution history of trace metals in sediments, as affected by the Rhine river. In "Environmental Biogeochemistry and Geomicrobiology", Vol.I, W.E. Krumbein (ed), 149-162.
SANFORD, W.E. & L.F. KONIKOW. 1989. Simulation of calcite dissolution and porosity changes in saltwater mixing zones in coastal aquifers. Water Res. Res. 25, 655-667.
SANYAL, S.K. & S.K. DE DATTA 1991. Chemistry of phosphorus transformations in soil. Advances in Soil Science 16, 1-98.
SAPEK, B., T. CHURSKI & A. SAPEK 1984. Distribution and translocation of mineral elements in peat profiles of the Wizna bog. Proc. 7th Int. Peat Congress, Dublin June 18-23 1984, Publ by Irish Nat. Peat Comm., 383-395.
SAUZAY, G. 1974. Sampling of lysimeters for environmental isotopes of water. In "Isotope Techniques in groundwater hydrology", Vol. II, IAEA, Vienna, 61-68.
SCALF, M.R., J.F. McNABB, W.J. DUNLAP, R.L. COSBY & J. FRYBERGER 1981. Manual of groundwater sampling procedures. NWWA/EPA Series, 93pp.
SCHEFFER, F. & P. SCHACHTSCHABEL 1970. Lehrbuch der Bodenkunde. Ferd. Enke Verlag, Stuttgart, 448p.
SCHINDLER, D.W. (1981) : Interrelationships between the cycles of elements in freshwater ecosystems. Ch. 7 in "Some perspectives of the major biogeochemical cycles", G.E. Likens (ed), SCOPE, 113-123.
SCHMIDT, K.D. 1977. Water quality variations for pumping wells. Ground Water 15, 130-137.
SCHNITZER, M. & E.H. HANSEN 1970. Organo-metallic interactions in soils : 8. An evaluation of methods for the determination of stability constants of metal-fulvic acid complexes. Soil Sci. 109, 333-340.
SCHOELLER, H. 1934. Les échanges de bases dans les eaux souterraines; trois exemples en Tunisie. Bull. Soc. Géol. Fr. 4, 389-420.
SCHOELLER, H. 1955. Geochemie des eaux souterraines. Revue de l'Instit. Francaise du Petrole 10, 230-244.
SCHOELLER, H. 1962. Les eaux souterraines. Masson, Paris, 642 p.
SCHOELLER, M. 1963. Recherches sur l'acquisition de la composition chimique des eaux souterraines. E. Drouillard, Bordeau, 231p.
SCHROEDER, M. 1988. 15 Jahre Messungen an der Grosslysimeteranlage St. Arnold. LWA Schriftenreihe 44, Landesamt für Wasser & Abfall Nordrhein-Westfalen, 66p.
SCHULZ, H.D. 1972. Grundwasserneubildung berechnet aus der Chlorid-Bilanz. Geol. Mitt. 12, 53-60.
SCHULZ, H.D. 1992. Water movement and geochemical reactions in the unsaturated zone of sands with low calcite content. In "Progress in hydrogeochemistry", G. Matthess, F. Frimmel, P. Hirsch, H.D. Schulz & H.-E. Usdowski (Eds), Springer Verlag, Berlin, 443-449.
SCHULZ, H.D. & E.J. REARDON 1983. A combined mixing cell/analytical model to describe two-dimensional reactive solute transport for unidirectional groundwater flow. Water Resources Res. 19, 493-502.
SCHWERTMANN, U. & H. FECHTER 1982. The point of zero charge of natural and synthetic ferrihydrites and its relation to adsorbed silicate. Clay Minerals 17, 471-476.
SELLERS, W.D. 1965. Physical climatology. Univ. Chicago Press, 272p.
SHIPOVALOV, G.V. 1984. Altitudinal hydrochemical zonations of groundwaters. Water Resources, 261-265.
SHOLKOVITZ, E.R. 1973. Interstitial water chemistry of the Santa Barbara sediments. Geochim. Cosmochim. Acta 37, 2043-2073.
SHOTYK, W. 1988. Review of the inorganic geochemistry of peats and peatland waters. Earth Sci. Reviews 25, 95-176.
SIEVER, R. 1962. Silica solubility, 0-200 °C and the diagenesis of siliceous sediments. J. Geol. 70, 127-150.

SLANINA, J., J. MOLS, J.H. BAARD, H.A. VAN DER SLOOT, J.G. VAN RAAPHORST & W. ASMAN 1979. Collection and analysis of rainwater; experimental problems and the interpretation of results. Intern. J. Environ. Anal. Chem. 7, 161-176.

SLOET VAN OLDRUITENBORGH, C.J.M. 1976. Duinstruwelen in het Deltagebied. Meded. Landb. Hogeschool Wageningen, 76-8.

SLOET VAN OLDRUITENBORGH, C.J.M. & E. HEERES 1969. On the contribution of air-borne salt to the gradient character of the Voorne dune area. Acta Bot. Neerlandica 18, 315-325.

SLUYTER, R. & K. OLSTHOORN 1992. Zwavel in fossiele brandstoffen. Lucht juni 1992, 42-45.

SMEENK, J.G.M.M. 1984. Organische microverontreinigingen en duininfiltratie. Ch4. in KIWA-Meded 81, 106-216.

SMEENK, J.G.M.M., O.I. SNOEK & R.C. LINDHOUT 1990. Van Rijn naar Rein; op zoek naar organische microverontreinigingen in Amsterdams drinkwater. H_2O 23, 126-135.

SMITH, W.H. 1976. Character and significance of forest tree root exudates. Ecol. 57, 324-331.

SNELTING, H. 1979. Miniscreens sampling system. Quart. Rep. Nat. Instit. for Water Supply in the Netherlands 16, 1-2.

SAUZAY, G. 1974. Sampling of lysimeters for environmental isotopes of water. In "Isotope techniques in groundwater hydrology", Vol. II, IAEA, Vienna, 61-68.

SPEELMAN, H. & H. HOUTMAN 1979. Grondwaterkaart van Nederland 1:50.000, kaartb;laden 24, 25 West en 25 Oost. Dienst Grondwaterverkenning TNO, rapport 119, 47p + 15 bijlagen.

SPEELMAN, H. & W. SENDEN 1979. Geo-elektrisch onderzoek Zandvoort-Amsterdam, kaartbladen 24 Oost en 25. Dienst Grondwaterverkenning TNO, 81p + 25 bijlagen.

SPREY, C., F.W. VAN DE VEGTE & E.G.H. VREEDENBURGH 1990. Het Noordhollands Duinreservaat : van grondwatergebruik naar grondwaterbeheer. H_2O 23, 601-608.

STEENKAMP, F.E.M., J. RUNHAAR, T.C.P. MELMAN & H.W.J. VAN DIJK 1981. In het spoor van de dragline; de gevolgen van vergravingen voor bodem en vegetatie. Duin 4, 10-18.

STEWART, W.D.P. 1965. Nitrogen turnover in marine and brackish habitats. I. Nitrogen fixation. Ann Bot. (N.S.) 29, 229-239.

STEWART, W.D.P. & M.C. PEARSON 1967. Nodulation and nitrogen-fixation by Hippophaë rhamnoïdes L. in the field. Plant & Soil 26, 348-360.

STIFF, H.A. 1951. The interpretation of chemical water analysis by means of patterns. J. Petrol. Techn. 3, 15-17.

STOKER, H.S. & S.L. SEAGER 1972. Environmental chemistry : air and water pollution. Scott, Foresman & Comp., Glenview Illinois, 186p.

STRAHLER, A.N. 1969. Physical geography. J. Wiley & Sons, NY, 733p.

STUMM, W. 1984. Interpretation and measurement of redox intensity in natural waters. Schweiz. Z. Hydrol. 46, 291-296.

STUMM, W. & J.J. MORGAN 1981. Aquatic chemistry, an introduction emphasizing chemical equilibria in natural waters. J. Wiley & Sons, NY, 2nd ed.,780pp.

STUURMAN, R.J. 1984a. Kwaliteit van doorval, bodemvocht en ondiep grondwater onder verschillende vegetatietypen in de Amsterdamse Waterleidingduinen. Doctoraalstudie IvA Vrije Univ. Amsterdam, 133p.

STUURMAN, R.J. 1984b. Regenwaterlensvorming op kunstmatig geïnfiltreerd, zijdelings afstromend Lekwater in de Duinwaterwinplaats van Gemeentewaterleidingen. Stagerapport GW, IvA Vrije Univ. Amsterdam, 81p.

STUURMAN, R.J., BIESHEUVEL, A. & VAN DER MEIJ, J.L. 1988. Grondwatersystemen in relatie tot ruimtelijke ordening en milieubeheer (aan de hand van ervaringen in Noord-Brabant). Dictaat GEOPLAN-cursus "Kwantitatief en kwalitatief grondwatergedrag en de anatomie van de aardkorst, 3 nov.'88.

STUYFZAND, P.J. 1977. Hydrochemical aspects of drinking water injection by a deep well in a semiconfined aquifer at Leiduin Pumpingstation near Zandvoort, North-Holland. Report GW, 130 p.

STUYFZAND, P.J. 1979. Tracerproeven ter controle van de bruikbaarheid van de preconcentratie op actieve kool mbv een mengsel reagentia voor de bepaling van Al, V, Cu, Co, Zn, Ni, Fe, Se, Mo, Cd, zeldzame aarden en U in grondwater. Intern rapport Instit.v.Aardwet. Vrije Univ. A'dam, 3 p.

STUYFZAND, P.J. 1982. Analyse van de problemen en mogelijkheden van waterwinning uit de onderkrijt-zandsteenlagen te Enschede, deel B : Geohydrochemie. KIWA-report SWO-83.201B, 74 p, in dutch.

STUYFZAND, P.J. 1983a. Belangrijke foutenbronnen bij bemonstering van grondwater via peil- en minifilters. H_2O 16, 87-94.

STUYFZAND, P.J. 1983b. Kwaliteitsveranderingen van voorgezuiverd Lekwater bij kunstmatige infiltratie in het duingebied ten westen van Castricum. Deelrapport 1 bij KIWA-Meded. 82, KIWA-SWE-366, 86p.

STUYFZAND, P.J. 1983c. Een zeer nauwkeurige berekening van het elektrisch geleidingsvermogen ter controle en aanvulling van wateranalyses. H_2O 16, 358-361 en 363.

STUYFZAND, P.J. 1984a. Kwaliteitsveranderingen van voorgezuiverd Lekwater bij kunstmatige infiltratie in de Amsterdamse waterleidingduinen ten zuiden van Zandvoort. Deelrapport 2 bij KIWA-Meded.82, KIWA SWE-367, 189 p.

STUYFZAND, P.J. 1984b. Kwaliteitsveranderingen van boezemwater bij kunstmatige infiltratie in het wingebied van de Leidsche Duinwater maatschappij. Deelrapport 3 bij KIWA-Meded. 82, KIWA SWE-368, 56 p.

STUYFZAND, P.J. 1984c. Kwaliteitsveranderingen van voorgezuiverd rivierwater bij kunstmatige infiltratie in het wingebied van de Duinwaterleiding van 's-Gravenhage. Deelrapport 4 bij KIWA-Meded. 82, KIWA SWE-369, 223 p.

STUYFZAND, P.J. 1984d. Effecten van vegetatie en luchtverontreiniging op de grondwaterkwaliteit in kalkrijke duinen bij Castricum : lysimeterwaarnemingen. H_2O 17, 152-159.

STUYFZAND, P.J. 1984e. Groundwater quality evolution in the upper aquifer of the coastal dune arae of the western Netherlands" IAHS Publ. 150, 87-98.

STUYFZAND, P.J. (ed) 1984f. Microverontreiniging en duininfiltratie. KIWA Meded. 81, 336 p.

STUYFZAND, P.J. 1985a. Hydrochemie en hydrologie van het duingebied tussen Egmond en Wijk aan Zee; kaartblad 19C. KIWA- rapport SWE-85.012 ,205 p.

STUYFZAND, P.J. 1985b. Hydrologie, herkenning en datering van Rijn-oevergrondwater. Ch.2 in KIWA Meded. 89.

STUYFZAND, P.J. 1985c. Anorganische bestanddelen van Rijnoevergrondwater. Ch.3 in KIWA Meded. 89.

STUYFZAND, P.J. 1986a. A new hydrochemical classification of water types : principles and application to the coastal dunes aquifer system of the Netherlands. Proc. 9th Salt Water Intrusion Meeting, Delft 12-16 may, Delft Univ. Techn., 641-655.

STUYFZAND, P.J. 1986b. Een nieuwe hydrochemische classificatie van watertypen, met Nederlandse voorbeelden van toepassing. H_2O 19, 562-568.

STUYFZAND, P.J. 1986c. Waterbalansen van en verblijftijden in vier, verschillend begroeide lysimeters nabij Castricum. KIWA SWE-85.013 ,53 p.

STUYFZAND, P.J. 1986d. Macroparameters bij duininfiltratie : kwaliteitsveranderingen van oppervlaktewater bij

kunstmatige infiltratie in de Nederlandse kustduinen. KIWA-Meded. 82 ,336 p.
STUYFZAND, P.J. 1987a. Effects of vegetation and air pollution on groundwater quality in calcareous coastal dunes near Castricum, the Netherlands: Lysimetric observations. Proc. Intern. Symp on Acidification and water pathways, Bolkesjo Norway 4-8 may 1987, Norw. Nat. Comm. for Hydrol. (ed), vol.2 , 115-125
STUYFZAND, P.J. 1987b. Een zeer nauwkeurige berekening van het elektrisch geleidingsvermogen ter controle en aanvulling van wateranalyses : 2e versie. KIWA-rapport SWE 87.006, 32 p.
STUYFZAND, P.J. 1987c. Influences of filtration and storage of groundwater samples on sample composition. Trends in Anal. Chem. (TrAC), 6, 50-54.
STUYFZAND, P.J. 1987d. Hydrochemie en hydrologie van duinen en aangrenzende polders tussen Zandvoort en Wijk aan Zee (kaartbladen 24F en 25A). KIWA SWE-86.016, 203 p.
STUYFZAND, P.J. 1988a. De alkaliteit, het redoxniveau en de verontreinigingsindex als parameters en keuzemogelijkheden in een hydrochemische classificatie van watertypen. H_2O 21, 640-643.
STUYFZAND, P.J. 1988b. Hydrochemie en hydrologie van duinen en aangrenzende polders tussen Noordwijk en Zandvoort aan Zee (kaartbladen 24H en 25C). KIWA-rapport SWE 87.007, 343 p.
STUYFZAND, P.J. 1989a. Hydrochemie en hydrologie van duinen en aangrenzende polders tussen Egmond aan Zee en Petten (kaartbladen 19A,B en 14C,D). KIWA-rapport SWE 87.001, 239p.
STUYFZAND, P.J. 1989b. An accurate, relatively simple calculation of the saturation index of calcite for fresh to salt water. J. Hydrol. 105, 95-107.
STUYFZAND, P.J. 1989c. Hydrology and water quality aspects of Rhine bank ground water in The Netherlands. J. Hydrol. 106, 341-363.
STUYFZAND, P.J. 1989d. Hydrochemical evidence of fresh and salt water intrusions in the coastal dunes aquifer system of the Western Netherlands. (Flemish) Natuurwetensch. Tijdsch. 70, 9-29.
STUYFZAND, P.J. 1989e. Quality changes of river Rhine and Meuse water upon basin recharge in The Netherlands' coastal dunes : 30 years of experience. In : "Artificial recharge of Groundwater", Proc. Int. Symp. Anaheim USA, 21- 28 august 1988, Johnson, A.I. & D.J. Finlayson (eds), Am. Soc. Civil Eng., New York, 233-245.
STUYFZAND, P.J. 1989f. Hydrochemische onderzoeksmethoden ter analyse van grondwaterstroming. H_2O 22, 141-146 & 166-169.
STUYFZAND, P.J. 1989g. A new hydrochemical classification of watertypes. IAHS Publ. 182, 89-98.
STUYFZAND, P.J. 1989h. Factors controlling trace element levels in ground water in The Netherlands. Proc. Sixth Int. Symp. Water Rock Interaction, Malvern (UK), August 3-8 1989, D.L. Miles (ed), Balkema Rotterdam, 655-659.
STUYFZAND, P.J. 1989i. Vergelijking van kunstmatige infiltratie via vijvers en putten in geohydrochemisch opzicht. H_2O 22, 721-728.
STUYFZAND, P.J. 1990a. Hydrochemie en hydrologie van het Boerendelgebied, een kwelplasrijk duinterrein benoorden het Wassenaarsche Slag. KIWA-rapport SWE-90.001, 122p.
STUYFZAND, P.J. 1990b. Hydrochemical facies analysis of coastal dunes and adjacent low lands : The Netherlands as an example. In "Dunes, European coasts", T.W.M. Bakker, P.D. Jungerius & J.A. Klijn (eds), Catena Supplement 18, 121-132.
STUYFZAND, P.J. 1990c. Een hydrochemische facies analyse voor hydro-ecologisch onderzoek : theorie en toepassing op Hollands kustduinen en aangrenzende polders. KIWA-Meded 114, 191-213.
STUYFZAND, P.J. 1991a. De samenstelling van regenwater langs Hollands kust. KIWA-rapport SWE-91.010, 70 p.
STUYFZAND, P.J. 1991b. Samenstelling, genese en kwaliteitsvariaties van ondiep grondwater in kustduinen. KIWA-rapport SWE-91.008, 175p.
STUYFZAND, P.J. 1991c. Sporenelementen in Rijnoevergrondwater in het rivierengebied. Ch.8 in KIWA-Meded. 118, 129-154.
STUYFZAND, P.J. 1991d. Sporenelementen in duinwater en kunstmatig geïnfiltreerd oppervlaktewater in de kuststreek. Ch.9 in KIWA-Meded. 118, 155-184.
STUYFZAND, P.J. 1991e. Sporenelementen in grondwater in Nederland. H_2O 24, 756-762 en H_2O 25 (1992), 20-25.
STUYFZAND, P.J. 1991f. Nonpoint sources of trace elements in potable groundwaters in The Netherlands. Proc. 18th Int. Water Supply Congress and Exhibition (IWSA) Copenhagen, 25-31 may 1991, Water Supply 9, SS10-11 -SS10-15.
STUYFZAND, P.J. 1992. De geohydrochemie als hydrologisch detective in Hollands kustvlakte. KNCV Symp. Reeks 4, 37-57.
STUYFZAND, P.J. 1993a. Behaviour of major and trace constituents in fresh and salt intrusion waters, in the Western Netherlands. Proc. 12th Salt Water Intrusion Meeting, November 1992 Barcelona, in press.
STUYFZAND, P.J., W. BASSIE & J. HOOTSEN 1984. Interacties tussen infiltratiewater en het abiotisch milieu. Ch.7 in "Invloeden van infiltratie van Haringvlietwater op het duingebied Schouwen", Rapport Watermaatschappij Zuid-West-Nederland, 100 p.
STUYFZAND, P.J. & J. BOL 1991. Grondwater in Holland. Grondboor en hamer, 45, 142-145.
STUYFZAND, P.J. & J.H. HEIJNEN 1984. Diep grondwater te Enschede door oxydatie van pyriet bedreigd. H_2O 17, 22-25.
STUYFZAND, P.J. & F. LÜERS 1991. Samenstelling van ondiep grondwater in de Luchterduinen, met aandacht voor de interactie met duinveen. KIWA-rapport SWE-91.016, 66p.
STUYFZAND, P.J. & F. LÜERS 1992a. Hydrochemie en hydrologie van duinen en aangrenzende polders tussen Callantsoog en Petten. KIWA-rapport SWE-92.008, 70 p.
STUYFZAND, P.J. & F. LÜERS 1992b. Bodemverzuring en herstel van kalkrijke kwel in de Luchterduinen ten westen van Hillegom. KIWA-rapport SWE 92.027, 42p.
STUYFZAND, P.J., F. LÜERS & H.G. DE JONGE 1993. Hydrochemie en hydrolgie van duinen en aangrenzende polders tussen Katwijk en Kijkduin. KIWA-rapport SWE-93.001, in press.
STUYFZAND, P.J., F. LÜERS & A.P. GROOTJANS 1992. Hydrochemie en hydrologie van het Kapenglop, een natte duinvallei op Schiermonnikoog. KIWA-rapport SWE-93.038, in press.
STUYFZAND, P.J., F. LÜERS & J. HRUBEC 1992. Bewaking en voorspelling van de beïnvloeding van bodem en water door kunstmatige infiltratie. KIWA-rapport SWE-92.023, 72p + 10 bijlagen.
STUYFZAND, P.J., F. LÜERS & E. NIJSSEN 1991. Ophoping en uitspoeling van nutriënten door kunstmatige infiltratie in het Boerendelgebied; een eerste verkenning. KIWA-rapport SWE-91.032, 80p.
STUYFZAND, P.J. & F.M.L MOBERTS 1987a. Hydrochemie en hydrologie van drie soorten (ver)nat duinterrein langs Hollands kust. KIWA SWE-86.006, 218 p.
STUYFZAND, P.J. & F.M.L. MOBERTS 1987b. De bijzondere hydrologie van kwelplassen in duinen met kunstmatige infiltratie. H_2O 20, 52-57 + 62.
STUYFZAND, P.J. & L. REINIERS 1990. Verzuring van grondwater in kalkarme duinen bij Schoorl met gevolgen voor sporenelementen. H_2O 23, 24-29 en 41.

STUYFZAND, P.J. & J.J. STEINMETZ 1990. Kwaliteitsaspecten van pandbodempassage als secundaire voorzuivering van infiltratiewater voor putten. KIWA-rapport SWO 89.326, 88p.

STUYFZAND, P.J. & R.J. STUURMAN 1985. Experimenteel bewijs en modellering van een stationaire regenwaterlens op kunstmatig geinfiltreerd oppervlaktewater. H_2O 18, 408-415.

STUYFZAND, P.J., J. VAN PUFFELEN & H.J.M. LIPS 1985. Anorganische microverontreinigingen. Ch.3 in KIWA Meded. 81, 54-105.

SUGAWARA, K., T. KOYAMA & K. TERADA 1958. Co-precipitation of iodide ions by some metallic hydrated oxides with special reference to iodide accumulation in bottom water layers and in interstitial water of muds in some Japanese lakes. J. Earth Sci. Nagoya Univ.6, 52-61.

SULIN, V.A. 1935. Waters in oil fields. Moscow, discussed in Konzewitsch (1967), opus cited.

SWNBL 1988. Water boven water. Studieresultaten 1983-1987 van de Studiecommissie Waterbeheer, Natuur, Bos en Landschap.

TANJI, K.K. 1969. Predicting specific conductance from electrolytic properties and ion association in some aqueous solutions. Soil Sci. Soc. Am. Proc. 33, 887-890.

TANJI, K.K. & J.W. BIGGAR 1972. Specific conductance model for natural waters and soil solutions of limited salinity levels. Water Res. Res. 8, 145-153.

TANJI, K. & L. VALOPPI 1989. Groundwater contamination by trace elements. Agriculture, Ecosystems and Environment 26, 229-274.

TEN HARKEL, M.J. 1992a. De ecohydrologische meetopstelling : studie naar chemische, fysische en biologische processen op een zuidhelling in de binnenduinen van Meijendel. Rapport Vakgroep Fys. Geogr. & Bodemk., Univ. v. Amsterdam, 223p.

TEN HARKEL, M.J. 1992b. Abiotiek-biotiek interacties in de droge duinen van Meijendel. Meijendel Meded. 24, 65-89.

TE WELSCHER, R.A.G. 1989. Het gedrag van organische microverontreinigingen tijdens duininfiltratie. 5e deelrapport, deel II, Gemeentewaterleidingen Amsterdam, 18p.

TE WELSCHER, R.A.G. & J.G.M.M. SMEENK 1988. Het gedrag van organische microverontreinigingen tijdens duininfiltratie. 4e deelrapport, deel II, Gemeentewaterleidingen Amsterdam, 20p.

THOMAS, A.G. 1986. Specific conductance as an indicator of total dissolved solids in cold, dilute waters. Hydrol. Sci. 31, 81-92.

TIJSSEN, S.B. 1970. Hydrographic and chemical observations in the Southern Bight, February, May, July and October, 1969. Annuals Biol. 73-81.

TIMPERLEY, M.H., R.J. VIGOR-BROWN, M. KAWASHIMA & M. ISHIGAMI. 1985. Organic nitrogen compounds in atmospheric precipitation : their chemistry and availability to phytoplankton. Can. J. Fish. Aquat. Sci. 42, 1171-1177.

TNO 1976. Geophysical well logging for geohydrological purposes in unconsolidated formations. Groundwater Survey TNO, Delft The Netherlands, 67pp.

TOLLENAAR, P. & H. RIJCKBORST 1975. The effect of conifers on the chemistry and mass balance of two large lysimeters in Castricum, The Netherlands. J. Hydrol. 24, 77-87.

TOTH, J. 1963. A theoretical analysis of ground water flow in small drainage basins. J. Geophys. Res. 68, 4795-4812.

TOUSSAINT, B. 1987. Erfahrungen mit Eignungsprüfungen von Messstellen zur Uberwachung der Grundwasserbeschaffenheit. Deutsche Gewässerk. Mitt. 31, 1-11.

TOWNLEY, L.R. & M.R. DAVIDSON 1988. Definition of a capture zone for shallow water table lakes. J. Hydrol. 104, 53-76.

UFFINK, G.J.M. 1990. Analysis of dispersion by the random walk method. Ph.D. Thesis Techn. Univ. Delft, 150p.

UGOLINI, F.C., R. MINDEN, H. DAWSON & J. ZACHARA 1977. An example of soil processes in the Abies amabilis zone of Central Cascades, Washington. Soil Sci. 124, 291-302.

ULLMAN, W.J. & R.C. ALLER 1985. The geochemistry of iodine in near-shore carbonate sediments. Geochim. et Cosmochim. Acta 49, 967-978.

ULRICH, B. 1983. Interaction of forest canopies with atmospheric constituents : SO_2, alkali and earth alkali cations and chloride. In "Effects of accumulation of air pollutants in forest ecosystems", B. Ulrich & J. Pankrath (eds), D. Reidel Publ. Comp., 33-45.

ULRICH, B. 1986. Natural and anthropogenic components of soil acidification. Z. Pflanzenernähr. Bodenk. 149, 702-717.

ULRICH, B., R. MAYER & P.K. KHANNA 1979. Deposition von Luftverunreinigungen und ihre Auswirkungen in Waldokosystemen im Solling. Schr.Forstlichen Fak. Univ. Gottingen & Niedersachs. Forstl. Versuchsanstalt Band 58, J.D. Sauerlander's Verlag Frankfurt a/Main, 291 p.

USDA 1960. Soil classification, a comprehensive system : 7th Approximation. U.S. Dept. Agric., Washington.

VAN AALST, R.M. & H.S.M.A. DIEDEREN 1982. De rol van stikstofoxiden en ammoniak bij de depositie vanuit de lucht van bemestende en verzurende stoffen op de Nederlandse bodem. IG-TNO rapport nr R 83/42, 30 p + 4 appendices.

VAN AALST, R.M. , R.A.M. VAN ARDENNE, J.F. DE KREUK & Th. LEMS 1983. Vervuiling van de Noordzee vanuit de atmosfeer. Rapport TNO Hoofdgroep Maatschap. Techn. nr. CL 82?152a , 123 p.

VAN AALST, R.M., J.H. DUYZER & G.M. MEYER 1984. Veldonderzoek naar droge depositie van gassen en deeltjes. In Adema & Van Ham 1984 (opus cit.), 74- 75.

VAN BEEK, C.G.E.M. 1987. Landgebruik en kwaliteit van het ondiepe grondwater. KIWA-Meded 99, Ch.5.

VAN BEEK, C.G.E.M. & W.F. KOOPER 1980. The clogging of shallow discharge wells in the Netherlands River Region. Ground Water 18, 578-586.

VAN BEEK, C.G.E.M. & J. VAN PUFFELEN 1987. Changes in the chemical composition of drinking water after well infiltration in an unconsolidated sandy aquifer. Water Resources Research 23, 69-76.

VAN BREEMEN, N. & R. PROTZ 1988. Rates of calcium carbonate removal from soils. Can. J. Soil Sci. 68, 449-454.

VAN BREEMEN, N., J. MULDER & C.T. DRISCOLL 1983. Acidification and alkalinization of soils. Plant and Soil 75, 282-308.

VAN BUUREN, J.T. 1988. Noordzee en eutrofiëring. H_2O 21, 591-595.

VAN DAM, D., G.W. HEIL, R. BOBBINK & B. HEIJNE 1990. Atmospheric deposition to grassland canopies : lysimeter budgets discriminating between interception deposition, mineral weathering and mineralization. Water, Air & Soil Pollution 53, 83-101.

VAN DAM, J.C. & J.J. MEULENKAMP 1967. Some results of the geo-electrical resistivity method in ground water investigations in The Netherlands. Geophysical Prospecting 15, 92-115.

VAN DE MEENT, D., J. VAN OOSTERWIJK & T. ALDENBERG 1984. RID-VEWIN meetnet regenwater 1978-1982, deel 1a : De meetgegevens. RIVM-rapport ECOWAD-84-01, 238p.

VAN DE PLASSCHE, O. 1982. Sea-level change and water-level movements in The Netherlands during the Holocene. Meded. Rijks Geol. Dienst 36-1, 93 p.

VAN DER GAAG, M.A. 1984. Enige toxicologische aspecten van kunstmatige infiltratie. Ch.6 in KIWA-Meded 81, 260-283.

VAN DER GOES, J., R. HIGLER, Y. VAN MANEN, R. RUESINK, H. VAN SLOGTEREN & A. ZOOMER 1981.

Duinrellen in Noord-Kennemerland. Rapport Werkgroep Duinrel, 44 p.
VAN DER JAGT, H. & P.J. STUYFZAND 1991. Analysemethoden voor sporenelementen in grondwater, atoom spectrometrie in het bijzonder. Ch.4 in KIWA-Meded 118, 53-65.
VAN DER KOOI, Th. & P.J. STUYFZAND 1987. CHEMCAL, a geographical database for hydrochemical analyses, including chemical, statistical and graphical manipulations. KIWA-manual.
VAN DER MAREL, H.W. 1949. Mineralogical composition of a heath podzol profile. Soil Sc., 193-207.
VAN DER MEER, K. 1952. De bloembollenstreek. De Bodemkartering van Nederland deel 11. Versl. Landbk. Onderz. 58.2, 's- Gravenhage. Ph.D. Thesis, Wageningen.
VAN DER MEULEN, F. 1982. Vegetation changes and water catchment in a dutch coastal dune area. Biol. Conservation 24, 305-316.
VAN DER MEULEN, F. 1988. Een mos verovert de duinen. Duin 1988, 10-12, in dutch.
VAN DER MEULEN, F., P.D. JUNGERIUS & J.H. VISSER (eds.) 1989. Perspectives in coastal dune management. Proc. European Symp., Leiden (The Netherlands), Sept. 7-11, 1987, SPB Acad. Publ. The Hague, 333p.
VAN DER MOLEN, W.H. 1958. The exchangeable cations in soils flooded with sea water. Ph.D. Thesis, Staatsdrukkerij, ,s-Gravenhage, 167p.
VAN DER MOLEN, W.H. 1989. Het zoute grondwater in West-Nederland : een gevolg van dichtheidsstromingen? H_2O 22, 330-331.
VAN DER NEUT, R. 1992. Onderzoek naar organische microverontreinigingen in neerslag in het duingebied bij Castricum. Afstudeerverslag, PWN-rapport, 24p. + 7 bijlagen.
VAN DER SLEEN, W.G.N. 1912. Bijdrage tot de kennis der chemische samenstelling van het duinwater in verband met de geomineralogische gesteldheid van den bodem. Ph.D.Thesis Univ. Amsterdam, Uitg. De Erven Loosjes Haarlem, 157p.
VAN DER SLOOT, H.A. 1976. Neutron activation analysis of trace elements in watersamples after preconcentration on activated carbon. ECN-Rapport ECN-1 (tevens Ph.D. Thesis), Petten, 215 p.
VAN DER SLOOT, H.A., D. HOEDE, J. WIJKSTRA, J.C. DUINKER & R.F. NOLTING 1985. Anionic species of V, As, Se, Mo, Sb, Te and W in the Scheldt and Rhine estuaries and the Southern Bight (North Sea). Estuarine, Coastal and Shelf Sciences 21, 633-651.
VAN DER SLOOT, H.A., J. ZONDERHUIS, C.A. VAN STIGT, J. WIJKSTRA, J.J. DEKKERS, J.J. DOCTER & G.D. WALS 1983. Analyse van sporenelementen in nederlands grondwater. Contract rapport voor RIVM door ECN, ECN-83-10, 22 p.
VAN DER VALK, A.G. 1974. Mineral cycling in coastal foredune plant communities in Cape Hatteras National Seashore. Ecol. 55, 1349-1358.
VAN DER VALK, L. 1992. Mid- and late-Holocene coastal evolution in the beach-barrier area of the Western Netherlands. Ph.D. Thesis Inst. of Earth Sci., Free Univ. Amsterdam, 235p.
VAN DER VEER, P. 1977. Analytical solution for a two-fluid flow in a coastal aquifer involving a phreatic surface with precipitation. J. Hydrol. 35, 271-278.
VAN DER WERFF, A. 1957. Diatom association. Verh. Kon. Ned. Geol. Mijnb. Gen., Geol. Serie 17, 184-189.
VAN DE VEN, G.P., J.P. BURGGRAAFF, P. HUISMAN, R. LAGEMAN, K.J. PROVOOST & L. SENTIS-SENDEN 1986. Atlas van Nederland : Water. Deel 15, Staatsuitgeverij Den Haag, 23p.
VAN DIEREN, J.W. 1934. Organogene Dünenbildung. Den Haag, Ph.D. Thesis Amsterdam.
VAN DIJK, H.W.J. 1984. Invloeden van oppervlakte-infiltraties ten behoeve van duinwaterwinning op kruidachtige oevervegetaties. Ph.D. Thesis LU Wageningen, 240p.
VAN DIJK, H.W.J. 1986. Oppervlakte-infiltratie en neerslagwater-lenzen in de duinen. H_2O 19, 276-278.
VAN DIJK, H.W.J. & J.A. MELTZER 1981. Hydrobiologie van natuurlijke duinmeren : een commentaar. H_2O 14, 564-566.
VAN DIJK, H.W.J. & T.W.M. BAKKER 1984. Duininfiltratie : invloed op balans en concentraties van voedingsstoffen. H_2O 17, 597-600.
VAN DIJK, H.W.J. & W.T. DE GROOT 1987. Eutrophication of a coastal dune area by artificial infiltration. Water Res. 21, 11-18.
VAN DIJK, J.C. 1992. Strategische keuzen van de waterleidingbedrijven : kwaliteit en/of kosten. H_2O 25, 582-592.
VAN DONGEN, P.G. 1969. Rapport inzake een geo-elektrisch onderzoek naar de diepte van het zoetwatervoorkomen in het duingebied en aangrenzend polderland tussen Zandvoort en Noordwijkerhout. Rapport TNO, Afd. Geofys. Onderzoek 44, 26p.
VAN DOORN, Z. 1951. Een hydrologische waarneming aan de lysimeters van het PWN te Castricum. Water (35)3.
VAN DUIJVENBOODEN, W. 1979. Diffuse en lokale verontreinigingsbronnen en hun effecten op het grondwater. H_2O 12, 525-529.
VAN DUIJVENBOODEN, W. (ed) 1989. De kwaliteit van het grondwater in Nederland. RIVM rapport 728820001, 307 p.
VAN ELBURG, H. 1986. Two-dimensional finite difference modelling of groundwater flow systems on micro and personal computers. In " Developments in the analysis of groundwater flow systems (Engelen, G.B. & G.P. Jones, eds), IAHS Publ. 163, 127-140.
VAN ELBURG, H., G.B. ENGELEN & C.J. HEMKER 1991. FLOWNET version 5.1, users manual : microcomputer modelling of two-dimensional steady state groundwater flow in a rectangular heterogeneous anisotropic section of the subsoil. Free Univ. Amsterdam, Instit. Earth Sciences, 31p.
VAN GAANS, P.F.M. 1989. WATEQX - A restructured, generalized and extended Fortran 77 computer code and database format for the wateq aqueous chemical mode for element speciation and mineral saturation, for use on personal computers or mainframes. Computers & Geoscience 15, 843-887.
VAN HOOK, R.I., M.G. NIELSEN & H.H. SHUGART 1980. Energy and nitrogen relations for a Macrosiphum Liriodendri (Homoptera : aphididae) population in an east Tennessee Liriodendron Tulipifera stand. Ecology 61, 960-975.
VAN JAARSVELD,D. & D. ONDERLINDEN 1986. Modelmatige beschrijving van concentratie en depositie van kolen relevante componenten in Nederland, veroorzaakt door emissies in Europa. PEO (uitg), RIVM-rapport 228202002, 67p.
VAN LEEUWEN, W. 1972. De verdamping in de duinwaterwinplaats van Gemeentewaterleidingen nabij Zandvoort. Stagerapport GW, NW nr. 30207, 41p.
VAN NIEVELT, B.F. 1941. Het lysimeterwaarnemingsstation in het provinciaal duinterrein onder Castricum. Water 25, 113-118.
VAN NOORT, P.C.M. 1985. Regenwaterkwaliteitsmetingen in relatie tot vermeerderd kolenverbruik. RIVM-rapport 840170001, 96p.
VAN OLDENBORGH, J. 1915a. Rapport omtrent de uitkomsten van een grondwater- en bodemonderzoek in het duingebied nabij Schoorl. Rijksbureau voor Drinkwatervoorziening, 147 p.
VAN OLDENBORGH, J. 1915b. Rapport betreffende eene centrale drinkwatervoorziening van Midden-Noordholland. Rijksbureau voor Drinkwatervoorziening, 79p.
VAN OLDENBORGH, J. 1916. Mededelingen omtrent de uitkomsten van door het Rijksbureau voor Drink-

watervoorziening ingestelde geohydrologische onderzoekingen in verschillende duingebieden. De Ingenieur 25, 458-467 en 26, 474-498.
VAN OOSTERHOUD, E., G.C. JANZE, W.T. DE GROOT & H.W.J. VAN DIJK 1982. Fosfaat en duin-infiltratie : een experimentele benadering. H_2O 15, 497-501.
VAN PUFFELEN, J. 1979. Berging van oppervlaktewater in de ondergrond. H_2O 12, 541-548.
VAN PUFFELEN, J. 1984. Kwaliteitsveranderingen van water bij diepe infiltratie met putten. KIWA-Meded. 79, 327-356.
VAN PUFFELEN, J. 1985. Kwaliteitsaspecten bij kunstmatige infiltratie van water in de duinen. H_2O 18, 50-54.
VAN PUFFELEN, J. 1986. Onderzoek naar de kwaliteit van de depositie in de duinen van Meyendel. Rapport Duinwaterleiding van 's-Gravenhage, 33p.
VAN REES VELLINGA, E., C.G. TOUSSAINT & K.E. WIT 1981. Water quality and hydrology in a coastal region of The Netherlands. J. Hydrol. 50, 105-127.
VAN SMEERDIJK, D.G. 1989. A palaeoecological and chemical study of a peat profile from the Assendelver polder (The Netherlands). Review of Palaeobotany & Palynology 58, 231-288.
VAN STRAATEN, L.M.J.U. 1954. Composition and structure of recent marine sediments in the Netherlands. Leidse Geol. Meded. 19, 1-110.
VAN STRAATEN, L.M.J.U. 1961. Directional effects of winds, waves and currents along the Dutch North Sea coast (Part 2). Geologie & Mijnbouw (40), 333-346 & 363-391.
VAN STRAATEN, L.M.J.U. 1965. Coastal barrier deposits in South- and North-Holland, in particular in the areas around Scheveningen and IJmuiden. Meded. Geol. Stichting, Nieuwe Serie 17, 41-75.
VAN STRAATEN, L.M.J.U. 1991. Stenen van de Hollandse stranden. Grondboor & Hamer 45, 125-129.
VAN WALLENBURG, C. 1966. De bodem van Zuid-Holland. STIBOKA, Wageningen, 101p.
VAN ZADELHOFF, F.J. 1981. Nederlandse kustduinen; geobotanie. Pudoc, Wageningen, Ph.D. Thesis.
VAN ZOONEN, P., E. BUIJSMAN & A.P.J.M. DE JONG 1988. Onderzoek naar het voorkomen van een aantal polaire bestrijdingsmiddelen in regenwater. Berichten uit het RIVM, 311-315.
VASAK, L., G.J.W. KRAJENBRINK & C.A.J. APPELO 1981. The spatial distribution of polluted groundwater from rural centres in a recharge area in the Netherlands, The Veluwe. In "Quality of groundwater", Studies in Envir. Sci 17, 341- 348.
VEELENTURF, P.W.M. 1982. Saltspray : het mechanisme, de betekenis als ecologische factor in duingebieden, en de veranderingen hierin na aanleg van het Slufterdepot voor de kust van Voorne. Rapport Vakgroep Fys. Geografie, Geogr. Instit. Rijksuniv. Utrecht, 109p.
VEER, M.A.C. 1991. De relatie tussen vegetatie en abiotische (bodem)parameters in vier duinvalleien; I. Inventarisende bodemanalyse, -kartering en -voorspelling. Rapport Gemeentewaterleidingen Amsterdam, 30p.
VERHOEVEN, B. 1962. On the calciumcarbonate content of young marine sediments. Neth. J. Agric. Sci. X, 58-71.
VERMEULEN, A.J. 1977. Immissieonderzoek met behulp van regenvangers : opzet, ervaringen en resultaten. Rapport PWS-Noord- Holland, Dienst voor Milieuhygiene, 109p.
VERRUIJT, A. 1971. Steady dispersion across an interface in a porous medium. J. Hydrol. 14, 337-347.
VERSLUYS, J. 1916. Chemische werkingen in den ondergrond der duinen. Verslag Gewone Vergad. Wis- & Nat. afd. Kon. Acad. Wetenschappen Amsterdam, 25-3-1916, XXIV, 1671-1676.
VERSLUYS, J. 1918. Hydrologie van het Nederlandsche Kustgebied. Water 1, 132-134, 151-152, 171-173, 187-189, 233-235.
VERSLUYS, J. 1931. Subterranean water conditions in the coastal regions of The Netherlands. Econ. Geol. 26, 65-95.
VERSTRATEN, J.M., J.J.H.M. DUYSINGS, L.A. BRUYNZEEL, W. BOUTEN & A.J. VAN WIJK 1984. Effect van de vegetatie (eiken, beuken, fijnspar) op de depositie van zuurvormende bestanddelen op de bodem. In "Zure regen, oorzaken, effecten en beleid", Adema & Van Ham 1984 (eds), PUDOC Wageningen, 113-120.
VISSER, W. 1969. Vaststelling van de immisie van luchtverontreinigende stoffen in de omgeving van Hoogovens. Onderzoek-rapport 30301-TR, Hoogovens, 44p + 51 tabellen + 38 figs.
VOGEL, J.C. 1967. Investigation of groundwater flow with radiocarbon. In "Isotopes in Hydrology", Proc. Vienna Symp. 14-18 Nov. 1966, I.A.E.A, Vienna, 355-369.
VOLKER. A. 1961. Source of brackish groundwater in Pleistocene formations beneath the Dutch polderland. Econ. Geol. 56, 1045-1057.
VOLLENWEIDER, R.A. (1976) : Advances in defining critical loading levels for phosphorus in lake eutrophication. Mem. Inst. Ital. Idrobiol. (33), 53-83.
VON BAUMHAUER, E.H. 1854. Analyse van het duinwater. Ned. Weekblad Geneesk. 4, 27-28.
VONG, R.J. 1990. Mid-latitude northern hemispere background sulfate concentration in rainwater. Atm. Envir. 24A, 1007-1018.
VON WOLZOGEN KÜHR, C.A.H. 1922. Het voorkomen van sulfaatreductie in diepere aardlagen. Water & Gas 6, 163-167 (in dutch).
VOS, G.A. 1984. Bodemkartering Duinwaterwinplaats Gemeente Amsterdam. STIBOKA-rapport 1782, 17p. in dutch.
VOSJAN, J.H. & K.M. OLANCZUK-NEYMAN 1977. Vertical distribution of mineralization processes in a tidal sediment. Neth. J. Sea Res. 11, 14-23.
VROM, 1992. Infiltratiebesluit Bodembescherming, houdende regels met betrekking tot infiltratie van uit oppervlaktewater verkregen water in de bodem. Ontwerp voor inspraak, Staatscourant 3 april 1992, nr 67.
WALLICK, E.I. & J. TOTH 1976. Methods of regional groundwater flow analysis with suggestions for the use of environmental isotopes. In : "Interpretation of environmental isotope and hydrochemical data in groundwater hydrology" IAEA Vienna, 37-64.
WALKER, S.E. 1983. Background groundwater quality monitoring : well installation trauma. Proc. 3rd Nat. Symp. on aquifer restoration and groundwater monitoring. Nat. Water Well Assoc., Worthington, Ohio, 235-246.
WALRAEVENS, K. 1987. Hydrogeologie en hydrochemie van het Ledo-Paniseliaan in Oost- en West-Vlaanderen. Ph.D. Thesis Rijksuniv. Gent, Belgium, 350p.
WARDENAAR, C.P. & J. SEVINK 1992. A comparative study of soil formation in primary stands of Scots pine (planted) and poplar (natural) on calcareous dune sands in the Netherlands. Plant & Soil 140, 109-120.
WARMERDAM, P.M.M. 1981. De invloed van de wind op regenwaarnemingen; een vergelijkend regenmeteronderzoek. H_2O 14, 16-20.
WEDEPOHL, K.H. (ed) 1978. Handbook of geochemistry. Springer Verlag Berlin, 5 Volumes.
WEICHART, G. 1973. Pollution of the North Sea. Ambio 2, 99-106.
WEGMAN, R.C.C., Ph. HAMAKER & H. DE HEER 1983. Bromide-ion balance of a polder district with large-scale use of methyl bromide for soil fumigation. Fd. Chem. Toxic. 21, 361-367.
WESTERHOFF, W.E., E.F.J. DE MULDER & W. DE GANS 1987. Toelichting bij de geologische kaart van Nederland

1:50000, Alkmaar West en OOst (19W-19O). Rijks Geol. Dienst, Haarlem, 227p.

WESTHOFF, V. 1989. Dunes and dune management along the North Sea coast. Perspectives in coastal dune management, F. Van der Meulen, P.D. Jungerius & J.H. Visser (eds), SPB Acad. Publ. B.V., The Hague, The Netherlands, 41-51.

WHITE, D.E. 1957a. Thermal waters of volcanic origin. Geol. Soc. Am. Bull. 68, 1637-1658.

WHITE, D.E. 1957b. Magmatic, connate and metamorphic waters. Geol. Soc. Am. Bull. 68, 1659-1682.

WHITE, W.B. 1984. Rate processes : chemical kinetics and karst landform development. Ch.10 in "Groundwater as a geomorphic agent", R.G. LaFleur (ed), Allen & Unwin, Inc., Boston., 227-248.

WICHMANN, K. 1980. Süsswasservorkommen auf den Nordseeinseln und ihre Nutzung zur Wasserversorgung. Wasserwirtschaft 70, 370-375.

WIERSMA, J. 1991. De ontwikkeling van de Hollandse kust; een kwestie van schaal. Grondboor & Hamer 45, 129-134.

WILLEMSEN. A. 1984. Verkennend onderzoek naar hydrogeochemische gevolgen van warmte-opslag in ondiepe aquifers. Rapport Heidemij, projectnr. 630-03252, 126p.

WILSON, K. 1960. The time factor in the development of dune soils at South Haven Peninsula, Dorset. J. Ecol. 48, 341-359.

WILSON, P. 1992. Trends and timescales in soil development on coastal dunes in the north of Ireland. In "Coastal Dunes", Carter, Curtis & Sheehy-Skeffington (eds), Balkema, Rotterdam, 153-162.

WIND, R. 1951. Een methode voor het verkrijgen van hangwater uit zandgronden. Water 35).

WIND, R. 1952. Verslag van een onderzoek naar de invloed van de vegetatie op de kwaliteit van het duinwater. TNO-Meded. (12), Instit. Toegepast Biol. Onderz. Natuur, Mariendaal, Oosterbeek, 127 p.

WIND, R. 1953. Opvangen van zout uit de lucht door een dennenbosje in de duinen. Water 37, 34-38 en 45-50.

WIND, R. 1954. Evaporatie, transpiratie en interceptie van een dennenbosje in de duinen. Water 18, 261-265.

WIND, R. 1958. The lysimeters in the Netherlands. Comm. Hydrol. Onderz. TNO, Verslagen en Meded. 3, 165-228.

WIND, R. 1960. De lysimeters in Nederland, II. Comm. Hydrol. Onderz. TNO, Verslagen en Meded. 4, 207-263.

WINTER, T.C. 1986. Effect of groundwater recharge on configuration of the water table beneath sand dunes and on seepage in lakes in the sandhills of Nebraska, USA. J. Hydrol. 86, 221-237.

WITKAMP, M. & M.L. FRANK 1969. Evolution of CO_2 from litter, humus and subsoil of a pine stand. Pedobiol. 9, 358-365.

WITT, H. & K.E. WIT 1982. Het verziltingsproces in de ondergrond van Noord-Holland. ICW Nota 1323, 34 p.

WOLTERS-NOORDHOFF 1990. Grote historische atlas van Nederland 1:50.000; I West Nederland 1839-1859. Wolters-Noordhoff bv., Groningen, 103p.

WOOD, W.W. & D.C. SIGNOR 1975. Geochemical factors affecting artificial groundwater recharge in the unsaturated zone. Trans. ASAE 18, 677-683.

WRIGHT, T.W. 1956. Profile development in the sand dunes of Culbin forest, Morayshire; II. chemical properties. J. Soil Sci. 7, 33-42.

YURTSEVER, Y. & J.R. GAT 1981. Atmospheric waters. In : Stable Isotope Hydrology, Techn. Report 210, IAEA, Vienna, 103-143.

YVENS, W.P.M.F., G.P.J. DRAAIJERS, W. BLEUTEN & M.M. BOS 1989. The impact of air-borne ammonia from agricultural sources on fluxes of nitrogen and sulphur towards forest soils. Catena 16, 535-544.

ZAGWIJN, W.H. 1974. The palaeogeographic evolution of the Netherlands during the Quarternary. Geol. & Mijnb. 53, 369-385.

ZAGWIJN, W.H. 1984. The formation of the Younger Dunes on the west coast of The Netherlands (AD 1000-1600). Geologie en Mijnbouw 63, 259-268.

ZAGWIJN, W.H. 1985. An outline of the Quarternary stratigraphy of The Netherlands. Geol. & Mijnbouw 64, 17-24.

ZAGWIJN, W.H. 1986. Nederland in het Holoceen. Geologie van Nederland (I), RGD Haarlem, Staatsuitgeverij 's-Gravenhage, 46 p.

ZAGWIJN, W.H. & C.J. VAN STAALDUINEN (eds.) 1975. Toelichting bij geologische overzichtskaarten van Nederland. RGD Haarlem, 134 p.

ZIMMERMANN, U., K.O. MÜNNICH & W. ROETHER 1966. Tracers determine movement of soil moisture and evapotranspiration. Science 152, 346-347.

ZIMMERMANN, U., D. EHHALT & K.O. MÜNNICH 1967. Soil-water movement and evapotranspiration : changes in the isotopic composition of the water. In "Isotopes in hydrology", Proc. Vienna Symp., IAEA, Vienna, 567-585.

UNITS AND ABBREVIATIONS

Prefixes for multiples and fractions

M	=	mega	=	10^6	μ	=	micro	=	10^{-6}
k	=	kilo	=	10^3	n	=	nano	=	10^{-9}
c	=	centi	=	10^{-2}	p	=	pico	=	10^{-12}
m	=	milli	=	10^{-3}					

Units of measurement

Length	m	metre
Area	m^2	square metre
Volume	m^3	cubic metre
	l	litre = 10^{-3} m^3
Mass	g	gram
Time	s	second
	min	minute
	h	hour
	d	day
	y	year
Temperature	K	Kelvin (273.15 K =
	°C	Celsius 0°C)
Pressure	Pa	Pascal = Newton/m^2
	bar	bar = 0.9869 atm = 10^5 Pa
Radioactivity	Bq	Becquerel [s^{-1}] (1 Bq = 7 pCi)
	TU	tritium unit (=0.119 Bq/l = 10^{-18} $^3H/H$)
	pmc	percent modern carbon
Voltage	V	volt
Electrical conductivity	μS/cm	microSiemens/cm (1 μS/cm = 0.1 mS/m)

Abbreviations, Greec alphabeth

α_L	longitudinal dispersivity of porous medium (m)
α_T	transversal dispersivity of porous medium (m)
α_x	correction factor for a contribution of sea salt = X/Cl^- in ocean water (Table 5.5)
γ_1	activity coefficient monovalent ion
γ_2	activity coefficient divalent ion
$\delta^{13}C$	relative deviation of $^{13}C/^{12}C$ isotope ratio (‰ ; Eq.1.2)
$\delta^{18}O$	relative deviation of $^{18}O/^{16}O$ isotope ratio (‰ ; Eq.1.3)
Δt	phase delay of temperature wave at depth z (s; Eq.6.12)
ΔTIC	change in TIC upon subsoil passage of pretreated Rhine water (mmol/l; Eq.7.4)
ΔX	concentration change upon subsoil passage of pretreated Rhine water (μmol/l; Eq.7.3)
ε	porosity (fraction by volume)
ϕ_o	piezometric head in (semi)confined aquifer at distance 0 (m+MSL)
ϕ_x	piezometric head in (semi)confined aquifer at distance x (m+MSL)
κ	thermal diffusivity (m^2/s; Eq.6.12-6.13)
Ω	angular frequency of oscillation, equal to 2π/wave period (rad/s)
λ	leakage factor ($\sqrt{[K_h D c_v]}$; m/d)
ρ_b	dry bulk density (kg/l)
ρ_f	density of fresh water (kg/l; Eq.3.3)
ρ_s	density of salt water (kg/l; Eq.3.3)
Σa	sum of anions (meq/l; Fig.2.7)
Σk	sum of cations (meq/l; Fig.2.7)
τ	time needed to attain a fraction of the ultimate depth of the fresh-salt water interface in equilibrium (d; Eq.3.11)
τ_{99}	time needed to attain 99% of the ultimate depth of the fresh-salt interface in equilibrium (d; Eq.3.11)

Abbreviations, Latin alphabeth

a	hydrochemical facies qualifier : agressive towards calcite (Table 2.15)
A	hydrochemical facies qualifier : Artificial recharge hydrosome (Table 2.14)
AAS	atomic absorption spectrometry
A_{Cl}	amplitude of concentration signal for chloride (µmol/l; Eq.6.15)
AD	anno domini, i.e. after Christ
AM	hydrochemical facies qualifier : artificial recharge hydrosome, composed of river Meuse water
A_o	amplitude of temperature wave at depth 0 (°C)
AOCl	active carbon adsorbable organohalogens (µg/l)
AP	hydrochemical facies qualifier : artificial recharge hydrosome, composed of polder/boezem water
AR	hydrochemical facies qualifier : artificial recharge hydrosome, composed of river Rhine water
A_x	amplitude of concentration signal for constituent x (µmol/l; Eq.6.15)
A_z	amplitude of temperature wave at depth z (°C; Eq.6.12)
B	width of dune belt (m)
BC	before Christ
BD_x	bulk deposition of compound x (mg $m^{-2}.d^{-1}$)
BEX	Base EXchange index (Eq.2.11)
BP	before present (with ^{14}C-datings generally referring to 1950 AD)
c	hydrochemical facies qualifier : calcareous, i.e. in near-equilibrium with calcite (Table 2.15)
c	thickness of capillary fringe (m)
C	concentration of conservative tracer
c'	relative concentration of conservative tracer (ad Eq.3.14)
C_f	relative concentration of conservative tracer in fresh fluid (ad Eq.3.14)
CFU	colony forming unit
C_{org}	organic carbon in solid phase
C_s	relative concentration of conservative tracer in salt fluid (ad Eq.3.14)
^{14}C	carbon-14 activity (pmc)
Ca^*	Ca^{2+} concentration corrected for contribution of sea salt (µmol/l)
CEC	cation exchange complex (meq/kg dry weight)
CIR	Centre for Isotope Research (University Groningen)
Co.	Company
COD	chemical oxygen demand by and expressed as $KMnO_4$ (mg/l)
C_s	concentration in solid phase (mg/kg)
c_v	vertical flow resistance (d)
C_w	concentration in water (mg/kg)
d	hydrochemical facies qualifier : deep anoxic (Table 2.15)
d	depth below water table (m)
D	hydrochemical facies qualifier : coastal dune hydrosome (Table 2.14)
D	thickness of specific aquifer or aquitard (m)
DIC	total dissolved inorganic carbon (mmol/l)
D_L	hydrodynamical, longitudinal dispersion coefficient (m^2/d; Eq.6.17)
D_T	hydrodynamical, transversal dispersion coefficient (m^2/d; Eq.3.15)
d.wt.	dry weight
%d	damping of concentration fluctuation (%; Eq.6.15 and 6.19)
D_{1-99}	total widt of transition zone in between c'=0.01 and c'=0.99 (m; Eq.3.18)
D_{10-90}	total widt of transition zone in between c'=0.1 and c'=0.9 (m; Eq.3.24)
D_{80}	thickness of a pure (<20% diluted) vegetation water lens (m; Eq.6.5)
D_d	diffusion coefficient (m^2/s)
DOC	dissolved organic carbon (mg/l)
D_s	thickness of aquifer system saturated with salt water (m)
D_x	thickness of rain water lens at distance X (m; Eq.3.21 and 3.23)
DWL	Duinwaterleiding 's-Gravenhage (changed in 1990 into DZH)
DZH	N.V. Duinwaterbedrijf Zuid-Holland (Dune Water Supply Co. of South Holland)
e	hydrochemical facies qualifier : marine cation equilibratrium, i.e. MCE = 0 (Table 2.7)
E	evapotranspiration (m/y)
%E	100*(E/*P*) in %
EC	electrical conductivity (µS/cm)
EC_{20}	electrical conductivity at standard temperature of 20°C (µS/cm)
ECN	Energie-onderzoek Centrum Nederland (Netherlands' Energy Research Foundation), Petten
E_H	redox potential (mV)
E_H7	redox potential at pH7 (mV)
EPI	Eutrophication Potential Index
erf	error function (Eq.3.17)
EWR	N.V. Energie- en Watervoorziening Rijnland (Energy and Water Supply Co. of Rijnland, Ltd)
f	hydrochemical facies qualifier : freshened, i.e. BEX > 0 (Table 2.7)
f	concentration factor by evaporation losses (Table 3.2)
F	formation (geological)
GC	gas chromatography

GH Gemeentebedrijf Hillegom (=municipal water supply of Hillegom)
GVh Gemeentebedrijf Voorhout (= municipal water supply of Voorhout)
GVs Gemeentebedrijf Voorschoten (= municipal water supply of Voorschoten)
GW Gemeentewaterleidingen (=municipal water supply of Amsterdam)
GWs Gemeentebedrijf Wassenaar (= municipal water supply of Wassenaar)
h thickness unsaturated zone (m)
^3H tritium activity (TU)
H_∞ elevation of ground water table at time t=∞ (m+MSL)
$H_2CO_3^*$ $CO_2 + H_2CO_3$
H_o elevation of ground water table at distance 0 (m+MSL)
HPLC high pressure liquid chromatography
H^+_{pot} potential acidity (Eq.5.6)
HSA Hydrological Systems Analysis
H_t elevation of ground water table at time t (m+MSL)
H_x elevation of ground water table at distance x (m+MSL)
HYFA HYdrochemical Facies Analysis
HWL high water line (mean)
i ionic strength
IAP ion activity product of mineral-water reaction in sample
IB ionic balance (% ; Eq.2.2)
ICP-AES inductive coupled plasma atom emission spectrometer
ID_x interception deposition of compound x (mg $m^{-2}.d^{-1}$; Eqs.6.20-6.24)
IGG-TNO Instituut voor Geohydrologie en Geo-energie, van TNO
IR infrared spectrometry
IvA Inst. of Earth Sciences (Vrije Univ. A'dam)
K^* K^+ concentration corrected for contribution of sea salt (µmol/l)
K_d distribution coefficient, i.c. the slope of the linear portion of the adsorption isotherm (l/kg; Eq.7.6)
K_h horizontal hydraulic conductivity (m/d)
KIWA KeuringsInstituut voor WaterleidingArtikelen (the Netherlands' Waterworks Research and Consultancy Institute)
KNMI Koninklijk Nederlands Meteorologisch Instituut (Royal Dutch Meteorological Institute), de Bilt
K_S solubility product of mineral in pure water at temp. T
K_v vertical hydraulic conductivity (m/d)
L hydrochemical facies qualifier : relict Holocene transgression hydrosome
L_∞ length of fresh water tongue below the sea at time t=∞ (m)
L^c as L, coastal type
LDM Leidsche Duinwater Maatschappij (changed in 1989 into EWR)
L^m as L, marsh type
m hydrochemical facies qualifier : mixed redox (Table 2.15)
M hydrochemical facies qualifier connate Maassluis hydrosome
Mg^* Mg^{2+} concentration corrected for contribution of sea salt (µmol/l)
Mig Perelman's migration coefficient (Eq.1.1)
MS mass spectrometry
MSL mean sea level
MW molecular weight (g/mol)
M_{xy} horizontal mixing length through sampling (m; Eq.6.7 and 6.8)
M_z vertical mixing length through sampling (m; Eq.6.7A and 6.8A)
n hydrochemical facies qualifier : nonpolluted (Table 2.15)
n number of samples
N natural groundwater recharge or precipitation excess (m/d)
N normal solution (gram equivalent)
Na^* Na^+ concentration corrected for contribution of sea salt (µmol/l)
o hydrochemical facies qualifier : (sub)oxic (Table 2.15)
OM organic material
p hydrochemical facies qualifier polluted (Table 2.15)
P hydrochemical facies qualifier : polder/boezem hydrosome
P gross precipitation (m/y)
PAHs polycyclic aromatic hydrocarbons
P_{CO2} partial CO_2 pressure (10^5 Pa; Eq6.9 and 8.55)
PDB Peedee Belemnite standard (for ^{13}C)
PE polyethylene
pH - log {H^+ activity}
PI pollution index (-)
POLIN pollution index, specified in Table 2.9
PVC polyvinylchloride
PWN N.V. Provinciaal Waterbedrijf Noordholland (= Provincial Water Supply Co. of North Holland Ltd.)
PWNH Provincie Noord-Holland, directie Water & Milieu (= Provincial Authority of North Holland, direction Water and Environment)
PWS Provincial Water Authority of N-Holland (PWNH since 1989)
q water recharge or discharge (m^2/d; Eqs.3.6-3.8, 3.19-3.20)
Q water discharge or abstraction (m^3/d)
Q_{CaCO3} decalcification flux (mg $CaCO_3$ $m^{-2}.d^{-1}$; Eq.6.26)
r hydrochemical facies qualifier : reduced, i.e.

anoxic (Table 2.15)

RE residue on evaporation at 180°C (Eq.2.5)

RGD Rijks Geologische Dienst (Geol. Surv. Neth.)

R_i retardation factor for constituent i (Eq.7.5)

RID Rijks Instituut voor Drinkwatervoorziening (since the early 1980s part of RIVM)

RIVM Rijks Instituut voor Volksgezondheid en Milieuhygiëne (National Institute of Public Health and Environmental Protection), Bilthoven

RIWA Samenwerkende Rijn- en Maaswaterleidingbedrijven (Cooperation of Rhine and Meuse Water Supply Companies)

RIZA Rijksinstituut voor Integraal Zoetwaterbeheer en Afvalwaterbehandeling

RUG Rijksuniversiteit Groningen (State University Groningen)

RWS Rijks Water Staat (= National Water Authority)

s hydrochemical facies qualifier: salinized, i.e. BEX < 0 (Table 2.7)

s total distance travelled in subsoil, within a vegetation water lens (m; Eq.6.4)

S hydrochemical facies qualifier : North Sea hydrosome

SI_c saturation index of water with mineral calcite (Eq.2.13)

SI_m saturation index of water with mineral m (Eq.2.13)

SMOW standard mean ocean water (for ^2H and ^{18}O)

SO_4^* SO_4^{2-} corrected for a contribution of sea salt (Table 5.5)

T absolute temperature (Kelvin)

T' wave period [d]

T½ half-life

t_d transit time of groundwater from water table to any position within a vegetation water lens (d; Eq.6.2)

TD_x total atmospheric deposition of compound x (mg $m^{-2}.d^{-1}$)

TDS Total Dissolved Solids in water (mg/l)

temp temperature (°C)

TEs trace elements

THMs trihalomethanes

TIC total inorganic carbon (= $H_2CO_3^* + HCO_3^- + CO_3^{2-}$) in mmol/l

TIN total inorganic, ionic nitrogen (= $NH_4^+ + NO_2^- + NO_3^-$) in mmol/l

TNO Organisatie voor Toegepast en Natuurwetenschappelijk Onderzoek (Netherlands' Organization for Applied Scientific Research), Delft

TOC total organic carbon (mg/l)

TotH total hardness (mmol/l)

t_t total transit time in subsoil, within a vegetation water lens (d; Eq.6.3)

t_v transit time of water in the vadose zone (d; Eq.3.1)

t_x transit time of water in the saturated zone at distance x (d; Eq.7.8-7.11)

UV ultraviolet

v migration velocity of tracer in water (m/d)

V mean moisture content of unsaturated zone (fraction by volume)

v_{CaCO3} decalcification rate (mm/d; Eq.6.27)

VEWIN VerEniging voor Waterleidingbedrijven In Nederland (Netherlands' Waterworks Association)

v_i migration velocity of constituent i (m/d)

VOCl volatile organohalogens

VROM Ministerie van Volkshuisvesting, Ruimtelijke Ordening en Milieubeheer

VU Vrije Universiteit (Free University), Amsterdam

v_w migration velocity of water (m/d)

VWM N.V. Voorburgsche Waterleiding Maatschappij

WDM Westlandsche Drinkwater Maatschappij

WLZK WaterLeiding Zuid-Kennemerland (Water Supply Co. South-Kennemerland)

WQI Water Quality Index (-)

WRK N.V. Watertransportmaatschappij Rijn-Kennemerland (Water Transport Co. Rijn-Kennemerland Ltd.)

X horizontal distance to starting point X=0 (m)

X^* concentration of ion X, corrected for a contribution of sea salt (Eq.5.7 and Table 5.5)

X_{cbd} concentration of constituent X corrected for bird droppings (mg/l; Eq.5.8)

z charge

z depth

Z_t depth to the fresh-salt interface at time t (m-MSL)

Z_∞ depth to the fresh-salt interface in equilibrium, i.e. at time t = ∞ (m-MSL)

SUBJECT INDEX

Abstraction of groundwater 98, 99
Accuracy of chemical analysis 48-50
Acid buffer
  sequence 221-223
  buffering in rain water 171-173
Acid facies 60, 61, 138, 139, 270
Acidification 270
Acidity of rain water 171, 172
  potential 172
Activity coefficient 49, 220
Alkalinity 53, 136
Allochthonous 61
Allogenic (def) 201
Analysis
  complete 43
  profundity of 123
  quality of 123
Anoxic (facies) 56, 57
Anoxic fouling 276, 277
Anion, dominating 53, 54
Aquifers in study area 76, 77
Aquitards in study area 76, 77
Artificial recharge
  flow systems 113
  general 30, 33, 98, 102-104
  hydrosome 142-150
  quality changes 33
Association of facies 63, 125
Atmospheric deposition
  air pollution 174-176
  biogenic contribution 173, 174
  contribution of mineral aerosols 173
  sea spray contribution 172, 173
  total 253
Atrophic water 60
Autochthonous 61
Base exchange index 54, 55, 288, 289
Base saturation 202-205
Bird droppings 173, 174
Boezem, definition 95
Bulk precipitation 167-170
Calais deposits 72
Calcareous (facies) 60, 61
Calcite saturation index 60, 61
Calcium carbonate; composition 199-201, 223, 224
Capillary fringe 82, 188
Carbon-13 38, 320-322, 326, 327, 331
Carbon-14 291, 292
Cation
  dominating 53, 54
  exchange 204, 246-248, 276
  exchange capacity 202-205, 264, 265
Chalcophile 37, 38
Classification of :
  elements (geochemical) 37, 38
  water types 51-55
  dune groundwater flow systems 112
Coastal dunes
  in general 28, 29
  of Western Netherlands 29-33
Coding of hydrochemical map units 63, 64, 130
Connate water 61
Conservation of samples 47, 48
Consistency (internal chemical) 50
Constituents
  major 36-38
  trace 36-38
  notation 36
Continental mineral aerosols 173
Conversion
  factors 38, 51
  of old-fashioned parameters 51
Damping 247-252
Dating of groundwater
  by carbon-14 291, 292
  by chloride 239, 240, 243, 289, 290, 302, 303
  by history matching 239, 240, 243
  by oxygen-18 290, 291
  by tritium 290, 302, 303
Decalcification
  boundary 223, 274, 284
  flux (definition) 257
  process 221, 259, 260, 274, 275
  rate 257-260
Deep anoxic (facies) 56, 57, 64
Denitrification 56, 57, 298, 315
Density of water 83
Differentiation of facies 63, 194
Diffusion (molecular) 89, 153
Dispersion
  by sampling 197-199
  effects of 249-252
  hydrodynamic 88-91, 196
Drente Formation 70-72, Encl. 1.4
Drilling fluids, effects of 44, 45
Dune
  calcareous 74, 75
  central comb dunes 73
  decalcified 74, 75, Encl. 1.1
  flow systems 111, 112
  hydrosomes 138-142
  infiltration 103
  lakes see flow-through dune lakes
  microparabolic 73
  older dune deposits 72
  top groundwater 165
  vegetation 75
  younger dune deposits 72
Dune valley
  groundwater 165, 166
  primary 73
  secundary 73
Dunkirk deposits 72
Eem Formation 70-72, Encl. 1.4
Eemian (period) 72
Electrical conductivity 49, 50
Enschede Formation 70, 72
Episode, in precip. chemistry 182-186

Error Function 89
Eutrophic water 60
Evapotranspiration 78-81
Evolution
  geological 91-95
  hydrochemical 267-279, 284-288, 298-302
  hydrological 91-108
  inversion in 65
  lines 64, 65
  prograde 65
  retrograde 65
Facies
  chain 42, 151, 152
  complex 41, 42
  definition 40, 51
  hydrochemical 40, 51-61
  parameters 51-61, 64
  sequence 42
  unit 42
Filtration of groundwater samples 46-47, 122
Flow
  branch 108
  density driven 92, 93, 113
  piston 32
Flow systems (groundwater)
  definition 108
  local 108
  maturity 108
  numbering 108, 109
  partial maturity 108
  regional 108
  subregional 108
  supraregional 108
Flow-through dune lake
  definition 117
  hydrochemical patterns 159-163
  hydro-ecological spinoff 166
  hydrological consequences 118-120
  modelling 119, 120
Fluctuations, annual
  bulk precipitation chemistry 182
  groundwater chemistry 237-240
  natural groundwater recharge 79, 80
  gross precipitation 78, 79
Fluctuations, seasonal
  atmospherical type 246-249
  biological type 246
  bulk precipiation chemistry 182-184
  hydrological type 249
  gross precipitation 78, 81
  groundwater chemistry 233-252
  natural groundwater recharge 81
  water table 81, 241, 241
Foredune ridge 73
Fouling of aquifer 276, 277
Freshened facies 54, 55, 275-278, 287-289, 310, 311
Fresh water lens
  shape 83-87
  size 83-87
  tongue 83-86
  time of formation 85-87
Gas wells 101, 102
Geohydrochemistry, definition 27
Ghyben-Herzberg principle 83, 84
Goldschmidt's geochemical classification 38
Harderwijk Formation 70, 72
Hardness of water 51
Historical hydrology 96-105
  early-historical hydrology 91, 93-96
History matching, technique of 239, 240, 243, 289-291
  sequential 239, 289
  spatial 239, 289
Holocene
  period 72
  transgression water 131-136
Hydrochemical
  district 41, 42
  facies 39, 40
  facies analysis (HYFA) 39-42
  maps 39, 40, 62, 63, 125, 126
Hydrological systems analysis 40, 108
Hydrophile 37, 38
Hydrosome, definition 41
Hyperoxic 57
Hyperthermal water 62
Hypertrophic water 60
Hypothermal water 62
Inheritance of BEX 55, 142, 146
Input function
  sulphate 238, 302
  chloride 238, 302
  tritium 302
Interception 80
Interception deposition
  calculation methods 252-254, 317, 318
  definition 205
  results of calculation 254-256
Interface fresh-salt water 83-87
Intrusion of
  fresh water 55, 310, 311
  salt water 55, 310, 311
Inversion of chloride
  connate type 135
  intruded type 136
Ionic strength 49
Ionic balance 48, 49
Kedichem Formation 70, 72, Encl. 1.4
Kreftenheye Formation 70, 72
Laws in geohydrochemistry 27
Leakage of risers 46
Le Chatelier & Van 't Hoff's principle 179
Lens
  dune water 83-91
  rain water 113-117
  peat water 230
  pure vegetation water 194
Lithophile 37-38
Litter leachate 210, 211
Lysimeters
  composition drainage waters 33, 214-216
  construction 190-192
  drainage quantity 78-81
Maassluis
  flow system 109
  Formation 70-72
  hydrosome 127, 131
Marine Cation Excess 54
Mass balance approach 313, 314
Maximum permissible concentrations 37
Mesotrophic water 60
Meteoric water 61
Methane 57, 127, 133, 136, 322, 331
Methanogenic facies 57
Meuse hydrosome 148, 149
Miniscreen 43, 44
Missing values, estimation of 50, 51

Mixing
by sampling 197-199
in porous medium 88-91
length (def) 197
non-prohibitive 57, 58
prohibitive 57, 58
Multilevel sampling 43, 44
Nature conservation 28-30, 104, 105, 162, 163, 166
N_2-fixation 206, 256, 257
Nitrification 205, 314
Nomenclature of hydrochemical map units 63
North Sea
chemical composition 133, 134
deposits 72
flow system 109-111
hydrosome 136-138
Oligotrophic water 60
Origin detection 61, 62, 125, 126, 138
Orthothermal water 62
Oxic (facies) 55, 56
Oxygen, dissolved 55, 56
Oxygen-18
in groundwater 125-127, 134, 138, 146, 154, 290, 291
in rainwater 181, 182, 184
units of measurement 38
PAHs 202, 205, 216
Palaeogeography of W-Neth. 94
Palaeohydrology of W-Neth. 91-96
Peat
aquitards 76
chemical composition 205
dune peat types 205, 227
dune peat 227-230
Penoxic (facies) 55
Perelman's migration coefficient 38
Persistence order of minerals 201
Phosphate classes 60
Phytolith 211
Piezometer nest 43
Piston flow 32
Pleistocene 68, 72
Podzolization 75, 260
Polder
definition 73
flow system 112, 113
hydrosome 142, 144-146
Pollution index 58, 59
Precipitation
bulk 167-170
excess 78
gross 78
monitoring networks 169, 175
wet-only 168-170
Pure vegetation water 194
Raining out 186
Rain water lenses
definition 113
dispersion across interface 117
evidence from dunes 114
modelling 115-117
Recharge
artificial see Artificial recharge
deep well 104, 105
depression focused 81
focus area 140, 155
natural 78-83
by spreading 103, 104
Redfield equation 276
Redox
cline 57
index 55-58
level 55-57
potential 55-56, 58
reactions 315, 316
sequence 55-57
Relict Holocene transgression hydrosome 131-136
Residue on evaporation 49-50
Retardation factor 293
Retention ridge 73
Rhine hydrosome 146-148
Roll-front 270, 284
Roll-front deposits 270, 284
Saalian (period) 72-
Salinization 97, 100, 101, 106, 107, 113, 114, 304
Salinized facies 54, 55, 300, 302, 304-311
Sampling
conservation 47, 48
devices 44
facility 43
problems, groundwater 44-50
problems, rainwater 168
Sea spray
contribution 54, 172
correction factors 54, 172
Sewage effluent
flow system 102, 111
hydrosome near Zandvoort 143
Siderite 156, 265, 277
Siderophile 37, 38
Silicates
primary 201, 224-226
secundary 201, 202, 225-227
Smoothing see damping
Soil moisture 82, 211-213
Spreading see Artificial recharge
Stem flow 80, 206
Storage in biomass 255, 256
Suboxic (facies) 56, 57
Sulphate
(meta)stable facies 57
reducing facies 57
Suspended fines
correction for dissolution 46, 47
in bulk precipitation 170
in groundwater 46, 47
Tegelen Formation 70, 72
Temperature
amplitude reduction 233, 234
classes 61
of air 68, 233, 234
of water 49, 61, 220
retardation in soil 233, 234
Throughfall 207-210
Trace elements
definition 36
in dune peat 205, 229, 230
in groundwater 37, 47, 121-311
in hydroxides 202
in precipitation 37, 171
in shells 200, 223, 224
in silicates 225, 226
Tracers for groundwater
anthropogenic 62
natural 62
origin detection 61, 62, 125, 126

semi-natural 62
transition (redox) 57
Transit time 81-83
Transpiration 80
Trends
bulk precipitation chemistry 179-181
atmospheric emission 179-180
river Rhine chemistry 158
groundwater composition 234-237
gross precipitation 78-79
groundwater table 100, 105, 107
Tritium
in dune groundwater 134, 282, 290
in Meuse water 126, 134
in precipitation 181, 182, 184
in Rhine water 302, 303
units of measurement 38
Twente Formation 70, 72
Uptake
by vegetation 206, 219, 220, 255, 256
preferential 206, 255, 256
Units of
analysis 38
measurement 359
Unsaturated zone (def) 188
Urk & Sterksel Formation 70, 72
Vadose zone (def) 188
Vegetation
effects on groundwater 32, 33, 219-221, 256
of coastal dunes 75
water (definition) 194
water lens 194-197
Volumetric compensation 113, 114
Washing out 186
Water balance 79
Water quality index 58-60
Water-rock interaction, reactions 316
Water type classification 51-55
Weathering sequence 201
Westland Formation 70-72, Encl. 1.3

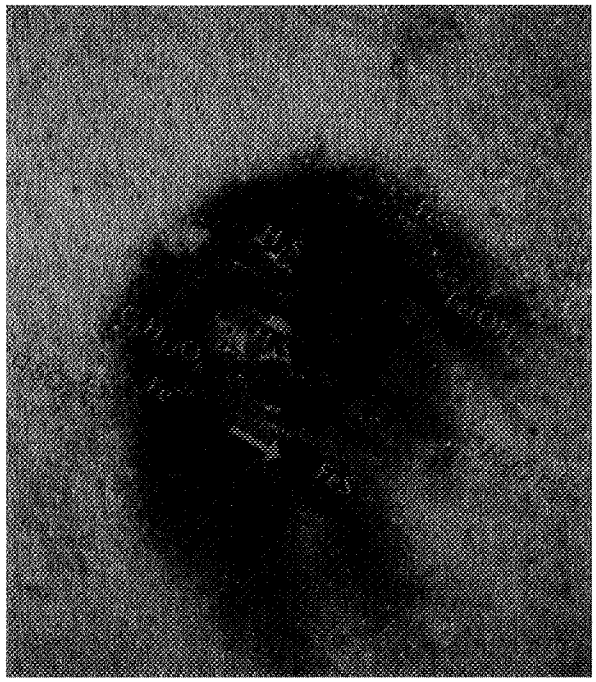

How can we map the chemical composition of groundwater in complex areas?

Where does the Rhine water that is recharged in the dunes but not recovered, remain, and how can it be recognized amidst coastal dune water of highly variable composition?

Why does groundwater under dune shrub strongly deviate from groundwater under Corsican pine?

How deep do environmental pollutants penetrate into the coastal dune aquifer system?

Why does acid dune water show high concentrations of heavy metals, and some deep dune waters high fluoride and phosphate levels?

How can hydrochemistry assist the hydrologist in depicting the true flow patterns and dating groundwater?

In this thesis, Pieter Jan Stuyfzand gives some answers to these and many other questions. An integrated approach of the hydrochemistry and hydrology of Holland's coastal dune area is presented, with emphasis on the chemical composition of groundwater.
A regional survey of the coastal dune area in between Camperduin (North Holland) and Monster (South Holland) forms the starting point of a detailed exploration of the processes that are responsible for the observed, extreme chemical variations of groundwater, both in space and time.

Due attention is paid to the hydrogeological structure, historical developments, groundwater flow, atmospheric deposition, the complex transformation of rain water into shallow groundwater, the chemical evolution within various water bodies down the hydraulic gradient over 0.8-10 km, and chemical mass balances.

The study area contains one of the most varied, extensive, unspoilt coastal dune areas in Western Europe, adjacent to the most densely populated and industrialized polder area of the world.
The high pollution levels of rain water and of the rivers Rhine and Meuse recharging the dune aquifers, make hydrochemical research highly relevant to the custody of both a vital drinking water supply and an already stressed nature reserve.

About the author : Pieter Jan Stuyfzand, born in 1953 (in the dune area), obtained his M.Sc. in physical geography (hydrology; cum laude) at the Institute of Earth Sciences, Vrije Universiteit, Amsterdam in 1978. Since 1981 he is employed as a geohydrochemist and hydrogeologist at KIWA Ltd, Research & Consultancy.

KIWA N.V., Research & Consultancy
Nieuwegein, The Netherlands

ISBN 90-74741-01-0